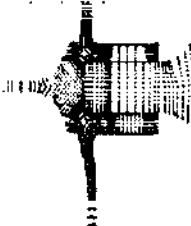
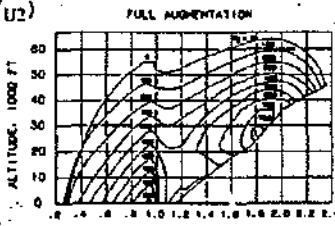


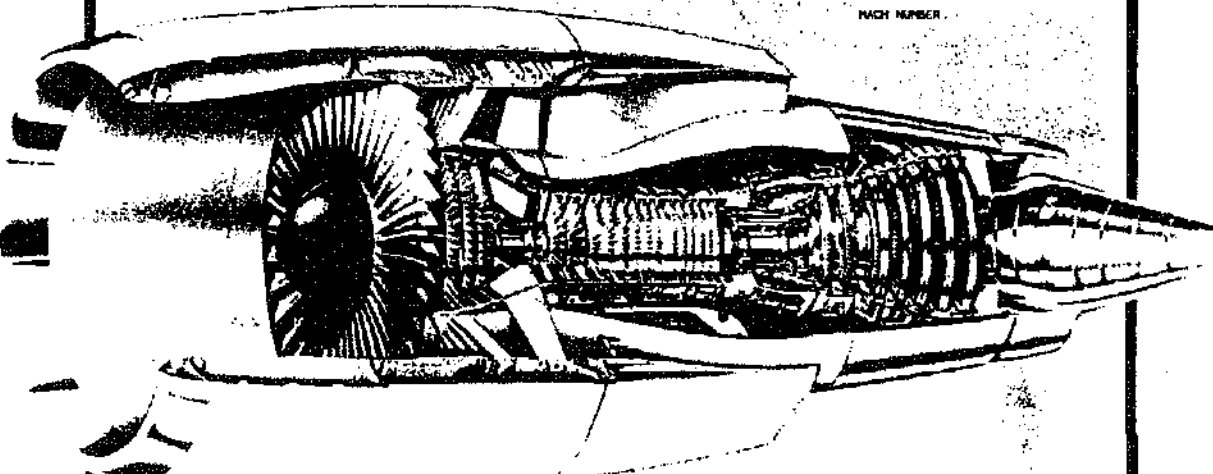
JET ENGINES AND PROPULSION SYSTEMS FOR ENGINEERS



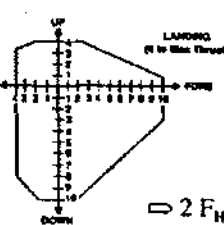
$$\Delta H = \omega r = \frac{W_f}{gJ} \omega r (V_{U1} - V_{U2})$$

$$\psi = \frac{g \Delta h_{TOT}}{2 \sum_{i=1}^n U_i^2}$$

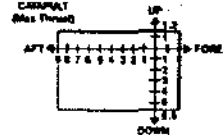




$$E_{\theta} = \frac{m \omega^2 r \cos \theta}{2}$$



S.L. = 2.8
1 = 0
2 = 0
3 = 14 RAD/SEC
4 = 24 RAD/SEC



$$\Rightarrow 2 F_{HXY} = Pr_n \int_0^{\pi} \sin \theta d\theta = Pr_n \left[-\cos \theta \right]_0^{\pi} = 2 Pr_n$$

HUMAN RESOURCE DEVELOPMENT



GE AIRCRAFT ENGINES

Jet Engines and Propulsion Systems For Engineers

Edited by

Thaddeus W. Fowler, Ed.D.

**Training and Educational Development
and the University of Cincinnati**

for

Human Resource Development

GE Aircraft Engines

©1989

Jet Engines and Propulsion Systems For Engineers

G. BERALDO

Munden

P. No. 11165

12/07/02

MTU

Edited by

Tel 03378 - 203170

Thaddeus W. Fowler, Ed.D.

**Training and Educational Development
and the University of Cincinnati**

for

Human Resource Development

GE Aircraft Engines

©1989

PREFACE

The purpose of this book and the companion course is to present to engineers the knowledge that has been gained about jet engines and propulsion systems over the past half century. The book and the course are not meant to present ideas at the highest quantitative level, but are rather to convey fundamental principles from the experts in one area to engineers in other domains. By doing this each can understand to some degree the problems encountered and approaches taken across the entire propulsion system. An increased level of insight and cooperation might come about toward developing even more refined engines and systems.

A number of people have worked together for well over a year to bring about the publication of this book. Each of the chapter authors are named at the beginning of their contribution. David T. Roessler was instrumental in coordinating the writing efforts and the course for which this book was written. Additionally, Rick Caudill, Manager of Structures Drafting, coordinated the production and reviewed the hundreds of drawings and charts in the text. Karen Grimme, Chris Licht, and Joe Lohre produced the drawings on an interactive graphics system. Jeff Hooper and Don Huber operated the computer system to plot each of the drawings. Typesetting and keylining were done by Dale Chance, Glenda Hammon, and Michael Thomas of O'Neil & Associates, Inc.

Thaddeus W. Fowler

TABLE OF CONTENTS

CHAPTER 1

AIRCRAFT MISSION REQUIREMENTS AND PRELIMINARY ENGINE DESIGN

Design Phases	1-1
Conceptual Design	1-1
Preliminary Design	1-1
Detailed Design	1-1
Aircraft Mission Requirements and Figures of Merit	1-5
Constraint Analysis	1-8
Mission Analysis	1-13
Engine Sizing and Cycle Selection	1-13
Cycle Modelling	1-26
Component Performance	1-28
Preliminary Component Design and Matching	1-30

CHAPTER 2

STATIC STRUCTURES

Introduction	2-1
Overall Engine Structure and Major Structural Components	2-1
Design Issues	2-6
Frames	2-7
Casings	2-18
Mounts	2-21
Containment	2-29
Structural Behavior and Analytical Methods	2-31
Maneuver Loads	2-33
Pressure Loads	2-33
Thermal Loads	2-33
Unbalanced Forces	2-34
Limit Conditions	2-35
Ultimate Loads	2-35
Fatigue	2-35
Damage Tolerance	2-36
Material Properties	2-36
Structural Testing	2-40
Summary	2-42

CHAPTER 3

FAN AND COMPRESSOR SYSTEMS

Introduction	3-1
Basic Aerodynamic principles, Components, and Definitions	3-1
Vector Diagrams	3-8
Blading	3-9
Basic Equations	3-10
Performance, Stall, Surge, and Stall Margin	3-11
Trends in Compressor and Fan Design	3-13
Design and Analysis Methods	3-15
Stall Margin Correlation	3-19
Efficiency Potential Correlation	3-20
Axisymmetric Analysis	3-23
Cascade Analysis and Blade Design	3-23
Fan and Prop Fan Configurations	3-28
Variable Geometry, Clearance, and Leakage	3-30
Multi-spool, Variable Geometry and Bleed	3-30
Leakage in Compressors	3-32

Clearance Control	3-33
Summary of Aerodynamic Design Considerations	3-33
Airfoil Physical and Functional Mechanical Design	3-33
Airfoil Mechanical Design Considerations	3-46
Airfoil Loading and Environment	3-46
Airfoil Failure Mechanisms	3-49
Ingestion	3-51
Airfoil Tradeoffs and Implications for Design	3-52
Rotor Physical and Functional Description	3-52
Rotor Design Considerations	3-56
Rotor Loading and Environment	3-56
Rotor Failure Mechanisms	3-60
Fatigue	3-60
Overspeed and Burst	3-60
Vibration	3-61
Rotor Tradeoffs and Implications for Design	3-61
Fan and Compressor Casings	3-62
Casing Design Considerations	3-63
Casing Failure Mechanisms	3-63
Buckling	3-63
Vibration	3-64
Other Failures	3-64
Casing Tradeoffs and Implications for Design	3-65
Fan and Compressor Variable Vane Actuation Systems	3-65
Actuation System Design Considerations	3-68
Actuation System Failure Mechanisms	3-68
Wear	3-68
Hammershock	3-68
Actuation System Tradeoffs and Implications for Design	3-68
Fan and Compressor System Design Considerations	3-68
Containment and Vibratory Weak Link Criteria	3-68
System Vibration and Balance	3-69
Stress Analysis of Rotor Disks	3-69
Numerical Example of Rotor Disk Stresses	3-70
Casing Containment Capability	3-73
Low Cycle Fatigue Life Analysis	3-74

CHAPTER 4

COMBUSTOR AND AUGMENTOR DESIGN

Combustor Aerodynamic Design	4-1
Introduction	4-1
Performance Requirements	4-1
Combustion Efficiency	4-1
Total Pressure Loss	4-1
Temperature Rise	4-1
Combustor Exit Pattern Factor	4-4
Combustor Exit Temperature Profile	4-4
Altitude Relight	4-4
Emission Requirements	4-5
Critical Design Parameters	4-5
Space Rate and Aerodynamic Loading Parameters	4-5
Reference Velocity	4-6
Combustor Dome Height	4-6
Combustor Dome Velocity	4-6
Combustor Length to Dome Height Ratio	4-6
Combustor Passage Velocity	4-6

Number of Fuel Injectors	4-8
Pattern Factor Correlations	4-8
Combustor Flow Distribution	4-9
Fuel Injection System	4-9
Dilution Zone	4-9
Liner Coolong	4-11
Combustor Mechanical Design	4-11
Combustor Analysis	4-13
Fuel Nozzle Design	4-15
Ignition System	4-18

CHAPTER 5

TURBINES

Turbine Aerodynamic Design	5-1
Introduction	5-1
Principles of Operation	5-6
Cycle (or Thermodynamic) Point of View	5-6
Turbine Aero Point of View	5-8
Radial Equilibrium	5-10
Performance Considerations	5-10
Basic Performance Parameters	5-10
Stage Flow Coefficient	5-11
Reaction	5-13
The Turbine Map	5-15
Turbine Loss Sources	5-15
Design considerations	5-24
Cooling Considerations	5-24
Turbine Testing	5-28
Turbine Mechanical Design	5-30
High Pressure Turbine Function	5-30
Design Considerations and Goals	5-30
Turbine Operating Conditions	5-31
High Pressure Stator Component Parts	5-33
HPT Combustor Casing	5-33
Inner Nozzle Support and Inducer	5-33
HP Nozzle	5-34
HP Turbine Shroud	5-34
Static Seals	5-36
HP Rotor Component Parts	5-36
Compressor Discharge Seal (CDP) Disk	5-37
Forward Shaft	5-37
Forward Outer Seal (FOS) Disk and Retainer	5-37
HP Disk	5-38
Aft Retainer	5-38
Aft Shaft	5-38
HP Blade	5-39
The Mechanical Design Process	5-39
The Basic Design	5-41
Preliminary Design	5-41
Engineering Drawings	5-42
Working The Details	5-42
Component and Factor Testing	5-47
Final Certification Analysis	5-47
Low Pressure Turbine Design	5-50
Low Pressure Turbine Rotor Components	5-50
Blades	5-50

LPT Disks	5-50
Interstage Seals	5-50
Blade Retainers	5-52
Shafting	5-52
Low Pressure Turbine Stator Components	5-53
LPT Nozzles	5-53
Shrouds	5-53
Interstage Seals	5-53
Pressure Balance Seal	5-53

**CHAPTER 6
ENGINE QUALIFICATION AND CERTIFICATION**

Engine Qualification	6-1
Master Test Plan	6-1
Program Master Plan	6-1
Engine Spec and Program Master Plan	6-1
Qualification for Production Release	6-1
Engineering Program Plan	6-1
Design Reviews	6-7
Component Qualification	6-7
Corrosion Qualification	6-13
Altitude Qualification	6-14
Endurance Testing	6-14
Operability Evaluation	6-14

**CHAPTER 7
BEARINGS AND SEALS**

Introduction	7-1
Mainshaft Bearing Types	7-1
Fatigue Life Considerations	7-4
Ball Dynamic Analysis	7-8
Heat Generation and Cooling	7-10
Clearance Control	7-13
Cage Slip	7-14
Preloading of Roller Bearings	7-15
Roller Skewing and End Wear	7-15
Static Capacity/Secondary Damage	7-16
Elastohydrodynamic Lubrication	7-16
Materials	7-18
Dynamic Seal Types	7-20
Labrinth Seals	7-20
Clearance Control	7-20
Stick Slip Instability	7-22
Out of Round Instability	7-22
Campbell's Criterion	7-23
1/Rev Excitation	7-23
Aeroelastic Instability	7-23
Rotor-Stator Interaction	7-23
Acoustic Coupling	7-23
Damping	7-25
Configuration and Materials Consideration	7-25
Carbon Seal Design	7-25
Circumferential Seals	7-25
Face Seals	7-27
Pressure Balanced Split Ring Intershaft Seal	7-27
Split Ring Unbalanced Intershaft Seal	7-27
Materials	7-27

Sump Design	7-30
Oil Scavenging	7-30
Fire Safety	7-30
Coking	7-30
Interference Fitting of Bearing Rings	7-30
Bearing Support Stiffness	7-31
Thermal Out of Round	7-31
False Bearings	7-31
Titanium Fires	7-31

**CHAPTER 8
SECONDARY SYSTEMS**

Introduction	8-1
Ait Systems	8-1
HPT Cooling System	8-1
LPT Cavity Purge System	8-5
Parasitic Leakage Purge System	8-5
Heating Systems	8-9
Anti-Icing/De-Icing	8-9
CDP Seal Bore Heating	8-9
TRF Hub Heating	8-9
Clearance Control Systems	8-9
Flange Cooling	8-10
LPT Case Cooling	8-10
HPC Bore Cooling	8-10
Seal Pressurization	8-10
Labyrinth Seals	8-14
Customer Bleed	8-16
Oil Systems	8-16
Lube Supply System	8-16
Lube Tank	8-17
Lube Pump	8-17
Lube Pipe Lines and Jets	8-17
Lube Scavenge System	8-19
Lube Scavenge Pump	8-19
Fuel Iql Cooler	8-19
Chip Detectors	8-19
Sump Vent System	8-21
Ait-Oil Separators	8-21
Oil Consumption	8-23
Oil Filtration	8-23
Lube Heat Rejection	8-23
Fire Safety Analysis	8-23
Sump/Support Heat Transfer Analysis	8-23
Axial Bearing Thrust Control	8-26
HP Rotor Thrust	8-26
Interfaces	8-26

**CHAPTER 8
INLETS AND EXHAUST SYSTEMS**

Aerodynamic Aspects of Inlets and Exhaust Systems	9-1
Introduction	9-1
Inlet Design	9-1
Elements of the Subsonic Inlet	9-1
Inlet Performance	9-1
Low Speed Design Considerations	9-4

Exhaust Nozzles	9-6
Elements of the Exhaust System	9-6
Flowpath Design Considerations	9-7
Exhaust System Performance	9-8
Thrust Reverser	9-8
Elements of the Thrust Reverser System	9-8
Reverser Flowpath Considerations	9-8
Reverser Performance	9-9
Nacelle Design	9-9
Elements of the Nacelle	9-9
Nacelle Performance	9-9
Installed Performance	9-10
Acoustic Considerations	9-10
Mechanical Aspects of Inlets and Exhaust Systems	9-11
Mechanical Design of Inlet	9-11
Lightening Zones	9-16
Commercial High By-Pass Fan Nozzle/Reverser	9-19
Fan Reverser	9-19
Fixed Structure Component System	9-22
Bulkhead Sidewalls	9-22
Inner Cowl	9-22
Outer Support Assembly	9-22
Vane Deflectors	9-22
Translating Cowl	9-22
Fan Reverser Opening System	9-22
Blocker Doors	9-22
Fan Reverser Control Actuation System	9-22
Supply Manifold	9-25
Deploy Operation	9-25
Stow	9-25
Commercial High By-Pass Primary Exhaust System Design	9-26
Lightening strikes	9-26
Abnormal Condition Requirements	9-26
Structural Property Variables	9-27
Weight and Producibility	9-27
Military Afterburning Variable Nozzle System	9-27
Components and Operation	9-29

CHAPTER 10

INSTALLATION AND CONFIGURATION

Commercial Propulsion System Installation	10-1
Commercial Nacelle Systems	10-1
Inlet	10-4
Engine Buildup (EBU) Hardware	10-5
Exhaust System	10-10
Military Engine Installations	10-10
Engine Installation Design Considerations	10-10
Installation Considerations Affecting Engine Maintainability	10-10
Engine Envelope	10-16
Engine-Airframe Interfaces	10-16
Configuration	10-25
Design Philosophy	10-25
Design Approach	10-25
Technical Requirements	10-33
Design Practices	10-33
Design Reviews	10-34

Design Tools, Assembly Aids, and Customer Mockups	10-36
Engineering Design Tool	10-36
Assembly Aid	10-37
Mockup	10-37
Production Engine Assemblies	10-37

CHAPTER 11
CONTROLS ENGINEERING

Introduction	11-1
Applications	11-1
Control System Requirements	11-1
Control Philosophy	11-5
Controls Terminology	11-5
Control Strategy	11-5
Developing Requirements	11-5
Control System Design	11-8
Stability and response	11-9
Definitions and Nomenclature	11-9
Design Requirements	11-14
Design Tools and Methods	11-16
Basic Engine Control Functions	11-17
Core and Fan Speed Control	11-17
Acceleration and Deceleration Control	11-19
Variable Stator Vane control	11-21
Speed and CDP Min and Max Limiting	11-23
Commercial Controls Objectives	11-26
Power Management Control	11-26
Idle Speed Control and Scheduling	11-35
Variable Bleed Valves (VBV's)	11-37
Turbine Clearance Control and Rotor Active Clearance Control	11-39
Reverse Thrust Scheduling	11-44
Military Control Objectives	11-45
Fan Inlet Guide Vane Control	11-45
Turbine Temperature Control	11-45
Fan Operating Line Control	11-46
Augmentor Fuel Scheduling	11-50
Special Functions	11-54
Component Design	11-55
Hydromechanical Control	11-57
Main Engine Controls (MEC's)	11-59
Hydromechanical Units (HMU's)	11-62
Augmentor Fuel Control	11-62
Other Control Components	11-66
Pumps	11-66
Actuators	11-69
Valves	11-71
Sensors	11-74
Electronic Controls	11-78
History	11-78
Environmental Design Factors	11-81
Temperature	11-81
Vibration	11-81
Lightening	11-81
Electromagnetic Interference	11-82
Nuclear Radiation	11-82

Digital Controls	11-82
Definition	11-82
Comparison to Analog	11-87
Redundancy Management	11-91
Adjustment Capability	11-92
Maintainability Features	11-93
Aircraft Bus Interfaces	11-94
Throughput	11-94
Resolution	11-96
Sampling and Digital-to-Analog Conversion	11-97
Software	11-99
Real-Time Software	11-99
Development Process	11-99
Functional Allocation	11-100
 CHAPTER 12	
LIFE ANALYSIS	
Qualification/Certification, Life Analysis	12-1
Commercial Life Analysis	12-1
Thermal Analysis	12-1
Stress Analysis	12-2
Flight Cycle	12-6
Materials Data	12-7
Military Approach	12-11
Life Analysis Summary	12-12
 CHAPTER 13	
PRODUCT SUPPORT	
Product Support	13-1
Maintenance	13-3
Field Related Problems	13-5
Engine Aging	13-6
Condition Monitoring	13-8
End User Assessment	13-9

Chapter 1

AIRCRAFT MISSION REQUIREMENTS AND PRELIMINARY ENGINE DESIGN

by Ronald Giffin and Vincent C. Hill

In general gas turbine aircraft engines may be categorized as belonging to commercial or military transports (Figure 1.1) high performance military fighters (Figure 1.2), or helicopters. Several options exist for converting engine power to propulsive power, and the most appropriate configuration is determined from the particular mission for which the aircraft is being designed and from the thermodynamic factors that control the power and efficiency of the engine.

The mission which an aircraft is designed to perform consists of a flight path with several distinct segments where specific performance requirements must be met. Aircraft are usually required to perform more than one mission where the most demanding mission results in the highest takeoff gross weight (TOGW) and is referred to as the design mission. An acceptable range of loading parameters (thrust loading, wing loading) is determined by incorporating all of the known performance constraints in an aircraft/engine system constraint analysis. Mission analysis is then used to iterate on an engine and airframe design that will satisfy the mission requirements. Performance is computed at constraint points where a particular fuel consumption rate, acceleration, or maneuverability is required. The design point of the engine cycle will correspond to the most demanding of these performance points or mission segments. If a candidate engine design does not satisfy all of the objectives, the engine size or cycle is reworked and the procedure is repeated. The process is inherently iterative and is characterized by the interaction of many technical specialties. The objective of this optimization process is to compare satisfactory candidate configurations and identify the one which best satisfies the mission requirements.

The preliminary engine design sequence is shown in Figure 1.3. Note that there are a number of opportunities for the engine and airframe company to interact and evaluate the "system" design and performance.

DESIGN PHASES

The design process is usually divided into three categories or levels of design: conceptual design, preliminary design, and detailed design. There is a certain degree of interaction between adjoining phases; and consequently, the boundaries are not always distinctly demarcated. There is no absolute procedure for the design of an aircraft engine, and the exact steps involved will depend upon the organizational architecture of the company as well as the specifics of the application. A new engine will always require more analysis than the modification of an existing power plant. What follows is more typical of the design of a new propulsion system.

Conceptual Design Mission objectives and requirements are defined. Parametric trade studies are conducted by both the airframer and engine manufacturer using preliminary estimates of aerodynamics, engine component characteristics, weights, etc. in order to establish the best engine/airframe match for the given mission. More than one engine type may be considered. Cycle selection and engine sizing studies are conducted to define the engine airflow capacity, bypass ratio, overall engine pressure ratio, and other independent design variables which maximize the figures of merit (FOM) upon which the system is evaluated while simultaneously meeting the mission requirements. Because of the strong interaction between engine and aircraft design variables, considerable interaction and iteration between the airframer and engine company is generally required. The process is one of compromise.

Preliminary Design The configuration established in the conceptual design phase is refined. More sophisticated procedures are used to optimize the design variables and minor adjustments are made in order to minimize the impact of any single variable on the figures of merit. Better estimates of component characteristics are incorporated into the cycle model and greater attention is given to secondary effects. Design tools are becoming more complex and increasing emphasis is placed on maintaining the aerodynamic and mechanical integrity of the design. Manufacturing, cost, and maintenance considerations are incorporated. The configuration is beginning to get locked in.

Detailed Design The configuration is "frozen". Detailed aerodynamic and mechanical design is completed. Accessories, controls, customer interfaces and other components are designed. All equipment and hardware items are specified and designed. Detailed drawings are made. Tooling and other production fixtures are made.



Figure 1.1 Commercial Transport

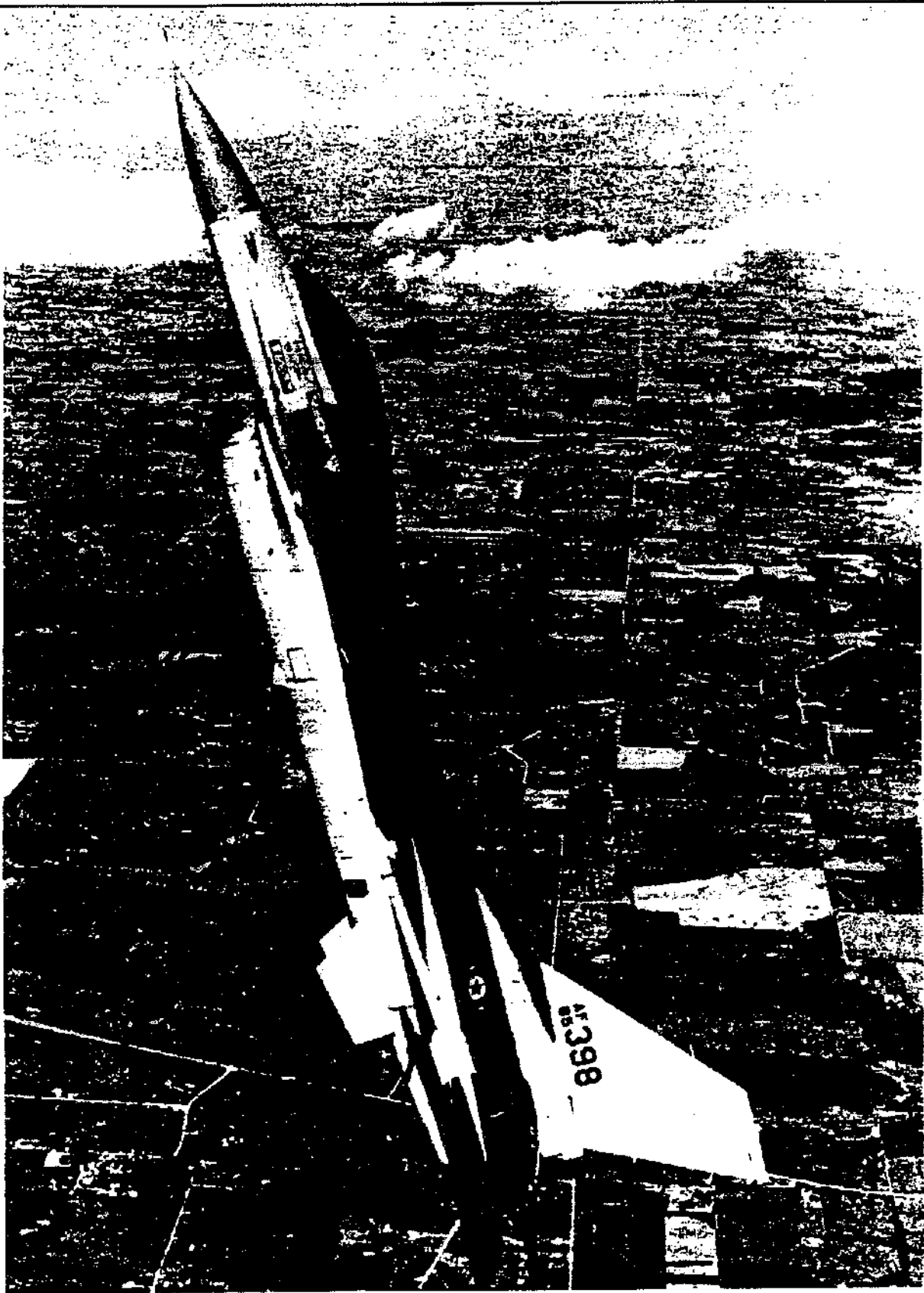


Figure 1.2 High Performance Military Fighter

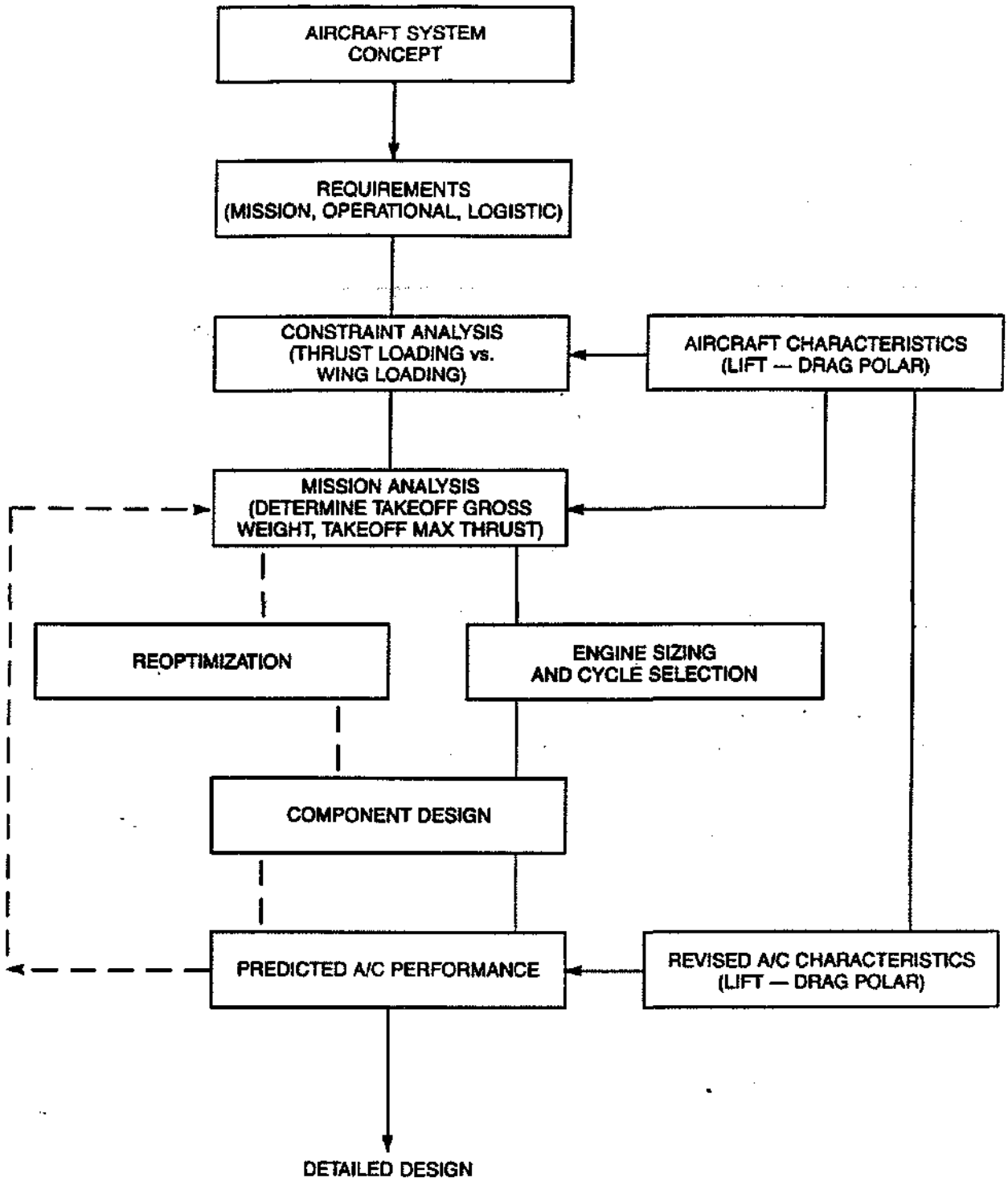


Figure 1.3 Preliminary Aircraft Engine Design Sequence

AIRCRAFT MISSION REQUIREMENTS AND FIGURES OF MERIT

The design process is driven by the aircraft mission requirements, which are specific requisites defining the expected performance characteristics of the aircraft system throughout the flight envelope. In addition to mission requirements there are also operational requirements which define the desired maintainability, logistic and serviceability characteristics of the aircraft. Both mission and operational requirements are specified prior to the design of the aircraft, are independent of the design, and are formulated by the end user or customer. Multiple mission and operational requirements invariably lead to conflicting design choices. This usually occurs during the conceptual and preliminary design phases when the realism reflected in the requirements is still being assessed. Consequently, mission requirements may often be reappraised and compromised as the design of the airframe and propulsion system progresses.

Figures of merit, on the other hand, are performance and operational characteristics dependent upon the specifics

of the aircraft design, but are not directly specified in the requirements. The designer uses the FOMs to evaluate competing designs which satisfy the requirements. In some cases, the distinction between a FOM and a requirement may not be obvious, especially if there is little or no operational experience associated with the system. Generally speaking, however, the mission and operational requirements drive the design options while the FOMs drive the selection from within these options. Formulation and recognition of the relative importance of the proper FOMs is critical to a successful design effort and requires a considerable understanding of the user's needs. Attention to the wrong FOMs can obviate an otherwise successful design.

Typical mission requirements and FOMs are shown in Table 1.1 for two representative aircraft systems: commercial transport and supersonic fighter. The general direction of this chapter will be to contrast these two respective aircraft systems in order to give the reader an appreciation of how the mission requirements and FOMs drive design decisions.

TYPICAL DESIGN REQUIREMENTS	
Commercial Transport <ul style="list-style-type: none"> • Range • Payload • Balanced Field Length • End of Climb Thrust • Engine Out Climb Gradient • Noise and Emissions • Growth Capability 	Military Fighter <ul style="list-style-type: none"> • Mission Radius • Payload • Sustained and Instantaneous "G" Capability • Specific Excess Power • Time to Accelerate • Maximum Mach Number and Dynamic Pressure • Field Length • Combat Ceiling • Growth Capability
FIGURES OF MERIT (FOM)	
Commercial Transport <ul style="list-style-type: none"> • Initial Investment • Direct Operating Cost • Cost Per Seat Mile • Fuel Consumption • Fuel Per Seat Mile 	Military Fighter <ul style="list-style-type: none"> • Life Cycle Cost (or Force Size for Fixed LCC) • Performance Parameters in Excess of Requirements • Takeoff Gross Weight • Alternate Mission Performance (Flexibility)

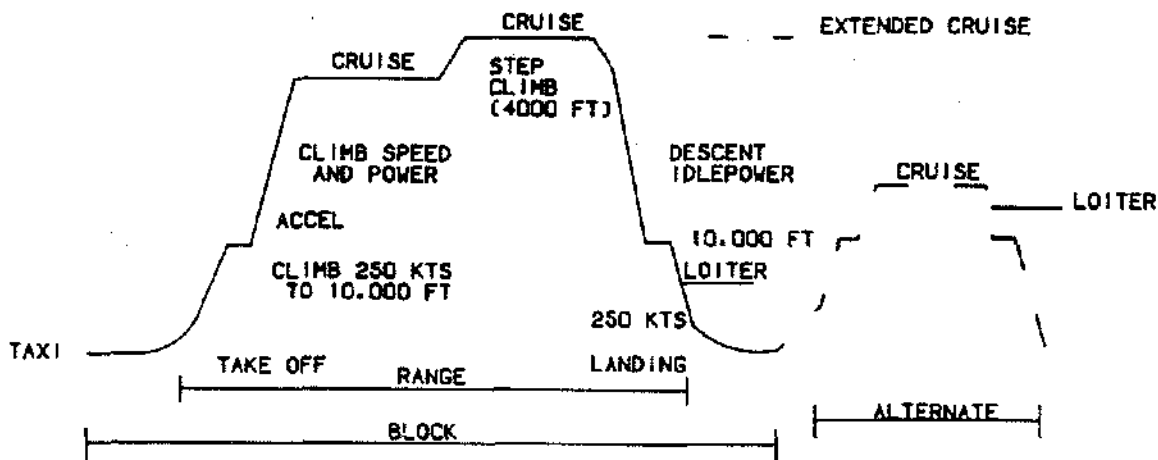
Table 1.1 Typical Mission Requirements and Figures of Merit

A typical commercial transport mission is depicted in Figure 1.4 and a range of tactical fighter missions is shown in Figure 1.5. The various branches of the military require multiple mission capability and place numerous operational requirements on the same airframe in order to reduce the number of aircraft types in their inventory. This is especially true of the Navy due to space, equipment, and manpower limitations imposed by carrier operations. Consequently, a tactical fighter will be required to perform a combination of the missions shown in Figure 1.5, and a particular design will be evaluated not only in its primary role but also on its performance in alternate missions.

In general, commercial systems will be evaluated primarily on economic factors; although environmental and safety constraints also receive considerable attention. Fuel costs, in some form, will be the principal FOM. However, purchase price, ease of maintenance, reliability, direct operating cost (DOC), life cycle cost (LCC), takeoff gross weight (TOGW), etc. all play an intertwining role in the design of the airframe and propulsion system. As an illustration of the relationship between requirements, FOMs, and the design, consider a commercial transport designed for minimum fuel burn. The

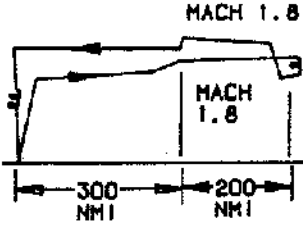
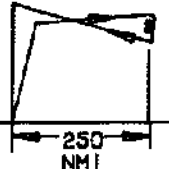
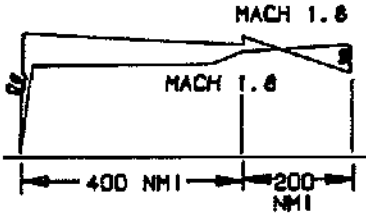
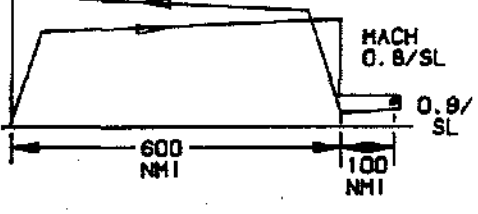
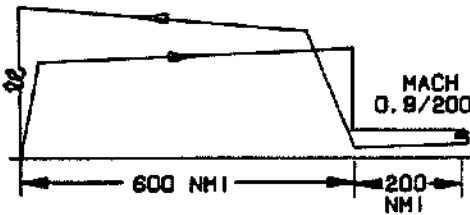
resulting aircraft will not be the same as one designed for minimum DOC or LCC. The minimum fuel burn aircraft will optimize at a lower flight speed, thrust to weight ratio, and wing loading; while the aircraft designed for minimum DOC or LCC will tend to optimize at higher values. If the range requirement is increased, fuel costs will dominate DOC and LCC and the design for minimum DOC or LCC will approach the minimum fuel burn design.

In contrast to a commercial system, a supersonic tactical fighter design requires optimization over a multiplicity of flight conditions. The aircraft may be required to perform an efficient subsonic cruise to a point of loiter or reconnaissance or penetrate supersonically to deliver weapons at an interior target. The aircraft may also be required to accelerate rapidly to either escape or overtake an adversary and to engage in transonic combat. Peacetime usage of the aircraft must also be considered in the airframe and engine design process. Peacetime duty cycles of both USAF and Navy aircraft have proven to be more severe than the design missions and must therefore be considered in determining both cyclic and time/temperature dependent design parameters.



- CITY PAIR FLIGHT
- - - REPRESENTS RESERVE FUEL ALLOCATIONS
 - ALLOCATION DEPEND ON FLIGHT - DOMESTIC/INTERNATIONAL
 - FUEL TO ALTERNATE AIRPORT
 - LOITER/HOLD AND EXTENDED CRUISE

Figure 1.4 Typical Subsonic Commercial Transport Mission

AIRFORCE	NAVY
<p style="text-align: center;">AIR - TO - AIR</p> <p>ACCEL 0.8-1.6/30,000 FT. 50 SECONDS TURN 0.9/30,000 FT. 4.5 G'S TURN 1.6/30,000 FT. 6.0 G'S STOL 1,500 FT</p>  <p style="text-align: center;">FEBA*</p>	<p style="text-align: center;">CAP (COMBAT AIR PATROL)</p> <p>ACCEL 0.8-1.6/35,000 FT. 75 SECONDS ACCEL 0.5-0.8/SL. 70 SECONDS P₃ 0.9/10,000 FT MAX F_N 850 INT F_N 300 TURN 0.6S/10,000 FT MAX F_N 6.5 G'S INT F_N 4.0 G'S</p>  <p style="text-align: right;">35,000 FT LOITER 2 HOURS</p>
<p style="text-align: center;">AIR - TO - GROUND (HIGH)</p> <p>ACCEL 0.8-1.6/30,000 FT. 50 SECONDS TURN 0.9/30,000 FT. 4.5 G'S TURN 1.6/30,000 FT. 6.0 G'S STOL 1,500 FT</p>  <p style="text-align: center;">FEBA</p>	<p style="text-align: center;">AWS (ALL WEATHER STRIKE) (LOW)</p> <p style="text-align: center;">SAME AS CAP</p> 
<p style="text-align: center;">AIR - TO - GROUND (LOW)</p> <p>ACCEL 0.8-1.6/30,000 FT. 60 SECONDS TURN 0.9/30,000 FT. 4.0 G'S STOL 2,000 FT</p>  <p style="text-align: center;">FEBA</p>	<p>ALTERNATES: DLI (DECK LAUNCH INTERCEPT) FE (FIGHTER ESCORT) AWS (HIGH) (ALL WEATHER STRIKE) ASW (ANTI SUBMARINE WARFARE)</p>

* FEBA - FORWARD EDGE OF BATTLE AREA

Figure 1.5 Tactical Fighter Missions

These requirements may be further complicated by the increasing need for:

STOL - Short takeoff and landing from restricted or battle damaged runways with very low approach speeds.

Stealth - Suppression of infrared and radar signatures, noise, and contrails to avoid detection and targeting by enemy systems.

Supercruise - The need for greater penetration Mach numbers both to enhance air-to-air combat capability and to reduce the surface-to-air missile launch window.

A particular aircraft mission (or collection of missions for a mixed mission aircraft) can be expressed in terms of equivalent flight envelopes, **Figures 1.6a and 1-6b**. The flight envelope determines the operating environment of the engine, which is of equal importance to the design. Ambient variations in temperature and pressure along with ram effects associated with the flight Mach number can produce high inlet temperatures and high pressure loads which the engine must be designed to sustain. At any flight condition, the flow conditions at the inlet can be calculated using standard aerothermodynamic relationships, while the pressure recovery in the inlet will be dependent upon the details of the inlet design. In order to standardize cycle calculations, the U.S. standard atmosphere is used to define pressure and temperature variations with altitude and a military specification (mil-spec) ram recovery is usually used to define the pressure recovery in the inlet, **Figure 1.7**; although specific recovery schedules may be supplied by an airframer when these effects are known or can be estimated.

Ram temperatures and pressures, as well as free stream dynamic pressure, are plotted in **Figure 1.8** using the U.S. standard atmosphere and mil-spec recovery definition. The dynamic pressure is significant to the structural design of the aircraft while temperature levels and pressure differences are considerations in the structural design of the engine. At low altitudes high ram temperatures and pressures are encountered at relatively low Mach numbers. These temperatures are critical to the design of the compression components and to the selection of materials, which must withstand these temperatures with minimal strength deterioration. The entire engine casing is also exposed to large pressure differentials at low altitude, high speed flight because the effect of a given engine pressure ratio on pressure differential increases with increasing inlet pressure.

Hot and cold day temperature excursions must also be factored into the engine operating envelope. At sea level

a hot day is defined as standard +31 °F and a cold day is defined as standard -65 °F, although average temperature variations diminish with altitude. The impact of hot and cold day operations on the flight envelope can be noted in **Figure 1.9**.

CONSTRAINT ANALYSIS

Once the mission requirements have been specified, a constraint analysis is used by the airframer to identify permissible aircraft thrust loading and wing loading. Thrust loading is defined as maximum take off net thrust developed on a standard day at sea level static conditions divided by the maximum take off gross weight of the aircraft, and wing loading is defined as the maximum take off gross weight divided by the wing area. Here the net thrust is referred to on an installed basis, which is less than the uninstalled net thrust produced by the engine when it is not attached to the aircraft.

Additional drag is generated on the external surfaces of the aircraft by the engine because engine airflow demand alters the airflow in the vicinity of the inlet and exhaust nozzle and may change the circulation characteristics of the fuselage, wing and tail. This drag is not accounted for in the aircraft drag model and must be estimated in addition to the aerodynamic characteristics of the airframe and the thrust lapse characteristics of the engine before a constraint analysis can be accomplished. Lift-drag polars for large cargo, commercial, or high performance fighter type aircraft can be estimated from available data bases or from experience. Similarly, the variation of engine thrust with altitude, Mach number and afterburner operation can also be estimated from available information and some basic cycle and technology assumptions.

Every performance requirement can be translated into a constraint boundary on a diagram of thrust loading vs. wing loading, **Figure (1.10)**. Any combination of thrust loading and wing loading that falls into the solution space satisfies all of the performance requirements. There are usually many acceptable solutions from this standpoint, however it is left to the design community to identify the best by maximizing the FOM's within the solution space. It is desirable to keep the thrust loading down in order to reduce costs and wing loadings should be consistent with design experience in order to ensure good handling qualities. This means that designers will focus on regions near the bucket in the solution space, although prudence must be exercised so that any movement of any of the constraint lines does not render a selection invalid.

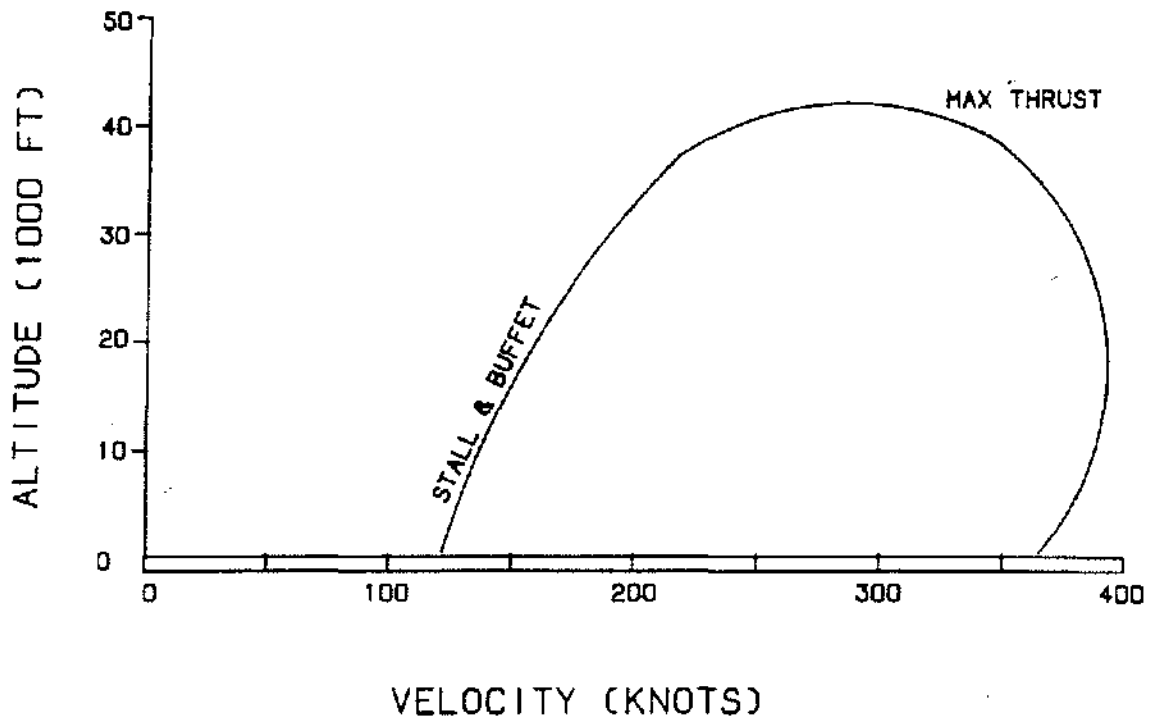


Figure 1.6a Typical Subsonic Aircraft Flight Envelope (Fairchild-Republic A10)

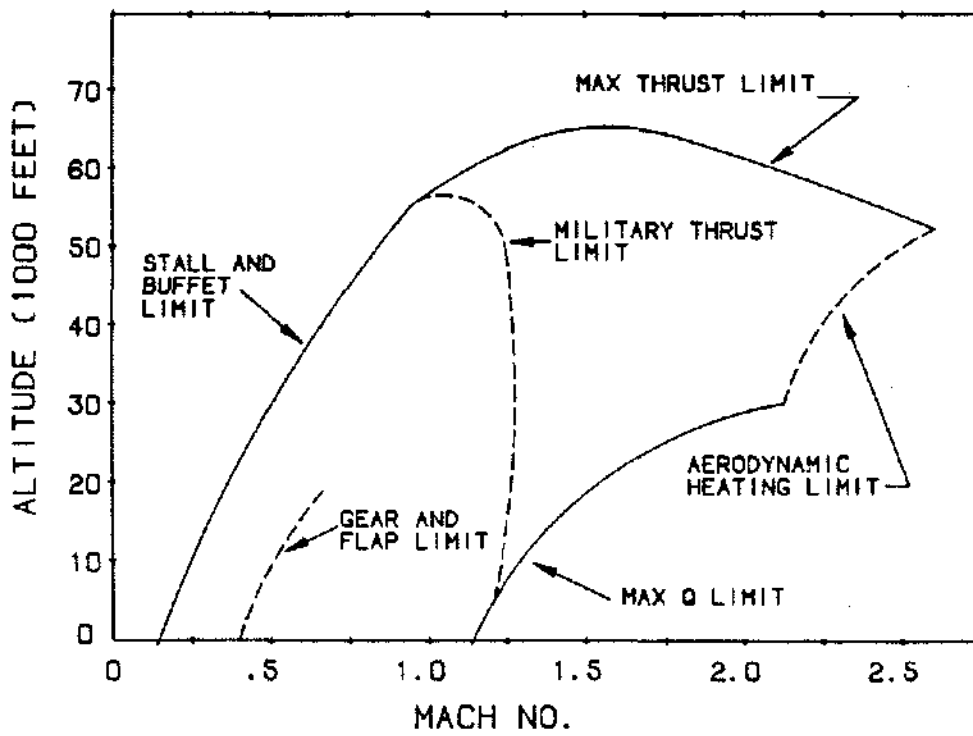


Figure 1.6b Typical Supersonic Aircraft Flight Envelope (Northrop F-20)

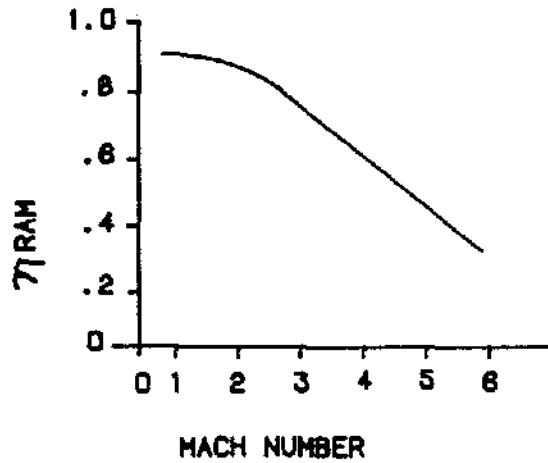
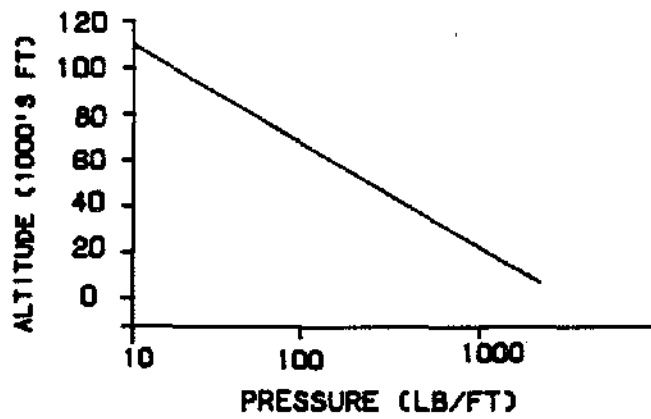
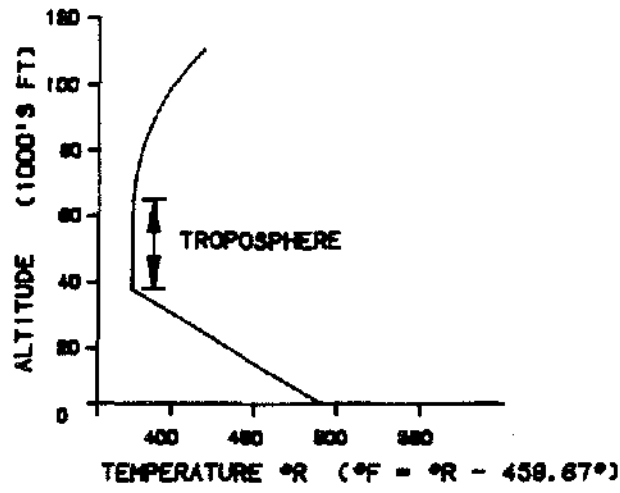


Figure 1.7 The U.S. Standard Atmosphere and a Reference Military Specification (Mil-Spec) Ram Recovery are Used to Standardize Cycle Calculations. These Schedules Define the Inlet Temperature and Pressure for a Given Altitude and Mach Number.

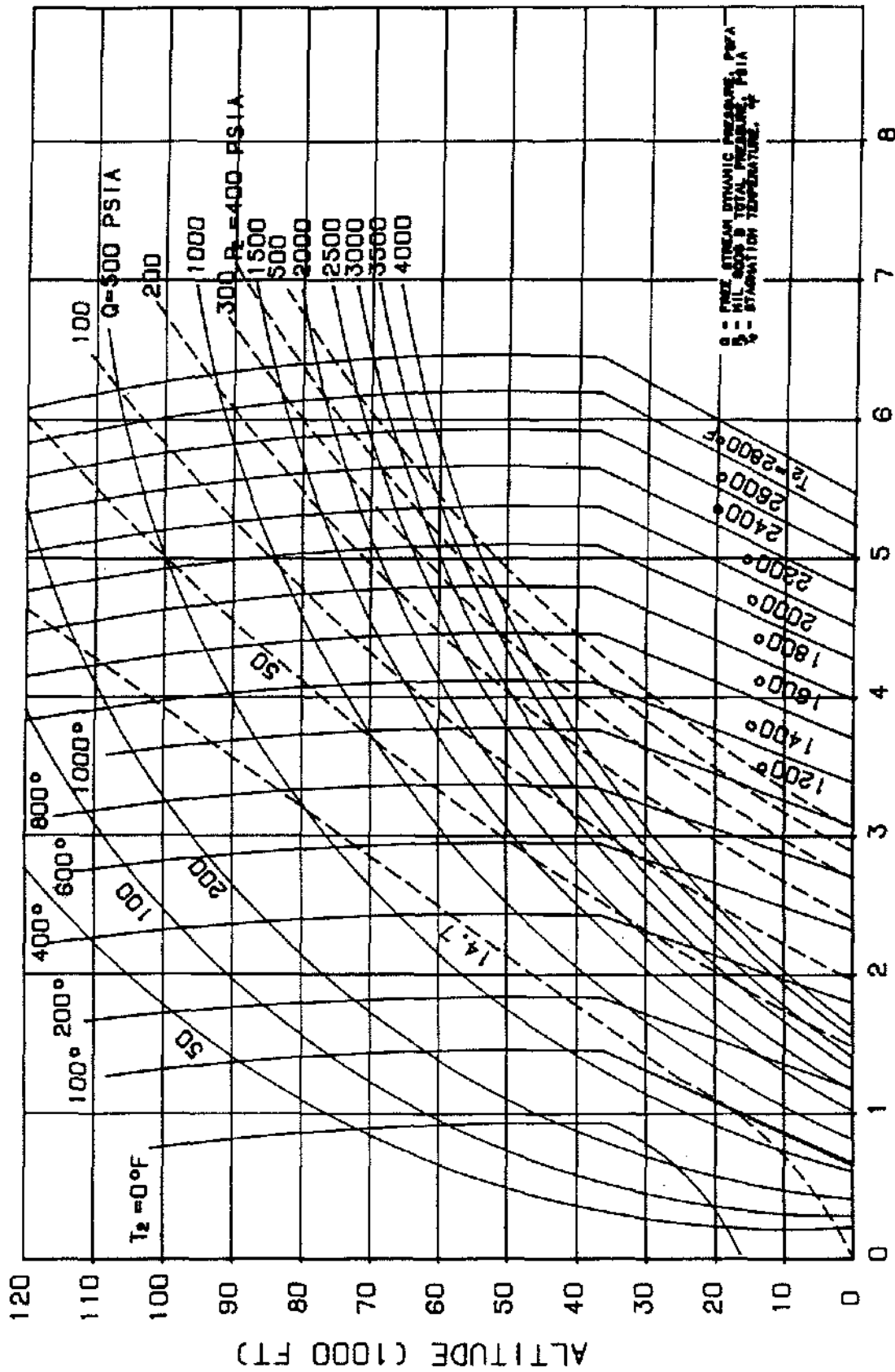


Figure 1.8 1962 U.S. Standard Atmosphere Geopotential Altitude

- MIL SPEC 5008C RAM RECOVERY
- HOT AND COLD DAY ENVELOPES ARE LIMITED BY THE ENGINE INLET CONDITION BOUNDARY AS DEFINED BY P1-T1 OPERATING ENVELOPE

——— STD DAY FLIGHT ENVELOPE
 ——— HOT DAY FLIGHT ENVELOPE (MIL-STD 210A)
 - - - - COLD DAY FLIGHT ENVELOPE (MIL-STD 210A)

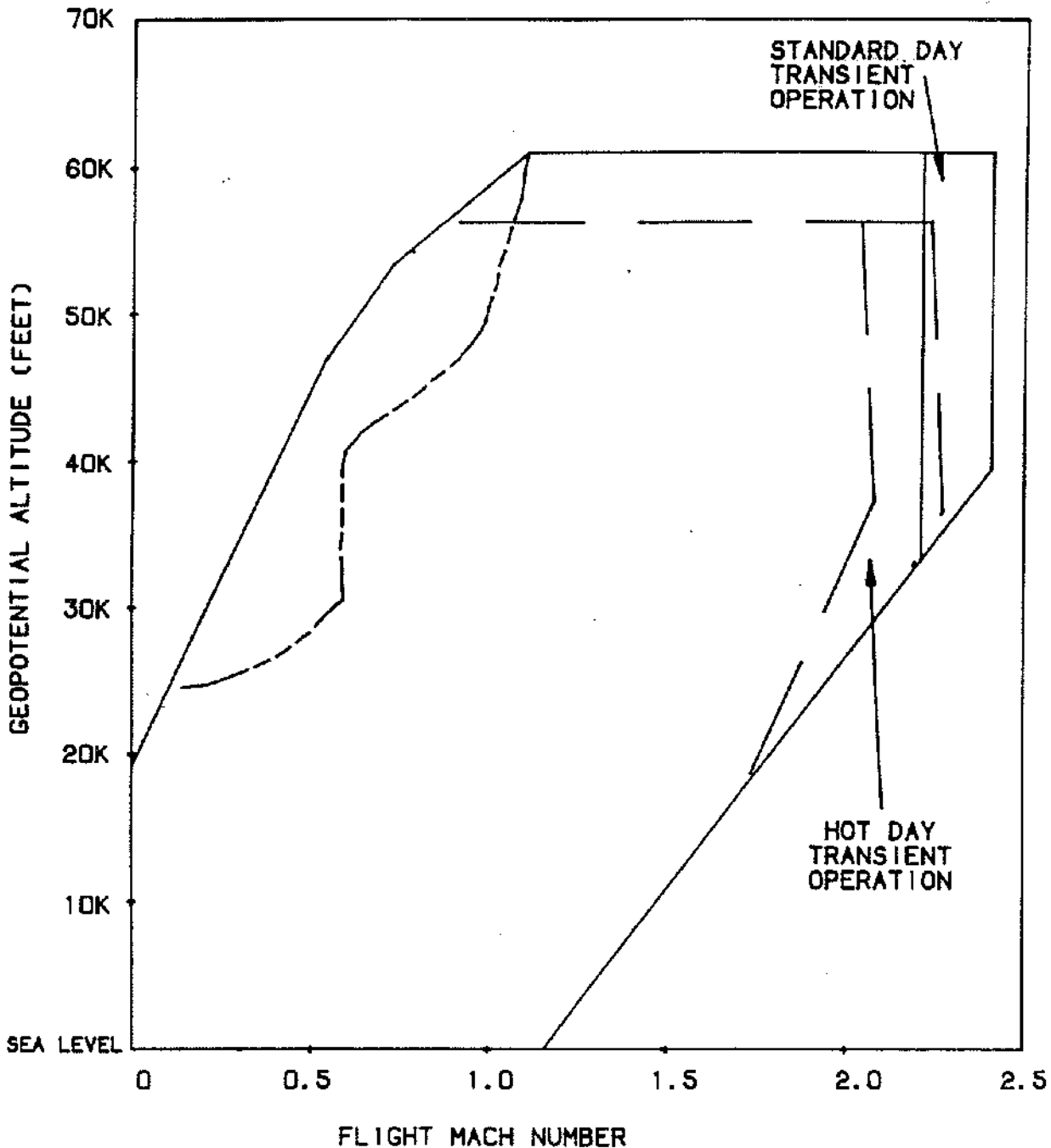


Figure 1.9 Hot and Cold Day Temperature Excursions Must Also be Factored into the Engine Operating Envelope.

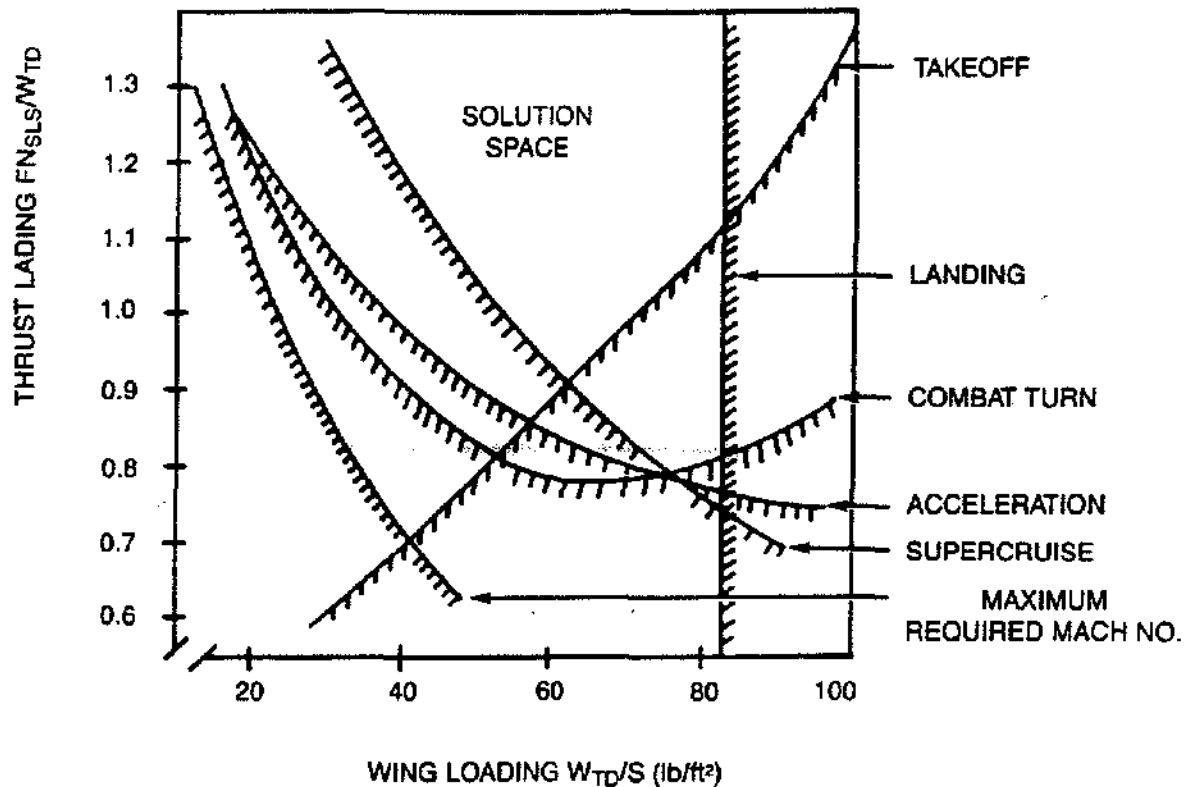


Figure 1.10 Typical Constraint Diagram for Tactical Military Aircraft

MISSION ANALYSIS

With values of wing loading and thrust loading determined from a constraint analysis, take off gross weight, maximum thrust and wing area are determined by "flying" the fictional aircraft through its entire mission. At any given point in the mission profile, the flight conditions (altitude, Mach number) are specified and the aircraft weight and drag are known from an assumed take off gross weight, the prior history of the mission and from the aerodynamic characteristics of the aircraft. The take off gross weight is the sum of the empty weight, the required fuel weight, the permanent payload weight (such as crew, passengers and their personal equipment) as well as any expendable payload such as cargo or munitions. The ratio of empty weight to take off gross weight will depend upon the type of aircraft and its mission. Fuel weight is gradually consumed during the mission and, except for any instantaneous release of cargo or munitions, the aircraft weight decreases at the same ratio. The instantaneous weight yields the required lift and corresponding drag — which is equal to the required installed net thrust. The instantaneous fuel consumption is determined by multiplying the net thrust by the specific fuel consumption (SFC). SFC is a complex function

of altitude, Mach number and throttle setting (which must be initially estimated from the assumed lapse characteristics of the engine). This procedure is progressively repeated at discrete points throughout the mission, the number of which depend upon the desired accuracy.

Besides yielding the empty to take off weight fraction and thrust required to complete a given mission, mission analysis reveals the best way to fly particular segments for minimum fuel burn or for minimum time to climb.

ENGINE SIZING AND CYCLE SELECTION

Although a lengthy treatment of engine performance is not intended, a brief overview of the relationship between fundamental cycle variables and engine performance is included to provide a measure of insight into the cycle selection and engine sizing process. The point here being that the engine size and cycle are not selected independently of one another. If they were for example, a high bypass ratio turbofan could simply be scaled up or down to satisfy the wide variety of commercial and military system applications. Usually, it is only one of the

requirements or constraints that directly sets the engine size. This implies that the other requirements relating to available thrust are exceeded; and as such, may be considered a figure of merit. Some growth potential is also generally designed into an engine because a larger derivative aircraft system is frequently pursued in commercial applications and because initial estimates in military systems are often optimistic, or capabilities are added along the way which increase the weight of the aircraft. Proper propulsion system sizing and cycle selection means choosing the engine airflow and thrust size to meet given mission requirements while simultaneously optimizing independent cycle variables to maximize the appropriate aircraft system figures of merit.

Engine performance is usually measured in terms of output (thrust or shaft horsepower), efficiency (specific fuel consumption), and weight. These and other cycle dependent variables are listed below.

- Net Thrust (lbsf)

$$F_n = W1(V_j - V_o) + A_e(P_j - P_o)$$

- Specific Fuel Consumption (lbs/lbs/hr)

$$SFC = \frac{W_f}{F_n}$$

where $W1$ = total inlet mass flow rate, V_o = flight velocity, V_j = exhaust jet velocity, A_e = exhaust area, P_j = exhaust jet static pressure, P_o = ambient pressure, and W_f = fuel flow rate.

- IR signature
- Weight
- Dimensions
- Noise
- Emissions
- Cost

Not all of the dependent variables will be of equal importance in a given application. For example, noise and costs are given more attention in commercial applications than in military systems. Conversely, IR signature receives a lot of attention in tactical military aircraft designs, but is not a consideration in the design of commercial systems. Typical independent variables considered in a preliminary sizing/cycle selection study include:

- Engine type (turbojet, mixed flow turbofan, VCE, etc.)
- Total inlet airflow ($W1$)
- Turbine inlet temperature ($T41$)

- Cycle pressure ratio (CPR)
- Bypass ratio (BPR)
- Fan pressure ratio (FPR)
- Scheduling parameters
- Augmentation ratio

Based on past experience, the preliminary designer will limit the engine types considered and the general range on the remaining independent variables. Scheduling parameters refers to the control the designer can exercise over operating lines, airflow schedules, geometry, and fuel flow schedules. Figure 1.11 shows the effects of turbine inlet temperature, cycle pressure ratio, and bypass ratio on thrust and specific fuel consumption for a high bypass ratio turbofan. Thrust is normalized by core airflow, as opposed to total inlet airflow, to restrict the comparison to a constant gas generator size. Note also that the information is presented for a specific flight condition. The trends will be similar for other flight conditions, however, the absolute magnitude of the cycle variables can vary dramatically. Engine thrust is relatively insensitive to cycle pressure ratio and extremely dependent upon turbine inlet temperature. SFC, on the other hand, is a strong function of bypass ratio, moderately sensitive to cycle pressure ratio, and only weakly dependent on turbine inlet temperature.

Insight into these relationships requires an understanding of the principle measures of the effectiveness of a propulsion system. One of the most direct measures of the propulsion system efficiency is the ratio of the work done by the propulsion system to the heat energy added. The work done by the propulsion system is the net thrust times the flight speed,

$$F_n V_o J,$$

expressed in BTU's, where J is the mechanical equivalent of heat (778 ft.lb/BTU). The heat added is the fuel flow W_f (lb/hr) times the lower heating value of the fuel h_f (BTU/lb). Hence, the propulsion system efficiency is

$$\eta_{ps} = \frac{3600 F_n V_o}{W_f h_f J}$$

By rearranging terms, the specific fuel consumption may be expressed in terms of the propulsion system efficiency.

$$SFC = \frac{3600 V_o}{\eta_{ps} h_f J}$$

(36,000 FT. 0.9 M)

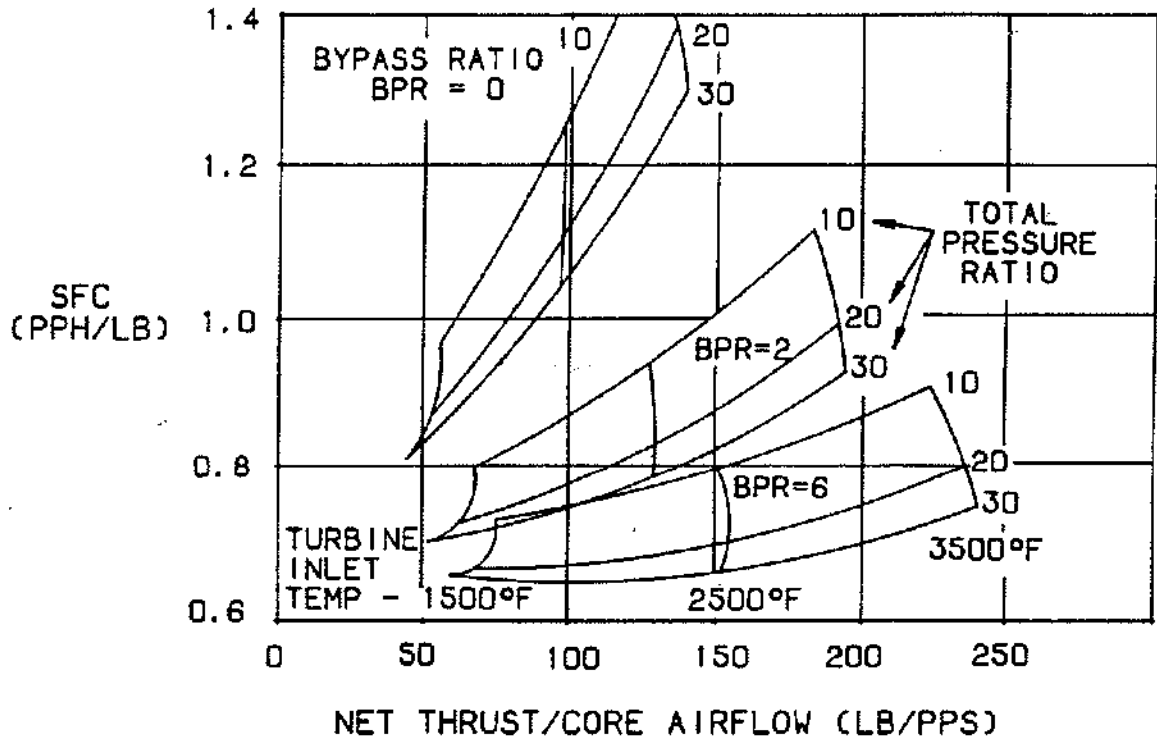


Figure 1.11 Effect of Cycle Parameters on Specific Fuel Consumption

Not surprisingly, this relationship states that higher propulsion system efficiencies are necessary to obtain reductions in specific fuel consumption. The overall propulsion system efficiency is shown for a variety of aircraft types in Figure 1.12. These trends can be explained by expressing the overall propulsion system efficiency in terms of its two constituent efficiencies: the thermal efficiency and the propulsive efficiency.

$$\eta_{ps} = \eta_{th} * \eta_p$$

The thermal efficiency is, as implied, a measure of the overall thermodynamic efficiency of the engine while the propulsive efficiency is a measure of how much of the engine output appears as useful work supplied to the aircraft. These efficiencies can be developed into the following expressions for interpretive purposes.

$$\eta_{th} = \frac{\text{Change In Kinetic Energy of Propellant}}{\text{Heat Addition}}$$

$$\eta_{th} = \frac{\dot{k}E}{W_f h_f} = \frac{\frac{V_j^2}{2} - \frac{V_o^2}{2}}{W_f h_f J}$$

$$= 1 - \frac{1}{\left(1 + \frac{k-1}{2} M_o^2\right) \left(\frac{P_3}{P_2}\right)^k}$$

where M_o = flight Mach number, P_3/P_2 = overall cycle pressure ratio, and f = fuel to air ratio, $K = (k-1)/k$ where k = ratio of specific heats.

$$\eta_p = \frac{\text{Power Delivered to Aircraft}}{\text{Change In Kinetic Energy of Propellant}}$$

$$\eta_p = \frac{F_n V_o}{\dot{k}E} = \frac{(V_j - V_o) V_o}{\frac{1}{2} (V_j - V_o) (V_j + V_o)}$$

$$= \frac{2 V_o}{V_j + V_o} = \frac{2}{1 + \frac{V_j}{V_o}}$$

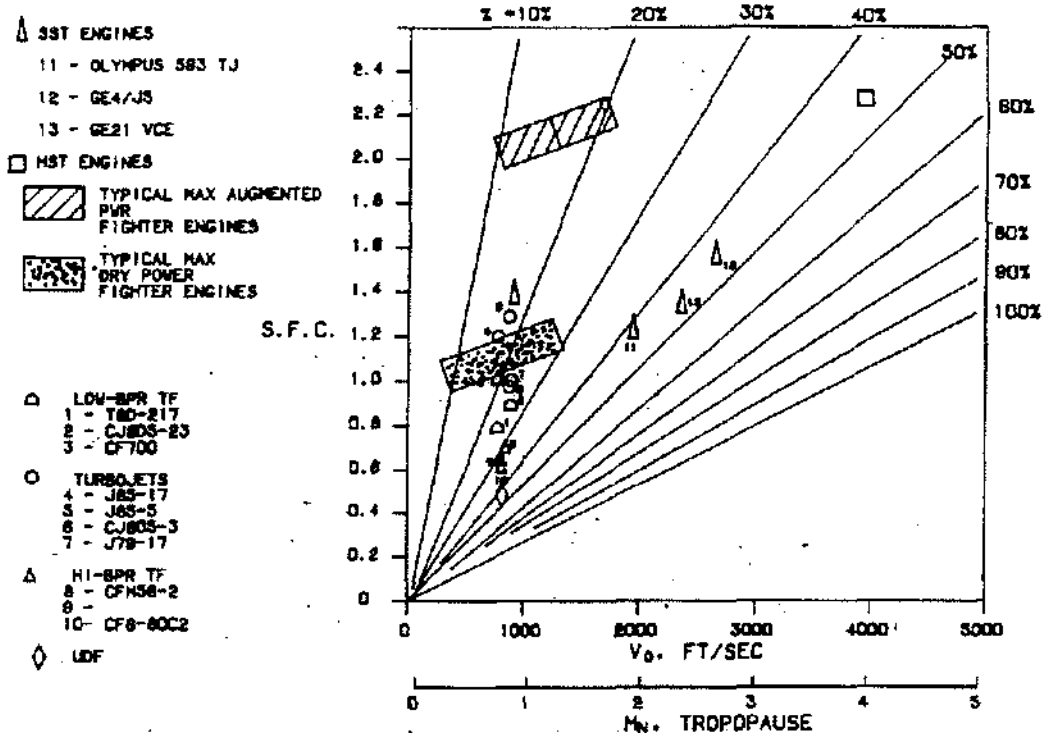


Figure 1.12 Overall Propulsion System Efficiency

Thus, the thermal efficiency increases with flight Mach number and cycle pressure ratio. From thermodynamics we know that in order to maximize the thermal efficiency the heat must be added at the highest possible pressure. Or alternatively, the thermodynamic efficiency of the cycle increases with the product of the ram temperature rise and cycle pressure ratio because for a fixed cycle temperature limit, higher combustor inlet temperatures result in a more "Carnot-looking" cycle. The propulsive efficiency is maximized when the exhaust jet velocity approaches the flight velocity. This of course reduces the thrust unless the total inlet airflow is increased. The thrust per pound of air is referred to as the specific thrust and is equal to the discharge velocity at static conditions. Note that at low flight Mach numbers high propulsive efficiencies imply low specific thrusts, and a high bypass ratio is a natural consequence. By employing a large diameter fan, a very large mass of air can be accelerated to relatively low discharge velocities, producing dramatic reductions in specific fuel consumption. These trends are conveniently summarized in Figures 1.13 and 1.14. Low values of specific thrust are desirable at low flight Mach numbers because the inherently better propulsive efficiency leads to a reduction in specific fuel consumption. As flight Mach number increases, the ability of high bypass ratio machines to

produce net thrust falls off rapidly and higher specific thrusts are needed to maintain high propulsive efficiencies and reduce SFC. This suggests that different aircraft missions and flight envelopes require different types of propulsion systems to maximize efficiency and performance (Figure 1.15).

An additional advantage of a high bypass ratio engine is the reduction in the jet noise, which dominates both sideline and community noise levels at takeoff. The reduction in discharge velocity produces an attendant reduction in turbulent and shear noise generation in the exhaust jet. During approach, when the engine is throttled back, engine noise is dominated by fan or compressor turbomachinery noise which can be shielded by using sound absorbing materials in the inlet and exhaust ducting. High blade counts in the turbine usually keep the associated turbomachinery noise out of the audible frequency range.

The higher bypass ratios lead to larger diameter engines, which are heavier in themselves, and incur additional installation penalties such as higher aircraft weight and drag due to larger nacelles. These penalties must be balanced against any uninstalled improvement in SFC. Although people generally tend to equate engine size with

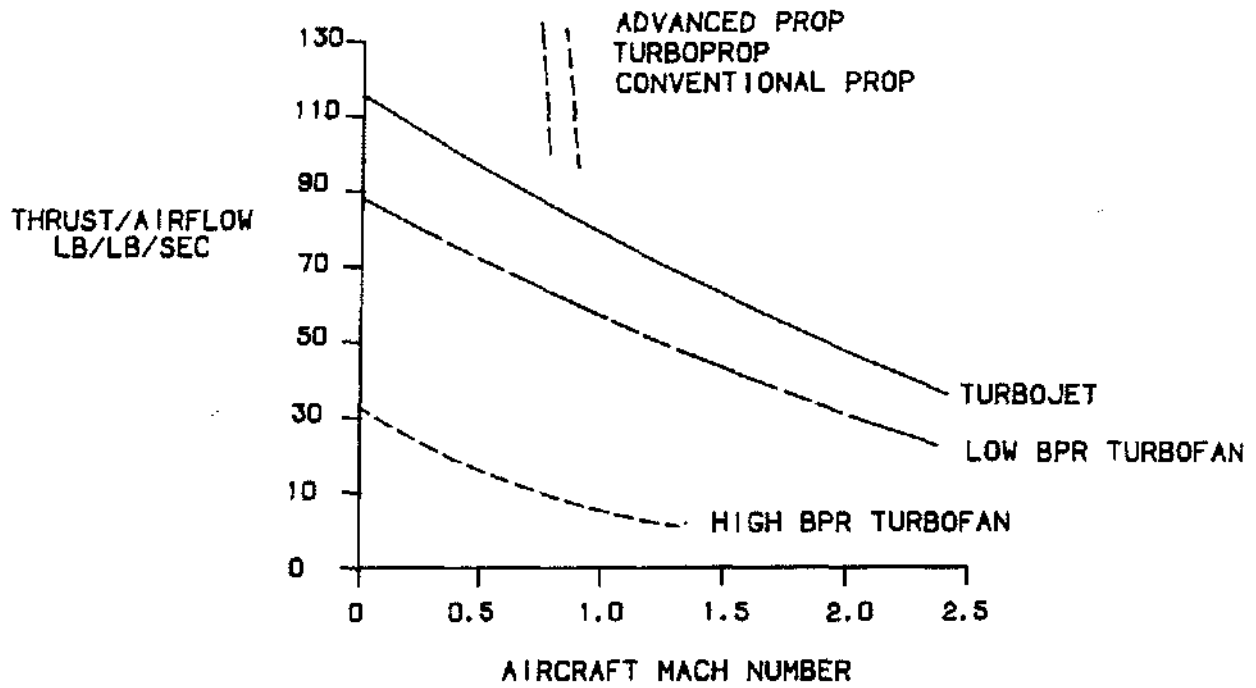


Figure 1.13 Low Values of Specific Thrust Give Higher Propulsive Efficiency at Low Mach Numbers.

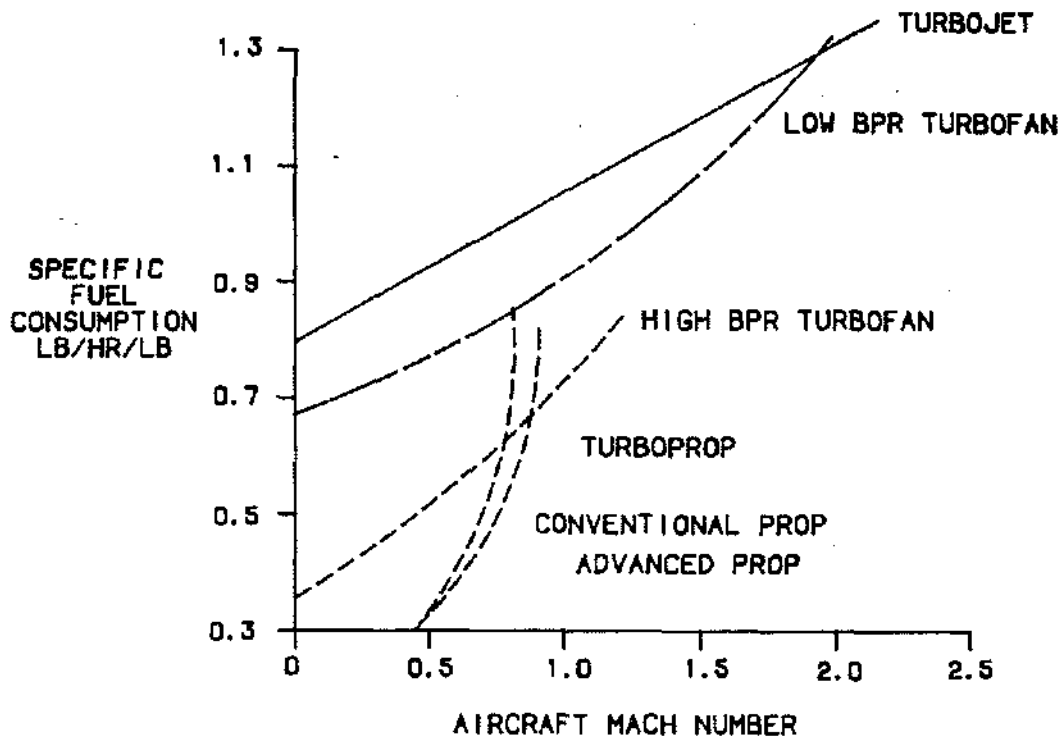


Figure 1.14 As Flight Mach Number Increases, Higher Specific Thrusts are Necessary to Maintain High Propulsive Efficiency and Reduce SFC.

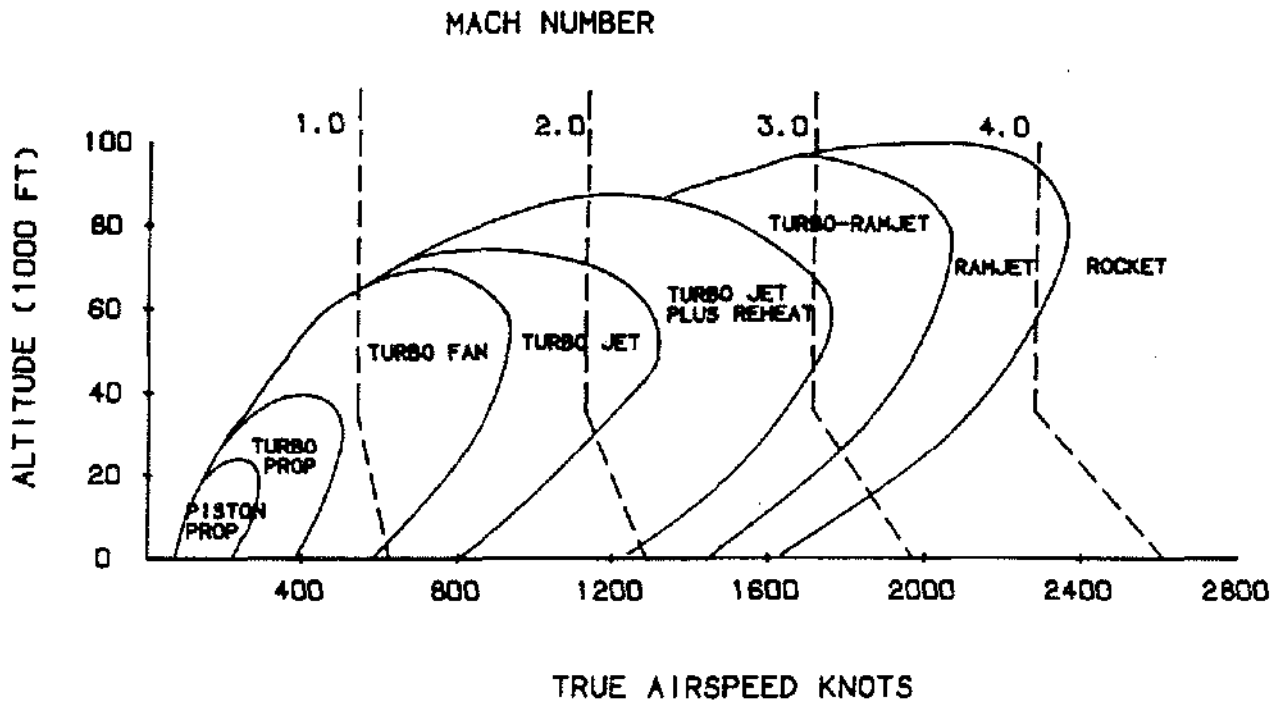


Figure 1.15 Typical Flight Envelopes — All Air-Breathing Engines are Speed and Altitude Limited. The Aircraft Flight Envelope is Used to Identify a Suitable Propulsion System for a Given Mission Specification.

maximum available thrust or shaft horsepower, airflow capacity is probably a better measurement of physical size. Selection of an inlet airflow and inlet Mach number implies a certain engine diameter through the compressible flow function relationship.

$$\frac{W \sqrt{T}}{A P} = \sqrt{\frac{k}{R}} \left[1 + \frac{(k-1)}{2} M^2 \right]^K$$

where W = mass flow rate, T = total temperature, P = total pressure, R = universal gas constant, A = annulus area, and $K = (k+1)/2(k-1)$.

The corrected flow per unit annulus area, or the specific flow, is a maximum of 49.92 pounds per second for an axial Mach number of unity (annulus choke). Since losses are proportioned to Mach number squared, Mach numbers much less than one are generally employed at the engine inlet. But the engine diameter is a function of annulus area and fan radius ratio, which in turn is a function of the available technology. Consequently, inlet Mach numbers are selected as high as is prudently possible in order to reduce engine diameter and weight. Wall

boundary layers and blade row physical blockages act to reduce the specific flow. Accordingly, specific flows of 40 to 43 lbs/sec/ft² are representative of fans, and values of 37 to 40 are representative of core compressors. Compressors have lower limits because of larger boundary layers in the transition ducts and physical blockages such as struts.

Engine weight is also strongly affected by the turbine inlet temperature and cycle pressure ratio. At a condition of constant thrust, weight is reduced by increasing turbine inlet temperature, which increases the exhaust jet velocities thereby reducing the airflow requirement. High strength superalloys, along with advances in turbine cooling technology, permit operation at higher temperatures and working stress levels. Increasing the cycle pressure ratio raises the engine weight by increasing the number of compression stages and the required thickness of the fan and compressor casings. Since the pressure rise per stage is a function of blade aerodynamics and rotor tip speed, high strength materials allow for higher rotational speeds which make it possible to achieve the same pressure rise with fewer stages.

In commercial systems, low values of cruise and loiter SFC are especially critical since the majority of on-board fuel is consumed cruising and because loiter SFC determines required fuel reserves. The actual fuel burn goes up by more than 1% for a 1% increase in SFC, because there is a multiplicative effect on fuel consumption. An increase in SFC necessitates that additional fuel be carried on board to satisfy range requirements. The additional fuel weight results in additional aircraft weight and thrust required to cruise. This effect is most severe for long stage lengths where on-board fuel is a higher percentage of TOGW. The optimum fan pressure ratio and bypass ratio is dependent upon the design cruise Mach number, the method of changing the fan pressure ratio (i.e. changing core size or temperature), and the appropriate FOMs. Fan pressure ratio and bypass ratio cannot be varied independently of one another because of diameter and loading limits on the low pressure turbine and because of the need to balance the static pressures of the core and fan stream at the mixing plane in a mixed flow turbofan. Some flexibility exists in selecting the mixing plane Mach numbers and areas, but the bypass ratio must decrease with increasing fan pressure ratio such that the turbine discharge total pressure remains compatible with the fan stream total pressure. Increasing the turbine inlet temperature permits higher bypass ratios at a given fan pressure ratio (Figure 1.16). Combinations of bypass ratio and fan pressure ratio will therefore depend upon the flight Mach number, critical thrust requirements, the technology level employed, and the desired SFC characteristics.

For a commercial system, critical thrust levels are determined by takeoff field length, engine out rate of climb, engine out ceiling, and desired cruise Mach number. The ratio of cruise thrust to sea level static thrust is referred to as the thrust lapse rate of μ ; engine and is markedly dependent upon the specific thrust, and hence, the bypass ratio and fan pressure ratio. Recalling the relationship for net thrust, and assuming the mass flow exiting the engine to be equal to that entering the engine (i.e. neglecting fuel flow and leakage) the specific thrust is:

$$F_{sp} = V_j - V_0 = V_j (1 - V_0/V_j)$$

At static conditions ($V_0 = 0$) the familiar sea level result is obtained. For a given flight speed the specific thrust loss is lower for high specific thrust engines (the lapse rate is high). Consider the situation shown in Figure 1.17 where two bypass ratio choices are being evaluated for a commercial transport application. Both engines have been sized to satisfy SLS thrust requirements. The illustration shows that engine A's bypass ratio is too low for the system. Not only does it suffer from internal SFC disadvantages, but it is too large of an engine and as a result, is throttled back beyond its SFC minimum at

cruise. Selecting the higher bypass ratio results in an inherent SFC improvement due to better propulsive efficiency, as well as a greater thrust lapse, placing the cruise operation at the SFC minimum.

The preceding example demonstrates the advantage of a high bypass ratio turbofan at a subsonic cruise condition where SFC was the primary FOM. A major consideration for sonic and greater flight speeds is the difference between the uninstalled and installed performance of the engine. The flow of subsonic air around an installed engine is relatively efficient. Supersonic flow around an installed engine results in penalties which are an order of magnitude larger. For this reason, engine diameters are kept to a minimum for supersonic applications. High levels of specific thrust necessarily follow, and the time or distance of the supersonic portion of the mission relative to the subsonic portion is an important consideration in the selection of the specific thrust. Typical values of sea level static specific thrust are shown in Table 1.2 for several representative commercial transport and military fighter engines.

The relative difference in specific thrust between dry and augmented operation punctuates the primary advantage of augmenting. The diameter and weight of an augmented engine is much less than that of a dry turbojet or turbofan producing the same maximum thrust. In addition, an augmentor provides the flexibility needed to optimize performance and FOMs throughout the flight envelope. High thrust loadings (available thrust/aircraft weight) are required for fighters in order to satisfy acceleration and maneuver requirements and to enhance combat performance. One of the operational characteristics encountered in high thrust loading systems is that the engines are throttled back from the SFC bucket at subsonic cruise. This problem is compounded by inlet spillage and afterbody drag problems due to low engine airflow demand. Consequently, a dry engine sized by a high Mach maneuver or acceleration requirement will be too large at cruise, and the aircraft performance would be too severely penalized by the resulting engine weight and because of poor off design operation of the engine components. Thus, augmentors are used to satisfy sizing point requirements without severely compromising the balance of the aircraft mission.

This advantage is partially offset by the poor thermal efficiency encountered during augmented operation, where SFC values are on the order of twice those encountered during dry operation. Note also that the augmentor increases the aircraft's vulnerability to an IR seeking missile. For these reasons, augmentors are only used for brief periods of acceleration, supersonic flight, or combat in order to gain speed for an intercept or to gain a position advantage in combat.

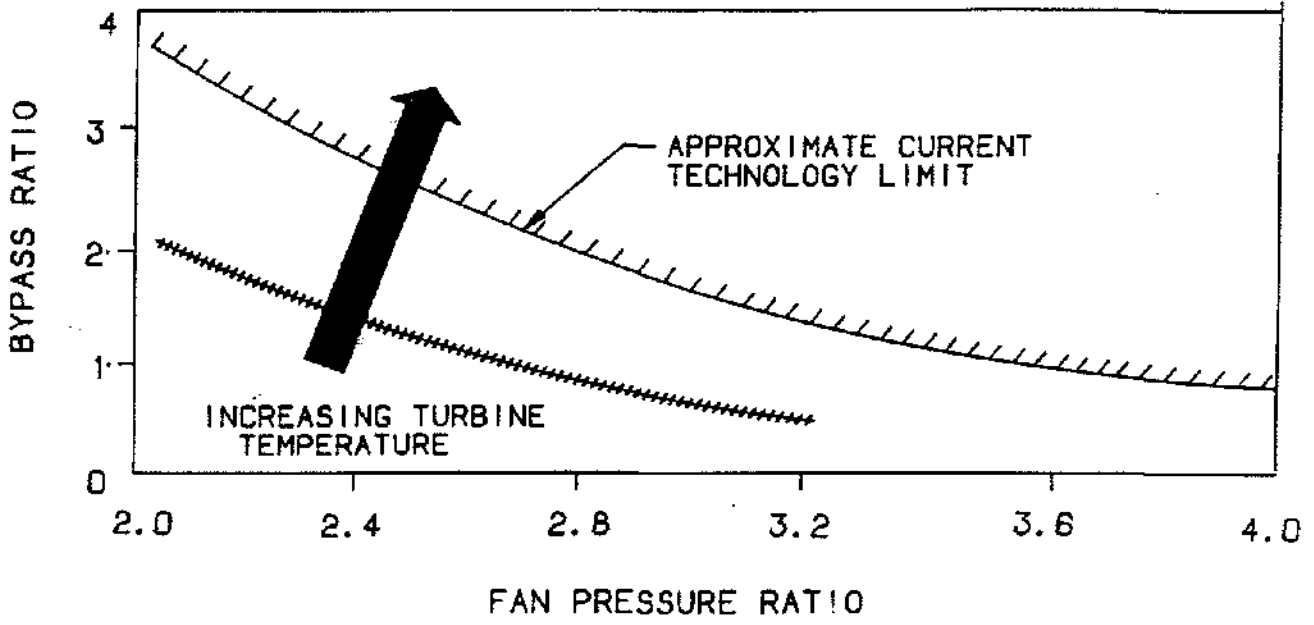


Figure 1.16 Fan/Core Matching Requirements Constrain Bypass Ratio and Fan Pressure Ratio Combinations.

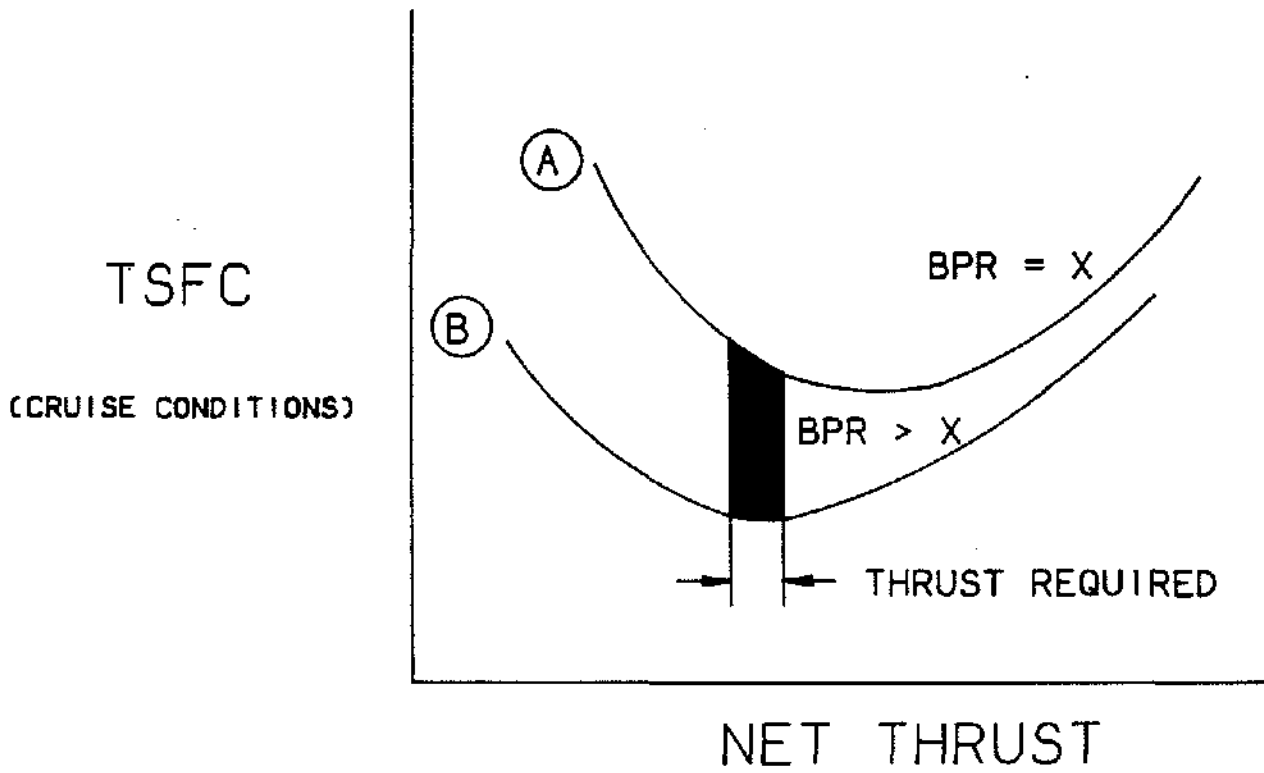


Figure 1.17 Bypass Ratio Selection Affects Engine Size and SFC Characteristics.

Engine	SLS Specific Thrust (lb Fn/lb W1/sec)	BPR (SLS)
UDFTM	8	35
CF6-80	30	5
F110 (Augmented)	105	0.8
F110 (Dry)	63	
F404 (Augmented)	115	0.3
F404 (Dry)	74	
J79 (Augmented)	105	0.0
J79 (Dry)	70	

Table 1.2 Specific Thrusts for a Variety of Engine Types

For a military fighter engine sizing requirements are usually expressed in terms of parameters which describe the energy states of the aircraft.

- Specific Excess Power (ft/sec)

$$P_s = \left(\frac{T-D}{W} \right) V$$

- Turn Rate (deg/sec)

$$TR = 57.3 \frac{g}{V} \sqrt{N_t^2 - 1}$$

- Turn Radius (ft)

$$R = \frac{V^2}{g \sqrt{N_t^2 - 1}}$$

- Sustained Gs (ft/sec²)

$$N_2 (\text{sust}) = \frac{L \cos \alpha + D \sin \alpha}{W} (T - D)$$

- Acceleration Time (sec)

$$V_2 - V_1 = \int_{t_1}^{t_2} \frac{g}{W} (T - D) dt$$

(time = $t_2 - t_1$ from $V_2 - V_1$)

where T = installed net thrust, D = aircraft drag, W = aircraft weight, V = true airspeed, g = 32.2 ft/sec².

α = angle of attack, and N_t = turn load factor = $(L + Fg \sin \alpha)/W$.

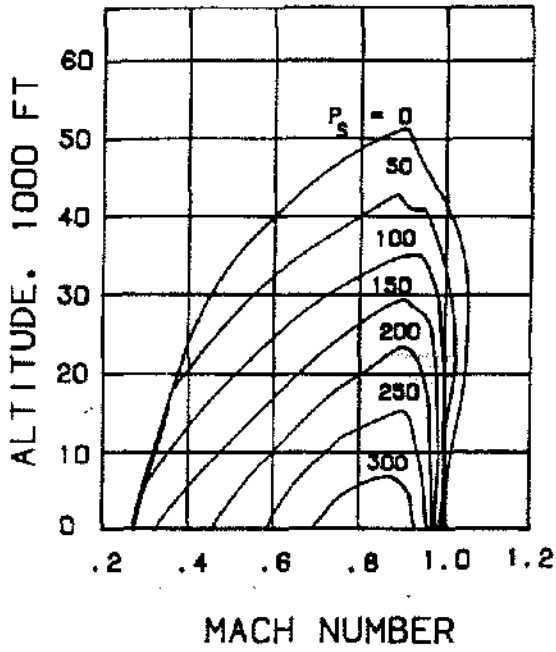
The specific excess power is a measure of the time rate of change of the energy per pound of aircraft weight and is equal to zero when the drag of the airplane and the maximum available thrust from the engine are equal. This indicates a condition at which the energy level of the aircraft can no longer be increased. Sustained "G" is the maximum number of G's that the aircraft is capable of in a constant airspeed level turn. The lift needed to balance the aircraft weight and centrifugal force causes a large drag increase which must be balanced by installed thrust. The equation for P_s may be manipulated to directly yield the required thrust.

$$F_{n \text{ req}} (M_o, h) = \frac{P_s}{V} W + D$$

Contours of constant P_s are plotted in Figure 1.18 for a constant aircraft weight. The impact of the augmentor on P_s is quite dramatic.

There are several systematic methods which may be employed in selecting a cycle and sizing an engine for a given application. A methodology commonly practiced is used in the following example to illustrate the technique relative to the design of a supersonic tactical military aircraft. The specifics of the application and mission are not important here because the procedure will be virtually identical regardless of the details. For any series of requirements, a family of candidate engines can be generated in the form of a matrix of compatible cycle variables for evaluation. This matrix facilitates the iteration process between the airframer and engine manufacturer by providing a basis for determining the effects of primary cycle variables on specific performance requirements throughout the envelope.

MILITARY (MAX. DRY) POWER



FULL AUGMENTATION

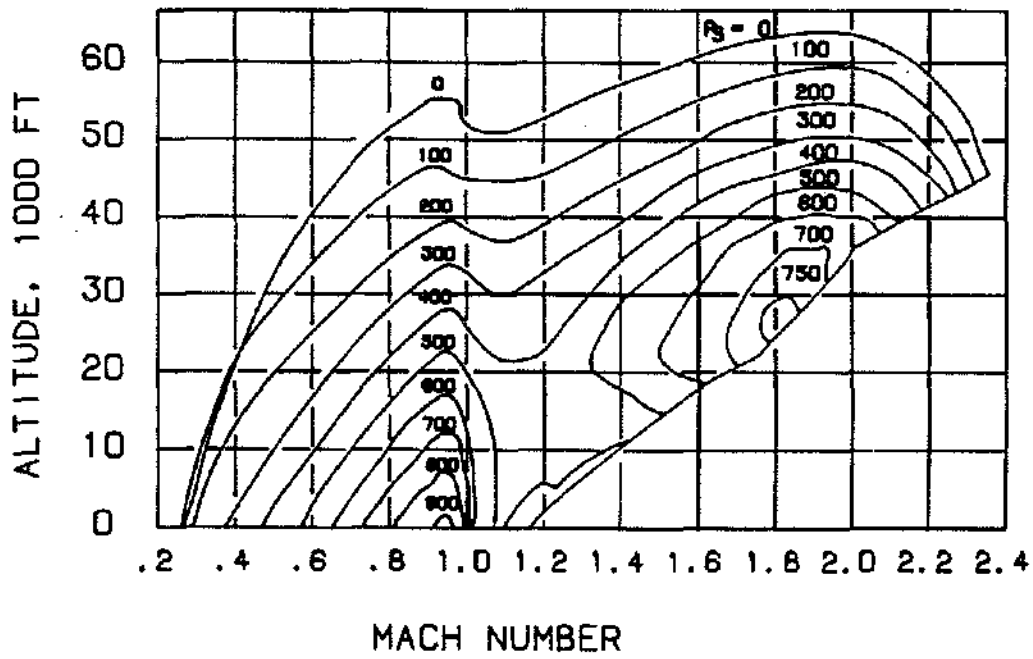


Figure 1.18 Augmentation in Order to Satisfy Energy and Maneuverability Requirement (P_s)

After defining a configuration based on previous experience, the anticipated technology level will define critical cycle parameters. The cycle variables directly impacted by technology level are: turbine inlet temperature (T41), compressor discharge temperature (T3), component efficiency levels, turbine cooling flows, and exhaust nozzle cooling flows. For a mixed flow turbofan, selecting the exhaust stream mixer, augmentor, and exhaust nozzle type completes the technology definition. Component matching criteria, inlet airflow schedules, minimum allowable fan and compressor stall margins, overspeed capability, etc. are all specified to complete the cycle definition. Having established these limits and cycle guidelines, the primary remaining unknowns are the design bypass ratio, and the fan and compressor pressure ratio. To facilitate this selection, a matrix of design bypass ratio/fan pressure ratio is constructed which is consistent with the cycle limits and matching guidelines. Figure 1.19 represents such a matrix for a family of engines with overall cycle pressure ratios between 18 and 30. Fan pressure ratios range from 3.6 to 4.3, and core compressor pressure ratios range from 5 to 7. These ranges were established by adding or subtracting a stage

to a reference compressor and by the preference for a single stage low pressure turbine. This is a consideration but not a constraint as the selection of the design bypass ratio will also impact the required turbine stage count.

The following observations can be made from the figure. For a given core pressure ratio, increasing the design fan pressure ratio will increase the overall cycle pressure ratio. The higher overall pressure ratio engines are restricted to lower flight Mach numbers as a result of the T3 limit. However, the T3 limit is reached at a lower ram temperature which allows the core size to be reduced (bypass ratio increased). Conversely, the lower overall pressure ratio engines can attain higher flight Mach numbers before the T3 limit is reached; but the higher ram temperature requires more core energy to drive the fan, and the core size must be increased for the specified T41 limit (bypass ratio reduced). If the overall pressure ratio is held constant (constant T3 and design flight Mach number), the fan pressure ratio has a large impact on the design bypass ratio. However, if the overall pressure ratio is allowed to vary, fan pressure ratio has a much smaller impact on design bypass ratio.

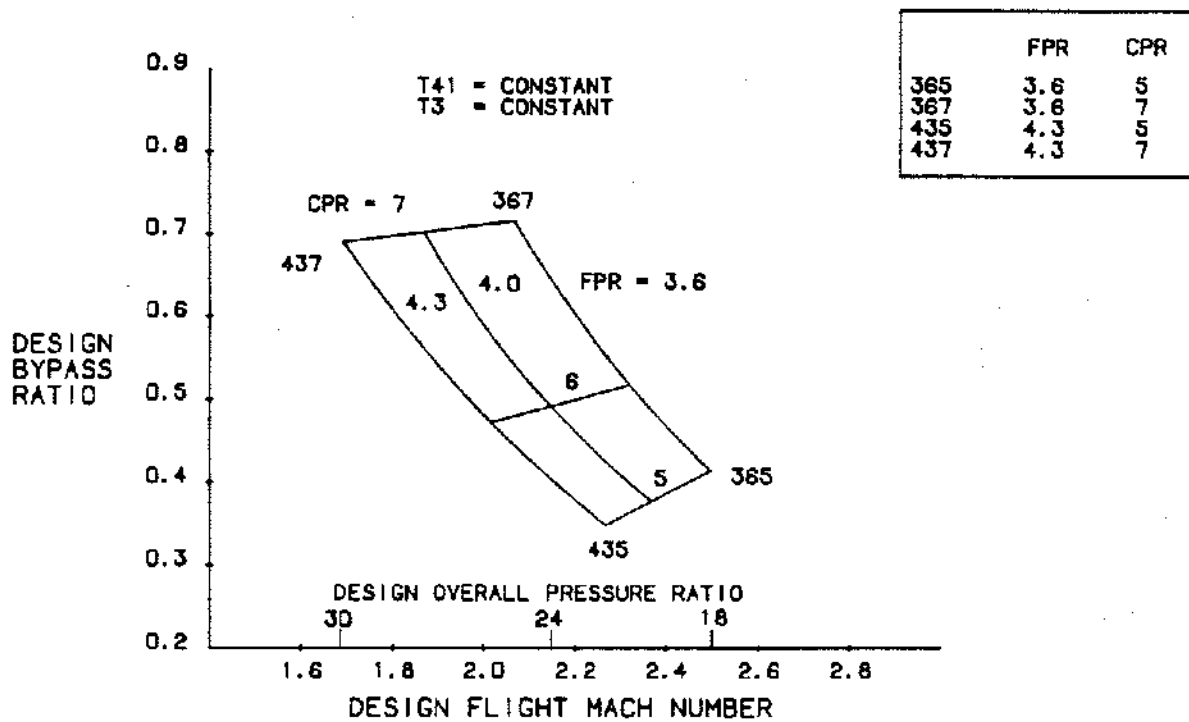


Figure 1.19 Cycle Matrix

For the cycles defined by the matrix, thrust ratios and specific fuel consumption are used to determine the relative performance between the cycles and to provide a basis for making a selection. Thrust ratios are defined as the ratio of thrust at a given flight condition to sea level static maximum augmented thrust.

Figure 1.20 presents thrust ratios for maximum dry operation at supersonic Mach numbers. The lower overall pressure ratio cycles have the highest thrust ratios because of their ability to maintain airflow out to higher Mach numbers. If, for example, a dry thrust ratio of 0.4 were required at Mach 2.15, a fan pressure ratio of four and a core pressure ratio of six would represent the most appropriate cycle for satisfying this requirement.

Figure 1.21 shows the maximum augmented thrust ratios for the matrix at the same supersonic Mach numbers. Again, the lower overall pressure ratio engines have greater thrust ratios. Furthermore, as fan pressure ratio is reduced (design bypass ratio increased), the engines have an increasing augmented thrust capability to progressively higher Mach numbers. The impact of the augmentor is reduced for lower bypass ratio engines be-

cause a larger percentage of the air in the augmentor has already been heated in the main combustor, reducing the oxygen content and temperature rise capability of the augmentor.

The effect of design overall pressure ratio and design bypass ratio on minimum SFC is shown in Figure 1.22. The higher bypass and higher overall pressure ratio cycles have the best SFC. Therefore, selecting the cycle with the highest overall pressure ratio consistent with the maximum flight Mach number and the maximum bypass ratio that satisfies the critical thrust ratio would provide the best uninstalled SFC. However, it should be noted that providing the minimum SFC at a rated thrust does not necessarily result in maximizing aircraft range. If an engine were designed to have minimum SFC at a subsonic cruise point, any changes in aircraft gross weight or drag would shift the resulting system away from the minimum SFC point. In addition, aircraft gross weight and L/D changes throughout the cruise segment of the flight as on-board fuel is consumed. Consequently, it is important that an engine have a relatively flat SFC characteristic at key cruise conditions (Figure 1.23).

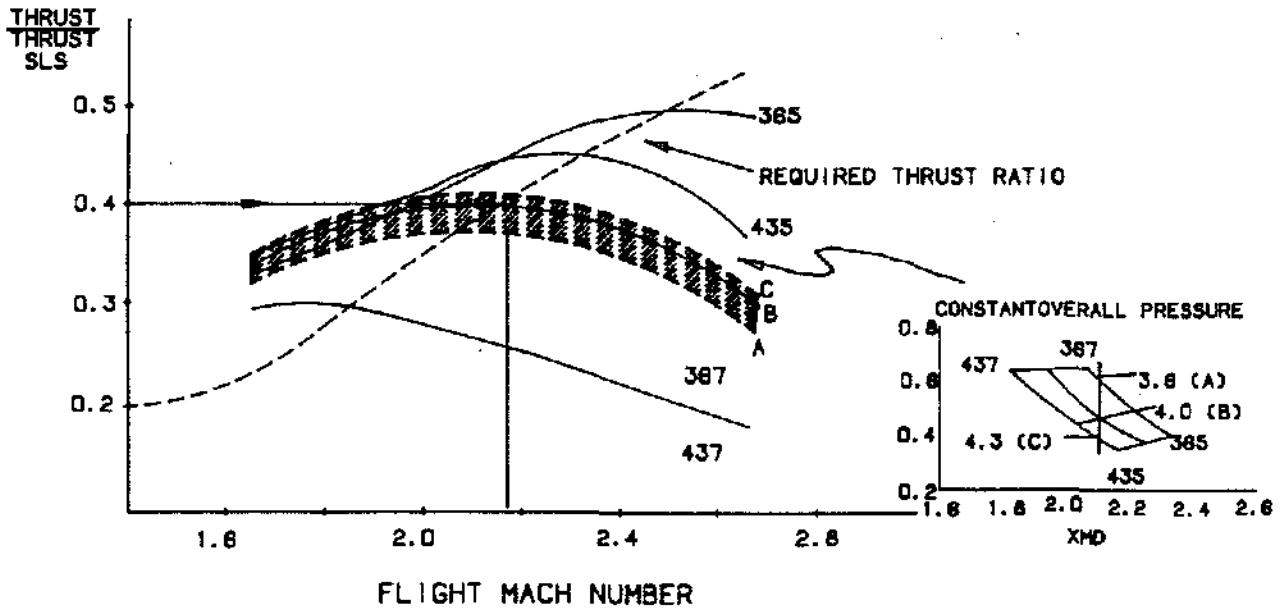


Figure 1.20 Maximum Dry (Non-Augmented) Supersonic Thrust Ratios

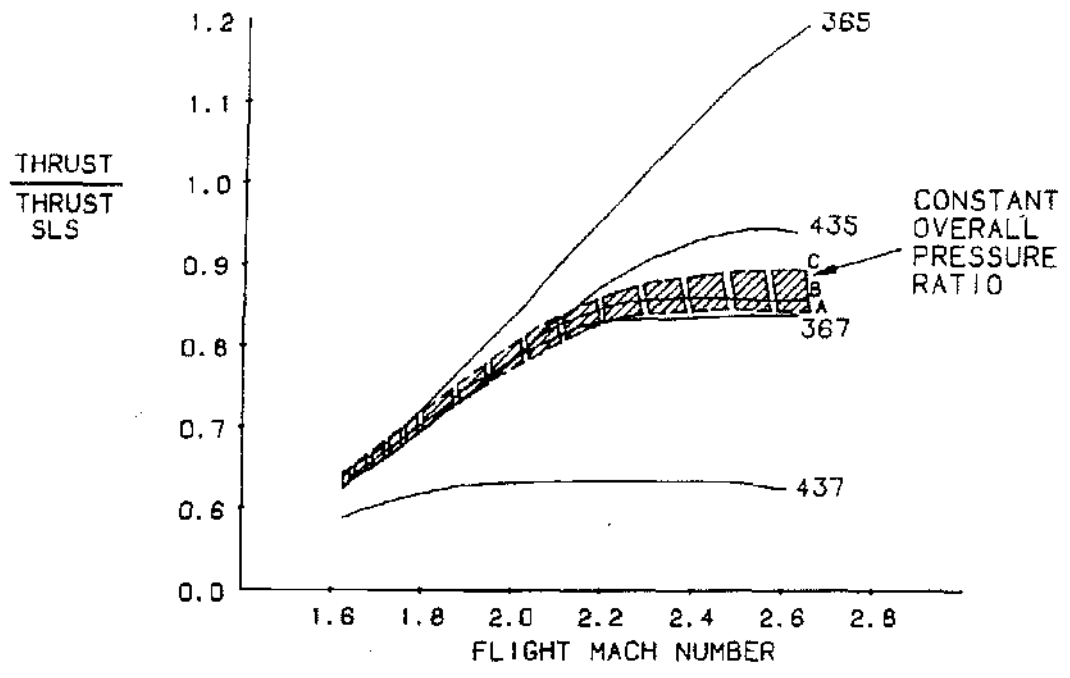


Figure 1.21 Maximum Augmented Supersonic Thrust Ratios

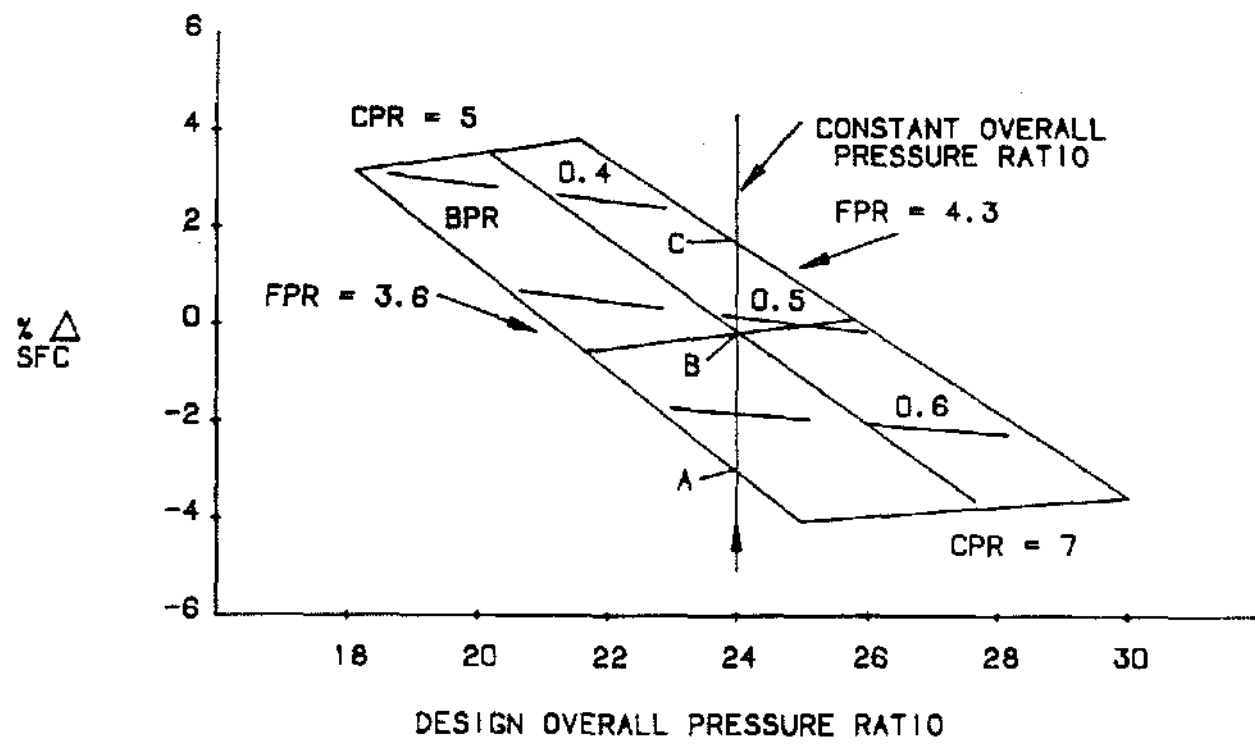


Figure 1.22 Minimum Specific Fuel Consumption for Subsonic Cruise

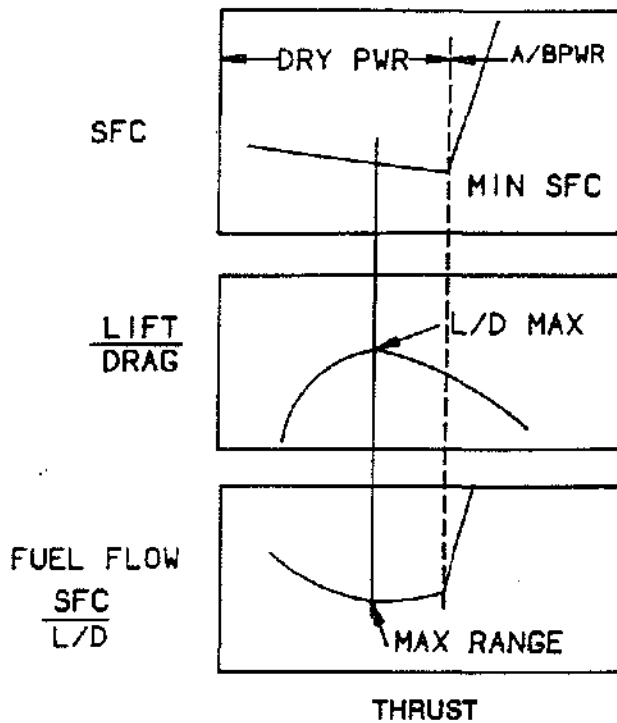


Figure 1.23 Maximum subsonic range does not necessarily occur at SFC minimum. An engine which has been sized by high Mach thrust or maneuverability requirements will be throttled well back from SFC minimum at cruise. An aircraft with a long subsonic cruise leg will be designed to cruise at wing L/D (lift to drag ratio) maximum.

Figure 1.24 shows a supersonic cruise condition that might be required of a multi-mission aircraft. The peak range condition does not occur at the SFC minimum or peak L/D. If the aircraft had a stringent supersonic cruise (supercruise) requirement, more emphasis would be placed on matching the SFC and L/D zero slope points to maximize range.

A concept which is now being extensively evaluated is the variable cycle engine. A variable cycle engine has the capability to vary primary cycle parameters such as bypass ratio, fan pressure ratio, and overall pressure ratio to optimize engine performance at both subsonic and supersonic flight conditions. The ability to vary these basic cycle parameters requires the addition of several variable geometry features. However, the addition of these variable geometry features introduces a host of design and control complexities. Consequently, a variable cycle engine would be most attractive on a mixed mission aircraft where fuel consumption is divided nearly equally between subsonic cruise and supersonic cruise flight conditions. Higher fan pressure ratios and lower bypass ratios are necessary for low specific fuel consumption at supersonic cruise while lower specific

thrusts associated with high bypass ratios and low fan pressure ratios are desired for subsonic cruise.

The ability to modulate the bypass ratio results in additional benefits in installed performance by reducing the inlet spill drag and afterbody drag. Inlet and exhaust systems that are sized at supersonic flight conditions have inlet airflow spillage and afterbody pressure drag at subsonic cruise conditions. These are referred to as throttle dependent drags because the magnitude of the losses is a function of the airflow demand and, hence, the power setting of the engine. Therefore, the ability to hold the design inlet airflow at off design Mach numbers and reduced power settings reduces the inlet spill drag. Holding the airflow by increasing the bypass ratio also increases the required exhaust system area, reducing the afterbody drag in the dry subsonic cruise mode by limiting the amount of nozzle closure.

CYCLE MODELLING

The engine cycle is a mathematical model of the aerothermodynamics of the internal flow in the engine. The

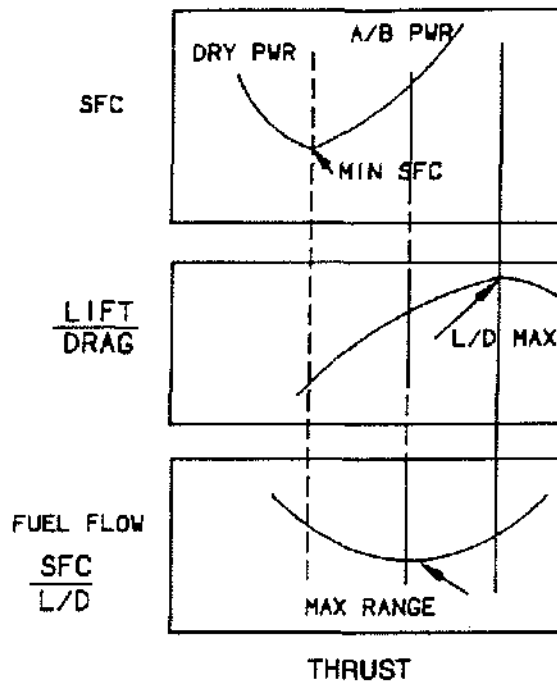


Figure 1.24 Maximum range at supersonic cruise conditions is hard to balance with subsonic cruise requirements. Maximum supersonic range is not coincident with either peak L/D or minimum SFC and usually occurs at partial augmentation. For a mission with an extensive supercruise leg, the airframe and engine would preferably be designed so that the wing peak L/D and min SFC Ppoints would be (almost) coincident with the maximum supersonic cruise range (matching zero slopes).

cycle model is used to determine all pertinent performance data for a given flight condition when the component characteristics and fuel flow are known. Although the fundamentals are the same, a turbofan, turbojet, and turboshaft engine all have unique modelling requirements; and a two spool engine model will be different than a single spool model. The cycle model strictly adheres to the principles of mass and energy conservation so that the difference between the gas flow exiting a component and that entering a downstream component must be equal after accounting for scheduled bleeds, leakage, and the addition of fuel or water to the mass flow. Two mechanically connected components must rotate at a constant speed ratio. The power delivered by a turbine must equal that required by the compressor, fan, or propeller to which it is connected less any power required to drive attached accessories and any parasitic losses such as fuel and oil pumps. These along with other mechanical and aerothermodynamic constraints are formulated into a series of nonlinear, simultaneous equations which the computer solves for a specific steady state operating point. And, in addition to calculating overall engine performance, flow rates temperatures

and pressures are also determined at any engine location defined in the model. This information is then used by component designers and other specialists to calculate pressure forces and thermal stresses on stationary and rotating parts as well as to design to expected levels of performance.

A typical steady state cycle model will consist of the following information stored as coefficients of polynomials or as tabular data along with appropriate interpolation routines:

- Thermodynamic properties of dry air as a function of altitude and temperature.
- Thermodynamic properties of water vapor in order to account for humidity or the effects of injecting water into the engine inlet for purposes of power augmentation.
- Thermodynamic properties for the products of combustion for the fuel to be used.

- The aerothermodynamic characteristics of all the engine components as a function of their principle independent variables,
- Modifiers to component performance due to Reynolds number effects, changes in blade and vane dimensions as a function of temperature and rotational speed, clearance effects, etc.
- Parasitic losses (friction, bearings, pumps, fuel/oil coolers, etc.),
- Leakage of air through flanges and seals and turbine cooling flows,
- Customer horsepower, bleed, and inlet recovery schedules.

COMPONENT PERFORMANCE

Although the accepted standards for presenting compressor and turbine performance can vary, the underlying fundamentals are the same. In order to preserve speed/

flow relationships under different operating conditions, performance is presented as functions of a corrected speed and a corrected flow parameter. By presenting performance in terms of these similarity parameters, kinematic similarity (velocity triangles) and dynamic similarity (ratios of different forces) are preserved, regardless of the actual flow conditions in the component. Another similarity parameter, the Reynolds number, is also included in component performance representations. However, Reynolds number effects are second order, and as such, are not explicitly incorporated into component maps but are applied as multipliers to map flows and efficiencies.

Typical compressor and turbine maps are shown in Figure 1.25 and 1.26, respectively. Compressors are, to a high degree of approximation, adiabatic so that the work interaction across the compressor can be expressed in terms of ideal energy (pressure ratio) and the adiabatic efficiency. Thus, for example, if the compressor is operated at the desired pressure ratio and speed, the flow and adiabatic efficiency are obtained from the map and the required work input and discharge temperature are determined.

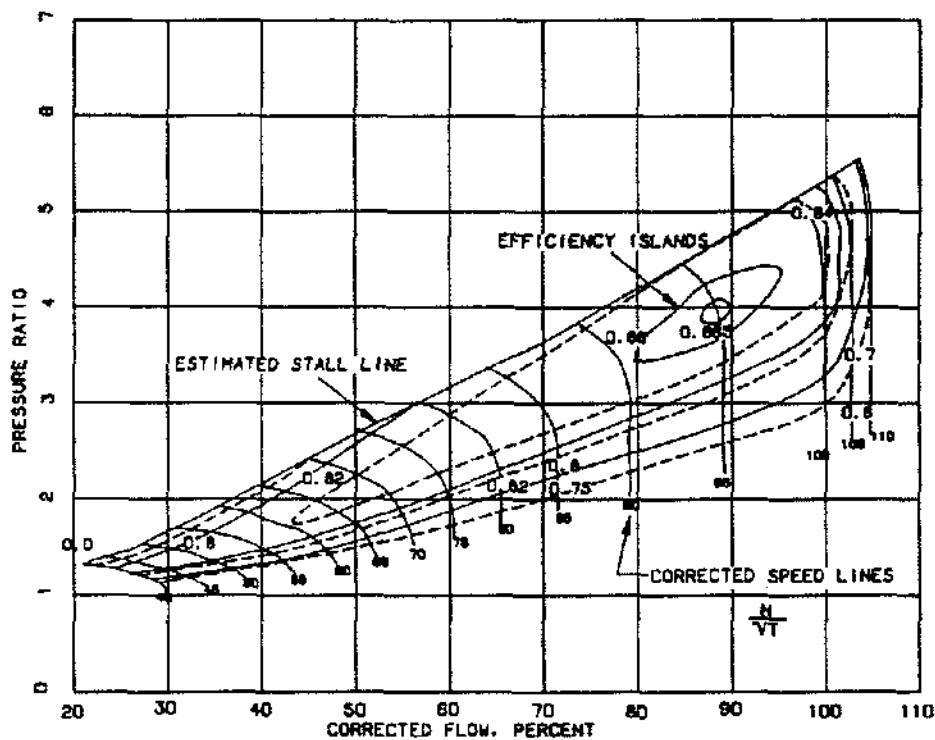


Figure 1.25 Typical Compressor Component Map

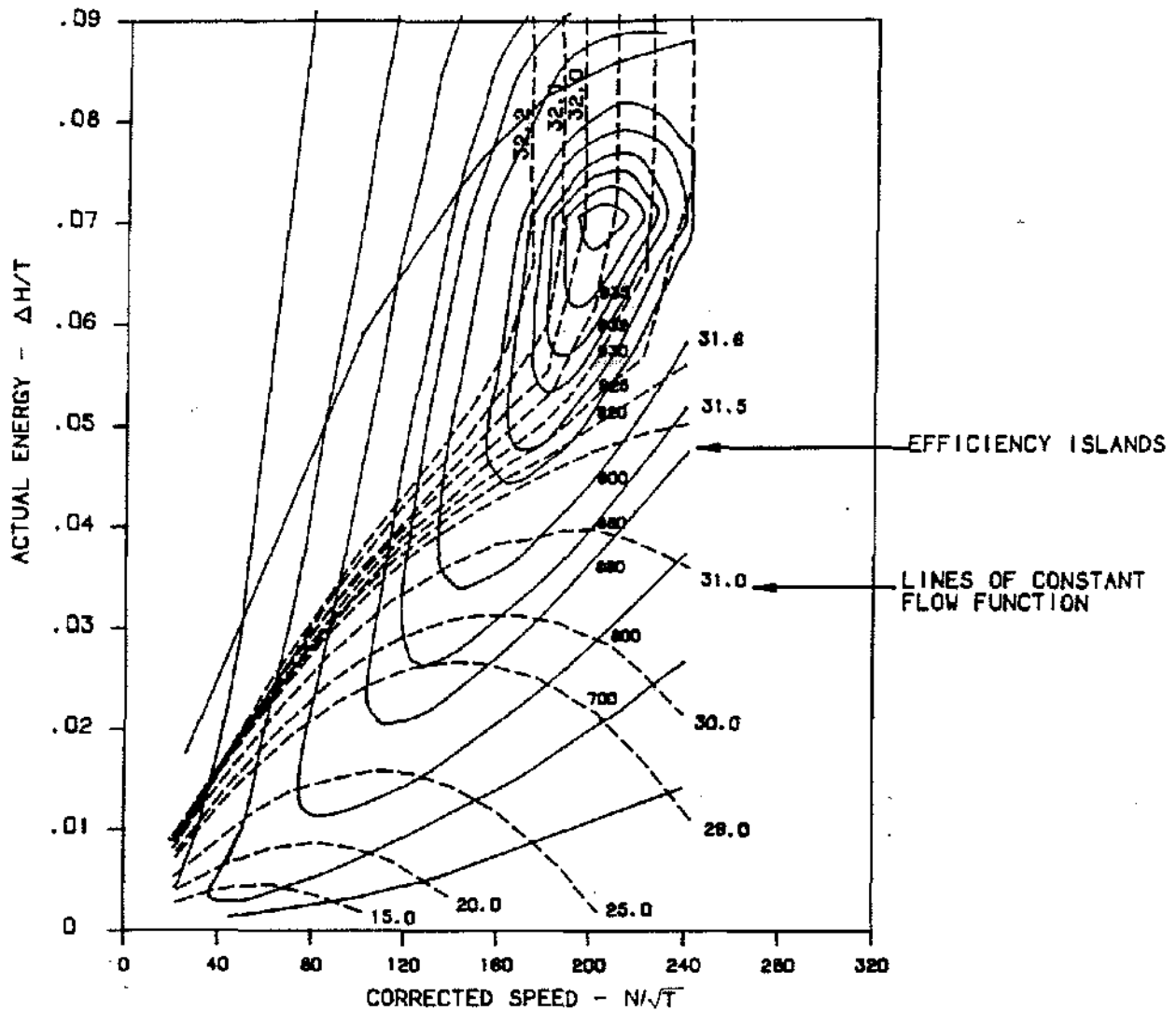


Figure 1.26 Typical Turbine Map

Unlike compressors, turbines are almost always cooled and therefore cannot be considered to be adiabatic. However, the adiabatic performance is usually presented and the estimation of the effects of the cooling air is determined separately and applied to the adiabatic map performance. The energy extracted (actual energy) in the turbine is normalized by the inlet temperature, and contours of constant adiabatic efficiency and flow function are plotted.

Component matching and off design performance are critical considerations when coupling compressors and turbines. Consequently, component performance must be presented over the full speed range of the engine so that the equilibrium operating line can be determined. At speeds below the design point, or at over-speed conditions, the operating line on the compressor may be too close to the stall line, and flow instabilities and surge may be encountered for flow perturbations or for inlet pressure and temperature distortion.

Combustor and augmentor performance is represented in terms of two measures of efficiency: the combustion efficiency or the ratio of actual heat release to the heating value of the fuel and the total pressure drop through the combustor or augmentor. The pressure losses arise from two sources: viscous or frictional losses and losses due to enthalpy addition at a finite Mach number. Through-flow Mach numbers in main combustors are very low so that the heat addition pressure loss is usually negligible. Mach numbers in the augmentor can be relatively high, however, because of limitations on the augmentor cross sectional area. Consequently, heat addition losses can become very significant; on the order of five percent.

Frame and duct pressure drops are losses between components which are not directly charged to any component. These losses are modelled as a function of the upstream velocity head and the effective area.

Exhaust nozzle performance is primarily dependent upon nozzle pressure ratio and geometry, and losses are principally due to under and overexpansion, angularity, leakage, and secondary flows. Variable geometry exhaust systems are required on many applications in order to provide nozzle throat area modulation and expansion area control. This is necessary to ensure high nozzle thrust coefficients over a wide range of operating conditions. As the sophistication of these systems increases, with increasing flight speed and vectoring/reversing capability for example, so does the sophistication of the modelling. For the sake of simplicity, however, all of the losses are collected and expressed in terms of the flow coefficient and the thrust coefficient. These parameters are usually applied as functions of nozzle pressure ratio, area ratio, vector/reversing angle, etc.

Since the engine is subject to a large number of mechanical and aerothermodynamic constraints, very close interfacing between cycle and component designers is necessary to ensure that these limits are not exceeded. If the engine is allowed to operate beyond its mechanical limits, it will fail; often catastrophically. Likewise, if the aerothermodynamic capabilities of the components are exceeded, the engine will not perform to design expectations. However, it is desirable to operate the engine at or near its limits at any operating point so that the maximum possible performance is achieved. The limiting values of individual constraints are not encountered simultaneously but are found at a variety of different operating conditions or during different control modes. For example, maximum core physical speed is reached at low altitude, high Mach conditions whereas the fan physical speed limit is encountered during a hot day takeoff.

These limits are established by the appropriate mechanical or aerothermodynamic design group and are subsequently included in the cycle model. Mechanical limits must be formulated in terms of equivalent cycle parameters so that they may be explicitly incorporated. Many aerothermodynamic limits appear implicitly in the component representations, but others, such as duct Mach numbers limits, need to be explicitly stated (see Tables 1.3 and 1.4).

PRELIMINARY COMPONENT DESIGN AND MATCHING

Quite obviously, the design and off design performance of the fan, compressor, and turbine have a significant effect on the overall performance of the engine. Steady state operation demands flow continuity and a power balance between components on the same shaft. Changes in engine inlet conditions and power settings produce migrations on component maps so that the performance characteristics of the turbine and compressor (or fan) must be very carefully matched, or else the engine will suffer from poor off design performance. The designers will try to match components so that the fan and the compressor are operating near their peak efficiency throughout the entire range of operation. This is accomplished by running the steady state operating line through the centers of the efficiency islands (so long as surge margin considerations allow). A great deal of experience and results from previous studies are needed to proceed quickly to a reasonable design, through a generalized method can be outlined to provide exposure to some of the complexities and constraints that are encountered in a typical design cycle.

The results from preliminary cycle studies will yield the inlet and exit flow conditions and the work requirements of the respective components, although these values are subject to change as the design is iterated. For turbomachinery preliminary analysis very often begins with a flow averaged radius analysis, after which radial variations are considered. The work coefficient, which characterizes the work interaction for rotating components, is used as a first order aerodynamic loading parameter.

$$\psi = g\Delta H/2U^2 \text{ (turbines)}$$

$$\psi = 2g\Delta H/U^2 \text{ (compressors)}$$

where ΔH = change in total enthalpy across the stage and $U = \omega r$ or the linear velocity of rotation at radius r .

Thus, the work coefficient is the ratio of work per unit mass flow divided by the wheel speed squared. Using

Mechanical Constraint	Cycle Parameter
Pressure and temperature extremes for engine inlet and casing (defined from flight envelope and inlet recovery)	T1 (min, max) P1 (min, max)
Compressor casing ΔP limit	PS3 (max), PS14
Compressor casing and cooling flow maximum temperature	T3 (max)
HPT and LPT average gas temperature limit at rotor inlet	T41 (max), T49 (max)
Augmentor liner temperature limit	T6 (max), T8 (max)
All rotor speeds	N (max)
Augmentor liner buckling load limit	ΔPS (max)
Maximum pressures and loadings on nozzle plugs, flaps, and reversers	P8-PAMB (max)
Exhaust nozzle area ratio limits for actuator and flap design	A9/A8 (min, max)
Minimum combustor pressure drop for backflow margin in turbine cooling circuits	(P3-P4)/P3 (min)
Combustor and afterburner fuel flows for control design and fuel/oil heat exchanger temperature limits	WF3 (min, max) WF6 (min, max)
Gearbox and shaft torque limits for power turbine output and customer power extraction	PWX (max)
Customer bleed rate, temperature and pressure limits	WB (max) TB (max) PB (min, max)

Table 1.3 Mechanical Design Limits

the Euler equation, which give the work input for a rotating blade row;

$$g\Delta H = \Delta(Uc_u)$$

where c_u is the tangential component of the fluid velocity.

In axial compressors and turbines it can be assumed that the radial shift in the streamline between the inlet and exit of a blade row is small, so that the change in the blade rotational speed along a streamline is negligible. The work coefficient becomes

$$\psi = \Delta c_u / 2U \text{ (turbines)}$$

$$\psi = 2\Delta c_u / U \text{ (compressors)}$$

Typical values of turbine work coefficient are around unity. Counter-rotating vaneless turbines are a factor of two higher. The same set of design rules apply to a counter-rotating design, but since the loss associated with the vane is absent, a higher work extraction and rotor loss can be tolerated without a reduction in the overall efficiency. Alternately, a low work extraction may be employed to achieve a higher efficiency. A representative value of compressor work coefficient is 0.8.

With the specific work established from the cycle, the designer selects the work coefficient and calculates the required wheel speed. The rotational speed of the spool is limited by the thermal environment of the turbine, and practical upper limits on turbine blade wheel speeds are 2,000 ft/sec at the blade tip.

Aerothermodynamic Constraint	Cycle Parameter
Maximum corrected speed and flow of each compression component	$N/\sqrt{\theta}$ (max)
Stall pressure ratio on each compression component for stall margin stack on operating line	P/P (stall)
Combustor and augmentor fuel flows for burner smoke, emissions and stability limits and augmentor thrust jumps	WF3 (min, max) WF6 (min, max)
Combustor and augmentor blowout parameter	CBOP (max) ABOP (max)
Turbine flow function limits which establish turbine area requirements	W41R (max) W49R (max)
Turbine corrected speed, work and pressure ratio limits	$N/T\sqrt{T}$ (max) $\Delta H/T$ (max) P/P (max)
Turbine exit Mach number limit	M5
Augmentor inlet Mach number limit	XM6BR (max)
Exhaust nozzle area requirements for complete expansion and nozzle stability	A9/A8 (min, max)
Duct Mach limits for sizing ducts	M(x) (max)

Table 1.4 Aerothermodynamic Design Limits

Turbine rotational speed constraints are usually expressed as the product of the annulus area and the square of the speed AN^2 . The actual limiting value of AN^2 will depend upon the turbine inlet temperature and the blade material. The numerical value of AN^2 rarely exceeds 5×10^9 , where the annulus area is expressed in inches squared. (An annulus area of 500 in² and an RPM of 10,000 yields $AN^2 = 5 \times 10^9$.) Another rotational speed limiting parameter is bearing DN, where D is the bearing race inner diameter in millimeters. DN then is simply a way of referring to the bearing peripheral surface speed. DN values are restricted to 2.2×10^6 , and it is usually only in small machines where this becomes a limiting parameter.

Once the AN^2 limit has been established, the annulus area is selected from the turbine exit Mach number considerations. Selection of a higher turbine exit Mach number reduces the annulus area and tends to enable

higher loadings, but reduces the efficiency and limits power extraction at high power due to annulus choke. Due to these considerations, axial Mach numbers at the turbine rarely exceed 0.5. With the annulus area so determined the spool rotational speed is calculated from the assumed value of AN^2 . With the wheel speed and rotational speed known, the radial location of the turbine may be calculated using

$$U = \pi RN/360$$

where U is in ft/sec, R is radius in inches, and N is revolutions per minute.

With the RPM of the spool determined the next step is to define the compressor configuration. The first step is to determine the annulus area at the compressor inlet. The compressor inlet corrected flow, given by the cycle, and an assumption of the inlet specific flow and radius ratio

determines the inlet dimensions from the following relationship:

$$A = \pi R^2 (1 - r^2)$$

where R is the inlet tip radius and r is the inlet radius ratio.

Using the rotational speed determined by the turbine, compressor blade speeds are calculated to check the reasonableness of the assumptions. Limiting values of compressor tip speeds are 1800 ft/sec at the inlet. Typical maximum rim speeds are 1200 ft/sec at the compressor exit where the gas temperatures are the highest, and a practical upper limit on the exit radius ratio is 0.92. Reducing the inlet radius ratio reduces the inlet tip radius and speed. Reductions in the rotational speed may also be employed to lower tip speeds but only at the expense of increasing turbine radius to achieve the necessary turbine wheel speed and loading. Generally speaking, the compressor inlet radius ratio needs to be increased until a limit on the inlet tip speed, exit rim speed, or exit radius ratio is encountered.

Axial compressor designs generally fall between two extremes; constant tip radius and constant hub radius. Constant tip configurations maximize the average wheel speed, which tends to reduce the stage count. Constant hub configurations maximize blade height, which tends to increase efficiency. For a given annulus area, clearance to blade height ratio decreases as blade height increases so that a smaller portion of the blade is subject to end wall effects. However, as blade height is increased, larger clearances are necessary to protect from rubs. Constant tip configurations require smaller clearances, but tolerances are harder to maintain at the larger diameters. Clearly, the problem is very complex. The application will ultimately determine which configuration is more suitable. Where weight and size are the primary

consideration, the stage count must be kept to a minimum; which suggests a constant tip configuration. When fuel economy and efficiency are the principle concerns, the design will tend toward a constant hub configuration. The GE25 (a turbojet) is an example of a near constant tip design, while the CFM56 is an example of a near constant hub design. The CF6, on the other hand, is an example of a near constant pitch design, the pitch line being the arithmetic average of the hub and tip radius.

Additional complexities arise for multiple spool designs, compressor flow extractions, and turbine cooling flows. Transition ducts require common interfaces, create pressure losses, and may require cooling. Close coupling of components may also restrict the work potential of components. When cooling the combustor liner and high pressure turbine, compressor discharge air is the only source of internal engine air with a high enough pressure to avoid hot gas backflow into the cooling circuit. (Compressor interstage bleed may be used for low pressure turbine cooling.) Therefore, the temperature of the compressor discharge air must be restricted to increase the effectiveness of the coolant flow. The coolant flow is a penalty to the cycle because only a portion or, in the limit, none of the energy invested in pumping this flow up to pressure is extracted in the turbine. The compromises are many and varied, and numerous trade-offs must be performed before a final configuration is defined.

Figures 1.27 and 1.28 are cross-sections of advanced turbofan engines superimposed on their contemporary counterparts. These engines will have higher pressure ratios, higher turbine inlet temperatures, and fewer turbomachinery stages. In addition, composite materials will be used extensively in the low temperature areas of the engine. These next generation engines will have higher thrust to weight ratios and improved installed performance and efficiency.

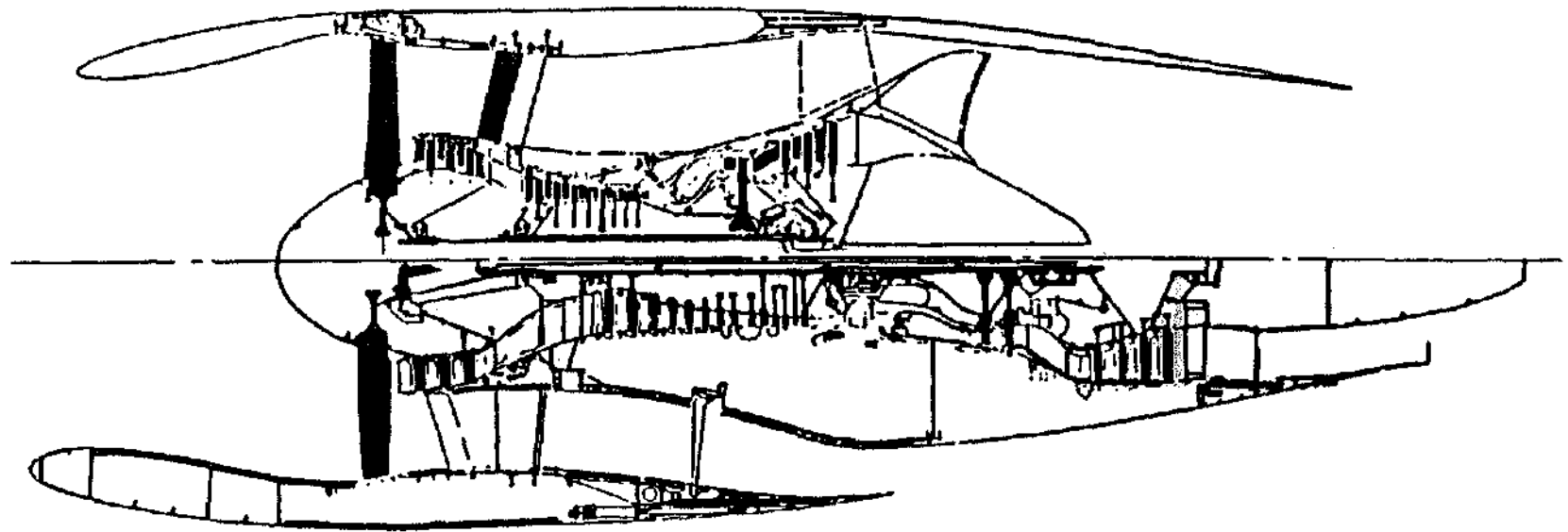


Figure 1.27 Comparison of an Advanced High Bypass Ratio Turbofan Engine with a CF6-50C Engine

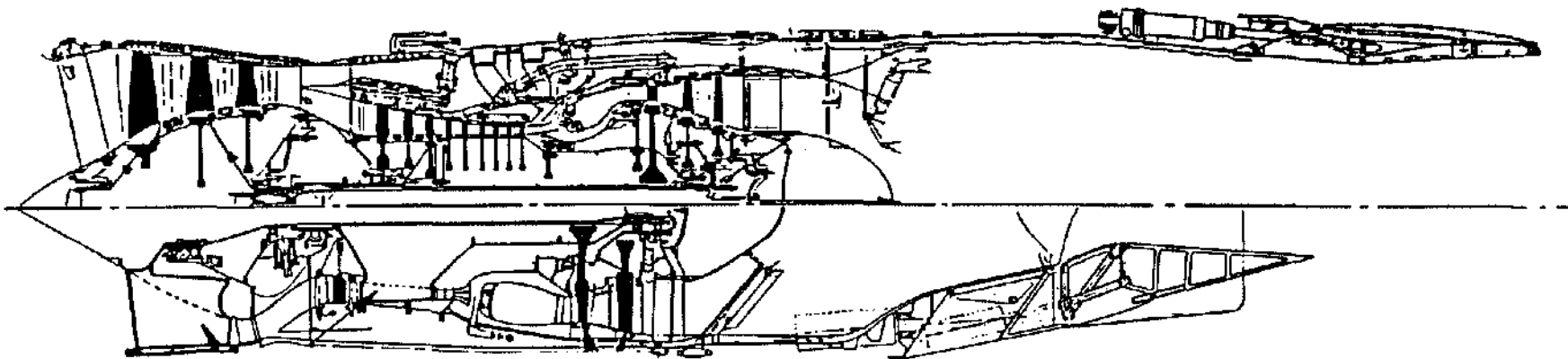


Figure 1.28 Comparison of an Advanced Military Fighter Engine with a F110-GE-100 Engine

Chapter 2

STATIC STRUCTURES

by Thomas S. Eichelberger

INTRODUCTION

The static parts of the engine are all of those parts that do not rotate. Static structures provide the overall backbone of the engine from mount-to-mount and extend fore and aft to support the inlet and the exhaust nozzle or reverser. Figure 2.1 is a typical high bypass commercial engine. Figure 2.2 is a typical military engine with a relatively low bypass ratio. In both the elements of the engine which constitute the basic backbone structure are labelled. These are the frames, casings, pressure vessels (including the combustor casings), the mounts (fore and aft), and any containment systems that are separate from the casings. In this chapter we are concerned with how the separate elements work together to provide the overall static structure of an engine.

What are the major design issues which dictate the nature of the frames, casings and mounts? What are the loads for which we must design? First of all, the static components must maintain alignment between the rotors and stators of the turbomachinery. In many cases, this dictates a need for stiffness, rather than strength, in the frames and in the casings between the frames. The major sources of load for the engine, which translate into forces on the structure, are the maneuver loads, acceleration and gyroscopic forces and moments through the bearings into the frame hubs, unbalance in the rotors, pressures internal to the flowpath, and thermal differentials induced by the hot gases flowing through the components.

Another requirement in the definition of static structures is the dynamic behavior of the engine and its possible interaction with the airframe in which it is installed. This is a major influence on the stiffness of frames between the sump hub and outer casing and the stiffness of casings between frames and mounts. All of this must be combined with design features and analysis which will enable the static structure components to handle differ-

ent types of loads. Extreme loads are called ultimate for which there is a criteria of no failure. Limit loads can approach yield, but there cannot be any permanent deformation. Normal operating loads occur every day in varying degrees during service and the predicted cyclic life must be compatible with the rest of the components of the engine.

OVERALL ENGINE STRUCTURE AND MAJOR STRUCTURAL COMPONENTS

The CF6-50 (Figure 2.1) is a high bypass fan engine which is used in primarily commercial applications, although it is also used on the 747 Flying Command Posts that are in the Air Force inventory. In the diagram it is shown with its full nacelle, some parts of which are supplied by the airframe manufacturer. Forward (on the left in GE engine drawings) is the inlet, made of aluminum sheet frames and skins with thinner barrel lined with acoustic treatment. The inlet and cowls, which form the outer flowpath for the fan and core discharge, are airframe designed and supplied. The fan and core thrust reverser are GE designed and supplied. The first engine static structural parts we see, as we follow the flow of air through the engine, are the fan cases which are bolted to the outer end of the fan frame struts and provide the support for the inlet. The inner part of the fan frame, or hub, provides the gooseneck shaped flowpath from the booster into the inlet of the high pressure compressor. The hub also supports the #1 bearing by means of a large aluminum cone and the #2 roller bearing by a cast steel cone. These two bearings hold the fan shaft and the front end of the low pressure shaft. The inner surface of the thrust reverser, while it provides the flowpath and acoustic treatment for the fan discharge, is not part of the basic structure of the engine. From the fan frame hub the main structural loadpath is the casing of the high pressure compressor, the compressor rear frame, a turbine mid-frame, and finally, the low pressure turbine casing. The compressor rear frame is also the combustor casing and the high pressure turbine casing. The turbine mid-frame carries the aft mounts. The low pressure turbine casing provides the support for the primary nozzle and, in this diagram, a turbine reverser.

Note that the fan frame hub carries the #3 ball bearing at the front of the high pressure compressor, and the compressor rear frame carries the #4 roller bearing between the rear of the compressor and the front of the high pressure turbine. The turbine mid-frame carries two roller bearings, the #5 bearing at the rear of the high pressure turbine and the #6 bearing at the forward shaft of the low pressure turbine. At the rear of the basic engine, just ahead of the turbine reverser, is the turbine rear frame.

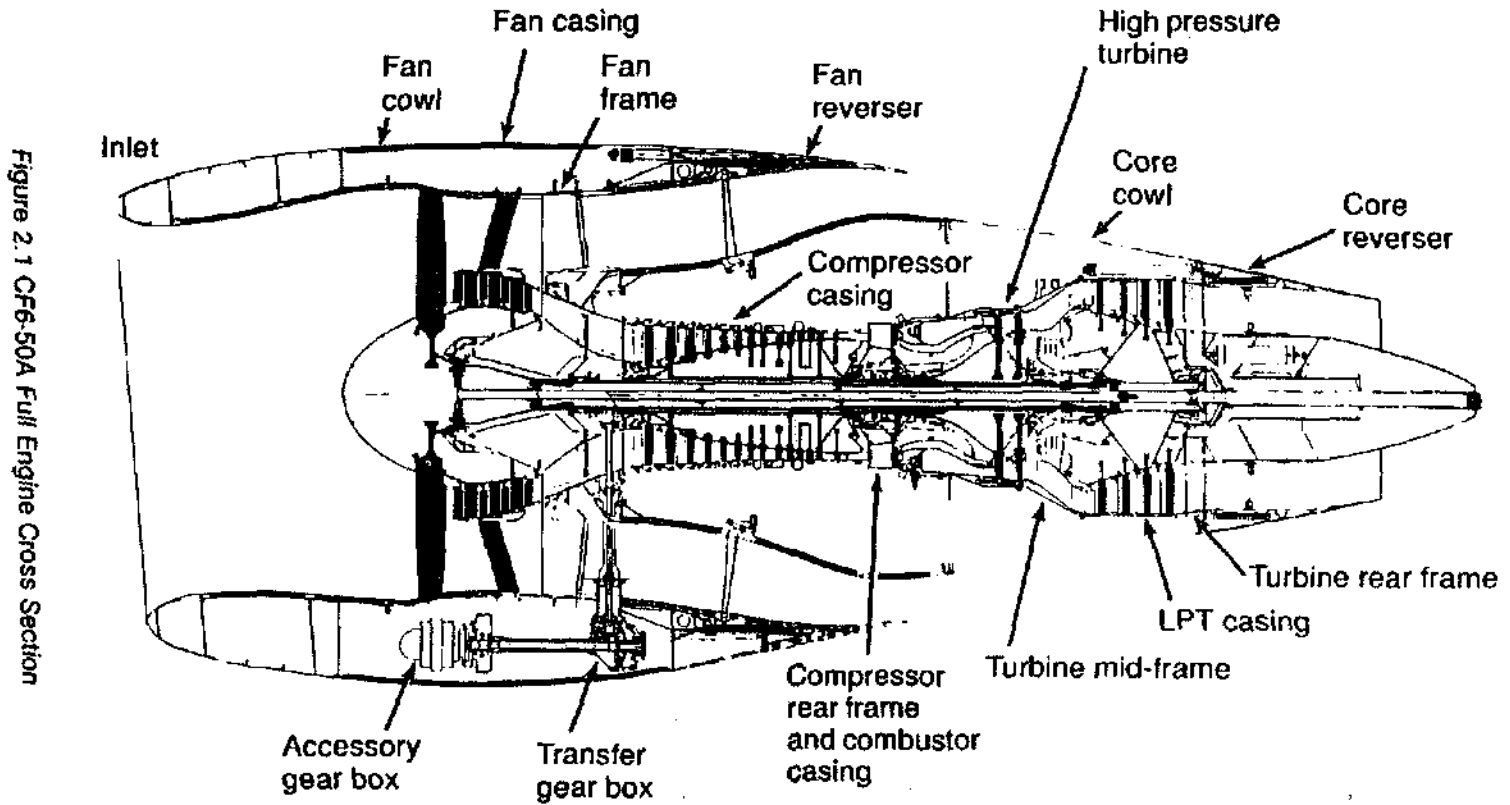


Figure 2.1 CF6-50A Full Engine Cross Section

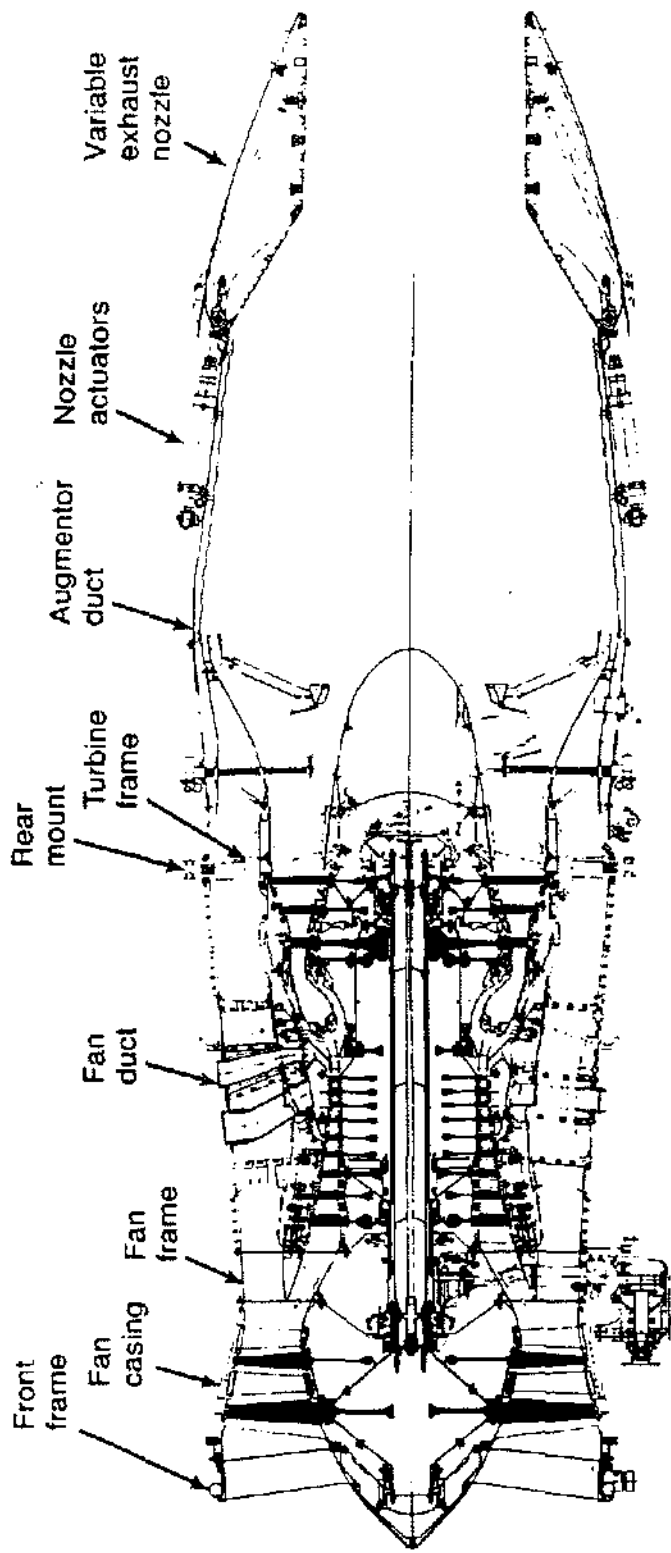


Figure 2.2 F101-GE-102 Augmented Turbofan

which supports the #7 roller bearing behind the low pressure turbine. Here, we have examples of a number of ways to support components. The fan is supported by the fan frame and is basically overhung from it on two bearings. The high pressure compressor and the high pressure turbine are both straddle mounted with bearings at the front and the rear, and the low pressure turbine is straddle mounted with bearings at the front and rear. This bearing arrangement on the rotors gives us a four-sump engine: A-sump in the fan frame, B in the compressor rear frame, C in the turbine mid-frame, D in the turbine rear frame. On the turbine mid-frame are the mount elements which are supported by links to the aircraft pylon. The forward mount is right behind the fan frame outside the forward flange of the compressor, but is not visible in this view.

While looking at the overall structure shown in Figure 2.1, note that in the A-sump, between the #2 and #3 bearings, there is a set of bevel gears connecting the high pressure rotor with a radial drive shaft at the 6 o'clock position. This shaft connects to a bevel gear transfer gearbox and then to a shaft running forward to the accessory gearbox, which on this engine is located in the fat lower lip of the nacelle.

The lower half of Figure 2.3, which shows the CF6-50 in more detail. (A little later on, we will study the top half of this figure, showing the -80A, which evolved from the -50.) On the fan frame hub, can be seen the bleed doors and bleed door mechanism between the acoustic panel and the hub outer wall. The doors or variable bleed valves (VBV) open in order to bypass excess booster flow, so that we do not overload and stall the high pressure compressor. The containment ring over the fan blades can also be seen. This stainless steel ring is sized to contain the energy that would be released if a fan blade should fail in the shank, just above the dovetail to the fan disk. Forward of the fan blades and between the fan blades and the outer guide vanes is the acoustic treatment in the fan flowpath. Just aft of the fan blade, is a deep stiffener ring that was added at the bolted joint between the containment ring and the aluminum midfan case. This stiffener ring raises the vibrational frequency of the containment system, so that it is not resonant with any vibrational mode of the fan rotor in the operating range of the engine. Just aft of the OGVs is the bolted joint between the aluminum fan mid-case and the aluminum aft fan case, which goes over the fan frame struts. Two deep rings over the fan frame struts distribute the reaction of those struts into the shell of the casing.

Recognize that the lower half of Figure 2.3 is really the 12 o'clock section of the -50 engine. The thrust mount is really pointing upwards since the engine is always

mounted either on the wing or in a tail engine position on a DC10. The mount is shown just outside the inlet guide vanes (IGV) of the high pressure compressor. The platform has a short fat pin, which takes the thrust in shear to the pylon foot; the platform is clamped to the pylon foot with two 7/8" bolts that belong to the airframe designer. The main thrust connection between the mount platform and the 12 o'clock strut of the fan frame is the short link between the two pins. This link or dogbone carries about 95% of the thrust load. The other 5% is carried through the bolted flange between the compressor and the fan frame. This bolted joint also carries vertical load and a slight amount of torque and sideload. This is "slight" because the forward pylon connection, to which it is attached, is quite flexible in torsion. The rear mount is shown at the 12 o'clock position on the turbine mid-frame. The mounting span of the engine between the front mount and the three rear mount links includes the compressor, the compressor rear frame combustor case, and the high pressure turbine section. Notice that the fan module is completely overhung from the front mount and the low pressure turbine, nozzles, and core reverser (if there is one) are overhung from the rear mount. This makes the -50 interesting from a dynamics point of view. The engine, which has some of the structural character of a dumbbell, is actually mounted near the nodal points of its fundamental bending mode, and therefore, the mount reactions are small under large unbalanced loading. Dynamically, the difference between that engine and the one shown at the top of Figure 2.3 is quite marked. Note that the front mount of the -80A is at the same axial location (the station of the shear pin is identical to that of the -50). However, the mount does not appear to be the same, and it is not. The differences in those mounts will be discussed in a later section of this chapter. The turbine mid-frame has been removed and the high pressure turbine of the -80A is cantilevered from a larger, heavier sump in the compressor rear frame. The low pressure turbine is supported by only one roller bearing in the turbine rear frame. You will note that the rear mount has now been moved aft of the low pressure turbine to the outer shell of the turbine frame. This increases the span between the mounts, and since it moves the mounting points away from the natural nodes, the reaction forces for the -80A under vibration are somewhat larger than for the -50 with the same unbalance in any one of the rotors.

Going back to the forward end of the engine, notice the difference in the containment systems for the fan blades. The -50 systems shown in the bottom half of Figure 2.3 is a steel containment ring, or shell, that runs from the front flange to the beginning of the acoustic panel behind the fan blades. This steel ring is designed to resist penetration by pieces of the fan blade and to absorb the total

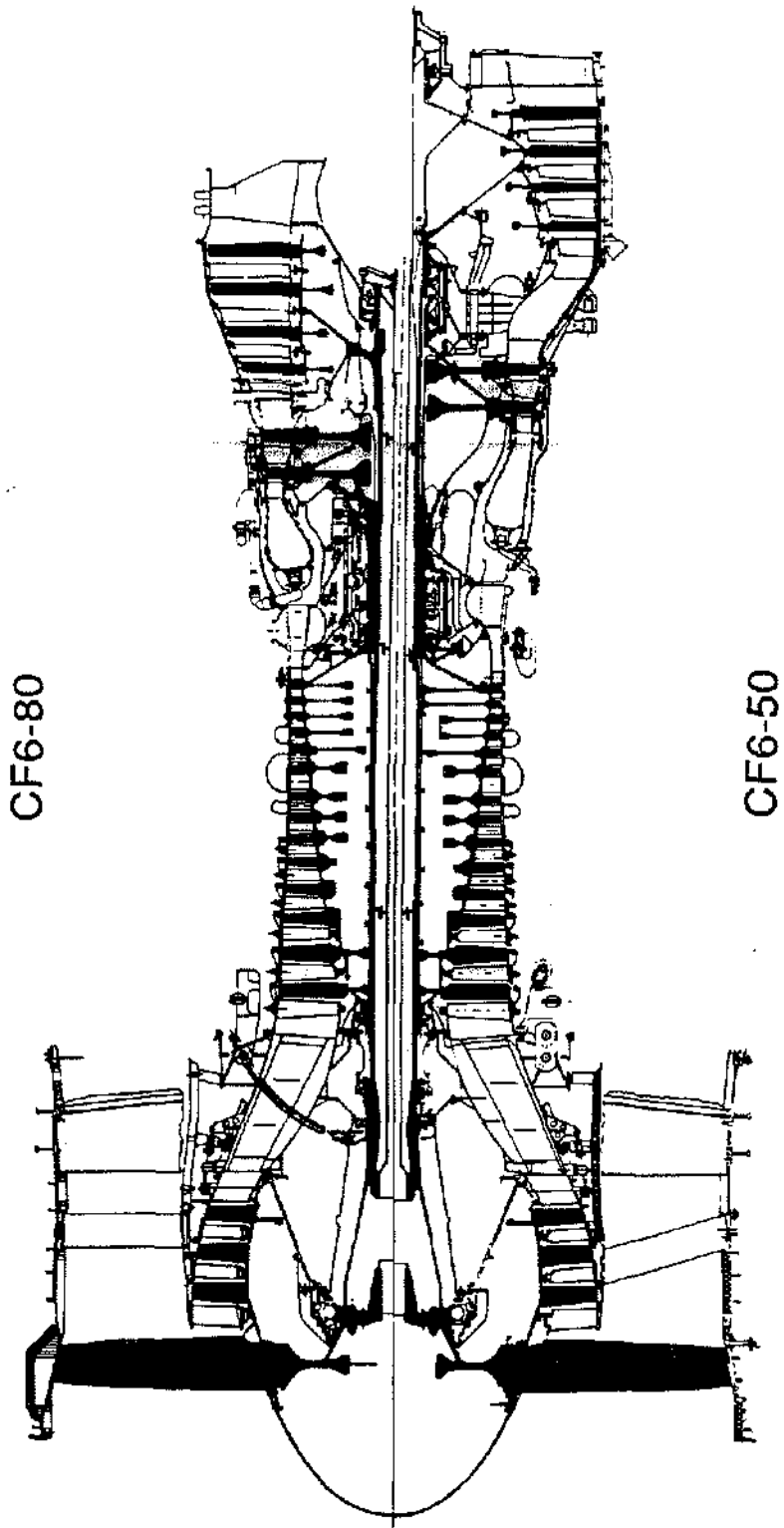


Figure 2.3 CF6-80 and CF6-50

energy of a fan blade released due to a shank failure at the disk dovetail. In the -80A containment system, shown at the top of Figure 2.3, the steel ring has been machined down until it is just a very thin shell, except for the section for about 2 inches behind the front flange where the steel itself must provide all of the containment capability. The containment of fan blade particles or the energy of an entire blade are absorbed by a Kevlar belt over the fan blades. The basic system consists of the thin steel shell, a deep section of aluminum honeycomb, and a graphite-epoxy outer band forming a sandwich that gives an equivalent stiffness to that achieved by the steel shell and the stiffener ring of the -50. The Kevlar containment consists of many layers of Kevlar cloth, in this case about 65 layers, that are woven to have the pocket shape that you see in the diagram. This containment system design is equivalent to the magician's trick of catching a bullet in a silk handkerchief.

Moving aft from the fan, the booster and the gooseneck passage into the high pressure compressor look very similar to that of the -50. The compressor flowpath contour appears to be quite similar, though the detailed aerodynamics of the airfoils is somewhat different. However, in the rear section of the -80A compressor the casing goes all the way to the 14th stage. There is no intermediate bolted joint like there was on the -50, which originally had a titanium forward case and an Inconel 718 aft case. The -80A has a steel case of M152 over the entire compressor. Extra length in the compressor flowpath has been removed and the CRF struts have been moved forward. The fuel nozzles and the combustor have been moved closer to the aft edge of the struts. All of these changes have significantly shortened the -80A engine. In the absence of a turbine mid-frame, with a gooseneck to the stage 1 low pressure turbine blades, the LPT of the -80A now has a near cylindrical inside diameter and a conical outside shape as opposed to the -50 which has the cylindrical outside diameter on the flowpath and a conical inside shape. The turbine rear frame serves as the support for the low pressure turbine as well as for the mounting of the engine to the pylon. Finally, the turbine frame has much longer struts in the axial direction because they serve as airfoils straightening the flow entering the exhaust nozzle.

Figure 2.2 is a supersonic, low by-pass, augmented turbofan for the military and powers the B1B bomber. Again, starting on the left at the forward end of the engine, there is a front frame. It supports a small sump and bearing so that this fan is what is known as "straddle mounted," with a bearing forward and aft. The aft bearing is carried in the fan frame. This engine does not have a booster or low pressure compressor. The small diameter basic structure of this engine is quite different from

the high by-pass commercial engines. There is a long fan duct that carries the flow from the fan back to the mixers, so that the core stream and the fan bypass stream are mixed just ahead of the augmentor. The duct that surrounds this fan flow is quite large in diameter and stiff. Consequently, the structural characteristics of this engine with the forward mount on the front frame and the aft mount on the mount ring outside the turbine frame are quite different from the structural characteristics of the large fan engine where the mounts are on the basic core structure. For this engine, the entire augmentor and nozzle assembly is cantilevered from the rear frame, which is just behind the low pressure turbine. There is no sump and bearings inside the combustor on this engine. The connection between the compressor and the high pressure turbine is a large tube or shaft. The bearing that supports the back end of the high pressure rotor is an intershaft bearing between the high pressure turbine aft shaft and the low pressure shaft. The LP shaft, in turn, is supported by a bearing from the turbine frame. This makes a very stiff HP rotor, but a somewhat softer support for the HP rear shaft than if there were a frame and bearings between the turbines. There are both advantages and disadvantages for an arrangement of intershaft bearings supporting a high pressure turbine as opposed to a sump and a high pressure turbine overhung from a compressor rear frame.

DESIGN ISSUES

Let us turn now to considerations of the details of the various static structural elements of the engine. As we look at how a variety of problems are dealt with, bear in mind the design issues that must be addressed in the design of all these parts.

Strength - Consideration must be given to the loads that must be carried, how the loadpaths transmit forces between elements, and the stresses that are involved versus the material properties of the parts.

Alignment - The static structures of the engines are major contributors to the performance and the retention of performance of an engine since they maintain alignment between the turbomachinery rotors and stators.

Stiffness - The stiffness of the static elements, their resistance to deformation or distortion under load, determines in large measure the alignment of the rotor and stator elements of the flowpath under normal operating conditions. By normal operation it is generally meant the steady-state conditions and the deflections that occur as a result of maneuver loads. A major secondary consideration in stiffness is related to the dynamics of the engine.

How will the engine, as an elastic structure, vibrate as a result of unbalance in the rotors or excitations from acoustic origin. Static components need to be designed for a usable cyclic life that is consistent with the rest of the engine major components, considering mechanical as well as thermal loading. It needs also to be recognized that most of the major structural elements are capable of being repaired. The considerations of life must include adequate strength against yielding under infrequent but high level forces (limit load) and the prevention of fracture or gross failure against the worst possible loads (ultimate load). In general, having met these yield and ultimate strength requirements, the design is really governed by low cycle fatigue generated within each flight cycle and high cycle fatigue, if there is continuing unbalance. As a final consideration, we must include damage tolerance and crack growth in service as part of the overall life considerations.

Materials - The choice of materials for the static structural elements needs to be considered. Selections are made of metals as well as composites and elastomers, taking into account material properties and behaviors, thermal expansion, load carrying ability, resistance to fatigue or crack growth, weight, and cost.

FRAMES

A frame in turbomachinery is a structure that supports bearings which in turn supports the rotors. Frame structures from different engines vary in characteristics, construction, and the way they adapt to mechanical and thermal loads. Figure 2.4 shows the common elements of a frame structure. If an element of an engine has an outer and inner casing and perhaps some vanes between them, but no bearing, it is generally referred to as a casing. An example of a casing would be the combustor case of the F101, F110, and CFM56 family. Here the frame consists of an outer shell, radial struts, and an inner shell that forms the flowpath and is an element of the hub structure. Figure 2.4 shows a welded, fabricated frame made up of rings, sheet metal and castings at the strut outer ends. With some modification of the design this frame could have been brazed together and made of sheet metal, fabricated struts, and castings similar to the F101 and F110 front frames. Frames have evolved from this fabricated construction to larger castings that were welded together, and finally to one-piece castings of very large diameter and great weight.

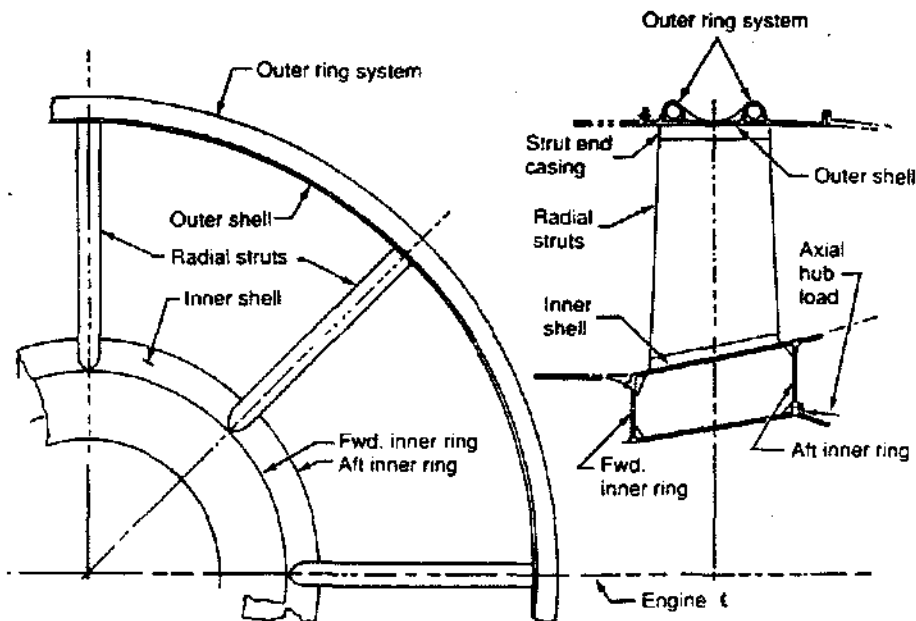


Figure 2.4 Typical Engine Frame
Eight Equispaced Radial Struts

Figure 2.5 shows the fan module of the F110 where the contributions of the front frame are quite apparent. The front frame supports the #1 bearing, the forward shaft of the fan rotor, and the variable inlet guide vanes. The guide vanes are necessary for the aerodynamic characteristics of the fan and help to prevent inlet distortion. Figure 2.6 shows some of the details of the front frame, including the vane bosses, the front mount (which takes vertical loads in the F-16 installations), and the oil supply and scavenge tubes shown partially disassembled. The frame is constructed by brazing fabricated brazed struts into a cast hub ring and a cast outer case. Figure 2.5 also shows the F110 fan frame and the way in which the core flow and the bypass flow are separated by the splitter. The hub of this frame supports the thrust bearing for the fan module. This fan frame is a one-piece titanium casting.

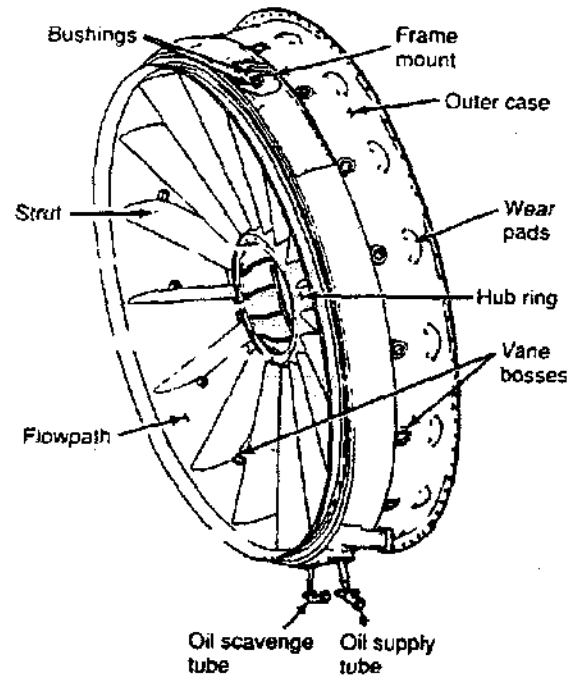


Figure 2.6 F110 Front Frame

At the other extreme of fan frame construction is the CF6-80C2 shown in Figure 2.7. This fan frame is also cast titanium. The hub is cast in one piece, probably the largest titanium casting in the world. The struts are also individually cast from titanium. The weld line can be

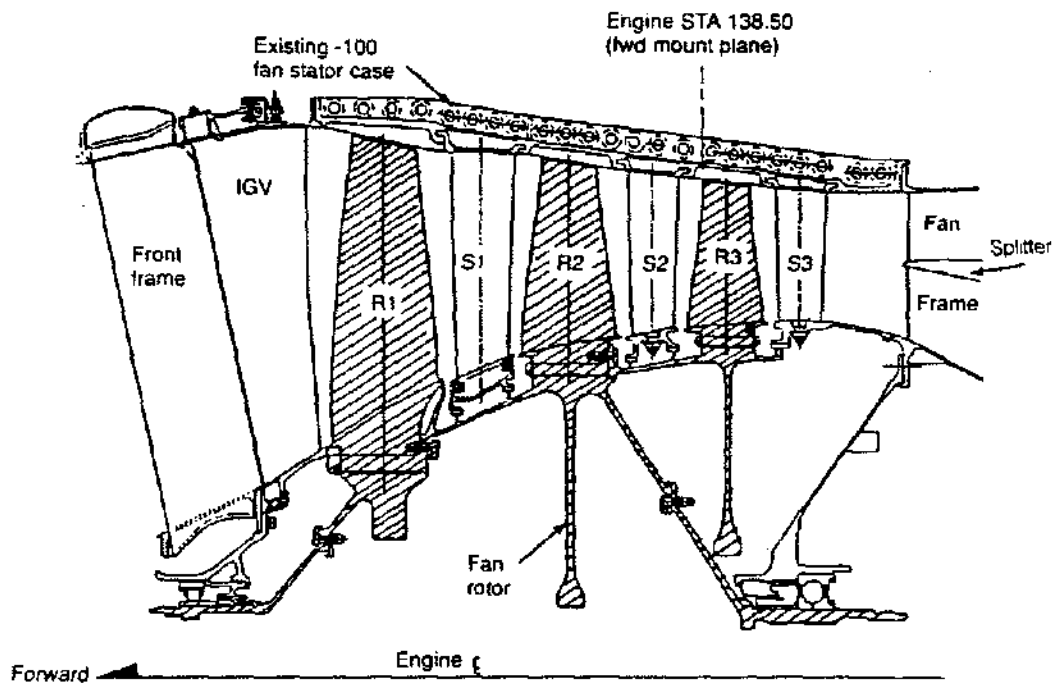


Figure 2.5 F110 Fan Schematic

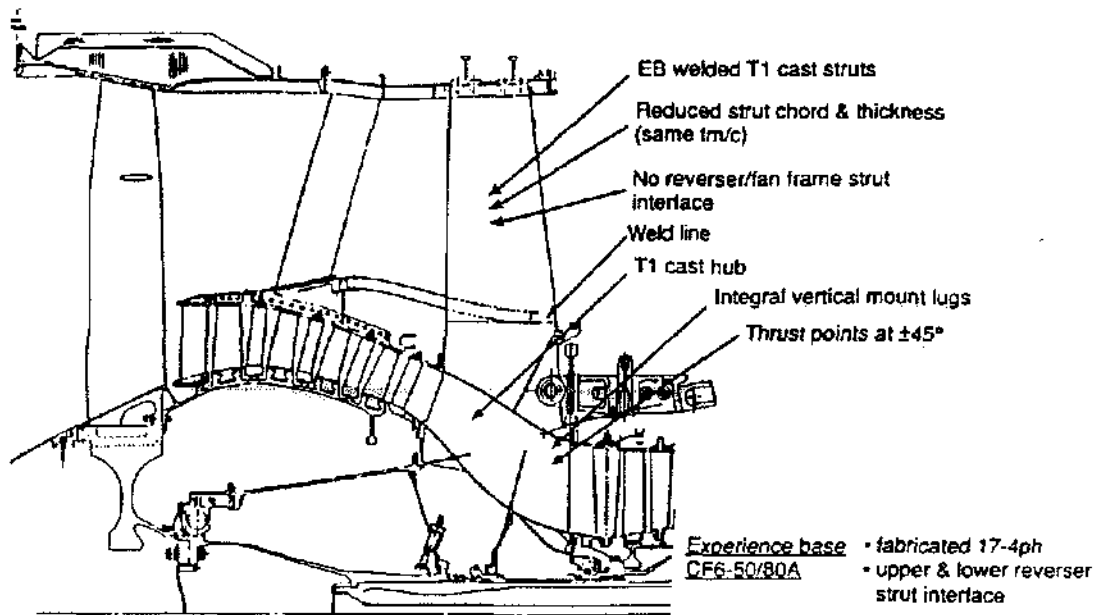


Figure 2.7 CF6-80C2 Differences With -80A

seen between the hub strut stubs and the struts proper just inside the acoustic panel on the 12 o'clock strut. When it was first proposed that this frame be titanium, the remark was made that, "Well, we had cast the entire F110 fan frame — hub, struts, outer case — all in one piece...." The statement made the -80C2 hub casting rather unremarkable until it was pointed out that the hub was bigger than even the outside diameter of the outer case of the F110 fan frame. The castings are chem-milled to remove the alpha case formed in the outer layers of the titanium, which is a serious detriment to long fatigue life. In the early 1970s the fan frames of the CF6-6 and -50 were fabricated by welding together 31 cast segments to form the hub of the frame. The struts were welded from eight stamped and bent pieces of sheet metal.

Another form of fan frame construction, using struts in the form of pinned links, is shown in Figure 2.8 for the TF/CF34 engines. The outer case is given additional support by the fan outlet guide vanes, which are bolted between the inner flowpath and the outer case. The actual hardware for this construction is shown in the photograph of the TF34 fanframe (Figure 2.9). The TF39 uses a similar A-frame strut system of pinned links.

As an indication of the value of one-piece castings consider the F101 fan frame which is fabricated from sheet metal and castings. It has 21 pieces welded together to

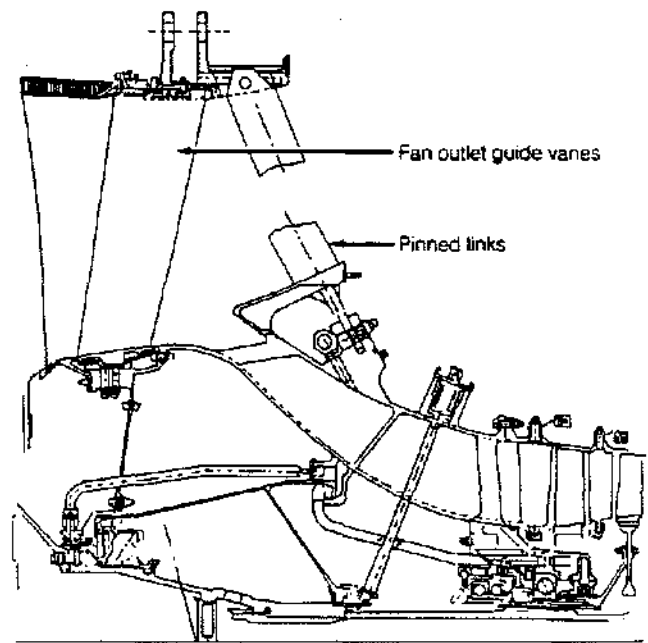


Figure 2.8 TF34 Fan Frame

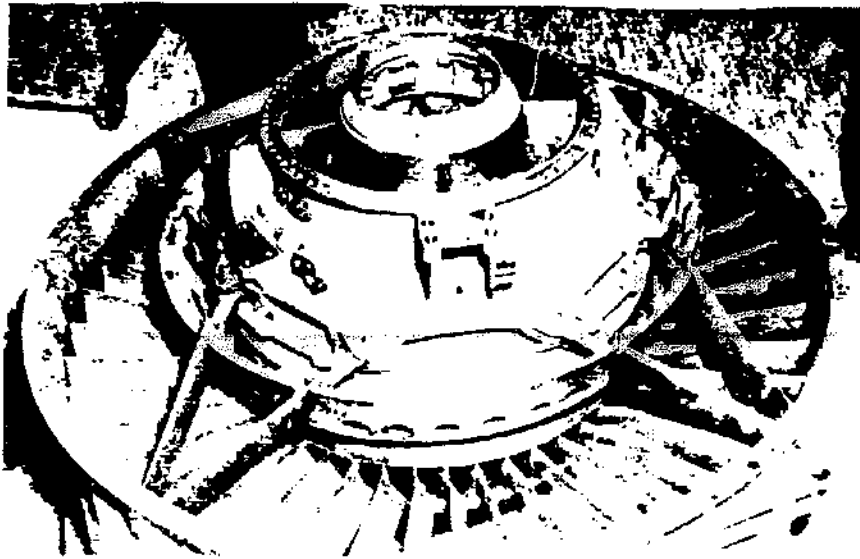


Figure 2.9 TF34 Fan Frame

form the hub, 27 pieces welded together to form the outer case, 24 pieces welded to form the 6 struts, and one splitter ring. A total of 73 pieces welded together to make one fan frame. As the 376th unit was produced, well down the learning curve, the shop cost was \$47,500. For the 100th unit produced of the one-piece cast titanium fan frame for the F110, the cost was only \$42,500 and decreasing.

Directly aft of the compressor is located the compressor rear frame (CRF), assuming the engine has bearings between the compressor and the high pressure turbine. **Figure 2.10** is the compressor rear frame for the CF6-80A. This is a short compact version of the frame that was used in the -50 family. The basic frame of 10 struts, the outer pressure shell, and the forward part of the combustor casing is cast in one piece of Inco 718. The aft section of the pressure shell is made out of rolled and welded rings and forged rings. On the left, the forward side of the frame, the flange and front of the shell is a flash-welded ring. In the CF6-50, the outlet guide vanes were nested in the split casing of the compressor. Here the outlet guide vanes are nested in the forward section of the CRF shell, trapped by the rear flanges of the compressor case. This isolates the pressure shell and the inside diameter of the flange from the main flowpath. In the -50 the flange inside diameter and shell were washed by the compressor discharge air and the large thermal gradient established during transients was a major cause of cracking of this flange, a serious short-life problem.

Note that there are three cones bolted to flanges on the inside of the frame; one on the inner flowpath supporting the compressor diffuser passage (CDP) seal, one bolted to the forward side of the hub supporting the forward end of the sump, and one bolted to a flange on the aft end of the hub supporting the sump and the high pressure turbine nozzle inner band. The thermal ΔT s associated with these bolted flanges and the stress concentration of the bolt holes have generated significant stresses and potential life problems for these frames.

Now compare **Figure 2.11**, which is the -80C2 compressor rear frame. The most significant change is that this is a one-piece casting from the sump support cone into the hub through the struts up to the outer shell of the frame and aft through the combustor casing, all the way to the aft flange at the high pressure turbine case. There is only one weld in the entire pressure shell, between the casting and the forged front flange. This forward flange connection is very similar to the -80A. There are no axial welds at all in this frame. Significant life improvements have been introduced in the way in which the sump support cone is cast integrally with the hub so there is no bolted joint. The CDP seal support flange comes off the hub rather than the inner flowpath, so that these thermal stress problems have been minimized. Where there was a bolted joint at the aft inner flange of the -80A, there is a welded combustor inner flowpath which carries the load back to the turbine nozzle. Finally, on the outer flowpath we have optimized the pads

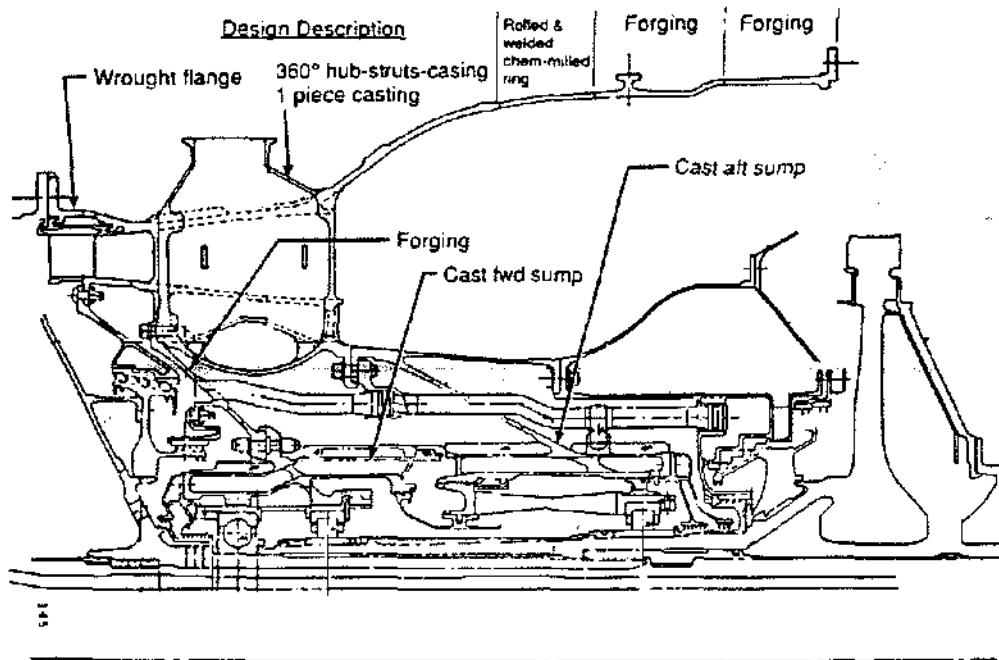


Figure 2.10 CF6-80 Compressor Rear Frame and B-Sump

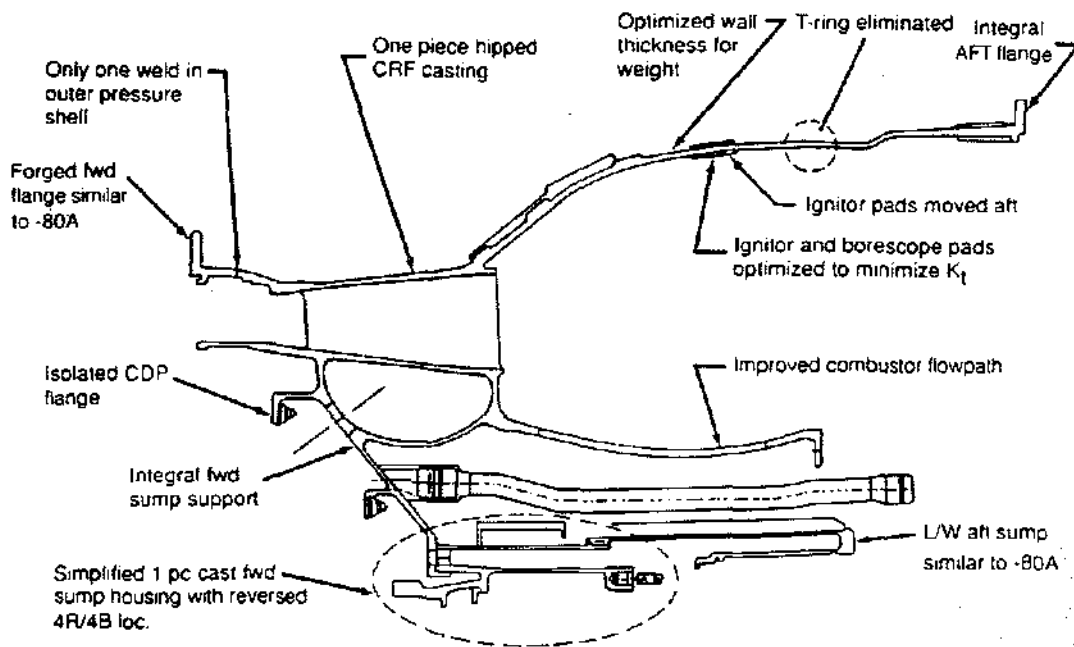


Figure 2.11 CF6-80C2 Compressor Rear Frame Design Features

for the fuel nozzles, ignitors, and borescope ports to minimize stress concentrations and increase life. Also, the ring that supported accessories on the outer shell is eliminated so there are no external vibratory inputs to the pressure vessel.

Figure 2.12 is the compressor rear frame of the TF34. It supports an overhung high pressure turbine very much like the -80A. While this engine is smaller in both size and thrust, the wheelbase between the roller bearings is greater than for the -80A, giving a more rigid support to the overhung high pressure turbine. Note, that the outer shell of the combustor case section of this frame is conical between cylindrical shell sections, so there is less flexibility in this part of the outer structure of the TF34 than there is in the outer structure of the core engine of the -50 and -80 engines.

In the TF39, CF6-6, and CF6-50 engines there is a hot frame between the high pressure turbine and the low pressure turbine (Figures 2.13 and 2.14). This turbine mid-frame supports the rear shaft of the high pressure turbine rotor with the #5 bearing and the front shaft of the low pressure turbine with the #6 bearing, both in the

same C sump. This frame also provides the flowpath from the high pressure turbine discharge to the larger diameter inlet of the stage 1 low pressure turbine. This permits an optimum design aerodynamically, but the reverse gooseneck involves considerable diffusion of the hot gas which is at about 1700°F. The thermal temperature differences during acceleration and deceleration are very large and a radial strut frame would typically have a very short life due to thermal fatigue. The mechanical load and thermal load problems were solved by adding a flowpath liner that was basically unstressed mechanically, except for the pressure loads, and would guide the flow and protect the struts and shells from the extreme temperatures of the gas path. The liner is welded sheet metal and wrought rings, and is cooled by compressor discharge seal leakage supplemented with bleed air from the 9th stage of the compressor. The mechanical structure consists of a hub ring casting, eight cast René 41 struts, and a fabricated outer case stiffened with hat sections, all welded together with strut end fittings that use expand bolts to tie the struts to the outer shell. These tangential struts have eight bolt pad attachments to the hub. In this way, as thermal mismatches between hub, strut, and outer casing occur, the struts expand and the inner

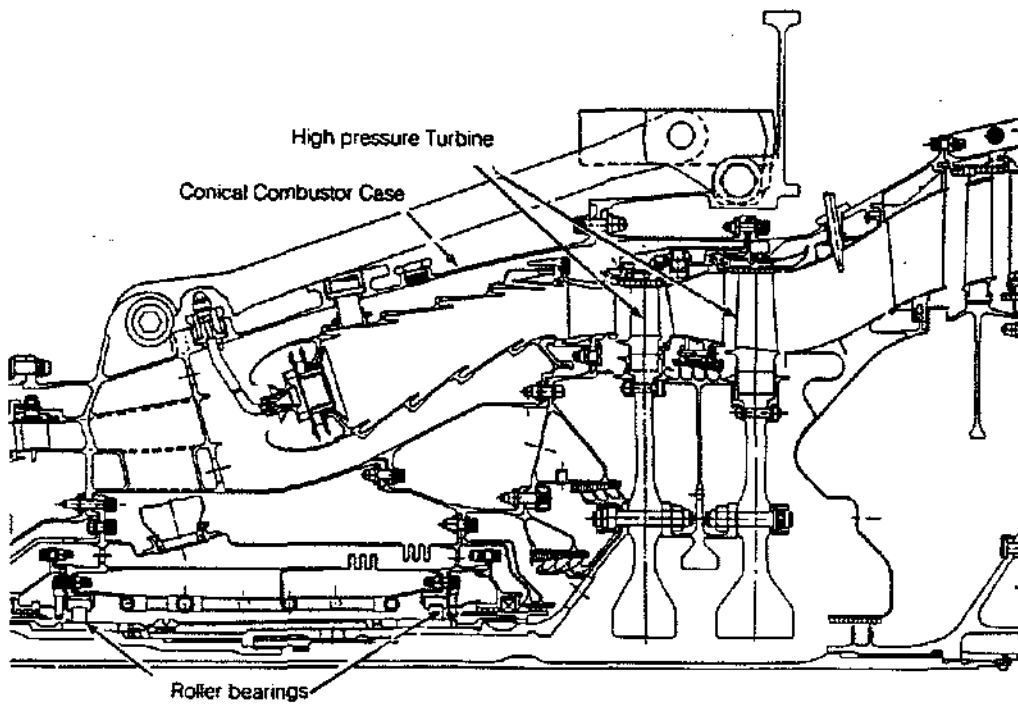


Figure 2.12 TF34 Compressor Rear Frame

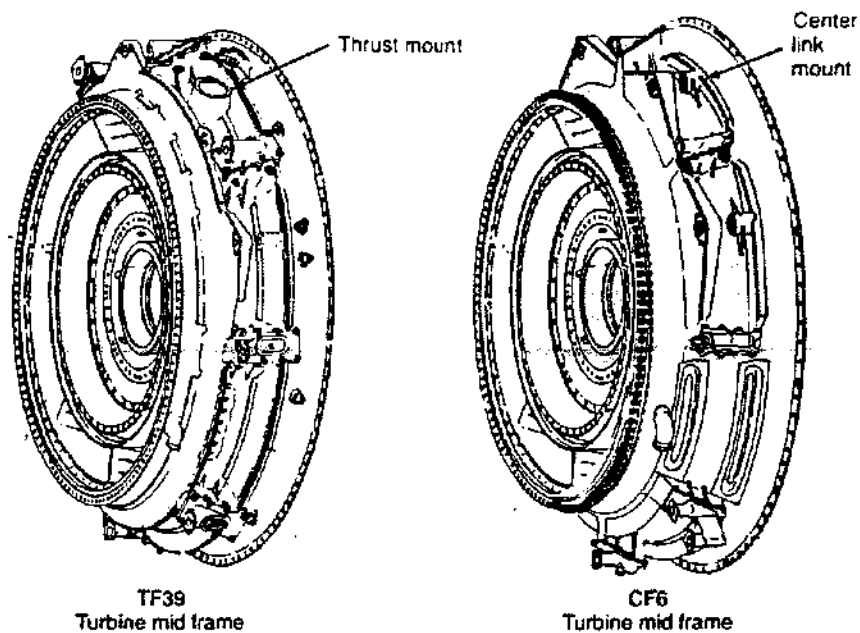


Figure 2.13 TF39/CF6 Turbine Mid-Frames

hub rotates. The thermal mismatches are accommodated for by the bending of the struts as opposed to the bending of the hub and outer shell and tension and compression of the strut.

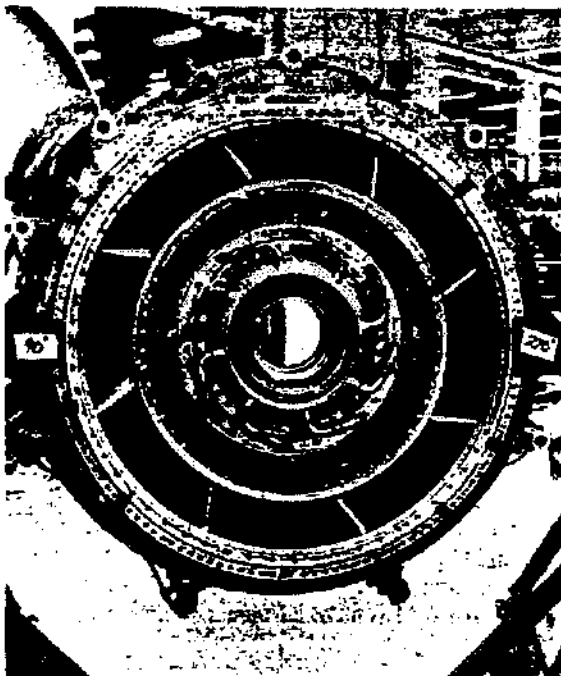


Figure 2.14 Turbine Mid-Frames

Figures 2.13 and 2.14 show the assembly of these frames. Figure 2.15 shows some of the internal pieces. In the case of the TF39 the thrust mount is at the top of the frame, consisting of a large spherical bearing holding a thrust pin from the pylon. While this is convenient for transfer of the thrust load from the engine to the C5 pylon, it bends the turbine mid-frame out of plane and induces local distortions in the turbine casings which are detrimental to turbine performance. When the -6 engine for the DC10 was designed, the thrust mount was moved to the front of the engine and a center link was added so that the turbine mid-frame takes outside load, vertical load, and the reactive torque of the engine. Unfortunately, this mount structure at the top of the mid-frame is quite heavy compared to the bottom 2/3 of the frame. There are large thermal distortions introduced into the frame which are carried into both the high pressure and low pressure turbines with subsequent loss of performance. However, this is not as bad as having the total thrust removed at this point, because that would add to problems of a non-symmetrical structure.

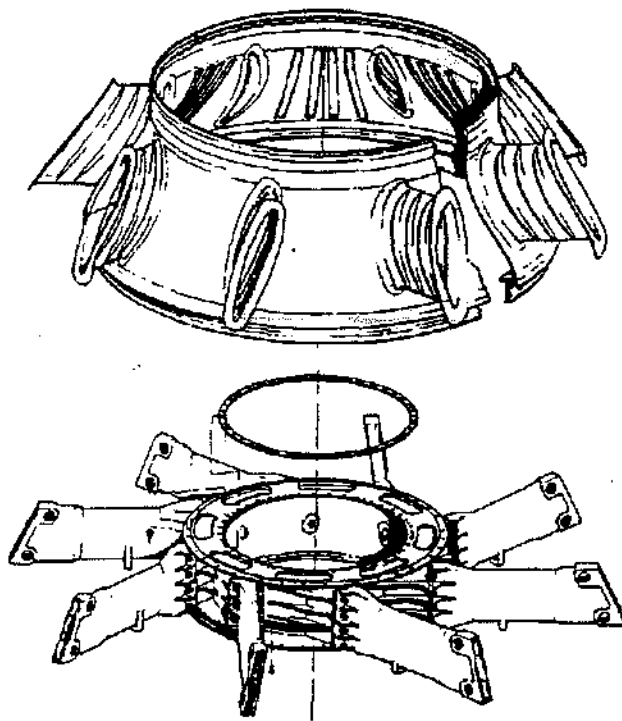


Figure 2.15 Turbine Mid-Frame Components

While we were able to eliminate the life problems and distortion of the turbine mid-frames in the -80A and -80C by moving the mounts behind the low pressure turbine and changing the support system for the rotors, the problem returned in the GE36, the Unducted Fan Engine. A structural frame was needed to support the gas generator, the propulsor, and provide a significant flowpath gooseneck to change diameters between them. Since the propulsor frame of the GE36 is the main support for the engine, a CF6 turbine midframe-type construction of the frame could not be fit inside the flowpath transition or liner. The frame is a one-piece HIP casting and the liner must be assembled around the frame structure. The method is still being developed with the possibilities of welding the liner segments together at the leading and trailing edges of the fairings, or of making the liner in sections which can be bolted together around the frame struts.

The last frame in any engine is the turbine rear frame and there are almost as many versions as there are

engine models. Let us take a quick look at the variations as a means of exploring the features that have been introduced and the ways in which their manufacture has evolved. Figure 2.16 shows the turbine frame on the rear of the LPT module. You can see that it provides mount fittings for installation on the pylon and a connection to the sump holding the #6 bearing to support the low pressure turbine shaft. This frame consists of a cast hub ring, a cast outer shell, and cast struts welded between the two rings. These details are shown in Figure 2.17, where it is apparent that tangential struts are used to accommodate the thermal transient problems. However, the outer structural flowpath is really polygonal from strut end to strut end so that any tendency to load the outer shell is taken in tension or compression of the sides of the polygon rather in bending a round shell. There is a transition from the polygonal sections to round bolted flanges, since it is difficult to make and seal polygonal bolted flanges. As casting technology has improved, this frame has been transitioned to a one-piece casting of hub, struts, mounts, and outer shell. This is the current method of manufacture. The next step in our development is shown in Figure 2.18, the -80C2 turbine rear frame. To avoid the performance losses associated with the tangential struts, which present restrictions in the flowpath in the acute angles, radial struts with a polygonal outer case again transitioning to round bolted flanges are used. In this figure, you can clearly see that the main rear mounts are over the ends of the struts. On the sides of the struts a small scoop is apparent. The function of this scoop is shown in Figure 2.19. Mainstream hot gas is scooped in, carried down the strut, and circulated through the hub to rapidly heat the hub (to cool it on decels), and thereby reduce the thermal mismatch between hub, struts and outer shell. Figure 2.20 shows the final feature of this development in which a thermal heat shield is added to the front of the hub. The cooling air from the low pressure turbine rotor is prevented from washing over the front surface of the hub and reducing the heating effect of the circulation inside of the hub.

Figure 2.21 shows another concept in turbine frames. This is again a case of a bolted core frame assembly with a sheet metal baffle on the leading edge of the strut and sheet metal aerodynamic fairing on the trailing edge. In the bypass stream outside of the core and between the frame and the mount ring on the outside of the fan duct the connections are adjustable links with rod-end bearings. Figure 2.22 is an axial view of this construction.

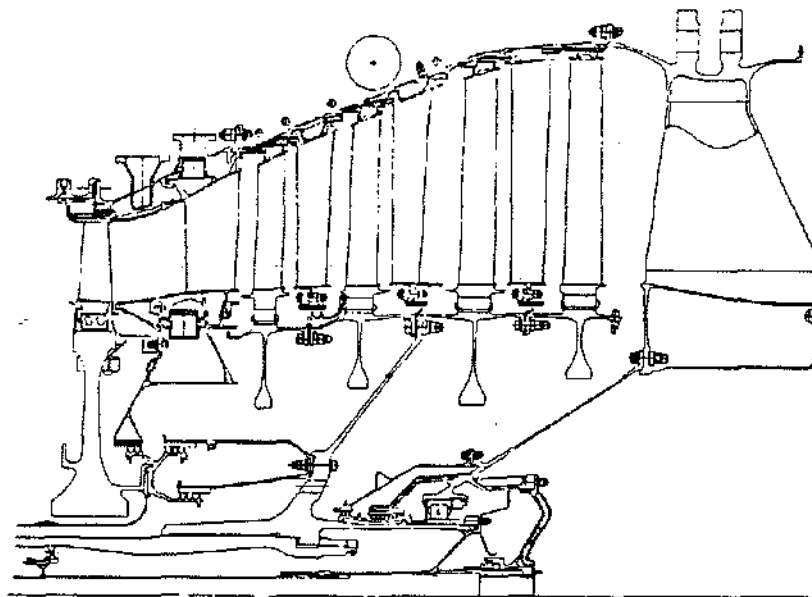


Figure 2.16 CF6-80A LPT Module

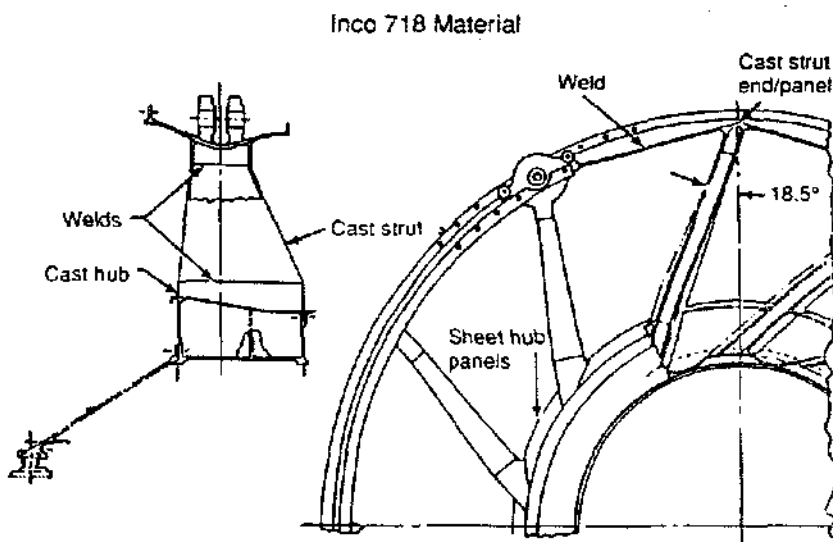


Figure 2.17 CF6-80A TRF Construction Production Design

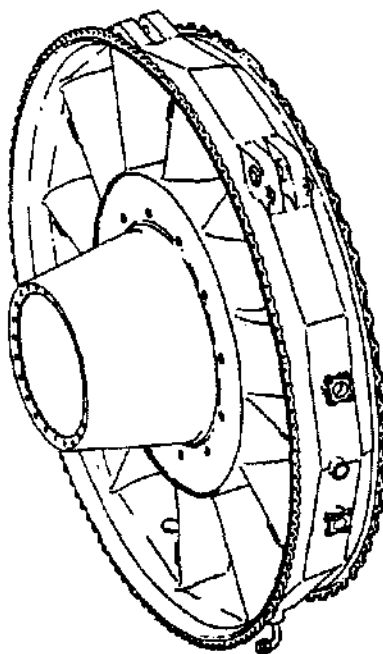


Figure 2.18 CF6-80C2 Turbine Rear Frame

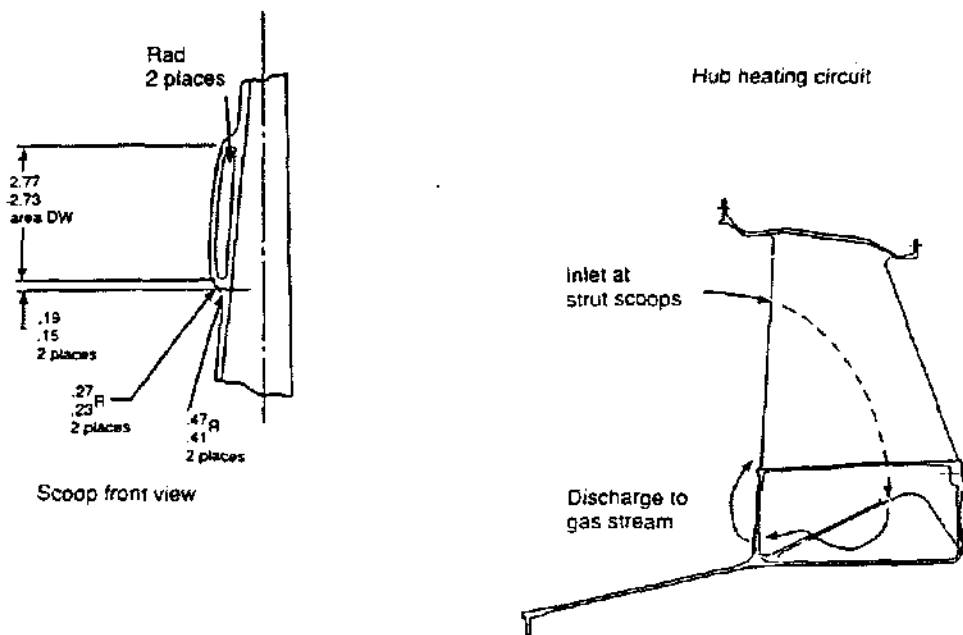


Figure 2.19 CF6-80C2 Turbine Rear Frame Strut Scoops

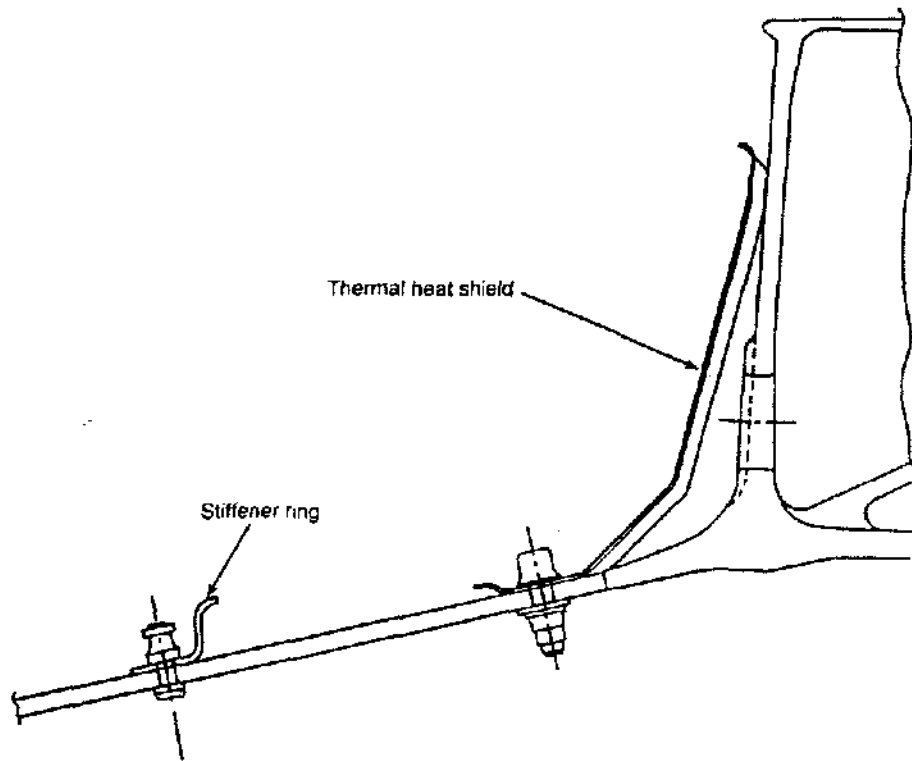


Figure 2.20 CF6-80C Thermal Heat Shield

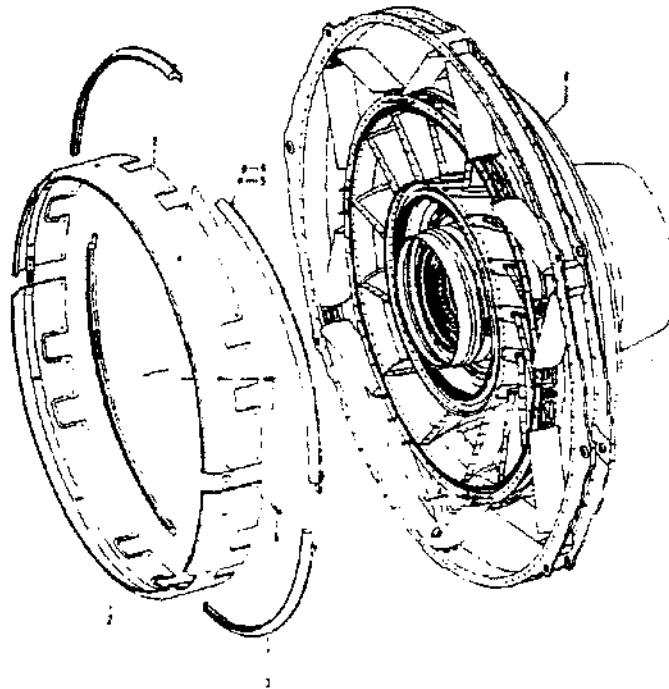


Figure 2.21 Turbine Frame Assembly

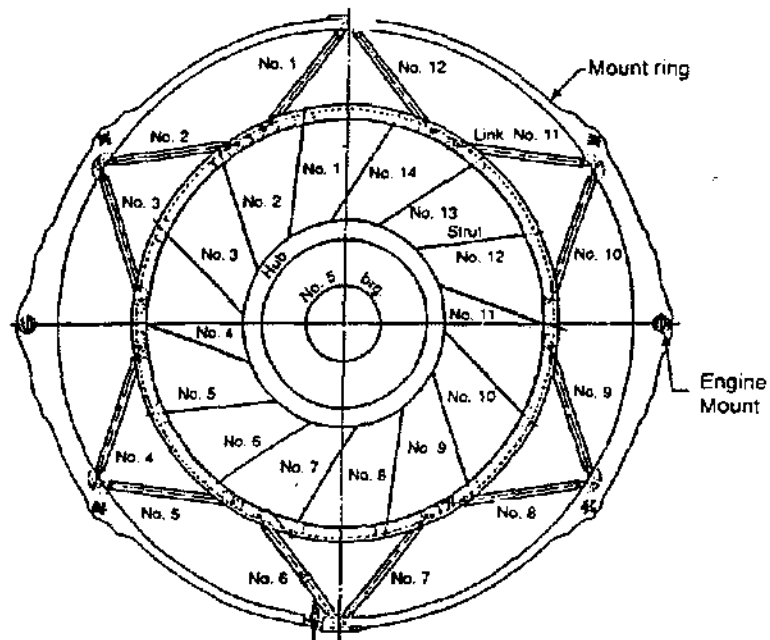


Figure 2.22 Turbine Frame Assembly-Fwd Looking Aft

CASINGS

The casings are the outer shells between the frames which form part of the structural backbone of the engine. Naturally, they take their first name from the component they surround: fan, compressor, combustor, high pressure turbine, low pressure turbine. The outer ducts may have similar designations, such as fan duct or bypass duct or augmentor duct. In addition to carrying the mechanical loads between the frames, inlets, and exhaust nozzles, the casings may very well be pressure shells containing low-pressure/low-temperature air or high-pressure/high-temperature air or gas. The casings are connected with bolted flanges which carry the major loads through the engine.

Figure 2.23 presents a good summary of the F110 casing locations and some of their features, since it shows both a cross-section and an outside view. The principal structural load path is clearly depicted from the front frame outer casing through the fan casing, the fan frame outer shell, and the fan bypass duct between the fan frame and the turbine frame. Supporting the cantilevered back end of the engine is a duct over the augmentor mixer and the augmentor duct extending back to the variable nozzle. It is quite apparent that these outer shells

are the primary means of support for the engine. The inner casings over the compressor, combustor, and turbines support the core turbomachinery and are critical to maintaining alignment and performance. One of the major considerations in the design of casings is its buckling strength or the capability of withstanding large compressive loads generally combined with bending. The lower half of Figure 2.23 shows how buckling capability has been treated in the fan bypass duct and extension duct with a waffle pattern of ribs and rings to reduce the size of the panels, that might buckle, and increase the stability of the duct. Figure 2.24 is a photograph of the fan duct showing the results of the chem-milling of this titanium shell in order to achieve adequate buckling capability at low weight.

It is not the intent of this section to deal in detail with the design of compressor and turbine outer casings. However, Figure 2.25 is worth examination as an indication of the problems faced in the design of pressure shells that are also in the main structural loadpath. This is the combustor casing in the military engine version of the CFM56 family. Note that the outer pressure shell separates from the compressor flowpath at stage 5, and the structural path continues up as a cone out and around the combustor liner. There are bolted joints that mu

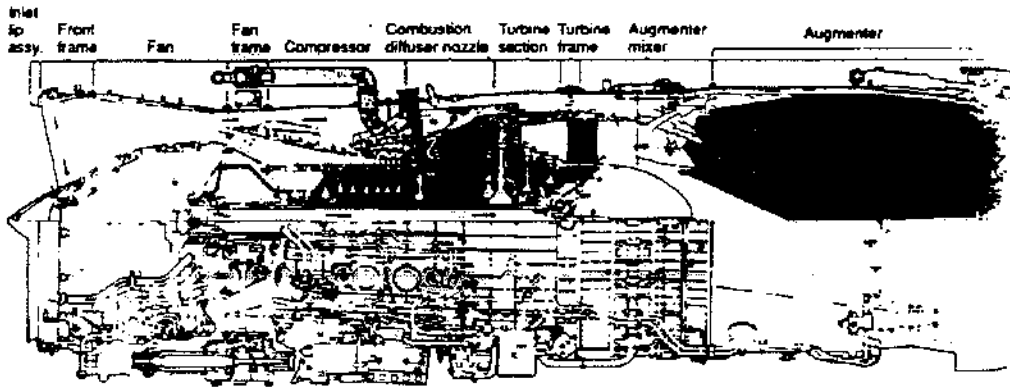


Figure 2.23 F110 Casing Features

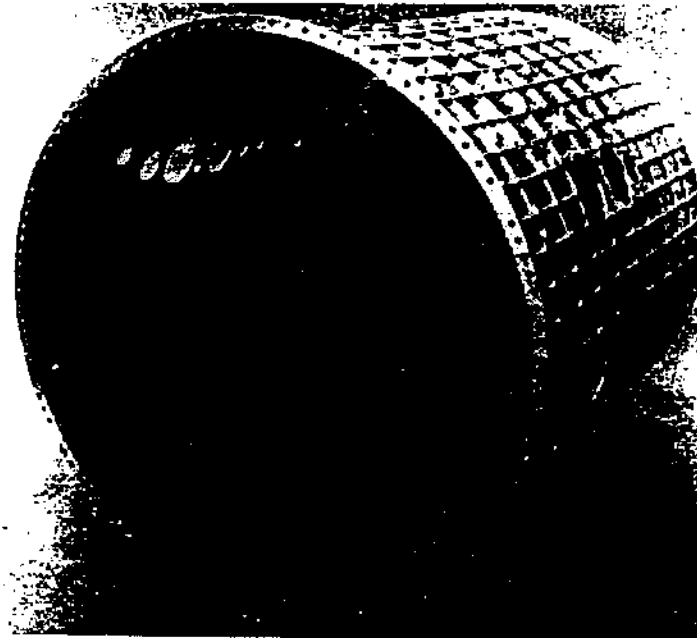


Figure 2.24 Fan Duct

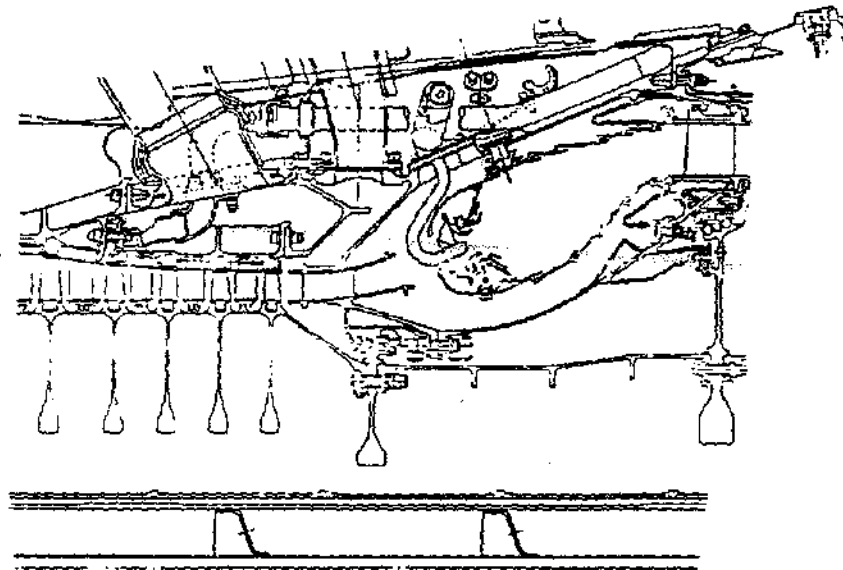


Figure 2.25 F101 Combustor Casing

withstand the bending forces on the engine under extreme unbalance as well as tie the pressure shell elements together to resist ΔP . In addition, the pressure shell elements themselves, which are cast structures, are penetrated by fuel nozzles, ignitors, borescope ports, and bleed ports for turbine cooling and customer air. Incidentally, we have learned the hard way that it is best not to put fuel nozzle ports, ignitor ports, and borescope ports in a straight line parallel to the axis of the engine; if a crack develops between them its effective length includes those ports. While cast properties are generally not as good as those for wrought materials, greater opportunity exists for optimum contouring and reinforcement of penetrations through the pressure shell to maintain stresses within the capability of the material. When pressure shells are made of wrought materials, they almost always have welds in them as part of the fabrication, and the cast properties of the weld plus the stress concentration effects of the weld geometry may very well offset any benefits of the wrought material.

Figure 2.26 shows the combustor frame of the TF34-100, an engine which is installed on either side of the A10 fuselage. Looking up at 6 o'clock, the clevises at 3 and 9 carry the thrust link from this frame up to the mount ring and the mounting struts to the aircraft. The two large cylinders with tube fittings on the side are oil

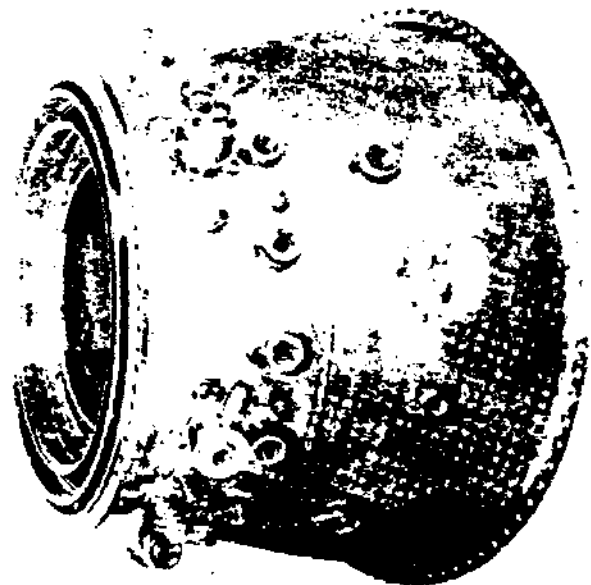


Figure 2.26 TF34-100 Combustor Frame

line connections for supply and scavenge. The pressure shell consists of only three pieces that are welded together: a wrought front flange welded to the outer casing and strut section with the fuel nozzle bosses shown behind the oil fittings, a mid-section, the entire one-piece aft half of the frame.

As a final comment on casings, consider Figure 2.27, which shows how the addition of a casing or duct permitted an engine to change from one configuration for F-15's and F-16's to an entirely different configuration to be used in the Navy's F-14. The engines themselves are essentially the same except for length and the accessory gearbox. The turbomachinery is the same and the augmentor and variable nozzle are the same, but between the duct over the mixer and the beginning of the variable exhaust nozzle, a 50" length of augmentor duct was added. This moved the front flange of the engine forward and the exhaust nozzle exit aft in order to fill a much longer hole in the F-14 where a competitive engine had originally been placed. These ducts must really be capable of resisting bending and buckling loads. Since the thrust mount for the Navy engine is forward over the fan and the rear mount has been moved all the way back to the new mount ring at the variable exhaust nozzle, the span between mounts has increased significantly. When the aircraft lands on a carrier, the arresting gear creates tremendous forward accelerations and the aircraft slamming onto the deck creates terrific downward accelerations. The ducts must be capable of carrying a great deal more bending moment than is the case in the Air Force engine. The differences in the mounts for these engines are discussed in the next section.

MOUNTS

There are probably as many different mount designs as there are engine models. Since we concluded the section on casings with remarks about the F110 family, we should look at the F110 mounts first. What must an engine mount system do? A mount should hold the engine in the aircraft in such a way as to minimize the distortion of the engine. That is to say it must minimize the overall bending of the engine structure and minimize local deflections at the points of attachment. The mount system also must be capable of carrying all of the inertial or maneuver loads to which the engine is subjected as well as normal and reverse thrusts. Generally, the first design criteria are the limiting ones in the life of the aircraft. These include limit loads with yielding, ultimate loads with no separation under crash, or major unbalance as would occur with blade loss. A second design criteria is cyclic loading without fatigue failures that would cause the engine to separate from the aircraft.

Figure 2.28 shows the F110 fan module with the three possible front mount stations designated. Table 2.1 and Figure 2.29 summarize the location and the forces that are reacted at the front and rear mounts for the various engine models and installations. F110-100 engines for either the F-15 or F-16 are identical, since they are shipped from the factory with a forward vertical load mount clevis on both the front frame and the fan frame. The same engine could be hung in either an F-16 or an F-15 depending on the mount used in the aircraft. The thrust mount locations for the aircraft are identical at station 200 on the rear mount ring that matches the turbine frame. As discussed in the section on casings, an extension duct was added to the F110-100 to make it into an F110-400. That extension duct carries with it an aft mount ring just ahead of the flange attaching the variable exhaust nozzle. But matching the engine to the bay in the F-14 aircraft results in the forward mount being on the side of the fan case directly over the leading edge of the stage 3 rotor blades. Major redesign was required on the case to avoid local distortions as a result of the mount, which carries thrust, side load, and vertical load. The thrust pin on the Inconel 718 mount yoke fits into a spherical bearing buried in the pocket (Figure 2.30). The spider web ribs spread that load more or less uniformly toward the aft flange. The upper and lower links, which are also Inconel 718, carry vertical and side loads into the casing at reinforced pads in such a way as to shear it tangentially into the casing shell. Figure 2.31 is a photograph of -400 engine, clearly showing the front mount on the fan case for a left-hand engine. (Yes, a left-hand installation, aft looking forward. Believe it or not, the engine mounting fittings are on the outside of the bay of the aircraft; not toward the center.)

If mounts for military engines are less than optimum because of the need to meet interfaces in existing aircraft, are the mounts for commercial engines any better? Well, they are getting better than they were fifteen years ago, starting with the TF39 and evolving to the CF6-6. It has already been mentioned that the -6 and early -50 engines used a front thrust mount that carried about 95% of the thrust into the 12 o'clock fan frame strut which distorted the top of the forward section of the compressor case. Additionally, in our consideration of turbine mid-frames, we looked at the heavy mount section required because the three mount clevises had to be between struts to permit the insertion of the expand bolts. Models of the -50 and all of the -80A engines use a load spreading front mount which carries the thrust load into the fan frame at approximately $\pm 27^\circ$ from top center and carries the vertical load into the compressor case at about 45° . This five link front mount system is shown in Figure 2.32. While this mount is not perfect, it does introduce an improvement in reduced local distortion

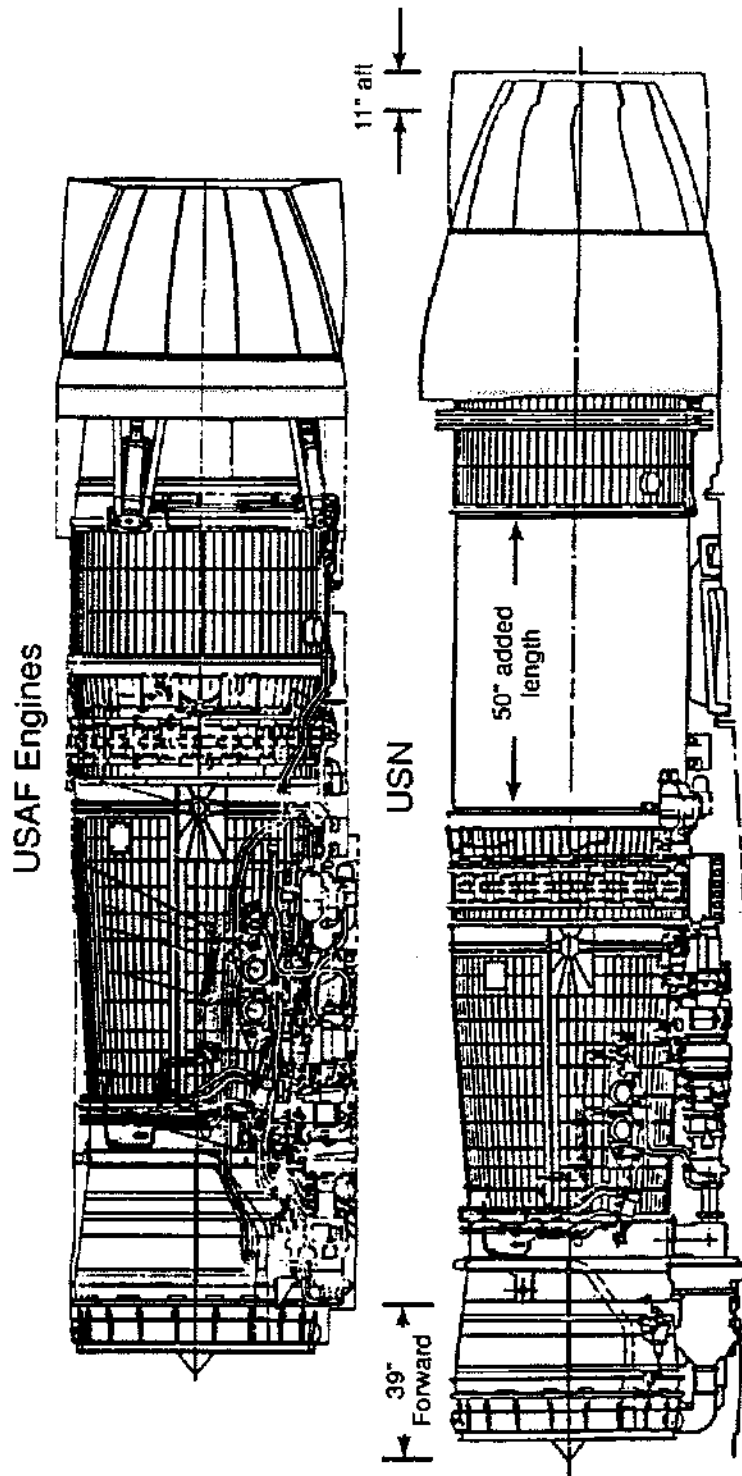


Figure 2.27 F110 Configuration for USAF/USN

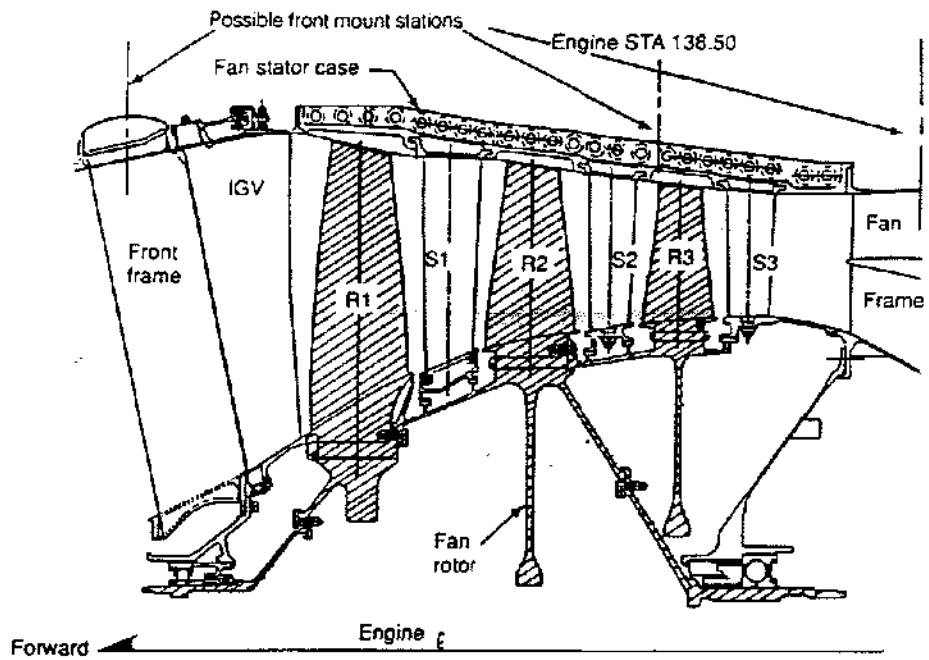


Figure 2.28 F110 Fan Schematic

ENGINE MODEL & AIRCRAFT	FORWARD MOUNT STATION FORCES	REAR MOUNT STATION FORCES
-100/F15	150.43 VERTICAL (FAN FRAME)	200.00 THRUST VERTICAL SIDE
100/F16	117.87 VERTICAL (FRONT FRAME)	200.00 THRUST VERTICAL SIDE
-400/F14	138.50 THRUST VERTICAL SIDE (FAN STG 3)	289.50 VERTICAL SIDE

Table 2.1 F110 Engine Model Mount Functions

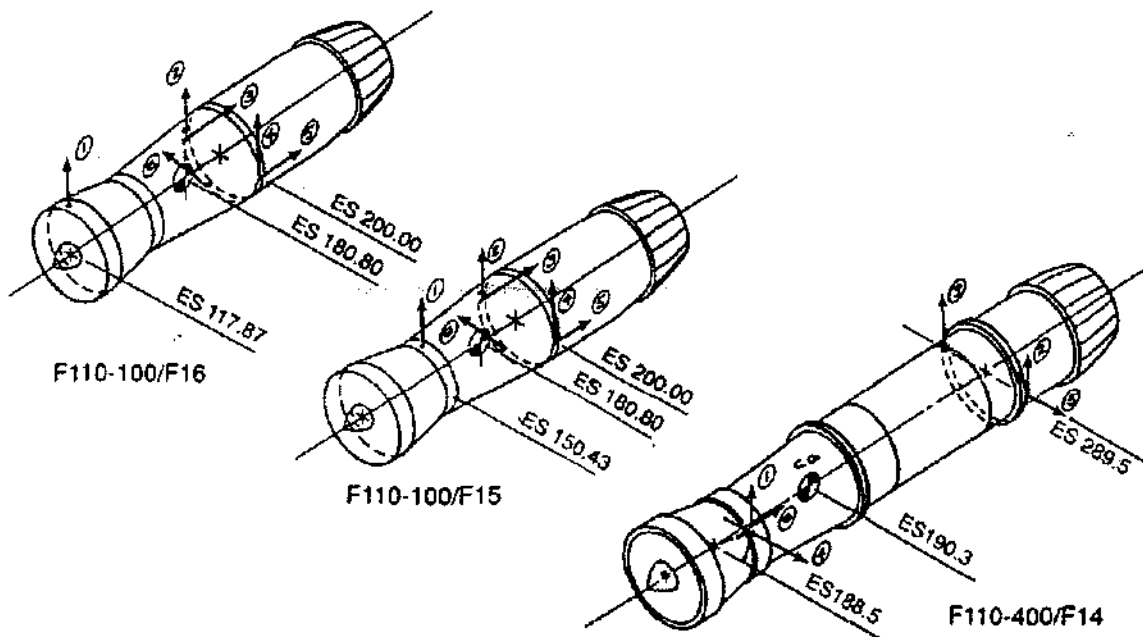


Figure 2.29 F110 Mount Locations and Reactions

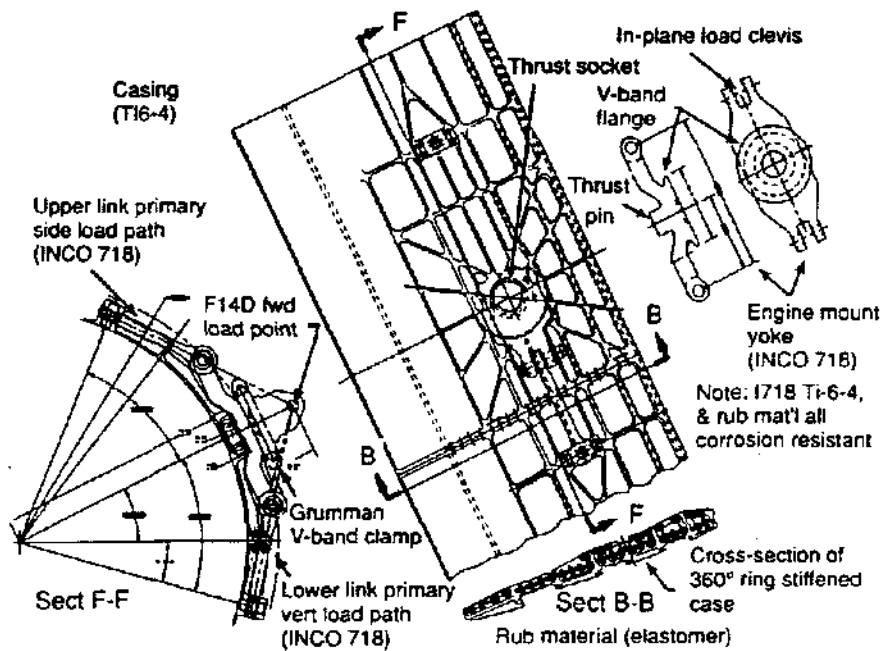


Figure 2.30 F110-400 Forward Mount System

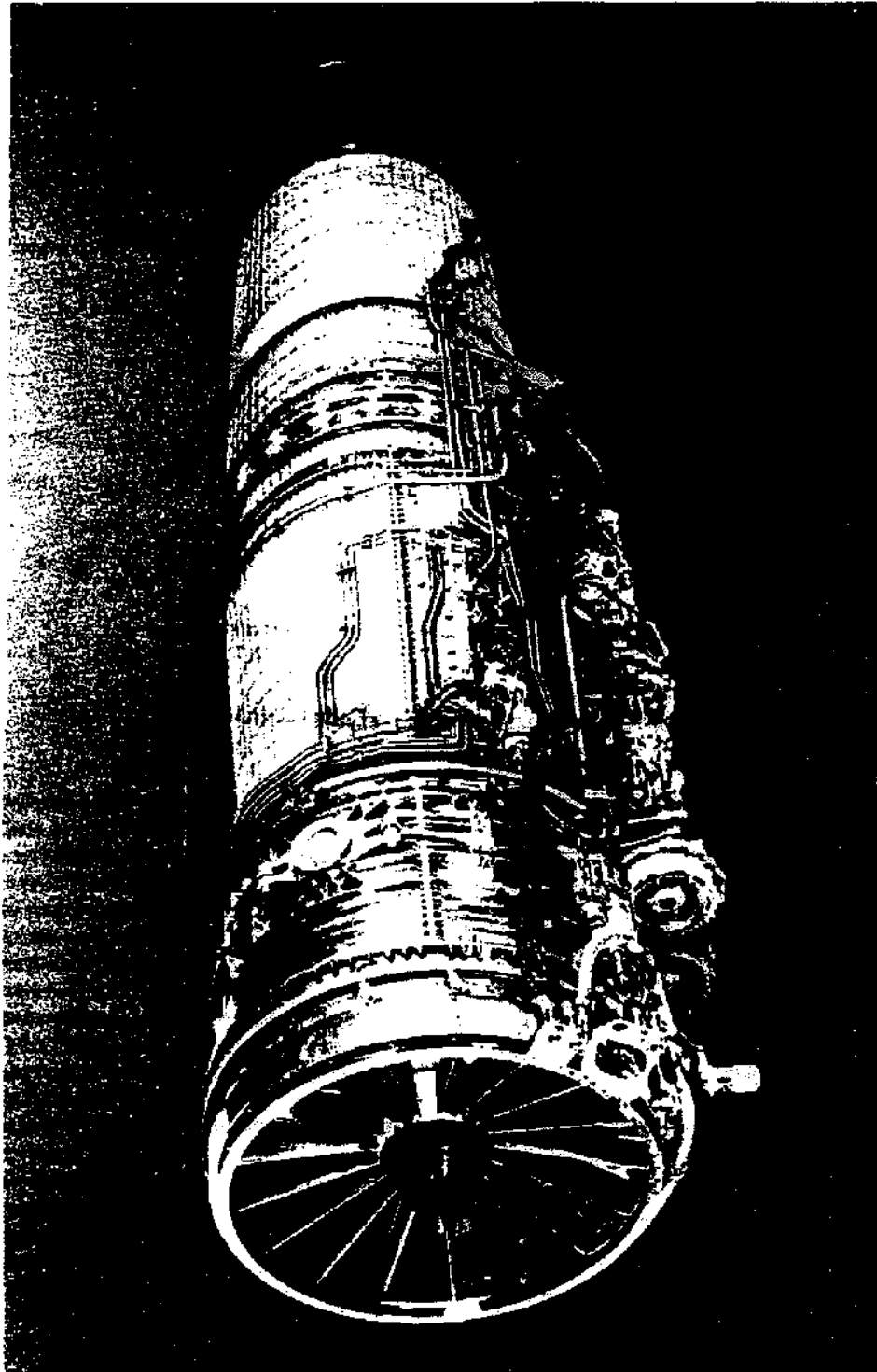


Figure 2.31 F110-400 Engine

CF6-80A/AI Fwd Engine Mount

Platform	Forged Ti 6-4
Links	Marage 300
Bolts	INCO 718 - tensitized
Sphr brgs	440C ball - CRM PLT
Bushings	7-4 PH race - dry film INCO 718

-50 same except platform shorter
& (2) bolts to pylon

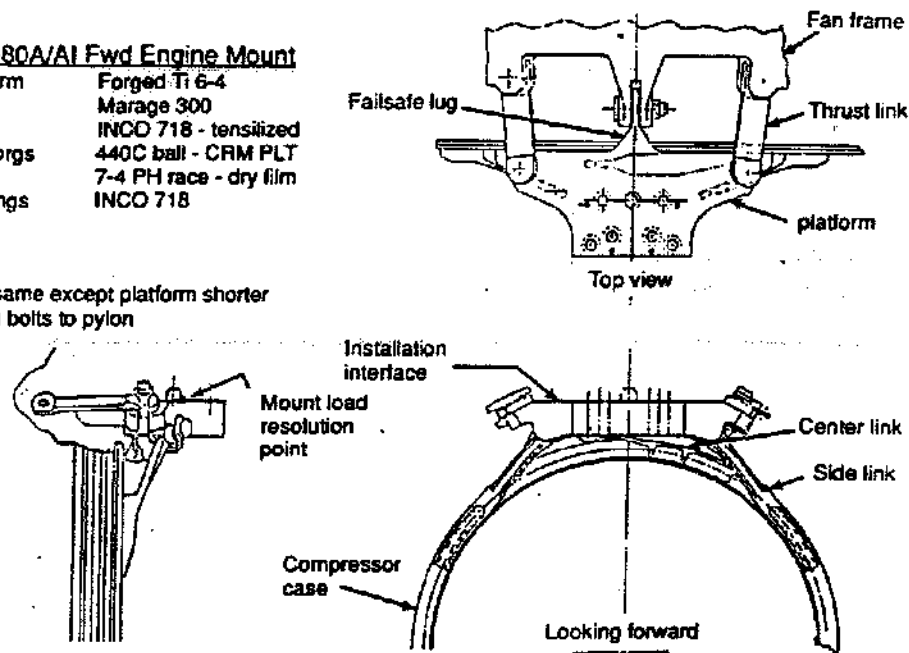


Figure 2.32 CF6-80A/AI Fwd Engine Mount

that permitted us to tighten the clearances in the forward compressor stages.

The aft mount that goes on the -80A turbine frame is shown in Figures 2.33 and 2.34. The mount clevises on the frame have moved to the ends of the struts, so that the loadpath from the rotor support consists of forces along the polygonal elements of the outer case and tension or compression loads along the strut centerlines. Bending in the frame elements due to thermal and mount loads has been significantly reduced or eliminated. The rear mount connection to the pylon consists of a two part assembly. The lower part is tied by means of the pin in a spherical bearing to the right frame clevis, so that both vertical and horizontal loads can be taken in any combination. On the left side there is a pivoting link between the clevis and the lower mount fitting, so that it can accommodate differential thermal expansion of the frame and the mount. The upper mount fitting has a bearing in both the right and left sides so that the lower mount fitting can pivot relative to the upper, accommodating differential thermal expansion of the engine relative to the pylon.

Finally, let us look at the front thrust mount for the -80C2 engine. Since this was a new engine, restrictions on the interface loads to the pylon were negotiable (as opposed to the -50 and -80A where the aircraft attachment already existed and was not capable of taking any moment). Figure 2.35 shows how the front mount is installed on the engine behind the fan frame and over the compressor case. Figure 2.36 shows this mount in greater detail. Vertical load is transmitted by four bolts between the platform and the pylon foot and then to the mount yoke. In the mount yoke the vertical loads are carried down links on both sides to clevises on the fan frame. Side load is similarly carried from the platform to the yoke and out through the fixed link on the left side of the engine. Thrust load is carried from the platform through the platform links to clevises on the mount yoke and then forward by means of thrust links to clevises that are part of the fan frame at $\pm 45^\circ$ from top center. The angle of the thrust links and the moment from the pylon makes this mount better than the -50 and -80A mounts in spreading the thrust load and reducing backbone bending.

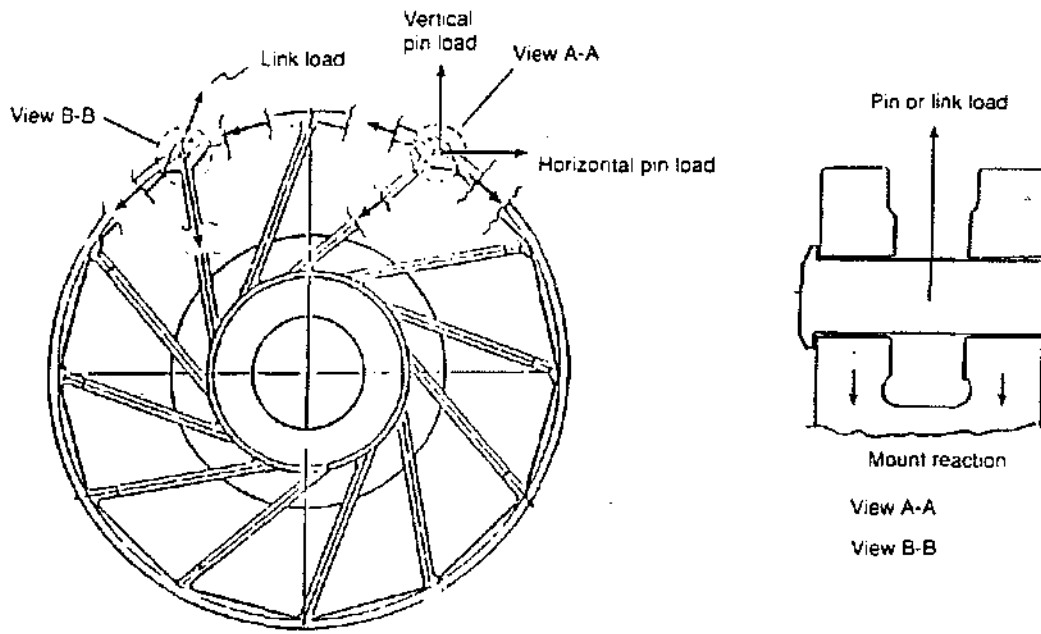


Figure 2.33 TRF Multiple Load Paths

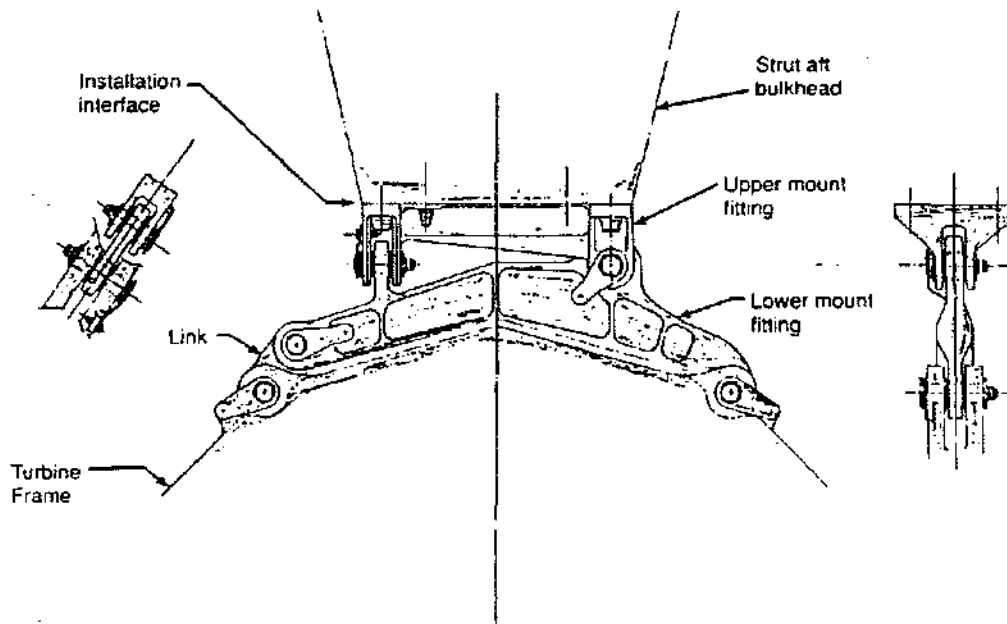


Figure 2.34 CF6-80A Rear Mount

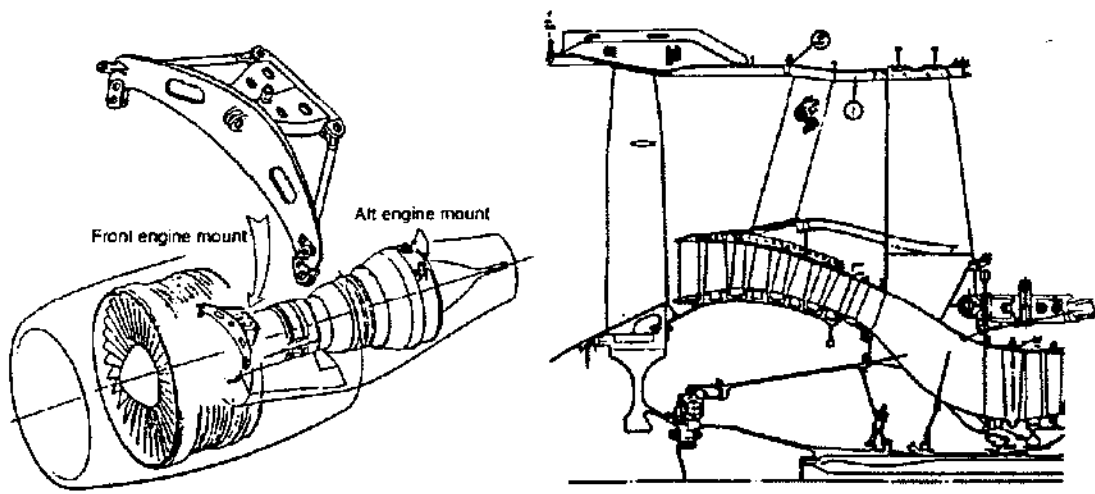


Figure 2.35 CF6-80C Engine Mounts

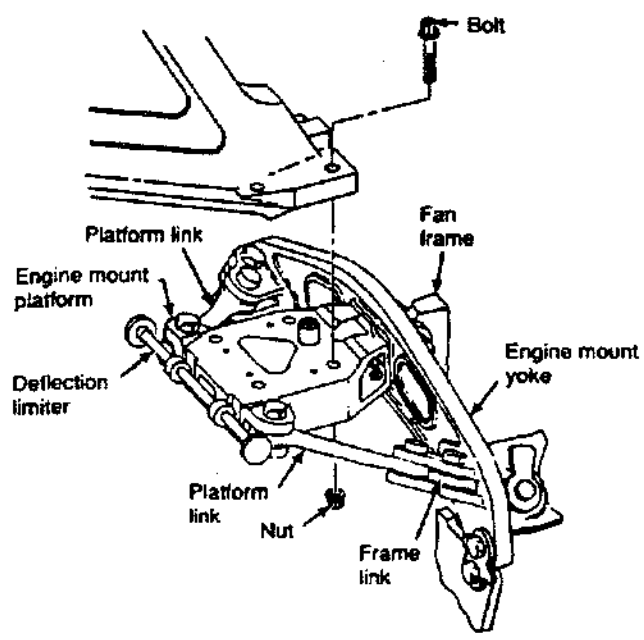


Figure 2.36 CF6-80C2 Front Mount

CONTAINMENT

In an earlier section of this chapter, we discussed briefly the difference between the steel containment ring over the fan blades of the CF6-6 and -50 and the Kevlar currently used in the new -80A and -80C engines. **Figure 2.37** shows the CF6-50 fan assembly, with its steel containment ring and stiffener. This steel ring was originally sized based on ballistic impact tests conducted at Watertown Arsenal with projectiles that struck a flat plate at various angles. The data from these tests is presented in **Figure 2.38** and **2.39** in which the kinetic energy of the projectile is related to the square of the thickness of the

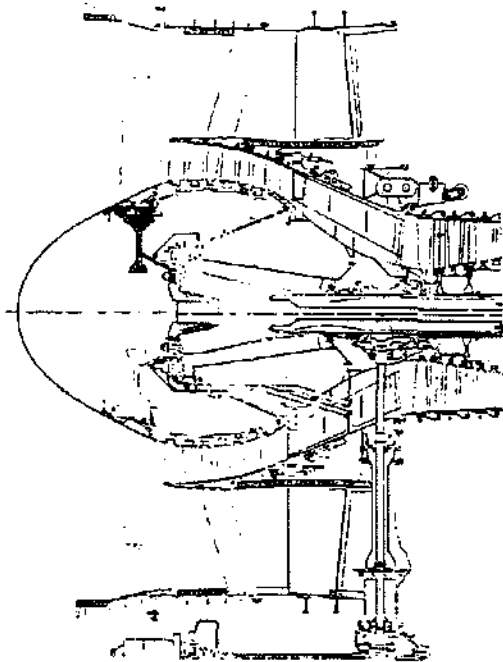


Figure 2.37 CF6-50 Fan Module

containment plate by the constant K , which is a function of the materials involved. When different containment material is used, this data can be scaled in an approximate way, recognizing that the energy to rupture is proportional to the area under the stress-strain curve to ultimate failure. A very hard, strong material may have a high ultimate strength but relatively little deformation to failure. A softer, more ductile material may have a lower ultimate strength but very high elongation in which case the total energy required to rupture a unit

volume is much greater. It was this sort of reasoning that led to the design of the -50 containment ring. The ring uses a high strength and highly ductile 18-3 MN stainless steel for the forward section of the ring which is welded to 304 stainless steel in the aft sections. The capability of this ring to contain fragments of fan blades was demonstrated in spin pit tests. It also was observed that the shank and platform of the released blade was pushed aft by the following blade. So, a short extension was added to protect the bolted joint and the aluminum fan case from such shank fragments.

In an attempt at major weight savings the -80A engine whirligig tests were undertaken to determine the amount of Kevlar cloth required to contain a blade. While the first tests were successful in preventing penetration of the cloth by blade fragments, the tests were not successful as a complete containment system. Since the cloth deflected a great deal more than was expected, blade fragments escaped axially, going aft. It was determined that Kevlar fibers could be woven in a shaped strip, so that when wound in a circular containment ring, they would form a pocket which would retain the fragments by catching them very much like a ball player's mitt. Since we needed to build a deep honeycomb sandwich on the outer ring to prevent resonance of ring modes and frequencies with the blade and disk, we had the Kevlar cloth woven to fit over the deep honeycomb. This proved to be totally successful in catching the first particle of blade penetrating the honeycomb sandwich and striking the Kevlar cloth. However, the Kevlar is very elastic, and when the first particle was trapped, it stretched the cloth radially and the ends pulled in axially and uncovered significant areas of the containment system. Subsequent particles were able to escape where the Kevlar cloth had moved axially. We solved this problem by bonding the layers of Kevlar together for about one inch on each edge with epoxy adhesive, forming a rim very much like the bead of an automobile tire. When the first fragment entered the Kevlar with this construction, the Kevlar still stretched in a radial direction, but the rigid ring at each edge formed by the epoxy bonded layers of cloth did not climb up and over the honeycomb sandwich. The necessary layers of cloth remained in place to catch subsequent particles that would have otherwise escaped radially.

It was also necessary to determine the angle required for containment forward and aft of the plane of rotation. **Figure 2.40** presents this problem in a comparison of the -50, the -80A, and ultimately the -80C containment casings. The -80A is the same size as the -50, and the weight saving was achieved by reducing the steel shell of the container to very thin gauge in the prime containment section and replacing the containment capability

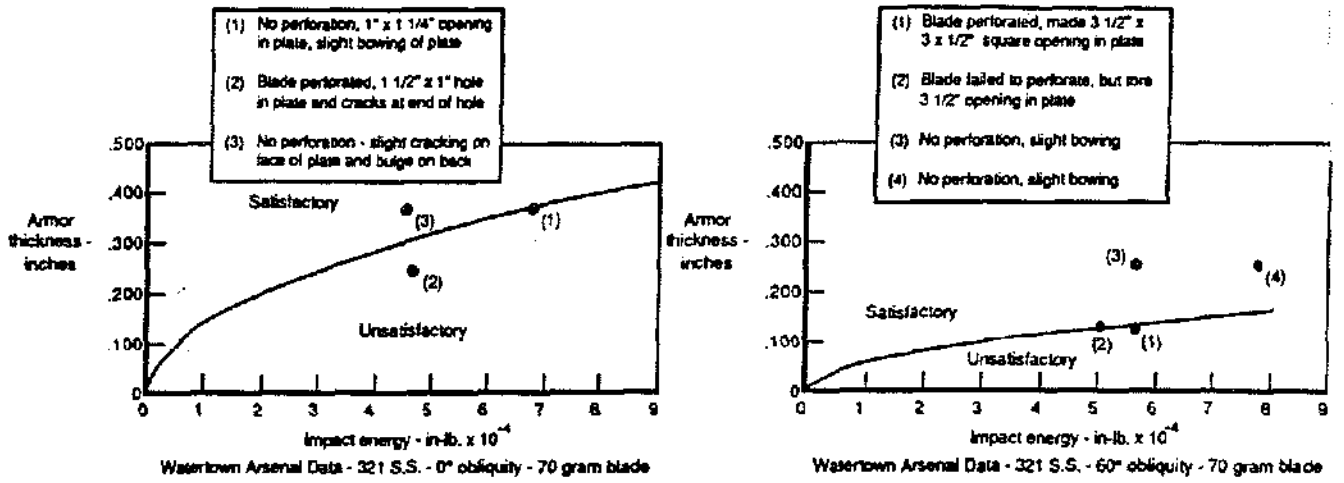


Figure 2.38 Ballistics Test Data

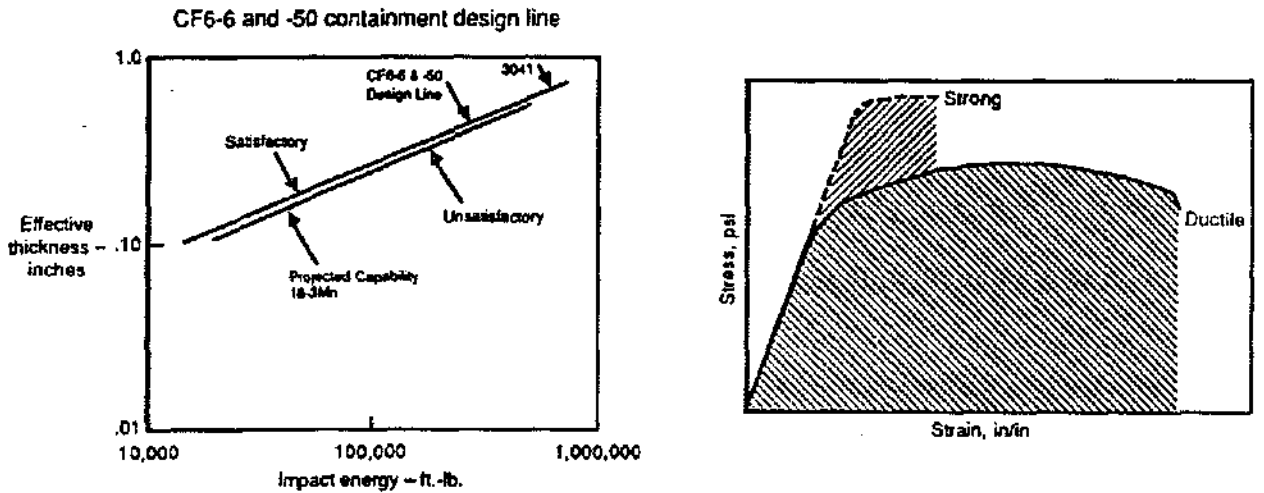


Figure 2.39 Scaled Rupture Data

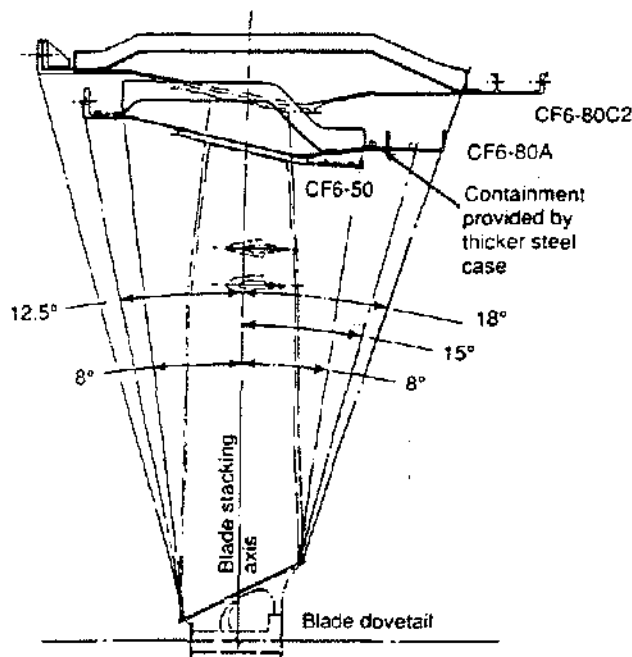


Figure 2.40 Kevlar Wrap

with the Kevlar belts over the honeycomb sandwich. To preserve the same containment capability forward and aft, the steel shell was thickened so that it was identical to the -50 at the forward flange in front of the Kevlar system. When we observed that the -80 system was marginal in containment in the aft direction, the steel shell also was thickened aft of the Kevlar. The Kevlar itself could not be extended any further aft because a mounting ring was needed to carry the fan mounted gearbox, which is a part of the -80A1 engines for the A310. This then established the criteria for the design of the -80C2. With no fan mounted gearbox the Kevlar was extended aft to provide the same 18° angle of protection as the steel shell for the -80A. In the forward direction, however, the design was considered to be inadequate because Kevlar did not extend to the same angle as had been covered by the steel in the -50 and the -80A. The inner aluminum shell and forward flange of the -80C2 is not considered to have any significant containment capability. The solution to this problem is shown in Figure 2.41. The forward flange of the -80C2 was moved forward by two inches and additional layers of Kevlar were carried forward with it. The lower sketch in the figure shows the final arrangement for the -80C2. The inner shell is a 2219 aluminum alloy, to which is bonded a 1/8 inch cell aluminum honeycomb covered with layers of graphite

epoxy to form the stiff sandwich. Cast titanium brackets are riveted and bonded to the inlet flange to reinforce it at the bolted connections to the inlet. Sixty-five layers of Kevlar cloth are used in the containment wraps. The final design on the -80C2 containment system is summarized in Figure 2.42.

STRUCTURAL BEHAVIOR AND ANALYTICAL METHODS

Thrust is the most obvious of the loads on engine structure. It is the reason the engine is on the aircraft in the first place. Thrust is developed not only from the exhaust gases exiting the nozzles, but also from the pressure distribution due to the airflow on the nacelles. It may be that in certain sections of the casings the loads will be tensile rather than compressive. The engine may be trying to pull instead of push, as it carries the net thrust out to the connection to the aircraft. In Figure 2.29 we showed examples of how thrust is carried to the aircraft for military engines. Now consider Figure 2.43 which shows the reactions between engine and pylon for the -80A engine. The forward thrust mount assembly carries axial thrust, vertical, and side loads. The swinging link and fixed link connections at the rear mount

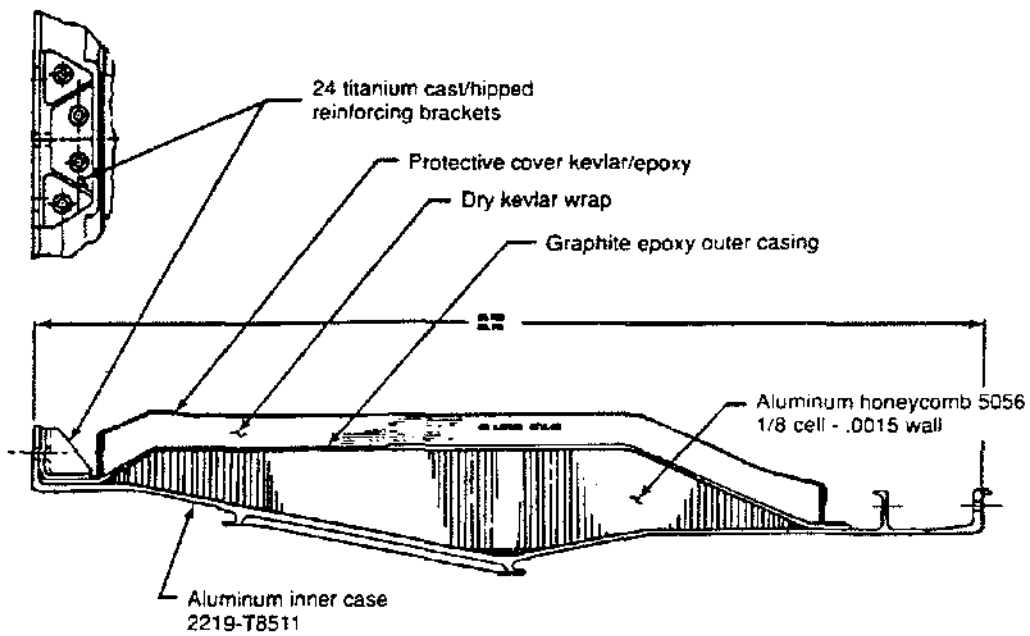
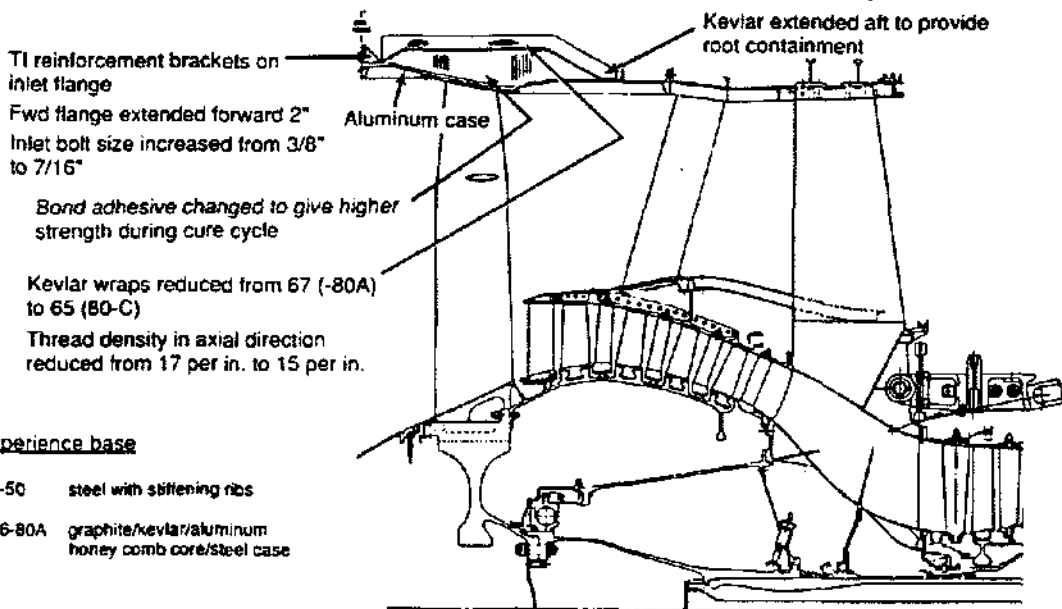


Figure 2.41 CF6-80C2 Fwd Fan Case Construction

CF6-80C2 Differences from -80A



Experience base

- CF-50 steel with stiffening ribs
- CF6-80A graphite/kevlar/aluminum honey comb core/steel case

Figure 2.42 CF6-80C2 Containment Case

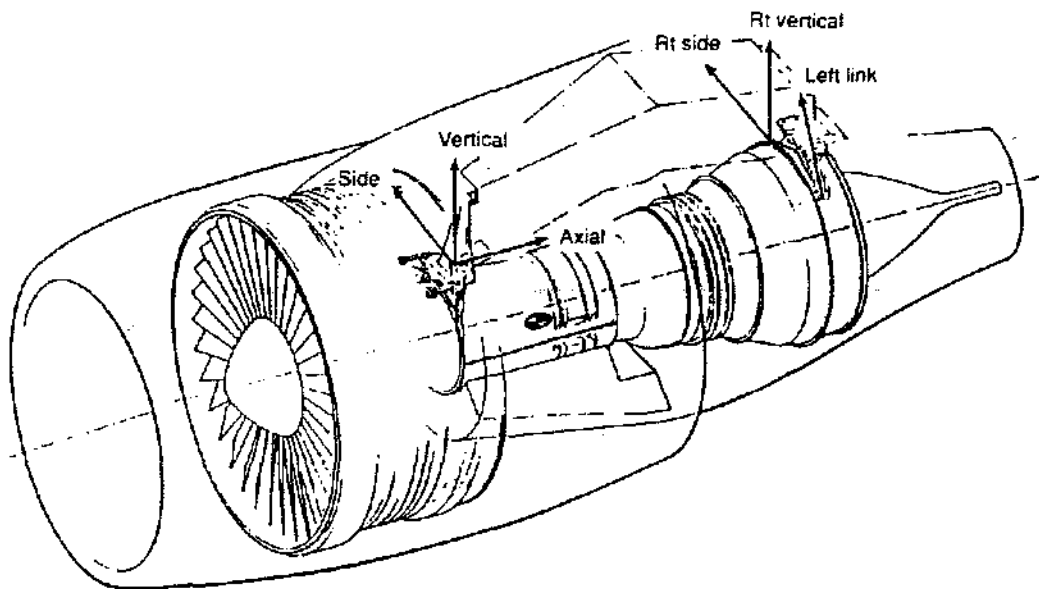


Figure 2.43 Interface Load Vectors

carry side and vertical load and reaction torque. Just as the thrust reaction for the F110-400 is displaced from the center line of the engine and results in significant bending due to axial forces, so in the CF6-80 and -50 the axial forces are reacted 20 inches from the centerline. For normal thrust alone there is a bending moment of one million inch-pounds applied to the engine at the front end of the compressor. In addition to thrust forces other forces act on the engine.

Maneuver Loads are the forces and moments generated by the inertia of the mass of the engine, both rotors and stators. Figure 2.44 taken from the basic specifications for military engines, shows the basic requirement for the F101, F110, F404, and TF34 families of engines. For a moment, imagine what the forces on the entire structure, and in particular the mounting, must be for the F110-400 Navy engine. These engines can be subjected to 9 Gs aft during catapult and as much as 10 Gs forward during arrested carrier landing. As the hook engages and the aircraft slams to the deck, there can be a 10 G down load tending to bend the engine between its mounts. For the internal frame structures the gyroscopic and inertia loads on the rotors are transmitted to the bearings and, hence, to the hubs of the frame and then out to the outer shells and mounts. These forces and the acceleration forces not only load the ball and roller bearings and the static structures, but also tend to bend and distort the rotors themselves.

Pressure loads are due to high differential pressures occurring in the rear stages of the compressor case through the combustor case and through the high pressure turbine structures. Lower ΔP s occur in the forward part of the compressor, in the low pressure turbines, and even in the fan cases and ducts. While the pressures in nacelles may be modest, diameters can be very large and the hoop stresses can be quite high. In the case of inlet structures or nacelles the normal ΔP may be only fractions of a psi. But, under burst duct or ruptured casing conditions the inlet and nacelle structures must be able to take several psi before vents open to relieve the pressure.

Thermal loading results from different temperatures in parts of a component made from the same material, different temperatures between connected parts as in the thermal expansion of an engine relative to the pylon or strut to which it is mounted, different coefficients of expansion between connected parts of different materials all at the same temperature, different coefficients of expansion along with different temperatures between elements made of different materials. Thermal loads and their resulting stresses are really the forces required to deflect all of the components so they will have the same dimensions between matching points. As we have looked at the various structural elements and how they have evolved, we have seen several ways in which thermal mismatch has been accommodated to minimize the

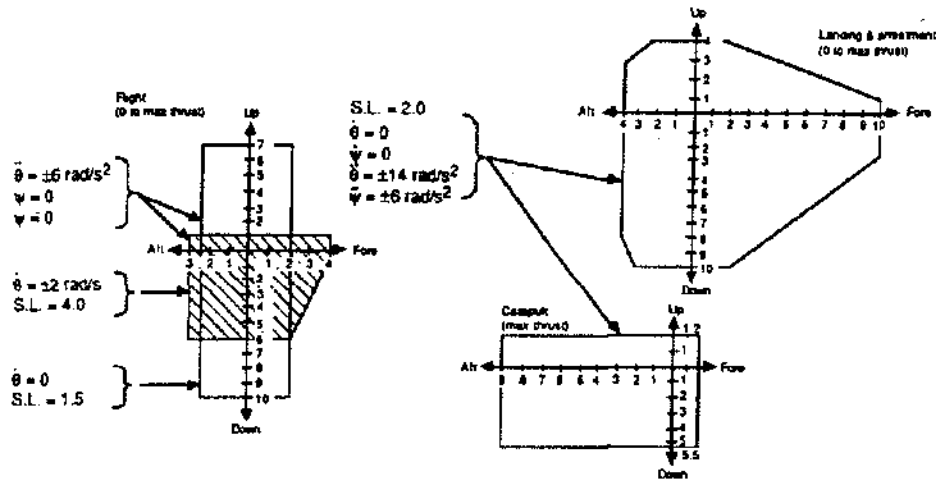


Figure 7-2

Figure 2.44 Externally Applied Forces

thermal forces. Another possibility is to select materials with low coefficients of expansion. However, the very low thermal expansion alloys often have very poor mechanical properties and are not suitable for prime structural elements. In some cases thermal mismatch can be accommodated for through the use of pivoting links with spherical bearings at the ends. Two examples of this treatment are the main mounting links between engine and aircraft and the outer links of the turbine frames on the F101 and F110 families. Here the hotter core engine is permitted to move freely relative to the colder outer duct.

Unbalanced forces in new engines occur as the result of variations in the weight of airfoils, eccentricities, and the lack of squareness in the manufacture of rotor components. The normal tolerance stack-up may result in a rotor with a slightly bent center line. The resulting unbalance is reduced to acceptable limits before the engine is shipped. But, in the course of service, airfoils may be damaged by foreign objects (hopefully, we never have any domestic object damage), erosion, deterioration of the tip caps of cooled airfoils, or fatigue or stress rupture deterioration which releases a part of the airfoil. Table 2.2 summarizes the requirements for unbalance that were developed for the CF6-50 models as a result of field problems of major unbalance. A similar table

should be prepared and added to the technical requirements for all engines as a guide to the design engineers. For every engine there should be some level of unbalance in each rotor for which the engine can operate indefinitely with no fatigue or other damage. At a high level of damage the engine should be able to operate for 30 minutes at various power levels and then be safely shut down with no fatigue or other damage. At the highest levels of unbalance at which the engine could continue to run and generate usable thrust, 30 seconds of operation should be expected until the crew can safely shut down. At the end of that operation, there may be some minor fatigue cracks in the static structure and perhaps some repairable failures of secondary components. However, there would be no loss of components or damage that could cause a fire, destroy bearings, or in any way threaten the aircraft. Finally, the ultimate unbalance, the worst load conceivable, is the release of a full fan blade at the disk dovetail along with all of the resulting secondary damage. We would expect major damage in the form of cracks and tears and probable destruction of bearings, but no loss of parts or failure of major load paths, no separation from the aircraft, no threat to the safety of flight, or fires. Depending on the level of damage, the engine would either shut itself down or would be shut down by the crew.

LARGE HIGH-BYPASS TURBOFAN (CF6-50 MODELS)

BLADE FAILURE/UNBALANCE	DURATION OF OPERATION	SHUTDOWN MODE	ACCEPTABLE DAMAGE
A) FAN -3000 GM-IN (TIP) BSTR -3000 GM-IN (> 1 STG 2 A/F) HPC -200 GM-IN (1/2 OF TIP, STG 1) HPT -600 GM-IN (> 1/2 of STG 1) LPT -1/5 AIRFOIL, ANY STAGE	UNLIMITED	NONE	NONE
B) FAN -15,000 GM-IN (OUTER PANEL) BSTR -15,000 GM-IN (6 STG 2 A/F) HPC -700 GM-IN (1/2 OF STG 1) HPT -4500 GM-IN (2 STAGE 2 A/F) LPT -8400 GM-IN (1 STG 4 A/F)	5 MINUTES AT T/O, 10 MINUTES AT CLIMB, 15 MINUTES AT CRUISE, SAFE SHUTDOWN.	CREW ACTION	NONE
C) FAN -50,000 GM-IN (BELOW DAMPER) BSTR -50,000 GM-IN (20 STG 2 A/F) HPC -3300 GM-IN (2 STG A/F) HPT -6750 GM-IN (3 STG. 2 AIRFOILS) LPT -17,000 GM-IN (2 STG 4 A/F)	15 SECONDS AT T/O, 15 SECONDS AT 50% T/O POWER; SAFE SHUTDOWN	CREW ACTION	MINOR DISTORTION AND/OR FATIGUE CRACKS; REPAIRS REQUIRED.
D) FAN -310,000 GM-IN (-6 AND -50, 2.5 BLADES) BSTR, HPC, HPT - ANY GREATER THAN C) FOR -80A, 250,000 GM-IN (2 BLADES) FOR -80C2, 260,000 GM-IN (1.5 BLADES)	NONE REQUIRED	SAFE SHUTDOWN BY ENGINE OR CREW	NO LOSS OF PARTS OR FAILURE OF MAJOR LOAD PATHS; LARGE CRACKS OR TEARS ACCEPTABLE.

Table 2.2 Typical Rotor Unbalance Design Requirements

Assume for the moment that the analysis has been performed and we know the stresses and deflections that results from the loads discussed. What are the criteria by which we measure success? How do we know whether or not our structure is adequate for the purpose?

Limit conditions for a commercial engine is defined as one which will occur once in the life of the engine and the criteria is that there shall be no permanent deformation and in some cases no loss of performance. There may be a number of limit loads defined in the engine technical requirements or in the customer's product specifications. No permanent deformation could be interpreted as no yielding anywhere. Usually, it means that there is no measureable deformation. Yielding can occur in very small areas of high stress. The "no loss of performance" is a much more severe criterion, because it means that the rotors cannot move into the stators and rub open clearances and thereby degrade the performance of the components. In some military specifications, limit is defined as occurring once per flight. This means that the small local high stress areas, which could be allowed to yield in a once-in-a-lifetime case, must now be considered relative to the fatigue strength of the material.

Ultimate loads are defined as those which might occur once in the lifetime of all the engines in the fleet for a particular aircraft. Significant plastic deformation can occur, but no fracture or other ultimate failures are allowed that would prevent carrying the full load, such as buckling. There may be a requirement that the engine continue to generate some fraction of its thrust capability.

Fatigue capability of the structure must be evaluated for low flight cycle fatigue variation of thrust, high maneuver loads, pressure, and thermal loading. Repetitive maneuver load information is supplied by the airframer manufacturer in the form of number of exceedances per flights or operating hours. Figure 2.45 is one such typical exceedance curve for vertical G's on a military fighter. These loads when combined with engine thrust loading produce a total mount reaction fatigue load spectrum for analysis. Figure 2.46 displays a resulting fatigue load spectrum for a typical military application at one mount location and direction. In some applications there are changes of power level and maneuvers which result in smaller secondary cycles. High cycle fatigue capability must be evaluated against the stresses which are induced by unbalance or frequently repetitive

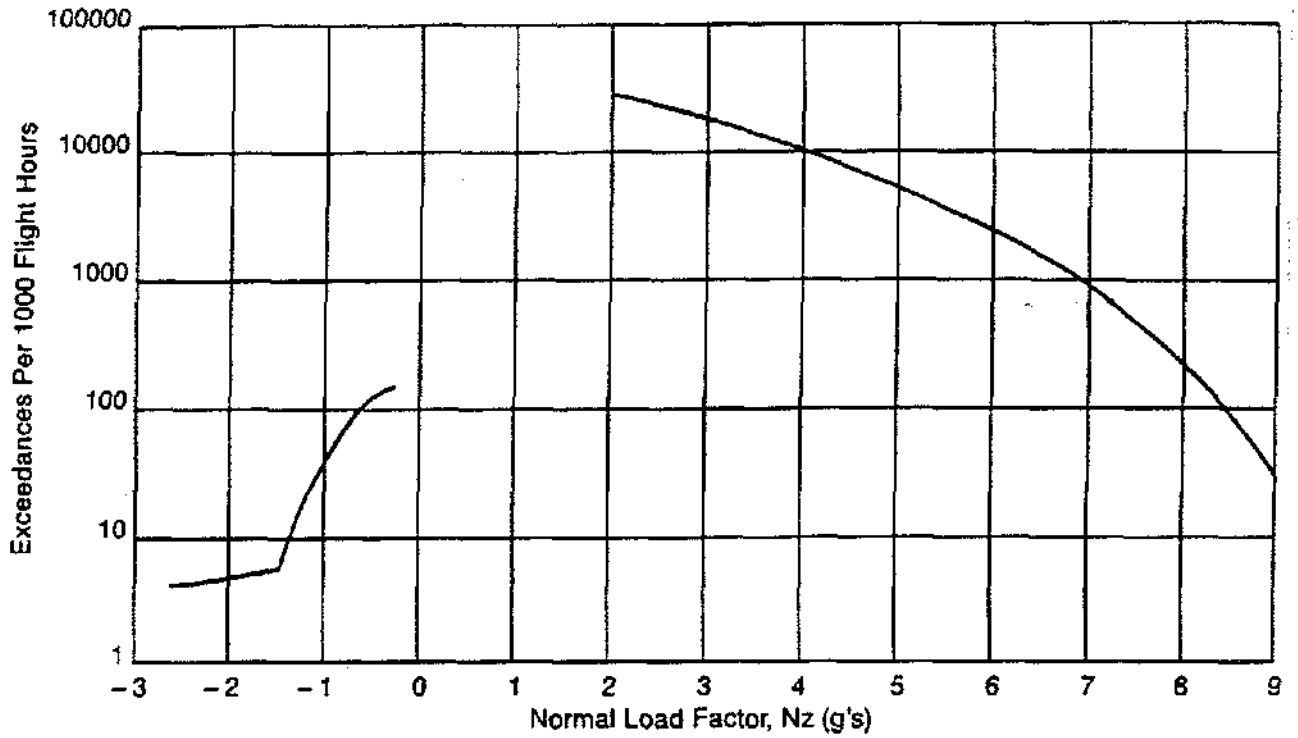


Figure 2.45 Normal Load Factor Exceedances Per 1000 Hours

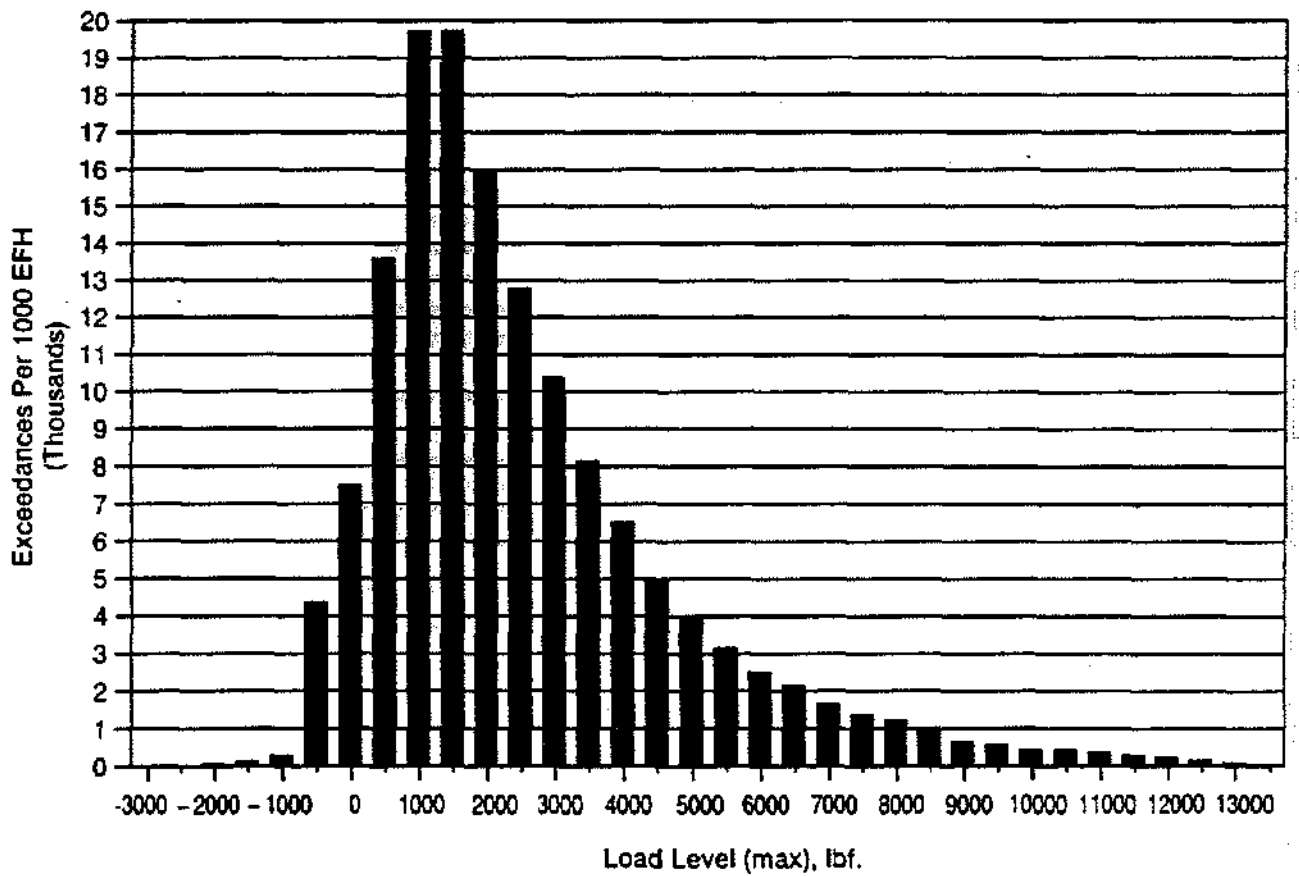


Figure 2.46 Right Axial Engine Mount Load

flight maneuvers such as gust loading. In general, high cycle fatigue is evaluated versus the endurance limit of the material for 10^7 cycles or more; low cycle fatigue is evaluated against the usual S/N curves for the material. Severe combinations of high cycle stress superimposed on low cycle stress may require the development of material property data for the particular case.

Damage tolerance or consideration of crack growth under cyclic loading, determination of critical crack size, and limitation of the crack to values that can safely carry expected loads is becoming an increasingly serious concern for both commercial and military engines. When a crack or defect cannot be allowed to grow safely for the life of the engine, assured inspection intervals must be defined to monitor the areas of concern.

Material properties that will be used to determine suitability of the design must be considered in the light of the environment in which the components must perform, specifically, the operating temperature, the possibilities of oxidation, the possibilities of corrosion, and the stability of the component.

How do we analyze the static structures of an engine? What techniques are available and how realistic are they? Initial sizing can be done with simplified stick and beam computer models, as shown in Figure 2.47. The outer shell rings can be represented as simple curved

beams. The forward and aft inner rings can be treated as curved beams with adjustment to the ring properties to account for the effects of the inner and outer shells. Straight bars or beams represent the struts. A very simplified model like this could be carried out on a time sharing computer program or a PC in the office. The various sketches show the forces and moments among the elements and the distortions of the inner rings for a uniform axial load applied to the hub.

The next step up in sophistication is shown in Figure 2.48 which was used in the initial analysis of the -80A turbine rear frame. The inner shells and cones are modeled by interconnecting plates, struts are represented as simple bars, the polygonal is modeled between the strut ends with plate elements, and the two link reactions are shown at the ends of the struts. On the left the line of action of the pivoting link and on the right the vertical and horizontal reactions of the fixed mount point are represented as forces. Models such as this are used to study overall stiffness and the forces and deflections developed between the struts and the outer shell elements of the polygonal ring. The values used as boundary conditions for the very detailed model of the strut end fittings and mount attaching clevises are shown in Figure 2.49. The stress distributions achieved with models of this degree of refinement can generally be used for realistic initial life calculations.

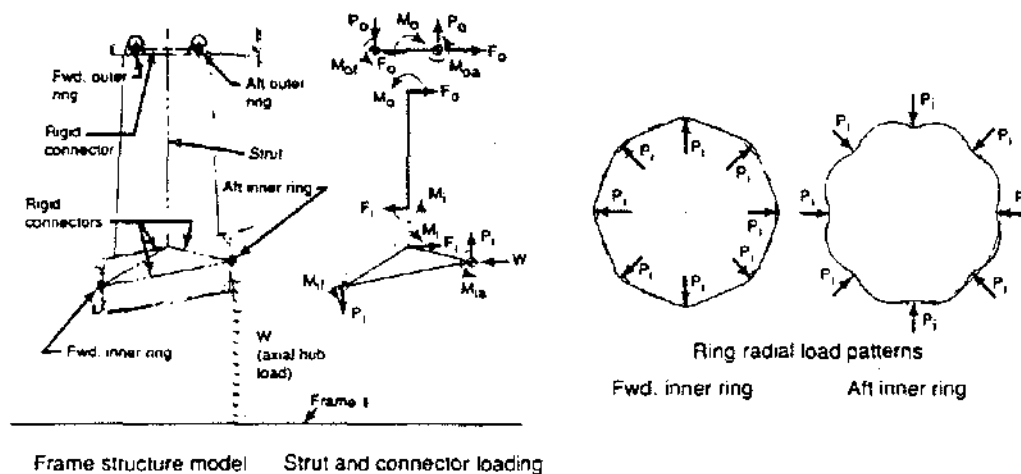
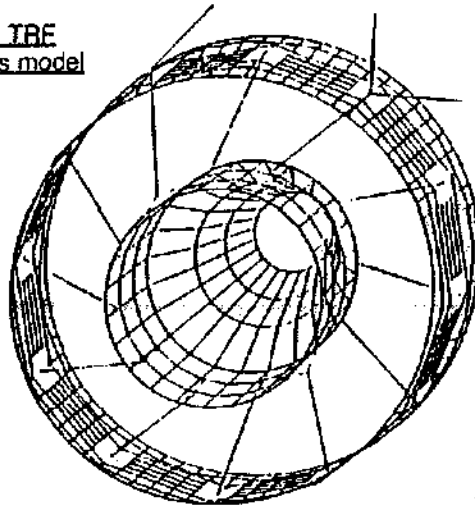


Figure 2.47 Stick and Beam Model

- 3 dimensional redundant structural analysis model

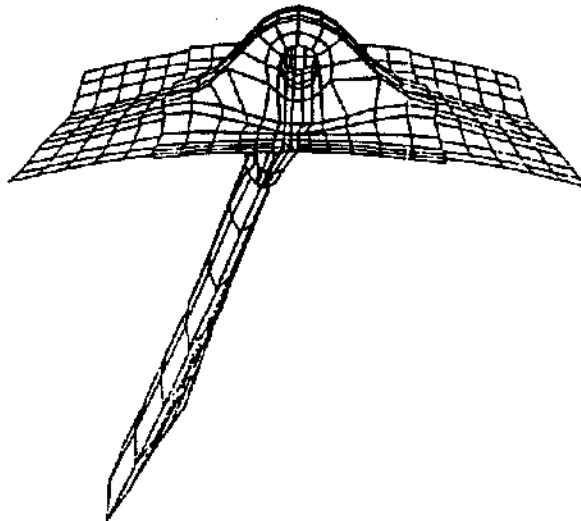
CF6-80 TRF
Plate mass model



- Deflections/stiffnesses
- General stress levels/internal load distribution

Figure 2.48 Redundant Structural Analysis Model

- 3 dimensional finite element model mount/strut section
CF6-80 TRF analysis model



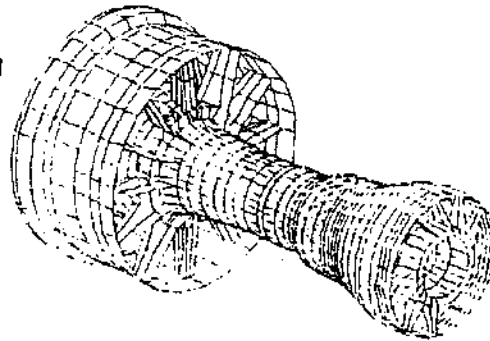
- Detail stress levels

Figure 2.49 Finite Element Analysis Model

To study the overall structural behavior of the engine, a technique has been developed and refined in which each major component of the engine is modeled (Figure 2.50). This model of the -80A clearly shows the Kevlar containment ring, the fan cases, the fan frame struts, compressor shell and combustor cases back through the compressor rear frame, combustor casing, and turbine casings of the tangentially strutted turbine frame. In the lower half of the figure, some of the shells have been cut away to show the inner structure, the frame struts, and the bearing support cones. Models like this can be used to determine the deflections of rotors and stators and the distortion of the casings and frames as they interact under inertia loads, pressure loads, thrust, and thermal mismatch. They are particularly helpful in conducting "What if..." studies to determine ways to minimize

distortion and deflection and improve performance by reducing running clearances between rotors and stators. Figure 2.51 shows all of the elements of a CFM 56-3 installation: the inlet and fan cowls, the basic engine structure, fan reverser and the core nozzle, the pylon attachment to the aircraft. These models not only permit study of the interaction of the major components of an aircraft installation; they also are suitable for use in dynamic studies. Figure 2.52 shows the first bending mode for the CFM56-3 engine. Such use of a finite element model permits the determination of the frequencies and the mode shapes for various natural vibration modes as well as response to force vibrations. These studies enable us to understand the dynamics of the engine and to make modifications to the design to reduce vibratory responses or change frequencies and mode shapes.

Engine structural model



Engine structural model

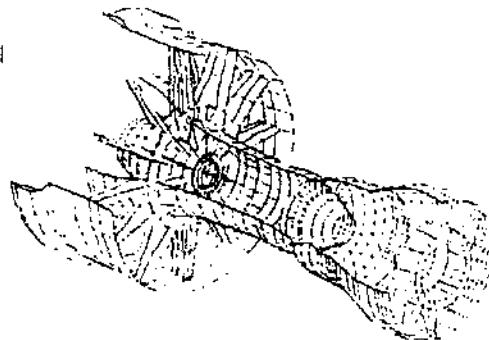


Figure 2.50 Overall Engine Structural Model

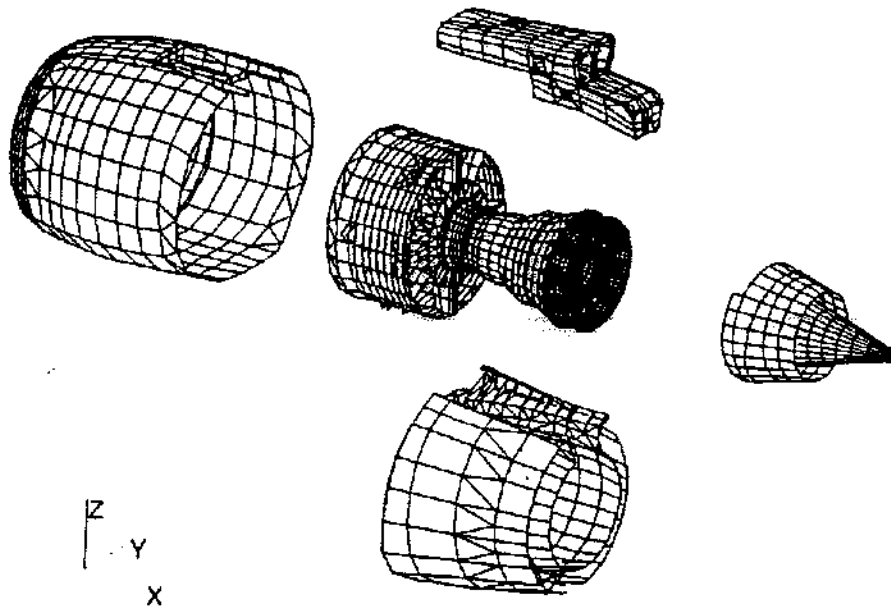


Figure 2.51 CFM56-3 3D Engine Model

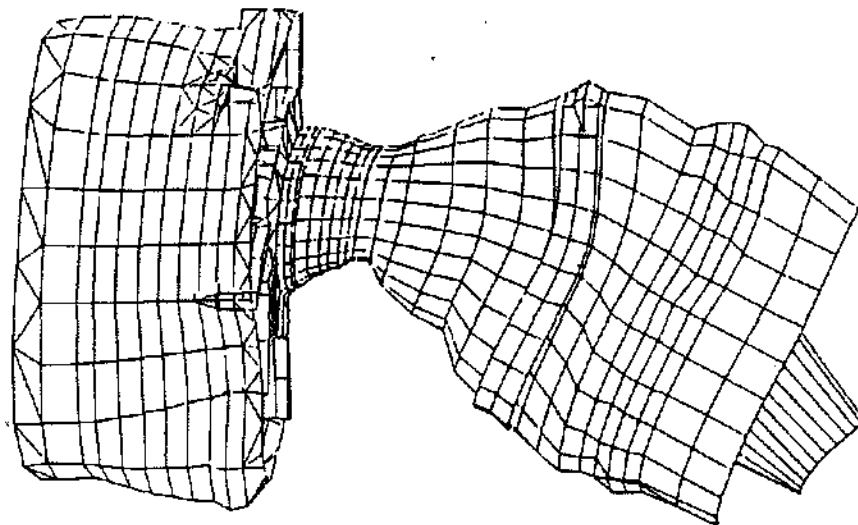


Figure 2.52 CFM56-3 First Engine Bending Mode

STRUCTURAL TESTING

Static structural testing comes in three forms, including component, engine, and extra severity testing. Component tests can be as simple as a clevis and link subjected to force to determine the shear capability of pins or bolts, the tearout of the lugs of the clevis or link end, or the stress distribution into the adjacent structure. Or the component test may consist of an entire frame loaded to simulate the application of thrust, maneuver loads, thermal mismatch, or pressure. Proof or burst pressure loads and hydrocyclic tests of combustor casings and compressor rear frames are almost routine, since it is unlikely that we will ever be able to measure in service the extreme conditions to which a military engine might be subjected. The fan duct (Figure 2.24) and the augmentor duct that are part of the engine were tested as components mounted between the adjacent frames and loaded to determine their ultimate buckling capability. As part of our understanding of the local distortions of the casing and the overall backbone bending of the engine, a CF6-50 engine static structure was once assembled in the Static Load Lab from engine inlet to turbine frame (Figure 2.53) and the entire engine carcass was then installed on a DC10 wing pylon with actual aircraft links and mount attachments. Bearings and shafts were installed in the sumps to represent the rotors of the engine, and radial bars were attached to the shafts carrying linear potentiometers to sweep over the inside surface of the casings and measure the actual deflections of the cas-

ings. These tests were fundamental to our understanding of the importance of spreading the thrust load and introducing mount side and vertical loads by shearing them tangentially into the shells at the points of attachment. Confidence in the overall computer models of the engine, shown in Figures 2.50 and 2.51, was generated when the result of those deflection calculations matched the experimental measurements that had been made on the actual engine structure.

Engine tests are generally of the stress/mechanical/performance (SMP) or cyclic endurance varieties. The static structures are evaluated by use of strain gauges, thermocouples, deflection measurements, or accelerometers. Extra severity tests can be performed either as component tests in which limit or ultimate loads are applied and failure or buckling capability is established. Or, in the case of containment studies a whirling rig is used to evaluate Kevlar containment for a full fan blade released at the fan disc dovetail at maximum speed. Extra severity engine tests are run to determine the capability of the engine to withstand the resulting damage from the ingestion of ice slabs and large birds. Of course, the most severe structural test to which the engine can be subjected is the release of a full fan blade at maximum operating speed. This test not only confirms the capability of the fan blade containment system, but also thoroughly checks the structural strength of the engine under extreme vibration. Here the engine is allowed to try to run for 15 seconds before the throttle is retarded.

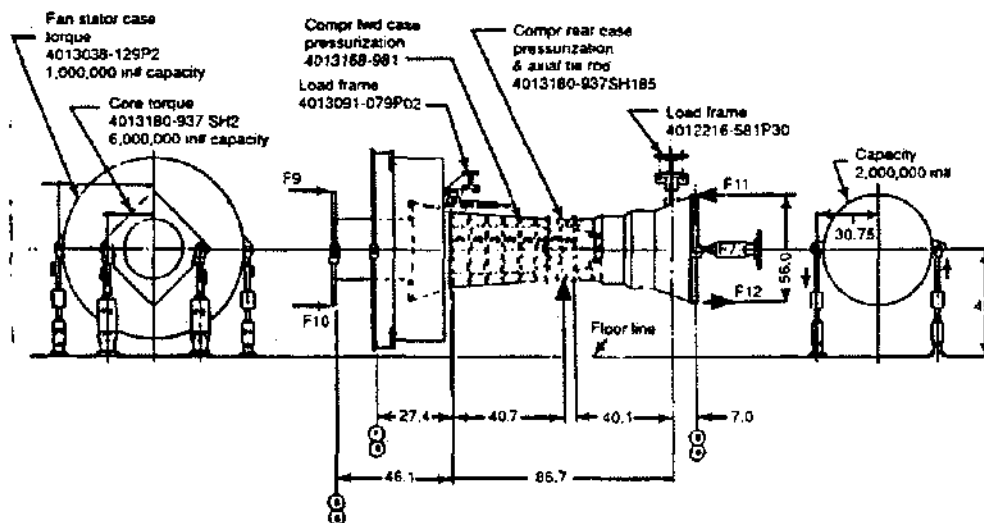


Figure 2.53 Static Load Test

Figure 2.54 shows the preparation for a typical component test of a major structural element. The first -80A turbine frame was produced by welding cast struts between a cast hub and the polygonal outer case (which had been formed by welding together twelve strut end castings). The ends of strut #12 and strut #2 carried the rear mount clevises. Failure of a strut-to-hub weld joint was simulated by sawing half-way through the strut

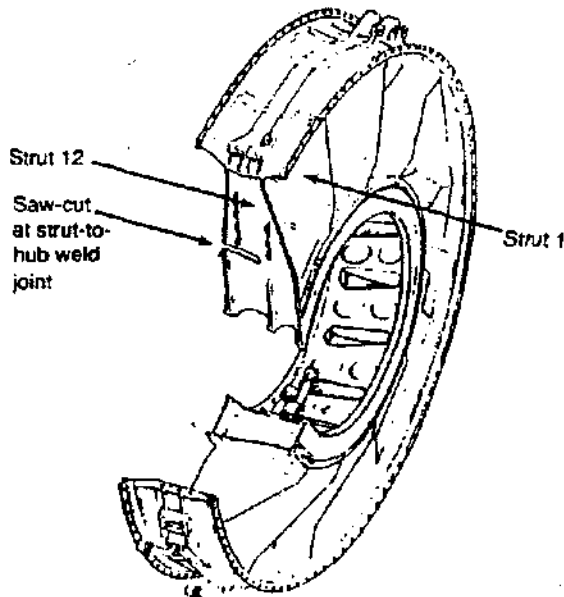
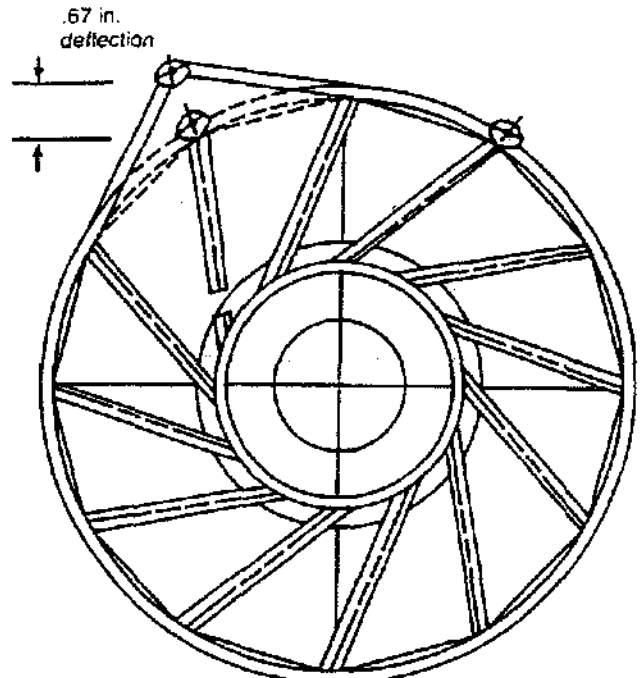


Figure 2.54 Induced Partial Crack in Weld Joint

along the line of the weld. Figure 2.55 shows the results of the failsafe test. Although the strut failed and the mount deflected two-thirds of an inch, the loads were supported by the redundancy of the outer shell and the other 11 struts. Figure 2.56 shows how a failure of an outer case panel weld was simulated by cutting through axially. The failsafe load was applied to the mount over strut #2 and again the test was successful. The load was carried by the redundancy of the strut, the flanges and the other remaining struts.



TRF deflected shape under max failsafe load

Figure 2.55 Failsafe Test - Severed Mount Strut

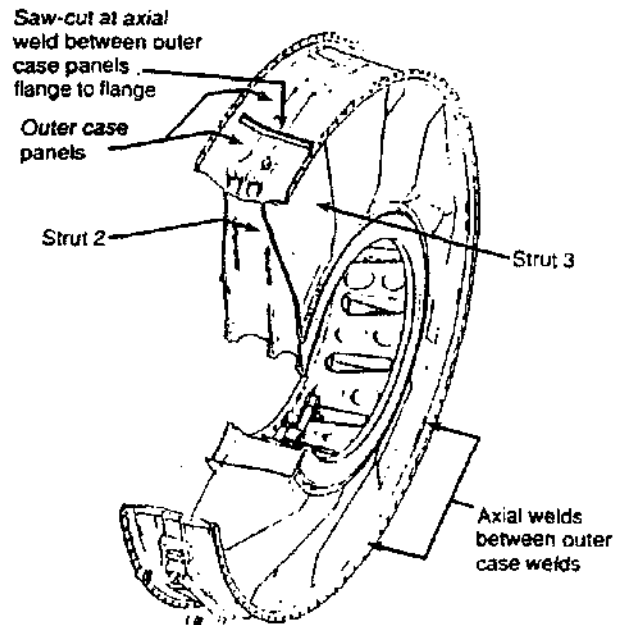


Figure 2.56 Induced Crack in Axial Weld

SUMMARY

In this chapter, you have been introduced to some of the problems to which the static structures are subjected and the various means by which they have been handled in various engines. We considered the overall static structural arrangement of typical military low bypass and commercial high bypass engines. Then we looked at some of the fundamental issues in the design of static structures and attempted to explain how they were han-

dled on engine frames of various types and designs. The mounting of engines in aircraft, both military and commercial was presented. Containment was considered in some detail. The various types of loading was examined along with the various methods by which analyses are performed to determine the capability of our structure to support those loads. Finally, we looked at the methods of testing by which we can confirm our analysis and substantiate adequacy of the structural components.

Chapter 3

FAN AND COMPRESSOR SYSTEMS

by David C. Wisler
(Aerodynamics Design Topics)

and

Leigh Koops, Al McDaniel, Jerry Juenger, Jay Cornell
(Mechanical Design Topics)

INTRODUCTION

The purpose of fans and compressors in turbojet engines is to impart energy to the airflow. This is accomplished by a rotor consisting of spinning wheels (or disks) filled with airfoil projections (blades) to increase the kinetic energy of the airflow and therefore bring about a total pressure rise. Directly following the rotor airfoils is a stage of stator airfoils (vanes). In this process both the rotor and stator turn the airflow, slowing the velocity, and yielding a rise in the static pressure of the airflow. Multiple stages or rows of rotor/stator stages are stacked in axial flow compressors to achieve exit to inlet total pressure ratios on the order of 8 to 12. Fans by comparison have fewer stages and are generally used to move large volumes of air with pressure ratios of 1.5 to 3.0.

Other components in fans and compressors include shafts connected to the turbine to turn the rotor and casings which act as pressure vessels to contain the air and support the stator vanes. In some engines many of the stator vanes are mechanically actuated to change their angle of pitch providing a better match of airfoil incidence angle at various engine operation points. These elements of fans and compressors are shown in Figure 3.1.

The design of air compression turbomachinery has advanced greatly since the early part of the 20th century when GE started to produce aircraft engine superchargers based on Dr. Sanford Moss's designs. These turbosuperchargers utilized a centrifugal compressor and an axial flow turbine, such as the one shown in Figure 3.2. Centrifugal compressors have design advantages of being compact and capable of high pressure ratios. During World War II, GE's experience in steam turbines and turbosuperchargers led to being selected to produce America's first jet engine, the I-A, which also utilized a centrifugal compressor. It became apparent that with the demand for higher thrust engines flying at higher

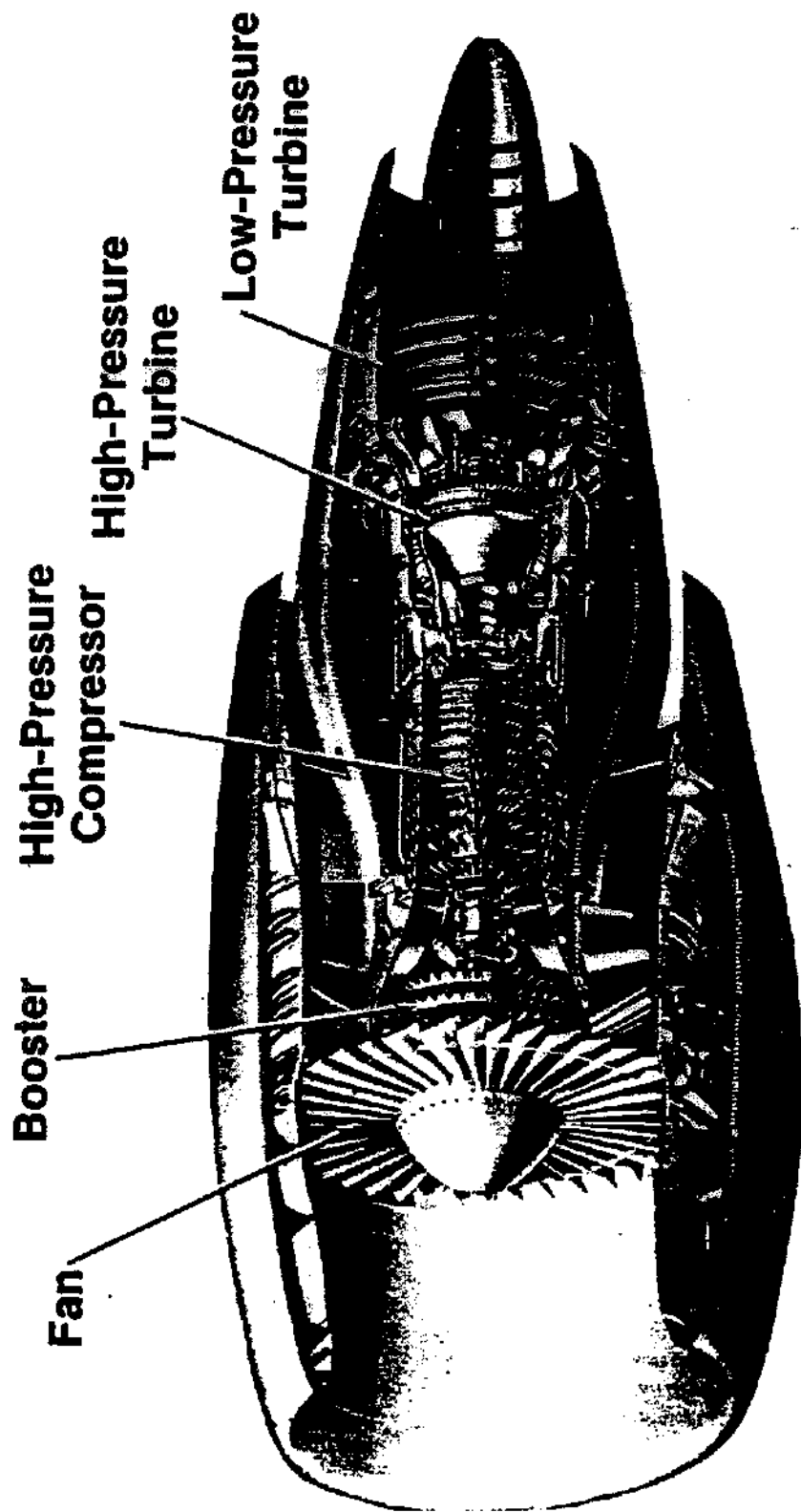
speeds that centrifugal compressors were not the proper choice due to the large frontal area and resulting drag. So, GE developed an axial flow compressor for the world's first turboprop engine, the TG100, designed in the mid-1940s. An example of an axial compressor can be seen in the J85 turbojet (Figure 3.3a) and a centrifugal compressor can be found incorporated in the CT7 engine (Figure 3.3b). Centrifugal compressors can now achieve a pressure ratio of 8:1 in a single stage, making them highly appropriate for applications such as helicopters.

Axial flow compressors advanced in the 1950s with the incorporation of variable stator vanes on the J79 engine. This allowed the turbojet engine to perform efficiently both at Mach 0.9 cruise speeds and at Mach 2.0 dash to combat speeds. Commercial derivatives of the J79, the CJ805 series of engines, were developed in the late 1950s. The aft fan version of the CJ805, shown in Figure 3.4, provided increased thrust and somewhat better SFC.

In the 1960s new transport engine designs at GE placed the fan at the front of the engine where some of the fan exit air could supercharge the compressor. The rest of the fan discharge air would "bypass" the compressor to provide additional thrust due to the movement of large volumes of air. The ratio of bypass airflow to core airflow in GE's first production high bypass turbofan engine, the TF-39, is 6.5:1. Further additions of stages to the fan rotor, such as the CF6-50 and CF6-80, where most or all of the exiting air would enter the core, are called "boosters."

In the 1980s advances were made in the area of composites. NASA funded research in propfans and a 1970's technology base of fan blade mechanisms with variable pitch came together to produce the latest advance in fan technology, the unducted fan or UDF. A cutaway diagram of the UDF is shown in Figure 3.5. The UDF resembles a large turboprop engine. One difference that can be noted is that the fan blades are swept back so that they resemble scimitars. This blade design allows the propulsion efficiency of the UDF fan to approach that of turboprops but maintains the peak performance at higher flight airspeeds. While turbofan engines are able to fly efficiently at still faster flight airspeeds, the vast improvement in SFC provided by UDF engines makes them an efficient propulsion choice for air transport designs for the early 21st century.

The first part of this chapter provides an overview of the aerodynamics of advanced compressor and fan systems. Topics include basic principles and definitions, an historical perspective of the trends in compressor and fan



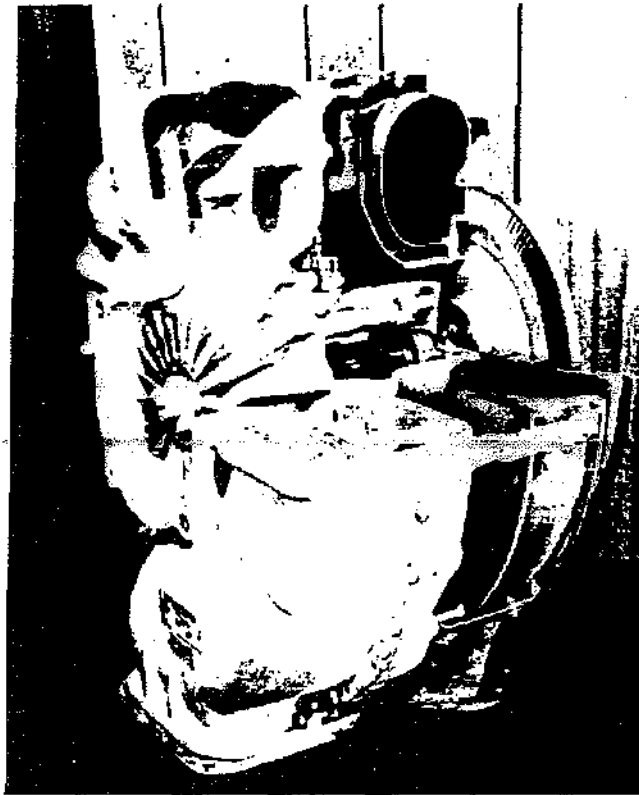


Figure 3.2 Turbosupercharger

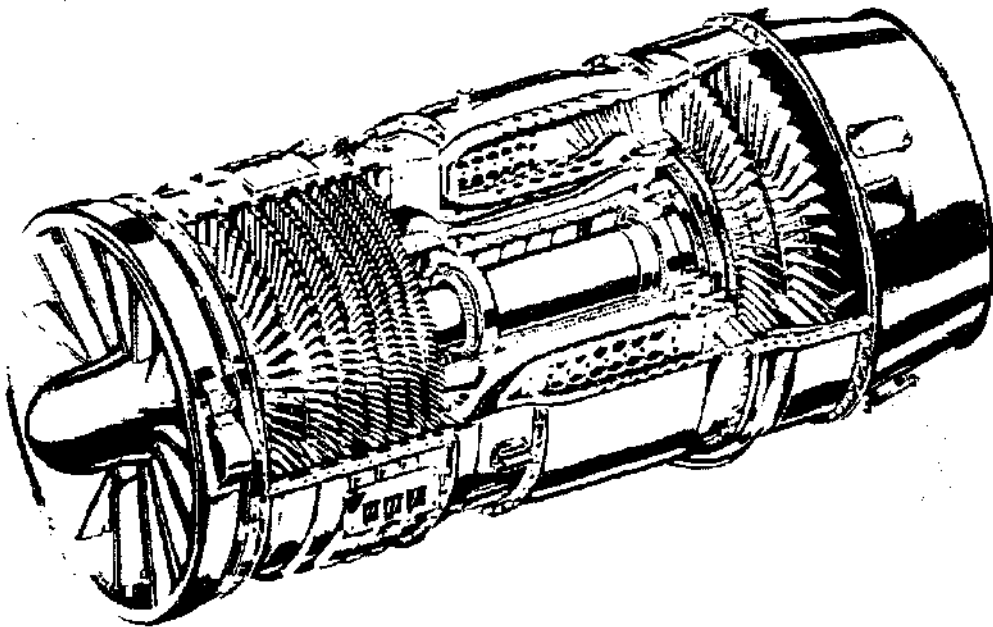


Figure 3.3a Turbojet Engine with an Axial Flow Compressor

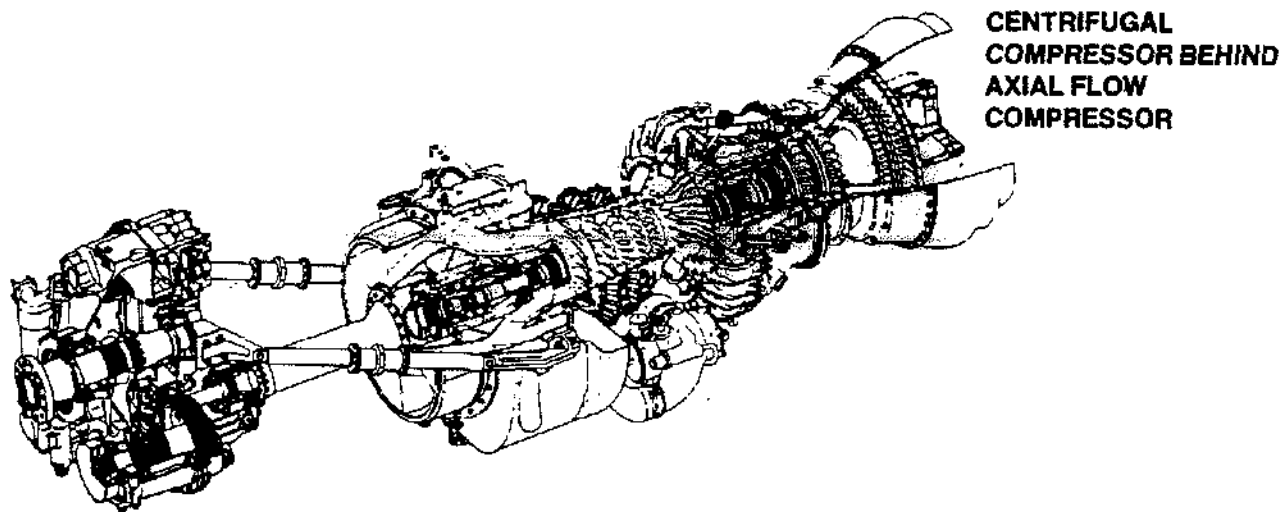


Figure 3.3b CT7 Engine Incorporating a Centrifugal Compressor

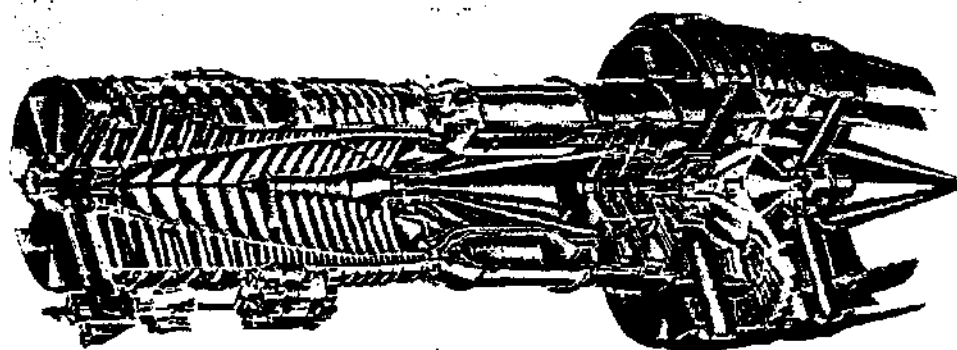


Figure 3.4 Cutaway Drawing of a GE CJ805-23 Aft-Turbofan Engine

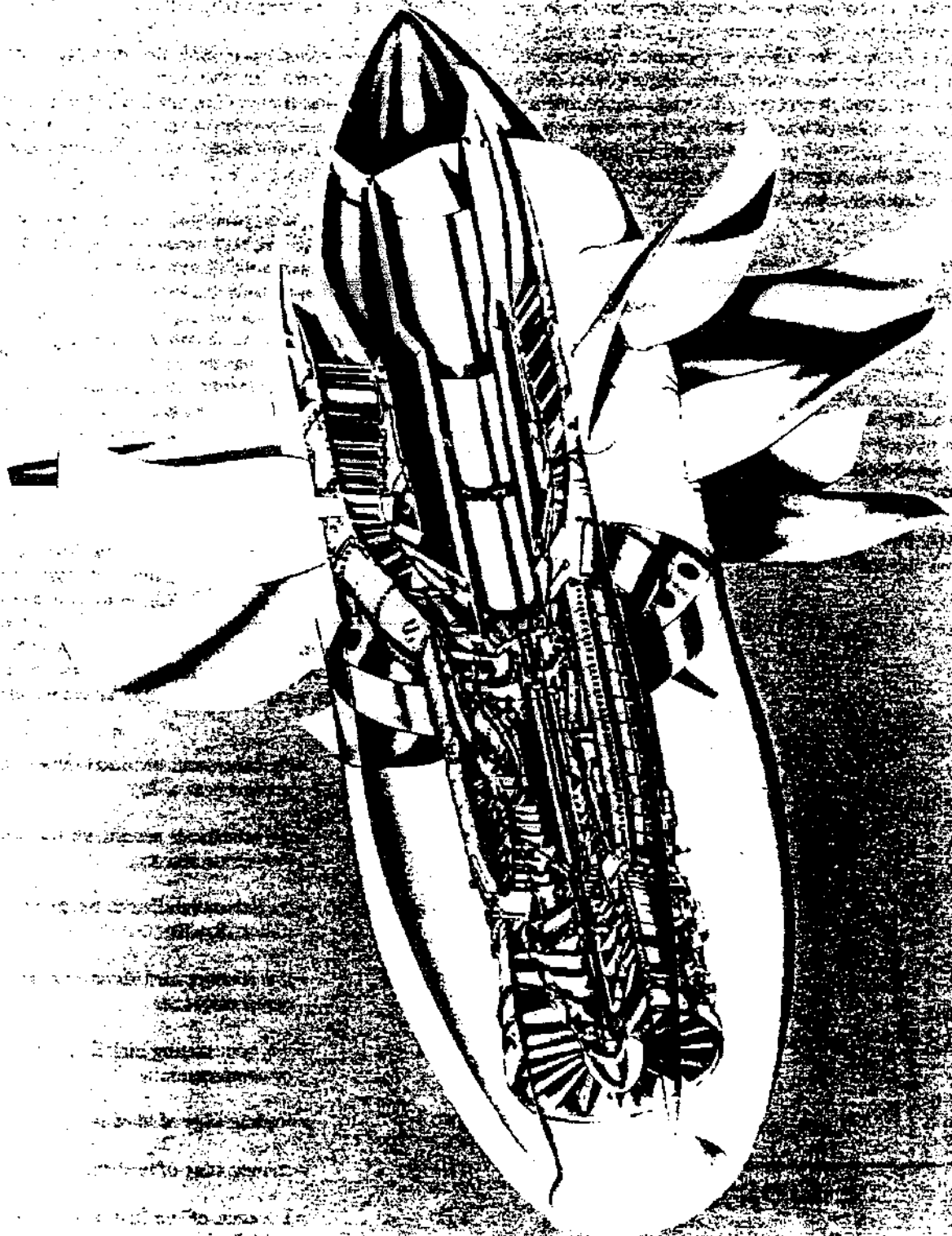


Figure 3.5 GE UDF Jet Engine

design, design and analysis methods including some current thinking in fan/prop-fan configurations, and lastly a presentation of variable geometry and the effects of tip clearance, shrouds, leakage, and clearance control on performance. The second part of the chapter deals with the mechanical design aspects of fans and compressors. It must be remembered that behind each of the topics discussed lies a wealth of proprietary technology used in the design of compressor and fan systems that cannot, for obvious reasons, be discussed.

BASIC AERODYNAMIC PRINCIPLES, COMPONENTS, AND DEFINITIONS

The fan, booster, and high-pressure compressor form the compression system. The basic task of the compressor is to add energy to the air stream with minimum loss, and thus raise the temperature and pressure of a specified amount of mass flow rate from State 2 to State 3 in the thermodynamic cycle determined during preliminary design, shown schematically in Figure 3.6.

Generally in a design process the overall pressure ratio and the mass flow rate are considered to be non-

negotiable items because they are principal factors affecting the cycle and thrust of the engine.

Designers have selected axial-flow or centrifugal compressors to achieve the high compression ratios required for turbojet and turbofan engines rather than piston-type compressors because of weight and size constraints. This overview will concentrate on axial-flow compressors.

The expanded view of an axial-flow compressor system in Figure 3.7 reveals that the compressor consists of an alternating sequence of rotating and fixed sets of airfoils. The sets of rotating airfoils are attached to a rotating spool, and the combination is called the rotor. The sets of fixed airfoils are spaced around the periphery of an outer stationary casing, and this combination is called the stator. One set of rotor airfoils (blades) and one set of stator airfoils (vanes) constitutes a stage. The number of stages varies, depending upon the pressure ratio required. Inlet guide vanes (IGVs) are a set of airfoils placed ahead of the first stage rotor to direct the air at the correct angle to this rotor.

A cross-sectional drawing of a typical axial-flow compressor including station location numbers along the flowpath is shown in Figure 3.8. A sketch showing the projection of the blading on the casing (outside looking radially inward toward the centerline) is also presented. Rotation is clockwise, aft, looking forward. Several important terms are used to identify various compressor components.

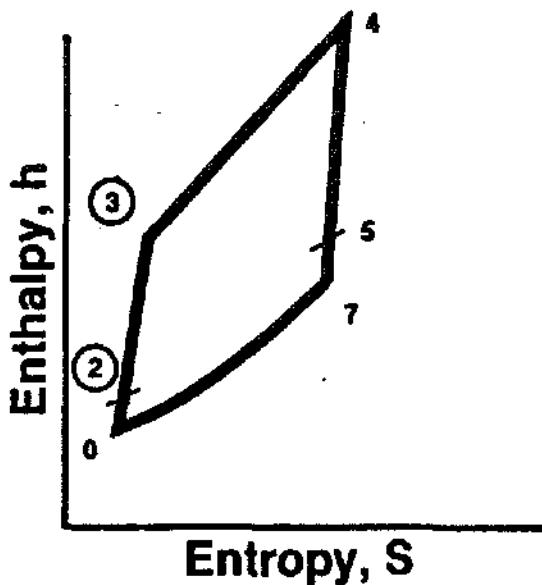
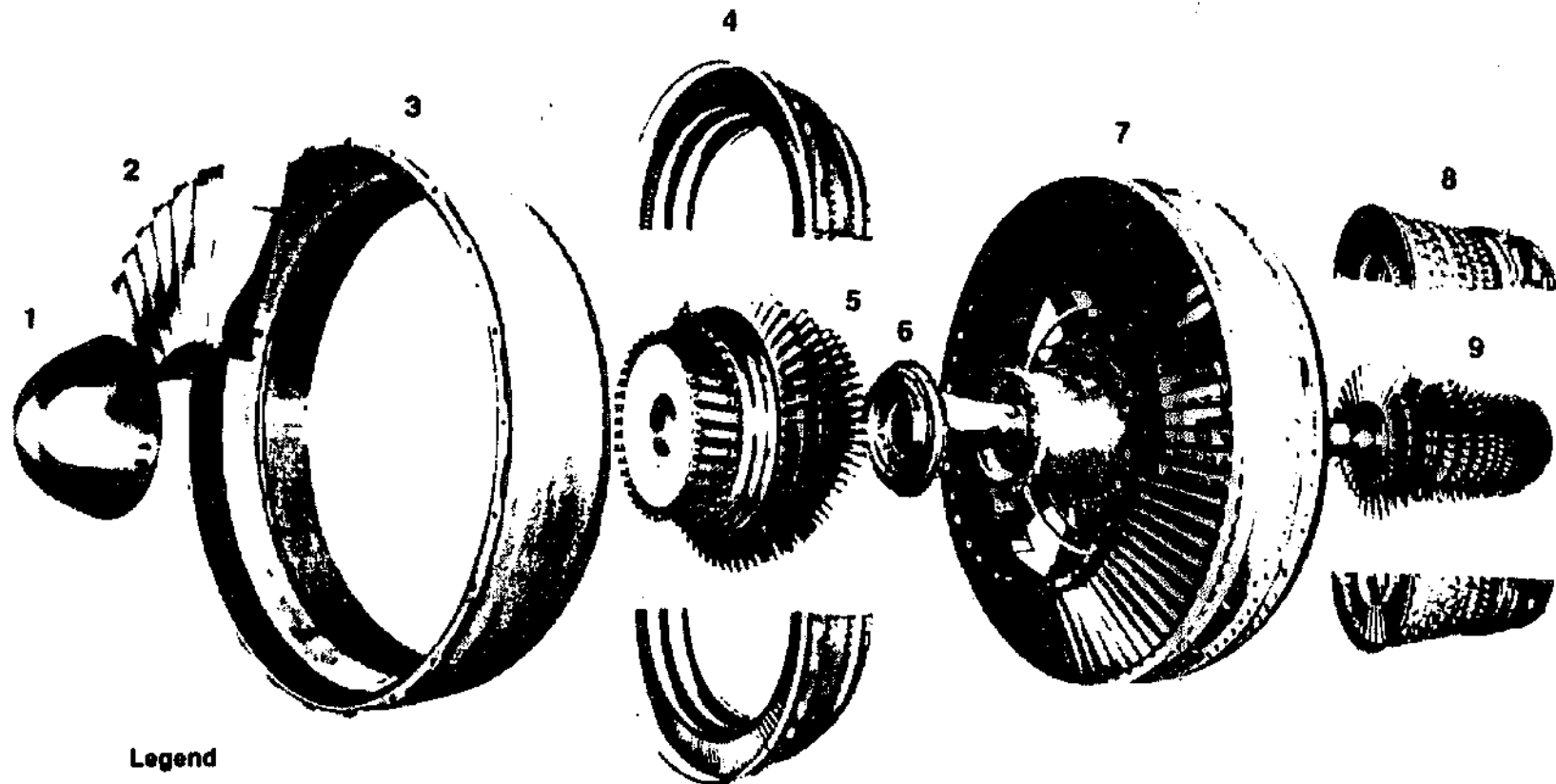


Figure 3.6 H-S Diagram Showing the Compression Phase of the thermodynamic Cycle

Casing	=the outer wall boundary of a compressor or fan, R_C
Hub	=the inner wall boundary of a compressor or fan, R_H
Radius Ratio	=the hub radius divided by the casing radius, R_H/R_C
Blades	=the rotating airfoils in the fan or compressor
Vanes	=the non-rotating airfoils in the fan or compressor
LE	=leading edge of blading
TE	=trailing edge of blading
1.0	=Location of the first stage rotor at LE hub
1.5	=Location of first stage rotor at TE hub



Legend

- | | |
|---|---|
| 1. Spinner Cone | 6. Fan Shaft |
| 2. Fan Blades (7 of 38) | 7. Fan Frame, All Case and Outlet Guide Vanes |
| 3. Fan Forward Case | 8. High Pressure Compressor (HPC) Stator |
| 4. Low Pressure Compressor (LPC) Booster Stator | 9. HPC Rotor |
| 5. LPC Booster Rotor | |

Figure 3.7 Exploded View of the Fan Compressor Assembly

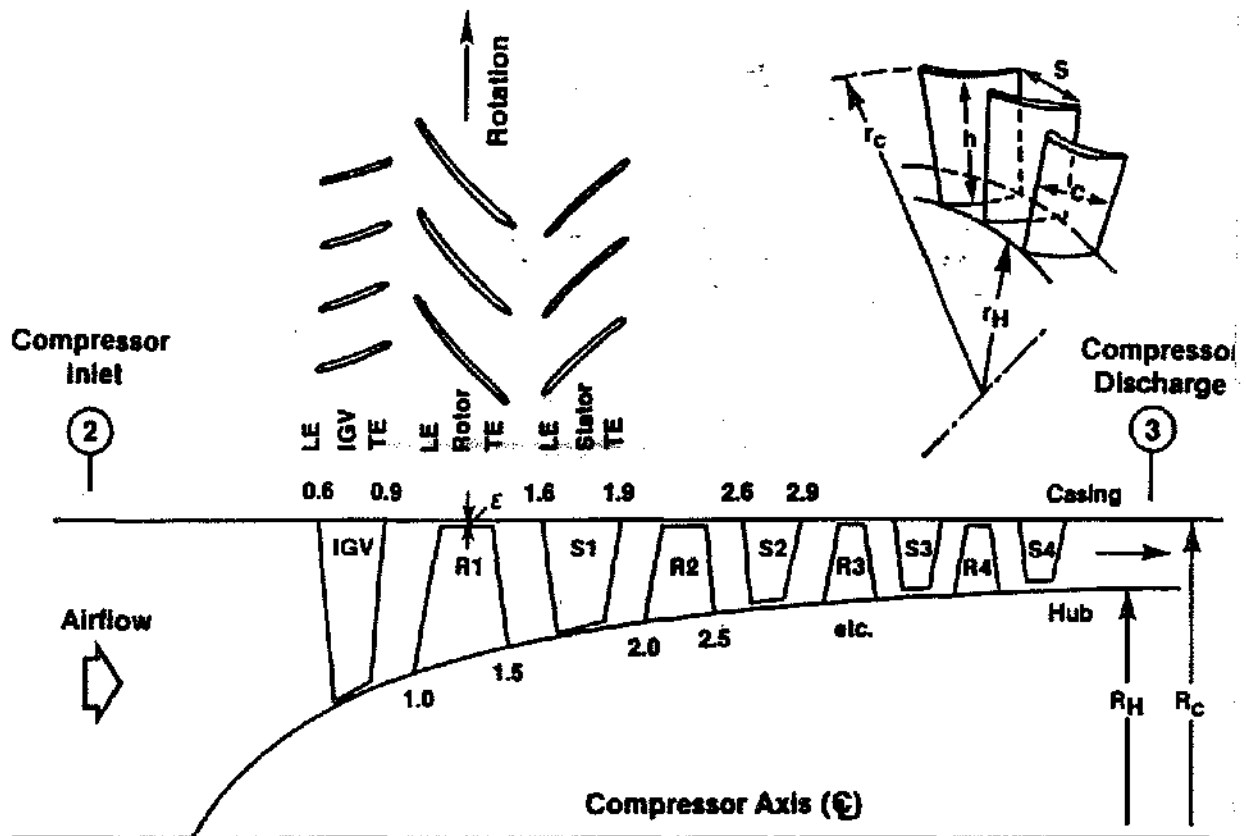


Figure 3.8 Cross-Sectional Drawing of a Typical Axial-Flow Compressor

- 1.6 =Location of first stage stator at LE casing
 1.9 =Location of first stage stator at TE casing

Stations for the second stage would be: 2.0, 2.5, 2.6, 2.9, where the number preceding the decimal indicates the stage number and the following number indicates the location within the stage

- Tip clearance =the radial distance between the airfoil tip and the adjacent flowpath, e

The basic principle of operation of a compressor is that kinetic energy (increase in tangential momentum) is imparted to the air by means of the rotating blades. This energy is then converted to a pressure rise by the diffusion process, which occurs in both the rotor blades and the stator vanes. The process occurs in a single stage and is repeated by succeeding stages until the desired pressure ratio is attained. The power to drive the compressor is derived from the turbine. An axial-flow compressor can

achieve high pressure ratios (e.g. 23:1) on a single spool at high levels of efficiency.

Vector Diagrams - Vector diagrams are extremely useful tools for describing the magnitude and direction of the air velocity at various locations in the compression system. They are used extensively by designers as the "set" the blading.

A velocity vector diagram, shown in Figure 3.9, relates the absolute velocity, C , the velocity relative to a frame of reference fixed to the moving rotor blades, W , and the velocity of the reference frame (i.e., wheel speed), U . Several quantities and relationships are also shown, including:

- W & β =relative velocity and air angle
 C & α =absolute velocity and air angle
 W_u =relative tangential velocity
 C_u =absolute tangential velocity

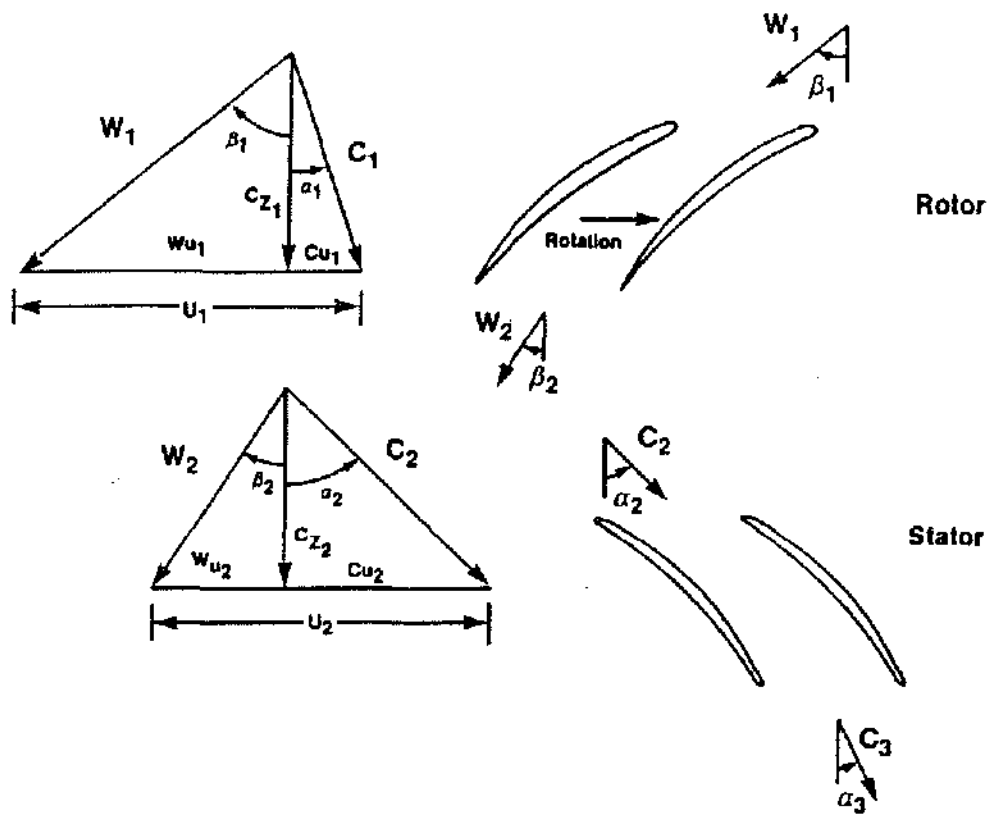


Figure 3.9 Vector Diagrams

U	=wheel speed
C_z	=axial velocity
$\Delta\beta = \beta_1 - \beta_2$	=flow turning in the relative frame
$\Delta\alpha = \alpha_1 - \alpha_2$	=flow turning in the absolute frame
α or β	=air angle, the angle between the air-stream and the axial direction, α , (absolute) for stators and β , (relative) for rotors
Flow Turning	=the difference between the inlet and exit air angle

Blading - The orientation of the airfoil relative to the vector diagrams and the shape of the airfoil have a dominate effect upon compressor efficiency. Airfoils and their orientation in the compressor are shown in Figure 3.10. Important definitions of terms associated with blades in compressors include:

Leading edge =the forward most portion of the airfoil

Trailing edge	=the rearward most portion of the airfoil
Chord, C	=the length of the straight line connecting the leading edge and the trailing edge of a blade or vane
Meanline	=a line bisecting the suction (convex) and pressure (concave) surfaces of an airfoil
Thickness envelope	=a distribution specifying the thickness at each point on the meanline. The thickness is applied perpendicular to the meanline.
Metal (meanline) angles	=the angle between the meanline of the blade and the axial direction, α^* for stators and β^* for rotors
Camber, ϕ	=the curvature of the meanline of an airfoil (often as expressed as $\beta_1^* - \beta_2^*$ for rotors or $\alpha_1^* - \alpha_2^*$ for stators), where 1 = LE and 2 = TE)

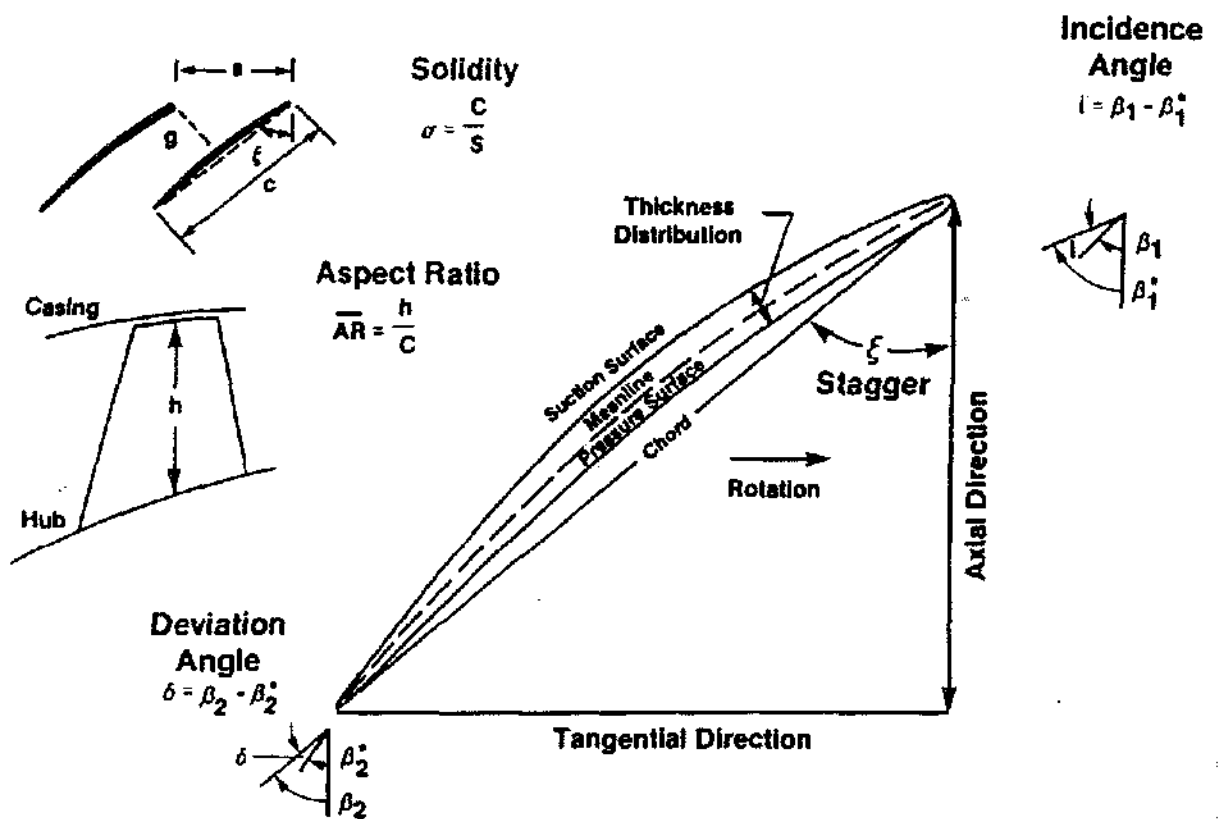


Figure 3.10 Blading

Incidence angle, i	=the difference between the inlet air angle and the leading edge meanline angle $i = \beta_1 - \beta_1^*$ or $\alpha_1 - \alpha_1^*$	Staggered spacing $= g = S \cos \xi$ (see sketch)
Deviation angle, δ	=the difference between the exit air angle and the trailing edge meanline angle $= \beta_2 - \beta_2^*$ or $\alpha_2 - \alpha_2^*$	Passage aspect ratio $= H/g$, blade length (height) divided by staggered spacing (see sketch)
Spacing, S	=the circumferential distance between two blades or two vanes. $S = 2r/N$ where N = number of blades or vanes	Stacking point $=$ the point on which the airfoil sections are stacked to form a blade or vane
Solidity, σ	$= \sigma = \text{chord}/\text{spacing}$	Basic Equations - The basic equations for computing the temperature rise obtained in a compressor for a given pressure ratio and efficiency are given in Table 3.1 and equations 3-1 and 3-2 where:
Aspect ratio	=blade height, h , divided by pitchline chord, c	Adiabatic efficiency is the ratio of the ideal enthalpy change to the actual enthalpy change between the same two pressures. This definition has the disadvantage of varying with pressure ratio, η_{ad} is usually shown on a compressor performance map.
Stagger angle, ξ	=the angle between the chord of a blade or vane and the axial direction	Polytropic efficiency is the ratio of the energy which contributes to the pressure rise to the total energy delivered to the compressor. η_p is used to compare one compressor to another.

BASIC EQUATIONS FOR COMPRESSORS

- Pressure Ratio of Compressor

$$\frac{P_{T3}}{P_{T2}} = \left[\eta_{ad} \left(\frac{T_{T3}}{T_{T2}} - 1 \right) + 1 \right]^{\gamma/\gamma - 1} \quad 3-1$$

$$\frac{P_{T3}}{P_{T2}} = \left(\frac{T_{T3}}{T_{T2}} \right)^{\frac{\gamma \eta_p}{\gamma - 1}} \quad 3-2$$

Where η_{ad} — Adiabatic Efficiency

η_p — Polytropic Efficiency

- Change in Tangential Momentum Across Rotor

$$(\Delta r c_u)_{Pitch} = \frac{g J C_p (r \Delta T_T)_P}{U_p} = \frac{g J C_p (\Delta T_T)_P}{\omega_p} \quad 3-3$$

- Pressure Ratio in Terms of Flow Turning

$$\frac{P_{T2}}{P_{T1}} = \left[1 - \frac{r \omega C_z (\tan \alpha_2 - \tan \alpha_1)}{H T_1} \right]^{\gamma/\gamma - 1} \quad 3-4$$

- Loss Coefficient

$$\bar{\omega} = \frac{P_{T_{in}} - P_{T_{out}}}{P_{T_{in}} - P_{S_{in}}} \quad 3-5$$

- Reaction

$$R = \frac{(\Delta P_S)_{rotor}}{(\Delta P_S)_{stage}} \quad 3-6$$

Table 3.1 Basic Equations for Compressors

The change in tangential momentum across each rotor can be computed from the temperature rise across the rotor using equation 3-3. The pressure ratio achieved can be related to the flow turning across a blade row ($\alpha_2 - \alpha_1$), equation 3-4.

The loss in a compressor is usually expressed in terms of a total pressure loss coefficient, $\bar{\omega}$, as defined in equation 3-5. For a rotor blade row, the relative total pressure is used, and for a stator the absolute total pressure is used.

The reaction of a compressor is defined as the static pressure rise occurring across the rotor blade divided by the static pressure rise occurring across the stage, equation 3-6.

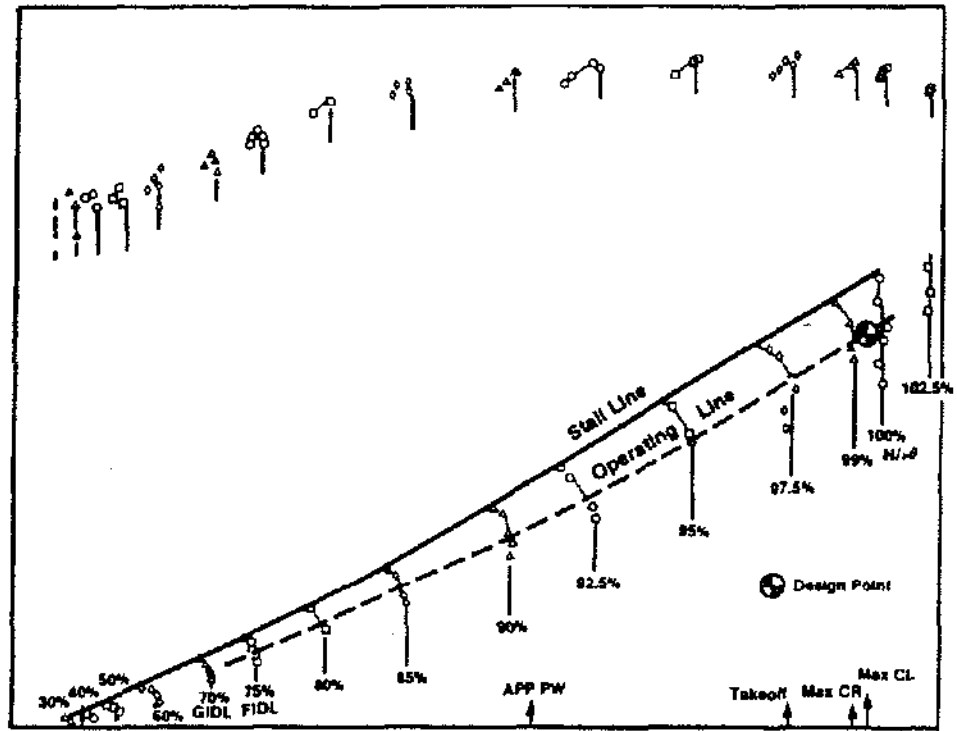
PERFORMANCE, STALL, SURGE AND STALL MARGIN

Compressor performance is usually presented in the form of a compressor map, as shown in Figure 3.11, in which pressure ratio and adiabatic efficiency are plotted as a function of corrected mass flowrate for various speed lines. Note the design-point goal and the stall line in the diagram.

Rotating stall and surge phenomena in axial flow compressors rank among the most serious problem areas in turbomachinery aerodynamics. Gas turbine engines may encounter severe performance and durability problems if

Adiabatic Efficiency

Total Pressure Ratio



Corrected Compressor Inlet Airflow (PPS)

Figure 3.11 Compressor Performance Map

the compressor is not able to avoid stalls or surges over its entire range of operation. In addition, the ability to recover from stall or surge, once encountered, is critical. These phenomena are described with reference to the performance map of Figure 3.12, which is a representative speed line from Figure 3.11.

As mass flow is decreased (throttle closed), pressure increases and the compressor will operate in a stable manner along the unstalled characteristic from points A - B. Further reduction in mass flow below point B will bring about rotating stall and the operating point will suddenly drop to a new stable condition in rotating stall, point C. If the mass flow is increased (throttle opened), the compressor does not jump back to point B, but operates along the stalled characteristic to point D. Further increase in mass flow beyond D causes the operating point to jump up to point E on the unstalled characteristic. Region B, C, D, E, B is the stall hysteresis region.

Stall (rotating stall more accurately) is a flow breakdown at one or more compressor blades. Typically, a rotating stall is a stagnated region of air which moves in the circumferential direction of rotor rotation, but at a fraction of the rotor speed. At a given throttle setting it does not move axially in either direction, although it may cause

pressure waves to move upstream (compression waves) or downstream (rarefaction waves).

Surge is a response of the entire engine which is characterized by a flow stoppage or reversal in the compression system. Upon surge, a compression component will unload by permitting the compressed fluid in downstream stages to expand in the upstream direction, forming a more or less planar wave which at high speeds often leads to flow reversal. The compressor can recover and begin again to pump flow. However, if the surge inducing cause is not removed, the compressor will surge again, and will continue the surge/recovery cycle until some relief is provided. Surge may be initiated by rotating stall.

One can distinguish between two types of stall. Blade stall is a two-dimensional type of stall, where a significant portion of the blade has large wakes due to substantial thickening or separation of the suction surface boundary layer. Wall stall is an endwall boundary layer separation.

Stall margin is a measure of the operating range between the design point and the in-stall point B. It is computed as follows:

$$\text{Stall Margin} = \left[\frac{\left(\frac{P}{P_{\text{STALL}}} \right) \times \frac{m \sqrt{\theta}}{\delta}_{\text{DESIGN PT}}}{\left(\frac{P}{P_{\text{DESIGN PT}}} \right) \times \frac{m \sqrt{\theta}}{\delta}_{\text{STALL}}} - 1 \right] \times 100\% \quad (3-7)$$

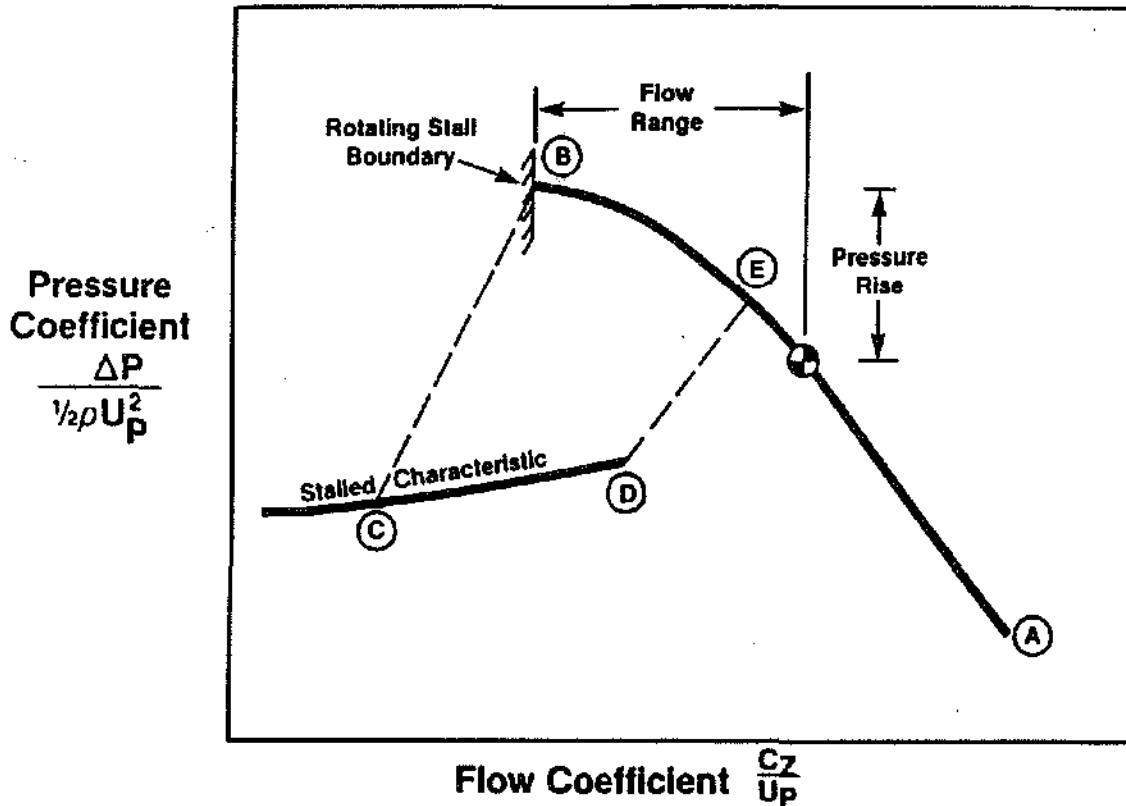


Figure 3.12 Performance Characteristics for Unstalled and Stalled Operation

Typical design values of stall margin range from 15 to 25%.

TRENDS IN COMPRESSOR AND FAN DESIGN

The general trends in compressor and fan design over the past 30 years (Figure 3.13) have been to higher speeds, higher spool pressure ratios, higher pressure rise per stage, higher aerodynamic loadings, lower aspect ratios, higher solidities, and improved configurations and blade shapes. Compressor pressure ratios for a single spool have been trending steadily upward. This is a result of the efficient use of higher blade speeds, variable stators, and bleed for off-design matching. Improved

materials and advanced mechanical design techniques are also being used.

Pressure ratios per stage (average loadings) have been increasing. This increase is partly because higher speeds are being used. But higher pressure ratios per stage are also because the non-dimensional loading (expressed as a static-pressure rise coefficient) has been increasing. Lower aspect ratios, plus higher-solidity and higher-stagger blading, are the major design advancements that make this possible.

The trend toward lower blading aspect ratios in multistage compressors is clearly seen. Average aspect ratios of about 1.4 are now common. The trend toward higher blading solidity in multistage compressors is also observed. Average solidities of 1.4 are now common.

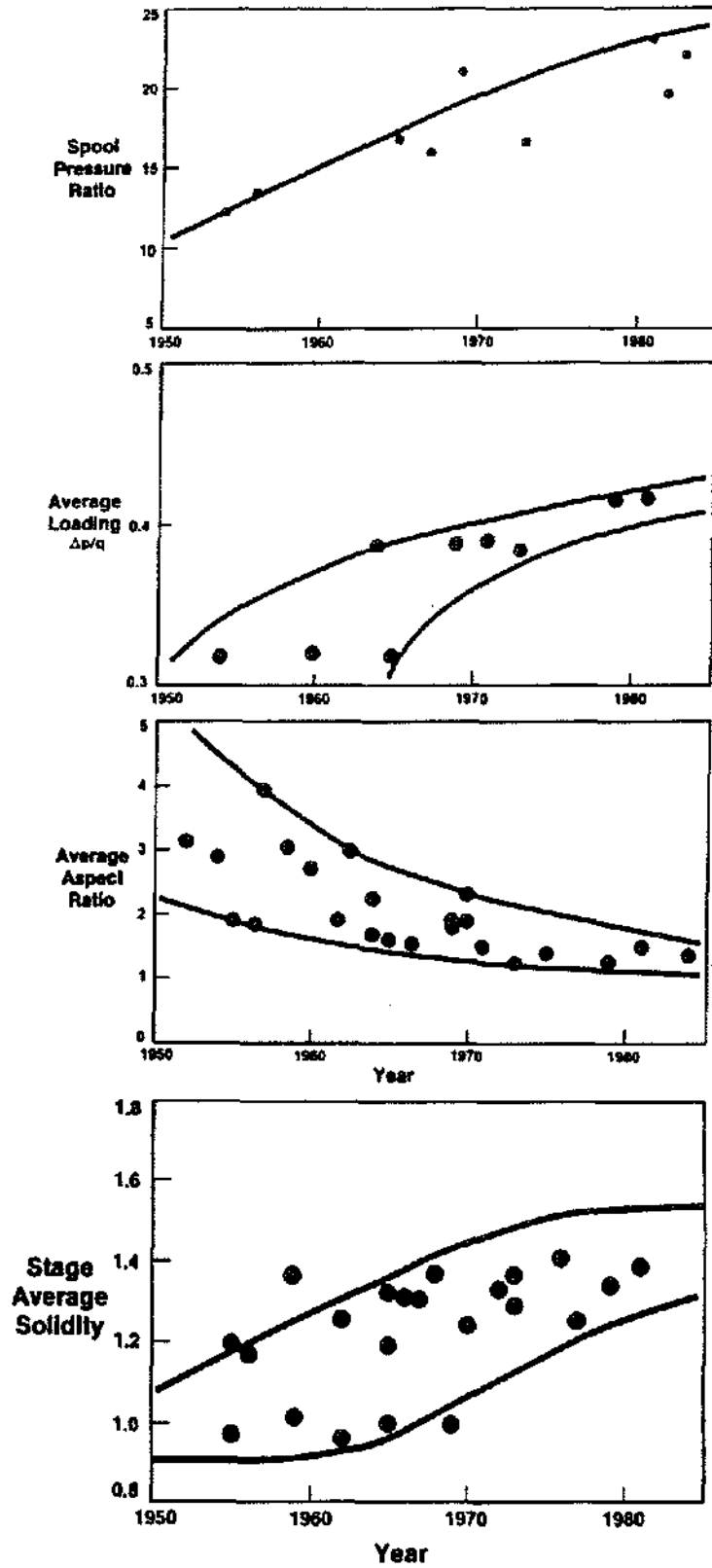


Figure 3.13 Compressor Design Trends

The trend toward higher tip speeds, higher pressure rise per stage and lower aspect ratios is shown for the first three core compressors in Figure 3.14. Each of the core compressors has a pressure ratio between 12:1 and 13:1. A time period of about 20 years is covered by these three designs.

The GE/NASA E³ core compressor is a recent design that continues the trends illustrated by the first three compressors. In this case, a pressure ratio of about 23:1 is developed in 10 stages, with even higher tip speeds and lower aspect ratio blading than used previously. A comparison of the J79 compressor rotor (1950s design) with the E³ compressor rotor (1980s design) in Figure 3.15 clearly shows the trend toward lower aspect ratio and higher solidities in the design of core compressors.

The generally beneficial effects of using lower aspect ratio blading are both aerodynamic and mechanical (Table 3.2). The historical trend toward lower aspect ratio designs results from designers exploiting these beneficial effects.

Table 3.3 gives more detail on the aerodynamic benefits given by lower aspect ratio blading. Most of the beneficial effects on efficiency are in themselves relatively small. And while the one bad effect, due to the thicker wall boundary layers, is fairly large, the sum of all the positive effects often gives lower aspect ratio stages better efficiency than higher aspect ratio designs. The increased stall margin achievable with lower aspect ratio blading results from many beneficial factors.

The flow in a multistage, axial-flow compressor is complex in nature because of the proximity of moving blade rows, the buildup of endwall boundary layers, and the presence of leakage and secondary flows. These regions of complex flows and associated high loss are shown in Figure 3.16. With the trends over the past two decades being to higher pressure rise per stage, higher aerodynamic loadings, higher speed, and lower aspect ratio, designers of advanced components are challenged to find configurations having improved aerodynamic performance while avoiding flow separation, increased loss, and stall margin penalties. For example, assessments of loss mechanisms suggest that approximately one-half of the total loss in the rear stages of a multi-stage compressor is associated with the endwall boundary layers. Thus, the trend toward lower aspect ratios increases the fraction of the total flow that is subjected to three-dimensional, endwall boundary layer effects. It becomes particularly important to devise ways to reduce endwall losses.

DESIGN AND ANALYSIS METHODS

The aerodynamic design of high-pressure, axial-flow compressors and high-thrust transonic fans is a very complex process. The flowfields, particularly in the endwall regions, are among the most complicated in engineering because of the presence of boundary layers, secondary flows, tip leakage, mixing, wake interaction, etc. The problem the designer faces is to orchestrate the large number of design choices (blade speed, number of stages, flowpath shape, vector diagrams, aspect ratio, solidity, stagger, Mach numbers, loading levels, and so forth) in such a manner as to achieve the desired pressure ratio and mass flow with adequate stall margin and high efficiency.

Designers of advanced compressors and fans are now challenged to find configurations that have increased durability along with improved performance. Simultaneously, they are asked to find design solutions that avoid weight or cost penalties. Compression systems also are increasingly being selected representing the best compromise between several often conflicting attributes. These attributes include efficiency, weight, length, and cost. The criterion used to select compressor design specifications is often an overall engine/aircraft system figure of merit such as thrust, weight, mission fuel burn, or direct operating cost. These FOMs are used rather than a factor that relates only to the compressor itself, such as pressure ratio per stage. Reliable design, analysis, and performance prediction methods are required to accomplish this optimization process.

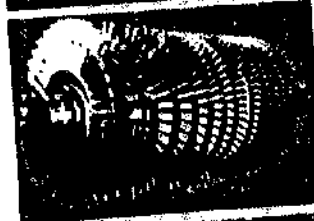
Compressors are designed by the indirect method. That is, first one defines the flowpath (casing and hub) radii and decides what thermodynamic and aerodynamic properties and work input (vector diagrams) one wants the air to have at each selected axial location (station) along the flowpath (see Figure 3.8). An iterative analysis is conducted in which the three conservation equations (mass, momentum, and energy) and state equation are satisfied at each station. Although there are no blades or blade shapes in the analysis, their presence is recognized by work input, turning ability, and loss. Then one designs the blades and vanes to achieve the desired thermodynamic and aerodynamic properties. The designer is constrained to achieve the non-negotiable items of overall pressure ratio and mass flowrate, discussed earlier. But, the designer is free to select negotiable items to achieve the desired performance. Negotiable items include flowpath, number of stages, number of blades/vanes, solidity, aspect ratio, vector diagrams, blade shape, etc.

**Energy Efficient
Engine (E³)**

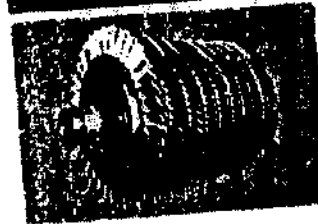
CJ805



CF6-50



CFM56



**Pressure
Ratio**

12.5

13

12

23

**Corrected
Tip Speed
(ft/sec)**

955

1180

1300

1495

Stages

17

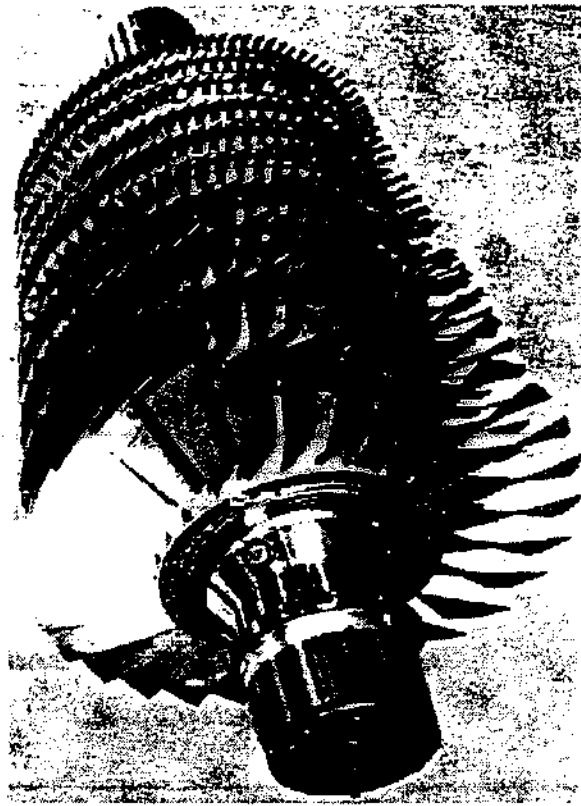
14

9

10

Figure 3.14 Compressor Design Trend

**E³ Rotor
(Early 80's)
23:1 P/P
10 Stages**



**J79 Rotor
(Late 50's)
12.5:1 P/P
17 Stages**



Figure 3.15 Comparison of J79 and E³ Rotors

EFFECTS OF LOWER ASPECT RATIO	
<u>Item</u>	<u>Effect</u>
• Durability	— More Rugged
• Number of Parts	— Fewer
• Cost	— Lower
• Weight	— About the Same
• Length	— About the Same
• Efficiency	— Often Better
• Stall Resistance	— Better

Table 3.2 Effects of Lower Aspect Ratio

AERO EFFECTS OF LOWER ASPECT RATIO		
<u>Item</u>	<u>Efficiency</u>	<u>Stall Resistance</u>
1. Higher Reynolds Number	Good	Good
2. Thicker Wall Boundary Layers	Bad	Good
3. Lower Annulus Wall Slopes	Good	Good
4. Lower Tip Clearance/Chord Ratio	Good	Good
5. Lower Axial Clearance/Chord Ratio	Good	Good
6. Lower Airfoil Thickness/Chord Ratio	Good	Good
7. Shocks More Oblique	Good	Good
8. Shrouding Not Needed	Good	—
9. Larger Twist Lean Angles	Bad	Bad
10. Better Airfoil Quality	Good	Good
11. Less Erosion	Good	Good
12. Smaller Relative Scale of Inlet Condition Nonuniformities	—	Good

Table 3.3 Aero Effects of Lower Aspect Ratio

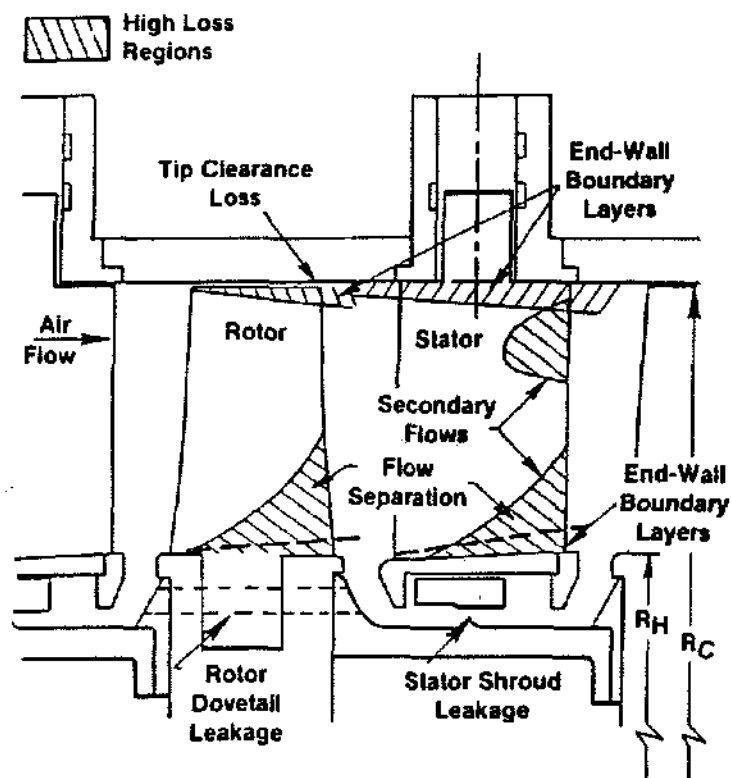


Figure 3.16 High-Loss Regions in Multi-Stage Core Compressors

No single solution of the equations of motion can, at this time, fully and exactly represent the flowfield. Consequently the designer must rely on data correlations and approximate solutions. Two very successful design correlations are stall margin and efficiency potential.

Stall Margin Correlation As discussed earlier, rotating stall and surge phenomena in axial flow compressors rank among the most serious problems in turbomachinery aerodynamics. Consequently, it is important to have a reliable method to evaluate the stall margin capability of a new compressor during the early preliminary design phase. The aerodynamic designer must be assured that critical design features such as blade speed, number of stages, aspect ratio, solidity, through-flow Mach number, and blade tip clearance are consistent with the stall margin requirements.

To satisfy this need, a stall margin correlation has been developed that gives the peak pressure rise coefficient achievable in the multistage environment where stall is usually caused by flow breakdowns in the endwall region. This is called CUS (Compressor Unification Study) at GE. Peak recover was found to be a function of a cascade geometrical parameter analogous to that used to correlate diffuser performance, with additional

dependence on tip clearance, bladerow axial spacing, Reynolds number, and the type of vector diagrams employed.

Since a stage of an axial flow compressor functions by diffusing the working fluid, its limiting pressure rise ought to be a function of cascade geometrical parameters that are analogous to those used to correlate two-dimensional diffuser data. It should be recalled that the diffusion process is one in which, as area increases, the velocity of a fluid decreases and the static pressure increases. This 2-D diffuser performance is often presented as shown in Figure 3.17, where contours of constant static-pressure-rise coefficient are plotted versus area ratio and length-to-inlet-width ratio. For a given diffuser length-to-inlet-width ratio, there is an area ratio for which the static-pressure rise coefficient is at a maximum. Further increases in area ratio only increases the amount of separated flow and actually decreases the pressure rise. In a compressor cascade the area ratio experienced by the fluid is not fixed by the blade geometry alone. Instead, it increases when the cascade is throttled to higher incidence angles and lower flow rates. Eventually the cascade stalls, and a maximum static-pressure-rise is obtained. In either a diffuser or a compressor cascade, both the maximum static-pressure rise and the

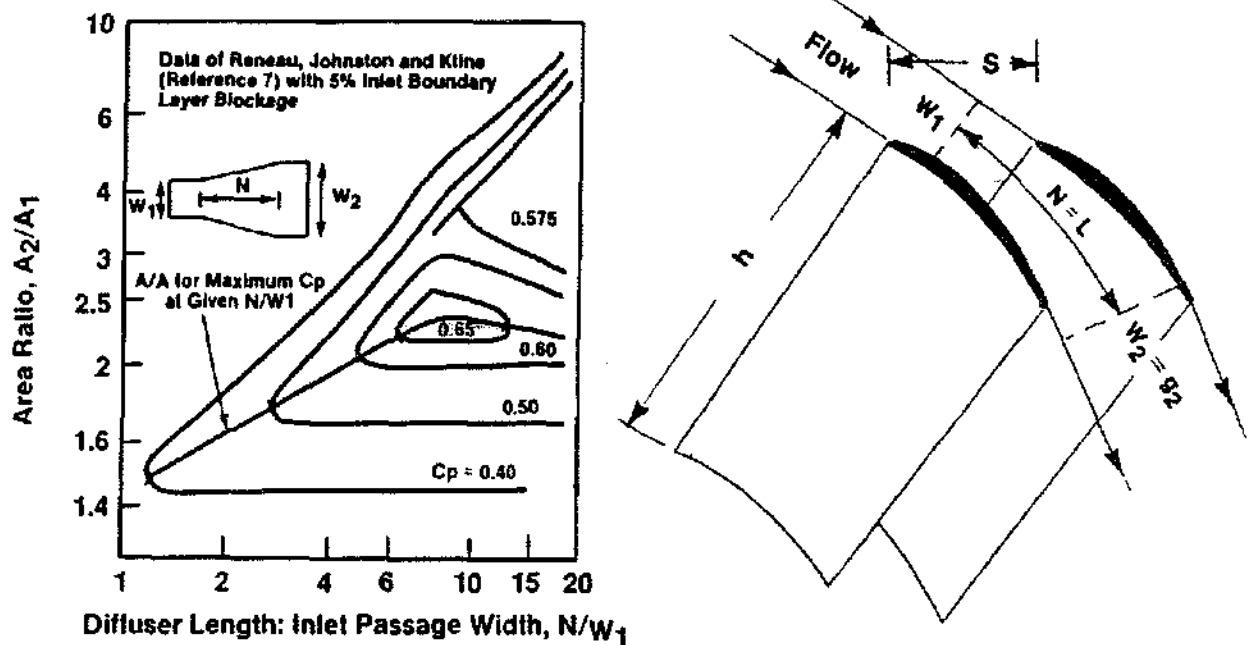


Figure 3.17 Diffuser Analogy for Compressor Bladerow

corresponding limiting area ratio should be functions of an appropriately formulated ratio of the diffusion length to some characteristic dimension of the flow's cross-sectional area. For a compressor cascade it is the exit flow area that remains roughly constant over the range of operation, while flow area at the inlet varies. Thus a correlating parameter for compressors is used that consists of the ratio of diffusion length to a cascade exit dimension (rather than an inlet dimension as is done for diffusers). The parameter is the arc, or meanline, length of the cambered airfoil divided by the staggered spacing at the cascade trailing edge, L/g_2 , involving aspect ratio and solidity. The similarity between diffuser geometry and compressor blading geometry is shown. This concept forms the basis of the compressor stall margin correlation.

The correlation of stalling static-pressure-rise coefficient versus diffusion-length to exit-passage-width parameter is shown in Figure 3.18. The correlation gives designers a means of predicting the maximum achievable pressure rise for well-designed axial flow compressors. Note that as solidity increases and aspect ratio decreases, the maximum pressure-rise capability of the compressor stage increases. This is the reason for the trend toward high solidity, low aspect ratio compressors.

Efficiency Potential Correlation A preliminary design model capable of predicting the maximum efficiency potential of an axial-flow compressor has also been developed. The model considers blade profile losses, leading edge bluntness and passage shock losses, endwall boundary layer losses, and part-span shroud losses (Figure 3.19). The model does not account for losses associated with off-design operation, blading unsuited to the aerodynamic environment, or poor hardware quality. The loss model is constructed using rational fluid-dynamic elements, such as boundary layer theory, wherever feasible in an attempt to minimize empirical influences. However, some empiricism inevitably enters.

Design parameters that affect the efficiency are numerous. They include vector diagram shape, aerodynamic loading level, aspect ratio, solidity, clearances, airfoil maximum and edge thicknesses, annulus area contraction, Mach number, Reynolds number, airfoil surface finish, and part-span shroud placement. The efficiency model is found to be in satisfactory agreement with multistage compressor experience that covers a wide range of these design parameters.

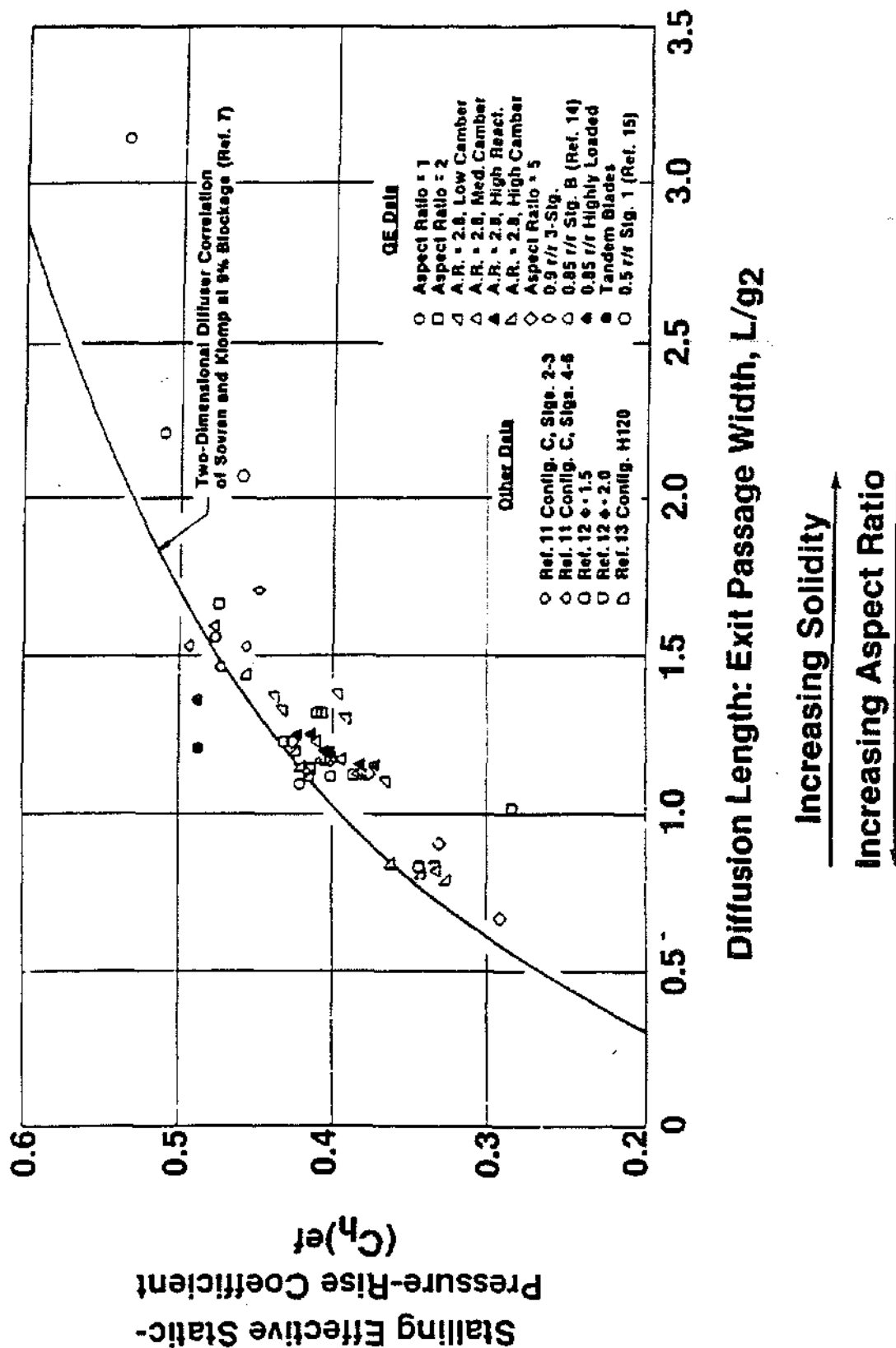


Figure 3.18 Stall Margin Data Correlation

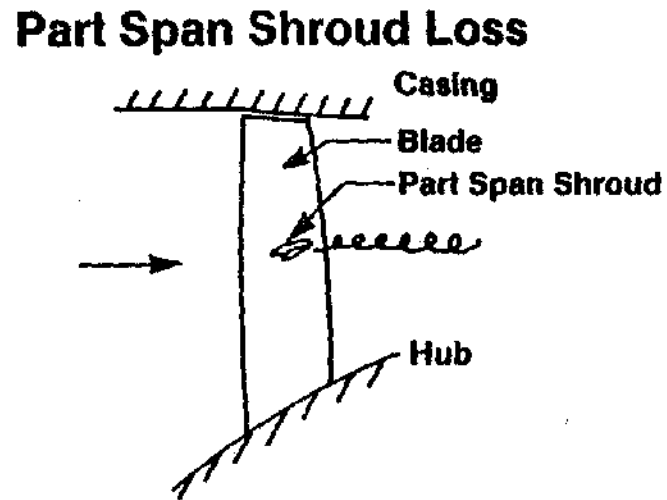
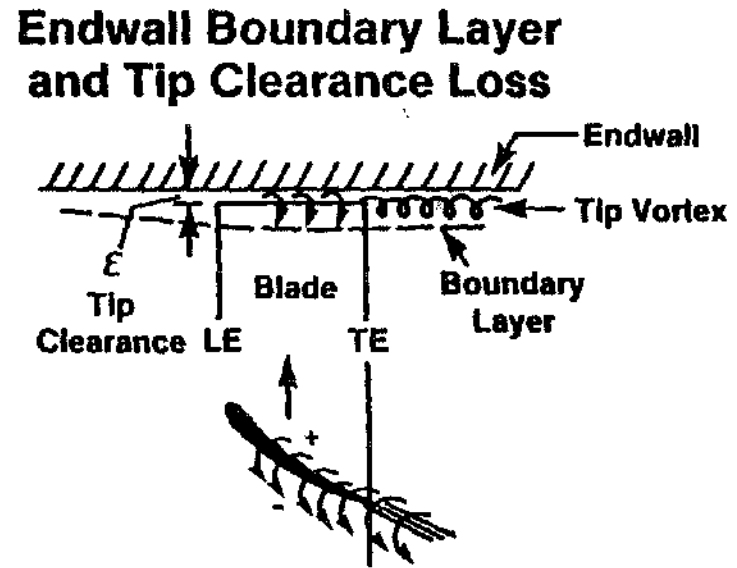
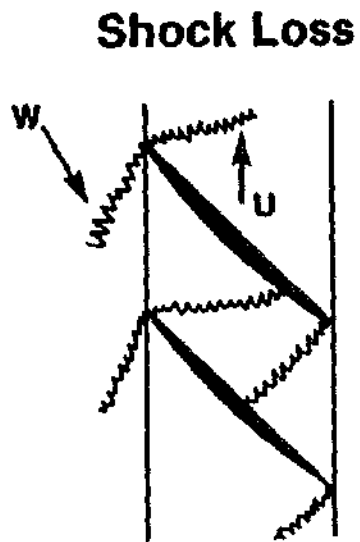
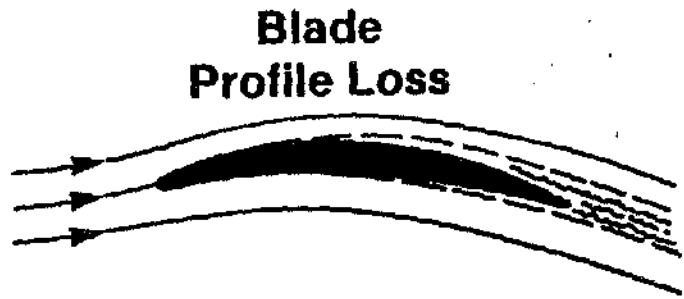


Figure 3.19 Aspects of the Efficiency Potential Correlation Model

Axisymmetric Analysis After selecting the approximate compressor configuration and determining that stall margin requirements have been met, the designer then begins the detailed design of the compressor using a so-called axisymmetric (throughflow) analysis. With this analysis the designer computes the thermodynamic and aerodynamic properties of the fluid at each axial station in the compressor. The radial variations of the fluid properties are computed in detail. The analysis is conducted by assuming circumferential averages so that no blade-to-blade information is computed. As with any sound aerodynamic analysis, the conservation equations of mass (continuity), momentum, and energy are satisfied along with the equation of state at each axial station along the compressor flowpath to determine the distribution of flow properties from hub to casing.

The calculation procedure centers around the solution of the radial equilibrium equation. The radial equilibrium equation is simply the radial component of the momentum equation written in a relatively cylindrical coordinate system r, θ, Z in which θ is measured relative to the rotating frame of reference and Z is measured along the compressor axis. It is the function of this equation to describe the radial variation of flow properties at each station. All phenomena affecting the momentum must be accounted for, including meridional streamline curvature, blade thickness blockage gradients, circumferential vorticity components, and non-radial blade elements. There may even be vorticity, entropy gradients, and stagnation enthalpy gradients in the fluid.

The iterative calculation scheme used, called CAFD (circumferential average flow determination), is iterative. The designer specifies the radial distribution of rotor work input and stator turning that is desired stage-by-stage. CAFD computes the vector diagrams (Figure 3.9) and other information associated with these specified quantities. How CAFD fits into the design scheme is shown schematically in Figure 3.20.

Cascade Analysis and Blade Design After the radial distributions of air angles and velocities (vector diagram information) are determined by CAFD, the blading can be designed. This is where the cascade analysis is utilized to give the flowfield solution between the blades and to find the pressure (velocity) distribution along the airfoil surface.

First a trial airfoil shape is constructed as follows: incidence angles, i , and deviation angles, δ , are selected so that the slope of the airfoil meanline at the leading edge and trailing edge can be established relative to the air angles (Figure 3.10). Then the meanline shapes and thickness distributions are defined to obtain an airfoil shape.

Incidence angles are selected to place the airfoil in the low-loss region of its performance envelope. Min-loss incidence is generally a few degrees negative for thin airfoils. Generally $-5^\circ \leq i \leq 5^\circ$.

Deviation angles present more of a problem because the air is not discharged at the trailing edge meanline angle, but rather at an angle which depends upon blading camber and solidity. Often, the semi-empirical Carter's rule is employed as a first guess where

$$\delta = m \phi \sqrt{\sigma} + X \quad (3-8)$$

where m is a deviation coefficient and X is an experimental adjustment factor to allow better correlation with experimental data. Generally $5^\circ \leq \delta \leq 20^\circ$.

With a trial airfoil constructed the pressure distributions on the airfoil surface are computed by the Cascade Analyses Streamline Curvature (CASC) computer program. This is shown schematically in Figure 3.20. The designer then looks at the "goodness" of the pressure distribution, some examples of which are shown in Figure 3.21. The magnitude of the leading edge loading is examined. Examples of nominal incidence and incidence that is too low or high are shown in Figures 3.21a, b, and c, respectively. Likewise the magnitude of the peak suction surface velocity at B and the diffusion on the suction surface B-C-D are examined. Adjustments in the airfoil shape (incidence angle, meanline shape or thickness distribution) are then made until the desired pressure distributions are achieved.

This type of analysis is conducted for every airfoil section that makes up each IGV, rotor, and stator in the compressor. The design process is an iterative one (Figure 3.20). After the blading is designed, the effect of the blading is input back into CAFD and the axisymmetric analysis is repeated, with that result feeding into CASC to redesign the blading. Another iteration loop "SECOND", shown in Figure 3.20, is used to compute secondary flow, but this is too complex for this discussion.

For transonic fans, like the E³ fan shown in Figure 3.22 and front stages of high pressure compressors, the additional features of shock waves must be included in the analysis.

High bypass fan blades typically have large amounts of radial twist and hub slope. The flowfield relative to the rotating blades varies from transonic/supersonic in the outer region to subsonic near the hub as shown in Figure 3.23. Different airfoil shapes are required in each flow regime to minimize losses and provide adequate passage areas. Incidence and deviation angles are

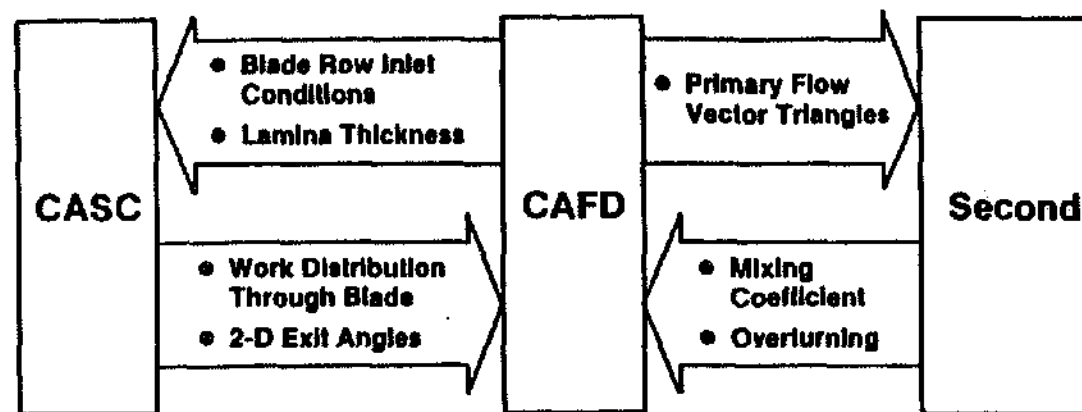
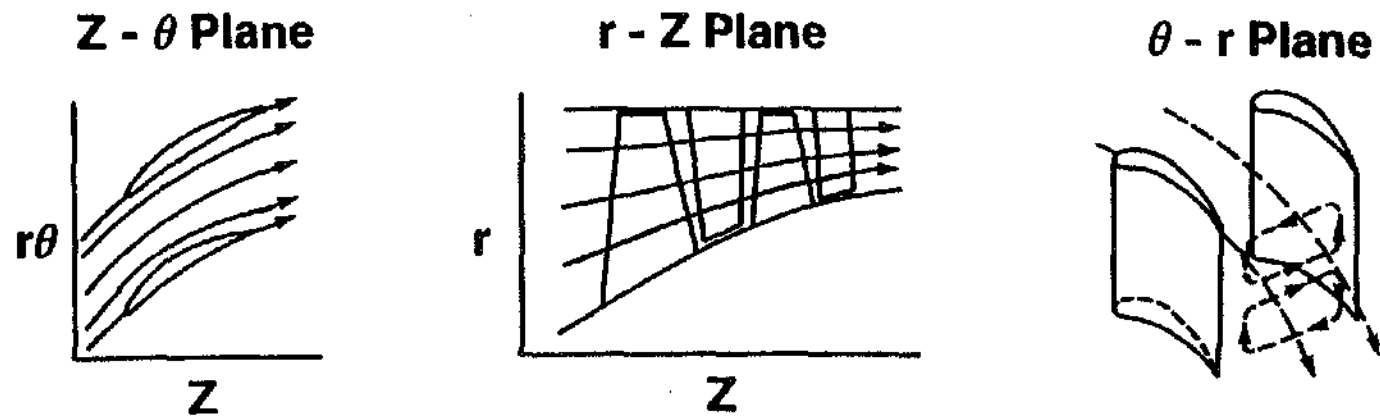
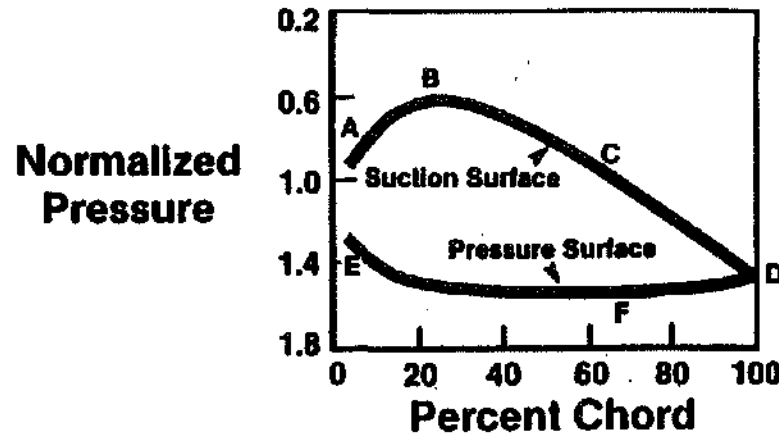
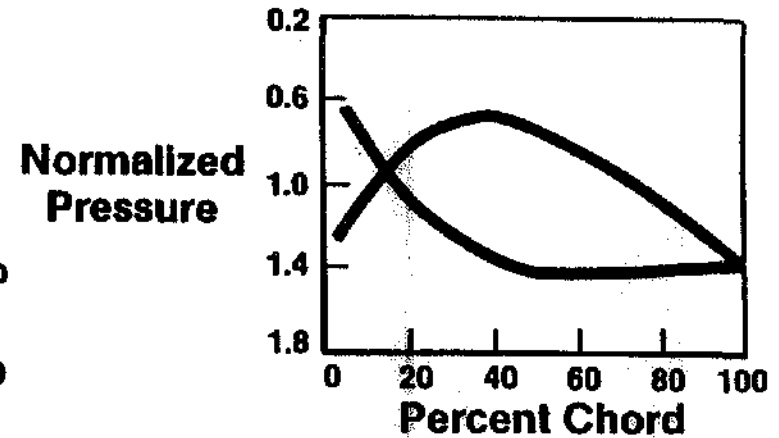


Figure 3.20. Turbomachinery Aerodynamic Analysis Quasi 3-D System

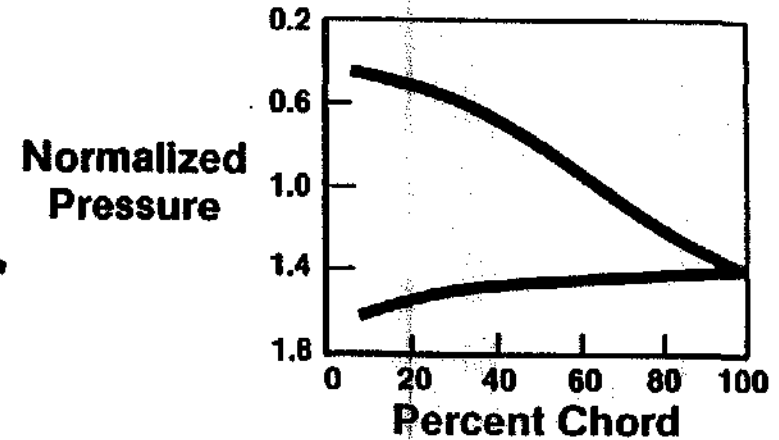


A) Nominal Incidence



B) Incidence too Low

- A-E Measure of Leading Edge Loading
- B Peak Suction Surface Velocity
- C Diffusion on Suction Surface
- F Pressure Surface
- D Kutta Condition Satisfied at Trailing Edge



C) Incidence too High

Figure 3.21 Blading Design-Surface Pressure Distribution

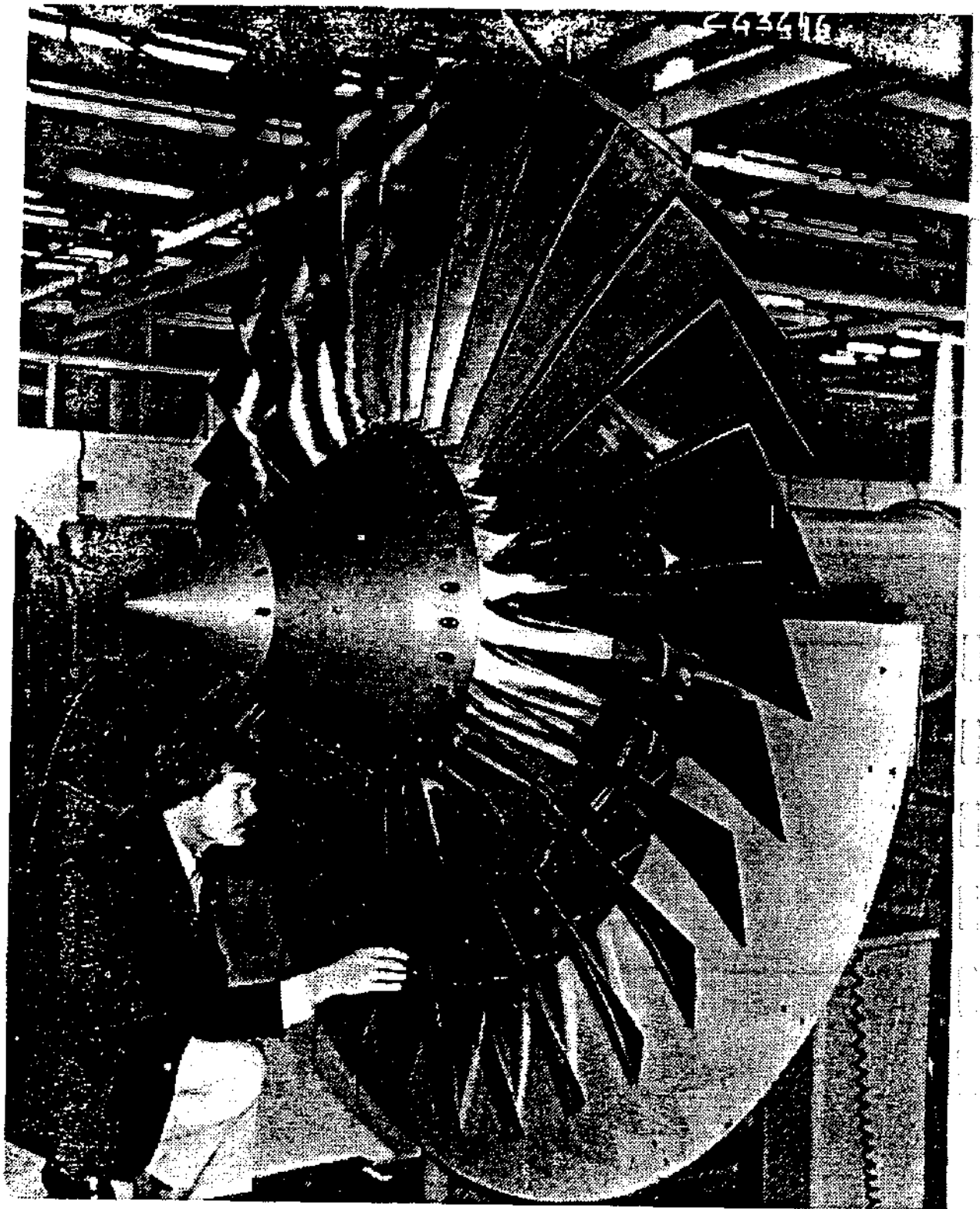


Figure 3.22 E3 Fan

Relative Inlet Flow

Supersonic
 $M' = 1.4$ to 1.1

Transonic
 $M' = 1.1$ to 0.9

Subsonic
 $M' = 0.9$ to 0.7

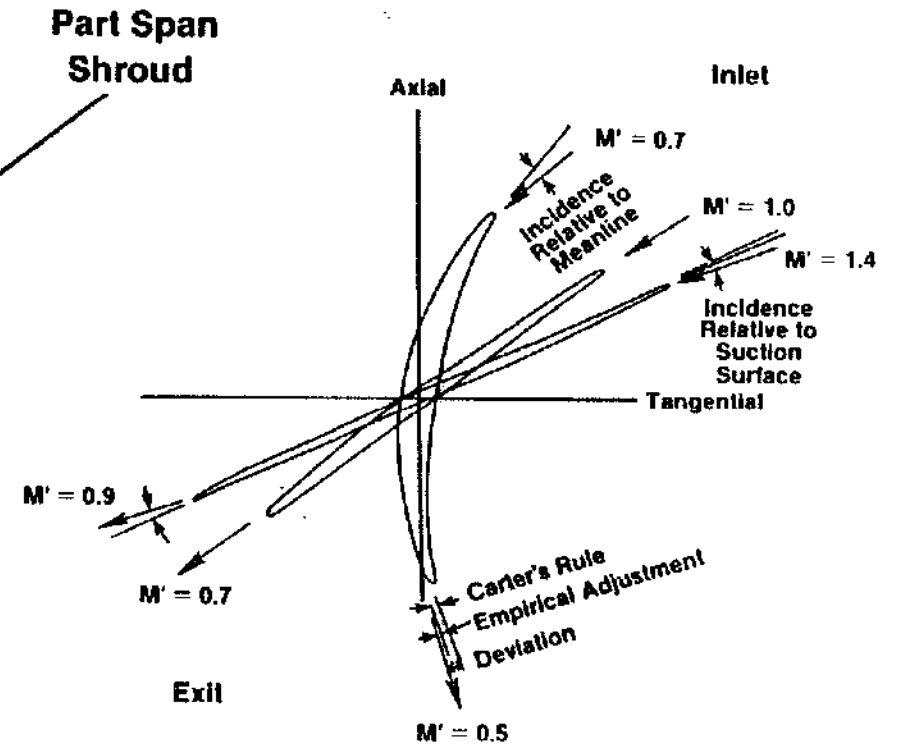


Figure 3.23 E³ Fan Blade

set by empirical correlations that provide smooth inflow and recognize effects of radius change and streamtube convergence.

Fan and Prop Fan Configurations A ducted, high bypass ratio, turbofan engine (Figure 3.1) accelerates a large mass of air to a relatively low velocity. This is a primary factor contributing to the turbofan's substantial efficiency improvement over turbojet engines, which accelerate a small mass at high velocity. Typical bypass ratios of modern engines are in the range of 5:1 to 8:1.

The GE/NASA E³ (Energy Efficient Engine) fan is an example of an advanced, high-bypass-ratio, single-stage design with a unique fractional-span stage arrangement that provides additional core-stream pressure ratio and particle separation. The E³ fan system, shown in Figure 3.24 features a combination bypass vane and strut frame, fan containment, and swept and leaned core OGVs. Fan specifications include: inlet radius ratio of 0.342, design tip speed of 1350 ft/sec, bypass pressure ratio of 1.65, inner 22% of flow supercharged to a pressure ratio of 1.67, bypass ratio of 6.8, a specific flow rate of 42.8 lbm/sec-ft².

New and improved blading arrangements that are finding increasing use include fractional stages for fans, integration of fan inner outlet guide vanes and the compressor inlet (goose-neck) duct, plus improved airfoil section shapes. The E³ fan uses a fractional hub booster stage. The feature whereby some of the flow from the fractional stage returns to the bypass stream provides a self-adjusting interspool bleed that protects the fractional stage from stall during engine transients without requiring variable geometry. It also provides a path for centrifuging dirt or FOD debris out of the core compressor inlet flow. Highly swept and leaned fan outlet guide vanes are used to guide the flow into the gooseneck inlet duct of the core engine without incurring excessive hub Mach numbers.

The propfan engine can increase the mass flow 5 to 6 times over that of modern turbofans, thus providing the potential for even greater propulsive efficiency (Figure 3.25). The efficiencies of both single-rotation (SRP) and counter-rotation propfan engines (CRP) are shown.

Figure 3.26 shows a General Electric Unducted Fan Engine (UDF). The bypass ratio of this engine is 35:

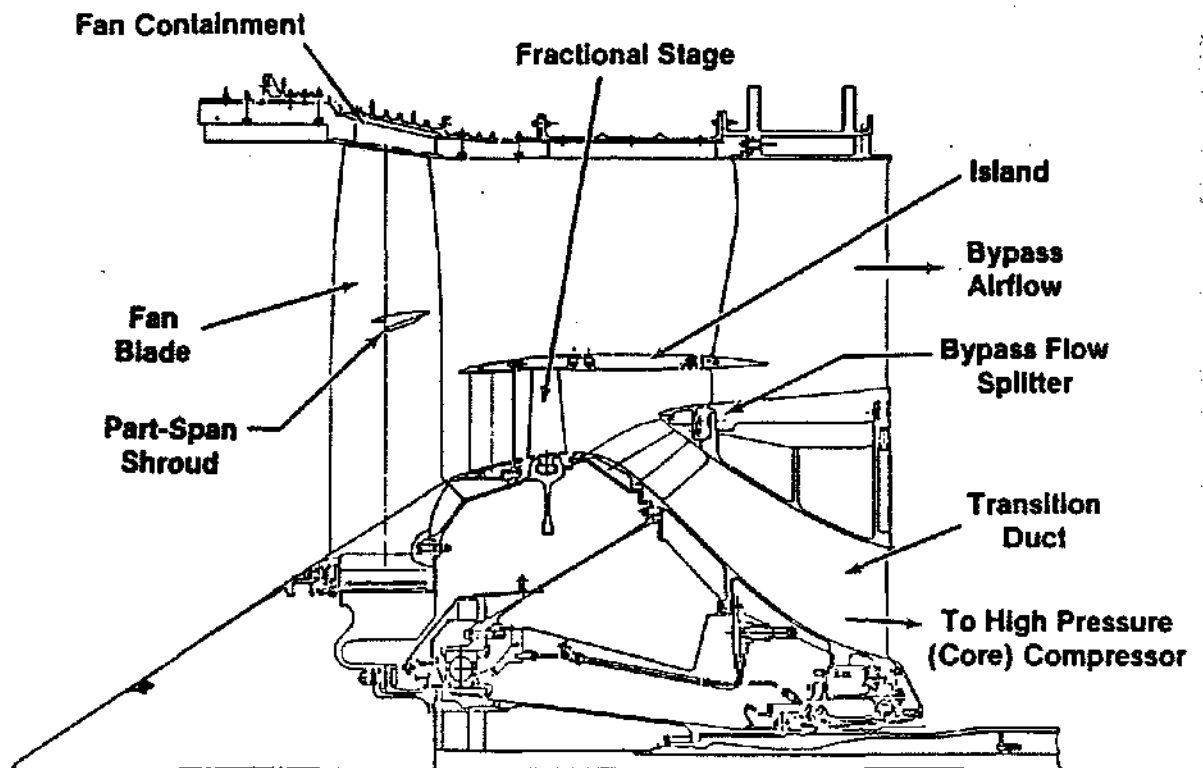


Figure 3.24 Energy Efficient Engine (E³) Fan System

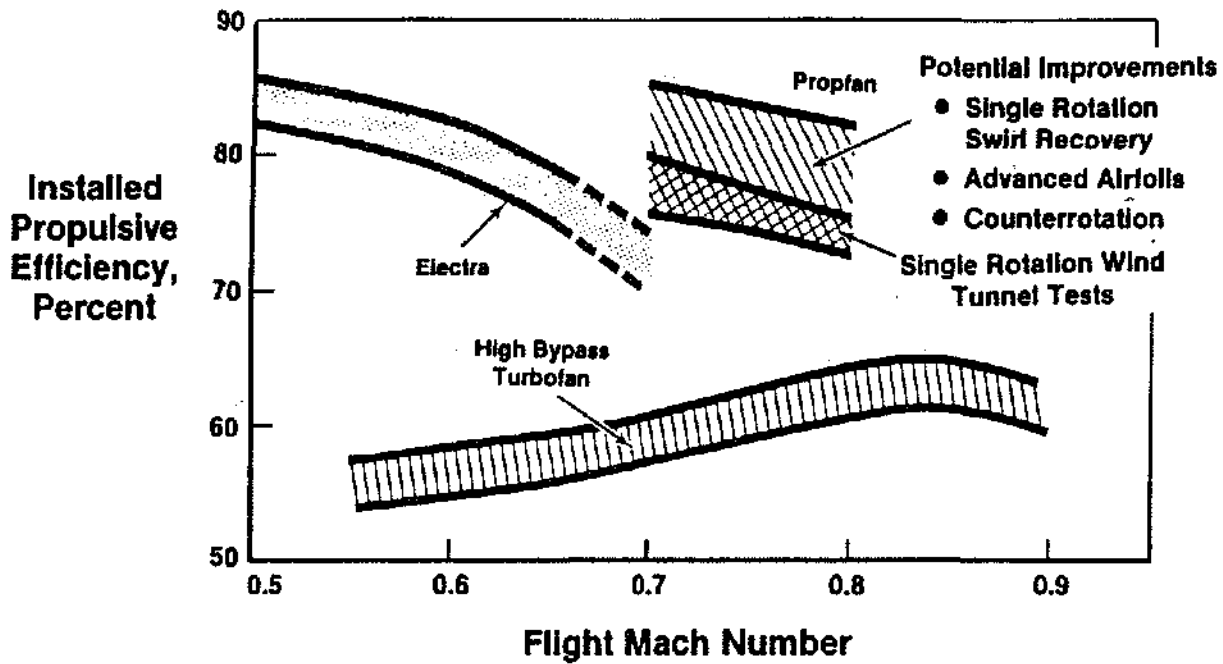


Figure 3.25 Proptan Efficiency

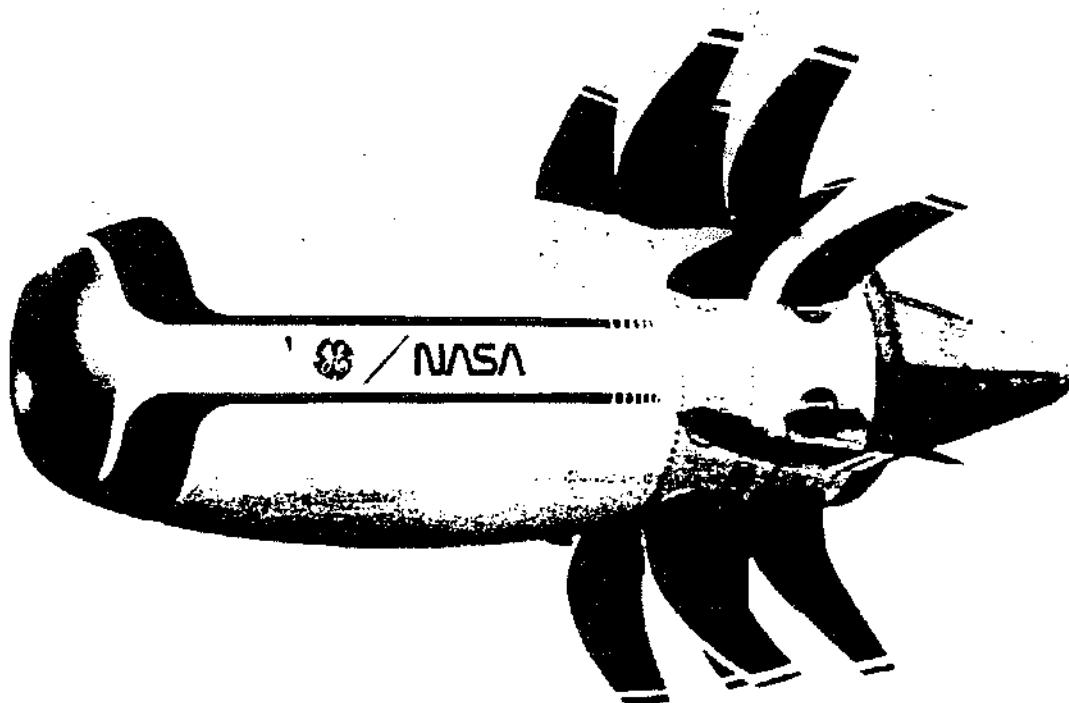


Figure 3.26 Unducted Fan Engine

Note the counter-rotating blades near the rear of the engine. The UDF is driven by a twin-spool core engine with a low-pressure counter-rotating turbine (Figure 3.27). In a conventional turbine the nozzle sees about as much torque as the rotors. In the UDF the turbine blades are rotating at the same speed but in opposite directions, so the effect is that of doubling the speed impact on the turbine. Thus, the design yields high power output with relatively low rotational speeds and no gearbox. Due to its variable pitch blades, the UDF retains thrust reversing capability.

To appreciate the impact of this design on fuel economy consider the following. If one started with a turbofan having a bypass ratio of six, then took the same core (all else being equal) and made a UDF out of it, the anticipated results would be 25% better SFC, a direct result of the UDF's extremely high bypass ratio.

VARIABLE GEOMETRY, CLEARANCE, AND LEAKAGE

Multi-spool, Variable Geometry and Bleed For better performance, the rotational speeds of the fan and compressor usually need to be different. In general the high pressure compressor (HPC) runs about twice as fast as the fan. This is accomplished by attaching the compressor and fan to different spools or shafts which run concentric to each other. Thus, in the dual spool configuration shown in Figure 3.28, the HPC is connected to the high pressure turbine by an outer spool and the fan/booster are connected to the low pressure turbine by an inner spool. In some configurations, three concentric spools are used.

Variable stators and inlet guide vanes are constructed so that the stagger angle of the vane can be varied in

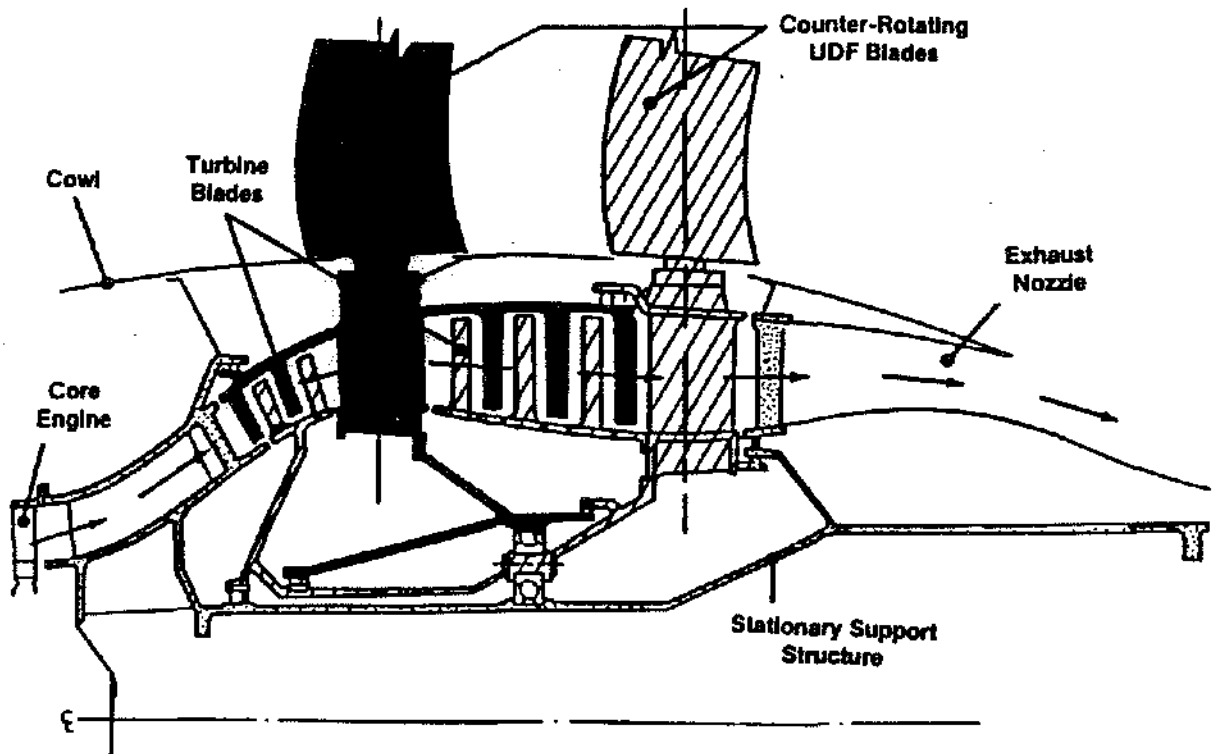
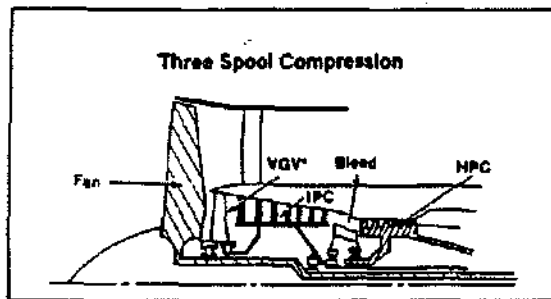
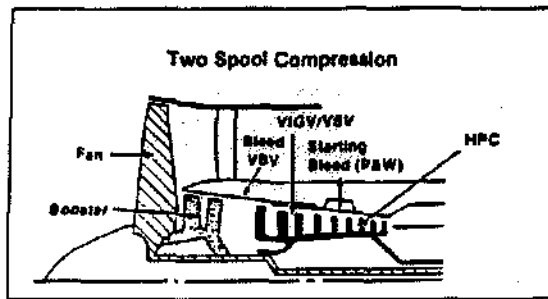


Figure 3.27 UDF™ Counter Rotation Schematic



HPC - High Pressure Compressor
IPC - Intermediate Pressure Compressor

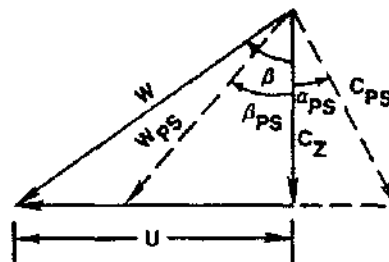
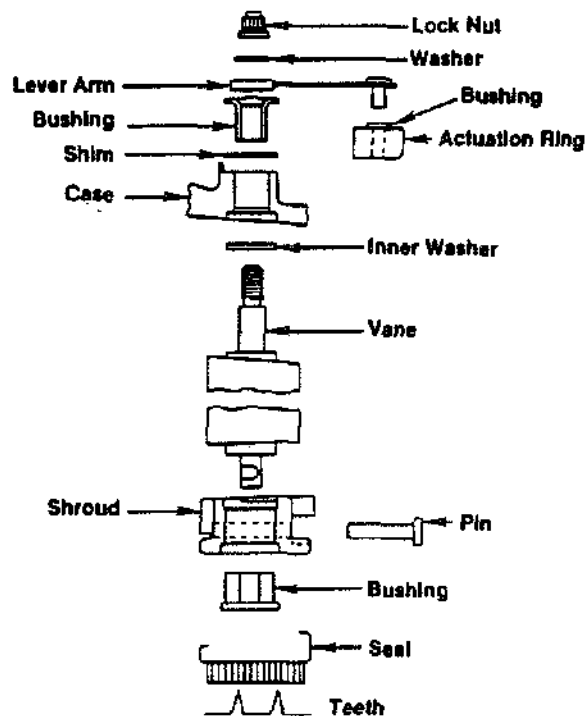
Figure 3.28 Multi-Spool Configurations

controlled fashion. This allows the vane to be re-aligned to the changing air angles that occur as the operating condition of the compressor or fan changes. An expanded view of a variable stator system is shown in Figure 3.29. The variable vane is rotated by means of the lever arm. These lever arms are attached to a ring on the outside of the compressor case Figure 3.30.

An example of a vector diagram showing the change in relative air angle and relative Mach number into the first stage rotor for two levels of preswirl is also presented in Figure 3.29. A variation in swirl from 0 to α_{ps} produces the change in W and β shown.

Bleed ports are shown in Figures 3.28 and 3.33. Bleed air is used for customer purposes, for turbine cooling, for active clearance control and in engine starting.

The need for variable geometry, multi-spoils, bleed, or some combination of them can be seen by considering the engine-start situation. At low rotational speeds the compressor cannot put as much work into the air as it can at high speed, and consequently cannot compress the air as much. The fixed area of the rear stages then limits the amount of air that can be pumped. The front stages try to pump the flow and in the process are back-



Effect of Variable IGV on Rotor Inlet W & β

— No Preswirl
--- Preswirl

Figure 3.29 Variable Stators and IGV's

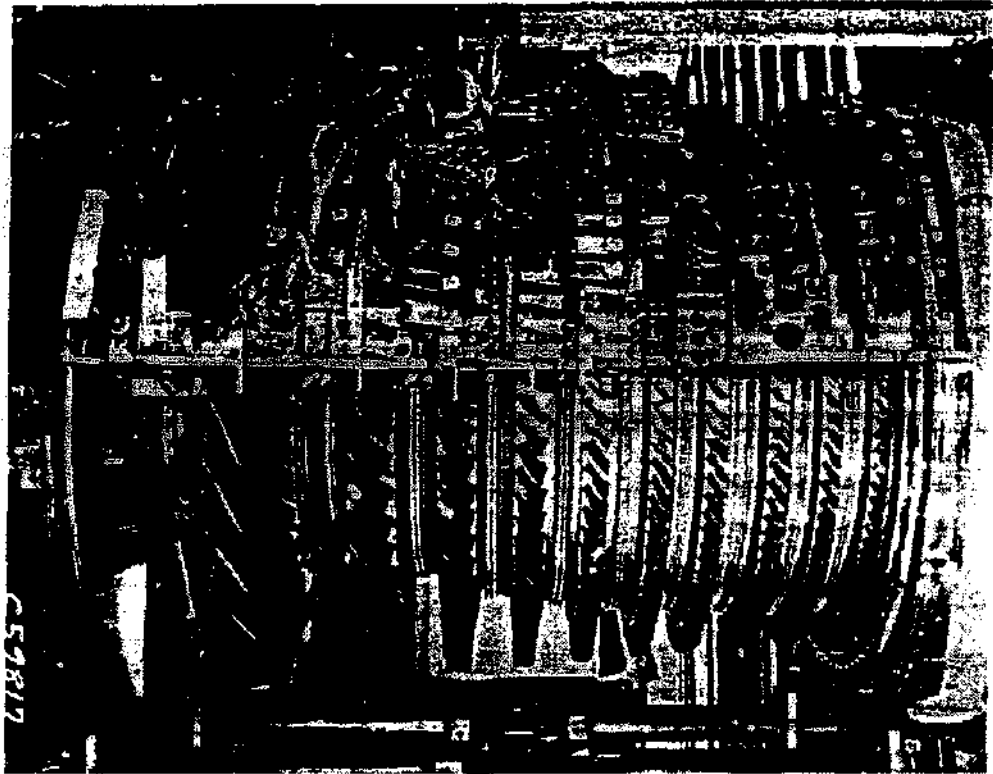


Figure 3.30 Compressor Rotor and Case

pressured trying to force the less-dense air through the rear stages. Mid-stage bleed allows this excess mass flow to be removed and the front stages to pump. As speed increases, work input increases, the air is compressed and goes through the area of the rear stages. At this point, bleed is no longer required. Variable geometry can also be used to control pumping in the front block. The higher the pressure ratio across a given block of stages on the same spool, the more severe the problem.

Leakage in Compressors Aircraft gas turbine engines have a large number of locations where air leakage can occur and the cumulative effect of leakage on engine power, thrust and fuel usage can be significant. Typical leakage paths are shown in Figure 3.34. In order to preserve efficiency in modern engines, which can have very high overall pressure ratios in the compression system (e.g. 38:1), close attention must be paid to leakage, seals and clearance. To compound the problem, evidence from airline reports notes that a typical high bypass ratio engine has an SFC increase of about 1 to 1 1/2% per year. Periodic overhauls do not fully recover this efficiency loss. The final result can be an engine with an

SFC 3 to 10% higher than that of a new engine. Sealing clearances also have a significant effect on compressor stall margin and are directly responsible for thrust droop.

Primary gas path seals perform two functions. They minimize gas recirculation between the blade tips and the wall for unshrouded airfoils, between shroud seals and labyrinth teeth, and across blade dovetail rotors and platforms. Primary gas path seals also minimize gas leakage out of the primary gas path (across flanges, variable vane pivots, and compressor end seals).

The leakage of gas across the airfoil tip from the pressure surface to the suction surface and the subsequent interaction with the endwall boundary layer of the primary gas stream and the production of secondary flows can produce substantial loss in efficiency and stall margin. In one research compressor data were obtained at two levels of tip-clearance-to-blade-height ratio, 1.38% and 2.8%. This increase in tip clearance costs 1.5 points in peak efficiency, 11.0% in stalling flow coefficient (flow range) and 9.7% in peak pressure rise relative to the nominal clearance.

Consequently, designers go to great length to minimize leakage effects. An advanced compressor shown in Figures 3.30 through 3.35 illustrates these measures. Figure 3.30 shows a compressor with the upper half of the split casing removed. The rotor blading and the labyrinth seal teeth are visible. The lower half of the casing shows the linkage mechanism for the variable stators and several bleed ports. Figure 3.31 shows the upper half of the casing. The stator vanes, the stator shrouds, and the shroud seal rub strips are visible. Figure 3.32 shows the IGVs, rotors, stators, stator shrouds, seal, and seal teeth.

Clearance Control The need for tight clearance from an aerodynamic perspective has already been established. One way to achieve this is through active clearance control. The variation in clearance between the casing and the rotor during engine operation is shown in Figure 3.36. The transient thermal response of the casing and the rotor and the centrifugal loading of the rotor are two of the most important factors in setting the final cruise clearance.

In general, the thermal response of the casing and the rotor are not the same because of differences in mass, cooling-air circulation, heat transfer, and material. The case tends to have a much faster thermal response to the gas stream temperature than the rotor. The rotor growth is initially due to centrifugal force during acceleration. If assembly clearances are too small, a rub will occur in the initial part of the acceleration due to the centrifugal force effect (Figure 3.36). On deceleration, the relatively fast thermal response of the casing will cause rubs if full power is demanded after a period of low power, such as an aborted landing. This happens because the relatively fast case response has reduced clearance to a magnitude less than the rotor displacement due to centrifugal force.

If very close cruise clearances are going to be maintained, then some type of clearance control is needed to eliminate the rub potential. This can be accomplished by using bleed air to control casing and rotor temperatures, and thereby clearances. The compressor shown in Figure 3.32 uses bleed air to control casing temperatures (diameter) and rotor diameter (bore cooling).

Summary of Aerodynamic Design Considerations Advances in technology over the past 20 years have led to substantial reductions in size, compactness, and weight in the modern compression system. In addition, significant improvements in efficiency have been obtained. These improvements can be seen (Figure 3.37) in the comparison of the engine cross-section for the E³ engine and the CF6-50 scaled to the same thrust.

AIRFOIL PHYSICAL AND FUNCTIONAL MECHANICAL DESIGN

Fan and compressor airfoils are broadly divided between rotating blades and stator vanes. The function of the airfoils is to increase the air flow velocity and pressure while the stator vanes help compress the air and direct the airflow onto the next stage of rotor blades at the proper angle preventing separated flow/stalls. Variable stators were introduced to provide an optimum airflow angle of attack over a wide range of operating conditions. Figures 3.38 and 3.39 and Table 3.4 define airfoil and shroud nomenclature.

Basic blade configurations include cantilevered, shrouded, or pin-joint designs (see Figure 3.40). The class of design is characterized by high and low ranges of the following parameters:

	LOW	HIGH
Aspect Ratio	<2.0	>2.0
Inlet Radius Ratio	<0.50	>0.50
Aerodynamic Tip Speed	<1350 fps	>1350 fps

With these combinations, eight design classes are possible, although two classes are not very common (i.e., the low aspect ratio, low radius ratio, low tip speed class and the high aspect ratio, high radius ratio, high tip speed class). Table 3.5 shows examples of each of the remaining six classes of design.

The type of airfoil is characterized by section meanline shape and chordwise thickness distribution (see Figure 3.41). The four basic airfoil section types used in GEAE designs are:

AIRFOIL TYPE	PRIMARY APPLICATION
NACA .65 series	Subsonic relative Mach no.
Double circular arc (or bi-convex)	Transonic region (0.8 < Mn < 1.2)
Quarter sine	Supersonic relative Mach no.
Custom	Supersonic regime or erosion/bird ingestion limited

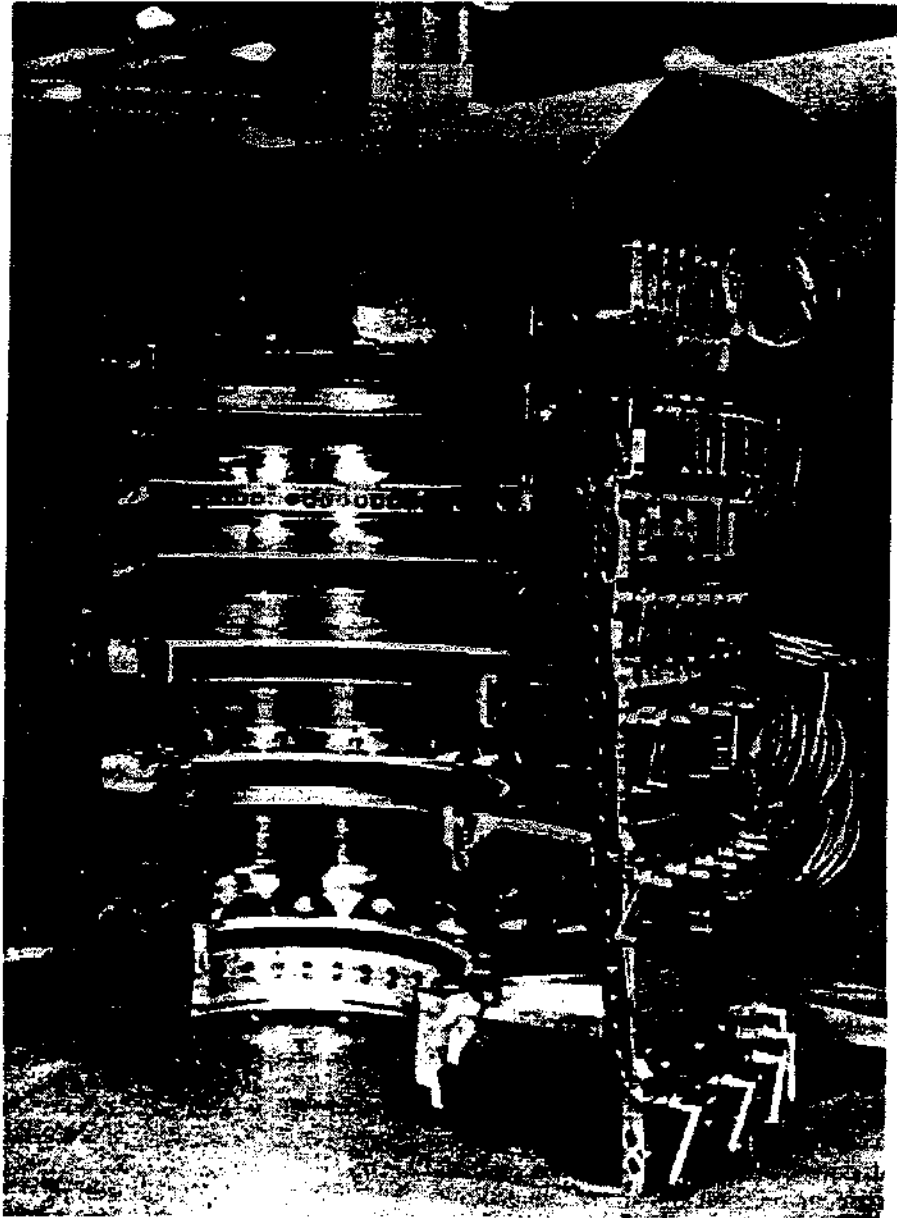


Figure 3.31 Compressor Case

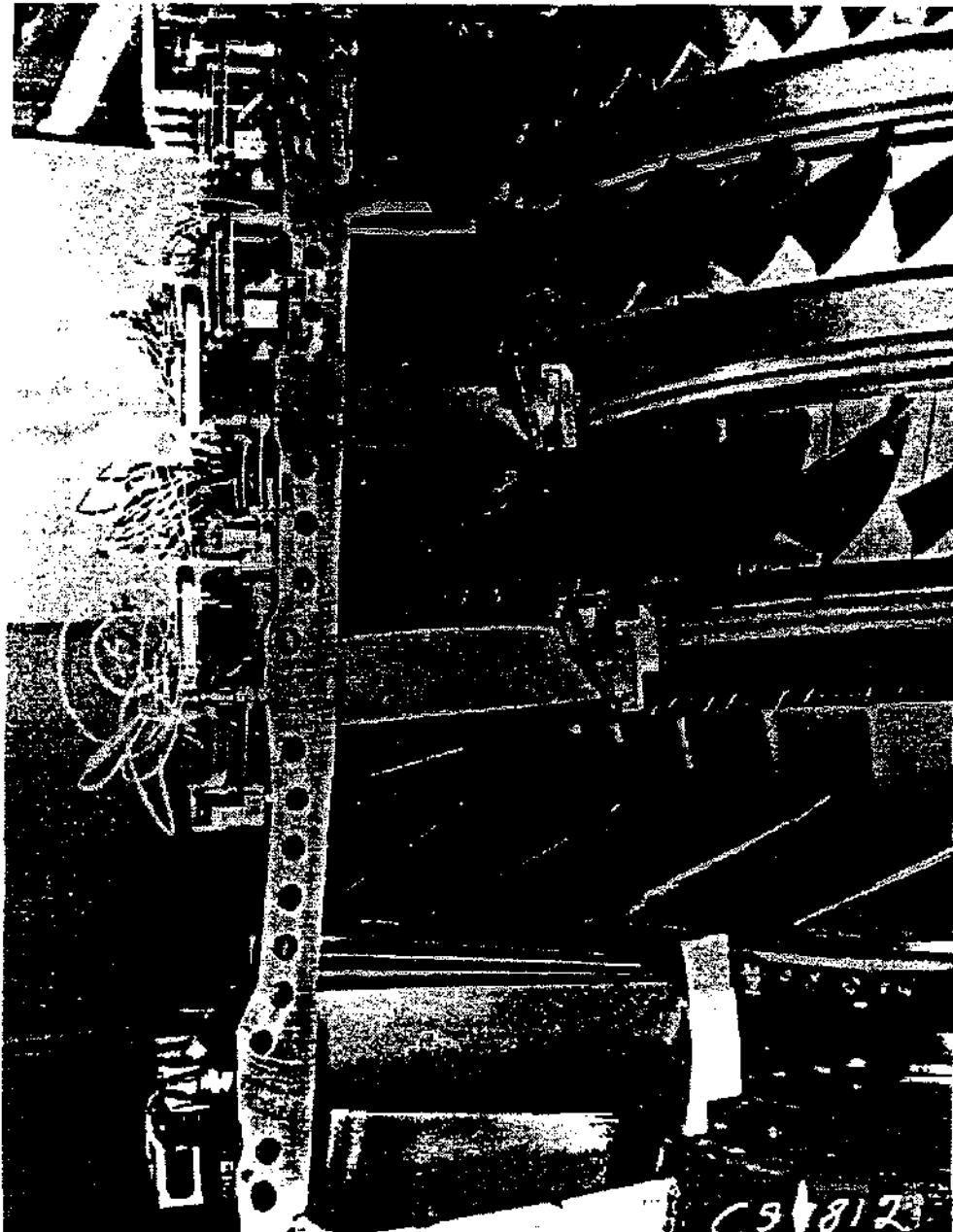


Figure 3.32 Compressor Blades, Vanes, and Shroud/Seals

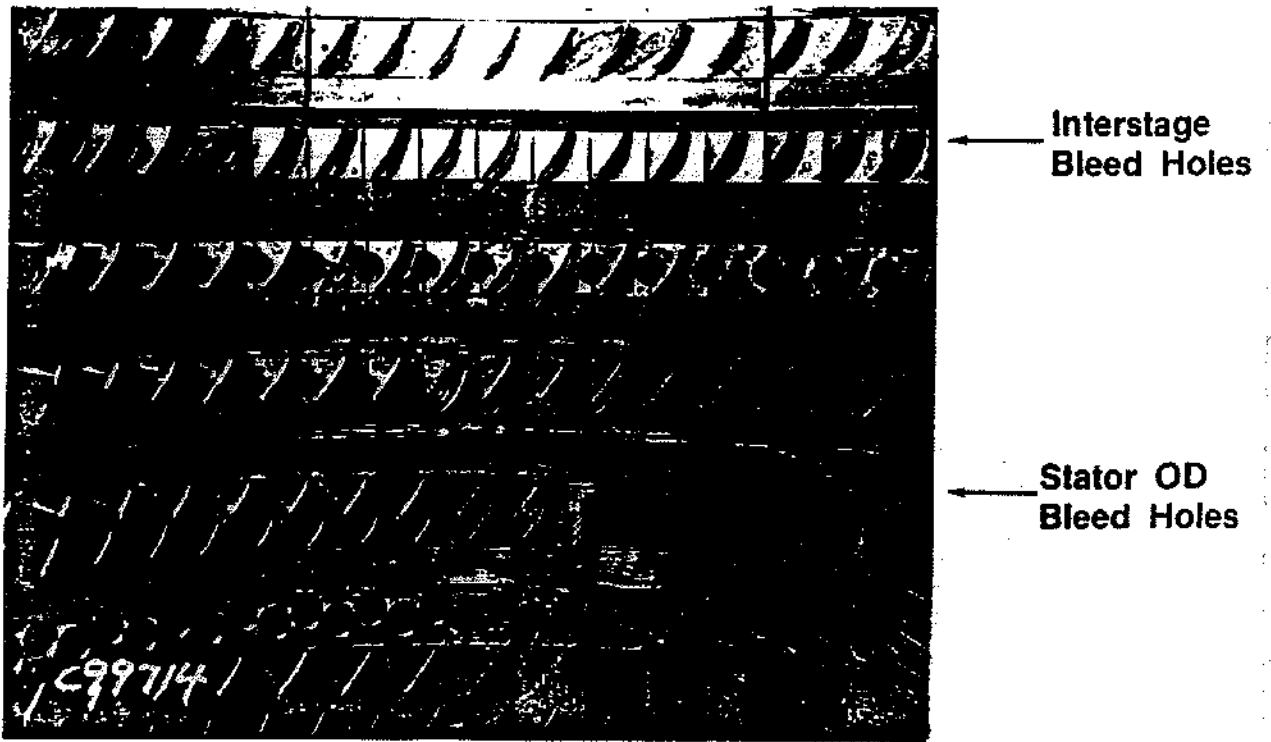


Figure 3.33 Compressor Bleed

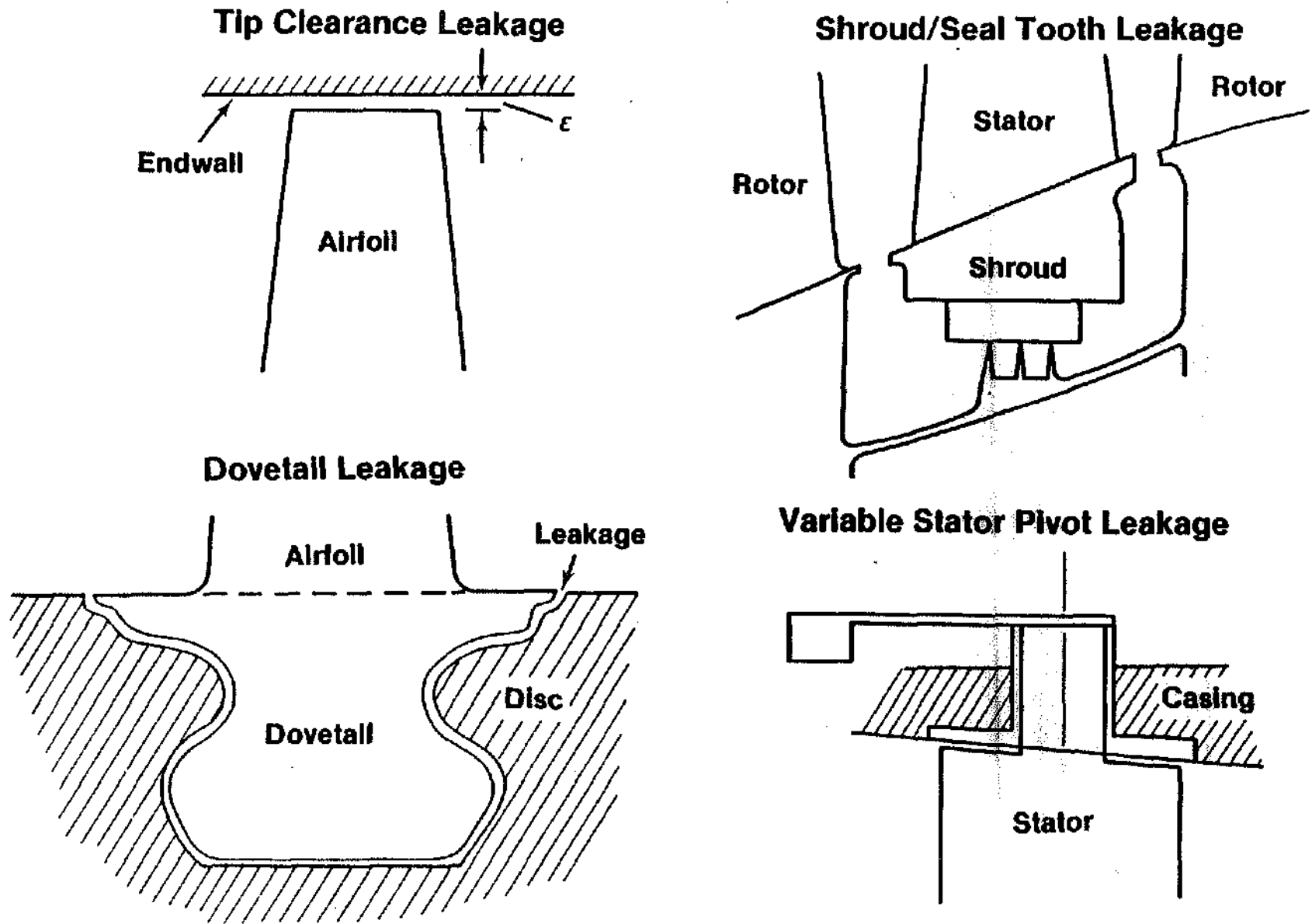


Figure 3.34 Leakage Paths in Compressors

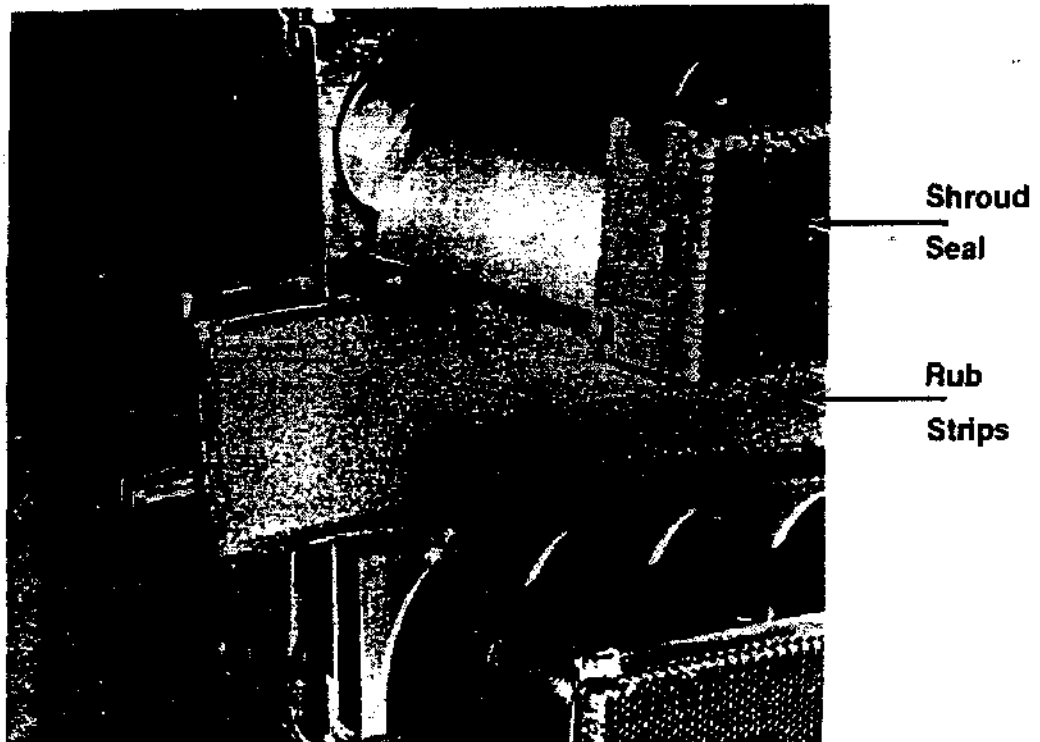


Figure 3.35 Shroud Seal and Rub Strips

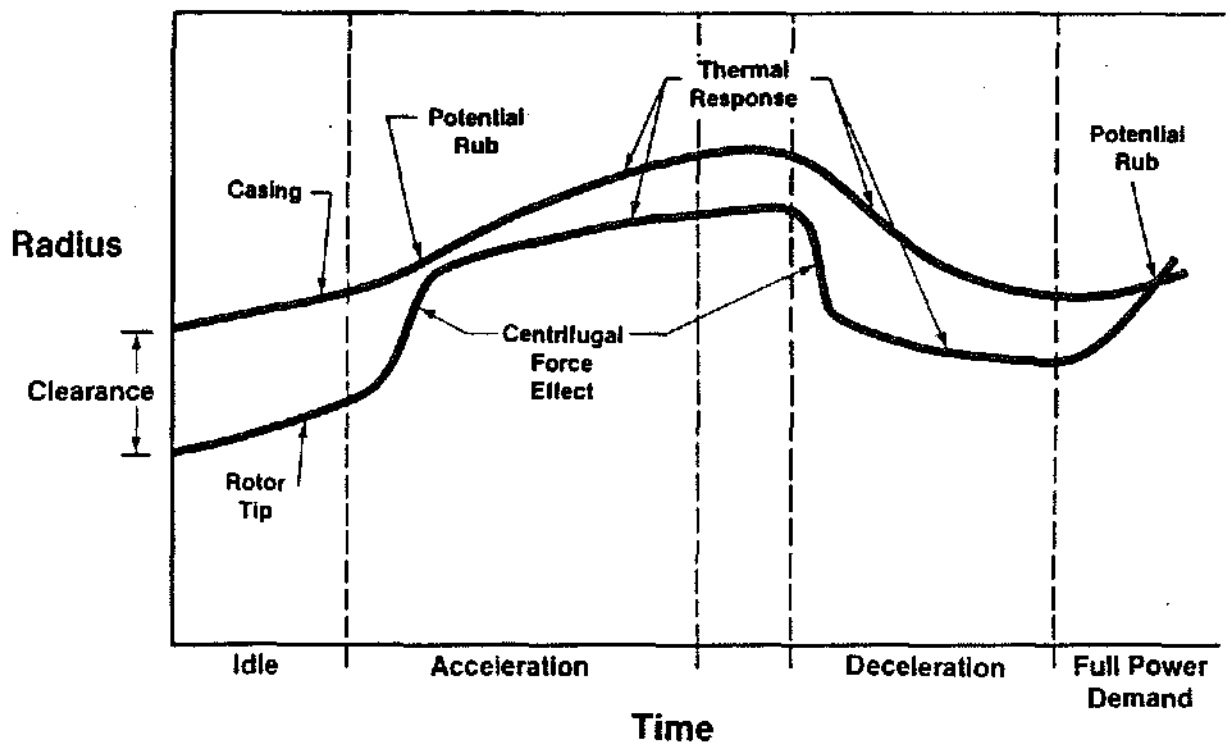
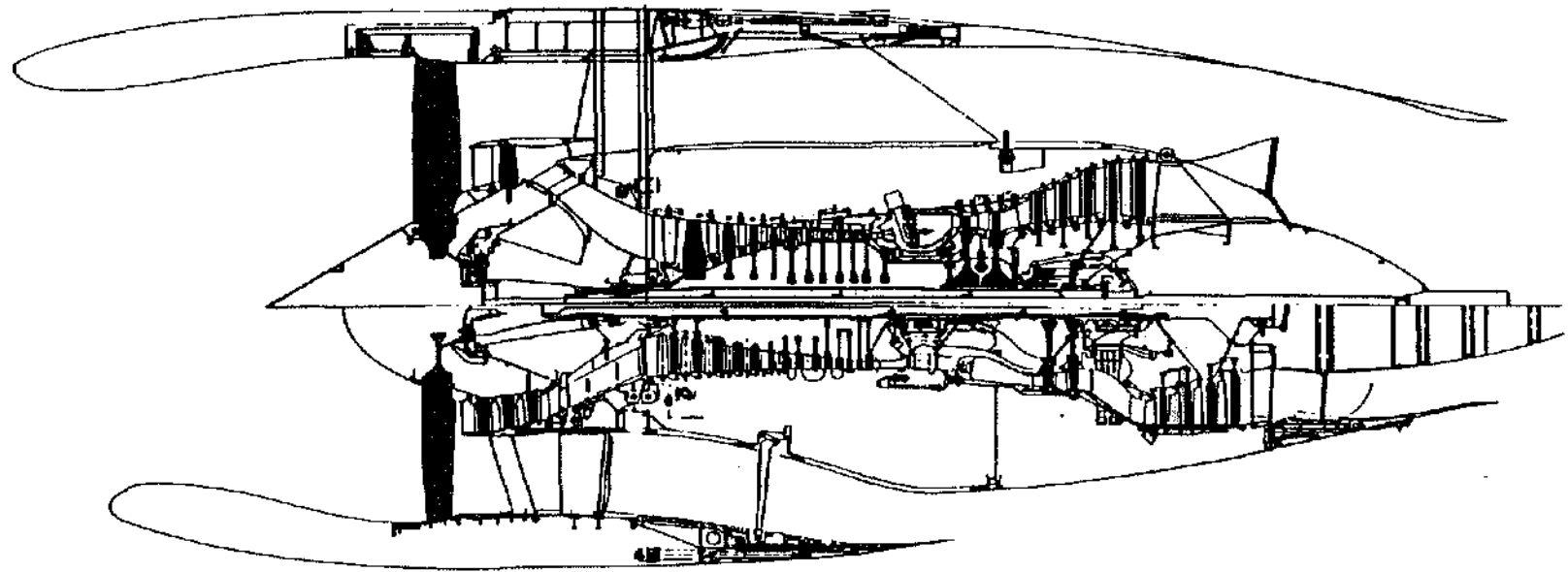


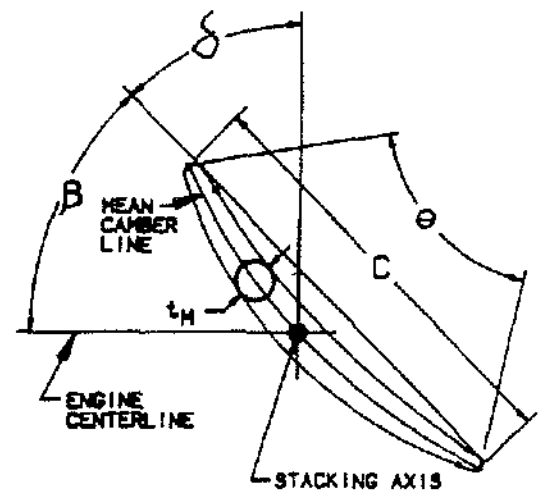
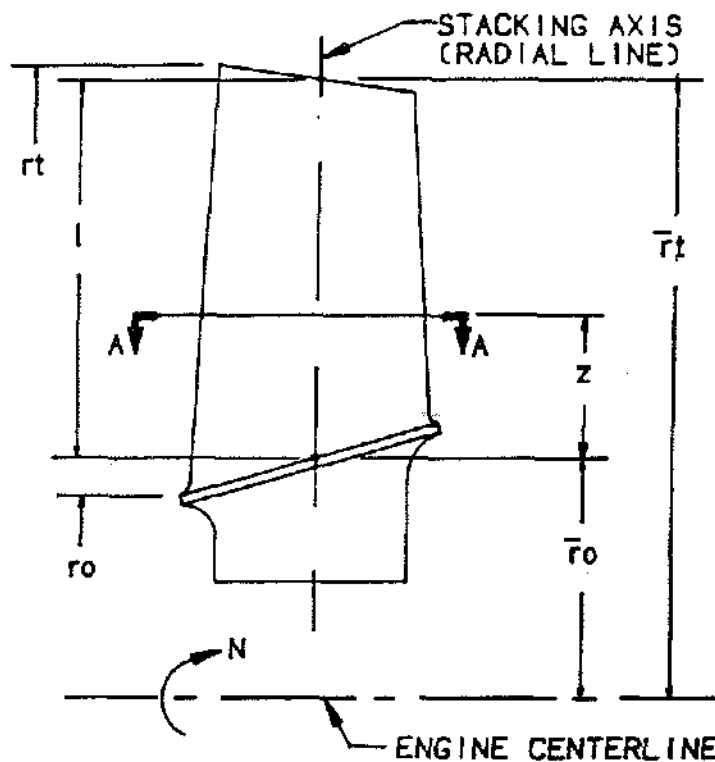
Figure 3.36 Casing-to-Rotor Clearance Variation During Transient Shows Need for Clearance Control

E³ Engine



**CF6-50C Reference Engine
(Scaled to E³ MxCI Thrust)**

Figure 3.37 E³ and Reference Engine Comparison



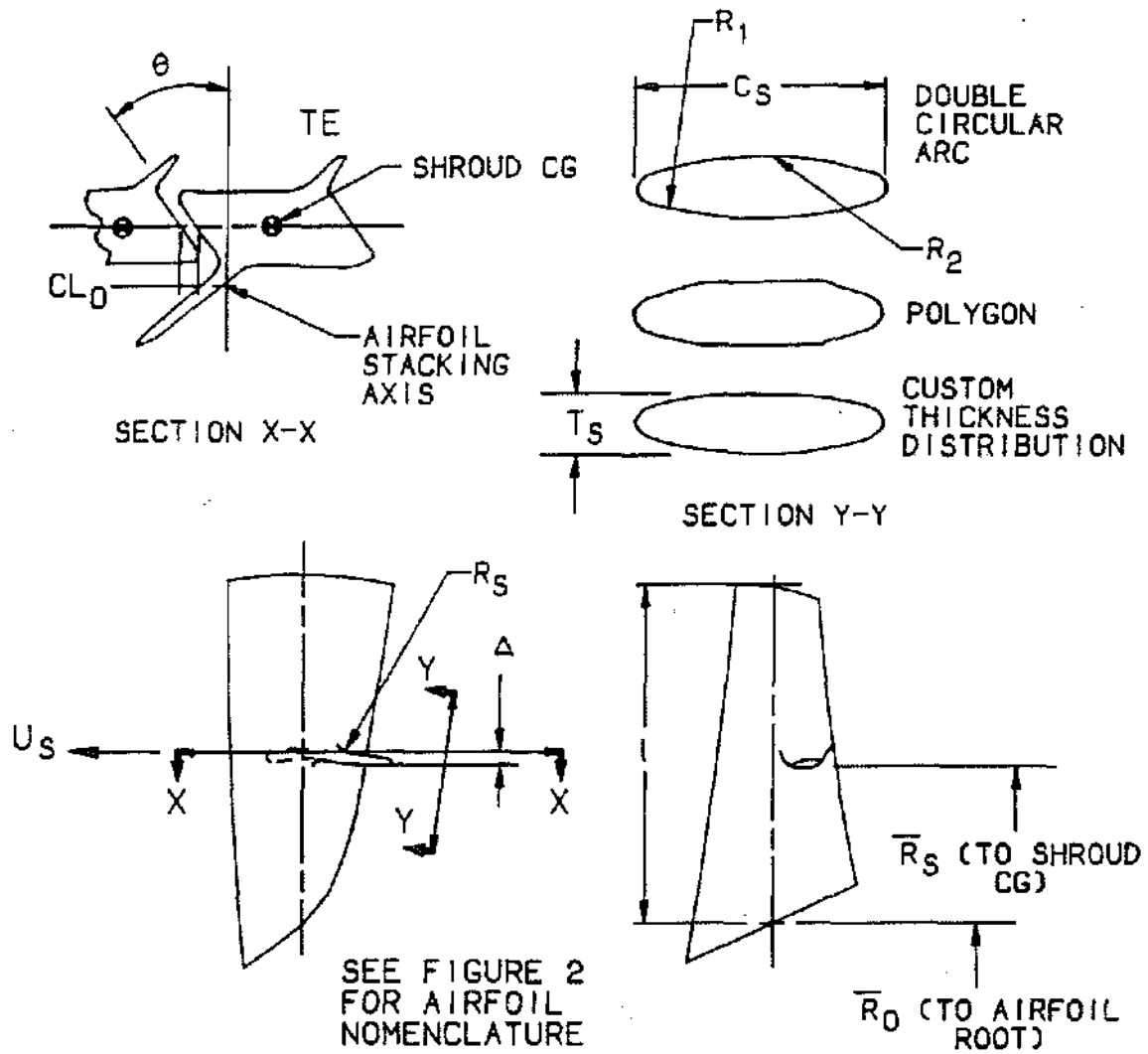
SECTION A-A

SUBSCRIPTS

- O = ROOT OR HUB
- t = TIP
- TE = TRAILING EDGE
- LE = LEADING EDGE
- SA = STACKING AXIS
- IN = INLET

<u>Nomenclature</u>	<u>Symbol</u>	<u>Units</u>	<u>Definition</u>
Number of Blades	N_B	—	Per Stage
Airfoil Section Max Thickness	t_M	Inches	See Figure
Camber	θ	Degrees	See Figure
Stagger Angle (Aerodynamic, Tangent)	β	Degrees	See Figure
Orientation Angle	δ	Degrees	$90^\circ - \beta$
Chord	C	Inches	See Figure
Aspect Ratio	AR	—	l/C
Radius Ratio (Avg)	R	—	\bar{r}_0/\bar{r}_t
(Inlet)	R_{in}	—	r_0/r_t
Percent Span	η	Percent	$(s/l) \times 100$
Spacing Between Blades	s	Inches	$2\pi(\bar{r}_0 + s)/N_B$
Solidity	σ	—	C/S
Blade Length (at Stacking Axis)	l	Inches	See Figure
Rotational Speed	N	RPM	See Figure
Tip Speed, Aerodynamic	U_t	FPS	$2\pi (r_t/12) (N/60)$
Tip Speed, Mechanical	\bar{U}_t	FPS	$2\pi (\bar{r}_t/12) (N/60)$
Wheel Speed	U	FPS	$2\pi ((\bar{r}_0 + z)/12) (N/60)$

Figure 3.38 Airfoil and Flowpath Nomenclature



Nomenclature

Symbol

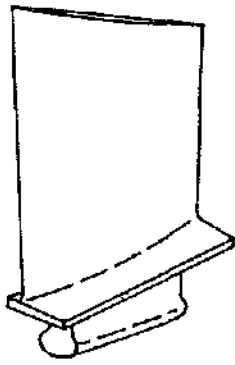
Definition

Chord	C_s	See Figure
Cross Sectional Area	A	—
Droop (Pre-Deflection Below A Circular Arc or Chord Line of A $2N_B$ Polygon)	Δ	See Figure
Interface Clearance at Assembly	CL_0	See Figure
Interface Angle	θ	See Figure
Location (% Span)	η_s	$(\bar{r}_s - \bar{r}_0) + l \times 100$
Shroud Fillet Radius	R_s	See Figure
Solidity (At Shroud Location)	σ_s	$C/(2\pi \bar{r}_s/N_B)$
Thickness, Maximum	t_s	See Figure
Wheel Speed at Shroud Location	U_s	$(2\pi \bar{r}_s/12) \cdot N/60$

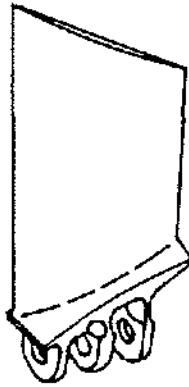
Figure 3.39 Part-Span Shroud Nomenclature

COMPONENT PARAMETERS (at Aerodynamic Design Point)		
Nomenclature	Symbol/Formula	Units
Flow (physical)	W	lb/sec
Pressure Ratio	P_r	—
Physical Speed	N	rpm
Corrected Speed	$100 \times (N/\sqrt{\theta})/(N/\sqrt{\theta})_{Ref}$	%
Specific Flow (frontal)	W/A_f	lb/sec-ft ²
Specific Flow (inlet)	W/A_1	lb/sec-ft ²
Corrected Flow	$W_R = W\sqrt{\theta}/\delta$	lb-sec
BLADE PARAMETERS		
Number of Blades	N_B	—
Aspect Ratio (root)	AR	—
Radius Ratio (inlet)	R_{in}	—
Radius Ratio (average)	R	—
Aerodynamic Tip Speed (at inlet plane)	$U_t = \frac{2\pi N}{60} \cdot \frac{r_t}{12}$	ft/sec
Mechanical Tip Speed (at stack axis)	$\bar{U}_t = \frac{2\pi N}{60} \cdot \frac{\bar{r}_t}{12}$	ft/sec
Root Radius (at stack axis)	\bar{r}_0	in.
Tip Radius (at stack axis)	\bar{r}_0	in.
Solidity (root)	σ_0	—
Solidity (tip)	σ_t	—
Maximum Thickness/Chord	t_M/C	—
Shroud Location Span	r_s	%
Chord	r_c	%

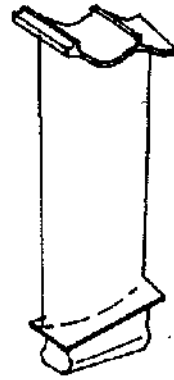
Table 3.4 Component and Blade Nomenclature Summary



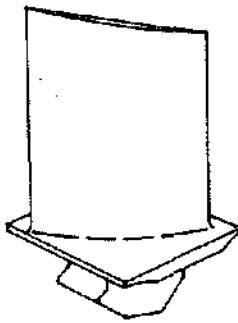
CANTILEVERED
AXIAL DOVETAILED



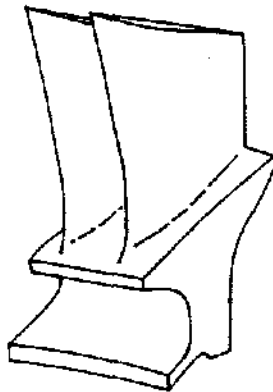
PIN JOINT



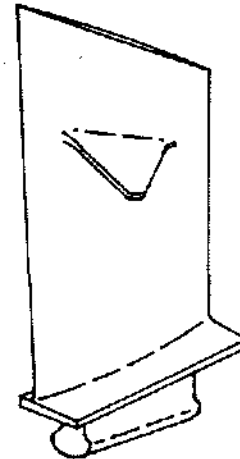
TIP SHROUD



CANTILEVERED
CIRCUMFERENTIAL
DOVETAILED



BLISK

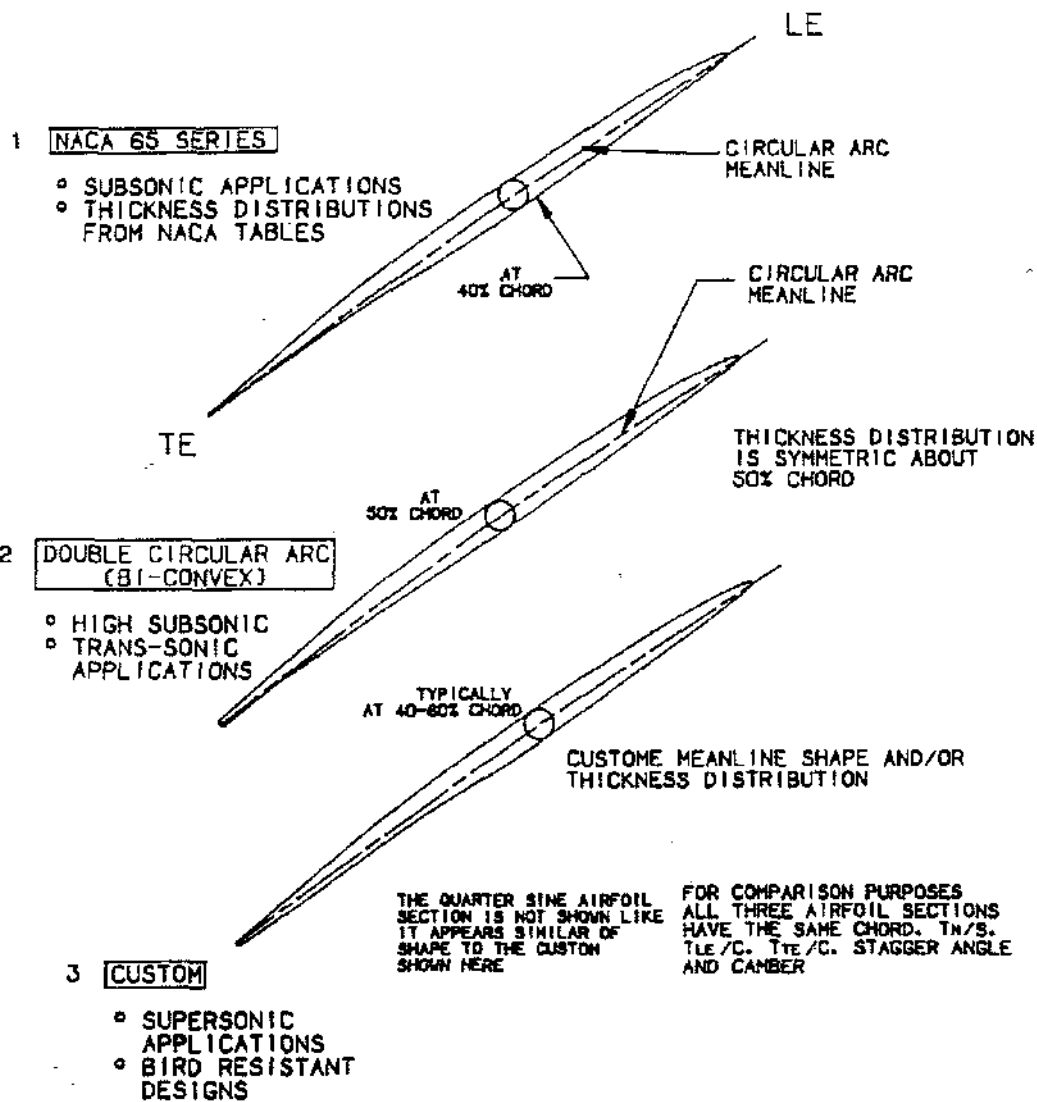


PART-SPAN
SHROUD

Figure 3.40 Basic Blade Configurations

Design Class			Engine	Component	Stage	Comments	Selected Primary Concerns
AR (Aspect Ratio)	R _{in} (Radius Ratio)	U _t (Tip Speed)					
Low	Low	High	F404	Fan	1	Part-Span Shroud	2/Rev Margin, Instability, Shank Flexibility-Stresses
			GE29	Compressor	1	Blisk	Panel Modes
			T700	Compressor	1	Blisk	Passing Frequencies
Low	High	High	F101/CFM56	Compressor	Front	Cantilever	Passing Frequencies
			F404	Compressor	Front	Cantilever	Passing Frequencies
			GE29	Compressor	Mid-Rear	Cantilever	Passing Frequencies
Low	High	Low	TF34	Compressor	Rear	Cantilever	Passing Frequencies
			F101, F404, CFM56	Compressor	Rear	Cantilever	Passing Frequencies
High	Low	High	CF6-6,-50,-80A,-80C	Fan	1	Part-Span Shroud	2/Rev Margin, Torsional Instability
			CFM56-2	Fan	1	Tip Shroud	2/Rev Margin
			TF34	Fan	1	Pin Joint	2/Rev Margin
			F110	Fan	1	Part-Span Shroud	2/Rev Margin, Instability, Shank Flexibility, and Stresses
High	Low	Low	J85-21	Compressor	Front	Pin Joint and Part-Span Shroud	Instability
			CF6-6,-50,-80A,-80C	Compressor	1	Part-Span Shroud	Instability
			CFM56-3	Fan	1	Part-Span Shroud	2/Rev Margin, Torsional Instability
High	High	Low	J85-21	Compressor	Mid-Rear	Cantilever	Instability
			TF34	Compressor	Front-Mid	Cantilever	Passing Frequencies
			CF6-6,-50,-80A,-80C	Booster	All	Cantilever	Passing Frequencies

Table 3.5 Blade Design Classes — Typical Examples



• For supersonic and recent transonic/subsonic airfoils, thickness vs % chord is given by a, b, and c

a.
$$\frac{T_C - T_E}{T_M - T_E} = \frac{X}{TK - 1} \left[(TK - X)^{TK - 1} \right]$$

where: • TK = 2 double circular arc
• X = Fractional distance from airfoil edge to thickness location

b. Quarter Sine Wave

$$\frac{T_C - T_E}{T_M - T_E} = \sin\left(\frac{\pi}{4} X\right)$$

c. Combinations of (a) and (b), and commonly combined with 65 series trailing edge

Figure 3.41 Airfoil Section Classes

Three basic root attachments are used in GEAE fan, booster, and compressor blades:

Single or double tang dovetails (axial, skewed axial, circumferential)

Pin joint

Blisk (Integral blade and disk)

Examples of each of these root attachments are shown in Figure 3.40.

AIRFOIL MECHANICAL DESIGN CONSIDERATIONS

Airfoil design is a collaborative effort by aerodynamics, aeromechanics, and mechanical design. No single design discipline has total control over any of the design parameters. Figure 3.42 and 3.43 show a generalized new design flowchart and a detail design flowchart, respectively.

The design of an airfoil is begun by setting a basic size based on required airflow and available space. In consideration of flow, efficiency, and stall margin requirements, aerodynamics design will set a preliminary flowpath. Parameters subject to significant iteration before the design concept is set to include the number of stages, blade/vane aspect ratios, inlet radius ratio, and tip speed.

In addition to these basic design parameters the design process requires consideration of resonant frequencies, steady-state and vibratory stresses/deflections, aerodynamic loading effects, aeroelastic instability/flutter, dovetail versus airfoil strengths, retention and locking, and shroud designs. For engine applications with noise emission requirements, the blade number, blade-to-vane spacing, and blade number to vane number ratios are additional issues, and the design process is not completed without consideration of materials and coatings, drawing delineation, manufacturing and quality control, and experimental verification.

When hardware becomes available, the next step in the design process is experimental verification of design calculations and demonstration that design intent was met. This is accomplished through bench and engine tests to determine:

Frequency and nodal patterns (mode shapes),

Steady-state and vibratory stress distributions,

Fatigue strength,

Structural strength (weak link determination).

The stress distribution at or near the airfoil root must be determined from component tests since classical analysis includes the assumptions that "plane sections remain plane" and that there are no abrupt changes in cross section. However, these "end effects" exist at changes in cross section including the shroud-to-airfoil transition and airfoil root-to-platform transition. Experimental verification may also include photoelastic model tests of critical stress areas using models cast in molds from actual hardware.

AIRFOIL LOADING AND ENVIRONMENT

Blade frequencies, stresses, and stability are affected by thermodynamic cycle, control system, and aerodynamic parameters. Airfoil loads are a result of gas loads and rotor centrifugal loads in the case of rotor blades. Gas loads induce several types of airfoil stresses including elastic steady-state bending stress, separated flow force vibration stress due to non-periodic flow separation, vibratory stresses due to stall (surge) loading, and "per-rev" induced vibratory stresses resulting from inlet airflow pressure/density variation (distortion). Blade metal temperatures can affect frequencies and stresses due to changes in the modulus of elasticity. Aerodynamic parameters such as incidence angle, mach number, and pressure ratio can affect aeroelastic stability.

Attention should be given to flight envelope and control system extremes. Off-design point gas loading estimate can be obtained using gas loading parameters which are a function of corrected speed and pressure ratio. In addition to steady-state loads, airfoils must accommodate vibrations induced by both upstream and downstream airfoil flow disturbances, bearing per rev excitation, and overall engine vibration.

Ultimate load conditions result from stalls and foreign object ingestion. These types of loads are very difficult to determine and design margin must be provided based on experience.

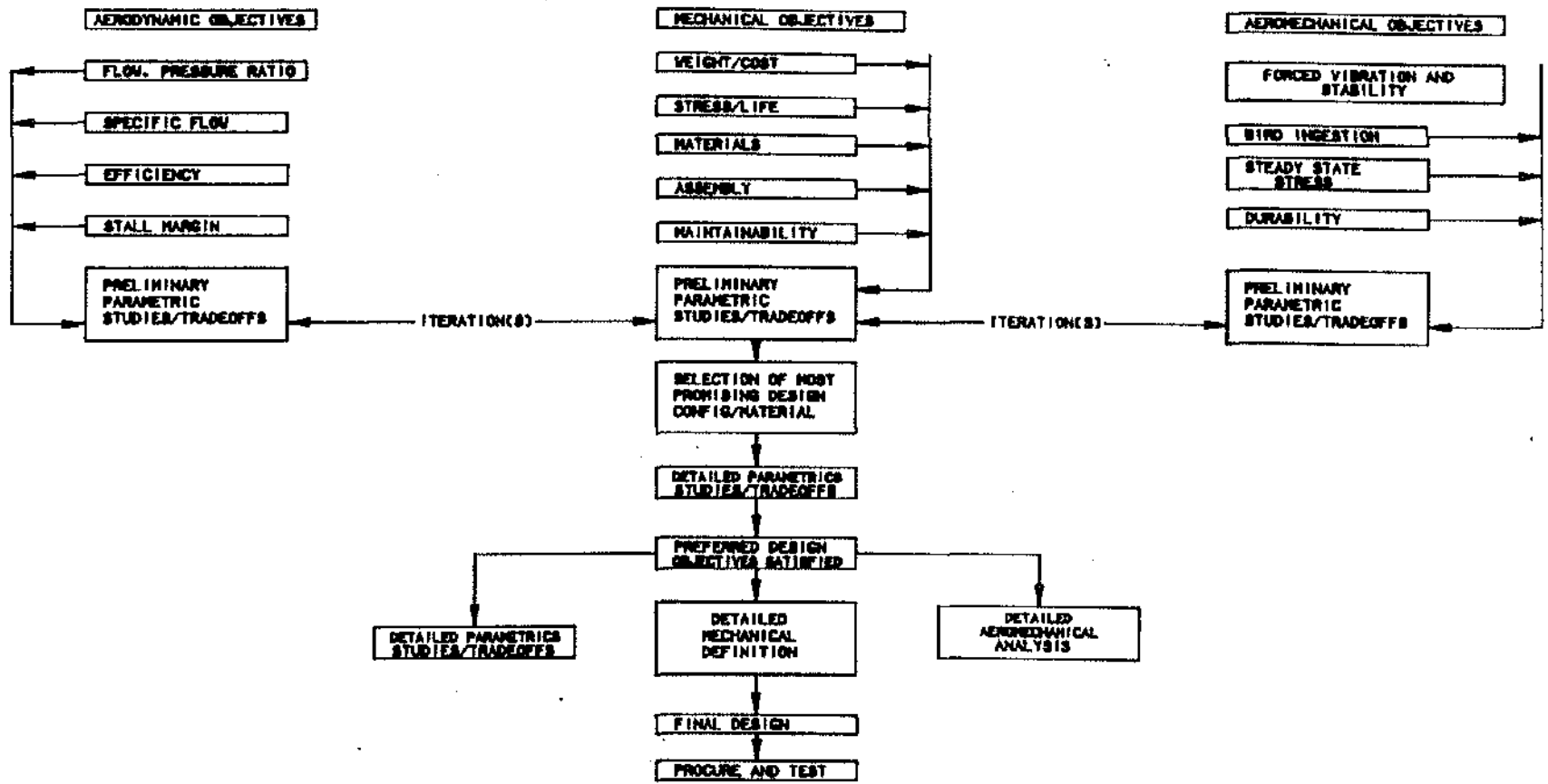


Figure 3.42 Generalized New Design Flowchart

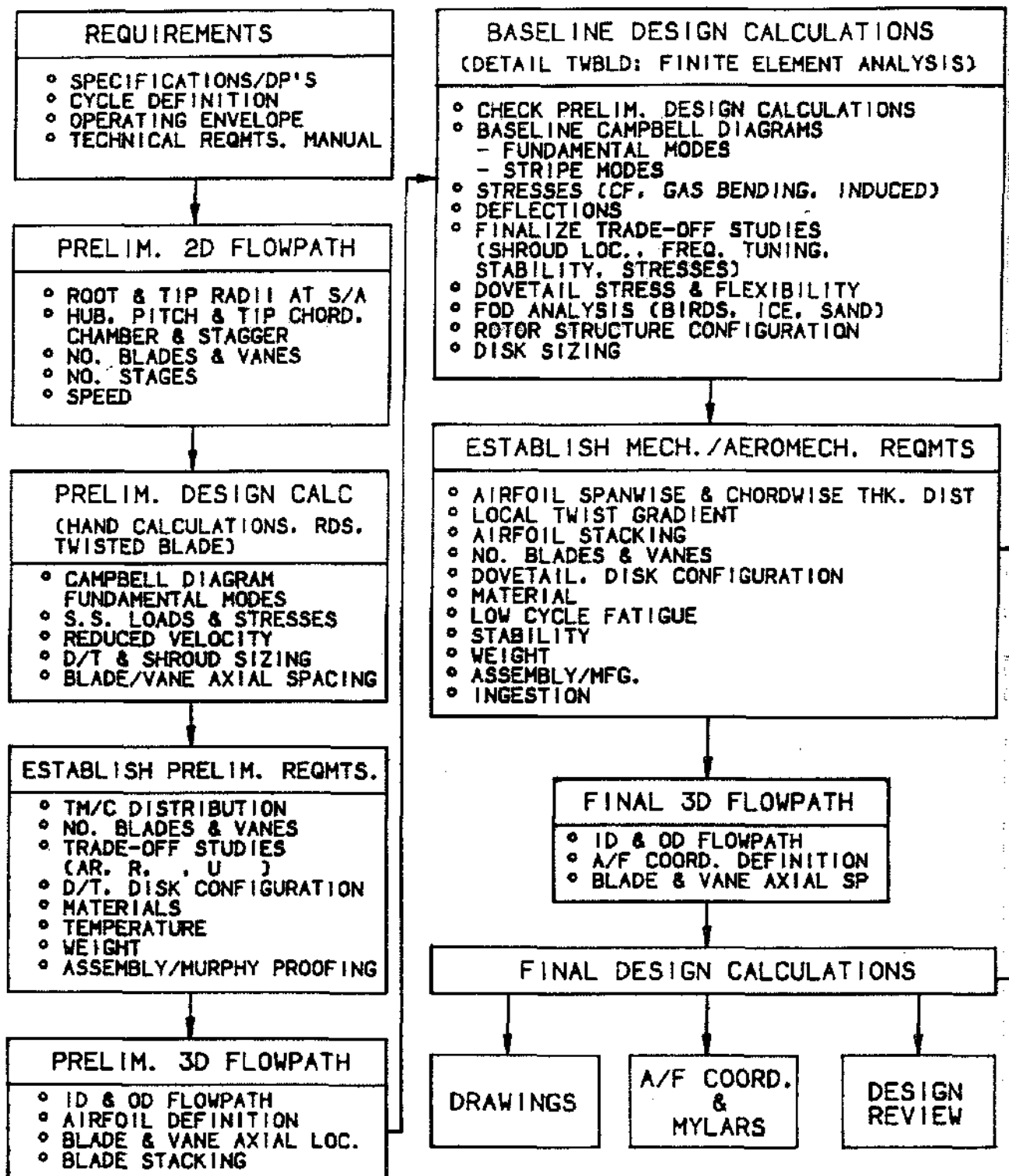


Figure 3.43 Detail Design Flowchart

AIRFOIL FAILURE MECHANISMS

Airfoil failures, i.e., cracking, separation or distortion beyond serviceable limits, may result from insufficient design margin for any of the above design considerations. Experience has shown, however, that most failures result from vibratory resonance, foreign object ingestion, or low cycle fatigue.

Vibration and Aeromechanical Instability Ideally, resonant mode vibration should be avoided between idle and maximum RPM for all possible sources of excitation. However, experience has shown that some resonance cannot be avoided but with careful design the resulting stress response may be acceptable. Figure 3.44 shows ideal fundamental mode shapes. Sources of low order excitation, e.g. inlet distortion, frame or vane struts, or bleed ducts, are of significant concern. Blade resonant frequencies and integral order blade stimuli must be plotted on Campbell Diagrams (see Figure 3.45).

System mode vibration results from elastic or aerodynamic coupling of blades within a stage and is identified by the blade mode and the mode shape of the rotor structure. For example, if the blades vibrate in their first mode (usually first flex) and the rotor structure vibrates

out-of-plane with two diametral node lines, this is the 1st - 2 diameter system mode. System mode characteristics are also plotted on Campbell diagrams as shown in Figure 3.46. The 1st - 2 diameter and 1st - 3 diameter modes are of primary concern but some higher modes have been observed in high bypass fans.

Maximum steady-state stresses due to centrifugal and gas loads are established to provide a vibratory stress allowance which does not exceed high cycle fatigue endurance limits. Since vibratory stresses are not known in the early design phase, these allowable steady-state stresses must be set sufficiently low to allow vibratory stresses within experience to provide infinite HCF life.

Under certain conditions, the air flowing over airfoil surfaces can interact with the vibratory behavior of the blade in an unstable (i.e. self-feeding) mechanism known as flutter. There are four basic concern areas relative to aeroelastic instability.

Subsonic stall flutter

Subsonic negative incidence and choke flutter

Supersonic stall flutter

Supersonic shock flutter

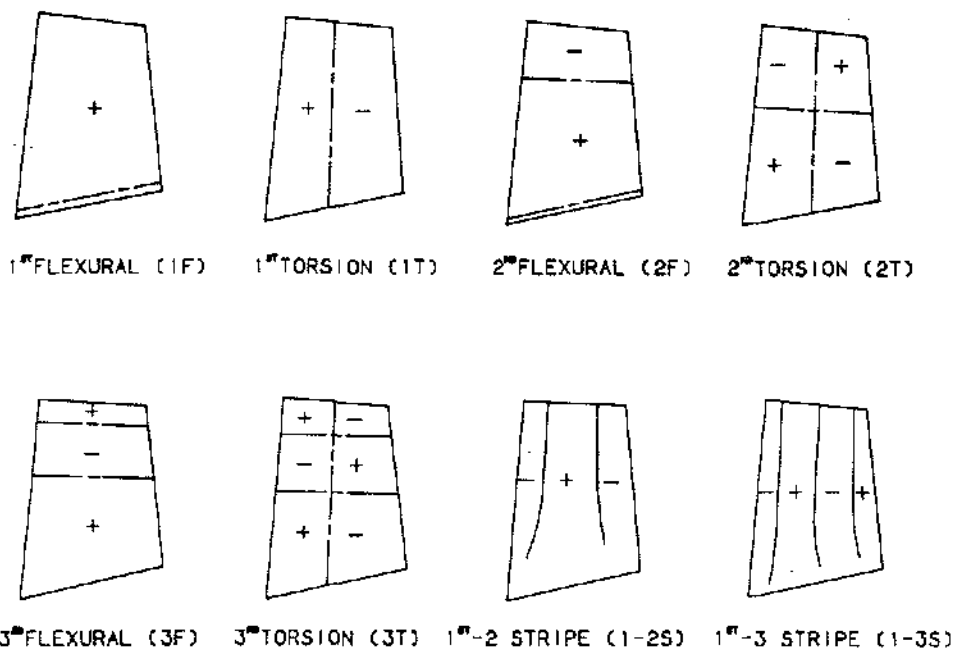


Figure 3.44 Ideal Fundamental Mode Shapes

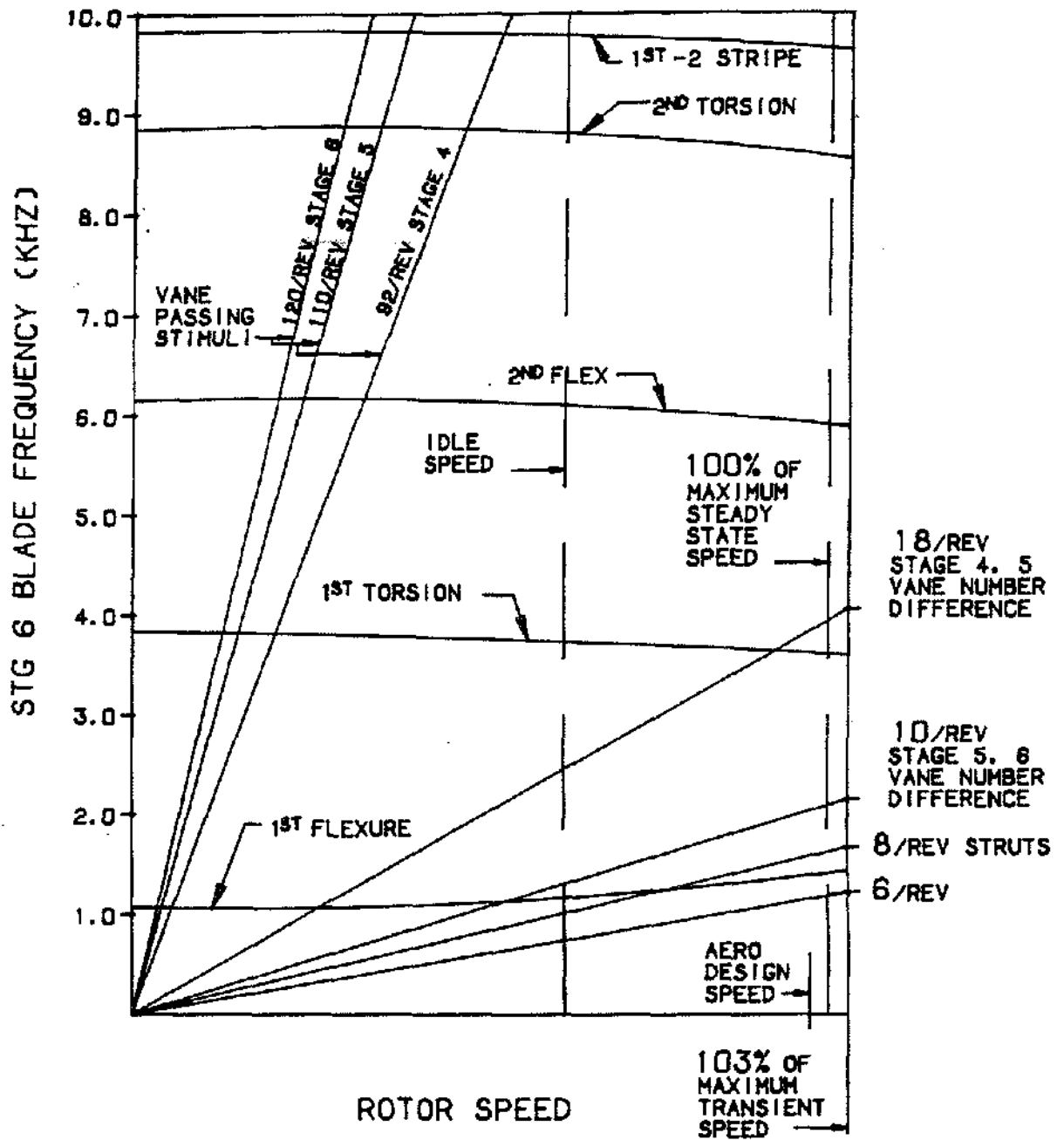


Figure 3.45 Campbell Diagram for a Typical Compressor Blade

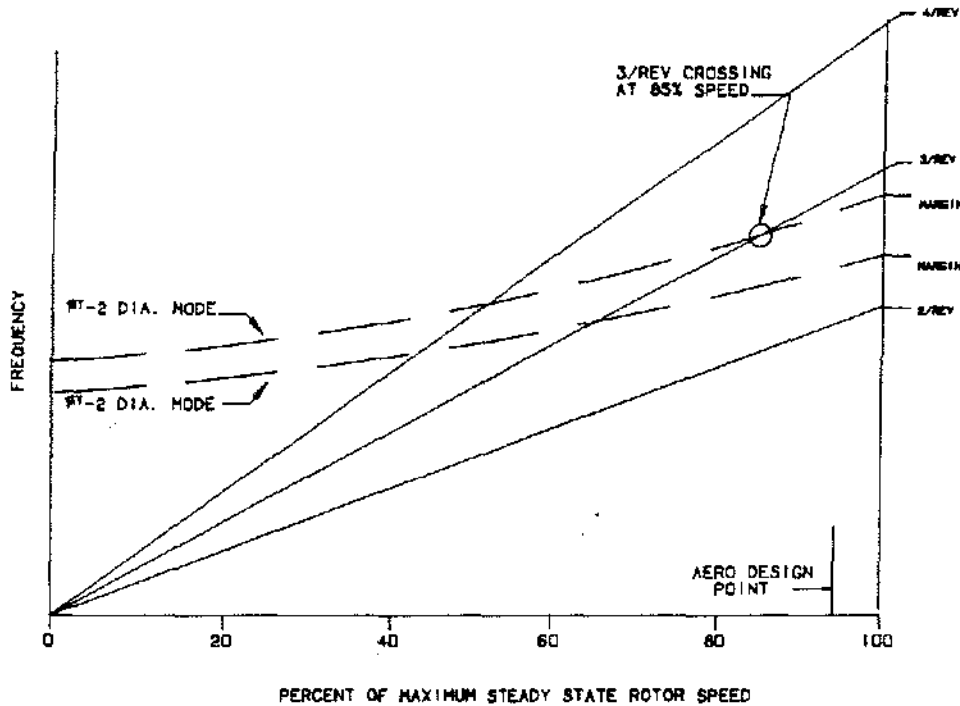


Figure 3.46 System Mode Campbell Diagram

Figure 3.47 shows a typical fan or compressor with instability regimes. The design objective is to be within experience if possible. This is accomplished by comparing the new design to similar designs with known instability boundaries based on several parameters including incidence angle and reduced velocity so that

$$\text{Reduced Velocity} = \frac{12V_{rel}}{\pi C f} \quad (3-9)$$

where V_{rel} = physical velocity of air wrt the airfoil (ft/sec), C = Chord (inches), and f = natural frequency of the mode of interest (Hz).

Ingestion Specific ingestion requirements vary from engine to engine based on engine size, type and contractual requirements but the general considerations are the same. Unprepared runways and runways in poorly controlled areas of the world present the danger of rock, sand and other debris. This trash can cause foreign object damage (FOD) to airfoil leading edges. In the case of a rock or other "hard body", a notch or tear can be produced in the leading edge which will be a stress riser and fatigue crack initiation site. In the case of sand, erosion of the airfoil leading edge reduces engine perform-

ance especially in compressors where the edges are thin and will erode quickly. For this reason military helicopter engines, such as the T700, have air-dirt separators in the engine inlets to prevent severe erosion from operation in desert or beach areas.

A major concern in large transport engines is damage to the fan blades from birds and ice. Engine certification programs require testing of all possible ingestion events. Hailstones are shot into engine inlets from air cannons that can simulate aircraft flight speeds up to about 950 ft/sec (650 MPH). Flying in icing conditions is tested by spraying water/air mixtures into engines during freezing temperatures. Ice shedding from nacelle inlets are simulated by throwing slabs of ice and ice spears into engines.

Birds are shot from air cannons to simulate various ingestion scenarios. Multiple small birds (2-4 oz) simulating a flying flock are ingested at takeoff speeds with minimal engine power loss requirements. Multiple medium birds (1-2 lbs.) are also ingested at takeoff speeds to simulate startled nesting birds with 75% of takeoff engine power typically required to be maintained to assure adequate aircraft climb. Large birds (4+ lbs.) are

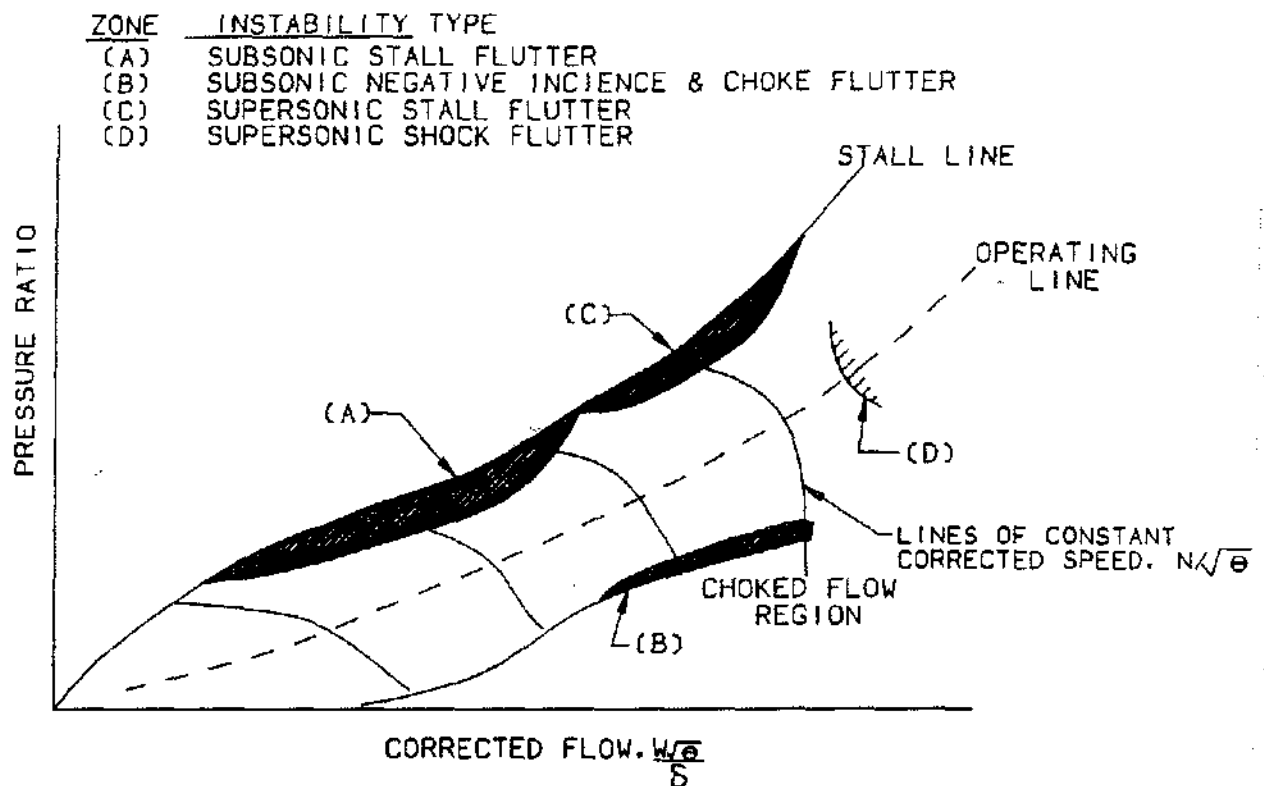


Figure 3.47 Typical Fan and Compressor Map with Instability Regimes

ingested singly at cruise flight speeds with safe engine shutdown requirements similar to containment tests. An interesting fact found by the British CAA in a study of aircraft bird strikes is that 80% of bird strikes involve birds weighing less than 4 lbs. and half of all bird strikes involve sea gulls.

Analytical models of bird and ice ingestion events treat them as "water balloons" impinging on the blade row. Indeed component tests using gelatin filled plastic bags have correlated very well with ingestion tests using real birds. The damage to the airfoil is characterized as "softbody" and produces bulges of the leading edge. The damage occurs very rapidly and analysis correlations of the material behavior draw on explosively formed metal manufacturing methods data. An analytical blade model showing a typical bulge analysis is shown in Figure 3.48. Detailed analyses taking into account the relative velocities of blade and bird to define incidence angle and the portion of the bird that is actually trapped between airfoils at the time of impact, show that the maximum impact damage generally occurs on the outer one-third of the blade at an aircraft (bird) velocity of 200 - 300 feet per second. Damage to static parts is maximized at max aircraft velocity, as one would expect.

AIRFOIL TRADEOFFS AND IMPLICATIONS FOR DESIGN

As discussed above, airfoil design requires trade-off between aerodynamic, aeromechanic, and mechanical design considerations. Trade-off studies for each of the four basic design parameters i.e., number of stages, aspect ratio, inlet radius ratio, and tip speed, are required to assure a well-balanced design.

Increasingly stringent maintainability and reliability requirements, higher stage pressure ratios, increased tip speeds and mach numbers and defect/ingestion tolerance has resulted in a trend toward lower aspect ratio ruggedized airfoils and fewer stages.

ROTOR PHYSICAL AND FUNCTIONAL DESCRIPTION

The prime functions of the rotor structure are airfoil retention, torque transmission, and provision of the inner flowpath surface. The rotor structure must be capable of withstanding the centrifugal forces produced by the dead weight of the airfoils as well as the body forces resultin

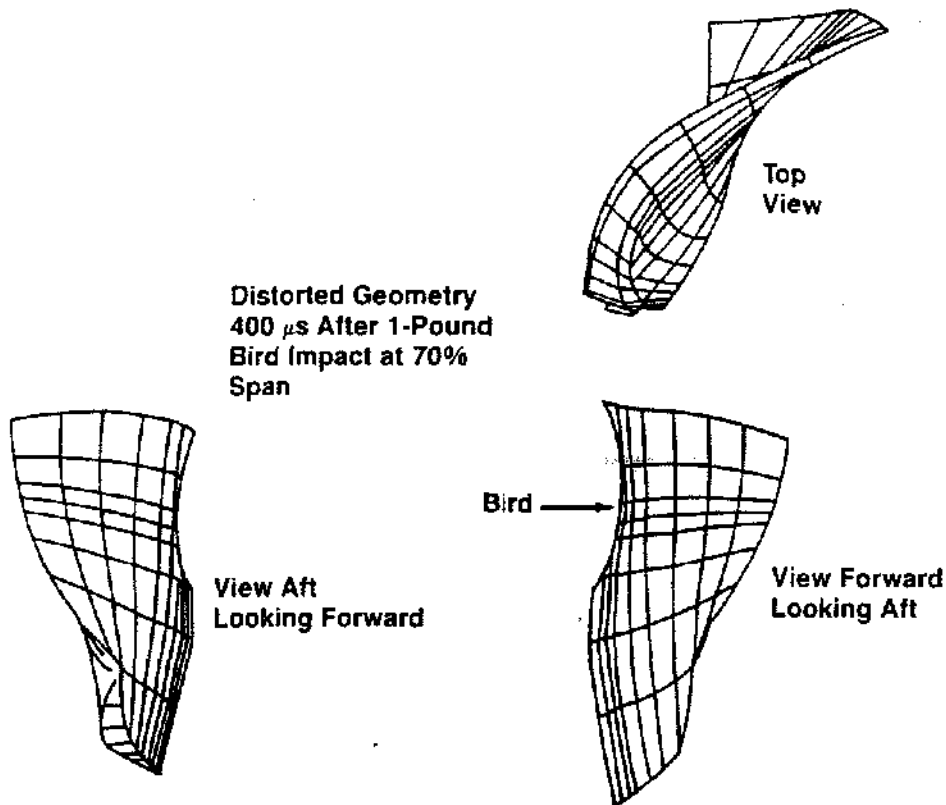


Figure 3.48 Bird Strike Finite Element Analysis

from the rotor structure's own inertia rotating at high speeds. Rotors either drive or are driven by other rotors which transmit horsepower as torque through connecting rotor shafts. Besides the mechanical functions described above, the rotor outside diameter must satisfy aeromechanical design requirements as well. In fact, the flow-path profile is fixed very early in the design; the mechanical designer is then left to design "from the outside-in" and design a structure to withstand the loading required to achieve the specified operational requirements. Geometrically, rotor structures are axisymmetric structures consisting of a combination of disks, shafts, spacers and rotating seals. A cross-section of the CFM56 high and low pressure rotor systems can be seen in **Figure 3.49**.

In most rotor structures, the performance requirements dictate the number of airfoil stages needed which in turn dictate a corresponding number of disks. In general, there are two types of disks; ring disks and disks which have a much larger radial length. The CF6-80C2 3-9 spool in the high pressure compressor rotor has examples of both of these type disks (see **Figure 3.50**). Stages 3-5 are ring disks while stages 6-9 are contoured disks with much smaller inside diameters. The three major sections of the contoured disk are referred to as the rim

(outside diameter, blade retention area), bore (inside diameter area), and web which connects the bore and rim of the disk. The function of the material in the bore of the disks provides a restraining force and allows rotors with higher blade tip speeds to be operated while maintaining sufficient blade/case clearance control and overspeed margin.

Rotors are supported from the static frames by bearings and shafts. Long rotor spools must be supported at both ends due to system dynamics and flight maneuver loads. Rotors such as the CF6-80C2 HPT rotor are cantilevered design with bearings at only one end of the rotor.

Rotating seals separate two different areas of the engine which are at different pressures such as low/high pressure air cavities or air/oil interfaces in sump regions. The rotating high pressure compressor discharge seal in the CF6-80C2 is shown in **Figure 3.51**.

Since typical rotor structure has been described as a combination of disks, shafts, and seals, one must consider the method of assembling these components. These components are usually bolted together but by differing methods. Three different methods of construction are: rabbet, dowelled, and curvic coupling construction.

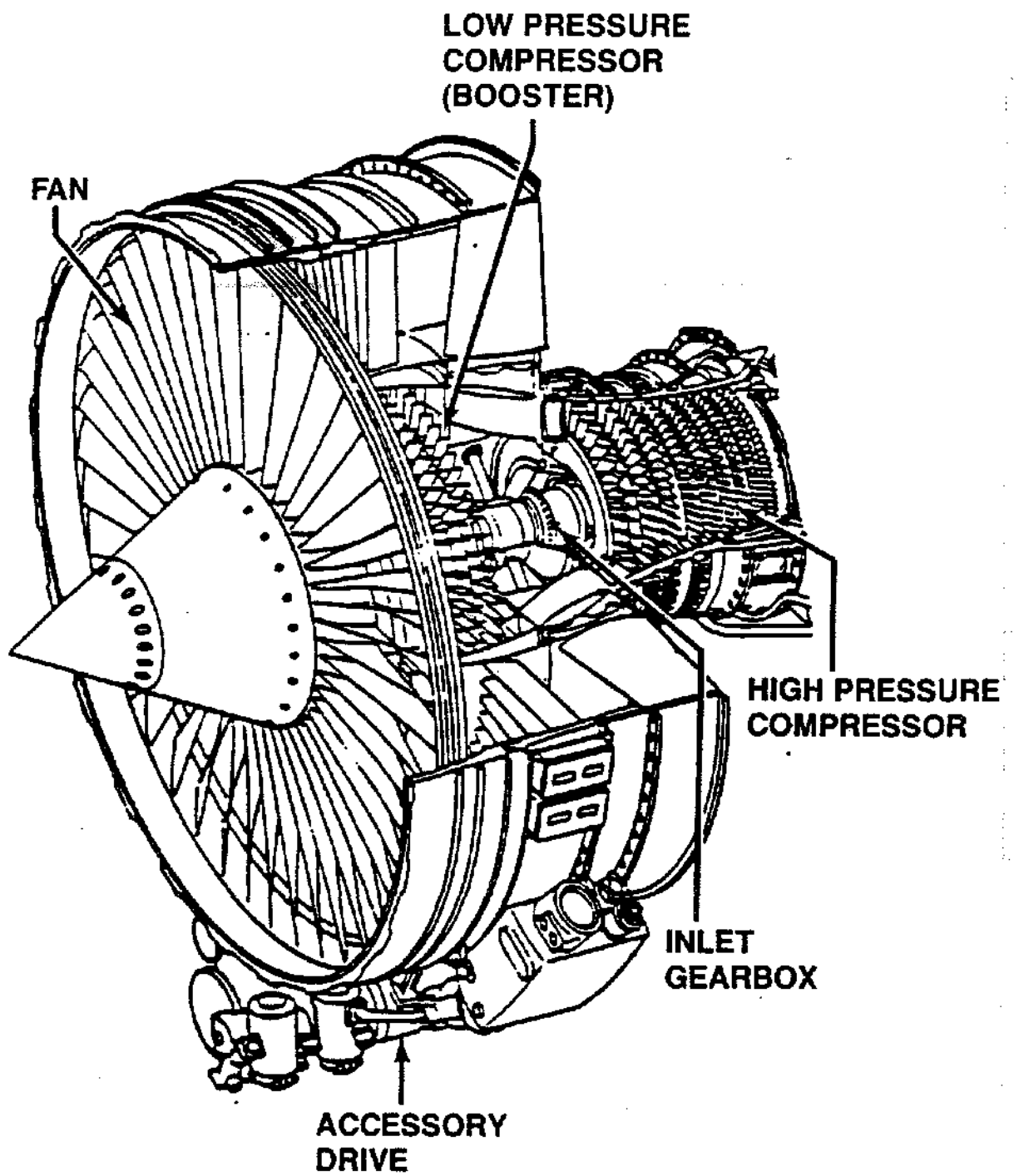


Figure 3.49 CFM Fan and Compressor

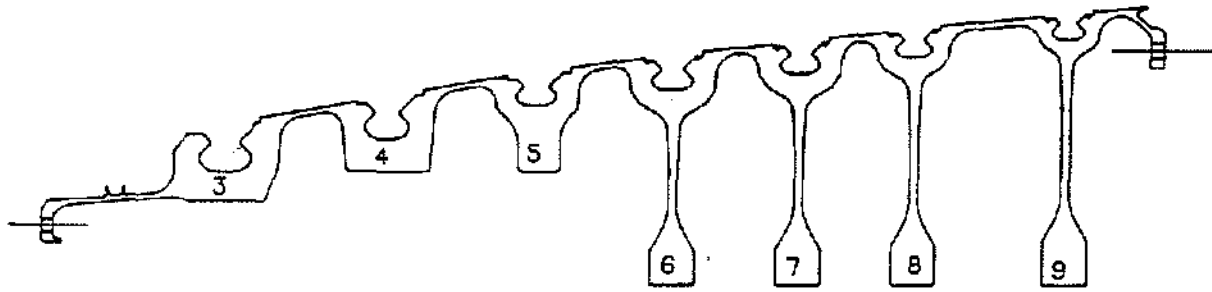


Figure 3.50 CF6-80C 3-9 Spool

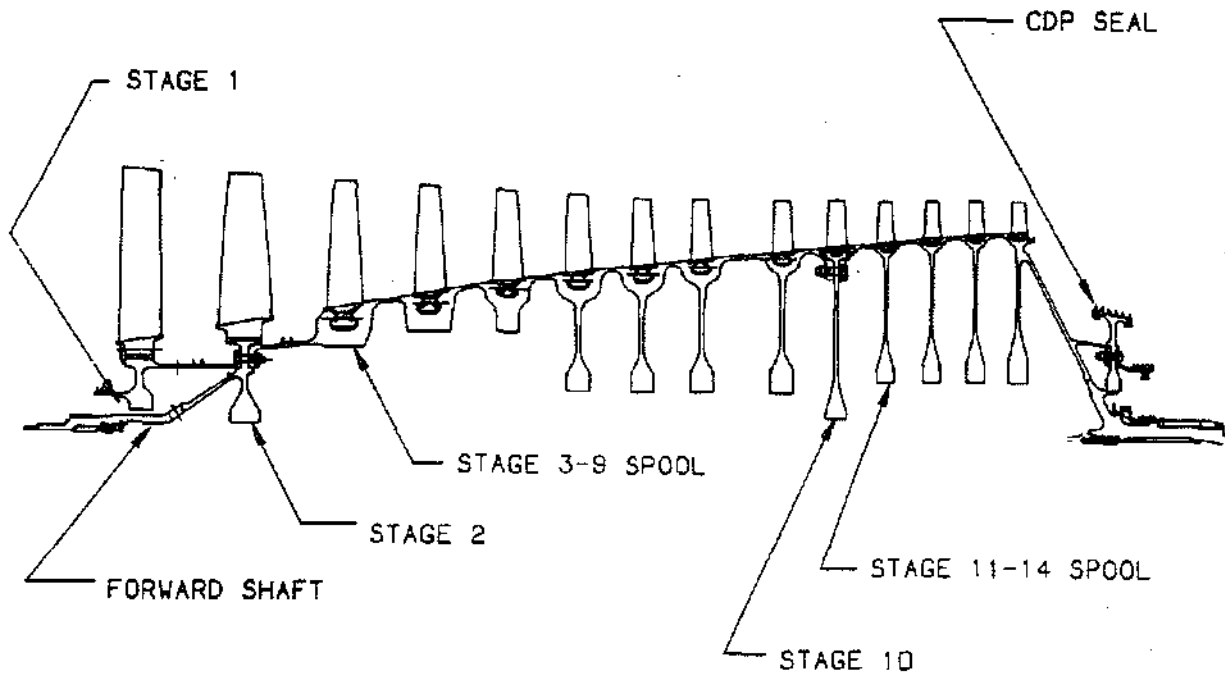


Figure 3.51 CF6-80C HPC Rotor Cross Section

The majority of bolted rotor designs rely on closely controlled locating mating diameters with a slight radial interference fit or "rabbet" to maintain rotor component alignment and concentricity. Rabbetted rotor constructions are usually preferred by commercial and long life application customers because they are more easily repaired at overhaul. Typical rabbetted rotors include all CF6 HPC and HPT rotors, CFM56 rotors and the F404 compressor rotor.

The most common alternative to rabbetted bolted joints relies on close tolerance bolt shank to hole fits to align rotor components as well as provide clamping preload. These dowelled rotors are preferred if single direction rabbet fits will not remain engaged during all operating conditions.

In applications where unique limitations make either rabbetted or dowelled joints impractical, curvic couplings are used in conjunction with long tie bolts to maintain axial preload. Curvic couplings are splines on the faces of adjoining components and are best suited for applications with high torque transmission. Examples of the three most common rotor constructions can be seen in Figures 3.52.

As mentioned previously, one of the primary functions of the rotor structure is airfoil retention. Two major blade attachment schemes are utilized in GEAE rotors; these are axial and circumferential dovetail attachment. Axial dovetail attachment is usually chosen in applications where centrifugal loading is high, airfoil root stagger is small and considerable dovetail strength is required. On the other hand, circumferential dovetails are more common where centrifugal loading is not as high, flowpath radius ratios are higher, and in multistage spools. Circumferential dovetail attachment design is usually less expensive to manufacture and does not require ancillary hardware for blade attachment. Blisks, (BLaded d)ISKS), are another example of airfoil retention. In this design, the airfoils are integral with the disk. This method of airfoil attachment has the advantage of higher performance due to reduced leakage and no ancillary blade retention hardware. Blisks have the disadvantage of requiring repair to a costly piece of hardware as opposed to individual blade replacement.

ROTOR DESIGN CONSIDERATIONS

Rotor Loading and Environment During operation, the rotor structure experiences several different types of loading. It is this loading which determines the cross-section of the rotor structure radially inward from the flowpath surface. These include mechanical loading

from centrifugal and pressure forces, thermal loading due to temperature gradients, and torsional loading due to torque transfer and vibratory forces.

The maximum physical speed of today's large high pressure rotors can be as high as 15,000 RPM. Since centrifugal forces are proportional to speed squared, tremendous forces are generated from both the dead loads of the airfoils as well as the body forces from the rotor structure itself. The tangential stress resulting from this inertial loading (not dead loads of airfoils) is determined by:

$$\sigma = \frac{\rho}{g} r_{cg}^2 \left(\frac{2\pi N}{60} \right)^2 \quad (3-10)$$

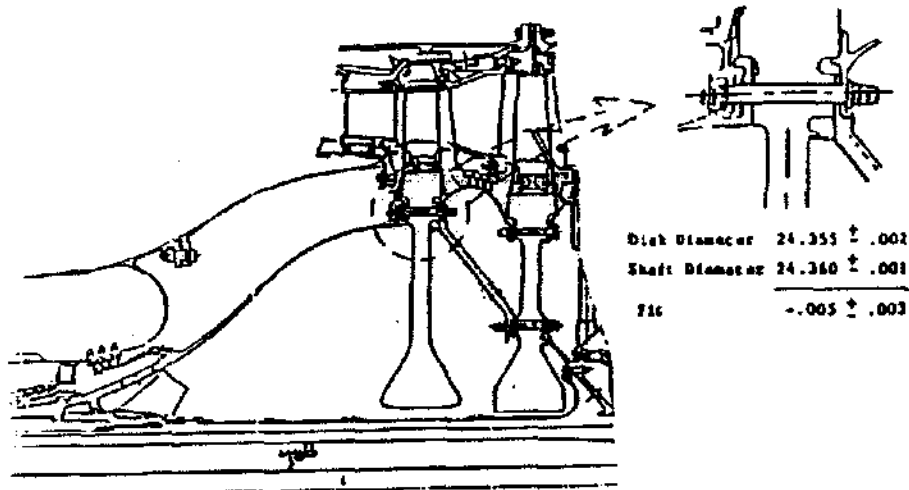
Accommodating these loads in an environment where the average temperature is high poses even a greater challenge to the mechanical designer. Metallic alloys lose strength with increasing temperature. Both creep and rupture can occur with loading at elevated temperatures. An ongoing research effort to develop alloys which maintain high strength at higher and higher operating temperatures is needed to develop more advanced engine applications such as for hypersonic flight.

A fundamental concept in the elastic behavior of material is that temperature gradients cause differential strain and thus thermal stress in a component. During normal operation, temperature gradients exist both radially and axially through the thickness of the rotor components resulting in significant thermal stresses. The magnitude of these thermal stresses are proportional to the temperature difference; that is,

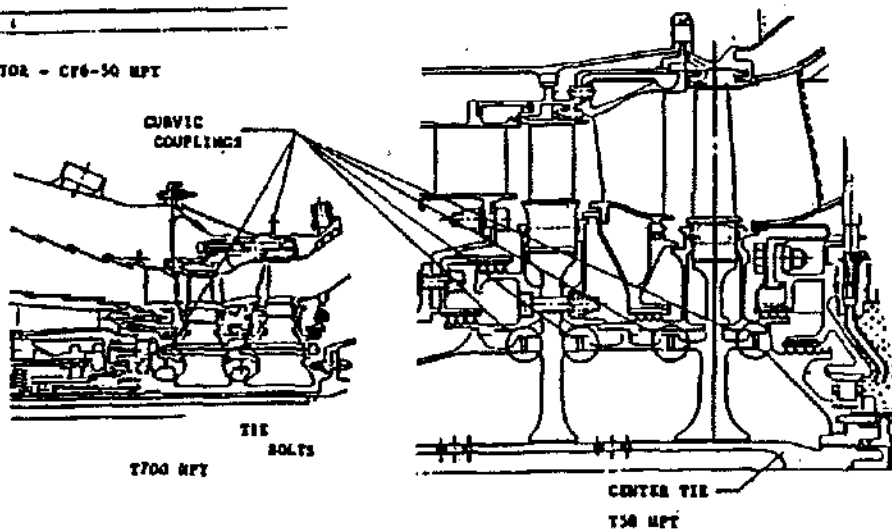
$$\sigma_T = E \alpha \Delta T \quad (3-11)$$

When rapid throttle movements are made, the rim areas of the rotor heat rapidly due to their close proximity to the flowpath gas. The areas further away from the hot flowpath gases heat slower resulting in large transient thermal gradients and thus thermal stress. This will be illustrated by an actual example later in this section.

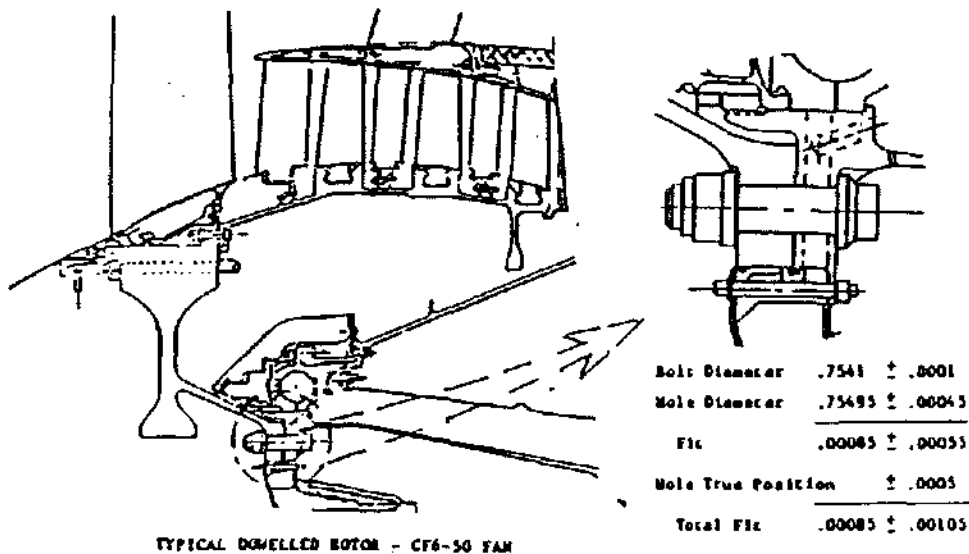
Since the prime purpose of fan and compressor rotors is to achieve a total pressure rise in the air stream, some degree of pressure loading is experienced by the rotor structure. Pressure loads are normally not a major contributor to rotor stresses except on large area conical shells subjected to compressor discharge pressure, airfoil induced rim overturning moments due to gas loads on the airfoil, and thin disks subjected to large pressure differences.



TYPICAL RABBETTED ROTOR - CF6-50 NPT



TYPICAL CUBIC APPLICATIONS



TYPICAL DOMELLED ROTOR - CF6-50 FAN

Figure 3.52 Common Rotor Attachments

The last type of loading to be discussed is torsional loading. Operational torque loading is determined from performance cycle data by

$$T = 63,024 \text{ HP/N} \quad (3-12)$$

where T = Shaft torque (in-lb), HP = Horsepower transmitted, and N = Rotational speed (RPM).

Torque loading is most significant in the design of shafts, curvic couplings, and bolted flanges, but is otherwise an insignificant component of loading in large diameter rotor structural components. Geometric discontinuities in torsional stress fields have high stress concentration factors (up to a factor of 6.0 for a round hole, for example) and must be carefully factored in the design of high torque load components such as shafts.

The interaction of these various different types of loading will be illustrated by examining the stress state of the CF6-80C2 stage 13 high pressure rotor disk throughout the CF6-80C2 typical flight cycle. The CF6-80C2 compressor rotor and flight cycle can be seen in Figure 3.53.

The typical CF6-80C2 flight mission can be described as eight minutes at ground idle prior to takeoff, two minutes at takeoff, twenty minutes in climb, twenty-six minutes at cruise, another twenty minutes for descent, three more minutes for approach, five seconds in thrust reverse and finally eight minutes at ground idle as the aircraft returns to the terminal. This cycle should be familiar to individuals who have been passengers on commercial aircraft.

Figure 3.54 plots the rotor speed, rim and bore temperatures, and total (mechanical and thermal) rim and bore tangential stress throughout the mission for the CF6-80C2 stage 13 compressor disk. This stress/temperature trace illustrates the characteristic response of a disk when subject to both mechanical and thermal loading.

The rim stress plots show the affect of the rim temperature increasing much faster than the bore. The rim is actually in compression during the maximum speed (take-off) point in the cycle due to the thermal stress being larger than the mechanical stress. As the disk bore heats up during the climb and cruise portions of the

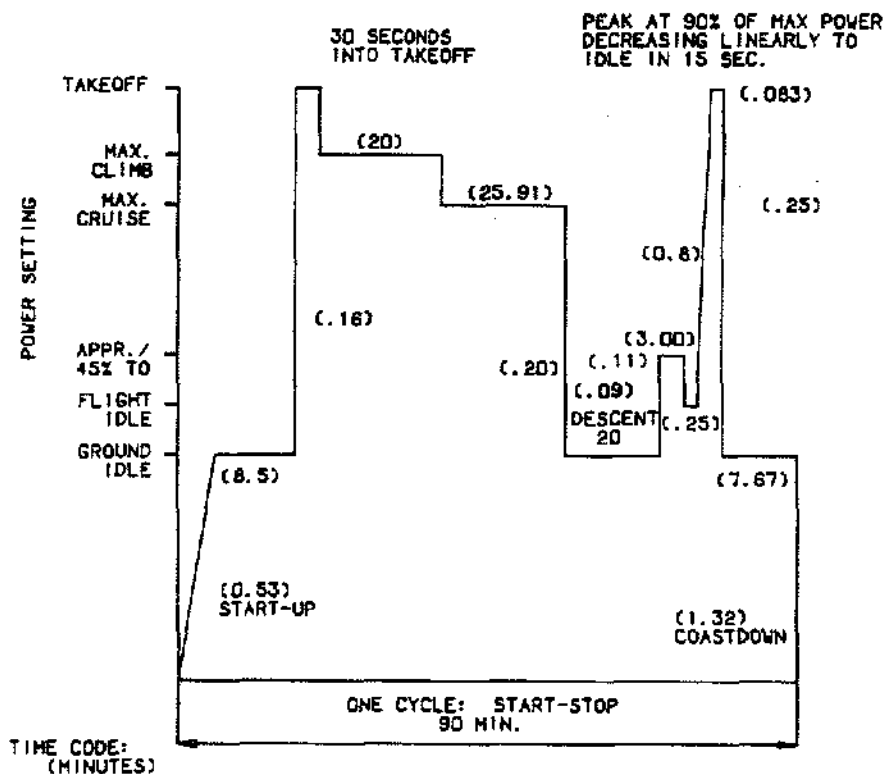


Figure 3.53 CF6-80C2 Flight Cycle

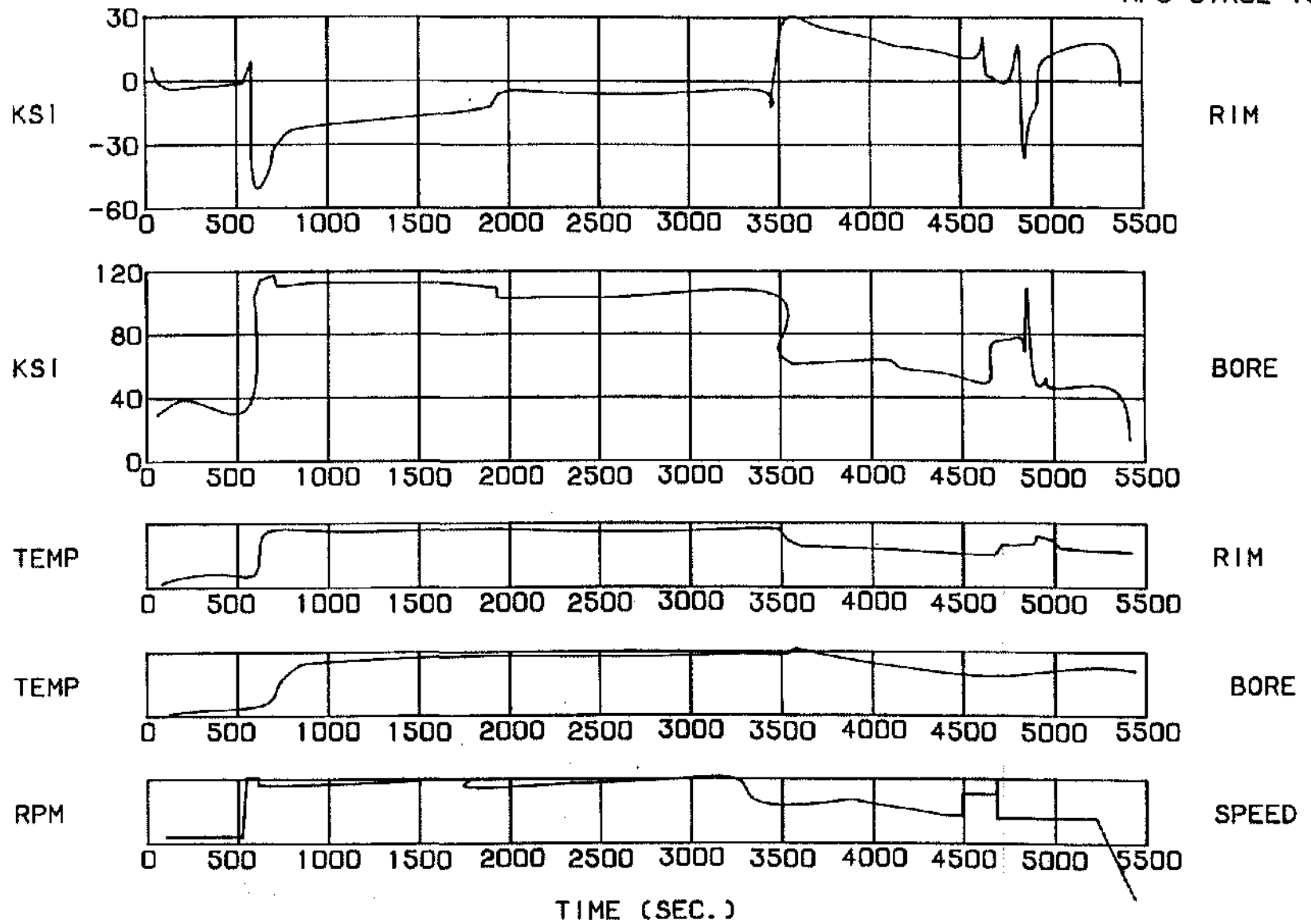


Figure 3.54 CF6-80C2 HPCR Mission Data Standard Day

mission, the thermal and mechanical stresses are of equal magnitude and the total stress is near zero. The throttle back to descent power at the end of cruise produces another transient response which is opposite to that seen in the throttle burst at take-off. The total stress is reduced by the lower rotor speed but the temperature gradient is reversed rim to bore; that is, the bore cools much slower than the rim resulting in the maximum tensile, tangential stress point in the mission. The high convective heat transfer coefficients in the rim coupled with lower thermal mass in the rim versus the disk bore makes these rim to bore temperature gradients unavoidable in rotor design. Complicating the design process, the rotor temperatures and thermal gradients are the least accurately known influence in rotor design, particularly in the early phase of the design when performance cycle variations, mission definition, and rotor cooling systems effectiveness are not fully evaluated. Since the temperature influence can be significant, it is necessary to use conservative assumptions during the initial design and pursue an aggressive program to refine the thermal loading assessment through instrumented engine testing.

ROTOR FAILURE MECHANISMS

Fatigue One of the most important design criteria for rotor structures is cyclic life. The two types of "life" most relevant to the design of fan and compressor rotor structures is low cycle fatigue (LCF) life and residual life. Low cycle fatigue refers to the behavior of materials under cyclic loading where the peak stress is much lower than that which would be completely safe if imposed in a unidirectional (static) application. Exposure to this cyclic loading results in fatigue damage and can ultimately lead to fatigue failure (i.e. fracture) in continued exposures.

The cyclic life of a feature on a rotor component is a function of the total stress range experienced by that feature. The total stress range is defined as:

$$\sigma_R = \sigma_{MAX} - \sigma_{MIN} \quad (3-13)$$

Typically, stress concentration factors must be applied to this stress range due to geometric discontinuities such as bolt holes, scallops, loading and locking slots in circumferential dovetail slots, etc. The alternating stress is defined as:

$$\sigma_{ALT} = \frac{1}{2} (\sigma_{MAX} - \sigma_{MIN}) = \frac{\sigma_R}{2} \quad (3-14)$$

while the mean stress is defined as:

$$\sigma = \frac{1}{2} (\sigma_{MAX} + \sigma_{MIN}) \quad (3-15)$$

The total stress range, alternating stress, mean stress, and the associated temperature history, coupled with the intrinsic material capability, determine the number of cycles which can be withstood before part cracking/failure can be expected.

The complement to LCF analysis and one receiving an increasing amount of attention, particularly in military applications, is residual life analysis, or crack propagation analysis as it is sometimes called. This analysis considers the life aspects of cracks propagating from surface and subsurface flaws in engine parts.

Rotor crack propagation life is predicted for two reasons: first, to determine the remaining part life after initiation of a crack in low cycle fatigue to allow the life management of field parts; secondly, to determine the functional life of parts made from materials whose processing and structure result in inherent defects from which fatigue cracks can develop. The results of the crack propagation analysis is used to set inspection intervals for the engines in the fleet.

Crack propagation analysis is similar to crack initiation life with two major exceptions. An initial defect size must be assumed and the residual life is a function of the stress intensity range rather than stress range. The stress intensity range is a function of the crack geometry as well as loading. That is:

$$K = c \Delta \sigma \sqrt{a} \quad (3-16)$$

where c = geometry constant based on crack shape, $\Delta \sigma$ = stress range normal to crack, and a = crack depth. This calculation must be done iteratively since, as the crack grows, the stress intensity changes since total crack length "a" and the field stress " $\Delta \sigma$ " at the crack front will change.

Overspeed and Burst Rotor structural parts, specifically disks, must be designed to have sufficient mechanical integrity to remain intact in the event of an abnormal engine overspeed condition. The burst speed of a disk is defined as the speed at which the stresses exceed the ultimate capability of the disk causing it to rupture or burst. Overspeed conditions can be caused by component and/or system failures such as main engine control failure, loss of throttle linkage or loss of fan nozzle. Adequate burst speed margin is a requirement of most certifying agencies (i.e. FAA) for commercial engines as well as military engines.

Techniques have been developed for calculating disk burst due to excessive hoop stress. These techniques utilize the maximum stress and temperature of the disk as

well as the bulk stress and temperature of the disk, the ultimate strength of the disk material (UTS), and a factor used to correlate General Electric's past experimental results from proof testing with the analytically predicted burst speed. Design Practice (DP) 3210 describes in detail the methodology for predicting burst speed.

Vibration Rotor component and system vibrational characteristics must also be considered in the mechanical design of compressor rotors. Natural frequencies and mode shapes are determined with finite element analyses to assure no disk or shaft critical speeds exist in the engine operating range. These results are usually verified with dynamic strain gages from full-scale engine testing. Stresses due to vibration must be superimposed upon the steady-state stresses to preclude high cycle fatigue (HCF) failures. Damping is provided by the bolted joints in fan and compressor rotors but in some components, such as rotating seals, additional damping is required and provided by damper rings and sleeves such as those shown on the CF6-80C2 CDP seal and vent seal and #4 air/oil seal (Figure 3.55). The sliding motion between the seals and damper elements result in a highly effective damping mechanism.

ROTOR TRADEOFFS AND IMPLICATIONS FOR DESIGN

Many of the design criteria previously discussed have conflicting implications relative to rotor design and require trade-offs to be made in the design process. A few of these trade-offs are discussed below.

In today's extremely competitive environment facing GEAE customers, reducing fuel consumption and operating costs are of paramount importance. More aerodynamically efficient and lower weight components are means to achieve lower fuel burn. This minimum weight constraint often conflicts with maintaining the disk bulk stress low enough to yield adequate burst speed margin. A simple method to increase disk burst speed is to add material to the bore of a disk but at the expensive penalty of increased component weight.

Another trade-off which must be considered in rotor design is that between "optimized" design and producibility. Producibility refers to the capacity of a component to be produced in a cost-effective and timely fashion. Today's design tools allow very elaborate part shapes and

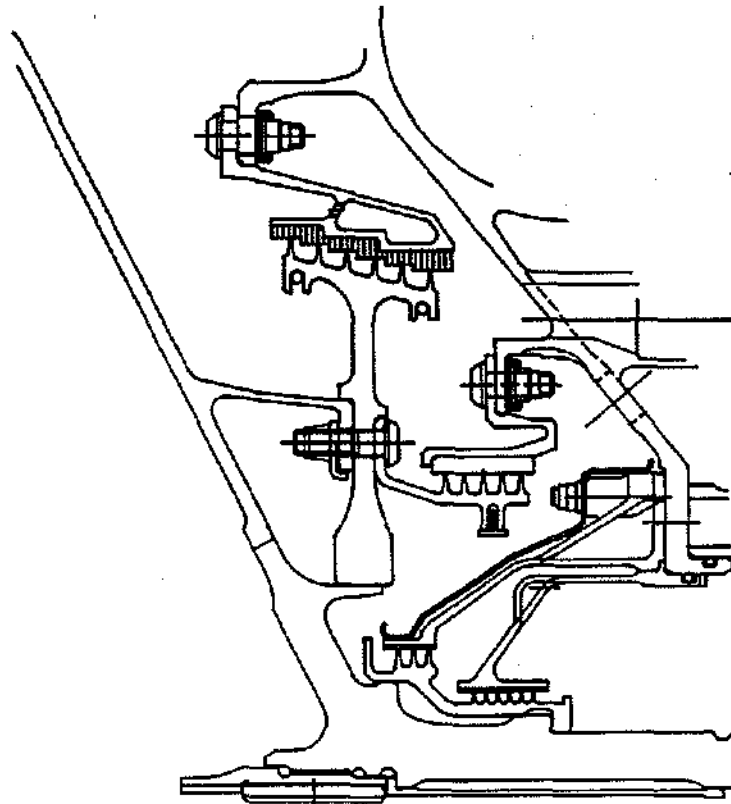


Figure 3.55 CF6-80C2 CDP Seal and Vent Seal

contours to be defined thus optimizing stress and increasing the cyclic capabilities of the rotor parts. However, these elaborate contours are also very expensive to manufacture and sometimes have little tolerance for the inevitable machine or operator error.

Increasing attention is being paid by customers to maintainability. While increasing the complexity of the design of the components and control systems can provide increased performance of the engine, it also increases the maintenance load and sometimes compromises system reliability. This is another trade-off in design; that is, between higher performance-complexity and maintainability. Fewer parts usually translates into decreased maintenance costs.

FAN AND COMPRESSOR CASINGS

Casings (or sometimes they are called pressure vessels) are generally cylindrical or shallow conical shells. In

general, a casing will have forward and aft flanges extending around the circumference in order to allow bolting to adjacent components, usually frames or other casings. Frequently, casings will also have axial flanges near the intersection of the casing with a horizontal plane through the engine centerline (i.e. the "horizontal split lines"). Externally, casings are usually studded with embossments (or "bosses") and holes used to supply bleed air, act as pivot points for drive mechanisms, and as openings for inspection access ("boroscope ports"). In addition, there may be a number of circumferential or axial stiffening rings which subdivide the casing skin into panel sections. Internally, casings may be of single or double walled construction, depending chiefly on the thermal environment. In split casings, it is usual to find grooves called "T-slots" running the circumference of the shell. As with the embossments on the outside of the casing, these T-slots are used for mounting other stator components, including vanes and blade tip shrouds. Figure 3.56 shows a compressor casing for the CF6 engine.



Figure 3.56 Compressor Stator

The primary function of a casing is to act as the structural backbone of the engine, transmit loads generated by the exhaust gases to the engine mounts, react aircraft maneuver induced loads with minimal deflection of the flowpath surfaces, and contain the hot, high pressure flowpath gases with minimal leakage. In addition, the casing must provide precisely located, stable mounting sites for a myriad of accessory components, brackets, tube clamps, pipes, and drive mechanisms. The inner surfaces ("ID") of the casing must provide mounts for both static and variable vanes, as well as defining the outer gas flowpath either with integral blade tip shroud material embedded in the casing wall or by providing mounting provision for removable shrouds. Finally, the case must act as a failsafe device in the event of a catastrophic failure of the rotor blades, preventing the escape of high velocity airfoil fragments.

CASING DESIGN CONSIDERATIONS

There are three primary fan and compressor case loadings: thrust and maneuver loads, pressure loads, and loads induced by the failure of internal rotating components. Thermal loads are not usually a major design factor except where bimetallic welds or rabbet joints exist. Engine thrust loads are usually transferred as compressive loads on the shell structure. Maneuver loads, which result from the reaction of the mount system to the "g" loads caused by slinging the massive engines about the aircraft centerline at speeds of several radians per second, combine with the thrust loads to cause various combinations of overturning moments, shear loads, and torque loads. These usually size the basic parameters of the casing.

Pressure loads on the casings result from the difference in internal and external gas pressures (ΔP). While pressures vary, becoming higher as one travels farther aft, tangential stress at a given location can generally be calculated according to:

$$\sigma = \frac{\Delta P r}{t} \quad \text{ok!} \quad (3-17)$$

where r and t define the shell wall meanline radius and thickness respectively. Casings must be designed to prevent tensile failure of the shell wall under pressures of up to two times the maximum operating pressure differential.

Casing walls are also expected to prevent the loss of failed rotor blades and the resulting secondary debris. Such fragments have a great deal of kinetic energy and if released they could (and have) penetrate the aircraft

structure causing damage to various aircraft systems. These fragments can be lethal even after passing through the aircraft fuselage and potentially, they could result in the loss of the airplane. In some cases, a band of composite material (usually KEVLAR) is added externally to the casing to satisfy the containment requirement without adding excessive weight to the basic shell design. It should be noted here that it is not practical to try to design casings which would be capable of containing a failure of the main rotor structural components. The weight penalty would be prohibitive. As a result, an extreme amount of effort is put into preventing such failures from occurring.

CASING FAILURE MECHANISMS

Containment Containment capability is determined by evaluating the energy absorption capability of the casing skin against the kinetic energy of the largest blade fragment which might be released during a failure. Energy absorption capability is a function of the skin thickness and the properties of casing material. Testing by the US Army at the Watertown Arsenal has established an empirical containment boundary (see Figure 3.57), above which the design must lie. The kinetic energy of a failed blade (E_b) is calculated for each stage at maximum rotor speed using:

$$E_b = \frac{1}{2} \frac{w}{g} v^2 \quad (3-18)$$

where w is the blade weight, g the gravitational constant, and v the tangential velocity at the blade center of gravity.

The casing thickness needed to contain a given energy blade is given by:

$$T_{eq} = K K_1 \sqrt{E_b} \quad (3-19)$$

where K is a material constant found from the Watertown arsenal or other similar testing (e.g. .00215 for titanium), and K_1 is the ratio of the modulus of toughness of the case material to a known test material. Calculation of actual casing thickness takes into account the hoop load carrying portion of any ring stiffeners as well as the thickness of the shell skin itself.

Buckling There are two types of instability against which the casing must be designed, general instability in which the entire shell structure collapses, and panel instability in which the local sections of shell skin

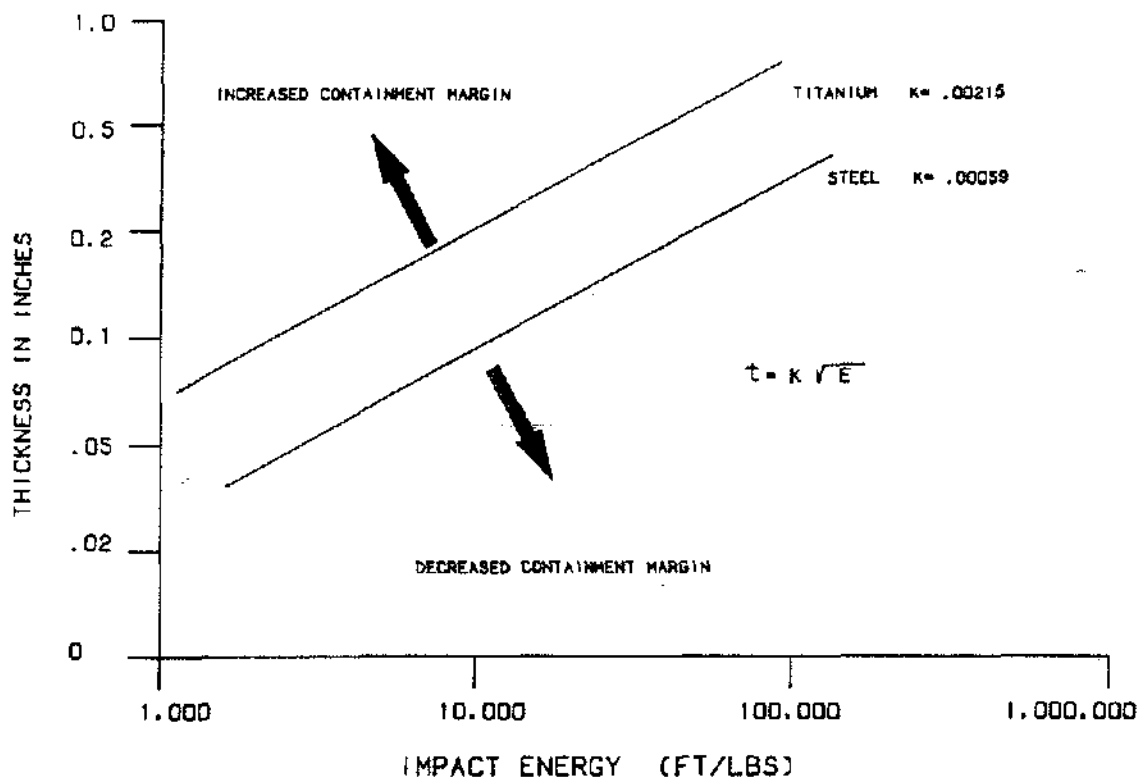


Figure 3.57 Empirical Containment Boundary

partitioned off by the stiffening rings and/or embossments buckle. The buckling of short cylindrical shells was extensively investigated by NACA (ref NACA TN 3786) in the late 1940s. Empirically derived buckling relationships were developed from which most shells can be correctly sized to provide the desired margins over engine loads. Interaction relationships between the overturning moments and torsional moments were also developed and are as follows (see Figure 3.58):

$$\frac{M}{M_0} + \left(\frac{T}{T_0}\right)^2 = 1 \quad (3-20)$$

where M_0 and T_0 are the values of these loadings that would individually cause general instability.

Vibration Casing walls located adjacent to the rotor blade tips are subjected to internal pressure pulses traveling with the rotor blades. In addition, low integral order rotor per rev and bearing passing frequency excitations are transmitted to the casing through its joints with the frames. Both the overall vibratory response of the casing and the response of local sections of the casing must be studied to insure that no interaction will exist with potential sources. This is generally done through

finite element analysis of the casing and the Campbell diagram approach.

Other Failures The ability of the casing to withstand overpressures without rupture and to operate without leakage under normal pressures requires that substantial attention be paid to the sizing of bolted joints. In addition to leakage, rotor failure also is a major joint design factor, for while the casing is not expected to contain major rotor structural failures, it is expected that flange joints will remain intact during such events.

The development of safe and effective rotor shroud materials is also an important issue in casing design. Materials must be sufficiently soft that they do not cause excessive heating or fracture of the blade tips and sufficiently hard that they do not rut or tear under blade rubbing. In the late 1970s, it was discovered that some tip coatings would explode if a sufficient quantity of coating dust was exposed to high temperature and pressure. This is precisely what can happen during a blade out failure during which the shroud coatings are severely rubbed out by the remainder of the rotor blades which are operating under high unbalance conditions. Since that time, combustion testing has been a key ingredient of all new coating development work.

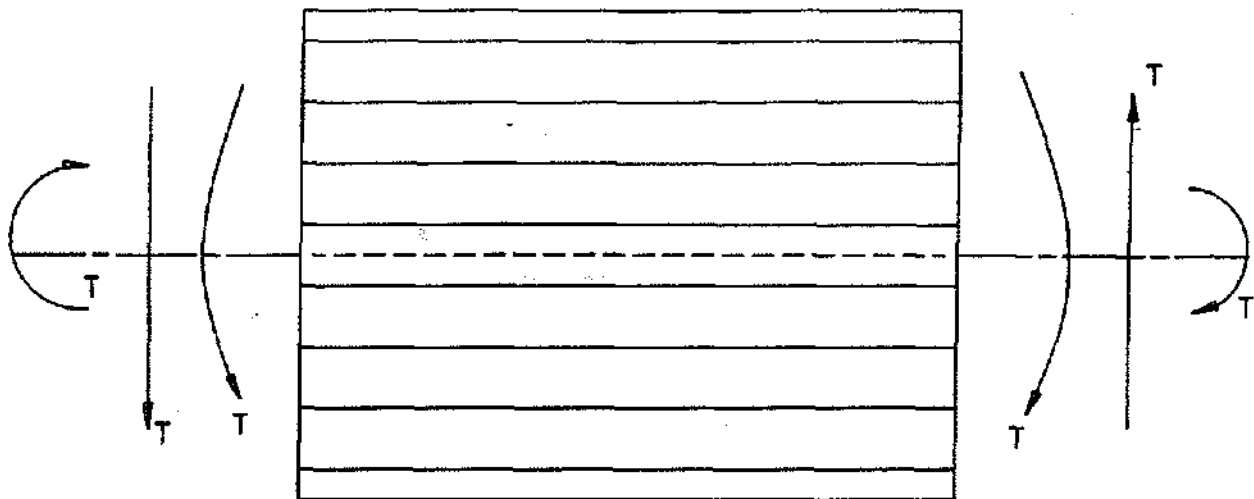


Figure 3.58 Casing Load Schematic

CASINGS TRADEOFFS AND IMPLICATIONS FOR DESIGN

The need for accurate mounting of vanes and accessories and a high degree of concentricity between the outer flowpath surface and the rotor bearing, and the minimization of weight results in considerable emphasis on manufacturing process development and control. The development of low density, very stiff structures is necessary to achieve these goals, and considerable effort has been expended in this direction. As previously mentioned, composite outer rings are beginning to be used to satisfy containment requirements, thus allowing a lighter weight design for the basic casing shell. Non-conventional manufacturing processes such as chemical milling and creep forming/diffusion bonding are also being used or tested. For the longer term, all composite casings are being considered, though issues of cost and dimensional control remain to be resolved.

FAN AND COMPRESSOR VARIABLE VANE ACTUATION SYSTEMS

Actuation systems are multi-component mechanisms which translate the electrical or hydromechanical output

of the engine control into mechanical rotation of stator vanes. As shown in Figures 3.59 and 3.60, the components of the system consist of an actuator, a drive or bell-crank mechanism, a unison ring for each variable stage, and a lever arm for each variable vane. In order to take up misalignments resulting from motion of the system and manufacturing tolerance, ball bearing joints are used in some places. Elsewhere, lined journal bearings are used.

By allowing the vanes to rotate, the operating efficiency of the compression components can be optimized at several points of the cycle instead of just at the cruise condition. This allows the aero-designer considerable freedom in his work. Typically, a test is conducted in the early stages of engine use in which the stator positions are modified systematically and both stall margin and performance are measured. From this test a "stator schedule" is established which optimizes performance while maintaining acceptable stall margins. This schedule is imbedded in the control logic, as a relationship between rotor corrected speed and actuator position. The function of the actuation system is to translate the motion of the actuator into the correct repositioning of the vanes.

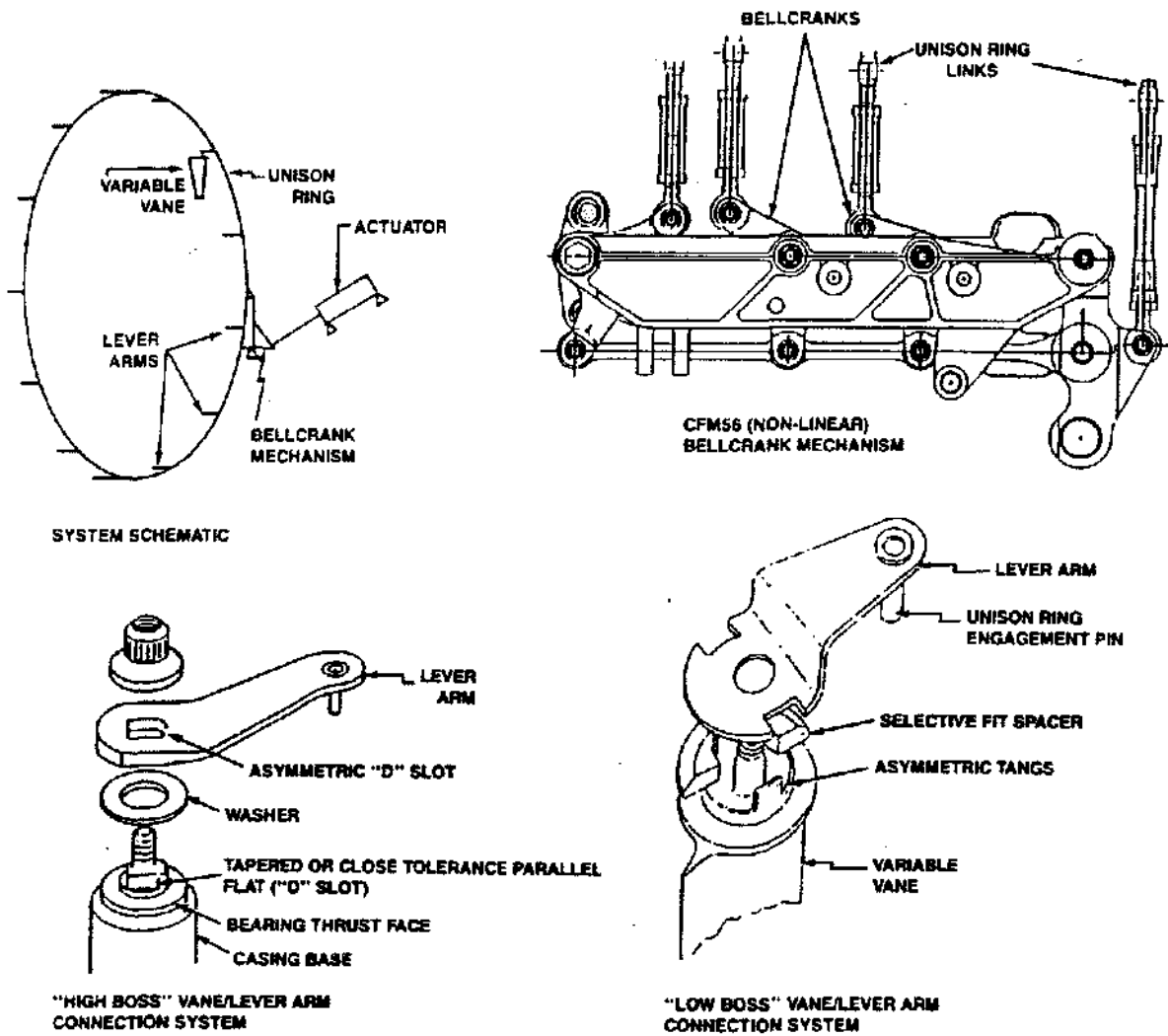
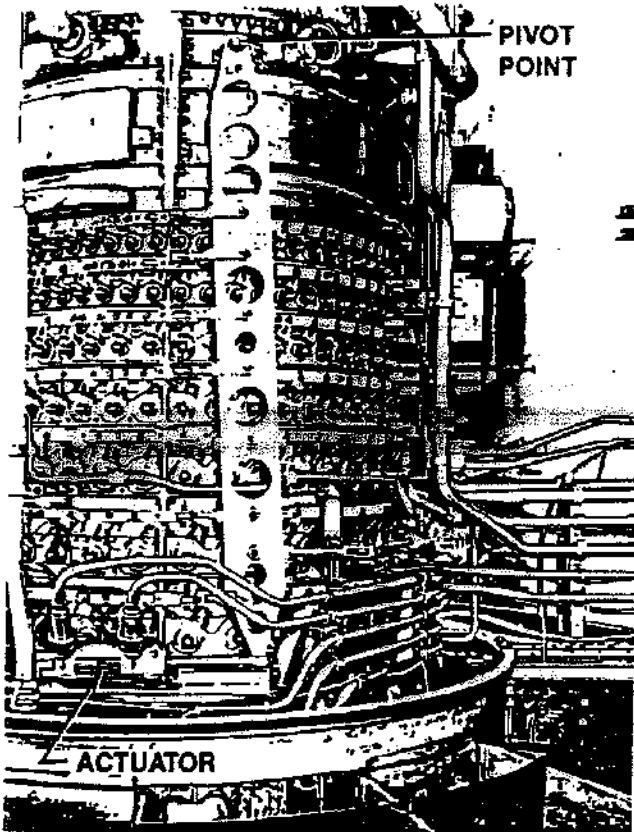


Figure 3.59 Actuation System Terminology



CF6 PUMPHANDLE SYSTEM

TF34 TORQUE SHAFT SYSTEM

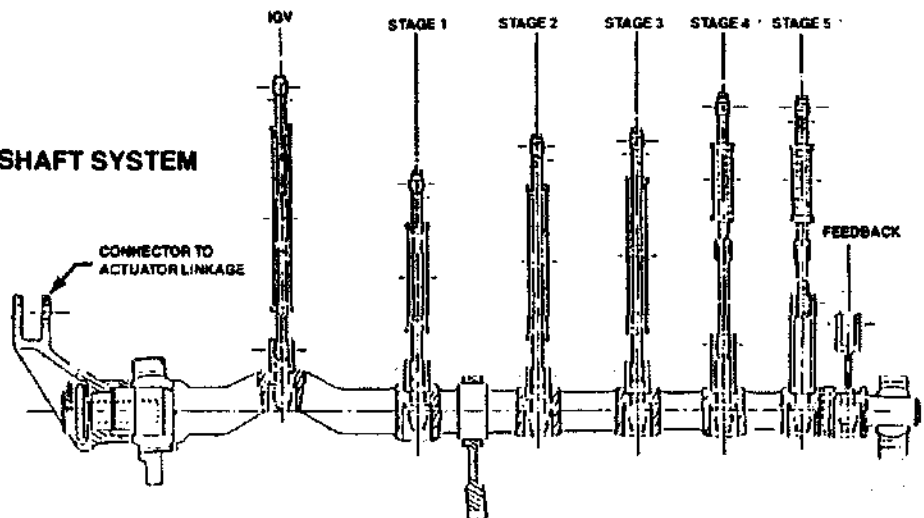


Figure 3.60 Linear and Torque Type Bellcrank Mechanisms

ACTUATION SYSTEM DESIGN CONSIDERATIONS

Normal operating loads on the actuation system are low, requiring only sufficient force to react the airfoil gas loads and to overcome friction in the system. However, stall and other abnormal operating conditions can result in overpressure pulses of up to ten times normal operating values. This results in designs which are very beefy and dovetail nicely with the need to minimize deflections of the system during normal operation since such deflections result in error in the vane positioning.

Because there are so many bearing surfaces in the actuation mechanisms, wear is also a major design issue. Most journal bearings and some ball bearing joints are lined with friction reducing materials such as Teflon® in order to extend the life of the mating metal parts. Mechanical vibration of any of the system components can accelerate the normal wear process by orders of magnitude, and hence it must be avoided in the design of components. Vibration stimuli include the vane natural frequencies and blade passing drivers on the vanes, and the engine per rev and bearing passing frequencies transmitted to the system components through the frames and casings to which they are mounted. In addition, flow pulsing in hydraulic actuators or overly sensitive control feedback systems can cause small motions or "dither" cycles of the system which have much the same effect as vibration on the wear of the system.

ACTUATION SYSTEM FAILURE MECHANISMS

Wear Key to the effective functioning of the actuation system is the minimization of hysteresis, a phenomenon which results in inaccurate positioning of the vanes, which can in turn result in dangerously high blade stresses. Hysteresis is primarily the result of looseness in the fit-up of the actuation system components and mechanical deflection of the components under load. While this can be minimized initially by designing the components to be very stiff and by specifying very tight tolerances on mating features, wear of these surfaces against one another will eventually occur.

Most fan and compressor actuation systems contain numerous interfaces in which metal against metal, metal against coated surfaces, or metal against special low friction inserts or bushings is gradually worn due to relative movement of the mating surfaces. It is important to fully test these interfaces and to quantify and document wear observed both in factory and flight testing (there is sometimes a wide variation in wear between the factory and field environments), since these data can have a profound impact on the rate of inspection and refurbishment

required in service. Undetected failure of these "minor" parts has led, on at least one occasion, to failure of the variable vane, ingestion of vane into the engine, and consequent massive damage to the compression section of the engine.

Hammershock For reasons not fully understood, it is possible to encounter strong shock waves in the gas flow which can result in large pressure pulses across the vanes and consequently very large loads on the components of the actuation system. Delayed augmentor lightoff, nozzle instability, and other causes which cannot generally be predicted during the design of the engine can result in pressures ten times higher than those expected in normal operation. In many cases, these loads size the actuation system components and the mounting of the components. Since this is in the same direction as the stiffness needed to minimize vane hysteresis, it does not usually result in a major weight penalty to the design.

ACTUATION SYSTEM TRADEOFFS AND IMPLICATIONS FOR DESIGN

Because of the need for increasingly efficient turbomachinery, it is likely that there will be a need for more, rather than fewer variable stages, on future engines. This will increase the complexity of the systems and increase the need for wear resistant materials that will function effectively at elevated temperatures. In most cases today, wear effectiveness is available, but at a very steep price. The designer must balance issues of initial cost against maintainability cost in selecting these materials.

With the advent of the UDF, practical application of blade actuation systems has arrived. The rotating environment greatly complicates the task of the actuation system designer, but performance and weight tradeoffs for a fully variable cycle engine are simply too good for this to stand in the way.

FAN AND COMPRESSOR SYSTEM DESIGN CONSIDERATIONS

Containment & Vibratory Weak Link Criteria Rotor mechanical designers must guard against catastrophic failure mechanisms. A common design practice in stationary steam and gas turbine applications set the rotors to release buckets from their dovetail attachments at a predetermined speed prior to rotor disk burst speeds. Thus eliminating the need to design containment casings for heavy rotor disk fragments which would have more

kinetic energy. In aircraft engines where engine operation and inlet conditions are significantly more varied than stationary engines the philosophy of having all blades flung from the rotor simultaneously is impractical. Therefore, axial flow compressors and fans are designed to have the casings contain all of the expected damage from ingestion events, such as tire treads and birds, which are certain to occur. All rotor fragments that are released are expected to exit away from the plane either forward or aft, and fragments exiting the engine radially must have little or no kinetic energy left to cause destructive damage to important airframe control lines or fuel tanks and lines. Further, flight weight aircraft engines employ a "weak link" criteria that simply stated is the airfoil shank is stronger than the airfoil, the blade attachment or dovetail is stronger than the blade shank, and the disk attachment is stronger than the blade attachment. This leads the design to have the lightest fragments fail first, if at all. Two benefits come from applying this criteria. First, in the event of a blade failure, less damage will be done from the smaller fragment, and the engine can be designed lighter as there will be lower unbalance loads and less containment capability required. Secondly, with the dovetail stronger than the airfoil the disk can be designed to prevent a "domino" effect where the loss of one blade results in a disk dovetail post failure which would result in the loss of another blade and so on.

System Vibration and Balance Modern jet engines are analyzed for overall system vibrations as complicated spring-mass systems. In these models, the interaction of rotor vibratory excitations and static structure flexibilities can be studied to find critical rotor speeds where bearing and engine mount loads are affected. Very often early in the design phase an important speed operating range is found to have a critical crossing. These can sometimes be moved out of the operating range by changing the stiffness of one or more components. In other cases, the engine control is modified to avoid steady-state operation at a known engine resonance speed. The system vibration models of development and production engines cover not only the engine system but also the mount attachments and airframe installations.

Manufacturing tolerances prohibit making perfectly balanced and centered parts and thus all high speed turbomachinery is balanced during assembly. Rotors weighing hundreds of pounds are dynamically balanced to obtain residual imbalances of 10 to 25 gm-in, which is equivalent to the weight of a penny displaced just 3 to 7 inches from the axis of rotation. Long flexible shafts and rotor spools require multi-plane balancing. Indeed, multistage non-integral compressor spools are balanced stage by stage. Then assembled together and rebalanced

as an assembly. This procedure tends to reduce bending stresses caused by local couples induced by imbalances during rotation.

Aside from vibratory excitations caused by rotor imbalances, the axial flow turbomachinery consisting of multiple stages of rotors and stators constitute the basic elements of an acoustic siren. The wide speed excursions and various combinations of rotor airfoil to stator airfoil ratios, present a device capable of generating a wide variation of frequencies. In point of fact, sirens are used in airfoil component testing to excite the airfoils natural frequencies. Thus engine development plans utilize three methods of designing to avoid harmful vibratory resonances: computer model vibratory analysis, component testing verification of the analytically found natural frequencies and mode shapes, finally, engine testing where actual vibratory responses and effects of damping can be studied.

Stress Analysis of Rotor Disks Before we begin the analysis of disks we will have a short review of the basic loads and stress equations governing this type of analysis. Modern turbomachinery designers rely heavily on large finite element computer models to aid in a detailed investigation of the design problem. However, the equations and concepts given here still find usefulness in checking the very large and costly computer model, so that the designer knows the answers are correct.

A rotor disk is nothing more than a big ring of material and the most significant stresses are the radial and tangential components. As a holdover from the days when barrels were commonplace, the tangential stress component is commonly known as the "hoop" stress. In simplified flat disk theory it is usually shown that the axial stress and the three shear stress components are zero by reasons of symmetry, but this is not the case in complicated geometries with complex loadings. Here we will develop equations that apply to flat disks as well as other shapes, but are limited in scope as they are one dimensional derivations.

Consider a ring of material which is pulled radially from the outside diameter with a uniformly distributed load, P , as shown in Figure 3.61. As the ring deflects radially outward under this loading, tangential forces (manifesting as hoop stress) are developed inside the ring to keep the ring in static equilibrium. The tangential force can be found from the free body diagram in Figure 3.61 by summing forces. Here we see that written as

$$\Sigma F_y = 0 = \int_0^\pi P \sin \theta r_0 d\theta - 2 F_{HOOP} \quad (3-21)$$

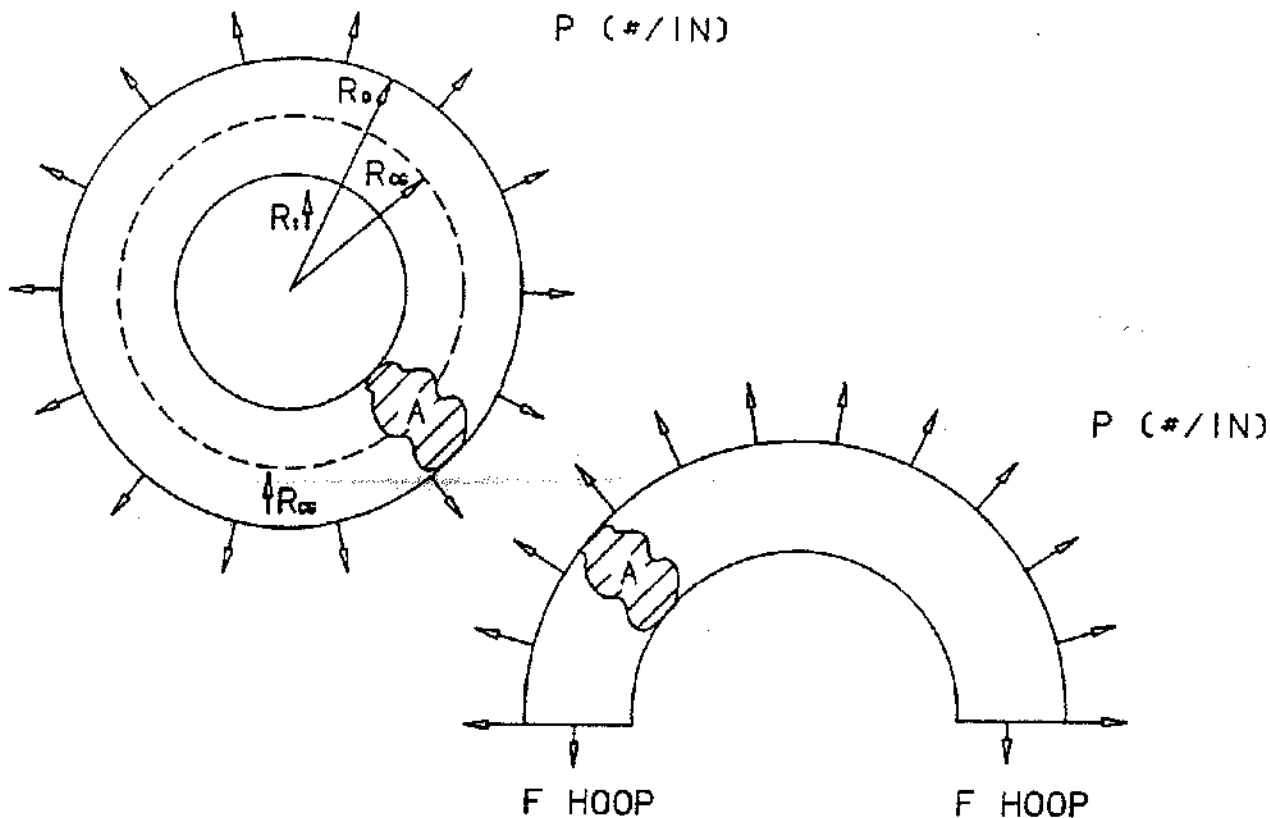


Figure 3.61 Radial Pull on a Ring

$$\Rightarrow 2 F_{HOOP} = Pr_o \int_0^\pi \sin\theta d\theta = Pr_o [-\cos\theta]_0^\pi = 2 Pr_o \quad (3-22)$$

$$\therefore F_{HOOP} = Pr_o$$

$$\sigma_{HOOP} = \sigma_\theta = \frac{F_{HOOP}}{A} = \frac{Pr_o}{A}$$

For a rotating ring the formula for hoop stress can be found in most handbooks as

$$\sigma_\theta = \frac{\rho \omega^2 r_{CG}^2}{g} \quad (3-23)$$

This result can also be derived from the load case by substituting $\rho A \omega^2 r_{CG}$ for P and r_{CG} for r_o in the above integral.

The thermal hoop stress in an axisymmetric ring at any radius is given by

$$\sigma_{THERMAL} |_r = E \alpha (T_{BULK} - T_r) \quad (3-24)$$

Where T_{BULK} is the volumetric average temperature in the ring, E is Young's Modulus and α is the coefficient of thermal expansion.

Hoop stress in a ring can also be obtained from the mechanical load radial growth (actually circumferential strain) as shown below.

$$\sigma_\theta = \frac{\Delta L E}{L} = \left(\frac{2\pi(r + \delta) - 2\pi r}{2\pi r} \right) E \quad (3-25)$$

$$\sigma_\theta = \frac{\delta}{r} E$$

Please note that, when working with total radial growths, the thermal component of growth is removed first. This is because uniform thermal growth does not create stresses. Thermal gradients produce stresses!

Numerical Example for Rotor Disk Stresses Consider a fan rotor stage whose blade tip diameter is 45 in with a blade tip speed of 1400 feet per second. The blade root is

located at the 22 in diameter with the blade shank and dovetail occupying the area from a 22 in diameter to a 18 in diameter, which is the rim of the live disk (actual hoop load carrying part). The geometry of the proposed disk is given in Figure 3.62 along with the material data and temperatures. There are 38 blades, each weighing 1.5 lbs, and the additional dead weight (parts that will not carry any of the hoop load) is approximately 20% of the blade weight. The total dead weight composed of the blades, dovetails, blade retainers, disk posts, etc. may be considered to act as a mass whose center of gravity is located at a 24.5 in diameter.

You are expected to find the average tangential stress in the disk, the mechanical and thermal hoop stresses in the disk bore and rim, the live disk rim radial stress, the stage weight, and the "upper bound" estimate for the disk burst speed.

A lot of preliminary calculations are needed to find the loading definitions to fit the equations we developed ear-

lier. First, find the rpm of the disk from the tip speed and tip diameter.

$$N = \frac{V}{\pi D} = \frac{1400 \text{ ft/sec}}{\pi 45 \text{ in}} \cdot \frac{60 \text{ sec}}{\text{min}} \cdot \frac{12 \text{ in}}{\text{ft}} = 7130 \text{ RPM} \quad (3-26)$$

Then, the angular velocity in rads/sec.

$$\omega = \frac{N\pi}{30} = 7130 \frac{\text{rev}}{\text{min}} \cdot \frac{2\pi \text{ rad}}{\text{rev}} \cdot \frac{1 \text{ min}}{60 \text{ sec}} = 746.7 \frac{\text{rad}}{\text{sec}} \quad (3-27)$$

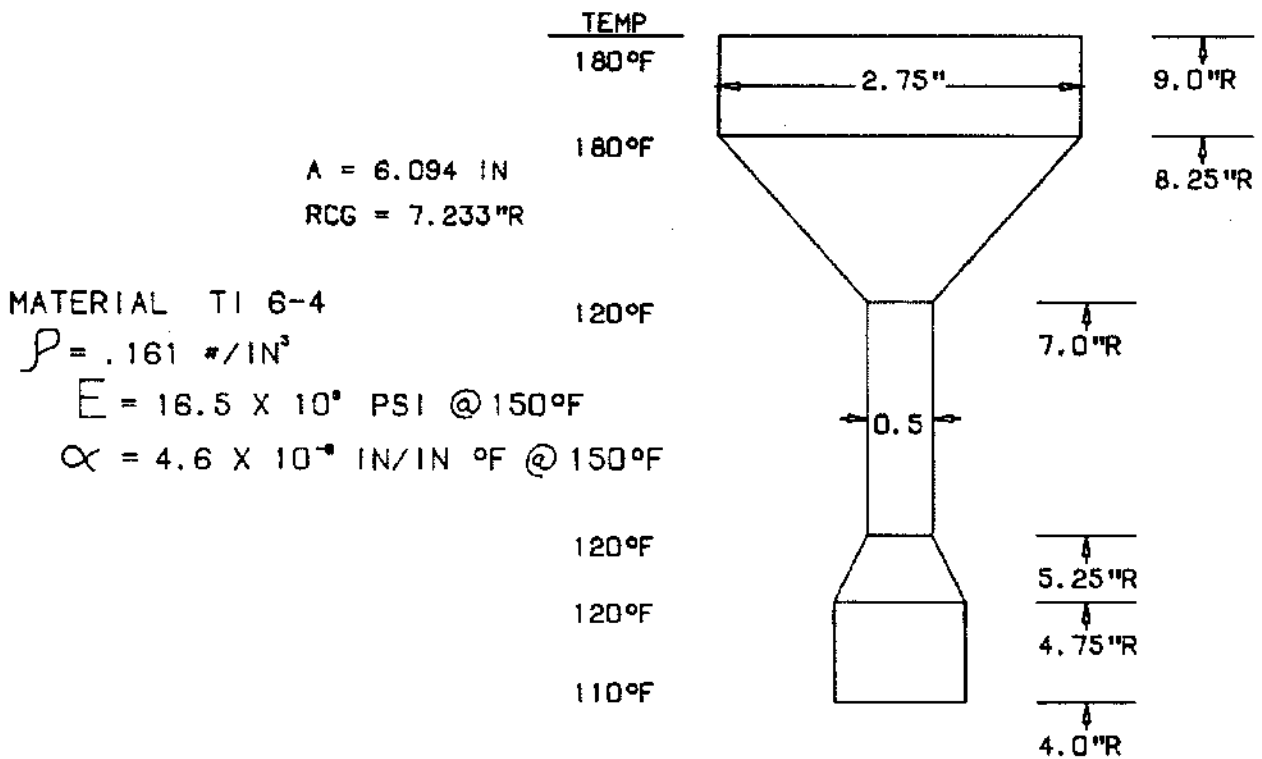


Figure 3.62 Live Disk Geometry

Then, the total rim dead load.

$$F_{CENT} = \frac{M\omega^2 r}{g}$$

$$= \frac{38_{BLDS} \cdot 1.5 \text{ lbs} \cdot 1.2 \cdot \left[746.7 \frac{\text{rad}}{\text{sec}} \right]^2 \cdot \frac{24.5}{2} \text{ in}}{386.4 \frac{\text{lb m} \cdot \text{in}}{\text{lb f} \cdot \text{sec}^2}}$$
(3-28)

$$F_{CENT} = 1.209 \times 10^6 \text{ lbf}$$

This is a big number that is typical of most engines. Now let us express it as a load per inch of circumference on the live disk rim.

$$P = \frac{F_{CENT}}{\pi D_o} = \frac{1.209 \times 10^6 \text{ lbf}}{\pi \cdot 18 \text{ in}} = 21,380 \frac{\text{lbf}}{\text{in}}$$
(3-29)

Ok, now we can use our earlier equations and find the average hoop stress by superposing the equations for hoop stress due to rim load and hoop stress due to rotation.

$$\sigma_{\theta AVG} = \frac{Pr_o}{A} + \frac{\rho\omega^2 r_{CG}^2}{g}$$

$$\sigma_{\theta AVG} = \frac{21,380 \text{ lbf} \cdot 9 \text{ in}}{6.094 \text{ in}^2}$$

$$+ \frac{.161 \text{ lb/in}^3 \left(746.7 \frac{\text{rad}}{\text{sec}} \cdot 7.233 \text{ in} \right)^2}{386.4 \frac{\text{lbm} \cdot \text{in}}{\text{lb f} \cdot \text{sec}^2}}$$
(3-30)

$$\sigma_{\theta AVG} = 43.7 \text{ KSI}$$

Using equation 3-25, we see that the bore and rim mechanical hoop stress can be obtained by radius ratioing if we ignore any differences in radial growth from the bore to the rim. Thus, we have

$$\sigma_{\theta BORE} = \sigma_{\theta AVG} \cdot \frac{r_{CG}}{r_{BORE}} = 43.7 \text{ KSI} \cdot \frac{7.233 \text{ in}}{4.0 \text{ in}}$$

$$= 79.0 \text{ KSI}$$
(3-31)

$$\sigma_{\theta RIM} = \sigma_{\theta AVG} \cdot \frac{r_{CG}}{r_{RIM}} = 43.7 \text{ KSI} \cdot \frac{7.233 \text{ in}}{9.0 \text{ in}}$$

$$= 35.1 \text{ KSI}$$
(3-32)

There is no average tangential thermal stress as the average tangential temperature is the same as the bulk temperature. So, calculating the thermal hoop stresses at the bore and rim from equation 3-24, we have.

$$\sigma_{\theta T BORE} = E\alpha (T_{BULK} - T_{BORE})$$

$$= 16.5 \times 10^6 \text{ PSI} \left(\frac{4.6 \times 10^{-6}}{^{\circ}\text{F}} \right) (150^{\circ}\text{F} - 110^{\circ}\text{F})$$

$$= 3.0 \text{ KSI}$$
(3-33)

$$\sigma_{\theta T RIM} = E\alpha (T_{BULK} - T_{RIM})$$

$$= 16.5 \times 10^6 \text{ PSI} \left(\frac{4.6 \times 10^{-6}}{^{\circ}\text{F}} \right) (150^{\circ}\text{F} - 180^{\circ}\text{F})$$

$$= -2.3 \text{ KSI}$$
(3-34)

The rim radial stress is simply a load per area calculation and can be quickly found by dividing P by the rim width.

$$\sigma_{r RIM} = \frac{P}{W} = \frac{21380 \frac{\text{lb}}{\text{in}}}{2.75 \text{ in}} = 7.8 \text{ KSI}$$
(3-35)

The stage weight is just the sum of the weights of all of the individual parts, and all are known with the exception of the live disk weight which is

$$\text{WEIGHT} = \rho A 2\pi r_{CG}$$

$$= (.161 \text{ lb/in}^3) 6.094 \text{ in}^2 (2\pi) 7.233 \text{ in}$$

$$= 44.6 \text{ lb}$$
(3-36)

And thus, the stage weight is 68.4 + 44.6 = 113.0 lbs.

Finally, a first pass calculation for disk burst that gives the "upper bound" burst speed occurs when the average tangential stress is equal to the ultimate tensile strength (UTS) of the disk material. Noting that the dead load and centrifugal load stresses are proportional to rotor speed squared, the burst speed can be found to be

$$N_{BURST} = N \sqrt{\frac{UTS}{\sigma_{\theta AVG}}} \\ = 7130 \sqrt{\frac{120 \text{ KSI}}{43.7 \text{ KSI}}} = 11,815 \text{ RPM} \quad (3-37)$$

A word about the accuracy of the stresses and burst speed just calculated is warranted. Comparison to a computer model is made in Table 3.6. This model includes the material property variation with temperature and accounts for the strain variation from rim to bore. As shown in the table, all of the stresses calculated for the example agree with the computer model answers within 2 KSI, except for the bore stress which is 13% high (9.2 KSI). The burst speed calculation that would give a maximum "safe" speed just prior to burst failure would be 10 to 15% below that calculated above. Whereas the "true" burst speed would fall somewhere between the two extremes.

Casing Containment Capability Suppose we are given a ribbed fan casing, shown in Figure 3.63, to analyze for containment capability and asked to find the mini-

mum thickness that can be used to stop the fan blade of the previous example when failure occurs during an overspeed event 20% above the design speed of 7130 rpm. Of course any weight savings found by using a thinner duct is to be calculated.

Let us begin by calculating the kinetic energy of the fan blade. Just prior to failure the kinetic energy is given by the rotational kinetic energy of the blade rotating about the engine centerline, and just after failure the blade kinetic energy is the sum of the translational kinetic energy and the rotational kinetic energy of the blade revolving about its own center of gravity. For ease of computing the kinetic energy of the blade just prior to release is used, and the resulting error is slight (less than 10%). Therefore, the blade kinetic energy is

$$E_b = \frac{m\omega^2 r_{CG}^2}{2} \\ E_b = \frac{1.5 \text{ lbm} \left[(7130 \text{ RPM}) 1.2 \left(\frac{\pi}{30} \right) \frac{24.5}{2} \left(\frac{1 \text{ ft}}{12 \text{ in}} \right) \right]^2}{2 \left(32.2 \frac{\text{lb} \cdot \text{ft}}{\text{lb} \cdot \text{sec}^2} \right)} \\ E_b = 19,500 \text{ ft} \cdot \text{lb} \quad (3-38)$$

We can see that the required thickness of the casing is

$$t_{SAFE} = .00215 \frac{\text{in}}{\sqrt{\text{ft} \cdot \text{lb}}} \sqrt{19,500 \text{ ft} \cdot \text{lb}} = 0.3 \text{ in} \quad (3-39)$$

DISK STRESS COMPARISON		
STRESS	HAND CALCULATION	COMPUTER
$\sigma_{\theta AVG}$	43.7 KSI	45.0 KSI
$\sigma_{\theta BORE}$	79.0	69.8
$\sigma_{\theta RIM}$	35.1	32.9
$\sigma_{\theta T BORE}$	3.0	4.1
$\sigma_{\theta T RIM}$	-2.3	-2.4
$\sigma_{r RIM}$	7.8	7.8

Table 3.6

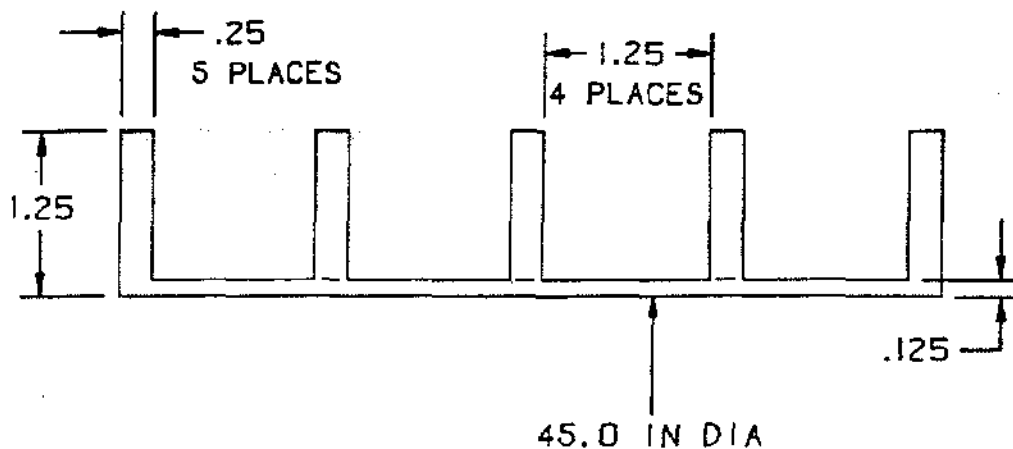


Figure 3.63 Ti 6-4 Casing Maximum Temperature = 300 F

This number is more than the minimum casing thickness of .125 in. However, this would ignore the beneficial effect of the ribs. Designers use an equivalent thickness in which ribs, that increase the hoop load carrying ability of the casing and are spaced so that the blade fragment cannot pass through them, are included. Quite simply, the total cross-sectional area is divided by the axial length to obtain an equivalent thickness. In our example this results in an equivalent thickness of

$$t_{eq} = \frac{A}{L} \frac{6.25 (1.25) - 4 (1.25 \cdot 1.125)}{6.25} = 0.35 \text{ in} \quad (3-40)$$

Therefore a thinner casing is warranted and by successive iterations (commonly known as trial and error) the minimum thickness of .065 in is found. This yields a weight savings of

$$\begin{aligned} \Delta W_T &= \rho \Delta A \pi D \\ \Delta W_T &= .161 \frac{\text{lb}}{\text{in}^3} \cdot 4 \cdot 1.25 (1.125 - .065) \pi 45 \text{ in} \\ \Delta W_T &= 6.8 \text{ lb} \end{aligned} \quad (3-41)$$

Low Cycle Fatigue Life Analysis Here we will consider a simplified mission, as shown in Figure 3.64, of a typical commercial flight. The top chart shown gives the basics of the flight and plots the engine power level. This chart could just as easily show thrust or engine rpm. The bottom chart gives the stress at the limiting location of the component in relation to the mission profile. The rotor is a single fan stage made of a new alloy called "unat-tainium" and the peak temperature excursion throughout the flight profile is limited to 150°F degrees. Calculate the LCF life from available material data given in Figure 3.65, and see if it meets the contract guaranteed life of 23,000 flight cycles. Bear in mind that FAA regulations require that the calculated life be divided by 3 to obtain the actual FAA approved life.

As shown in Figure 3.66 we have reduced the previous stress chart of the flight profile to three stress cycles that represent the cyclic content of the fan rotor. Also given in this chart are definitions and calculations for the alternating stress, mean stress, and A-ratio of the various stress cycles. Using the Goodman diagram of Figure 3.65, a broad range of life values can be found. The figure shows that for an A-ratio = 1.0 and alternating stress of 50 KSI that the cycles to failure (NF) is 100,000. For

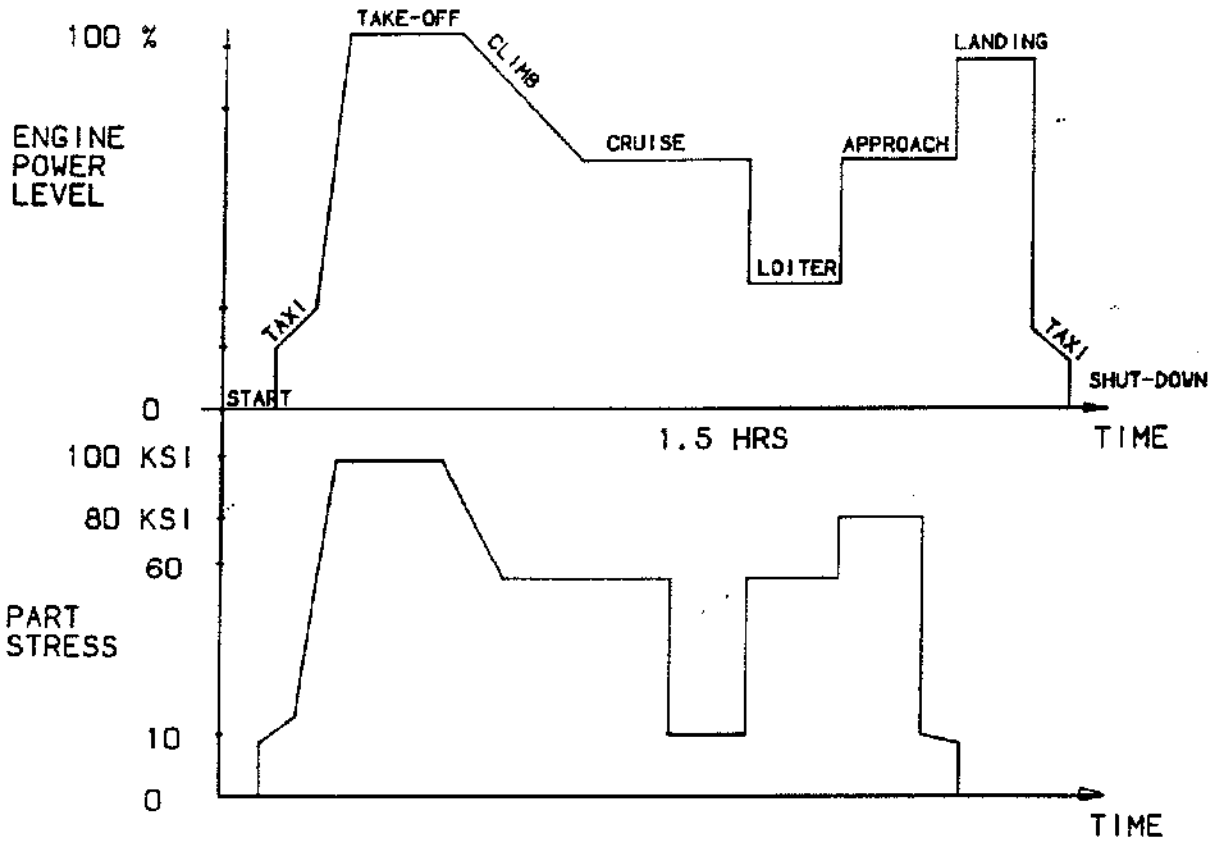


Figure 3.64 Simplified Commercial Mission

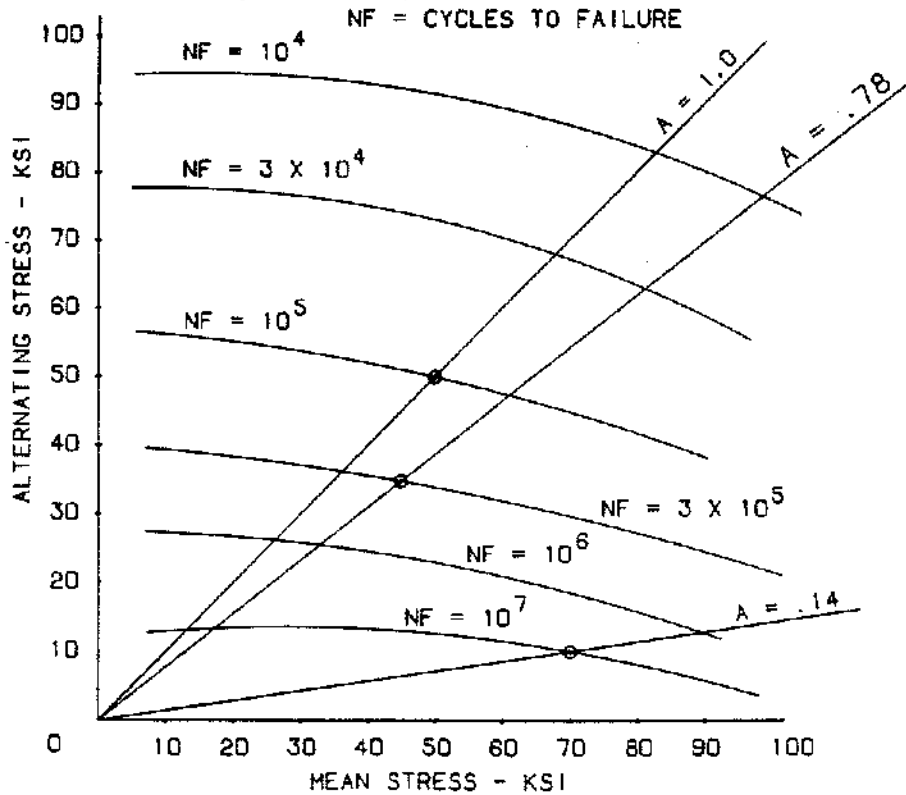


Figure 3.65 Goodman Diagram for Unattainium at 150 Degrees F

A-ratio = .78 and alternating stress of 35 KSI, $N_f = 500,000$ cycles, while A-ratio = .14 and alternating stress of 10 KSI yields $N_f = 10,000,000$ cycles.

So far so good, all of the cycles to failure exceed the 23,000 flight cycles by more than a factor of three, but how about when they are combined as they are in the flight mission? This is where we use a "linear damage" assumption, commonly known as "Miner's Rule". Simply stated, each stress cycle uses a portion of its total

useful life and that portion is equal to the inverse of the total allowable cycles. For instance, the A-ratio = 1.0 cycle would use 1/100,000th of its useful life during each flight. We can further assess which stress cycle consumes most of the available life of the part. This is brought out more clearly in Table 3.7 in which we see that the design life of 23,000 flight cycles uses only 27.8% of the available life for the fan rotor and meets the overall life objectives of the engine contract.

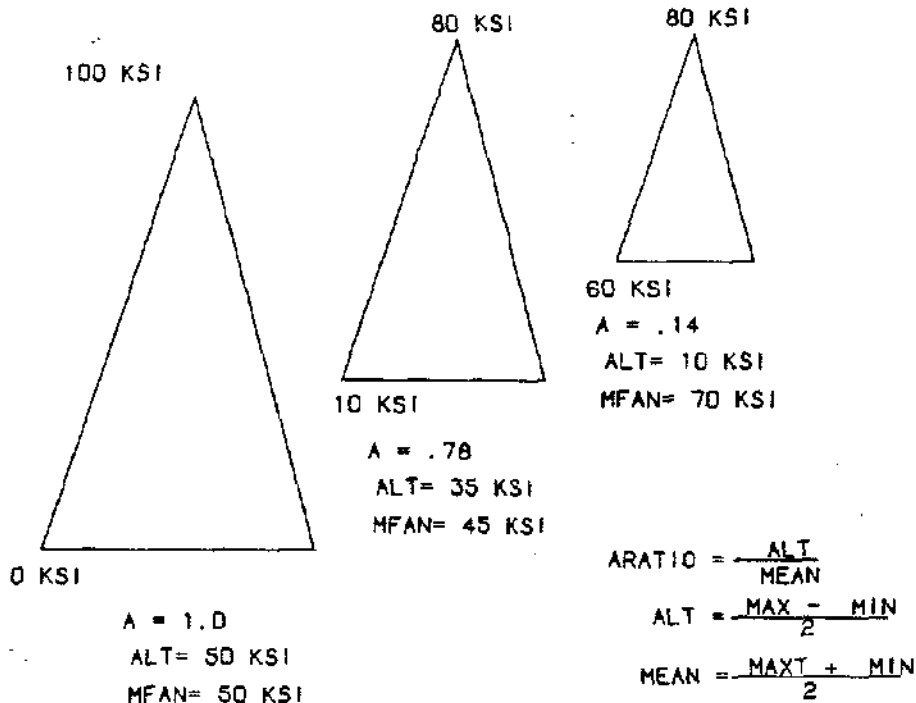


Figure 3.66 Fan Rotor Stress Cycles

STRESS CYCLE	REPEATED DURING MISSION	NUMBER OF ALLOWABLE CYCLES	PER CENT LIFE USED
0-100-0	1	100,000	23.0
10-80-10	1	500,000	4.6
60-80-60	1	10,000,000	0.2
Total Life Used =			27.8 %
Per Cent Life Used = $\frac{23,000 \text{ flights} \times \text{Repeated During Flight}}{\text{Number of Allowable Cycles}}$			

Table 3.7 CF6-XX LCF Life Analysis Summary

Chapter 4

COMBUSTOR AND AUGMENTOR DESIGN

by Paul Sabla
(Aerodynamic Design Topics)

and Dick Stenger
(Mechanical Design Topics)

COMBUSTOR AERODYNAMIC DESIGN

INTRODUCTION

The combustion system receives engine airflow from the compressor, adds heat energy to this airflow and delivers the hot gases to the turbine. Gas turbine combustors must supply uniformly mixed hot gases to the turbine at temperatures that are generally below stoichiometric fuel-air mixture combustion temperatures. Efficient burning, however, over a wide range of operating conditions, requires that the burning occur with fuel-air ratios that are close to the chemically correct or stoichiometric values. At stoichiometric conditions, the maximum amount of heat is released and all of the available fuel and oxygen is consumed. As shown in Figure 4.1, below stoichiometric, excess air acts as a diluent and reduces the heat released. Over stoichiometric, excess fuel acts as a heat sink, thus reducing the heat released. A typical combustion system cross-section is shown in Figure 4.2 along with the nomenclature for the various parts of the system.

Combustion systems are usually divided into two major regions, or zones, of about equal volume, that perform different functions. The upstream region is the primary combustion zone where nearly stoichiometric burning takes place with the correct fraction of air flow. The downstream region is the secondary or dilution zone, where the excess air is mixed with the hot combustion products to provide the desired turbine inlet temperatures.

Average flow velocities in typical combustors range from 60 to 100 ft/sec., but turbulent flame speeds are considerably less. For flame stability, a sheltered region must be used that provides space for the recirculation of hot combustion products and turbulent diffusion of these products into regions of unburned fuel-air mixtures, thereby providing continuous re-ignition and smooth burning. Many different techniques have been used to achieve a stable reverse flow pattern in the primary com-

combustion zone, but the method most commonly used is to form a swirling flow, or vortex, that creates a low static pressure region in the center of the vortex which induces a reverse flow of hot gases from downstream regions. Whatever technique is used, the flow pattern must be very stable over a wide range of operating conditions and must have the correct proportions of fresh air, fuel-air mixture and burned products. It has been found from past experience that a strong recirculating flow pattern with large reverse flow velocities provides very compact flame zones and high heat release rates.

PERFORMANCE REQUIREMENTS

The combustion system must operate over a very wide range of conditions and be capable of starting and accelerating the engine. To satisfy the objectives of engine operation, certain design requirements must be met. Several important design parameters are shown in Table 4.1.

Combustion Efficiency Combustion efficiency, which is defined as the ratio of actual to theoretical heat release, must be as high as possible over the operating range of the engine. Efficiency requirements for a new combustion system design are initially selected by the engine cycle design group and then modified as the combustor design progresses to factor in realistic estimates based on a more finalized version of the design.

Total Pressure Loss The total pressure loss of the combustion system is defined as the difference between the averaged stream total pressure at the compressor exit station and the turbine inlet station. This loss includes the diffuser total pressure loss, and is usually expressed as a percentage of the compressor exit total pressure, P_{T3} . In general, higher pressure losses result in better combustor performance and the combustor size and weight can be reduced. But, of course, higher pressure losses reduce the engine cycle performance. The pressure loss is very nearly proportional to the square of the compressor exit Mach number, and is a weak function of the combustor temperature rise.

Temperature Rise The combustion system temperature rise requirement is determined by the engine cycle design and turbine design groups. The value, ΔT , is the difference between the combustion chamber exit temperature, T_4 , and the compressor exit temperature, T_3 . If the required ΔT is greater than about 2600 °F, combustion efficiency may become less than the chemical efficiency due to the adverse effect of the exit temperature profile.

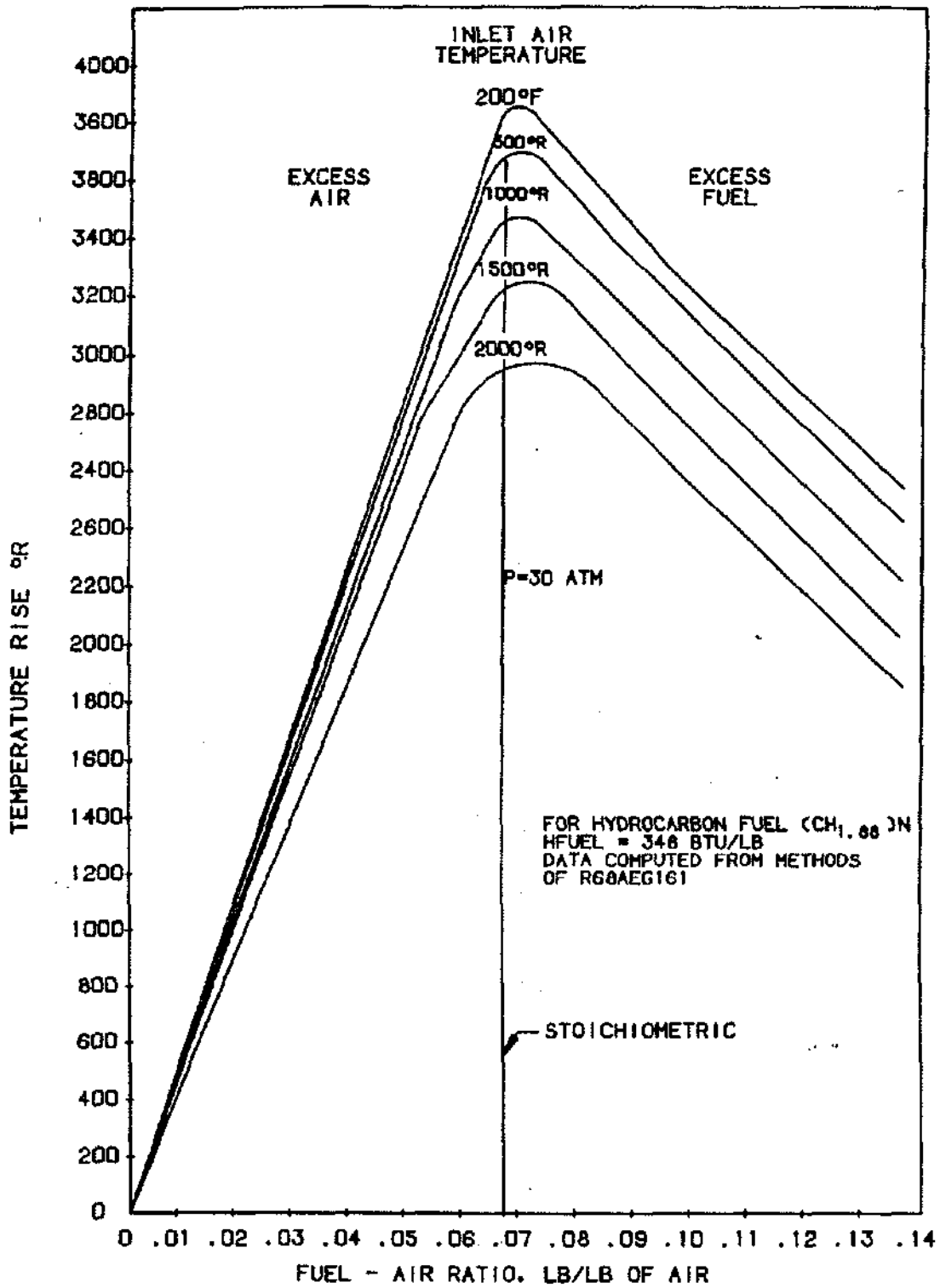


Figure 4.1 Combustion Temperature Rise

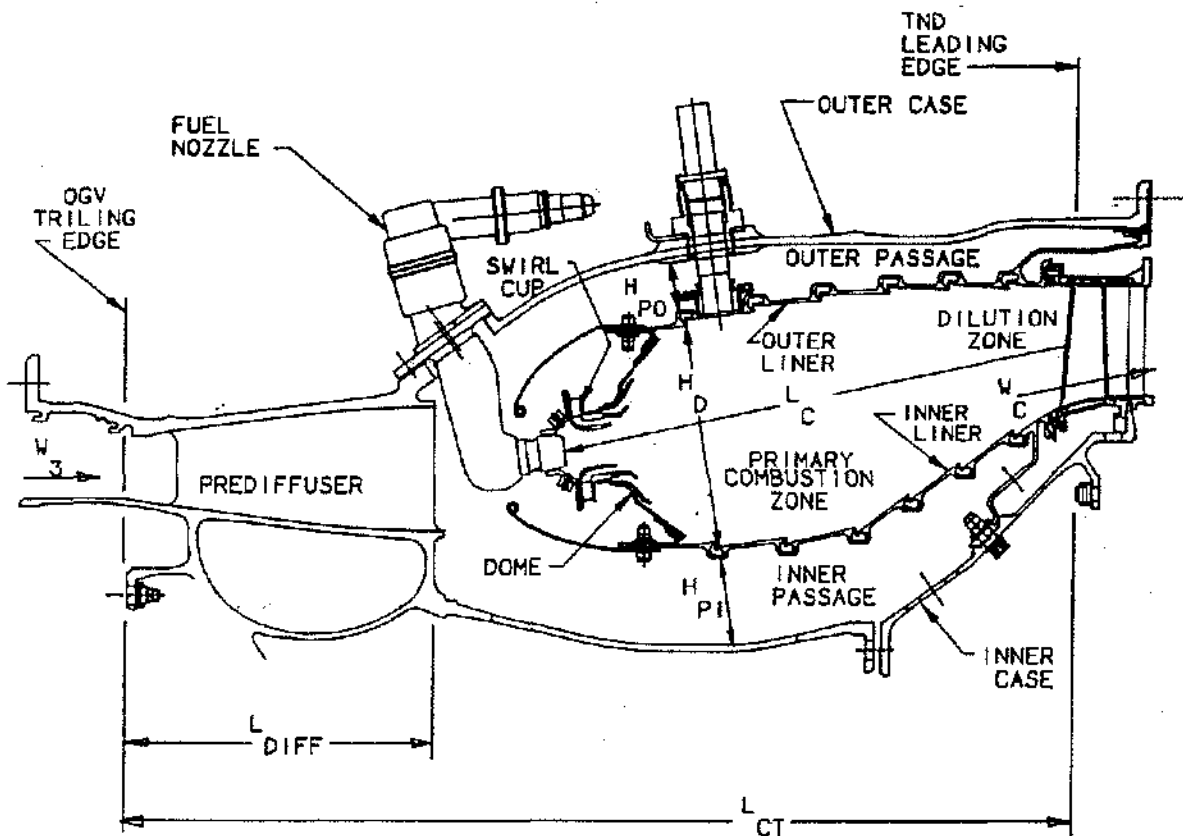


Figure 4.2 Typical Main Combustor Flowpath Design

COMBUSTION SYSTEM DESIGN REQUIREMENTS

- High Combustion Efficiency - $\eta_C \geq 99.8\%$
- Low Total Pressure Losses - $\Delta P_T/P_{T3} \sim 4 - 6\%$
- Uniform Exit Temperature Distribution - P. F. ~ 0.2
- Altitude Relight Capability - Up To 30,000 Feet
- Short Length - Light Weight
- Long Life
- Low Cost
- Maintainability
- Emissions Requirements

Table 4.1 Combustion System Design Requirements

Combustor Exit Pattern Factor A combustor exit pattern factor requirement is usually established in conjunction with the turbine designers. It is based on past experience with similar combustors and on parametric correlations that have been formulated from a large amount of test data. Pattern factor is a measure of the maximum temperature existing at the combustor exit plane. Pattern factor has a major effect on the life of the turbine nozzle vanes, unless the vanes are designed for stoichiometric temperatures. Many different combustor design parameters have an effect on pattern factor.

Combustor Exit Temperature Profile The combustor exit radial temperature profile is defined as the average of all of the circumferential temperature readings at each radial measurement station at the combustor exit plane. This profile, which is a measure of the temperature experienced by the turbine rotor vanes, is plotted against the radial distance from the turbine inlet root radius to the tip radius position. Combustor exit temperature profile factor is the highest temperature of the average temperature profile. Temperature profile requirements are

determined by the turbine design group with the close coordination of the combustion system designer. The curve on the left in Figure 4.3 shows a typical desired profile. The curve on the right is the locus of the maximum profile peaks. Any profile, for which the average temperature meets requirements and which falls below the locus of profile peaks, satisfies the combustor exit temperature profile requirements.

Altitude Relight Aircraft engine combustion systems are usually required to have the capability of relighting at specified high altitudes for windmilling conditions with cold, low pressure air and with cold fuel. This requirement is usually defined in the form of a required relight flight condition map. An example of a relight map is presented in Figure 4.4. The most difficult light-off conditions are usually encountered at the upper left corner of the map, where the air pressure is lowest and the combustor pressure drop is small. This altitude relight requirement is usually established by the engine project group to meet the requirements of the customer.

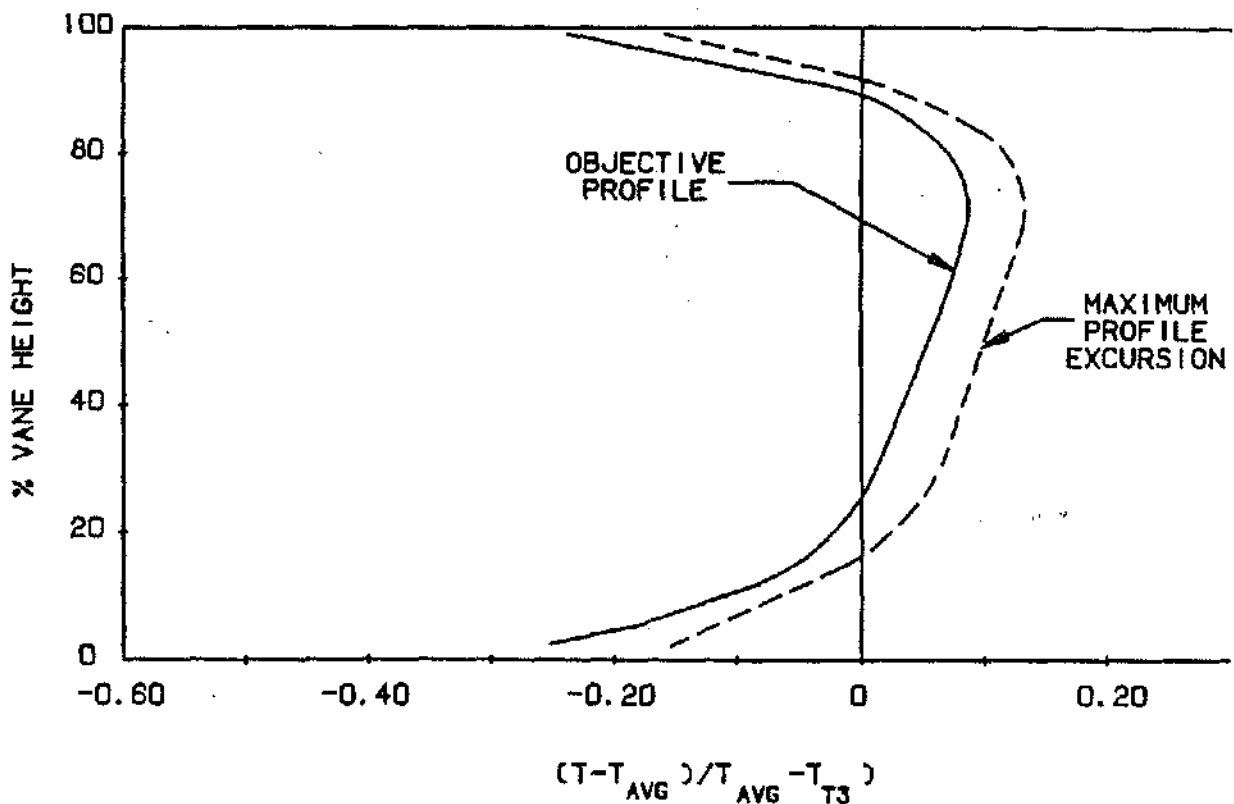


Figure 4.3 Typical Combustor Exit Temperature Profiles

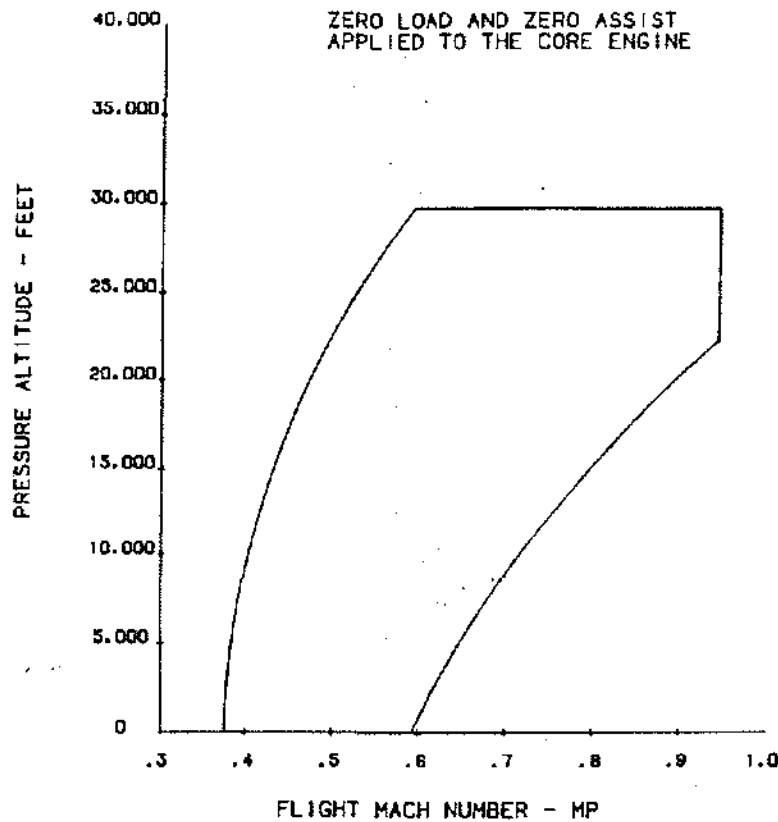


Figure 4.4 CF6-80C2 Windmilling Air Start Envelop

Emission Requirements Requirements for the maximum emissions of undesirable atmospheric pollutants from jet engines are established by government agencies. The U.S. Environmental Protection Agency establishes emission limits for commercial engines and military agencies establish limits for military engines. Emission limits are established for smoke, the oxides of nitrogen (which usually reach maximum values at take-off conditions), carbon monoxide, and unburned hydrocarbons (which are usually predominant at ground idle conditions). Since some of the basic combustion system design parameters have a strong effect on emission levels, the emission requirements must be considered during the preliminary design phase of the combustion system.

CRITICAL DESIGN PARAMETERS

There are certain key parameters used to evolve the combustor design. These parameters help determine the size and aerodynamic performance of the design. Table 4.2 lists the critical parameters and typical values for conventional combustion systems.

Space Rate and Aerodynamic Loading Parameters The combustion system space heat release rate is a measure of the concentration of the energy released inside of the combustor. Space rate is calculated as follows:

$$SR = \frac{3600(\text{Fuel Heating Value}) * (\text{Fuel/Air}) * W_3}{P_{T_3} / 14.7 * Vol_c}$$

where Vol_c is the interior volume of the combustion liner in cubic feet. In general, combustors for large engines should have relatively low space rates and combustors for small engines can have relatively high space rates. Space rate is inversely related to residence time, and directly related to temperature rise, ΔT , as follows:

$$SR = k \frac{\Delta T}{T_3} * \frac{1}{t_c}$$

where k is a constant for a particular combustion system design. This relationship suggests other loading parameters which may be used to correlate combustion system

CRITICAL DESIGN PARAMETERS

- Space Heat Release Rate - Btu/hr - Atm-Ft³
- Reference Velocity
- Combustor Dome Height
- Combustor Length to Dome Height Ratio - L_c/H_D
- Combustor Dome Velocity
- Passage Velocities
- Number & Spacing of Fuel Injectors
- Pattern Factor Correlation Parameters

Table 4.2 Critical Design Parameters

performance, such as the aerodynamic residence time parameter:

$$\tau_c = \frac{\rho_3(\text{vol}_c)}{w_c} = \left[\frac{1}{2} \left(1 + \frac{w_c}{w_D} \right) \right] \text{sec}$$

which is inversely related to space rate but does not depend on ΔT , where w_c = combustor airflow and w_D = dome airflow.

Reference Velocity Combustion system reference velocity is a measure of an "average" velocity through the entire cross-sectional area between the inner and outer casing walls of the combustion chamber. This velocity affects the residence time of fuel-air mixtures in the burner and the basic flame stability of the system. Although the reference velocity does not describe a physical velocity at any particular place in the system, this parameter is easily defined and provides a convenient method of comparing different designs.

Combustor Dome Height The physical dome height, H_D , of the combustor is an important parameter because the value of this parameter has a significant effect on the altitude relight capability of the combustion system. A correlation of maximum relight altitude with combustor dome height is presented in **Figure 4.5**. Although many other design parameters have an effect on altitude relight capability, the dome height must be large enough to permit the combustion system to satisfy the altitude relight requirements of the engine.

Combustor Dome Velocity The combustor dome velocity is defined as the average velocity for all of the com-

burntor dome flow, immediately downstream of the dome, between the inner and outer combustor liners. In general combustion flame stability is reduced as dome velocity is increased, which affects altitude relight capability, combustion efficiency (especially at high values of ΔT), and pattern factor.

Combustor Length to Dome Height Ratio All combustors must have sufficient volume and length to accommodate a low velocity flame stabilization region and a higher velocity mixing region where the hot combustion products are mixed with the excess dilution air. The total volume necessary to do this job depends on space rate, residence time, and other loading parameters, but the overall flow patterns required are well established. The desired flow patterns, which consist of a recirculating pattern in the primary zone and an air jet penetration pattern in the mixing region, determine, to a large extent, the overall shape of the combustor as defined by the combustor length to dome height ratio. L_c/H_D ratio will be nearly constant for all of the different combustor flowpath concepts, and since these basic flow patterns can be scaled to larger and smaller sizes, the L_c/H_D ratio is essentially independent of engine size. For values of L_c/H_D greater than 3.0, the liner cooling flow increases and begins to cause a serious increase in pattern factor. Values below 2.5 but not less than 2.0 may be used if the reference velocity is low, the fuel injectors are closely spaced, or the combustor pressure drop is high. As combustor technology has advanced, smaller, more compact combustors with reduced L_c/H_D have evolved as shown in **Figure 4.6**.

Combustor Passage Velocity Liner passage velocity for a combustion system is the velocity of the flow between

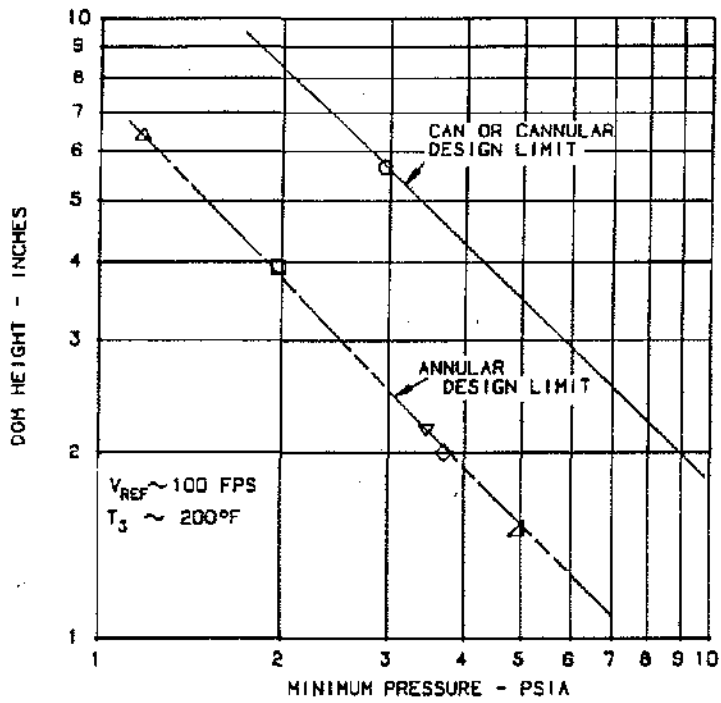


Figure 4.5 Dome Quenching Effect Correlation

* WITH EQUIVALENT PERFORMANCE CAPABILITIES

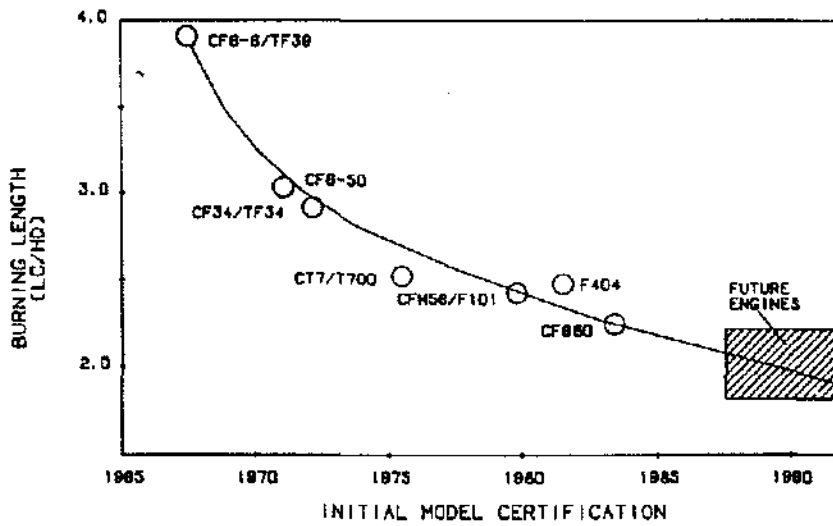


Figure 4.6 Progress and Trends in Combustor Lengths

the inner liner and inner casing and between the outer liner and outer casing of the system. The passage velocities change as the flow in the passage changes and as the passage area changes along the length of the passage. But the passage velocity is defined as the velocity at the dome exit plane with the total passage airflow. The passage velocities should be low enough to provide a uniform flow to the combustor with high static pressures and low total pressure losses in the passages. They should be high enough to provide good convective cooling of the combustor liner. The effects of passage velocity on liner convective cooling are established by the cooling system designer.

Number of Fuel Injectors Ideally, for good combustion system performance, the fuel should be injected from a large number of closely spaced injection points. However, practical considerations usually limit the number of fuel injectors which may be used. Fuel injectors, along with the swirl cups which are used with each injector, are costly and heavy. Also, a large number of injectors increases maintenance time and costs. The ratio of combustor length, L_c , to circumferential spacing of the fuel injectors, b , is a critical design parameter. If the fuel in-

jectors are too widely spaced and the L_c/b parameter is too low, high temperature regions may appear downstream of each fuel injector at the turbine inlet plane which may cause the pattern factor to be too high to meet requirements. The L_c/b parameter usually ranges from about 2.5 to about 4.5.

Pattern Factor Correlations Several combustor exit pattern factor correlations have been developed, based on various combinations of the critical design parameters. A correlation which includes a large number of important design parameters is illustrated in Figure 4.7, where pattern factor is shown as a function of a severity parameter. This severity parameter is defined as:

$$S = \frac{\text{S.R.} \left(\frac{w_{Lc}}{w_c} \right) \left(\frac{V_p}{V_{ref}} \right)^{1/2}}{10^{n_d} \left[\left(\frac{L_c}{H_D} \right) \left(\frac{L_c}{b} \right) \left(\frac{\Delta P}{P} \right) \right]^{1/2}}$$

where n_d is an estimated diffuser efficiency factor.

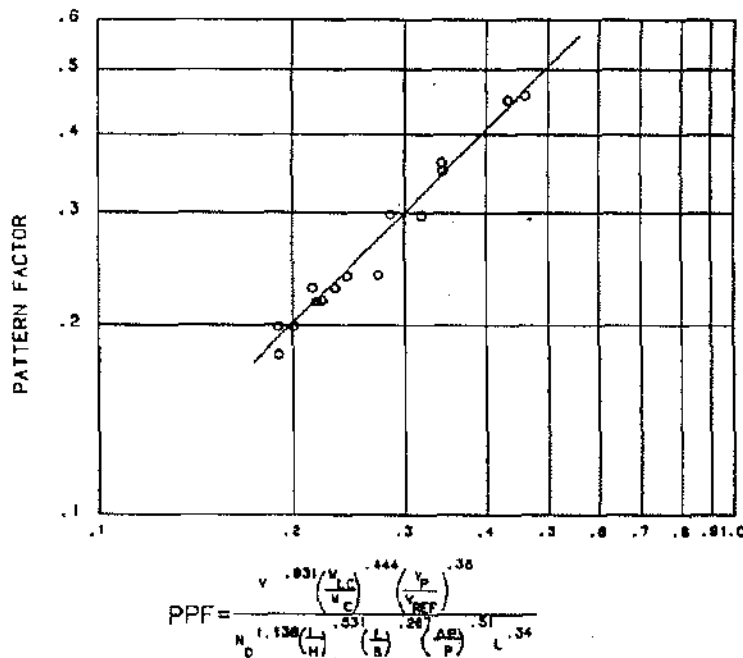


Figure 4.7 Pattern Factor Correlation

COMBUSTOR FLOW DISTRIBUTION

In order to meet the design requirements and satisfy the critical design parameters described earlier, the combustor airflow must be proportioned properly throughout the combustor flowpath. The three major flow divisions in the combustor system are the primary zone, dilution zone, and liner cooling. The combustor primary consists of the dome flow and part of the air that enters through mixing jets located at the forward end of the combustor. High combustion efficiency over a wide range of fuel-air ratios can be maintained by the proper combination of basically good flame stability, uniform dispersion of fuel vapor, and nearly stoichiometric mixtures of fuel and air in the dome. Flame stability, as mentioned earlier, is maintained by swirler vortex flow which establishes a recirculation zone.

Intimate mixing of the fuel and air can be achieved with high turbulence levels superimposed on the basic flow pattern in the primary zone of the combustor. Both small scale turbulence and large scale turbulence are needed to obtain very rapid and efficient combustion. Small scale turbulence provides better dispersion of the fuel droplets or fuel vapor into the adjacent air, and large scale turbulence transports pockets of hot burned products into fresh mixture to provide the widely scattered ignition sources that are needed for rapid burning of the fresh mixture. High turbulence levels can be obtained by several different techniques. Jets of air directed into the primary zone generate turbulence. A cross-flow pattern between adjacent streams generates turbulence. A strong cross-flow pattern can be obtained between air swirlers arranged around the circumference of a combustor dome. As the intensity of the turbulence increases, the mixing action becomes more rapid and the flame zone becomes more compact and more efficient. For each of these turbulence generating techniques, the intensity of the turbulence is directly proportional to the jet flow velocity, or swirl vane discharge velocity. Jet flow velocity is proportional to the square root of the pressure drop across the combustor dome.

Fuel Injection System A combustor that is designed to have good performance at high temperature operating conditions may not necessarily have good ignition characteristics or good low temperature rise performance. High combustion efficiency, low emissions, and uniform exit temperature distributions are more readily achieved with very uniform dispersions of the fuel throughout the primary combustion region. However, for good ignition performance, a heterogeneous mixture that provides a range of fuel-air ratios is more likely to have the correct fuel vapor-air mixture at the ignition source. At lightoff conditions, the flow velocities are low and the fuel and

air are cold which means that fuel vaporization rates are very low and a relatively large proportion of liquid fuel is needed to obtain the correct amount of vapor fuel. Because of surface quenching effects, lightoff is generally more difficult in small engines since the combustors liners generally have high surface to volume ratios. Ignition problems must, therefore, be carefully considered in the selection and design of the fuel injection system and primary combustion zone.

Typical engine operating conditions range from low temperature rise idle points to very high temperature rise sea-level-takeoff points. For the low temperature rise cycle conditions, the fuel flow is low and the combustion zone is generally lean. To maintain high combustion efficiency under these conditions the fuel dispersion should preferably be concentrated at the dome end of the combustor and the air flow pattern should supply only as much air to the mixture as is needed for stable combustion. As the engine temperature rise is increased, the fuel dispersion should reach deeper into the combustor and the air flow pattern should supply more fresh air to the mixture. This "staged" system of fuel penetration and fresh air supply should be designed into the primary zone of the combustor as a basic part of the fuel dispersion and air flow pattern. The conventional pressure atomizing fuel nozzle and liner hole pattern arrangement accomplishes this "staged" mixture by having higher fuel nozzle spray velocities and deeper spray penetration at higher fuel flows along with increasing amounts of air injection as the flame zone moves downstream. It is clear, therefore, that the fuel nozzle plays a critical role in combustion performance.

Dilution Zone The hot gases leaving the primary combustion zone of a gas turbine combustor are at very high, nearly stoichiometric temperatures. To achieve the required turbine durability, these gases must be uniformly cooled to a lower temperature level with the desired exit temperature profile and peak temperature factor or maximum local hot spot temperature. Temperature profiles and flow conditions at the exit of the combustor primary zone have a strong effect on the mixing and dilution requirements in the mixing zone. Since the relatively cool mixing air will quench combustion reactions that have not gone to completion, the mixing air should not be introduced until all of the fuel has been burned, especially at the high temperature rise operating conditions. Otherwise, the combustion efficiency would be reduced. If the temperature profile at the exit of the primary zone is very non-uniform, or has large random time variations, the mixing problem is considerably more severe and the mixing zone design must account for these profiles or variations. This problem is further complicated in very high temperature rise combustors where a large propor-

tion of the total air flow is used in the primary zone to burn the fuel and a much smaller proportion of the air is left for the dilution flow mixing. As shown in Figures 4.8 and 4.9, both uniform mixing and cooling air quantities can strongly affect combustion efficiency as the combustor exit approaches stoichiometric.

Traditionally, dilution of the hot gases in the mixing zone of the combustor has been accomplished with jets of air that penetrate across the hot gas stream and spread through the hot gases by a turbulent diffusion process. The number, size, and location of these dilution holes are very important variables in the design of the combustor mixing zone. The total open hole area required for the dilution flow is determined by the amount of the combustor air flow that is available for dilution, the pressure drop across the combustor liner in the mixing zone, the air density, and by the flow coefficients of the mixing holes. This total hole area could be divided into a small number of large holes or into a large number of small holes. The flow from large holes penetrates deeper into the hot gas stream but the flow from small holes mixes more rapidly. Obviously, for any particular design, there is a combination of hole size and number of holes that gives the best mixing performance. Jet flow penetration into cross flowing streams has been the subject of a number of experimental studies. The results of these studies indicate that the depth of penetration is

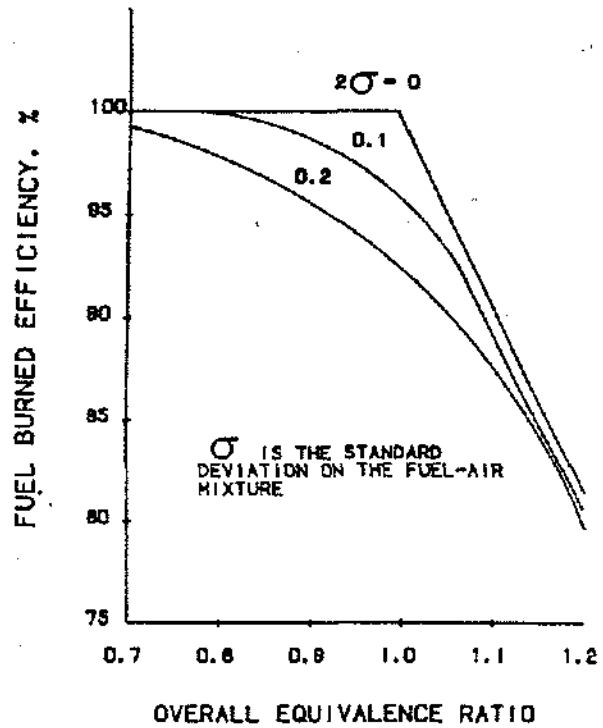


Figure 4.8 Combustion Efficiency at High Equivalence Ratios

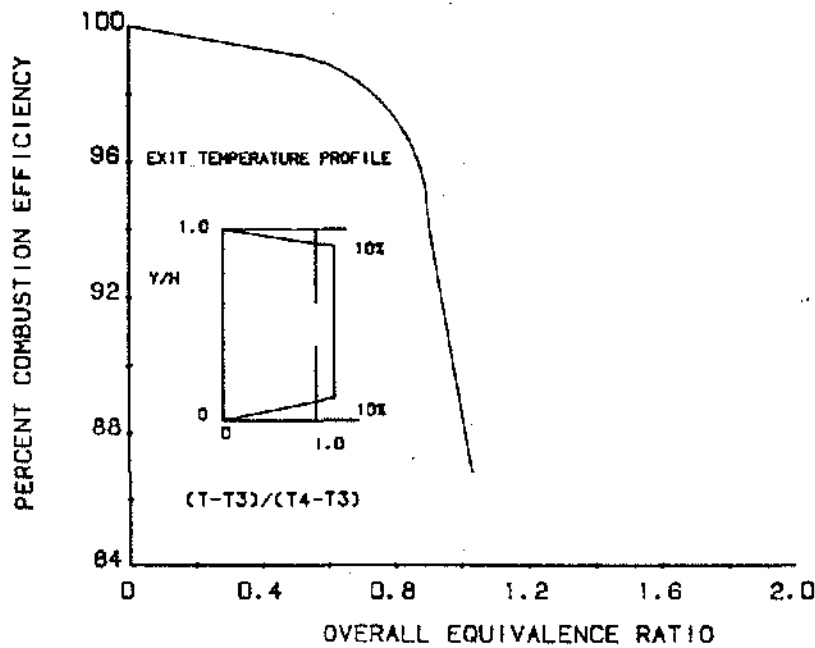


Figure 4.9 Combustion Efficiency with 20% Thermal Boundary Layers

directly proportional to the hole diameter and proportional to the cold stream to hot stream momentum ratio to an exponential power.

The introduction of combustor dilution air through holes located at discrete intervals around the circumference of the burner creates an alternating pattern of hot and cold flow around the burner. These hot and cold flow streams mix by turbulent diffusion as the flow moves downstream. The mixing region must be long enough to achieve the desired level of uniformity. More rapid mixing can be obtained by using a larger number of smaller holes that are spaced closer together circumferentially, but when the holes are smaller the penetration depth is reduced. If the holes are too close together, the hot gases from the primary zone will not flow between the cold jets and will be deflected over the outer surface of the jets, as if the jets had formed a continuous circumferential slot.

Liner Cooling The liner cooling flow, usually expressed as a percent of combustor flow, is the film cooling air required by the inner and outer combustor liners from the downstream edge of the dome to the turbine inlet plane.

Hot gas temperatures within the primary zone of a gas turbine combustor can reach very high values. Temperature levels as high as 4000°F are not unusual. Particulate matter within the combustor that reach these high temperature levels radiates a large amount of heat energy to the combustor liner walls. Also, local high velocity regions within the combustor can cause high convective heat transfer to the liner walls. If the combustor liner walls are not properly cooled, distortion and cracking of the liner material can occur. In extreme cases, the liner material can melt, leaving burned-out regions in the liner walls. For long life, the liner wall temperature should not exceed a value of about 1600°F at any point on the wall surface and temperature gradients should be minimized as much as possible.

In some cases, convective cooling of the outer surface of the liner may be sufficient to handle the liner heat load, but with compressor exit temperatures as high as 1000°F, film cooling of the inner surface is usually required. With film cooling, the entire inner surface of the liner is covered with a thin film of air that removes the radiation heat load and protects the liner from high velocity hot gases.

COMBUSTOR MECHANICAL DESIGN DESCRIPTION

The CF6-80C combustion system is shown on Figure 4.10 as it is installed in the engine. The diffuser is part of the combustor casing and is a single cast structure with integral struts. The combustor is mounted redundantly at its downstream end with a clamped flange at the outer diameter and a bolted joint at the inner diameter. Leaf seals are mounted on the leading edge of the turbine nozzle and mate with the combustor.

Fuel is delivered to the combustor through 30 dual cone fuel nozzles which are inserted through the casing and into the swirl cups. Ignition is accomplished using two igniters located on the first panel of the combustor outer liner.

The combustor is an assembly which consists of five individual pieces. The frame for the combustor is the dome. The inner and outer cowls and inner and outer liners are bolted to the dome at its inside and outside diameter as shown. The bolts and self locking nuts are tack welded to prevent them from separating and causing turbine foreign object damage.

The two combustor cowls are sheet metal parts which may be stamped in a die or formed by a spinning process. The leading edge of the cowls are reinforced by a wire that is rolled in place. This provides vibrational damping for the cowl structure.

The combustor dome consists of a single spectacle plate which is a die formed sheet metal part (Figure 4.11). Individual swirl cup packages are brazed into the spectacle plate. These swirl cup packages include the primary swirler with its retainer, the counter rotating secondary swirler, the venturi, and the splash plate. These assemblies are brazed together and the retainer is welded into position on the front surface of the venturi.

The two combustor liners are fabricated from individual machined forgings welded together. Cooling air is introduced through holes which are drilled by gang electric discharge machining (EDM) or some other high speed process. Dilution air is introduced through several bands of holes in the liners. It serves to mix the reacting gases to provide the required design profile at the turbine.

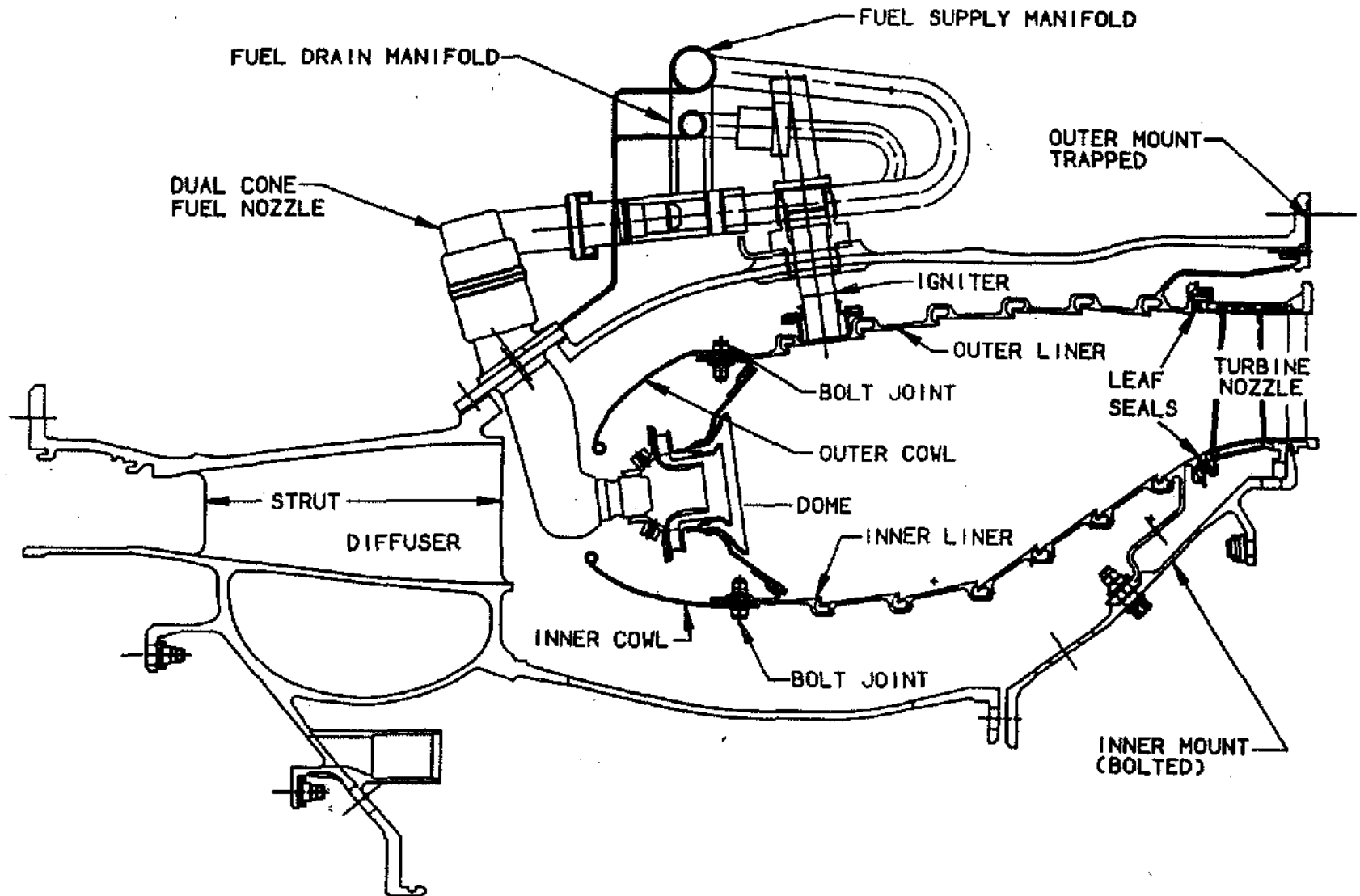


Figure 4.10 CF6-80C Combustion System

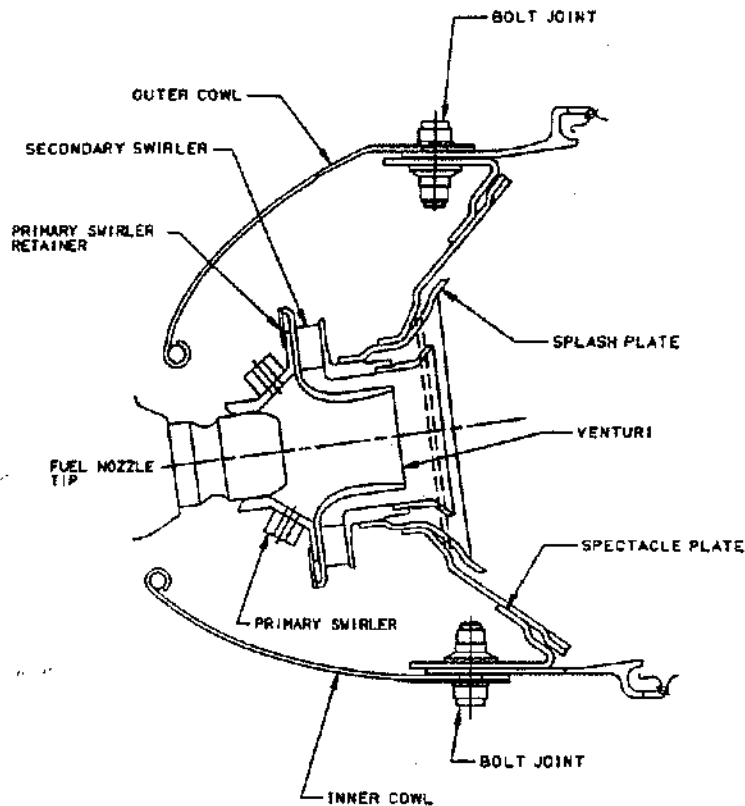


Figure 4.11 CF6-80C Combustor Dome

The cooling nugget on the CF6-80C is of the super slot variety as shown on Figure 4.12. The cooling air supply is introduced through holes in the downstream face of the ring. The air impinges on the forward face of the cavity where it provides cooling on the support ring and the cooling lip. It then flows around the radius through the cooling slot and forms a film of air to cool the downstream panel.

COMBUSTOR ANALYSIS

The analytical tool for assessing combustor life is the "CLASS MASS" program. The combustor structure is modeled using the finite elements shown on Figure 4.13. Appropriate boundary conditions are applied at the downstream mounts. The program calculates steady state stresses, deflections, and other conditions at all extremes of the operating envelope. It also analyzes the vibration response characteristics.

Most of the life consumption in a combustor is associated with low cycle fatigue (LCF) due to the thermal gradients produced by the combustion reaction as the en-

gine is operated through a complete cycle from cold (ambient) to take off power and back to cold. Partial cycles impose less damage. A cycle from idle to takeoff to idle will consume approximately 25% of the life consumption of a complete cycle.

Life consumption is dependent upon the specific thermal cycle imposed on the parts. The severity of the hot streaks is predicted by the "THTD" heat transfer program. This program models the combustor using experimentally derived cooling effectiveness data and hot streak conditions that are empirically derived. The analysis provides the temperature distribution in the material shown on Figure 4.14. This temperature data is then used in the "Class Mass" program to evaluate the basic stress levels. Life consumption is obtained from this information together with the appropriate materials data curves.

Normally in the development program for new engines instrumentation is applied to an early engine to measure temperature and pressure data which may be compared to predictions. If necessary, the predictions are modified and the life assessment is repeated.

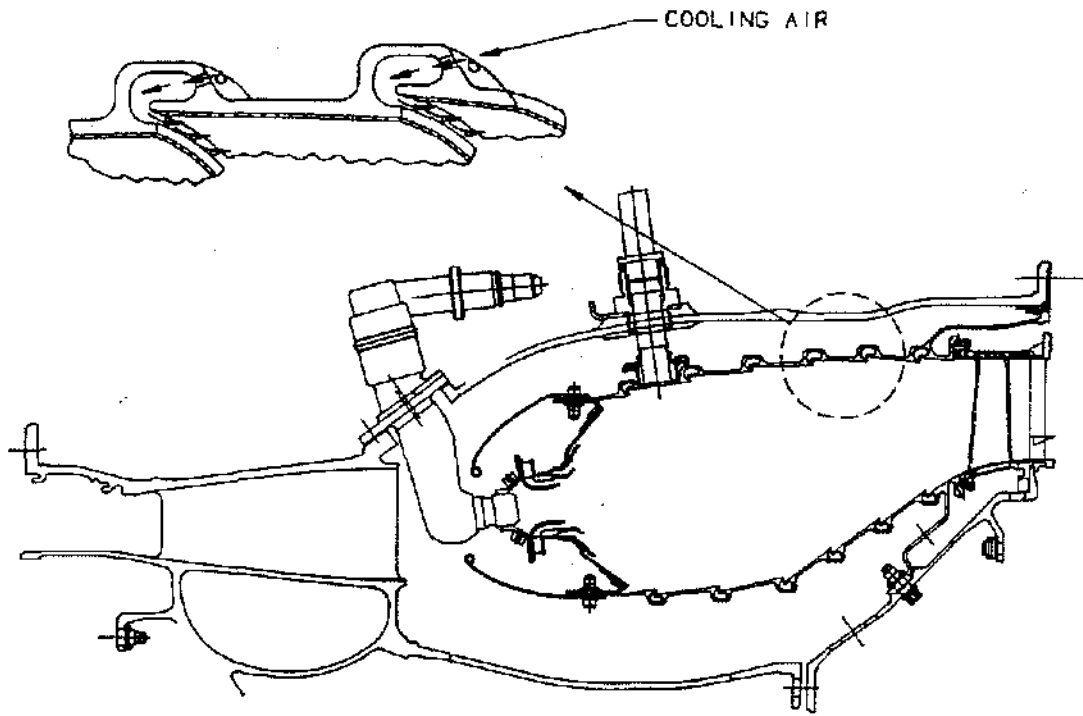


Figure 4.12 CF6-80C combustor Cooling Nugget

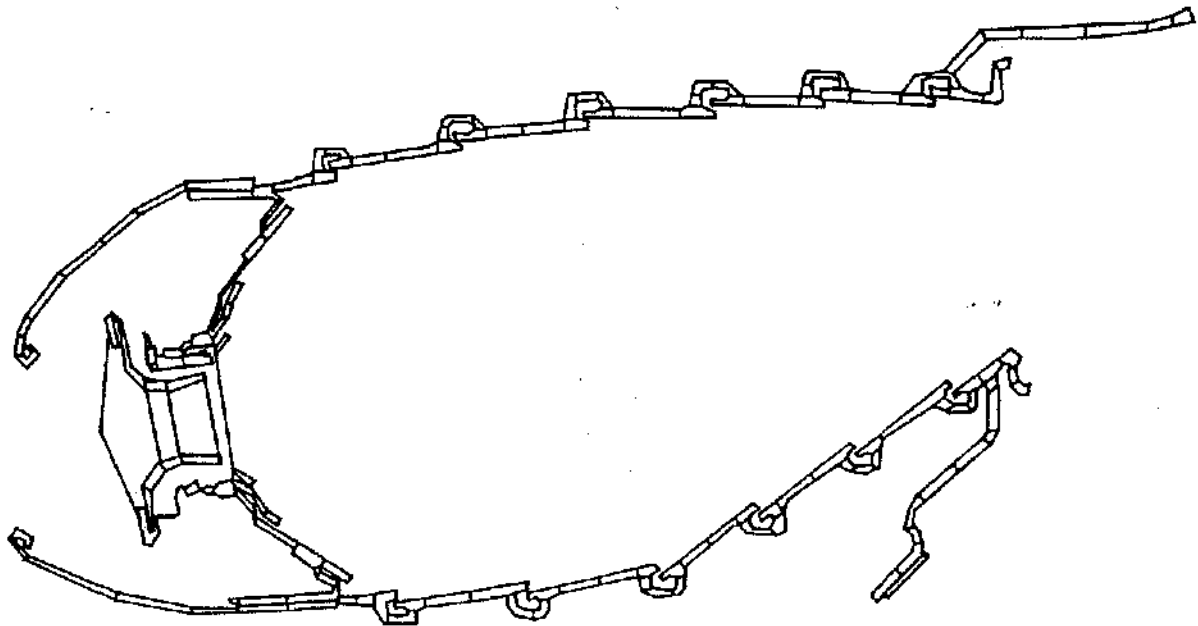


Figure 4.13 Combustor Class Mass Model

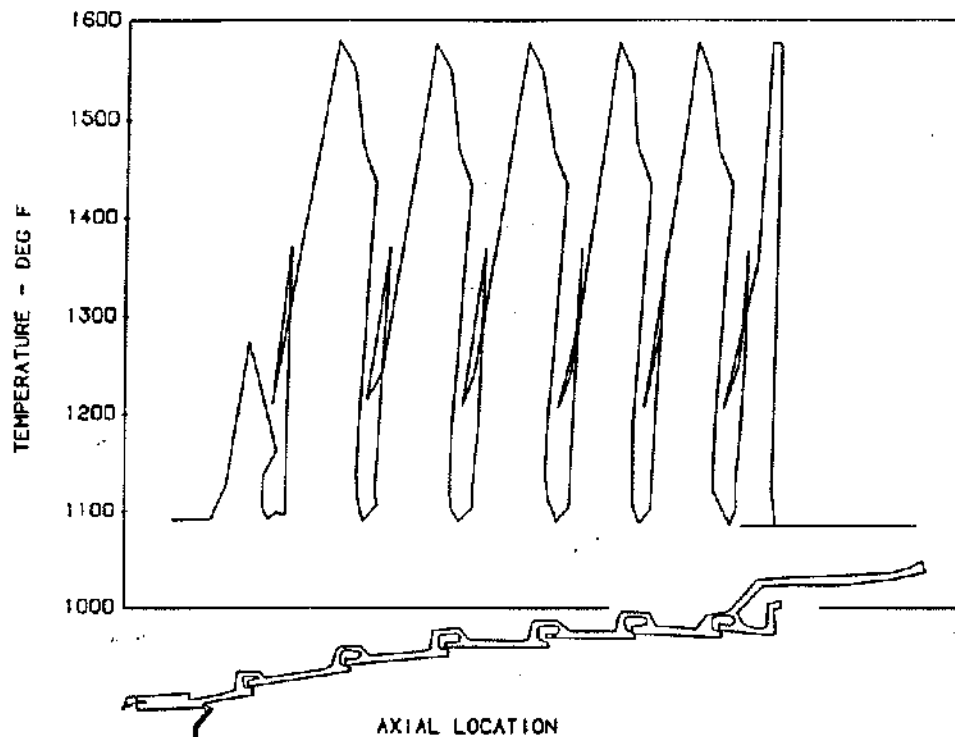


Figure 4.14 Typical Combustor Outer Liner Temperatures

Combustors are frequently coated on the flame side with thermal barrier coating which reduces the heat transfer rate to the liners and dome. This reduces the peak temperature, the thermal gradients, and serves to diminish the severity of any hot streaks that may be present.

Combustors are subjected to borescope inspection at regular intervals. The combustor condition is compared to allowable limits for cracks, burned areas, etc. Combustors are removed from the engine only after a specific limit is exceeded. Frequently combustors are "zero timed" by repair when an engine is disassembled for some reason.

Combustor life is normally presented as total life with allowable repair. Combustor crack length versus cycles is presented in Figure 4.15 and compared to the limiting length value.

Combustors are designed so that they may be repaired several times before they are scrapped. Current commercial combustors can operate trouble free more than 10,000 hours and may be repaired at least 4 times giving an effective life greater than 50,000 hours. To repair a combustor the part is disassembled into its component parts and the thermal barrier coating is removed by a

stripping process. Cracked areas may be welded. Any severely cracked or burned areas that are encountered are cut out and a new piece is welded into position. Wear areas in the dome are renewed as required. The part is then recoated with the thermal barrier coating and reassembled.

FUEL NOZZLE DESIGN

Fuel is introduced into the CF6-80C combustor through 30 dual cone fuel nozzles. Figure 4.16 shows a typical fuel nozzle. The term dual cone means that the fuel is introduced through two spray nozzles in the tip. A primary nozzle is used for starting and low fuel flows. It is designed to provide a fine spray during engine starting when the flows are low. Surrounding the primary nozzle is the secondary nozzle through which fuel is introduced as the flow is increased above idle. Both the primary and secondary nozzles include spin chambers which swirl the fuel and produce fine spray after the flow passes through the final orifice. The flow to the primary nozzle is delivered through a passage in the stem. A valve is located in the head of the nozzle assembly. It pressurizes the fuel manifold, preventing flow leakage through the

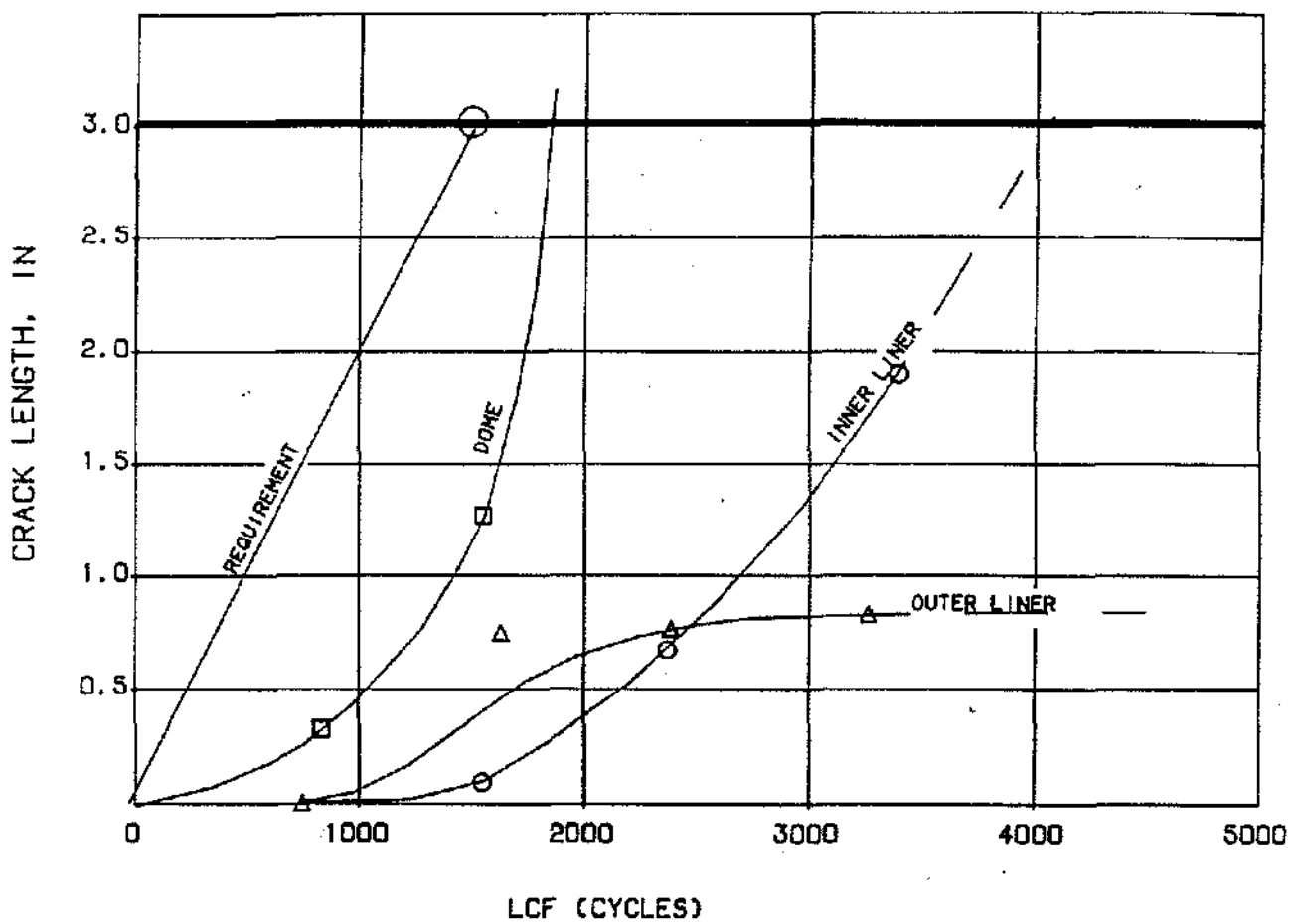
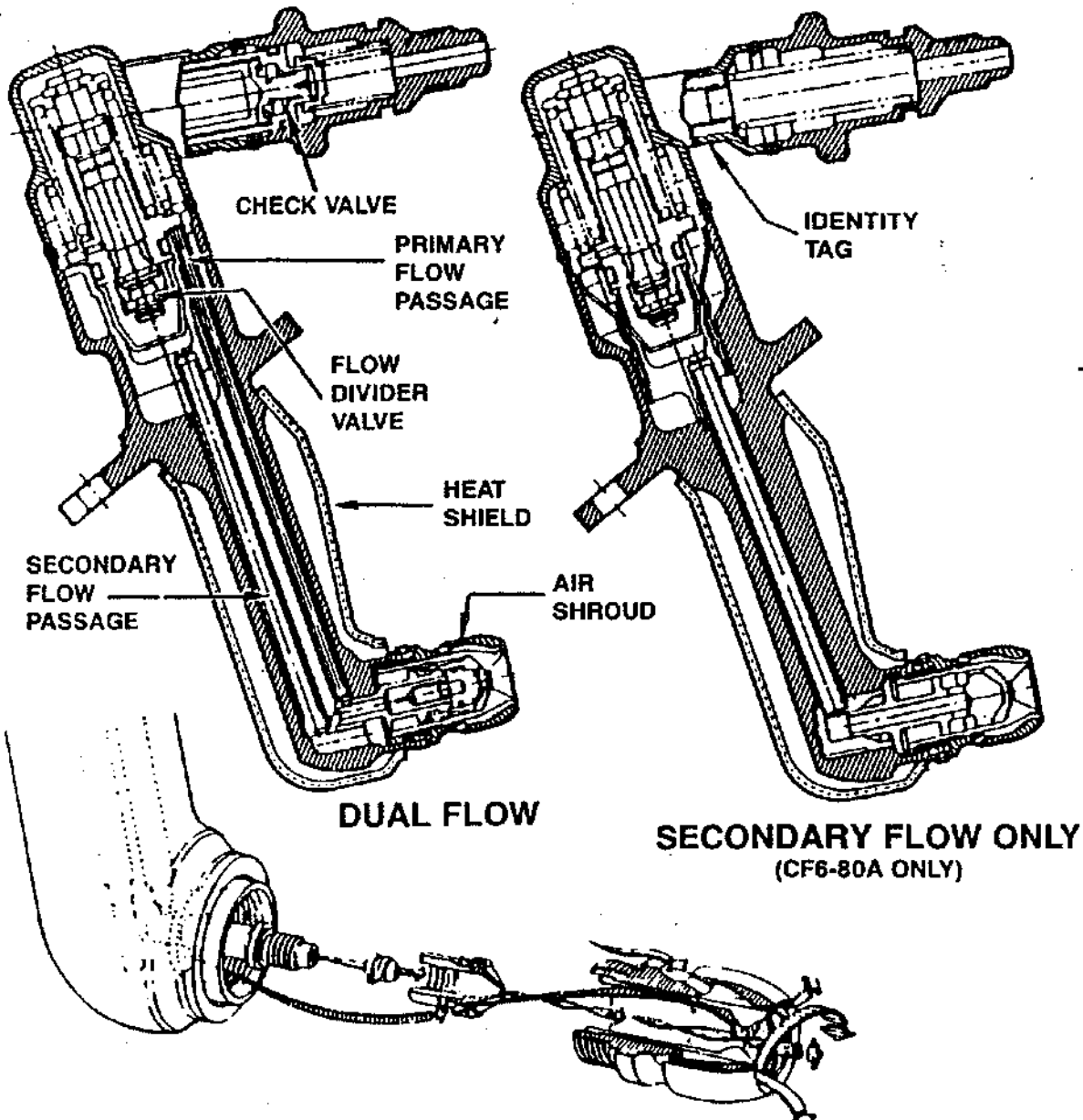
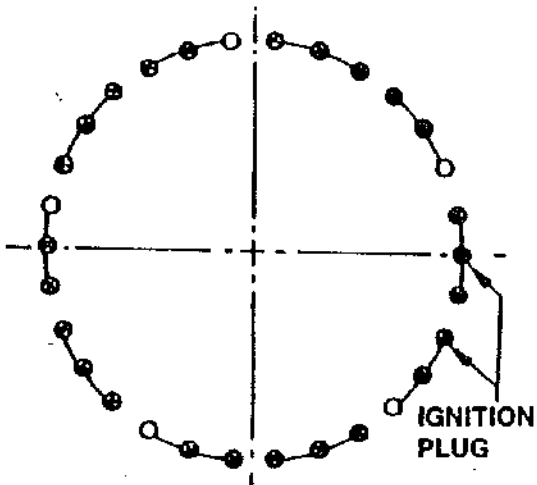


Figure 4.15 Relationship of Combustor Component Crack Length and Low Cycle Fatigue Cycles



CF6-80 FUEL NOZZLES



FUEL NOZZLE CONFIGURATION
AFT LOOKING FORWARD

- ⊗ PRIMARY/SECONDARY
- SECONDARY ONLY

Figure 4.16 Fuel Nozzle Schematic

nozzles at pressures below 20 psi. This feature prevents fuel from draining out of the manifold to minimize ignition delay on subsequent starts and to prevent fuel from draining overboard. The flow to the secondary nozzle passes through the secondary flow distributor valve. This valve has a variable area slot that is opened as the fuel manifold pressure increases. The resultant fuel flow-pressure curve is shown in **Figure 4.17**. As flow is introduced into the system, the pressure increases to 20 psi when the check valve opens and introduces flow to the nozzle. Further increases in engine flow raises the pressure and the secondary valve is opened supplying fuel to the secondary nozzle as indicated.

Dual cone fuel nozzles are normally made from 300 series stainless steel or Hastelloy X forgings. Castings are to be avoided since they are subject to leakage. The tip and cover on the valve cavity are welded. Hardened materials are used for the flow metering parts and for the tips.

The nozzles are subjected to a thorough heat transfer analysis to maintain low fuel temperatures and to prevent carbon formation inside the nozzles. Both internal and external heat shield are used to minimize fuel temperatures. A concept used on many of the current production engines to prevent flameout is called "sector burning" or "pilot burning." Here several special fuel

nozzles that have higher flow primary nozzles than the other nozzles are utilized to produce a fuel rich zone during throttle chops. The rich flow exists only during low speed operation. At higher speeds the flow-pressure curve matches the other fuel nozzles to prevent hot streaks.

IGNITION SYSTEM

The ignition system used on the CF6-80 engine consists of two exciters, two leads, and two igniters (**Figure 4.18**). The igniters are mounted on the combustor casing into sliding ferrules on the first panel of the combustor. A seal is provided on the casing. The exciter is connected to the igniter by the ignition lead. The downstream portion of the lead is air cooled. The exciter is mounted on the outer surface of the fan casing. The exciter receives signals from the cockpit and provides a spark of approximately 1.5 joules of delivered energy at 16KV once per second. The circuit operates as a capacitor discharge system.

The igniter is shown on **Figure 4.19**. The electrical pulse is delivered through the center electrode and produces a spark as it jumps across the gap between the center electrode and the outer shell. Aluminum oxide insulators are used between the electrodes.

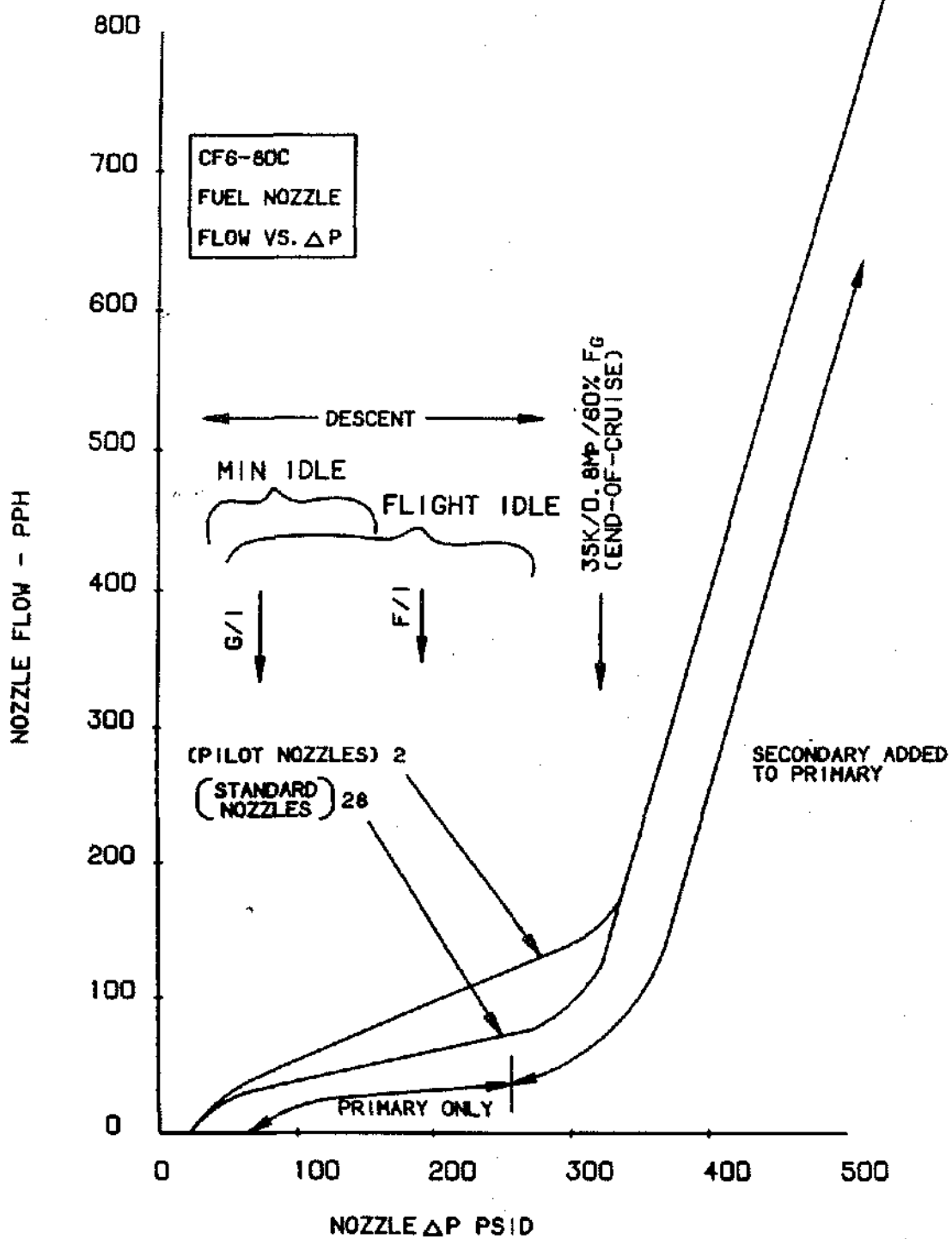


Figure 4.17 Fuel Nozzle Metering Characteristics

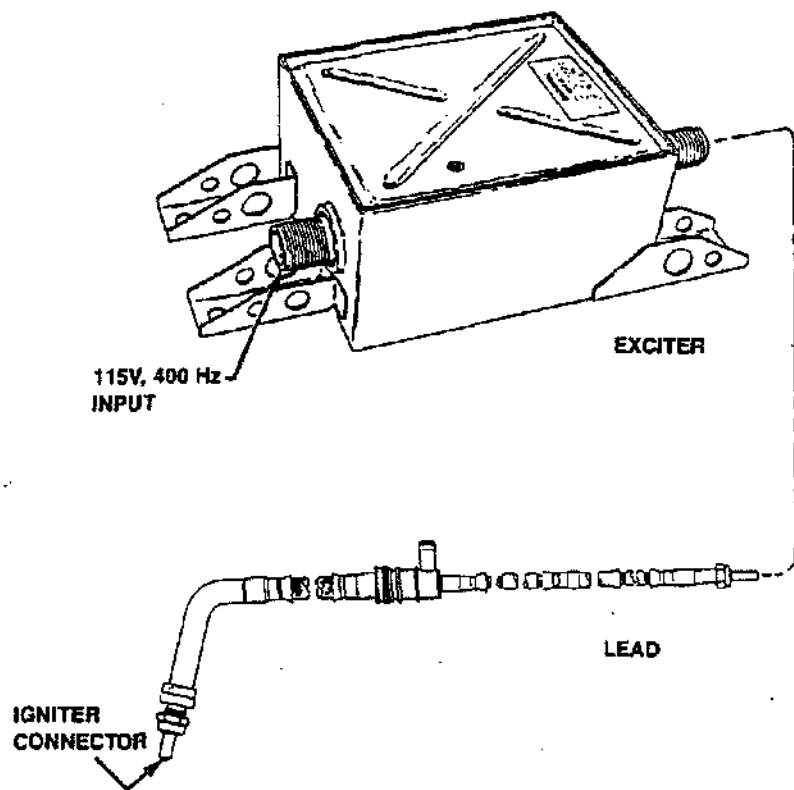


Figure 4.18 Ignition Exciter and Lead

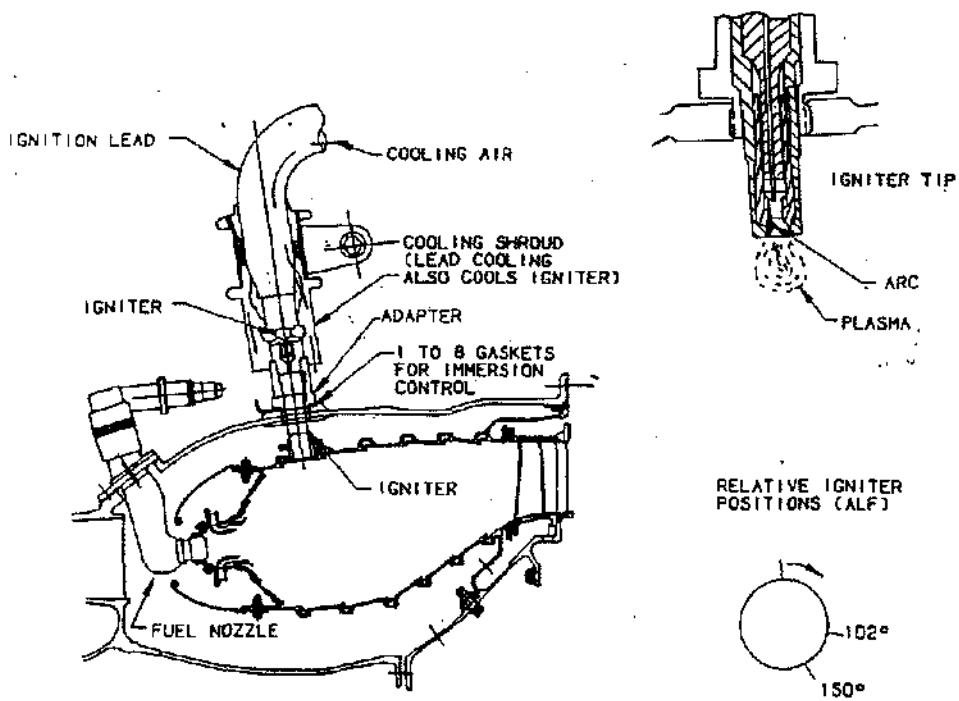


Figure 4.19 Igniter Installation

Chapter 5

TURBINES

by David Cherry
(Aerodynamic Design Topics)

and

Thomas B. Knost and Philip Stoughton
(Mechanical Design Topics)

TURBINE AERODYNAMIC DESIGN

INTRODUCTION

The turbine is probably the most general energy conversion device in use today. Its basic function is to convert thermal energy into mechanical energy through an expansion process by impinging the working fluid into a bladed rotor as shown schematically in Figure 5.1. Turbines are used in a variety of applications. Table 5.1 lists several specific applications and illustrates the range of size, speed and power.

While turbines in general can be radial flow, Figure 5.2, or axial flow, Figure 5.3, most aircraft gas turbine engines today employ axial flow turbines. This is because for a given turbine diameter they can accommodate considerably higher mass flow rates, their rotating parts are more readily air-cooled, which allows higher temperature operation, and they are more readily adapted to multi-stage applications, where two or more stages are put in series and power from all stages is delivered to a common shaft.

The function of the turbine section of the aircraft gas turbine engine is to extract just enough power from the fluid (air/gas) to drive the fan or compressor (or gearbox, in the case of marine industrial or turboprop applications) and then to pass the fluid onto the downstream component (e.g. exhaust nozzle, augmentor or another turbine) as efficiently as possible.

Since the turbine is only one of a series of interconnected components in the engine, it must be properly designed to ensure that its flow capacity, power output and efficiency level are consistent with the cycle calculation which is being used to size the other components.

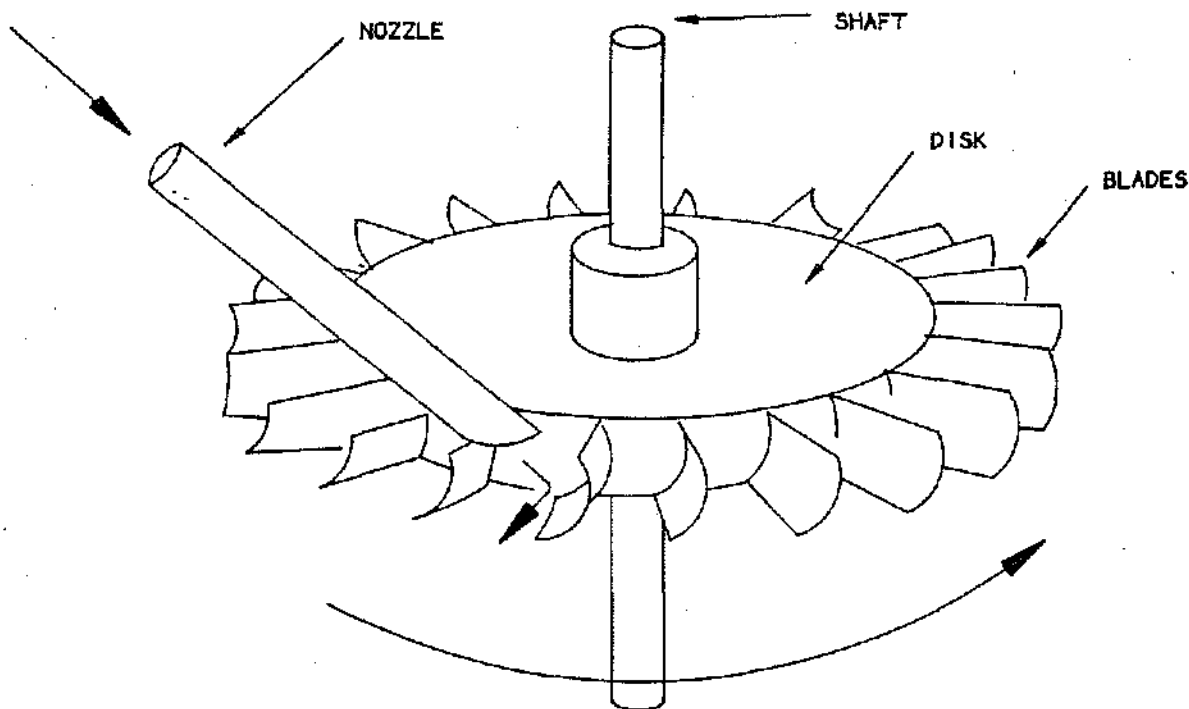


Figure 5.1 A Simple Turbine 1) Thermal energy converted to kinetic energy in nozzle. 2) Kinetic energy converted to mechanical energy in bladed rotor.

Application	Turbine	Working Fluid	Dia	Length	Nominal T41	— Power — MW	HP	Speed RPM	Flow PPS
Small Helicopter Engine	T700 HPT	Fuel/Air	8"	4"	—	—	3,000	45,000	8
Large Turbofan Engine	CF6-80C HPT	Fuel/Air	35"	9"	2500°F	—	80,000	10,000	260
Land Gas Turbine	MS-7F	Fuel/Air	112"	49"	2300°F	135	181,000	3,600	900
Power Plant	LST-G/Fossil	Steam	115"	95'	1000°F	820	1,100,000	3,600	792
Power Plant	LST-G/Nuclear	Steam	175"	100'	550°F	1339	1,800,000	1,800	4722

Table 5.1 Examples of the Range of Application of Axial Flow Turbines

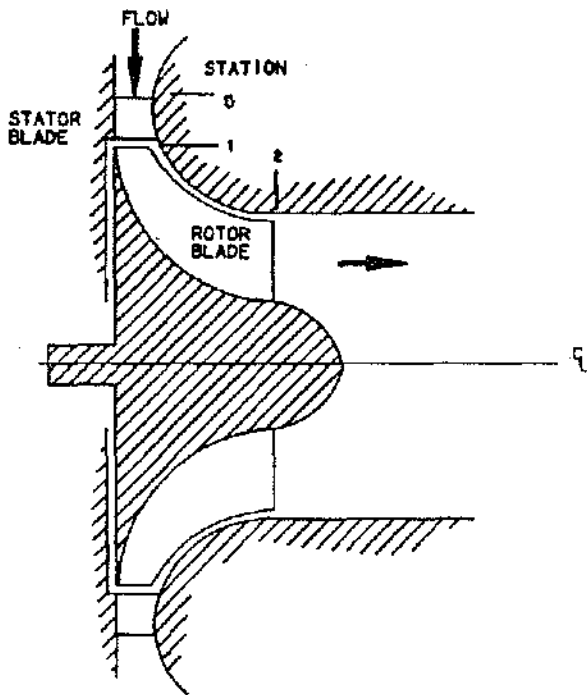


Figure 5.2 A Radial Inflow Turbine Stage

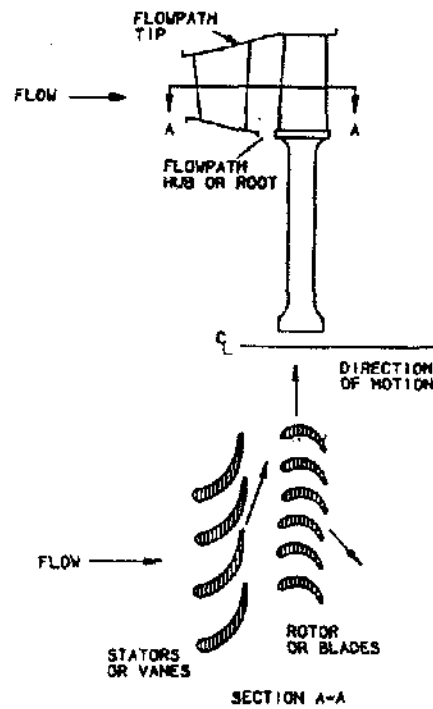


Figure 5.3 An Axial Flow Turbine Stage with Airfoil Sections

This is the function of the turbine aerodynamic design process.

An axial turbine consists of one or more "stages" in series and connected to a common shaft. Each stage of an axial turbine consists of one row of stationary airfoils (called nozzle vanes or stators) followed by one row of moving airfoils (called rotor blades) which are attached to a rotating disc. See again Figure 5.3.

Every aircraft gas turbine engine has a so-called High Pressure Turbine (HPT) to drive its compressor. The HPT sits just behind the combustor in the engine layout and experiences the highest temperature and pressure levels (nominally 2400 °F. and 300 psia respectively) developed in the engine. The HPT also operates at very high speeds (10,000 RPM for large turbofans, 50,000 RPM for small helicopter engines). In order to meet life requirements at these high levels of temperature and stress, HPT's today are always air-cooled and constructed from advanced alloys. Figure 5.4 shows an assembly of nozzle vanes and a rotor assembly for a typical HPT. Figure 5.5 shows how cooling air, bled from the compressor exit and transported to the turbine around the combustor, flows through internal passages in the airfoils (cooling by convection) and then onto the

airfoil surfaces providing an insulating film (so-called film cooling). On the order of 20% of compressor inlet flow may be used to cool state-of-the-art HPT's.

The HPT is alternately termed the core turbine or the gas generator turbine. Typical GE HPT flowpaths are shown in Figure 5.6.

While a straight turbojet engine will usually have only one turbine (an HPT), most engines today are of the turbofan or turboprop type and require one (and sometimes two) additional turbine(s) to drive a fan or a gearbox. This is called the Low Pressure Turbines (LPT) and immediately follows the HPT in the engine layout. Since substantial temperature and pressure drops occur across the HPT, the LPT operates with a much less energetic fluid and will usually require several stages (up to six in GE AE products) to extract the power.

Typical GE LPT flowpaths are shown in Figure 5.7. LPT hardware is shown in Figure 5.8. Note, that the rotor blades have interlocking tip shrouds to reduce tip leakage losses and to add stiffness to the longer airfoils. These are possible because of the lower temperature and speeds in the LPT compared to the HPT.

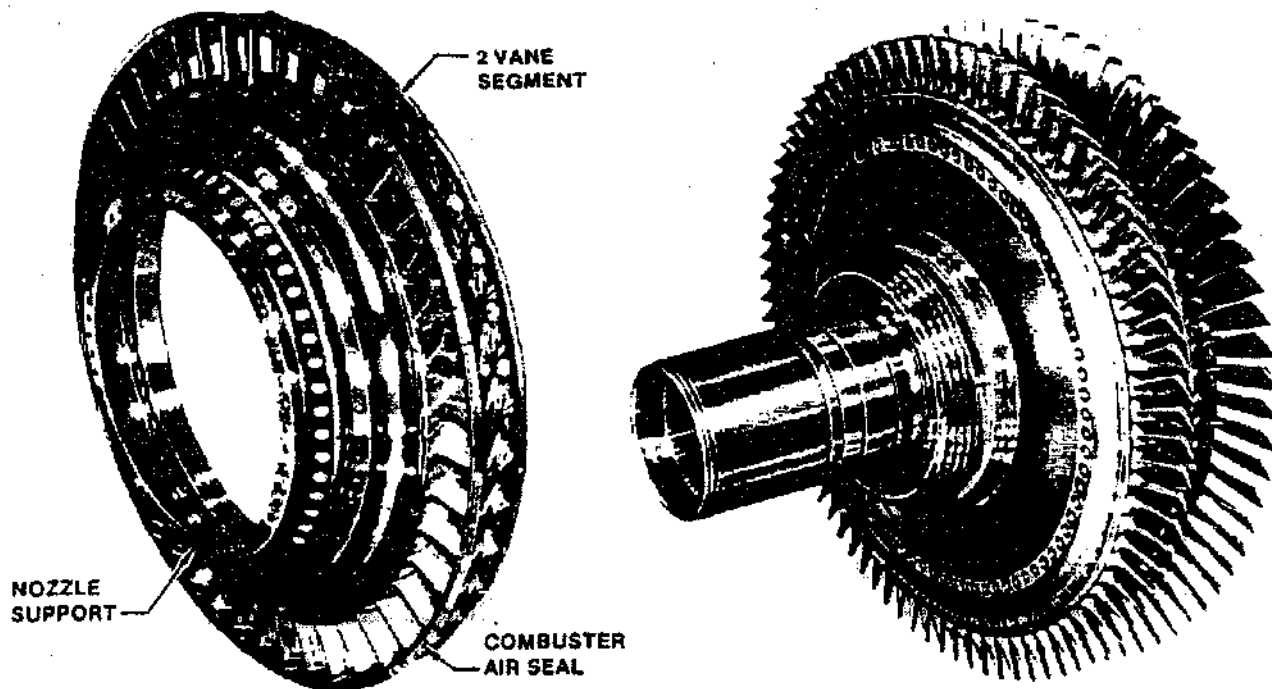


Figure 5.4 Typical HPT Nozzle and Rotor Assemblies

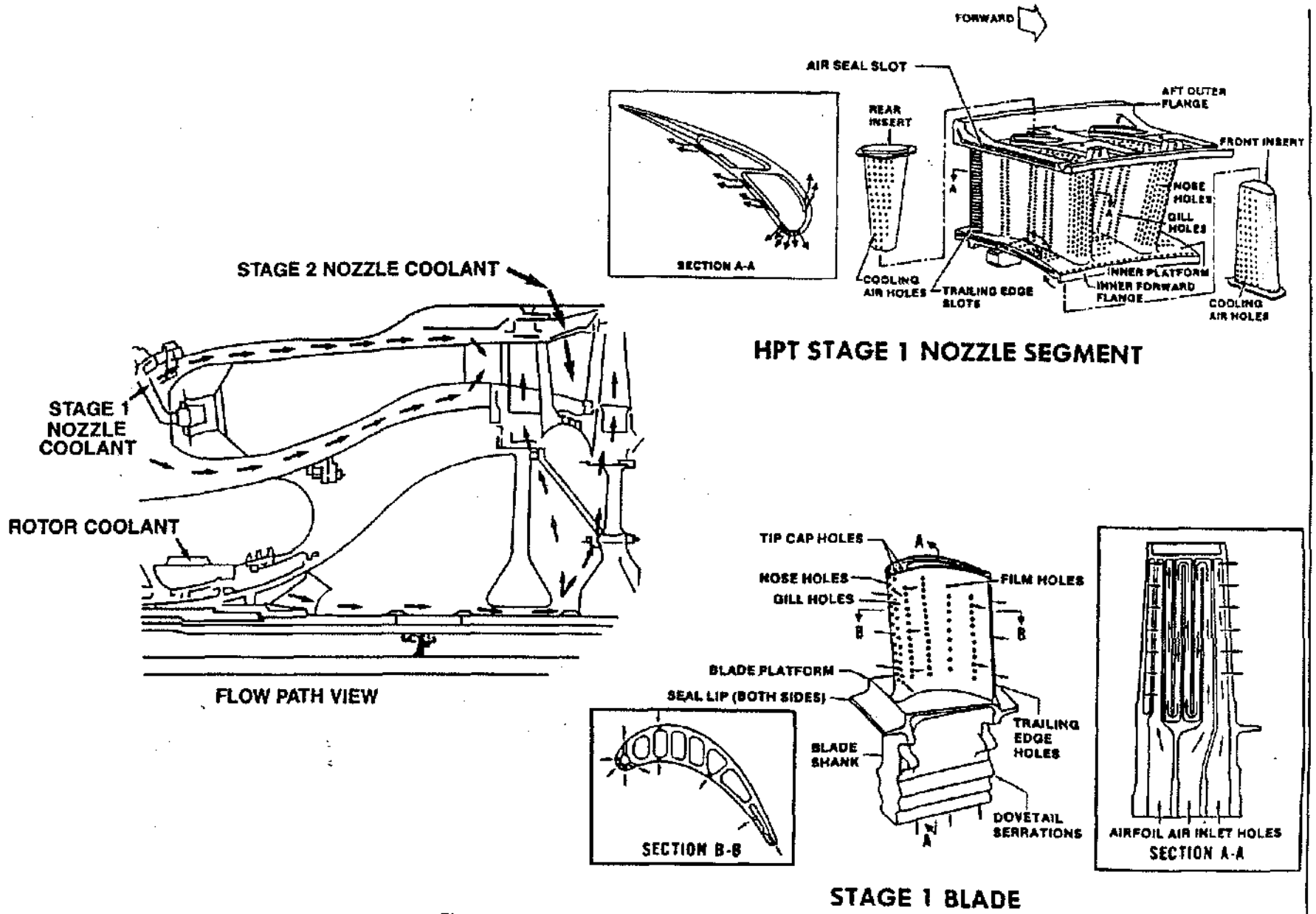
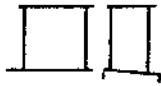


Figure 5.5 An Air-Cooled HPT (Typical CF6/TF39)

F101/F110/CFM56



CF6-80C2



F404



T700

Figure 5.6 Flowpath Schematic for Typical GEAE HPT's

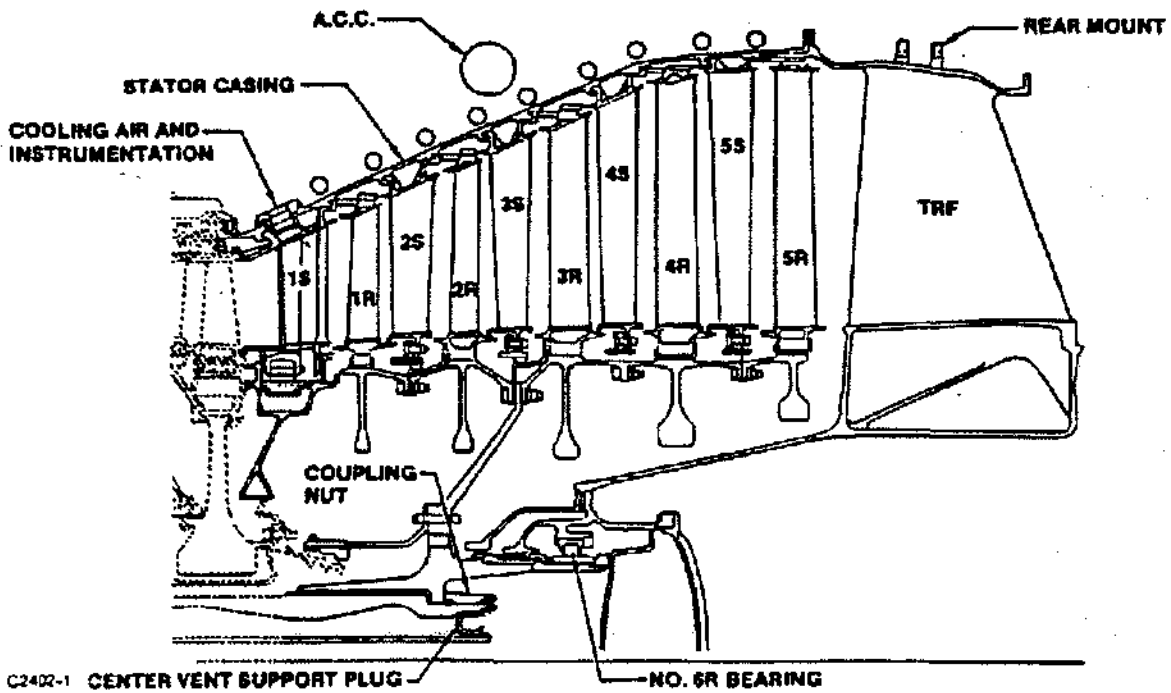


Figure 5.7 Five-Stage LPT Flowpath (CF6-80C2)

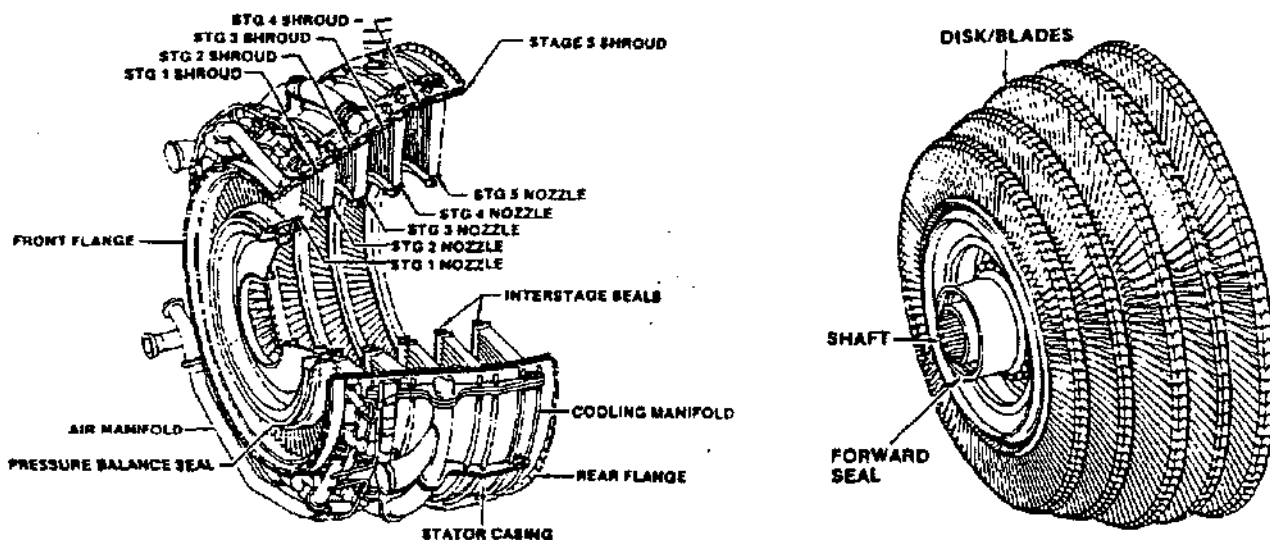


Figure 5.8 Typical LPT Nozzle and Rotor Assemblies

The characteristic annulus flare in multistage LPTs occurs because, as the pressure drops across each turbine bladerow, the decrease in fluid density requires more volume per pound of fluid.

PRINCIPLES OF OPERATION: Cycle (or Thermodynamic) Point of View

The cycle treats the turbine as a thermodynamic "black box" which yields power according to the following relation:

$$\Delta H = W_1 C_p (T_{T1} - T_{T2}) \quad (5-1)$$

where ΔH = turbine power (BTU/sec), W_1 = turbine stage 1 rotor inlet flow (lbm/sec), C_p = specific heat at constant pressure (BTU/lbm °R), T_{T1} = turbine stage 1 rotor inlet temperature (°R), and T_{T2} = turbine exit temperature (°R).

More familiar units for absolute power are brake horsepower:

$$HP = \frac{J}{550} \Delta H \quad (5-2)$$

where HP = turbine horsepower, and J = mechanical equivalent of heat (778 ft-lb_f/BTU).

Note from equation (5-1) that turbine power is directly proportional to flow and since turbine flow in lbm/sec varies with inlet conditions, it is traditional to express power on a specific basis as follows:

$$\Delta h = \frac{\Delta H}{W_1} = \frac{550}{J} \frac{HP}{W_1} = C_p (T_{T1} - T_{T2}) \quad (5-3)$$

where Δh = turbine specific power (BTU/lbm).

This is the actual power needed to drive the compressor; however, since the turbine is less than 100% efficient (i.e. since there are losses in the turbine blading, disks, bearings, etc.), we need to define an ideal power which tells the cycle how much specific power a "no loss" turbine would produce at a given inlet temperature and pressure ratio:

$$\begin{aligned} \Delta h_i &= C_p (T_{T1} - T_{T2i}) = C_p T_{T1} \left(1 - \frac{T_{T2i}}{T_{T1}} \right) \\ &= C_p T_{T1} \left[1 - \left(\frac{P_{T2}}{P_{T0}} \right)^{\frac{\gamma-1}{\gamma}} \right] \quad (5-4) \end{aligned}$$

where Δh_i = ideal specific power available from isentropic (i.e. no loss) expansion of turbine flow from P_{T0} to P_{T2} , T_{T2i} = ideal turbine exit temperature ($^{\circ}R$) - lower, than T_{T2} and never achieved in a real machine, P_{T0} = turbine inlet pressure (lb_f/in^2), P_{T2} = turbine exit pressure (lb_f/in^2), and γ = ratio of specific heats. While the ratio P_{T2}/P_{T0} is utilized in the expression for ideal energy, the inverse of that ratio, P_{T0}/P_{T2} , is usually quoted as the turbine pressure ratio or expansion ratio.

It is left to the turbine aero designer, then, to tell the cycle what fraction of this ideal power will actually be achieved for the current application. This is basically an experience factor, termed the "turbine efficiency":

$$\eta_{TT} = \frac{\Delta h}{\Delta h_i} \quad (\text{dimensionless}) \quad (5-5)$$

Turbine efficiency is determined by test, by estimating losses in each bladerow or by comparison to previous designs.

A final expression for turbine power (cycle viewpoint) can be obtained by combining equations (5-3, 5-4 and 5-5) as follows:

$$\Delta h = C_p \eta_{TT} T_{T1} \left[1 - \left(\frac{P_{T2}}{P_{T0}} \right)^{\frac{\gamma-1}{\gamma}} \right] \quad (5-6)$$

Thus the power per pound available from the turbine can be increased by (a) increasing turbine inlet temperature (usually limited by materials capability), (b) increasing turbine pressure ratio, P_{T0}/P_{T2} , (c) increasing turbine efficiency, and (d) increased C_p .

Option "d" is of academic interest only, since for aircraft gas turbines, C_p is always within the range of .24 to .30. In an application which could utilize a fuel such as liquid hydrogen ($C_p = 3.5$), however, tremendous power per pound is available from a very small package.

Equation (5-6) states that if turbine performance (i.e. efficiency) is below predicted level for some reason (e.g. excess tip clearance or cooling flows, deteriorated seals, poor design execution), then either temperature level or pressure ratio must be increased to compensate. Since turbine pressure ratio is often set by component matching considerations, it is usually turbine inlet temperature which must increase to deliver adequate power to the compressor (and thus allow the engine to achieve thrust). This not only increases fuel burn, but also degrades turbine component lives.

Recall that turbine horsepower can also be augmented by increasing the mass flow, W_i in equation (5-1). In the aircraft gas turbine, this is of little real consequence since the compressor requires power input proportional to flow. In industrial gas turbine applications, however, mass flow through the power turbine can be augmented using steam injection (from a boiler fired by turbine exhaust for example) resulting in significant increases in horsepower for the same fuel burned.

Before leaving this section, it should be noted that equation (5-1), while correct for an uncooled turbine, requires modification when applied to HPTs or cooled LPTs because, in an air-cooled turbine, not all of the temperature drop is a result of power production. There is a "dilution" effect on gas temperature which occurs as a result of introducing relatively cold compressor discharge air into the turbine gaspath. This could be approximated rather simply in equation (5-1) (which is essentially just a heat balance equation) as follows:

$$\Delta H = W_i C_p (T_{T1} - T_{T2}) - \underbrace{W_c C_p (T_{T2} - T_{TC})}_{\text{dilution term}}$$

where W_c = cooling flow, lbm/sec , and T_{TC} = temperature of cooling flow ($^{\circ}R$). Note that the dilution effect is an "adder" to the basic power equation and really doesn't affect our prior discussion. Elaboration on the effects of cooling flow will be provided later.

PRINCIPLES OF OPERATION: Turbine Aero Point of View

While the turbine power calculation in the cycle deck recognizes flow, temperature level, pressure ratio and efficiency level, it is oblivious to such mechanical and aero considerations as number of stages, wheel speed, airfoil turning, etc. In this section, we will derive an expression for turbine specific power, Δh , in terms of velocities, flow turning and wheel speeds within the turbine which will determine the actual "look" of the blading required to achieve the cycle Δh given by equation (5-6).

With reference to Figure 5.3, let's consider the mid-span portion (Section A-A) of a typical axial flow turbine stage. Figure 5.9 shows an expanded view of A-A with so-called vector or velocity diagrams denoting the direction and magnitude of the velocities entering and leaving each of the bladerows.

Absolute velocities and flow angles (i.e. those seen by a stationary observer) are denoted by V and α respectively. Relative velocities and flow angles (those seen by an observer moving with the same tangential speed as the rotor blades) are denoted by R and β . Note that angles α and β are measured from the axial direction. Axial stations corresponding to vane leading edge, vane exit and blade (also stage) exit are denoted by subscripts 0, 1 and 2 respectively. Axial and tangential components of velocity are denoted by subscripts Z and u respectively. Note that, since the rotor blade is "running away" (in the tangential direction) from the vane, it sees a velocity, R_1 , which is lower in magnitude and at a more axial angle than the vane absolute exit velocity, V_1 .

The tangential force on the rotor caused by the vector diagrams of Figure 5.9 is:

$$F_u = \frac{W_1}{g} (V_{U1} - V_{U2}) \quad (5-7)$$

where F_u = tangential force (lb_f), g = gravitational constant ($32.174 \text{ lbmft/lb}_f\text{sec}^2$), V_{U1} = vane exit tangential velocity (ft/sec), and V_{U2} = blade exit (absolute) tangential velocity (ft/sec).

This says that force is simply a change in momentum (a basic law of physics). We consider the tangential component since it produces torque on the shaft; however, the tangential and axial forces on both bladerows need to be considered by mechanical designers for structural and bearing design.

Next, consider the torque (force x distance) transmitted to the shaft by the force, F_u :

$$\mathcal{T} = F_u \times r = r \frac{W_1}{g} (V_{U1} - V_{U2}) \quad (5-8)$$

where \mathcal{T} = torque ($\text{ft}\cdot\text{lb}_f$) and r = radius of Section A-A (ft). This torque, acting through an angular displacement, is analogous to work and the rate of producing work is power. Thus, the absolute power for the stage of Figure 5.9 is:

$$\Delta H = \omega \mathcal{T} = \frac{W_1}{gJ} \omega r (V_{U1} - V_{U2}) \quad (5-9)$$

where $\omega = \frac{2\pi \cdot \text{RPM}}{60}$

is rotational speed ($1/\text{sec}$), RPM = turbine speed (revolution /min).

Expressed as specific power:

$$\Delta h = \frac{\Delta H}{W_1} = \frac{r}{gJ} U (V_{U1} - V_{U2}) \quad (5-10)$$

where U = tangential velocity of rotor at radius r , $U = \omega r$ (ft/sec). The vector U is sometimes termed "wheel speed".

For a single turbine stage, we can compare equation (5-6) with equation (5-10) and get

$$\begin{aligned} C_p \eta_{TT} T_{T1} \left[1 - \left(\frac{P_{T2}}{P_{T0}} \right)^{\frac{\gamma-1}{\gamma}} \right] \\ = \frac{1}{gJ} U (V_{U1} - V_{U2}) \end{aligned} \quad (5-11)$$

Increases in either inlet temperature, T_{T1} , or expansion ratio, P_{T0}/P_{T2} will be manifested as increased velocities inside the turbine and thus more $V_{U1} - V_{U2}$.

A fundamental concept obvious from inspection of equation (5-11) is that a high efficiency turbine stage (high η_{TT}) will more effectively convert the potential thermal energy of that stage (set by a given temperature level and expansion ratio) into actual tangential momentum exchange across the rotor by producing a larger $V_{U1} - V_{U2}$ than a design with lower η_{TT} . That is, it more effectively converts thermal energy into mechanical energy.

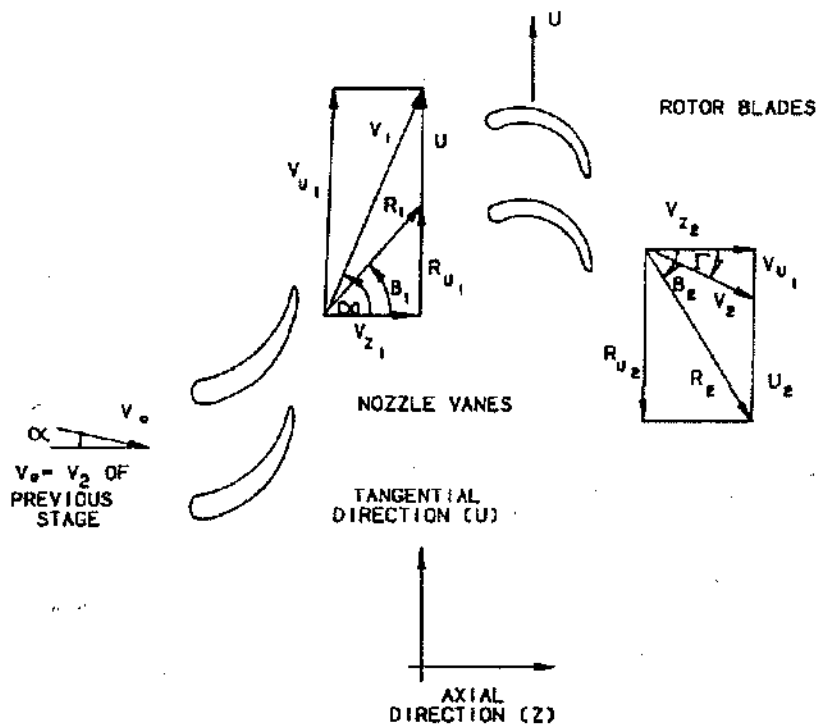


Figure 5.9 Typical Turbine Vector Triangles

While Figure 5.9 is a schematic of sorts, it does present the velocity vectors V_{U1} and V_{U2} in the proper perspective relative to one another for a typical stage. That is, V_{U1} is always in the direction of rotation while V_{U2} is usually opposite rotation, and V_{U1} is usually much larger in magnitude than V_{U2} . The fact that V_{U2} is usually negative means that the magnitudes of tangential velocities are additive in equation (5-10).

There is a practical limit, however, on the amount of V_{U2} that can be designed into a stage because, as V_{U2} increases, the absolute angle leaving the turbine (called 'swirl') increases. If there is a nozzle or an augmentor downstream of the turbine stage, then swirl is kept in the range from 0° to 5° . If there is a frame or another turbine stage downstream, then the swirl can be as high as 30° . In any case, most of the potential for tangential momentum exchange in the turbine rotor must come from V_{U1} because of this limitation on V_{U2} .

With this in mind, we can now describe the real function of the turbine bladerow types. The stator's prime function (at least from an aero viewpoint) is to set up the very high level of tangential momentum (i.e. large V_{U1}) required by the rotor to achieve the stage target Δh . Note

from Figure 5.9 that this is achieved by a combination of turning and acceleration ($V_1 > V_0$). Secondly, the stator (especially the first stage stator) serves as a flow control device which sets the flow capacity of the turbine. The rotor's function is to "catch" the high momentum flow from the stator, and once again through a process of turning and accelerating, to produce the tangential momentum change ($V_{U1} - V_{U2}$) within stringent swirl limitations.

As will be seen later, the losses in turbine blading generally increase as turning ($\alpha_1 - \alpha_0$ for the stator and $\beta_2 - \beta_1$ for the rotor) or velocity levels (V_1 or R_2) are increased. Because of this, there is a limit to how much Δh can be extracted from a turbine stage for any given temperature level and wheelspeed because η_{TT} drops faster than $V_{U1} - V_{U2}$ increases (equation (5-11)). Thus, if the cycle demands a certain Δh and if temperature levels and speeds are already at their maximum, the only alternative is to add another stage.

The single most effective "handle" that the turbine designer has on just how much Δh can be efficiently achieved in a stage is called stage loading, to be discussed under Performance Considerations.

PRINCIPLES OF OPERATION: Radial Equilibrium

The vector diagrams shown in Figure 5.9 occur only at the pitchline. Variations from pitchline vector diagrams at the hub (inner wall) and tip (outer wall) are substantial and must obviously be considered when designing the airfoils.

The variations in velocity and angles from hub to tip at any axial station inside the turbine is governed by the radial equilibrium (or momentum) equation which can be stated (in a very simplified form) as:

$$\frac{dp}{dr} = \frac{\rho}{g} \frac{V_u^2}{r} \quad (5-12a)$$

where $\frac{dp}{dr}$ = radial static pressure

gradient (lb/ft³) and ρ = density (lbm/ft³).

The left hand side of equation (5-12a) is the radial static pressure gradient required to counteract the centrifugal force of the flow swirling in the annulus at tangential velocity, V_u , at radius, r . While other forces are present, the centrifugal force described by the right hand side of equation (5-12a) predominates in an axial flow turbine stage.

Figure 5.10a shows the static pressure gradients behind a typical HPT vane and blade. Note that the gradient for the vane is more severe due to the larger magnitude of V_u there.

With some manipulation the dp/dr term in equation (5-12a) can be replaced with a thermodynamically equivalent function of enthalpy, entropy and velocity. The result, for a turbine with Δh constant along the span is the following ordinary differential equation:

$$\frac{dV_z^2}{dr} = - \frac{1}{r^2} \frac{d(rV_u)^2}{dr} \quad (5-12b)$$

A very common approach used in most early gas turbines was to design for constant axial velocity, V_z , along the span which tends to make the flow per unit area uniform along the annulus height. To satisfy this simplified form of radial equilibrium for that condition requires that the product of radius and tangential velocity, rV_u , also be constant. This is the so-called free vortex approach to radial equilibrium and it results in the vector diagrams for hub, pitch and tip sections of a typical tur-

bine stage shown in Figure 5.10b. Note that V_z is constant for all three sections, but that V_u and U vary with radius. Figure 5.10c shows blading designed to fit the vector diagrams of Figure 5.10b. Note the characteristic twist from hub to tip caused by variations in V_u and U as a function of radius.

One parameter that affects the amount of twist in the blading is the radius ratio defined as the ratio of hub radius to tip radius. A low radius ratio design will have more twist because hub and tip are further away from the pitchline, with more variation in V_u and U . LPT blading tends to be much lower in radius ratio, and therefore more highly twisted, than higher radius ratio HPT blading.

Experience has shown that a free vortex turbine is a very adequate performer, although recent technology says that something like a one point improvement in efficiency can be obtained by slight deviations from free vortex aerodynamics.

In spite of the considerable variation in vector diagrams from hub to tip, it is still true that the pitchline vector diagrams represent a good average for the turbine stage. Consequently, most performance parameters, some of which are discussed in the following section, are quoted based on pitchline values.

PERFORMANCE CONSIDERATIONS: Basic Performance Parameters

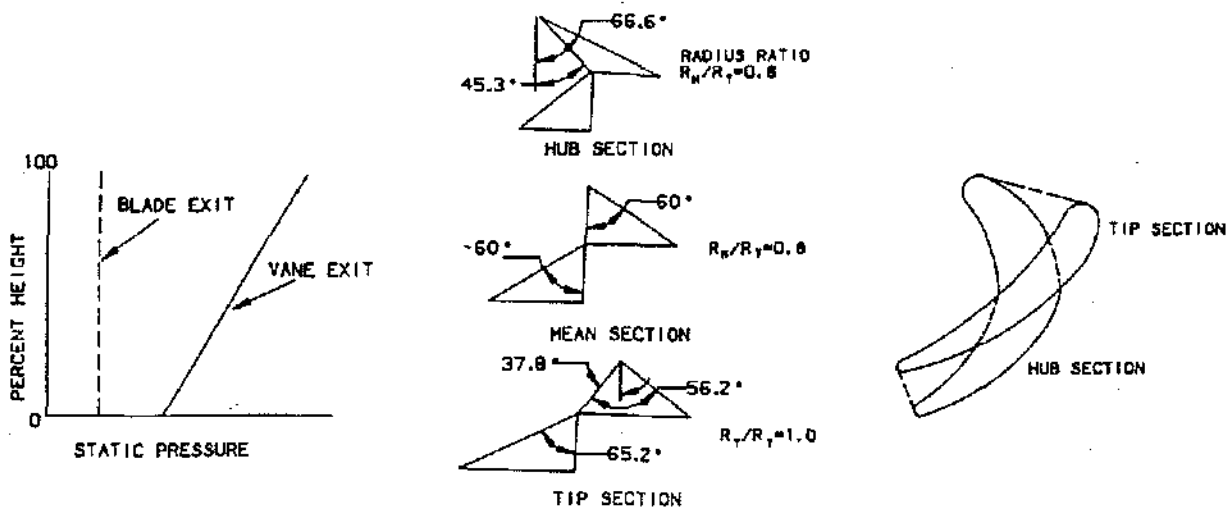
We will now discuss three parameters which, when taken together, completely define the pitchline (mid-span) vector diagrams and set the efficiency potential of the stage. These are loading, flow coefficient and reaction.

Stage Loading Turbine stage loading is the single most effective indicator of efficiency potential. It is defined as the ratio of actual specific power, Δh , to the specific power of a reference stage operating at the same wheel speed, U . The reference stage, by definition, has zero swirl ($V_{u2} = 0$) and zero "reaction" (no static pressure drop across the rotor so that $R_1 = R_2$). It can be shown that, for the reference stage, equation (5-10) reduces to:

$$\Delta h = 2U^2/gJ$$

so that, by definition, GE's stage loading parameter, ψ , becomes:

$$\psi = \frac{gJ\Delta h}{2U^2} = \frac{V_{U1} - V_{U2}}{2U} \quad (5-14)$$



a) Hub-to-Tip Variation In Static Pressure For A Turbine Stage Designed For Zero Exit Swirl

b) Vector Diagrams For A Free Vortex Turbine Designed For Zero Exit Swirl

c) Hub And Tip Airfoil Shapes Corresponding To the Vector Diagrams In 10b

Figure 5.10 Effects of Radial Equilibrium in a Turbine Stage

A trend of efficiency versus loading is shown schematically in Figure 5.11. Thus loading is a figure of merit, of sorts, which says that a highly loaded turbine stage, which must produce high work (via high turning and high velocity levels) because of lower wheel speed (rate of doing work), is inherently less efficient than a more lightly loaded stage. Another interpretation is that airfoils in a highly loaded turbine stage must produce higher lift (i.e. tangential force) and there is a limit beyond which an airfoil can no longer efficiently produce that lift.

If, as often happens, the total Δh required by the cycle is greater than that which can be produced by a single stage at wheel speed, U , then one or more stages must be added to achieve the Δh at an acceptable level of overall loading for the multistage group.

Loading for a group of two or more turbine stages is defined as follows:

$$\psi = \frac{gJ\Delta h_{TOT}}{n \sum_{i=1}^n U_i^2} \quad (5-15)$$

where Δh_{TOT} = total Δh required by the cycle, n = number of turbine stages, and U_i = wheelspeed of the i^{th} stage.

Loading levels for GE HPT stages are in the range from 0.6 to 1.0. Loading levels for GE LPT stages vary from 0.6 all the way to 1.7, with multi-stage averages in the range of 0.7 to 1.3. Note that turbine loading can be increased by decreasing stage RPM and/or diameter (both resulting in lower U) or by increasing extraction, Δh .

Stage Flow Coefficient Another parameter which affects turbine performance potential, almost as significantly as loading, is the stage flow coefficient, ϕ , defined as the ratio of axial velocity to wheel speed:

$$\phi = \frac{V_z}{U} \quad (5-16)$$

Figure 5.12 illustrates the effect of flow coefficient on the shape of the vector diagrams for two examples, both with the same stage loading.

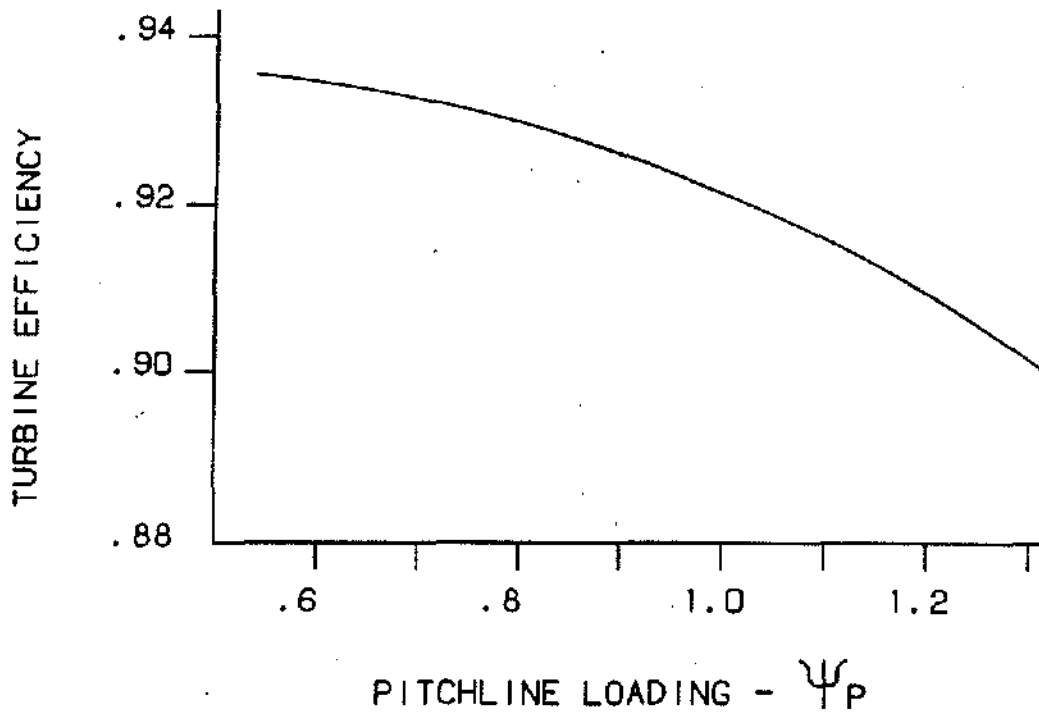


Figure 5.11 A Trend of Efficiency vs. Loading For a Hypothetical Turbine Stage

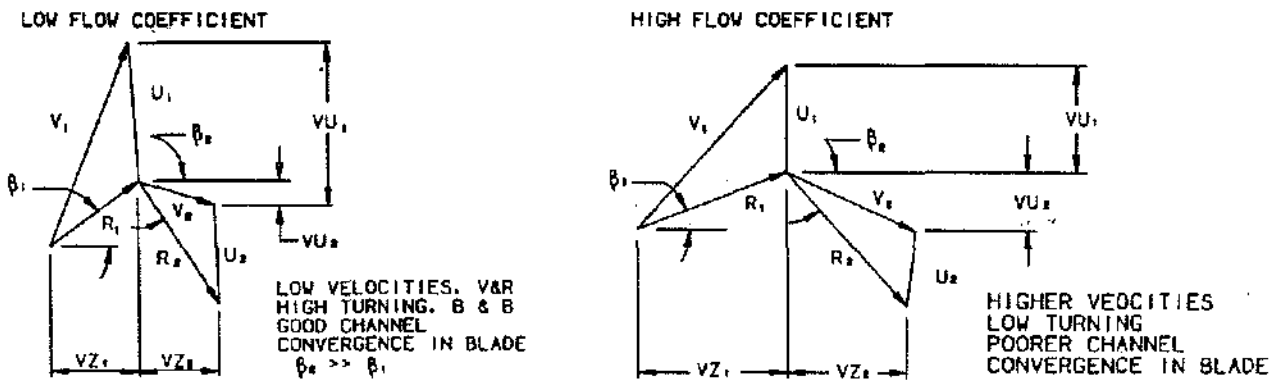


Figure 5.12 Effect of Stage Flow Coefficient. VZ/U On Vector Diagram Shapes For Constant Stage Loading. $\Delta VU/ZU$

Note that the stage with large axial velocity relative to wheelspeed (a high "through-flow" or high flow coefficient design) has less blade turning (α_1 and β_2 more axial) but higher velocity levels than its low through-flow counterpart. We will see in section on turbine maps that excess turning causes high loss, thus there is a lower limit on flow coefficient. On the other hand, since friction losses in turbine blading are generally proportional to velocity squared, there is also an upper limit. This implies that, for any given level of loading, there is an optimum value for flow coefficient which balances turning losses and friction losses.

This is illustrated in Figure 5.13 for a typical turbine stage. If we take a vertical slice through the efficiency contours on this plot (i.e. at a constant value of ϕ), then we get a trend of η versus ψ which looks like Figure 5.11. Note, however, that if we take a slice at some other level of flow coefficient that trend will be different. The reason for this basic relationship is once again, the balance between turning and friction loss.

In the course of laying out a flowpath, the turbine designer will use a chart similar to Figure 5.13 to guide the selection of annulus area in each stage. For a given flowpath mean diameter, a large annulus area will yield low

axial velocity and thus low flow coefficient. Generally, since a taller annulus results in increased blade root stress and (possibly) more rotor weight, the designer will pick a value to the right of the aerodynamic optimum of Figure 5.13 (the system optimum).

Reaction The cycle sets the pressure drop across the turbine and this, together with the number of stages sets the pressure drop across each of the individual stages in the turbine. It remains to the aero designer to split this stage pressure drop between the vane and the blade. A parameter called "reaction" defines the pressure drop across the blade as a fraction of the pressure drop across the stage. In detail, enthalpies are used rather than actual pressures, since these relate more directly to acceleration across the turbine bladerows.

By strict definition then, reaction is the ideal static enthalpy drop across the blade divided by ideal total-to-static enthalpy drop across the stage. This can be expressed in terms of flowpath pressures as:

$$R_x = \frac{P_1^x - P_2^x}{P_{T0}^x - P_s^x}$$

where P_1 = rotor inlet static pressure, P_2 = rotor exit static pressure, and $x = (\gamma - 1)/\gamma$.

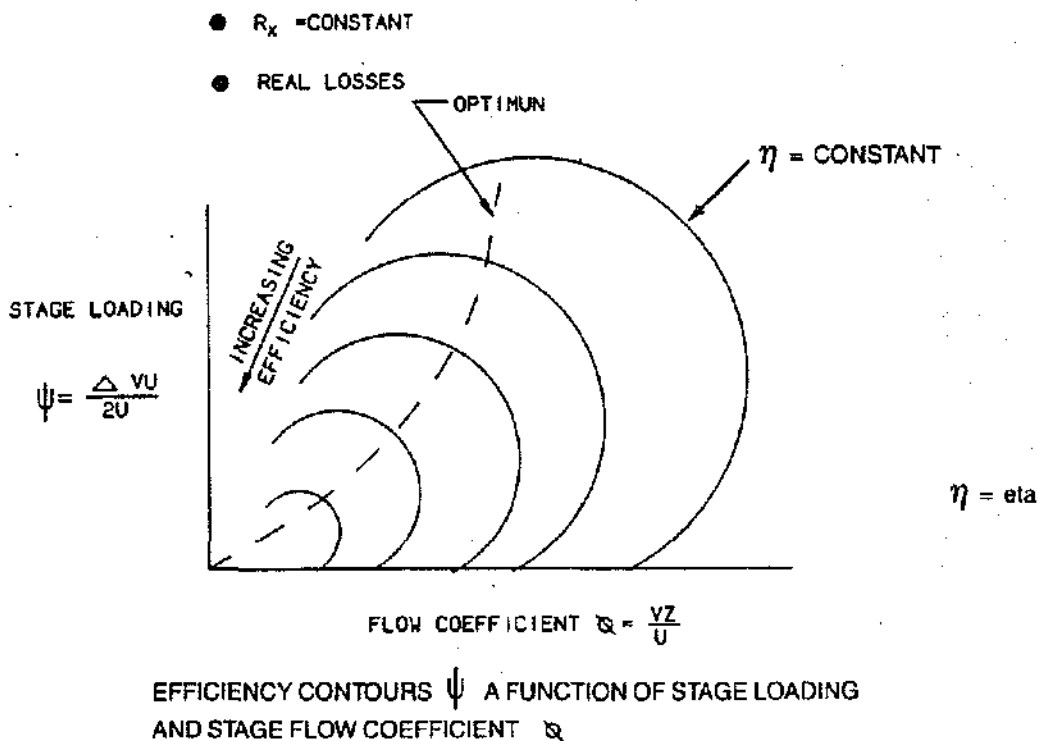


Figure 5.13 Vector Diagram Characteristics

Zero reaction stages take all the static pressure drop across the vane and none across the blade. These are also called impulse stages because all the force on the rotor results from the impulse of the high velocity stator exit flow impinging on the rotor and there is no additional reaction force due to expansion off the rotor. Most early turbine designs (and some modern steam turbine designs) are of this type. Advantages are that the axial thrust on the bearings of the turbine rotor are less with an impulse stage. Further, nozzle vanes with very high exit velocities can attain very high levels of performance and, as loading requirements approach 2.0, this is the most efficient way to get the necessary tangential momentum exchange. Too much reaction at too high a loading results in excess swirl and increased losses across the tips of unshrouded rotor blades.

At the low to moderate levels of loading encountered in aircraft gas turbines, however, some degree of positive reaction (say up to about .5) usually results in best efficiency because there is a more uniform distribution of acceleration between the vanes and the blades. Also, rotor axial thrust tends to be cancelled by the compressor.

Negative reaction, where a pressure rise actually occurs across the rotor blade, is usually avoided in modern gas

turbine design because of the poor rotor blade performance that results.

Recall from Figure 5.10a the very large gradient in static pressure, P_1 , behind the vane due to radial equilibrium considerations. Note that, since P_1 is lowest at the hub, the blade hub section will always have the lowest reaction.

Consequently, while loading and flow coefficient are quoted at the pitchline, GE AE practice is to quote reaction at the hub section. Given the combination of high turning (see Figure 5.10c) and low reaction at the hub, the blade hub section is a relatively difficult section to design.

Hub reactions for GE HPT's are in the range from 0.25 to 0.40, with LPT's falling in a slightly lower range. Figure 5.14a shows the spanwise variation in reaction for a turbine designed to the vector diagrams of Figure 5.10b.

Figure 5.14b shows examples of zero, positive and negative reaction turbine blades.

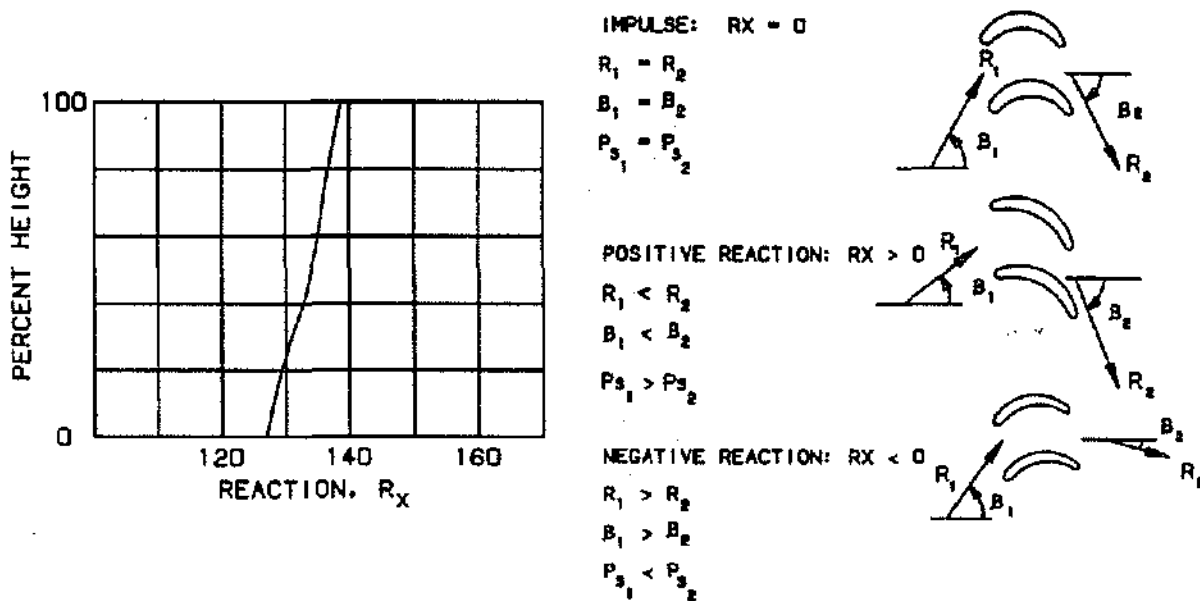


Figure 5.14 Typical Spanwise Variation of Stage Reaction and Effect of Reaction On Blade Channel Designs

The Turbine Map Figure 5.15 shows a typical turbine map which presents turbine efficiency contours plotted on a background of energy function, $\Delta h/T_{T1}$, and corrected speed, $N/\sqrt{T_{T1}}$. Recall from equation (5-6) that Δh is directly proportional to T_{T1} so use of $\Delta h/T_{T1}$ makes the map more generally applicable. Further, since velocities inside the turbine are proportional to the square root of temperature, use of $N/\sqrt{T_{T1}}$ ensures that the wheelspeed vector U will always be in proportion to the velocities (V_z , V_u , etc.). Consequently, the turbine vector diagrams will retain their similarity at any point on the map regardless of temperature level.

The reader should note some similarity between the turbine map, with its high-efficiency ridge (or backbone), and Figure 5.13, with its locus of optimum efficiency. While loading and flow coefficient do affect the shape of the map, there is the additional consideration in Figure 5.15 of angle of attack (or incidence) loss incurred by running a fixed geometry turbine away from its design point. Figure 5.16 shows how flow coefficient affects angle of attack and, therefore, the fall off of efficiency from the backbone.

Another key parameter required by the cycle from the turbine map is flow function, $W_1\sqrt{T_{T1}}/P_{T0}$. Figure 5.16 shows how this varies over the map for an LPT.

Flow function variation is less pronounced for HPT's since their vanes tend to operate at or near choke over most of the map.

PERFORMANCE CONDITIONS: Turbine Loss Sources

There are three classes of losses which occur in the process of converting thermal and kinetic energy inside the turbine into mechanical energy to the shaft. They are spanwise aero losses (Class I), endwall aero losses (Class II), and mechanical and coolant delivery losses (Class III). Spanwise aero losses (i.e. losses which occur along the entire span of a turbine airfoil) include profile loss, shock loss, Reynolds number and roughness loss, angle of attack loss, and airfoil cooling loss. Endwall aero losses (i.e. losses confined to the hub or tip of the airfoil) include secondary flow loss (including wall slope loss), tip clearance loss, band or shroud cooling losses, cavity purge and interstage seal losses, and loss due to recirculation in wheelspace cavities. Mechanical and coolant delivery losses are bearing, disk windage, and coolant pumping losses. Only Classes I and II will be considered, since Class III losses are generally not directly controllable in the aero design.

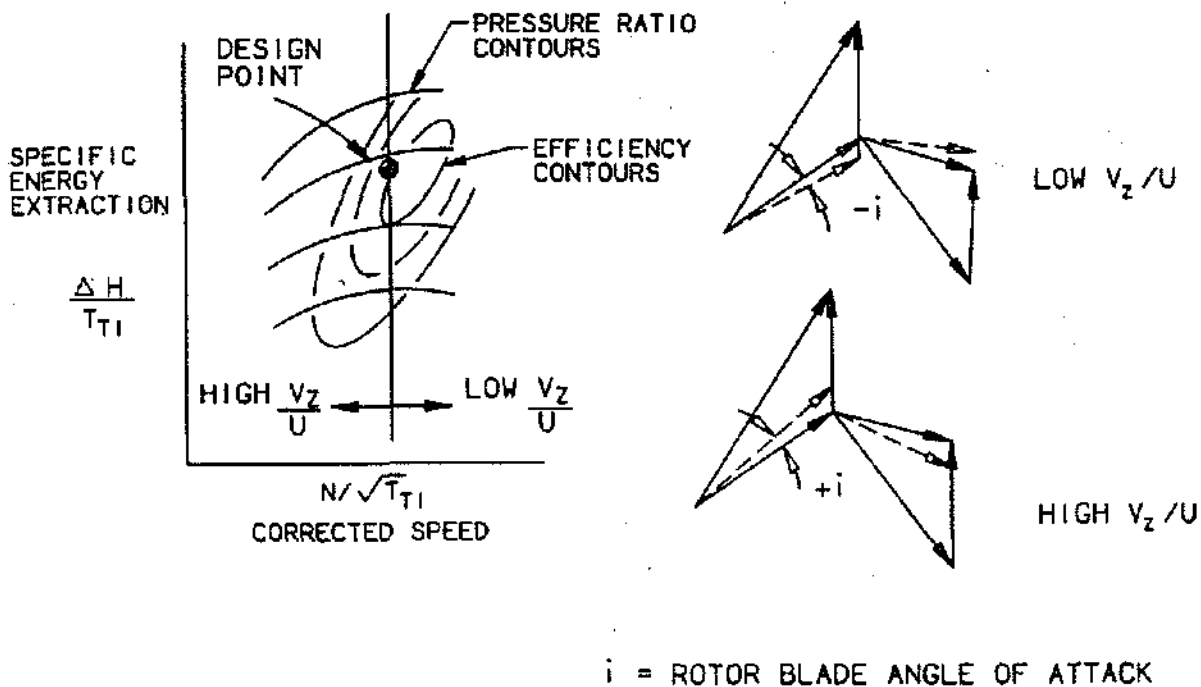
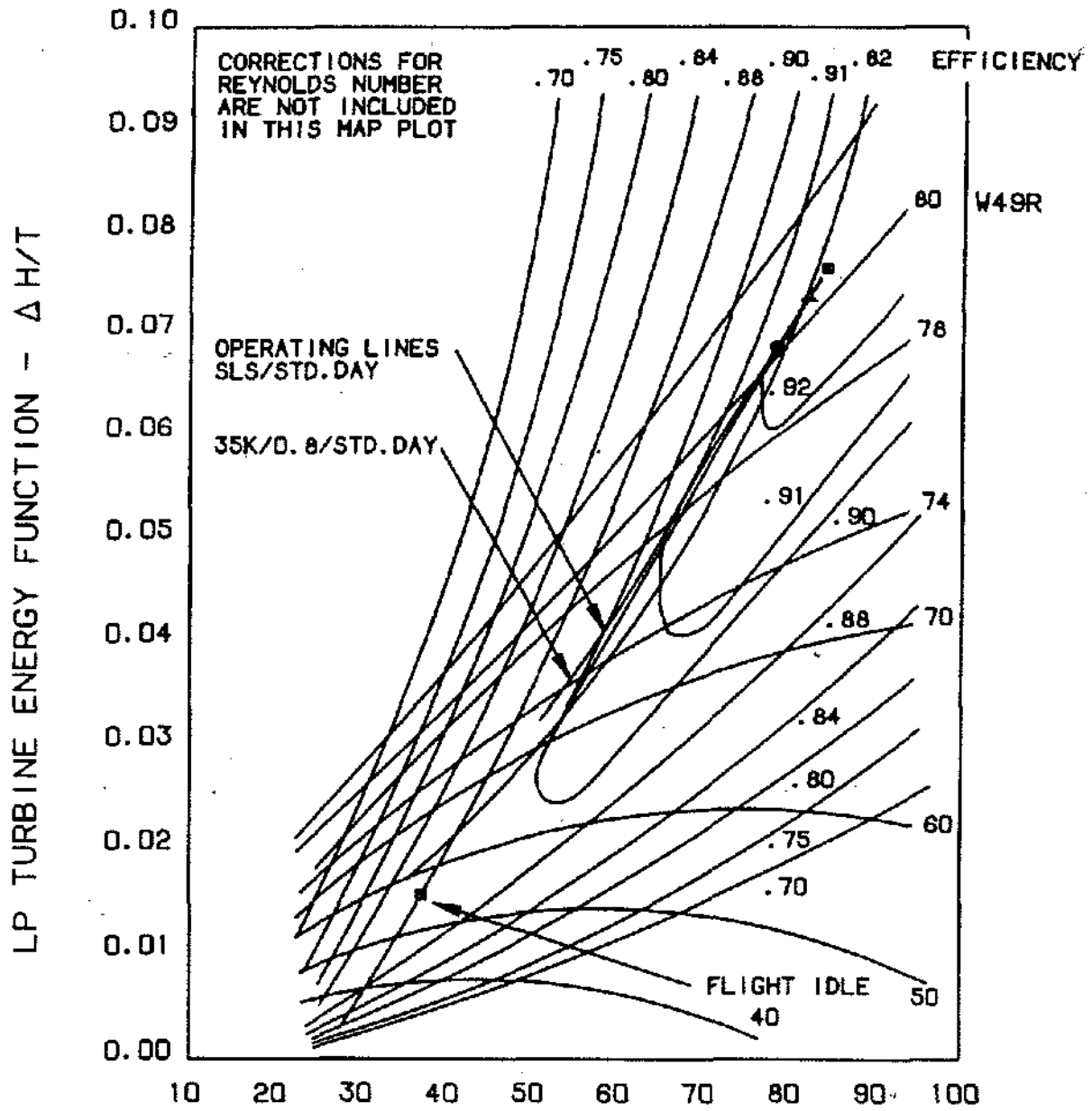


Figure 5.15 Typical Turbine Map Showing Efficiency Variation and Off-Design Angle of Attack Tendencies

$$W49R = \frac{W\sqrt{TY}}{P_T} : \text{FLOW FUNCTION}$$



LP TURBINE CORRECTED SPEED - N/\sqrt{T}

- TAKE-OFF
- MAX CLIMB
- ▲ MAX CRUISE

Figure 5.16 LPT Map Showing Flow Function and Efficiency

Turbine blading losses in Classes I and II are expressed in terms of efficiency loss where

$$\Delta\eta_{BR} = 1 - \frac{V_a^2}{V_i^2}$$

where $\Delta\eta_{BR}$ = loss in bladerow kinetic energy, V_a = actual velocity leaving bladerow, and V_i = ideal velocity leaving bladerow. Bladerow efficiency, $\Delta\eta_{BR}$, should not be confused with stage efficiency, η_{TT} , defined in equation (5-5).

Profile loss for a subsonic airfoil occurs due to friction drag on the airfoil surfaces and to expansion around the trailing edge. Figure 5.17a shows how profile loss will manifest itself as a wake in total pressure at the airfoil trailing edge. Figure 5.17b shows how profile loss is affected by solidity (chord/tangential spacing) and blade row turning. If solidity is too low (i.e. if there isn't enough lifting surface per airfoil) then the flow will actually separate off of the airfoil surface. Too high a solidity just increases the wetted area and results in more friction. An optimum solidity is usually based on test experience. Figure 5.17c shows how increases trailing edge thickness affect profile loss.

In several single stage turbine designs at GE, the stator and rotor exit velocities, V_1 or R_2 , are supersonic (exit Mach numbers as high as 1.2, but suction surface Mach numbers can reach 1.4 locally). In this case, a shock loss is incurred as the supersonic flow adjusts around the thick trailing edge. Figure 5.18a shows this schematically.

Profile losses are usually obtained in tests at high Reynolds numbers. If the turbine operates at low Reynolds numbers, where the effect of viscosity become more noticeable, then the profile friction loss will increase per Figure 5.18b. LPT stages operating at altitude or turbines in very small engines may lose from 0.5 to 3.0 points in efficiency due to low Reynolds numbers.

A rougher airfoil will have a higher friction coefficient than a smooth airfoil and, as Figure 5.18 shows, this effect is more pronounced at higher Reynolds number levels.

Angle of attack losses are incurred as the turbine moves away from its design point (see Figure 5.15). Figure 5.19 shows how this affects bladerow efficiency.

Mixing loss caused by injecting relatively low momentum cooling flow through film holes (see Figure 5.5) is a function of the amount of cooling flow, the angle of in-

jection and the ratio of coolant to mainstream momentum. The first stage vane of an HPT may lose 1.5 points due to this effect.

Secondary flow losses occur when mainstream flow near the hub and tip is slowed by wall friction and then swept across the channel from the pressure side to the suction side of the airfoil. It then forms a vortex as shown schematically in Figure 5.20a. Figure 5.20b shows how secondary flow losses show up as holes in the spanwise profile of η_{BR} . Figure 5.20c shows how the ratio of bladerow chord to height (called the aspect ratio) affects secondary flow loss. LPT stages are more efficient than HPT stages of similar loading because they tend to be much higher in aspect ratio and their secondary flows are confined to a smaller percentage of the annulus.

Figure 5.20d shows how wall slope can accentuate secondary flow loss, a factor that limits the outer wall slope in LPT's. Ideally, the CF6-80 type LPT's would like more wall slope to get more wheelspeed for a given RPM. However, experience has shown that wall slope beyond about 25° will eat up any performance increase from reduced loading.

Tip clearance is a major loss source in turbines, but especially so in HPT's, where blade tips are unshrouded and where a finite clearance is a much larger percentage of annulus height. Clearance loss, in fact, is correlated as a function of percent clearance (100 x clearance/blade height) as shown in Figure 5.21a. Figure 5.21b shows how clearance changes affect the flowfield behind an HPT stage.

Stator band or blade shroud cooling air contributes a momentum mixing loss similar to that discussed for Class I cooling loss.

All wheelspace cavities in HPT's and LPT's are purged with small amounts of cooling air and these create mixing losses when they finally mix with the mainstream air.

While all turbine cooling and purge flows do cause some mixing loss, they also contribute to turbine power since most of them ultimately go through the turbine blading. However, only the HPT stage one nozzle cooling enters the turbine with full tangential momentum (V_{t0}). This is termed "non-chargeable" flow because it is charged to the turbine and not to the cycle. The remainder of the cooling flow is "chargeable" to the cycle to simplify bookkeeping. The partial availability of the chargeable flow is reflected in the turbine efficiency definition as explained in Figure 5.22.

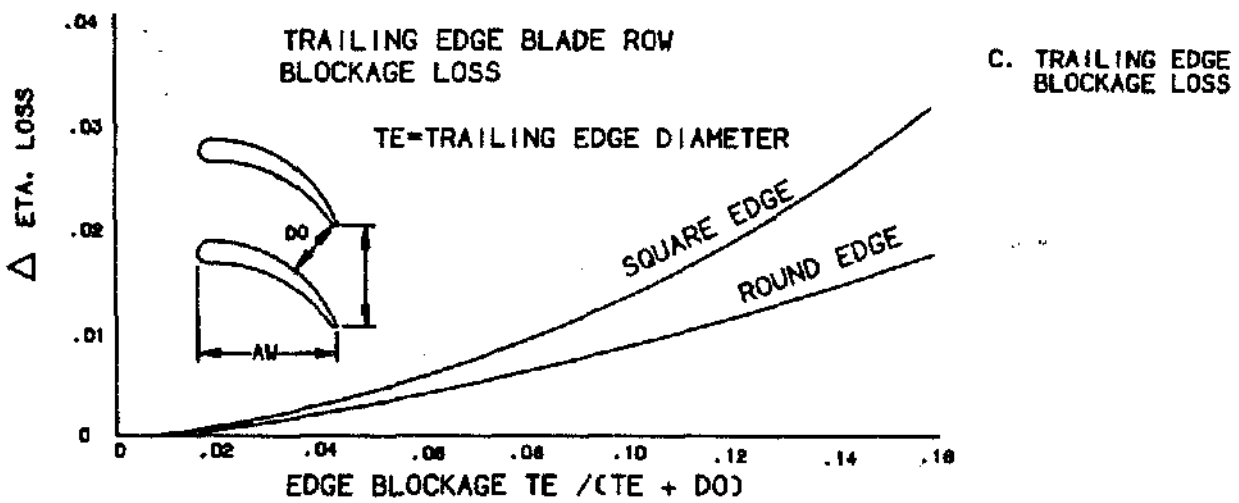
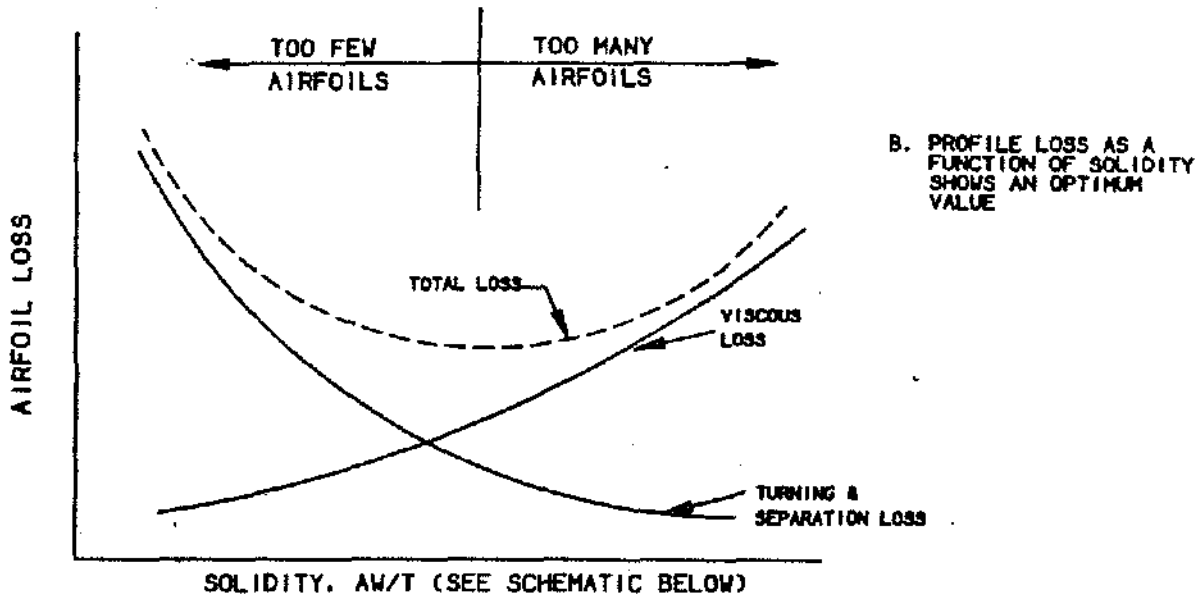
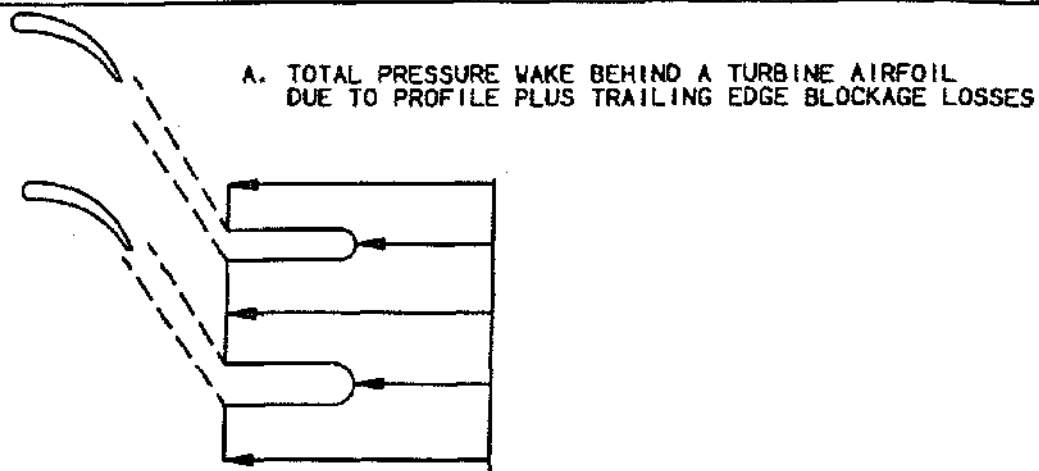


Figure 5.17 Turbine Losses

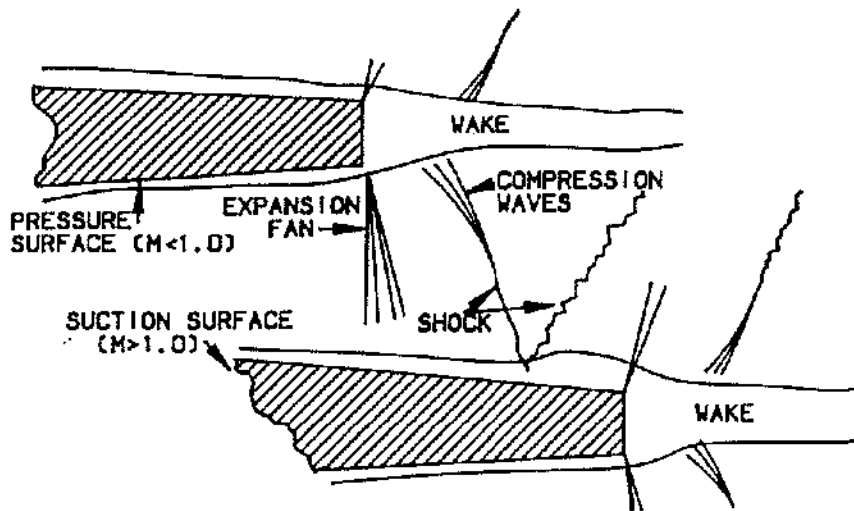


Figure 5.18a Schematic Showing How Supersonic Flow Adjusts Around the Trailing Edge Region of A Turbine Airfoil. Loss is Incurred Through Oblique Shocks and Shock/Boundary Layer Interaction.

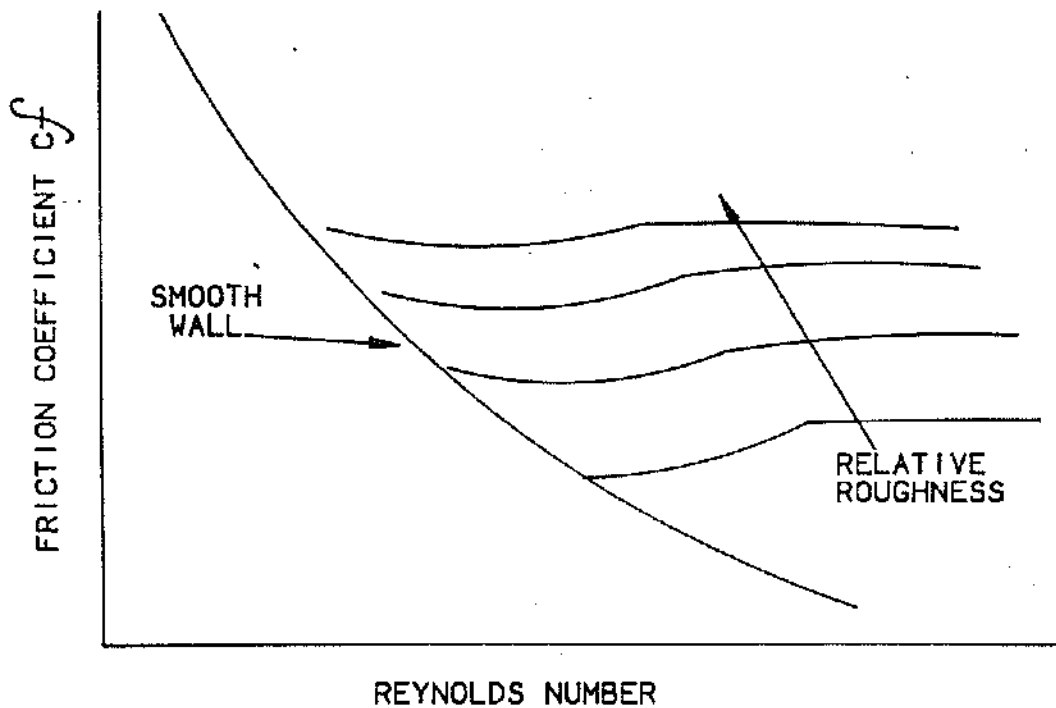


Figure 5.18b The Effect of Reynolds Number and Roughness on Friction (And Therefore Loss) For A Turbine Blade

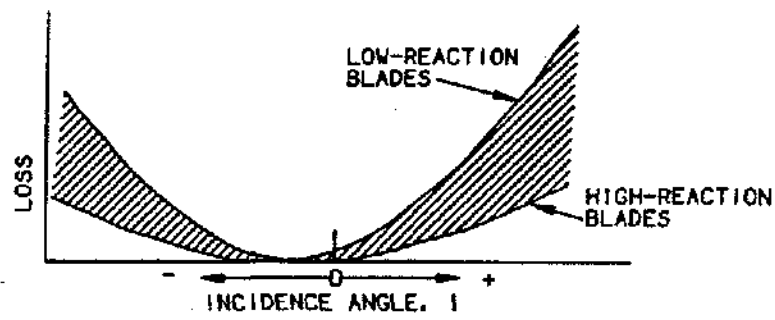


Figure 5.19 Angle of Attack Loss on Turbine Airfoils

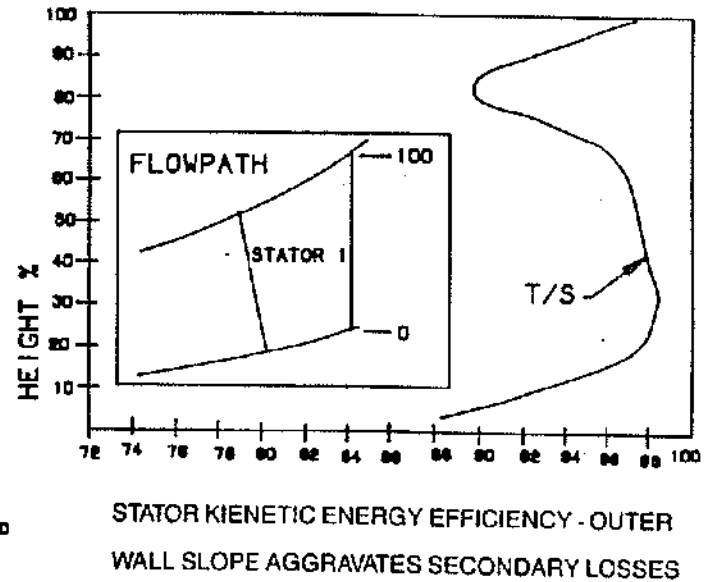
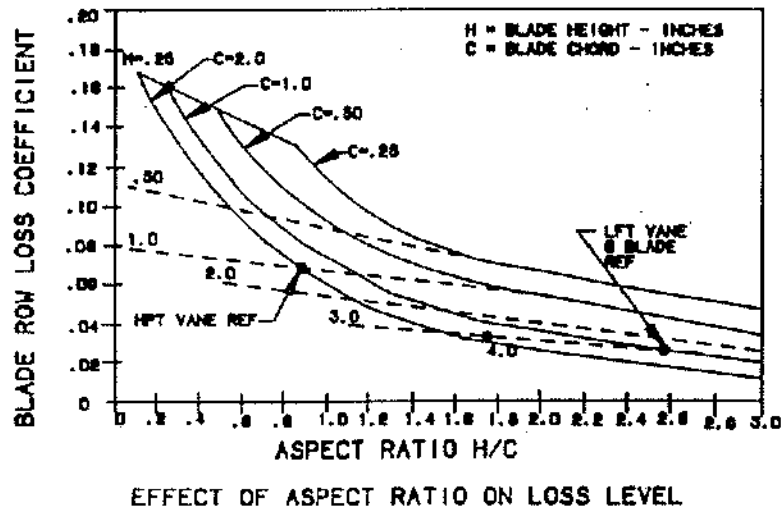
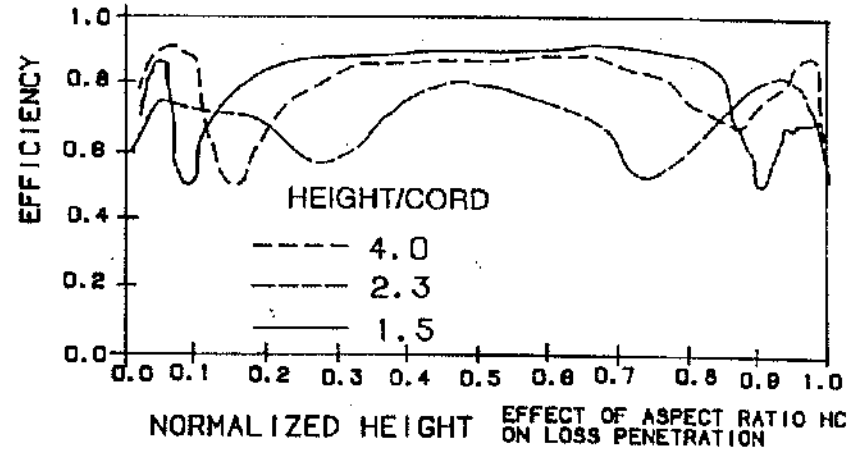
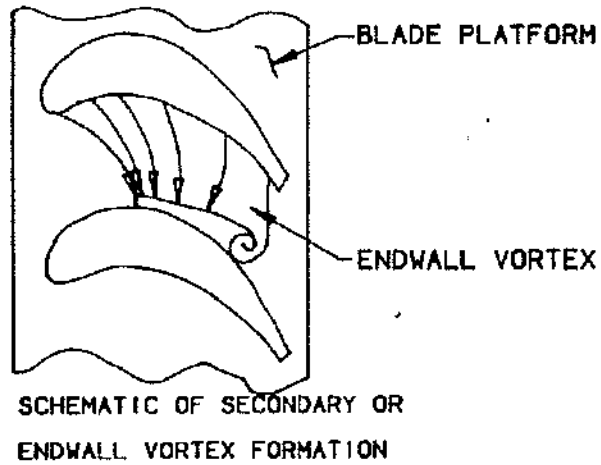
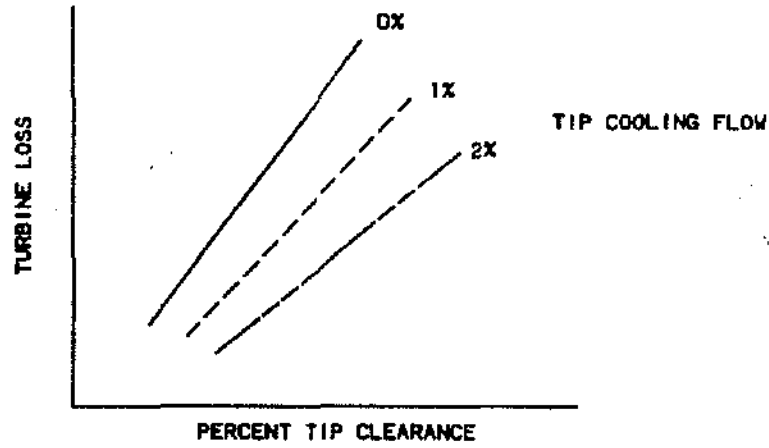
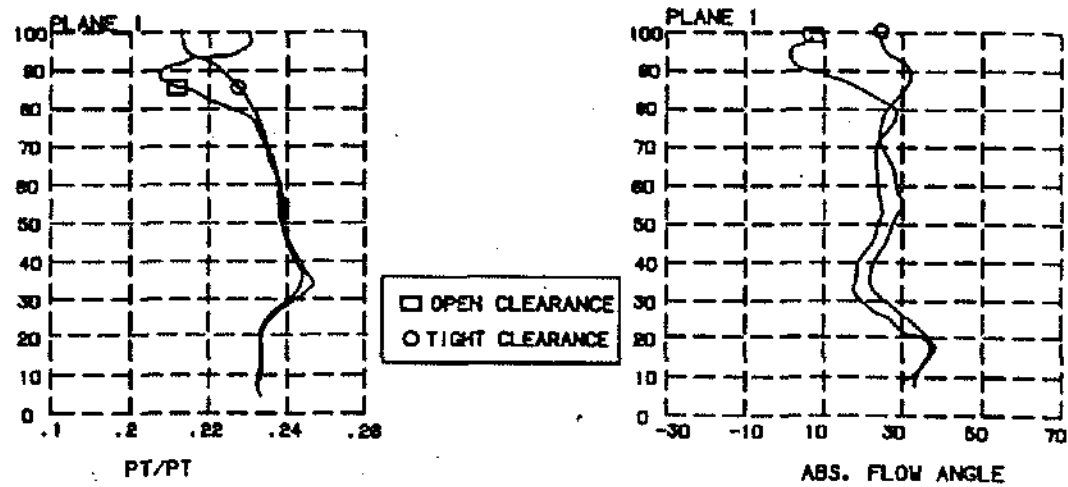


Figure 5.20 Secondary or Endwall Losses in Turbine Blading

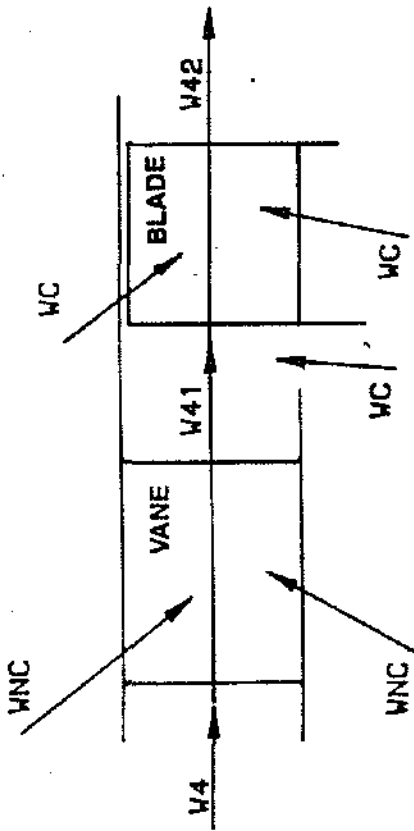


STAGE EFFICIENCY LOSS AS A FUNCTION OF PERCENT CLEARANCE



SINGLE-STAGE HPT EXHAUST PRESSURE AND FLOW ANGLE DISTRIBUTIONS FOR TWO LEVELS OF TIP CLEARANCE

Figure 5.21 Single-Stage HPT Exhaust Pressure and Flow Angle Distributions for Two Levels of Tip Clearance



- W4 = COMBUSTOR EXHAUST FLOW
- W41 = W4 + ΣWNC • ROTOR INLET
- W42 = W41 + ΣWC • TURBINE EXHAUST
- WNC = CYCLE NON-CHARGEABLE COOLING
- WC = CYCLE CHARGEABLE COOLING
- ΔH 41-42 (= H 41 - H 42)
- ΔH C-42 (= H C - H 42)

- H41 = TOTAL ENTHALPY AT 41, BTU/IBM
- H42 = TOTAL ENTHALPY AVAILABLE IN IDEAL EXPANSION OF FLOW FROM SOURCE PRESSURE TO EXHAUST PRESSURE, P42

GE CYCLE EFFICIENCY

$$\eta_{TT} = \frac{550}{J} \frac{HP}{W41 \Delta H41-42}$$

THERMODYNAMIC EFFICIENCY (P&WA, NASA)

$$\eta_{TH} = \frac{550}{J} \frac{HP}{W41 \Delta H41-42 + \sum WC \Delta HC-42}$$

- HP = TURBINE HORSEPOWER DELIVERED
- = COMPRESSOR GASPATH POWER + ACC DR.
- = TURBINE GASPATH POWER - PUMPING

NOTE: FROM CYCLE VIEWPOINT, TURBINE WORKS ONLY WITH W41. CHARGEABLE FLOWS SIMPLY BYPASS THE TURBINE AND REENTER AT 42. THE PARTIAL AVAILABILITY OF THE CHARGEABLE FLOWS TO DO WORK IN THE TURBINE, TOGETHER WITH THE WORK REQUIRED TO PUMP THESE FLOWS FROM THEIR SOURCES TO THE POINTS OF ENTRY, ARE REFLECTED BY TURBINE AERO INPUT IN η_{TT}

Figure 5.22 From Cycle Viewpoint, Turbine Works Only With W41. Chargeable Flows Simply Bypass the Turbine and Reenter at 42. The Partial Availability of the Chargeable Flows To Do Work in The Turbine, Together With The Work Required To Pump These Flows From Their Sources To The Points of Entry, Are Reflected By Turbine Aero Input in η_{TT}

DESIGN CONSIDERATIONS

Figure 5.23 is an overview of the turbine aerodynamic design process. Starting with cycle data and various geometric or mechanical design constraints from step 1, the designer proceeds to step 2 where the turbine flowpath and free vortex vector diagrams are optimized. Methods to estimate the Class I and II losses and their effect on turbine efficiency are included in a free vortex computer program.

Once the flowpath and vector diagrams have been roughed out in step 2, a refinement takes place in step 3. This is basically an upgrade of the free-vortex analysis (simplified radial equilibrium per equation (5-12b)) to a so-called through-flow analysis (full radial equilibrium per Reference 3).

Figure 5.24 shows results from a through-flow analysis. This is the information that will be used to design and analyze the blading, step 4.

Figure 5.25 shows the result from a streamline curvature analysis of a typical HPT blade. This analysis yields Mach number distributions on the airfoil surfaces. Included in the figure are key points which are checked by the aero designer before the blading is released to mechanical and heat transfer design.

COOLING CONSIDERATIONS

There are several major steps in the preliminary heat transfer design of an air-cooled HPT. The first step is to determine peak gas temperatures in front of each blade row, including the effect of combustor circumferential and radial hot streaks, possible deterioration in coolant delivery system (worn seals), general engine deterioration and hot day operation. Figure 5.26 shows heat transfer design temperature profiles for a two-stage HPT.

The convective gas side heat transfer coefficient, h_g , distribution for each exposed surface is determined. For the airfoils, the aero Mach number distribution (similar to Figure 5.25) is used to get h_g from empirical correlation of Reynolds number and Prandtl number. Figure 5.27 shows typical h_g distribution. This is integrated over the airfoil surface length to get a total "heat load", $hgAg$ (BTU/hr $^{\circ}$ F) on each airfoil.

The level of cooling effectiveness required is calculated using:

$$\eta_c = \frac{T_g - T_b}{T_g - T_c}$$

where η_c = cooling effectiveness, T_g = gas peak temperature for bladerow from step I, T_b = bulk metal temperature, and T_c = coolant temperature. T_b is the average (bulk) temperature that the airfoil material must be cooled to. This is a function of stress level, material properties and target life over a given mission.

A cooling technology curve, like Figure 5.28, is used knowing the required cooling effectiveness and the heat load parameter is read.

$$HLP = \frac{2W_c C_{pc}}{hgAg}$$

where HLP = heat load parameter, W_c = coolant flow (lbm/hr), and C_{pc} = specific heat of coolant. HLP is the result of applying a heat balance between the gas side and the coolant side of the airfoil. It gives the ratio between the heat the coolant must carry away (BTU/hr $^{\circ}$ R) to maintain η_c to the heat load, $hgAg$, from step II. Finally, W_c is determined from HLP and $hgAg$. This is a preliminary number.

Detailed heat transfer design entails iterative studies of both steady state and transient temperature calculations driven by knowledge of the gas side heat transfer from above and assumed cooling hole and cooling cavity distributions. Empirical data on film effectiveness, effects of rotation, pressure drops in cooling passages, ways to promote turbulence (for enhanced coolant side heat transfer), etc. are used in the course of these studies. Iteration is required to establish the cooling circuitry which yields a satisfactory temperature distribution with no hot spots beyond material capability, no gradients in metal temperature which violate mechanical limitations and which meets the bulk temperature target. The result is a final cooling design for the bladerow and a value for W_c which should be pretty close to W_c from step V of the preliminary sizing process.

In addition to gaspath heat transfer, all structural and rotating parts such as disks, retainers, shroud and nozzle supports, etc. much undergo transient analysis. Relative to the elapsed time required for aerodynamic design execution, heat transfer design is a longer process because of the magnitude of work required and because of iteration with mechanical design personnel.

OVERVIEW

1 INPUT

- Cycle Data (P , T , $\Delta h/T$, N/\sqrt{T} , $W \sqrt{T}/P$)
- Geometric Limitations (new or derivative ?)
- Mechanical/Heat Transfer

2 PRELIMINARY DESIGN (TP3)

- Flow Path and Vector Diagram Trade Studies
 - number of stages
(loading/pressure ratio)
 - annulus area distribution
(aspect ratio, slopes, AN^2)
 - energy splits
 - reaction and solidity levels
 - coolant effects
 - specific design features
(x-duct, counter-rotation, vaneless, etc)
- Initial Input To Support Groups

3 THROUGHFLOW ANALYSIS (CAFD)

- General Upgrade of Preliminary Design, including
 - intra-bladerow stations
 - slope/curvature effects
 - non-uniform loss, coolant penetration effect
 - updated by blade-to-blade analysis (CASC)

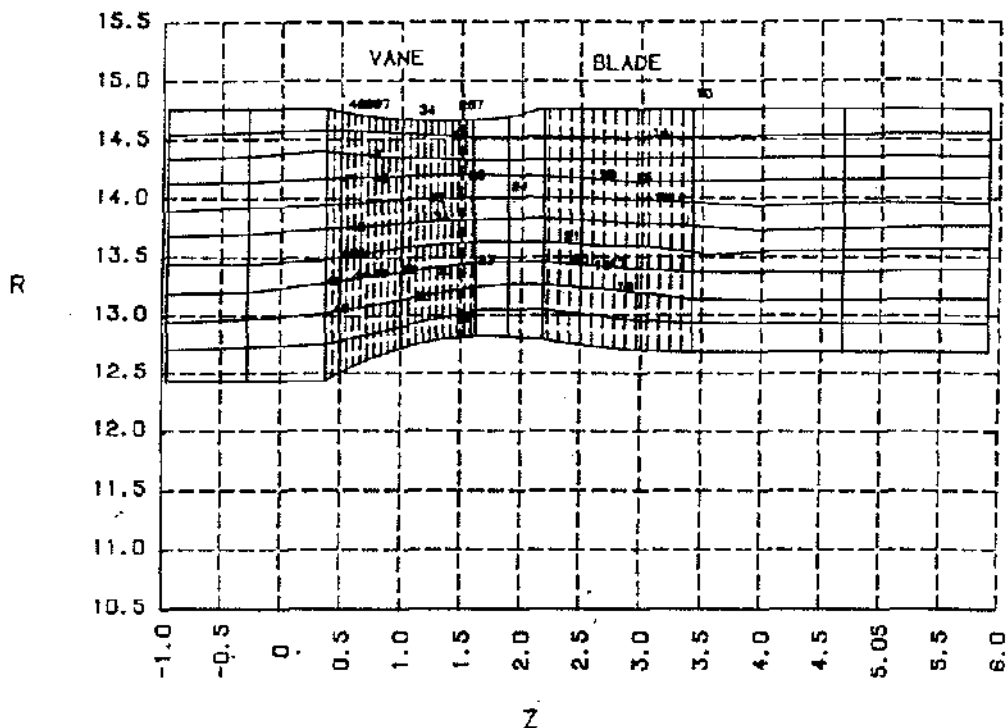
4 BLADING DESIGN AND ANALYSIS (BLADES/CASC)

- Blade-to-Blade Analysis on CAFD Streamsurfaces
 - lamina distribution updated per CAFD
- 3D Analysis as Appropriate

5 OUTPUT

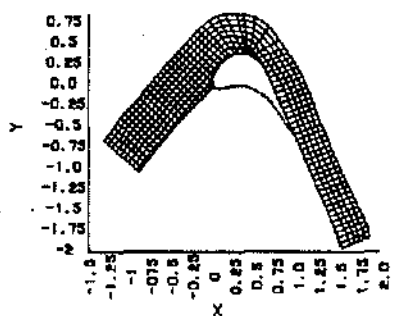
- Airfoil Definition to CAD
 - cooling cavities
 - hollow section properties
 - mechanical/heat transfer analysis
- Detailed Vector Diagram Output
 - blade forces and interstage pressures
 - blade relative pressures/temperatures

Figure 5.23 Turbine Aerodynamic Design Process



CALCULATION GRID FOR GE'S THROUGHFLOW
CALCULATION PROGRAM (CAFD) SHOWING
CONTOURS OF STATIC PRESSURE

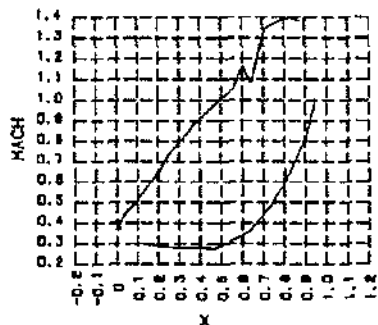
Figure 5.24 Calculation Grid For GE's Throughflow Calculation Program (CAFD) Showing Contours Of Static Pressure.



JSL=6 REGION=BLADE 1 HACH1=0.3343
 ITERATION E52MX Q52MX DVMAX DPTE
 14 0.0034 0.0008 -25.9183 -4.32
 AT 322 183

PARAMETERS

CNVF BETAM2 P52 H2H1 SSDF
 0.700 -66.62 9.68 0.964 T
 IPS ICHK NODENS NDAHCV
 2 3 2 7

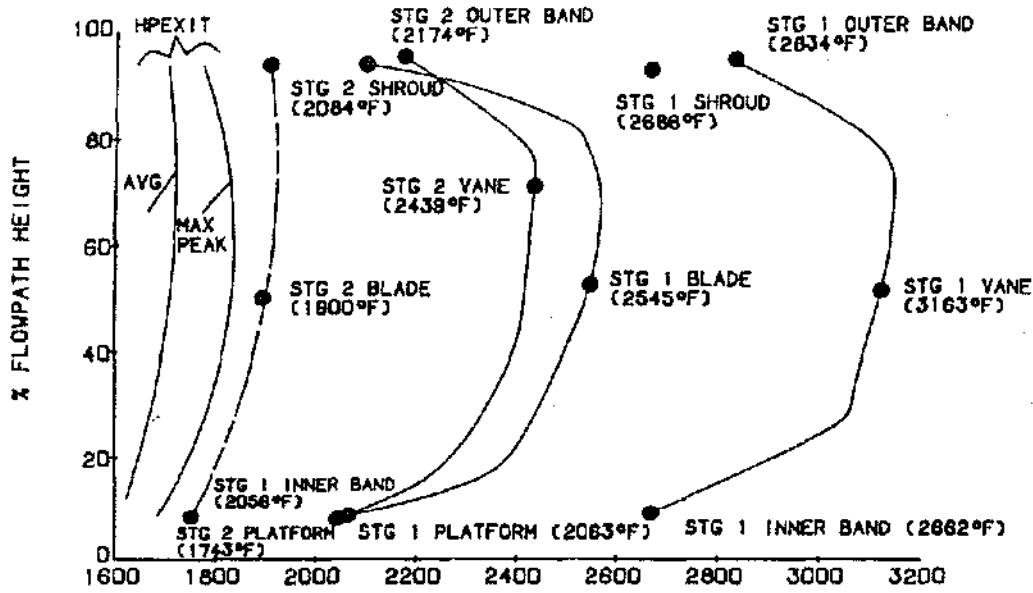


KEYNAME	ENGINE	MODEL	COMPON'T	DISCIPL.	CONFIG.	REGION	ID
INPUT	DEMO	USAF	HPT	AERO	I	BLADE1	13

Figure 5.25 Results From GE Streamline Curvature Analysis For A Typical HPT Blade

122F DAY

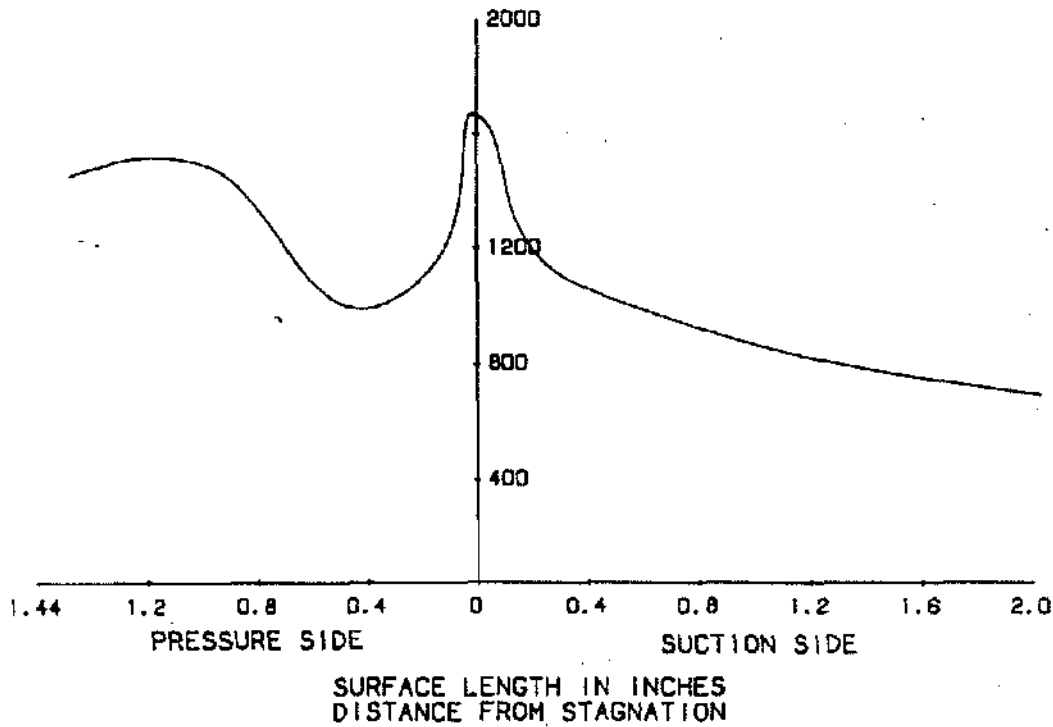
M = .3 SEA LEVEL T/O
 $T_{4.1} = 2590F$



T_{GAS} - TURBINE DESIGN GAS TEMPERATURE

HEAT TRANSFER DESIGN TEMPERATURE PROFILES (°F)
 FOR STATE-OF-THE-ART COMMERCIAL TWO STAGE HPT

Figure 5.26 T_{GAS} — Turbine Design Gas Temperature Heat Transfer Design Temperature Profiles (°F) for State-of-the-Art Commercial Two Stage HPT



CONVECTIVE HEAT TRANSFER COEFFICIENT, HG, FOR
 TYPICAL HPT BLADE (MID-HEIGHT)

Figure 5.27 Convective Heat Transfer Coefficient, HG, for Typical HPT Blade (Mid-Height)

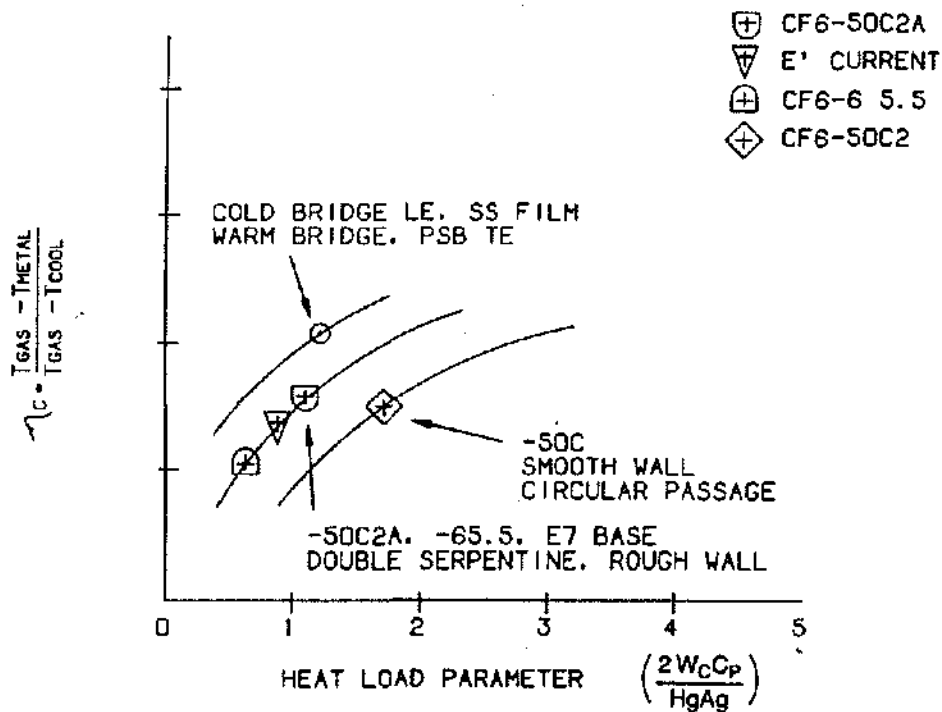


Figure 5.28 Cooling Effectiveness vs. HLP for HPT

TURBINE TESTING

Because of the elevated temperatures in modern gas turbine engines, instrumentation for performance verification is limited at best and often nonexistent. For this reason, reduced temperature turbine component testing is often carried out in special facilities in Evendale or Lynn to get detailed measurements not possible in an engine environment. Recall that a turbine can be run at reduced temperature as long as $\Delta h/T$ and N/\sqrt{T} are consistent with the corresponding engine point.

Figure 5.29 is a picture of the Evendale test facility. Figure 5.30 lists required measurements to get definitive performance data. Results from tests in these facilities have allowed GE turbine design engineers to refine details of turbine construction that impact performance and to develop design methodology and performance prediction techniques that would otherwise not have been possible.

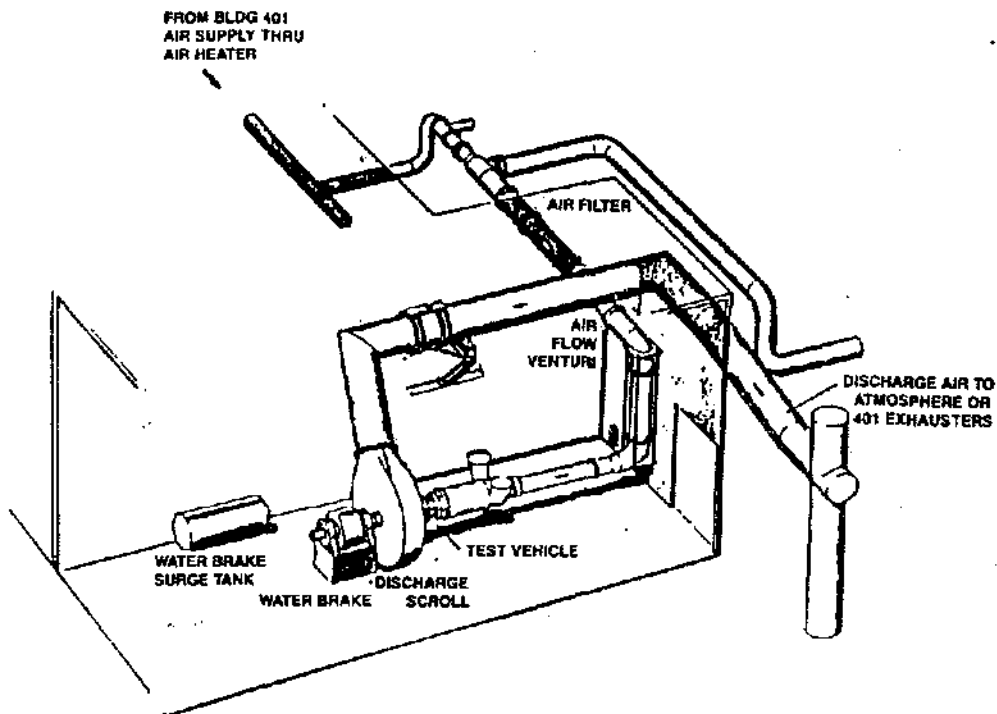


Figure 5.29 Air Turbine Test Facility Cell A7

PRIMARY TEST MEASUREMENTS

- Inlet
 - Flowrate (Choked Venturi)
 - Total Pressure (Frame Inlet or Traverse)
 - Total Temperature (Frame Inlet)
- Exit
 - Total Pressure (Arc Rakes and/or Traverse) To Calculate Isentropic Δh
 - Torque To Calculate Actual Δh
 - Total Temperature (Arc or Radial Rakes) To Check Torque
- Internal
 - Flowpath Inter-Stage Static Pressures To Calculate Reaction
- Cooled
 - Temperature, Pressure and Flow For Each Cooling Circuit

Figure 5.30 Measurements Required To Define Aerodynamic Performance of a Turbine Rig in Cell A7

TURBINE MECHANICAL DESIGN

INTRODUCTION

The high pressure (HP) turbine is usually separated into two components, one composed of static parts and the other of rotating parts. For purposes of this discussion the static component will be referred to as the high pressure turbine stator (HPTS) and rotating components as the high pressure rotor (HPTR).

Mechanically and aerodynamically those components compliment and support each other to extract work from the flowpath gas to efficiently provide an energy source for the HP compressor. This discussion will focus on the topics of the HP Turbine function, design considerations, typical operating conditions, description of major component parts and their role, and the mechanical design process. Towards the end of the chapter the low pressure turbine will be presented more briefly.

As you will soon see, the HP Turbine is an energy conversion machine that operates in a demanding environment which presents many design and manufacturing challenges.

HIGH PRESSURE TURBINE FUNCTION

A turbine is first and foremost an energy conversion machine. Energy stored in the gas flowing through the engine is converted to mechanical energy (horse power) delivered to the HP compressor. Therefore, the HP turbine structure must define the flowpath for gas to support this conversion process. Furthermore, the turbine must support engine loads which include weight, thrust, internal pressure and thermal stresses generated by the operating environment.

Turbine operating conditions are very severe, temperatures can become excessive and must be held to limits consistent with available material capabilities. This is achieved by providing secondary air flow to internal cavities. The turbine must be constructed to provide a conduit for these cooling secondary flows.

The turbine must also seal the engine internally to prevent the reservoir of high pressure compressor discharge air from dissipating internally. Gas flow must be confined to the flowpath for energy conversion purposes. Unfortunately, this sealing process is never perfect and so the turbine uses the resulting leakage as the source of secondary cooling air flow. The turbine structure is responsible for managing this leakage. Taking too much

flow, hurts engine efficiency. Not taking enough can adversely impact component life. Leakage control is achieved by placing limits on seal clearances between the static and rotating structures. Clearances can be controlled either actively or passively.

There are a variety of auxiliary HP turbine functions which dictate its final structural form. First, the combustor is nestled within the turbine and so ports must be provided for supplying fuel. Ports are also required for customer bleed air, so that passengers on the airframe can breathe air at pressures conducive to life. Occasionally, for maintenance purposes it is useful to be able to view engine hardware through ports provided for boroscope, a fiber optic device for looking into engine cavities. After satisfying these functional duties, the HP turbine must provide for its mechanical structural integrity.

DESIGN CONSIDERATIONS AND GOALS

The history of past experience and the lessons learned has shown that there are five major considerations in successfully designing HP turbines. These include performance and mechanical integrity, which are dictated by technical requirements. Performance is related to engine efficiency and is usually thought of as the ratio of fuel consumed to thrust generated, expressed as specific fuel consumption (SFC). The remaining three considerations are dictated by business need; the need to be competitive. These include weight, ease of assembly & maintenance, and cost/productibility.

The competitive aspects of turbine design begin with weight. Obviously, the lighter the better and the ratio of thrust to weight is a valuable reference. Today, the CFM56-5 engine delivers 25,000 pounds of thrust at a design weight under 5000 pounds for a thrust to weight ratio of around five. An engine that is easy to maintain and manufacture are clear factors in remaining competitive and profitable in today's aggressive business environment. Without these five engine requirements being satisfied, failure follows quickly.

Four of these requirements become fairly well understood in a relatively short period of time. After designing, building, and operating a relatively few engines it is possible to quantify parameters relating to performance, weight, maintenance, and cost. Given their importance, ongoing programs refining and improving these competitive requirement assure a non-eroding competitive position in the market place.

The requirement of mechanical integrity has both short and long term aspects. Short term factors include being able to hold up to limit loads of overspeed, maximum thrust, overtemperatures, tolerance for foreign object damage (FOD), and high cycle fatigue life associated with known engine unbalances and other excitations. Achievement of these requirements is demonstrated during factory engine development programs.

Another short term factor is dust tolerance. A jet engine can be thought of as a giant vacuum cleaner. Air contains dust, dirt, and other materials held in suspension. These materials must be purged and not accumulated, since collecting such stuff generates both mechanical or efficiency related problems. Again, during the factory development program achievement of this requirement can be accomplished.

The toughest requirements to satisfy with total confidence are the longer term issues. Problems that can show up after hundreds, maybe thousands, of engines are manufactured, sold, and in operating services. These are a mechanical designers nightmare. One such problem is component fatigue and rupture life. HP turbine components must withstand the highest speed, pressure,

and temperature the engine has to offer. This environment can cause turbine components to deform destroying performance, and if unchecked can lead to rupture and component/engine disfunction. Repeated engine usage (e.g. each aircraft flight) causes cyclic application of stress and temperature to all engine parts. The HP turbine experiences the greatest range of stress and temperature of all engine components and can fail from low cycle fatigue. The bursting of casings and disks involve safety issues as well as expense and loss of credibility with customers. Such occurrences must be avoided at all costs.

TURBINE OPERATING CONDITIONS

The operating conditions for HP turbines are severe. Since operating conditions vary from engine to engine, the CFM56-5 will be used as a representative illustration. This HP turbine is a single stage component and is shown in Figure 5.31. Major flowpath parameters are displayed in Table 5.2. Examples of internal cavity temperatures and pressures used to cool turbine blades, nozzles, rotor structure, and provide control of clearances are given in Table 5.3.

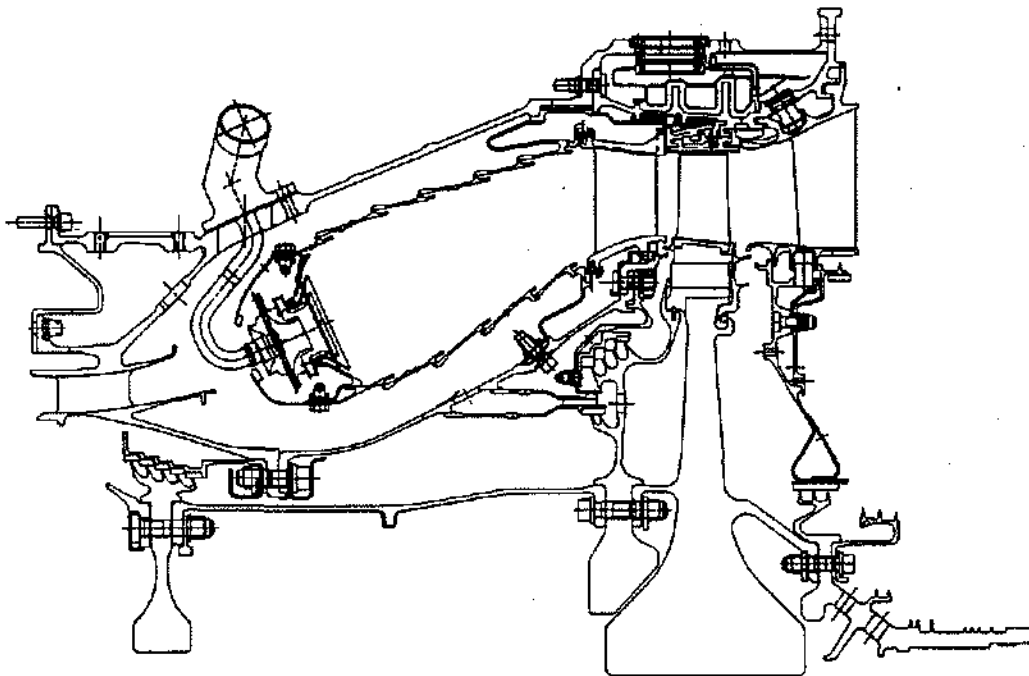


Figure 5.31 HP Turbine Rotor and Stator

PARAMETER	VALUE	COMMENTS
CORE SPEED (N2)	15183 RPM	REDLINE
COMBUSTOR EXIT (T4) TEMPERATURE	2750°F	
TURBINE INLET (T41) TEMPERATURE	2580°F	REDLINE
TURBINE EXIT (T42) TEMPERATURE	1800°F	
COMPRESSOR EXIT (P3) PRESSURE	400 PSI	REDLINE
TURBINE EXIT (P42) PRESSURE	100 PSI	

Table 5.2 CFM56-5 Flowpath Parameters

CIRCUIT	PARAMETER VALUES
BLADE COOLING TEMPERATURE PRESSURE	1000°F 200°PSIA
BORE COOLING TEMPERATURE PRESSURE	350°F 30°PSIA
ROTOR CAVITY PURGE TEMPERATURE	1350°F
TURBINE CLEARANCE CONTROL TEMPERATURE	300-900°F

Table 5.3 Major Secondary Flow Parameters

To relate these conditions to metal stress and temperature consider the following items. A HP turbine blade weighs 145 grams or .32 pounds held in your hand. When spinning at redline speed this blade effectively weighs 29,250 pounds. Now, 80 blades make one set, and so the HP turbine disk is holding in place a set of HP blade weighing 2,340,000 pounds. In turn the mechanical component of disk stresses due to blade weight and spinning disk are,

Web Stress
Hoop 60 KSI
Radial 130 KSI

Bore Stress
Hoop 130 KSI

The HP turbine blade has a bulk average temperature of 1700°F and an average centrifugal root stress of 36 KSI. While this is not the whole story for either disk or blade stress it gives some idea of how operating conditions translate into component stresses.

HIGH PRESSURE STATOR COMPONENT PARTS

The HP turbine stator is composed of many parts. However, it has five major components, including the HP combustor casing, the inner nozzle support and HP inducer, the HP nozzle, the HP turbine shroud, LP nozzle support and HP turbine clearance control, and static seals for compressor discharge pressure (CDP) and the forward outer seal (FOS). Each of these parts is an assembly of smaller parts, investment casting, weldments, or a combination of each.

For purposes of illustration our discussion will focus on a single stage HP turbine. An example of such a machine is found in the CFM56/F101 family of engines and will be used as a basis for our discussions.

HPT Combustor Casing The major load carrying stator component is the casing (Figure 5.32). It is bolted to the HP compressor and LP stators, forming a significant portion of the engine carcass. As a function of how the engine is mounted to the airframe, the carcass will carry uniform, bending, and a variety of self-equilibrating

loads. The casing is also a pressure vessel that contains the pressurized air supplied by the HP compressor (P3).

The casing is surrounded by air at various temperature and it supports various engine components, each having their own operating temperature. Therefore it has a thermal distribution which varies in time and produces a significant portion of the casings stress field. Clearly the bulk stress field at location varies with time and is composed of mechanical and thermal components. The casing is manufactured as a weldment composed of investment castings. Due to the need for moving bleed air and engine fuel through the casing wall, the casing has many embossed holes interrupting its load carrying shell. These embossments provide local stiffening for the shell and reduce concentrated stresses which accumulate around holes.

Inner Nozzle Support and Inducer As its name suggests this component (Figure 5.33) supports the HP nozzle as well as the inducer, combustor, and two static seals which provide pressure balance for the rotor thrust bearing. It is bolted to the HPT casing, nozzle, and the combustor.

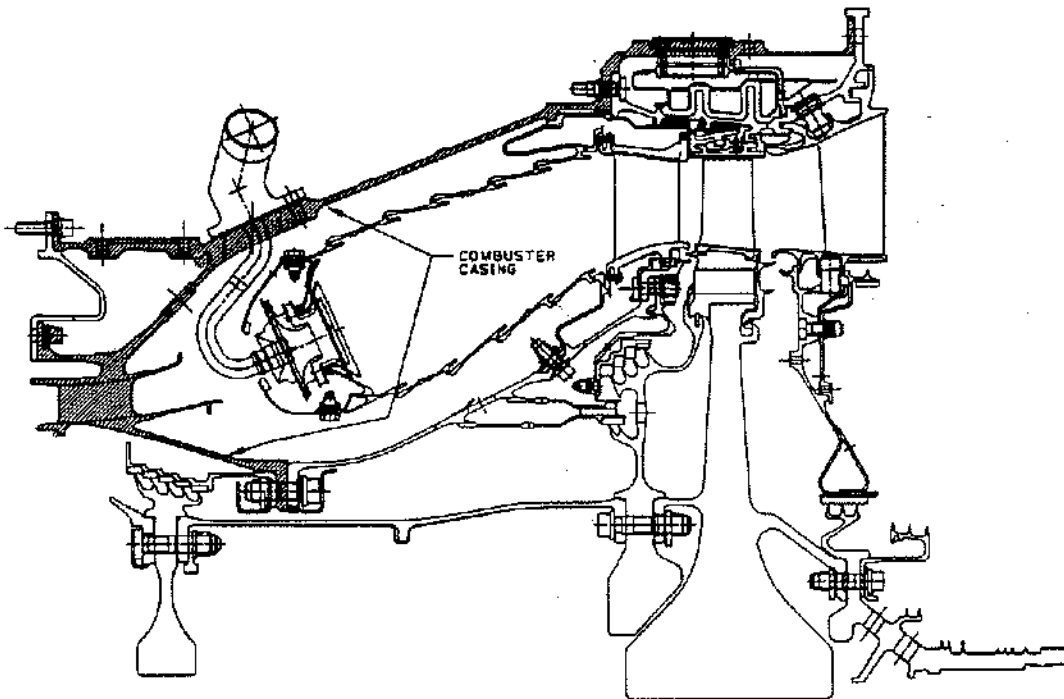


Figure 5.32 HP Combustor Casing

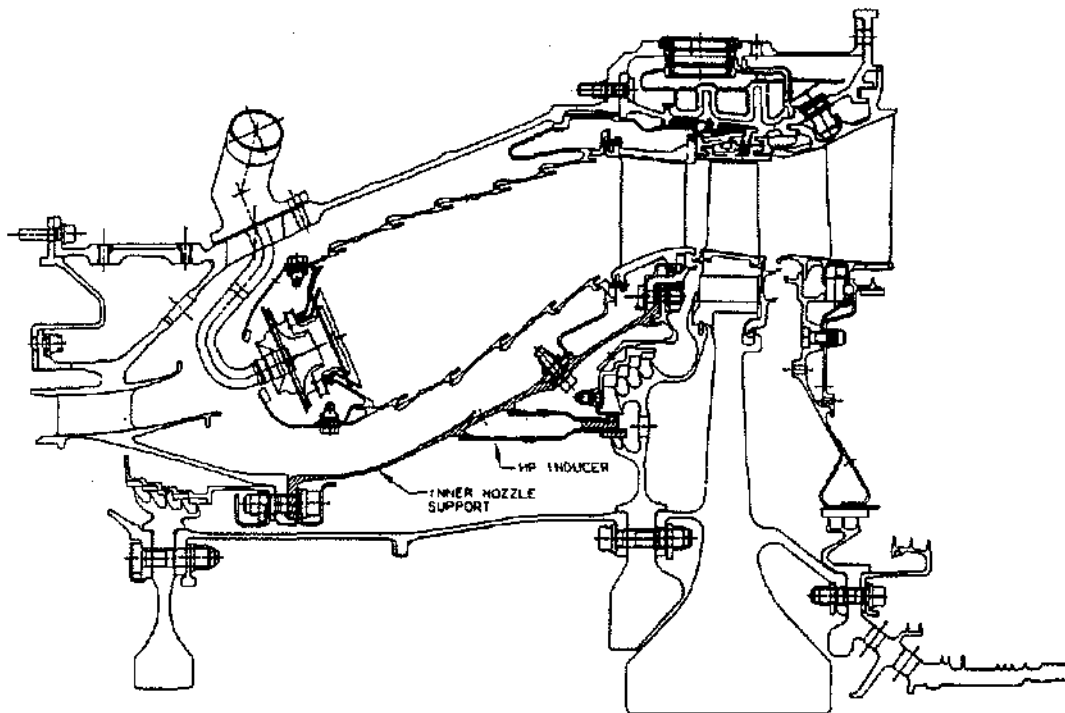


Figure 5.33 Inner Nozzle Support and HP Inducer

Like the HPT combustor casing, this component experiences mechanical and thermal loading which varies transiently with engine operation. The inducer is a device which supplies HPT blade cooling air to the rotating turbine structure. (see Figure 5.37). This component turns the axial flow of blade cooling air in a circumferential direction, accelerating it to meet the rotating structure. This induced circumferential motion reduces the temperature of the air relative to the rotor and improves its cooling capacity.

HP Nozzle The HP nozzle (Figure 5.34) receives the active flowpath gas stream at the combustor exit temperature of 2750°F and approximately the compressor discharge pressure of 400 PSIA. Simply, its function is to turn the gas stream accelerating it to meet the spinning rotor. While all this is happening it just sits there and takes the heat. Current materials technology require that the nozzle be a hollow structure to facilitate internal cooling air. Cooling air is bled from the combustor cavity at 1100°F to cool this structure. It has a bulk average temperature of 1700°F.

The nozzle is an investment casting made from high-strength and high temperature nickel based alloys. The

aerodynamic design of this component determines the degree of turbine reaction which has major impact on turbine performance. The radial relationship between the nozzle and turbine blade also has major impact on performance. If the gas stream sees major steps or cliffs which disrupt its smooth flow, the energy conversion process loses efficiency. The mechanical designer must position the cold as-assembled components so that when deformations from speed, pressure, and temperature move both the rotor and stator they finally end up in the correct relationship.

HP Turbine Shroud The HP turbine shroud and the HP blade (Figure 5.35) form the portion of the flowpath where gas stream internal energy is converted to horsepower. If shrouding does not fit tightly to the HP blade tip, gas can go over the blade tip and escape without sharing its energy with the rotor. This loss of efficiency has caused mechanical designers to dream up all kinds of tricks to minimize this gap.

A major part of this problem arises from transient and steady state positioning of the HP blade. As a function of changing engine speed and temperatures, deformation of the HP disk varies the blades position in the flowpath. To

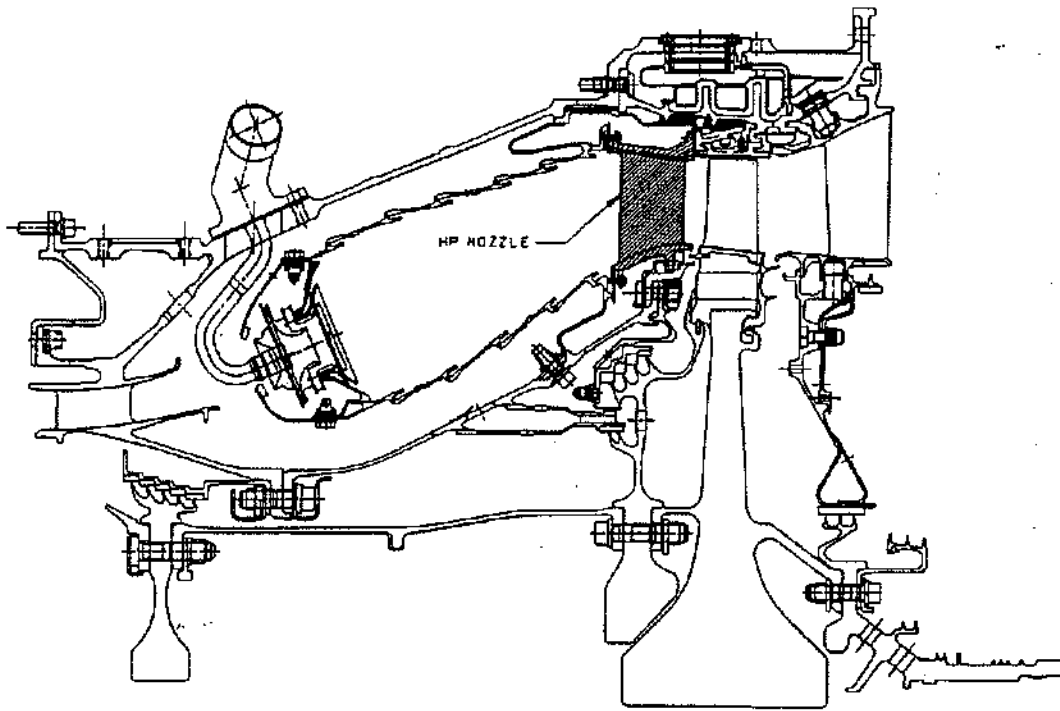


Figure 5.34 HP Nozzle

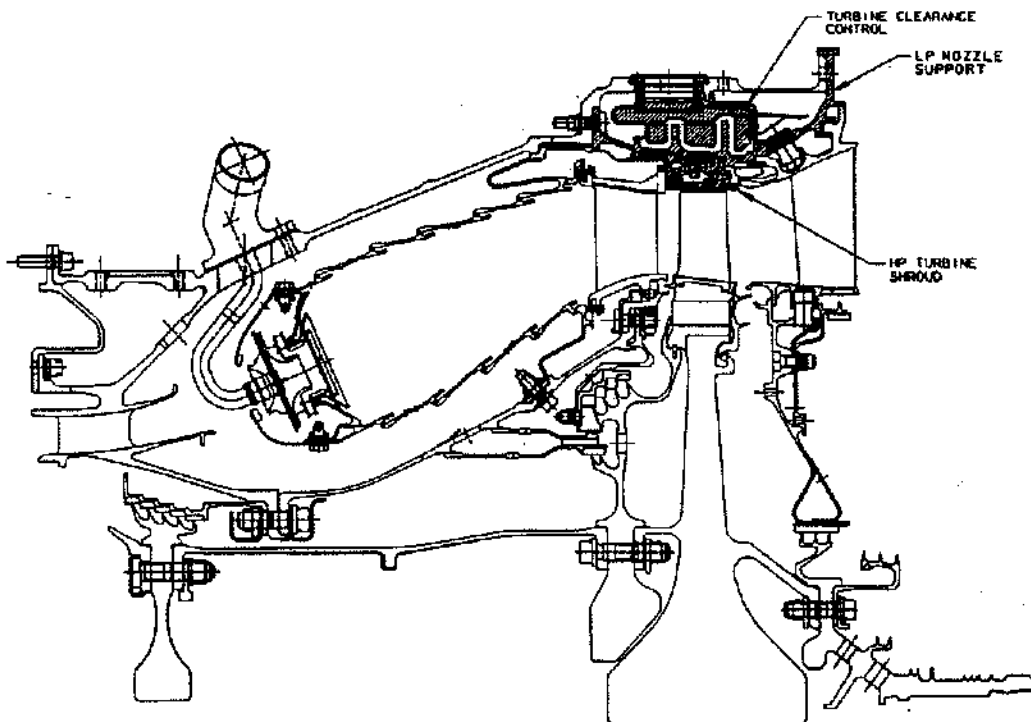


Figure 5.35 HP Turbine Shroud, LP Nozzle Support and Turbine Clearance Control

match this variation the engine control meters compressor bleed air which is piped to the HP shroud, (Figure 5.37). Alternate heating and cooling cause the shroud support structure to expand and contract to meet changing rotor deflections and thereby improve turbine efficiency. This process is called active turbine clearance control (TCC). Typical bleed air temperatures are given in Table 5.2.

Static Seals Bolted to the inner nozzle support are two cantilever static structures which provide sealing for internal turbine cavities (Figure 5.36). The forward inner seal (CDP seal) keeps the compressor discharge air from by-passing the combustor flowpath. Seal leakage is then introduced to another larger cavity which is also sealed. This second seal is called the forward outer seal (FOS) and its purpose is to hinder the leakage air from finding its way back to the flowpath. However, this is not a perfect seal, its leakage purges the cavity immediately forward of the HP blade-disk. Without this purge, flowpath gases would be ingested into this rotor cavity. Rotor materials are no match for flowpath temperatures and this purge is critical to successful operation of the highly stressed rotor structure. This is an example of competing requirements. Performance goals demand a stop to all leakage, mechanical goals demand that flowpath cavities

be purged to protect the rotor. Actually, the engine performance usually tells the designer how to manage this critical leakage/purge problem. The diameter of both these seals is critical in determining pressure balance and the magnitude of axial thrust load supported by the rotor thrust bearing.

HP ROTOR COMPONENT PARTS

The HP rotor is composed of seven components which are either disks, shafts, blades and blade retainers shown in Figure 5.37. They form an integral structure which is subject to large centrifugal loads and have large thermal gradients. All of this translates into stress fields which can be the source of low cycle fatigue. Great care is exercised in designing these component because their failure can lead to disastrous consequences. Rotor components, excluding the blade, are machined from nickel based forging having high tensile and fatigue strength capability. While the HP blade is a casting made of high temperature/strength nickel based alloys. Functionally, the rotor positions the HP blade in the flowpath and transmits torque and axial load to the compressor and forward axial thrust bearing.

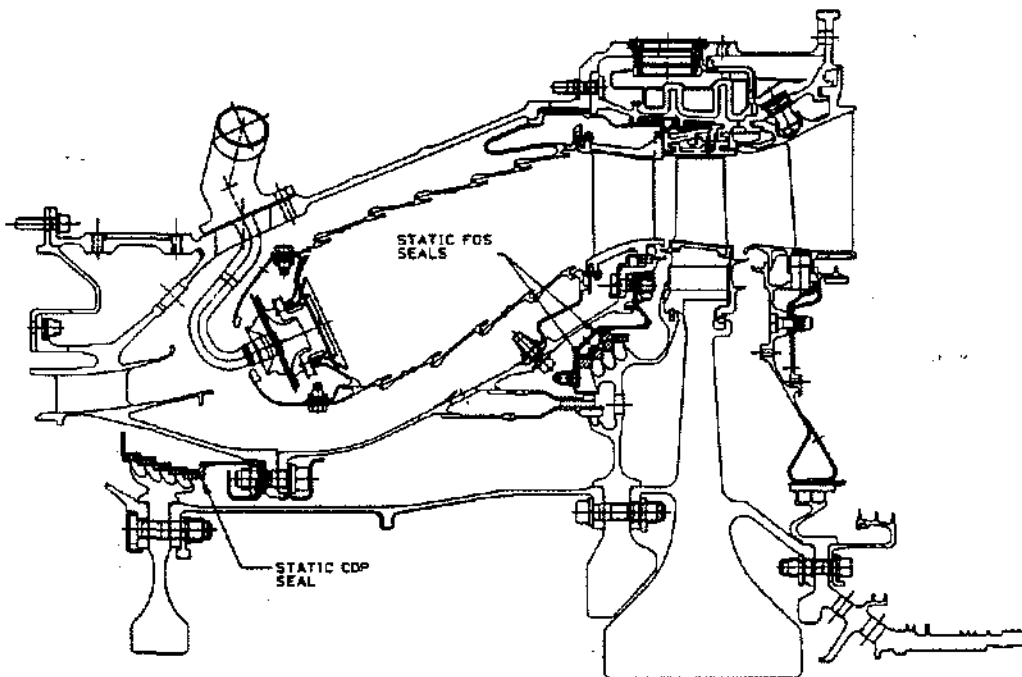


Figure 5.36 Static CDP and FOS Seals

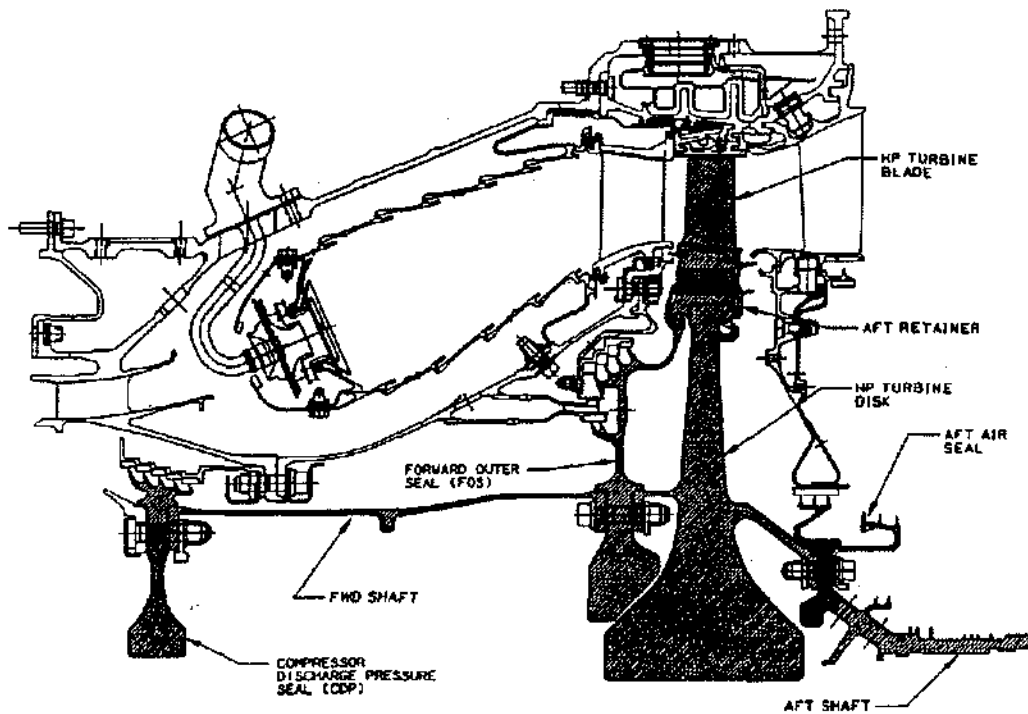


Figure 5.37 HP Turbine Motor

Compressor Discharge Seal (CDP) Disk This component is sized to provide a seal for compressor discharge air as discussed earlier. A disk is required to support the rotating seal head and to keep the concentrated stresses in the bolted flange to levels low enough to avoid low cycle fatigue. Another factor in the size and proportion of this disk is to keep critical rotor vibratory frequencies out of the range of operating speeds.

Forward Shaft The purpose of this shaft is to provide a torque and axial load carrying structural member between the HP disk and HP compressor. Again this component is proportioned to avoid critical rotor vibratory modes and low cycle fatigue.

Forward Outer Seal (FOS) Disk and Retainer The rotor disk is relatively complex as disks go. As with the CDP seal disk, it provides support for the second (outer) cavity sealing head, sometimes called the "four tooth seal".

Cantilevered off of the seal head is a flexible arm supporting the forward blade retainer. This structure provides assurance that the HP blades will not move forward in the flowpath. The retainer portion of this

structure is rabbeted to the HP disk. Rabbeted construction has three basic purposes. It provides additional radial support as the FOS arm could not withstand bending stresses associated with centrifugal loads. Secondly, this construction assures that rotor parts do not shift under heavy centrifugal loads. Shifting would destroy the impeccable balancing of these high speed components. Imbalance associated with shifting of rotor parts would cause heavy one per rev vibratory loads, generate excessive seal leakages, and could generate high cycle fatigue. Finally, rabbeted construction provides a seal for the blade cooling circuit. Blade cooling air would be dumped into the FOS cavity without this seal (see Figure 5.38). Besides being a performance loss, without the cooling air the HP blade would overheat and rupture.

The web of the FOS disk has holes placed slightly below the inducer center line. These holes permit the inducer to pressurize the blade cooling circuit. Remember the inducer accelerates the blade cooling air to meet these rotating holes and thereby expanding (cooling) the air. Since the air is now moving at wheel speed it can get on board the rotor without heat being generated through windage. This is a double benefit: less drag on the rotor (more efficiency) and increased cooling capacity for the

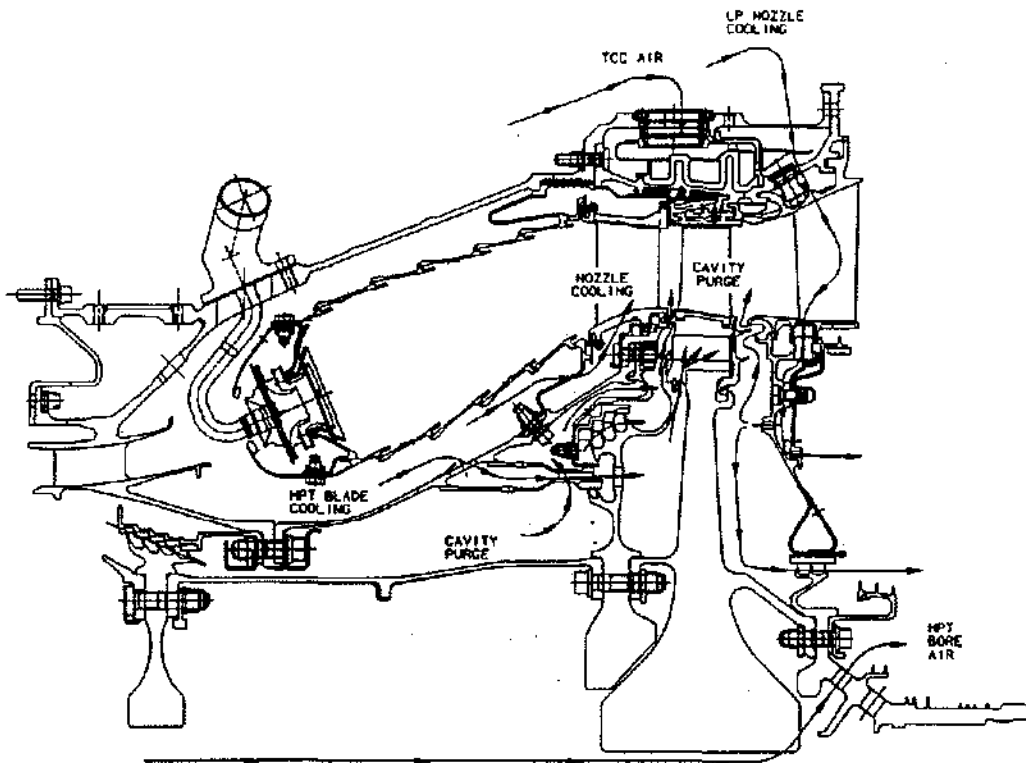


Figure 5.38 Secondary Air Flow

HP blade. Placing these holes below the center line of the inducer helps keep dust out of the blade cooling circuit. The air can turn the corner and the dust if it is heavy enough will be centrifuged back to the flowpath.

Radially, inboard of the inducer holes, is a two tooth seal which prevents blade cooling air from leaking into the CDP cavity or hot CDP cavity air from leaking into the blade cooling circuit as a function of pressure gradients.

The FOS disk bolts to the HP disk and forward shaft. The complex shape of the FOS disk can result in unnecessary thermo-mechanical bending stresses. When these features are carefully positioned with respect to each other these stresses can be minimized. This is called "stacking the disk". A full understanding of the time varying thermal gradients and mechanical loading is the key to successfully "stacking the disk".

HP Disk This component supports the blade dead load (over 2 million pounds), along with the radial rabbet loads from the forward and aft retainers. The HP blades are held by a two tanged fir tree arrangement shown in Figure 5.39. The large radial blade load and disk mechanical and thermal stress result in a very large bore

hoop stress. This stress is reduced by increasing the bore width (see Figure 5.37). Disk flange arms facilitate bolting other shafts and disks to the HP disk. Again this disk is proportioned to avoid critical vibratory modes in the engine operating speed range.

Aft Retainer This component is rabbeted to the HP disk and is charged with providing an axial stop for the HP blade. It also provides sealing for the HP blade cooling circuit. When forward and aft retainers seal properly, the blade cooling circuit is pressurized by the inducer and the hollow HP blade is convectively cooled.

Aft Shaft This rotating structural member provides support for the HP rotor as its journal houses a radial bearing. The shaft also meters the bore cooling circuit. Shaft holes permit bore cooling air to leave the HP rotor and pass on to the LP rotor, (see Figure 5.38). As with the CDP and FOS disks, this shaft has seal teeth which interact with the static and rotating low pressure (LP) turbine, thereby sealing HP and LP secondary flows from each other. Again, this component is proportioned to avoid critical rotor vibratory modes in the operating speed range.

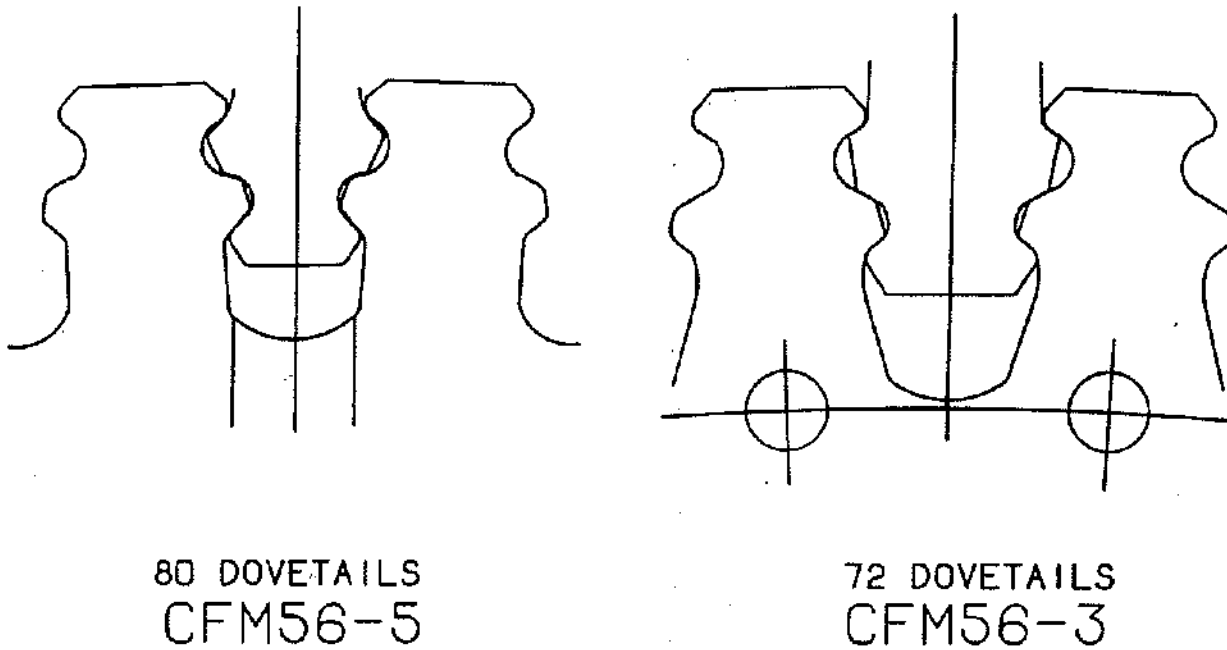


Figure 5.39 Comparison Between CFM56-3 and CFM56-5 Dovetails

HP Blade The HP turbine has eighty hollow cast turbine blades. The internal passages have been designed to provide for an efficiently cooled turbine airfoil. These circuits are shown in Figure 5.40. Convection is the prime heat transfer mechanism. After the cooling air speeds through the blade passages, it is returned to the flowpath gas stream through small holes in the airfoil and tip cap.

Air exiting the airfoil forms a thin film of air around the blade to minimize disruption to gas streamlines and to shield the external blade surface from hot flowpath gases. Thin trailing edges and gas path stagnation at blade leading edges cause these locations to be the hottest. Airfoil holes are usually placed in these locations with design intent being to minimize airfoil thermal gradients.

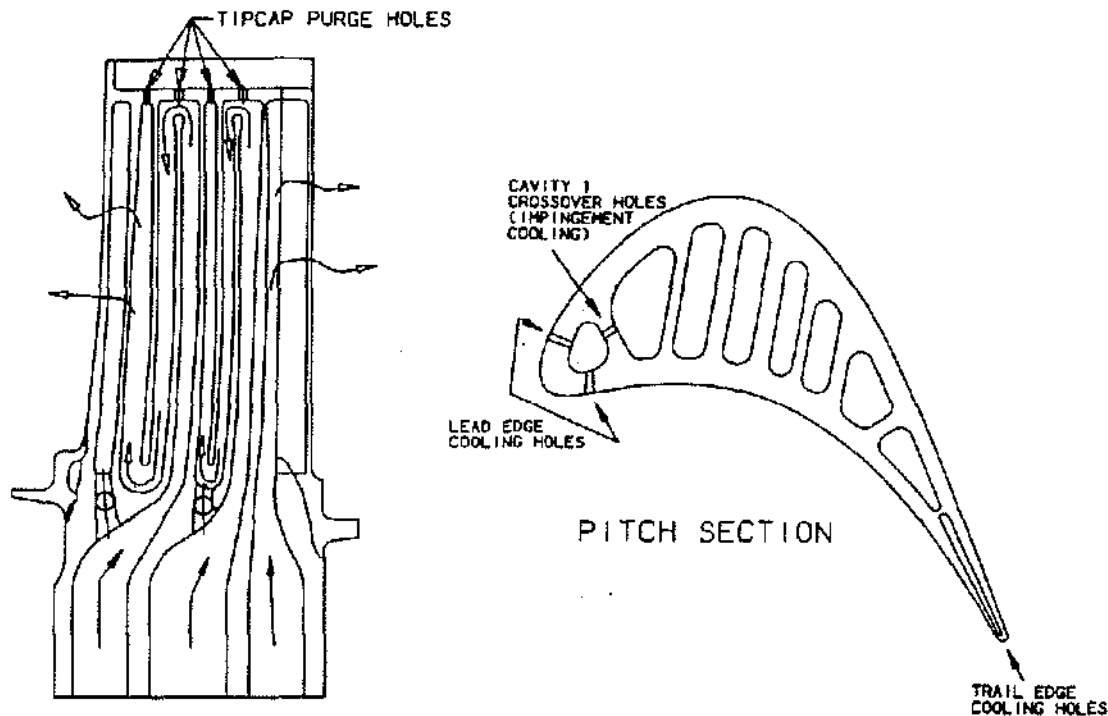
There are three functions for the air exiting the blade tip. The first function is to cool the tip cap, the second is to purge internal blade circuitry and reduce internal pressure loss, and thirdly it purges the blade of dust. If dust accumulates in blade cooling passages or blades cooling holes the result will be a hot blade and rupture/fatigue.

The blade, like the turbine disk, must be stacked carefully to reduce bending stresses caused by gas path pressures and centrifugal loads. The aggressive thermal environment can even cause tough blade alloys to oxidize or corrode away so the blade receives a CODEP coating to protect parent blade metal.

THE MECHANICAL DESIGN PROCESS

The design of HP turbines is a challenging problem, that has very little margin for error. Complex thermomechanical stresses generated in engine operation can produce failure in meeting design goals and sometimes actual engine disfunction. The road to a successful design is attention to detail. Over looked items usually lead to serious problems.

While the dream of every turbine designer is a clean sheet of paper, the reality is a nightmare of deciding where to start. Then, there are seemingly endless iterations of refinement and discovering how to compromise the conflicting design goals and constraints of weight, performance, and durability.



3 CIRCUIT HPT BLADE COOLING

Figure 5.40 Cooling Circuitry for CFM56-5 HPT Blade

While flowpath hardware (nozzles and blades), as well as stator and rotor hardware each have their own particular design problems. They also have similarities. To illustrate the process let us focus on the rotor to get a sense of how a mechanical design evolves.

An overview of design and development includes the following activities:

- Basic design concept
- Preliminary sizing
- Engineering drawings
- Working the details
- Component and engine testing, and
- Final certification or qualification analyses

All designs rely on four critical items, teamwork, experience, demonstration, and verification. A turbine mechanical designer is a conductor of a large orchestra composed of specialist in areas like:

- Cycles and performance
- Aerodynamics
- Secondary flow

- Heat transfer
- Materials application
- Drafting
- Testing
- Computer methods
- Stress and vibration analysis, and Manufacturing

The designer must meld the design inputs and constraints from each of these areas into a harmonious result.

Experience is found in a variety of places technical specialists, other mechanical designers, GE design practices, reviews held by the Chief Engineer's office, and individual designer's own personal reservoir of knowledge and insight. No matter how strong the designer's knowledge and insight is, it will be insufficient to producing a viable design. Experience in applying engineering principles will result in a sound design concept, only when all resources are utilized in a detailed fashion.

A design concept can be refined and verified through repeated modeling and analysis. This is an integral portion of design verification. Application of design analysis

methods tempered by lessons learned is also a powerful cost effective method for accumulating and applying actual design experience. Final demonstration of all designs is achieved through component and engine testing. The engine always processes a level of wisdom that humbles the best thought out designs.

The Basic Design Systems engineering has prime responsibility for the total engine system meeting its requirements. Their relationships with cycles, performance, aerodynamics, and mechanical design specialists gives broad form to the engine and its requirements. Key items here are:

- Number of turbine stages
- Flowpath dimensions
- Aerodynamic shapes for the nozzle and blade
- Numbers of nozzles and blades
- Engine speed and thermodynamic parameters, and
- Locations of frames and bearings

Once the size and performance parameters of the HP turbine are established by systems engineering the mechanical design process can begin.

Preliminary Design The core engine rotor structure is usually supported at its extremes by bearings, one of which is an axial thrust bearing, (Figure 5.41). For the CFM56/F101 family of engines the forward bearing supporting the HPC rotor, is the axial thrust bearing. This bearing supports the net axial load on the core rotor. The sources of this load are HPC and HPT blade loading and internal pressures acting on the rotor structure. This bearing is also the reference point for axial growth of the rotor, an important factor in establishing rotor seal design. With the inputs provided by Systems Engineering, the mechanical designer begins discussions with Systems, Secondary Flow, Heat Transfer, Bearings Design and Performance specialists to define the secondary flow aspects of the turbine structure. Fundamental engine issues are being settled here. Major issues include:

How much bleed air will be used to cool and purge each rotor-stator cavity and the HP turbine blade?

Where will the bleed air be extracted?

How will the bleed air be reintroduced to the engine flowpath?

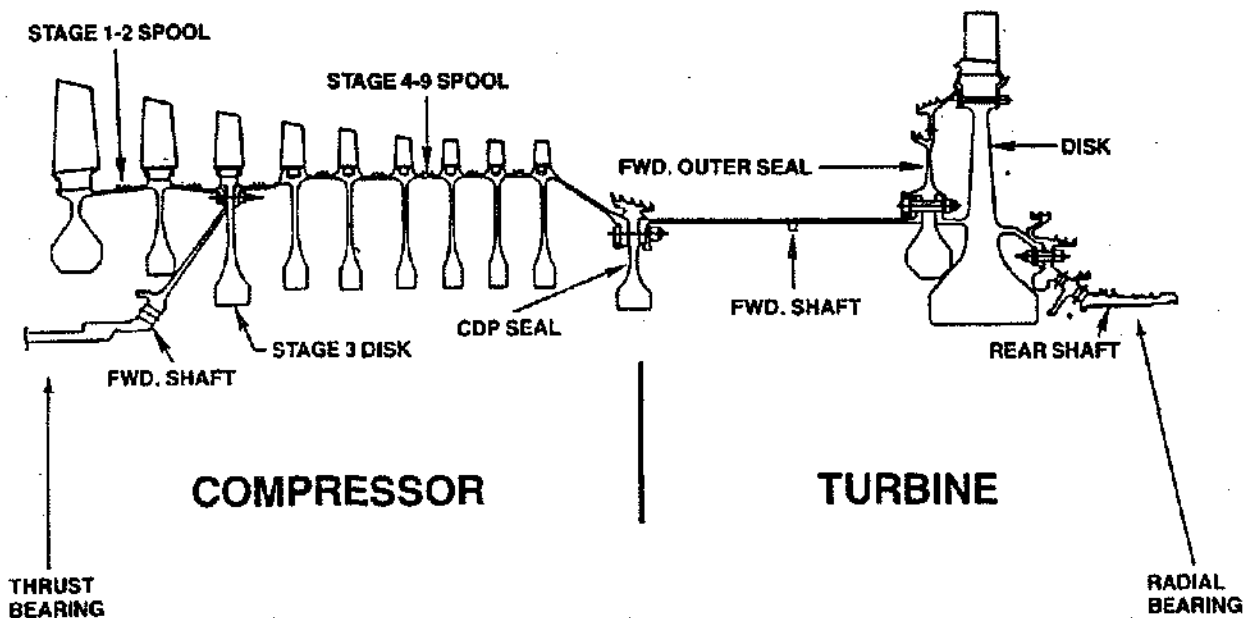


Figure 5.41 CFM56-3 High Pressure Rotor Bearing Support

Given the above, what is the impact on engine performance?

How can engine performance be improved?

What will be the diameter of the compressor discharge and the pressure balance (forward outer) seals?

Is the resultant axial load within the bounds adequate for bearing life?

Does this secondary flow system present insurmountable mechanical problems?

Resolving these fundamental issues requires creative thought, evaluation of many alternative concepts through an iterative process, and then arriving at a design based on mutual compromise.

During this process, estimates of internal cavity flows, pressures and temperature are made by secondary flow specialists. The heat transfer specialists estimate metal temperature distributions for generic acceleration from steady state idle to steady state takeoff and a deceleration back to idle.

With these estimates and engine speed (a thermodynamic parameter) the mechanical designer begins to size the various turbine rotor disks. Disks are usually required to support rotating seal heads and large dead loads like those created by the rotating turbine blades. The designer must assure that each disk has adequate overspeed margin to its burst speed, and then estimate radial and axial deflections for rotating seal heads as well as the HP turbine blade. These displacements when compared to deflection estimates made by those designers responsible for the HP stator provide insight to potential seal clearances. These clearances usually require the secondary flow analysis to be repeated, and so on until the rotor-stator interaction is understood and secondary flow and performance constraints are satisfactorily met. This process requires many months of work until the final design concept is worked out.

Engineering Drawings During this early period the mechanical designer will work out associated details relative to sizing shafts and bolting issues. In sizing each HP turbine component the designer must also assure that adequate materials are selected for each component, operating bulk temperature and stress distributions are kept to levels consistent with creep, rupture, and low cycle fatigue life requirements, disk and rotor vibratory modes are kept outside the engine operation range, and drafting

is generating engineering drawings to support technical work.

An early milestone is the material release drawing for forgings and castings. Lead time for these items can be from six months for forgings to one year for castings and must be allowed to achieve the overall engine schedule. Experience, intuition, and engineering estimates are used to provide detail component definition for fillets, hole size, and other features which can result in significant level of concentrated stress.

After much design work and discussion, involving design and design analysis reviews with the Chief Engineer's office and other experienced mechanical designers, the final engineering drawings are released for each component. Again, timing is important due to manufacturing lead time. A sufficient period is required for tooling, gaging, and machining. Typical process requirements are from three to six months.

Working the Details From the release of engineering drawings to the first chips made cutting the initial turbine components, a time period is provided for detailed design analysis of the HP turbine rotor. Early in the engine program, Systems Engineering has defined a design flight cycle or cycles for engine wide application (Figure 5.42 and Table 5.4). This operating cycle is a generic description of revenue service engine usage. It is used by design and component systems specialists to establish the transient and steady state turbine operating environment. Rotor heat transfer specialists construct a transient heat transfer model of the rotor (Figure 5.43). The resulting transient metal thermal distribution shown in Figure 5.44 is for the "end of takeoff" mission point. This model is based on steady state parameters determined by secondary flow specialists for the design flight cycle (Figure 5.45).

Mechanical Design specialists then generate a structural rotor model (Figure 5.46) composed of shells, rings, and two dimensional finite element members. Transient thermal distributions are then input to the rotor model for approximately 100 time points of interest. This structural model provides basic understanding of bulk stress behavior of the rotor with time (Figure 5.47).

To determine levels of concentrated stress around fillets, holes, slot bottoms, and complex non-symmetric rotor features more detailed models are required. Now, two and three dimensional finite element models are generated to fully describe component geometries and predict correct values of concentrated stresses. Shown in Figure 5.48 is the bolted joint where the forward shaft and

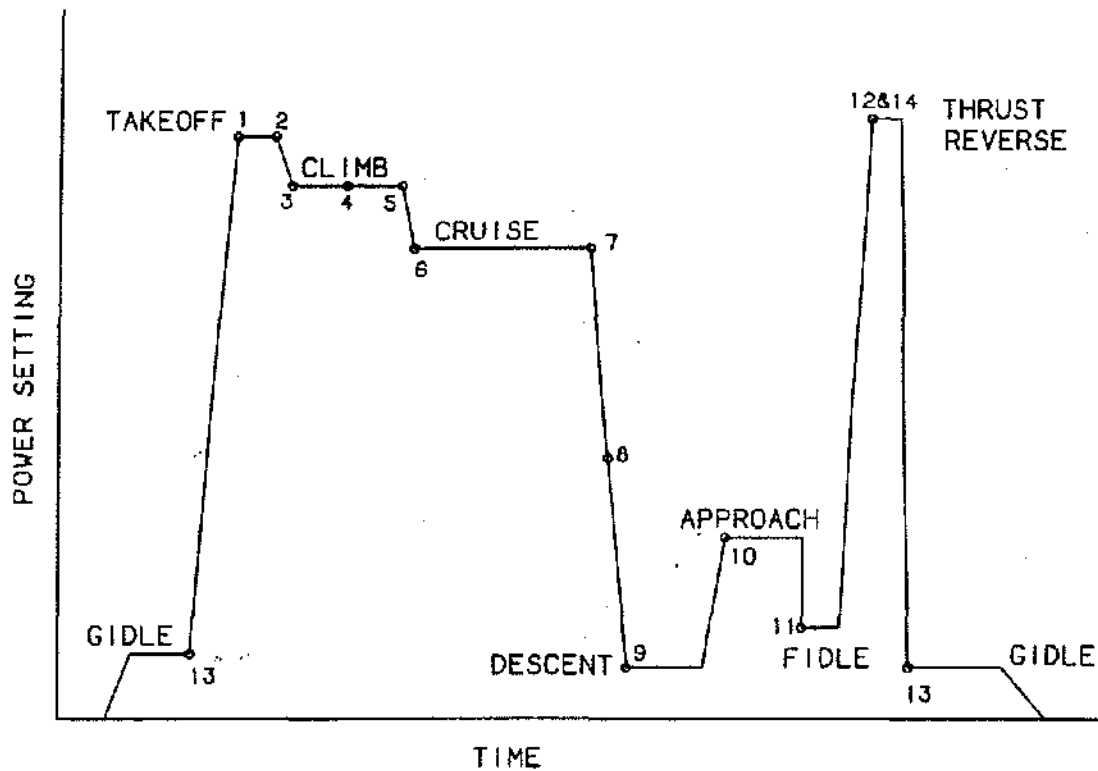


Figure 5.42 CFM56-5 Design Flight Cycle Profile and Points

POWER	ALTITUDE (FEET)	MACH NO.	L/M/N/O* DTAMB (°F)	INTERVALS OF TIME (MIN)
TAKE-OFF	0	.35	-9/11/27/66	1.39
END TAKE-OFF	1500	.40	-9/11/27/66	
CLIMB	10000	.61	10/15/20/40	20.0
	20000	.733	10/15/20/40	
	30000	.850	10/15/20/40	
CRUISE	30000	.850	10/15/20/40	19.24
DESCENT	30000	.859	10/15/20/40	14.0
	20000	.733	10/15/20/40	
	10000	.610	10/15/20/40	
APPROACH	5000	.3	10/15/20/40	5.0
FIDLE	0	.2	-9/11/27/66	0.11
THRUST REVERSE	0	.2	-9/11/27/66	0.26
GIDLE	0	0	-9/11/27/66	5.0

* RELATED TO STD DAY (59°F)

Table 5.4 CFM56-5 Aircraft Altitude, Speed, and Time Intervals

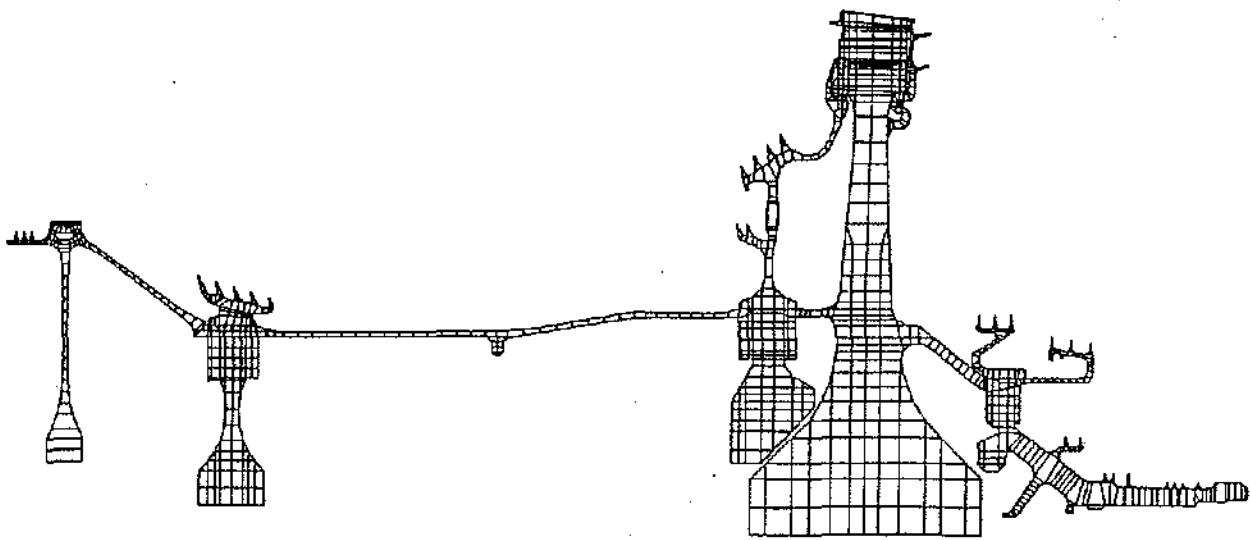


Figure 5.43 CFM56-5 HPT Rotor Heat Transfer Model

HEAT TRANSFER ANALYSIS AT END OF TAKE-OFF

NODAL TEMP
 0 250.
 . 400.
 . 550.
 . 700.
 . 850.
 . 1000.
 . 1150.
 . 1300.

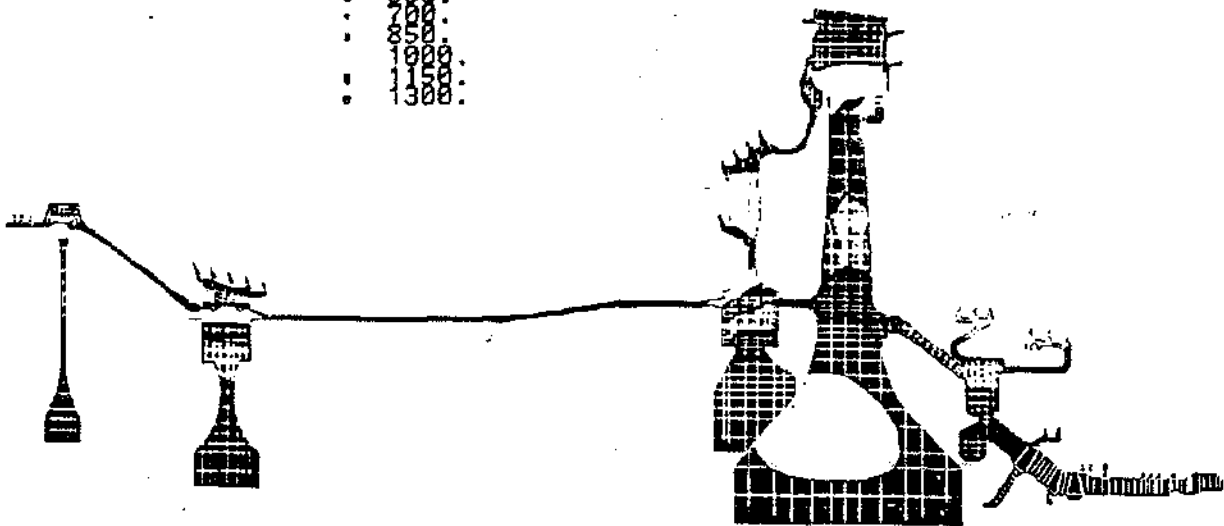


Figure 5.44 HPT Rotor Temperature Contour Plot

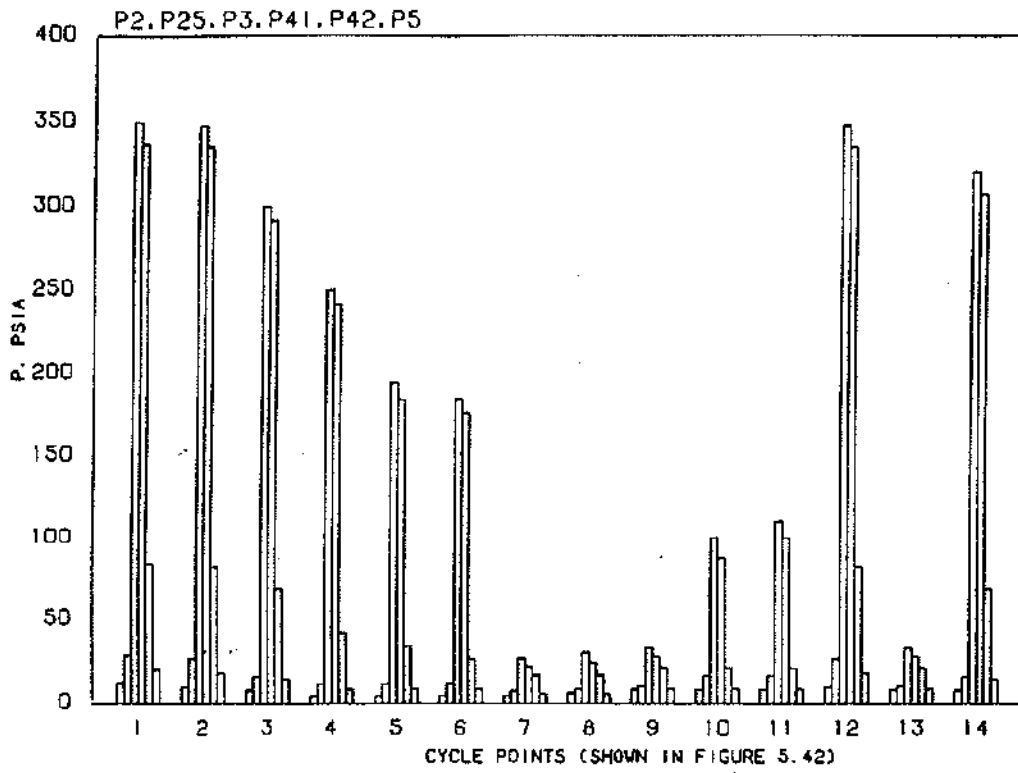


Figure 5.45 CFM56-5 Typical Cycle Pressures from Secondary Flow Models

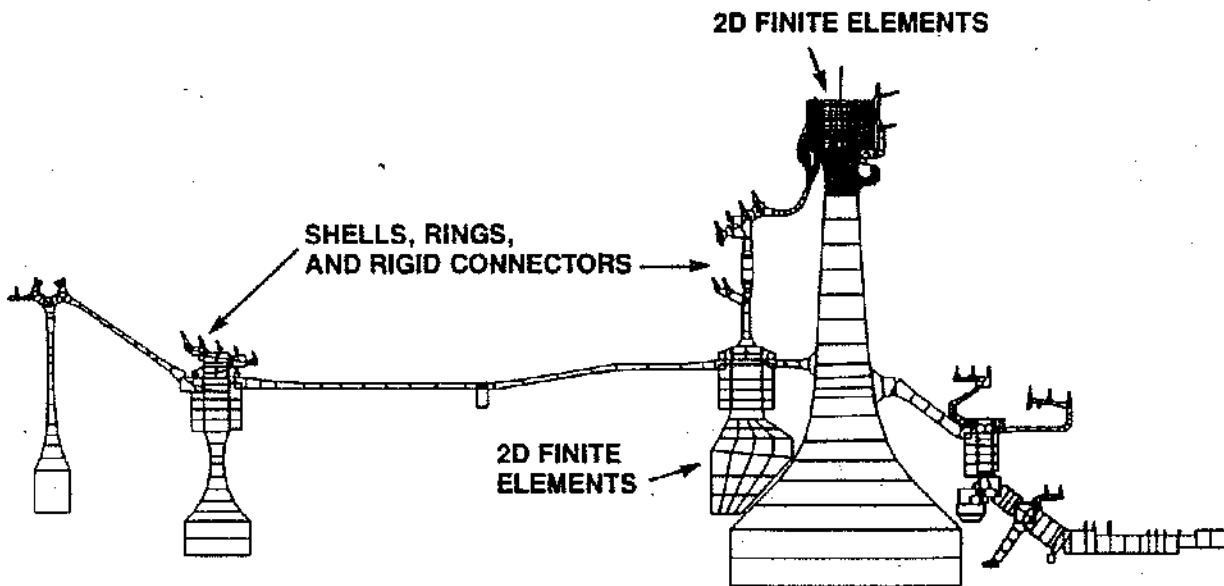


Figure 5.46 CFM56-5 HPT Rotor Structural Model

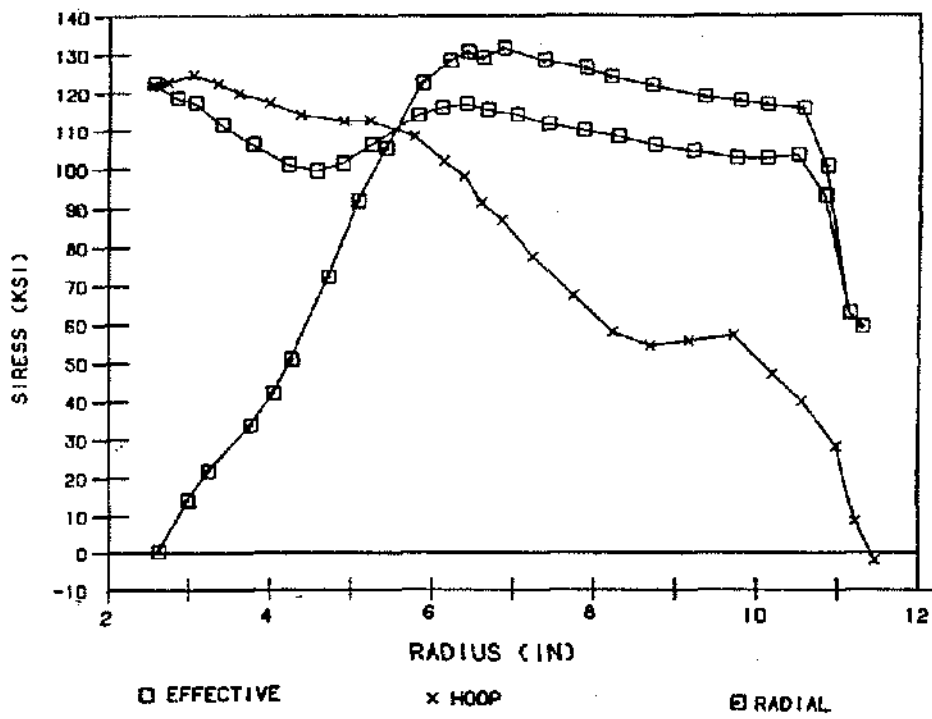


Figure 5.47 CFM56-5 HPT Disk Shell Stresses End of Takeoff

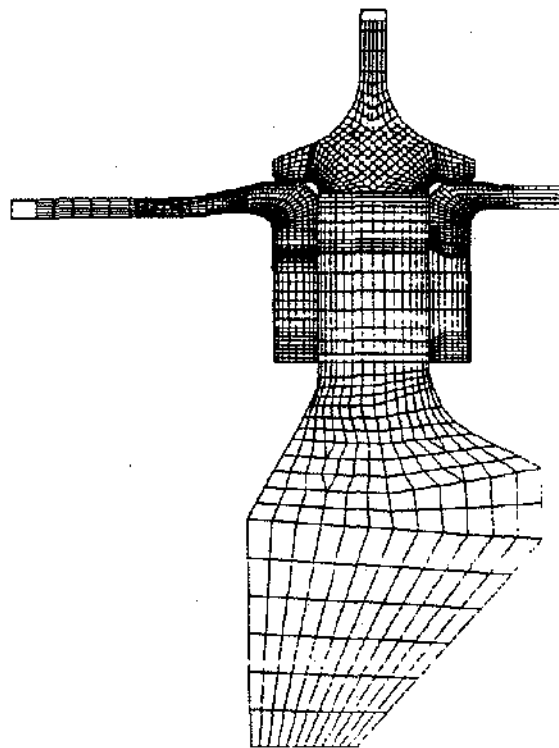


Figure 5.48 Finite Element Model of Joint Where Forward Shaft and Forward Outer Seal Are Bolted to the Forward Flange of the HPT Disk.

forward outer seal are bolted to the forward flange of the HPT disk. In Figure 5.49 a model of the shaped bolt hole in the forward outer seal is shown. Finally, the complex geometry of the HP turbine disk rim is analyzed via a three dimensional finite element model shown in Figure 5.50.

These are only a handful of analysis models used to confirm that design intent has been met. When problems are uncovered, design changes are made prior to hardware manufacture, so that factory test programs can proceed based on hardware configurations slated for production.

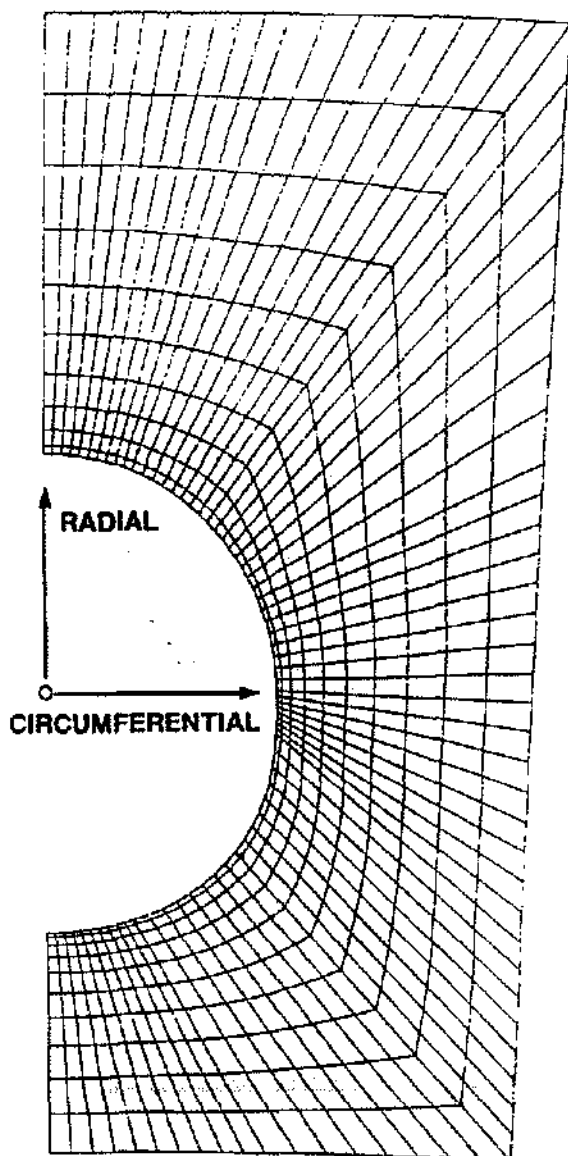


Figure 5.49 Model of Shaped Bolt Hole

Component and Factory Testing During the entire design process the mechanical designer utilizes testing wherever possible to demonstrate achievement, or provide assurance, of design intent being met. Two important kinds of testing illustrate this point. First, photoelastic testing, is used during preliminary and detailed design. It provides a tool for evaluating complex geometry features such as an HP turbine disk rim shown on Figures 5.51 and 5.52. This is a three dimensional photoelastic HP turbine disk with a variety of disk rim air slot and slot bottom geometries. This plastic model provided information to select the most optimum combinations of geometry and to validate stress analysis tools. A shortcoming of this kind of testing is that it only evaluates mechanical loading. However, it validates an analysis method, which is then applied to the full thermal and mechanical conditions.

Secondly, a factory engine test is run to verify the heat transfer model and its ability to predict transient and steady state thermal distributions. Hardware for this test is instrumented with air and metal thermocouples, cavity pressure gages, and metal strain gages. Strain gages are used to assure that the designer has successfully avoided critical rotor frequencies in the engines operating speed range. Figure 5.53 shows typical rotor thermocouples as well as predicted versus measured thermal response.

Completion of a certification or qualification program requires that engines must be demonstrated at a variety of severe conditions. These include ice and bird ingestion, "A" and "C" cycle endurance, fan blade out vibratory testing, and overtemperature testing at redline speed operation. This kind of engine testing uncovers problems for early resolution, verifies engineering models, and provides the ultimate evidence of an engine ready for customer utilization.

Final Certification Analysis Having fine tuned the HP turbine components based on comprehensive analysis work, further detailed design reviews, and factory engine verification testing, the analysis process begins again. As verification testing is completed, analysis models are updated and the mechanical designer then generates the stress, deflection, and life results that will be the basis for engine certification.

As the rotor mechanical designer is busy calculating temperatures, loads, deflections, stress, and life capability, the HP blade and stator designers are engaged in similar work. This process usually can be completed in a three year period. As the characteristics of the HP turbine are understood, they are presented to Systems Engineering so that the turbine can be integrated into an engine system.

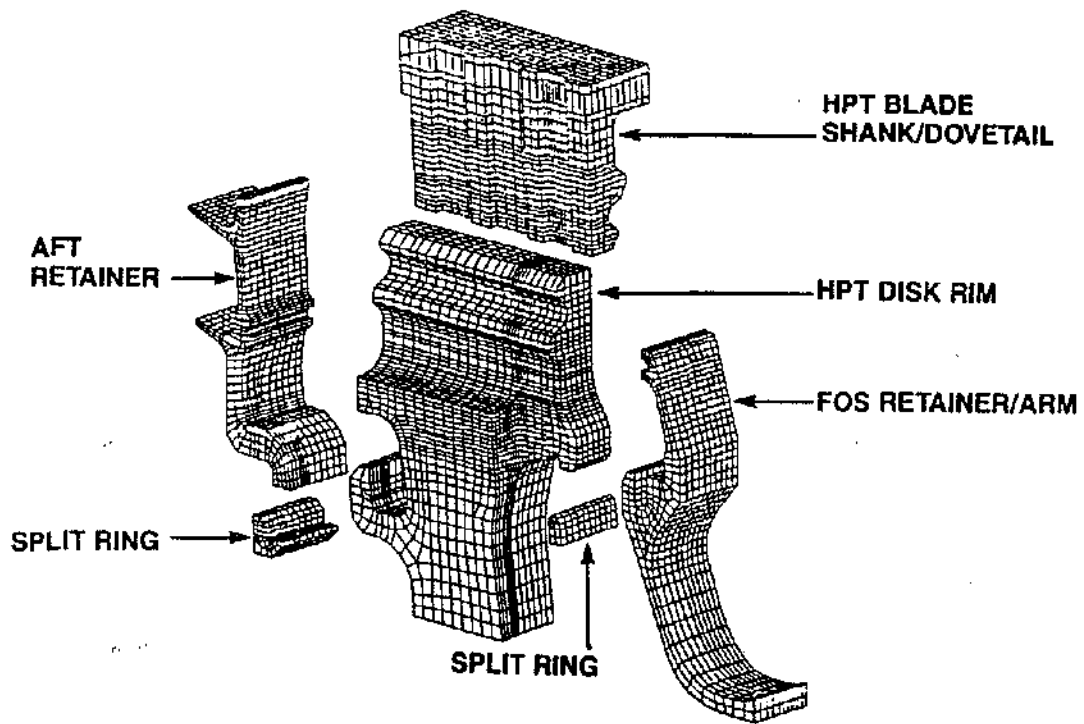


Figure 5.50. CFM56-5 HPT Disk Rim 3-D Model

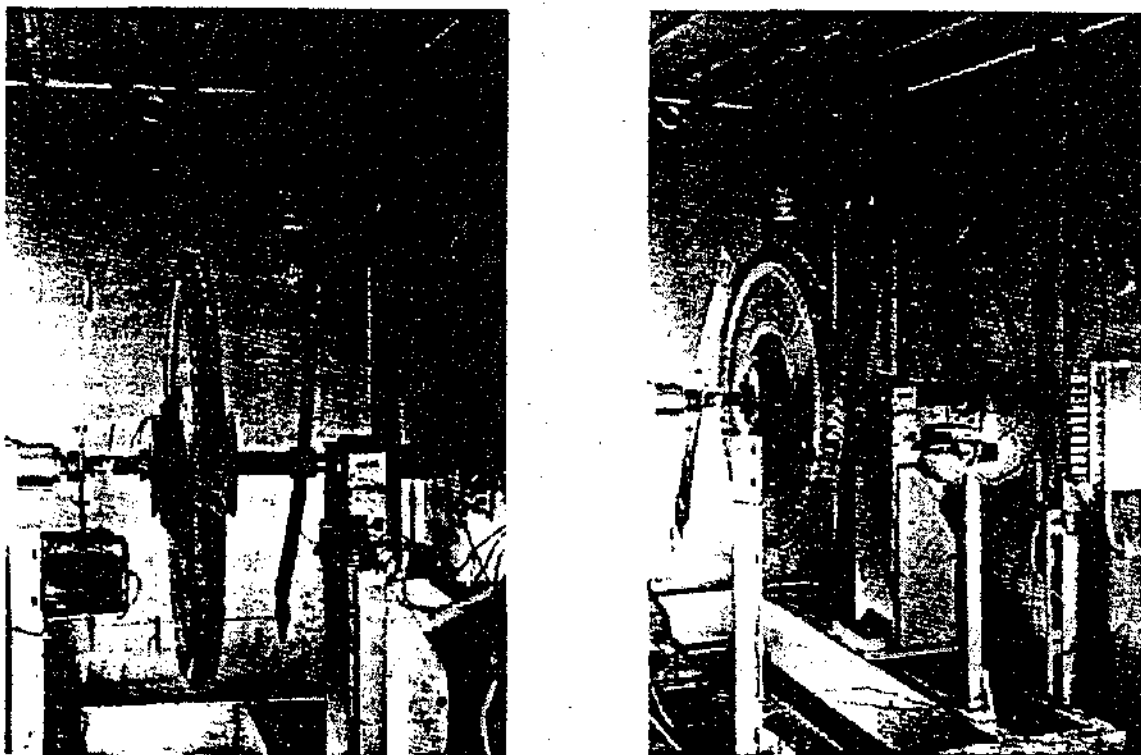
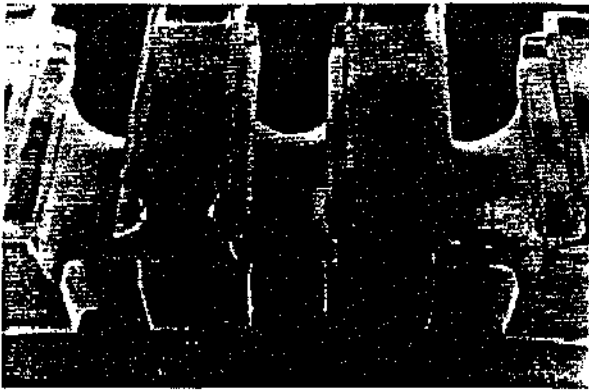
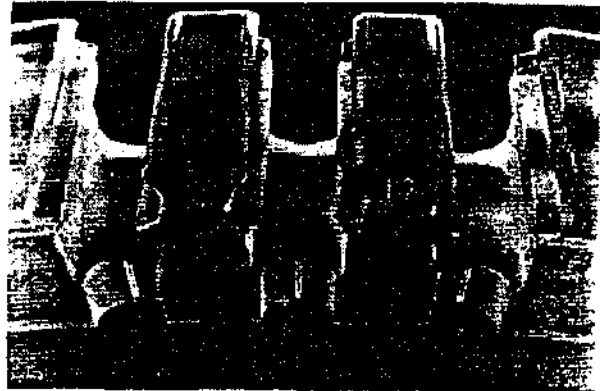


Figure 5.51 3D Full Scale HPT Disk Photoelastic Test



■ FLAT BOTTOM AIRSLOT WITH ROUND SLOT BOTTOM



● ROUND BOTTOM AIRSLOT WITH FLAT SLOT BOTTOM

Figure 5.52. Airslot/Dovetail Configurations

- HP TURBINE INSTRUMENTED ROTOR
- TOTAL OF 40 METAL AND 17 CAVITY THERMOCOUPLES

- PRESSURE GAGES
- ▲ METAL T/C TEMPERATURES
- △ AIR T/C TEMPERATURES

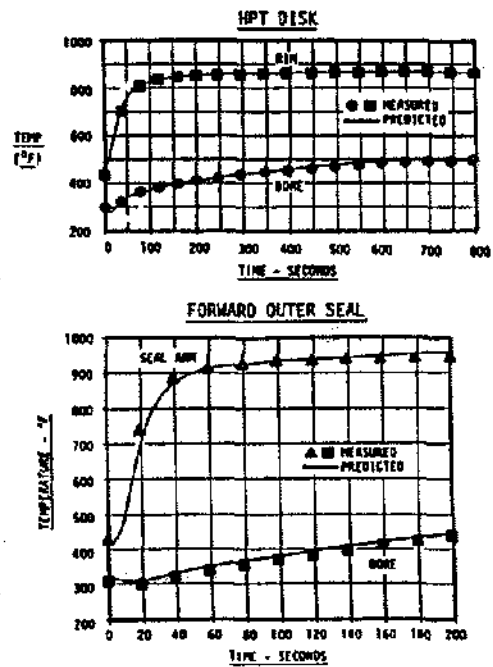
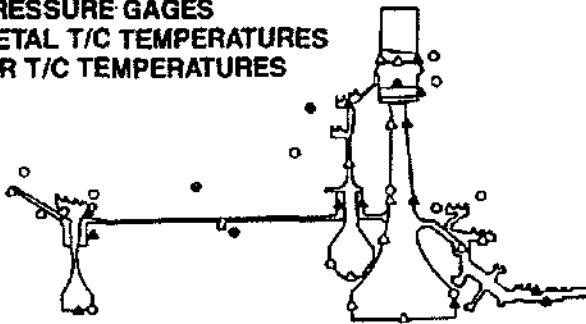


Figure 5.53 Heat Transfer Rotor Instrumentation and Engine Temperature Measurements vs Prediction

LOW PRESSURE TURBINE DESIGN

The function of the low pressure turbine is to extract energy from the flowpath gas, providing torque to drive the fan and booster. The torque is transmitted through the fan midshaft which runs through the center of the engine. At first glance, the mechanical design of low pressure turbine components seems easier than that of high pressure turbine components because operating speeds and temperatures are lower. However, since materials and component lives are essentially the same, low pressure turbine components operate at similar stress and temperature levels as high pressure turbine components.

Early in the design phase of the low pressure turbine, the flowpath shape, rotational speed, and number of turbine stages are determined. These decisions are based primarily on cost, weight, performance, and fatigue life trade studies.

A high performance LPT is characterized by multiple stages, high operating temperatures, and low stage loading (high rotational speed and/or large diameter) (see Table 5.5). Unfortunately, these characteristics are in conflict with the mechanical designer's constraints of low weight, low cost, and long life. The technical requirements assist the designer in achieving the right compromise for each engine program. The trend at GEAE in recent years has been towards higher stage loading with fewer stages.

ENGINE	NO. OF LP TURBINE STAGES
TF39	6
CF6-6	5
CF6-50	4
CF6-80A	4
CF6-80C	5

Table 5.5 Trends in number of LPT stages

LOW PRESSURE TURBINE ROTOR COMPONENTS

Most of GE's LPT rotor configurations are of similar design. A progression of refinements is evident when comparing one configuration to its predecessor. The CF6-80C2 represents GE's latest large commercial LPT design and will be used as an example of typical construction and features.

Figure 5.54 shows a cross-section of the CF6-80C2 Low Pressure Turbine. Figure 5.55 is an enlarged view of a typical stage (stator & rotor) illustrating several of the performance improvement features of the CF6-80C2 LPT.

Blades The CF6-80C blades are thin, high aspect ratio, tip shrouded blades. Unlike HPT blades, the LPT blades do not require internal cooling air, thus simplifying the mechanical attachment design. Interlocking tip shrouds are used to provide damping, and to form the outer band of the flowpath. On the outer periphery of the tip shroud are seal teeth which rub into the open cell honeycomb shrouds to reduce the amount of flowpath gas leaking past the airfoils. The blades attach to the disk by use of two tanged axial dovetails.

LPT Disks The primary function of the disks is to support the dead load of the blades. The large radial load imparted to the disk rim by the blades plus the rotational speed and temperature gradient in the disk determines the overall disk geometry.

Current LPT disk web thicknesses are generally no less than .1" thick. The TF39 LPT disks had webs sized at .060" and were subjected to manufacturing induced "oil canning" problems plus operational blade-disk vibratory problems.

The largest unconcentrated stresses in the disk generally occur at the bore. The lightest disk design will be one where the bore diameter is as low as possible. Geometrical, manufacturing, or assembly features generally dictate the practical limits of disk bore diameter. For example, the CF6-80C2 stage 1 disk bore is set at its current diameter to allow access to the stage 1-2 joint during the rotor balance operation. Figure 5.56 shows the stress and temperature distribution for a typical LPT disk.

On all of GE's commercial LPT rotors, the disks are bolted together at flanges located away from the disk web at the ends of the "spacer arms." Locating the bolt holes away from the structural portion of the disk, avoids potential stress concentrations in this region.

Interstage Seals The interstage seals on the CF6-80C2 LPT rotor are sandwiched between the LPT disk flanges. The forward stages each contain two seal teeth and serve to restrict gas flowpath air from bypassing the airfoils. These seals extend aft, and mate with the adjacent disk post to provide a passage for cooling air to the disk slot bottom and prevent the LPT blades from sliding forward out of the disk.

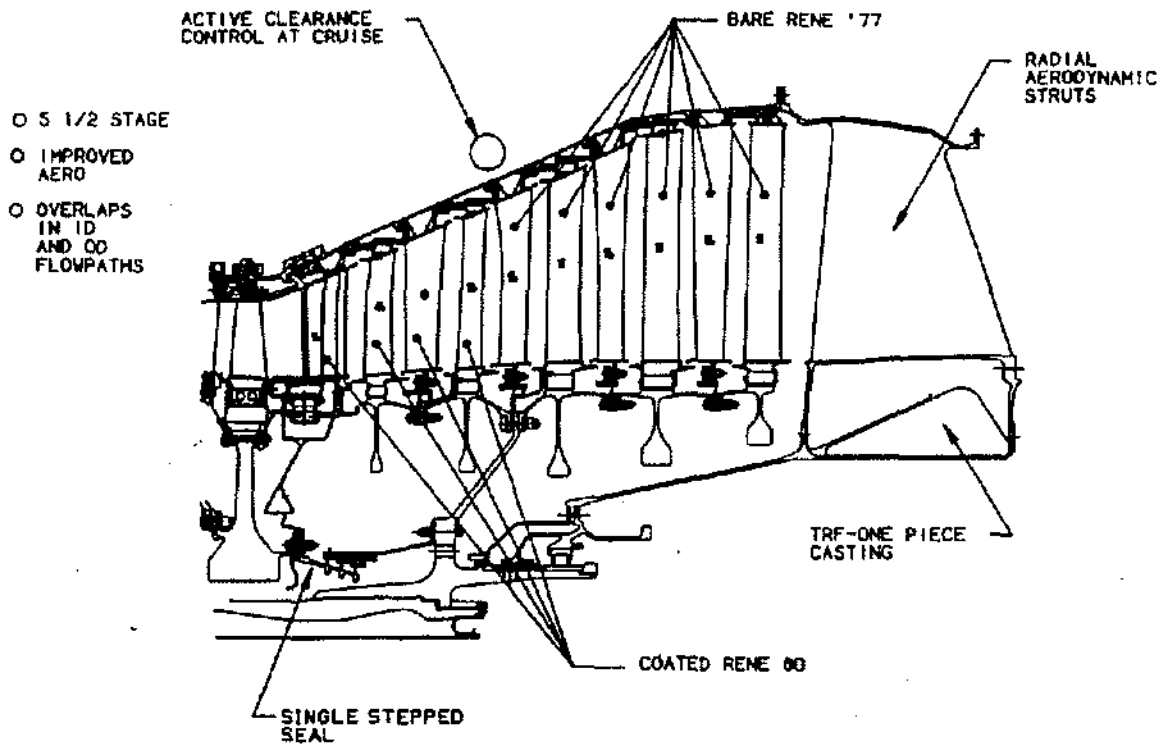


Figure 5.54 CF6-80C2 Low Pressure Turbine

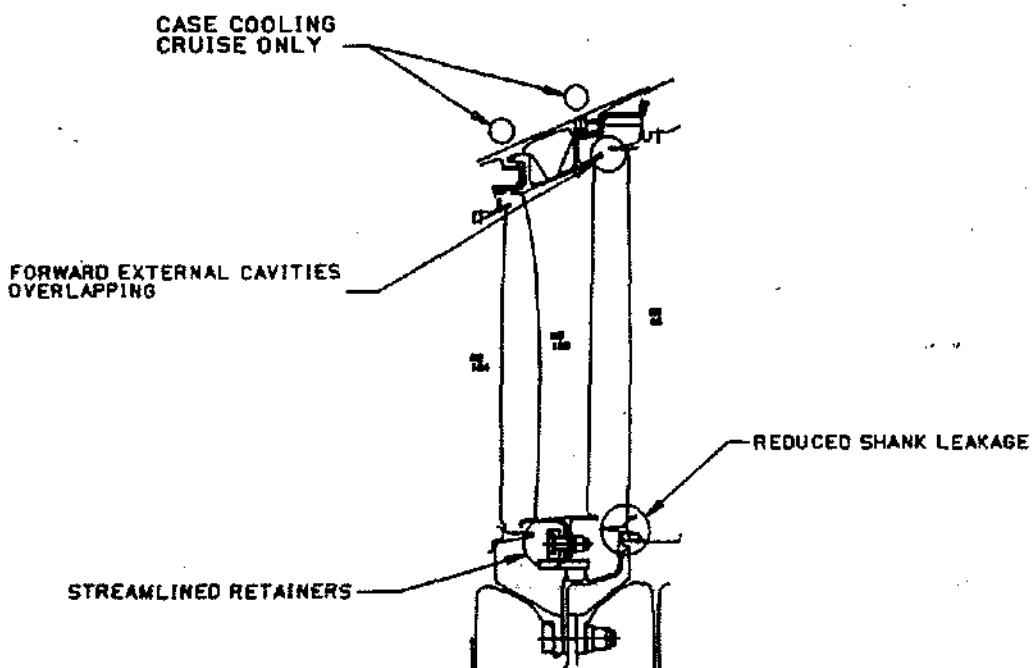


Figure 5.55 CF6-80C2 LPT-Typical Stage

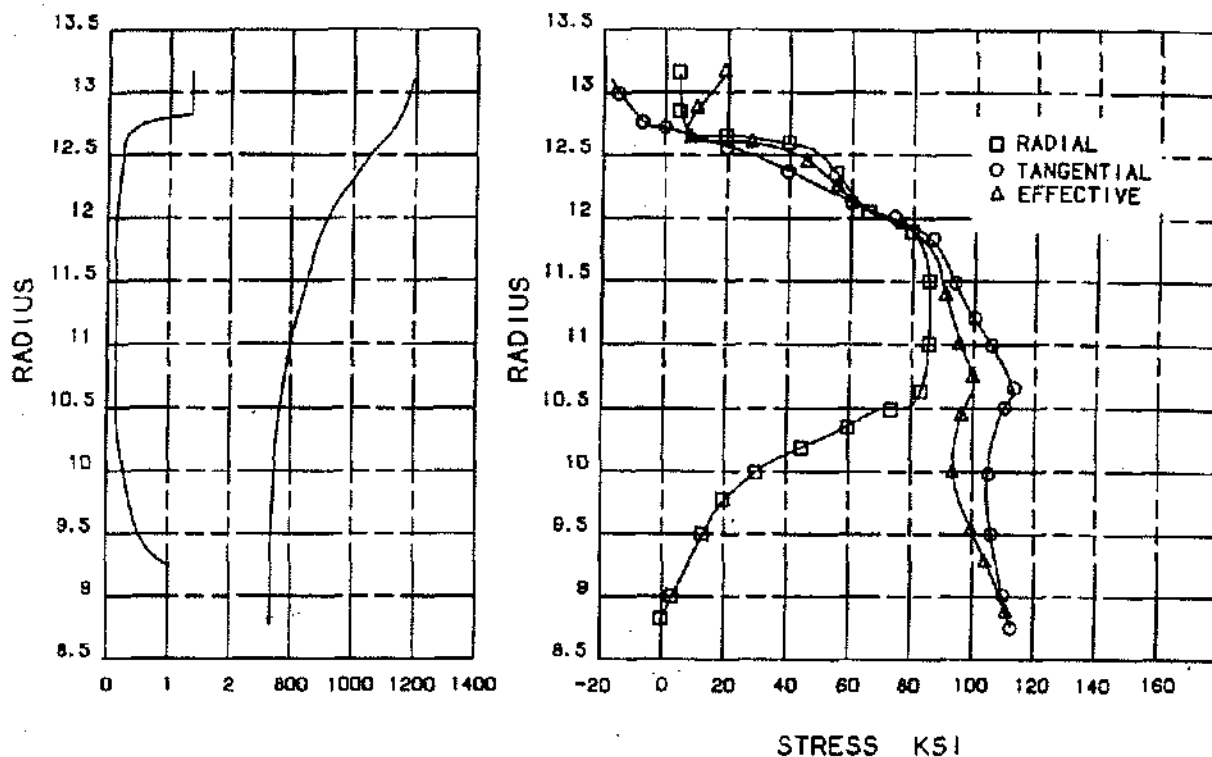


Figure 5.56 CF6-80C2 LPT Stage Three Disc Stresses

The aft interstage seals are one-tooth, sheet metal seals. Because flowpath gas temperatures are reduced in the aft stages, no cooling air is required for the disk slot bottoms. Single tooth sheet metal seals were chosen based on cost and weight benefits over the performance advantage of having two teeth.

Blade Retainers Most of GE's commercial LPT rotor blade retainers have been the bend-up clip design. Blade retainers are installed in the gap between the blade bottom and the disk slot bottom. One end of the retainer is pre-bent prior to installation and the other end is bent after installation. The blade retainers are made from annealed Inco 718, because of the cold working required at assembly.

The CF6-80C only uses these bend up retainers on stages 1, 4, and 5. As mentioned earlier, the stage 2 and 3 blades are retained in the forward direction by the interstage seals. They are retained in the aft direction by a stop designed into the blade skirt, and disk dovetail post which prevents the blade from moving aft.

Shafting The LPT shaft and fan mid shaft transmit torque from the LPT to drive the fan. On the CF6-80C2 LPT shaft bolts between the stage 2 and stage 3 disks and is coupled to the fan midshaft via a spline. The aft extension on the shaft provides the journal for the No. 6 bearing and supports the associated sump air and oil seals. A vent seal is attached on the forward side of the cone which is required as part of the LPT rotor cooling air supply circuit.

Earlier GEAE commercial LPT rotor designs (TF39, CF6-6, AND CF6-50) consisted of two LPT shafts. The CF6-80A engine was the first commercial LPT rotor to use a single shaft design. The elimination of the turbine midframe and associated bearings, made this cost and weight reduction idea feasible.

The fan midshaft mates to the LPT shaft and the fan shaft through splines. The fan midshaft is made from Marage 250 steel, because of its high shear strength capability. A center vent tube is assembled through the middle of the fan midshaft which allows a common forward and aft sump vent at the exit of the engine.

Chapter 6

ENGINE QUALIFICATION AND CERTIFICATION

by Robert Jutras and Rick Sherrer

ENGINE QUALIFICATION

One of the major objectives of an engine development program is the qualification or certification of that engine. Qualification is conducted in accordance with the qualification provisions detailed in the engine specification. Sufficient technical data must be accumulated to demonstrate that the engine meets all requirements described in the engine specifications relative to structural integrity, performance, operability, weight, maintainability, reliability, safety and durability.

The qualification activities to be performed on an engine program are described in the Master Test Plan. The Master Test Plan describes the engine test, component tests, and similarity and analysis reports required to satisfy the requirements identified in the Engine Spec and the Program Master Plan (PMP). The flow of information for satisfying each requirement is provided along with the specification paragraph stating the requirements. The strategy or method of accomplishment for qualification of components and the engine generally falls into the following categories:

- S By similarity to an existing program
- A Analysis used to show compliance
- CT Component Test
- ET Engine Test
- FT Flight Test

Development programs will normally take full advantage of knowledge and experience gained from previously successful programs. This allows specific qualification requirements to be fulfilled by similarity, thereby reducing time and program cost. When qualification by similarity is not applicable, an attempt should be made to qualify by analysis. If the analytical tools are not available, or the analysis is complicated, time consuming and expensive, an alternative such as component testing or engine testing should be considered.

Qualification for Production Release (PR) generally consists of test requirements for controls and accessories (C&A) components, engine components, engine tests, and flight tests. The management flowdown of the technical requirements for component and engine testing is shown in Figures 6.1 and 6.2 respectively.

The Management System for work planning and flowdown of requirements is in accordance with AEBG policies, documents, and other operating procedures and instructions. It assures coordination of activities with interfacing organizations to ensure compatibility of objectives, schedules, and procedures through the Program Master Plan (PMP). Engineering Technical Requirements provide detail contract specifications for engine design and associated requirements. Engineering Program Plans (EPP) (AEBG 730.10) are generated by prime and sub-tier contributors to meet the objectives stated in the EMP (Figure 6.3). The EPP includes program plans and milestone charts to describe the work effort, schedule, cost breakdown and substantiation of costs.

Work packages to meet program objectives are communicated and funded through Work Requests (WR) and Work Authorizations (WA) as shown in Figures 6.4 and 6.5 respectively. Work authorizations may fund manpower, specific hardware procurement or non-recurring development costs at vendors. Work authorizations provide specifics of the work effort to be accomplished and timing required. Test Project Sheets (TPS) are usually initiated by Design Engineering to define and communicate requirements for engine tests, flight tests and component tests. These Test Project Sheets (see Figure 6.6) are funneled through the Operations Group to assure they meet the program objectives and are then sent to Evaluation for execution. A Test Plan is written to provide a detailed definition of the development test program. This plan may include engine identification, types of planned testing (e.g. cyclic endurance, performance, etc.), instrumentation, and major milestones. This plan must be jointly approved by Evaluation, Engineering, and Project Management.

Evaluation Engineering, after receiving the Test Plan and related test project sheets, is responsible for the preparation and coordination of Test Requests. These Test Requests are provided to the Test Facilities group and define specific requirements for a development engine test and reflect the Test Plan and agreed upon TPS's. Instrumentation Requests are generated by Evaluation Engineering according to the agreed upon test plan and provided to Instrumentation System Engineering for implementation.

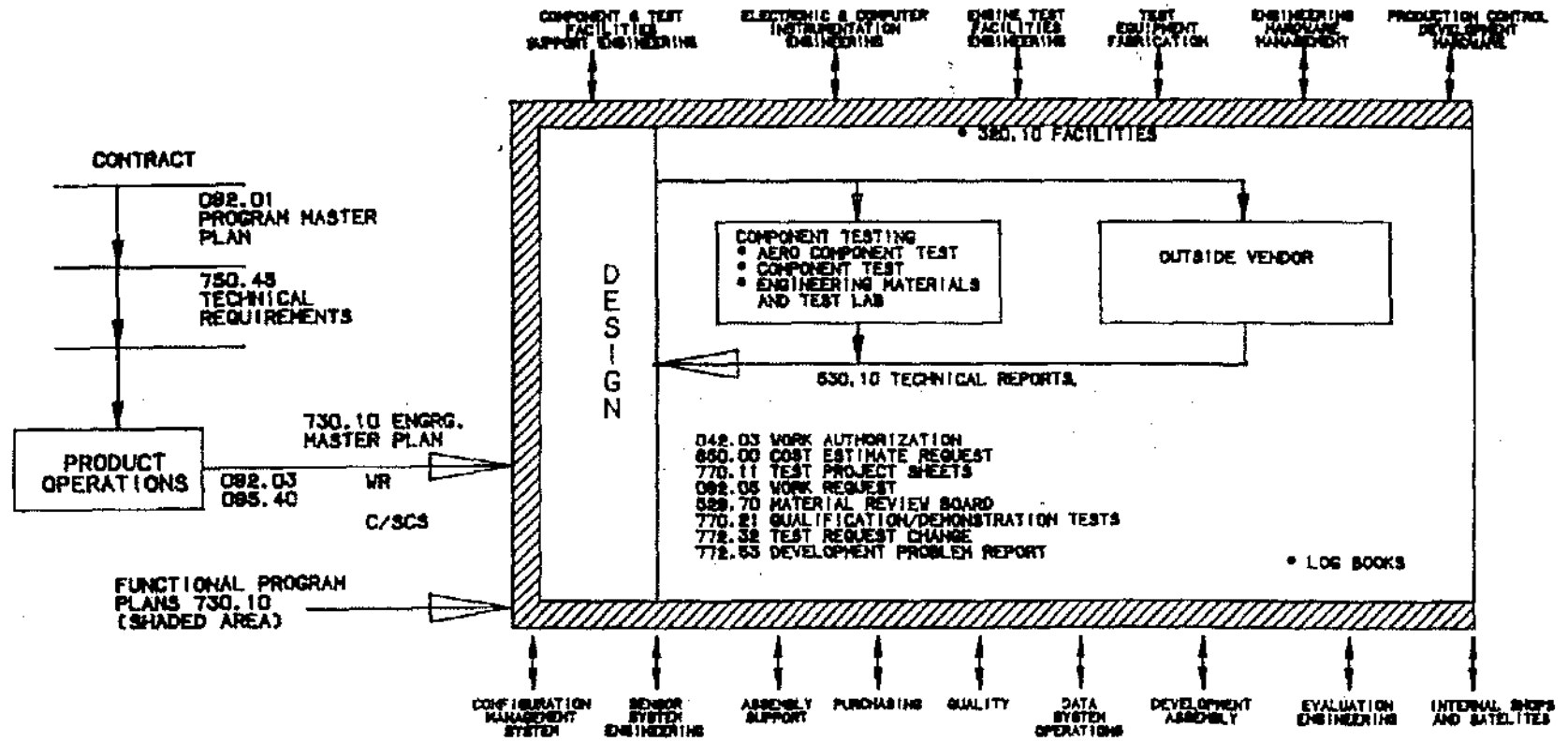


Figure 6.1 Management Flowdown for Component Tests

LOW PRESSURE TURBINE STATOR COMPONENTS

Stator Case The LPT stator case is the load carrying structure between the HPT stator case and the Turbine Rear Frame. The casing contains internal hooks to which the LPT nozzles attach. Borescope inspection ports are provided at stages 1, 2, and 4.

The LPT stator case is fabricated by EB welding a series of rings together, with an Inco 718 casting for the front of the casing. The hotter, middle sections are Waspalloy and the aft sections are Inco 718. The LPT stator case must be designed to withstand engine dynamic loads, (including fan blade-out loads) internal pressure loads, and must be able to contain a turbine blade in the event of a failure. The elimination of the turbine midframe also results in increased structural loads in the casing.

The CF6-80C2 LPT casing (as well as the CF6-80A casing) is a 360° structure. Earlier GE commercial LPT casings (TF39, CF6-6, CF6-50) were designed as two-piece fabrications. They consisted of an upper and lower half which were bolted together by an axial horizontal splitline flange. This is the same design concept used in the compressor.

The upper and lower half casing had advantages from an assembly and maintainability viewpoint. The entire rotor could be assembled and balanced followed by the stator assembly being assembled around it. It was also relatively easy to disassemble one of the stator halves to perform a visual review of the entire rotor assembly for suspected field damage.

The CF6-80A and -80C2 engines eliminated the need for the turbine midframe (between the HPT and LPT), which resulted in a significant cost and weight benefit. Because the LPT case was now bolted directly to the HPT case, significant out of roundness distortion in the HPT stator was observed during the early development stage of the -80A engine (the early -80A LPT case was a two piece upper and lower design). This distortion was attributed to the thermal lag in the LPT split line flanges causing an ovalization in the HPT stator. For this reason, the -80A and -80C2 LPT cases are 360° structures. The assembly procedure involves alternately stacking rotor and stator stages, and balancing the rotor with the stator. Although the tooling is more extensive, the assembly time for the rotor and stator has been reduced.

LPT Nozzles LPT nozzles consist of a sector of six vanes, which are Rene 77 airfoils. Their function is to direct the flowpath air from the preceding row of turbine blades to the next row of blades with maximum effi-

ciency. The nozzles are assembled to the stator case by rocking-in each segment onto the hooks inside the case. Pins are pressed into the stator case which serve to position the nozzle segments and react to the tangential loads.

Shrouds The shrouds attach to the case and nozzle segments to provide a rubbing surface for the blade seal teeth. The shrouds are fabricated by brazing Hast-X honeycomb foil to Rene 41 or Waspalloy sheet metal segments. The design intent is for the blade seal teeth to rub into the shrouds, thus reducing the amount of air that can bypass the turbine airfoils.

A secondary function of the shrouds is to thermally shield the case from the hot flowpath gas. In earlier engine designs, insulation blankets were trapped between the shrouds and case. In the -80C LPT design, the shrouds were purposefully designed with an axial interference between adjacent nozzle stages to create a dead cavity. This concept results in a cost reduction and appears to be working very well to date. Figure 5.57 shows the shroud and nozzle attachment area in greater detail.

Interstage Seals The stationary interstage seals perform the same function as the shrouds; they reduce flowpath gas from bypassing the turbine airfoils. The interstage seals are located at the inner flowpath. The interstage seals are fabricated sheet metal segments with Hast X honeycomb foil brazed to the inner diameter. The stage 2 seal segments span two nozzle segments while the stage 3, 4, and 5 seals span four nozzle segments. Each seal segment is connected to the adjacent segment using a sliding connection and specially designed retainers, which provide damping from potential vibrations.

Pressure Balance Seal The pressure balance seal is a 360° fabricated structure which is located at the I.D. of the stage 1 nozzles. The function of the pressure balance seal is to minimize cooling flow requirements and reduce flow sensitivity to seal area variations. Cooling air for the aft side of the stage 2 HPT disk and the LPT rotor is routed from the compressor through external pipes to the LPT case at the stage 1 nozzles. Air travels radially inward through the stage 1 nozzles into the pressure balance seal. The cooling air exits the forward side of the pressure balance seal through angled holes which impart a large tangential velocity to the air. This develops a forced vortex into the HPT-LPT cavity; a radial pressure gradient is developed which pumps cooling air into the flowpath discouraging hot flowpath ingestion into the turbine. The forced vortex also serves to reduce the flow sensitivity to cooling flow area variations at the inner diameter of the pressure balance seal.

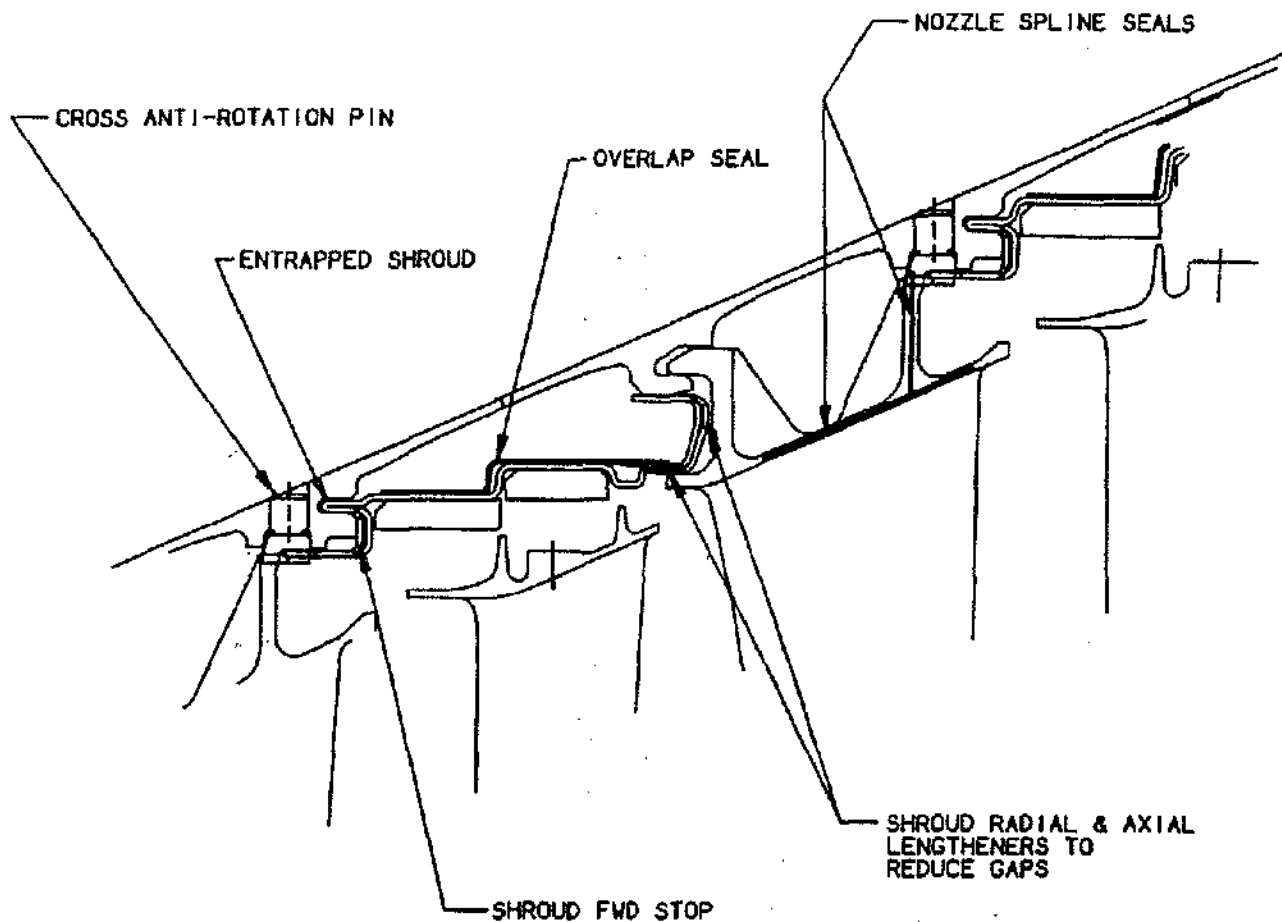


Figure 5.57 CF6-80G2 LP Turbine Stator Cross Section Leakage Improvements

There are many similarities between low pressure turbines and high pressure turbines. Because of the differences in temperatures, pressures, and speeds of rotation,

low pressure turbine design departs from the design of high pressure turbines in the several areas described.

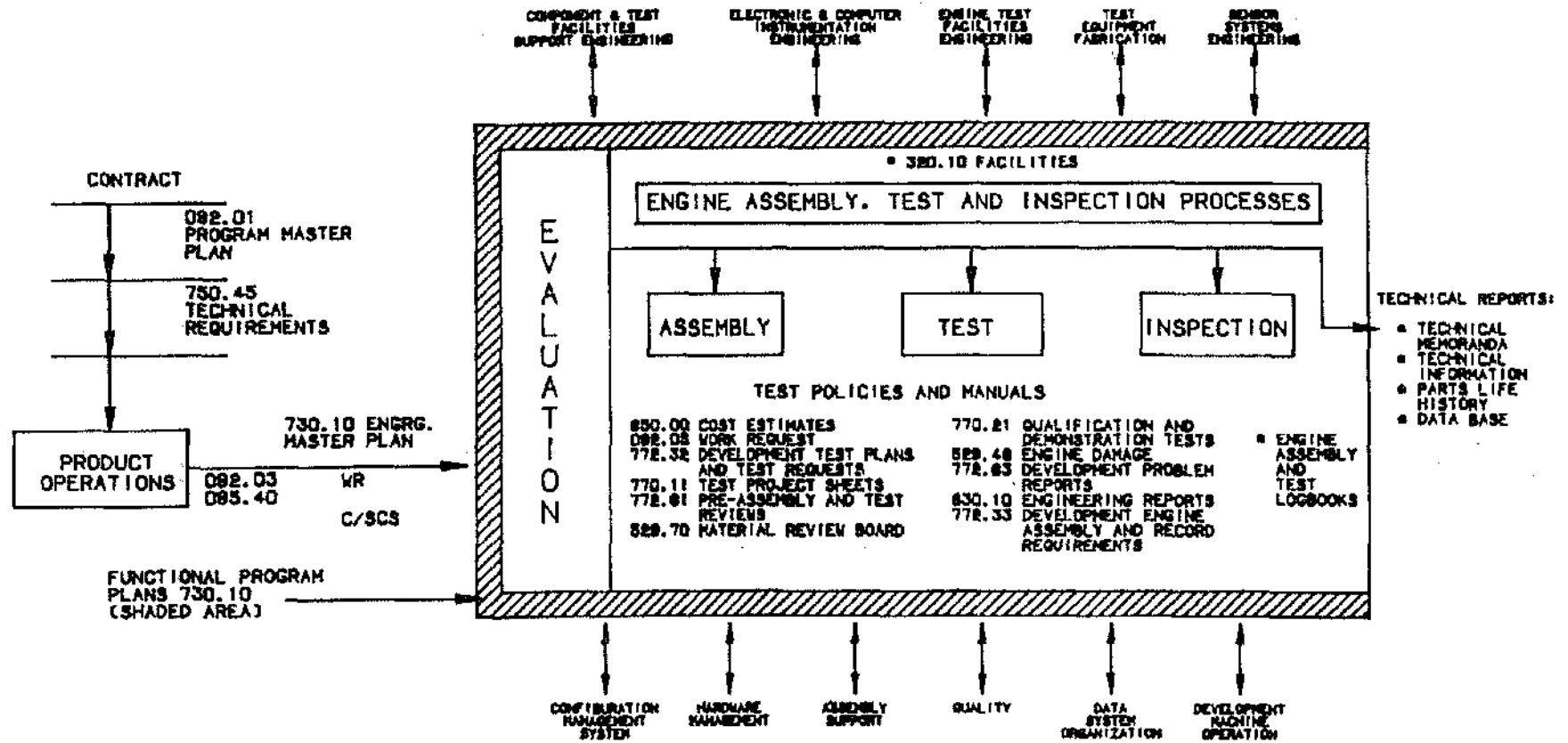


Figure 6.2 Management Flowdown for Engine Tests

ENGINEERING MASTER PLAN (EMP)

ENGINE QUALIFICATION AND CERTIFICATION

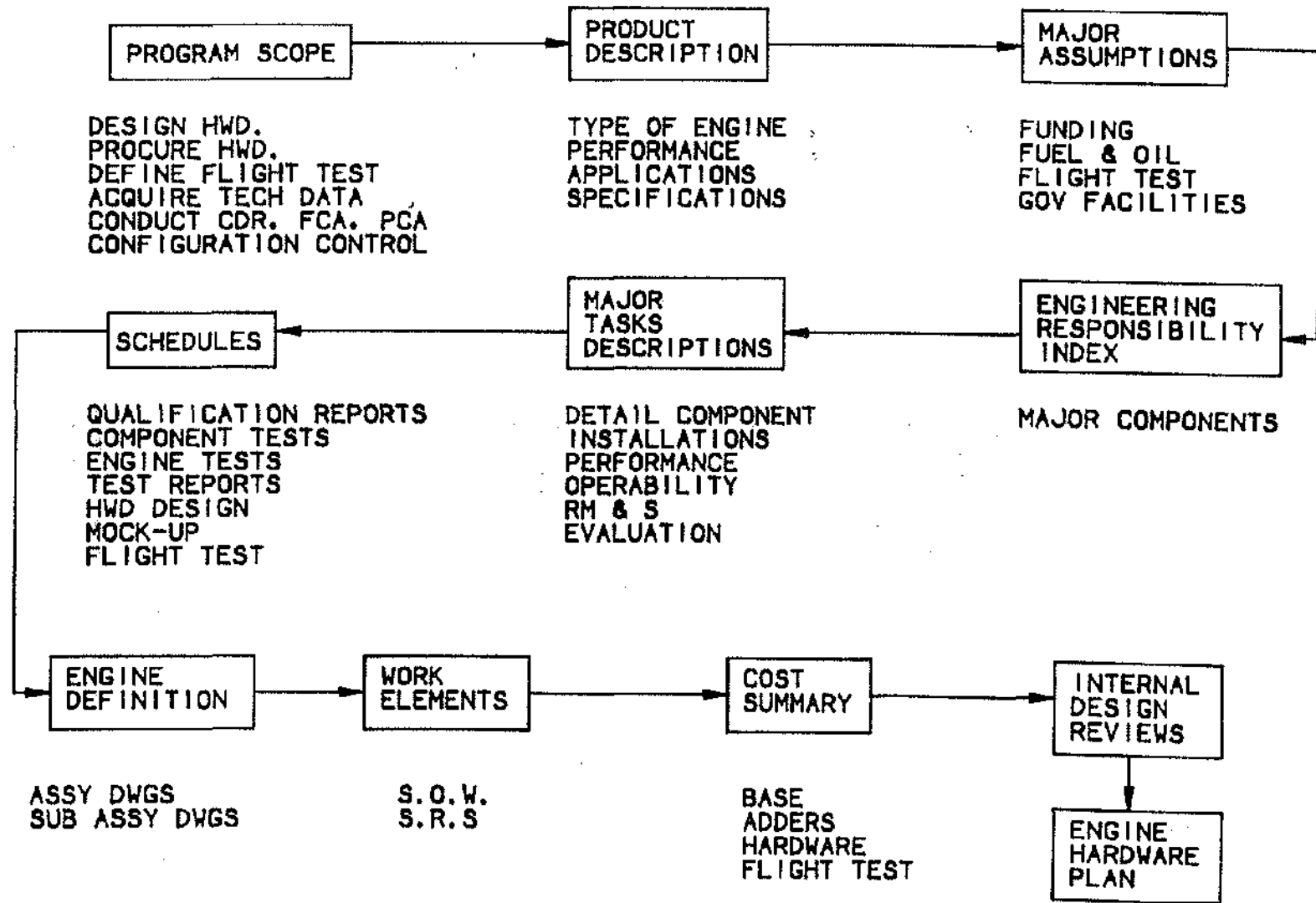


Figure 6.3 Program Plans

WORK REQUEST

TO WHOM	WORK INFORMATION REFERENCE NO.	WORK REQUEST NO.
WORK CENTER / PROJECT	ACCOLLECTOR'S NO.	ACKNOWLEDGEMENT YES <input type="checkbox"/> NO <input type="checkbox"/>
DATE	DATE REQUIRED	TO

APPROVALS

DATE	DATE	DATE
1. SPECIAL REQUEST	2. ORIGINAL BACKGROUND	3. SPECIAL INSTRUCTIONS
<p style="font-size: small; margin-top: 10px;">4. INFORMATION</p>		

ON FILE 150

Figure 6.4 Work Request

WORK AUTHORIZATION

Complete all items
Enter NA if not applicable

See AEBG Instruction 092.03 for
use and preparation

TO NAME - ORGANIZATION LOCATION	JOB NO. 000	ISSUES	CLASS	CLASS NO. (SIC)	DISPATCH OR	NO.
FROM NAME ORGANIZATION LOCATION PHONE NO.	PLANT AREA	REPORT NO.	PLANT'S DESIGN	PLANT/REPAIR NO.		
AUTHORIZED LINES		DATE / APPROVAL		LENGTH / SCALE		STATUS
PRICE	TOTAL TO DATE					
DATE	ORGANIZATION	NAME	NO.	NO.	NO.	NO.
CLASS	QUALIFY LEVEL	REQ. INSTRUCTION	REQ. NO.	DATE / RIGHTS APPLICABLE	SIGNATURE	
DESCRIPTION (FROM RELEASE DATE)	CLASS (10% SPECIAL REQUIREMENTS)	REQ. INSTRUCTION	SIGNATURE	DATE	APPROVAL	
REASON FOR IDENTIFICATION OF USE (SEE PART 10 OF AEBG INSTRUCTION 092.03)	CLASSIFICATION	QUANTITY LEVEL	LOCATION	CLASS NO. (SIC) / DISPATCH OR NO.	FOR USE SPECIFY DRAWING NUMBER, SOURCE AND DATE (10/11)	
DATE	CLASS	QUANTITY LEVEL	LOCATION	CLASS NO. (SIC) / DISPATCH OR NO.	FOR USE SPECIFY DRAWING NUMBER, SOURCE AND DATE (10/11)	
DESCRIPTION I NATURE OF JOB II REASON FOR JOB III SPECIAL INSTRUCTIONS IV DISPOSITION						
DATE REQUIRED	DELIVER TO	PRICE	FLOOR	CLASS NO.	APPROVALS	
DESCRIPTION					CLASS NO.	DATE
					CLASS NO.	DATE
					CLASS NO.	DATE
					CLASS NO.	DATE

ON FILE 001

Figure 6.5 Work Authorization

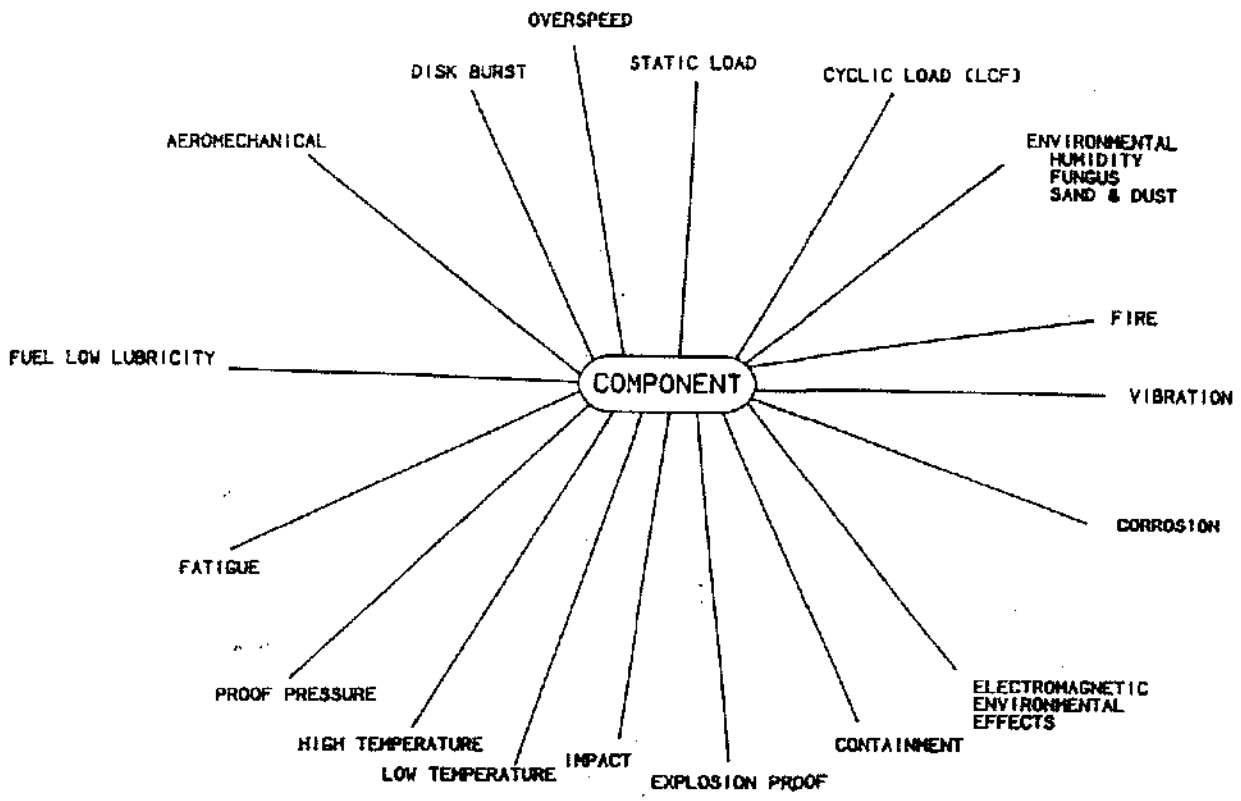


Figure 6.7 Component Test Requirements

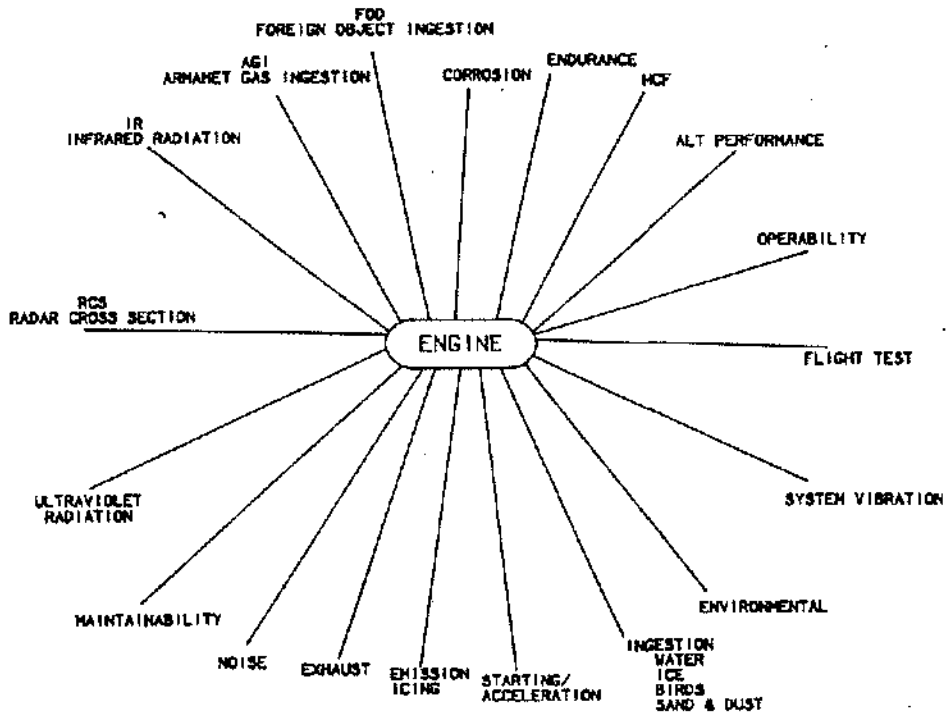
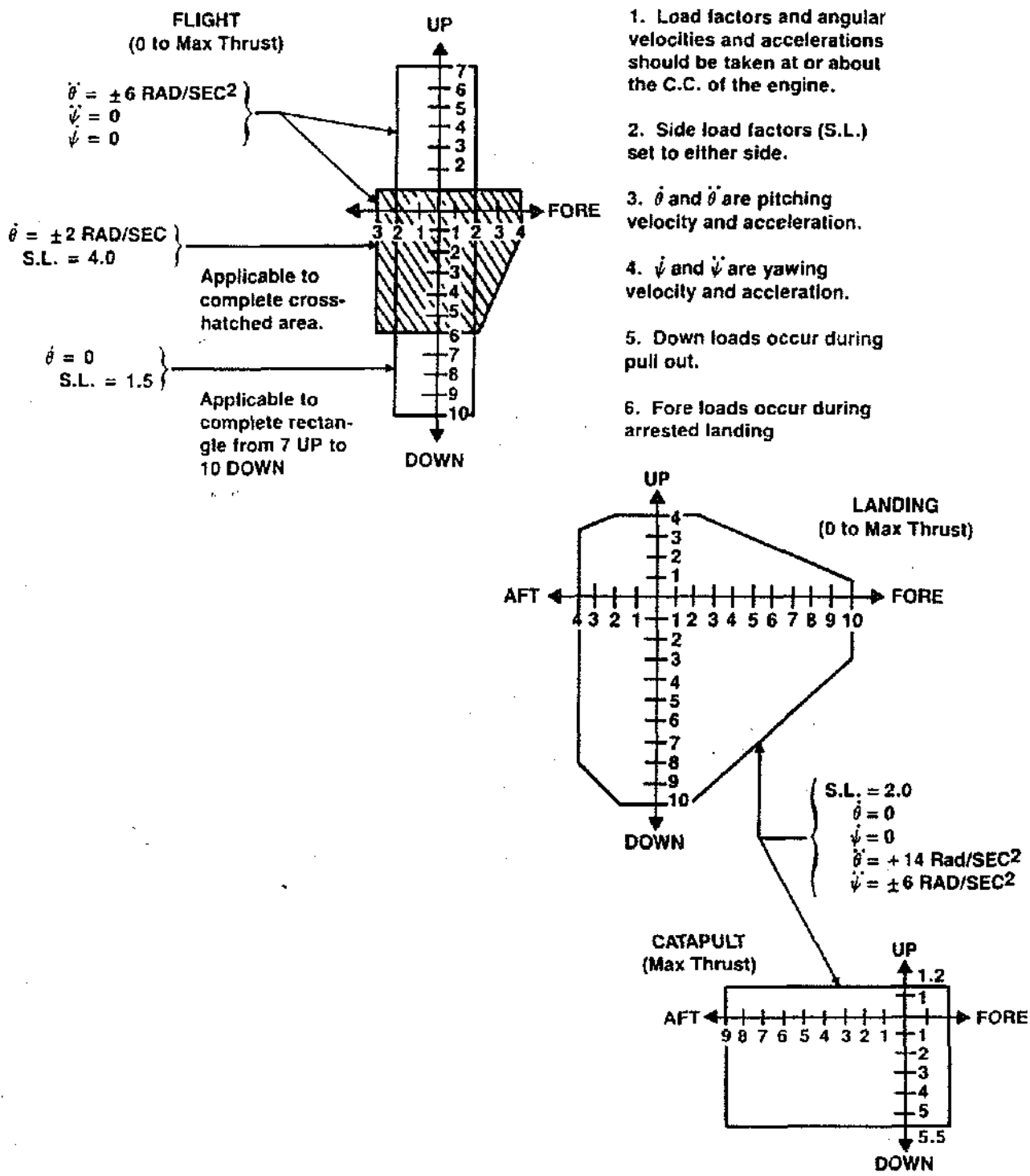


Figure 6.8 Engine Test Requirements

COMPONENTS		SUB-SYSTEMS	
ACCY DRIVE INTERNAL G/B ACCT DRV GRZ BEVEL GEAR ACCT DRV RAD DRV SHAFT ACCY G/B HORIZ SHAFT ACCY G/B HRZ SHAFT HSG A/C ACCESSORY GEARBOX AUGMENTOR MIXER AUGMENTOR DUCT AUGMENTOR FUEL MANIFOLD AUGMENTOR FUEL TUBES AUGMENTOR FUEL VALVE AUGMENTOR IGNITOR AUGMENTOR LINER AUGMENTOR SPRAYBARS COMBUSTOR (IGNITION) COMBUSTOR CASE COMPRESSOR BLADE/VANE COMPRESSOR BLEED TUBES COMP ROTOR 1 & 2 SPOOL COMP ROTOR SIG 3 DISK COMP ROTOR 4-9 SPOOL COMP ROTOR FWD SHAFT COMPRESSOR STATOR DISTRIBUTORS (AUGMENT) ENGINE ACCY GEARBOX EXHAUST NOZZLE DUCT EXHAUST NOZZLE LINER EXHAUST NOZZLE SHROUD	EXHST NOZZLE EXT DUCT EXHST NOZZLE EXT LINER EXHST NOZZLE OUTER FLAP EXHST NOZZLE PRIM FLAP EXHST NOZZLE PRIM SEAL EXHST NOZZLE DIVERG FLAP EXHST NOZZLE DIVERG SEAL EXHST NOZZLE ACTUAT RING EX/NOZ ACTUAT LINK & BRAC FAN BLADES & VANES FAN FRAME FAN IGV FLAP FAN OUTER DUCT FAN ROTOR STG 1/FWD SHFT FAN ROTOR STG 2 DISK FAN ROTOR STG 3 DISK FAN ROTOR AFT SHAFT FAN STATOR CASE/FWD MNT FAN STATOR VANE FRONT FRAME HPT BLADE/VANES HPT ROTOR/FWD/AFT SHAFT HPT STATOR/NOZZLE IDG PIPING LPT BLADE/DOVETAIL LPT ROTOR/SHAFT LPT STATOR/VANES TURBINE FRAME	Valves, Fan and Core Spraybar Valves, Local Distribution Control, Fuel, Hydromechanical (MEC) Control, Electronic (AFTC) Control, Augmentor Fuel Pump, Augmentor Fuel Pump, Hydraulic Pump, Lube/Scavenge Pump, Main Fuel Pump, Total Fuel Boost Valve, De-icing Core Stator Actuator Variable Stator Vane Feedback Cable Engine Monitoring System Processor Gearboxes Sensor, Flame Ignitor, Main Augmentor Filter Augmentor Filter Electrical Harness Alternator	Actuator, Exhaust Nozzle (AB) Actuator, Fan IGV Cooler, Lube Oil/Fuel Cooler, Hydraulic Oil/Lube Oil Cooler, Lube Oil/Air - (IDG) Detector, Turbine Met Temp (Pyrometer) Exciter, Ignition Sensor, Fan Discharge Temperature (T25) Sensor, Fan Speed Sensor, Inlet Temperature (T2) Transducer, Exhaust Nozzle(AB) Feedback Tank, Lube & Hydraulic Aircraft/Eng Interface Mounts, Thrust Fitting and Links Filter, IDG Oil Line, Fuel & Motive Flow Pump, Supply Ejector, Air/Oil (IDG) Cooler Regulator, Ejector (9th Stg Bleed Air) Flowmeter, Fuel

Table 6.1 Major Components and Subsystems Requiring Qualification



1. Load factors and angular velocities and accelerations should be taken at or about the C.C. of the engine.
2. Side load factors (S.L.) set to either side.
3. $\dot{\theta}$ and $\ddot{\theta}$ are pitching velocity and acceleration.
4. $\dot{\psi}$ and $\ddot{\psi}$ are yawing velocity and acceleration.
5. Down loads occur during pull out.
6. Fore loads occur during arrested landing

Figure 6.9 Externally Applied Forces

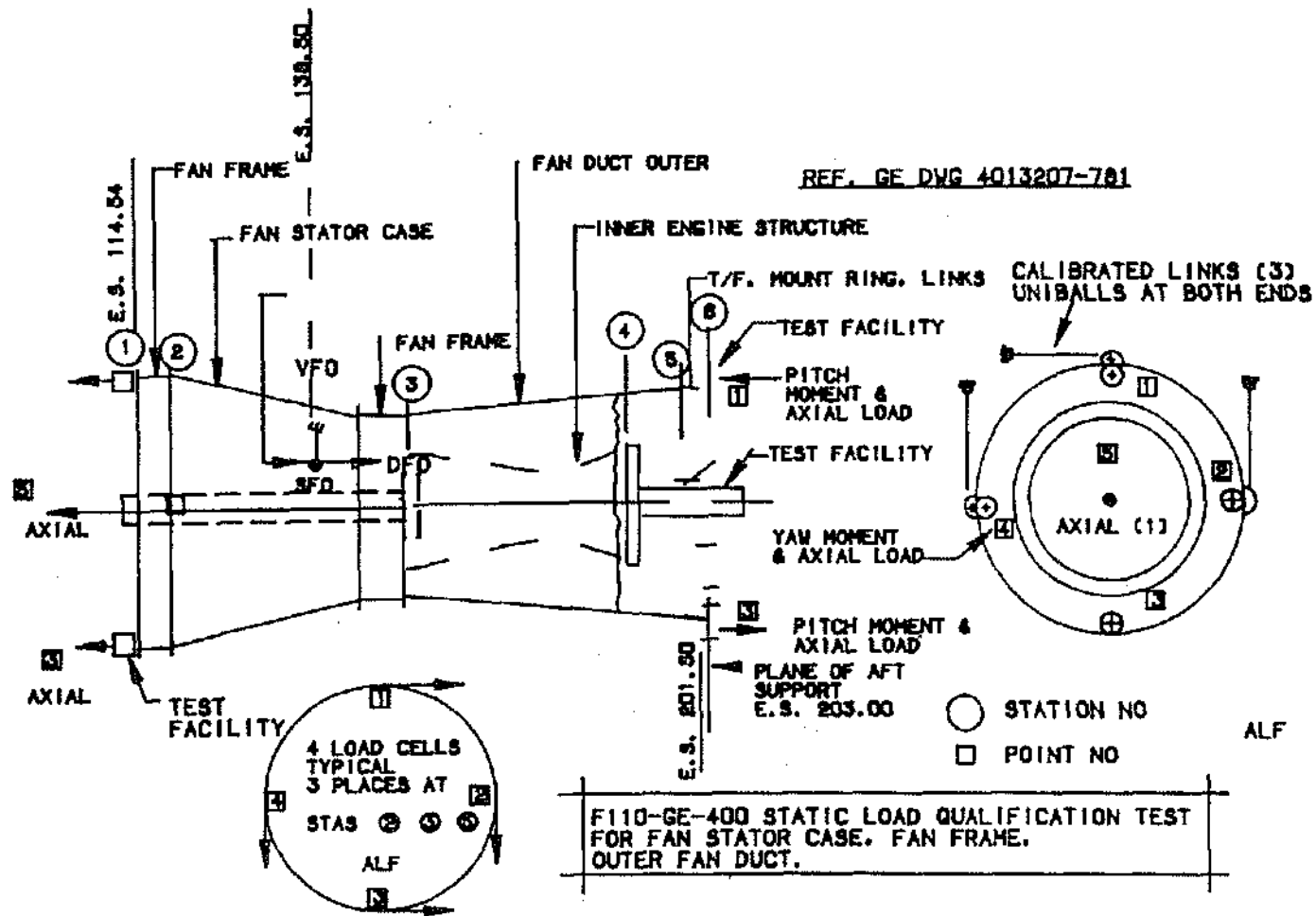


Figure 6.10 Test Setup

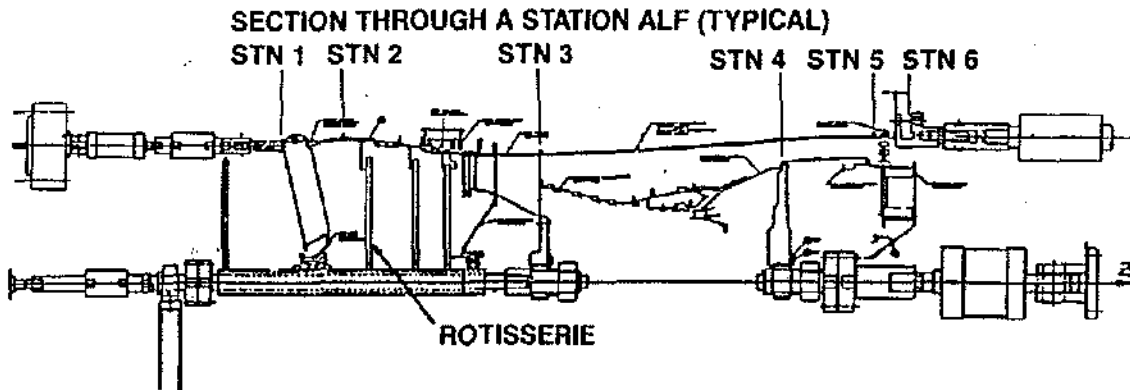
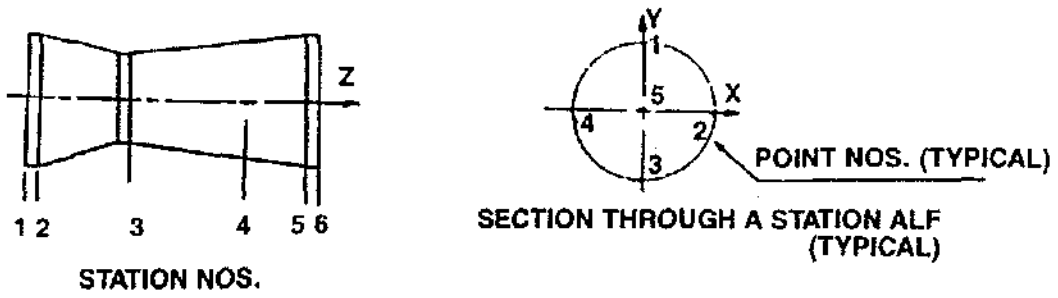


Figure 6.11 Cross Section of Facility Test Stand

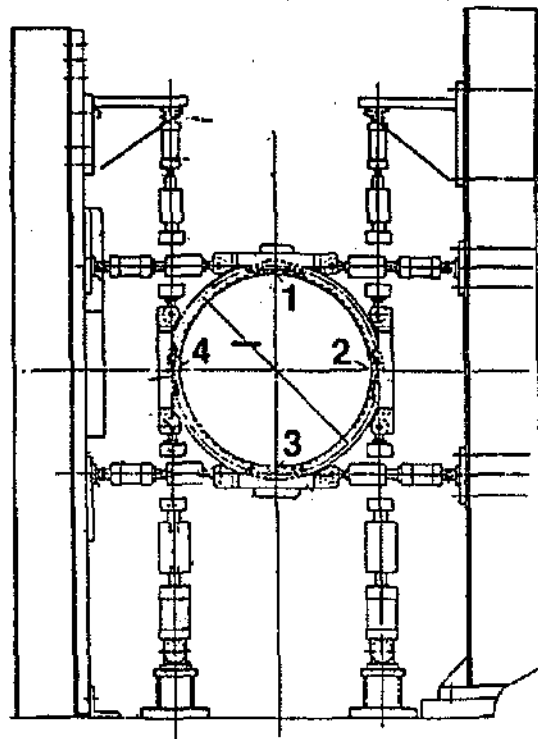


Figure 6.12 In-plane Applied Loading Assembly at Stations Two and Three

The accessory drive system consists of a gearbox to drive the engine accessories and a power takeoff shaft, or an aircraft accessory gearbox coupled to the engine gearbox through a drive shaft. These components require qualification demonstration of many aspects such as attitude capability, static torque, vibration, heated oil, etc. The gearbox system can be qualified either through component test or a combination of component and engine tests.

Controls and accessories components consists of many components which require qualification testing to meet specification requirements, see Table 6.2. Specific test requirements are delineated in the Master Test Plan relative to the various subsystems of the C&A component which include the fuel system, ignition system, de-icing system, hydraulic system, and engine control system including temperature sensing and actuation components. The component testing is called Simulated Operational Test (SOT). This test is to simulate the engine function with the components in their normal selective relationship. Each component is operated according to an appropriate mission related test cycle to demonstrate its endurance capability within its operating environment (temperature, pressure, fuel, oil, etc.).

All engine electrical and electronic components can be subject to an Electromagnetic Environmental Effects (EEE) Test. An example of these components is provided in Table 6.3. Typical requirements for C&A components are shown in Figure 6.1.

The engine qualification generally consists of:

- Corrosion test
- Altitude qualification
- Endurance testing
- HCF for tubes and pipes
- Operability tests
- Accessory drives, engine control and lube system qualification

Corrosion Qualification A corrosion qualification test is usually required on an engine that will be operated in a marine environment to demonstrate engine performance and integrity after exposure to salt-laden air. The typical test cycle (see Figure 6.13) is an accelerated mission consisting of twenty-five cycles each lasting forty-eight hours in which the engine accumulates one hundred fifty hours of operation. The remainder of the time, the engine is exposed to various combinations of temperature, humidity and salt environments.

MAIN ENGINE CONTROL	IGV ACTUATOR
AFT CONTROL	ENGINE FUEL/OIL COOLER
T25 SENSOR	IDG FUEL/OIL COOLER
EMSP	HYDRAULIC OIL COOLER
PYROMETER	M1 SENSOR
ELECTRICAL CABLES	T2 SENSOR
VSV FEEDBACK	ANTI-ICE VALVE
AUGMENTOR FUEL PUMP	LUBE AND SCAVENGE PUMP
MAIN FUEL PUMP	AUGMENTOR FUEL CONTROL
FUEL BOOST PUMP	LUBE/HYDRAULIC OIL TANK
HYDRAULIC PUMP	FLAME SENSOR
VSV ACTUATOR	IDG AIR/OIL COOLER
AUGMENTOR FUEL FILTER	IDG EJECTOR AIR VALVE
ALTERNATOR	IDG OIL FILTER
AB ACTUATOR	LUBE PRESS TRANSMITTER
AB LVDT	

Table 6.2 Controls and Accessories Components List

MAIN ENGINE CONTROL	T2 SENSOR
AFT CONTROL	AUGMENTOR FUEL CONTROL
EMSP	FLAME SENSOR
PYROMETER	IDG EJECTOR AIR VALVE
ELECTRICAL CABLES	ANTI-ICE VALVE
HYDRAULIC PUMP	IGV ACTUATOR
ALTERNATOR	LUBE LEVEL SWITCH/TEMP
A8 LVDT	SENSOR/PRESSURE TRANSMITTER
N1 SENSOR	CORE FUEL FLOW METER

Table 6.3 Potential Components Requiring Electromagnetic Environmental Effects Tests

Altitude Qualification This qualification is to demonstrate steady-state performance, altitude starting and transients, inlet compatibility and windmilling characteristics throughout the flight envelope. See Figure 6.14 for typical flight envelope. The altitude test consists of operation and air starting checks at several conditions including effects of power extraction, inlet recovery, bleed air extraction, inlet distortion and windmilling on engine performance and stability. The operating envelope of the engine is verified by testing at the extremities of the flight map. Engine steady-state and transient characteristics are determined at each test point over a range of power settings with and without customer bleed and power extraction.

Endurance Testing Here the engine is subjected to an Accelerated Simulated Mission Endurance Test (ASMET) or an Accelerated Mission Test (AMT) to evaluate the engine durability, reliability and maintainability requirements. These endurance cycles are based on the aircraft mission mix and includes simulation of flight missions and ground cycles. The objective is to accumulate the established Total Accumulated Cycles (TAC) specified in the requirements. TAC's are a measure of accumulated damage done to the engine and are defined in terms of low cycle fatigue cycles (LCF), full thermal cycles (FTC) and cruise to intermediate cycles (CIC). LCF is defined as startup to intermediate power or above, and shutdown. An FTC is defined as idle to intermediate power or above, and back to idle. A CIC is defined as cruise power setting to intermediate power or above, and back to cruise power setting. For engine life requirements,

$$TAC = LCF + 0.25 (FTC) + 0.025 (CIC)$$

An example of how a mission cycle is converted to an ASMET cycle is shown in Figures 6.15 and 6.16.

There are many ways of converting from a mission cycle to an accelerated cycle depending on the objectives. For example, if the objective is to demonstrate rotor durability you would want to keep all idle to intermediate excursions and minimize max A/B excursions while if the durability of the exhaust nozzle were to be demonstrated, you would include all max A/B excursions while minimizing idle to intermediate transients.

The endurance test may be conducted at various inlet pressures and temperatures, horsepower extraction and fuel temperatures for selected number of cycles. Customer bleed and the de-icing system may be required for a selected number of cycles.

As part of the qualification endurance test, a high cycle fatigue (HCF) test is usually included to assure that the tubes and pipes don't have detrimental resonances in the engine operating range. The HCF, known as the stair-step bodie, is typically run in two parts, the up-leg and the down-leg. The up-leg is normally done at the onset of the endurance test and the down-leg at the end. An example of an HCF cycle is shown in Figures 6.17 and 6.18 for the up-leg and down-leg respectively. The HCF cycles consist of a sequence of rotational speeds of one hour duration ranging from idle to maximum speed in increments of 200 rpm. The down-leg is offset by 100 rpm from the up-leg so as to cover every 100 rpm from idle to the maximum operating speed. This sequence will provide adequate data to evaluate the tube and piping characteristics and identify potential problems.

Operability Evaluation The operability evaluation is normally conducted in the altitude qualification test to evaluate the effects on transient operation and steady-state performance.

SALT	200PPB	0	200	0	200PPB	0	200	0
TEMP	15°C (59°F)	AMB	15°C (59°F)	43°C (110°F)	15°C (59°F)	AMB	15°C (59°F)	43°C (110°F)
HUMID	73%	AMB	73%	80%	73%	AMB	73%	80%

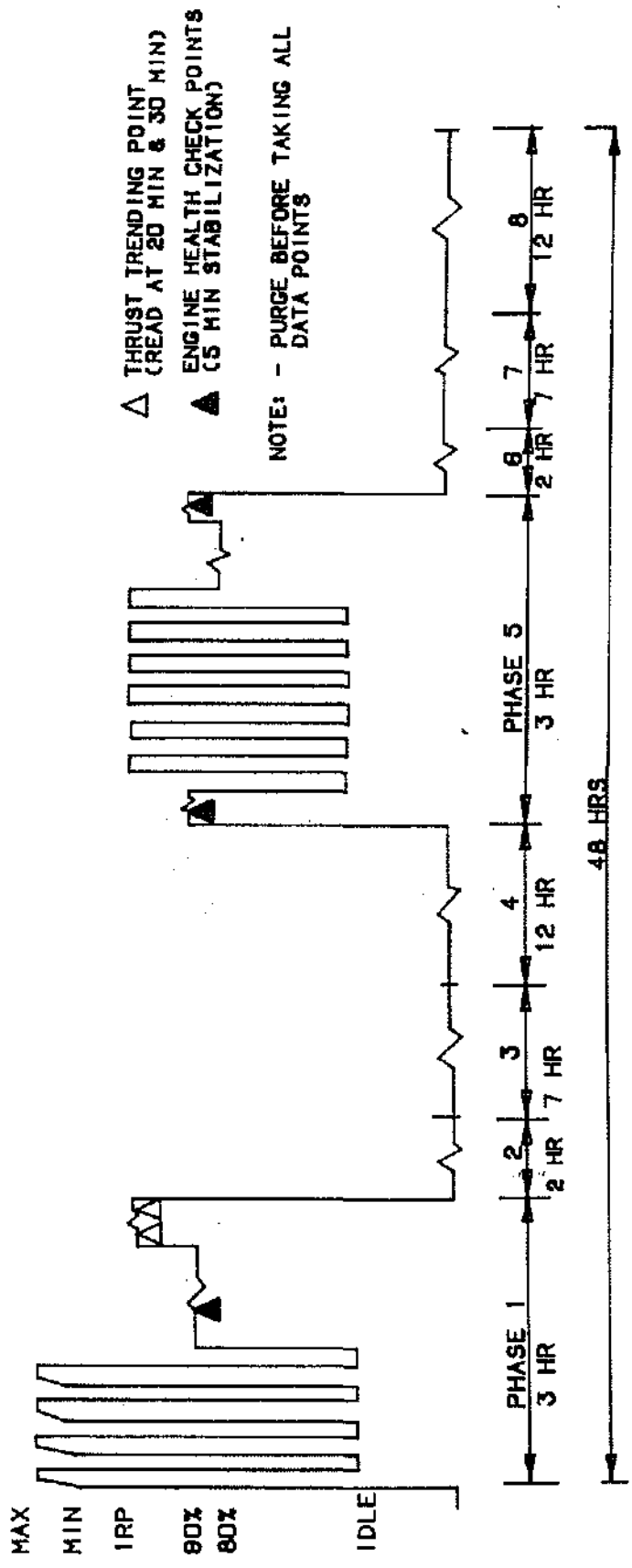
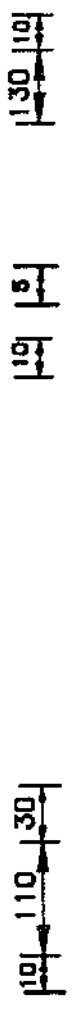
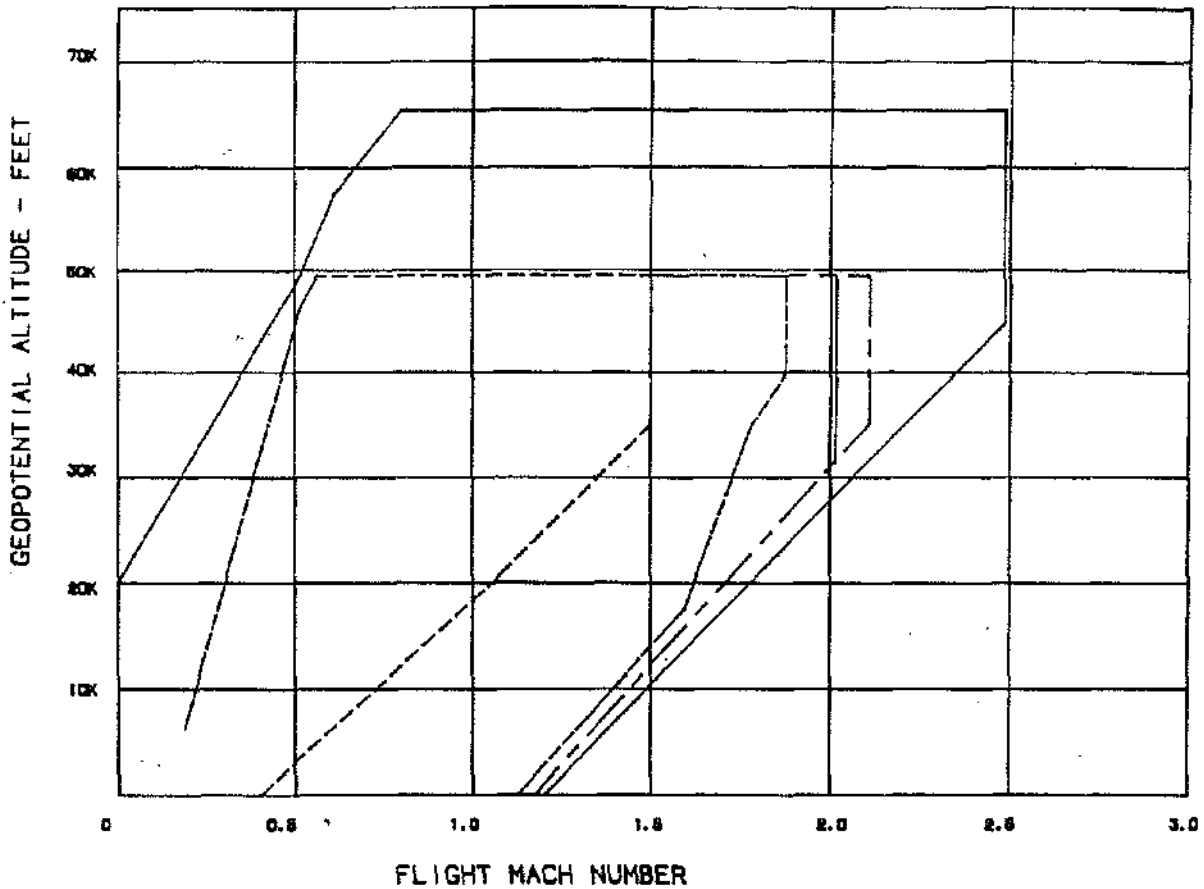


Figure 6.13 Typical Corrosion Cycle

- STANDARD DAY FLIGHT ENVELOPE
- - - - - AFTERBURNER FLIGHT OPERATING LIMIT
- A/C ENVELOPE CLEAN STORES (1978 NATOPS)
- - - - - F14D GOAL



REFERENCES

- (1) STANDARD DAY FLIGHT ENVELOPE. SPEC.NO. E2272. FIG. 13. 4/25/86
- (2) AFTERBURNER FLIGHT OPERATING LIMIT. SPEC.NO. E2272. FIG. 13. 4/25/86
- (3) A/C-ENVELOPE CLEAN STORES, NATOPS FLT. MANUAL. FIG. 1-107. 2/1/78

Figure 6.14 Typical Operating Envelopes

AIR COMBAT MANEUVERS MISSIONS

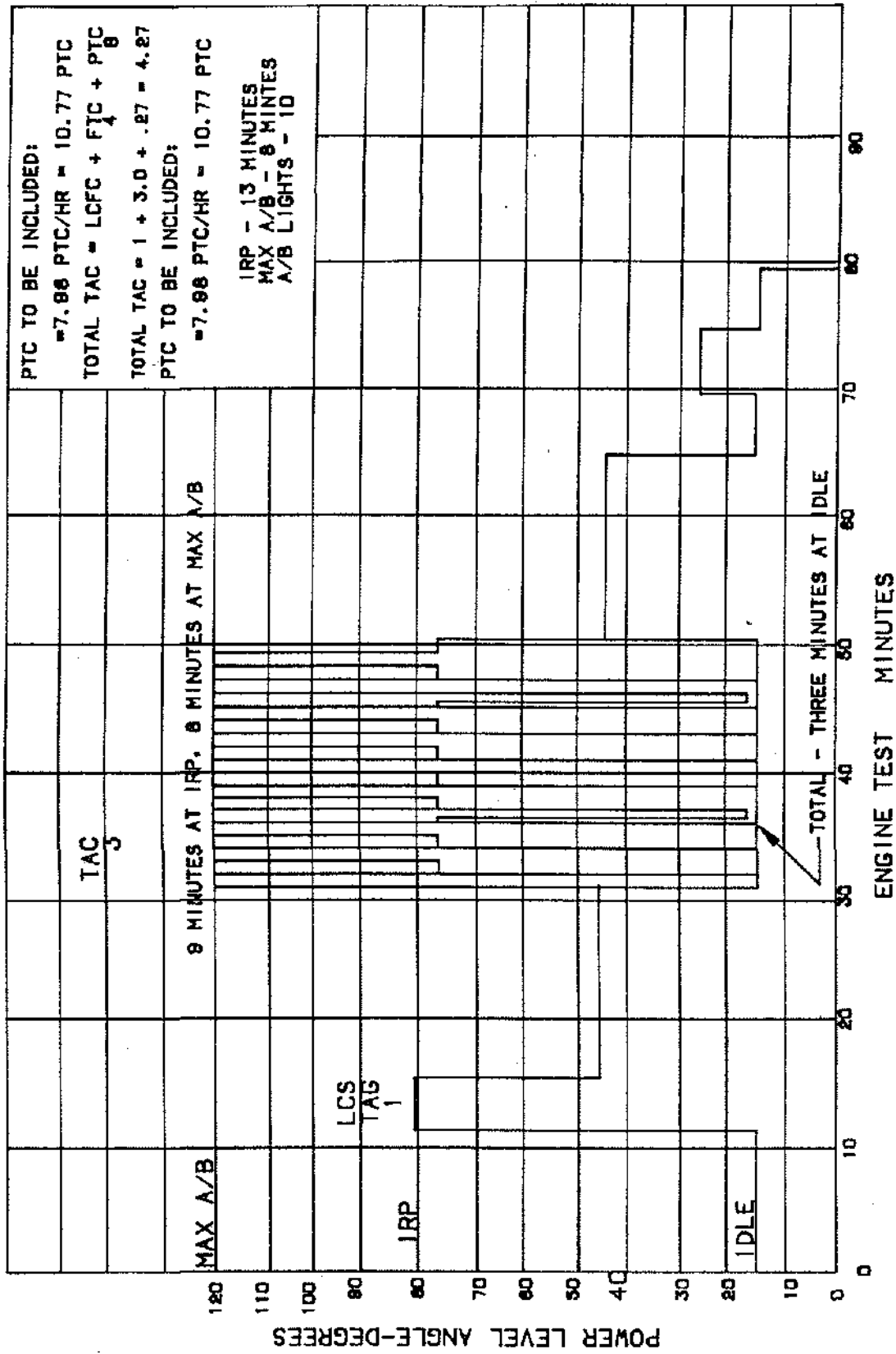


Figure 6.15 Mission Cycle

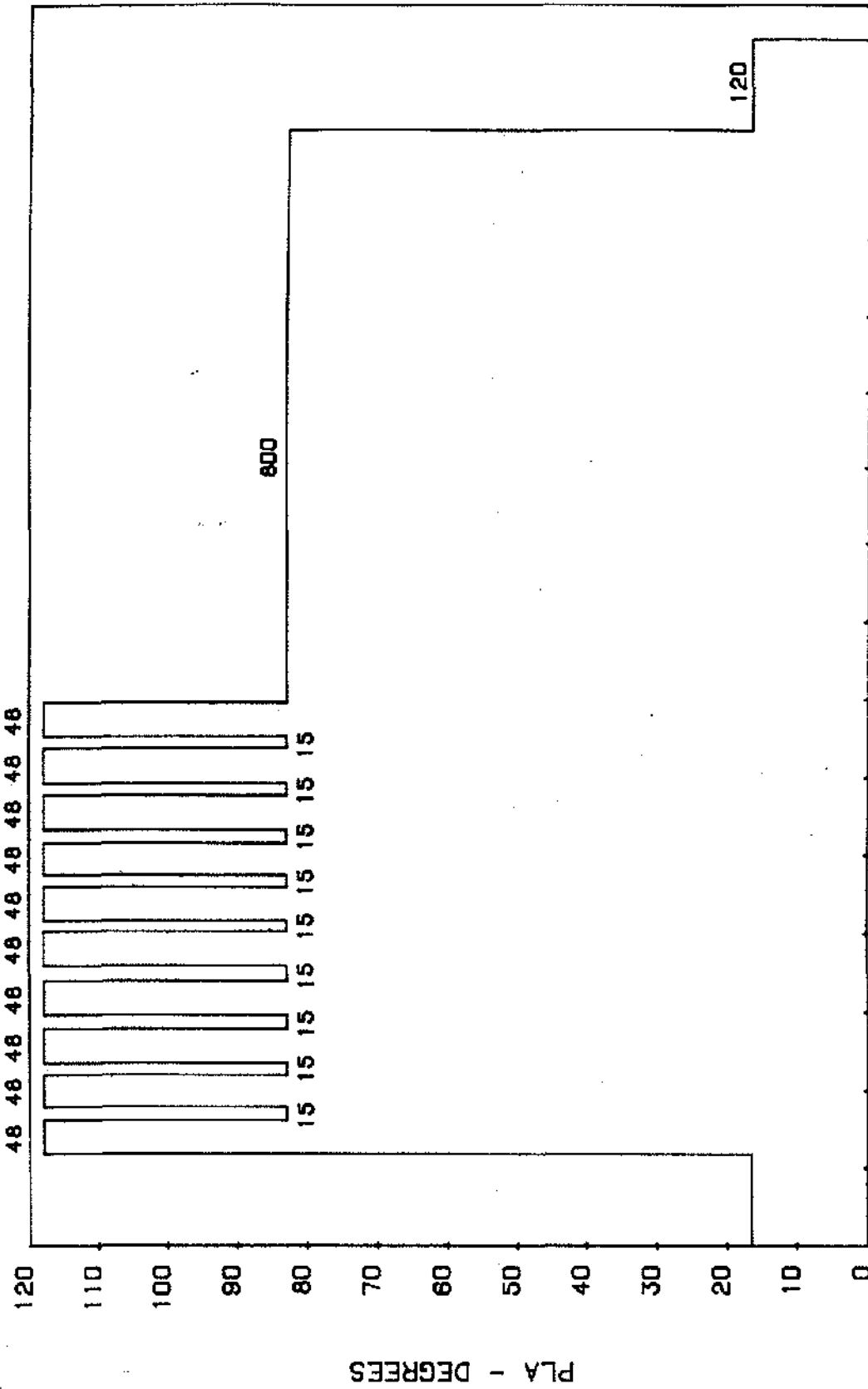


FIGURE 6.16

TIME - SECONDS

Figure 6.16 ASMET - Air Combat Maneuvers

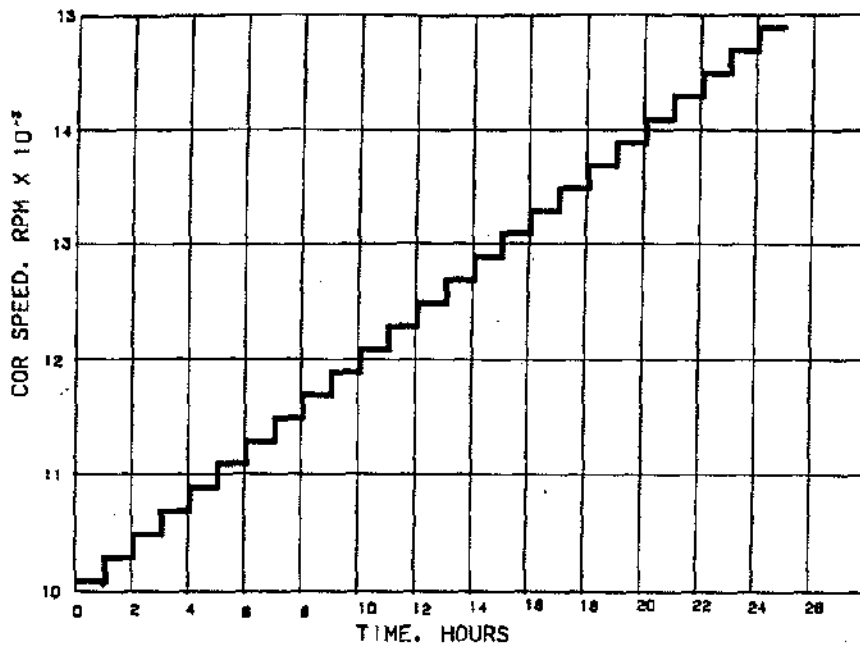


Figure 6.17 HCF Up-Leg Cycle

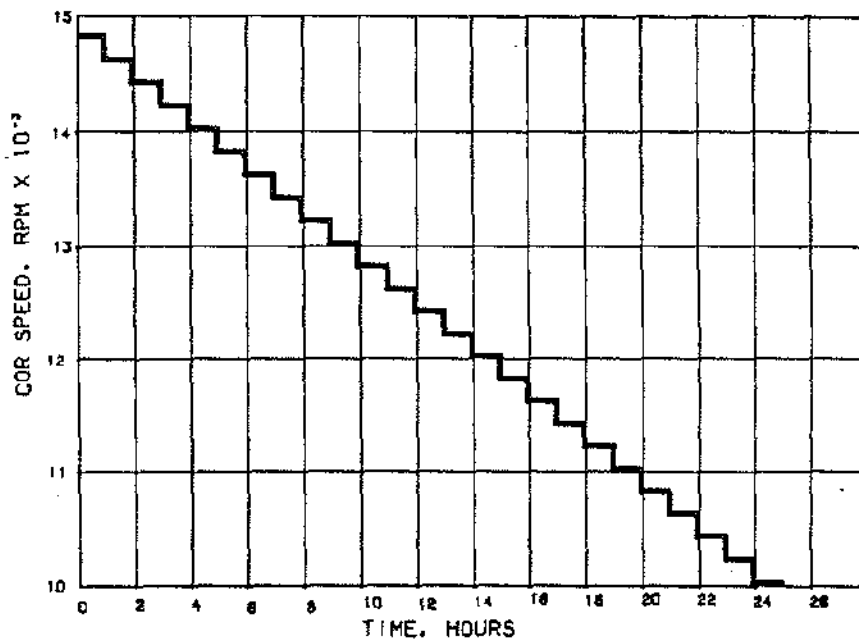


Figure 6.18 HCF Down-Leg Cycle

Accessory Drive Testing The accessory drive system, as mentioned earlier, is tested on a component rig for attitude and static torque evaluation and demonstration. The operational capabilities of the accessory drive system are verified during engine testing, altitude or endurance testing. The accessory pads can be loaded via water brakes or actual components to provide the desired load

as a function of speed. If overload conditions are required to be demonstrated, the test may require altitude testing to generate the appropriate conditions or demand on the selected pads. The lube system and engine control system are qualified on both the endurance and the altitude qualification tests.

Chapter 7

BEARINGS AND SEALS

by Paul R. Bissett

INTRODUCTION

Mainshaft bearings are used to accurately locate the main engine rotors with respect to the stators. They provide the capability to utilize small axial and radial operating clearances in the turbomachinery flowpath (seals, blades & vanes) which is vital for good engine performance. Bearings in aircraft gas turbines are almost exclusively of the rolling element type and usually are either cylindrical roller or ball bearings of the split ring type. Ball bearings can provide either axial or radial rotor support whereas roller bearings are only capable of significant radial support.

The basic reason for the use of rolling element bearings in aircraft engines are to minimize weight (particularly on thrust bearings), minimize friction and power loss, reduce oil flow and cooling requirements, and to have the capability to withstand significant short time overloads such as maneuver loads, hard landing loads and high unbalance loads due to turbomachinery damage (airfoil loss).

In many ways, jet engine bearings are similar to those used in automobiles and industrial equipment but three key differences exist. Jet engine bearings usually are required to operate at significantly higher speeds, higher loads and higher temperatures than other industrial bearings and as the trend for more efficient engines or higher performance airplanes continues, the operating environment for the bearings becomes more and more severe.

The temperature capability of the bearings is, however, quite limited in comparison to many areas of the engine flowpath that are in close proximity to them. Bearings in use today can operate at up to 600 °F but are cooled with synthetic oils that are limited to 400 °F. If gears are present in the bearing cavity or sump, then temperatures must be limited to 350 °F. By comparison, compressor exit temperatures often exceed 1100 °F and turbine inlet

temperatures exceed 2000 °F in the flowpath which may be located only a few inches from the bearing sump.

In order to prevent overheating of the bearings, gears and lubricating oil, sealing systems must be provided to prevent this hot flowpath air from reaching the bearing sumps and the lubricating oil flows must be sufficient to carry away heat generated internally by the bearings because of their speed of rotation. The design of the sealing and cooling systems themselves are covered in a later chapter. The design of the hardware comprising those systems will be covered in principle in this chapter.

Seals may be divided into two broad categories namely non-contacting (labyrinth) and contacting (rubbing) types. Within each category exist several different types. Engines for subsonic applications can be designed to run efficiently and reliably utilizing all labyrinth seals whereas supersonic applications normally require the use of at least some contacting seals - usually carbon rubbing seals - in order to limit air flows and temperatures which get severe at high mach number operation. Carbon seals generally leak much less air than even the best labyrinth seal designs and sometimes are preferred for reasons of cycle efficiency. However, because they rub and wear during operation they have finite life whereas labyrinth seals always operate with a small clearance between rotor and stator and normally do not wear if correctly designed. An example of each seal type is shown in Figures 7.1 and 7.2. A further function of the sealing system is to limit axial loads on the ball thrust bearings which is done by optimum choice of seal diameters to balance aerodynamic loadings on the rotors. This allows maximum bearing life to be achieved. A complete sump and sealing system, including mainshaft bearings is shown in Figure 7.3. This is the B-C sump area of the CF6-80C2 large commercial turbofan.

MAINSHAFT BEARING TYPES

Ball bearings are primarily used to carry axial or thrust type loads but may also be used for radial shaft support. An example of a typical high speed split inner ring thrust bearing is shown in Figure 7.4. It comprises a one piece outer ring, one piece cage (which is considered desirable for strength reasons when running at very high speeds), a number of perfectly spherical balls and an inner ring made in two halves with an axial split line. The reasons for this is to allow a maximum number of balls and a one piece cage to be used and still be able to assemble the bearing. Maximizing the number of balls gives the bearing the longest possible life at any specific loading. An added benefit is that by using special grinding techniques the axial end-play or float in the bearing

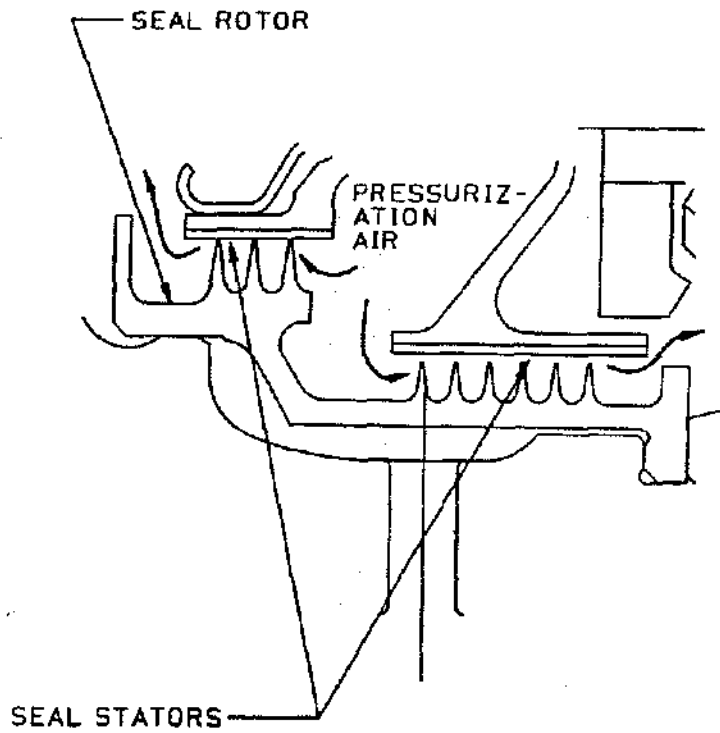


Figure 7.1 Typical Labyrinth Sump Seals

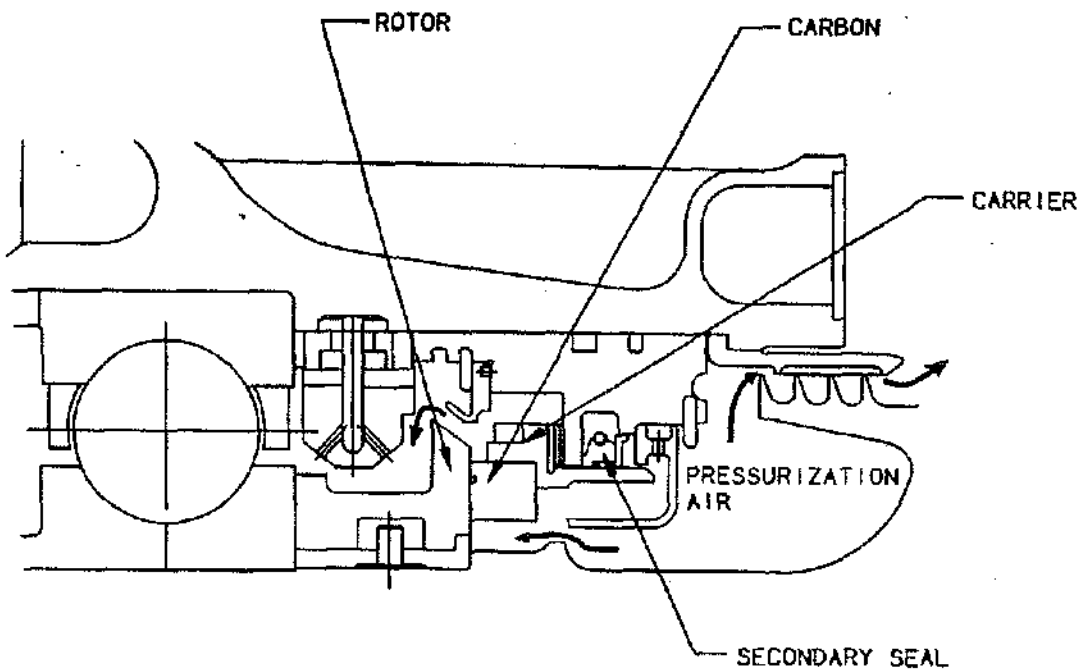


Figure 7.2 Typical Carbon (Face) Sump Seal (F101 #3 Seal)

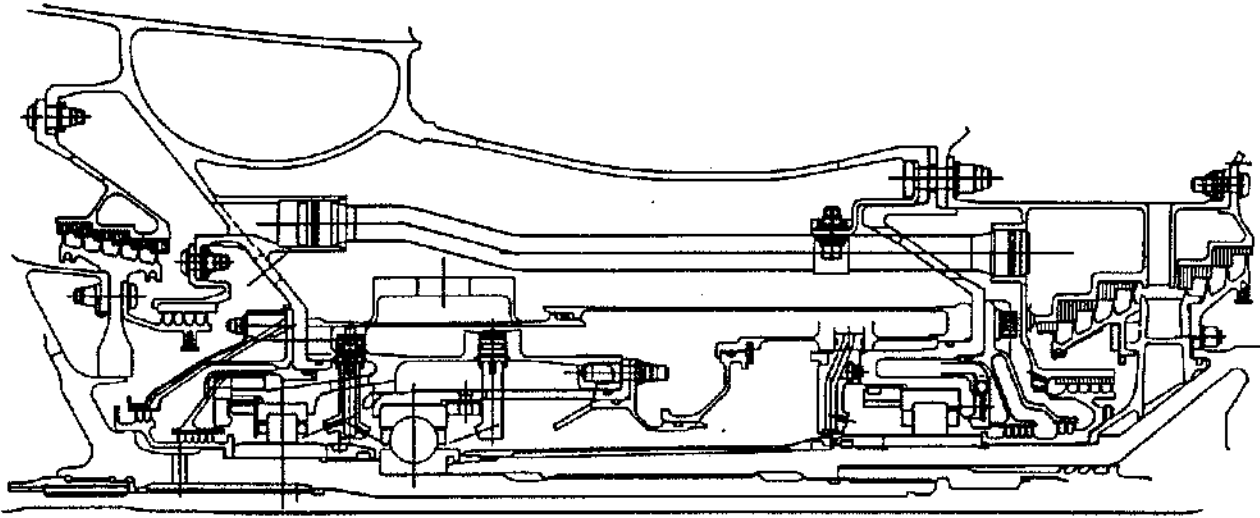


Figure 7.3 B-C Sump of CF6-80C2

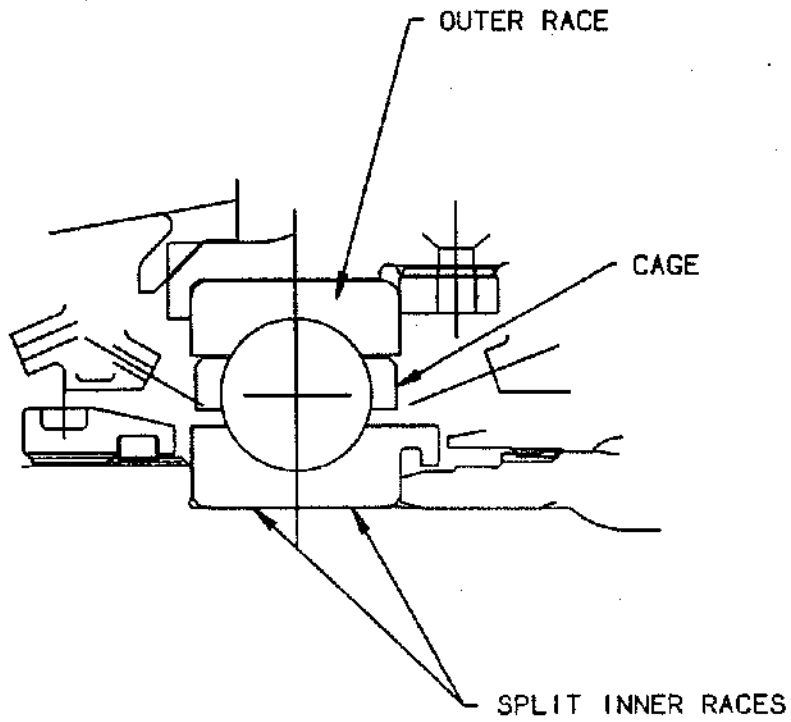


Figure 7.4 Typical High Speed Thrust Bearing

can be reduced in the split ring design which reduces axial travel in the turbomachinery rotors. Most ball bearings designs utilize a single row of balls but duplex or tandem designs which are essentially two bearings side by side have been successfully used (see Figure 7.5)

Figure 7.6 shows a typical high speed roller bearing, designed only to accept radial loads. It comprises a one-piece outer ring, one-piece cage, rollers and one-piece inner ring. Because the assembly slides together axially there is no reason to split either of the rings in order to use the one-piece cage with a maximum number of rollers. All components in both bearings with the exception of the cages are made from hardened tool steel and manufactured to extremely small tolerances; often less than half of one thousandth of an inch. Balls and rollers are matched in size to within millionths of an inch. Cage materials vary somewhat but the modern tendency is toward low carbon high strength steel of medium hardness, covered with a thin silver plating. Materials are covered in more depth later in this chapter.

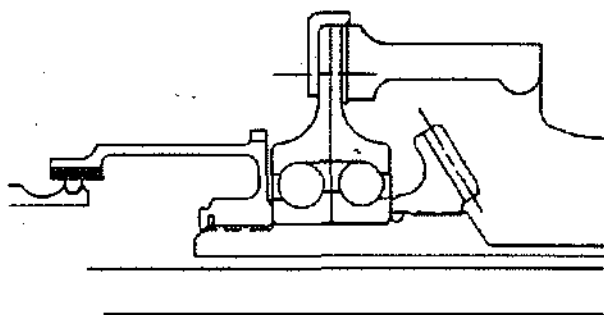


Figure 7.5 Duplex Ball Bearing Supporting Horizontal Bevel Gear On CF6-6

FATIGUE LIFE CONSIDERATIONS

The first step in the design process for either a ball or roller bearing is to establish the life requirements which should be consistent for all bearing positions in the engine. Commercial engines for airline applications usually require an L_{10} life of at least 35,000 hours while on military engines the figure is often considerably lower. It should be understood that bearing L_{10} life is the calculated time period in which 10% of a given population of bearings will have experienced high cycle fatigue failures in normal service. The remaining 90% will exceed this service life. The designer should obtain the required L_{10} life from the technical requirements for the particular engine model being designed. These lives are established to yield an acceptable failure rate per million flight hours based on an assumed average operating time on the bearings.

Next it must be realized that engines rarely operate so that speeds, loads and temperatures on the bearings are

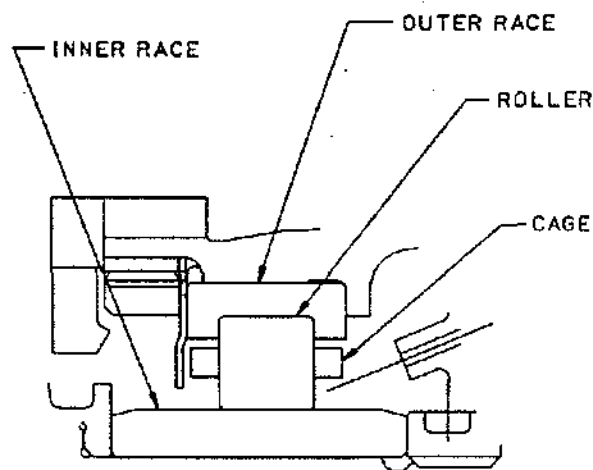


Figure 7.6 Typical High Speed Radial Roller Bearing Design - CF6-80C2 No. 4R.

constant. All three will vary depending on the power setting and altitude of the aircraft. Typical mission profiles for commercial and military aircraft are shown in Figures 7.7, 7.8 and 7.9. Bearing lives are calculated for each mission point and then combined to obtain an overall composite mission life via the following simple equation:

$$L_{10} = \frac{1}{\frac{t_1}{L_1} + \frac{t_2}{L_2} + \frac{t_3}{L_3} \dots}$$

where L_{10} is the mission L_{10} life, L_1 is the L_{10} life at condition 1, t_1 is the mission time fraction at condition 1, L_2 is the L_{10} life at condition 2, etc. Note that $t_1 + t_2 + t_3 + \dots + t_n = 1.0$ where n is the total number of mission points.

It must also be realized during the initial design process that other constraints often exist that influence the available envelope for the mainshaft bearings. Shaft stiffness stress and critical speed requirements generally dictate minimum acceptable shaft diameters which thereby defines minimum allowable inner ring bore diameter. Space available between the sump and flowpath in some cases may restrict the size of the bearing outer ring O.D. Having roughly defined bearing I.D. and O.D. further practices are applied to keep ball and roller sizes within prescribed limits. For reasons beyond the scope of this text, ball diameter should not be less than 0.1 times the bearing pitch diameter (i.e. the mean diameter between I.D. and O.D.) nor should it be greater than 0.5 times the difference between the outer radius and inner radius of the bearing. Maximum roller size should also be limited to 0.4 times the difference between the bearing outer and inner radius. Within these basic constraints the internal geometry of the bearing may be varied and optimized to yield satisfactory calculated fatigue life. Simple hand calculations may be used to get rough estimates for initial sizing for low speed bearings.

The following equations and factors are taken from the AFBMA Standards Section No. 9. The life calculated by this method is given in hours by the following equation for ball thrust bearings.

$$L_{10} = \frac{16667}{N} \left(\frac{C}{P} \right)^3$$

where C = Basic Dynamic Capacity - LBS, N = Shaft RPM, and P = Equivalent Load - LBS.

The above equation applies for inner or outer race rotation. The applied loads are converted to an equivalent load as follows:

$$P = XV F_r + Y F_a$$

where X = Radial Factor, Y = Thrust Factor, V = Rotation Factor, F_r = Radial Load - LBS, and F_a = Thrust Load - LBS. The value of the X and Y factors are a function of the ratio of the applied loads. (curve not shown)

The basic dynamic capacity for a radial or angular contact ball bearing is given by,

$$C = f_c (\cos\beta)^{-1.7} Z^{2/3} D^{1.8}$$

where β = Operating Contact Angle - Degrees (see Figure 7.10), Z = Number of Balls, D = Ball Diameter - Inches, and f_c = a factor which depends on geometry of the bearing components, the accuracy of various bearing parts and the material. (curve not shown). For balls greater than one inch in diameter, the diameter exponent is 1.4 instead of 1.8.

The above equations should not be used when bearings operate above 1.0 million DN specific speed. DN is defined as the product of bore size in millimeters and shaft speed in revolutions per minute. Computer analyses are commonly available to accurately predict ball loadings and life on high speed bearings and are also able to allow geometry optimization for other considerations that come into play at high speeds. The limited applicability of the hand calculations is because the centrifugal loads of the balls themselves which are not considered in the AFBMA equations. They do however serve to illustrate that bearing capacity and life improve as the number of balls, ball diameter and contact angle increase. Limitations on the above parameters are placed by other high speed operational considerations which will be discussed later. Number of balls in a bearing is limited only by the need for sufficient cage strength and initially can be estimated by

$$Z = \frac{dm}{(.01 + 1.18D)}$$

where Z = number of balls, dm = pitch diameter, and D = ball diameter.

For cylindrical roller bearings the following equations and factors are taken from the AFBMA Standards Section 11.0. The life as calculated by this method is given in hours by the following equation:

$$L_{10} = \frac{16667}{N} \left(\frac{C}{P} \right)^{10/3}$$

where N = Shaft RPM; P = Applied equivalent radial load - lbs, and C = Basic Dynamic Capacity.

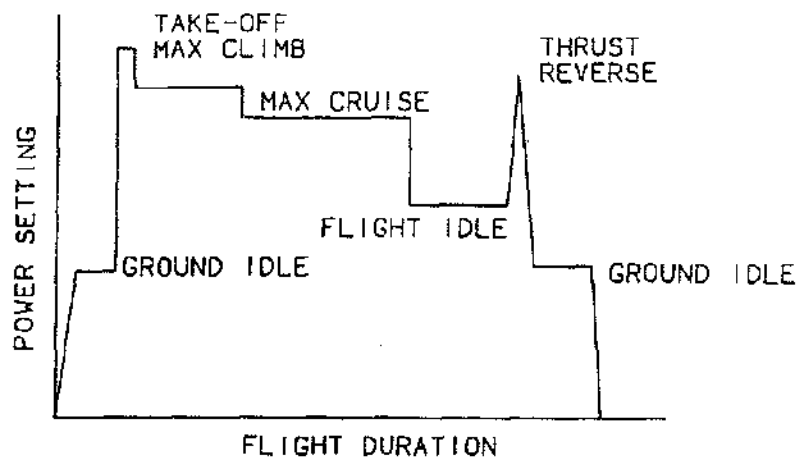


Figure 7.7. Commercial Airline Flight Profile

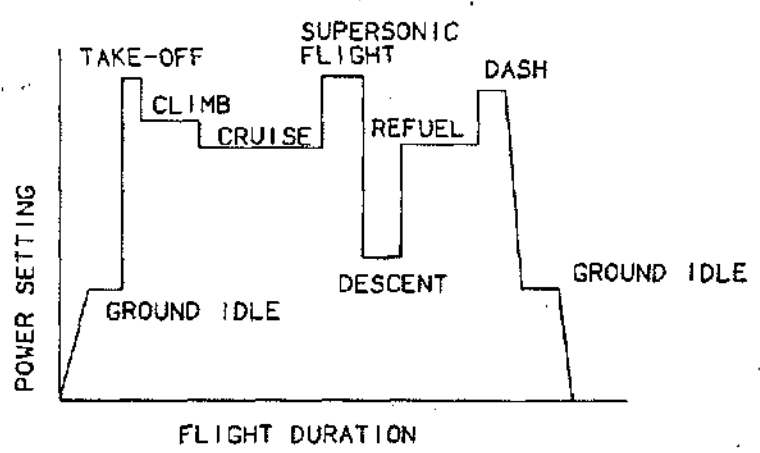


Figure 7.8 Military Duty Cycle

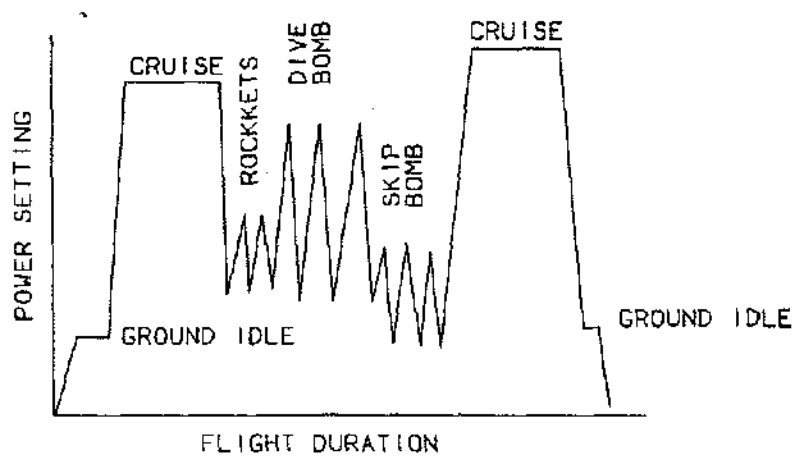


Figure 7.9 Military Multi-Mission Duty Cycle

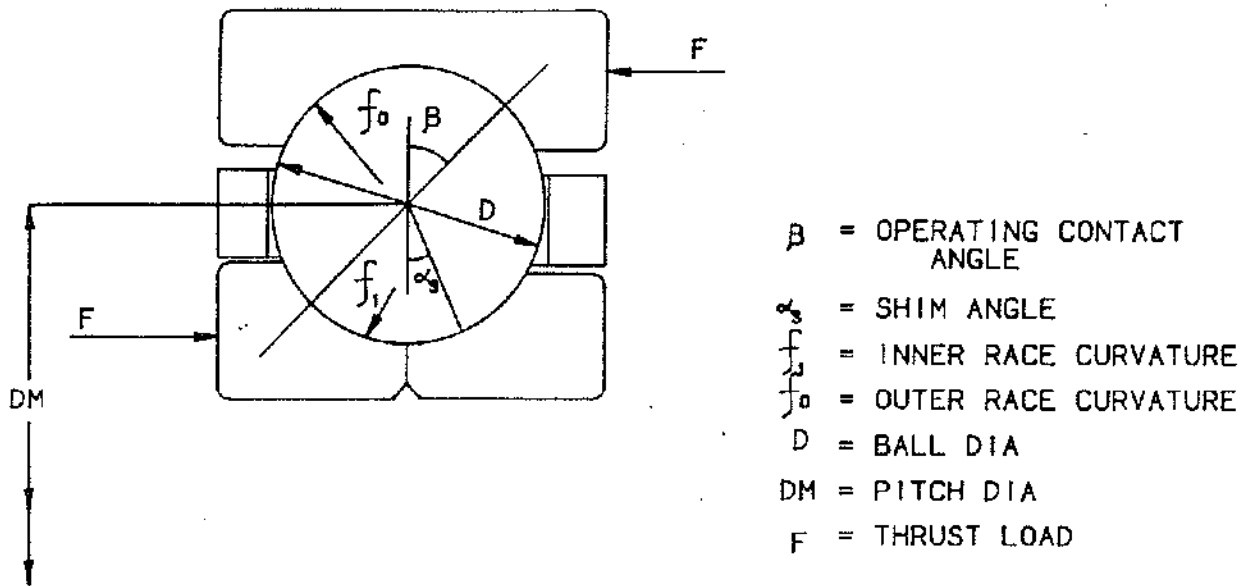


Figure 7.10 Ball Bearing Internal Geometry

The above equation applies for inner or outer race rotation. The applied load (F_R) is modified as follows:

$$P = V F_R$$

where $V = 1.0$ for inner ring rotation relative to the applied load and $V = 1.2$ for inner ring stationary in relation to the load.

The basic capacity for cylindrical roller bearing is given by:

$$C = f_c (l_e)^{7/9} Z^{3/4} D^{29/27}$$

where f_c = a factor defined by the geometrical shaft of the load carrying surfaces of the rollers and races and the accuracy of the roller grinding (curve not shown), l_e = effective length of contact between one roller and that ring where the contact is the shortest (overall roller length minus roller corner radii), Z = number of rollers, and D = roller diameter.

Again the reader is cautioned that this method is useful only for rough sizing of low speed bearings but serves to show the trend of increasing life with increasing roller

diameter, roller length and number of rollers. These parameters are also limited by other high speed considerations which can only be effectively addressed by computer analysis and will be discussed later.

Finally it should be noted that the previously described calculation techniques were originally formulated many years ago. Since that time, bearing materials have vastly improved and also the influence of elastohydrodynamic film thickness (discussed later) on fatigue life has become more clearly understood.

Therefore today's bearings demonstrate much longer actual lives than calculation would indicate. It is common to multiply the calculated life with a "life factor" depending on materials being used and elastohydrodynamic (EHD) film thickness. It is not uncommon for life factors of 20 to 50 to be obtained in actual service.

BALL BEARING DESIGN

The details of high speed ball bearing design are well beyond the scope of this text, involving extensive trade-offs between fatigue life, ball dynamics and heat

generation. This process requires a computer model to analyze and a considerable amount of experience to interpret the results based on knowledge of prior successful designs. It is however possible to describe the principles involved in relatively simple terms. Refer to Figure 7.10 for terminology used.

Ball Dynamic Analysis If the outer ring is stationary and the inner ring rotates it must first be appreciated that the balls and cage will rotate about the shaft centerline at a speed different from that of the inner ring. This speed can be estimated by hand calculation reasonably accurately using the following equation:

$$N_c = \frac{N_i}{2} \frac{(1 - D \cos \beta)}{dm}$$

where N_c = cage speed in rpm, N_i = inner ring speed in rpm, D = ball diameter, dm = pitch diameter, and β = contact angle in degrees. For a typical thrust bearing these values may be: $dm = 10.0$, $D = 1.25$, $\beta = 30^\circ$, so that $N_c \approx 0.45 \times N_i$.

If both inner and outer races rotate (at N_i and N_o rpm) the equation becomes

$$N_c = \frac{1}{2} \left[N_i \frac{(1 - D \cos \beta)}{dm} + N_o \frac{(1 + D \cos \beta)}{dm} \right]$$

and the ball speed about its own roll axis is given by:

$$N_r = \frac{1}{2} \frac{dm}{D} \frac{(1 - D \cos \beta)}{dm} \frac{(1 + D \cos \beta)}{dm} (N_o - N_i)$$

Even though the cage generally rotates at less than half the speed of the shaft (for a stationary outer ring), at high speeds in excess of one million DN, the cage speed is high enough to impose significant centrifugal loads on the balls. Figure 7.11 illustrates the results of this effect.

The low speed bearing on the left has very little centrifugal load on the balls and the operating contact angles on inner and outer raceways are nearly equal. The actual ball loads on inner and outer raceways would also be nearly equal and given by:

$$P_i = P_o = \frac{F}{Z \sin \beta}$$

where P_i and P_o are the inner and outer raceway contact loads, F = the net thrust load on the bearing, Z = number of balls, and β = operating contact angles (inner and outer).

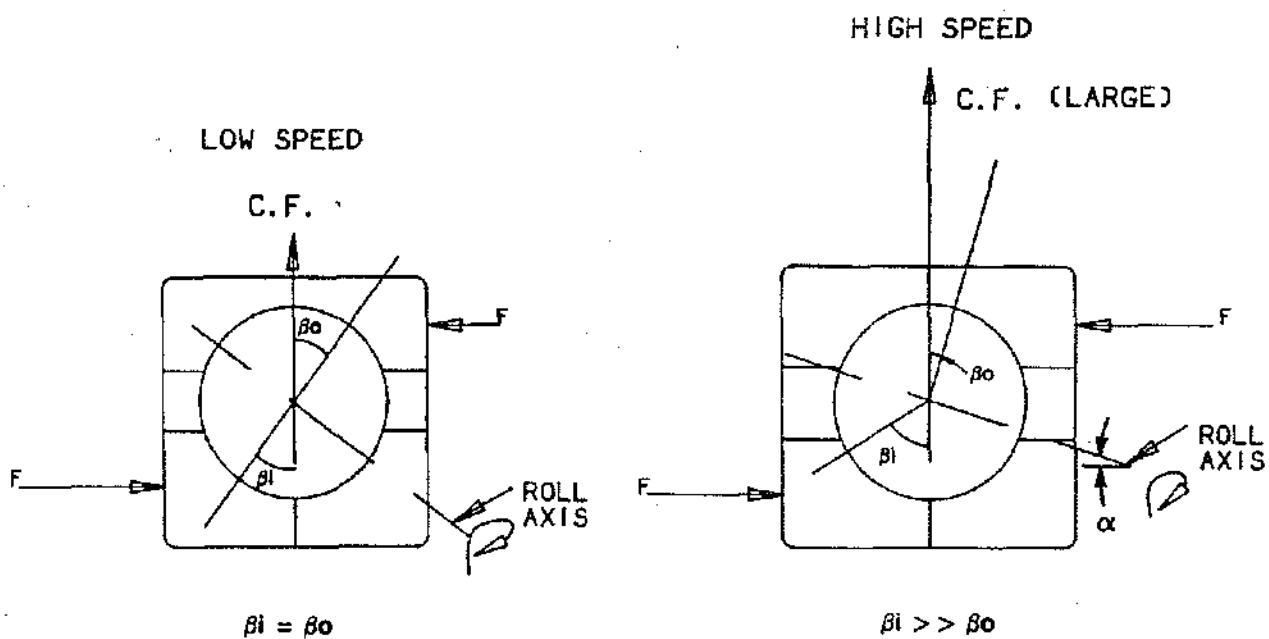


Figure 7.11 Speed Effects On Operating Contact Angles

This of course only holds true for a bearing taking pure thrust and no radial load so that all balls are equally loaded. At high speed the bearing on the right has significant centrifugal (C.F.) load vectors on each ball. This causes unequal inner and outer contact angles in order to balance the extra radial ball load. The outer race contact angle must get smaller and the inner will correspondingly increase because the total bearing clearance is assumed unchanged. The ball rolling axis will align primarily at right angles to a line normal to the outer race contact and thus increased sliding and heat generation must occur at the inner race because of it's physical displacement from the roll circumference. At high contact angles and high speeds the sliding and heat generation can degrade the lubricant films in the contacts and cause bearing damage.

This effect can be reduced by reducing the design contact angle but this of course reduces fatigue life as previously shown. Making raceway curvatures larger (less conforming) will also reduce heat generation at the contacts but this also involves a fatigue life penalty. It will also be noted that during one cage revolution the roll axis of the ball travels in a cone shaped trajectory with the apex of the cone at the centerline of bearing rotation.

Thus during one revolution the roll axis must swing through a total angle of 2α . This requires a gyroscopic moment to achieve and the moment must be provided by friction forces at the raceway contacts. At very high speeds the available forces may not be sufficient and gyroscopic spinning will occur at the contacts. This in some cases may cause distress due to additional heat generation and lubricant film breakdown. Gyroscopic spinning can be reduced by reducing the contact angle but as previously stated, a fatigue life reduction results.

A further consideration is maximum ball excursion occurring in the bearing. Figure 7.12 shows a bearing with combined radial and thrust loading (F_R & F_A). The radial load is supported by a number of balls in an arc as shown with the highest loaded ball being directly under the load and the balls in the rest of the bearing giving little or no radial support. This results in a contact angle change as the balls travel through the radial load zone. The contact angle reduces to balance the increased radial forces on the balls in the load zone. Because of this, the balls in the load zone slow their orbital velocity according to the previously shown equation for cage speed whereas the rest of the balls want to run faster. This deviation from nominal cage speed is the ball excursion

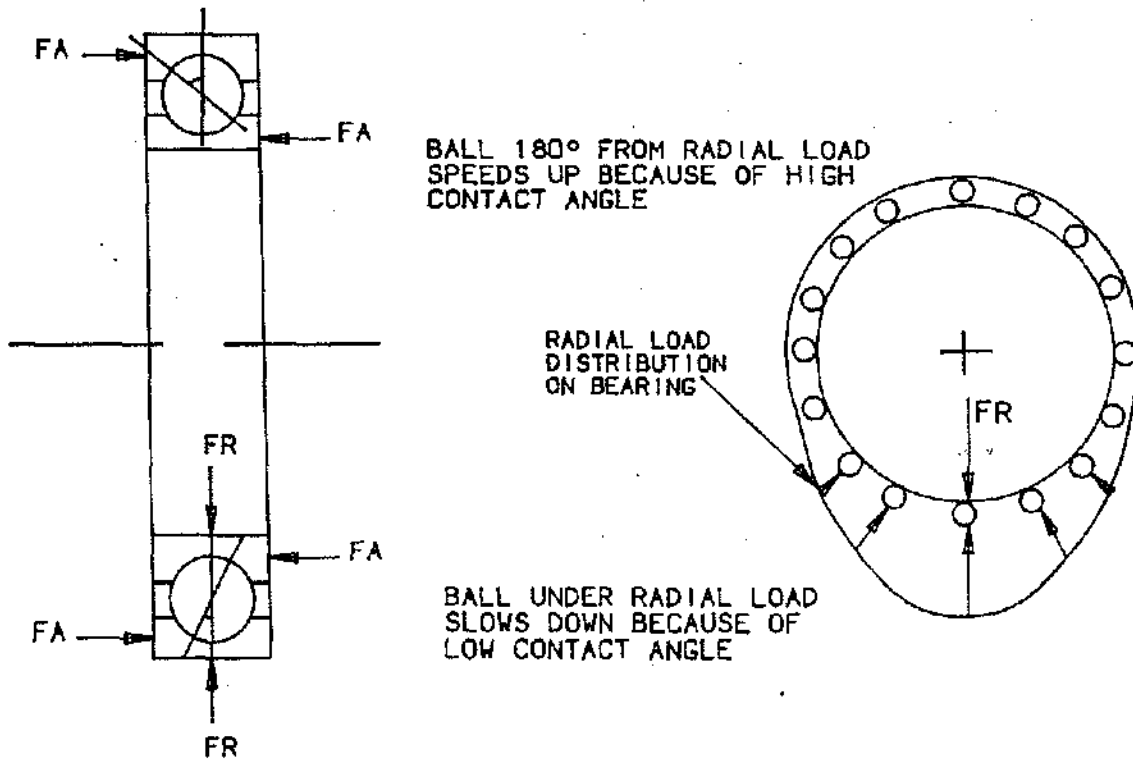


Figure 7.12 Ball Bearing With Combined Radial & Thrust Loads

and is usually expressed as the circumferential distance the ball will deviate from its nominal position during one half cage revolution. In a real bearing the balls are only free to do this until they use up the clearance which exists in the cage pockets and then they must slide in order to orbit at the average cage speed. At high speeds and with combinations of approximately equal radial and thrust loads the cage loadings and rapid sliding that has to occur can quickly cause bearing failure. Misalignment of the inner and outer races causes similar effects to occur, again because of contact angle changes from ball to ball (see Figure 7.13).

If it is not possible to get a more favourable loading situation or reduce misalignment to acceptable values the designer must allow for ball excursion in other ways. A first step may be to increase the ball to cage pocket clearance which may also involve reducing the number of balls in order to maintain sufficient cage strength (web thickness). If this approach is not practical, the calculated excursion may be reduced by reducing contact angles, and increasing one of the raceway curvatures (usually the inner). Once again, all of the above actions will reduce the calculated fatigue life. As a general rule

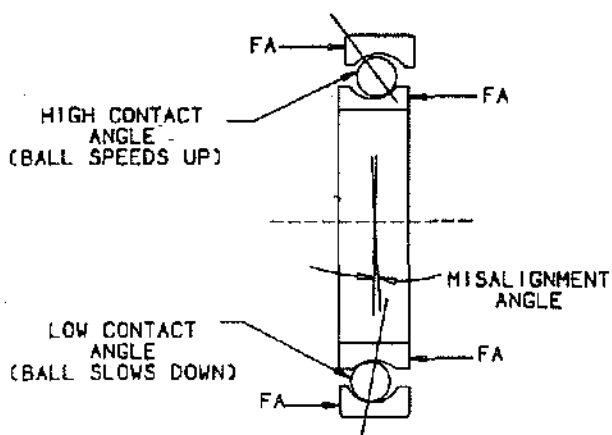


Figure 7.13 Ball Bearing With Angular Misalignment Between Inner & Outer Races

the excursion should be kept to a value equal to or lower than the pocket clearance. However it has been found that when loading is light and the bearing is well lubricated, excursions much higher than the pocket clearance may be tolerated without damage. One notable example is the large no. 1 fan thrust bearing of the CF6-50 engine which has calculated ball excursions in the neighborhood of one inch under certain load conditions but has minimum pocket clearance of 0.030 inch.

This section has attempted to show that the successful design of a high speed mainshaft ball bearing involves many trade-offs in which geometry is varied and optimized not only to maximize fatigue life but also to obtain satisfactory dynamic characteristics. The equations involved are extremely complex and can only practically be solved iteratively using computer models. The results of the computer analyses require considerable depth of experience to evaluate and a large reliance is put on previous successful designs and lessons learned on other engines. Unfortunately there are no standard text books available to the designer that would help in the optimization process other than G.E. design practice 3255 - Main Bearing Design.

Heat Generation and Cooling. The following remarks apply to both ball and roller bearings and are intended to give the reader a concept of why heat generation and cooling is of vital importance to a successful high speed bearing design. The details of how cooling flows are estimated and how lubrication systems are designed are covered in Chapter 8.

When speeds are very low such as in wheel bearings of automobiles, the heat generated by the bearings is minimal. It occurs primarily because of rolling friction losses at the raceway contacts and sliding friction between balls or rollers and the cage. The amount of lubricant required in such cases is very low and can often be accomplished by packing with grease which is prevented from leaking by seals. The small amount of heat generated is conducted into shafts and housings and then dissipated by natural convection. In jet engines this approach is not permissible because of the speeds involved, the rate of heat generation is much higher; 5 to 10 horsepower being not uncommon and this requires a more efficient removal system. Secondly, because the sumps are often in the hot sections of the engine there are no heat sinks available in the immediate vicinity to remove heat by convection. Therefore, copious quantities of oil are used to remove the heat generated, being pumped into and out of the sump by engine driven pumps. The oil is in a closed system and after being removed from the sump it passes through a cooler where it is cooled by the main engine fuel flow. Chapter 8 deals with the lubrication system in detail. The main point to be remembered here

is that without an efficient oil cooling system the bearings would reach such high temperatures that failures would occur in an extremely short time. The amount of oil actually needed for lubrication is extremely small compared to that needed for cooling because the lubricant films in the raceway contacts usually are only a few millionths of an inch thick, regardless of oil flow. This will be discussed later.

One final point worth noting is that in high speed applications a new significant source of heat generation is that energy required to pump the oil from the bearing itself. Because of the high oil flows required there is a drag loss, often called "churning loss" that occurs because of the balls or rollers ploughing through the oil that is momentarily trapped in the bearing prior to being flung out by centrifugal force. At very high speeds this can be the highest source of heat generation in the bearing. It has in fact been shown by rig test that as oil flow is varied from low to high values, bearing race temperatures at first fall, but after reaching some minimum value, actually begin to rise again as the churning losses overpower the oil's ability to remove the heat generated. It is clear that optimization of oil flow is a key factor in maintaining a cool and thermally stable bearing system.

Static Capacity/Secondary Damage Static capacity is defined as that static load which corresponds to a permanent deformation of ball and race at the most heavily stressed contact of .0001 of the ball diameter. The basic static capacity in pounds is given as:

$$C_0 = 1780 ZD^2 \cos\beta$$

where Z = number of balls, D = ball diameter in inches and β = contact angle in degrees.

The significance of this parameter is in the consideration of overload conditions. Mainshaft bearings are subject to occasional overloads due to turbomachinery damage which is normally because of airfoil loss from the fan, compressors or turbines. The unbalance loads caused by such events have to be reacted by the bearings and up to certain values (defined in the engine technical requirements) should not cause permanent bearing damage. It has been found by rig and engine test that at speed, a bearing is able to withstand a load up to twice its calculated static capacity provided the outer race is mounted in a fairly rigid housing. If the outer race is supported on an oil film as is often the case to reduce normal vibration amplitudes, then the bearing load capability is reduced to 1.6 times to static capacity. This design consideration in some cases may be the one that basically sizes the bearing capacity required, rather than fatigue life considerations. Which criterion is most important can only be assessed by looking at the maximum values of blade-out

loads at each bearing position on the engine and comparing them with respective static capacities. The importance of static capacity and blade-out capability is that some airfoil loss events are not unusual, particularly on fans and turbines and if the bearing fails due to overload it is a sudden rapid failure where the rollers or balls groove deeply into the raceways. This can cause far more severe turbomachinery damage than the initial event and is of course very undesirable. The bearings should therefore have enough static capacity for reasonable unbalance events which are usually defined in the engine technical requirements.

ROLLER BEARING DESIGN

Of the foregoing remarks on ball bearings, many such as manufacturing accuracy, heat generation and cooling and static capacity/blade out capability apply equally well to roller bearings. However, high speed roller bearings present their own unique challenges in obtaining successful operation.

The roller bearing shown in Figure 7.6 is typical of those on many General Electric jet engines having roller guide flanges integral with the outer ring. The flanges have a very small (typically 0.001 to .002 inch) clearance with the ends of the rollers which serve to guide them on the raceway and overcome their natural tendency to skew as they orbit in the cage. The inner diameters of the guide flanges usually have a small clearance with the cage (typically .015 to .030 inch) and keep it centered with the raceways. The clearance between the cage and the inner race is typically much larger (.200 to .300 inch) in order to give large target area for oil impingement from the lubrication jet(s). The rollers normally are retained by machined tangs on the cage cross bars which run between the rollers. This makes the rollers, cage and outer ring a non-separable assembly.

Another common configuration when jet lubrication is not used would have the roller guide flanges on the inner ring and the guiding surface for the cage between the cage I.D. and guide flange O.D.s. In this case the inner ring, rollers and cage form the non-separable assembly and the outer ring is a plain cylinder. This configuration is particularly suited to an internal lubrication system whereby multiple oil holes are drilled from the bore of the inner ring to the intersection of the guide flanges and raceway and oil is allowed to flow from the shaft and through the race to lubricate and cool at the ends of the rollers where it is most needed. An example of this is shown in Figure 7.14. It is often a more efficient lubrication system because it uses centrifugal force to aid in pumping the oil through the bearing. There are no hard

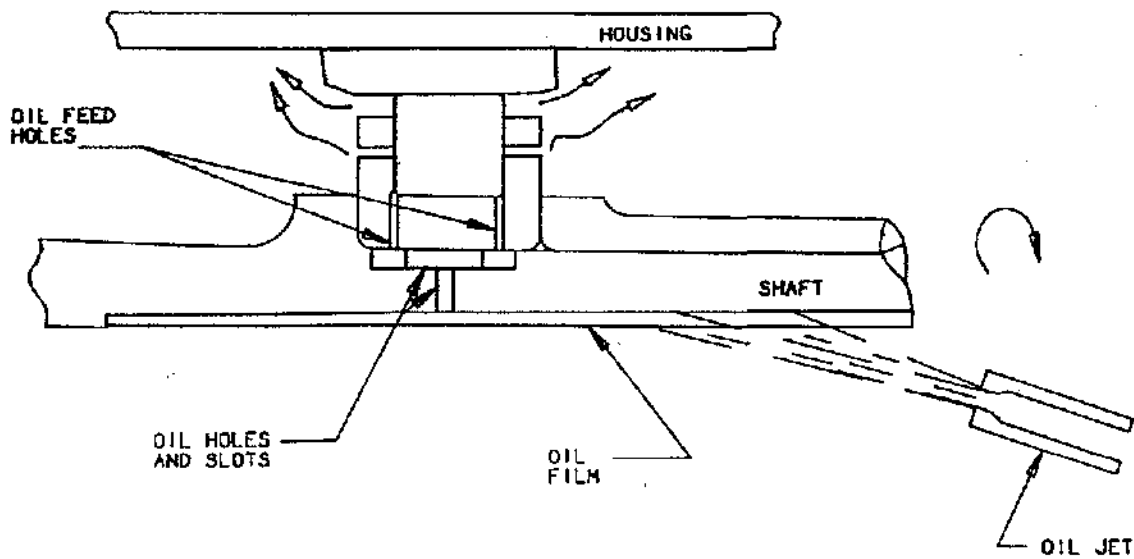


Figure 7.14 Under-Race Oil Cooling Scheme For A High Speed Roller Bearing

and fast rules for which type of bearing will work best in any application and the designer should be guided by successful applications in other G.E. engines. There are also other designs, though less common where the roller guide flanges are on the outer ring and the cage is inner-ring guided and vice versa.

Low speed industrial bearings sometimes feature cage guided rather than flange guided rollers but this is not an aircraft engine practice.

Figure 7.15 shows details of a high speed roller. Generally the ratio of length to diameter is kept close to unity as the best compromise between maximum fatigue life and reducing propensity to skewing. This is often termed a "square" roller by designers. Skewing will be discussed later. It will be noted that the roller is not perfectly cylindrical but is uniformly crowned at each end. This reduces its load carrying ability under perfect alignment conditions but prevents stress concentrations from occurring at the ends when alignment of the raceways is not perfect - which is normally the case. The radius of the crown is usually quite large (20 - 30 inches). A centrally located portion of the roller is uncrowned and is often referred to as the "flat length". This is normally 50 - 65% of the roller effective length. Accurately ground corner radii are at the junction of the crowned

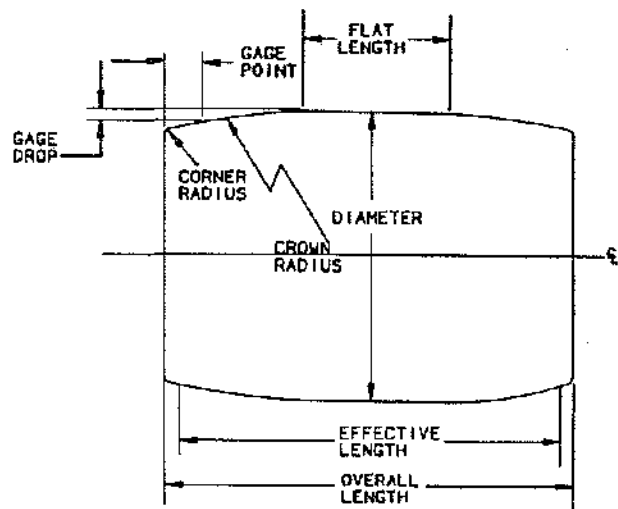


Figure 7.15 Roller Nomenclature

portion and the roller end faces. The total roller length minus twice the corner radius defines the effective length. Rollers for high speed bearings are made to extremely tight tolerances in order to maintain good dynamic balance at high speeds of rotation and to give a uniform stress distribution axially and circumferentially within the bearing. Diameters are usually matched within 50 millionths of an inch, lengths within .0001 inch and corner radii runouts are often .001 inch or less. Similar tight controls are placed on raceway taper, waviness and other characteristics affecting roller stress distribution.

Clearance Control Figure 7.16 shows a plot of bearing life versus operating IRC (Internal Radial Clearance) for a typical high speed roller. Maximum life occurs at zero clearance when the zone of loaded rollers maximises at near 180°. As the clearance becomes negative, life falls rapidly because the radial tightness can only be absorbed by stretching the races in the hoop direction and by increased deflection at the roller/raceway contacts. A bearing is very stiff in both these deflection modes so that high raceway stresses result and the fatigue life drops. Another phenomenon that occurs as soon as the

bearing is about .001 inch negative in IRC is micro-pitting of the raceways. The full understanding of this mechanism has yet to become clear but it appears to be a lubricant film breakdown caused by small amounts of sliding in the raceway contacts under high Hertzian (contact) stresses. The film breakdown momentarily allows metal to metal contact at the surface asperities leaving minute pits as the asperities weld, work harden and tear out of the raceways. If allowed to continue, the micropits progress quite rapidly to surface fatigue and the bearing will fail at a much shorter life than the calculated subsurface fatigue life. In order to avoid this phenomenon the minimum calculated IRC at any operating condition and under the worst tolerance stack-up should never be less than zero. As clearance increases to a positive value, calculated life falls slightly because fewer rollers support the applied load and raceway stresses are increased. In fact the actual life obtained will again fall rapidly as the clearance increases beyond .002 inch because of premature skidding failures which will be discussed later. Therefore a high speed roller bearing may have to have its clearance or IRC controlled very carefully within the band of 0.0 - 0.002 inch in order to operate successfully. This includes all tolerance and thermal

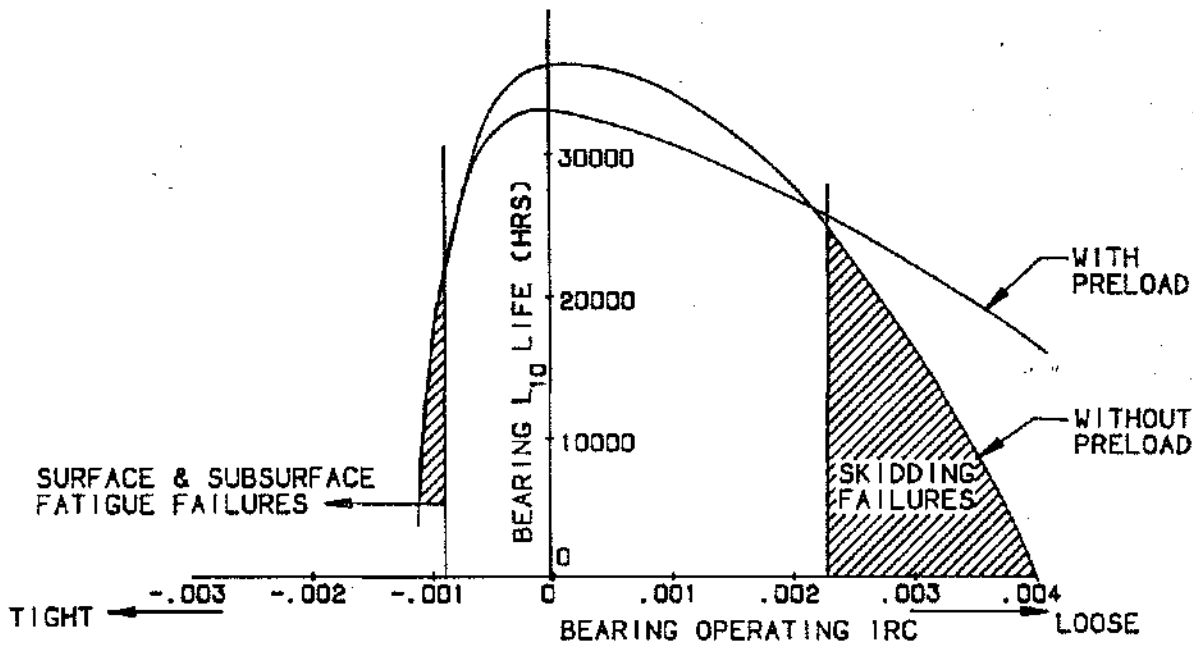


Figure 7.16 Roller Bearing Life Versus Operating Clearance (IRC)

effects and usually presents a considerable challenge to the designer. Even with very tight control of mechanical tolerances the overall stack-up often approaches .002 inch. Accurate knowledge of operating temperatures of shaft, bearing rings, rollers and support housing are vital in estimating operating IRC. An error of only 25 °F can cause a .001 inch error in calculated IRC, and this constitutes 50% of the total allowable range. Current state of the art heat transfer techniques are not capable of yielding the required accuracy and it is usually necessary to determine IRC and race temperatures from early development engine testing and make adjustments from there if necessary. If the acceptable range of IRC is too small to be practically attainable, the upper bound may be extended by using a radial preload to suppress skidding damage at higher IRC values. This is illustrated also in Figure 7.16 and does involve some life penalty because of the preload involved. Preloading is discussed in a later section.

Cage Slip The theoretical cage speed for a roller bearing may be calculated accurately by the following equation:

$$N_c = \frac{1}{2} \left[N_i \frac{(1 - D)}{d_m} + N_o \frac{(1 + D)}{d_m} \right]$$

where N_c = Cage speed in RPM, N_i and N_o are inner and outer race speeds in RPM, D = roller diameter inch, and d_m = bearing pitch diameter inch.

This is very similar to the equation for a ball bearing except that there is no contact angle involved. It should be appreciated that the torque to drive the cage at this theoretical or sometimes termed "epicyclic" speed, comes only from the loaded rollers. In a bearing with positive clearance and say 30 rollers, there may be only 6 carrying any load. The remainder of the rollers are pushed by the cage through the non-loaded zone of the bearing until they reach the load zone and begin to drive the cage again. The non-loaded rollers constitute a drag torque on the cage which is made up of rolling friction losses, cage friction losses and churning losses (see Figure 7.17). As speed increases all three components increase and may reach a level at which the driving rollers cannot provide enough torque to maintain equilibrium so cage speed falls until equilibrium is restored. This phenomenon is known as cage slip and is usually referred to as a percentage which is given by:

$$\text{Cage Slip \%} = \frac{(N_c - N_a)}{N_c} \times 100$$

where N_c = epicyclic cage speed and N_a = actual cage speed.

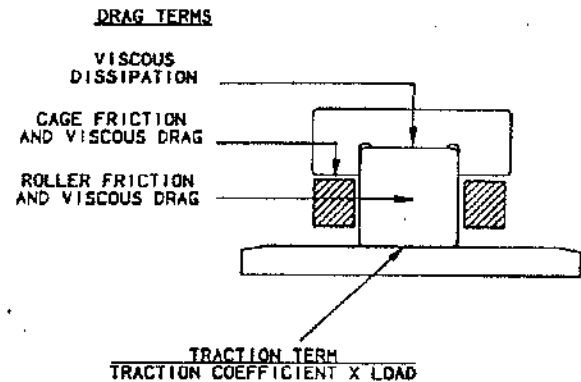


Figure 7.17 Schematic Showing Drag Terms and Traction Term. If Drag Terms > Traction; Skid Occurs. (Inner Race Rotation)

Small values (5-10%) of cage slip are normal in high speed bearings and are not of concern. The design practices recommend a maximum of 15% though higher levels can be tolerated under special conditions. The danger of running high slip rates is that if load is suddenly applied to the bearing, damage may occur to the rollers and inner race as they try to accelerate the cage to its new equilibrium value. Such damage is often termed skidding damage and takes the form of rapid wear to the inner race and even more rapid uniform roller wear. This would of course result in a large increase in IRC and an even higher cage slip rate. It is not unusual for a skid damaged bearing to have all rollers worn uniformly by several thousandths of an inch on their diameters, but little else obviously visually wrong with the other bearing components.

The key to avoiding skid damage is either to avoid high rates of load application at high steady state slip rates or, if this is not possible, limit the slip rate itself below 10-15%. This may mean for instance that on a military fighter engine application where the main bearings may be subject to frequent sudden maneuver loads, slip rates must be limited more than in a bomber or commercial airliner application where sudden maneuvers and power level changes are infrequent.

Preloading of Roller Bearings As stated in the last section, cage speed normally seeks a value that puts driving and drag forces in equilibrium. If this speed results in unacceptable slip, then corrective action is necessary, and load is the only really significant parameter that can be varied to increase the drive or traction forces in the bearing. Drag may be reduced by reducing the total number of rollers or using inner ring roller guide flanges but this may not always be practical for other reasons. In such cases a preload may be built into the bearing system so as to guarantee a minimum load regardless of the normal externally applied loads (lg, unbalance, backbone bending and maneuver). Three basic techniques are available to achieve this: mechanical offset, bilobe, and trilobe.

The first method can only be used on a system with three or more bearings on one shaft because it achieves the preload by radially offsetting a bearing against the others, causing deliberate misalignment loading which is always present. This technique appears simple at first but it requires accurate knowledge of bearing housing spring rates, tolerance stackup and external loads, all of which may conspire to negate the preload. If these factors can be controlled to be a small influence on overall preload, then the mechanical offset technique is usually very cost effective, requiring that the bearing housing diameter is off-centre by a small amount from the housing rabbet diameter. It is used on the CFM56-5 engine to preload the 3R roller bearing.

Using a bilobe to give preload is a well known technique that has been in use for many years on engines such as the CF6-6, -50, T64, TF39, LM2500 and CF6-80C2. It consists of an accurately ground profile on either the outer raceway, outer ring O.D. or outer ring housing to give a radial pinch at two points on the bearing 180° apart. This guarantees a minimum internal load on the bearing, regardless of externally applied loads. The ground profile of the race is made so that a gradual transition occurs into the region of maximum pinch or preload. Early bilobed bearings were sometimes made by physically deflecting a race into a bilobe, grinding it perfectly round, then allowing it to spring back into a "mirror-image" bilobe. However, nowadays, more accurate cam grinding techniques are generally used.

The trilobe is less commonly used, being found in production only on the T700 and CF6-80A/C2 engines. It is similar in concept to the bilobed design except that there are three equally spaced lobes or load zones instead of two. These are always manufactured by cam grinding rather than the deflection method. Trilobes are used when high preload values are needed because the bearing rings have five times the bending stiffness in three point versus two point bending. Therefore for a specific

value of lobe height on the ring, much higher preload values result.

The choice of preload method used is influenced by factors such as operational IRC variation, preload value needed, engine assembly sequence, sump thermal distortion and others. Some of these factors also influence how a bilobe or trilobe is incorporated i.e. ground into the raceway, outer race O.D. or housing. Sometimes the same profile is ground on to raceway and O.D. so that the ring cross section is constant. This maintains the outer ring O.D. roundest in the assembled condition which may be desirable in some cases.

Computer analyses are available to predict cage slip and the effect of preload. The method of attaining that preload and the manufacturing and assembly considerations are then determined by the designer based on a trade-off of the aforementioned factors. Figure 7.18 shows schematically the typical roller load distributions resulting from the various preload methods, as determined by the computer analyses.

Roller Skewing and End Wear All rollers have a tendency to skew about their roll axes unless geometry and alignment is perfect and raceway taper non-existent. In practice these factors causing skewing are always present to some degree and at high speeds the skew rates and loadings on the rollers can get quite high. That is why accurately machined guide flanges are configured into high speed roller bearings for successful operation. Clearance between the roller ends and flanges is maintained at a low (.001 - .002 inch) value so as to limit the skew angle through which the roller may travel before correcting forces are generated. In addition the roller and raceway geometry is accurately maintained and external factors such as misalignment and thermal taper minimized to reduce the tendency to skew. If this practice is not followed, rapid wear of the roller ends and guide flanges can occur until the forces are being primarily resisted by the cage. At this point a rapid cage fatigue failure will take place leading to a general failure of the bearing. In addition to the aforementioned precautions, a small taper or layback angle is usually ground into the guide flange surfaces to enhance oil film generation and reduce wear.

In general the designer must rely on experience and good design practices to avoid skewing wear problems. Although computer codes exist to predict roller skewing moments, they do so usually by a static force balance routine which will predict trends but not accurate absolute values. For a true estimate of the forces involved a full dynamic analysis is required, and while they do exist, they try the capacities of even the more powerful computers and are therefore not useful as design tools.

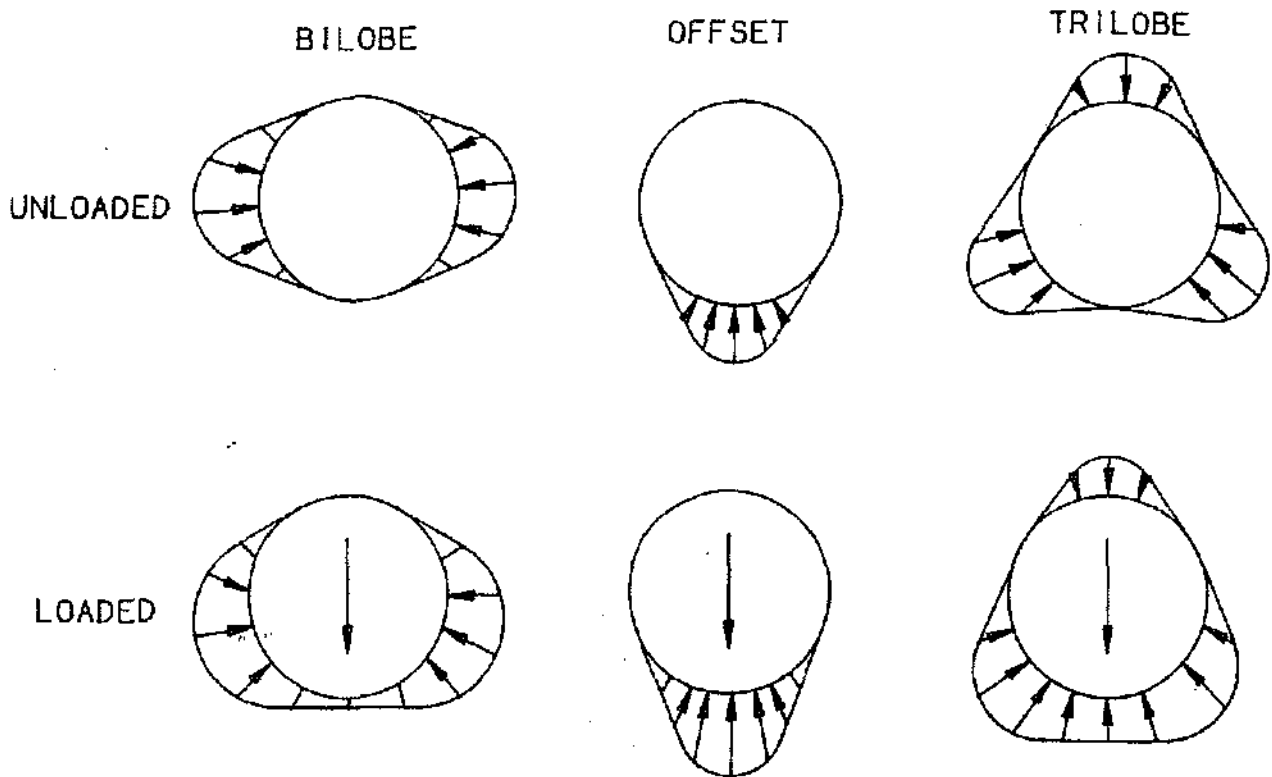


Figure 7.18 Roller Load Distributions For Different Preload Schemes

Small routines do however exist to optimize flange geometry for reduced wear and should be used if skewing becomes a concern.

Static Capacity/Secondary Damage. Almost all of the previous remarks on this subject with regard to ball bearings also apply to roller bearings. In fact roller bearings always see the effects of high unbalance whereas because of redundant spring mounts commonly used to radially "float" ball thrust bearings, they often experience no radial overload at all. Again, in order to limit secondary damage to the engine, sufficient static capacity must be built into the bearing so that the dynamic loads do not exceed twice the capacity. The equation for capacity in this case is given by:

$$C_0 = 3120 Z l_e D$$

where C_0 = static capacity - lbs, Z = number of rollers, l_e = roller effective length - inches, and D = roller diameter - inches. As with ball bearings, if the outer race is mounted in an oil film rather than being rigidly mounted, the allowable load is only 1.6 times C_0 .

ELASTOHYDRODYNAMIC LUBRICATION

The field of elastohydrodynamic (EHD) lubrication is vast and any detailed description is well beyond the scope of this text. It will only be attempted to explain very simply the principles of EHD and why knowledge of it is so crucial to bearing design. The EHD lubrication regime exists between the boundary lubrication regime, where significant asperity contact and surface wear usually occur, and the full film regime where classical hydrodynamic theory predicts complete surface separation and no wear. It was observed for many years that often highly loaded lubricated contacts such as gears, cams and rolling element bearings exhibit no signs of wear during operation which would indicate full separation of the rolling surfaces even though hydrodynamic theory could not predict sufficient film thickness. Various modifications to the theory were sought and after considerable theoretical and experimental research the key limitations to classical theory were thought to be those of rigid surfaces of contact and constant lubrication viscosity regardless of contact pressure. At the relatively low

pressures existing in hydrodynamic bearings, these assumptions were fairly accurate, but in rolling element bearings and gears where contact pressures often exceed 200,000 psi they were questionable. Theoretical analyses were able to establish contact shapes and areas under load, and high pressure viscometers were used to experimentally verify a large increase in viscosity with pressure. This led to a simple approximation for viscosity at pressure:

$$\mu = \mu_0 e^{\alpha p}$$

where μ = viscosity in centipoise (Cp), μ_0 = viscosity at atmospheric pressure (Cp), α = pressure viscosity coefficient for each oil type, and p = contact pressure in psi. With realistic values of pressure and pressure viscosity coefficient, this equation would predict a viscosity increase of three orders of magnitude or more.

Using this model and accounting for elastic contact deflections, full film lubrication could be predicted in even very highly loaded contacts. In 1959 Dowson and Higginson published the following semi-empirical formula for film thickness in a "line" contact (i.e. curved surfaces infinitely long)

$$h_0 = \frac{1.6 (\mu_0 U)^{-.7} \alpha^{-.6} R^{.43}}{E^{.03} W^{.13}}$$

where h_0 = minimum EHD film thickness, μ_0 = viscosity at atmospheric pressure, U = average entrainment velocity into the contact, α = pressure viscosity coefficient, R = radius of equivalent cylinder for the contact, E = elastic modulus of equivalent cylinder, and W = load per unit width of the contact.

As can be seen from the general form of the equation, for constant contact geometry (R) the film thickness is strongly dependent on viscosity, entrainment velocity and pressure viscosity coefficient but weakly and inversely dependent on Young's modulus and unit loading. Figure 7.19 shows contact shape and pressure distribution for the dry "Hertzian" and lubricated EHD conditions. The entrainment velocity is the average of u_1 and u_2 . These surfaces in the converging inlet to the contact pull oil into the entrance to the contact and raise both pressure and viscosity. When the oil enters the Hertzian part of the contact, pressure and viscosity become so high that there is no time for the oil to flow back out of the contact and the film supports the load. It should be remembered that the film is extremely thin compared to the size of the contact. If the contact was as long as a football field, the film would still only be ankle deep! Accurate knowledge of the EHD conditions existing in a bearing is important because it can predict the likelihood of excessive metal to metal contact and wear, has a big

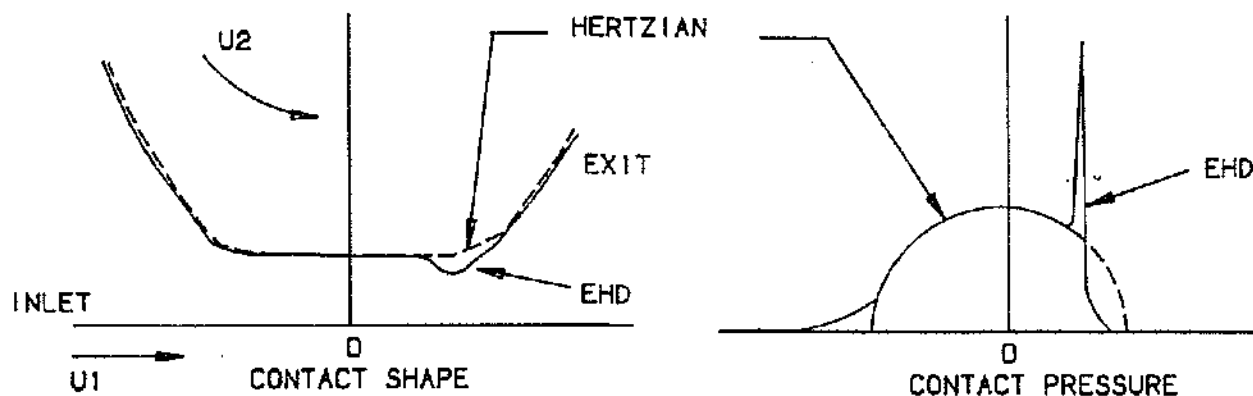


Figure 7.19 Contact Shape and Pressure Distributions - Hertzian and EHD

influence on fatigue life and is needed to make meaningful cage slip calculations.

One other term that must be introduced is specific film thickness, often referred to as lambda ratio (λ). It is defined as the ratio of calculated minimum film thickness to the composite surface roughness of the two surfaces separated by the oil film.

When the calculated λ is above 1.6, full surface separation exists and wear of the surfaces should not be observed. At ratios less than this, progressively more and more asperity contact occurs between the surfaces and increasing wear is observed. In addition, Figure 7.20 illustrates the effect on bearing fatigue life factor of λ . Using curve A for ball bearings using C50TF56 premium M50 steel the life factor increases from 11 to 34 as lambda increases from 1 to 2. In other words the bearing life would increase by more than 3 times.

Conversely as λ drops from 1.0 to 0.5, the life factor falls from 11 to slightly less than 2 which is a life degradation of approximately 6. In fact at such low λ 's the failure mode of the bearing would be primarily surface initiated rather than subsurface initiated fatigue. This illustrates the tremendous influence of EHD film thickness on life.

One final consideration is the friction forces usually termed traction coefficients that are present at the lubricated contacts. It is essential to have knowledge of these in order to calculate drive and drag forces on the cage. Attempts in the past to analytically predict the traction coefficients using simple analytical models have not been successful, particularly at high rates of slip. Finite element approaches have proven more exact but not practical to incorporate into the bearing design codes, so in general either data banks or curve fits of experimental data have been utilized to produce the coefficients. It is vital to have accurate knowledge of the traction coefficient as a function of oil type, temperature, contact stress and slide to roll ratio in order to make any cage slip predictions or specify preload. Another offshoot of such analysis would be the calculation of power loss or heat generation for the bearing by a summation of all the power losses at the raceway and cage contacts. Such models have been developed in the past but are of limited use because of the large proportion of heat generation due to churning as mentioned earlier which makes the analysis still highly dependent on empirical data.

MATERIALS

Materials development for jet engine bearings has involved the introduction of new materials, and improved processing to get fewer impurities in the steels, both of which were aimed to improve subsurface fatigue capacity of bearings. The development continues with added goals of improved crack growth resistance and corrosion resistance. G.E. and other U.S. engine manufacturers have almost exclusively used low alloy tool steels containing molybdenum for bearings, whilst European manufacturers concentrated on development of steels alloyed with tungsten. This basic difference came about primarily because of the strategic availability of the two elements, particularly during World War II. Only the molybdenum based alloys will be discussed in this section. Early jet engines used air melted SAE 52100 material as this was the U.S. industry standard material. It is a low alloy steel which is through hardened and tempered to approximately 58 on the Rockwell scale (Rc58). It's hot hardness is limited and it is not suitable for operation above 350°F. As jet engine performance improved on the '50's and early '60's it became apparent that improved hot hardness was needed and a new alloy, AISI M50 with a 600°F capability was developed. At the same time, vacuum melting of specialty steels was becoming more commonplace and the new alloy was introduced in vacuum processed form. The new processes were also applied to SAE 52100 resulting in Consumable Electrode Vacuum Melt or CEVM 52100 steel. This gave both alloys a considerable fatigue life boost of 5 to 10 times over air melted 52100 with M50 having an even greater advantage because of the ability to attain higher hardness (Rc 62 at room temperatures). Further process development showed fatigue life improvement if the steel was subjected to a second vacuum melt to further cleanse the microstructure. This resulted finally in the Vacuum Induction Melt - Vacuum Arc Remelt or VIM-VAR M50 steel which is today's current standard for G.E. main-shaft bearings which under ideal lubrication conditions can give between 18 to 36 times the life of the baseline air melt 52100 steel.

As bearings continue to be run at higher and higher DN's, hoop stresses in the rotating races must also increase. This has exposed a basic shortcoming of through hardened materials which is lack of crack growth resistance, often termed fracture toughness. Although M50 has an ultimate tensile strength of about 300 KSI, at only 10% of this value, a small subsurface fatigue crack quickly will propagate to critical size, resulting in spon-

USE CURVE:

- A = MAINSHAFT BALL BEARINGS USING C50TF56 (PREMIUM STEEL)
- B = MAINSHAFT ROLLER BEARINGS, GEARBOX BEARINGS, MAINSHAFT BALL BEARINGS WITHOUT C50TF56

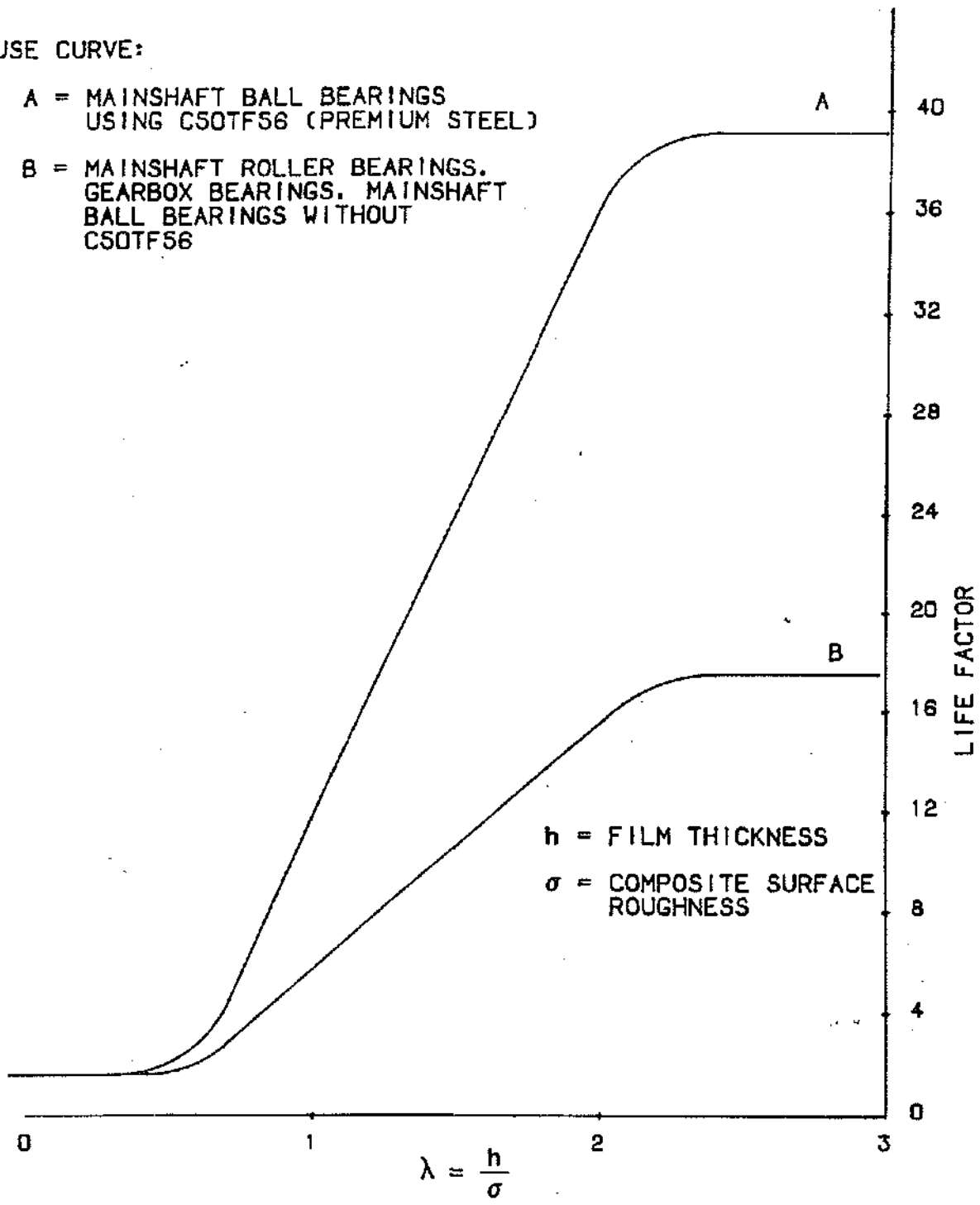


Figure 7.20 Lambda vs. Life Factor For Ball and Roller Bearings

taneous ring failures. This occurred early in CF6-80A commercial service at the number 5R bearing position, resulting in several cases of severed turbine shafts when pieces of fractured races became trapped after fracture and melted the shafts from frictional heating. At that time (late 1982) a new fracture tough bearing steel was under development by G.E. and FAFNIR Bearings on USAF R&D contract. It was a carburizing version of M50 called M50-NIL or M50-Nickel Low carbon. Instead of being hardened completely through in a conventional vacuum furnace, the M50-NIL is carburized to a depth of .030 - .040 inch below the surfaces of the rings by exposing them at temperature in a carbon-rich (usually Methane) atmosphere. Subsequent heat treat results in hard surface "case" which transitions to a relatively soft "core" at the .030 - .040 depth. The case has very high residual compressive stresses to a considerable depth which yields exceptional resistance to fatigue as well as resistance to crack growth. The relatively soft ductile core provides further capability to arrest crack growth and avoid spontaneous failures. Rig testing of M50 & M50-NIL bearings at artificially high hoop stresses and with deliberately induced defects (cracks) showed the M50-NIL bearings lasted from 5 to 200 times as long before failure. More importantly the M50-NIL failure mode was always normal progressive fatigue spalling, not the spontaneous fractures exhibited by M50. Fatigue spalling may take several hundred hours before cage fracture and rapid failure occurs. During the fatigue progression, many small chips are released into the oil system and are readily detectable during routine inspections of the magnetic chip detectors present on all engines. Thus complete and expensive bearing failures may be completely avoided. Development of M50-NIL was accelerated following the CF6-80A experiences and first introduced to production in 1985 at the number 5R position on the CF6-80C2. It is predicted to become the new "standard" G.E. bearing material for severe applications. Work continues to simplify it's rather complex heat treatment process and give it corrosion resistance using surface treatment techniques. Corrosion is still the number one cause for rejection on bearings being inspected for further service. This is a significant cost of ownership to engine operators. Further in the future ceramics such as Silicon Nitride may be developed for high speed, high temperature applications such as hypersonic engines.

Cage materials have also evolved over the years as materials for races and rolling elements have progressed. Early cage materials were either low carbon steels or bronze. Later iron-silicon-bronze and S. Monel became the standard as a good compromise between strength and wear resistance. Today's G.E. standard is heat treated SAE 4340 steel at about Rc36 hardness and covered with

a thin silver plate coating for wear resistance. The 4340 steel is about the strongest material available at the relatively moderate temperatures bearings run at. It also has very good fatigue resistance.

Some effort is still being expended to find alternate coatings to silver which has a tendency to trap hard particles in the oil which then damage balls, rollers and raceways but no immediate replacement is foreseen at this time.

DYNAMIC SEAL TYPES

This section will be broadly divided into non-contacting labyrinth seals and contacting carbon seals. Other categories exist, but are not used in mainshaft applications of G.E. engines, nor is any discussion included on static seals such as "O" rings, piston rings, omni-seals, etc. Dynamic seals are basically flow restrictors and in jet engines are used between a rotating and stationary part or between two independently rotating parts to minimize the flow of air or hot flowpath gases. The objective of the designer is to provide a geometry that presents the maximum resistance to flow throughout the life of the engine.

LABYRINTH SEALS

A labyrinth seal consists of one or more pointed teeth usually on the rotating seal member, running in close proximity to a cylindrical or stepped cylindrical stator with air or gas flow between the two members. On intershaft seal applications the cylindrical "stator" referred to above, also rotates independently of the toothed seal member. Figures 7.21a through 7.21f show various types of labyrinth seals used in G.E. engines to keep sumps oil tight, provide cool buffer air for bearings and support structures and to minimize leakage of high performance derivative flowpath air.

In general the low ΔP seals that seal air with a low performance derivative are referred to as non-critical seals while critical seals include the few engine seals characterized as causing significant performance penalties with high air leakage.

Clearance Control A labyrinth seal restricts air flow one or more times depending on number of teeth used between rotor and stator. As the leakage flow passes through the minimum clearance point at the tooth tip the leakage flow accelerates to its maximum value which may be sonic in the case of a critical seal. Downstream of the seal or between teeth the velocity decelerates to a very low value so that each tooth imparts approximately

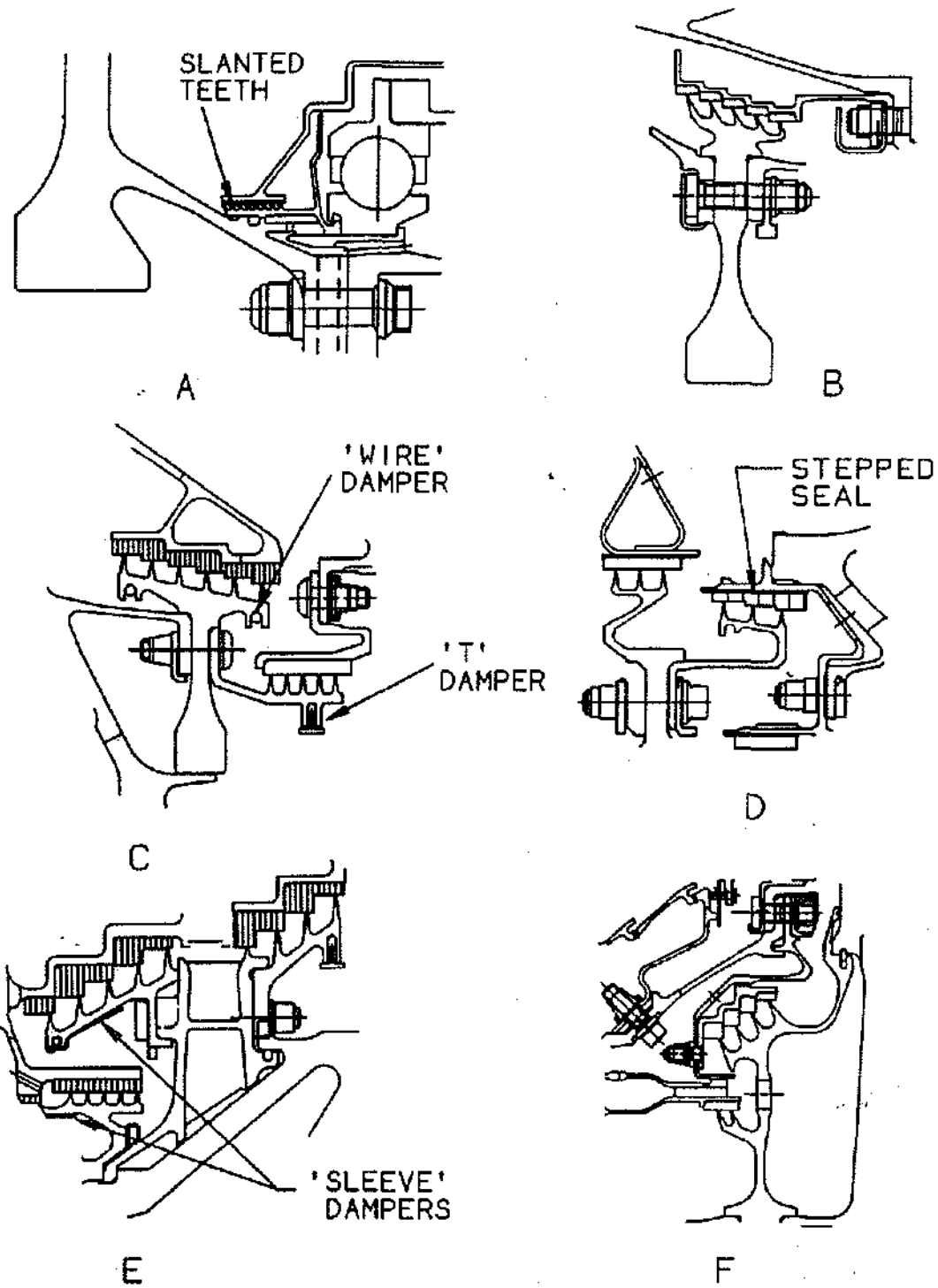


Figure 7.21 Labyrinth Seal Types

one velocity head of pressure loss to the leakage flow. In a multiple tooth seal, because pressure is decreasing as the flow passes successive teeth, the velocity must increase and therefore the pressure loss increases with successive teeth. Thus in say a six tooth seal, the bulk of the total ΔP across the seal occurs on the two or three teeth on the low pressure or downstream side of the seal.

The flow rate through the seal for constant upstream temperature and pressure ratio is a direct function of seal flow area which of course is directly related to clearance. In addition, flow is related to a configuration factor K , which is itself a function of clearance. Therefore the key to minimizing flow through a seal is to design mechanically for the minimum possible operating clearance under all conditions of interest. This includes attaching the seals to their support structures in a way that they are minimally affected to vibration, rotation, axial motion, or transient radial clearance changes.

The first step in the design process should be to consider the stack of mechanical tolerances between rotor and stator to determine minimum practical assembly clearances for the seal. This should take into account part eccentricities, out of round and size tolerances to determine the required value. Changes in the mounting system should be considered at this time to minimize or eliminate stack up where possible. Heat transfer and deflection analysis of the configuration should then be conducted to determine the closure effects on clearance. As a minimum the designer should consider sea level static ground idle and hot day take-off conditions as this will normally cover the range of thermal extremes experienced by the seal. The results of this analysis may dictate a change in the cold clearance or a change in material of rotor or stator in order to maintain optimally matched parts and minimum operating clearance on all teeth. If applicable a buckling analysis should be made at maximum ΔP conditions.

In addition, a transient heat transfer and deflection analysis must then be conducted to see if under burst or chop conditions excessive clearance closure might occur which would result in rubbing and increase the steady state clearance. Both radial and axial relative rotor/stator excursions should be examined to estimate the true operating clearance. Another result of the transient deflection analysis will be max transient stresses so that low cycle fatigue (LCF) life of the part may be assessed. Iterations may be required at this point to optimize the seal for both leakage and life. One further note of caution is that on supersonic engine applications there may exist more severe thermal excursions than hot day take-off at altitude and high mach number so this should be considered during the analysis.

In addition to the above effects there are other transients such as maneuvers and hard landings that may cause rotor to stator deflections and rubs. These effects also may require clearance increases to accommodate. The overall objective on a well designed seal is that at all teeth locations a light 360° rub should be observed on the actual stator hardware after running all the above conditions. Adjustments are generally made during engine development programs to achieve the objective. These may take the form of an overall clearance change, or diameter changes on individual teeth in the assembly. However, before the development phase begins, the designer must complete further analyses to assure that the seal has stable thermal operation and is free from mechanical and acoustic vibration problems, any of which could either physically break the parts or at least adversely affect the operating clearance. These phenomena are covered briefly in the following sections.

Stick-Slip Instability This form of instability is generally the result of a rotor/stator rub at low speed where rubbing friction is relatively high and therefore is more likely to affect fan and L.P. rotor seals. It can affect any seal because the rub generates vibration at high frequency (analogous to the screech of chalk on a dry blackboard) and energy is automatically fed in at some natural frequency of the excited part. If this phenomenon becomes a problem to seal operation the only practical way to avoid it is to increase cold clearance so that rubbing is avoided or delayed until a higher speed is reached when the friction force vs. rub velocity curve has flattened out. A lower friction rub material such as Teflon may also be substituted provided that operating temperatures are low enough.

It should be noted that rubbing seals should also be stable when rubbing at high speeds. In general this involves making the stator the outer seal member and making it thermally responsive so that heat generated during the rub causes it to grow away from the rotor and clear the rub. It also requires sufficient tooth height on the rotor so that the generated heat is also conducted into the teeth where it may be dissipated into the leakage air by convection from their flanks. This prevents heat from reaching the main rotor structure which would cause more thermal expansion and aggravate the rub. Guidelines for the choice of tooth pitch and height are given in the labyrinth seal design practice, DP3352.

Out of Round Instability If a seal is subjected to a local rub over a relatively small arc of its circumference, the local resultant heating will have a tendency to make the seal member go out of round. The basic support structure of the seal must be stiff enough in circumferential bending to restrict the out of roundness to a very small

Damping Normally coulomb or friction dampers are the only practical way to provide sufficient damping for seal structures. Common forms of damper are the wire, the "T" damper and the sleeve. Examples of these are shown in Figure 7.21. They are loaded either mechanically or centrifugally into a slot or channel in the seal and achieve their effectiveness by rubbing against the seal at the surface of contact, should the seal begin to vibrate. In order to get best effectiveness the damper should be placed as far radially from the neutral bending axis as possible where relative motion between seal and damper will be greatest during any vibration. It is also a requirement that they be positively retained so that they do not ever exit the seal and cause internal engine damage. The details of damper design require consideration of centrifugal loading available and the ratio of the damper mass to the vibrating mass of the seal.

Configuration & Material Considerations As stated at the beginning of this section, the key objective of the designer is to provide the seal configuration with the maximum resistance to flow, within the space available. As shown in Figure 7.21, sometimes radial steps and slanted rotor teeth are incorporated to assist in killing the flow velocity head as it exits each tooth. At large clearances in the big high ΔP critical seals, honeycomb backing strips are superior to plain rub strips. These are usually brazed in place. The more critical the seal from a performance standpoint, the more likely these additional features will be seen.

Materials used in labyrinth seals vary depending on the temperature environment. In the cold locations ahead of the H.P. compressors, seal rotors are often titanium but as temperatures rise the designers must resort to higher temperature steels such as 17-4 Ph, A286, Inconel 718 or Rene 41. Stators vary similarly from high temperature filled epoxy moldings in cooler locations to Inconel 718 and Rene 41 in hot locations. Hastelloy X is probably the most common honeycomb material in hot locations. Plain oil seal rub strips are often micro-balloon filled epoxy or teflon at low temperatures and sprayed Nickel-Graphite or Metco 601 in high temperature locations. Good thermal matching between rotor and stator should always be the designer's prime objective in the choice of the best materials for the seal structure. Adequate rub compatibility is the objective in the choice of rub strip.

CARBON SEAL DESIGN

There have been many different carbon seal designs in use and under consideration over the years and to de-

scribe the merits of each type would be almost impossible in this section. Discussion must be limited therefore to commonly used configurations in production G.E. engines. All main shaft carbon seals are in sump seal applications with their primary function being to prevent oil leakage from the sump. Large diameter high ΔP air to air seals have been designed and tested but none have ever been used on a production basis. Carbon seals normally have a leakage rate very much lower than a comparable labyrinth seal of the same diameter and therefore are attractive for critical seal locations to improve engine performance. However rubbing velocities at large diameters on gas generator seals are prohibitively high for attaining long wear lives on contacting seals and hydrodynamic or hydrostatic solutions to the problem usually require more precise geometry and lower distortion and misalignment values than practically attainable. In addition temperature requirements on critical seals often exceed 1000 °F which is unsuitable for carbon if long life is an objective.

For these reasons there are no carbon seals in critical locations but as sump seals, where rubbing velocities and temperature environments are much more moderate they offer a more reasonable and sometimes the only solution to the requirements of the design. This is particularly true in supersonic applications where sump pressurization pressures sometimes are prohibitively high for labyrinth seals and would cause unacceptable sump vent flows and oil consumption.

Circumferential Seals Figure 7.23 shows a cross section of a circumferential seal which may be utilized in tandem as shown or singly depending on the application. It consists of a number of accurately machined carbon segments which are held radially inwards by a circumferential spring and by the pressure of the air being sealed so as to become loaded on to the race and form a sealing surface against the IDs of the carbons. In tandem applications, axial compression springs load the carbon segments apart axially to keep them seated against the housing and in single applications a wave spring is often used between the carbons and one end of the housing for this purpose. Carbons always are anti-rotated to the housing, often with simple straight pins. The windback is a device consisting of coarse internal thread in close proximity to the shaft on the oil side of the innermost carbon seal. It is capable of driving oil back into the sump at low speeds and seal ΔP s, should the seal become flooded.

Various methods of overlapping the ends of the carbon segments are used with the aim being to keep end gap air leakage as low as possible. The rather complex looking

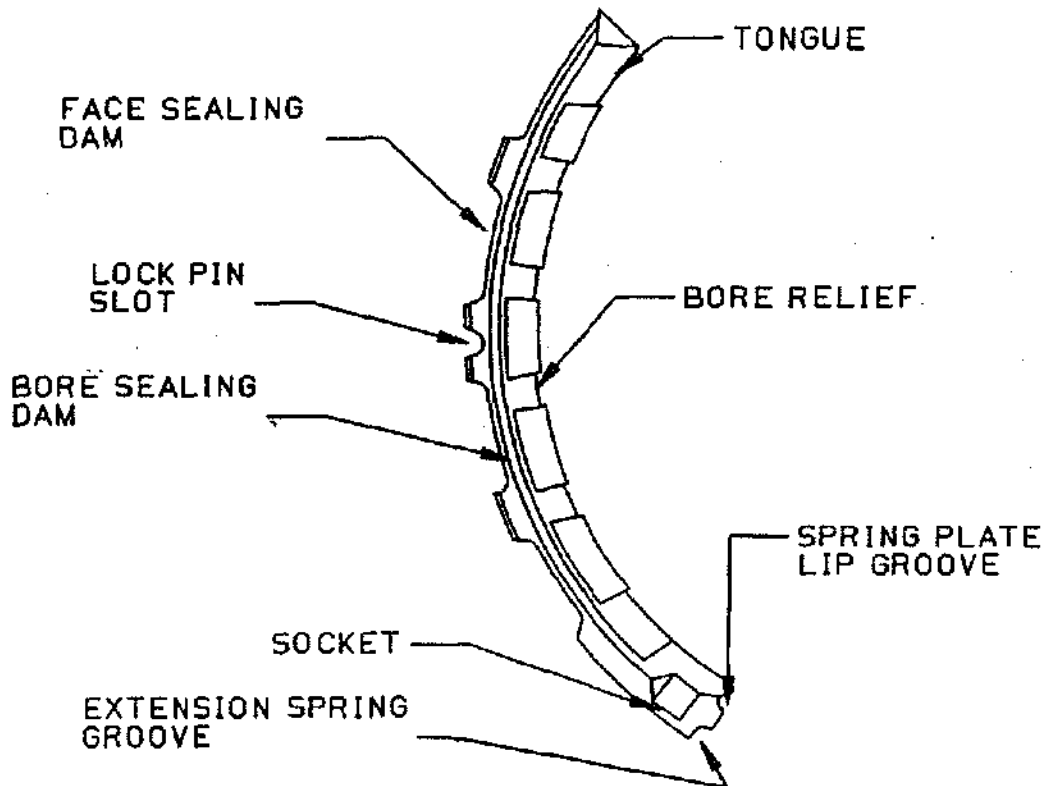
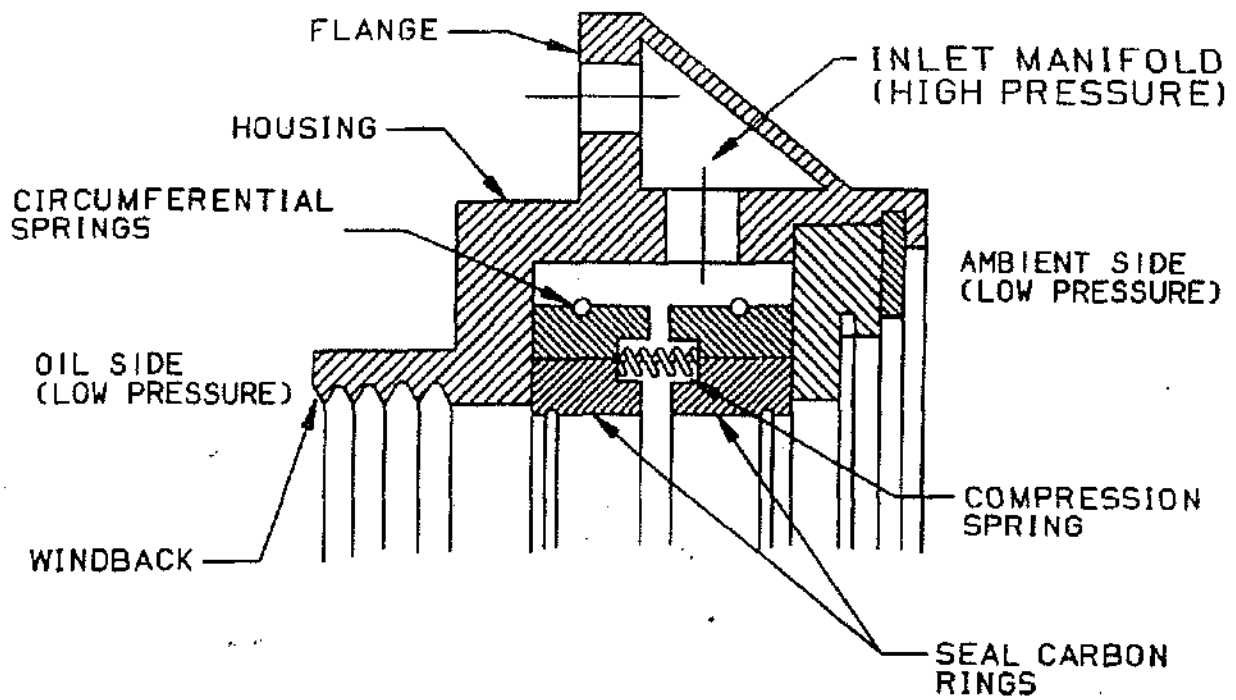


Figure 7.23 Tandem Circumferential Carbon Seal

value or it will aggravate the rub and go unstable usually causing a thermal runaway failure. In the early 1970's some analytical work was done at G.E. to establish a design criterion that would give protection from this problem. In order to do a rigorous analysis, the rub temperature profile and arc length must be known which are usually difficult to quantify. However, the study referenced used real data from successful and unstable seal designs in order to set guidelines. Basically it is recommended that the seal inner diameter be no greater than 93% of the outer diameter for assured out of round stability. For seals in the 93% - 97% range a more rigorous analysis must be performed assuming 100°F temperature increase over a 90° arc and allowing a specified out of roundness per inch of seal radius. Seals over 97% ID/OD are deemed unstable and should never be used. Those cases in the 93% - 97% range that do not meet the criteria may be made acceptable by adding stiffening rings at one or more axial locations as shown in Figure 7.21. DP3352 contains details of this process.

Campbell's Criterion Campbell's Criterion, for a rotating seal structure requires that:

$$f_n > n N_{max}$$

where f_n = natural frequency of the structure (CPS), n = number of circumferential waves, and N_{max} = maximum rotational speed (r.p.s.).

If the seal meets this criterion (with usually a 20% margin) then it should not be vulnerable to resonance problems. Such problems can occur because any force fixed in space can feed energy into a rotating structure at its natural frequency when the backward travelling wave speed as seen by a stationary observer is zero. Normally the analysis is carried out by finite element or shell analysis to determine natural frequencies of the part for each number of circumferential waves and then displaying graphically as in Figure 7.22 to determine margin which should be at least 20% by analysis. This can be verified by a simple component test to determine actual natural frequencies. A minimum of 15% margin is required by test.

Campbell's criterion is also applied to static seals, though in this case a rotating force is needed before energy can be fed into a static structure, which is not an uncommon situation in jet engines. If Campbell's criterion is not met, then the design must be changed to raise the natural frequencies, at least through $n = 10$. The higher order vibration modes above 10 require too much energy to become excited and are therefore not of concern.

1/Rev Excitation A seal must be designed to have its minimum natural frequency (in cps) greater than the maximum speed in rps. Note that this is distinctly different from Campbell's criterion, but when Campbell's criterion is satisfied, 1/Rev is automatically satisfied.

Aeroelastic Instability Aeroelastic instability is a self-excited vibration phenomenon. It occurs when small vibration deflections in a seal cause pressure distribution changes across the seal that tend to increase the initial deflection and feed energy into the vibration. The tendency for this to happen is higher as seal clearance decreases and as previously stated, minimum possible clearance is normally the designer's goal. An empirically derived criterion called "w/r" is used to assess the propensity for instability. For w/r values less than 0.4×10^{-3} instability should not be a problem. Above this value dampers must be incorporated as described at the end of this section. If the seal is supported to its mounting structure on both ends, a w/r value of 2.0×10^{-3} may be considered acceptable.

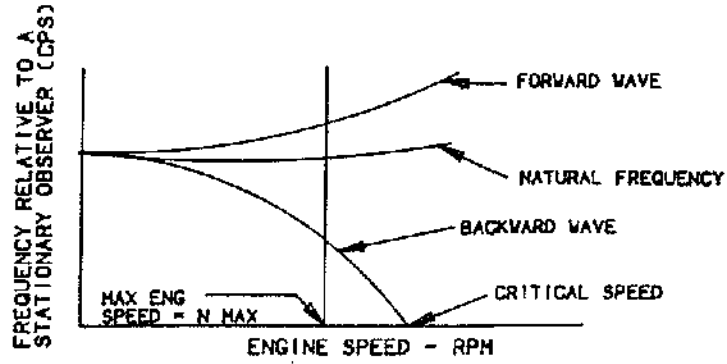
It should be also noted that seals that are supported on the discharge (downstream) side are inherently more stable than those supported on the upstream side so this should be always incorporated where feasible.

Rotor-Stator Interaction This phenomenon occurs when travelling vibration waves in both rotor and stator have the same number of circumferential waves, rotate in the same direction and frequencies coincide within the engine operating speed range. Normally 20% speed margin is required at least on the lower ordered modes below $n = 6$. If this cannot be achieved, damping is required.

In some cases, at higher engine speeds the backward travelling wave of the rotor becomes a forward travelling wave, resonant with forward travelling waves of the stator. Avoidance of all interaction is often extremely difficult but is essential for $n \leq 6$ on undamped seals.

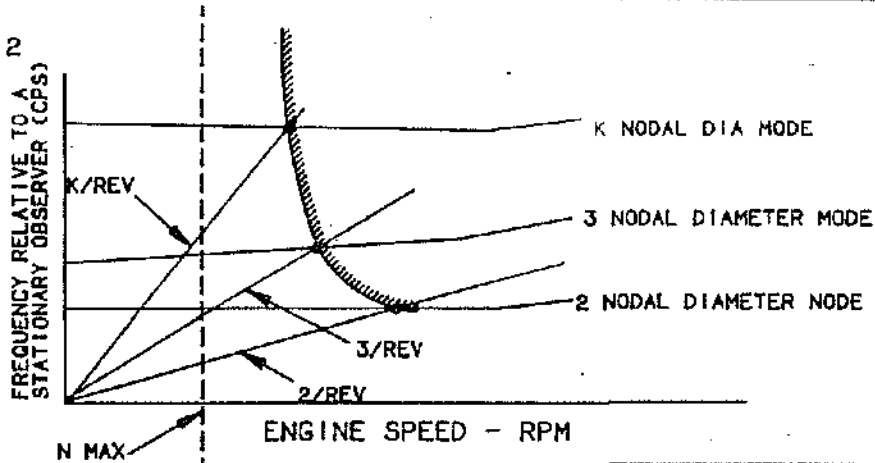
Acoustic Coupling This phenomenon is the interaction between the acoustical natural frequencies of the cavity downstream of the seal and mechanical seal frequencies. It can be caused by an aerodynamic instability which excites an acoustical cavity adjacent to the seal at one of the cavity's natural acoustic frequencies. If the frequency coincides precisely with a mechanical frequency of the seal, then vibration may occur. A twenty per cent speed margin is required for coincidence of acoustic and mechanical frequencies. If this cannot be met, damping should be incorporated on critical seals.

METHOD 1



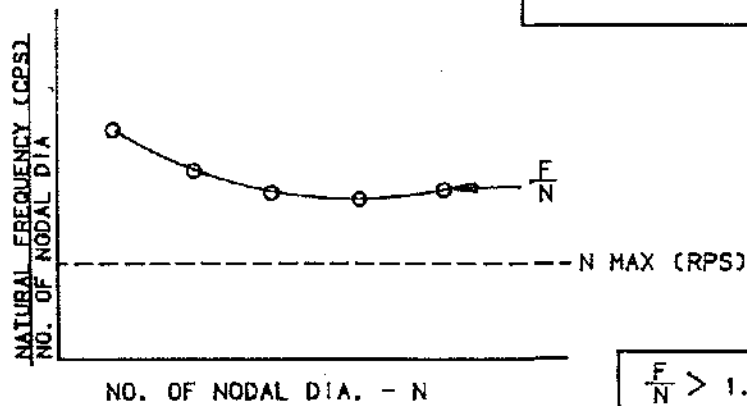
$$\text{CRITICAL SPEED} > 1.15 N \text{ MAX}$$

METHOD 2



SHADED REGION SHOULD BE TO THE RIGHT OF N MAX WITH 15% MARGIN

METHOD 3



$$\frac{F}{N} > 1.15 N \text{ MAX}$$

Figure 7.22. Graphical Models of the Campbell Criterion

grooves machined into the bore of the typical carbon segment also shown in Figure 7.23 serve the purpose of pressure balancing the seal to limit the pressure loading on the bore and face sealing lands. This is the key to successful seal designs and requires careful consideration of all operating conditions to ensure a minimum but not excessive loading is always present to keep the seal closed on to the shaft and housing. Computer codes are normally employed to optimize the carbon loadings and analytically explore the whole mission for specific seal geometry. Circumferential bore seals are used in many G.E. engines to seal between a static housing and a single shaft. Because of the individual carbon segments they are not suitable for high speed intershaft applications where both seal members must rotate. These type of seals are used widely on J79, F101, F110, CF6, T700, J85 and T64 engine families.

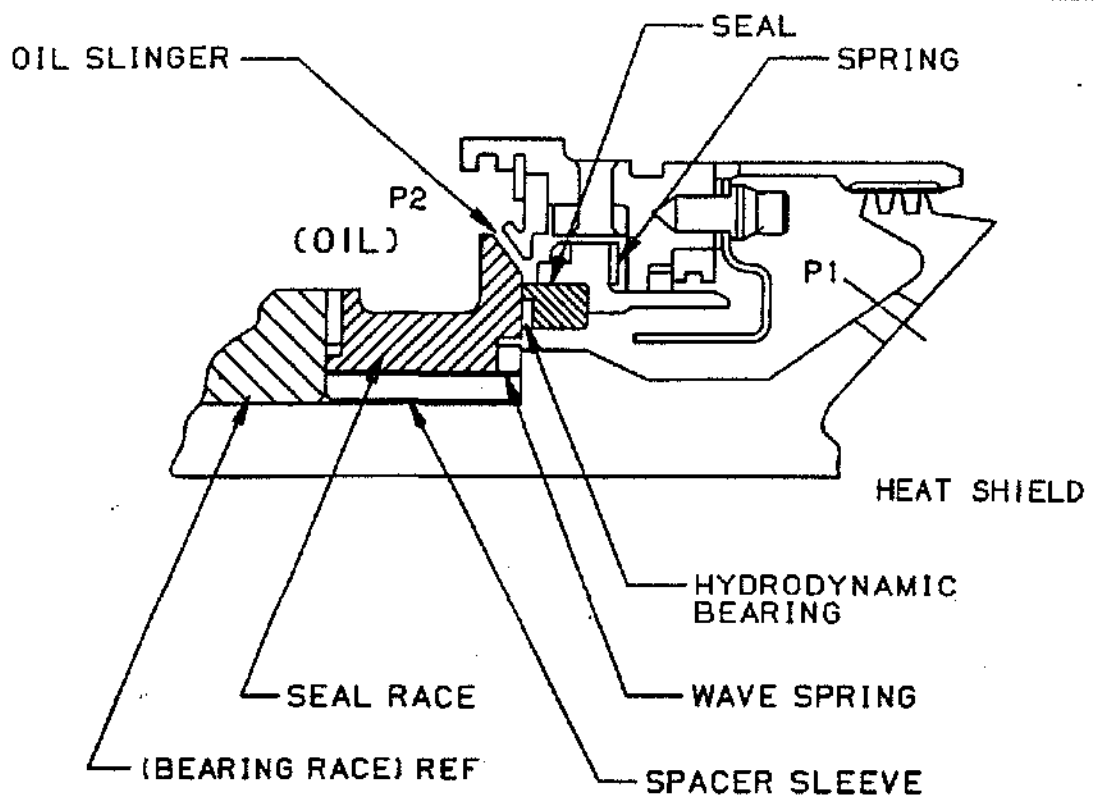
Face Seals Face seals as the name implies do the sealing function on the radial faces of the carbon and race rather than on the bore of the carbons as in segmented circumferential seals. They are capable of running at moderate speeds of around 200 ft/sec rubbing velocity but with hydrodynamic assist from tapered pads on the seal face (carbon or race) this can be extended to 600 ft/sec. The advantage they have over circumferential seals is that they are easier to pressure balance over a wide range of ΔP s and can therefore withstand up to 350 psi compared to 50-60 psi with the circumferential seal. Also because of the one piece carbon ring, they can be used in intershaft applications at low to moderate speeds. Figure 7.24 shows the F101/F110 No. 3 seal which is the only current G.E. application of a single shaft hydrodynamic face seal. Also in Figure 7.24 is shown schematically pressure diagram of the forces tending to open and close the seal. Normally the seal is balanced so that the total closure force is slightly higher than the opening force at all operating conditions so that the seal dam always has an extremely light pressure on its face. The hydrodynamic air bearing pads are precision machined into the carbon or race face and have geometry such that air is drawn by viscous action into a slightly converging space circumferentially as the race rotates, thereby generating hydrodynamic pressure or lift. This ability to ride the carbon on an air film is what gives the design greatly extended speed capability over a plain rubbing face seal. An additional advantage of the face seal design is that because of the oil slinging action of the rotating race tending to throw oil back into the sump, it will seal down to zero ΔP compared to about 2 psi ΔP for the circumferential seal. This type of seal can also be balanced hydrostatically but there are none of this type in service on G.E. engines.

Pressure Balanced Split Ring Intershaft Seal Although face seals can be used in intershaft locations, the relatively low tensile strength of most carbon materials limits the speed at which the rings can be rotated before hoop stresses get too high. On the split ring design the carbon ring is split radially at one point rather like an automobile piston ring and is lightly compressed into a steel carrier so that centrifugal loading produces only compressive stress rather than hoop tensile stress in the carbon. This allows speeds of 300-400 ft/sec to be attained. In addition, if there is sufficient ΔP across the seal, it can be pressure balanced so as to use hydrostatic pressure forces to reduce the face loadings and provide long carbon wear life. Figure 7.25 shows such a seal in the F101/F110 number 4 intershaft location together with the force balance diagram of all the forces acting on the carbon ring. As in the case of the designs previously discussed, the details are quite complex and reference to detailed manuals should be made if more information is needed.

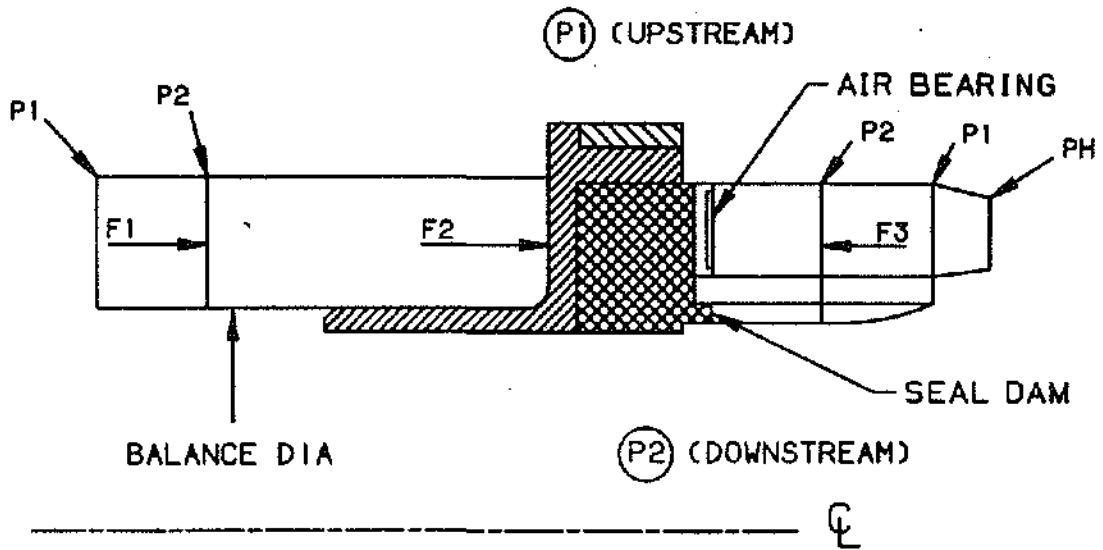
Split Ring Unbalanced Intershaft Seal When ΔP s are low across the intershaft seal, force balancing becomes impractical and the normal course of action is to use an unbalanced split ring seal as shown schematically in Figure 7.26. As can be seen the radial and axial forces have unbalanced components which limits the useful ΔP that it may be used at to about 20 psi. They have however been run at extremely high speeds of up to 800 ft/sec with good results. Such designs are used on T64 and F404 engines.

Materials Bore rubbing and face seals have almost universally used hard chrome plated steel for the seal races while the No. 3 face seal on the F101 engine uses flame sprayed chrome carbide. It is normal to specify a hard surface coating for good wear resistance both of the seal race and the carbon itself.

Carbons are basically in three categories depending on temperature of operation and oxidation resistance required. For up to 600°F, resin bonded grades are suitable but coal tar and pitch binders can extend operation to 800°F. For temperatures in the 800 - 1200°F range phosphor salts are employed to maximized oxidation resistance. Various proprietary additives are used to enhance wear resistance together with special heat treatments. Over the years, literally hundreds of carbon grades have been developed and generally the advice of the carbon manufacturer is sought in order to pick the best candidate grade for each application. It is normal to rig wear test the best candidates before committing them to an actual seal design.

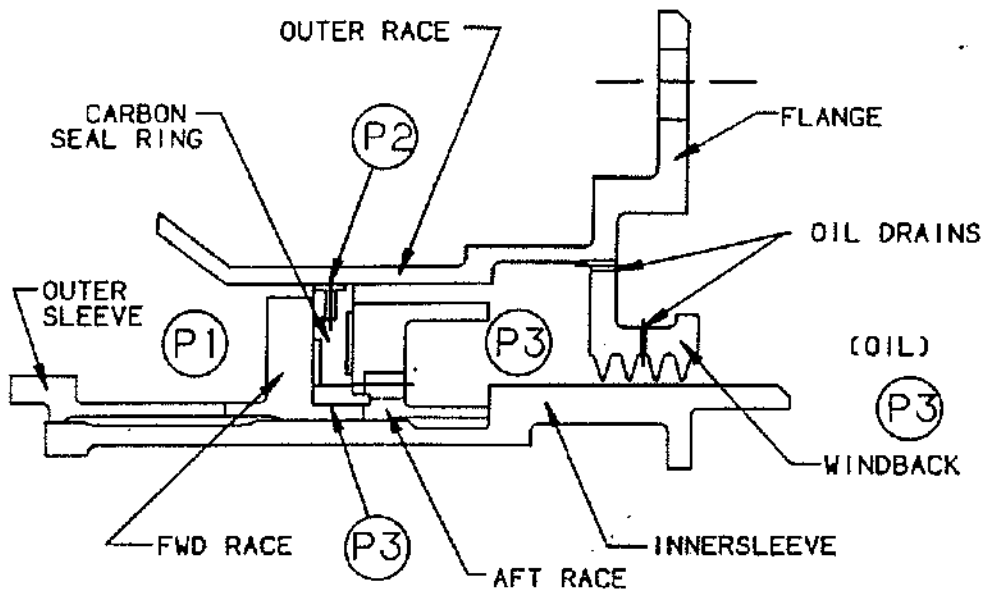


(P1 > P2)

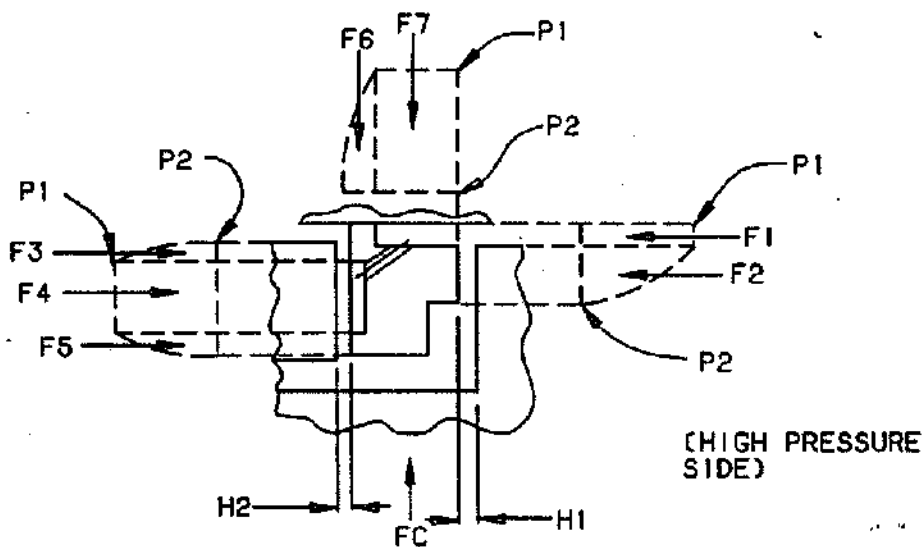


PH = BEARING PRESSURE
 F1 + F2 = F3 (@ EQUILIBRIUM)

Figure 7.24 Hydrodynamic Face Seal Assembly and Pressure/Force Diagram



P1 P2 P3



$$F1 + F2 = F3 + F4 + F5. \text{ WHEN } H1 = H2$$

$$FC - F6 + F7 = \Delta FR$$

FC = CENTRIFUGAL FORCE

Figure 7.25 Force Balanced Split Ring Intershaft Seal and Force Balance Diagram

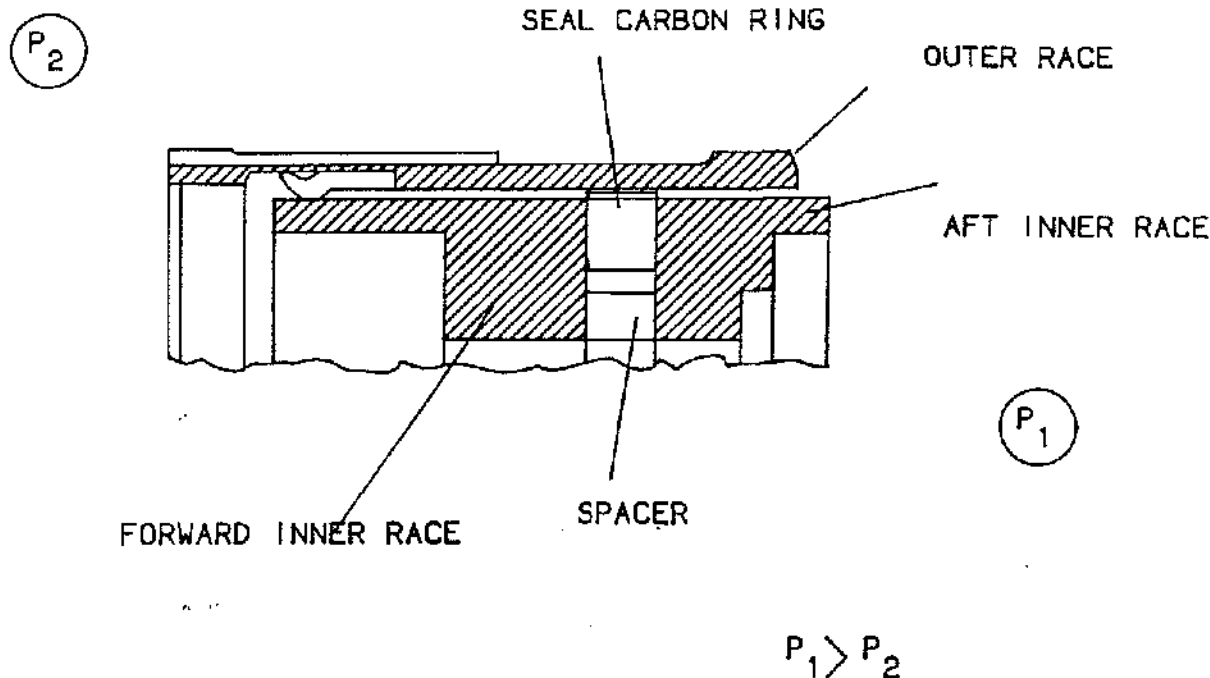


Figure 7.26 Split Ring Intershaft Seal

SUMP DESIGN

Overall sump design requires some discussion because these considerations often influence the design of bearings, seals and housings. For a complete description of these criteria reference should be made to materials on sump design in DP1422.

Oil Scavenging The placement of the oil scavenge port in a sump should have a relationship to the oil seals so that it is always covered with an oil puddle before the oil can get deep enough to flood the oil seals. This must be true at all possible operating attitudes of pitch and roll, otherwise oil leakage may occur.

Fire Safety Sumps in hot areas of the engine must have provision to get any sump leakage oil overboard and it must never be allowed to become trapped in areas hot enough to result in auto-ignition. This usually requires additional seals and overboard drains from a cavity surrounding the sump. In any case a fire safety analysis must always be conducted.

Coking Steady state and transient sump wall temperatures must be kept below 400°F in order to avoid the

long term build up of varnish and coke. Coke is a black hard deposit which is formed when engine oil is exposed to high temperatures. It is undesirable because it can block oil lines, scavenge ports and filters resulting in complete bearing failures.

Interference Fitting of Bearing Rings Bearing rings are always installed with an interference fit on shafts and in housings to prevent spinning and fretting. Sufficient fit must be used to offset the reducing effects of temperature and rotation. Fretting is a form of abrasive wear that occurs due to microscopic movement between surfaces and can affect bearing bores and ODs if residual fit pressures on the mounting surfaces are too low. Computer analyses are available to determine the amount of fit required. The interference fits cause small changes in the diameter of the bearing rings themselves and this must be accounted for in the clearance analysis of the bearings. In addition there may be an influence on the bearing clearance due to mechanical and thermal effects on structures remote from the bearing itself. These "remote effects" must also be accounted for in the bearing clearance analysis.

Bearing Support Stiffness In preloaded roller bearings the bearing housing stiffness often plays a role in attaining the required preload as described earlier. It is vital that the housing be designed so that the circumferential bending stiffness is as uniform around the bearing as possible. Avoidance of local bosses, flanges and cutouts is essential to ensure that local "hard spots" do not occur because they can cause significant dynamic overloads on the rollers, leading to micro-pitting and rapid failure. This failure mode was primarily responsible for several occurring early in CF6-80A revenue service at the number 5 bearing location.

Thermal Out of Round In some instances, sumps thermally distort to a non-round condition. The CF6-50 and CF6-80 "B" sumps do so because of service lines and ducts at the 6 and 12 o'clock positions. This causes the sumps to ovalize and expand more in the vertical plane than in the horizontal. Wherever this is thought likely to be a possibility a 3-D analysis should be conducted to assess the magnitude of the non uniform deflection. If it is significant when compared to bearing operation IRCs, this effect must be included in the calculation of roller load distribution, preload and L_{10} life.

False Bearings Seals and sump housings must be designed so that axial interference between a rotating and stationary part can only occur after the rotor has moved axially a distance that would involve significant rubbing between airfoils and vanes in the engine flowpath. On large Evendale engines this distance has usually been determined by taking the minimum axial distance between any blade/vane row at the maximum end of its tolerance

range and adding 0.25 inch. Therefore on at least one blade/vane row, 0.25 inch minimum of the blades and vanes must be worn away during a rotor shift before rotor contact with a seal or sump housing can occur.

The reason for this is that if a shaft separation should occur and a turbine becomes disconnected from a compressor or fan and is also by reason of the separation free to move axially, the first rotor to stator contact should be in the flowpath where a large braking force will occur and overspeed will be prevented. If contact were to occur first at a lower diameter on a seal or sump, sufficient energy is usually present to melt the contact surfaces and momentarily make a low friction bearing which would support the rotor long enough to allow overspeed to occur. This liquid metal bearing is what is referred to as a "false bearing" and because of its low friction and relatively small diameter, it provides very little of the desired braking effect on the rotor.

Titanium Fires Titanium is commonly used for seal rotors, bearing housings and other sump hardware in relatively cool areas of the engine. Designs must be such that two titanium parts may never rub together since this would most likely result in a titanium fire in the engine. For the same reason, uncoated titanium seal teeth should only be allowed to rub into soft coatings such as teflon, microballoon epoxy, Metco 601 or 75/25 Nickel-Graphite. If the rub material is metallic honeycomb or hard 85/15 Nickel-Graphite the teeth must be thermal spray coated with harder material such as aluminium oxide or borazon.

Chapter 8

SECONDARY SYSTEMS

by Martin R. Brown

INTRODUCTION

Secondary systems refer to those flow systems which are not part of the primary gas turbine flowpath but whose function is required to support overall engine operation. Systems typically include compressible or incompressible flow and heat transfer analysis. The objective of the system designers is to assure that the functional requirements of a system can be achieved. These designers do not have responsibility for the hardware in these systems but are expected to insure that required flows temperatures and pressures are met.

Generally, computer models of the systems are constructed. Flowpath data (pressure, temperature) are used as source and sink boundaries in air models and system internal cavity pressure and temperatures calculated from engine geometry and heating/cooling flow requirements. Similar methods are used for oil wetted systems using lube pump maximum flowrate at a particular oil temperature as a design condition. Instrumented engine tests are monitored to verify the validity of the computer models. **Figures 8.1 and 8.2** show some of the systems on the CF6-80 engine design giving an indication of the variety of the systems involved on just one family of engines.

Since the secondary systems designer has a model of the engine internal cavities, it is possible to calculate cavity loads which are major contributors to axial thrust bearing loads. By combining cavity loads and turbomachinery flowpath loads the overall resultant bearing thrust loads are obtained. These loads are supplied to bearing designers so bearing lives can be estimated.

Early in the development of an engine the air model data is published in the form of an issued print so other designers will be aware the system details. A similar print is issued for the oil system.

AIR SYSTEMS

A secondary air cooling system is one which uses air-flow to remove heat buildup to prevent or limit hardware life damage. This type of system differs from a purge system which uses an air source to "pressurize" a cavity to prevent hot flowpath air from entering that cavity. The HPT system that will be described is an example of a cooling circuit. A purge system will also be described.

HPT Cooling System Figure 8.3 shows the flow circuit and hardware for a high pressure turbine cooling system. Any air that is bled off the primary flowpath and used for a secondary purpose has a negative effect on engine fuel consumption. The prime objective of this HPT cooling design is to provide cooling air sufficient to meet blade life at a minimum cost to engine performance. This requires a thorough understanding of the pressure, temperature, seal flows, seal deflections, and blade flow effects that will be expected.

Understanding these design details necessarily takes a significant amount of communication between secondary systems, turbine designers, seal designers, and cycle groups. A starting point might be to agree on the design point for this system. For instance, is hot day takeoff an adequate design point or should deteriorated engine operation be considered. Failure modes might include a lost seal rubstrip or lost turbine tip caps which would to change the system flow requirements. These decisions are usually made based on past experience with similar systems.

A major factor in a design of this type is the effect of dirt ingestion on the turbine cooling circuit. Turbine blades have many small passages which could become blocked and make it mandatory that ingestion be minimized. This portion of the design is not easily solved by analytical methods and the designer must rely heavily on component testing and engine development tests to assure satisfactory operation of the system.

Another significant design item in this circuit is an efficient inducer design to be sure cooling air is transferred effectively from the stationary to the rotating member. Properly designed, the inducer will not be greatly affected by open seal clearances or other engine hardware tolerances as engine cycles accumulate.

Secondary Systems responsibilities in the design of this cooling circuit would be to communicate with other involved designers, define and direct component testing, define the inducer characteristics, estimate all design

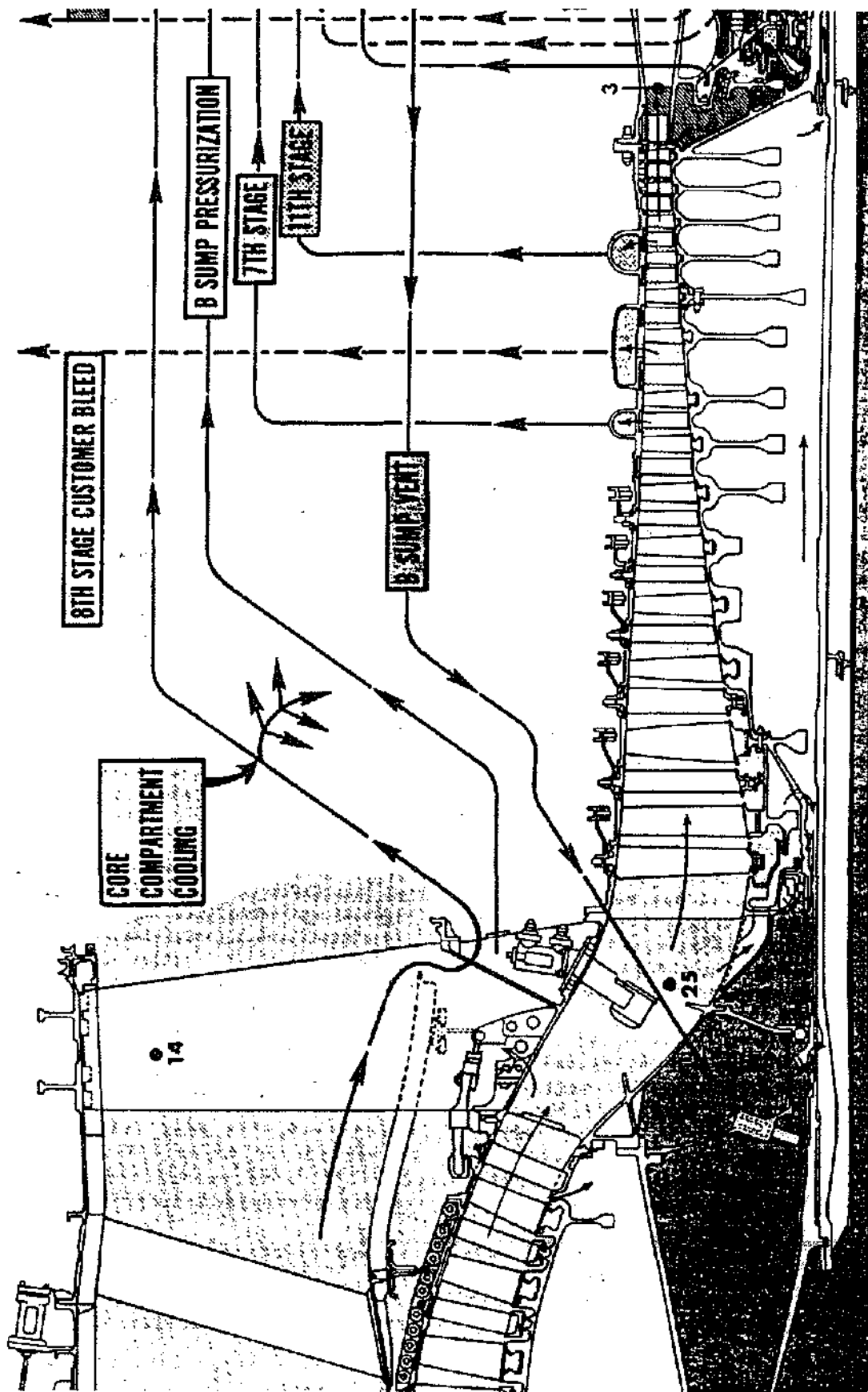


Figure 8.1 CF6-80C2 Secondary Systems

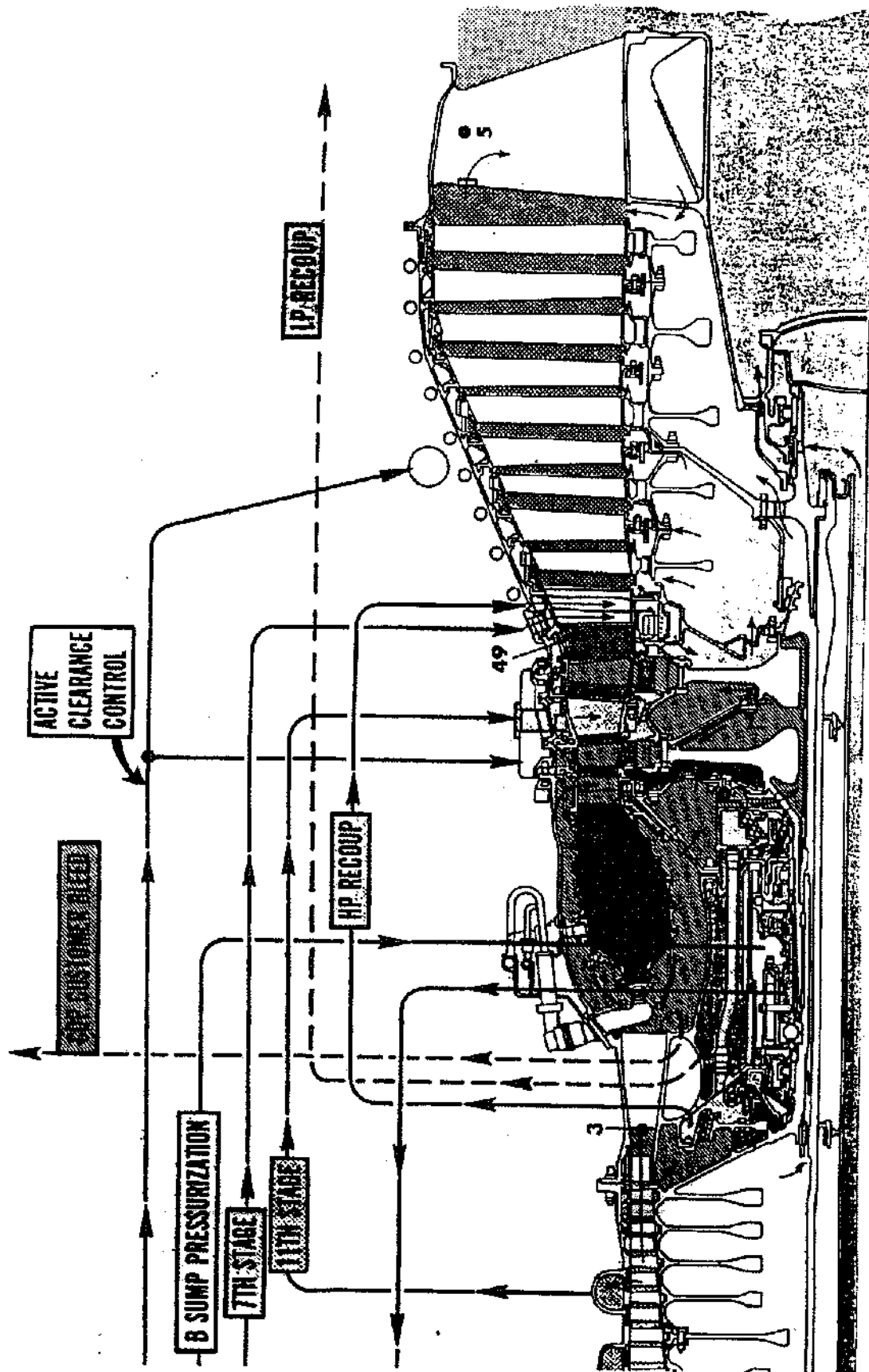


Figure 8.2 Additional CF6-80C2 Secondary Systems

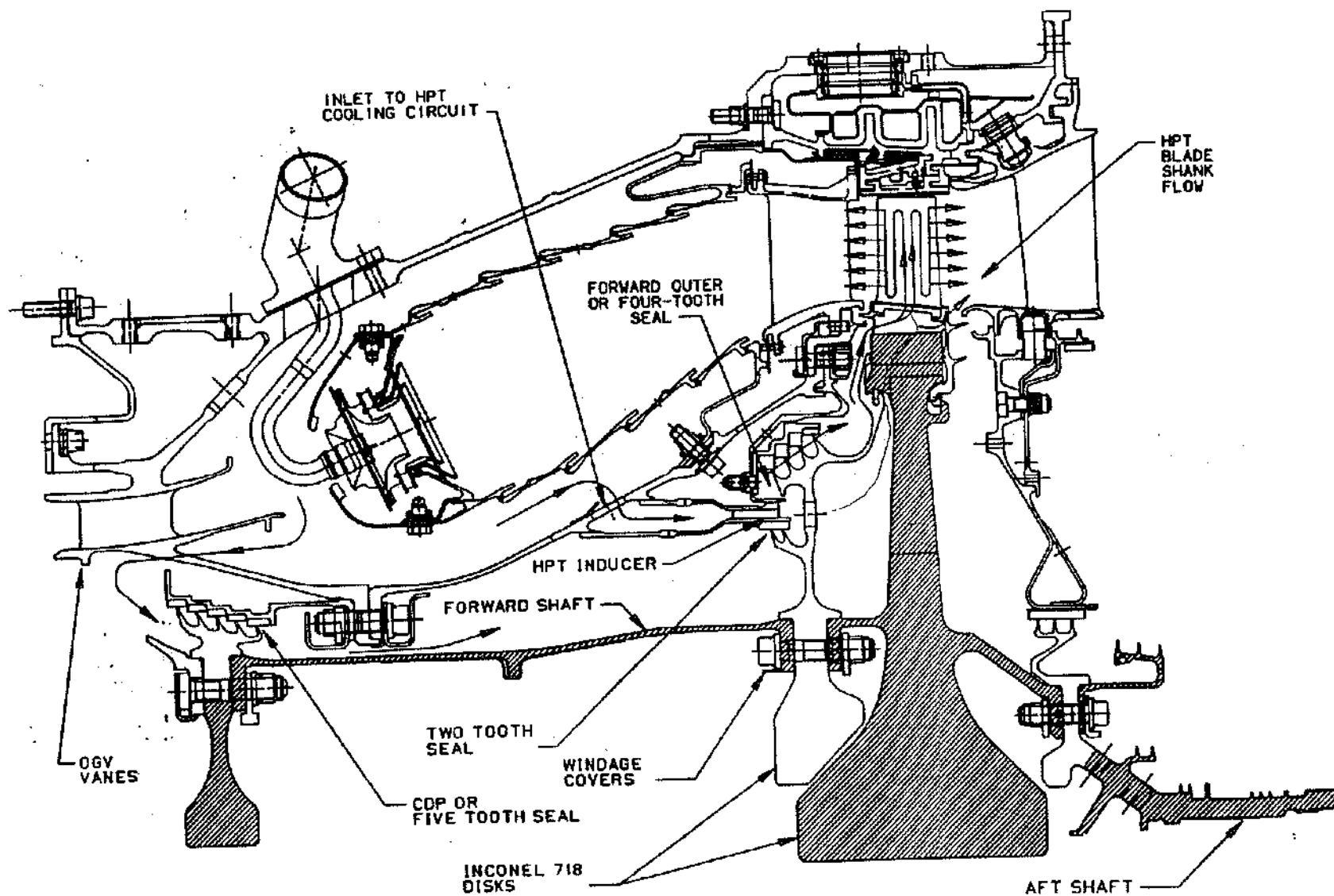


Figure 8.3 HPT Cooling-Circuit Hardware

and off design airflow, pressure, and temperature levels plus insure that seal configurations selected do not adversely affect other secondary systems such as rotor thrust bearing axial load.

LPT Cavity Purge System The CF6-80 engine design uses 7th stage compressor air to purge the HPT and LPT turbine disk cavities. This system is shown in detail in Figure 8.4. Air is bled from two locations of a 360 degree circumferential compressor case manifold to a 360 degree manifold at the turbine case, then through 13 pipes to 13 sets (6 vanes per set) of turbine vanes. Purge air flows through passages in the forward half of the vanes radially inward to the pressure balance seal internal cavity. The air is then directed forward to purge the cavity aft of the HPT. After purging the HPT, a major portion of the air flows under the pressure balance seal to purge the LPT rotor where approximately half the air flows to the turbine flowpath and the remainder leaks through the interstage seal between the HPT and LPT rotors.

This system was developed on the CF6-80A engine and incorporated in the CF6-80C2 version. The system involves the typical flow problem of delivering a required flowrate at a desired pressure or temperature but includes features which limit the amount of flow used. First, the same air that purges the HPT cavity is used to purge the LPT cavity. Second, the 7th stage air entering the HPT cavity is swirled in the direction of rotor rotation to create a vortex. Air which has significant angular momentum in a cavity with large radial dimensions can develop a free or forced vortex with an accompanying radial pressure gradient.

Understanding the reason for adopting the vortex system requires a look at the running clearances of the HPT/LPT interstage seals. As shown on Figure 8.2 the HPT rotor is a cantilevered rotor held by the 4R, 4B, and 5R bearings in the compressor rear frame. During takeoff, the gyro loads cause significant rubs on these seals. If the vortex system was not used, the system would leak more flow than required for purging these cavities. Figure 8.4 shows the design intent pressure gradient aft of the HPT plus test results of early and final development testing. Also shown is pressure data from an -80C2 engine. Note that without the vortex established the pressure ratio across the vortex seal inner diameter would be $1.24 \times (102.6/82.6)$ instead of $1.10 \times (91.3/82.6)$ which represents a significant difference in airflow. Once the pressure gradient is defined, the vortex seal becomes a "flow splitter" dividing the purge flow between the HPT and LPT cavities. Developing this system required considerable coordination effort between secondary systems, turbine aero, and turbine mechanical designers.

Parasitic Leakage Purge Systems High pressure compressor discharge seal leakage airflow, usually referred to as HP RECOUP air, is a significant factor in determining engine fuel consumption. Using engineering guidelines, seal configurations are designed to give the least leakage possible. The leakage that does occur is collected by the addition of another set of vent seals as shown in Figure 8.5. Rather than dump this air overboard, since it represents a significant amount of cycle work, it is directed back into the cycle at some convenient and useful location.

One example of such a system is shown on Figure 8.2 and in more detail on Figure 8.4. This CF6-80A/80C2 configuration uses HP recoup air to purge the inner and outer cavities around the stage 1 LPT nozzle. One drawback of the recoup air is that since it is seal leakage air its level is unpredictable because seal clearances change with time depending on how the engine is operated. An advantage is that as engine run-time increases, the seals tend to "wear in", opening up the seal clearances, and the purge flow increases. Another advantage of this particular design is that the recoup air acts as a buffer between the flowpath air and the 7th stage purge air. If the 7th stage air is decreased for any reason, any 1500°F flowpath air that is ingested into the cavities will be diluted by the 1000°F recoup air.

Another example of a recoup purge system is shown on Figure 8.6. This CF6-6 design uses air from the same leakage source to purge the turbine mid-frame liner cavity. This liner is used to protect the load carrying strut from the hot HPT exhaust gas temperature. Keeping these struts cooler helps keep oil lines that are routed through these struts from exceeding oil coking temperatures of approximately 450°F.

In addition to estimating parasitic flows, sizing piping and system orifices to be sure the air is properly distributed, the secondary systems engineer is responsible for calculating system effects of failure modes. Typical failure modes for this type of system might be supply pipe failures or liner/outer case cracking. Each of these failures presents a different problem for the engine. In the pipe failure case, hot flowpath air could backflow through the cooling circuit causing overtemperature of the parts the system was designed to protect. An analysis to define the effects and optimum location for one-way check valves in this system would be required. Liner/case cracking limits are usually a compromise between limits allowable for safe hardware operation and limits allowable before another system is affected. For instance, outer case cracking may adversely affect under-cowl cooling temperature since it would leak directly into that region.

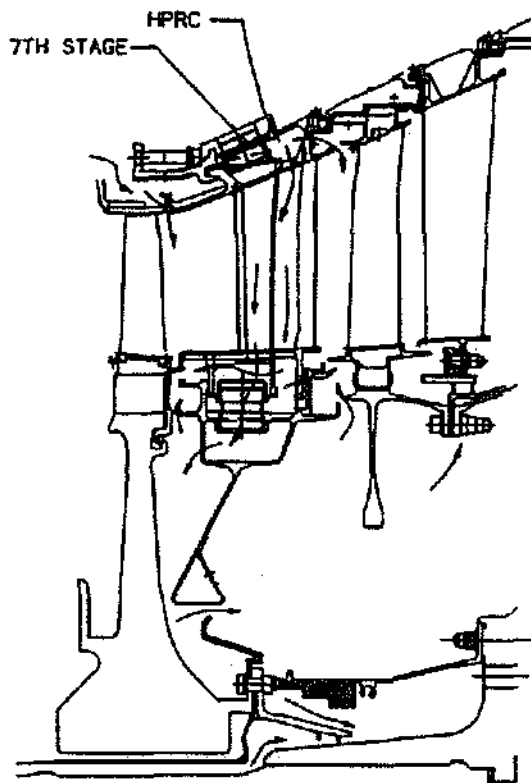
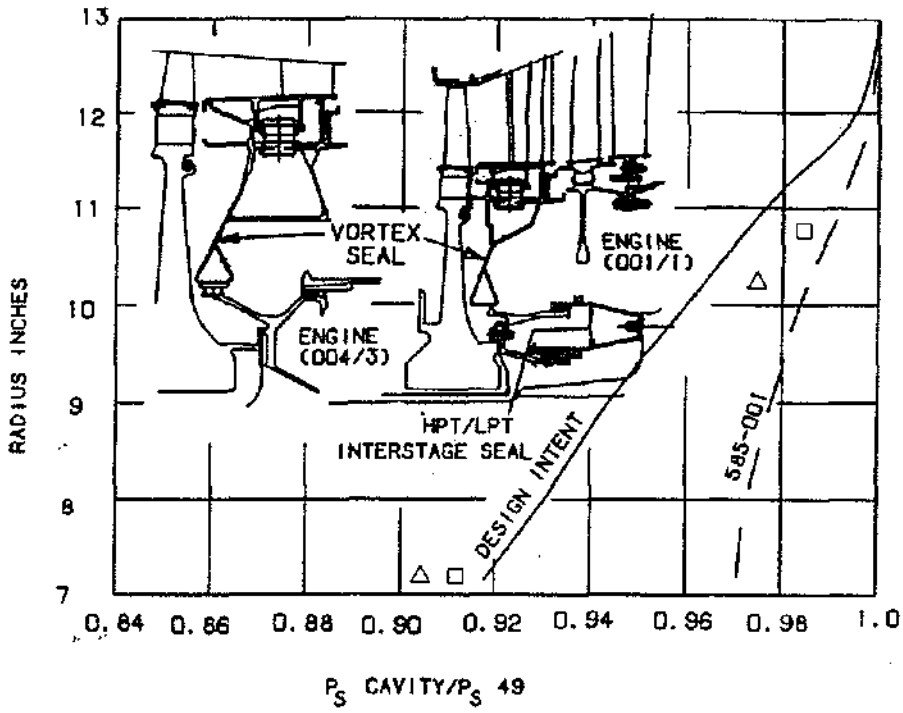


Figure 8.4 LPT Cavity Purge System

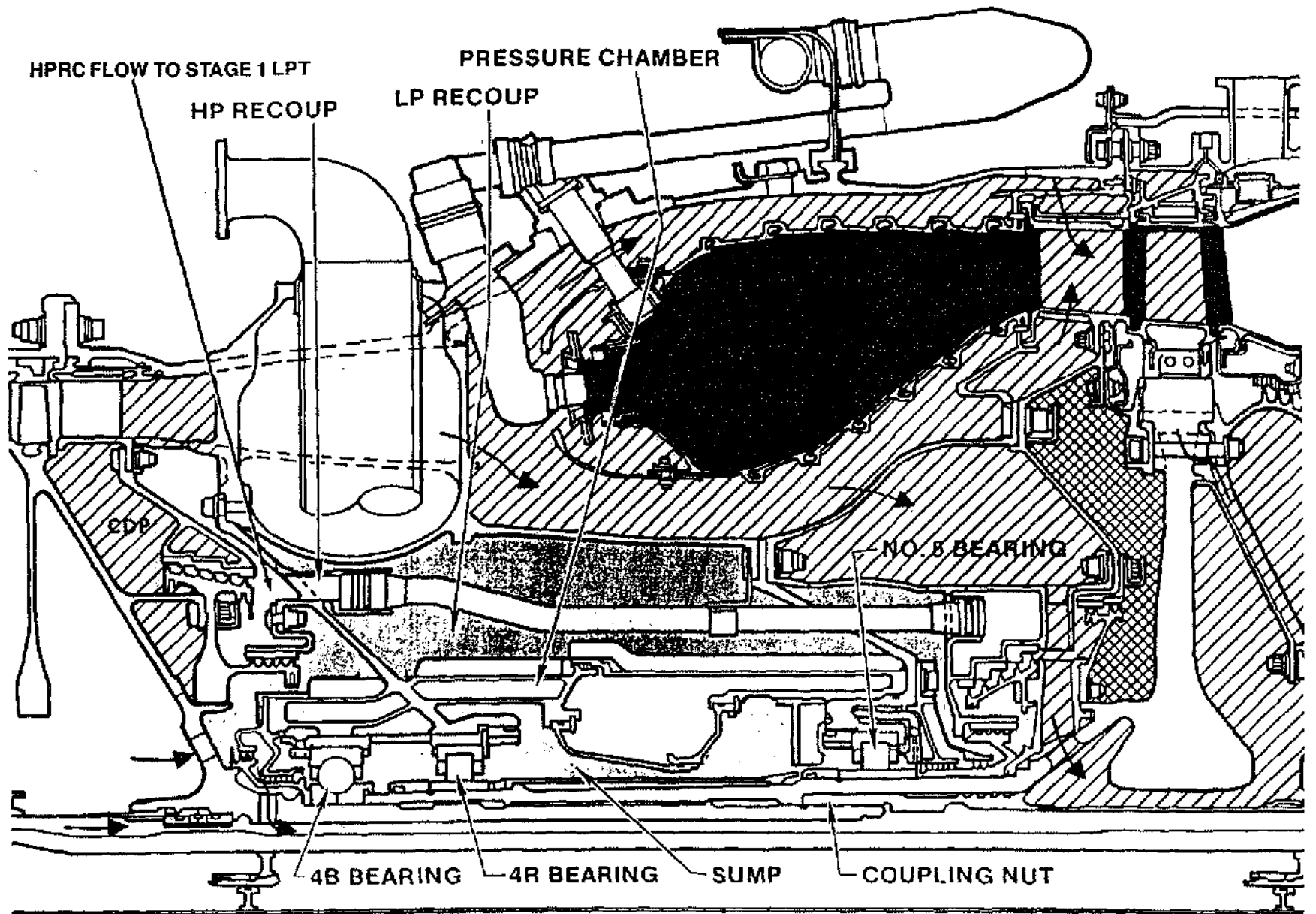


Figure 8.5 Parasitic Leakage Purge Systems

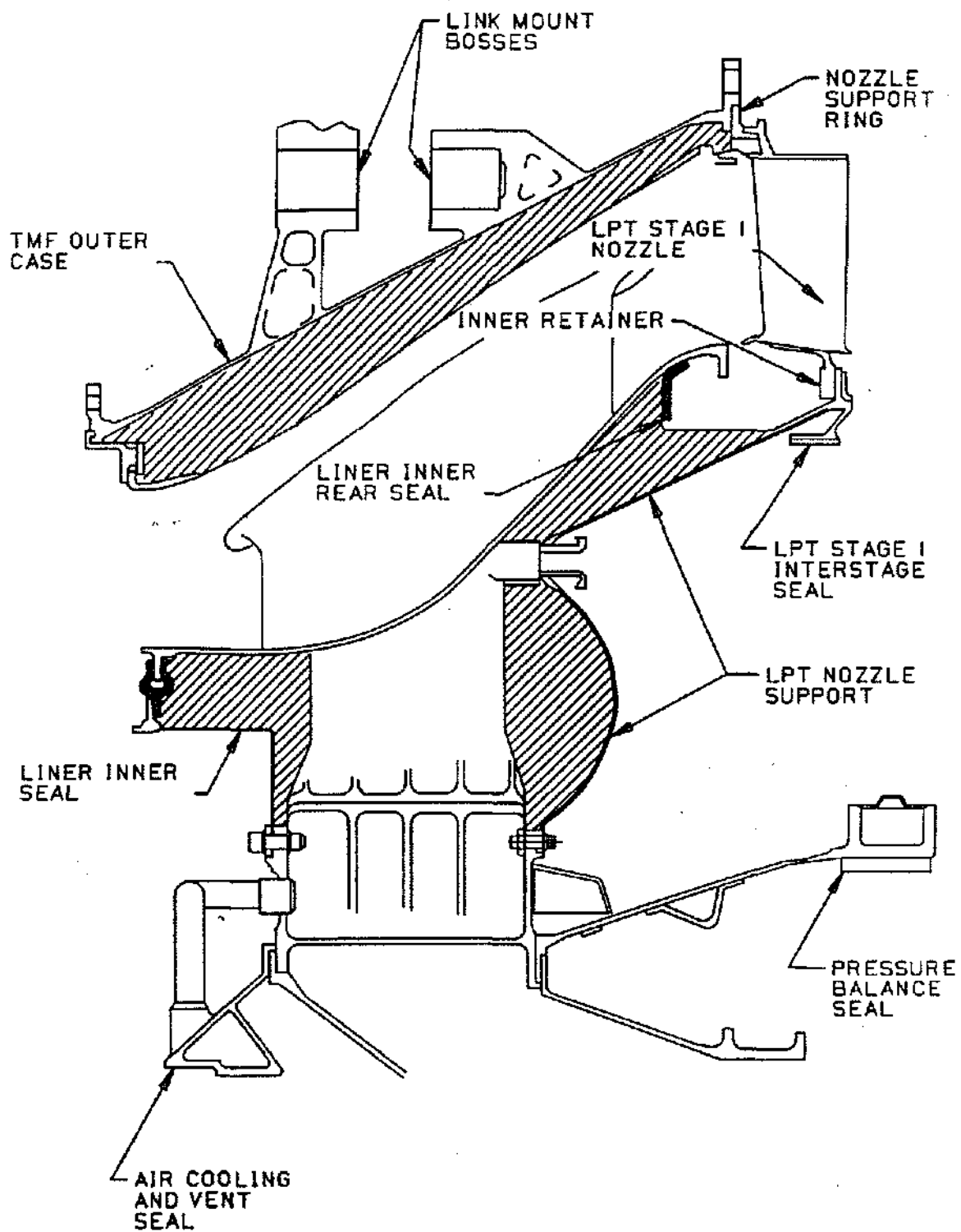


Figure 8.6 Recoup Purge System

Heating Systems A heating system is one which extracts heat from one part of the cycle and pipes it to a cooler, low pressure section of the engine. Examples include anti-icing or de-icing, compressor bore heating (see clearance control), CDP seal bore heating, and TRF hub heating.

Anti-Icing/De-Icing Anti-icing systems prevent ice buildup and require more heating air (and engine SFC) than de-icing systems which allow cyclical ice buildup and shedding. Choice of systems is determined mostly by the type of mission required and the particular engine configuration. Engines with hardware that is sensitive to ice impact require anti-icing systems. Each of these systems require a significant level of engine testing to verify ice formation characteristics and system operability.

CDP Seal Bore Heating Figure 8.7 is a cross section of the CF6-80C2 forward compressor discharge seal showing the flow direction of the CDP bore heating air. The purpose of this air is to increase the heat transfer into the rotating seal disk so its transient response is more closely matched to the response of the seal rim. Secondary Sys-

tems responsibility in this design is to size the circuitry for the configuration chosen to ensure the required flow is delivered. The steady state and transient heat transfer responses of the system are the responsibility of the heat transfer engineer. This data is forwarded to the mechanical design engineer who performs the stress and life calculations.

TRF Hub Heating A system similar to the CDP heating is also used on the CF6-80C2 turbine rear frame. This circuit is shown in Figure 8.8. Scoops in the side of the turbine frame struts feed hot cycle air radially inward to the frame hub for improved hub response. Hardware life can be increased appreciably by use of these relatively simple systems.

Clearance Control Systems In clearance control systems, air at different temperature than normal is used to cool or heat hardware to control radial growths impacting rotor clearances. Either cooling or heating systems have been designed for high pressure turbines and compressor bore cavities of various engines as described below.

CF6-80C2

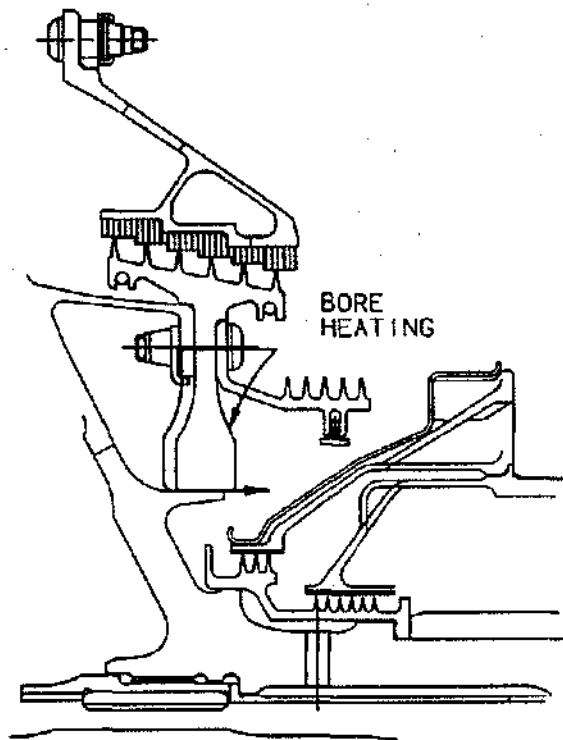


Figure 8.7 CDP Seal Bore Heating

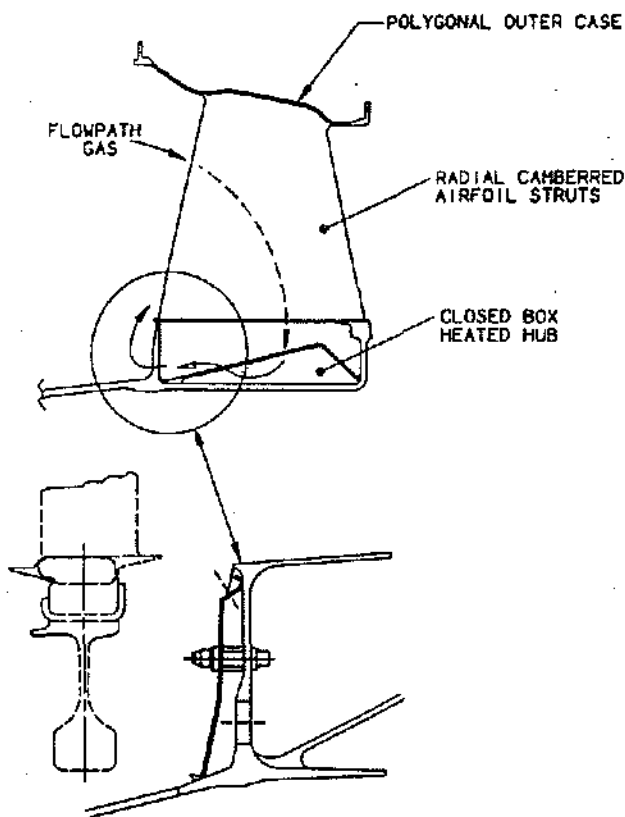


Figure 8.8 Turbine Rear Frame Hub Heating

HPT Flange Cooling The CF6-80C2 engine uses fan discharge air to cool the flanges above both stages of the HPT. This cooling system shown for the left side on Figure 8.9 controls turbine blade tip operating clearances for improved engine performance. A similar piping circuit supplies the right hand side. The clearance control piping is in parallel with the core compartment cooling system which cools various components inside the cowl. The secondary system engineer models the complete circuit to determine pressure losses so that components will receive required flow levels and clearance control manifolds will receive flow at proper pressures needed for impingement cooling. The impingement circuits and flange responses are the design responsibilities of the heat transfer engineer.

The CFM56-5 engine has a somewhat more complicated system in that it uses a combination of 5th and 9th stage

air to more closely control the heat flux delivered to the flanges. Thermocouples at the flanges provide feedback to the digital control for heat flux adjustment during engine operation.

LPT Case Cooling LPT case cooling systems are typically "bird cage" style as shown on Figures 8.2 and 8.9. These systems are generally steady state systems turned on above a particular altitude with flow levels set to optimize clearances at cruise. Again the design responsibilities are divided between secondary systems, heat transfer, and mechanical design groups.

HPC Bore Cooling Compressor bore cooling circuits are some of the most challenging secondary circuits to design because measured pressures, temperatures, and airflows within the circuit are difficult to obtain. Essentially all elements in the system are rotating so slip rings or telemetry modules are required for all instrumentation readouts.

The CF6-80C2 bore cooling circuit is shown on Figures 8.1 and 8.2. This circuit uses booster discharge flow to limit the growth of the compressor disks so major excursions in compressor blade tip clearances are prevented. The air then passes under the B/C sumps and HPT, providing cooling for the LPT shaft and discharges at the exit of the last stage of the LPT. This system has little clearance change effect on hardware other than the compressor.

The CFM56-5 engine has a much more effective bore cooling circuit. Figure 8.10 shows a cross section of the Rotor Active Clearance Control (RACC) This system uses 5th stage air to heat up the hardware shown on the figure. As shown, the compressor, CDP seal and turbine clearances are all affected so much larger performance benefits are realized.

Seal Pressurization Seal pressurization circuits serve two functions. The primary purpose is to keep the lubrication oil in the sumps at all attitudes and altitudes expected during the typical mission. The CF6-80A attitude envelope, which is typical of most commercial engines, is shown on Figure 8.11. Second, the circuit insulates the hot sumps from radiation of combustors and turbines. A schematic depicting sump philosophy is shown on Figure 8.12. A second set of seals is placed around the sump oil seals and pressurization air from some appropriate source is introduced between the two sets of seals. The figure shows labyrinth seals but either carbon or "lab" seals can be made to work well.

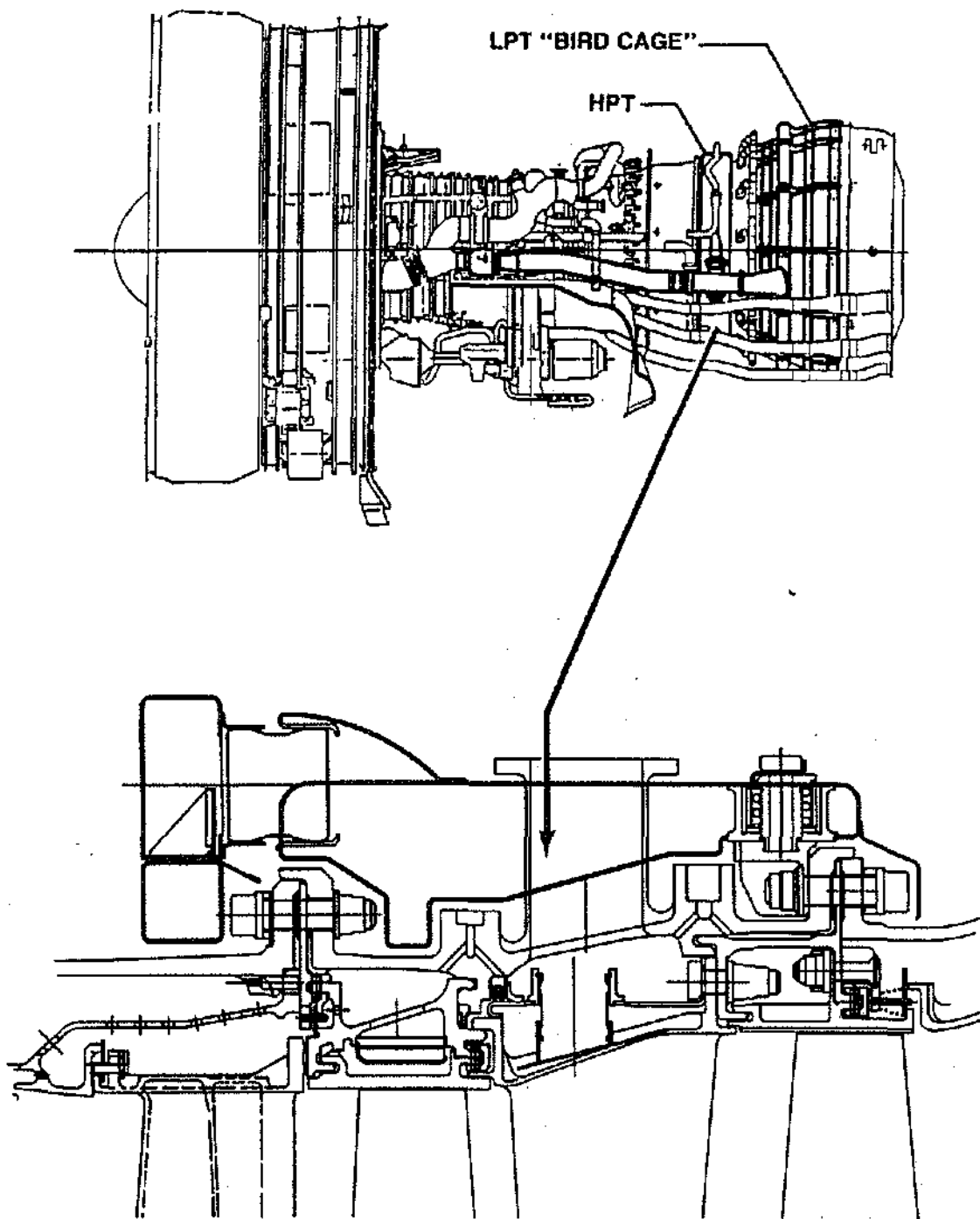


Figure 8.9 HPT Active Clearance Control

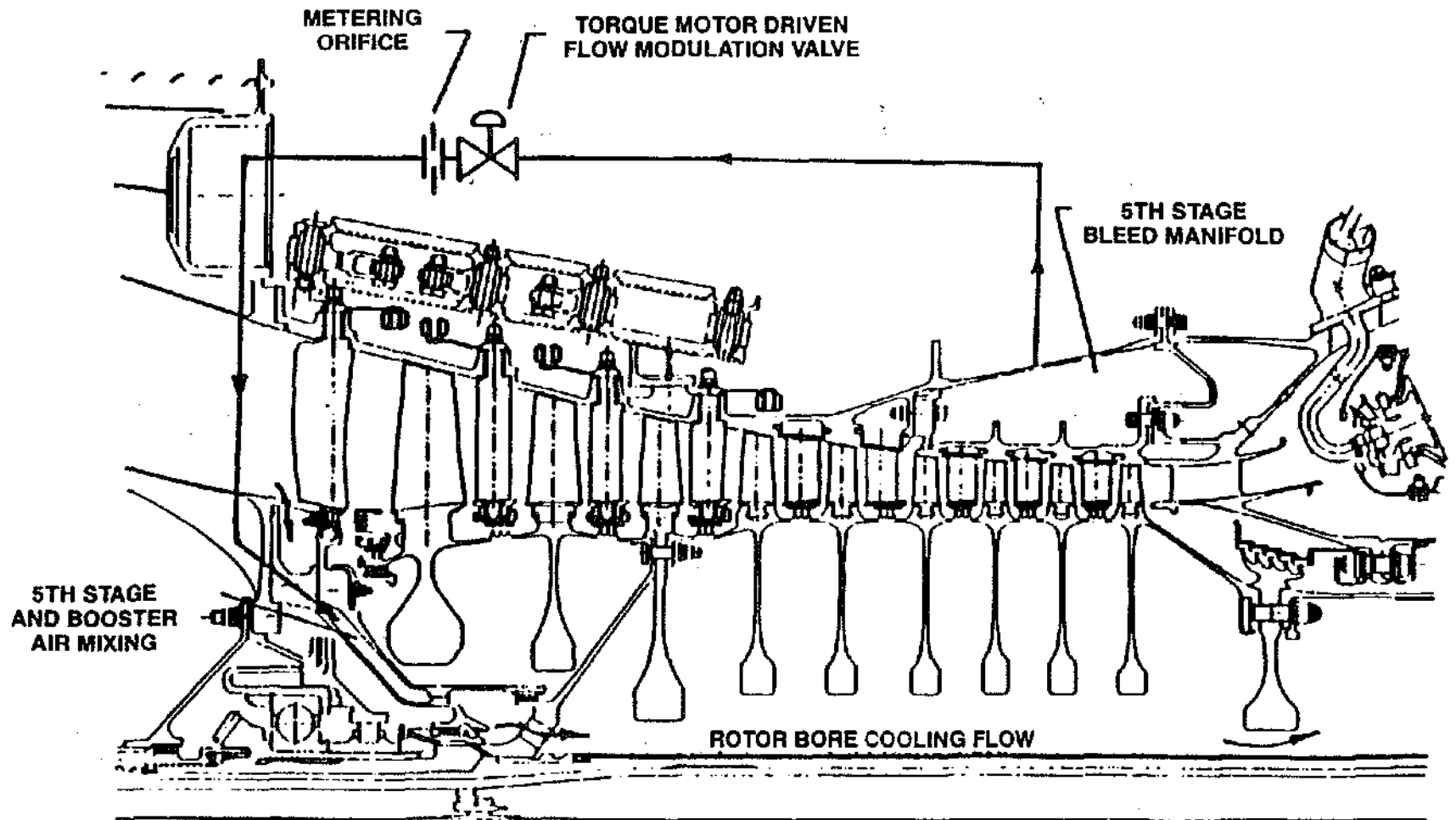
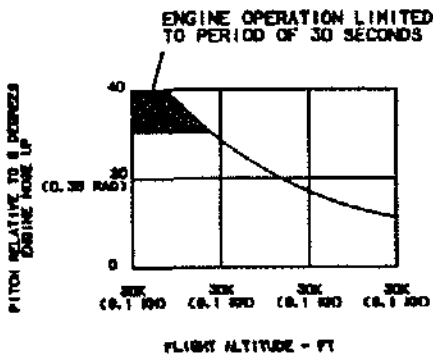
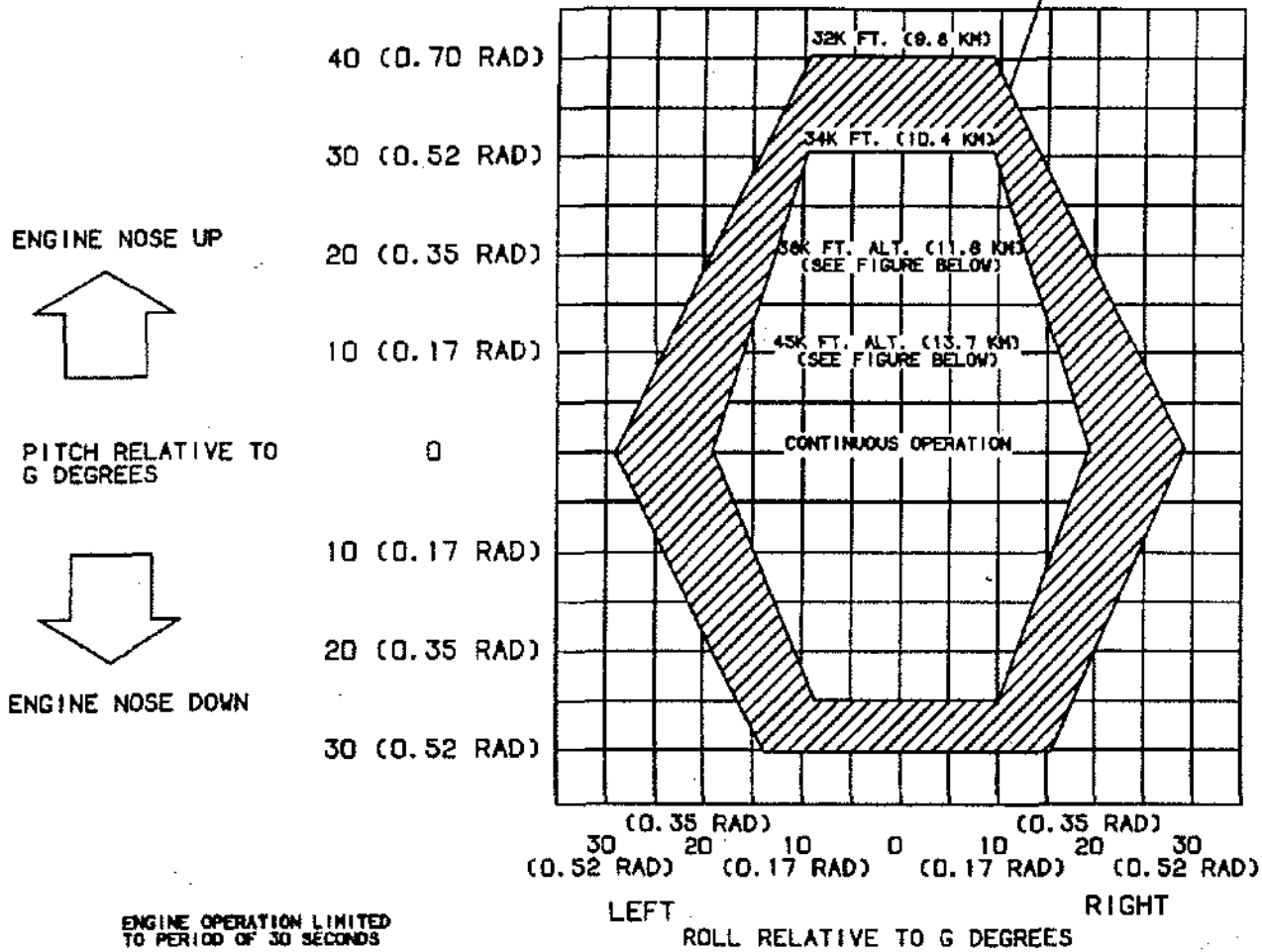


Figure 8.10 Rotor Active Clearance Control

ENGINE OPERATION LIMITED TO PERIOD OF 30 SECONDS



NOTES:

1. CONTINUOUS OPERATION IN ENCLOSED CLEAR AREA AND 30 SECONDS OPERATION FOR SHADED AREAS
2. NEGATIVE G IS LIMITED TO 30 SECONDS
3. ZERO G IS LIMITED TO 30 SECONDS
4. PITCH AND ROLL ARE DEFINED AS THE ANGLES BETWEEN NORMAL VERTICAL AXIS OF THE ENGINE AND THE RESULTANT WEIGHT VECTOR OF ANY RETAINED FLUID

Figure 8.11 CF6-80 Flight Attitude Envelope

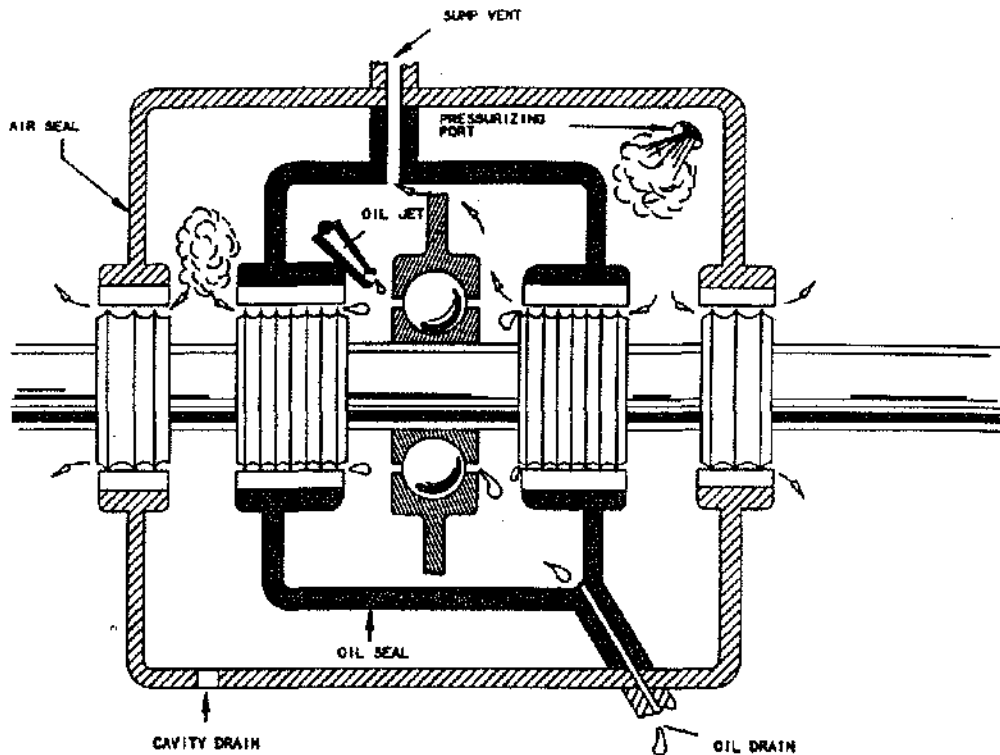


Figure 8.12 Sump Philosophy

Labyrinth Seals One of the drawbacks of labyrinth seals is that they always require more pressurization air. However, once the system is properly designed, the seals are extremely trouble free and require very little maintenance. A functional design using "lab" seals can be seen on Figure 8.5. Some pertinent criteria include pressurization air temperature of less than 600°F, the seal cannot be submerged in oil, by current practice four to seven teeth are utilized, thermally self-clearing of seals during rubs (teeth on rotating shaft), no pressure reversal, inherently higher air leakage rates, and low heat generation.

Once the secondary system designer determines the basic seal definition such as number of teeth, type of rub material, stepped or straight-through flow, it is up to the bearings and seal designer to do the mechanical design. His function as described in that portion of this course is to define material, evaluate thermal and vibratory response, provide weight, cost and a variety of other tasks.

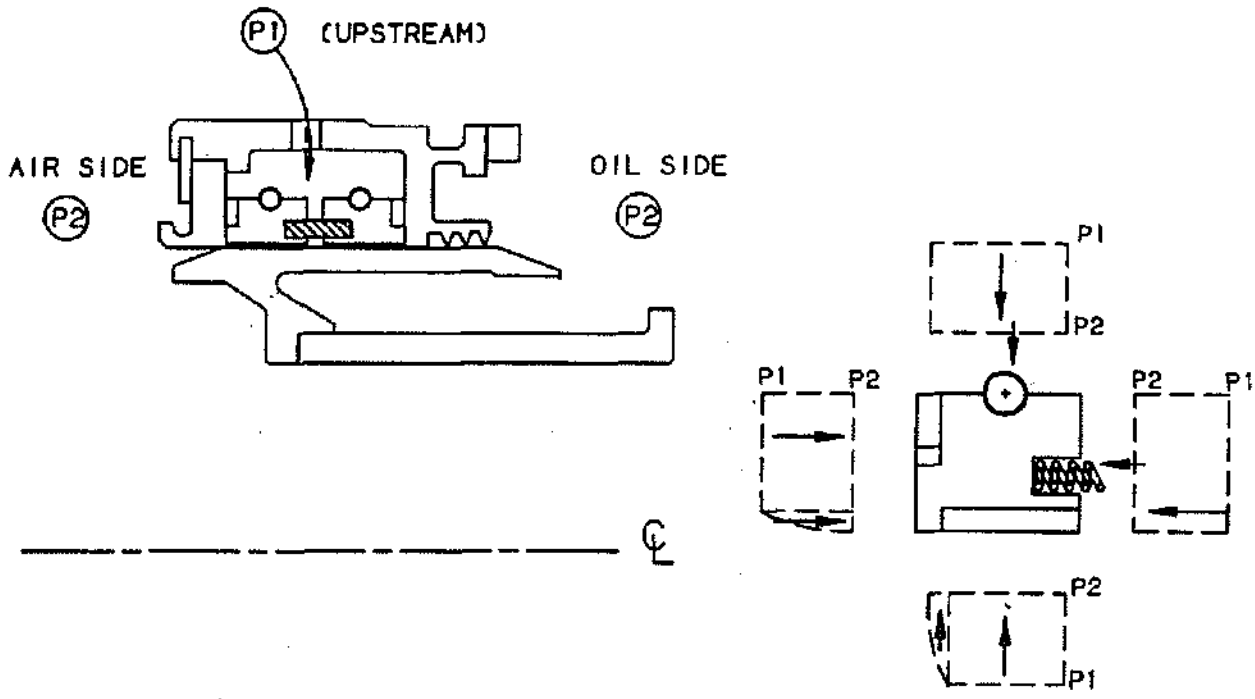
Carbon Seals There are two main types of carbon seals: circumferential (bore rubbing) and face rubbing seals. Bore rubbing seals are preferred if engine speed, maintenance requirements, and life requirements can be met.

Carbon seals can also be gas or liquid seals. In general, main shaft sump seals are gas seals in that they are required to limit the amount of air entering the sump. Gearbox seals are liquid seals since they limit oil leakage out of the gearbox.

Major carbon seal problems are due to assembly damage or hangup in service due to oil coking. Particular attention must be taken in the design process to assure proper cooling and ease of assembly. Figure 8.13 gives a typical cross section of each of the two types of seals. Detailed engineering guidelines are available on carbon seal design.

Some major points for circumferential seals are pressurization air temperature less than 850°F, 80 psid pressure maximum steady state, maximum surface speed of 420 feet per second, non-exuding carbon, and the ability to be used singularly or in tandem. Face rubbing seals are designed for use at pressure levels above 80 psid, a pressurization pressure limit of 150 psid, and oil must not reach load springs unless spring temperatures are less than oil coking level of 400°F. An in-depth thermal analysis of rub face is required.

CIRCUMFERENTIAL SEAL



HYDRODYNAMIC FACE SEAL

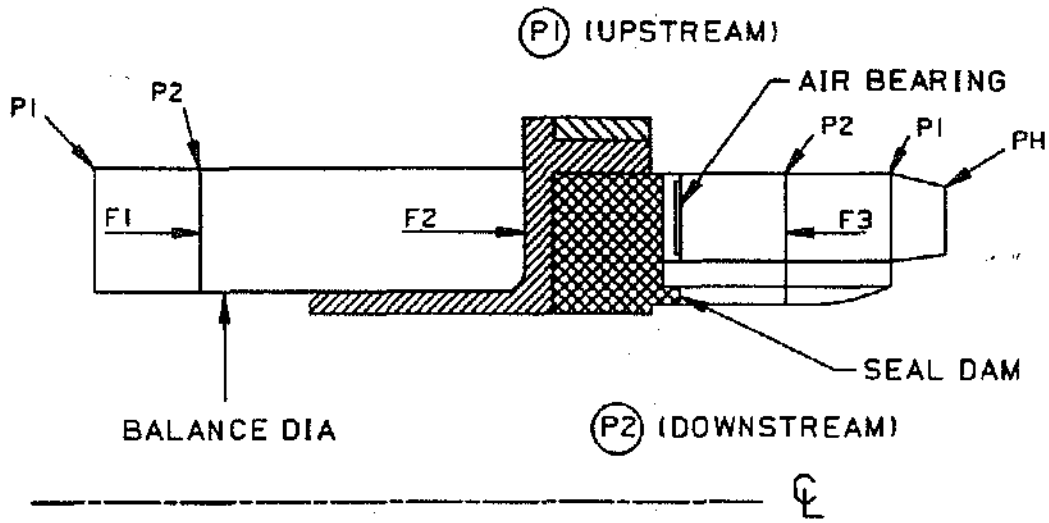


Figure 8.13 Carbon Seals

Customer Bleed Customer bleed is compressor bleed air extracted through piping to supply aircraft with air for cabin pressurization/air conditioning packs, avionics cooling, or other miscellaneous uses. Secondary systems design does not have responsibility for sizing this engine piping but is occasionally called on to model these systems for problem analysis. A schematic representation is shown in Figure 8.14.

OIL SYSTEMS

Engine oil systems consist of several subsystems. Each of these subsystems and the components involved are described below. The purpose of these systems is to lubricate and cool the bearings and cool sump walls. Oil is the transport medium which transfers heat obtained in the sumps to the engine fuel system or in some cases the ambient airstream. A typical lube schematic is shown in Figure 8.15. Oil stored in the tank is delivered through the lube supply system to the sumps where it drains by gravity to the scavenge system and returned to the tank

by the scavenge pump. The oil is filtered on either the supply or scavenge circuit, or both, to less than 45 micron particle size. Also included in the supply or scavenge circuit is a fuel oil heat exchanger. System flowrate is sized to accept engine heat load with 50 to 100 Fahrenheit degree temperature rise.

Lube Supply System The lube supply system consists of the oil tank, lube supply pump, filter, piping and bearing oil jets. Lube supply systems can be either full flow or pressure relieved systems. The pressure relieved system limits the lube pressure to some maximum desired level by means of a pressure relief valve in the pump. In the full flow system, lube pressure is a function of pump flow, oil restrictions, and oil temperature. Since the lube jets essentially act as a fixed orifice, and pump flow is determined by pump speed, the lube pump is sized to give the desired flow at 100% speed and pump pressure falls out as a by-product. This is the preferred system, since any plugged jets or broken lines will show up as an abnormal oil pressure. Typical supply pressures are from 40 to 80 psid.

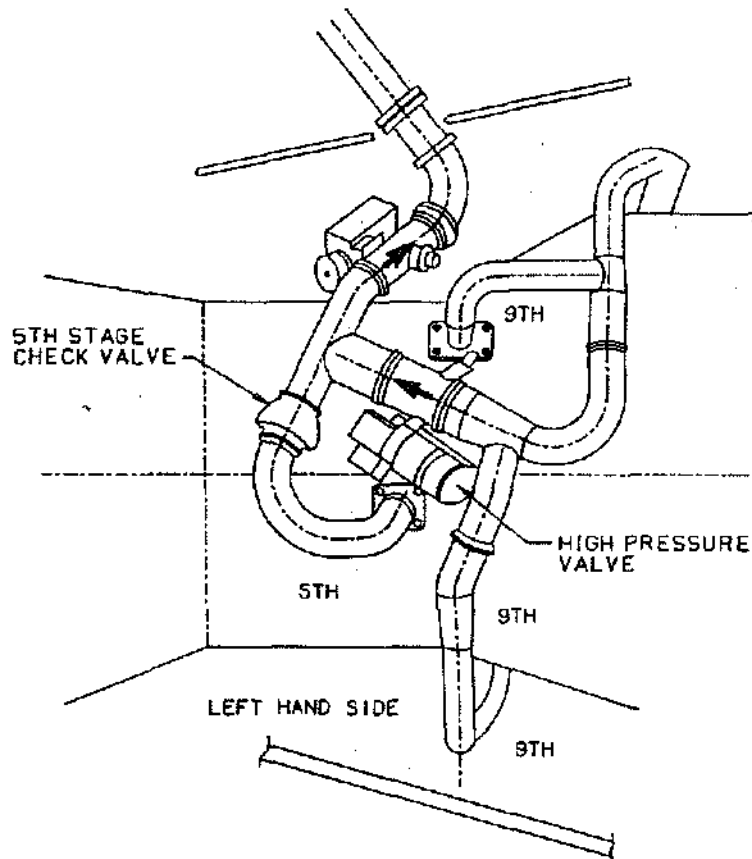


Figure 8.14 CFM56-5 Customer Bleed System

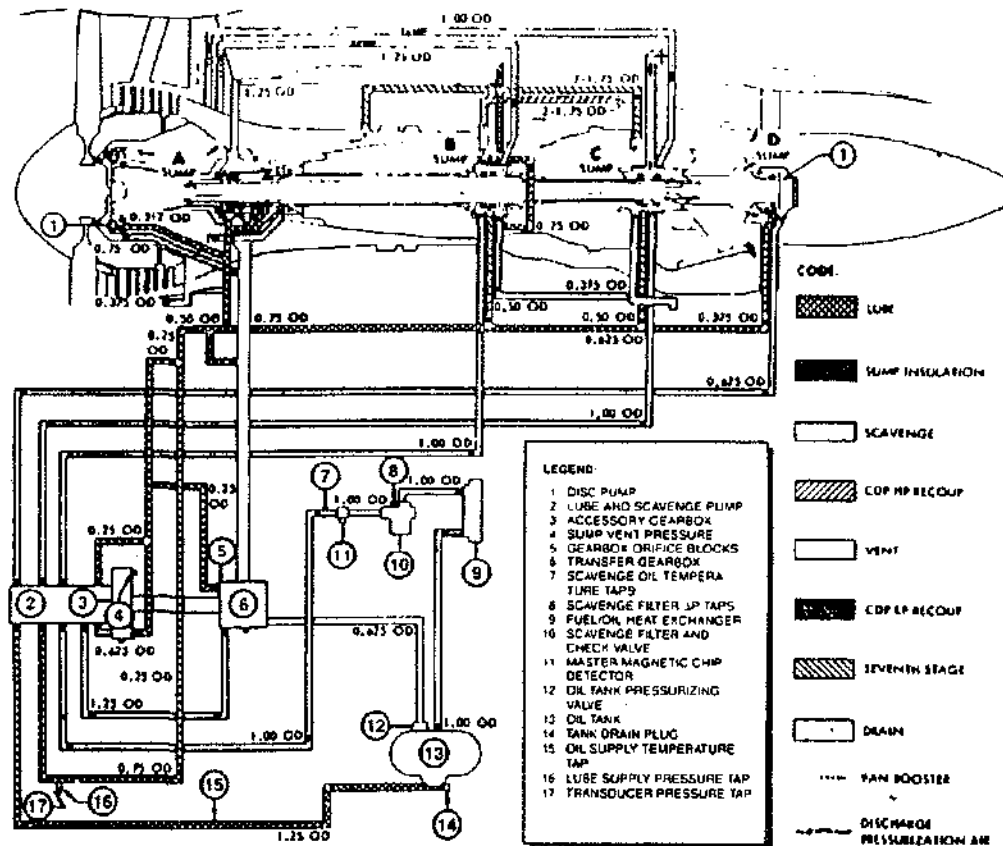


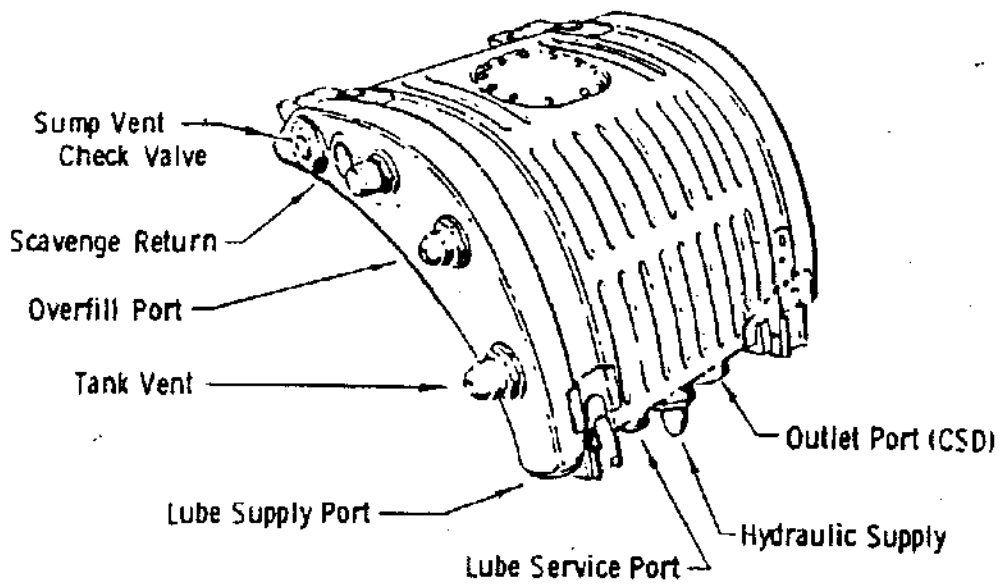
Figure 8.15 Lube System Schematic

Lube Tank The functions of the lube tank are to store oil, deaerate scavenge oil, accommodate inverted operation (if required), vent excess air, provide adequate supply pump inlet pressure, and provide for oil sampling. Lube tank size is determined by estimated engine oil consumption, system gulping (oil quantity in transient operation), all attitude reserve, and expansion space for oil thermal excursions. Oil tank shape is frequently determined by available space, particularly in military applications. A good example is the J79 tank shown in Figure 8.16. That same figure shows an internal schematic of the tank giving an indication of the complexity of tanks for engines requiring inverted flight.

All tanks have a tank pressurizing valve which builds up tank pressure so a positive pressure will always be maintained on the supply pump element to prevent cavitation even at high altitudes. The source for this pressure is air that is returned to the tank with the scavenge oil. The air is routed through a deaerator inside the tank then vented back to the gearbox or overboard through an air/oil separator. Depending on the application, tanks can have manual oil level indicators or electrical cockpit indication. All tanks have remote fill/overflow ports for servicing with a lube cart.

Lube Pump The lube and scavenge pump elements are usually housed in the same casting. A typical cross section is shown in Figure 8.17. Pumping elements can be vane, gear or gerotor (internal gear) type elements. Each type is shown in Figure 8.18. Once the engine requirements have been established, the pump specification can be issued and the vendor competition and selection completed. Then the development testing and engine qualification testing follows. The pump body is sometimes used to provide other functions such as chip detector mounting, inlet screen mounting, cold start bypass relief valve, filter mounting, filter bypass mounting, filter service shutoff valves, or core speed sensor drive/mounting.

Lube Pipe Lines and Jets Lube supply lines are sized to deliver required oil flowrates to the sumps at a maximum velocity of 10 feet per second. This assures that the majority of the system pressure drop will take place at the lube jets. The use of stainless steel tubing is required. Supply lines are routed near the bottom of the engine to minimize effects of soakback temperature increase after shutdown. Lube jet minimum diameter is limited to 0.025 inches to minimize jet plugging.



J79 OIL TANK SCHEMATIC

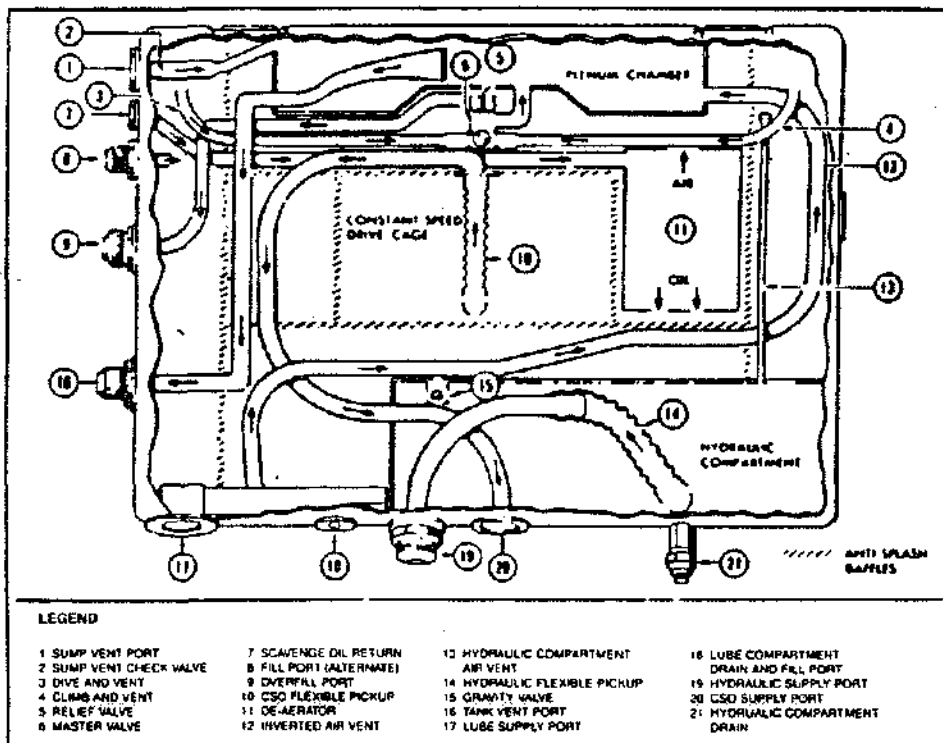


Figure 8.16 J79 Oil Tank

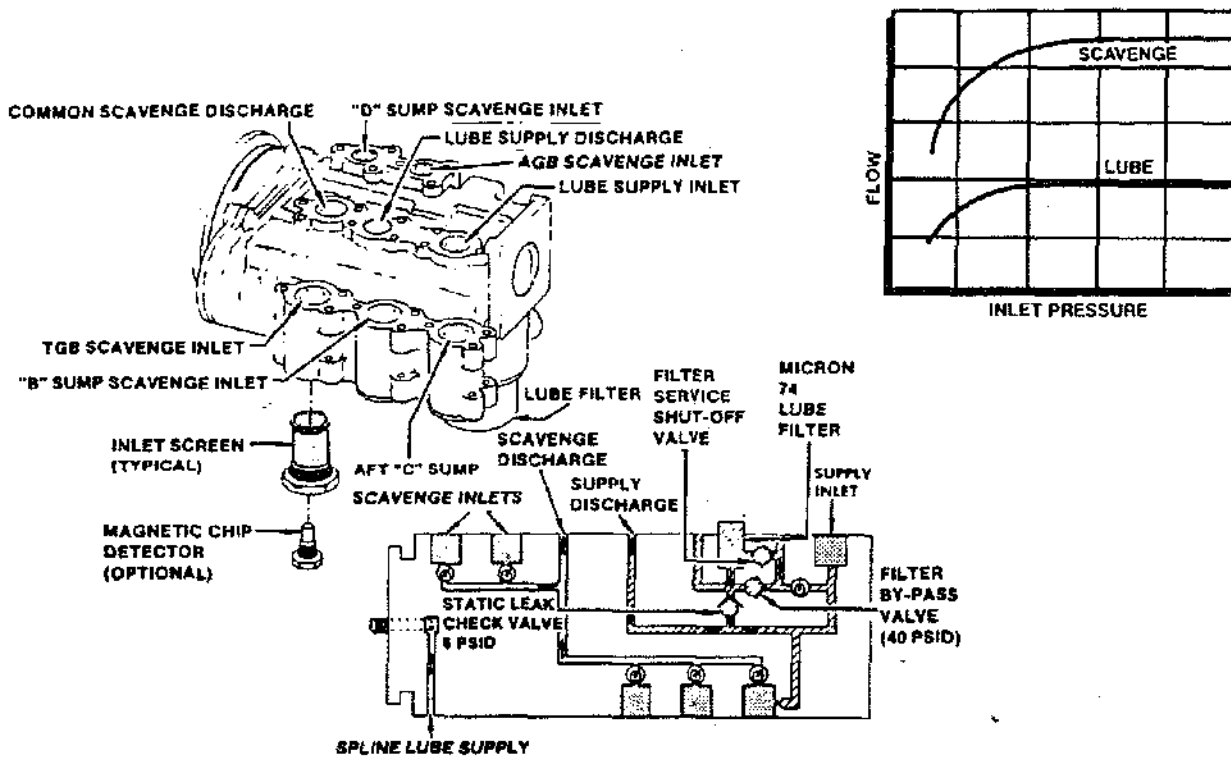


Figure 8.17 Lube and Scavenge Pump

Lube Scavenge System The oil scavenge system consists of the gravity drain regions in the sumps including piping to the pump, scavenge pump, filter, and heat exchanger. The purpose of this system is to prevent oil storage in the sumps and transport the sump generated heat to an outside cooling source.

Lube Scavenge Pump Scavenge pump elements can be of the same types as supply elements but are sized to have three times the capacity of the oil delivered to the sump being scavenged. This excess capacity assures dry sump operation so that bearings do not run submerged in oil which could cause excess heat generation. This excess capacity is the primary reason a deaerator is required in the lube tank. Scavenge elements should be primed by gravity. The elements are usually required by specification to be self priming to inlet pressures as low as 1.5 psia. The discharge side of the elements must be submerged in oil. Scavenge element seizure should cause failure of the supply pump as well to prevent the possibility of sump flooding.

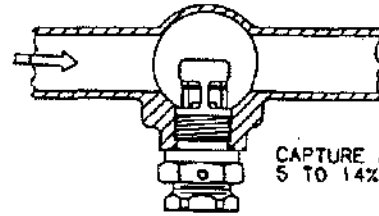
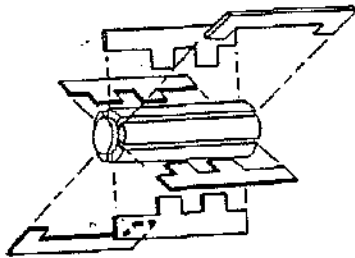
Fuel Oil Cooler The oil cooler regulates the temperature of engine oil by transfer of heat from the oil to the engine

fuel. The properly designed cooler thermodynamically responds to changes in heat load (oil flow and temperature) and heat sink (fuel flow and temperature) so as to maintain required engine oil temperatures. Heat transfer performance requirements for the oil cooler are established by systems analysis of the engine. Overall considerations of engine weight, available envelope space, cost, and reliability are also considered in establishing fuel oil cooler performance requirements.

Limits of fuel and oil pressure drop are imposed on the cooler as well. Other important considerations are failure effects such as fuel leaking into oil or to external regions, maintainability (cleanability), and repair.

Chip Detectors Chip detectors are magnetic devices installed in main or individual scavenge lines or in the bottom of oil tanks or gearboxes to collect wear particles. These devices all collect particles by means of a magnet and are useful for collecting chips greater than 50 micrometers. Also available are electric chip detectors with connections for remote (cockpit) indication. Several varieties of magnetic chip detectors are shown on Figure 8.19.

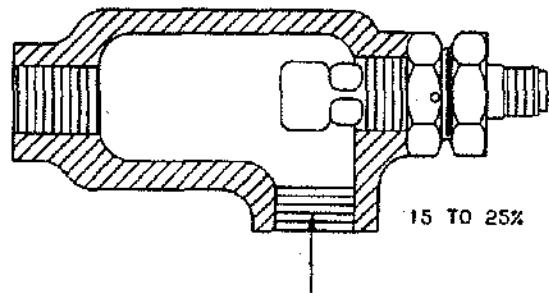
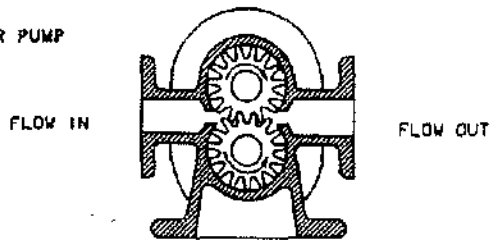
VANE PUMP



CAPTURE EFFICIENCY
5 TO 14%

(A)

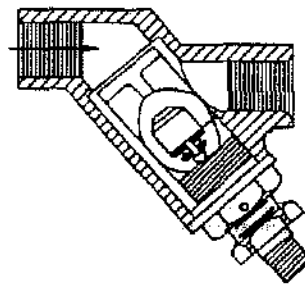
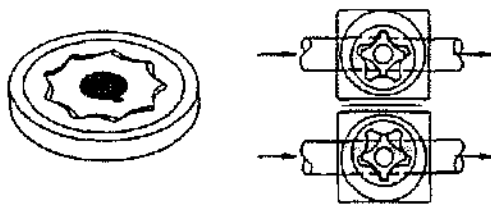
GEAR PUMP



15 TO 25%

(B)

INTERNAL GEAR PUMP



100% (PARTICLES
LARGER THAN
SCREEN MESH)

(C)

Figure 8.18. Various Types of Pumping Elements

Figure 8.19 Chip Detectors

Sump Vent System Sumps can be either vented or non-vented designs. A schematic of a vent system is shown on Figure 8.20. The aft most sump on Figure 8.2 is an example of a non vented sump. The sump vent system provides the following functions: to maintain sump pressure below pressurization air levels, to maintain scavenge pump inlet pressure above the minimum acceptable performance level, to provide acceptable oil consumption rates, and to provide transient capability.

Air contained in the vent system is supplied by leakage across sump oil pressurization seals. If the vent circuit exiting the sump is oversized, the sump pressure will be low. This causes increased seal flow which in turn increases oil consumption by carrying more oil particles overboard. The low sump pressure also is detrimental to scavenge pump performance. If the vent circuit is too small, the sump pressure will be too high, forcing the oil out through the oil seals. The secondary systems designer must size these vent areas so that proper balance is maintained during both steady state and transient operation.

Non-vented sumps have quite different design requirements. These sumps must necessarily be small in volume and located in low pressure areas, usually in the forward or aft end of the engine. These sumps rely on the excess capacity of the scavenge pump to prevent oil leakage from the sump. Ambient temperature is limited to 600°F. Vent flow is directed overboard usually through an airoil separator which removes oil particles from the air to minimize oil usage.

Air-Oil Separators Lack of adequate air-oil separator capacity has been the most common cause of high oil consumption on jet engines. Static separators usually mounted in lube tanks, have low air capacity, typically 30 standard cubic feet per minute (SCFM). Dynamic separators, usually built into a gearshaft or main rotor shaft, can have capacities up to 250 SCFM. Dynamic separators are used in most recent engines. A schematic of a gearbox mounted and intershaft mounted separator are shown in Figure 8.21. Both are examples of dynamic separators.

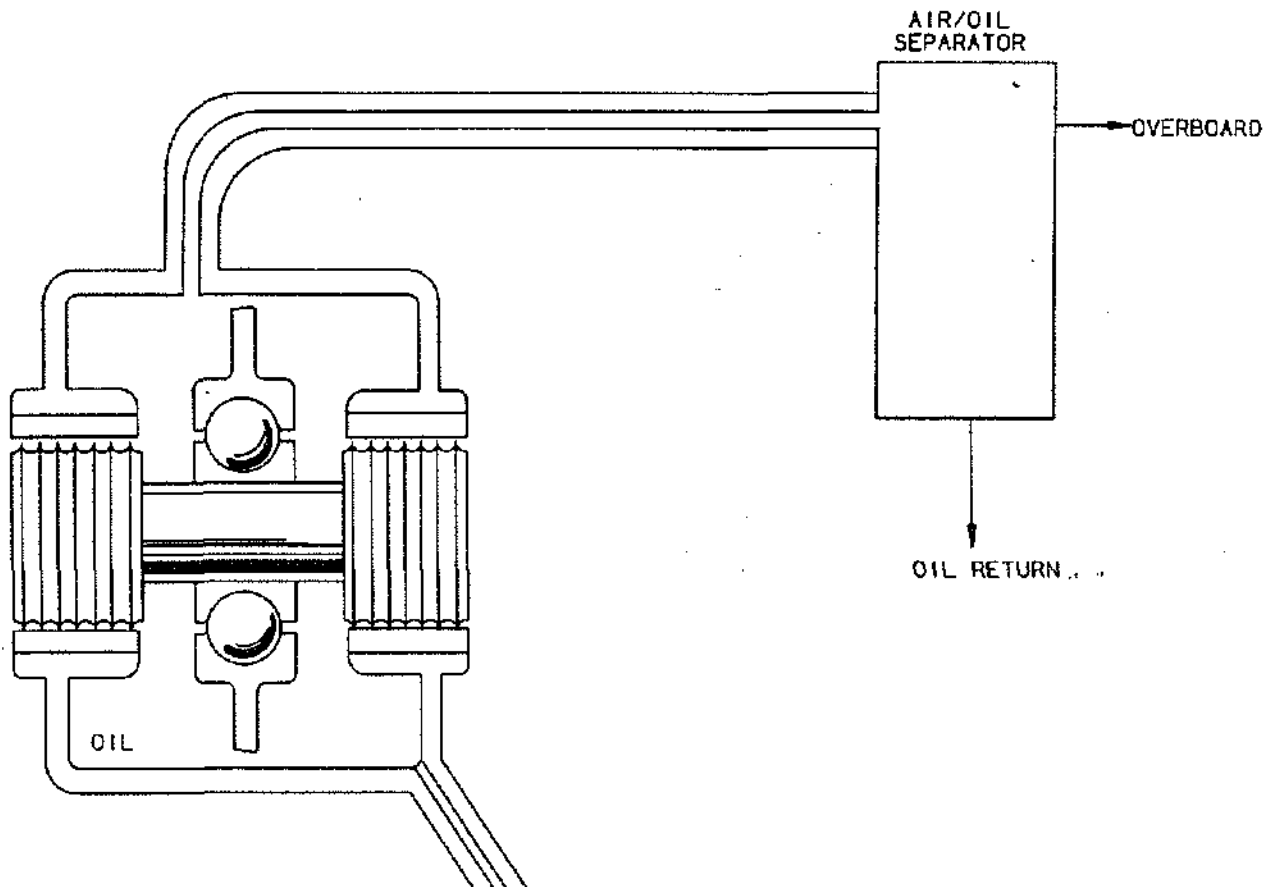
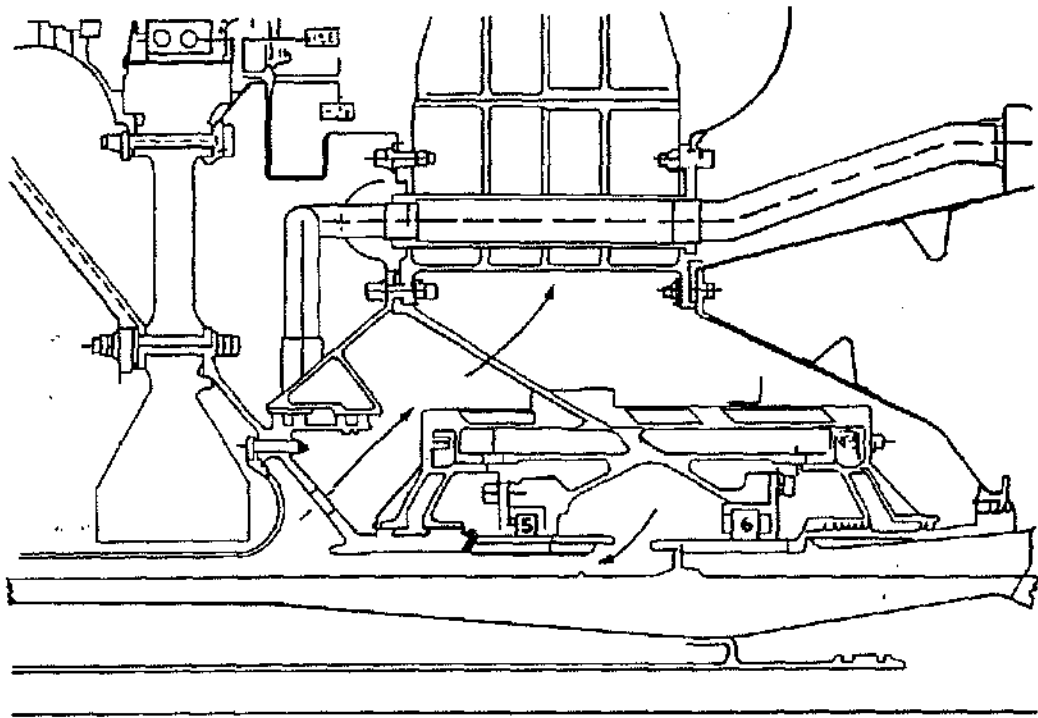


Figure 8.20 Vent System

INTERSHAFT AIR/OIL SEPARATOR



AIR/OIL SEPARATOR

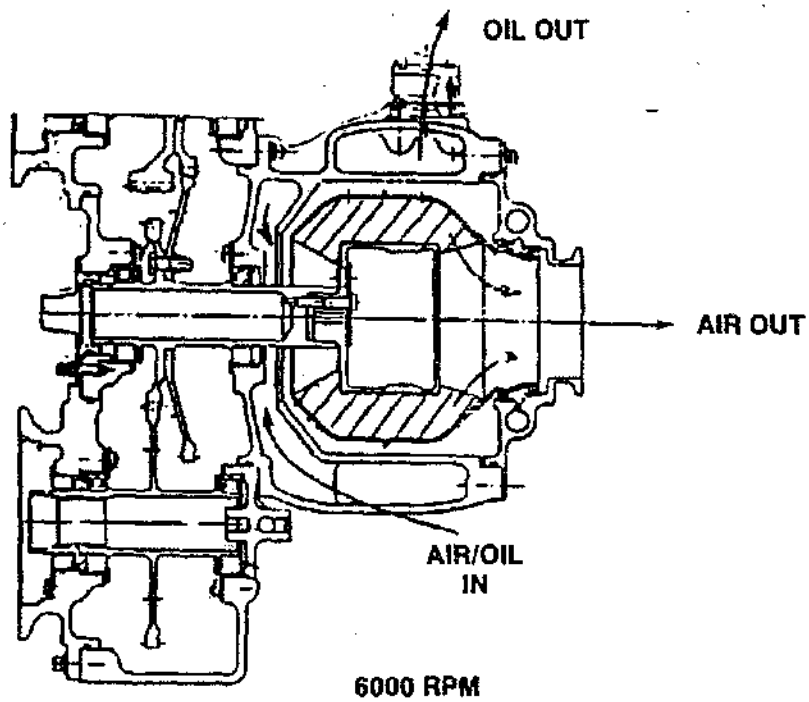


Figure 8.21 Air-Oil Separators

Oil Consumption For engine designs with labyrinth seals, oil consumption is largely a function of vent air-flow and temperature. Over the total life of the engine the seals tend to wear so vent flowrates gradually increase. For this reason, oil consumption quoted in engine specifications is usually a maximum guarantee level. Typical consumption numbers for a variety of engine designs range from .05 to .30 gallons per hour.

Oil Filtration Serviceable contamination filters should be provided in judicious locations throughout the lube system. Coarse filters for items such as weld splatter or machining chips should be backed-up by fine filters for materials such as sand or engine wear particles. The fine filter is the "working" filter which establishes the system cleanliness level. This method should provide long reliable lube system life.

Prior GE experience has been with fine filtration in the supply system alone, scavenge system alone, and in both supply and scavenge systems. The advantages of fine filter in scavenge system alone are wear particles are removed closest to the point where generated, filter debris shows up sooner for trouble indication, and the filter provides engine contamination protection for cooler, tank, anti-static/leak valve and supply pump. Advantages of fine filter in supply system alone are that it provides filtration immediately before distribution to oil-supplied components so that both engine generated debris or possible contamination from tank servicing is eliminated.

If circumstances dictate the use of only one filter, it must be the supply filter that is used on the basis of maximum component protection. However, design practice is to provide both a coarse supply and a fine scavenge filter.

Lube Heat Rejection One of the major functions of the secondary systems engineer is to calculate the heat load of the oil system. Estimates of heat transferred to the oil by bearings, seals, sump walls, pressurization air, pumps and gears must be made for extreme ambient air and extreme fuel temperatures expected during in service operation. Typical results of these estimates are shown on Figure 8.22. This data is then used to estimate the oil heat load effects on the fuel system to prevent associated problems such as fuel nozzle coking.

Once the analysis has been completed, a computer model of the system is constructed in a computer language compatible with airframe companies systems. Airframe designers have pumps and cooling equipment that interact with the fuel and need our input to optimize their systems.

Fire Safety Analysis Secondary systems engineers have the responsibility to analyze the potential for combustion in the sumps and surrounding areas. The analyses must include normal operation and any malfunction of systems or hardware. Assuming that a problem, or potential problem, has been isolated to a particular flow circuit and fuel source, the following process is applied: obtain information on suspected operating condition and location, obtain drawings and estimates of system flow, pressure and temperature, split the flow into a series of chambers, and analyze each chamber for conditions of flammability, ignition and stability.

Flame can be either pre-mixed, which is a homogeneous fuel vapor/air mixture, or of the diffusion type which is a localized liquid fuel puddle source. In each case, all conditions of flammability, ignition and stability must be met. This method provides either a zero or 100% probability of fire. These methods are explained in detail in reference material.

SUMP/SUPPORT HEAT TRANSFER ANALYSIS

Accurate prediction of metal and air temperatures for bearings, sumps and surrounding cavities is critical to the design of these components. Setting bearing operating clearance, determining air/oil seal clearances, estimating axial travel of rotor relative to stator, and stress analysis are four major uses for the data.

Detailed heat transfer in the bearing region is extremely difficult due to the complexity of the oil flow regime in and around the bearings. A cross section of one of the more complicated bearing and support models is shown in Figure 8.23. This 1100 node model was used to predict steady state bearing, seal, and support temperatures plus transient temperature changes in seal and support structure. Component rig testing was used to determine the bearing heat generation characteristics for input into the model.

Once a complete nodal model of the system was available, secondary systems air and oil models and engine test data were used to calculate flows in sumps and surrounding areas. These flows were then used to calculate heat transfer coefficients. GE's heat transfer program, THTD, was run to calculate local metal temperatures for comparison to measured engine data. The heat transfer coefficients were adjusted as required until a temperature match was obtained. Boundary temperatures and pressures used in this analysis were normalized by major

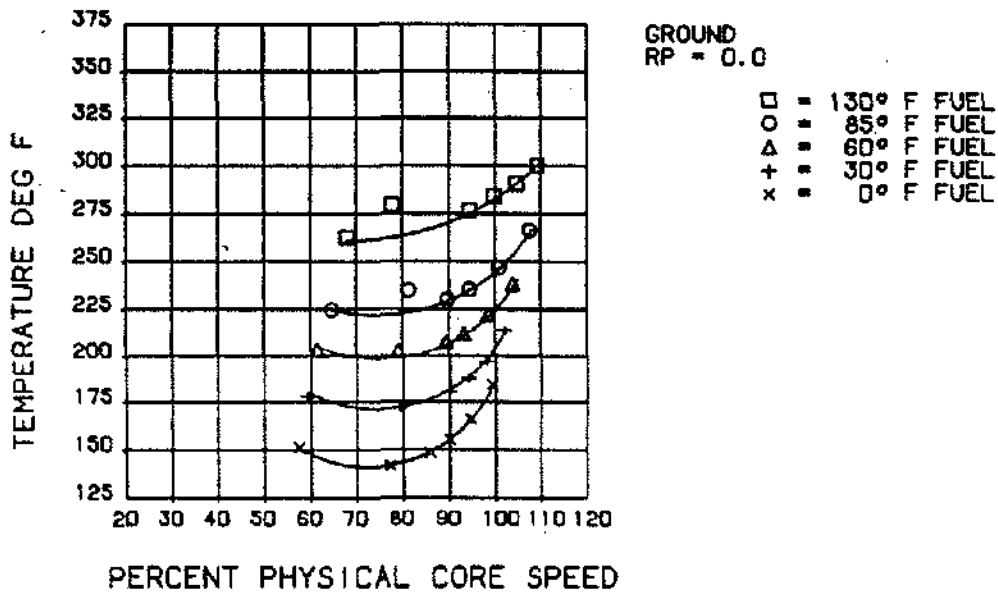
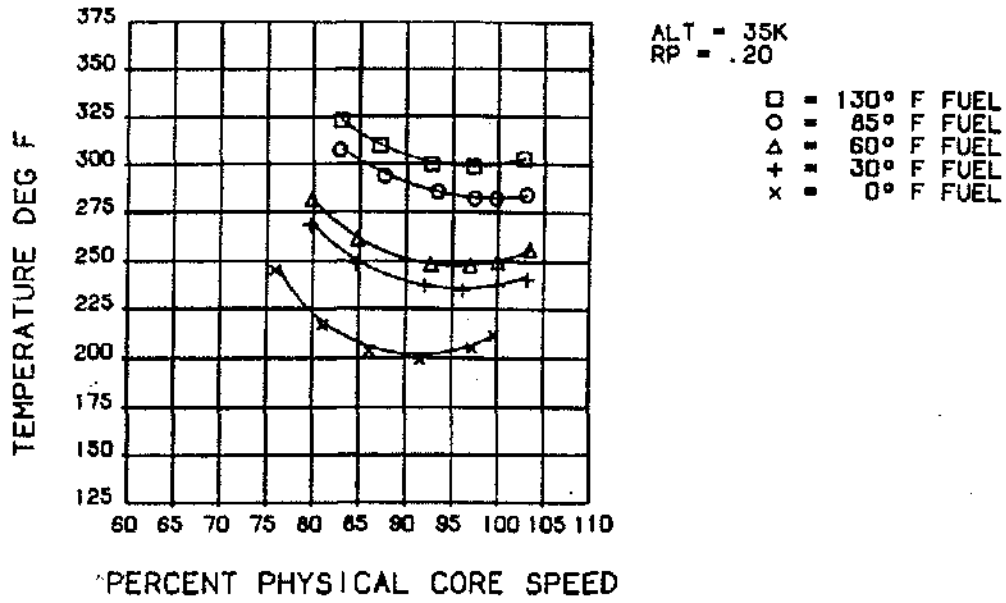


Figure 8.22 Calculated Lube Scavenge Temperature For Various Fuel Temperatures

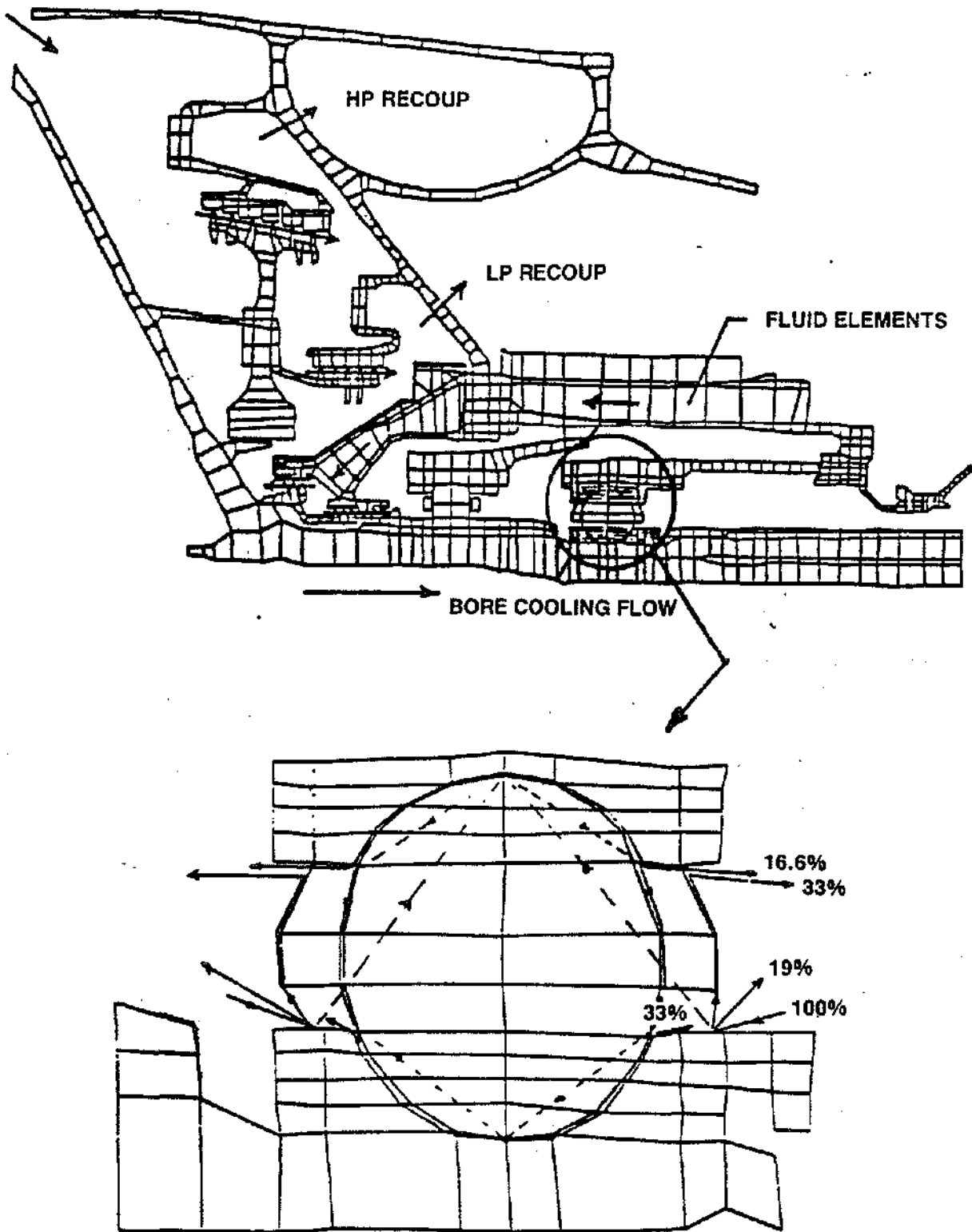


Figure 8.23 Forward Sump Heat Transfer Model

engine parameters such as engine inlet or compressor discharge temperature so predictions for cycle points could be made.

The nodal model for this effort is shown in **Figure 8.23** for the b-sump. A similar model exists for the c-sump. Using these models, metal temperatures for particular sump components were predicted at cycle points requested by mechanical designers and the results forwarded to them for use in their design effort.

Another very important heat transfer function, particularly for new engine designs, is to estimate the maximum oil wetted metal temperature expected for a sump configuration. Lubricating oils currently in use tend to generate varnish and start to form coke in the 440°F to 450°F temperature range. Severe coking can cause plugged lube supply and scavenge circuits, cause carbon seals to hang up or just be a general maintenance or cosmetic nuisance.

Design practice is to limit oil wetted metal temperatures to 400°F. This is easier to accomplish during engine operation than during post shutdown periods when all the heat stored in the engine tends to radiate to the sumps with no flow mechanism to cool the sumps. This phenomenon is known as soakback. If not designed for it can drive sump wall or tube temperatures above coking levels.

AXIAL BEARING THRUST CONTROL

Balancing the axial thrust loads which develop in the flowpath and internal cavities of jet engines is critical to obtaining acceptable thrust bearing lives. Since the secondary systems air model includes all major cavities, a simple summation of pressure times projected area for all pertinent cavities will give the resultant load on all rotating hardware. Factoring in the compressor and turbine aerodynamic blade loads yields the axial forces on the engine thrust bearings.

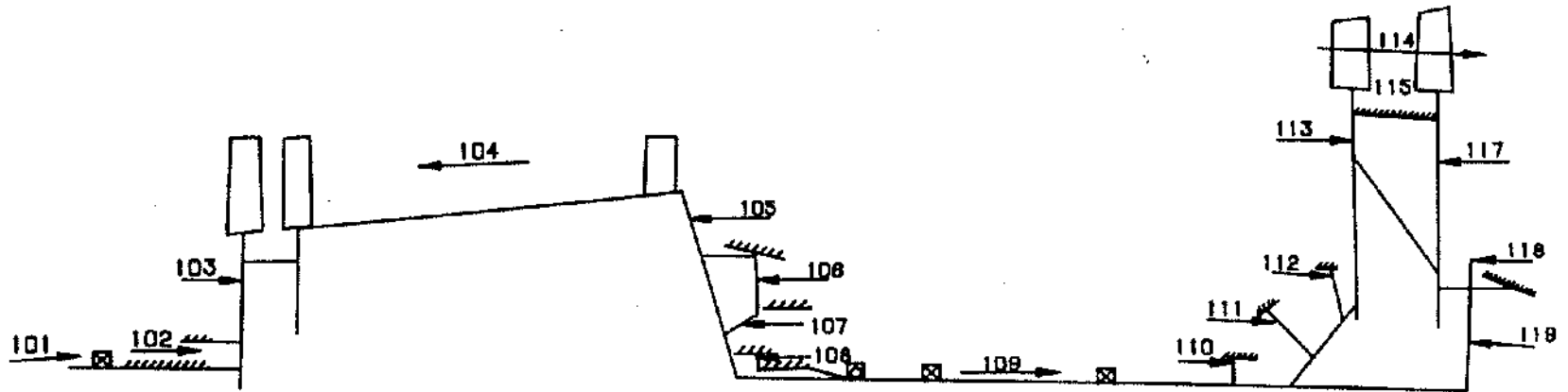
HP Rotor Thrust Table 8.1 shows a schematic and tabulation of pressures, areas, and forces involved in obtaining the resultant loads on the high pressure rotor bearings of the CF6-80C engine at takeoff. Note that the resultant load (-4561 lb.) is small relative to the major cavity loads. This is typical of HP rotor bearing axial loads. Also, note that maximum cavity loads are substantially higher than either compressor or turbine total airfoil aerodynamic loads. Compare forces 104 and 114 with force 113 on **Table 8.1**. The accuracy of predicting these cavity pressures is a critical factor in predicting bearing loads.

Once the bearing load is predicted and determined to be too high for acceptable bearing life it can usually be adjusted to required levels by moving a critical seal to a larger or smaller diameter thus changing its projected area. For instance, in **Table 8.1**, changing the diameter of the seal which affects forces 105 and 106 would be used to balance the load on the HP thrust bearing. In drastic cases if more adjustment is necessary, several seals or even turbine airfoil changes may be required to obtain desired bearing loads. **Figure 8.24** shows a comparison of four different engines axial HP load and how they change with engine speed.

LP Rotor Thrust Prediction of the low pressure rotor thrust bearing load is generally much easier mainly due to the lower pressure levels involved. The principles remain the same. **Figure 8.25** shows the low pressure rotor thrust for the same CF6-80C engine. Note that the predicted load is very close to the measured data presented in the figure.

INTERFACES

Performing the above design functions necessarily involves interactions with many other specific groups internal and external to the company. **Figure 8.26** is a schematic showing typical types of functions or subjects involved on the radial lines and the groups interfaced with during those functions.



NO	RI	RO	CHAM	AREA	PRESS	FORCE
101	3.190	3.845	30	14.48	19.69	-285
102	3.845	4.840	33	27.16	33.07	-898
103	4.840	6.944	5	77.89	24.71	-1925
104	1	1	--		--	+5783
105	7.640	11.825	7	253.92	384.65	+9332
106	6.375	7.650	36	55.70	102.82	+5727
107	4.650	6.375	59	59.75	22.75	+1359
108	4.000	4.650	41	17.66	26.65	+471
109	4.000	4.075	58	1.90	20.93	+40
110	4.325	5.050	62	21.35	21.32	-451

NO	RI	RO	CHAM	AREA	PRESS	FORCE
111	5.050	6.200	39	40.64	105.14	-4273
112	6.200	7.470	40	54.34	318.95	-11308
113	7.470	14.040	10	448.39	253.99	-118879
114	1	1	--		--	-31856
115	12.890	11.825	11	85.04	186.08	+17448
116	12.890	4.000	12	93.77	128.76	-8282
117	6.830	13.680	51	64.23	76.22	+41339
118	4.425	13.543	54	429.66	83.70	+7118
119	2.925	6.830	50	85.04	25.09	+869

Table 8.1 Variables Affecting Loads On High Pressure Rotor Bearings

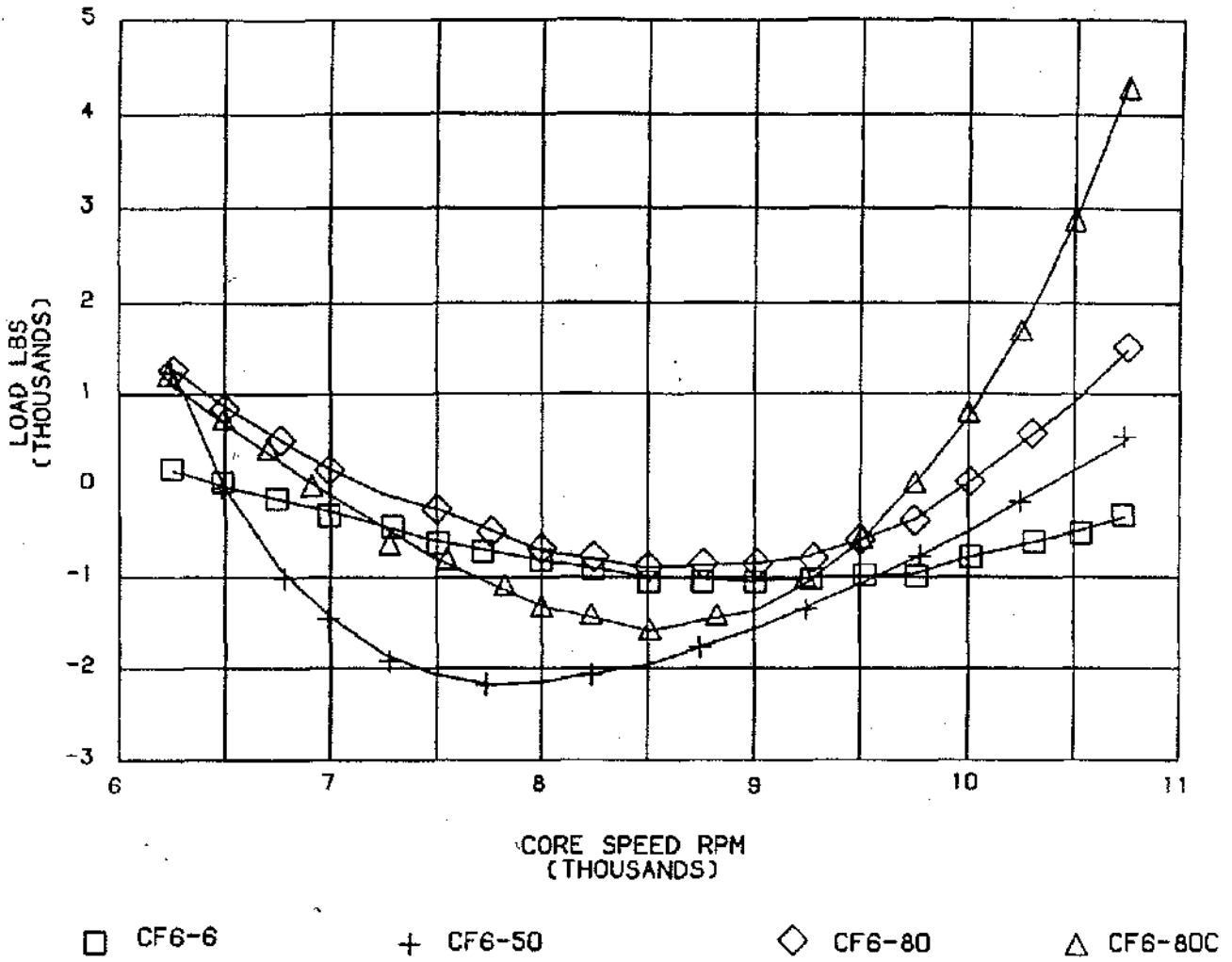


Figure 8.24 CF6 HP Axial Thrust Comparison

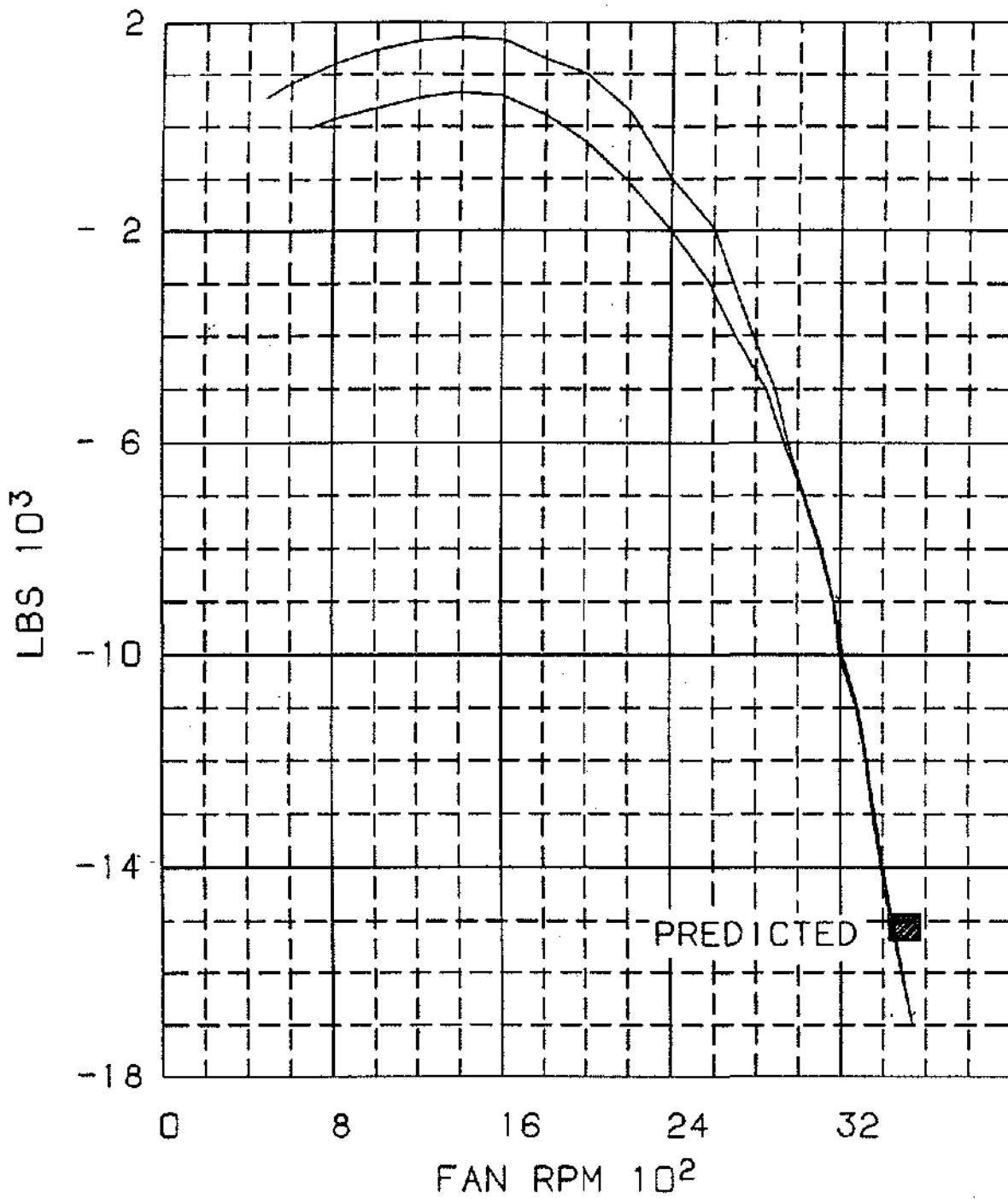


Figure 8.25 1B Axial Rotor Thrust For Various Fan Speeds

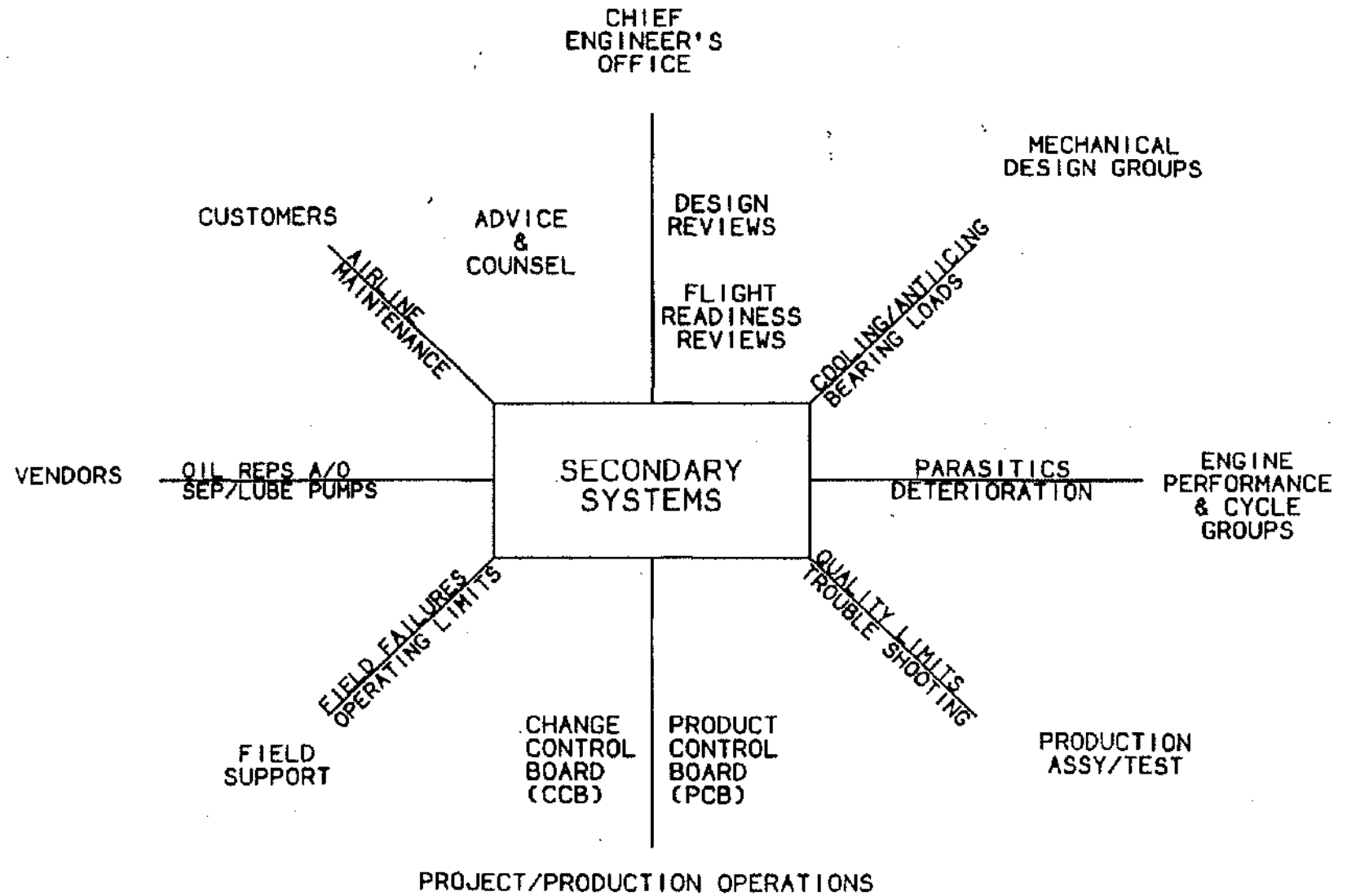


Figure 8.26 Secondary Systems Interfaces

Chapter 9

INLETS AND EXHAUST SYSTEMS

by Alfred Lingen
(Aerodynamic Aspects)

and Robert G. Beedon
(Mechanical Aspects)

AERODYNAMIC ASPECTS OF INLETS AND EXHAUST SYSTEMS (NOZZLES AND REVERSERS)

INTRODUCTION

The major purpose here is to provide familiarity with the terminology involved in the aerodynamics of inlet and exhaust systems. Because inlet and exhausts are the major components of nacelle designs for subsonic aircraft, overall nacelle considerations will be discussed also. The design process will be presented in three phases: (1) the front of the nacelle or the inlet, (2) the back of the nacelle or the exhaust system, and (3) the joining of front with back including the attachment to the aircraft.

The inlet component provides the flowpath through which the flow accelerates to the engine fan face for low flight speeds and decelerates for high flight speeds typical of cruise conditions. The design is such that the flow process is accomplished with near ideal efficiency producing inlet recoveries in excess of 0.995 for all flight conditions. The losses are primarily skin friction losses.

The exhaust system in forward-thrust is designed to provide a similar, near ideal flowpath to accelerate the flow from fan exit and turbine exit to ambient conditions. Typical cruise exhaust coefficients are in excess of 0.980, where as in the case of the inlet, the losses are primarily due to skin friction.

The exhaust system has another function, thrust reversal which is accomplished by turning the fan flow to a forward direction while leaving the core engine flow undisturbed. In reverse mode, the major performance consideration is maintaining adequate flow area while turning the fan flow in the forward direction and pointing the fan flow in the circumferential direction for minimum interference with the airframe.

The most important overall issue in the nacelle design is minimum volume for best weight and drag. Be reminded that the nacelle contains the engine plus the installation

(pipes, harnesses, etc. required to run the engine) and the engine build up, EBU (pipes, harnesses, etc. required to run the aircraft).

INLET DESIGN

Elements of the Subsonic Inlet For simplicity, the design elements are described for flow entering the engine and then for the external flow. The sketch of Figure 9.1 is provided to clarify nomenclature.

The highlight is the leading edge of the inlet when perceived as an airfoil with a cylindrical chordal plane. For the internal flow, the highlight is followed by a contraction to the smallest area or the throat. Usual practice is to use a slender ellipse as the contraction shape which has a length to radial height ratio in excess of 2. At times ellipse exponents higher than 2.0 are used to thicken the contour at the leading edge as a better match to the exterior lip shape. The inlet throat is followed by a diffuser which leads the flow to the engine fan face. The diffuser shape is ordinarily cubic with horizontal tangency at the throat and at the fan face. The diffuser length ordinarily provides a half diameter of flowpath length for acoustic treatment. Diffusion is calculated taking the fan spinner into account and the wall contour is kept to an equivalent cone angle of 10 degrees or less in the interest of avoiding separation in the diffuser.

The external flow is pushed aside by the inlet outer lip. Early designs were very slender elliptical shapes. Subsequently, these shapes were modified in order to provide equivalently slender but somewhat sharper nosed contours.

The outer lip shape must be thick enough to provide for cancellation of additive drag (avoidance of spillage) and long enough to avoid a drag-rise condition at the cruise Mach number. Contained volume requirements may dominate as in the case of a fan-mounted gearbox or use of Kevlar containment. In these cases the aerodynamic minimum thickness requirements are exceeded and the design has greater drag than necessary. Design values for aerodynamic considerations are illustrated in Figure 9.2 where length and diameter relationships are mapped for best spillage and Mach capability.

Inlet Performance The major performance parameters for cruise conditions are inlet recovery and spillage drag. Inlet recovery is defined as the ratio of the average stagnation pressure at the fan face (recovery condition) to the free-stream stagnation pressure. The subsonic inlet is a flowing pitot tube. Recovery losses are confined to boundary layer friction as affected by the diffusion

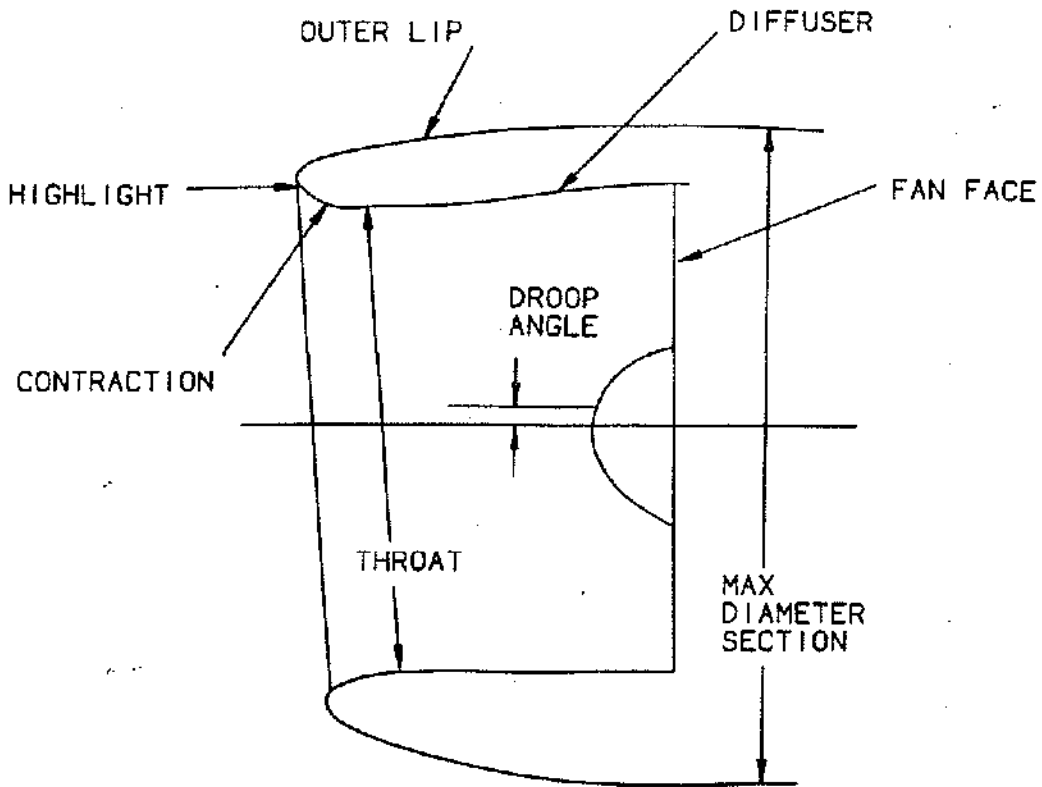


Figure 9.1 Elements of Subsonic Inlet

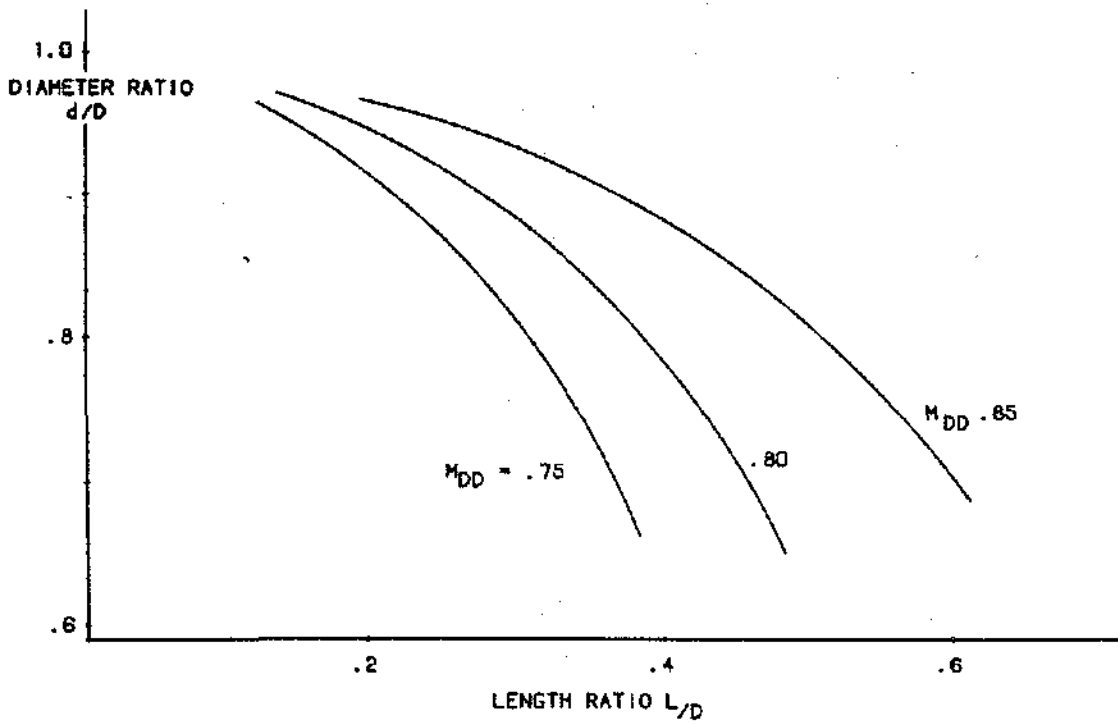


Figure 9.2 Inlet Critical Mach Relationships

from inlet throat and the presence of roughness attendant to acoustic treatment. Inlet recovery is a key measurement in the scale model tests that document the inlet performance. From 10 to 30% scale models are ordinarily tested in wind tunnels to obtain inlet performance. Recovery measurements are made and converted to full scale values in two steps by modifying the loss term for (1) the change in skin friction coefficient resulting from the model to full-scale Reynolds number relationship and (2) the friction increase due to the presence of the acoustic treatment.

Spillage drag takes some careful explanation. The sketch of Figure 9.3 is presented for illustrative purposes. Again at the important cruise point, the ingested mass flow usually has a smaller area than the highlight. For this type of condition, the flow diffuses or increases in area as it reaches the lip. The ratio of ingested stream tube area to the highlight area is conventionally called the mass flow ratio. The increase in area involved implies a change in momentum which is called the additive drag. If the lip were sharp, this additive drag would be a system penalty (as it is in supersonic inlets). But the sub-

sonic inlet lip is far from sharp and the external flow accelerates around the outer lip from the stagnation point creating low pressures which result in a thrust direction force commonly called lip suction. For ingested flows having areas just smaller than the highlight, the lip suction is easily equal to the additive drag and there is no spillage drag. As the ingested mass flow is reduced, the additive drag increases and the flow acceleration around the lip has a bigger and bigger job to do to generate more and more lip suction to cancel the greater additive drag. Lip design and, finally, flow separation limit the lip suction and create spillage drag by allowing the lip to cancel all but a portion of the additive drag.

Spillage drag characteristics are another key measurement in scale-model inlet tests that document the inlet performance. Rakes are used at the trailing edge station of the fan cowl to assess drag by accounting for the actual momentum deficit around the entire circumference. Flowing the inlet at varying mass flows for each free-stream Mach of interest produces the typical spill drag map presented in Figure 9.4. Spill drag increases for decreasing massflow ratio and for increasing Mach number

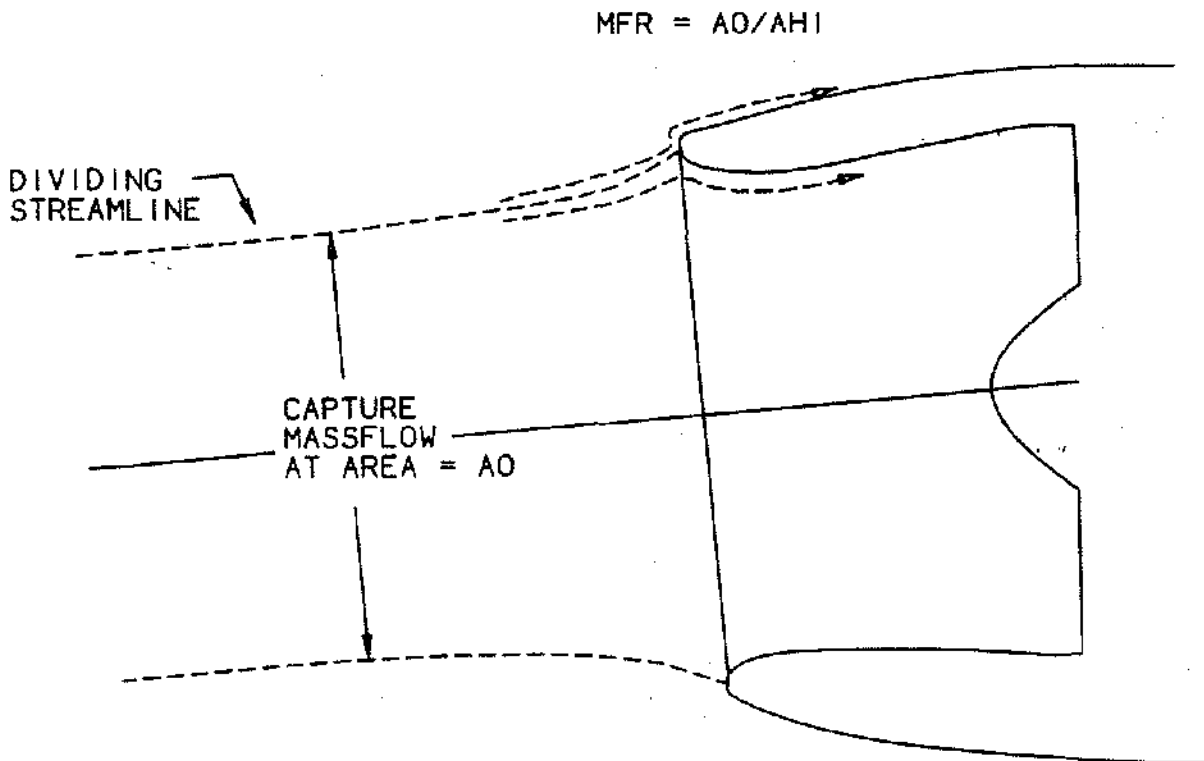


Figure 9.3 Definition of Masterflow Ratio

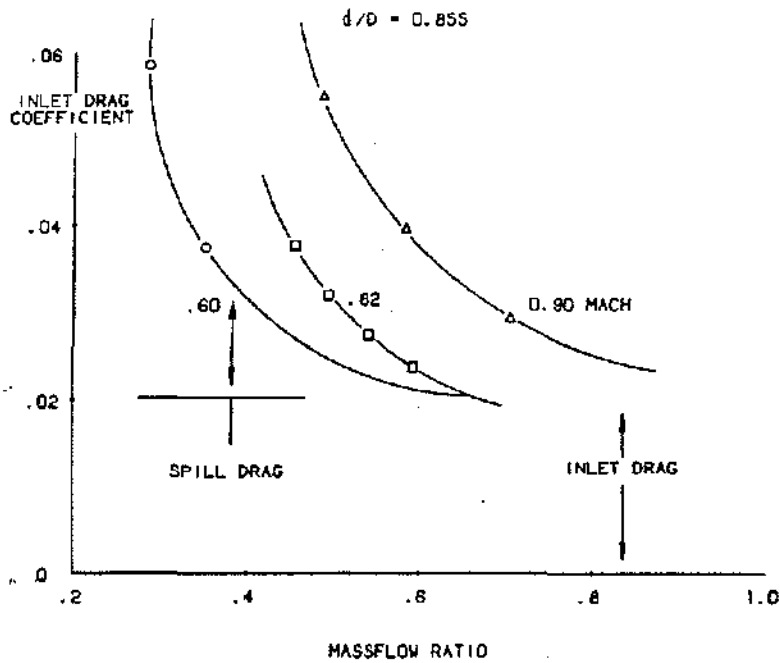


Figure 9.4 Typical Spill Drag Variation

for a given inlet design. Highlight to throat diameter ratio decreases (thinner lips) will have increasing spillage at given massflow ratio and Mach number. Also, variations in length far from the values noted in Figure 9.2 will result in higher spillage drag than that given.

The selection of an inlet throat size is usually done as a compromise between recovery and spill drag at cruise conditions and angle of attack performance at low speed. A typical result curve for the cruise trade is presented in Figure 9.5. At small throat areas spillage drag is minimized. As throat size is increased, the recovery losses go down because of both decreasing throat Mach number and decreasing diffusion from the throat to the fixed value of fan area. But with large throats come larger highlight areas for the given ingested stream size (decreasing mass-flow ratio) and attendant increases in spill drag. The best performance valley is the preferred region of throat size selection that is also guided by low speed considerations. These low speed considerations will be discussed next.

Low Speed Design Considerations At low speed, the ingested stream tube is larger than the highlight for maximum thrust conditions. Spillage drag is impossible and recovery is determined by the mechanisms noted above.

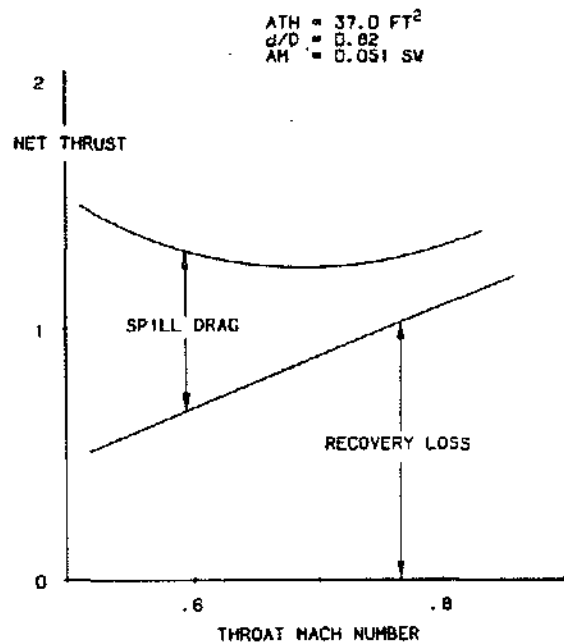


Figure 9.5 Inlet Throat Selection

However, the aircraft system requires operation at high angle of attack. Normal takeoff angles are in the vicinity of 20 degrees at Mach 0.25 while hot day, high altitude takeoffs might require angles of 26 or more degrees at Mach numbers above 0.30.

Capacity to handle high angle operation without large flow separation and attendant fan face flow distortion is the major consideration of the lip design. While takeoff angle of attack is the prime determiner of the lower lip geometry, similar considerations for crosswind operation determine the side lips of the inlet. The round or near round cross-section shapes desirable for structural reasons produce a uniform contraction inner lip.

Conventional turbofan engines have angle of attack requirements much like the one illustrated in Figure 9.6. The high altitude, hot day conditions which are extreme from the Mach number and angle of attack requirements involve the highest inlet corrected flows in the flight path. Since a low throat Mach number is most desirable for best inlet performance at these low speed high angle conditions, the throat selection is made at the largest value in the best performance valley from the cruise

trade off mentioned in the previous section. Some discussion of low speed characteristics of inlets at angle of attack is needed here to put the throat selection into perspective with the engine requirements.

Rotating machinery operates nicely with uniform inflow. When the inflow becomes non-uniform the operation is driven in the direction of the surge line of the rotating machinery. As distortion increases, the surge line itself migrates to lower pressure for a greater massflow. Other engine surge margins are also required and the minimum surge margin usage comes with minimum inflow distortion. At GE the distortion is described with factors called IDC and IDR (Index Distortion Circumferential and Radial).

At angle of attack the stagnation streamline of the air entering the inlet is below the highlight and the flow accelerates around the lip to the inlet throat and then diffuses to the fan face. Increasing angle of attack requires an increasing amount of flow acceleration to the throat. The lip has a bigger and bigger job to do, which is directly analogous to that discussed previously under spillage drag. When the lip can no longer do the job, flow sepa-

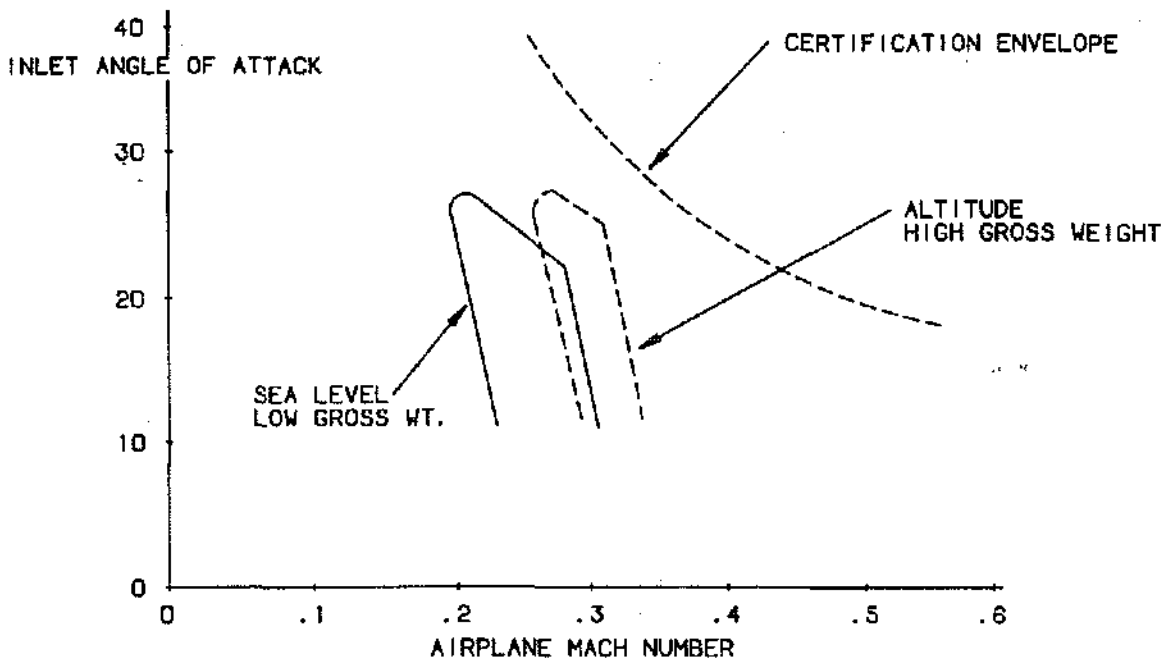


Figure 9.6 Inlet Angle of Attack Requirements

ration occurs in the diffuser and a distorted inlet flow is produced. Since the low pressure from the separation is at the bottom of the fan face and decreases quickly around the circumference, the parameter IDC is of interest. Presented in Figure 9.7 is the variation of angle of attack with throat Mach number for IDC of 10% for a typical turbofan inlet. Capacity for angle of attack decreases slowly with increasing throat Mach number to a value near Mach 0.75 when a knee in the curve is evident. Operation at or above the knee is accompanied by supersonic flow (Mach 1.2 to 1.4) and separation near the inlet throat. The sharply decreasing angle regime is analogous to a choking restriction at the inlet throat. From the above, throat Mach numbers below 0.75 are selected for the required inlet operation with judicious margin for airflow growth as engine thrust requirements increase.

Lip contraction from highlight to throat affects the angle of attack capability at a given throat Mach number. A typical variation for flight Mach 0.25 is presented in Figure 9.8 where a linear variation indicates compound interest type of improvement of achievable angle as contraction ratio is increased at a constant fan face distortion

value. Note that contraction ratio is restrained from large values by cruise spill drag considerations and the inlet design selection involves trading contraction ratio and throat Mach number.

EXHAUST NOZZLES

Elements of the Exhaust System The various elements of the turbofan engine exhaust system comprise the rear-most portion of the nacelle and provide exhaust flow paths for the fan and primary or core flow. Some features of the fan flow path are involved with the thrust reversal function and will be discussed separately in a later section.

The fan exit is forward and outboard of the low pressure turbine exit. The fan flow path is turned outboard to provide contained volume for core engine installation and for reasons which are obvious in the subsequent section on thrust reversal. The fan flow path then turns inward and the outer wall is joined by the aft portion of the nacelle outer cowl at a point selected to limit the outer cowl boat tail angle to 12° while providing a generous fairing

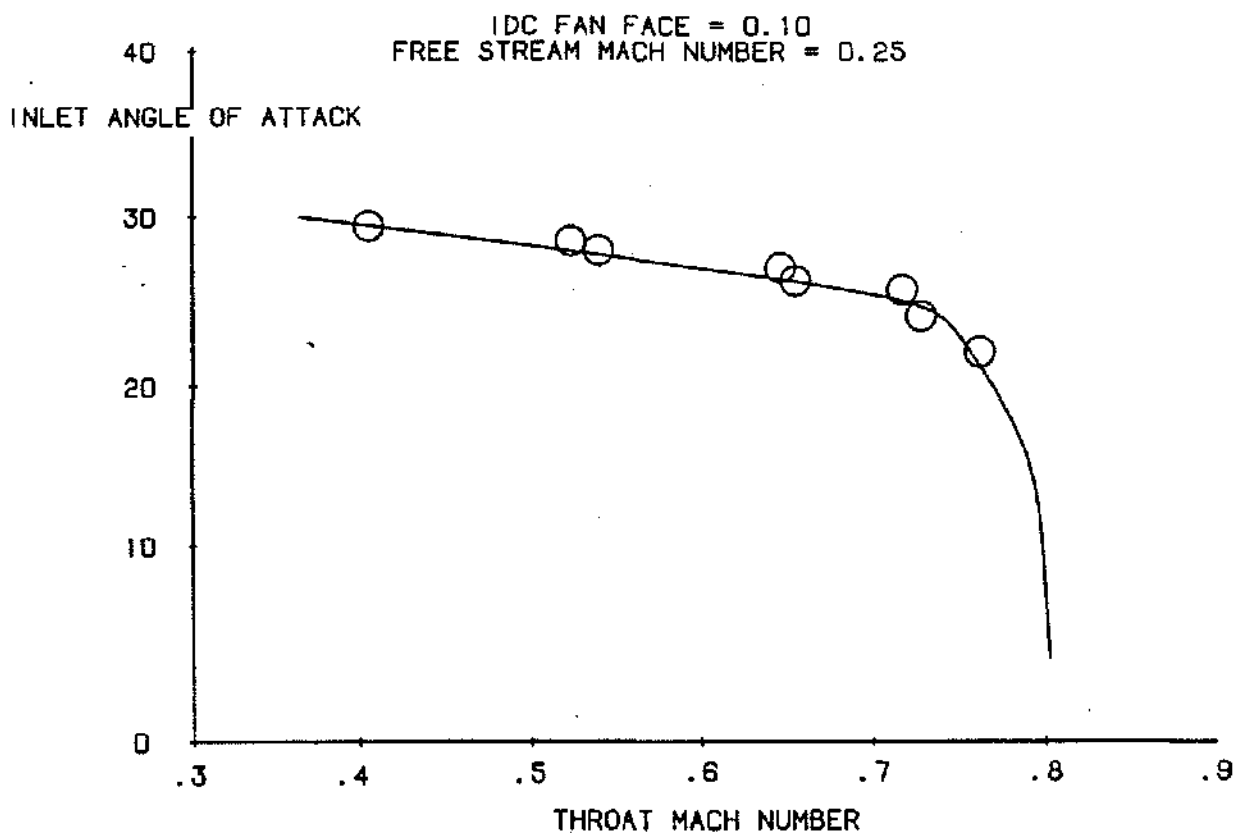


Figure 9.7 Inlet Angle of Attack Capability at Low Speed

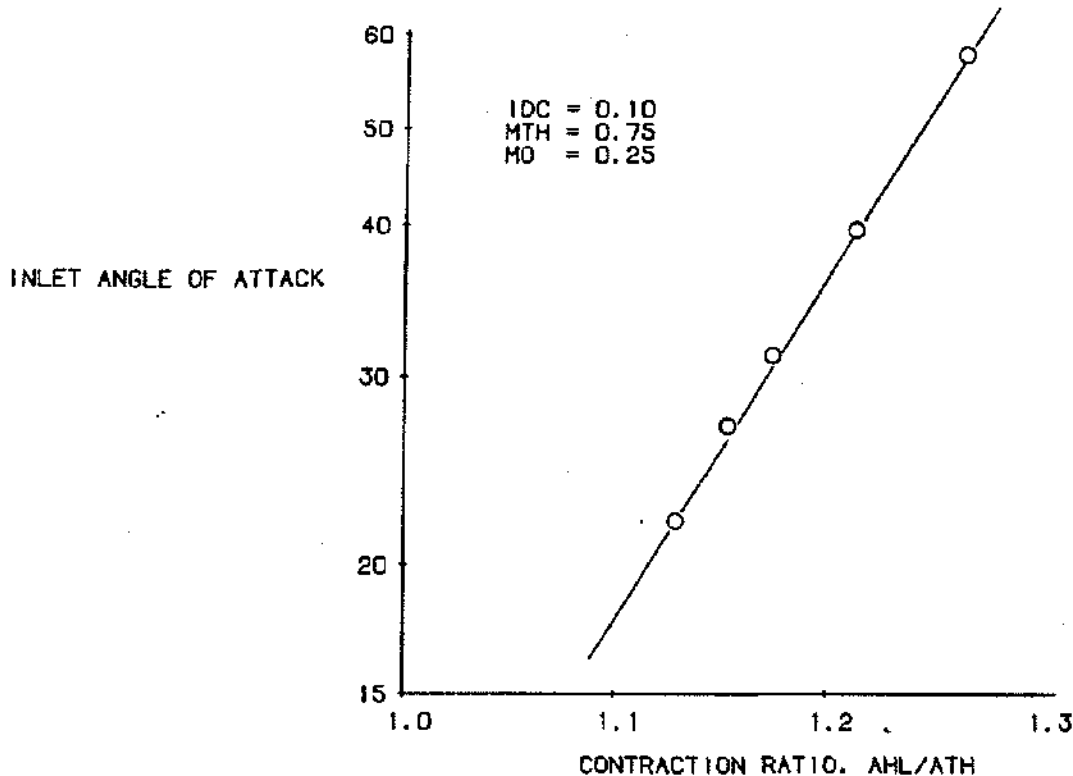


Figure 9.8 Contraction Ratio Effect On Angle

of the external contour. Because of the forward position of the fan exit, the inner wall of the fan flow path also turns inward to form a core cowl of inclination which suits the matching of the core cowl to the core nozzle outer wall. Contained volume requirements dictate the maximum diameter at the fan nozzle throat. The core cowl downstream of the fan throat guides the fan flow inward on a conical surface to join the core nozzle outer wall. The flowpath designs avoid mismatches in flow direction where the various flows come together.

Flowpath Design Considerations Considerations of design are directly similar for the core nozzle and fan nozzle. A minor difference is that the center plug of the core nozzle can be steeper for the same aerodynamic effect because the annular core exit flow goes round at the end of the plug. Accordingly, the outer streamline can match the core cowl convergence best when the core plug angle exceeds the core cowl angle by 4 or 5 degrees.

In each of the two nozzles, the throat is preceded by turning from an outward direction to a direction which matches the downstream surfaces. Some of the turning is designed into the throat to provide a desired variation of

flow coefficient with pressure ratio. Further tailoring of the flow coefficient is provided by designing convergent divergent nozzles where the throat is followed by a small divergence of 1 to 3%. In this manner, the fan nozzle area "opens up" at take-off pressure ratios and "closes-down" at cruise conditions while the core nozzle is kept from feeling the influence of the fan flow.

But the fan nozzle is not completely annular. Attachment of the engine to the airplane is accomplished through a pylon, the structure of which mounts the core engine to the aircraft wing, forming a large upper bifurcation of the annular flow path. A lower bifurcation is also involved to allow the fan exhaust to be formed in two D-shaped ducts which are cowl doors hinged at the pylon to provide access to the core engine for maintenance.

The design process for exhaust systems is iterative in nature. From various candidates, the most compact lines are selected which meet the criteria of external boat tail and minimum overall duct loss based on conventional flow codes and attendant boundary layer solutions. Curvatures are limited to avoid separations on all internal and external surfaces.

Exhaust System Performance Candidate exhausts are subjected to 10% scale model tests for evaluation in which cold flow at uniform conditions is employed and overall thrust and separate fan and core flow measurements are made. Test results ordinarily verify the flow code results and are then converted to coefficient form for use in performance cycle calculations.

The flow coefficient is defined as the actual flow measured divided by an ideal flow resulting from the same upstream conditions and the geometric nozzle area. Isentropic expansion from upstream pressure to throat conditions is involved in this coefficient. When the throat conditions are not sonic, the ambient pressure is used as the ideal throat pressure independent of the actual nozzle geometry.

The thrust coefficient is defined as the measured thrust divided by an ideal thrust resulting from the expansion of the actual measured flow from the upstream conditions to ambient pressure. Throat conditions are not involved in the thrust coefficient.

Turbofan exhausts involve two separate flows: the fan and the core. Scale model testing begins by flowing the core system only (without fan flow) and evaluating the flow and thrust coefficients of the core nozzle. The testing then proceeds to dual flow operations where the fan and core flow are measured separately and an overall thrust measurement is made. The core flow coefficient is then determined and used in the cycle work. The effects of fan flow on core flow coefficient are known and may call for iteration of the core nozzle design in that the fan flow effect may vary the core effective area in an undesirable way. The fan thrust coefficient is found using the assumption of super position. Calculated core thrust from the core only run is used directly to subtract a core thrust from the overall thrust measurement, thus determining a fan nozzle thrust. As a result, fan nozzle thrust coefficients contain any interaction term or effect of fan flow on core thrust even though they are used for separate cycle calculations of fan and core thrust.

A straightforward method is used to convert the model scale coefficients to full scale values. The coefficients are first divided into throat condition coefficients and pressure drops using skin friction drags calculated for the cold-flow test conditions. Pressure drop is calculated for all surfaces downstream of the "charging" station as the total pressure measurement station is called. The throat condition coefficients are then assumed to apply directly to the full scale exhaust system. Calculated skin friction values for full scale conditions are then used to correct the coefficient basis to upstream conditions. Additionally, further calculated pressure drops are added as

appropriate to account for steps and gaps in the flow path as well as surface roughness conditions for the actual structure and applicable acoustic treatment.

THRUST REVERSER

The thrust reverser which is discussed here is the identical hardware to that described under exhaust nozzle. The discussion below refers to the hardware fully actuated to the reverse thrust position. Further, the discussion is confined to the reversal of the fan flow only as is current day practice for high bypass engines.

Elements of the Thrust Reverser System When the outer shroud of the exhaust system translates aft, blocker doors close off the downstream flow path and cascade boxes are exposed through which the fan flow exits in a forward direction.

The smooth annular surface over which the flow turns outboard into the cascades is playfully called the Dagmar. The Dagmar is the suction surface of the radial turning vane for which the blocker doors and the inner flowpath are the pressure surface and as such must be carefully designed. Hence, the fan flow first turns radially outward where it approaches the entry of the cascade boxes.

The cascade boxes are comprised of turbine-stator type turning vanes which accelerate the flow to the minimum section at the exit. Most of the cascade boxes have radial outward exhaust in a direction 40 to 50 degrees from axial. Some boxes provide other than radial outflow by skewing of the turning vanes or by providing turning by virtue of axial vanes in an arrangement that resembles an eggcrate.

Alternative tailoring of the reverser outflow is possible through the use of different axial angles. For example, the DC10 tail engine calls for boxes at the bottom which turn the flow less than 90° to direct flow aft in the proximity of the horizontal tail surfaces.

Reverser Flowpath Considerations The flow process in the reverser is in two steps: 1) flow turning in an axial plane to the entrance of the cascades and 2) flow through the cascades. The first process in the axial plane is usually modeled in a two dimensional computer flow code with the assumption that the flow has axial symmetry. Major concerns are avoidance of separation on the Dagmar to provide full flowing area at the cascade entrances and thereby, ensure that minimum reverser length is required.

The cascade boxes are truly two dimensional. Standard turbine design practice is used for blade shape and solidity determination. Solidity is defined as the ratio of vane chord to axial spacing. Entry angles are taken from the radial plane flux plot and the design values of exit angle result from the amount of reverse thrust required. It is usual to have tailored entrance angles and uniform exit angles. Also, greater amounts of turning require higher solidities. Axial and non axial stiffening are usually required for structural integrity and the cascade box flow size is increased to account for this blockage using empirical factors which depend on the stiffener cross-section shape.

Reversal of the fan stream affects the core nozzle in that fan stream influence is removed. The core flow only coefficients measured in the exhaust system scale model tests are used to calculate core nozzle thrust in reverse mode in cycle decks.

Reverser Performance Reverse thrust of the engine system alone results from three sources. The unaffected core engine thrust is more than overcome by the fan flow exhausting forward and by the fan and core flow ram drag. The ram drag is the largest of the forces. However, operation on the aircraft is not quite that simple.

Reversers are deployed after aircraft touchdown and are used down to speeds just above the speed at which the reverse flow is re-ingested or cross ingested so as to affect engine operation. The range of speeds may be from 120 knots down to 60 knots. In this speed regime, the aircraft drag is a large retarding force. But the reverse flow shrouds a part of the aircraft and changes the aircraft drag. It seems important to discuss how the total interaction is defined.

Aircraft landings are first made without reverser. Aircraft velocity and runway distance are the measured parameters from which retarding force is derived. The retarding forces are due to brake action forces and aircraft drag while the idle thrust is the engine contribution. Component brake data and wind tunnel drag data converted to full scale are redundancy checks on the measurements. Knowing the two major components, the reverse thrust is added to the test and analyzed in a particular manner. The static reverser thrust of the engine is used as known and together with brake forces, a modified aircraft drag is derived. The difference between the original measurement and that with reverser active is the reverser interference drag. Reverser interference is a large fraction of aircraft drag and there is, therefore, considerable payoff in tailoring circumferential reverse flow to minimize the interference.

Static performance measurements are a key input to the aircraft system performance. Static reverse thrust tests are run on a conventional sea level test facility modified to prevent reverse flow ingestion by use of a long entrance pipe to cover the inlet bellmouth. Moving the inlet source two diameters upstream was found to prevent exhaust ingestion over the entire speed range. Engine thrust measurements are made in forward and in reverse mode and cycle analysis is used to separate core thrust from the overall reverse thrust measurements. The large effect of the re-ingestion tunnel on thrust is obtained from the forward mode tests.

NACELLE DESIGN

Elements of the Nacelle The upstream part or front of the nacelle is the inlet outer cowl. The outer lines of the inlet are ordinarily not round to accommodate accessories (engine installation items). The downstream part or back is the outer line of the exhaust system or thrust reverser. For structure efficiency reasons, the reverser translating surfaces are kept axisymmetric. The front to back fairing job is made more complicated by inlet droop.

To improve installed performance under the wing at cruise and provide help for high angle operation at low speeds, the inlet is ordinarily drooped i.e. the inlet centerline is bent downward at a point near the fan face. Installed performance at cruise is helped for cases where the engine gearbox is mounted outboard of the fan case. The drooping of the inlet might be looked at as cambering the nacelle, thereby better suiting the outer lines to the bottom gearbox bulge. However, droop angles of 3 to 5 degrees are employed to suit the inlet face to the actual flow direction ahead of the wing at cruise conditions thereby minimizing the nacelle installation drag.

Nacelle design amounts to providing smooth lines front to back (from inlet to reverser) while keeping important contours unaffected. Smoothness is required in the longitudinal and in the circumferential lines. Conventional lofting techniques are employed where equation fits are made region by region to the desired coordinates with slope and curvature reconciliations between regions. In this process, the first 60% of the inlet outer lip is maintained as originally designed as is the exhaust boattail.

Nacelle Performance The first consideration of nacelle performance has to do with nacelle drag in isolation. The effect of the aircraft environment is the second consideration.

Isolated nacelle performance is basically the drag of the nacelle on a free-stream environment. The nacelle can be looked at as an airfoil wrapped around a cylinder. The drag is comprised of flat plate friction for the wetted area dependent on free-stream conditions plus an increase in this friction due to the higher Mach numbers created by thickness. Because of the high fineness involved, pressure drags are small in most cases except those with very high speed cruise e.g. the B747 cruising at Mach 0.86. The latter case requires careful design of the inlet upper lip to avoid large pressure drag resulting from the wave drag attendant to local Mach numbers in excess of 1.0.

Wind tunnel tests for aircraft drag polars, as the basic airplane performance maps are called, are conducted with full airplane models which have the nacelle cowl lines modeled in flow through nacelles, that is, inlet airflow is simulated but the exhaust system airflow is not. The drag of the nacelles is included in the zero-lift drag assessment of the entire airplane.

Installed Performance Auxiliary wind tunnel tests are also conducted, usually in a larger scale with airplane half models. This is done in order to provide better exhaust simulation through the use of more elaborate flow through nacelles which model the exhaust core cowl and the core plug. Also, turbine powered simulators (TPS) are used to model the exhaust directly, by providing high pressure air from the simulator exit. These so called propulsion tests mount the fuselage to the tunnel wall and measure half-airplane forces with or without the fuselage on the balance. In either event, difference measurements are made to define the several installation drags because absolute values from these measurements are difficult to interpret.

The simplest installation drag is determined from the difference in drag of the half-model tested with and without the nacelles installed. The difference value after correction for the static thrust of the exhaust is formally called the installation drag. More elaborate test programs take the additional step of testing the nacelle/pylon separately in a free-stream environment to experimentally assess the "isolated" nacelle drag. When this latter measurement is subtracted from the installation drag, a residual drag is produced which is called interference drag. Interference drag is the remainder after all the component ingredient drags are accounted for in the test series.

Recent experiences have confined installation and interference drag measurements to flow through models having a practical degree of exhaust geometry simulation

without exhaust pressure simulation. This simplification was made in the interest of improving the quality of the drag measurement after elaborate series were run with and without exhaust pressure simulation by use of a TPS with basically the same result for the lowest drag configurations.

Interference drag can be positive or negative, that is, the combination drag can be higher or lower than the separate parts added. Negative interference drag can occur with high technology wing designs which were done with a nacelle in place. The spanwise lift distribution does not improve when the nacelle is removed. Hence, the wing drag for a given lift coefficient is higher without the nacelle installed and the separate parts are too large by the amount that the nacelle improved the lift distribution. More usual wing designs are done without the nacelle in place and, therefore, do not have the potential of negative interference drag. The losses involved in interference drag for nacelle/pylon/wing regions are due to high velocity flow from the proximity of curvatures on the component parts of the installation and from the aggravation of such effects by the presence of a partly open channel. Because of the aft sweep of the wing, the "worst" channel is on the inboard pylon side. Lowest drag installations have the engine exhaust forward of the wing leading edge, thus avoiding the inboard channel effect. The channel effect which is associated with high drag is characterized by a convergent-divergent area distribution with sonic velocities from combination curvatures at the minimum area and acceleration to local supersonic flow with shock waves for readjustment of pressure to conform to the wing pressures. These high drag conditions are ordinarily repaired by re-contouring airplane surfaces.

Acoustic Considerations The incorporation of acoustic panels for fan noise suppression into the inlet and exhaust only intrudes on the aero design process in the case of the inlet. Typical fan exhaust systems have large amounts of flowpath surface which provide ample opportunity for suppression area. But in the inlet an accommodation is made and the inlet diffuser length is set by the requirement for noise suppression. Considerations of type and extent of treatment are discussed in a later chapter.

The performance effect of the treatment is an increase in wall friction due to the added surface roughness of the treatment and the "puffing" effect of the suppression mechanism. Specific application to inlet recovery and exhaust system loss were denoted in prior sections.

MECHANICAL ASPECTS OF INLETS AND EXHAUST SYSTEMS

MECHANICAL DESIGN OF INLET

The inlet is designed to meet, and is certified to, the requirements of FAR 25. In part, this includes the loads and environmental factors, lightning protection, materials and fabrication methods, failsafe requirements, and ice protection. The inner barrel is the main structural member of the inlet. It is also acoustically treated to attenuate the fan noise.

The CF6-80C2 inlet (see Figures 9.9 and 10) consists of the lip, forward bulkhead, inner barrel and mounting flange, aft bulkhead, and the anti-ice spray tube and duct as shown in Figure 9.11. Borescope ports are incorporated in the forward bulkhead to provide a means of inspecting the anti-ice spray tube and the supporting links. Similarly access panels are provided in the outer barrel and the aft bulkhead to inspect the interior of the inlet and the anti-ice duct slip joint (see Figure 9.12).

As the CF6-80C2 inlet weighs about 525 pounds, hoist points are provided for the attachment of fittings for lifting slings. Two index pins are provided on the attach flange to facilitate alignment to the engine fan case. A phone and ground jack are provided at the bottom of the inlet. These features are shown in Figure 9.13. The inlet also includes provisions to pin the inlet cowl cover to the inlet as shown in Figure 9.14.

The acoustic considerations set the length of the inner barrel rather than the aerodynamic considerations. The state-of-the-art acoustic treatment is linear 2DOF shown in Figure 9.15. The structural requirements for the inner barrel and the engine attach flange are set by the blade-out loads. The approximately one-inch thick aluminum honeycomb sandwich used to satisfy the acoustic criteria will also satisfy the structural requirements. Twenty-four 7/16 inch diameter bolts are required to meet the blade-out loads assuming any one bolt is ineffective because it is loose or missing. Comparatively large flange mounting brackets (see Figure 9.16) are required between the flange and the aluminum honeycomb sandwich to spread the high point loads at the bolt into the sandwich structure. The airlines want to be able to install, remove and otherwise perform maintenance on the fan blades without removing the inlet from the engine. Accordingly, this generates a requirement that two-250 pound men must be able to walk on the inside diameter of the inlet. This requirement can be met if the honeycomb sandwich is made up of face sheets equal to or greater than .032 inch and the honeycomb is 3/8 inch or

smaller. Fortunately, these parameters are near optimum for the acoustic treatment and the requirement is easily met.

The inlet is drooped approximately 4 degrees so the airflow will be normal to the lip at the cruise angle of attack. This droop could interfere with removal of the fan blades as they must come straight forward to disengage the dovetail. To eliminate this potential problem, the aft end of the inlet typically has a straight cylindrical section to facilitate removal of the fan blades. The inner barrel is also formed from three segments spliced together (see Figure 9.17) to limit crack or delamination and propagation resulting from bird strikes, ice, or slush ingestion. The inner barrel is also designed to withstand limit load with any one segment failed and, hence, is also failsafe. Aerodynamic loads (principally a comparatively high vertical load during take-off rotation) and maneuver loads are the operating loads that are considered in the fatigue analyses.

The inlet lip assembly consists of the lip, anti-ice spray tube and supporting links, and the forward bulkhead. The lip assembly provides the required ice-protection for the engine. The lip assembly is also required to meet the prescribed FAA requirements for hail and bird-strike resistance and lightning protection. The inner barrel skins of the sandwich structure must be aluminum (metallic) for lightning considerations.

The anti-ice spray tube is fabricated from Inconel 625 and contains two rows of holes to impinge engine bleed air on the inside of the lip to provide the necessary ice-protection. The anti-ice spray tube is supported by a series of links in a manner that permits the tube to expand freely to the bleed air temperature without inducing thermal stresses. The lip is fabricated in four segments because it is non-symmetrical. It is fabricated from 2219 aluminum alloy and will meet the bird-strike and hail resistance requirements if the minimum thickness is .063 inch after all forming and processing is completed. The forward bulkhead is fabricated from Ti 6-4 to withstand the temperature of the engine bleed air without convective cooling that the lip experiences. There are slots through the forward bulkhead at the periphery of the inside diameter to exhaust the anti-ice air into the aft compartment forward by the inner barrel, outer barrel and the forward and aft bulkheads. Borescope holes are provided in the forward bulkhead to provide access to inspect the links that support the anti-ice spray tube. The inlet lip assembly is riveted to the inner barrel assembly.

The outer barrel assembly is a fairing that provides the external flowpath between the lip assembly and the aft

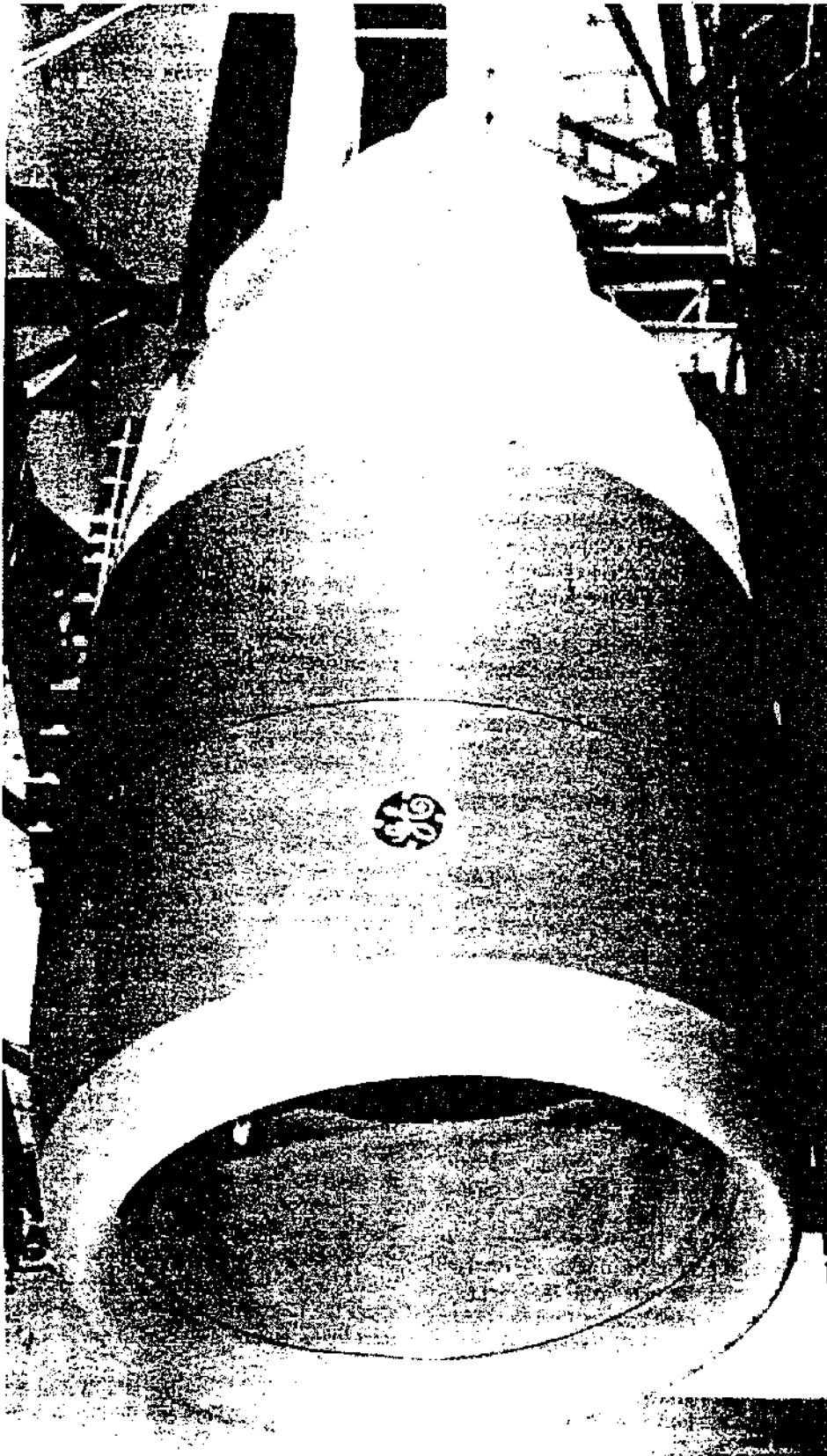


Figure 9.9 CF6-80C2 Nacelle Left Hand View Looking Aft

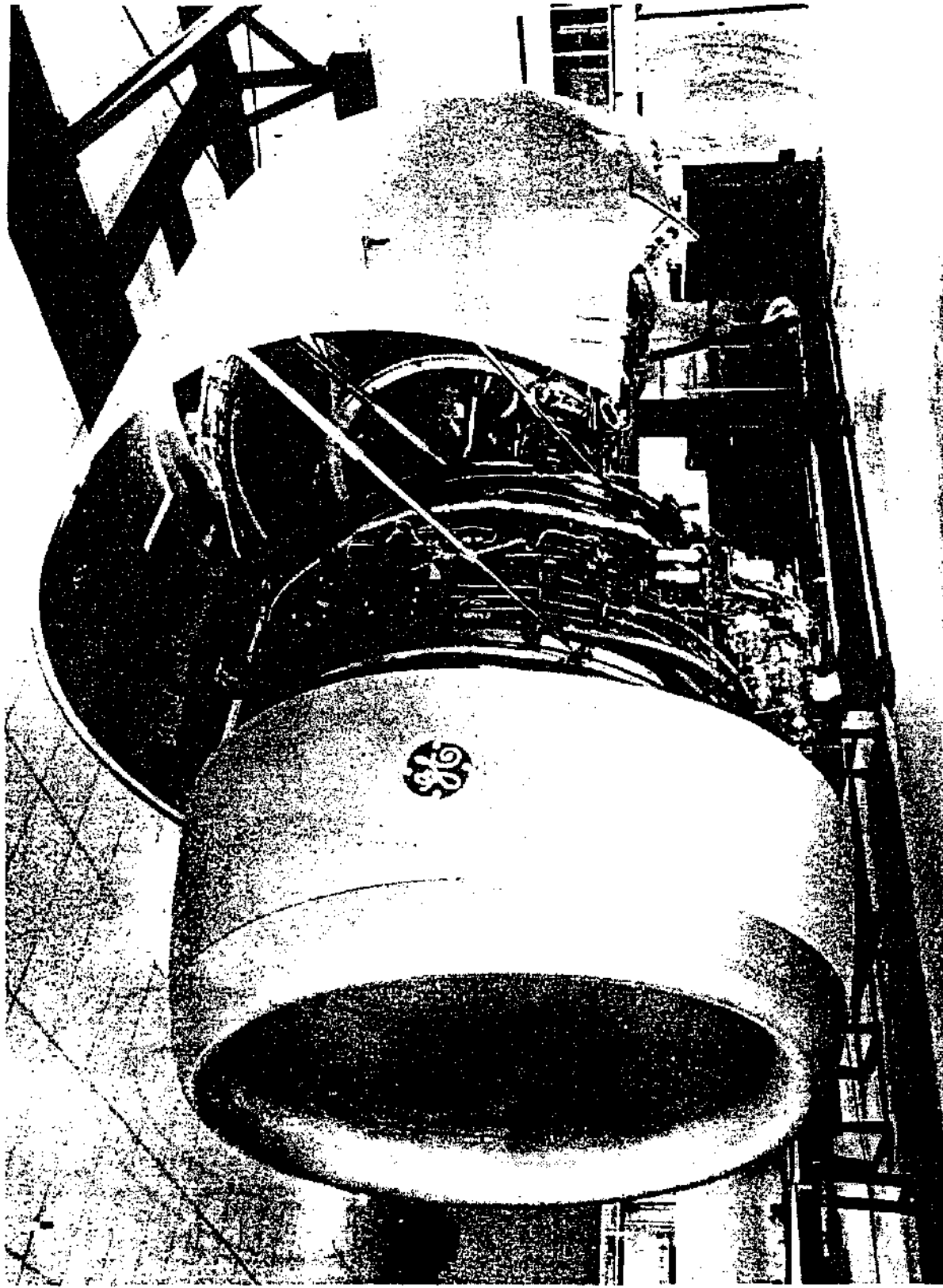
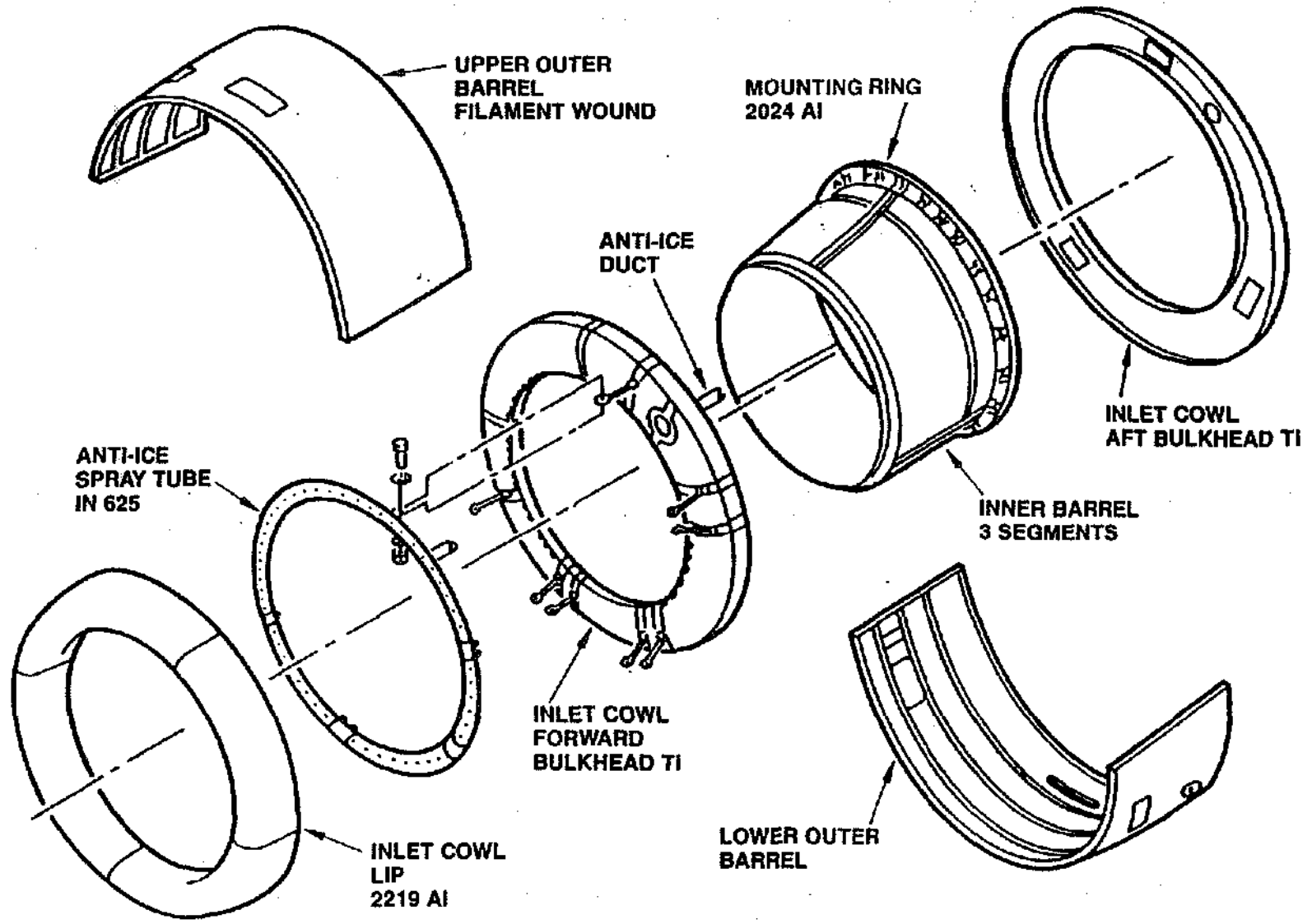


Figure 9.10 CF6-80C2 Inlet Cowl Right Hand Side



PRINTED IN USA

Figure 9.11 Inlet Cowl Details

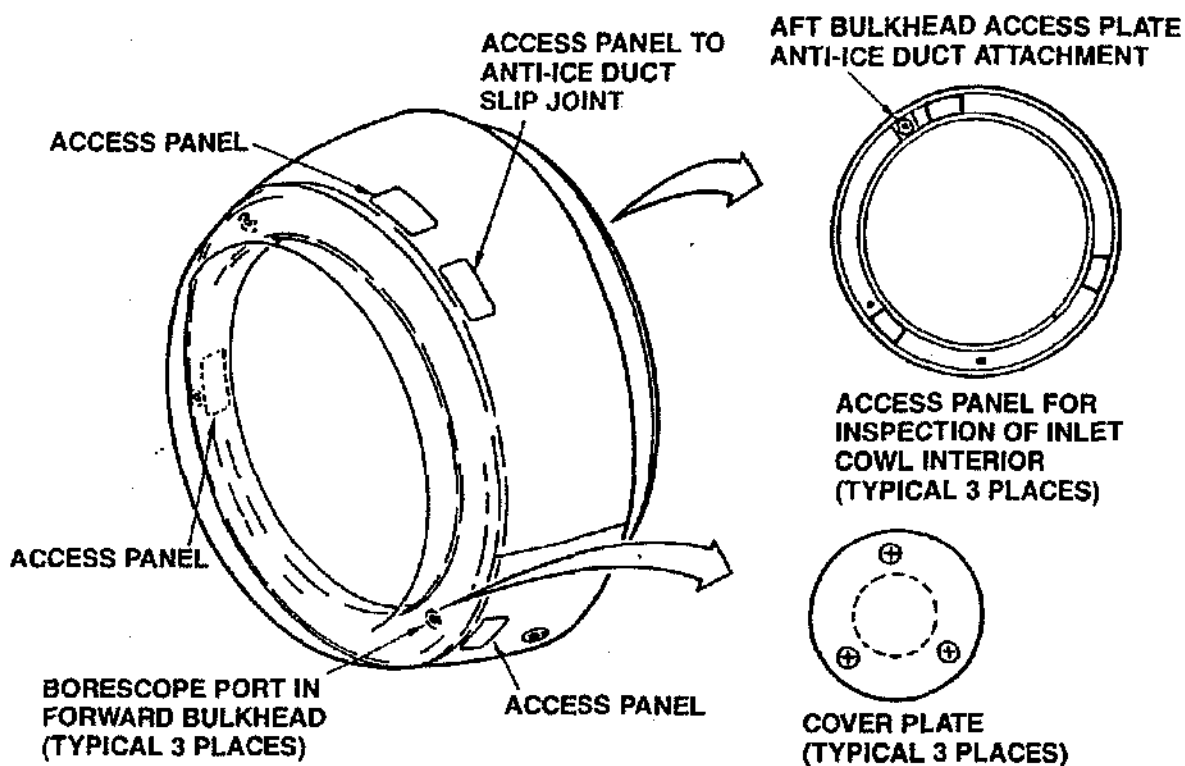


Figure 9.12 Inlet Cowl Access Panels

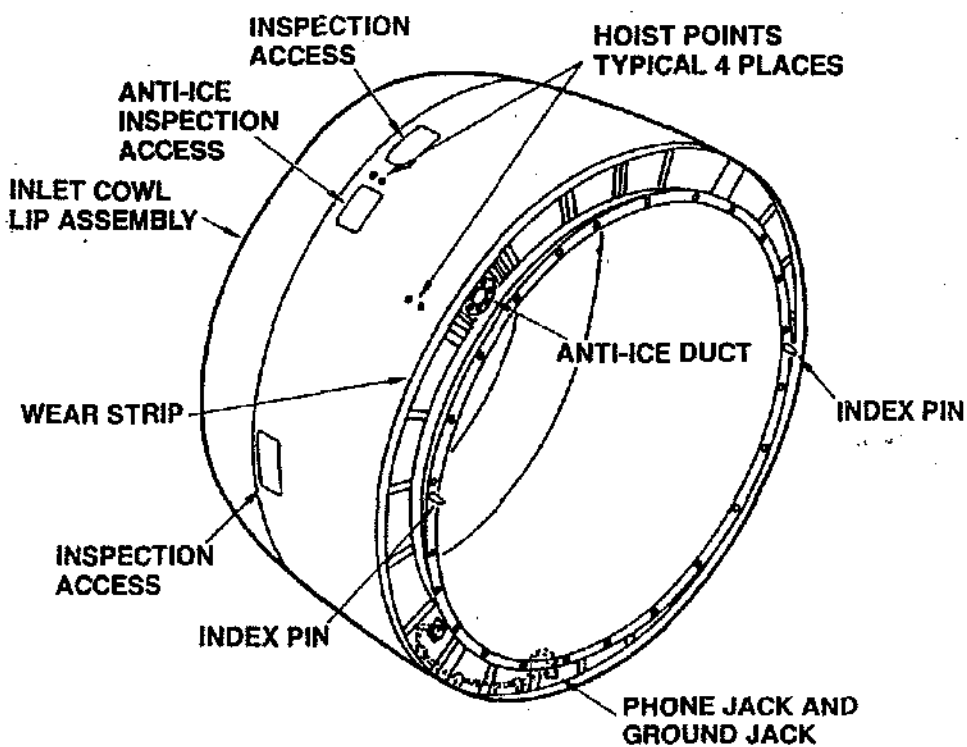


Figure 9.13 Inlet Cowl Assembly

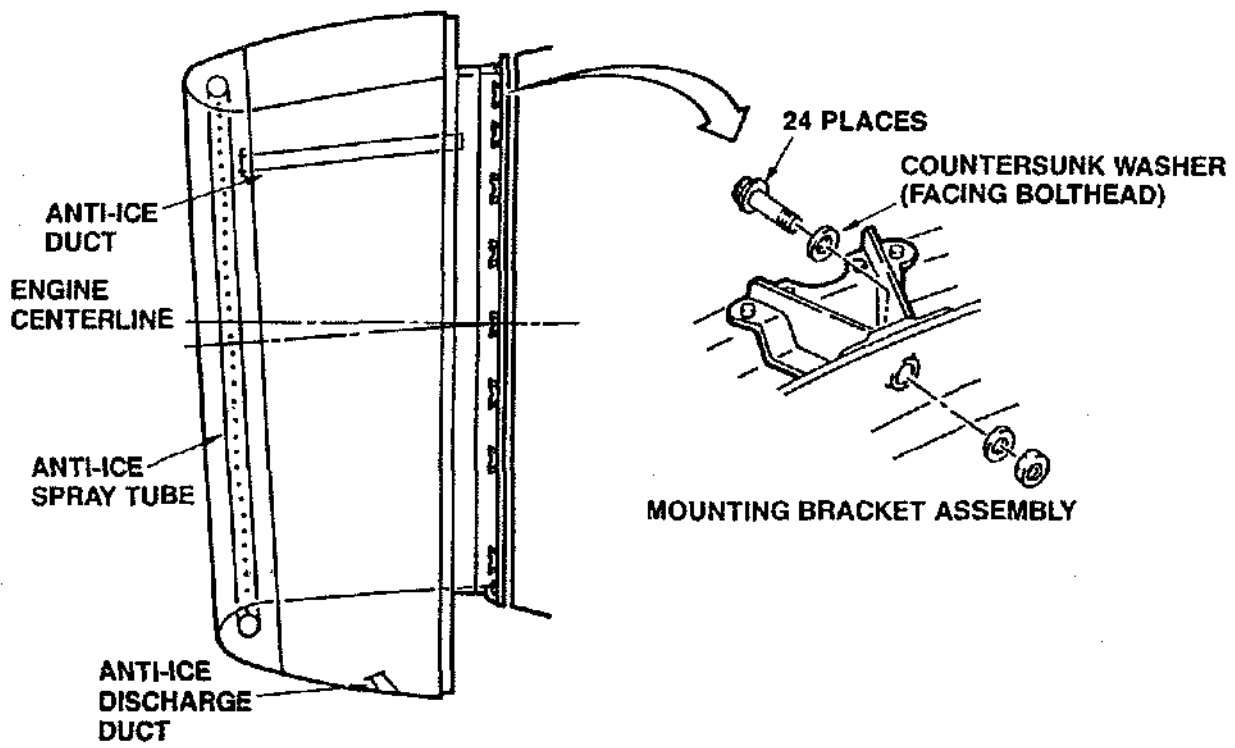


Figure 9.16 Inlet Cowl Installation

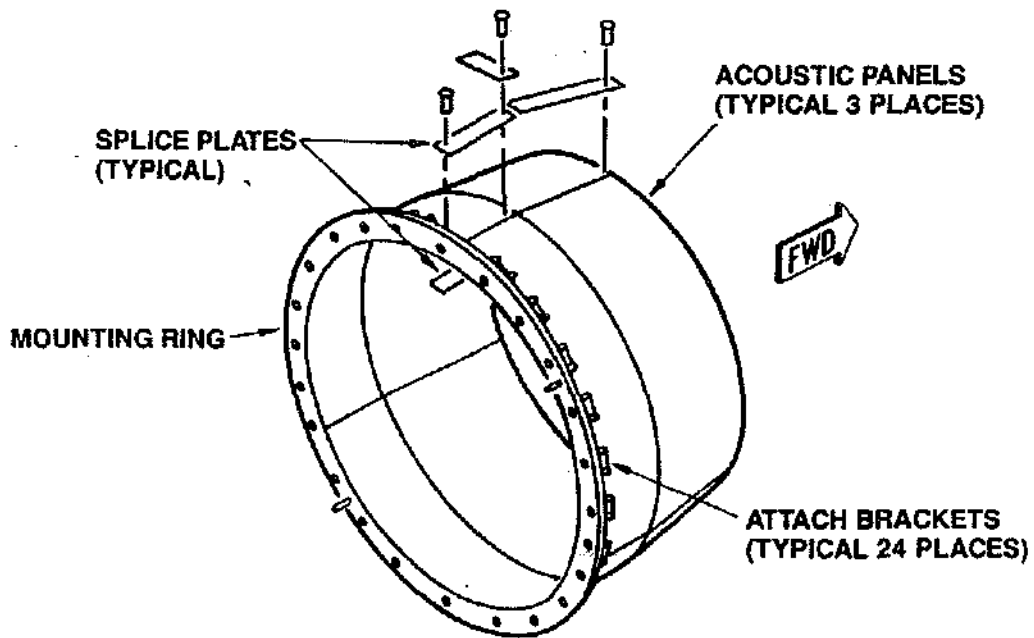


Figure 9.17 Inlet Cowl Inner Barrel

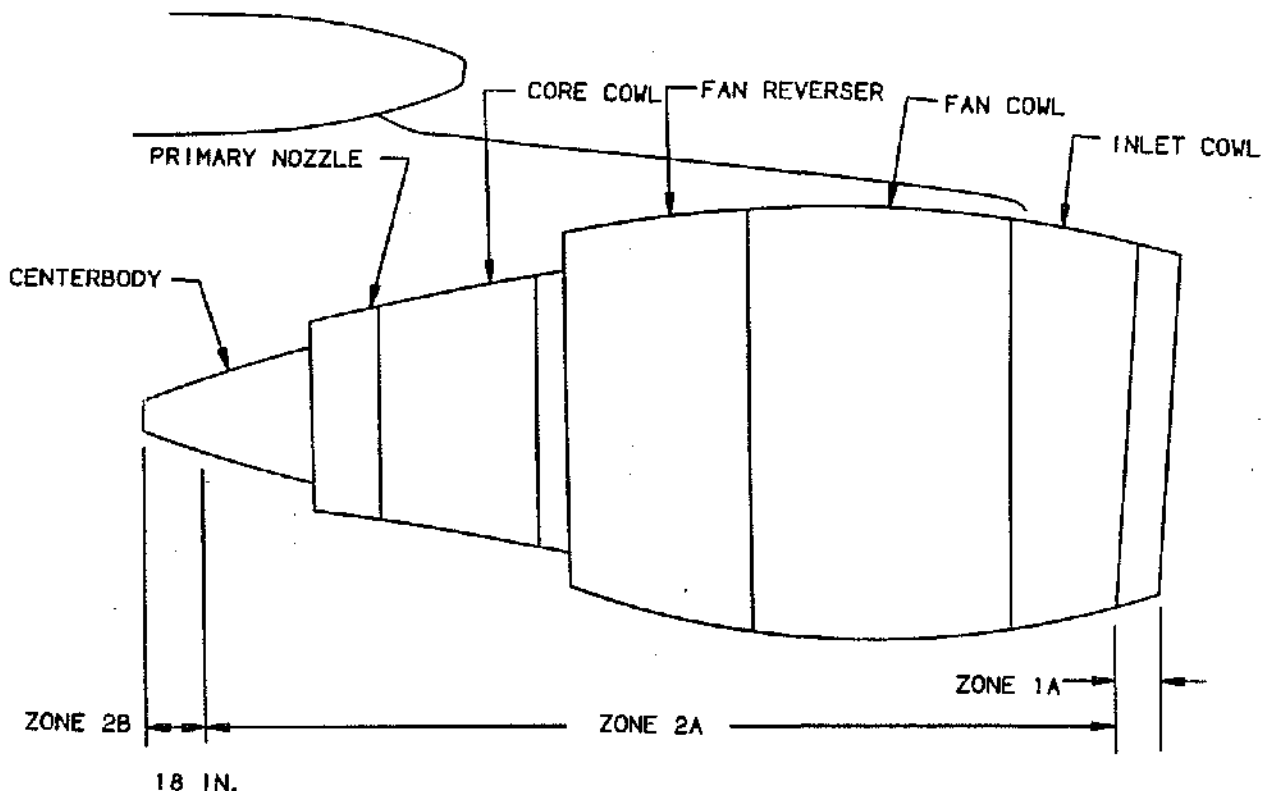


Figure 9.18 Lightning Strikes Zones For Wing Mounted Engines

COMMERCIAL HIGH BY-PASS FAN NOZZLE/REVERSER

The exhaust/reverser systems consist of three main subsystems: The fan nozzle with reverse thrust features incorporated, the control and actuation system, and the fixed geometry core exhaust nozzle. The fan nozzle/reverser, which is mounted on the aft flange of the fan aft case and hinged to the pylon, forms the fan-stream exhaust nozzle when stowed and reverses the direction of the fan-stream flow when deployed (Figure 9.19).

The fan nozzle and thrust reverser is composed of a left and a right hand fan reverser assembly (Figure 9.20). Each fan reverser half assembly forms a kidney shaped flow passage to the nozzle exit plane. The interruption of a continuous annulus is necessary to allow aircraft strut attachment at the top and engine service line routing at the bottom.

Operation in reverse mode is possible at all forward indicated ground speeds of the aircraft. However, normal operation in reverse mode at ground speeds lower than 80 knots without power reduction is dependent on results of evaluation of flow patterns created by the interaction of the fan reverser, core exhaust system, and aircraft

flow fields. These values are determined during tests of the aircraft/propulsion system. The system is not designed for normal reverse operation in flight. However, it is required to be capable of sustaining an inadvertent deployment without separation of components which could affect safety of flight. Translation of the outer cowl is accomplished through an air driven actuation system comprised of an airmotor and three interconnected ball screw actuators per half.

Fan Reverser The fan reverser, like the fan cowl and the core cowl, is also part of the pylon assembly and is not removed with the engine, while the inlet and the core fixed nozzle are removed on engine change. It is constructed in two halves, hinged to the aircraft pylon at the top, and latched together at the bottom to permit opening the reverser for engine access or removal. Each half-duct forms the inner and outer surfaces that direct the fan air-stream, and contains the blocker doors, cascade sections, outer and inner cowling, actuators, and necessary structural components. During deployment, the translating cowl is driven aft, rotating the blocker doors into the fan stream and exposing a series of louvered cascades which turn the blocked air-stream outward and forward (Figure 9.19).

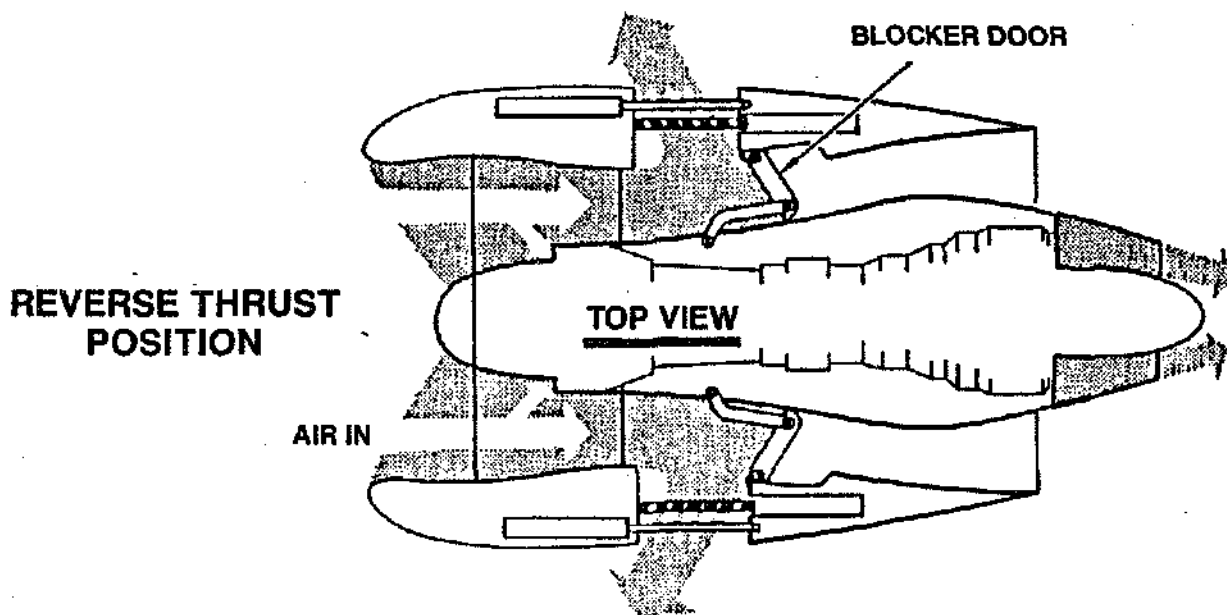
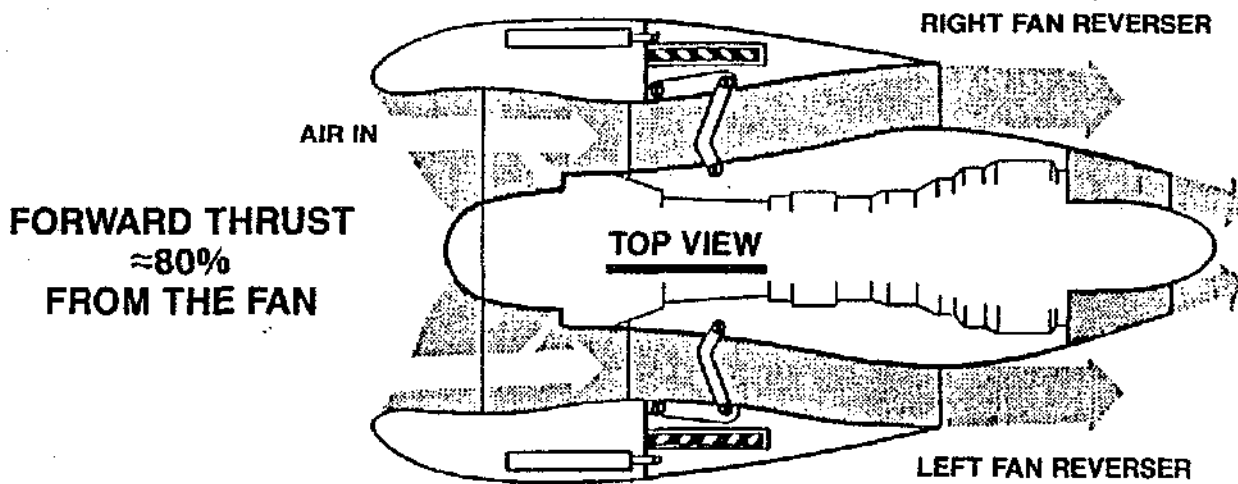


Figure 9.19 Exhaust/Reverser System

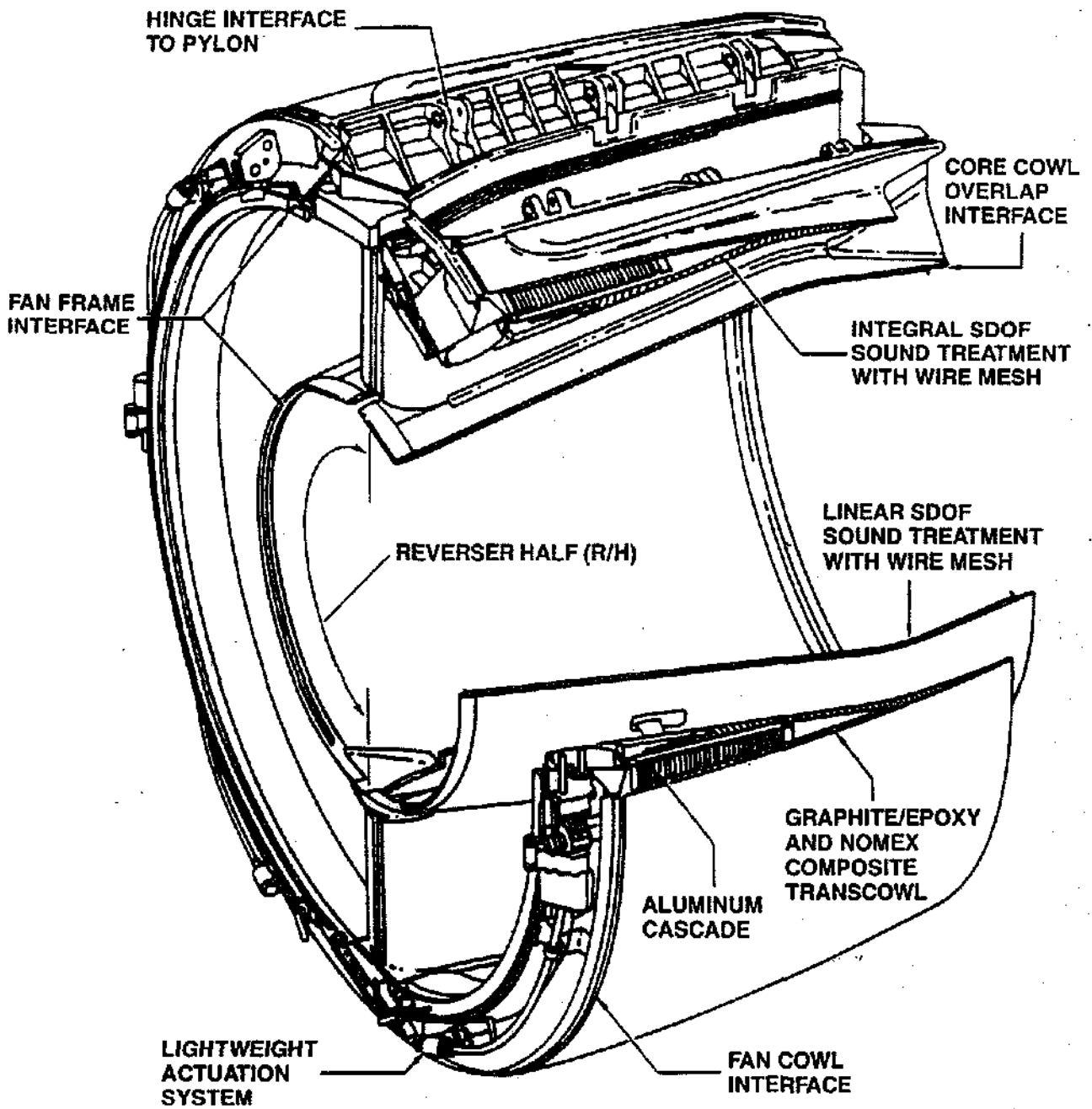


Figure 9.20 Fan Reverser

Fixed Structure Component Description The fixed structure halves (Figure 9.21) are riveted, bolted and bonded together to form a single fabrication. The aluminum surfaces of the inner cowl exposed to the engine compartment environment are protected with an insulating ablative coating for temperature/fire protection.

Bulkhead Sidewalls The duct sidewalls, upper and lower, are aluminum honeycomb bulkheads which connect the inner and outer flowpath surfaces formed by the inner cowl and the translating cowl. They form airfoil shaped flow splitters which provide cavities for the aircraft strut structure and engine service tube and cables. The upper sidewall includes three hinge clevis forgings, power opening actuator support/reaction forging and three deflection limiters and wear pads. The lower duct sidewall includes two deflection limiter wear pads, three lower latch assemblies with alignment pins and two hinged lower access panels; the forward panel also serves as an engine cavity pressure relief door.

Inner Cowl The inner cowl is an aluminum honeycomb bondment providing an aerodynamic inner flow surface for the fan duct and a core engine forward cowl. The inner cowl also incorporates acoustic treatment as part of propulsion system sound suppression. The cowl is bolted to the duct sidewalls. On the forward inner edge of the cowl, a partial tanged flange engages a groove on the fan frame. Six hinges for blocker door link assemblies are attached to each inner cowl. An air extraction duct penetrates the inner cowl for the fan air pre-cooler, and a hinged access door is provided for servicing engine accessories. Zee rings riveted to the inner surface provide additional stiffening to the honeycomb. The flowpath surface is perforated to provide engine noise suppression.

Outer Support Assembly The outer support assembly is a riveted and bolted framework of aluminum sheet and extrusions to support and position the translating cowl actuation system and the vane deflector assembly. It is bolted to the duct sidewalls. It is supported and stiffened by a forward latch ring assembly which engages a vee on the outer aft fan case and latches at twelve and six o'clock positions to the fan case. Tee slots provide guideways and support to the translating cowl.

Vane Deflectors Vane deflectors are aluminum castings. The blank off panels are aluminum. The deflectors and panels are bolted to the support assembly to provide various optional patterns of air deflection. The system pattern for each half, are selected based upon engine position, inboard or outboard half, and for aerodynamic and braking effect. The deflectors and panels are individually replaceable.

Translating Cowl The translating cowl bondment is constructed of graphite/epoxy with a Nomex core. Fiberglass is used on the flow path face sheet for acoustically treated flow surfaces. The structure provides an outer flow path for the air, a smooth low drag outer cowl and a pocket to enclose the vane deflector assembly in the stowed position. The transcowl is positioned by three ball-screw actuators with its rod end bearings locked into steel fittings by removable pins. The translation is guided by teflon coated Tee hinged rails at upper and lower ends engaging the lined tee slots of the support assembly. Hinge clevises provide the forward pivot for the deployment of the blocker doors. In the stowed position, a bulb seal bolted to the transcowl at the forward edge of the blocker door support ring provides an aerodynamic seal between the fan flow stream and the deflector vane cavity.

Fan Reverser Opening System Each fan nozzle/reverser half incorporates attachment fittings for a strut mounted hydraulic actuator. The respective power opening actuator (Figure 9.22) is driven by a portable hydraulic pump which attaches to a coupling located on the lower fan case. Each reverser half must be opened independently for maintenance access to the core engine. Hold open rods are provided and required for each reverser half for use after the reverser half has been fully opened by the hydraulic system.

Blocker Doors The blocker doors (Figure 9.22) are pivoted into the fan exhaust to block the normal flow path, requiring the fan air to turn and exit through the vane deflector assembly. They are a composite structure of fiberglass face sheet, graphite/fiberglass back pan with aluminum hinge castings bonded into place. The doors are hinged on their forward edge to the translating cowl and bolted into the blocker link housing near the aft edge. The blocker link acts as a radius rod controlling the rotation of the blocker door into the fan air as the transcowl is deployed. The blocker doors are spring loaded in the stow position to provide a seating force.

Fan Reverser Control Actuation System The fan reverser (F/R) transcowl is driven to deploy or stow position by three ball-screw actuators on each fan reverser half (Figure 9.23). The power to drive the actuators is aircraft ECS (Environmental Control System) bleed air ducted to each of two pneumatic actuator drive motors located at the center positions of the fan reverser transcowl.

These units are referred to as center drive units (CDU). The center drive units are interconnected to the end actuator gearboxes through flexible cables. The pneumatic supply and the direction of drive motor rotation is controlled by dual cockpit commands to the pressure regula-

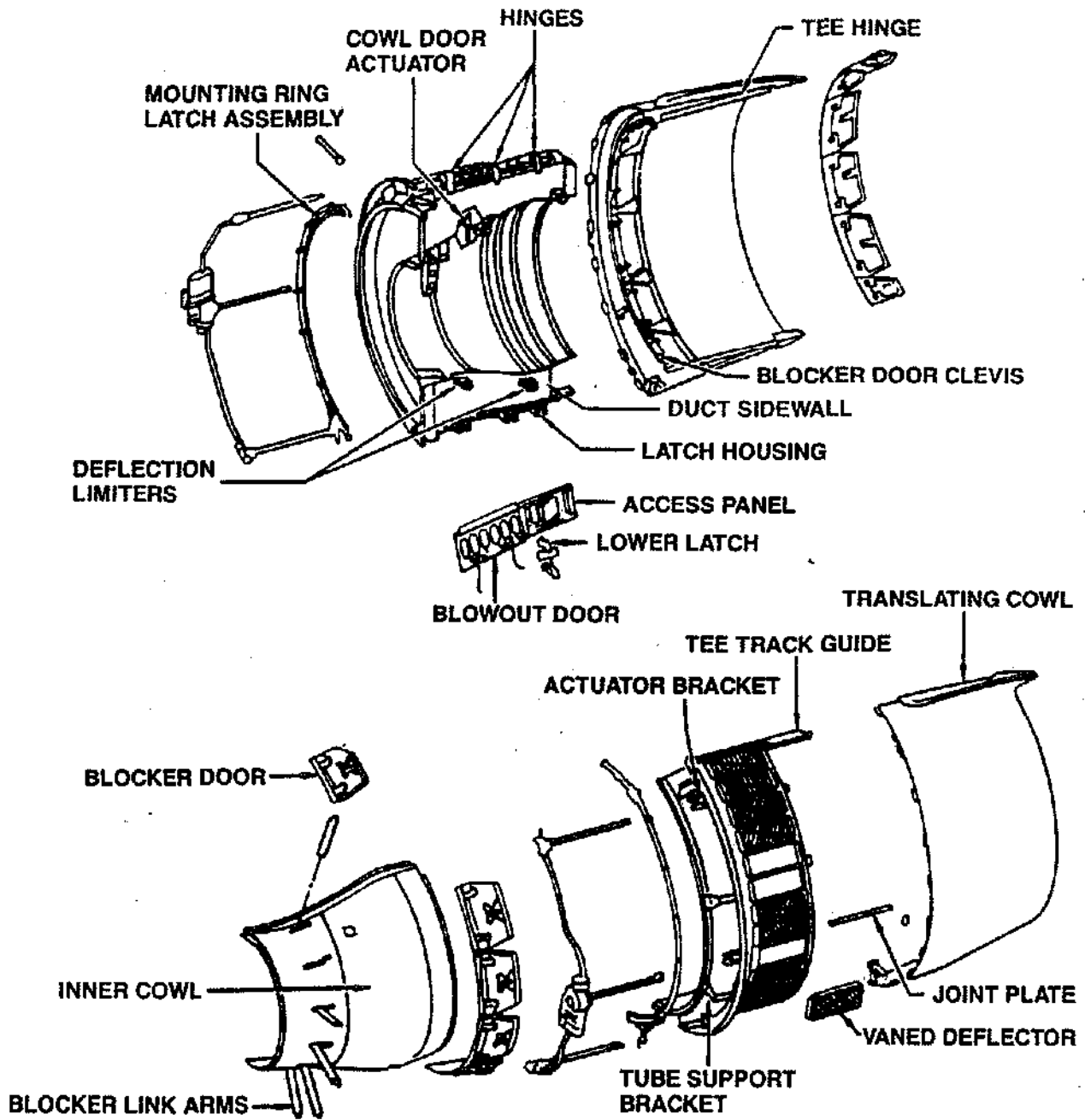


Figure 9.21 Fan Reverser Exploded View

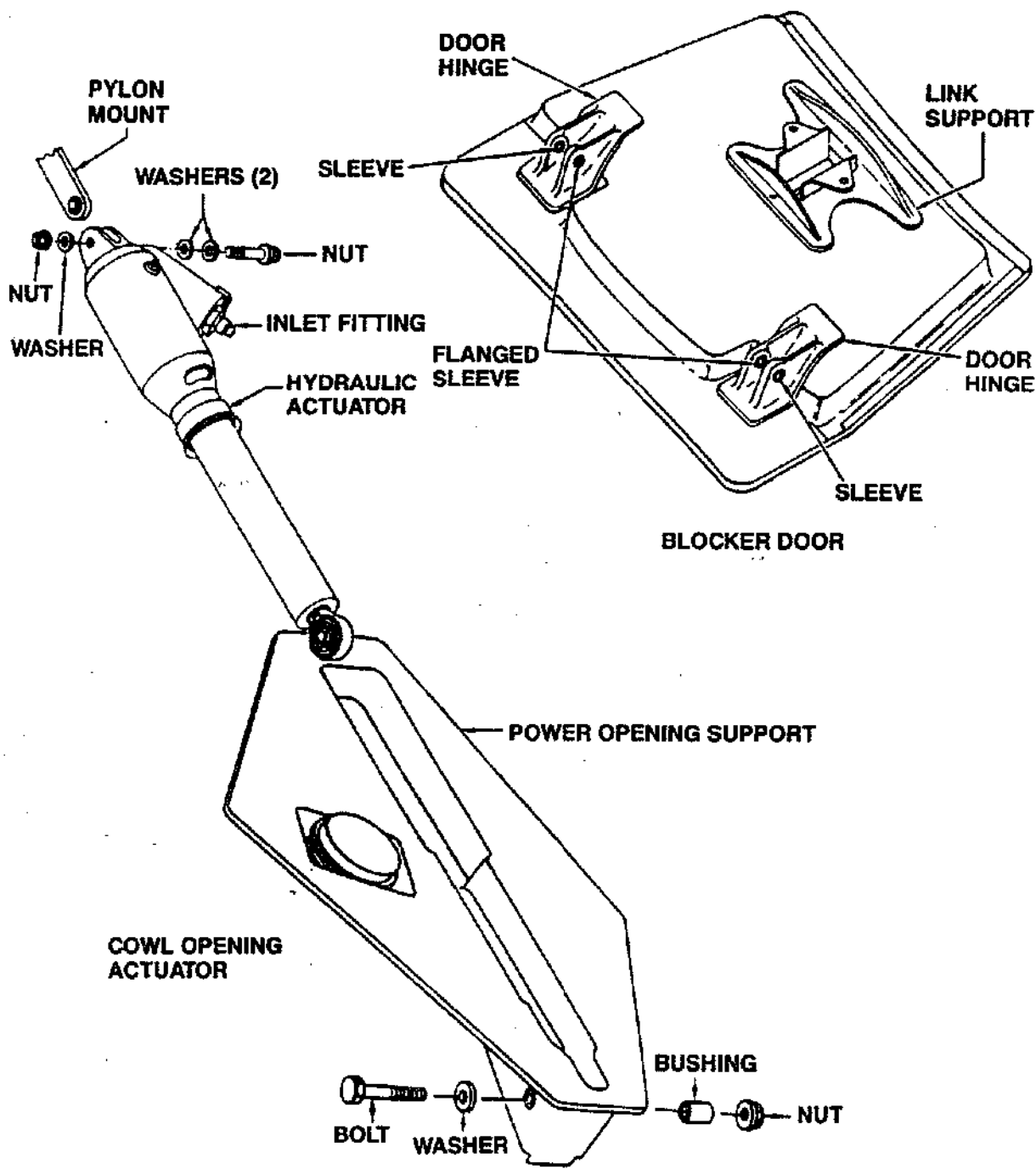


Figure 9.22 Reverser Opening Actuator and Blocker Door

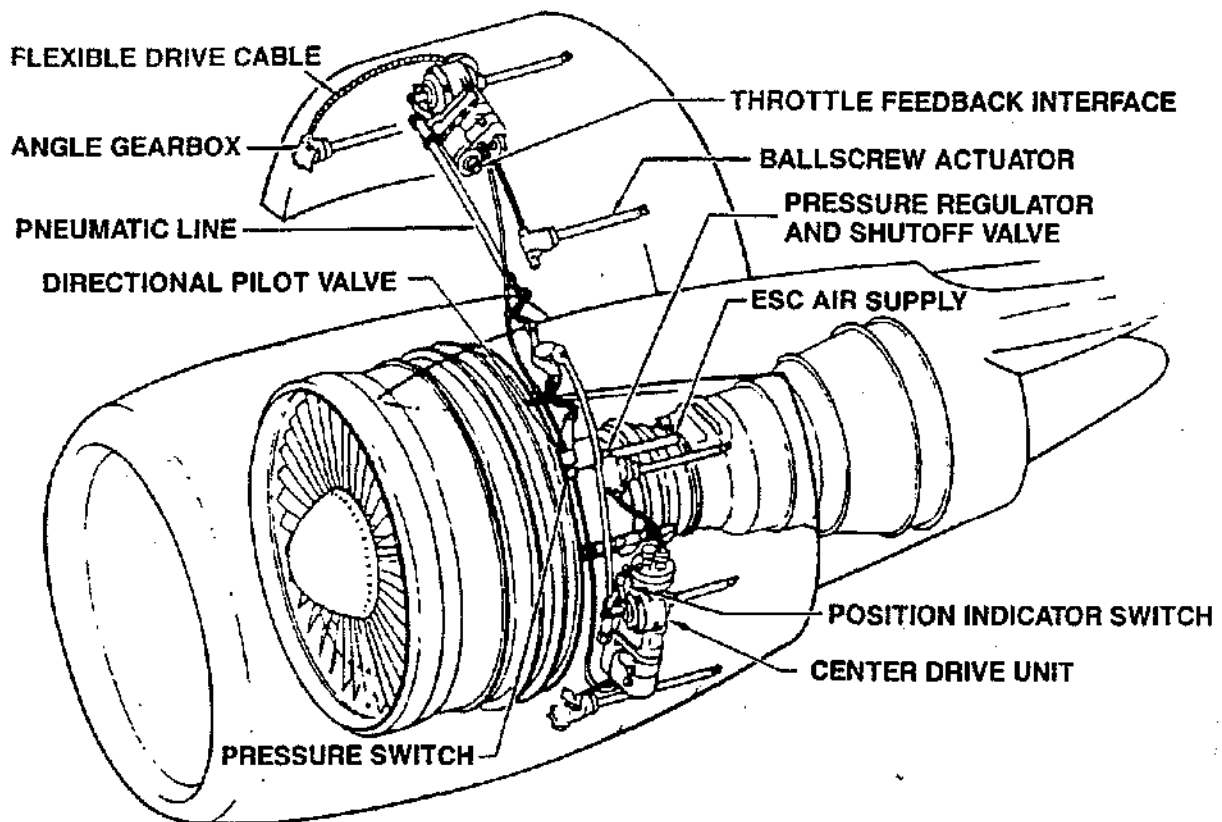


Figure 9.23 Thrust Reverser System

tor and shutoff valve (PRV) and the directional pilot valve and pressure switch (DPV). Cockpit indication of transcowl position is provided by electrical limit switches which are cam operated by the pneumatic CDU's. Throttle feedback actuators, part of the CDUs, position the aircraft push-pull cables proportional to the transcowl position. In a normal stow or deploy, the feedback mechanisms removes a throttle block permitting full engine rpm following 82% translation to deploy and 92% translation to stow. In the event of inadvertent deploy, the push-pull cable will override the pilot command and drive the power lever to engine idle speed position. The recent introduction of the "FADEC" system (Fully Automatic Digital Electronic Control) provides the positioning feedback electronically instead of through push-pull cables.

Supply Manifold A pneumatic supply manifold supplies air to the two CDU's. Installed in the duct are a Y-check valve for automatic ground test capability, a pressure regulator and shutoff valve, a wye to split the supply, two flexible hoses and a directional pilot valve (DPV) on the left hand reverser half. The DPV in turn ports control signals to each CDU.

Deploy Operation To deploy the system, the main throttle must be moved to the idle position which then allows the reverse levers to be moved into the reverse idle position. The fan reverser throttle feedback prevents the reverse lever from being pulled beyond the idle position. With the lever in the reverse idle position, the deploy command switch is closed. This energizes the thrust reverser pressure regulator valve solenoid. The pressure regulator opens and permits ECS air to flow to the system (Figure 9.24). When the pilot moves the reverse levers to the throttle interlock, the mechanical action closes a switch and provides an electrical signal to the directional pilot valve solenoid which closes its vent and opens its supply port. Each of the directional control valve pistons is then pressurized, and each directional control valve rotates to a deploy mode, admitting pressure to the drive motors and releasing the brake on each drive motor. With the motor pressurized and the brake released, the drive unit actuators proceed to actuate the system to the deploy position.

Stow To stow the system, the pilot returns the throttle handles to the forward thrust position. The Pressure Regulator Valve (PRV) solenoids are now energized through the closed stow switch circuits and the PRV valve opens and regulates as in the deploy mode.

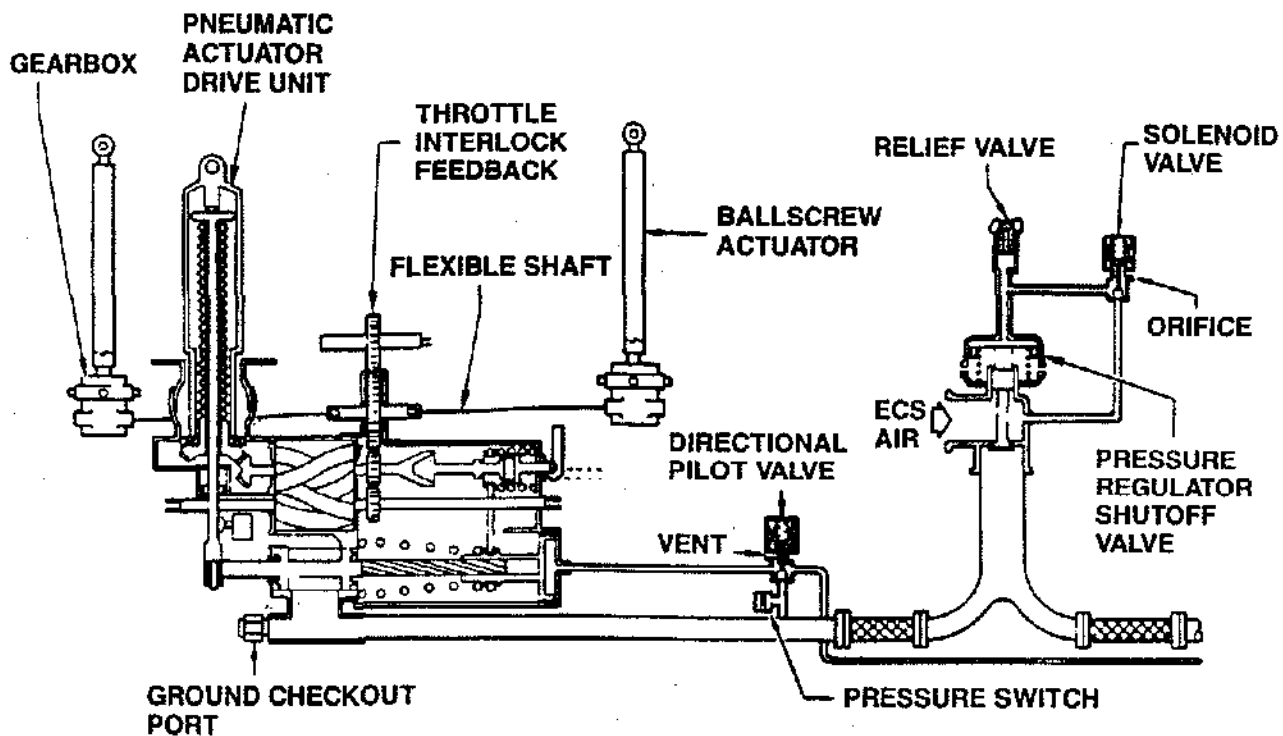


Figure 9.24. Simplified Thrust Reverser Actuation System

COMMERCIAL HIGH BY-PASS PRIMARY EXHAUST SYSTEM DESIGN

The primary nozzle assembly consists of a centerbody and an outer barrel fairing (Figure 9.25). The nozzle directs the primary exhaust gas aft and regulates the gas stream flow. The outer surface of the outer fixed cowl provides a continuation of the fan flowpath aft of the core cowl doors when the fan reverser is stowed. The centerbody is Inco 625 material comprising a forward flange for attachment to the engine inner exhaust nozzle frame, a forward sheet metal formed/brazed section and an aft sheet metal formed/brazed section with an opening at the aft end for the engine center vent system. The nozzle outer barrel assembly is comprised of an outer cowl bolted to the inner barrel portion called the primary nozzle. The outer cowl is a sheet metal welded and riveted fabrication made from 6AL 4V-Ti material while the primary nozzle is a sheet metal welded and brazed fabrication made from Inco 625 material. There are three ports on the inner barrel to introduce engine low pressure recoup air into the primary airstream. Wear pads are attached to the outer cowl to support the aft end of the core cowl doors. In addition to the basic design considerations of pressure, thermal and fatigue loading of exhaust

system components there are design conditions or requirements imposed by regulatory agencies (FAA, DGAC, etc.), aircraft manufacturers, aircraft users and operational experience.

Since the outer surface forms part of the nacelle, the interfaces with strut and other nacelle components must generate minimum disturbance to the aerodynamic contour. Leakage from the nozzle flow path is an engine performance loss which must be minimized. This requirement becomes challenging with nozzles containing the reverse thrust function where components are designed to deploy and stow every flight.

Lightning Strikes Nacelle surfaces exposed to lightning strikes must demonstrate the capability to endure prescribed levels of strike without damage which would impair flight safety. Grounding paths are required which protect aircraft and engine electrical systems.

Abnormal Condition Requirements Requirements imposed by regulatory agencies, airline users and aircraft producers for flight safety reasons often provide the structural loading definition which sizes components and provides design margin for the normal flight mission ele-

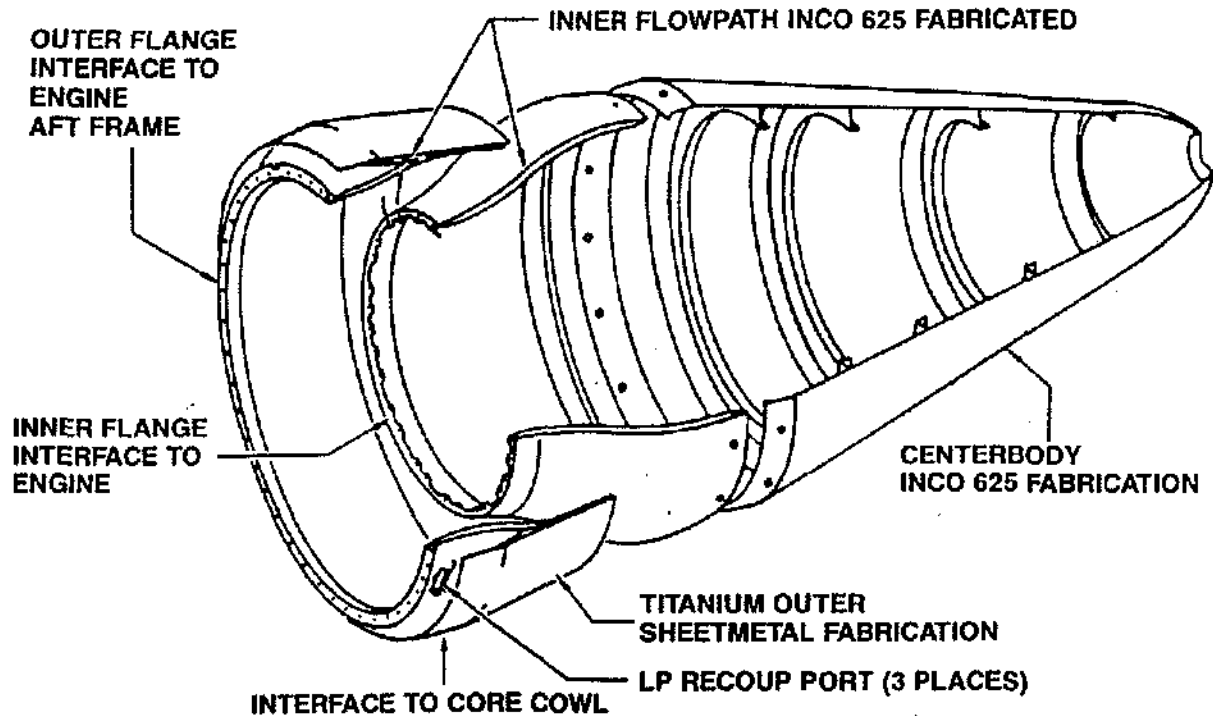


Figure 9.25 Primary Exhaust System

ments. Included in these conditions are: operation with hinge or latch disconnected, duct burst conditions in the engine cavity, inadvertent deployment of the fan reverser in flight, rejected take-off conditions and engine rotating part failure conditions.

Structural Property Variables Since many of the major components are honeycomb core bondments, they are subject to process control variables and environmental exposure deterioration. Design properties utilized for these materials and adhesives are reduced to cover maximum temperature and environmental exposure conditions along with a design margin defined to cover process variables.

Weight and Producibility All parts of aircraft propulsion systems are designed to maximize use of the material properties so that weight is minimized. The producibility factor affects the material capability usage in many cases since repeatable construction is necessary for system performance and manufacturing cost control. Continuous coordination between the design and manufacturing functions is required during the design release phase to optimize the cost/weight relationship.

MILITARY AFTERBURNING VARIABLE NOZZLE SYSTEM

The military afterburning variable nozzle system Figure 9.26 provides for a number of functions. It limits exhaust gas temperature (EGT) at military and afterburner power settings to a preselected value. Near linear thrust change from idle to military thrusts must be provided by mechanically scheduling nozzle position. The nozzle provides a temperature limiting schedule that maximizes engine performance over the wide range of military engine speeds. Nozzle area needs to be able to be changed based on the rate of change of engine speed, to provide maximum stability of engine speed during afterburner transients (particularly useful at higher altitudes). The nozzle need to anticipate changes in EGT to provide fast nozzle response during EGT transients. The nozzle need to reset exhaust gas temperature to a lower value during high compressor discharge pressures (CDP) while in afterburner operation.

The afterburning nozzle section contains a casing which is the structural pressure vessel and transmits nozzle loads, a cooling air dispersion liner, flame holders, and

LEGEND

- | | | | |
|---|---|--|--|
| 1. COS SUPPLY PORT | 8. SERVO FUEL FROM MAIN FUEL CONTROL | 30. ACTUATOR BLEED PORT TO REAR GEARBOX | 16. TO TACHOMETER GENERATOR, FILTER BYPASS INDICATOR SWITCH, MAIN IGNITION UNIT AND ANTI-icing VALVE |
| 2. TO ANTI-icing INDICATING SWITCH | 7. REFERENCE LINE TO MFC BYPASS LINE (ENGINE BOOST) | 11. THROTTLE CABLE | 18. COOLING FLOW TO AIR FUEL PUMP (AFC BOOST) |
| 3. CDP LINE TO AFTERBURNER FUEL CONTROL | 5. SEAL DRAIN TO OVERBOARD DRAIN MANIFOLD | 12. NOZZLE PUMP BELT PRESSURE RELIEF TO SCAVENGE | 17. COOLING FLOW FROM MAIN FUEL PUMP |
| 4. NO. 3 BEARING SUPPLY VENT LINE | 6. NOZZLE PUMP MAGNETIC DRAIN PLUG | 13. HYDRAULIC PUMP INLET SCREEN | |
| 5. NOZZLE ACTUATOR PRESSURE TAP PORTS | | 14. TO SECONDARY MAIN IGNITION UNIT | |

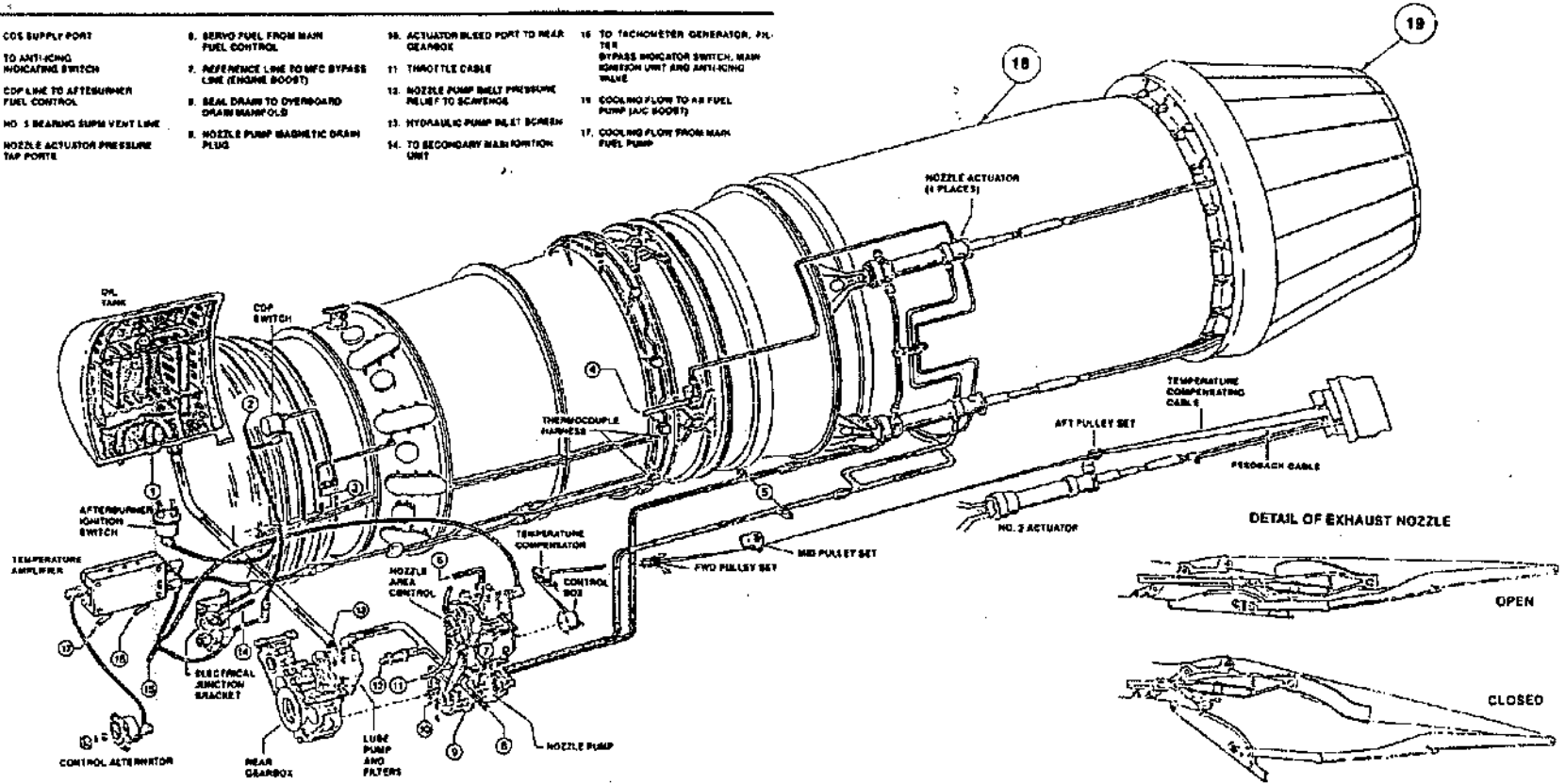


Figure 9.26 Military Afterburning Variable Nozzle System

fuel injecting spray bars. This section provides the chamber for utilizing the energy available in the gas generator exhaust gases. When the aircraft requires the thrust increase, fuel is injected into the turbine discharge flow, ignited and directed to the programmed nozzle area.

The nozzle (Figure 9.26, item 19) is comprised of a double row of "sliding iris" flaps. The arrangement provides a mechanism which varies the exit area as directed by the actuators and control system. The system depicted obviously needs an intricate control and sensing system. The structural design considerations include significant thermal excursions during operation, mechanism durability in a severe thermal and fatigue loading atmosphere, and definition of the assembly mechanism for nozzle area variation with engine operational demands.

Components and Operation Variable nozzle operation is controlled in two ways; mechanical operation (mechanical schedule) and temperature limiting. During mechanical operation the variable nozzle is controlled by throttle angle compared to a mechanical feedback from the variable nozzle. These two parameters are sensed

and compared by the nozzle area control (NAC). If the throttle angle calls for a nozzle position different from actual (feedback), the nozzle area control output rod retracts or extends. When the output rod moves, it positions the nozzle pump control lever and causes the pump to supply oil under pressure to the nozzle actuators. The nozzle actuators move the variable nozzle flaps thus varying the nozzle exit area.

The major components that make up the temperature limiting section are the thermocouples, control alternator, temperature amplifier, and the nozzle area control. Thermocouples produce a millivolt signal proportional to the exhaust gas temperature. The control alternator produces the electrical power necessary to operate the temperature amplifier. The temperature amplifier receives a small electrical signal from the thermocouples and compares this signal with a reference voltage. The resultant signal is amplified and at times biased before being sent to the nozzle area control torque motor within the nozzle area control. The torque motor converts the signal from the temperature amplifier into a proportional mechanical displacement, which in turn provides the input to the overtemperature servo portion of the nozzle area control.

Chapter 10

INSTALLATION AND CONFIGURATION

by Eugene J. Antuna, John A. Gill and A. G. Creque
(Installation Topics)

and John F. Cataline and John J. Souhrada
(Configuration Topics)

COMMERCIAL PROPULSION SYSTEM INSTALLATION

Providing engines to the aircraft industry is more than designing and manufacturing an engine that operates well in the test cell. Whether the application is a single engine fighter or a four engine widebody commercial aircraft, the engine is no better than its installation in the aircraft (Figure 10.1).

An installation program normally starts when an aircraft manufacturer (or sometimes an engine manufacturer) identifies a need in the market place for a new aircraft. The aircraft manufacturer, along with General Electric Project Marketing Operation, identifies the requirements for such an engine. The engine preliminary design organization defines potential cycles and physical definition of the engine.

Utilizing the early engine definition, the installation design features must be determined. Important first considerations are in providing proper attention to engine mounting, ground support equipment requirements (GSE), costumer bleed and power extraction requirements, acoustics, external and internal flow-lines, and other major physical and functional interfaces with the aircraft.

Early in the program the aircraft manufacturer and GE Projects arrive at a business agreement on the types of hardware to be supplied by each party. This may range from supplying a bare engine to providing engines with nozzles, afterburners, or reversers to providing complete propulsion systems which include all hardware from the strut or pylon outboard. Once the application is defined, a set of product requirements can be prepared.

The first step in the installation design is to establish the aero lines. The aero design considerations are discussed elsewhere, but in reality involves a series of trade studies including type of flow (mixed or separate), structural

requirements impact (mounts, gearboxes, etc.), acoustic treatment (area and type), reverser type (cascade, target, etc.), and containment.

Aside from the basic engine dimensions, engine mounts and gearboxes are the structural areas which most commonly establish the minimum cross section for the aero lines. Therefore, first activities normally involve identifying a preliminary mount system which meets the load and pylon or strut system dynamics requirements (Figure 10.2). This requires close integration with the aircraft manufacturer to define mutually acceptable operating loads and interface stiffness which will result in acceptable dynamics and acoustics to both the aircraft and engine.

In the area of the gearbox the requirements for both the engine and aircraft must be considered. Assuming engine requirements are available, the electric power and hydraulic requirements must be established with the aircraft manufacturer. Taking these requirements and working with the gearbox design group, a gearbox can be designed and located on the engine consistent with both engine mechanical and aero considerations.

After establishing the major structural requirements, studies with the aero group engineers can then be conducted with appropriate trades being made relative to weight, cost, and performance. Other aero considerations such as installed performance and engine to nacelle to pylon spacing, which could have impact on the lines must also be considered at this time along with other potential hard points to be sure that all aspects of the installation have been considered.

Now that the major structure has been defined, the other systems must be evaluated. The next major item to consider is the aircraft bleed systems for environmental control, aircraft anti-icing, and starter air supply where applicable. With the trend toward more fuel efficient engines with reduced air flows and increased aircraft bleed flow requirements (especially in commercial applications) compressor bleed capability is being severely strained. This often requires study of alternate anti-icing systems and more efficient bleed systems.

Location of bleed system interfaces varies by application depending on the contractual agreements. This may vary from some ports on the compressor case to a single interface providing regulated pressure from a series of two or three stages controlled from an engine mounted electronic control. Recent systems have provided aircraft anti-icing air for wings and struts from these same integrated air bleed systems for simplicity.

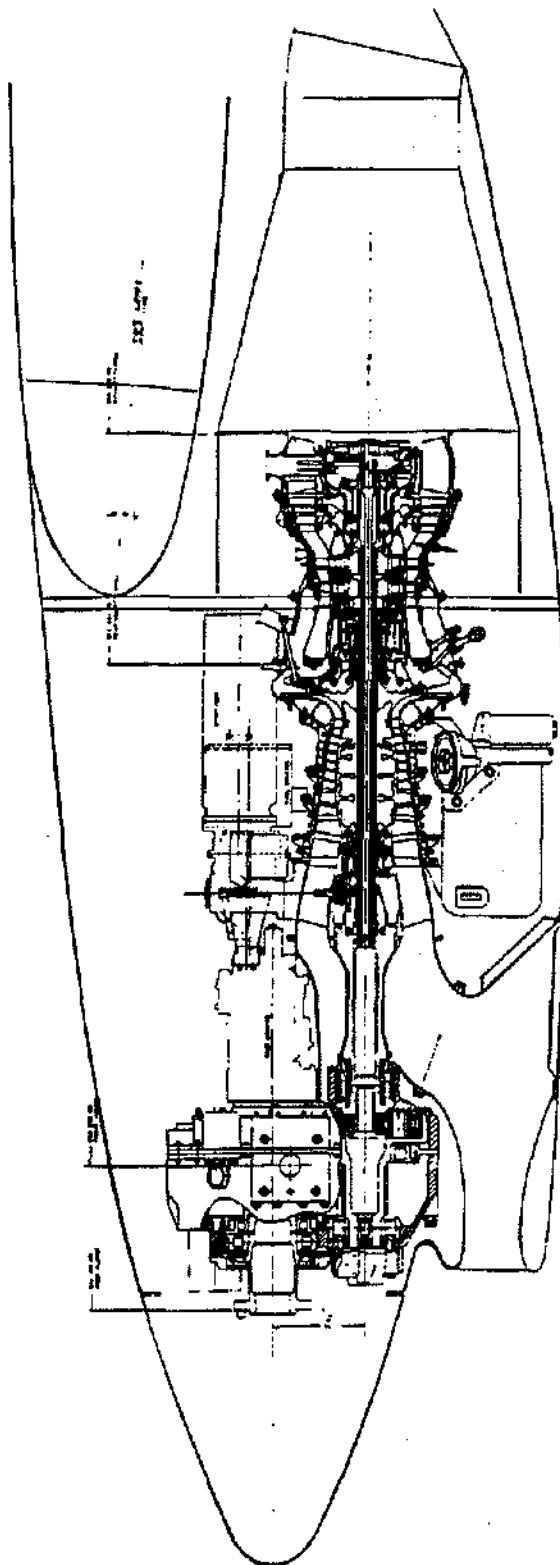


Figure 10.1 CT7 Installation with Close Coupled Gearbox

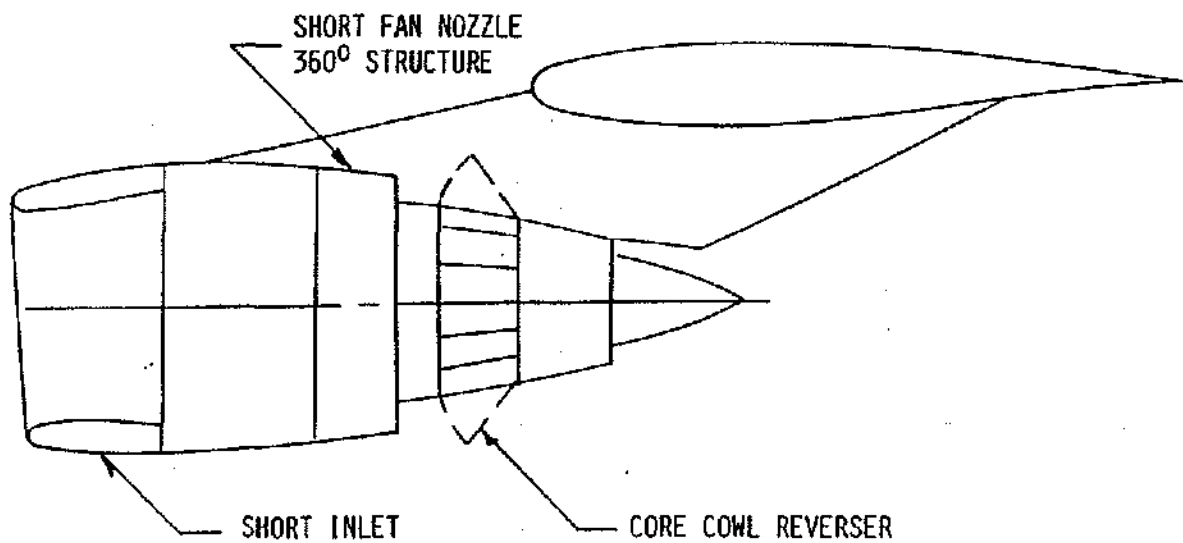


Figure 10.2 Large Fan Installation Studies

Other important considerations relative to the installation design effort include mission type (carrier, inverted, military), weapon system placement, cooling or ventilation system requirements, type of installation (wing or fuselage), gearbox location (engine or fuselage), removal requirements, instrumentation, access requirements, special exhaust requirements (military), and envelope limitations. In addition there are a number of other systems which must be defined and functional and physical interfaces identified. Among these are fuel and oil monitoring, fire detection, drains, fuel shut-off, throttle control, electrical power, and hydraulic power.

Once the systems have been defined by a coordinated series of design and system trade studies, these agreements between the engine and aircraft manufacturers are documented in physical and functional interface drawings and system descriptions. With these agreements detailed design of the various systems and components can proceed.

Maintainability and commonality play a major role in most product installation designs. Maintenance plays a major part in establishing the direct operating costs to the customer and in some cases is a contract guarantee. Layout of features and access provisions which are sub-

ject to maintenance is therefore a significant consideration. Early planning and reviews with users are necessary to be sure that adequate attention is paid to this item. Maintainability demonstrations using full size propulsion system mockups are conducted for the purpose of showing proper attention to this important feature and demonstrating removal and installation times of complete engines and components.

For airline customers using the same engine on different aircraft commonality is a very important consideration. Keeping the installations as common as possible, reduces the number of spare engines and components required which is a major airline investment. It also improves airline flexibility in moving engines between applications. Commonality is also a major benefit to manufacturing since with fewer differences a final model decision can be delayed farther down the production line, providing more flexibility to the shop and lower product cost.

The installation engineering function, consistent with its role as design interface with the aircraft manufacturer plays a major role as design interface with the aircraft certification programs. Problems involving either physical or functional interfaces are followed by this group

until solutions are identified and implemented. It involves a high degree of coordination with Engineering, Project, and Product Support functions and continues throughout the life of the program.

Installation functions are also responsible for preparing and maintaining the installation manuals and drawings which on commercial programs specifies the bounds for certified use of the product. These documents control such installation features as installation loads, operating temperatures, and operating pressures. At the same time the function maintains control of the qualified or certified structure tree or model lists which states installation items such as reversers, nozzles, and kits which are approved for use on the appropriate engine models.

In virtually all new engine programs, due to the complexity of the program, it is necessary to establish an integration plan between the engine and aircraft manufacturers. This plan may vary in formality, but it is necessary to protect the schedules and commitments of both parties. In general an integration plan is a document which details how the specification or contract is to be implemented by both parties.

The integration plan covers all aspects of the installation program from initial trade studies, to program review dates, to compliance and flight test, to engine and aircraft certification or qualification. The plan provides the discipline under which the program is conducted.

Periodic installation and program reviews are conducted to document progress to the integration plan, resolve technical and program issues, and document agreements. Engineering Coordination Memos (ECM's) document engineering communications, but the final mechanical, electrical, and functional interface agreements are documented in the functional and mechanical interface documents.

The engine or propulsion system mockup provides a first checkout of the interfaces, but the first real test is at the customer flight test. This is the first time that production engines or propulsion systems are fully mated with the production aircraft and all systems are operational. The installation and external system design personnel work closely with their airframe counterparts to quickly resolve technical problems which could delay an expensive aircraft flight test program.

This close technical coordination is continued through the production startup. Interface changes always occur between the flight test and production phase and may require modifications to the interfaces. These changes must be evaluated, released, mocked up, and production

hardware modifications scheduled. In addition, if any aircraft qualified or certified hardware is being provided along with the engine, this certification must be completed prior to delivery to the customer. Even after the product is delivered to the customer, close contact with Product Support is required to ensure a smooth integration of the product into service.

COMMERCIAL NACELLE SYSTEMS

In today's tight marketing world, most engine manufacturers are taking advantage of the cost and commonality that can be obtained by providing a complete Propulsion System (Table 10.1) for a commercial aircraft as opposed to the engine only. A Propulsion System, when done correctly, can be used in different aircraft installations therefore offering the airlines a much needed way to reduce their inventories on spare parts and replacement hardware. GE is currently providing common propulsion systems for installation on Airbus, Boeing and Douglas Commercial Aircraft.

A typical commercial nacelle system is shown in Figure 10.3. In addition to the engine this includes the (A) inlet, (B and C) cowling, (D) Aircraft Engine Buildup (EBU) hardware, and (E) an exhaust system as shown in Figure 10.4. These items combine to complete the package for a typical commercial propulsion system. The description of these components and their functions is below.

Inlet The purpose of the inlet is several fold. The aero lines must be selected to bring air on board the engine with a minimum loss and flow separation as each has an impact on efficiency and engine blade/vane excitation. The inner barrel of the inlet is normally acoustically treated to suppress fan/booster tones so as to meet FAR requirements: These three items form the criteria for which the inner lines are defined. The outer lines are defined to minimize drag throughout the inlet angle of attack, crosswind, windmilling and mach number envelope.

The inlet is normally anti-iced to prevent formation of ice which could disrupt its aerodynamic function or break loose and damage engine or aircraft components. This is usually done thermally with either engine bleed air or resistance heating. Significant analysis and test is required to demonstrate FAR 25 compliance with this requisition.

Maximum loads generally result from engine imbalance (blade out), thermal stresses (anti-icing) and near field acoustic noise. Inlet lips and structure are normally aluminum or titanium to withstand impact loads, the inner

PROPULSION SYSTEM = ENGINE + NACELLE SYSTEM + EXHAUST SYSTEM

- INLET
- FAN COWL
- CORE COWL
- EBU SYSTEM
 - ELECTRICAL
 - HYDRAULICS
 - PNEUMATIC
 - FIRE DETECTION
- MOUNT SYSTEM
- FAN REVERSER
- EXHAUST NOZZLE
- EXHAUST PLUG
- PYLON/STRUT FAIRINGS

*Table 10.1 Commercial Propulsion System
Large Fan Engine*

barrel is normally sandwich honeycomb type construction for acoustic and load carrying capability and the outer skins filament wound or layed-up composites.

Cowls The cowling forms the outer aerodynamic flow path for the nacelle and together with radial bulkheads establish the compartments around the engine. These cowls and bulkhead walls must be either fireproof (2000°F for 15 min.) or fire resistant (2000°F for 5 min.) depending on the type of fire zone.

The cowl loads generally consist of pressure, thermal and some redundancy load distribution with the engine and aircraft. If load sharing with the engine is utilized to reduce engine deflections this must be considered. The cowls often contain special provisions like service access or blowout doors, opening features and bleed intake or outlet vents which must be considered structurally and aerodynamically. This hardware is tooling controlled, made of composites or aluminum, and must be closely dimensionally controlled for interchangeability.

Engine Buildup (EBU) Hardware (Figure 10.5 and Figure 10.6) The engine buildup hardware (EBU) is that required to integrate aircraft and engine systems. It consists of such functions as the bleed air system, electrical power system, hydraulic power system, throttle and fuel systems, fire detection and extinguishing systems, and drain systems. These designs require a high degree of physical and functional integration with the aircraft company and knowledge of both system and component design. Design fields involved include mechanical, electrical, fluid flow and heat transfer considerations.

Depending on the installation, some parts of the EBU may be Buyer Furnished Equipment (BFE). These items could include such items as bleed valves, generators, hy-

draulic pumps and starters. When they are so supplied, the engine manufacturer is still responsible for their installation and operating environment.

These designs must be physically and functionally integrated with the engine systems to obtain the proper balanced design. This is further complicated by the fact that maximum engine commonality must be maintained among multiple aircraft applications.

Engine mount hardware is supplied as either part of the engine or as part of the EBU. Historically on large commercial engines, the front mount is part of the engine and the rear mount part of EBU. This hardware is made up of the attach pieces between the engine and aircraft interfaces. The configuration of the mount system is very important relative to propulsion system performance due to its impact on engine bending (clearances) and nacelle lines (drag). From a maintainability standpoint, they must permit easy installation/removal of the demountable power plant and permit necessary access to the engine.

Design of the mount hardware must consider the large variety of static and fatigue loads which both the aircraft and engine can impose on the structure both separately and together. Defining the static and fatigue load spectrums is a complicated joint effort between the aircraft and engine manufacture because it requires extensive understanding of both the engine and aircraft operation and physical characteristics on both sides of the interface. Design loads must consider all potential facets of operation including such things as blade out, aerodynamic, gusts, inertia, seizure, crash, etc. For safety considerations, mount systems are usually designed with redundant load paths so that a single failure does not result in loss of the powerplant from the aircraft.

NACELLE SYSTEM

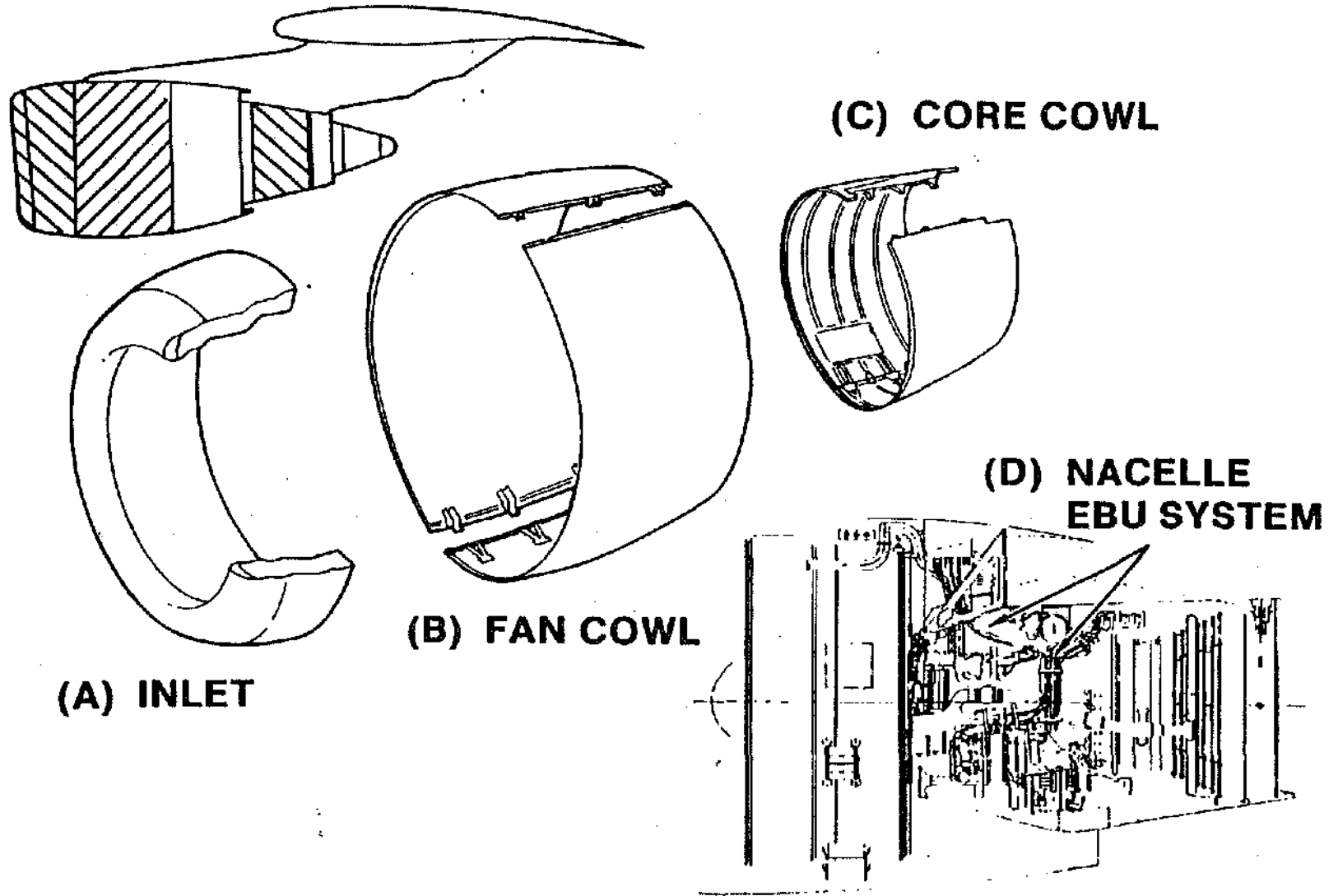
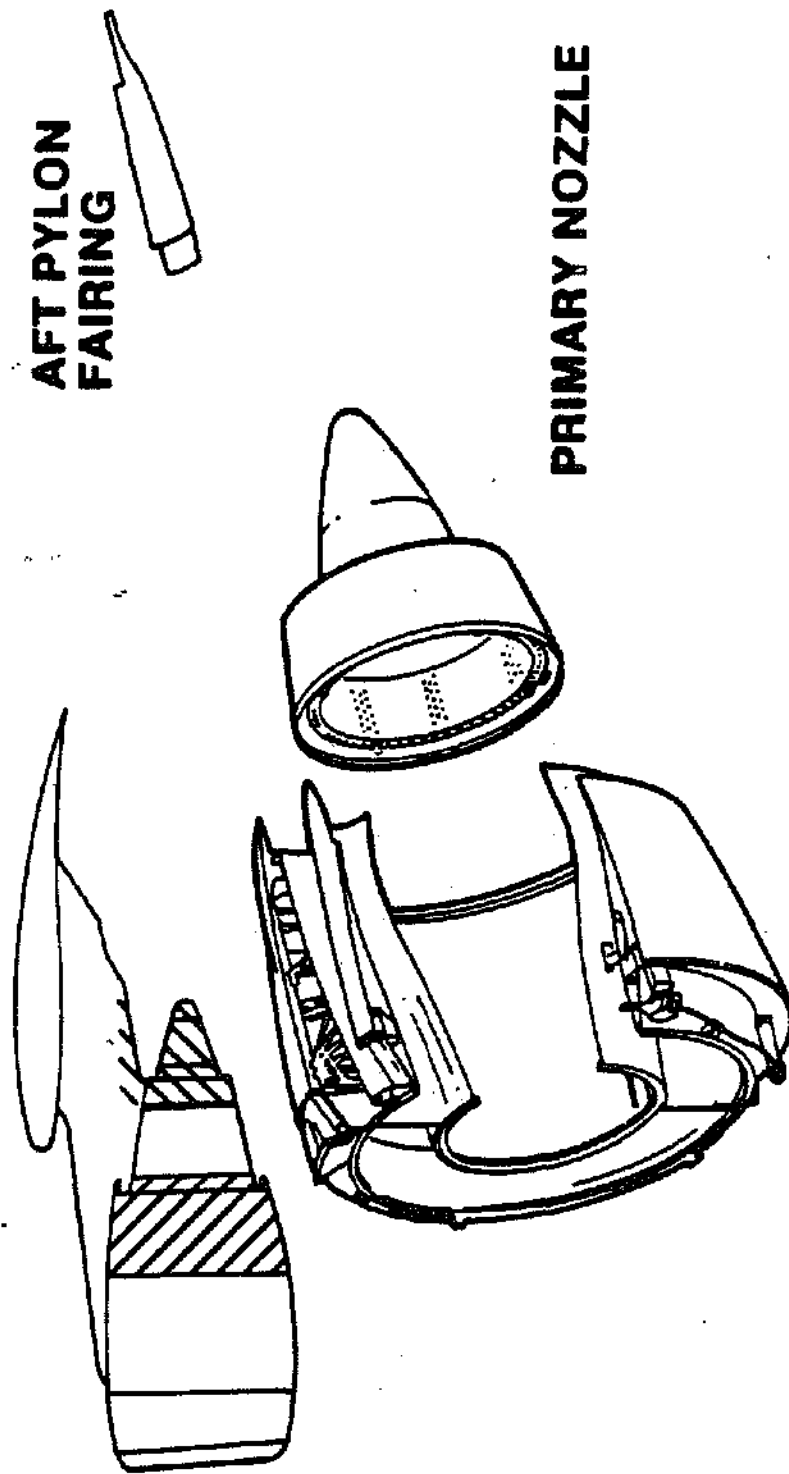


Figure 10.3 Nacelle System

EXHAUST SYSTEM



**AFT PYLON
FAIRING**

PRIMARY NOZZLE

FAN REVERSER

Figure 10.4 Exhaust System

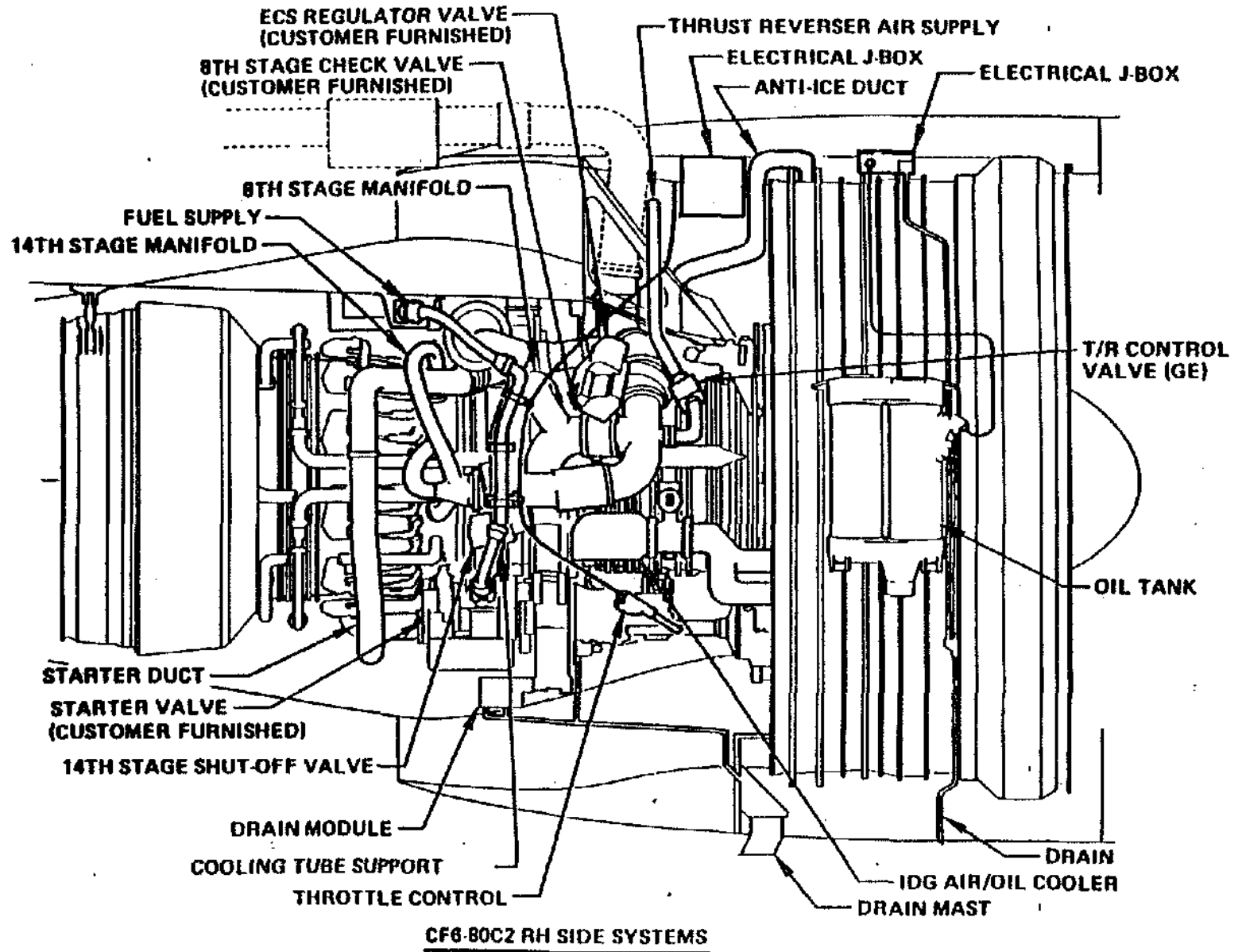


Figure 10.5 CF6-80C2 RH Side Systems

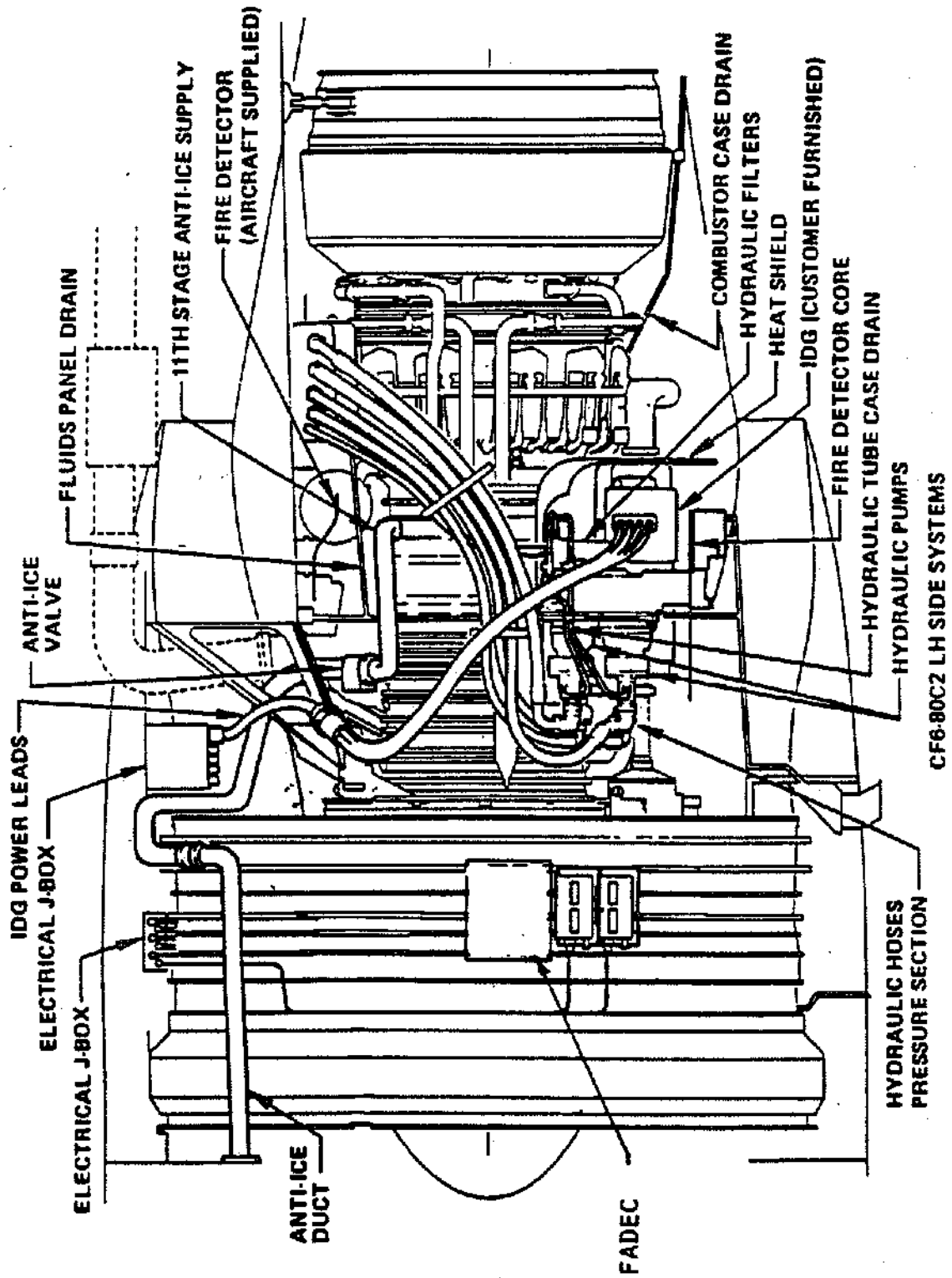


Figure 10.6 CF6-80C2 LH Side Systems

Exhaust System For each engine flow stream exhausting to atmosphere, a nozzle is required in order to obtain high discharge velocities and an efficient cycle. On separate flow fan engines, a nozzle is provided for both the primary and fan flow paths. On mixed flow fan engines, only one mixed flow nozzle is required. Examples of CF6-80C2 engines with separate and mixed flow are shown in Figures 10-3 and 10.4. On commercial engines the nozzles are normally fixed and are either converging or converging-diverging depending on the cycle and pressure ratio.

Primary nozzles are of the extended or submerged plug type and in most cases made of an Inco 625 fabrication, or titanium sheet. In some installations the primary jet stream can be spoiled or reversed to minimize stopping distance, however, this is not normally a cost effective feature.

On large fan engines like the CF6, the fan nozzle and the fan reverser are combined into one component. The purpose of the reverser is to shorten the aircraft landing stopping distance by providing reverse thrust and increasing aircraft drag. Reversers operate by diverting the flow stream either radially or forward. Popular types of reversers include cascade or target with cascade being the more popular due to the ability to better tailor the flow to different applications and overall effectivity. The CF6 type reversers are "D" duct type mounted from both the pylon and engine and stay with the pylon during engine removal and open in halves for engine maintenance. The fixed structure of the reverser is aluminum or steel with a composite transcowl and blocker doors. The actuation system is normally air driven on GE designs but some other industry designs are hydraulic.

MILITARY ENGINE INSTALLATIONS

Installation design considerations for a military engine differ significantly from those for commercial customers. The operating environment for military engines is much more demanding and severe. Military engines must tolerate high flight maneuver and landing loads (-4 to + 10 g's), unusual aircraft operating attitudes (vertical climbout, inverted, nose down, etc.), high flight speeds, and rapid changes in altitude, pressure, and temperature. Combined with conflicting aircraft requirements for reduced frontal area to minimize drag (e.g., a restrictive engine envelope cross section), rapid engine installation, ease of installed engine maintainability, and engine commonality with two or more different aircraft, the installation engineer must evaluate numerous design trade-offs to successfully integrate the engine with the airframe.

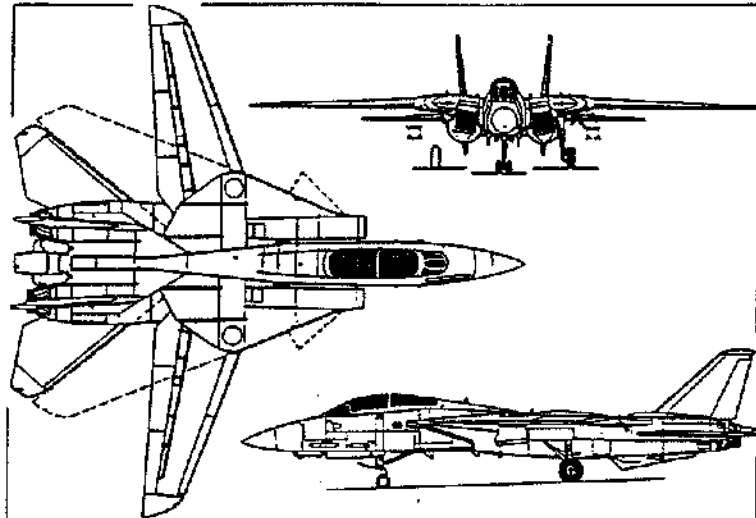
The general airframe configuration and engine arrangement for several military aircraft are illustrated in Figures 10.7 and 10.8. Obviously, the location and placement of the engines differ from aircraft to aircraft depending on mission requirements. The propulsion system can be a substantial part of the overall aircraft design in terms of percent of total aircraft volume and weight. A properly designed engine installation greatly enhances aircraft performance, mission readiness, and combat survivability.

Engine Installation Design Considerations Numerous installation design requirements must be evaluated to ensure compatibility of the engine with aircraft structure and systems. Major items which must be addressed from an engine manufacturers viewpoint include:

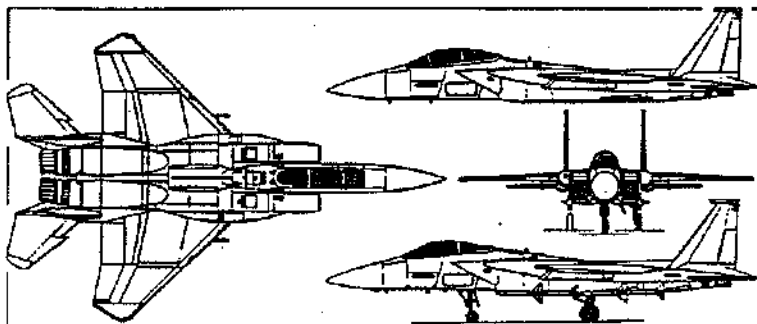
- Engine installation equipment and methods
- Engine envelope restrictions due to aircraft structure
- Installed engine accessibility and maintainability
- Engine bay environment including temperature and pressure profiles, ventilation and cooling, vibration acoustics, and drain and vent pressures due to aircraft external flow field
- Aircraft structural compatibility including mount system configuration and worst-case load limits, engine weight and center of gravity, relative clearances between the engine and airframe during flight maneuvers (due to deflection of the engine and airframe), and engine thermal expansion
- Engine-airframe interface configurations and interface load conditions
- Neutral engine configuration for installation in either left or right engine bays

Installation Considerations Affecting Engine Maintainability The military customer, like the commercial airlines, places a premium on the ease of maintenance in the field. Often engine repairs are performed on the aircraft flight-line. Engine repairs may be needed at remote and austere air bases and the aircraft may be exposed to weather extremes, so a large measure of an engine's reputation is based on how easily repairs can be performed and how infrequently they are repaired.

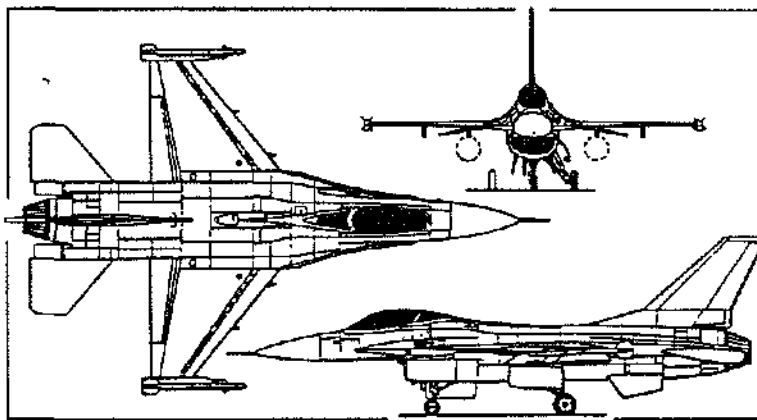
Numerous design studies are performed to locate external components for installed accessibility and repair. Service points and external components are located on the engine for easy access through aircraft doors and service panels. The F110-GE-100 engine, as shown in Figures 10.9, 10.10, and 10.11, was configured for component removal and replacement based on access doors and panel locations already existing on the F-15 and F-16 aircraft. Figures 10.14, 10.15, and 10.16 show access panel locations for the F-16C/D aircraft.



Grumman F-14A Tomcat carrier-based multi-mission fighter (Pilot Press)

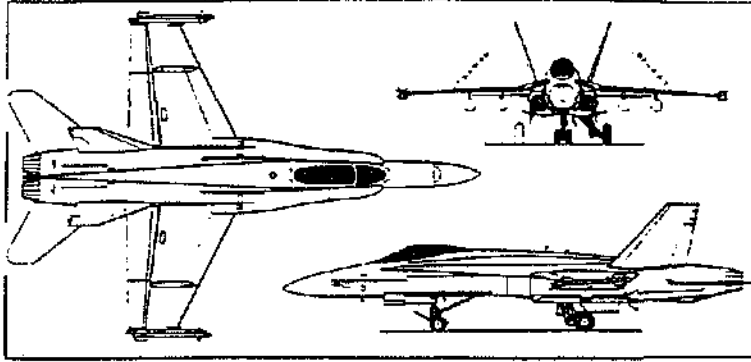


McDonnell Douglas F-15C Eagle single-seat air superiority fighter, with additional side view (top) of two-seat F-15B (Pilot Press)

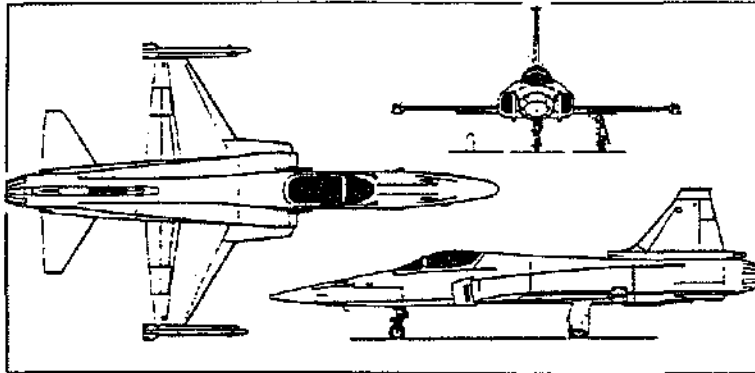


Three-view drawing of General Dynamics F-16A Fighting Falcon (Pilot Press)

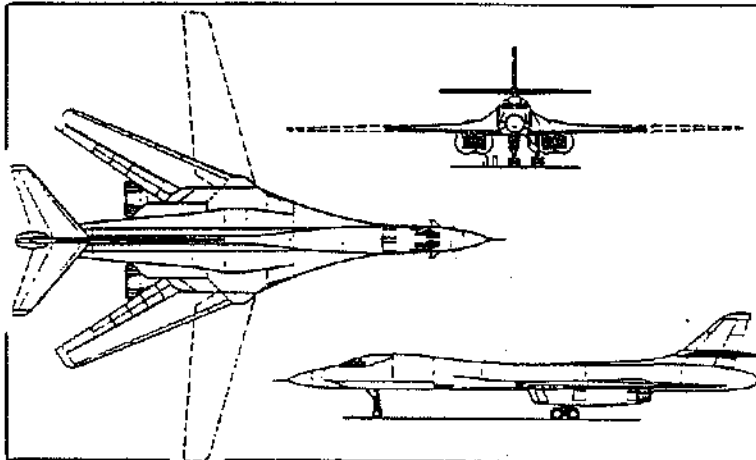
Figure 10.7 Examples of Engine-Airframe Configurations



McDonnell Douglas F/A-18A Hornet (two General Electric F404-GE-400 turbofan engines) (Pilot Press)



Northrop F-20 Tigershark export fighter (General Electric F404-GE-100 turbofan engine) (Pilot Press)



Rockwell International B-1B long-range multi-role strategic bomber (Pilot Press, provisional)

Figure 10.8 Examples of Engine-Airframe Configurations

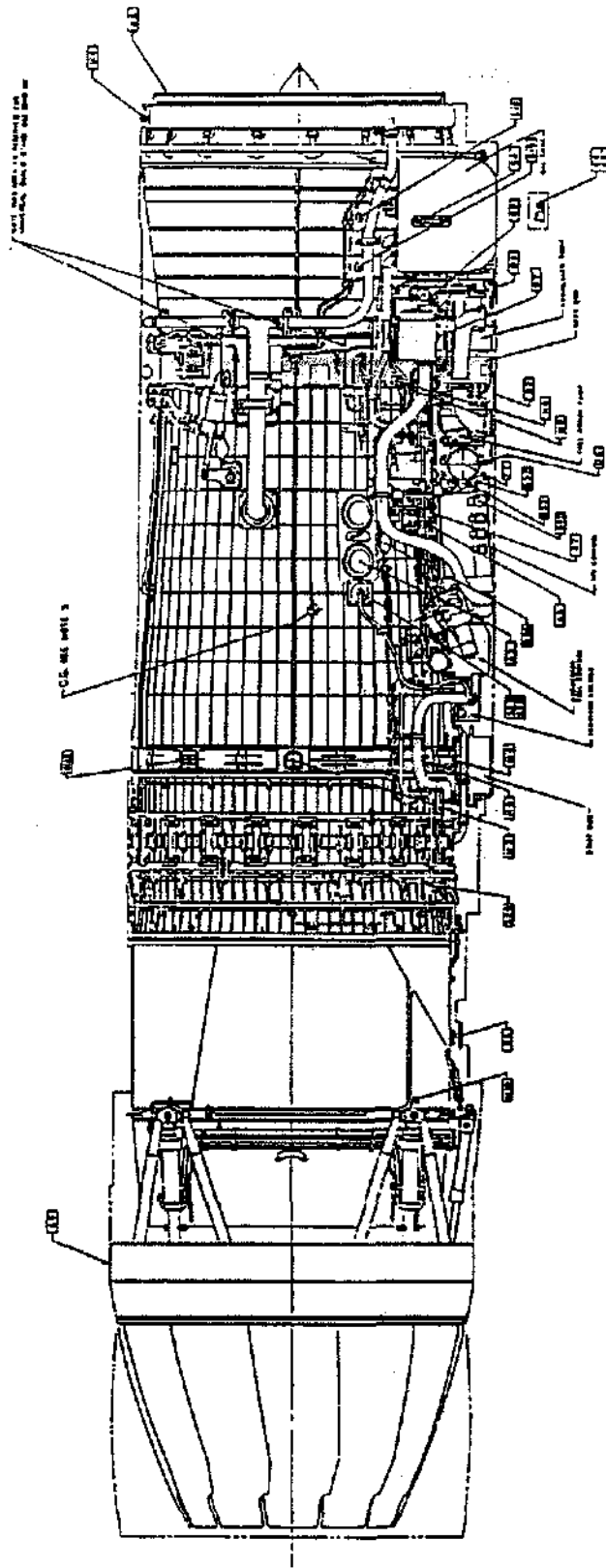


Figure 10.10 F110-GE-100 Engine Configuration and Interface Locations (Right Side View)

Engine Envelope The engine envelope is a geometric description of the three dimensional space occupied by the engine. Its description is contained as part of the engine installation drawing provided to the airframe manufacturer. The engine envelope establishes a surface boundary within which all engine hardware is contained and is used to ensure the fit and installation of the engine with the aircraft. Engine envelope dimensions describe a cold, non-operating engine (68 °F) and do not include deflections caused by flight maneuver loads, customer installation adjustment space, installation or removal clearance, or engine thermal growth (except for the nozzle which is described "hot"). The intricacy of the F110-GE-100 engine envelope description is illustrated in Figure 10.12. It is easily visualized in the three-dimensional wire frame computer graphics representation shown in Figure 10.13.

The engine envelope is established by the Installation Design group in the early phases of the design program. All external hardware when assembled to the engine (i.e., controls and accessories, tubes, clamps and brackets, and electrical cables, etc.) must remain within the envelope.

The aircraft manufacturers use the engine envelope to design the surrounding aircraft structure, locate hardware within engine bays, and perform engine installation and removal studies. Typical design practice for the airframe designer is to provide a 1.0 inch clearance between the engine envelope and internal aircraft engine bay structures to accommodate relative deflections during aircraft flight maneuvers. During engine installation or removal, however, a minimum clearance of 0.5 inches is permissible. Engine hardware penetrating the engine envelope constitutes an envelope violation. Envelope violations are corrected through either hardware rework, component redesign, or revisions to the engine envelope which must be approved by the airframe manufacturer.

Engine-Airframe Interfaces Each engine contains numerous interface points where mechanical or electrical connections are made with aircraft systems. Interface locations on the F110-GE-100 engine are shown in Figures 10.9, 10.10, and 10.11. Quick-disconnect design features are utilized wherever possible to speed engine interface hook-up with the aircraft. There are a number of key interfaces for the F110 engine.

Flight Mounts The engine flight mount arrangement used with the F-16C/D aircraft is shown in Figure 10.17 through 10.20 and comprises a forward (M1) located on the top of the front frame, two thrust mounts (M2 and M3) located on opposite sides of the turbine mount ring,

and a side mount (M4) located on the right side of the turbine mount ring roughly 70° down from the horizontal engine centerline. The F-15 aircraft will use the same flight mounts except that the top mount (M1) utilizes the fan frame upper mount clevis. The mount load combination is statically determined to isolate air frame structural loads from the engine.

Main Fuel Inlet The fuel inlet interface (F1) is a 3.0 inch inside diameter 90° elbow at the fuel boost pump inlet. A threaded sleeve and O-ring in the aircraft fuel line mate with the external threads on the engine fuel inlet coupling, as shown in Figure 10.21. A spring loaded locking on the engine fuel inlet coupling prevents the aircraft fuel line sleeve from loosening. The aircraft fuel line includes ball-swivel joints and a pressure compensating slip-joint to permit relative engine movement and to allow the fuel line to be rotated for clearance during engine installation and removal.

Power Takeoff (PTO) Flange Engine shaft power to drive aircraft accessories is transmitted from the engine accessory gearbox PTO flange (P1) through a lightweight PTO shaft to an aircraft accessory drive gearbox (ADG). The PTO shaft used in the F-16C/D aircraft is shown in Figure 10.22. Aircraft electrical generators and hydraulic pumps are mounted on the ADG. Alternately, aircraft starting power is supplied to the engine through the PTO shaft. Radial disks are located at each end of the PTO shaft to permit angular misalignment between the engine and the ADG. Maximum PTO shaft speed for the F110-GE-100 engine is 14,682 rpm and can supply up to 150 shaft horsepower to drive aircraft accessories.

Fan and Compressor Bleed Air Ports (A1, A2, A3, and A9) Engine compressor bleed air is supplied to operate the aircraft environmental control system (cabin pressurization and air conditioning) and sometimes to provide pneumatic power to other aircraft systems such as engine bay ventilation ejectors. The F110 bleed port configuration, shown in Figure 10.23 is an "E-seal" configuration. A metal seal is sandwiched between the engine and aircraft bleed duct flanges. V-band clamps secure the engine and aircraft bleed duct flanges together.

Electronic Fuel Cooling Inlet and Return Couplings (A7 and A8) Engine electronic components are normally cooled by fuel circulated in a separate close-loop series circuit. Fuel for engine electronic component cooling is supplied by teeing into the main fuel feed lines upstream of the engine fuel inlet interface. Depending on the engine application, the warm fuel can be returned either directly to the engine fuel tanks or consumed by the engine. The F110-GE-100 engine uses special push/pull quick disconnect couplings at the electronic fuel cooling

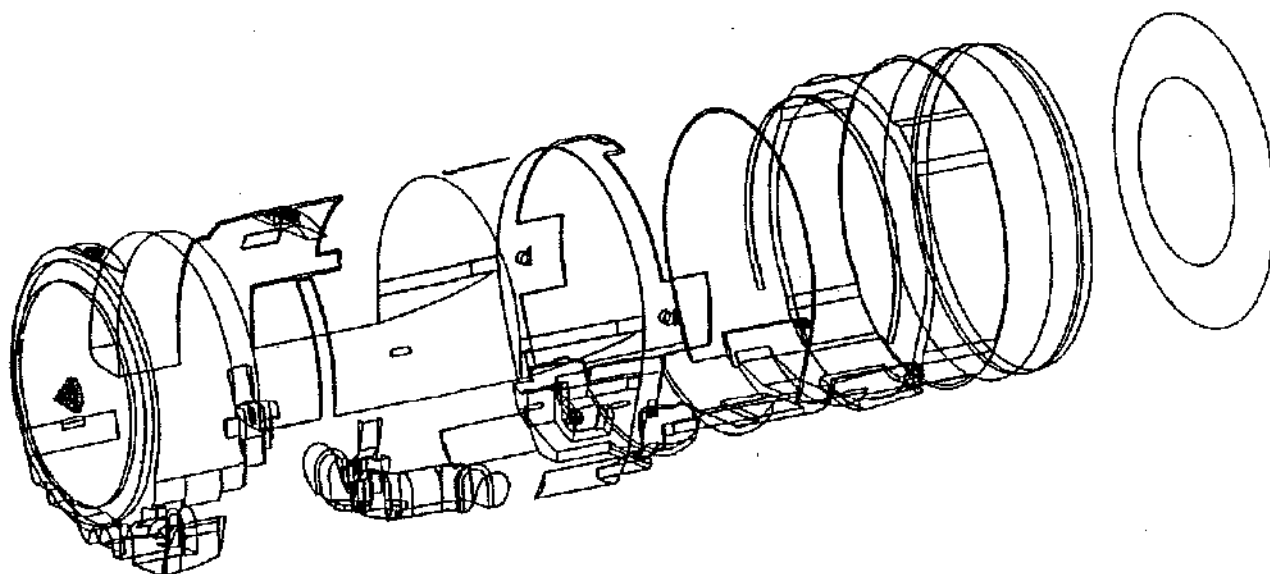


Figure 10.13 F110-100 Engine Envelope (Left Side Three Dimensional Representation)

circuit inlet and discharge interfaces, as shown in Figure 10.21. The fittings are "Murphyproofed" by using a female fitting at the inlet coupling and a male fitting at the discharge coupling. The couplings are self-sealing to prevent fuel seepage when disconnected.

Electrical Interface Connectors (E1 and E2) Threaded electrical connectors are utilized at the engine-airframe electrical interfaces, which may be located on the engine electronic control or conveniently relocated to a more accessible location using a wiring harness. When specified, MIL-STD-38999 Series III quick disconnect connectors are used, which have a coarse thread and fully engage in one turn or less.

Exhaust Nozzle Shroud (A4) The exhaust nozzle shroud provides smooth aerodynamic transition between the aft fuselage moldline and the exhaust nozzle outer flap contour, while accommodating engine or airframe deflections and engine thermal growth. The nozzle interface between the engine and airframe is a series of cantilevered metal flaps or "Eagle feathers," as depicted in Figure 10.24, which are secured against the exhaust nozzle shroud by a circumferential strap. Spacers between the metal flaps and the nozzle shroud provide a small gap (0.25 inches) through which the engine bay ventilation air exits.

Power Lever Shaft and Throttle Linkage (A5) The engine power setting (thrust level) is controlled by varying the angular position of the power lever shaft on the main engine control (MEC). The power lever shaft is mechanically connected to the cockpit throttle quadrant through a push/pull cable and rack and pinion rotary actuator. A spring-loaded torque shaft connects the aircraft rotary actuator with the splined power lever shaft. The F16C throttle quadrant and engine bay throttle shaft are shown in Figure 10.25. The cockpit throttle quadrant is calibrated by "rigging" the power lever shaft at the "intermediate" power setting position and adjusting the throttle cable linkage.

Fluid Drains and Vents (D1, D2, and D3) Lubricating oil that leaks past bearing cavity seals and fuel leakage from various components is collected at fluid drain masts located along the bottom of the engine. These fluids are normally dumped overboard through penetrations in the aircraft skin or stored in aircraft accumulator tanks. Also, sometimes bearing seal pressurization air is vented overboard through the engine main drain masts. In the aircraft engine bay a drain bellows seats against the engine drain mast to collect the fluids (Figure 10.26).

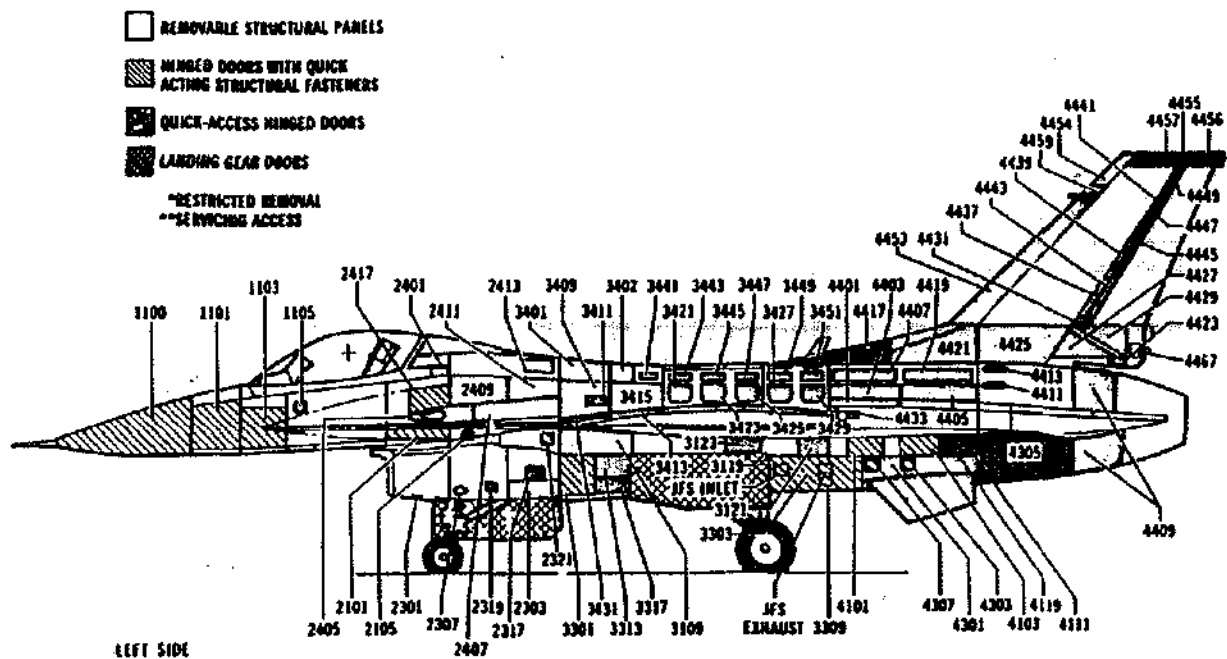


Figure 10.14 F-16C/D Access Doors and Panels (Left Side)

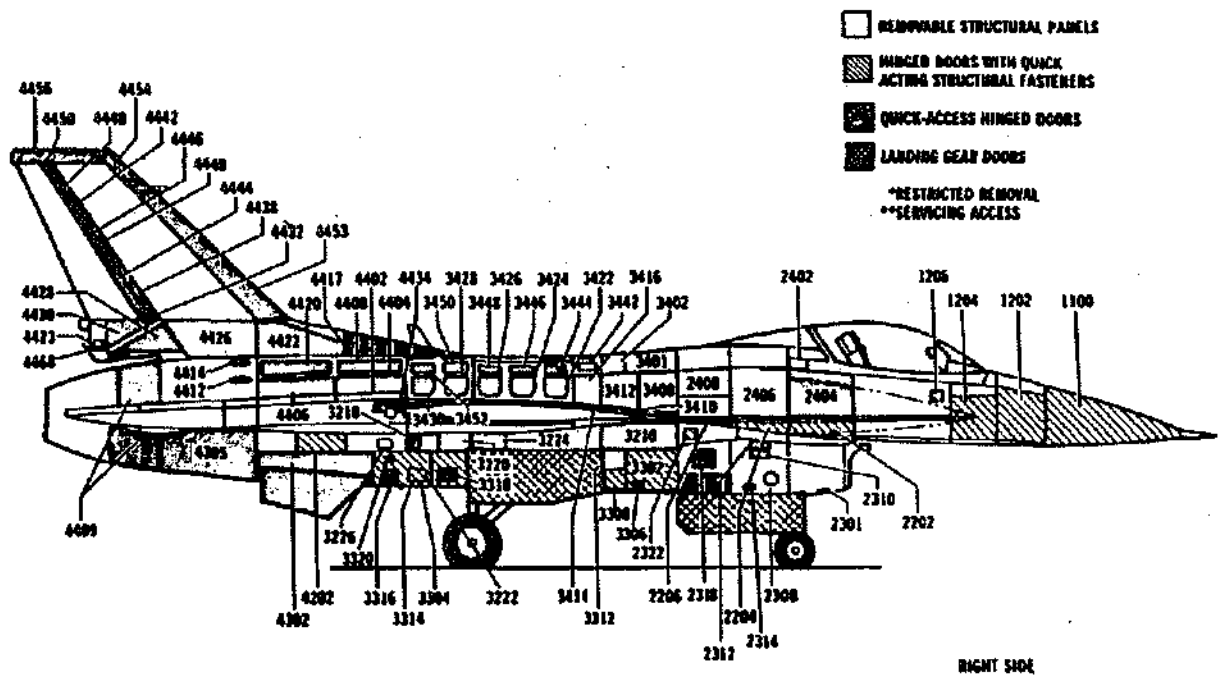


Figure 10.15 F-16C/D Access Doors and Panels (Right Side)

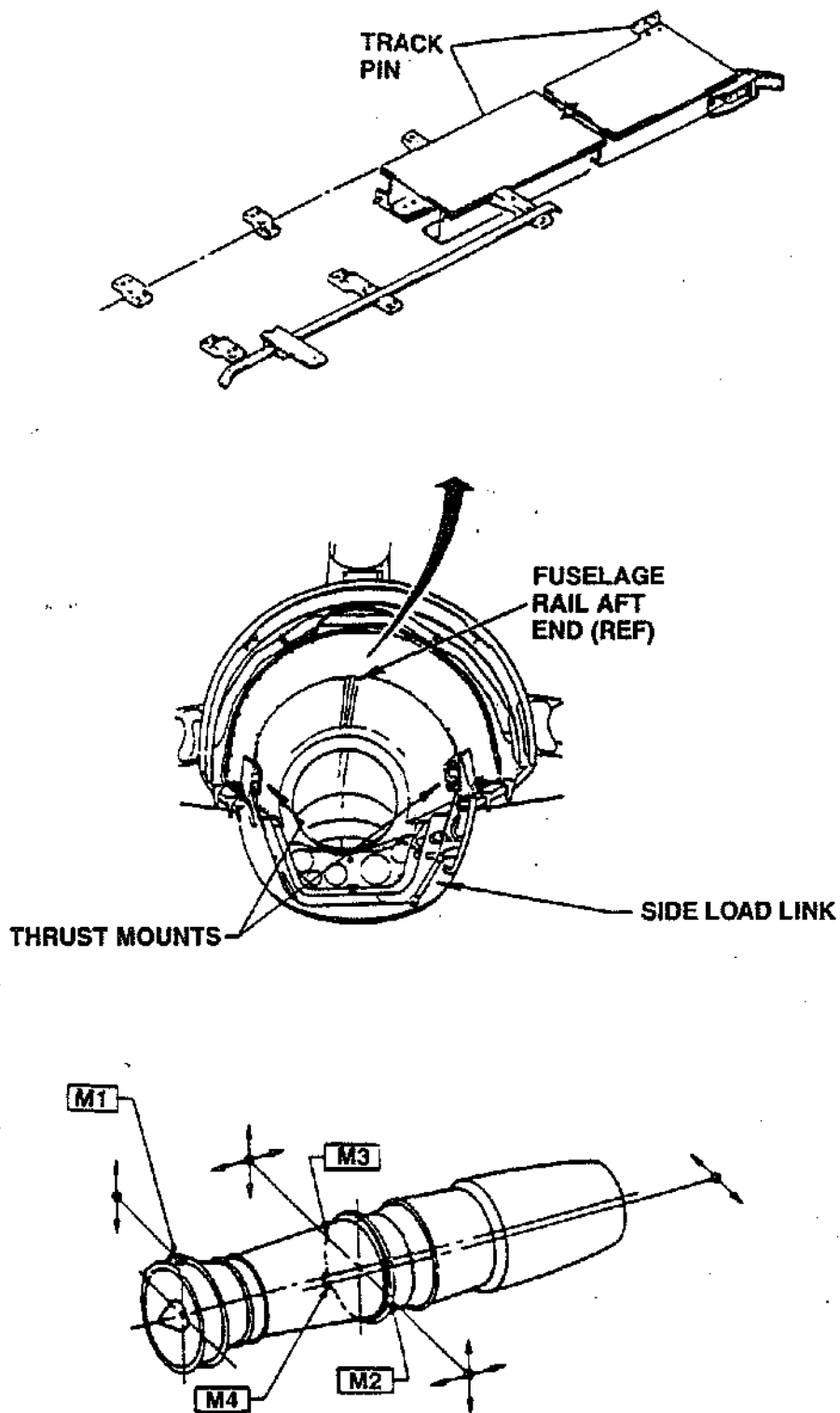


Figure 10.17 F110-GE-100 Engine Mount System Arrangement for the F-16C/D Aircraft

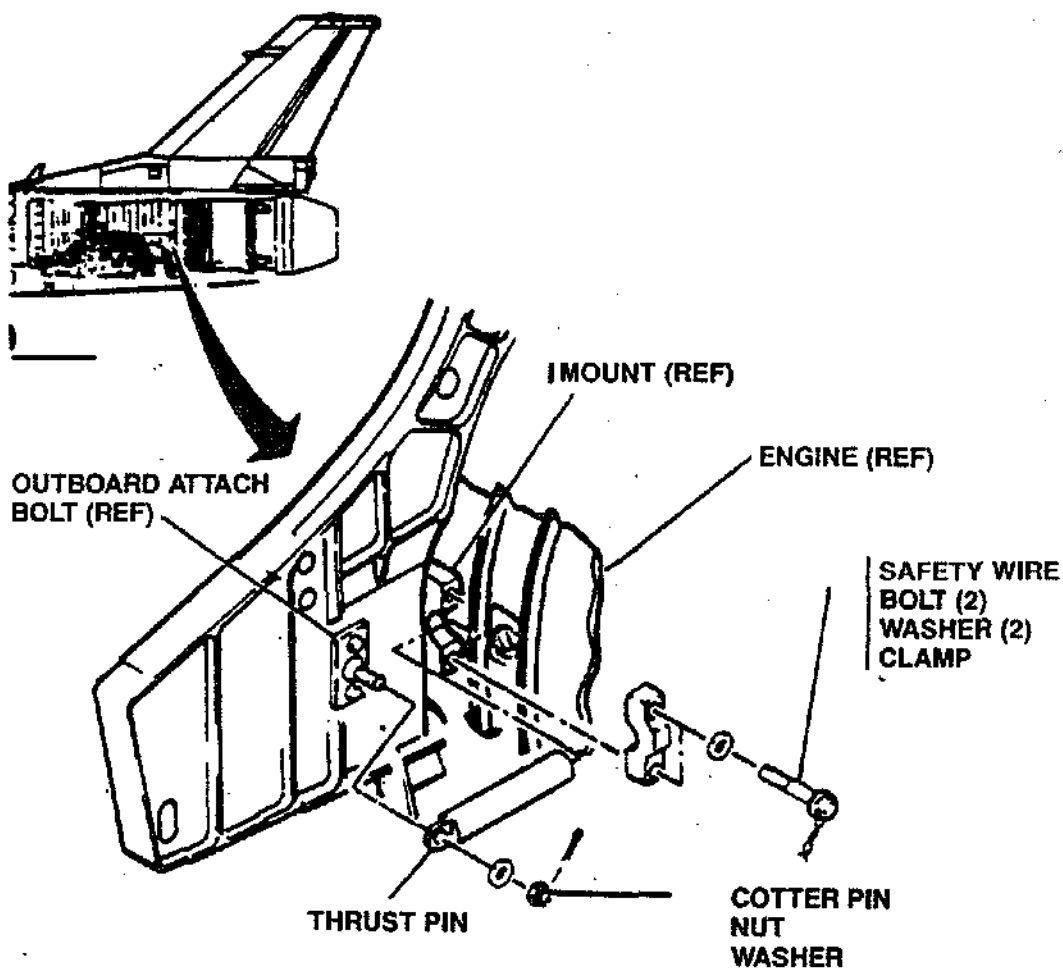


Figure 10.18 F-16/F110-GE-100 Thrust Mounts

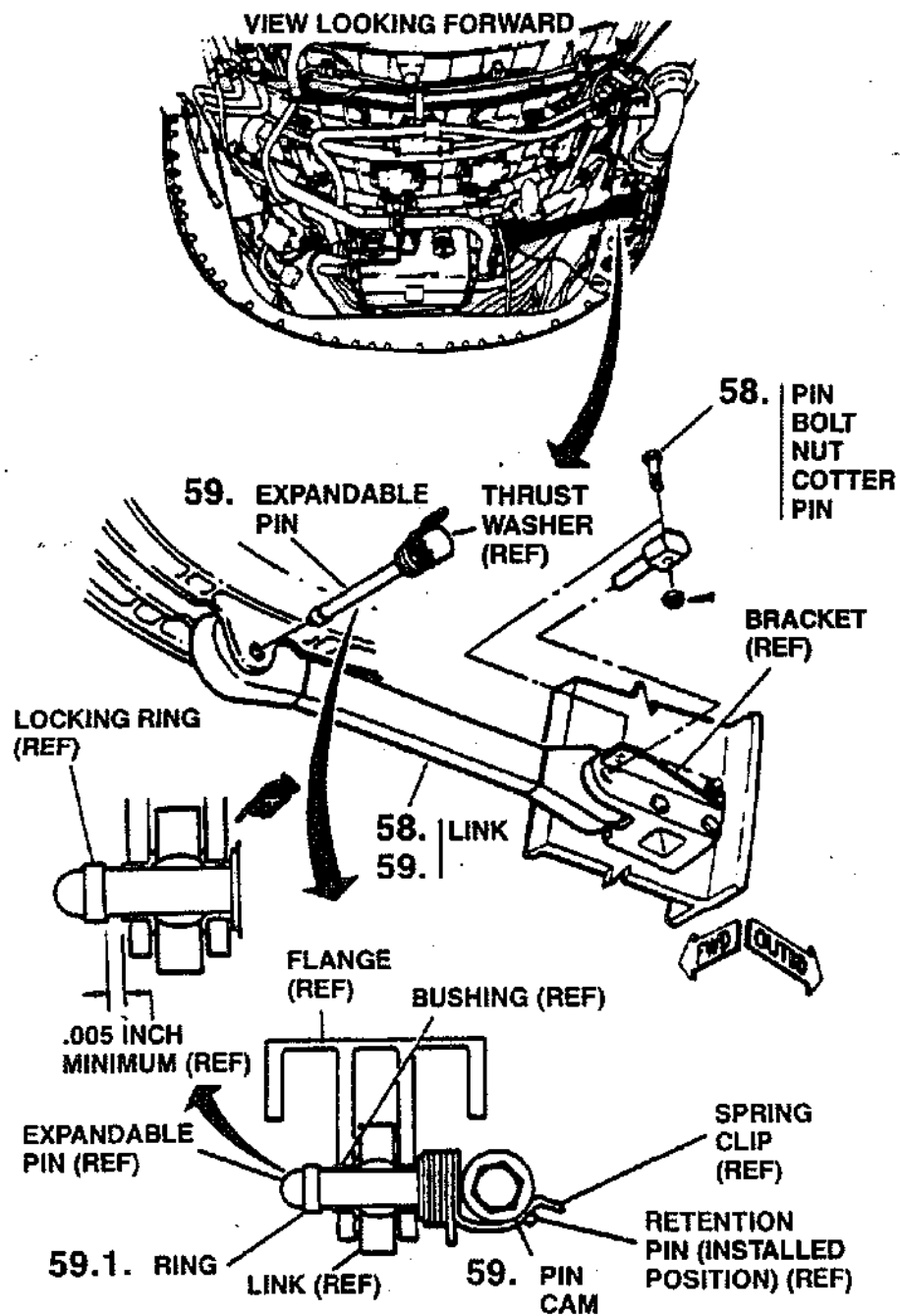


Figure 10.19 F-16/F110-GE-100 Side Load Link

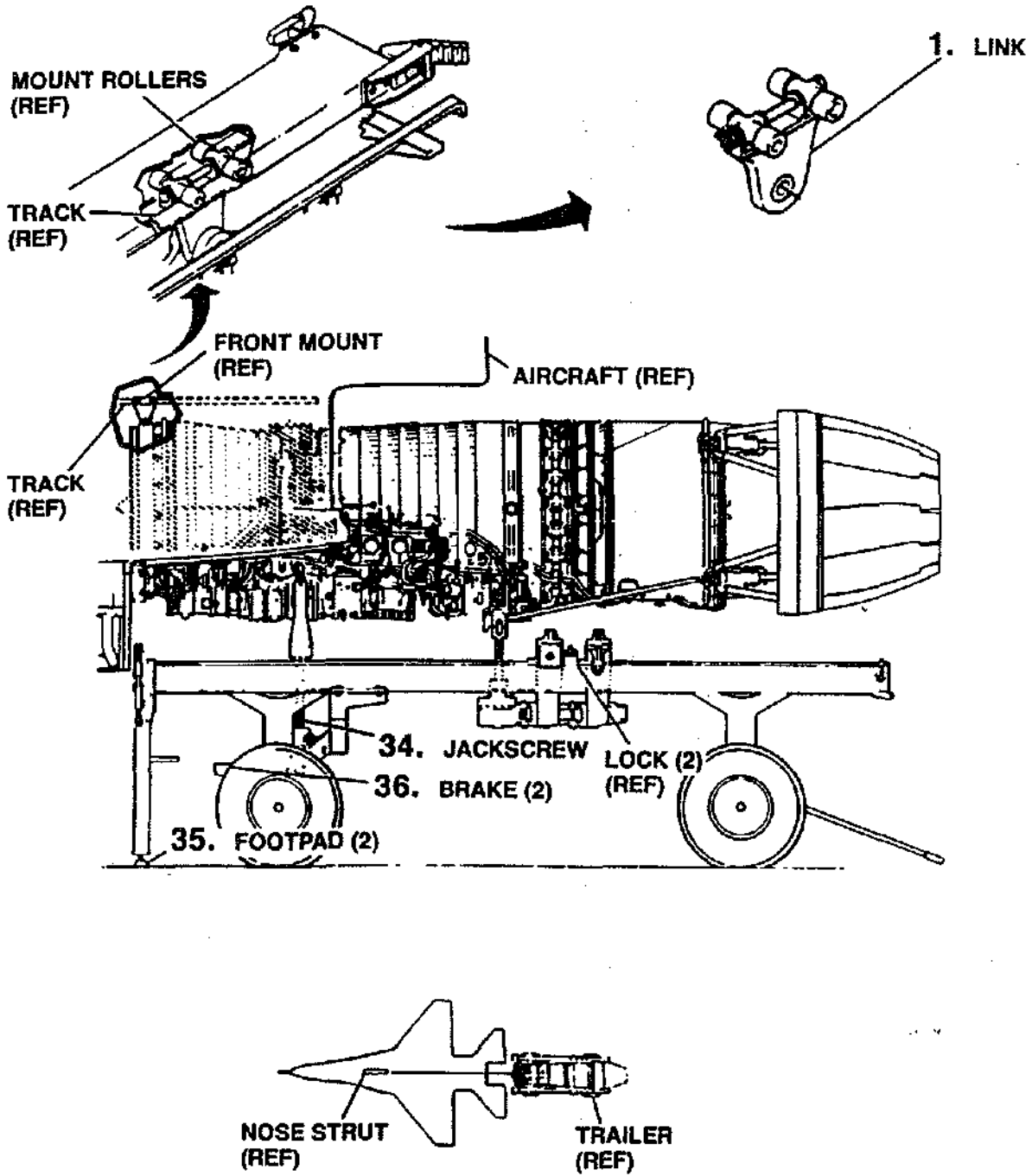


Figure 10.20 F-16/F110-GE-100 Front Mount

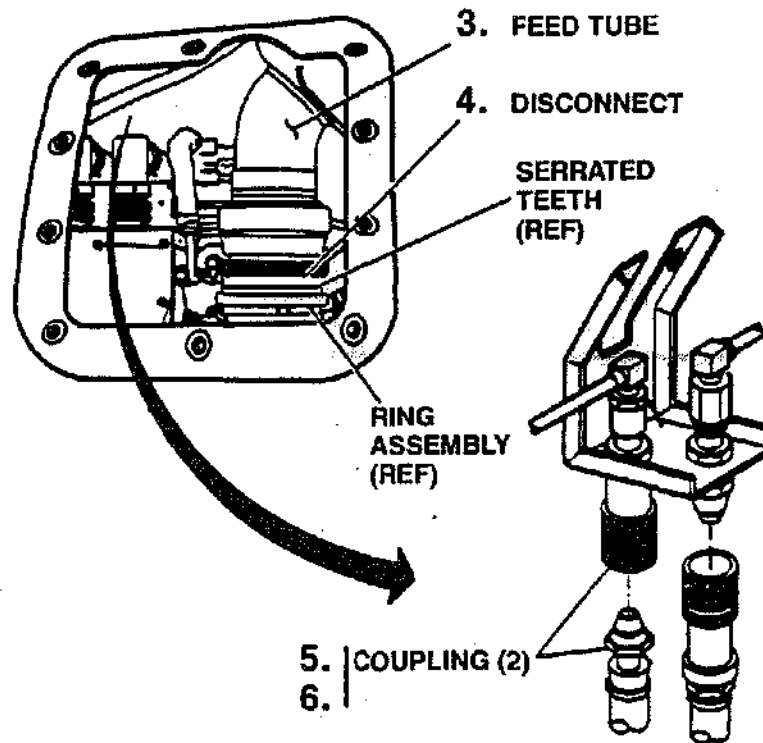


Figure 10.21 F110-GE-100 Fuel Inlet and Electronic Fuel Cooling Interface Couplings

CONFIGURATION

Design Philosophy As with other design areas, the design philosophy for configuration design is to produce hardware that is low cost, light weight, manufacturable, and highly reliable. With the advent of the F110-100 engine in the F-16 fighter single engine safety concerns have brought to engine piping the proper technical recognition.

Other considerations such as meeting engine-aircraft envelope, meeting the technical design requirements, and having the capability of operating in an unfriendly engine environment play a significant role in the design of configuration hardware.

Since the early 1970's when the F101/B-1 program was initiated, significant work has been done to investigate the use of more exotic materials such as titanium and Inconel 625 for configuration hardware due to weight and material strength considerations. At present, GEAE military engines utilize titanium for approximately 60% of configuration tubes and 321 stainless steel and inconel

625 for the remainder. All brackets and supports are inconel 625. GE commercial engines, namely the CF6-80 family, utilize 321 stainless steel and inconel 625 for tubing and inconel 625 for brackets and supports. Unique cast aluminum clamps and "broom handle" spring clips have been developed for tubing and electrical cable supports respectively.

Configuration hardware receives rigorous design analysis, design reviews and engine/component testing to assure it is capable of meeting the design requirements with adequate safety margins.

Design Approach The approach to configuration hardware design is a series of steps with checks along the way which when followed rigorously will lead to a design that will satisfactorily meet all requirements.

To initiate a configuration design project, the first pieces of information to obtain are the engine description, key dimension drawing, and engine installation envelope. These pieces of information set the space boundaries available for packaging the engine accessory gearbox,

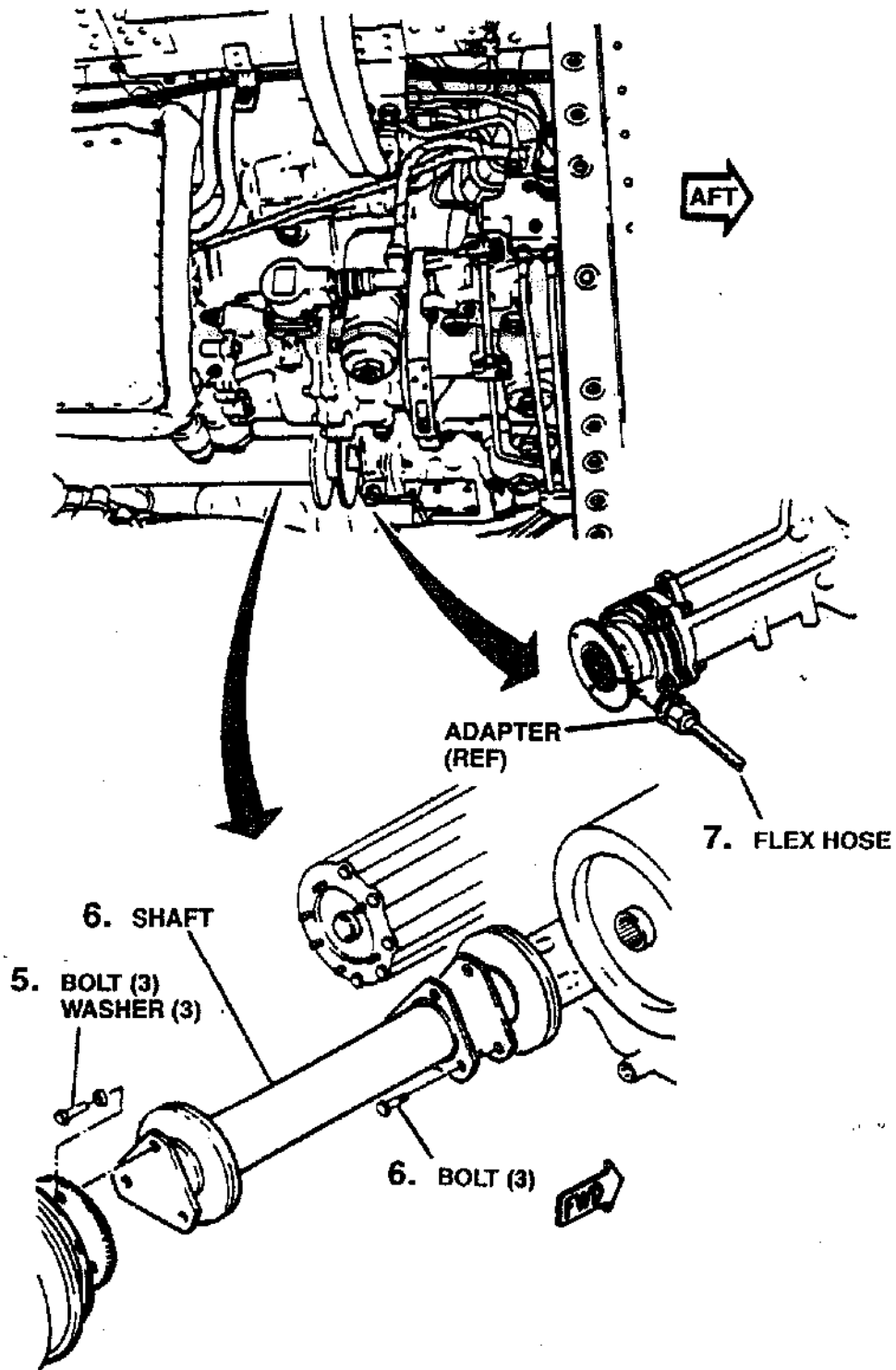


Figure 10.22 Power Takeoff (PTO) Shaft for the F-16C/D

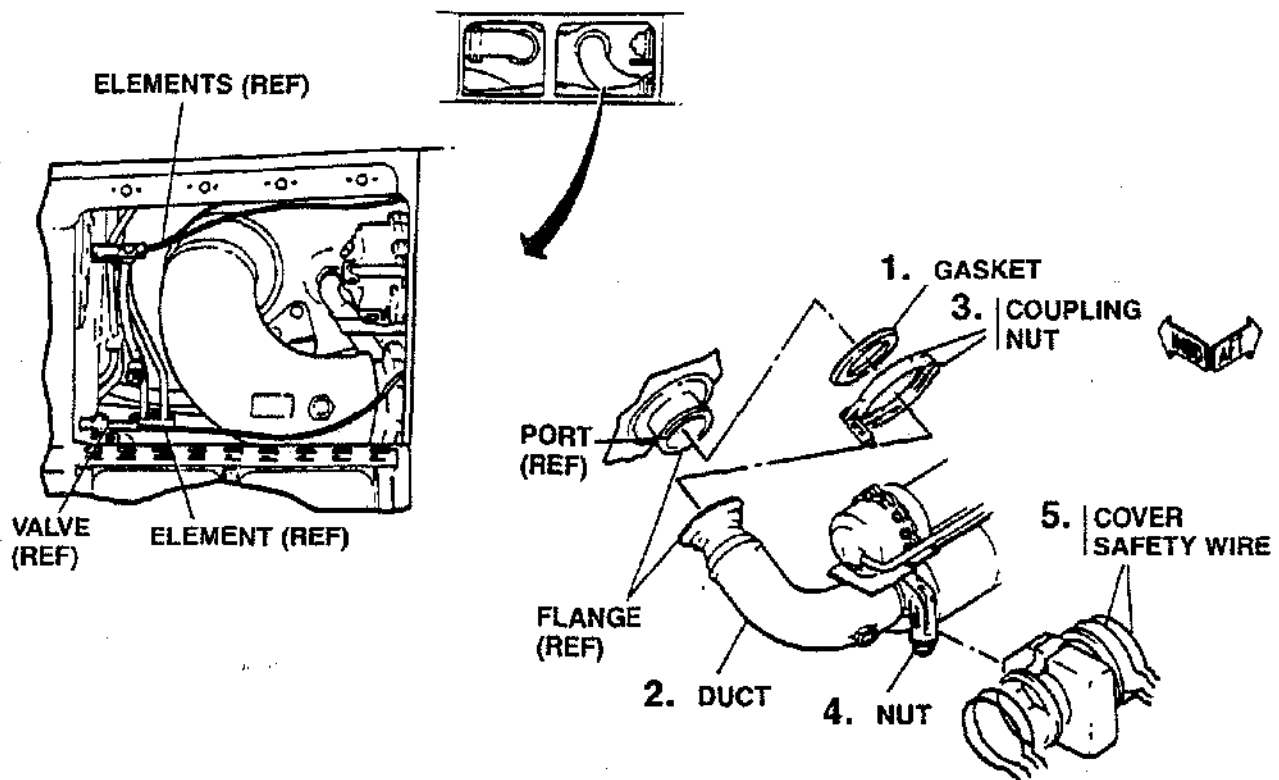


Figure 10.23 F-16/F110-GE-100 Compressor Bleed Air Supply Ports

controls and accessory components and configuration hardware. Then the engine technical requirements data must be obtained to provide information on the engine operating conditions such as pressures, temperatures, vibration and hardware life requirements. The next piece of design information required is the systems schematics which are provided by various engine systems groups and controls and accessories systems.

Now comes the planning for the configuration design work. A well thought out plan of attack is the real foundation for developing a good configuration design. An engine rollout drawing (Figure 10.27) is a very useful tool for this phase of design. The engine is un-rolled, if you will, into a flat pattern view. Then controls and accessory components are placed and packaged to obtain the most efficient piping routing. Attachment ports are located on the components and the engine frames at this time. The key objective is to obtain the most orderly piping routing. Once again, this is where good preliminary planning will produce good results.

The rollout is converted into conceptual hardware using an engine mockup as an engineering tool. An effective

visualization of the overall conceptual configuration is then obtained (Figure 10.28).

The next phase of configuration design is to have Drafting produce the piping layouts and detail drawings. Utilizing the rollout, the engineering mockup, design practices, technical requirements and giving thought to vibration characteristics and thermal stresses, the configuration design engineer can aptly direct the drafting designers to produce a successful piping design (Figures 10.29 through 10.31).

During the layout phase, it is necessary to do a thorough job of analysis to determine the vibration and thermal stresses in the piping. Utilizing the Goodman diagrams (Figure 10.32) for the various materials, safety factors and life capability of the hardware is determined.

The next important step is to have a thorough design review conducted by experienced engineering experts, namely members of the Configuration Design Board. This assures input for "lessons learned", standardization, and "good design practice" are obtained and responses documented.

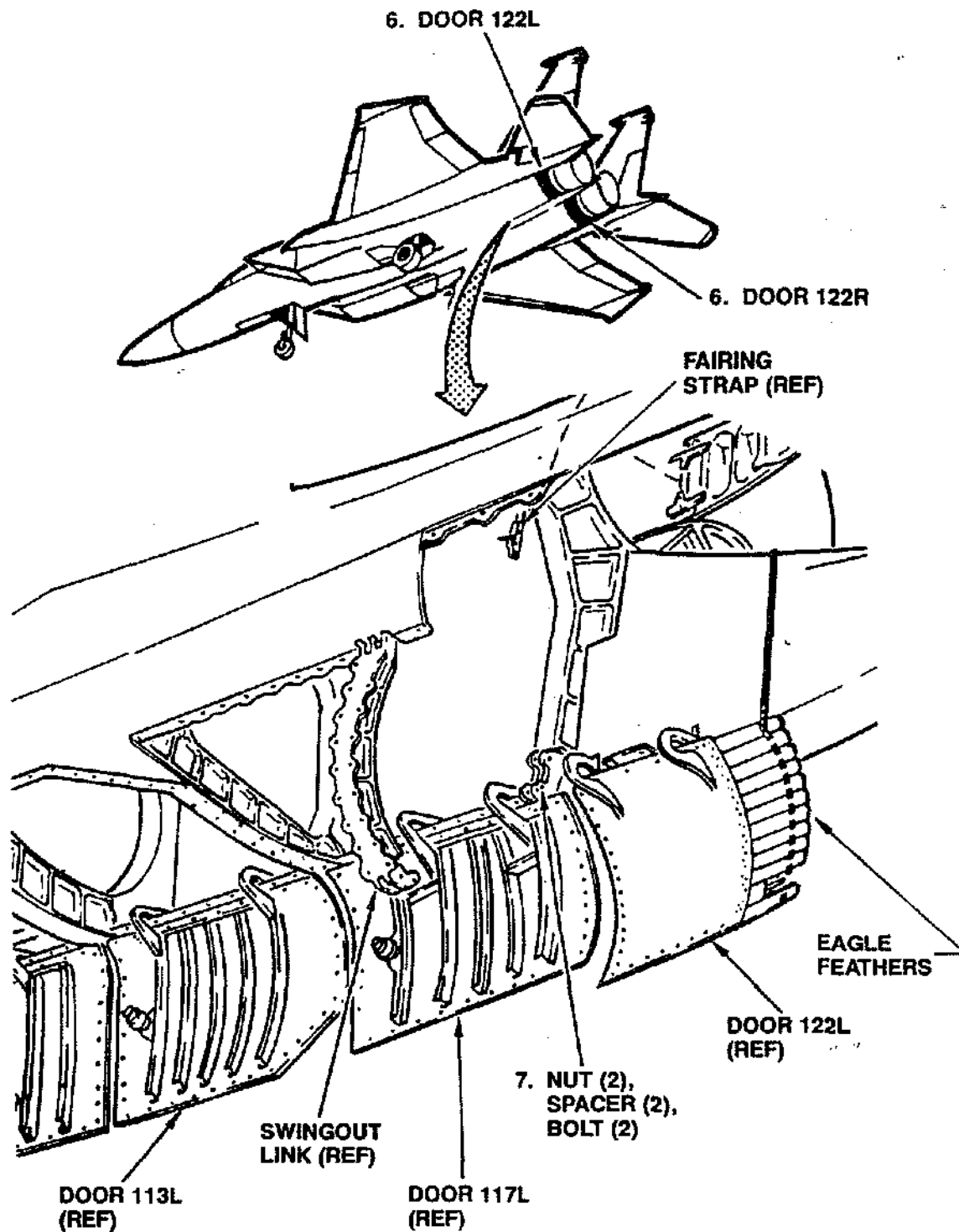


Figure 10.24 F-15C/D Engine Bay Access Doors and Exhaust Nozzle Shroud, "Eagle Feathers"

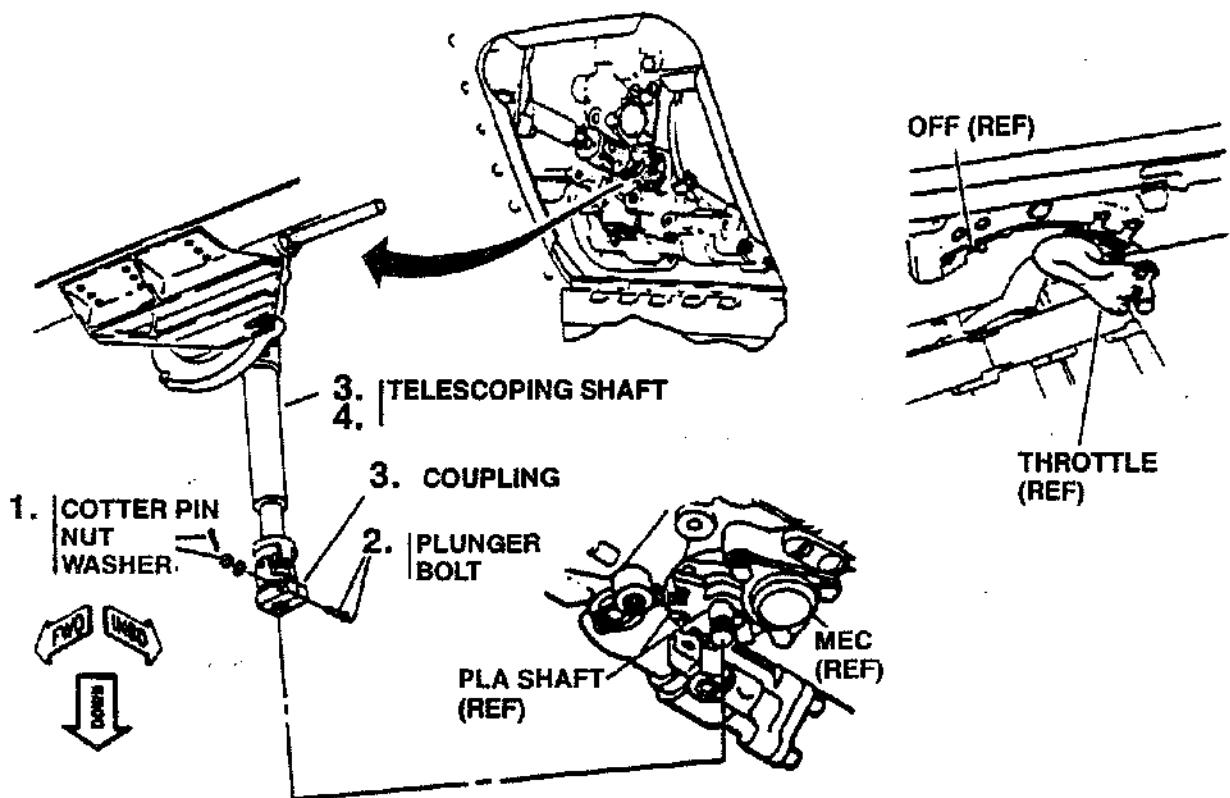


Figure 10.25 F-16C/D Cockpit Throttle Quadrant and Engine Bay Throttle Shaft

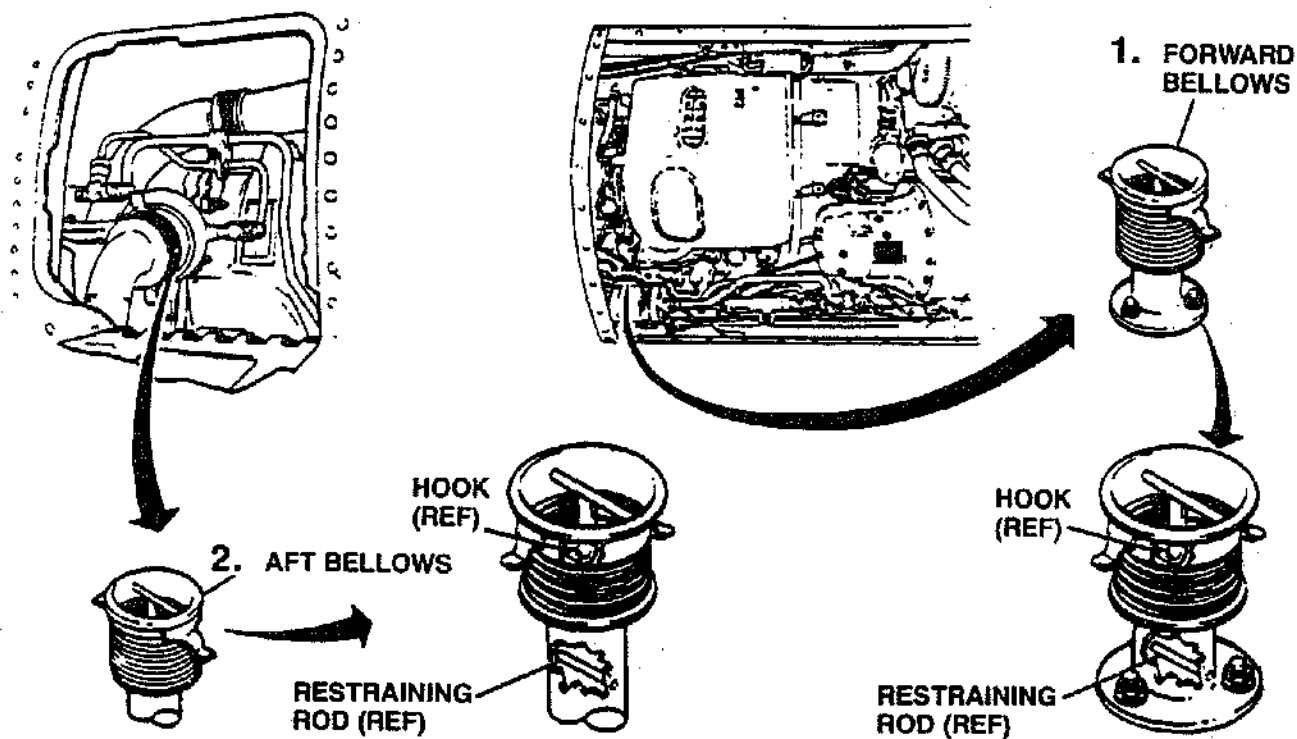


Figure 10.26 F-16C/D Engine Overboard Fluid Drains

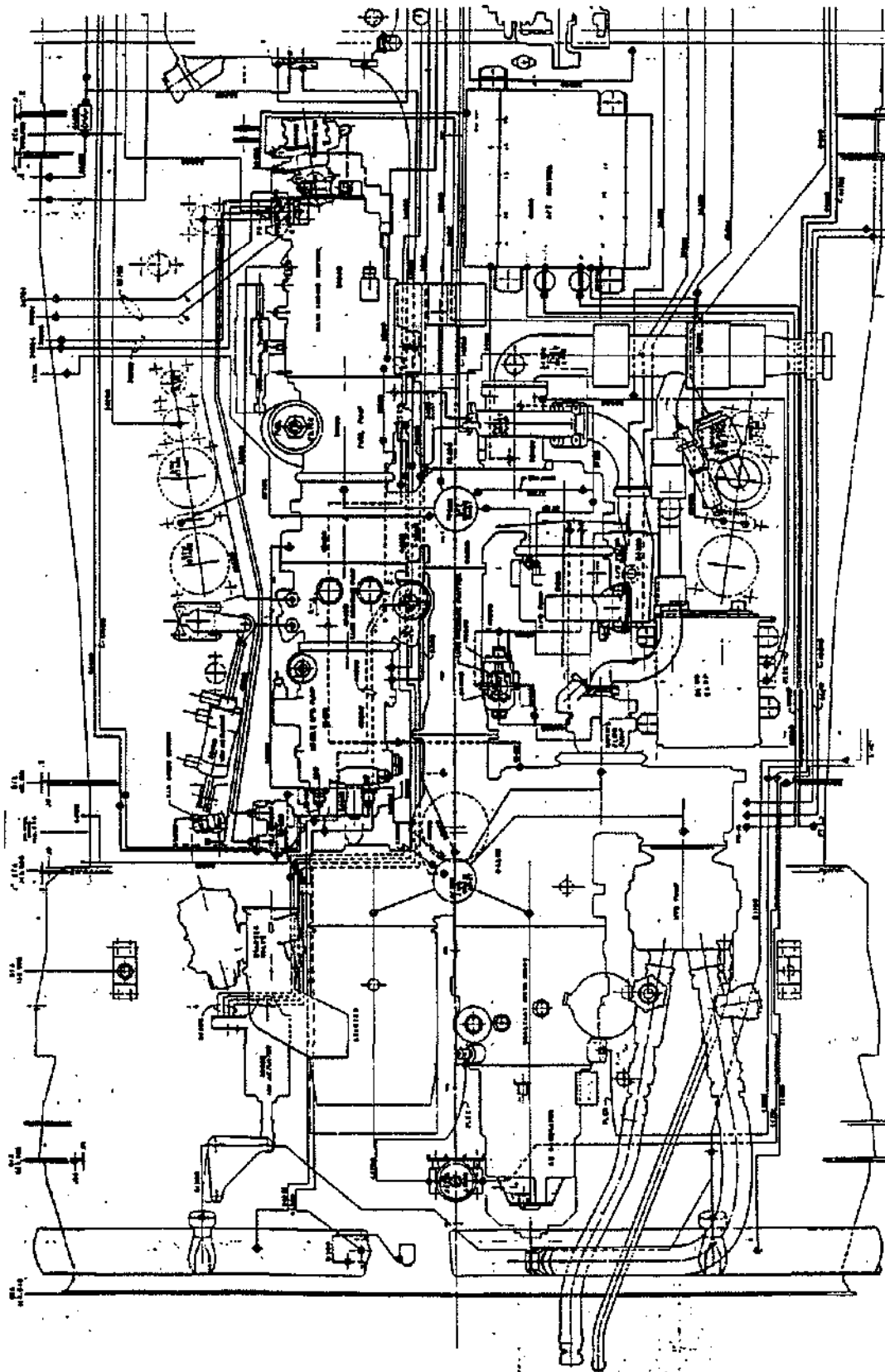
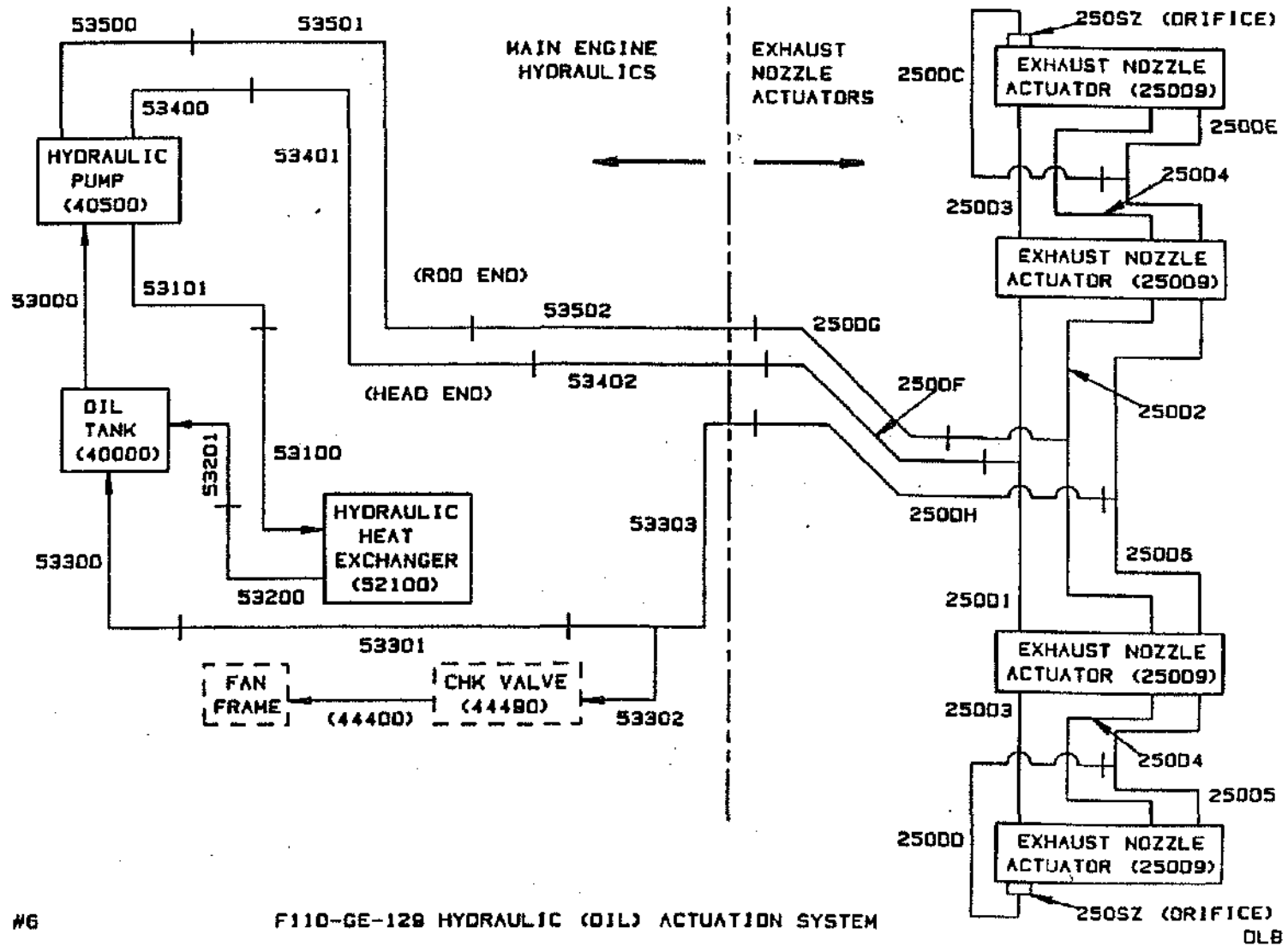


Figure 10.27 F110-400 Rollout Drawing

- 53000
- 53100
- 53101
- 53200
- 53201
- 53300
- 53301
- 53302
- 53303
- 53400
- 53401
- 53402
- 53500
- 53501
- 53502
- 25001
- 25002
- 25003
- 25004
- 25005
- 25006
- 2500C
- 2500D
- 2500E
- 2500F
- 2500G
- 2500H
- 25009
- 250SZ



SKETCH #6

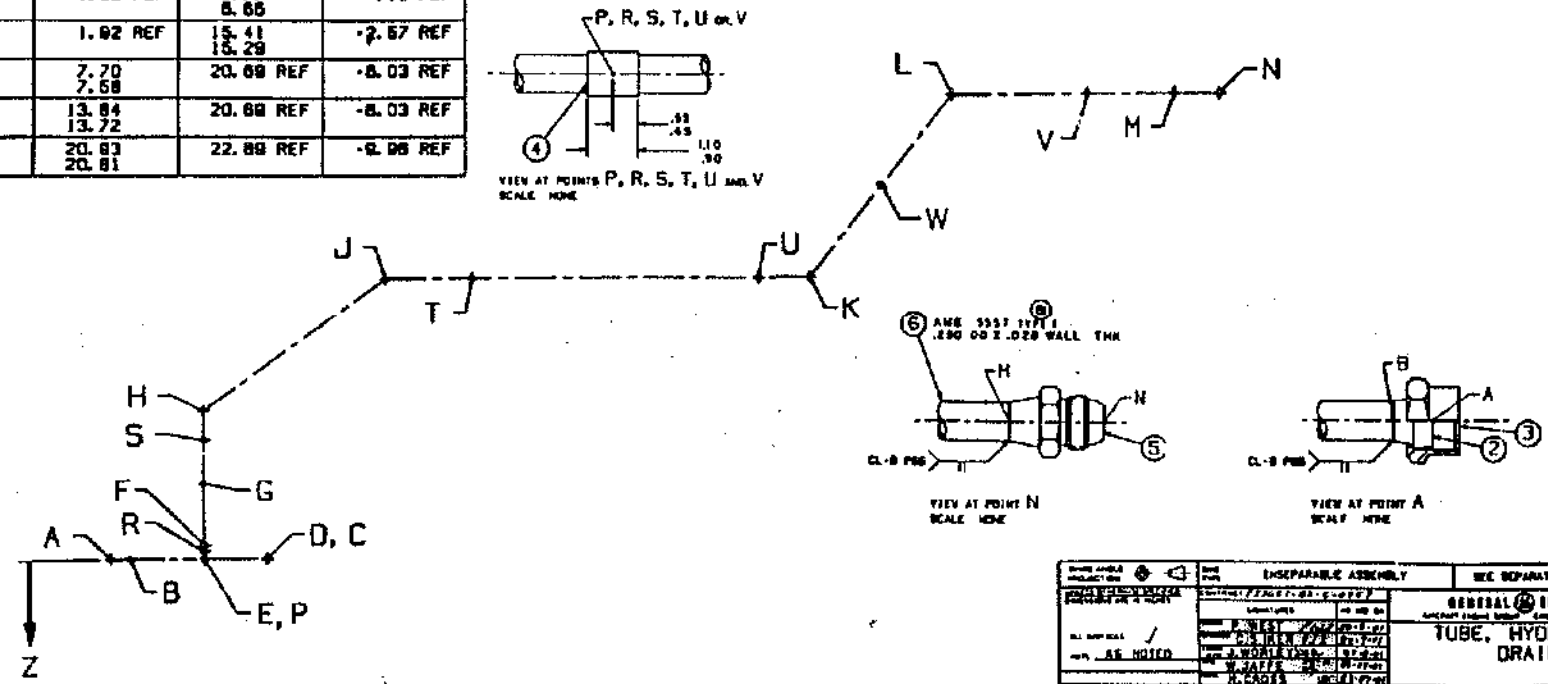
F110-GE-129 HYDRAULIC (OIL) ACTUATION SYSTEM

DLB

Figure 10.28 Configuration Schematic

COORDINATES - INTERSECTING - END POINTS			
POINT	X	Y	Z
A	.00 BSC	.00 BSC	.00 BSC
C	3.27 BSC	.00 BSC	.00 BSC
D	3.27 BSC	2.63 BSC	.00 BSC
E	1.92 BSC	4.16 BSC	.00 BSC
F	1.92 BSC	6.74 BSC	-.28 BSC
G	1.92 BSC	13.64 BSC	-1.62 BSC
H	1.92 BSC	18.66 BSC	-3.20 BSC
J	5.78 BSC	20.69 BSC	-8.03 BSC
K	14.88 BSC	20.69 BSC	-8.03 BSC
L	17.94 BSC	22.89 BSC	-8.98 BSC
N	23.89 23.78	22.89 22.83	-10.02 -9.90
P	1.92 REF	.00 REF	.00 REF
R	1.92 REF	8.77 8.65	-.18 REF
S	1.92 REF	15.41 15.28	-2.57 REF
T	7.70 7.58	20.69 REF	-8.03 REF
U	13.84 13.72	20.69 REF	-8.03 REF
V	20.83 20.81	22.89 REF	-9.98 REF

REF EDP NO. F101-227 F101-231 BEND DATA							
STR LG REF	TURNABLE			BEND			
	BETWEEN PLANES	ANGLE REF DEG MIN	AT PT	ANGLE REF DEG MIN	RADII BSC	ARC LG REF	
2.37	-----	-----	C	90 0	.50	.78	
1.91	B, C, D- C, D, E	0 0	D	40 58	.50	.38	
1.86	C, D, E- D, E, F	188 28	E	41 8	.50	.38	
4.33	D, E, F- E, F, G	88 62	F	12 0	.50	.10	
4.87	E, F, G- F, G, H	0 1	G	12 0	.50	.10	
3.17	F, G, H- G, H, J	278 42	H	38 12	.50	.33	
5.97	G, H, J- H, J, K	348 67	J	52 18	.50	.46	
8.67	H, J, K- J, K, L	183 38	K	58 48	.50	.48	
4.92	J, K, L- K, L, M	180 0	L	58 44	.50	.48	
4.68	-----	-----	--	-----	-----	-----	-----
RUN OF TUBE B THRU M				DEVELOPED LENGTH		45.93 REF	



GENERAL ELECTRIC		GENERAL ELECTRIC	
TUBE, HYDRAULIC DRAIN		TUBE, HYDRAULIC DRAIN	
E 07482		9398H36	
2 X F110-6E-100		1 93303	

Figure 10.29 Simplified Tube Drawing

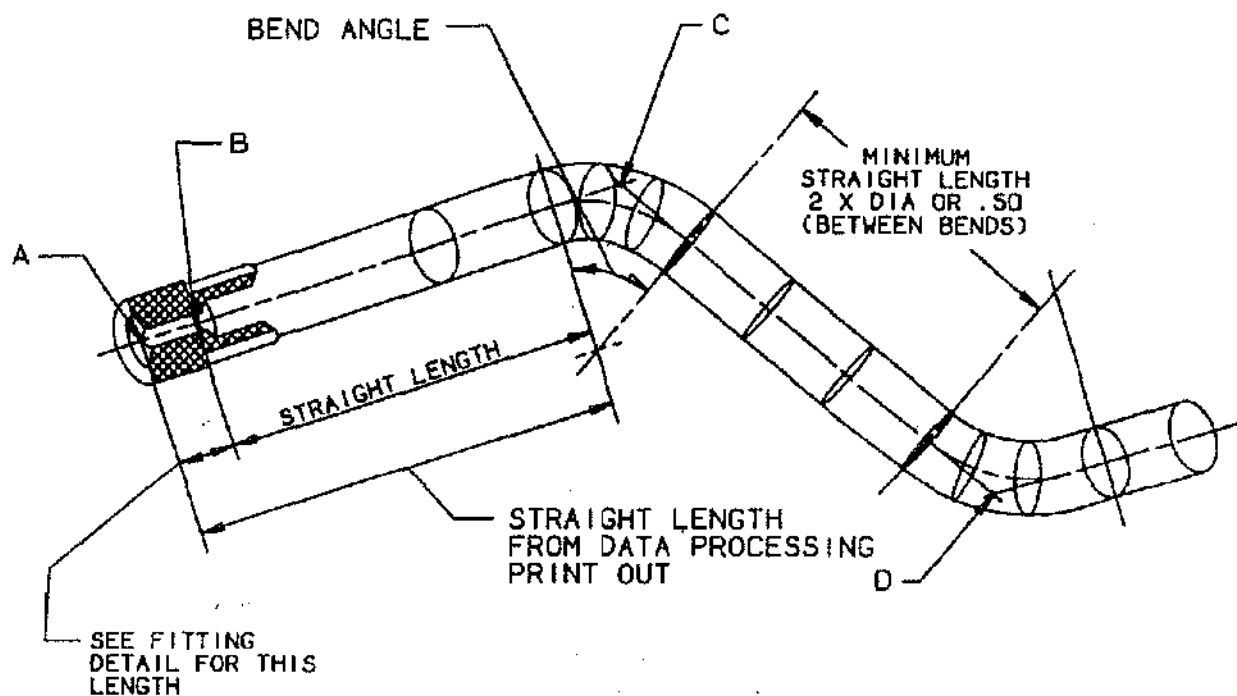


Figure 10.30 Tube Terminology Definitions

The engine mockup once again is an important engineering tool to obtain a trial fit and an overall review of the engine configuration prior to release of hardware for manufacturing. Component vibration tests are conducted on certain critical design hardware to provide assurance the designs can withstand the worst engine environment. By following these design steps and checks, the configuration design will operate successfully during all phases of engine operation.

Technical Requirements Overall configuration requirements are established by reviewing the engine model specification, the engine contract, and the engine technical requirements manual. Applicable installation and configuration requirements are then summarized along with system schematics (fuel, lubrication, hydraulic, and pneumatics systems) and recorded in the appropriate design record books (DRB). Other requirements are based on engine system operating requirements such as temperature, pressure, critical frequency ranges and useful life.

A complex array of configuration tubes, hoses and ducts are used to convey engine operating fluids from tanks or reservoirs to pumps through filters, sensors, and control systems to engine locations where they will be used or

consumed. Engine tubing and all connectors must be prime reliable where fluid leaks could result in engine bay fires or loss of engines. Flammable fluid lines are located or shielded to prevent leakage from contacting hot engine surfaces. Tubing needs to be located for easy access and maintenance to insure proper assembly. All fasteners and couplings are torqued with necessary seals in place. Tubing is analyzed for vibratory stress between supports, stress due to tube-to-engine differential thermal growth and built-in assembly stresses due to deflection at bracket and clamp locations, and misalignment plus hoop stress due to internal pressure. Finally, tubing is designed for minimum weight, number of parts, and life cycle cost.

Design Practices The external configuration design practices are based on extensive operating experience. They give guidelines and recommendations for tubes, hoses, ducts, brackets, clamps, and other hardware in terms of material section, manufacturing processes, fitting types, design operating conditions, analysis methods, and test or substantiation. Many other important applicable design practices and specifications are listed in the manuals and cover items such as general mechanical design, interpretation of drawings, standard torque valves, welded joints, stress concentrations, engine

THE TURNABLE ANGLE IS MEASURED WHEN LOOKING IN THE DIRECTION OF THE ARROW TOWARD THE PREVIOUS BEND OR ANGLE AND IS MEASURED CCW FROM THE PLANE FORMED BY THE PREVIOUS BEND ANGLE (X,Y PLANE)

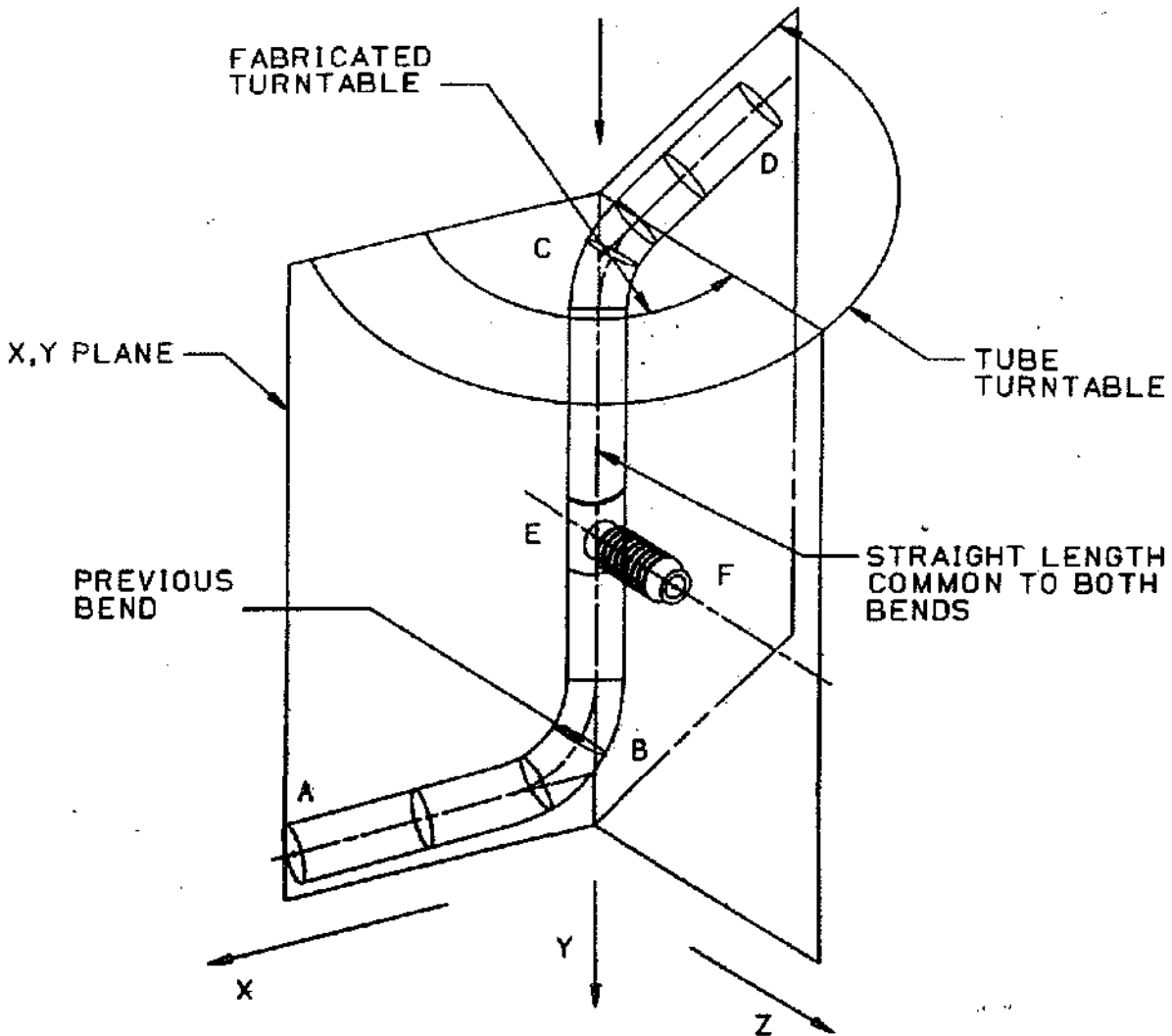


Figure 10.31 Turntable Angle Definitions

installation and fire protection, formed tubing, and sheet metal. These subjects and many others are covered in the "BLUE" AEBG Engineering Standards books. They are written to control or guide design, manufacture, development, and qualification of high quality and reliable external configuration hardware.

Design Reviews Installation and configuration preliminary design reviews are conducted periodically within the design organization using overall experience to assist and assure uniformity of interpretation and application of design practices. A design board meets periodically to review the installation and configuration design prac-

GENERAL ELECTRIC
 AIRCRAFT ENGINE BUSINESS GROUP
 CINCINNATI, OHIO / LYNN, MASSACHUSETTS

SECTION E-7-m DRAWING 1-7.1a

MATERIAL PROPERTIES HANDBOOK		T1-3AL-2.5V TUBING	
APPLICABLE TO		PROPERTY	
M.T. 1300F - 2 HRS - AC OR VC		FATIGUE LIMIT DIAGRAM: LOAD	
CHEM MILLED		TEMPERATURE	NO. HOURS/CYCLE
PEENED: .250" DIA. / .028" W.T.		75F	4
11-15N USING .008" TO		TEST TYPE	
.011" DIA. GLASS BEADS		LOAD CONTROL, 4-POINT BENDING	
DEGREES OF FREEDOM		FREQUENCY	HOLD TIME
5	NO. OF TESTS		RAMP TIME
		TEST MODULUS: E (10 ⁶ PSI)	CROSS SECTION: A"
		ORIENTATION	
NO. OF TESTS IN MODEL			
— : \bar{x} -K5 (95/99)		— — — : \bar{x} -3s	— — — : \bar{x} (AVERAGE)
		- - - - : EXTRAPOLATED	

A=4.0 A=1.0

STRESS IN SEC MODE - ROD END HYDRAULIC TUBE

ALLOWABLE MAT'L STRESS

A=1.50

A=1.25

A=1.00

A=0.75

A=0.50

A=0.25

A=0.00

THE INFORMATION CONTAINED HEREON IS PROPRIETARY INFORMATION		5455, 5452, 5524	1488R1	PD1488R2
REVISION BY	DATE	APPROVED BY	ISSUE DATE	PAGE
S.L. AWALT	5/10/73	G.E. BEST	7/29/63	2 of 2

Figure 10.32 Typical Goodman Diagram

tics and requirements. Flight readiness reviews are held prior to the first use of an engine on a military or commercial aircraft. These reviews are conducted by Chief Engineer's office.

In addition design reviews are conducted with customers, airframe manufacturers, the Air Force, and other government agencies to review assembly and maintenance procedures and coordinate other engine system requirements.

Engine flight experience over more than 35 years has established designs, materials, and features that have been used successfully for extended service. Aircraft and government contracts may dictate use of standard features throughout the engine, such as "no lock/safety wire," assembly without a torque wrench or assembly with a minimum number of tools, and many others that could affect design details.

DESIGN TOOLS, ASSEMBLY AIDS, AND CUSTOMER MOCKUPS

Visualization of the way parts fit relative to other parts is and always has been a major concern to engineers. In the world of designing and installing engines for and into today's aircraft, the fit of configuration parts to each other is only the beginning. The configuration design engineer must address the requirements of his hardware relative to fit and function as well as the requirements imposed by aircraft installation and envelope restrictions, maintainability provisions, ground handling equipment interfaces and access requirements, minimum clearance requirements to other tubes as well as electrical cables and other components. In addition, clamping and the overall aesthetics of packaging a many tubes, manifolds, electrical leads, and their fastening hardware must also be considered.

The best of current layouts still utilize two dimensions and lack depth delineation. New methods and tools are in the process of being developed in computer graphics and hold great promise of enhancing visualization through shaded solid modeling and other techniques using computer methods.

Fit and function demonstrations and checks are required prior to introduction of production engine hardware. The purpose of this section is to provide an explanation of the system available to satisfy the fit requirement. Function demonstrations and checks must be satisfied using test rigs or engine testing.

All hardware designed by Nacelle and Installation Products Operation personnel must be fit and function demonstrated or checked prior to release for use. The vehicles to be used to accomplish the fit portion of the task are: engineering design tools, assembly aids, customer mockups, and production engine assemblies.

Engineering Design Tool An engineering design tool is a full scale, dimensionally accurate model of the designated engine. It may be 180° or 360° of that area of the external engine where C&A components and configuration hardware are mounted. High bypass (commercial) engines will normally be a 360° sector, and low bypass (military) engines will normally be a 180° sector. The engineering design tool is used during the design or redesign phase of an engine program to expeditiously determine C&A component arrangements or geometric requirements and tube routing.

Several new techniques have been used in the development of the engineering design tool. Plastic tubing or bent wire is used to determine tube routing, which allows the engineer a quick method of optimizing the arrangement, routing, clamping, and clearances relative to engine C&A components and piping. The plastic or wire definition is captured in tube coordinate format by a vector reading device and a metal tube is made.

The metal tube is then trial fitted on the engineering design tool and further modifications made as required. The final definition is then released to Drafting to use as input to generate the drawing which is released to make the production parts. The plastic or wire is left in place while the metal part is being made, to occupy the space so the design of other parts can continue.

Synthetic cord or roping is used to finalize electrical cable routing. Commercially available, synthetic mesh rope or cord selected to approximate twisted pair electrical lead, is bundled as a simulated electrical cable to determine routing, branch locations, lengths, and bracket locations. Connectors are added and keyway orientations are determined which completes the definition of the cable. The completed cable is taken off, measured and reinstalled on the vehicle until mockup cables are available. The measurements are transcribed into drawings and issued as the production definition.

Existing C&A components can be used as dies to generate additional components where minor or no change is involved. Experience to date shows about ten percent of the cost and one fourth the lead time involved in procuring mockup hardware is due to procurement of parts from vendors of C&A components.

Assembly Aid An assembly aid is usually the engineering design tool updated as required with C&A components and configuration hardware made to issued production drawings, or otherwise-sameas-mockup drawings, containing specific exceptions that may be taken. Quality Class "C" metal mockup hardware or Quality Class "P" production parts, downgraded to Quality Class "C", must be used for any hardware with defined interface requirements.

The assembly aid is utilized by Assembly Planning and Maintainability as a visual guide, as well as a reference for clarity in writing assembly and maintainability procedures. The assembly aid serves an additional role of continued use as an engineering design tool on an as-required basis. Therefore, it is a requirement that all drawings be issued and an assembly drawing and parts list be prepared and issued for this tool.

Mockup A mockup is a specific scale (usually 1/1), dimensionally accurate model of the exterior features of individual parts or assemblies of an engine. Customer mockups may be required to duplicate actual engine weight and center of gravity in order to demonstrate installation handling characteristics. This is accomplished by adding ballast and adjustment provisions.

The mockup is used for form and fit verification of the production engine. It must therefore represent the best definition known, of the production engine. The verifi-

cation process starts with the initial customer acceptance review, which involves a formal presentation of what was incorporated in the mockup, followed by the customer's critique including "chits" on those specific items thought to be deficient. Specific areas covered include: conformance to installation envelope, access to interfaces, maintainability features, ground handling requirements, tube clearances, actual or potential chafing, and conformance to design practices. These "chits" must be satisfied or a plan initiated to accomplish the work required.

The process continues with reviews at the airframer, usually by installing the engine mockup into the aircraft or a mockup of the aircraft. Installation is performed using ground support equipment, thereby performing a checkout of that hardware as well.

Production Engine Assemblies Production engine assemblies are real, functional engines, assembled as serial number engines. The use of production hardware makes this the most desirable and least available alternative. The added danger of possible contamination imposes very strict controls on this method. All mockup hardware assembled to a production assembly must be made of material compatible to attaching hardware, be painted or coated yellow, and cleaned to production parts standards. In addition, a controlled on/off list is maintained of all items removed or added.

Chapter 11

CONTROLS ENGINEERING

by Terry J. Sharp, Daniel I. Wiggins

and Kenneth F. Cook
(*Electronic Controls*)

INTRODUCTION

Controls Engineering encompasses a broad spectrum of activities focused on the development of control strategies and the design of the components which control the performance and safety of the engine. Controls Engineering interfaces with almost every organization in the company (Figure 11.1), and provides a wide range of jobs from the proposal phase to manufacture and field support of the product. The specific products of Controls Engineering are the control system design and the design of the components which comprise the system.

The control system design includes definition of the control mode and logic (control strategy), definition of the system mechanization mix (quantities and types of controls, sensors, actuators, pumps, etc.) dynamic design for stability and transient response, and definition of component to component, component to engine, and engine to aircraft interfaces.

The majority of controls components are designed and supplied by outside vendors according to Controls component specifications and source control drawings. Some components are designed internally and manufactured and assembled by outside vendors. A considerable dollar volume of controls components are supplied by other GE businesses such as the Aerospace Control Systems Department (ACSD), Binghamton, N. Y. and Ft. Wayne, Indiana which supplies analog electronic controls, digital electronic controls, engine monitoring system processors, and electrical cables. The Aircraft Instrument Department (Wilmington, Mass.) provides optical pyrometers for turbine blade temperature measurement, and GEAE at Lynn, Mass. manufactures our augmenter fuel controls and other valving which are designed at Evendale.

Controls Engineering is involved with the design of military, commercial, and marine and industrial product lines. There are two basic functions; control system de-

sign and component design. The functional hardware designers interface with outside vendors to obtain the controls components which comprise the control systems. An exception to this is those components which are designed internally.

The control system designers are responsible to design fuel, hydraulic, pneumatic and electrical systems based on engine specification requirements. They also integrate all control activities and interface with Project, Product Operations and the Customer.

Applications Controls Engineering designs the control systems for a wide variety of engines for land, sea, and air applications. These include:

- Dry turbofans for commercial airliners, military transports, and military tankers
- Augmented turbofans for military fighters and bombers
- Turboshfts for land electrical power generation and pipeline pumping
- Turboshfts for naval propulsion (which are now powering approximately 225 ships for 17 navies)

The evolution of controls technology during the past two decades has been from full hydromechanical control or hydromechanical control with single function analog electrical trim, to hydromechanical control with extensive analog electrical trim or hydromechanical control with digital electrical trim, to full authority digital control (with and without hydromechanical backup). This evolution is shown on Table 11.1. The control strategy which has been employed has been influenced by the evolutionary paths taken by commercial and military technologies and application requirements, and special considerations associated with single engine applications.

Control System Requirements The basic requirements of a jet engine control system are as follows:

- Regulate steady state and transient power output over the available power range.
- Maximize engine cycle efficiency
- Provide required transient thrust response during power changes
- Provide stable operation under all operating conditions
- Maintain safe operating limits.

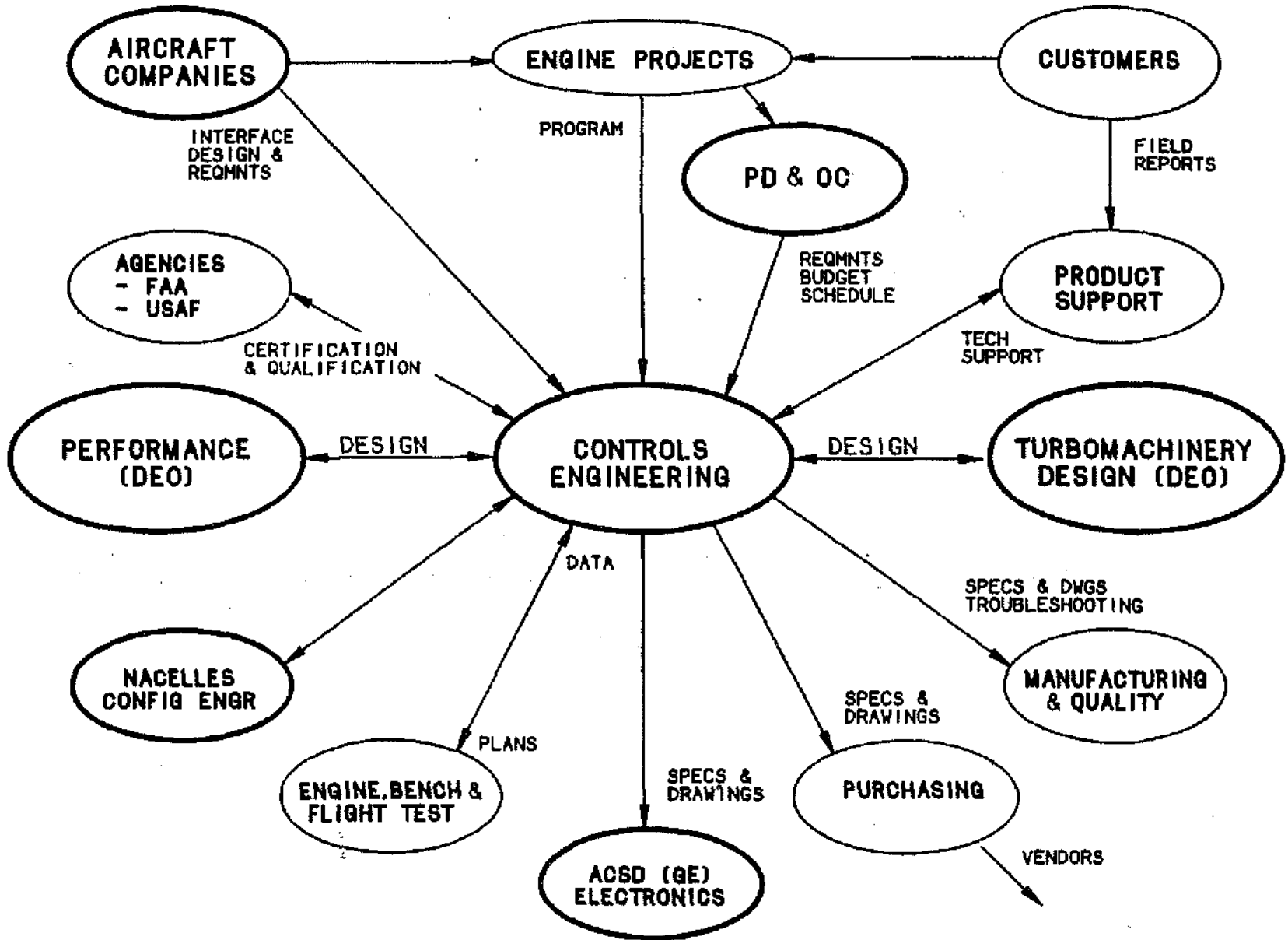


Figure 11.1 Controls Engineering Interfaces

Control Type	Applications	Controlled Variables
Hydromechanical control with computation by levers, mechanisms, and fluids (fuel).	TF39, CF6-6, CF6-50 (military transport and commercial aircraft).	Hydromechanical control of core speed, compressor stators, accel/decel fuel flow on TF39 and CF6-6. The CF6-50 also has variable bleed valves (VBV's).
Hydromechanical control with extensive analog electrical functions	F101-GE-102 (B1B bomber)	Analog electrical control of intermediate fan speed turbine blade temperature (T4B), augmenter fuel flow, nozzle area, fan IGV's and ignition. Hydromechanical control of core speed (idle and part-power), compressor stators, min and max PS3.
	F110-GE-100 and F110-GE-400 (F-16 and F-14)	Analog electrical control of fan speed (full range), core speed limiting, T4B, augmenter fuel flow, nozzle area, fan IGV's, min and max PS3, and accel/decel fuel flow, with hydromechanical control of compressor stators. A backup (secondary mode provides hydromechanical control of core speed, accel/decel fuel flow, compressor stators, and min and max PS3, with an analog electrical fan speed limiter. The fan IGV are fixed partially open, the nozzle is fixed full closed and the augmenter is disabled.
	CFM56-3/3 (commercial aircraft, military, tankers, reconnaissance aircraft)	Analog electrical Power Management Control (PMC) of fan speed. Hydromechanical control of core speed, compressor stators, variable bleed valves (VBV's), accel/decel fuel flow, and turbine clearance control.
Hydromechanical control with digital electronic override/trim functions	CF6-80A and CF6-80C2	Digital electronic Power Management Control (PMC) of fan speed, idle core speed reset, starting, and ignition. Hydromechanical control of core speed, accel, decel fuel flow, compressor stators, variable bleed valves (VBV's) and rotor active clearance control.

Table 11.1 Recent Evolution of Control System Technology (Sheet 1 of 2)

A8	Nozzle Area
AFC	Augmenter Fuel Control
AFTC	Augmenter Fan Temperature Control
AIS	Augmenter Initiation Signal
AOA	Angle-of-Attack
BF	IGV Position (Deg.)
CBP	Customer Bleed Pressure
CDP,PS3	Compressor Discharge (Static) Pressure
CIT	Compressor Inlet Temperature
CITS	Central Integrated Test System
DEC	Digital Electronic Control
Delta P/P	(PT25 - PS14)/PS14
ECC	Engine Cycle Counter
ECU	Electronic Control Unit
EGT,T56	Exhaust Gas Temperature
EMSP	Engine Monitoring System Processor
EPR	Engine Pressure Ratio
FDS	Flame Detector Signal
FADEC	Full Authority Digital Electronic Control
FICA	Failure Indication & Corrective Action
FN	Net Thrust
HMU	Hydromechanical Unit
HPT	High Pressure Turbine
IFSD	In Flight Shut Down
IGV	Fan Inlet Guide Vanes
LPT	Low Pressure Turbine
M	Mach Number
MEC	Main Engine Control
MN,M	Mach Number (Aircraft)
NC,N2	Core Speed
NF,N1	Fan Speed
ϕ (PHI)	WFR/PS3C (A/B Fuel Ratios)
PLA	Power Lever Angle
PMC	Power Management Control
Po	Ambient Pressure
PRU	Pressure Ratio Units ($\Delta P/P$)
PSM,PS14	Fan Discharge (Static) Pressure
PT2	Engine Inlet Total Pressure
PTM, PT25	Fan Discharge Total Pressure
RVDT, LVDT	Rotary/Linear Variable Differential Transformer
SG	Specific Gravity
T2	Engine Inlet Temperature
T25,FDT	Fan Discharge Temperature
T4B	HP Turbine Blade Metal Temperature
TLA	Throttle Lever Angle
TM	Torque Motor
To	Ambient Temperature
VBV	Variable Bleed Valves
VSV	(Core) Variable Stator Vanes
WFM	Main Engine Fuel Flow
WFR,WF6	Augmenter Fuel Flow
WFT	Total Fuel Flow (WFM + WFR)
WOW	Weight on Wheels

Table 11.2 Glossary

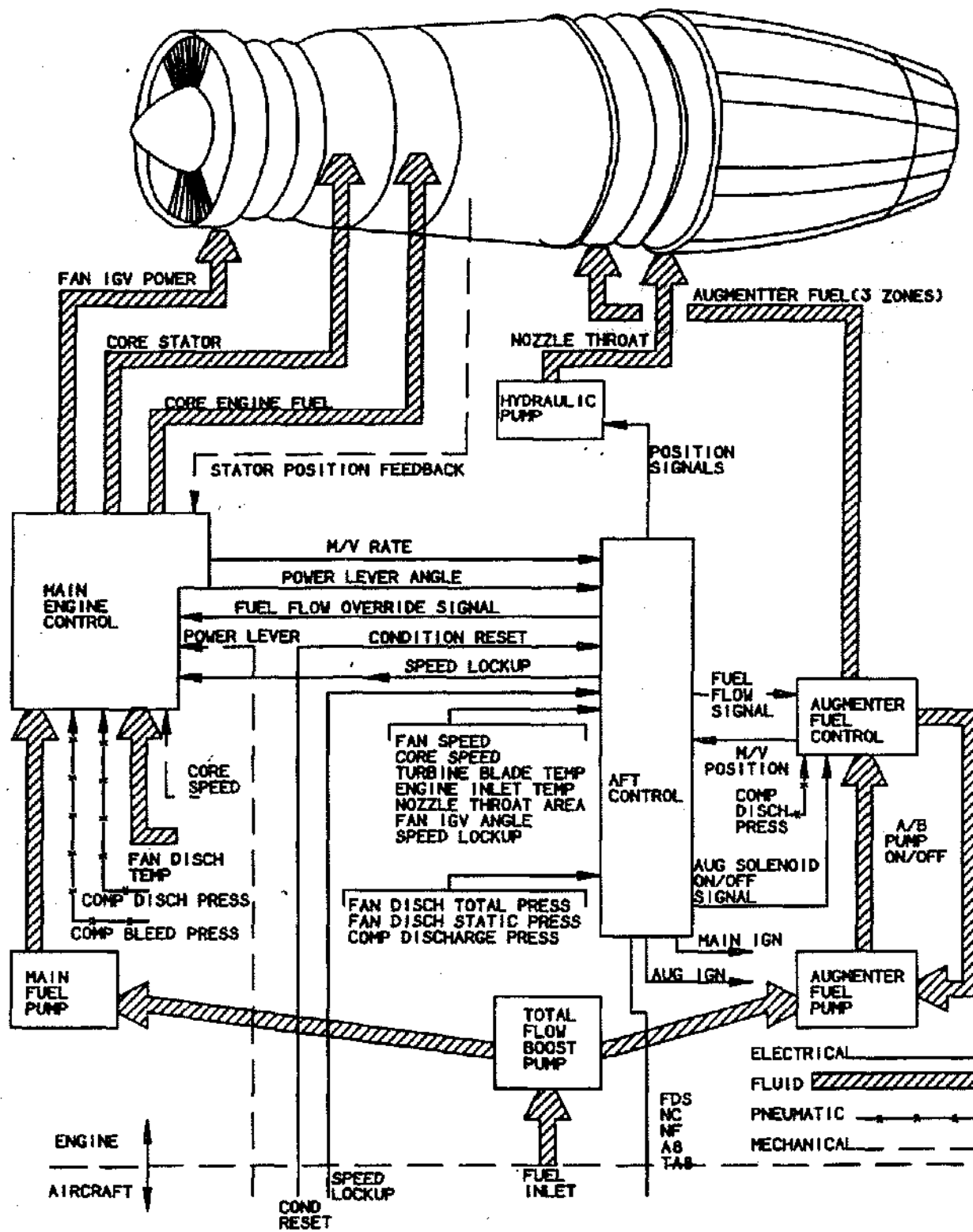


Figure 11.2 Control System Schematic

Parameters in this category include mach number, ambient pressure and temperature, weight on wheels (WOW), bleed, thrust command/limit and any special function inputs.

The control system requirements come from two basic categories: regulation of power and efficiency; maintenance of safe operating limits. The control strategy for each application must take into account all of the specific requirements for each category. These two categories are interrelated since the design must provide fully regulated thrust while also preventing exceeding engine speed, pressure, temperature, and stall limits.

The complexity of a control system is directly related to specifications defined by the customer, requirements imposed by the cycle, safety and special requirements or functions (e.g. additional stall margin resets, SFC reduction features - turbine clearance control, bore cooling, etc.).

Generally, the engine control must provide steady state thrust characteristics proportional to rotation of the engine power lever. This thrust to power lever characteristic must be essentially linear, accurate, repeatable and be distinguished by dwell bands or "flats" at certain thrust

levels. A linear thrust-power lever relationship is required to enhance fine thrust tuning. The engine control system must set and maintain an accurate thrust level to prevent asymmetric thrust in multi-engine applications. Various dwell bands are necessary to allow the pilot to set specific thrust levels by feel of the power level in detents or gates.

The best means of thrust control for dry turbo fans is to schedule fan speed as a function of power lever angle. For augmented engines linear thrust control of the augmentor is accomplished by scheduling the augmentor fuel air ratio as a function of power lever.

Control System Design Engine control systems are designed to regulate engine power and efficiency by manipulating the available variables as a function of sensed parameters. The manipulated variables are varied to schedule or set the controlled variables. Control system design does not determine the set of manipulated variables. These are defined by cycle design. Controlled variables and sensed parameters are selected by the control system designer to meet system requirements. Figure 11.3 shows the basic process of control system implementation.

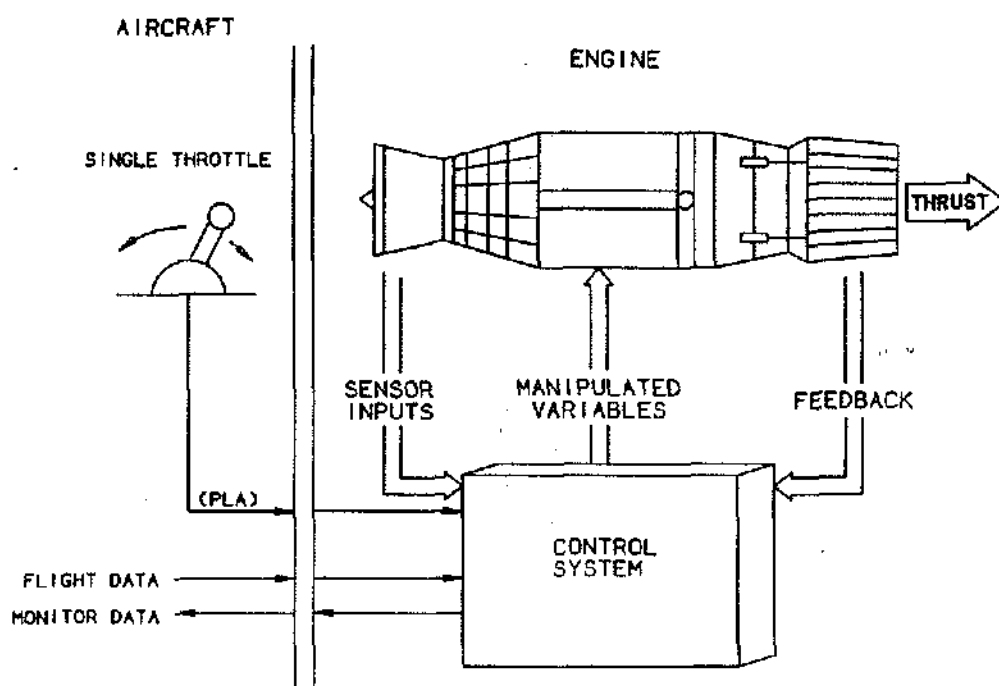


Figure 11.3 Control System Implementation

The controlled variables are selected to provide accurate control of engine power output, engine transients, and engine operating limits. Factors which affect the selection of the controlled variables are as follows:

- Influence on thrust setting accuracy
- The parameters which must be sensed (measured) in order to define the required control system schedules in terms of the controlled variables.
- Unique engine component requirements to maximize efficiency and ensure stall-free operation - For example, all of our modern engines require compressor stator and/or variable bleed control. Military engine installation factors require fan IGV control for distortion attenuation.
- Installation and application requirements - Most aircraft require maintenance of bleed pressure at some minimum acceptable levels, and many supersonic aircraft require maintenance of engine airflow limits.
- The requirement to protect the engine from over-speed, overtemperature, stall, and blowout

The controlled variables which are in common use on today's turbofan engines include fan speed (N1, NF), core speed (N2, NC), HP turbine blade temperature (T4B), exhaust gas temperature (EGT), compressor discharge pressure (PS3), augmenter fuel flow (WFR), fan discharge Mach number (M25, $\Delta P/P$) (the latter two on augmented engines), and fan and compressor variable geometry (IGV's, VSV's, and VBV's).

The manipulated variables, those parameters which are modulated directly by the control system to maintain control of the above controlled variables are as follows:

- Main fuel flow (WFM)
- Augmenter fuel flow (WFR)
- Exhaust nozzle area (A8)
- Compressor variable stator vanes (VSV's)
- Fan variable inlet guide vanes (IGV's)
- Variable bleed valves (VBV's)
- Thrust reverser

Sensed parameters are selected to support the engine control mode, provide accurate scheduleability over all flight conditions and provide limits protections. Various sensed parameters used on military and commercial engines are: inlet temperature and pressure (T2, P2), ambient pressure (Po), aircraft mach number (M), compressor inlet temperature (T25), bleed pressure, compressor discharge pressure, fan and core speed, fuel metering valve position and exhaust nozzle area.

STABILITY AND RESPONSE

Usually we tend to think of a jet engine's operation in terms of steady state conditions. A jet engine's performance capability is also stated in steady state parameters for comparison of one engine to another. Although an engine spends the majority of its operational life at steady state conditions the transient response is an extremely important design criteria. An engine must start, accelerate, decelerate and handle a variety of varying inputs both externally and internally while providing smooth and stable operation. Even while running steady state the engine is in a very dynamic mode. All of the various control "loops" are functioning independently, setting controlled variables which interact with one another.

Dynamic analysis and simulation are design procedures that are used on all jet engines in the development of control systems. Stability and transient response are very important steps for designing, developing, evaluating and optimizing the engine-control system interaction. This type of analysis spans from simple linear models of components, to complete detail control system and engine mathematical models. This type of analysis capability is invaluable in the development stages of a new engine and for assessing the effects of a control loop change on a mature engine. Using dynamic analysis to design the control system or investigate a stability or response issue saves both time and money over testing on an actual engine or a component rig.

Definitions and Nomenclature Before getting into design requirements and methods in more detail its appropriate to discuss some basic definitions and nomenclature. First and basic to all control systems is the *control loop*. The control loop includes the reference inputs which are used in computing the schedule. It may include the control and/or engine dynamics. Within the control loop a manipulated variable is positioned to set the controlled variable. Figure 11.4 shows a basic closed loop control and the primary functions.

There are two basic types of control loops; "*open loop*" and "*closed loop*." A closed loop is where the output is monitored either continuously or on a sample basis. This output, of the controlled variable is compared to the scheduled value of the controlled variable (or demand), through feedback to a summer. The difference is the error. The output is continuously changed to minimize the error. Examples of closed loop controls used on current engines are: fan and core speed control, variable stator (VSV) position, variable bleed valve (VBV) position, inlet guide vane (IGV) position, and fan discharge mach number (or delta P/P).

CLOSED-LOOP CONTROL:

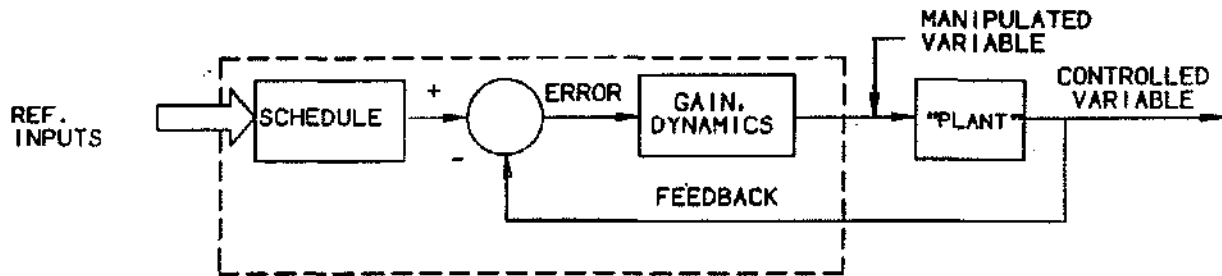


Figure 11.4 Basic Feedback Loop

An open loop control is much simpler. The output parameter is set based on a precalculated schedule. There is no feedback sampling of feedback output. This type of control is used for turbine clearance control and bore cooling control. Most jet engine control loops are closed loop because they allow more accurate steady state and transient setting of the controlled variable.

Using the analogy of driving an automobile, we can show the distinction between the open and closed loop controls. In a normal driving situation, your brain decides what path you wish the car to take. This desired path is compared to the actual path sensed by your eyes and the difference in direction is sent via nerves to the arm muscles which amplify the "error signal" and turn the wheel in the appropriate direction. This action continues until the actual path coincides with that dictated by the brain. This is closed loop control. If, on the other hand, we were to drive by a calibrated degree wheel on the steering column without looking where we were going, this would be open loop control insofar as the vehicle path is concerned.

Control loops are defined and represented by *block diagrams*. These diagrams can be as simple as one loop (Figure 11.4) or as complex as an entire control system.

The block diagram is made up of various elements such as summers, integrators, differentiators, gains, multipliers, min and max selectors. The basic representation of each element is shown in Table 11.3. An integrator and differentiator are basic *transfer functions*, which are described by Laplacian algebra. The Laplace transform is a method of transforming differential equations, which describe the control system as algebraic expressions. These transfer functions describe the control systems response to various inputs (steps, ramps, sinusoids, etc). A reverse transformation can be made to show the system outputs as a function of time. In control design and analysis the transfer function is a very important tool to understand the response of a complex control function.

An example of simple transfer functions are differentiators and integrators. *Differentiators* are used to calculate fuel metering valve rate which is used to maintain loop stability. An example of *integrator* in the control system is an actuator. The input is a rate of change of volume (fluid) which the actuator integrates into a displacement.

A transfer function is a mathematical expression representing the steady state and transient behavior of a physical system. For a simple example consider the


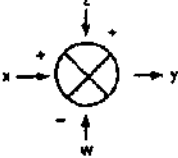



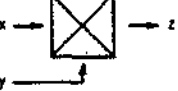
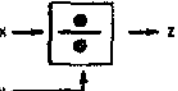
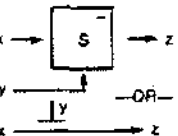
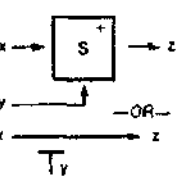
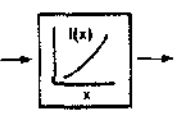
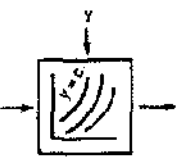
NAME	BLOCK	EQUATION
1) INTELLIGENCE PATH		$x = y$
2) SUMMER		$y = x + z - w$
3) COEFFICIENT (GAIN)		$y = Kx$
4) INTEGRATOR		$y = K \int x$
5) DIFFERENTIATOR		$y = K \frac{dx}{dt}$
6) MULTIPLIER		$z = xy$
7) DIVIDER		$z = \frac{x}{y}$
8) SMALL SIGNAL SELECTOR (MIN SELECT)		$z = x, \text{ IF } x < y$ $z = y, \text{ IF } y < x$
9) LARGE SIGNAL SELECTOR (MAX SELECT)		$z = x, \text{ IF } x > y$ $z = y, \text{ IF } y > x$
10) FUNCTION GENERATOR (2D)		$z = f(x)$
11) FUNCTION GENERATOR (3D)		$z = f(x,y)$

Table 11.3 Control Loop Block Diagram Basic Elements

spring-dashpot system shown in Figure 11.5. If the dashpot force equals the spring force then

$$K(X_i - X_o) = B(dx_o/dt)$$

Using the Laplace transform for the derivative

$$K(X_i - X_o) = BSX_o$$

Solving for the transfer function

$$X_o/X_i = \frac{1}{(B/K)S + 1} = \frac{1}{TS + 1}$$

Where $T = B/K$ is the *time constant*.

Now we have an expression (transfer function) of an input (X_i) to an output (X_o). This is called a *first order lag*, which is the most common transfer function. If this type of transfer function was subjected to a step input the output would respond exponentially. The time it takes for the output to reach 63.2% of its final value is equal to the time constant. The output lags the input.

A *lead* (or lead-lag) circuit has a transfer function

$$X_o/X_i = \frac{T_1S + 1}{T_2S + 1}$$

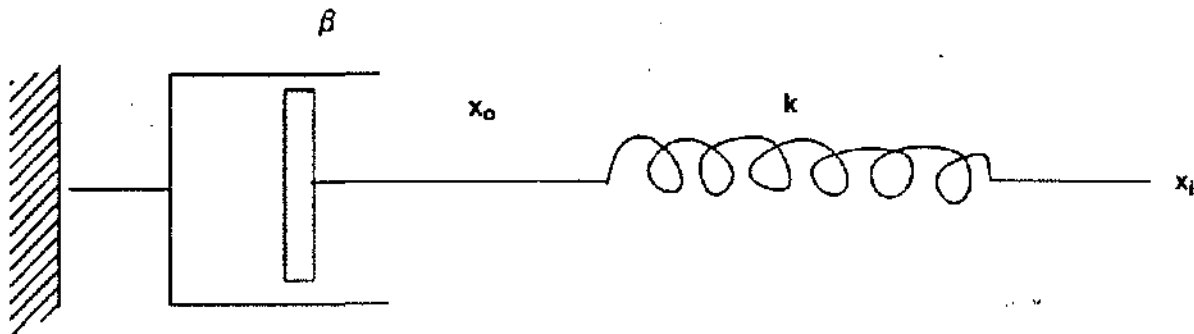
where $T_1 > T_2$. For this type of circuit the response to a step input is an initial over shoot (lead) of the input value and subsequent exponential settling to a final value.

For a transfer function written

$$X_o/X_i = \frac{K_1}{TS + 1}$$

K_1 is the steady state position *gain*. This is constant, input to output ratio of a device steady state. The gain can also be a single element of a system in the block diagram.

We have shown that transfer functions are a way of describing the input-output relationship of a system, and we have discussed the special case of a step input. There is also special interest in knowing how a system responds to a sinusoidal input. Two terms need to be defined that describe the "frequency response" of a system: (a) the amplitude ratio and (b) the phase shift. The output waveform of a linear system that is driven with a sine wave is also a sine wave. The output will have the same frequency, but will have a different amplitude and will be shifted in time relative to the input.



$$k = \text{SPRING RATE, } \frac{\#}{\text{in}}$$

$$\beta = \text{DAMPING COEFFICIENT, } \frac{\# - \text{sec}}{\text{in}}$$

Figure 11.5 Spring-Dashpot System

The *amplitude ratio* is normally expressed in *decibels* (db). When the input is oscillated in sinusoidal fashion measurements of peak-to-peak input and output are made. With these values the amplitude ratio is calculated by

$$K = 20 \log_{10} \frac{\text{Peak-to-peak output}}{\text{Peak-to-peak input}}$$

Thus if peak-to-peak output equals input the amplitude ratio is zero db. *Phase shift* is usually defined in terms of an angle, in degrees. A negative angle denotes the output lags the input (phase lag). Phase angle is obtained by inputting an oscillating (sinusoidal) signal into a device. The corresponding output is also recorded. The time lag between the input and output is measured. This is divided by the total time for one cycle. Since a complete cycle is 360 degrees this fraction is multiplied by 360. The obtained value is the phase shift. The amplitude ratio and phase shift normally vary as a function of input frequency. The amplitude ratio and phase shift of a system can be measured by subjecting it to a frequency response test. There are also mathematical methods to compute amplitude ratio and phase directly from a transfer function.

Consider the block diagram shown in **Figure 11.6**. This is a closed loop system with negative feedback, since the feedback is a negative adder to the summer. Note there are three elements in the *feed forward* portion of the control loop:

- Gain: K_1
- Lag: $K_2/(T_1S + 1)$
- Integrator: K_3/S

The *open loop transfer function* (OLTF) is defined by multiplying the elements:

$$\text{OLTF} = \frac{K_1 K_2 K_3 K_4}{S (T_1 S + 1)}$$

The *closed loop transfer function* (CLTF) is a little more complicated:

$$\text{CLTF} = \frac{\text{Feed Forward}}{1 + \text{OLTF}}$$

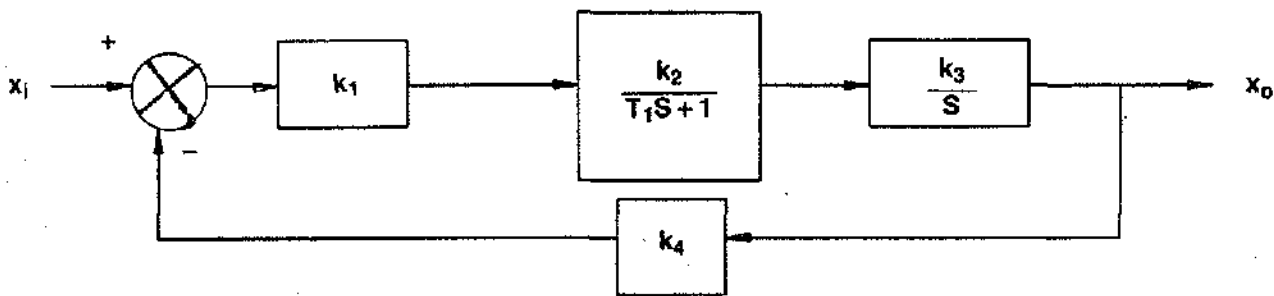


Figure 11.6 Closed Loop System

Normally open loop transfer functions are used to evaluate stability and response. Closed loop transfer functions are used if they are part of a larger loop.

Figure 11.7 shows a block diagram for a portion of a control system. At first glance it appears very complex. If each element of the diagram is evaluated one by one using the elements in Table 3-1 and the transfer function information, the complexity is reduced considerably.

Design Requirements The first design requirement is to design for stability which includes minimizing steady state thrust variation. Slight variations in inputs from sensors, schedule computing hardware or software, engine flow dynamics positioning valves or actuators and feedback signals occur continuously. Thus the term steady state is somewhat of a misnomer. The control loops and entire system must be able to react to these variations without causing unstable operation.

Tied into this requirement is the need to minimize variations in controlled parameters and engine parameters. Designing the control loop response is tricky since the engine has to react quickly to meet thrust transient, stall margin and other operational requirements. If a control loop responds too fast, instabilities can occur. The stability of a control loop depends on the gain-phase-frequency relationship of the open loop transfer function. A Bode plot can be used to show these relationships graphically. This plot is simply the amplitude ratio (gain) and phase shift of a transfer function for various sinusoidal input frequencies. A basic Bode plot is shown in Figure 11.8. Note that at a given input frequency the gain and phase shift can be obtained. The frequency is normally plotted on a log scale.

The relative stability of a control loop is expressed in terms of *gain margin* and *phase margin*. The gain margin is defined as the negative gain of the open loop transfer function at a phase angle of -180 degrees. Phase margin is defined as the difference between -180 degrees and the phase shift at a gain of zero db. These are shown graphically in Figure 11.8. General design criteria for stability is to optimize the response such that the phase margin is 40 to 60 degrees and gain margin is 6 to 10 db.

Excessive gain or excessive phase can cause loop instabilities. Non-linearities can introduce gain and phase effects that cannot be accounted for by linear analysis. There are some analytical methods for dealing with non-linear systems, but it's generally more practical to resort to non-linear computer models of the system.

Up to this point we have basically discussed the stability requirements for a single loop. In the actual control sys-

tem many control loops are "nested" within another loop, or directly effected by outputs of other coupled control loops. Thus the designer must also prevent interaction between control loops that may cause instabilities. This becomes a very complex task on engines with many independent control loops. For example, on an augmented turbofan, changes in fan speed, exhaust nozzle position and augmented fuel flow all affect one another.

The other design requirement is to design for proper transient response. Transient response of an engine and its control system includes a variety of requirements. The control system must be designed to provide acceptable thrust response during transients, throughout the flight map. This includes response to accel's, decel's, starting, engine load variations and changes in inlet conditions. For example, during flight maneuvers the conditions at the engine inlet can vary significantly even if the throttle is held constant.

Analysis of transient response is also used to measure steady state and transient tracking errors of control schedules. The design goal is to minimize this tracking error. If control loops track too far off schedule this could cause performance loss or even excessive stall margin consumption. Related to this requirement the control/engine transient response is designed to provide acceptable overshoot and undershoot of end points of a transient. This is a trade off since we also want quick transient response which tends to cause overshoot or undershoot. Here, we are concerned with possible combustor flameouts, compressor or fan stalls, speed or temperature overshoots, etc.

Another important design step is to assess control system response to failures. The system must be designed so that selected control or engine component failures do not result in catastrophic engine failure. The control system is designed to react to these failures and provide a smooth transition to the failure mode operation. Similar to this transient response requirement is the need to provide smooth transition during mode transfers used in military control systems.

The F110 - 100 engine, for example, has a primary (normal electronic) control mode and a secondary mode which provides a "get home" capability if a failure occurs in primary. Secondary mode is selected by the fault logic or manually. When this occurs the hydromechanical control takes over speed scheduling, the exhaust nozzle goes full closed, fan IGV's slew to a fixed position and the afterburner is disabled. The control system response must control this transfer while providing acceptable engine operation.

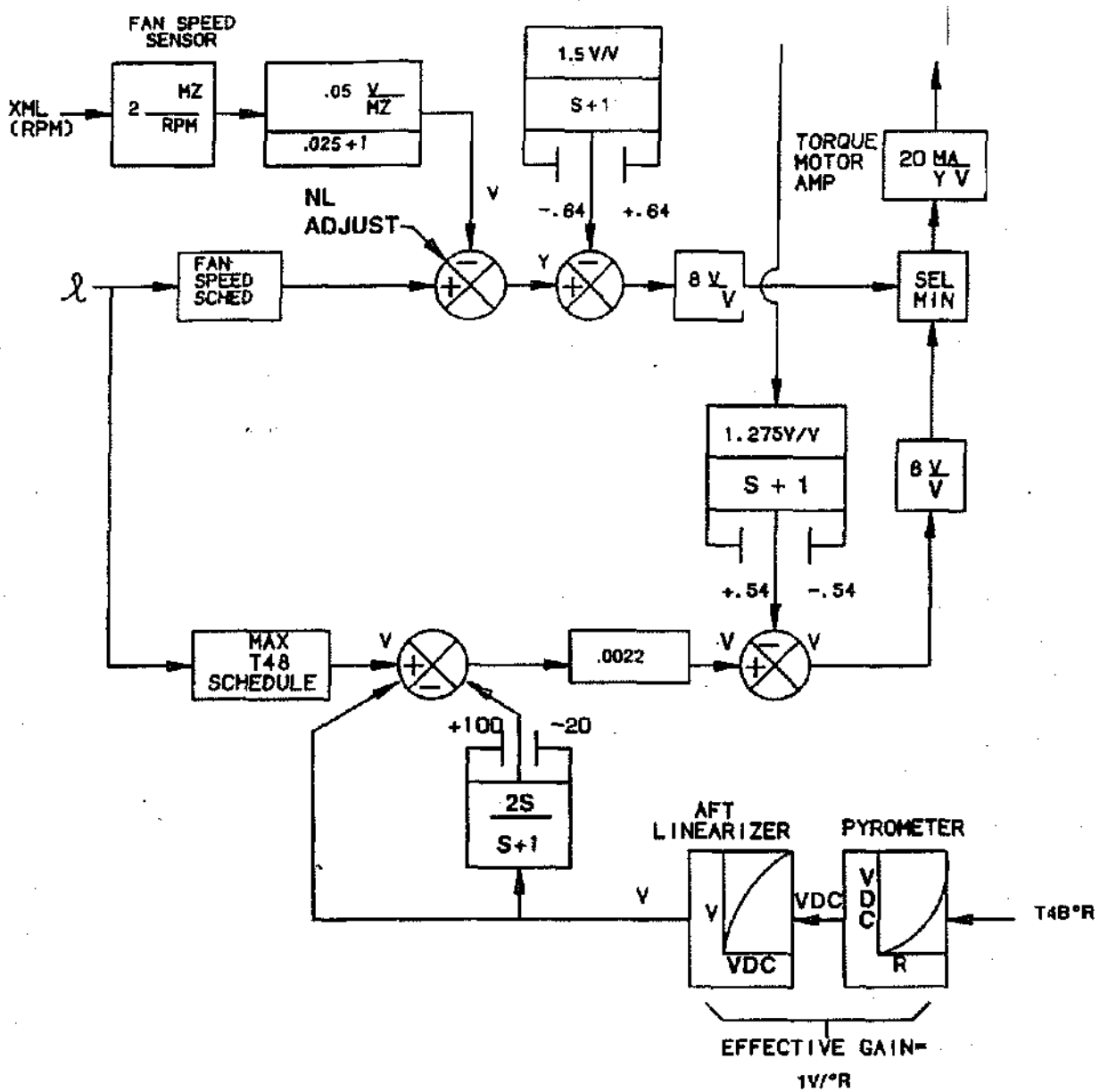


Figure 11.7 Control Subsystem Block Diagram

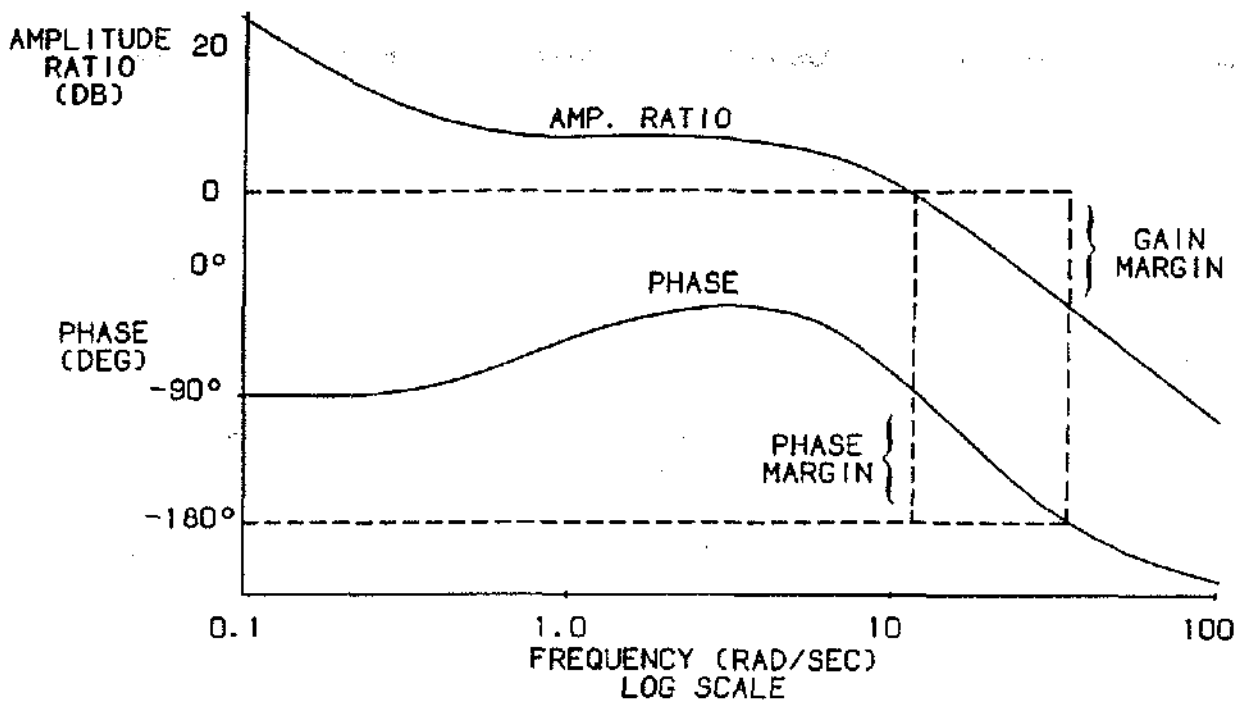


Figure 11.8 Bode Plot

A recent addition to the dynamic analysis responsibilities is to complete the FICA model design. FICA is the Failure Indication & Corrective Action model. This is a simple engine and control system model used in recent digital controls. For certain component failures the control can revert to operation using model inputs. The model must be designed with most of the previously mentioned transient response requirements so the engine can operate stably.

Design Tools and Methods The basic design methods used for stability and response analysis are linear and nonlinear control analysis. Linear analysis is used primarily for investigating stability. Most components in a control system, including the engine itself, can be simplified by linear models. Complete control position loops can also be represented by linear models. Using these models and equivalent open and closed loop transfer functions a linear analysis can be accomplished, as previously described. The linear analysis of each loop is used to "tune" the loop constants and dynamic compensation.

The next step is to perform the nonlinear dynamic analysis. This is accomplished using detailed control loop

simulations. A mathematical model of the entire control system is developed from a complete description of the hardware and software. The software sampling frame times and dynamic characteristics of the hardware are reflected in the model. Previously ignored effects such as fluid compressibility, piston inertias, loads, volumes, pressure drops and valve non-linearities are included. This mathematical model of the control system includes the algorithms and equations defining the control loops, sensors, actuators and valves.

All jet engines have a number of controls which are closed loop through the engine. Examples are speed, turbine temperature and duct airflow control. Thus the engine is an integral part of these control loops. In order to do a complete non-linear analysis the control system model must be combined with the engine model.

A mathematical model of the engine is constructed describing the thermodynamic and mechanical processes governing the operation of the engine. This includes the principles of compressible fluid flow, combustion, and work and energy balances. The model may be a "first principles" model using basic thermodynamic and dynamic equations or "table driven" using empirically

derived data or a combination of both. The end result is an engine model that accurately predicts the dynamic response of the engine to inputs such as fuel flow, and variable geometry. This model is usually an adaptation of the steady state engine cycle model.

Engine transfer functions describing the response of the controlled parameters to small fuel flow changes can be developed. The transfer functions for these linear engine models are obtained by perturbing the engine thermodynamic model to derive unbalanced torque partial derivatives. Zero unbalanced torque is steady state speed operation, a positive unbalanced torque will accelerate the engine and negative decelerates. These transfer functions provide a linear representation to small changes. From this analysis a linear engine model is built.

The control system and engine non-linear models can be used to simulate transients (accel, decel, etc.), failure reactions, mode transfers and other operational functions. This type of model is invaluable for initial engine/control system development and for analyzing production field problems. Initially these models are used to evaluate control logic, and optimize schedules, transient response and logic. Later in an engine development program the model has many other uses.

Testing response to failure scenarios on engine would be very difficult and expensive. In some cases, such as fan overspeed or turbine over temperature protection verification, the risk or expense is too great to test on engine. The model makes it easy to simulate "what if" situations. The engine transient model is also used to evaluate signal processing, fault detection, signal selection and FICA models. Another important use for the model is to evaluate the engine/control system transient response (e.g. thrust transient times) versus engine specification requirements.

Once an engine is in production, if field problems are experienced, or modifications to a control mode or hardware are required the transient model provides a very cost effective way to check out changes. Having a model of the engine and control system makes it easy to simulate design improvements or modifications, with virtually no risk. Obviously stability and transient response analysis and design is a very important part of any engine control system design.

BASIC ENGINE CONTROL FUNCTIONS

Certain control functions are basic to most of our current military and commercial engine control system designs. These include: fan and/or core speed scheduling, acceleration and deceleration fuel scheduling, variable stator

vane scheduling, minimum and maximum fuel flow, core speed and compressor discharge pressure settings. Each military and commercial engine program has other unique control system requirements. For example, military engines may require design for control of augmentor fuel flow, variable exhaust nozzle or variable inlet guide vanes. While unique commercial requirements include power management, variable bleed valves, turbine clearance control and thrust reverse. These will be discussed further in the next two sections. The control system designer's job is to optimize scheduling and control of these variables to meet the engine performance objectives.

Core and Fan Speed Control The primary function of an engine control system is to provide linear and accurate thrust control with a single throttle input. For a jet engine thrust is easily controlled by regulating air flow. Early studies for turbojets examined various methods of controlling thrust such as rotor speed, turbine inlet and exit temperatures and compressor discharge pressure. Each variable was studied for sensitivity to component efficiencies (compressor, turbine, etc.), ability to provide safe operating limits, mechanization consequences, and schedulability. It was found that controlling rotor speed was the most accurate method of setting thrust. Also, the best manipulated variable to set rotor speed is fuel flow.

Compressors can be described by a "map" of pressure ratio versus corrected air flow, as shown in Figure 11.9. Here, the operating line is a locus of points for normal steady state operation. The compressor is pumping into the turbine nozzle. The back pressure it "sees" goes up like a square function. Eventually the operating and stall lines intersect at some corrected rotor speed. This characteristic necessitates the requirement for corrected speed limiting. If the control only regulated physical speed, a compressor stall could occur on cold days when a low inlet temperature would result in high corrected speeds. Use of corrected parameters as controlled variables allows for normalization of compressor performance.

By scheduling corrected speed as a function of power lever angle (PLA) the pilot has direct control of corrected air flow or thrust. A PLA versus core speed schedule can be developed which provides a constant thrust at any angle. To maintain constant corrected speed at a given PLA, physical speed is increased for increasing compressor inlet temperatures (CIT), as displayed in Figure 11.10. This type of schedule is optimized to give a linear thrust demand - power lever curve. As altitude increases (lower P_0) the absolute thrust values for idle and max thrust are reduced, but thrust linearity is preserved.

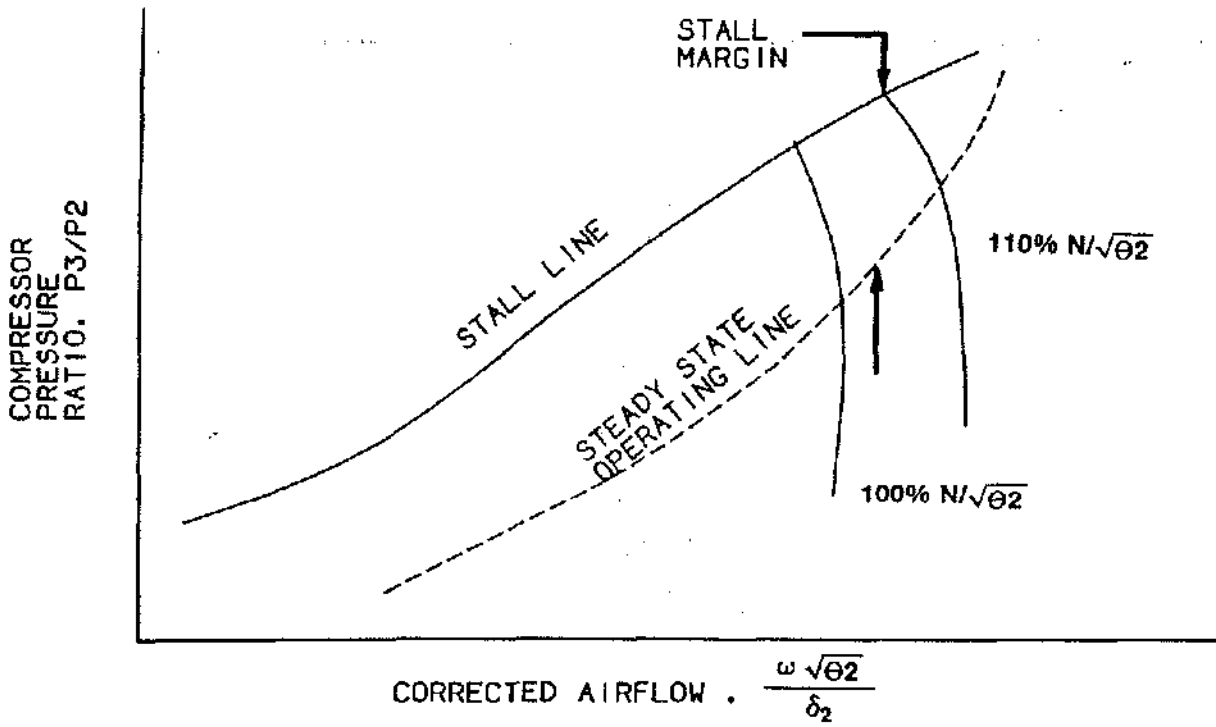


Figure 11.9 Basic Compressor Map

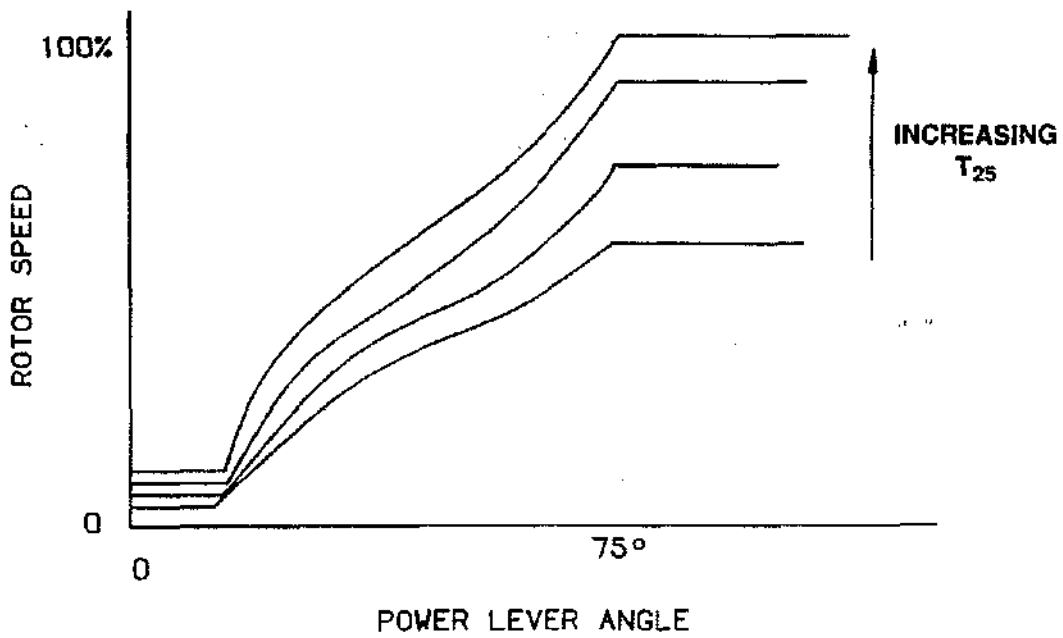


Figure 11.10. Rotor Speed Schedule

In designing core speed schedules, the designer must also take into account bleed air and horsepower extraction requirements. The core is required to drive all engine and aircraft mounted accessories on the gear box. Optimization of these schedules requires close integration between controls and cycle designers.

On modern turbofan engines, thrust is more accurately controlled by setting fan speed. This is because all of the airflow is pumped by the fan rotor. The core rotor only handles a portion of the air flow. Since fan and core speeds are coupled, thrust can still be accurately modulated by scheduling core speed as a function of PLA. Using the cycle deck to obtain an energy balance between core and fan speeds, for various conditions a speed-speed curve can be generated. This is a curve of corrected fan speed versus corrected core speed, or corrected core speed versus thrust. The controls designer uses this data to define a schedule similar to Figure 11.10. Temperature lines are now lines of constant compressor inlet temperature (CIT, T25) which is a function of T2 and fan speed.

Earlier turbofan engines such as TF39, CF6-6, and -50 used core speed control exclusively. (The pilot set EPR

or fan speed with the throttle.) Speed is affected by various parameters like engine component efficiencies and stack ups, altitude, mach number, schedule tolerances and deteriorations. Thus core speed is not an optimum manipulated variable to set fan speed. A transition was made for the F101, CFM56-2/-3, CF6-80A and -80C engines to provide a limited override of the core speed schedule. These override controls allow for direct scheduling of fan speed in a limited PLA range, usually in the takeoff or max climb PLA regions. Fan speed is typically controlled as a function of T2 which results in corrected fan speed control.

Acceleration and Deceleration Control One very important function of the control system is fuel scheduling for starting, accelerations (accel) and deceleration (decel) of the engine. The accel fuel schedule is designed to provide necessary fuel flow for smooth starting and rapid rotor acceleration. It must also maintain adequate compressor stall margin and transient overtemperature protection of turbine components. The decel schedule is designed to permit quick core speed reduction, while protecting from possible lean combustor blowouts. This is shown graphically in Figure 11.11.

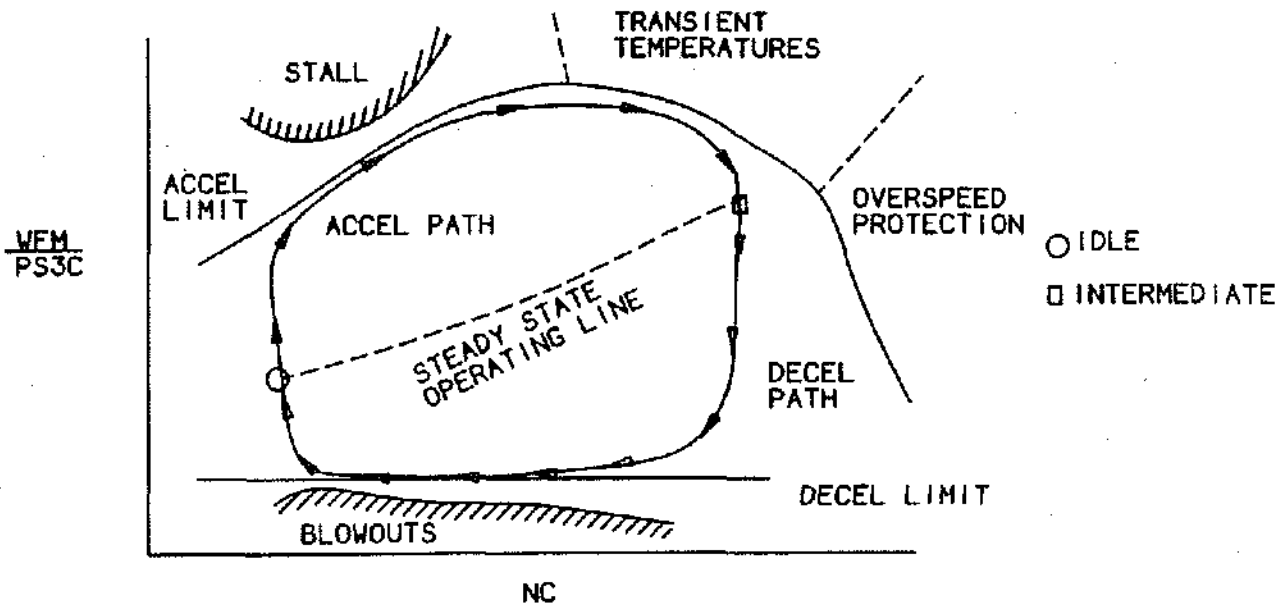


Figure 11.11 Acceleration/Deceleration Objectives

When an engine is at a steady state condition, there is an energy balance where the control meters fuel to maintain a constant rotor speed. In order to reach a higher steady state rotor speed, fuel flow must be increased to produce an unbalanced torque. It is this unbalanced torque which causes rotor acceleration. From the compressor map, the compressor pressure ratio is a function of corrected air-flow and speed. At a given steady state point, the required fuel flow is known from the cycle. Thus a map of corrected rotor speed and fuel flow can be used to determine compressor pressure ratio (CPR).

Basic studies have shown that because of this relationship acceleration of the core can be controlled most accurately by scheduling fuel flow over compressor discharge pressure (WF/PS3) as a function of corrected core speed. This gives the designer the best control over stall margin. Stall margin is defined as the margin between the operating point and the stall line. It is zero on the stall line. Design of an accel schedule requires definition of a WF/PS3 (fuel-air ratio) schedule which produces the fastest acceleration while maintaining sufficient stall margin and overtemperature protection.

A simplified typical accel fuel schedule is shown in Figure 11.12. Note that at a given corrected core speed (NCK) WF/PS3 varies according to CIT. Since the compressor is a corrected parameter machine, the accel schedule is also optimized through corrected fuel flow.

Designing a new acceleration schedule is a reverse process. Dynamic Analysis runs an engine (math) model with stall margin as an input to define initial accel schedule lines. Once the core is defined, extensive engine testing is accomplished to define the steady state stall line. This can also be defined as a line (band) of corrected WF/PS3 stall points for various corrected core speeds. The designer can work backwards from this data to refine the accel schedule. A stall limit line is defined with a minimum allowable stall margin. From here additional stackup tolerances and parameters are subtracted, which can consume stall margin (WF/PS3). Items in this category are open variable stator vanes (VSV's), compressor inlet distortion, deterioration, horsepower extraction and engine to engine variation of compressor components and turbine nozzle area (A4). Next the accel fuel schedule tolerance is subtracted. At this point, the tran-

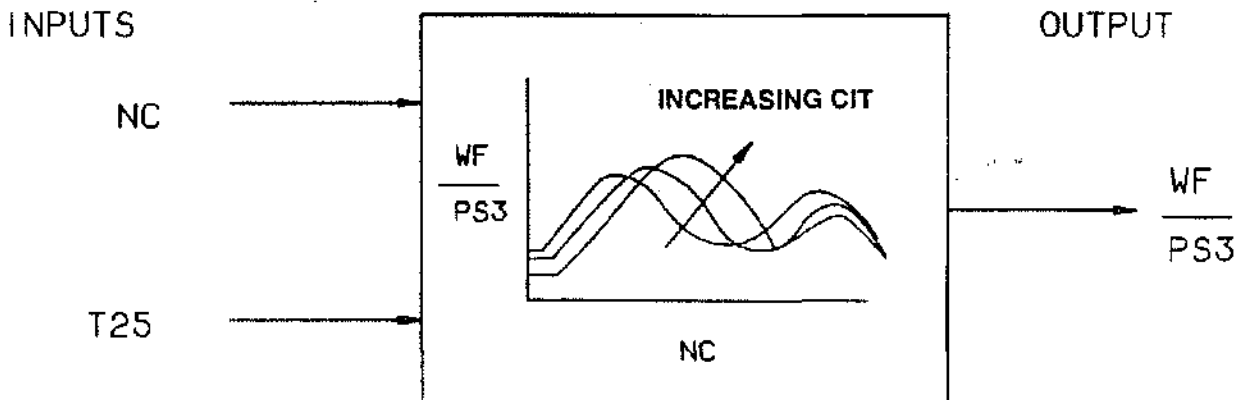


Figure 11.12 Typical Accel Fuel Schedule

sient cycle deck is used to optimize the schedule by running simulated transients at various flight or operating conditions. This also allows for checkout of interaction and effects of control loop dynamics. Additional optimization may also be required to assure compliance with FAA or military thrust transient requirements. This may involve changes in idle speed schedules, accel path, tolerances or other control dynamics.

It can be seen from Figure 11.12 that at high corrected core speeds the fuel schedule is "leaned out". These lines are designed by transient analysis to prevent turbine inlet temperature from exceeding design requirements.

The start schedule is just a low speed extension of the accel schedule. The design process for this schedule is similar to the accel schedule. Some unique considerations required to optimize this schedule are fuel-air ratios required to light off the burner at various altitude/temperature conditions, rich light off stalls, started assisted versus windmill starts, fired and unfired torque requirements and ground and air start time requirements. Other considerations are the speed to introduce fuel flow and sensitivity of a high speed compressor to low speed stalls. Usually extensive testing is performed on the engine to define the low speed stall line and the optimal start fuel schedule.

If the engine has bleed air extracted during an accel, energy available to accel the engine is lost. Also stall margin is increased. To recoup the lost accel time and offset the increased stall margin, the accel fuel schedule is normally enriched under bleed conditions. The amount of enrichment is usually a function of the percentage of core flow extracted.

The primary constraint for design of the decel schedule limit is blowout of the main combustor. Other important design considerations are decel times and possible speed hangups. Two different designs are used. The simplest approach is a constant WF/PS3 ratio. The other approach is to use a fraction of the accel fuel flow (usually 0.4 to 0.6).

Variable Stator Vane Control The primary objective of compressor design is to meet a high speed (takeoff or cruise) design point. Unfortunately a compressor designed for high efficiency at high speeds is also very inefficient and prone to stall at low speeds. At low corrected speeds the front stages of the compressor are pumping more airflow than the rear stages can handle. This raises the pressure ratio of the front stages driving them toward stall. The compressor stall line is effectively made up of a family of individual stall regions for each stage.

The stall phenomena of a compressor is the same as experienced on a wing. As the pressure rises across a stage, the effective angle of attack must increase to do more work on the fluid. As the limiting angle of attack is reached, as shown in Figure 11.13, flow begins to separate from the trailing edge upper surface. This causes a drop in the coefficient of lift (C_L), thus stage pressure ratio. Once a complete flow separation occurs, this chokes (limits) the flow path resulting in complete flow breakdown in the compressor. Following a corrected speed line of the compressor map in Figure 11.9, it is also evident that increased pressure ratio will result in stall.

There are three conventional solutions to deal with this stage mismatch. They are compressor bleeds, dual rotors and variable guide or stator vanes (VSV). If a bleed valve is placed in the front stages of the compressor, it is possible to open at low speeds and vent excess airflow overboard. For high pressure ratio compressors there is usually no "best" location for a single bleed, therefore, multiple bleeds are needed. The disadvantage is the lower propulsive efficiency because energy is used to pump the air up to the bleed point, then dump through the valve. The bleed concept is used on some GE engines along with VSV's to improve starting stall margin.

If the compressor is split into two halves, each driven by a separate turbine, the stage matching problem can sometimes be improved. At low speeds, the front stages runs at a lower speed thus pumping less flow. Normally an intercompressor bleed is still required to match high altitude and transient flow maps.

Since the basic problem is caused by the front stages of the compressor, another solution is to limit the low speed pumping capability of these stages. By closing down the inlet guide vanes to each stage, the angle of attack, airflow pumped and therefore stage pressure ratio is reduced. Figure 11.14 shows two separate stall lines of fixed stator compressors designed for high and low pressure ratios. The use of variable stator vanes allows the designer to tailor high speed-high pressure ratio compressor to operate like a low pressure ratio machine at low speeds. VSV's are employed on most GE engines since the J79.

To optimize the VSV position, tests are run to define the stall point for each stage at various corrected core speeds. This process is applied to each successive stage back to the point where the low speed pumping problem no longer exists. The F101/CFM56 nine stage compressor, for example, only varies the first four stages of compression. With this data, schedules can be developed defining stator angle versus corrected core speed for each stage. These schedules are designed to maintain a desired stall margin and maximize compressor efficiency.

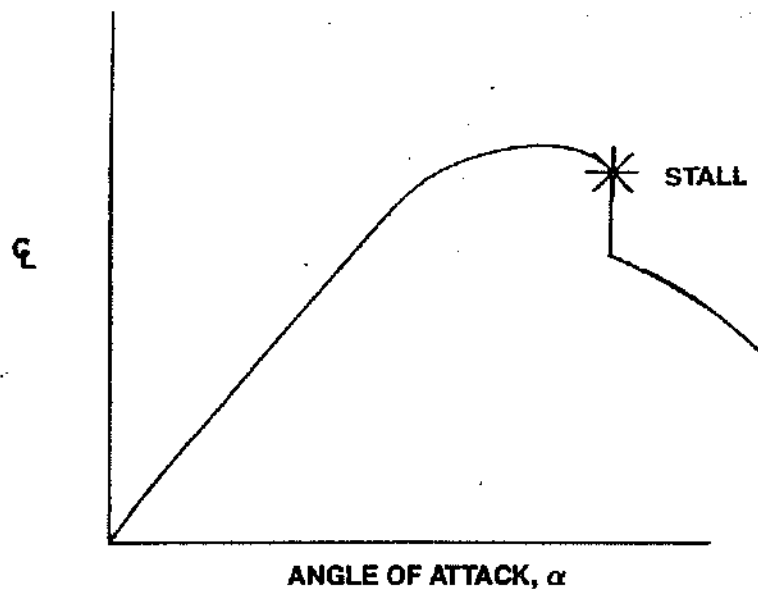


Figure 11.13 Effect of Angle of Attack on an Airfoil

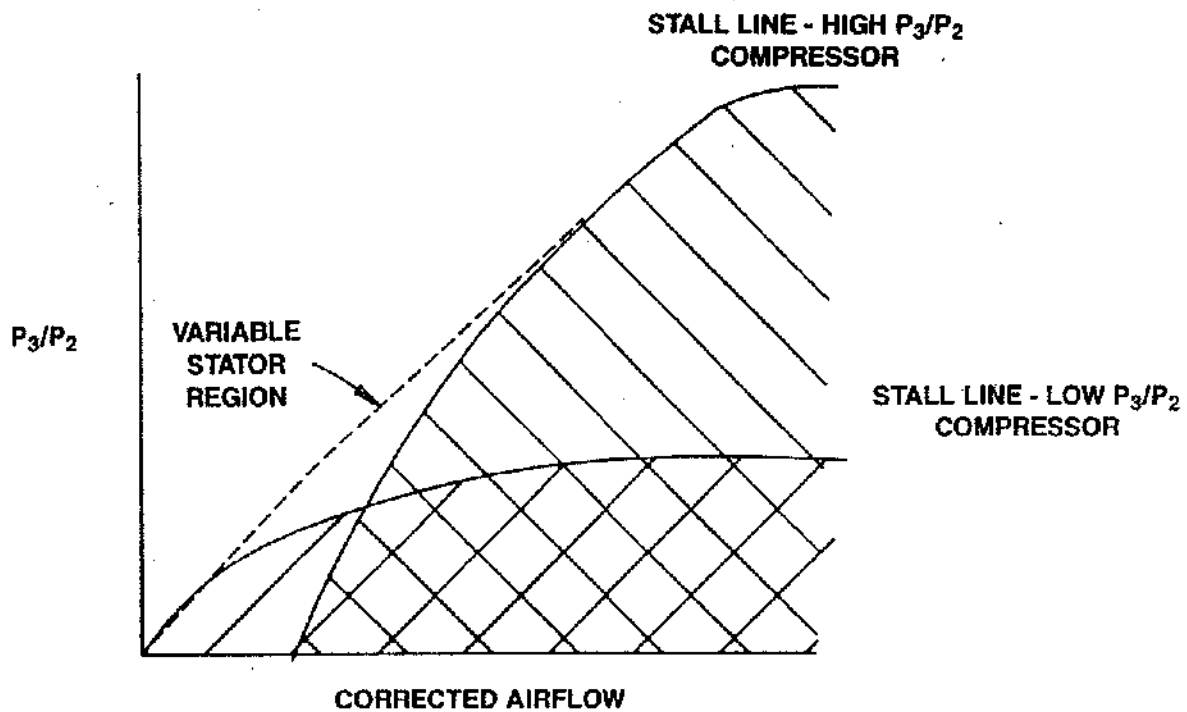


Figure 11.14 Fixed Stator Compressor Stall Lines

Definition of these schedules also requires factoring in engine deterioration effects, engine to engine variation and control tolerances. Once the schedules are optimized, the stator vanes can be mechanically linked together so a single actuation point will position each stage correctly. The front stages will have a wider positioning range than the rear stages. Thus, the stator vane rotation decreases as you get further into the compressor.

A typical VSV schedule is shown in Figure 11.15. Normally the angle called out on these schedules is only the first variable stage. Note also a failsafe can be designed into the schedule if a T25 sensor fails to a full cold shift. The normal failure mode of the T25 sensor is to indicate cold (-65°F to -80°F). The failsafe flat allows for adequate compressor performance during standard day conditions when the VSV's would be too far open otherwise.

Speed and CDP Min and Max Limiting Control systems are also designed to assure both maximum and minimum limiting of important parameters. Limiting the maximum values of the engine speed and compressor discharge pressure (CDP or PS3) is essential to prevent

catastrophic failures. Maintaining a minimum value for these parameters is usually required to allow the engine to meet external demands. The system is designed so these limits are included in a hierarchy which selects the controlling loop. Figure 11.16 shows the ten control loops used to select main fuel flow for the F110-100 engine. The selection of the controlling loop is accomplished by a series of minimum and maximum selectors.

Note that the min core speed and min PS3 limits are fed into a max selector, while max core speed and PS3 are fed into a min selector. The selection process is prioritized such that these limits will not be exceeded. The actual mechanization can be hydromechanical or electronic.

The purpose of limiting the maximum core speed is to protect the turbomachinery. Use of this limiter is not required unless the normal speed scheduling is malfunctioning. Typically the accel schedule is designed to limit WF/PS3 ratios at high core speeds. The schedule sets a value below the required to run (operating) line which reduces engine speed. If this system operates normally, speed will be reduced before an overspeed can occur. As

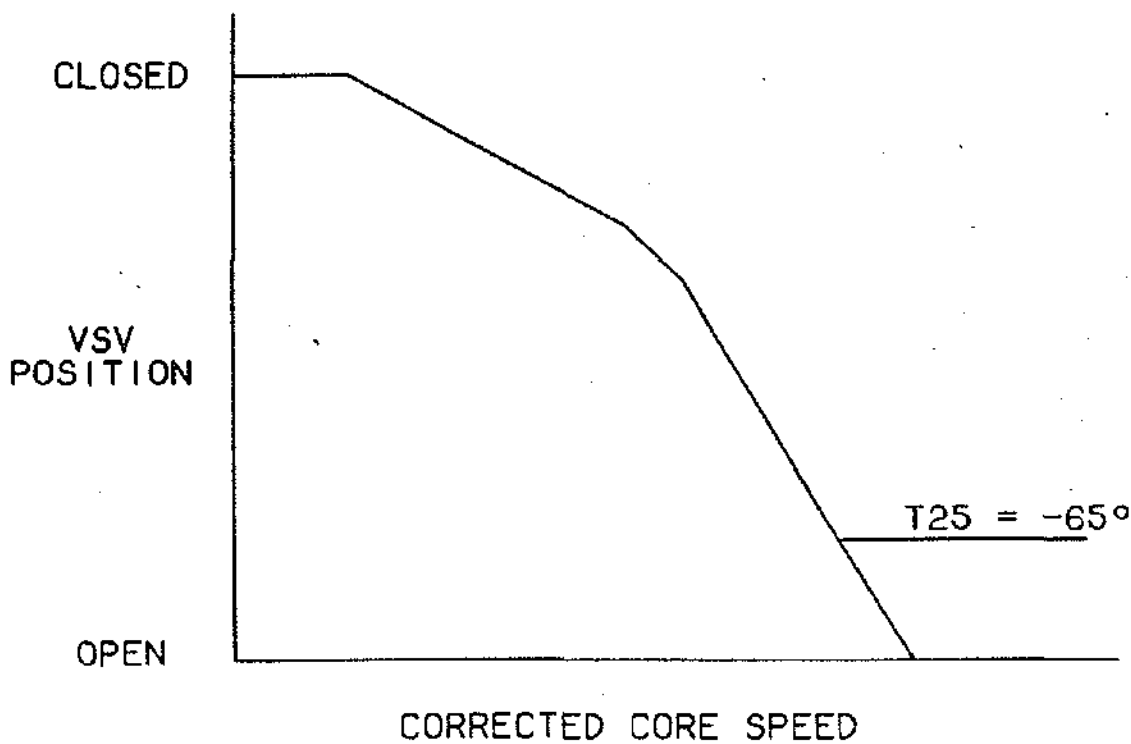


Figure 11.15 Typical VSV Schedule

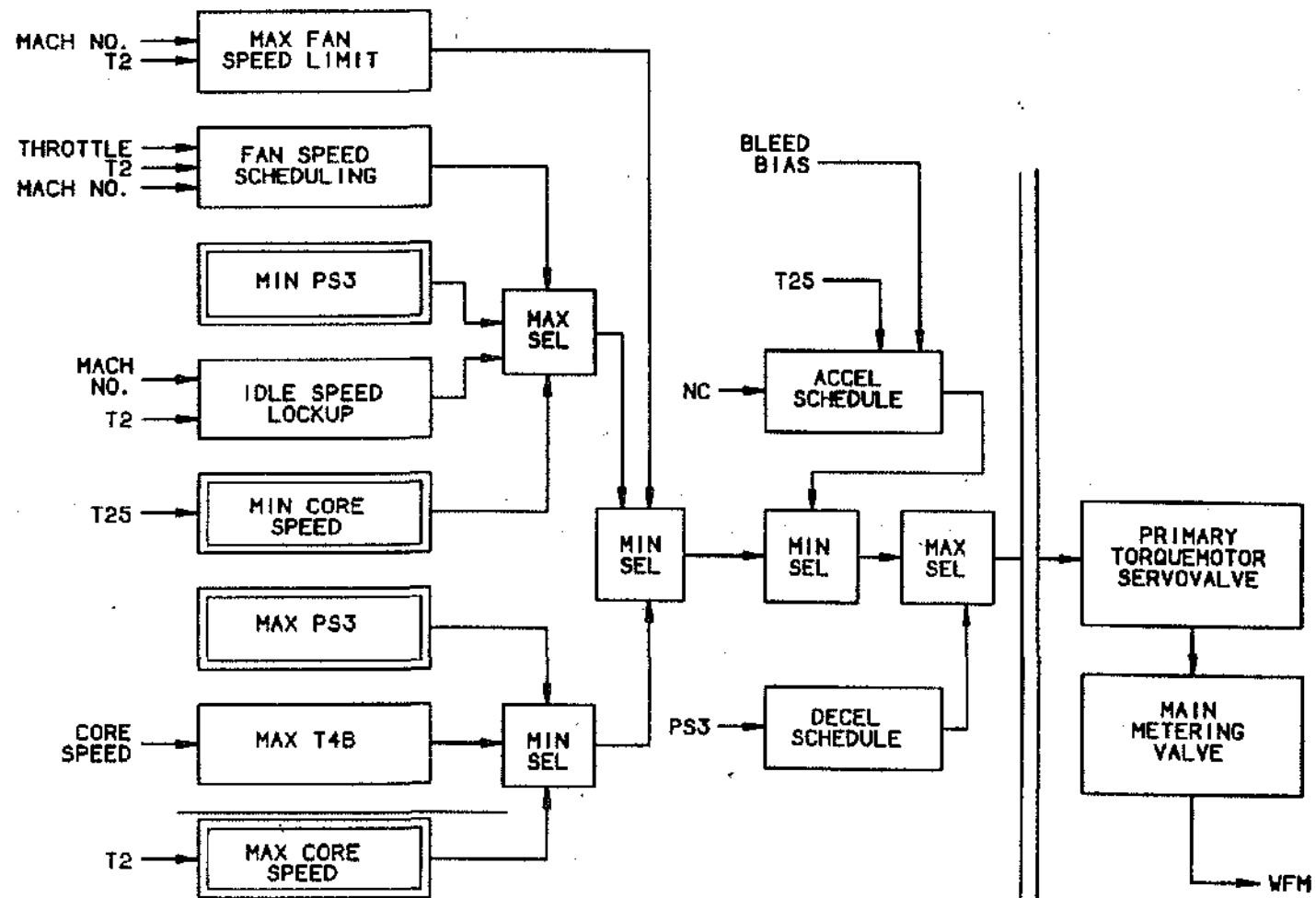


Figure 11.16 F110-100 Main Engine Fuel Flow-Primary Mode

a final line of protection, overspeed trip mechanisms are designed into the hydromechanical control to shut off fuel flow in case of a run away speed condition. Capability is also designed into the system to "recycle" and attempt a restart of the engine after the trip is actuated.

With today's sophisticated electronic controls, limiting of maximum core speed and fan speed can be added electronically. The added flexibility of electronic controls also allows for complex limiting functions which are dependent on various inputs. For example limiting of the minimum core speed (idle) is required to meet various operational constraints. Some are: acceleration time requirements, min idle thrust, stall avoidance on snap accels, horsepower extraction and bleed requirements. Commercial applications may also require separate ground and flight idle schedules due to unique FAA regulations. Minimum core speed is usually scheduled as a function of compressor inlet temperature (T25).

The aircraft environmental control system operates on bleed air from the engine. For this system to operate properly, the bleed air pressure must be above some minimum level. Normally, on the ground and at low alti-

tudes, speed scheduling will provide adequate bleed pressure. Operation at high altitudes and low PLA's (speeds) can cause the supplied bleed pressure to fall below the minimum required. This can be remedied by adding a function to sense PS3 and maintain a minimum value. If PS3 starts to fall below min, the control will override the speed control and increase speed to keep PS3 at the min setting.

Due to high ram pressures, when an aircraft operates in the lower right corner of the flight envelope, PS3 can get very high. If design limits are exceeded the structural integrity of the rear frame and combustion casing is in jeopardy. To protect the engine, a max CDP limiter must be incorporated in the control. This is normally accomplished by introducing a "false" PS3 into the acceleration schedule, rather than add another complex function. At high PS3's a lower value of PS3 is used in calculating acceleration fuel flow. Figure 11.17 shows how this is accomplished. The actual PS3 and PS3' are equal up to a point. Then as actual PS3 goes up PS3' is reduced. This causes the accel schedule to lean out until it eventually intersects the operating line, limiting the engine. The engine will settle at

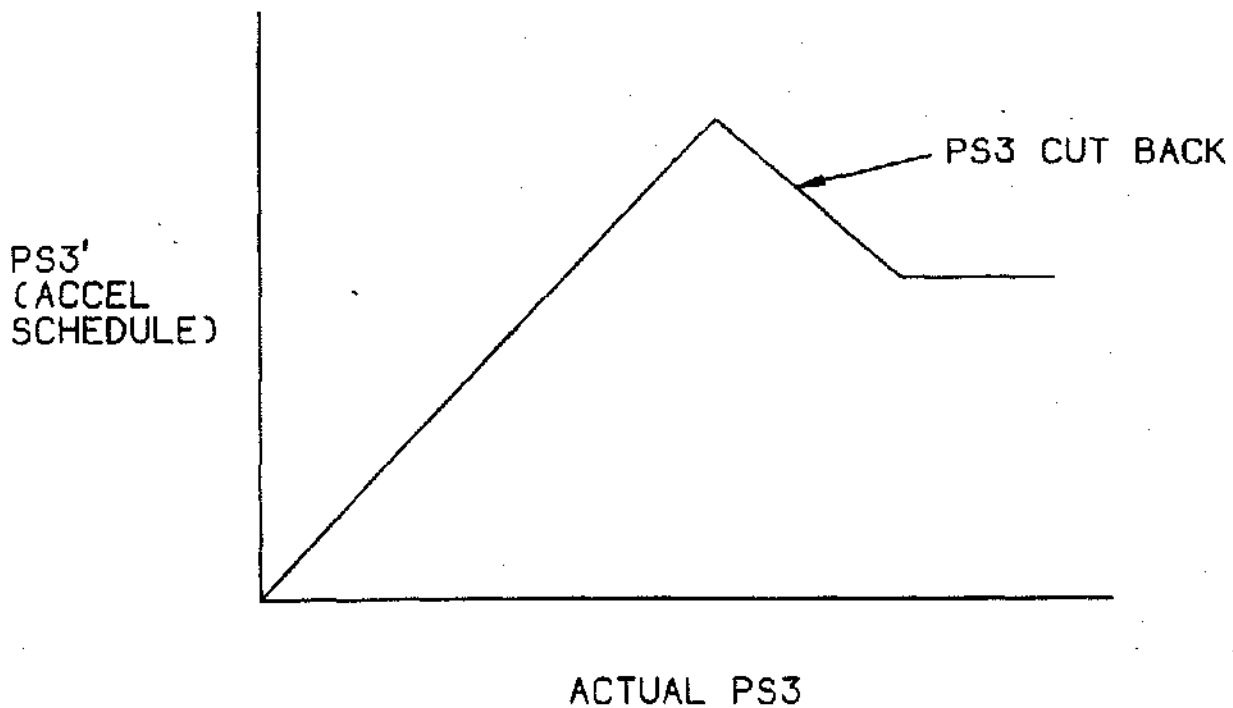


Figure 11.17 Maximum PS3 Limiting

a new operating line with a lower actual PS3. On more modern engines PS3 levels are limited electronically by sensing the pressure and adjusting fuel flow accordingly.

Two other control limits deserve mention in this section, i.e., min and max fuel flow. The maximum fuel flow is a fixed value set by the maximum safe flow capability of the fuel pump. The min fuel flow limit does not allow fuel flow below a prescribed level and can override the accel or decel schedules. This value is set to assure adequate fuel flow for lightoff during ground and air starting.

COMMERCIAL CONTROLS OBJECTIVES

Some control system functions and strategies are unique to commercial engine applications. These include power management control, selectable idle thrust, modulated idle speed, variable bleed valves (VBV's), turbine clearance control, core rotor active clearance control, and reverse thrust scheduling. With the exception of the last item, the objectives of these functions are to provide the minimum fuel consumption for the particular aircraft application and mission.

Power Management Control Performance of commercial aircraft engines are generally specified to the airframe manufacturer for several key thrust settings, or ratings. These ratings include takeoff thrust (TO), go-around thrust (GA), maximum climb thrust (MCL) and maximum continuous thrust (MCT). Some of the design criteria for commercial controls systems are integral to these rating structures, for instance:

- Takeoff thrust (or corrected fan speed) and go-around thrust must be achievable at all takeoff flight conditions
- Takeoff thrust should occur at approximately the same throttle lever angle at any takeoff flight condition
- Full throttle thrust must not exceed takeoff rated thrust by more than a minimum amount
- MCL and MCT ratings are usually required to be a fixed throttle angle regardless of flight condition, i.e. a maximum performance climb from 1500 feet to maximum aircraft operating altitude can be performed without throttle resets

Takeoff rated thrust is the highest thrust rating quoted by the engine manufacturer for operational use by the aircraft manufacturer. The thrust rating is based on a maxi-

mum allowable exhaust gas temperature (EGT) level at which the engine is allowed to operate for five (5) minutes. Engine thermodynamics are such that for a constant EGT value, engine thrust varies inversely with ambient temperature (see Figure 11.18). Typically, the max operating EGT level for an engine model is specified at sea level altitude and a specific ambient temperature, which is higher than standard atmosphere conditions (usually between +27 to +36 degrees F. delta temperature). This condition is referred to as "corner point day". Corner point day is established by the aircraft manufacturer to cover hot day aircraft performance requirements with no operating penalty, i.e. max payload, range, takeoff field length, etc.

At ambient temperatures below corner point takeoff thrust is a constant value for a given altitude, or so called "flat rated" (see Figure 11.19). At temperatures above corner point takeoff thrust rating is reduced to hold EGT constant at the corner point value (see Figure 11.19). The constant corrected thrust characteristic of flat-rating results in a constant takeoff corrected fan speed for a given altitude (see Figure 11.20). The takeoff thrust available at altitudes other than sea level is a function of the particular engine cycle performance at the corner point EGT level at the particular altitude.

Takeoff power management is normally developed and certified by analysis of test data taken during aircraft certification flight testing. A typical power management chart for takeoff rating is shown in Figure 11.21. This chart is in the form used in aircraft flight manuals, with airport outside air temperature (OAT) on the x-axis and Takeoff rated Fan Speed (%N1) shown on the y-axis. Note that above the corner point temperatures for each altitude, all the altitude lines virtually collapse to one line, i.e. a constant EGT value.

Go-around thrust is essentially an in-flight takeoff rating used during missed approaches or aborted landings. While takeoff power management is based on setting power by 0.1 aircraft Mach number on takeoff roll, go-around thrust is based on approach airspeeds of 0.25 to 0.3 Mach number.

In recent years, some airlines and aircraft manufacturers have negotiated increased takeoff and max continuous thrust levels in certain areas of the aircraft operating envelope to tailor an the aircraft performance for some particular combination of airport elevation, ambient temperature, and flight route. The resulting rating, typically called a "bump" rating, allows the customer to operate the engine at increased thrust and EGT levels, typically on hot days, at high altitude airports. This permits the aircraft to takeoff with higher payload or fly a

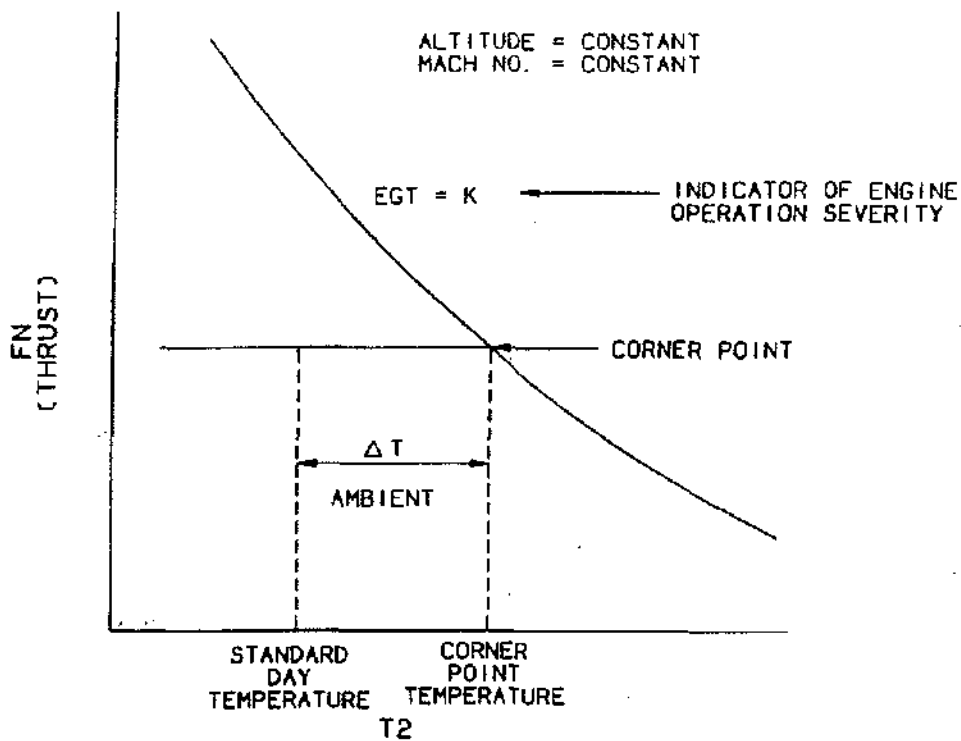


Figure 11.18 Engine Thermodynamics

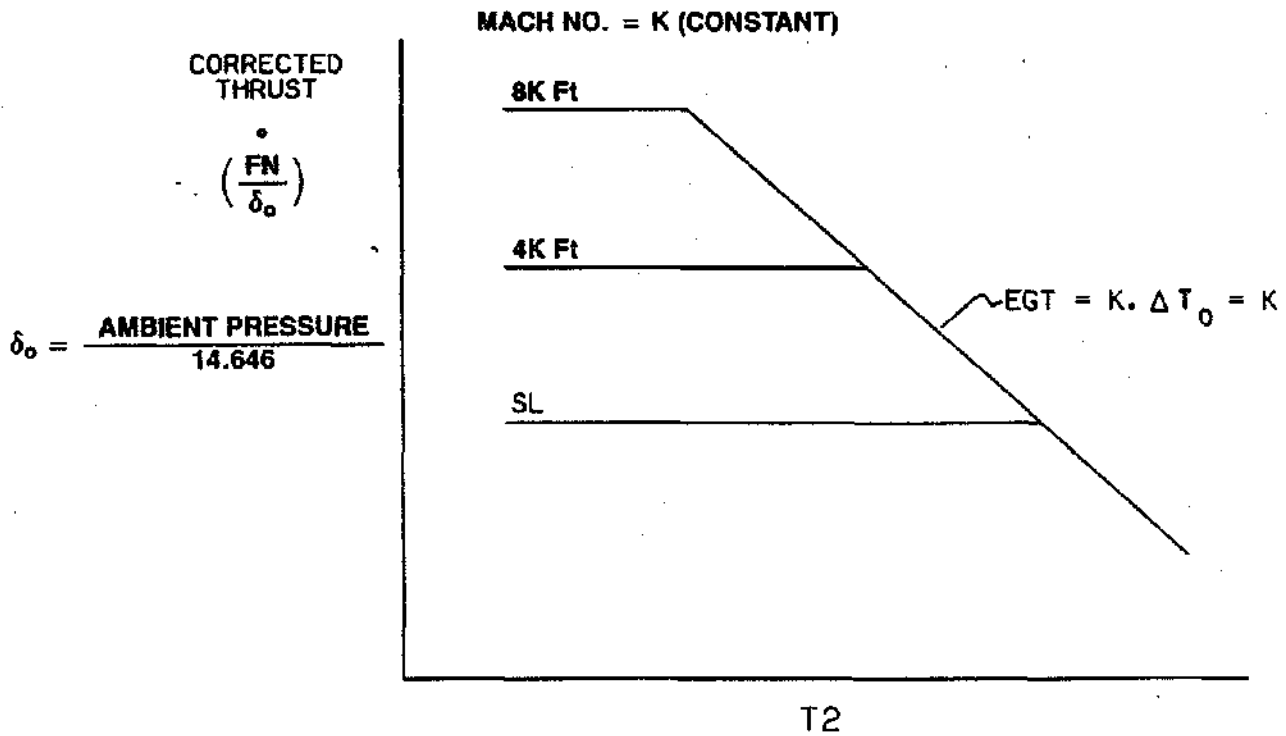


Figure 11.19 Altitude Effects on Take-off Rating

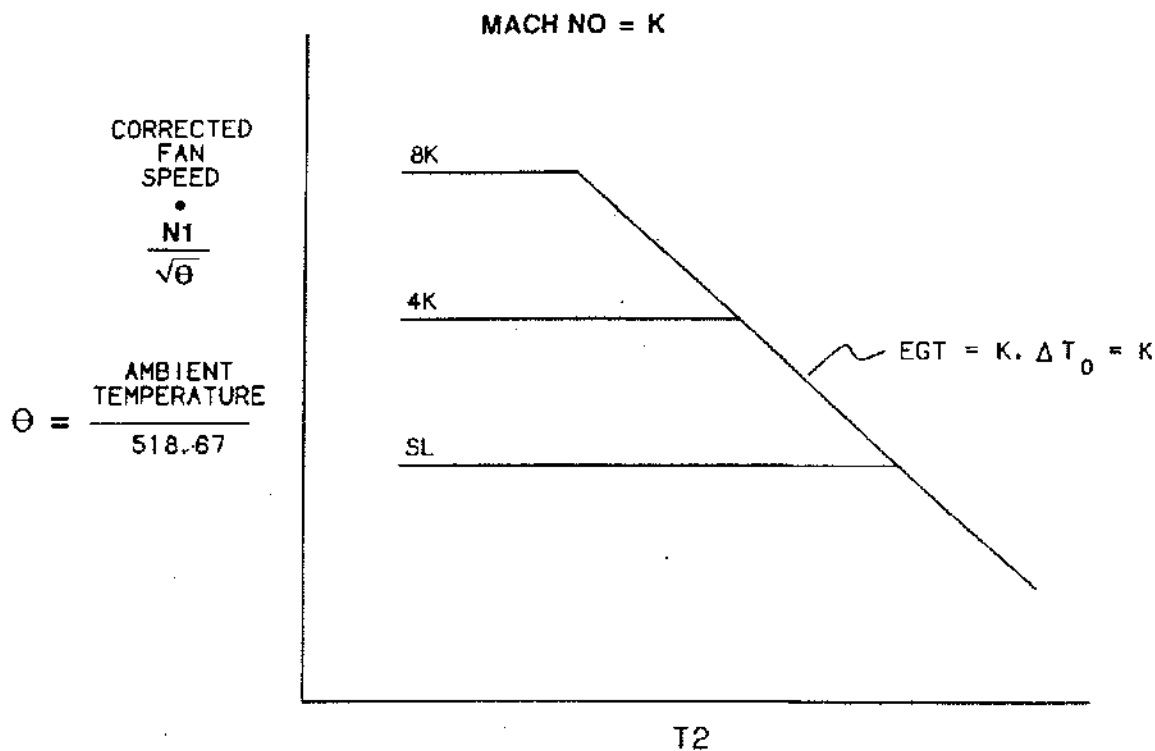


Figure 11.20 Altitude Effects on Take-off Rating

longer flight route under these conditions than would be allowable using the normal "non-bumped" thrust rating. An example of this is the takeoff rating of the CFM56-3-B1 engine on the 737-300, which is tailored for up to 7-8% increase in hot day takeoff thrust at airport elevations between 3000 ft. and 10000 ft. such as Denver (5330 ft.), Albuquerque (5350 ft.), and Mexico City (7340 ft.). Hot day conditions, i.e. above corner point temperature, at these airports are prevalent during late spring, summer, and early fall, so to maximize aircraft payload capability for long range flights an increased takeoff thrust is desirable. The "bump" rating meets these needs nicely, however, the increased complexity of the resulting rating must be factored into the control schedule design. Figure 11.22 shows the complexity of a "bumped" takeoff rating. This chart represents the takeoff corrected fan speed settings versus ambient temperature relationship for this rating. Note that the corrected fan speed at a constant altitude below corner point temperature is constant, which results in constant thrust. Note also that the constant altitude lines do not collapse to one constant EGT line until well beyond the corner point temperatures. An approximate constant EGT line is illustrated on the chart; the rating points to the right of this line are "bumped" above normal.

MCT rating, which is normally defined by the aircraft manufacturer as the thrust needed for one-engine out climb performance above a specified terrain elevation, is the highest allowable thrust level at which the engine may be operated continuously. The corner point temperature for MCT is usually lower than for takeoff, typically a delta ambient temperature above standard day of +18°F. The EGT level for MCT is normally a constant value for a defined climb profile on a corner point day up to the terrain clearance elevation. Above that altitude, MCT rating, and the associated EGT level, decrease to a value equivalent to MCL rating. MCL rating, on the other hand, is the thrust required by the aircraft manufacturer to meet specified aircraft climb performance with all engines operating. Power management for these two ratings are developed and certified during aircraft certification flight testing. A typical power management chart for MCL is shown in Figure 11.23 and 11.24. Arriving at a power setting fan speed for max climb (or max continuous) requires that the minimum N1 value be determined between the two charts.

It can be seen from the above discussion of the complexity of the various thrust ratings, a control system which meets the above controls design criteria must include

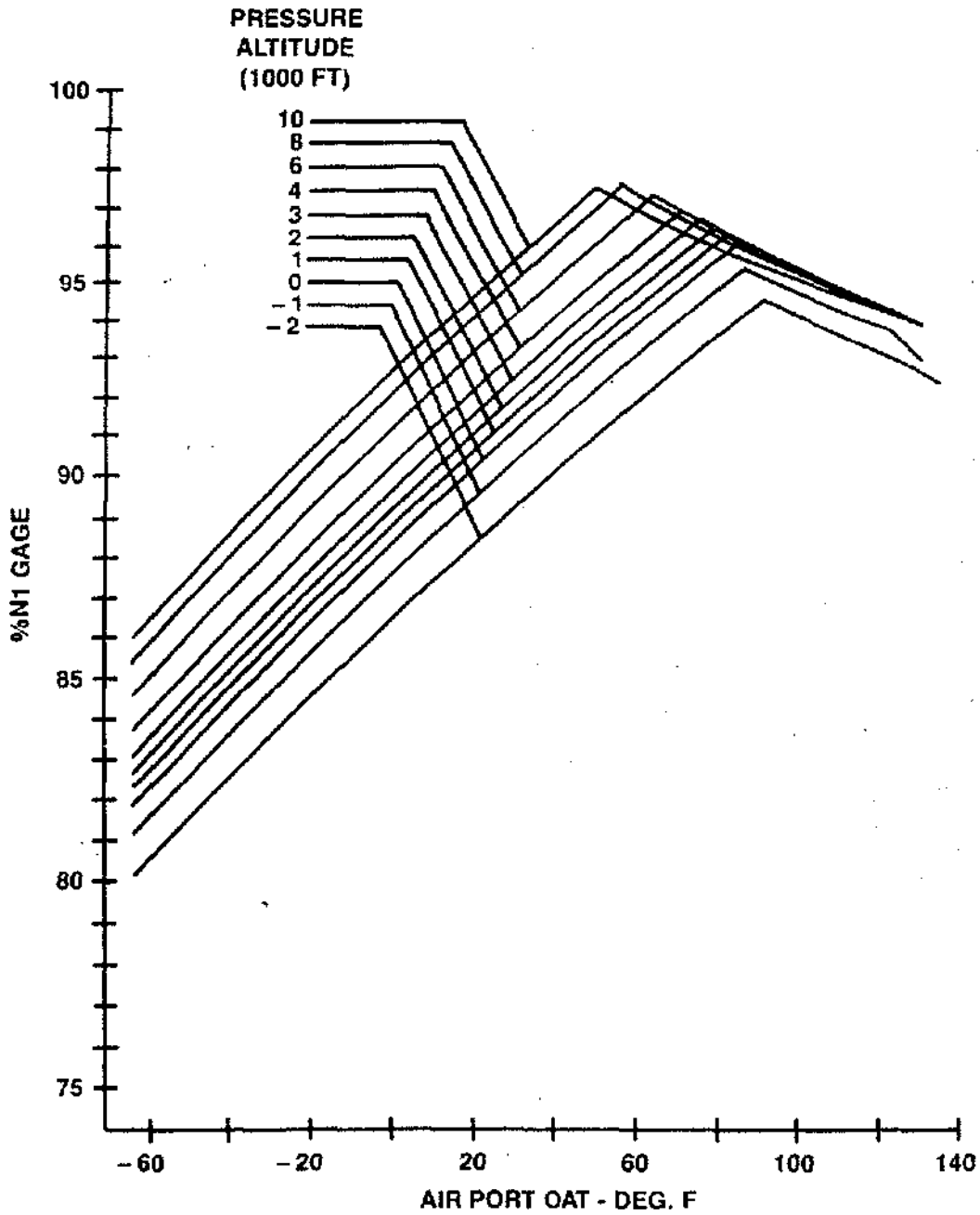


Figure 11.21 Typical Take-off Power Management Chart

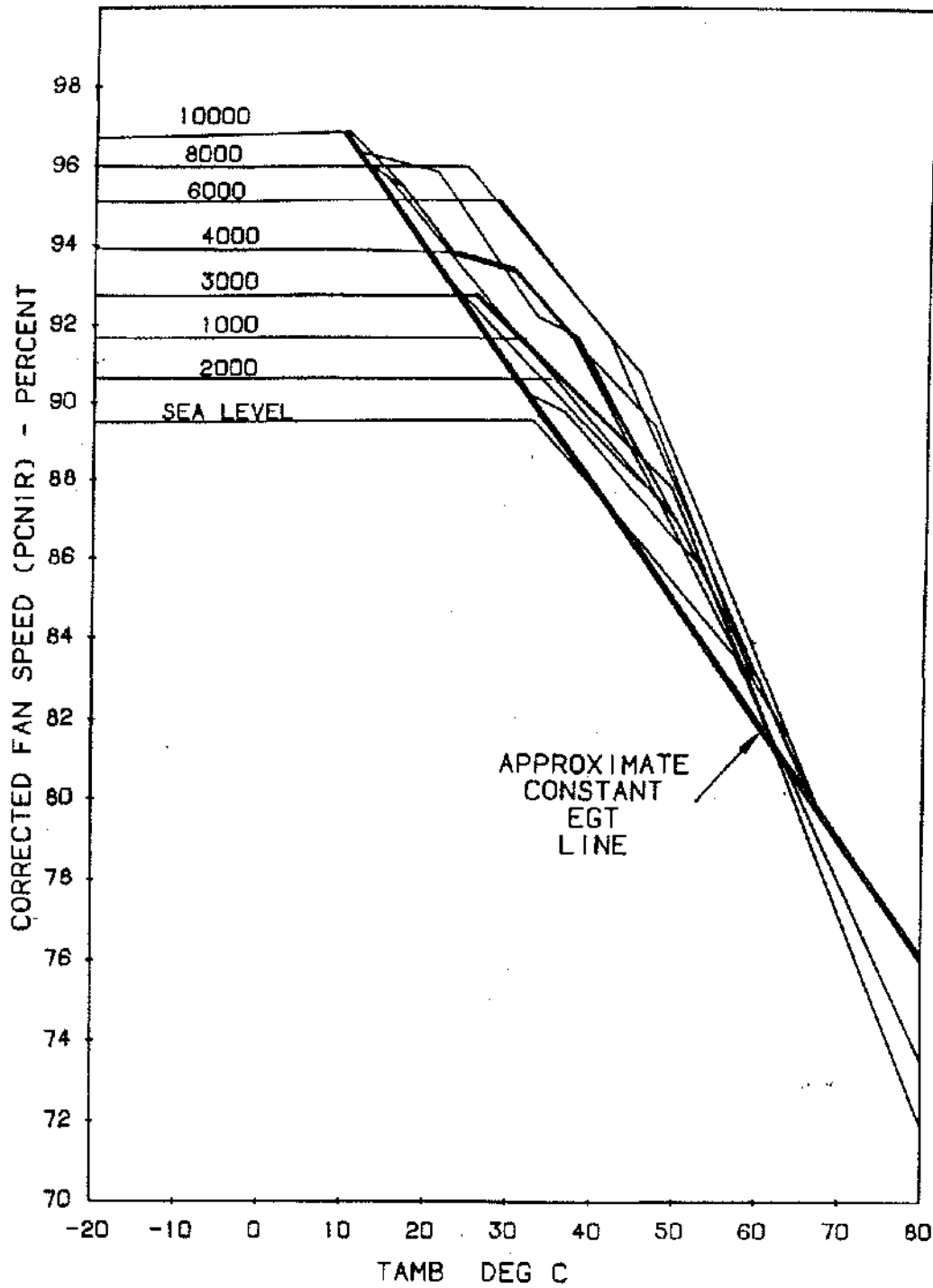


Figure 11.22 "Bumped" Take-off Rating

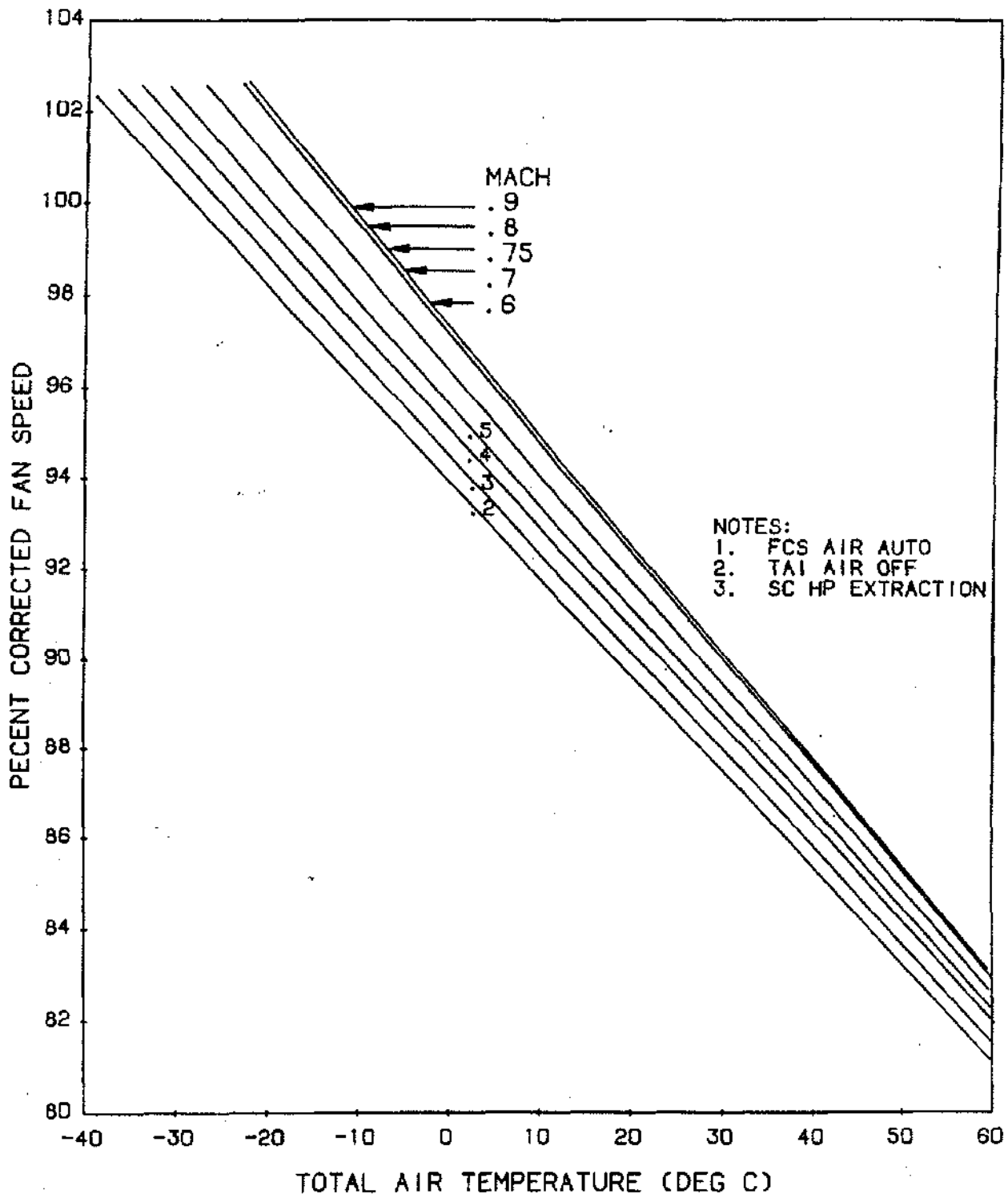


Figure 11.23 Max Climb Rating (Mach No., Temperature)

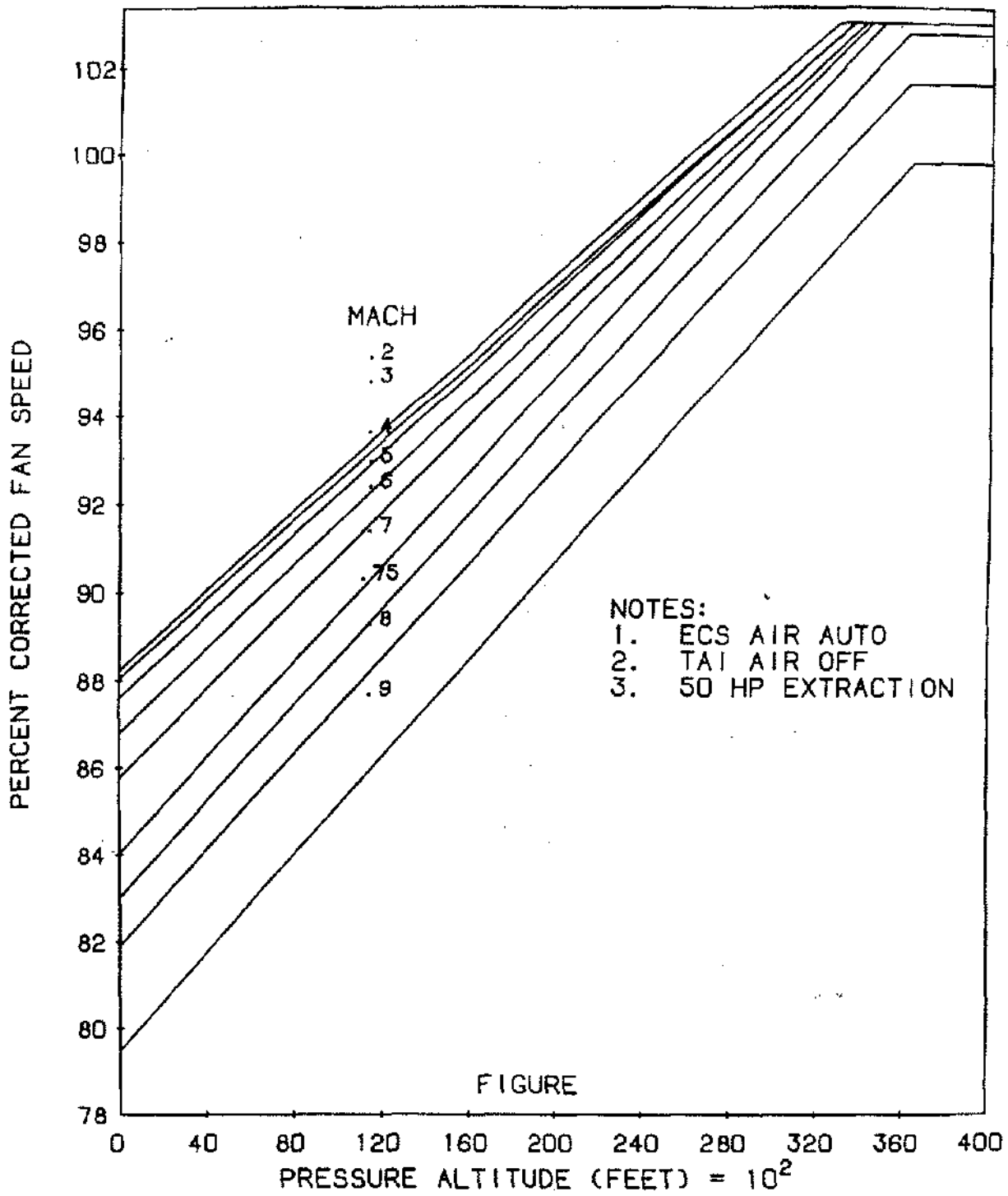


Figure 11.24 Max Climb Rating (Mach No. Altitude)

power management architecture and have input signals for the essential sensed parameters. Of particular importance is the direct measurement and accurate control of the primary thrust setting parameter, fan speed (N_1). To accomplish this objective, commercial control systems designed in the mid 1970's included a limited authority fan speed control called a Power Management Control (PMC).

Early commercial control system designs, such as the CF6-6 and -50, had a simple hydromechanical core speed control, which set a given N_2 at a PLA, regardless of ambient temperature or altitude. Power management charts for aircraft which used these engines were still based on setting a fan speed as a function of ambient temperature, altitude, or total air temperature, altitude and aircraft Mach number. Setting power on these early commercial engines required that the flight crew determine the appropriate N_1 setting for the given takeoff or climb conditions from a flight manual chart or via a cockpit thrust management computer. The crew then set the throttles until the desired N_1 had been obtained. The control system schedules were designed to ensure that adequate N_2 speed could be achieved to meet power

management N_1 requirements at any flight condition in the aircraft operating envelope.

First generation PMC's, like the CFM56-2 and -3, are analog electronic controls with inputs signals of N_1 , PLA, fan inlet temperature and fan inlet static pressure. The main output signal is a feedback error signal to the hydromechanical N_2 control torque motor to trim the N_2 demand. Early PMC's have limited interface with aircraft systems except for on/off function, PMC inoperative indication, and N_1 demand signal to the cockpit. Figure 11.25 shows a schematic of the corrected N_1 (NIK) speed governor system in the CFM56 analog electrical PMC. Scheduling of NIK is set by PLA, biased by inlet static pressure (P_{12}), and limited by inlet total temperature (T_{12}). A block diagram of this PMC is shown in Figure 11.26.

Later generation PMC's are digital electronic designs with more sophisticated power management architecture, made possible by direct communication of the PMC with aircraft air data computer systems, etc. via a digital data bus. Digital PMC's receive aircraft Mach number, total pressure, total air temperature, and static

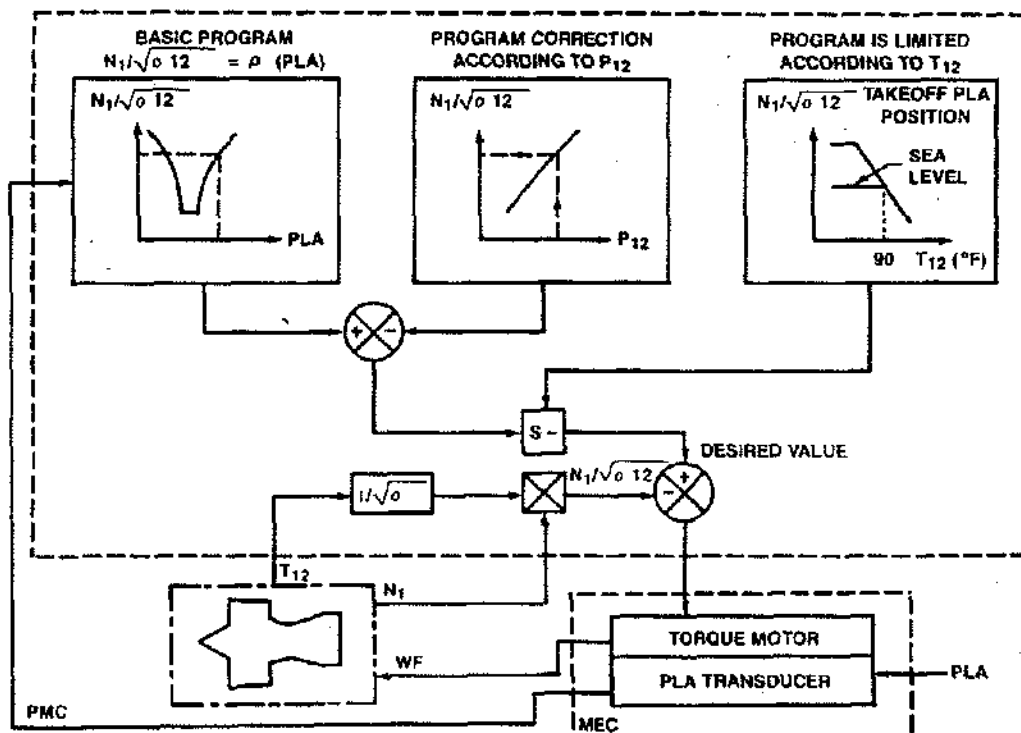


Figure 11.25 N_1K Speed Governing System

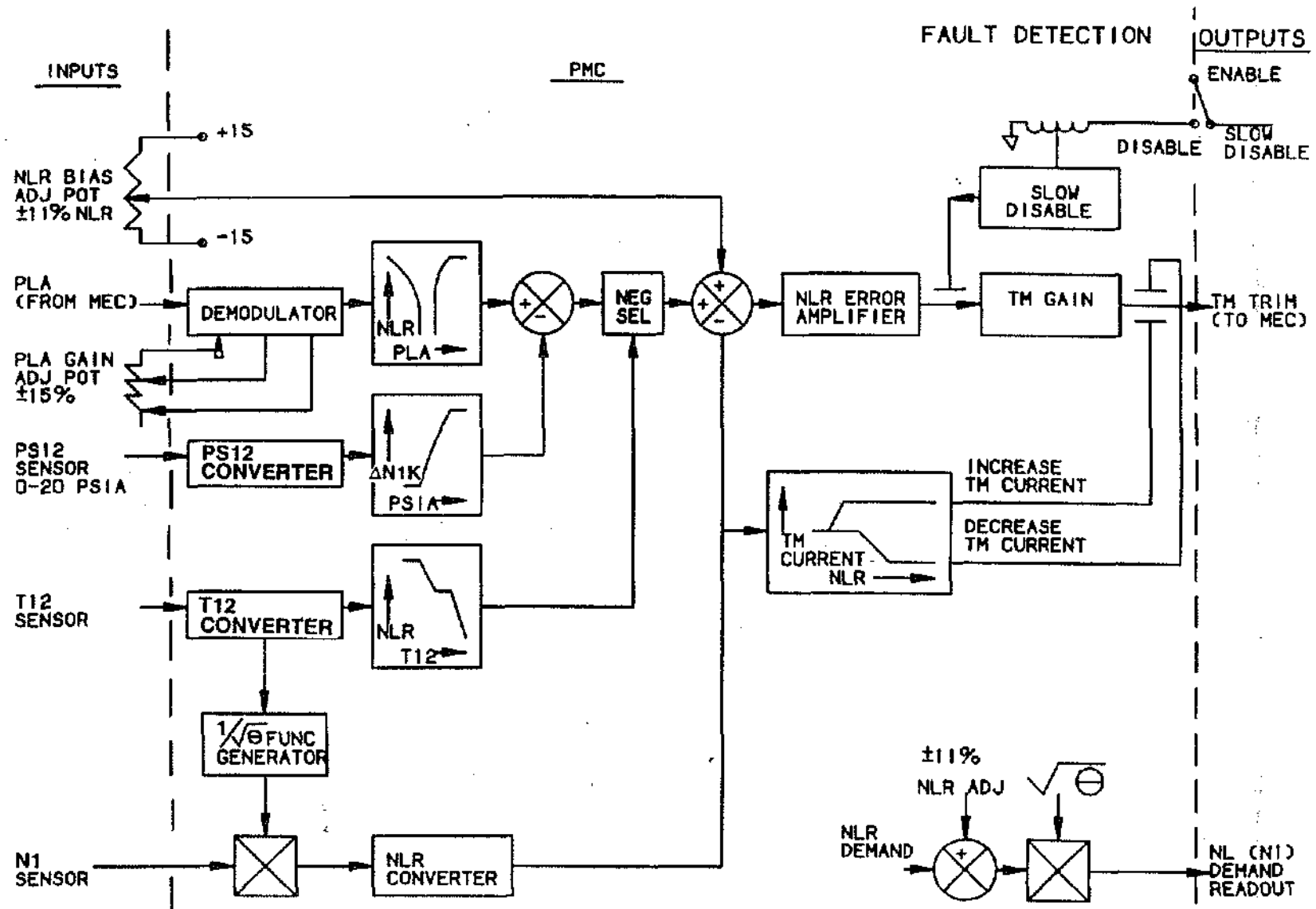


Figure 11.26 PMC Block Diagram

pressure (altitude) via the data bus. This system allows direct implementation of power management tables into the PMC. Rating logic, an example (-80A PMC) of which is shown in Figure 11.27, is significantly more complex in the newer digital PMC's.

Commercial control systems with PMC's still maintain a full function hydromechanical core speed control which governs core speed, schedules transient fuel flow, schedules engine variable geometry, and, in some cases, controls turbine clearance control valves. Commercial aircraft can still be dispatched and operated with the engine's PMC's inoperative should the need arise. Benefits of the PMC/MEC control system over hydromechanical control only are:

- Improved engine operational characteristics
 - Reduced takeoff N1 and EGT overshoot
 - Control scheduling matched to aircraft thrust requirements, power management
 - Reduced mission fuel burn
 - Improve engine on-wing life
- Reduced pilot workload
 - Reduced throttle stagger
 - Single throttle setting for takeoff and climb
- Improved aircraft/engine integration
 - Autothrottle system
 - Maintenance systems/ground test

Since the PMC is designed to incorporate power management architecture into control schedules, today's control system designers must work closely with performance analysis group to ensure that engine thrust rating logic is properly implemented in the control. This requires a great deal of integration between the two engineering functions, not only during the design of the control system, but also throughout the development and certification flight test programs, culminating in certification of the engine model on a particular aircraft.

Idle Speed Control and Scheduling Most commercial control systems have at least two idle speed control schedules, which normally are selectable by an aircraft input signal. Generally, a minimum idle speed schedule and an approach idle speed schedule are provided in the control system. On engines with a PMC/MEC control system, these schedules are usually a corrected core speed schedule implemented in the hydromechanical control. The idle speed schedules are usually negotiated between the engine manufacturer and the airframe manufacturer to meet certain objectives. In broad terms, the requirements used to define idle speed schedules are as follows:

- Idle speed on the ground must be less than a prescribed max thrust (usually around 4 to 6% of takeoff thrust) for minimum brake wear and positive aircraft control on wet or icy runways and taxiways. Ground idle settings are generally lower on recently certified commercial aircraft. Ground idle speed on cold days is limited by a minimum physical core speed stop in the control system, required to keep engine-driven aircraft electrical generators operating properly.
- Idle speed during descent must meet a combination of objectives: (a) must be low enough to provide minimum possible fuel burn during descent, (b) must be high enough to ensure adequate engine bleed pressure and flow capability to power aircraft air conditioning and pressurization systems, (c) must be low enough to provide minimum level of thrust required to meet emergency descent profile (in case of aircraft cabin decompression) time requirements compatible with aircraft emergency oxygen system capacity, (d) must be high enough to provide adequate thrust response from idle to meet aircraft performance needs

As can be seen, there are conflicting objectives for defining the idle setting for descent. In most cases, trade-offs are required to arrive at a compromise idle speed schedule which meets the most important objectives. The resulting schedule sometimes requires a separate mechanism in the control with pressure and temperature inputs. In MEC's, this mechanization takes the form of an additional 3-dimensional cam surface. This is sometimes referred to as a "modulated" idle schedule. A comparison of idle descent paths for typical approach and minimum idle schedules is shown in Figure 11.28. The unmodulated min idle case shown is the characteristic which would have resulted, if a modulated idle schedule cam had not been incorporated into the control. Idle speed during approach and landing is generally a higher thrust setting than the idle thrust setting for descent and ground taxi operation. Typical values for approach idle thrust range from 8% to 15% of takeoff thrust.

Approach idle is determined, for the most part, by the go-around thrust (FAA) requirements for the particular aircraft/engine application. The FAA regulations require that for the maximum certified landing weight of the aircraft, sufficient thrust must be available eight (8) seconds after initiating an aborted approach/go-around maneuver from approach idle to arrest aircraft descent and establish a specified aircraft climb angle. The go-around requirement is usually considered for a case of maximum landing altitude, minimum landing airspeed, maximum customer bleed extraction, and maximum accessory horsepower extraction from the engine. All of these factors tend to reduce engine thrust response. The

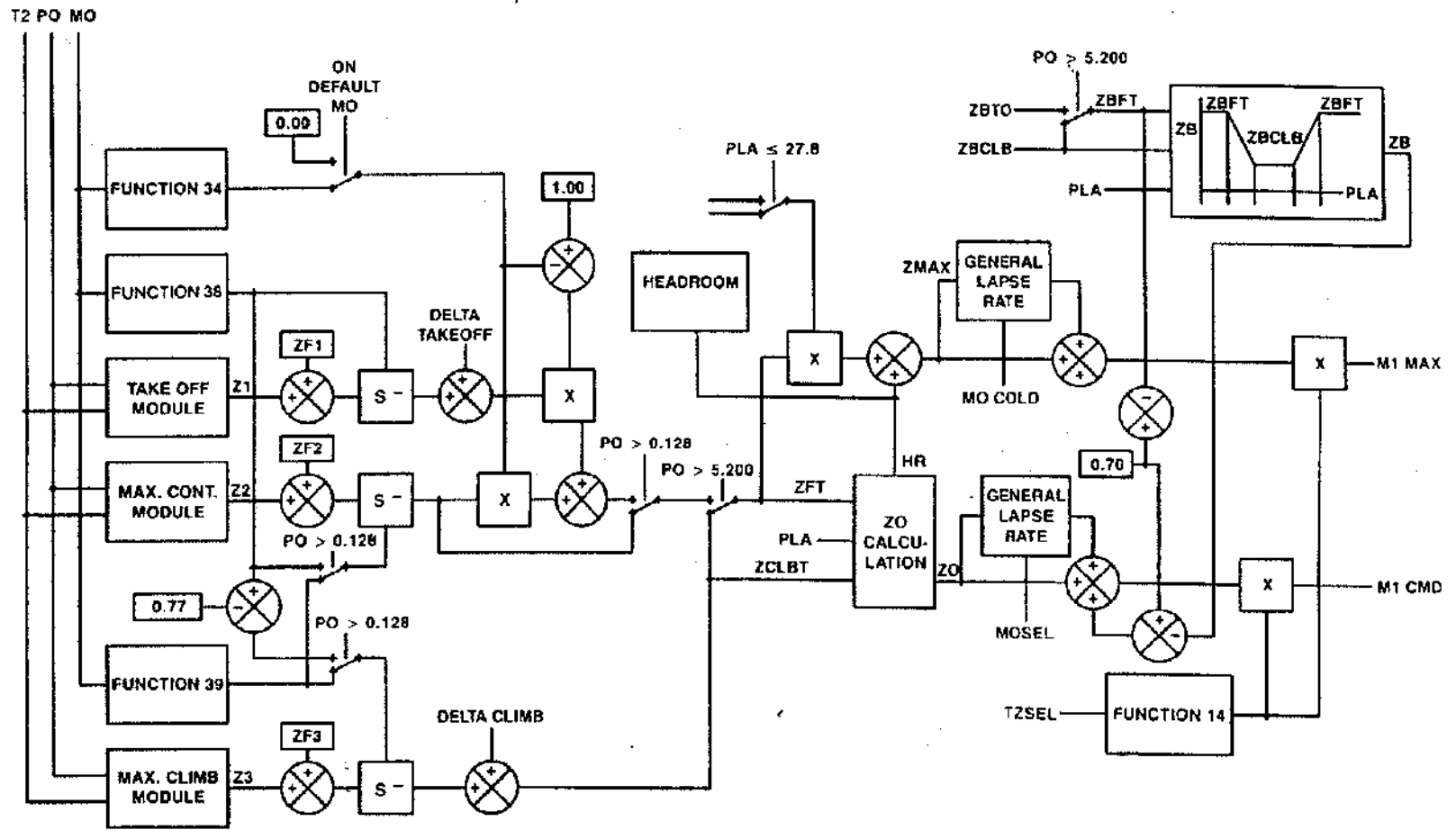


Figure 11.27 Typical Digital PMc Rating Logic

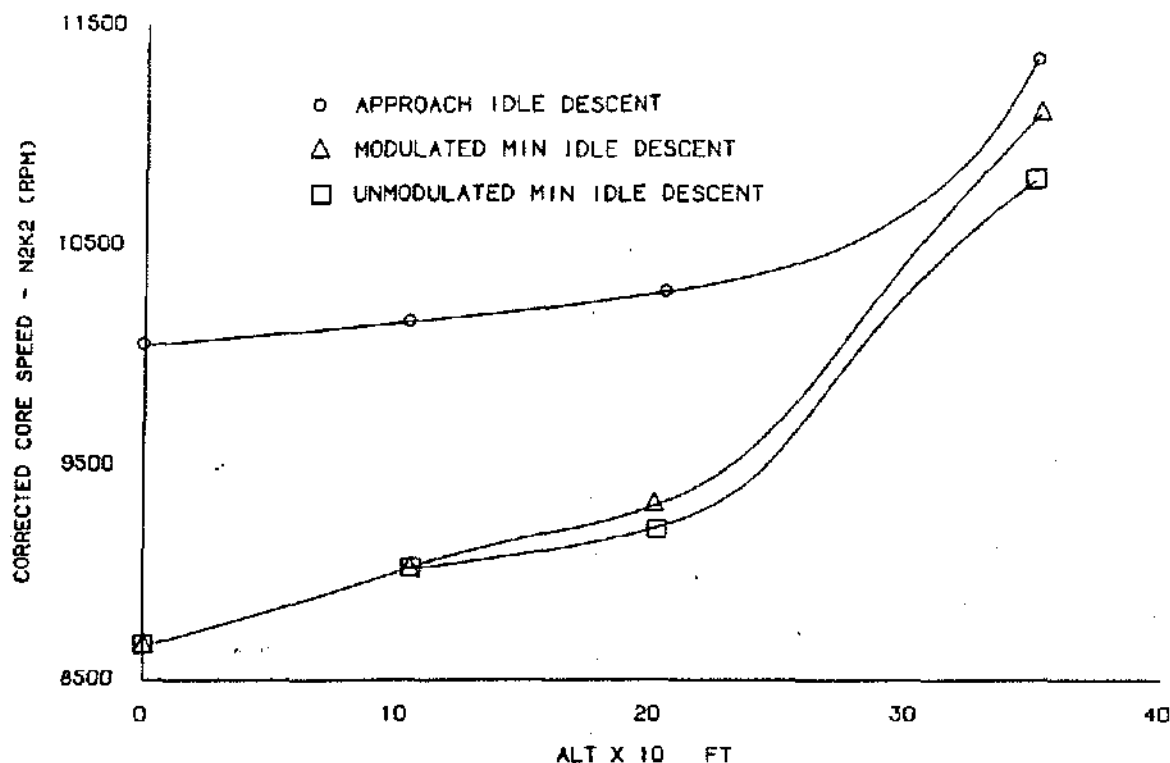


Figure 11.28 Idle Descent Paths

thrust required to be available eight (8) seconds after a go-around maneuver is a negotiated value between the engine and aircraft manufacturers. Typical values for this thrust requirement on present day commercial aircraft range from 78% to 95% of full go-around thrust.

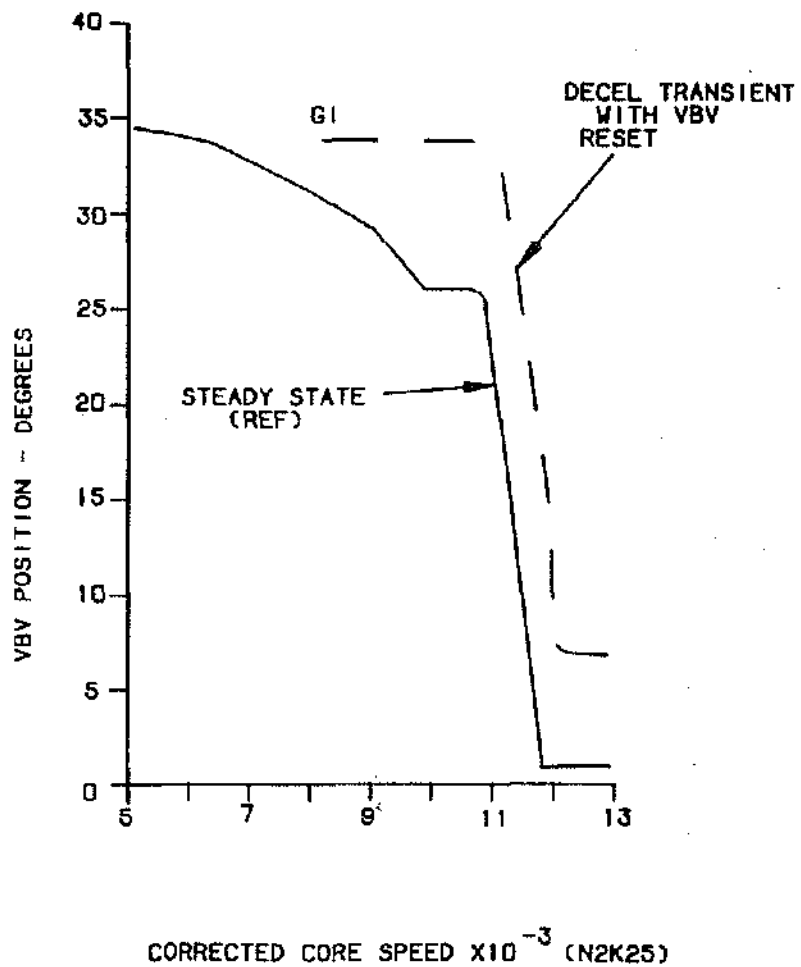
Current commercial aircraft require relatively low approach idle thrust settings to permit a wide range of thrust modulation during approach. Since lower idle speeds generally result in reduced engine thrust response, a thorough analysis of a specific engine's approach idle go-around performance must be completed before a final value can be agreed upon with the aircraft manufacturer.

Most modern commercial control systems combine the scheduling of ground idle and descent idle requirements into one function. As mentioned previously, this function is often mechanized by a separate cam with ambient temperature and pressure inputs. Figure 11.29 shows a block diagram of a typical idle speed governor system, in this case the CFM56-3 hydromechanical system. The modulated idle function is a 3-dimensional cam represented by the box labelled "MOD IDLE MULT" in the figure. Approach idle scheduling is often implemented

by using the ambient temperature and pressure speed schedule biasing provided on the normal 3-dimensional speed schedule cam (shown as the box labelled as SCHED in the figure). The selection of the two idle settings is provided for by an electromechanical solenoid on the hydromechanical control. The selection of normal (ground/descent) idle or high (approach) idle is accomplished via an aircraft signal to the solenoid.

Variable Bleed Valves (VBV's) Most of today's commercial aircraft gas turbine engines are high by-pass ratio turbofan engines. The core (high pressure) compressor inlet is "supercharged" by the low pressure (LP) compressor, which consists of the hub section of the fan and a multi-stage booster. The LP compressor, which comprise 4 to 5 stages, contains no variable stator vanes. The resulting booster airflow versus speed characteristic at low speed and part power is higher than the corresponding airflow capacity of the high pressure compressor at the same engine operating condition (see Figure 11.30). This characteristic raises the booster operating line since the high pressure compressor acts as a flow restriction as viewed by the booster. At some conditions the booster operating line may be raised to the point of stall which is obviously unacceptable.

DECEL TRANSIENT & THRUST REVERSE EFFECT



ALTITUDE BIAS (STEADY STATE)

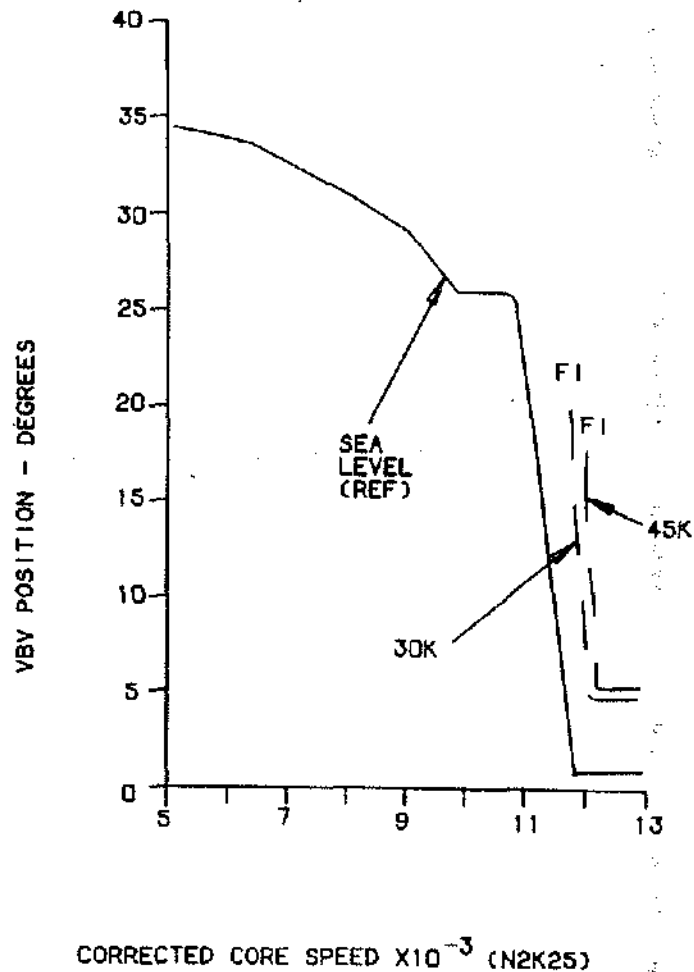


Figure 11.33 VBV Schedule and Modifiers

To provide adequate stall margin for the booster, a Variable Bleed Valve (VBV) system is incorporated into the fan frame of the engine downstream of the booster discharge. These valves, which are actually hinged doors in the outer flow wall of the goose neck, are moved by a fuel actuator-driven mechanical system (see Figure 11.31 and 11.32). The VBV's are scheduled by a cam and pilot valve as a function of corrected core speed in MEC equipped engines. A typical VBV schedule is shown in Figure 11.33. The system is designed to open at idle and part power to bleed some booster discharge flow into the fan flow path, which unloads the booster and lowers the operating line. At high power conditions, where there is a better flow pumping match between the booster and the high pressure compressor, the VBV's are scheduled closed to improve engine performance.

Also shown on in Figure 11.33 are several VBV schedule modifiers, which are used in various commercial control applications. The decel transient reset opens the VBV schedule transiently to account for VBV operating line upward migration due to fan and core rotor speed mismatches during decelerations. During a decel the core rotor (being lower in inertia) will spool down faster than the low pressure rotor. This results in additional transient mismatch in flow pumping capacity of the booster and high pressure compressor, which tends to raise the booster operating line during a decel. The VBV reset mechanism in hydromechanical controls is based on sensing the rate of closure of VSV's (decel direction) above a defined threshold. When the VSV closure rate exceeds the threshold, the VBV schedule is reset open to provide additional transient booster stall margin. This function is often referred to as the VBV "kicker". Electronic controls may use measured rotor speed mismatch to modulate the transient VBV scheduling.

The reverse thrust VBV reset opens the VBV schedule during thrust reverser operation. Again, the idea is to lower the booster operating line, in this case to account for potential booster stall line degradation due hot gas reingestion into the booster during high power thrust reverse operation.

Altitude biasing of the VBV schedule is used on some commercial control systems to modulate the VBV schedule open as a function of altitude. This is required on some engines, particularly on low stall margin boosters, to account for booster operating line upward migration caused by altitude and Mach effects on the engine cycle.

Turbine Clearance Control and Rotor Active Clearance Control Turbine clearance control and rotor active clearance control are functions that have been added to recently developed and certified commercial control sys-

tems. Both features are designed to actively control either turbine blade tip clearances, compressor blade tip clearances, or the use and amount of engine cooling or parasitic flows. The objective of these functions is to improve overall engine cycle efficiency by improving compressor or turbine efficiency or by reducing use of parasitic flow when nonessential.

Turbine clearance controls vary from engine model to engine model in implementation. Early CFM56 engines employ a hydromechanically controlled open loop system, where a double air valve is commanded open or closed as a function of core speed. The air valve schedules are implemented in the hydromechanical control via cams and pilot valves. The double air valve (see Figure 11.34) ports either fifth stage compressor air, ninth stage (compressor discharge) air, or a mixture of fifth and ninth air to the HP turbine internal shroud support cooling manifold. The system provides the proper air temperature to the shroud support to keep turbine clearances open far enough to prevent blade tip rubs at high power and to reduce clearances at cruise to improve engine fuel consumption. Figure 11.35 shows how the cooling modes affect turbine blade tip clearances.

CF6-80C2 engines employ a different technique to control clearances in the turbines. HP and LP turbine clearances are controlled via external impingement of fan discharge air on the HP turbine and LP turbine cases. The fan discharge cooling air supply to the HPT and LPT case cooling manifolds is commanded on and off by a system of valves which are controlled by ambient pressure and core speed inputs to the hydromechanical control. At altitudes above 20,000 ft. and between 82 and 98% N2 the MEC sends output signals to the air valves to shut-off core compartment cooling and provide turbine case cooling to reduce clearances. This improves cruise fuel efficiency by reducing unnecessary core compartment cooling use and by improving turbine efficiency.

Full Authority Digital Engine Control (FADEC) equipped engines (CFM56-5A, -5C, and -80C2F) employ more complicated clearance control techniques than those discussed above. In some applications, a simple turbine clearance model is used in conjunction with measured HP turbine shroud ring temperature, fully modulated turbine cooling valve position and output temperature feedback, and thermal history of the engine to provide the optimum cooling flow and temperature for transient and steady state turbine clearances.

High pressure rotor active clearance control is a function that has been incorporated on recent commercial engines, which employ FADEC. The purpose of the rotor

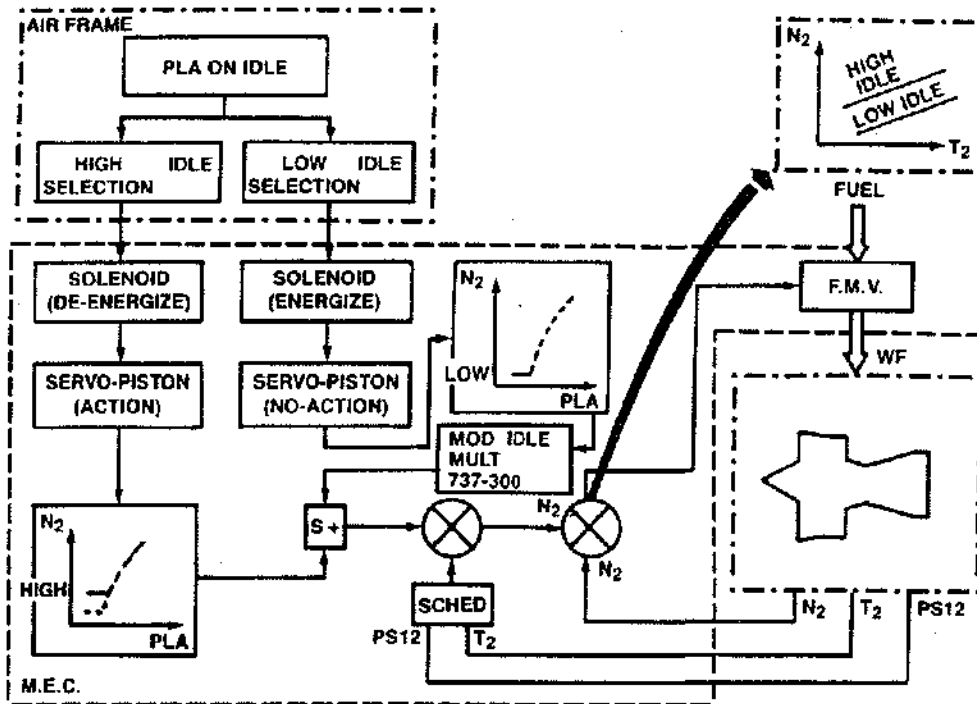


Figure 11.29 Idle Speed Governing System (N2K2)

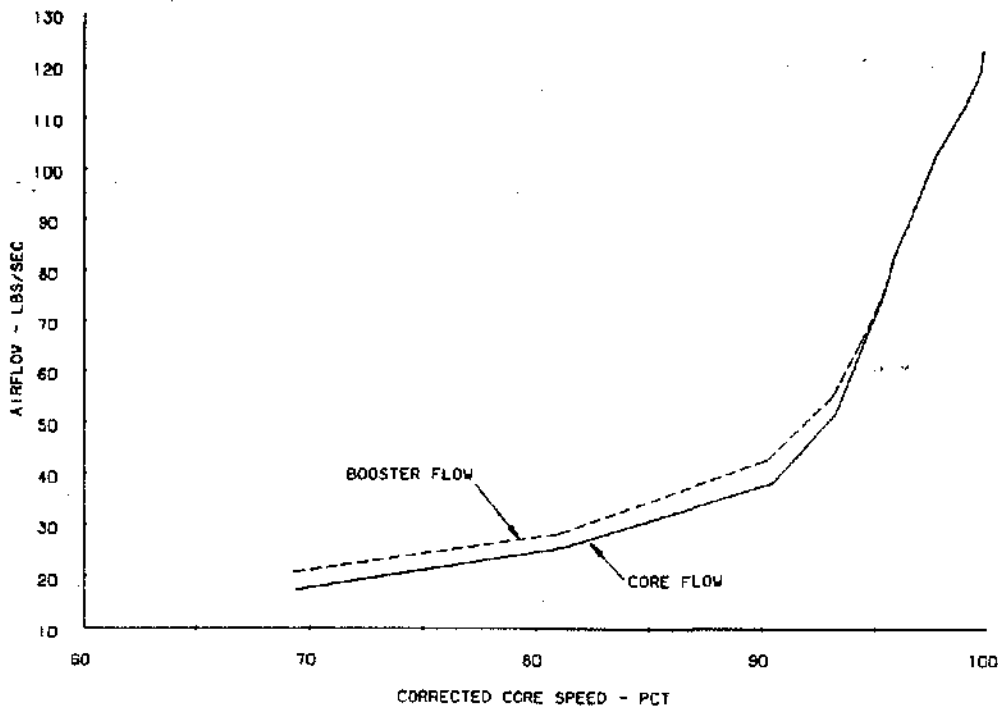


Figure 11.30 Airflow vs. Corrected Core Speed

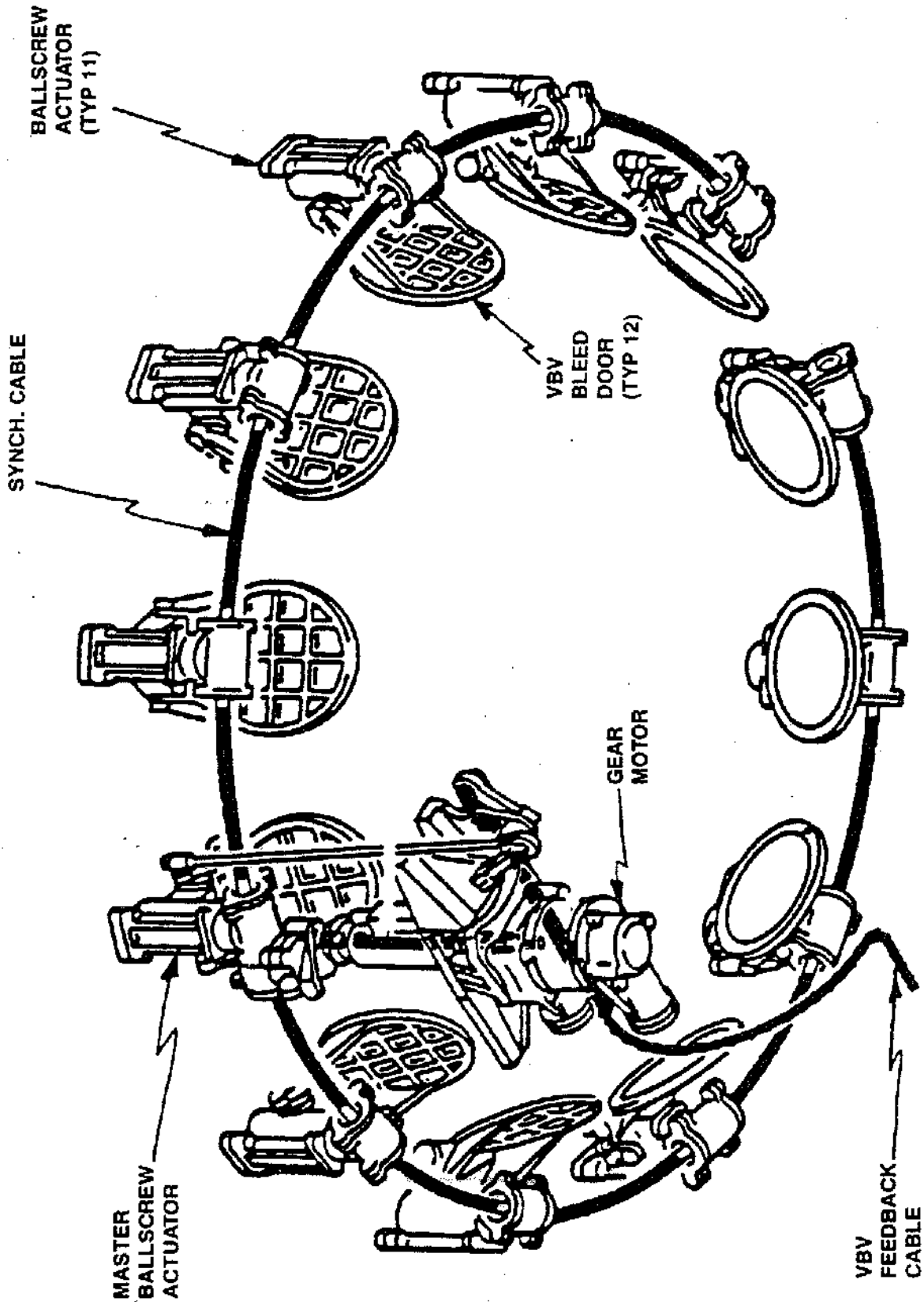
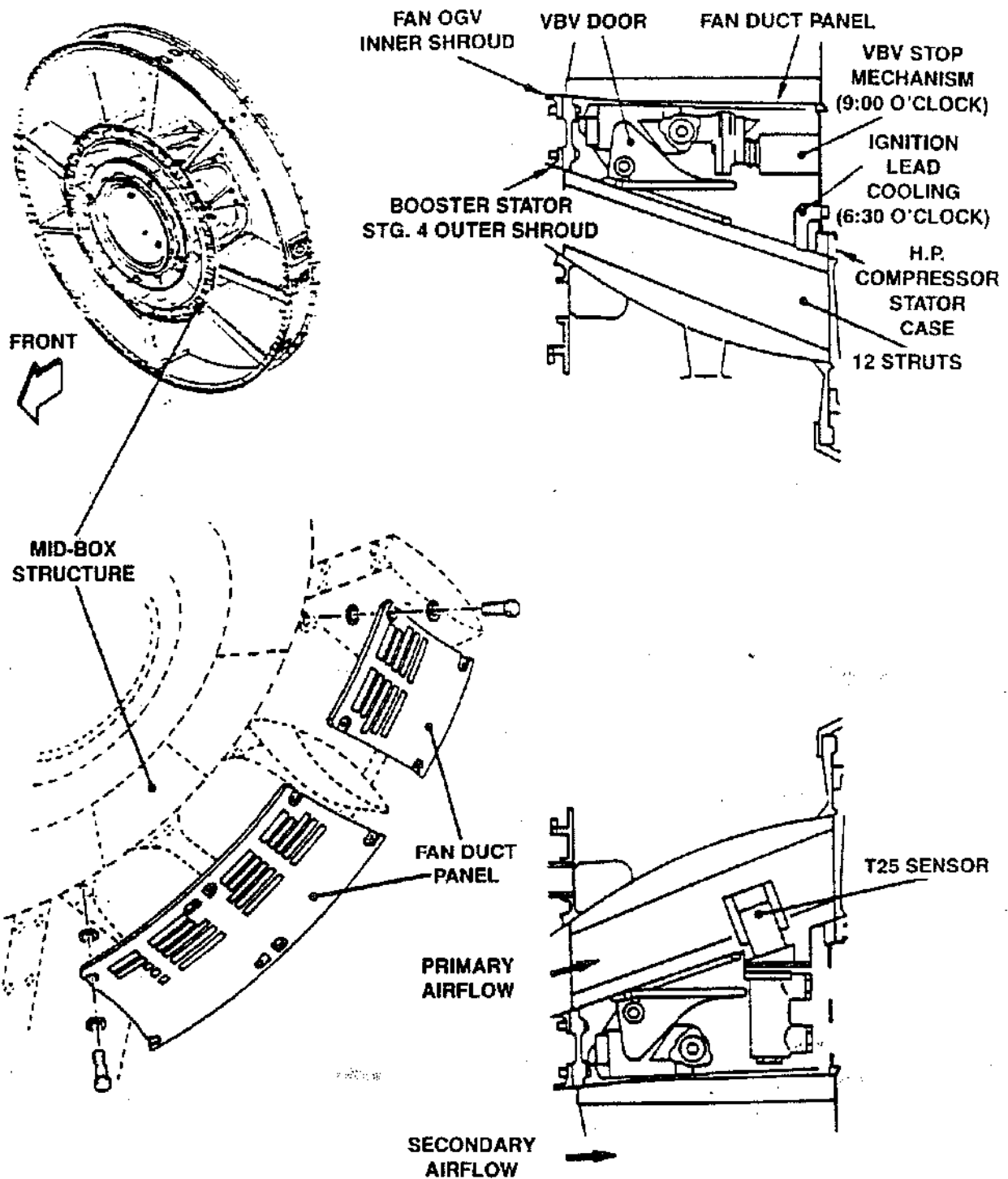


Figure 11.32 VBV Actuation System



FAN FRAME MID-BOX STRUCTURE

Figure 11.31 VBV Location in Fan Frame

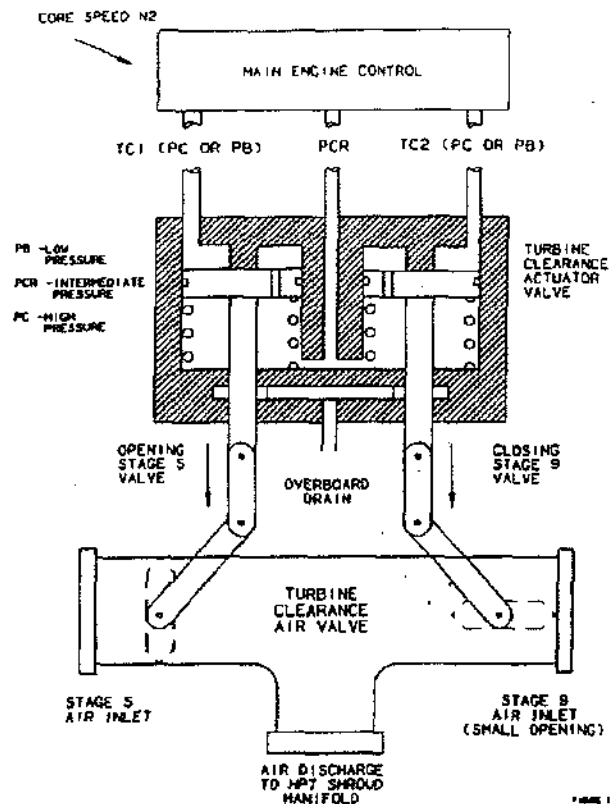


Figure 11.34 TCC Valve

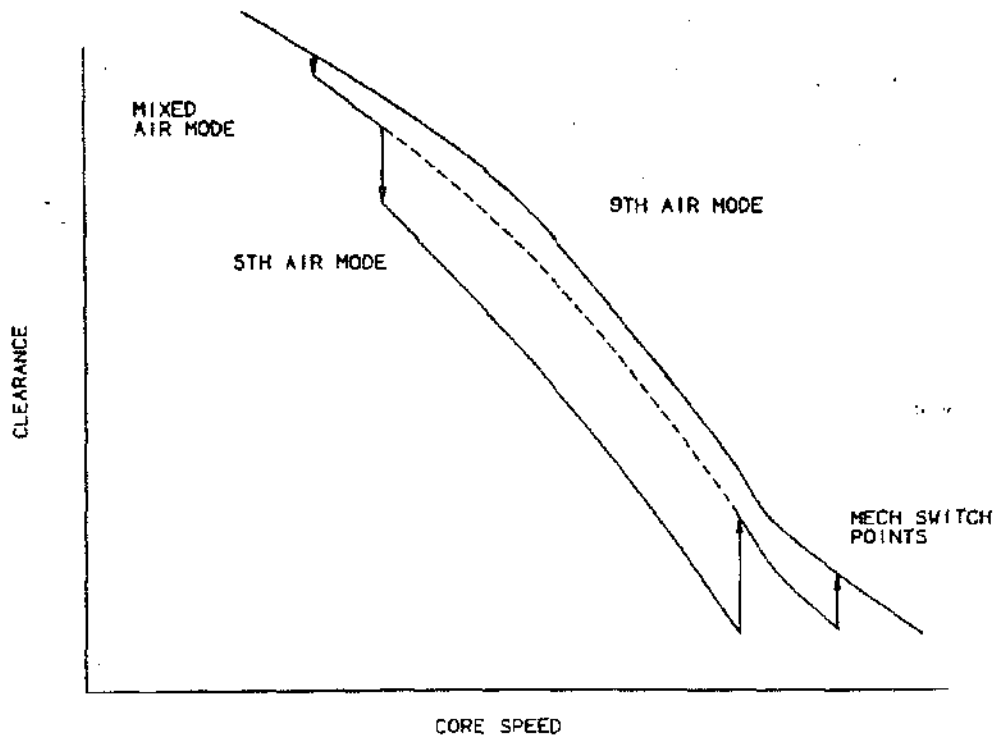


Figure 11.35 HPT Steady State Tip Clearance

clearance control system is provide hot air to the bore cooling air circuit of the high pressure rotor during cruise operation to heat the rotor. This action expands the core rotor and decreases blade tip clearances, which results in improved component efficiency and decreased engine fuel burn. The system includes appropriate control laws in the FADEC and a fuel pressure actuated air valve to control the bore heating air.

Reverse Thrust Scheduling Most commercial engine applications are equipped with a thrust reverser system, which is designed to provide additional retarding force from the engine to slow the aircraft during a landing roll. Mechanization of the thrust reverse control on the aircraft side is accomplished by providing a separate reverse thrust lever as part of the cockpit thrust control lever. When the forward thrust lever has been retarded to idle and after the reverser is deployed, an interlock system allows the pilot to increase engine reverse thrust by pulling up on the reverse thrust levers. This allows the throttle lever on the engine control to be rotated through the reverse side of the speed demand (either

core or fan) schedule (see **Figure 11.36**). As shown in the figure, a typical commercial control uses a throttle lever rotation range of 130 degrees. The forward thrust speed schedule is incorporated in the range from 55-60 degrees to 130 degrees, while the reverse thrust speed schedule uses 45 degrees to 0 degrees. The reverse thrust schedule is usually a mirror image of the forward thrust schedule, thus, like the forward thrust schedule, it provides nearly linear thrust versus throttle angle.

Normally, as part of an aircraft certification flight test program a maximum reverse thrust value will be defined, which is usually somewhat less than full reverse thrust. This limit is generally determined by the maximum engine reverse thrust level which can be maintained down to a forward airspeed of 50 to 70 knots without reingestion of hot gas into the engine. The specified max reverse stop is implemented into the control system by way of a (vendor) adjustable throttle lever stop in the hydromechanical control or by software in digital controls.

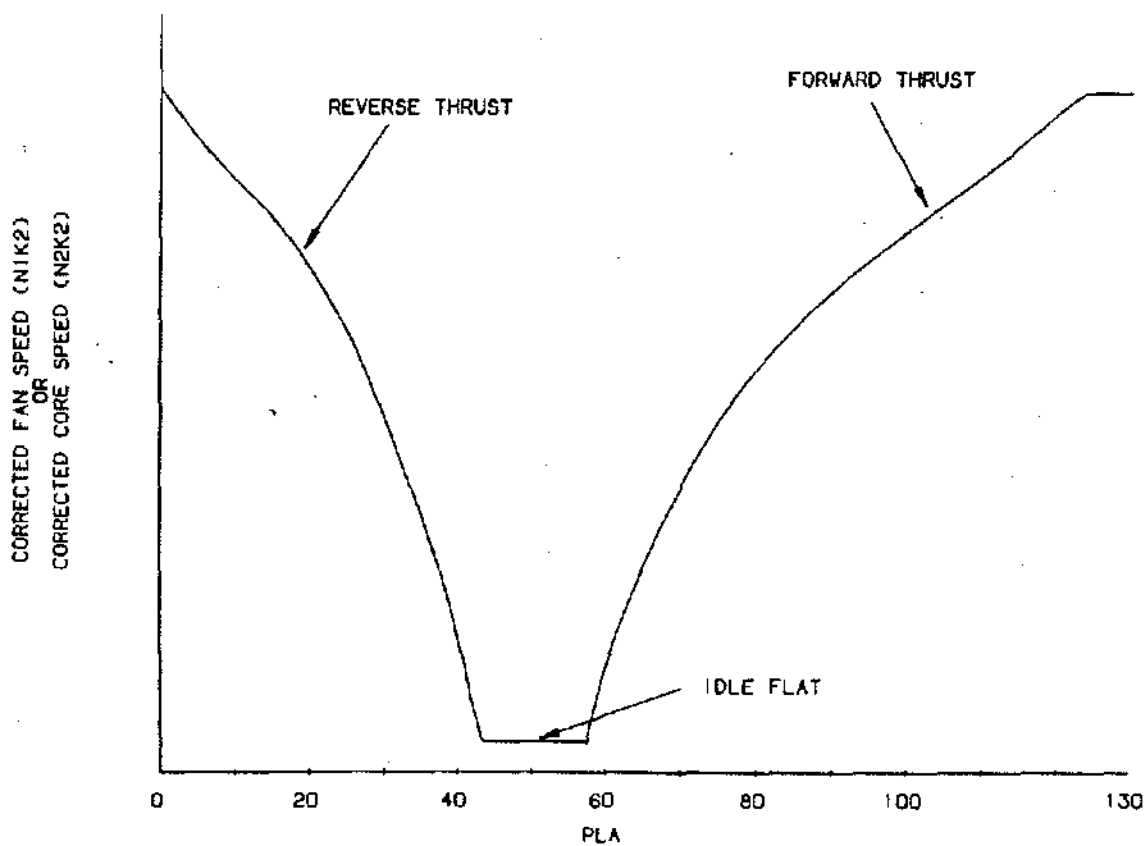


Figure 11.36 Speed Scheduling - Forward and Reverse Thrust

MILITARY CONTROL OBJECTIVES

Due to the unique missions of military aircraft the engine design is quite different than commercial engines. Military engine specifications define operational requirements that have a strong effect on the control system design. While a commercial program is concerned primarily with fuel burn and reliability, the military requires high thrust to weight ratios and quick thrust response. In order to meet these spec requirements special controls hardware and functions are designed just for military engines. Some components unique to military engines are variable inlet guide vanes, variable exhaust nozzle, an augmenter (A/B) and turbine temperature pyrometers. Each of these requires special controls hardware and control system design efforts. Also, each engine application may require various special control functions to meet aircraft integration and flight envelope or maneuvering capabilities. Another very important consideration for military engine/control system design is safety for single engine applications. This is a major driver for a control system design. To meet prime reliable requirements the F110-100 control system has two control modes. First, a primary control mode which is the normal mode. Also, a secondary control mode is available to control the engine and provide reliable "get home" thrust, should the primary experience a failure. The secondary mode is selected automatically by the control if a failure occurs, or it can be pilot selected. The F110 control system secondary mode provides 70% of intermediate thrust up to 30,000 feet. On a more sophisticated engine, with digital controls (F110-129) there are two other hybrid modes available which allow partial primary control. Table 11.4 lists the various control loops and control modes for this engine.

The remainder of this section will cover some of the control functions common to most military engines. This is by no means inclusive of all military control functions.

but addresses the features most often used on a military engine. Each engine model and application has a unique control system tailored to its needs. Coverage of all these other functions is not appropriate for this summary discussion.

Fan Inlet Guide Vane Control Scheduling variable guide vane position in front of the fan rotor has the same effect as VSV's in the compressor. The inlet guide vanes (IGV), one behind each front frame strut, can be positioned, to control fan stall margin over the speed range. It is not practical for large fan diameter commercial engines to add all the extra hardware, weight and system complexity required for IGVs. These engines spend most of their operating life at a specific cruise condition, for which the fan can be optimized. Military engines, on the other hand, have relatively small diameter fans and are required to operate efficiently over a wide range of speeds. Incorporating IGV's allows for optimization of the fan performance over a wide speed (pressure ratio) region. The variable guide vanes act like VSV's and control the airflow through the fan, therefore providing stall margin control.

Control of fan airflow (and stall margin) is much more important on military engines where inlet distortion occurs. Both pressure and temperature distortion at the engine inlet face can occur. This distortion is due to extreme aircraft maneuvers and long serpentine inlets unique to military aircraft. Distortion is basically a gradient of temperature or pressure across the engine inlet plane and can create local "pockets" of high or low pressures or temperatures. As the distortion goes up the fan operating line moves up, consuming stall margin.

The fan IGV position is normally scheduled as a function of corrected (to inlet temperature) fan speed (See Figure 11.37). This assures control of fan airflow since air density will change as a function of inlet temperature. The

Major control loop	Control mode			
	Primary	Hybrid VSV	Hybrid	Secondary
Fan IGV's	DEC	DEC	DEC	Fixed closed
Core VSV's	DEC	MEC	MEC	MEC
Main engine fuel flow	DEC	DEC	MEC	MEC (DEC NF limit)
Augmenter fuel flow	DEC	DEC	DEC	Not available
A8 area	DEC	DEC	DEC	Fixed closed

Table 11.4 Control Mode Overview

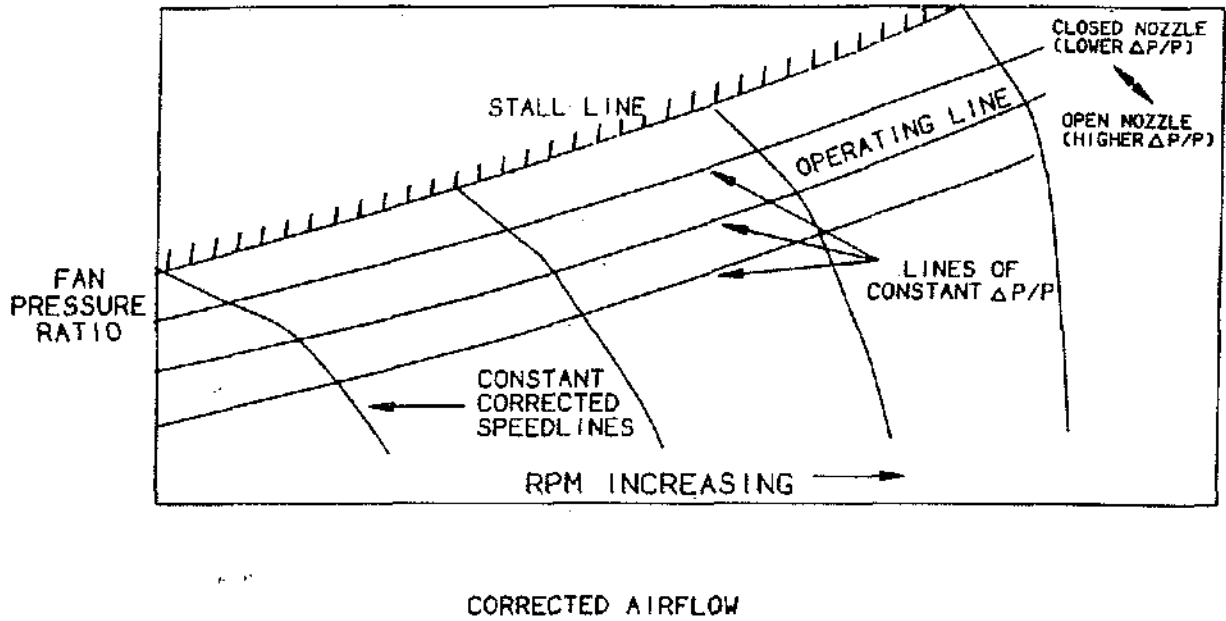


Figure 11.39 Basic Fan Map

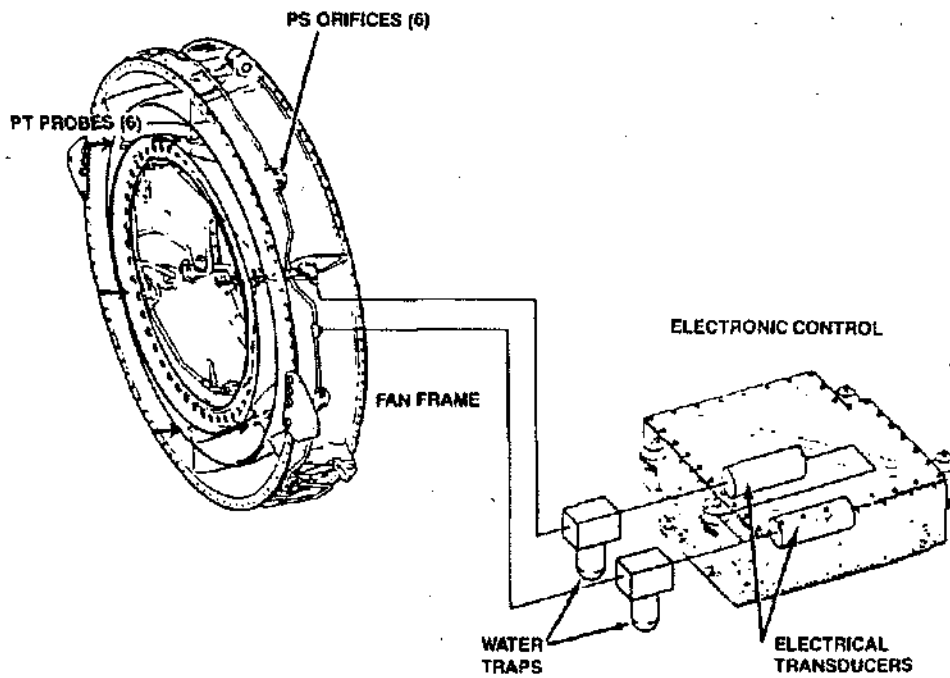


Figure 11.40 Fan Operating Line Control Signal Acquisition

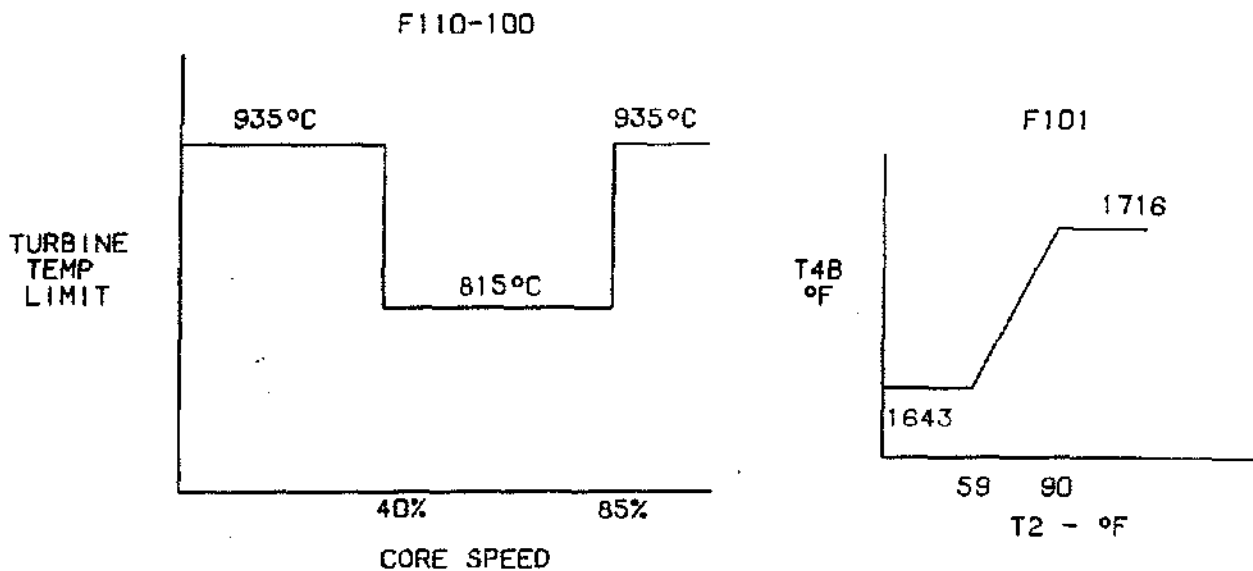


Figure 11.38 T4B Limiting Schedules

due to effects such as poor correlations, effects of component variations and low gains relative to A8. Even scheduling fan pressure ratio (P_{25}/P_2) did not provide close control over fan operating line due to small pressure ranges, which effected accuracy.

Further studies found that lines of constant corrected (to fan discharge conditions) fan airflow run parallel to the stall line. Sensing corrected airflow would be difficult. If the fan discharge duct area is known then corrected airflow can become a flow function:

$$FF = \frac{W T}{PA}$$

The flow function is a function of mach number, which is a function of total (P_T) and static (P_S) stream pressures. Thus, if the fan discharge total to static pressure ratio is known then a duct mach number - flow function - operating point is known. Since fan duct mach numbers are low (.40 to .70) the P_T/P_S ratio is small. Sensing low pressure ratios accurately, requires a sophisticated sensor. Additional studies indicated that very good accuracies could be obtained using the parameter:

$$\text{Delta } P/P = \frac{P_T - P_S}{P_S}$$

Fan discharge total pressure (P_T) minus fan discharge static pressure (P_S) divided by fan discharge static pressure (P_S). Which is equivalent to:

$$\frac{P_T}{P_S} - 1$$

Delta P/P is sometimes called duct mach number for this reason. This parameter is used as the controlled variable and A8 the manipulated variable on all GE augmented turbofans.

Figure 11.39 shows a basic fan map and the constant lines of delta P/P. Note that they run parallel to the stall line and lower delta P/P lines are closer to stall (higher operating line). This can be rationalized by taking, closing A8 to the limit. Of course there would be no flow (cause stall) thus total equals static pressure and delta P/P goes to zero. Opening the nozzle does the opposite; unloads the fan. (lower operating line) less flow restriction which yields higher velocity (mach number) duct flow.

The pressure measurement for this system is provided by 6 total and static pressure taps in the fan frame which are manifolded for averaging, as shown in Figure 11.40.

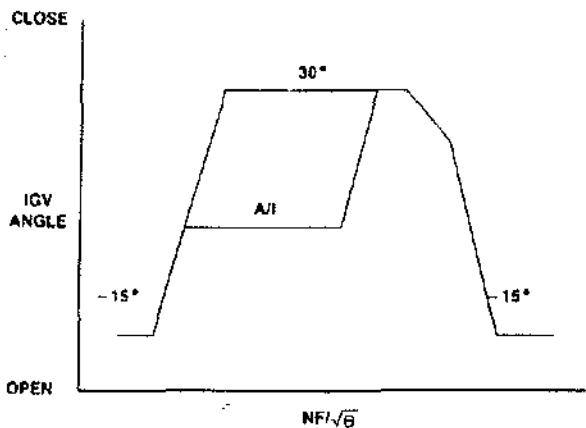


Figure 11.37 F101 Fan IGV Schedule

actual guide vane position is defined by the fan aero and operability designers. The guide vanes are "ganged" to a unison ring which can be positioned by a single rotational input. Actual scheduling is provided by the electronic control using fuel powered actuators. This is a closed loop control with electrical position feedback.

Referring to Figure 11.37 note the schedule starts open, goes closed, then open. The low speed open schedule is designed so the IGV's are open at shutdown, to ease inlet inspections of the fan. The schedule has a closed "flat" so the fan does not become choked (flow limited). Also, an anti ice (A/I) reset is provided. This schedule sets the vane angle at zero degrees when in icing conditions. The low angle gets the vanes out of the direct airflow and prevents ice build up. The control system is also designed so that electrical or mechanical failures will cause the IGV's to slew to a safe position.

Turbine Temperature Control Due to the high thrust requirements of military engines the turbines operate at higher temperatures than commercial engines. Turbine temperatures are controlled indirectly on commercial engines through power management. These schedules are designed to limit exhaust gas temperature (EGT) overshoot which relates to turbine temperatures. For military engines there is less turbine temperature margin while operating on the normal fan speed schedule. To protect the high pressure turbine from excessive over temperature the control system incorporates a turbine blade temperature (T4B) limiting function.

If by deterioration high compressor bleed or horsepower extraction, hot day operation, or an unusual event, T4B reaches the limit, the control will prevent further over-temperature. This is normally accomplished by overriding the fan speed schedule and reducing fuel flow. Depending on the engine and special requirements the limits are designed as a function of T2 or core speed. Figure 11.38 shows two typical T4B limiting schemes. Note that the F101 has a limit which varies with T2, while the F110 has flat limits for bands of core speed. The F101 previously had a flat limit of 1716°F. The lower limiting at low inlet temperatures reduces turbine deterioration while maintaining required thrust levels. Between 40% and 85% core speed T4B is limited to 815°C on the F110 engine to enhance air starting.

An optical infrared pyrometer is used to measure actual blade temperature. This signal is fed to the electronic control which reduces core fuel flow to limit turbine temperature. The control loop, therefore, is closed loop through the engine. Since the engine time constant is relatively slow, T4B anticipation logic is included in the control to prevent excessive overshoot during bursts.

Fan Operating Line Control The fan operating line is similar to the compressor operating line. It is defined in the same manner; fan pressure ratio (P25/P2) versus corrected airflow. As the fan operating line increases it gets close to stall (consumes stall margin). The ideal fan operating line sets the fan pressure ratio as high as possible to optimize fan performance and thrust while maintaining adequate fan stall margin. The fan operating line can easily be controlled by varying the exhaust nozzle area (A8). The exhaust nozzle acts like a throttling valve which causes a back pressure in the fan exit duct, this increases the fan pressure ratio as A8 closes down and vice versa. Having the capability to control fan operating line is especially important for a augmented engine since the augments is directly coupled to fan discharge. Therefore, A/B lights and fuel flow changes are "felt" directly by the fan and could cause excessive back pressure (stall).

During development of the augmented turbofan engine, various parameters were considered for nozzle area/fan operating line control. Among those considered were T5, P3/P6, NF and P25/P2. All of these were rejected

These pneumatic signals are transmitted to the electronic control where absolute (P_S) and differential ($P_T - P_S$) transducers are mounted. The electronic control calculates the delta P/P ratio and signals nozzle position adjustment to set a scheduled value of delta P/P. Modulation of A8 serves as an excellent method of controlling delta P/P, therefore fan stall margin.

Delta P/P is normally scheduled as a function of corrected fan speed or T_2 . Different engines have other schedules to optimize performance. Usually the control is designed to select the highest value (max select) when more than one schedule is used. An example of an exhaust nozzle control block diagram is shown in Figure 11.41. This application has three schedules. The basic schedule biased by T_2 is usually in control. The scheduled value of delta P/P increases for high T_2 's to increase stall margin for supersonic flight conditions. The idle schedule (low PLA's) is designed to cause the exhaust nozzle to drive full open which reduces thrust, at low flight speeds or on the ground. A $P_T - P_S$ reset schedule is also provided for operation in the upper left corner of the flight map. In this region the fan stall line is

lower, thus delta P/P is increased to offset consumed stall margin.

Since the exhaust nozzle has physical limits on open and closed area, A8 "roof" and "floor" schedules are included in the control. The floor is a lower electrical limit and the roof an upper electrical limit. A8 position is sent to the control via an electrical feedback transducer mounted in an A8 actuator. Usually the nozzle position is controlled by delta P/P. When setting a scheduled value of delta P/P would violate the roof or floor limit, control reverts to the roof or floor schedule. (See Figure 11.41)

The floor schedule (fixed value) prevents operation on the physical actuator stops. The roof schedule varies as a function of PLA. It allows setting a large opening at idle (to reduce thrust). A lower A8 schedule is allowed for other non A/B, PLA settings. This prevents A8 from going wide open under certain delta P/P failure modes, which would cause a thrust reduction. Since burning A/B fuel flow causes a throttling effect on the fan, the nozzle must open further to maintain delta P/P. This requires

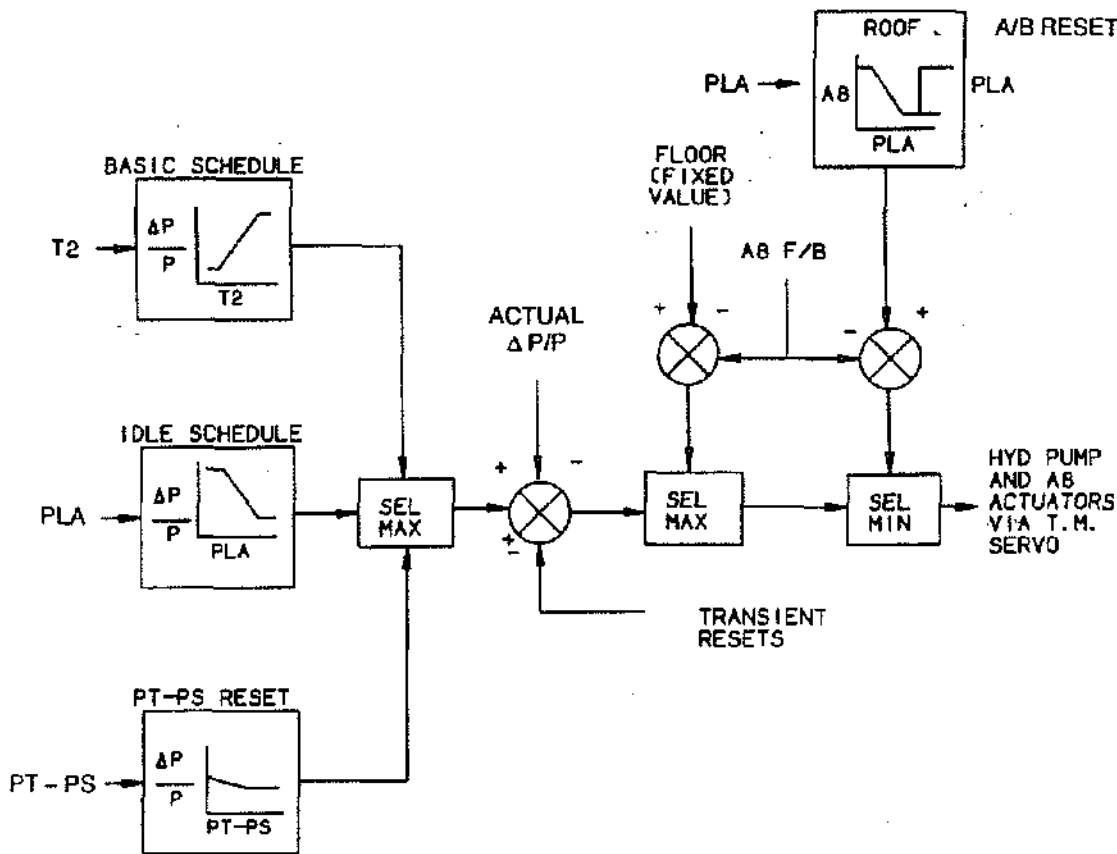


Figure 11.41 F110-100 Exhaust Nozzle Control Diagram

a higher roof setting for A/B operation, than dry operation. A roof reset is provided in the control to allow the larger roof.

Augmenter Fuel Scheduling In setting the controlled variables for an augmented turbofan engine a good parameter for controlling thrust is fuel/air (f/a) ratio. Controlling this parameter also can be used to maintain certain stoichiometric limits. To schedule actual fuel air ratio ($WFR/W6$), we would need to measure airflow in the augmenter ($W6$). (WFR stands for fuel flow - re-heat.) Fortunately there is another way. A predictable relationship exists between $PS3$ and $W25$ (core airflow). If the bypass ratio is known, then the ratio of $W6$ to $W25$ is known. Therefore, fuel-air ratio for the augmenter can be approximated by scheduling A/B fuel flow to compressor discharge pressure, ($WFR/PS3$).

To maintain linear thrust control as the pilot moves the throttle $WFR/PS3$ can be scheduled linearly. But, as engine inlet temperature changes so does air density which effects net thrust. In order to compensate for $T2$ effects, the $WFR/PS3$ schedule is biased as a function of $T2$. This is shown in Figure 11.42, a typical A/B fuel sched-

ule. Notice that the schedules are higher for higher $T2$'s (reduced air density). The hydromechanical augmenter control regulates actual fuel flow using a $PS3$ signal to "multiply" $WFR/PS3$. Thus, at a given $WFR/PS3$ schedule, actual fuel flow delivered increases with increasing compressor discharge pressure.

In a turbofan engine the afterburner fuels two air-streams; a hot stream which is the core engine exhaust gas, and a relatively cold stream which is the fan bypass air. GE turbofan engines use three sequentially modulated fuel zones:

- Local ($WFRL$) - The fuel flow used for lighting the A/B. It is delivered behind the core and fuels the light off pilot burner. This flow is usually a constant $WFR/PS3$ ratio from lightoff to max A/B.
- Core ($WFRC$) - This is additional fuel delivered directly behind the hot gas exit of the LP turbine.
- Fan ($WFRF$) - Fuel mixed with fan discharge air, in the outer diameter of the augmenter.

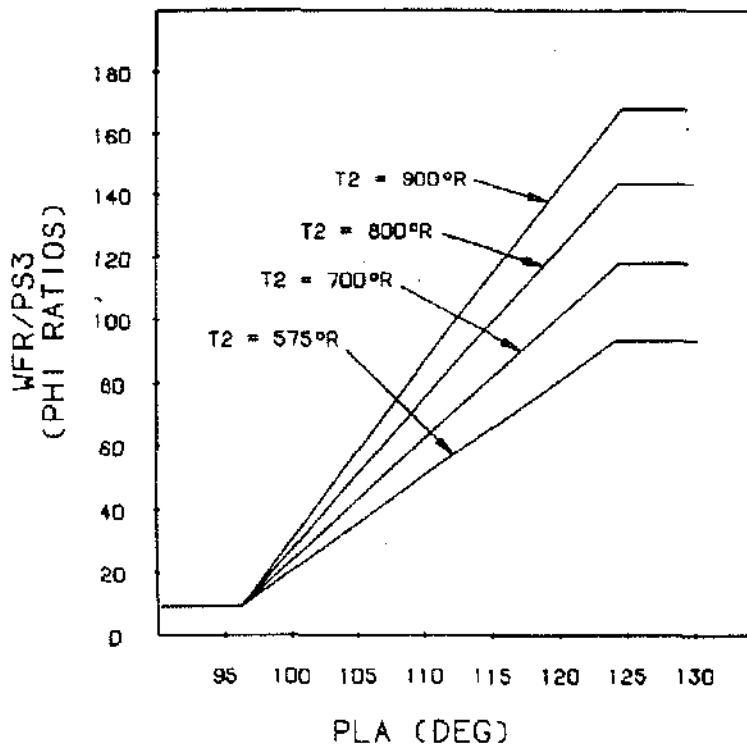


Figure 11.42 A/B Fuel Schedule

The schedule is designed to sequence these zones for smooth operation over the PLA range, throughout the flight map. The control system utilizes; an electronic control to turn on the augmenter fuel pump (to initiate fuel flow) and to schedule WFR/PS3, an augmenter fuel control (AFC) to regulate actual fuel flow and separate flow zones, and a flame detector to signal lightoff. The AFC contains the metering valve and supplies an electrical feedback position to the electronic control for closed loop WFR/PS3 positioning.

When A/B is selected the control "holds" fuel flow at the min (or local) level, regardless of throttle position. Once light off is confirmed by the flame sensor, the electronic control allows increased scheduling of A/B fuel. This hold at min A/B assures a "soft" light with minimum consumption of fan stall margin. If fuel flow was allowed to increase before light off a hard (rich) light could occur, possibly causing fan stall or damage to augmenter hardware.

After light off the core fuel flow increases with PLA to a point where the core WFR/PS3 level saturates. As throttle angle is further increased the core WFR/PS3 level is

constant. As higher WFR/PS3 is demanded the AFC begins to deliver fan flow which continues until the max value on the PLA schedule is reached. This can be seen graphically in Figure 11.43, for the F110-100 at one PS3 (sea level static) condition.

For fighter applications the transient time required to go from A/B lightoff to maximum A/B flow is approximately two seconds. Mixed flow afterburning turbofan engines are vulnerable to fan stalls during A/B lights and fuel flow transients. In order to meet this thrust transient requirement and good operability over the entire flight envelope, the control system provides a variety of special functions. One of the most important features is exhaust nozzle "pre-open". When A/B is selected by the throttle the control system adds a small reset to the delta P/P schedule (A8 open), prior to light off. This enables entry into A/B with no transient consumption of fan stall margin. When the augmenter fuel lights it expands and causes a back pressure on the fan which drives delta P/P down transiently faster than the A8 loop can respond. Pre-open sets a lower fan operating line, so initial light off does not drive below the normal operating line. A time trace of a typical transient from light off to max A/B is illustrated in Figure 11.44.

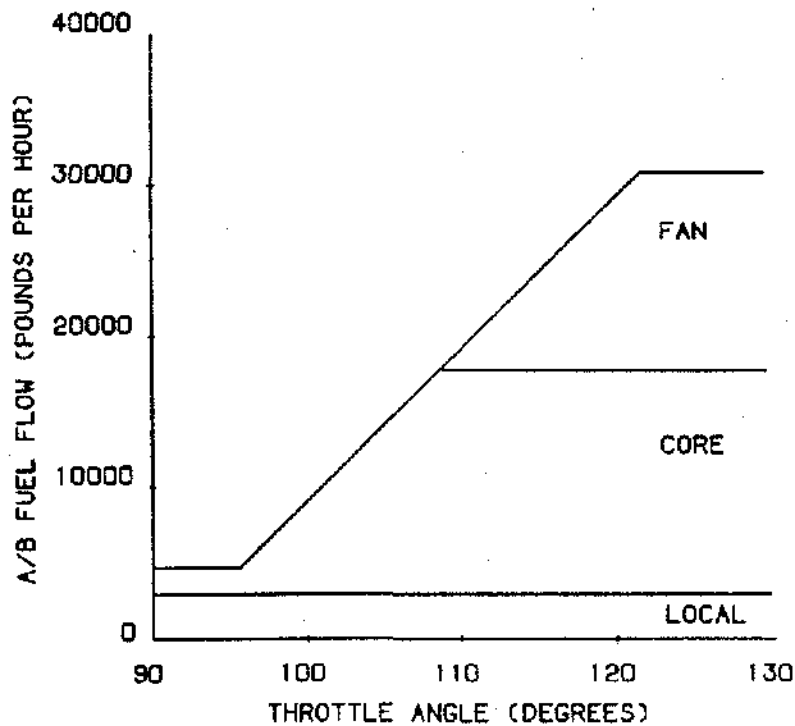


Figure 11.43 A/B Fuel Flow Distribution Take-Off Standard Day

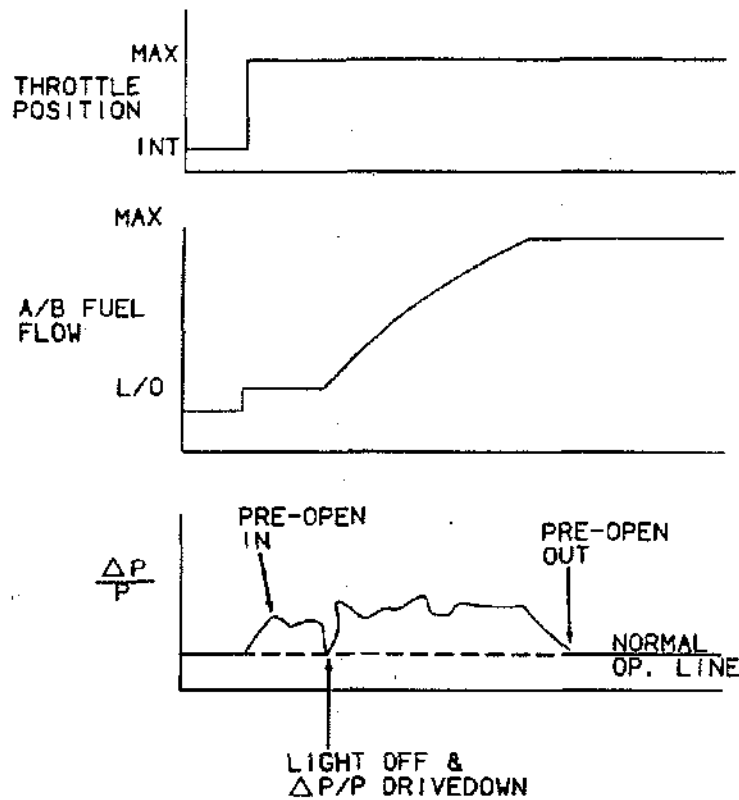


Figure 11.44 Afterburner Transient Sequence

As WFR/PS3 is being ramped up during a transient added fuel is burning and causing back pressure. The delta P/P control loop must continually open A8 to maintain operating line. Since delta P/P is closed loop through the engine it is too slow to maintain adequate stall margin. To help this situation pre-open is "kept in" until the A/B fuel metering valve rate falls below a certain level. An additional function, A8 anticipation is also incorporated to modify the delta P/P demand signal to maintain transient fan stall margin. Figure 11.45 shows the block diagram for this function. This function increases delta P/P demand (therefore error) as the metering valve rate increases. The actual rate of the A/B metering valve is also controlled on accels and decels to provide stable burning and reduce "screech" potential. This rate is normally a constant or controlled as a function of PS3. Another very important function in the A/B control system is the automatic blowout detection and re-light logic. If the flame detector senses an augmentor blowout, the electronic control automatically begins slewing the metering valve to min A/B. Pre-open is initiated and augmentor ignition turned on when WFR/PS3 has reached a low, safe light off setting. This is all done

automatically and requires no pilot action. If the throttle remains at the same position this logic will re-light the augmentor and accel back to the original setting, if the initial blowout cause is no longer present.

In the upper left hand corner of the flight envelope (high altitude - low mach no.) the low fan discharge temperature and pressure are not suitable for stable A/B burning. Attempting full fan burning in this region can result in fan stalls. The control system can provide sensing and logic to automatically cut back fan flow. This is called rich stability cutback. On the F101 and F110-100 and -400, this is accomplished by sensing PS3. At a predetermined PS3 level the fan spray bars are not fueled. On the F110-129, fan flow is not cut off but modulated as a function of fan discharge total pressure (PT25). Figure 11.46 shows a flight envelope with lines at constant PT25 and the rich stability cutback region. This section should give the reader an appreciation for the complexity of the A/B control functions, all of which were not covered. Due to the effect A/B operation has on the fan operating line, close control of this system is essential for unrestricted throttle capability.

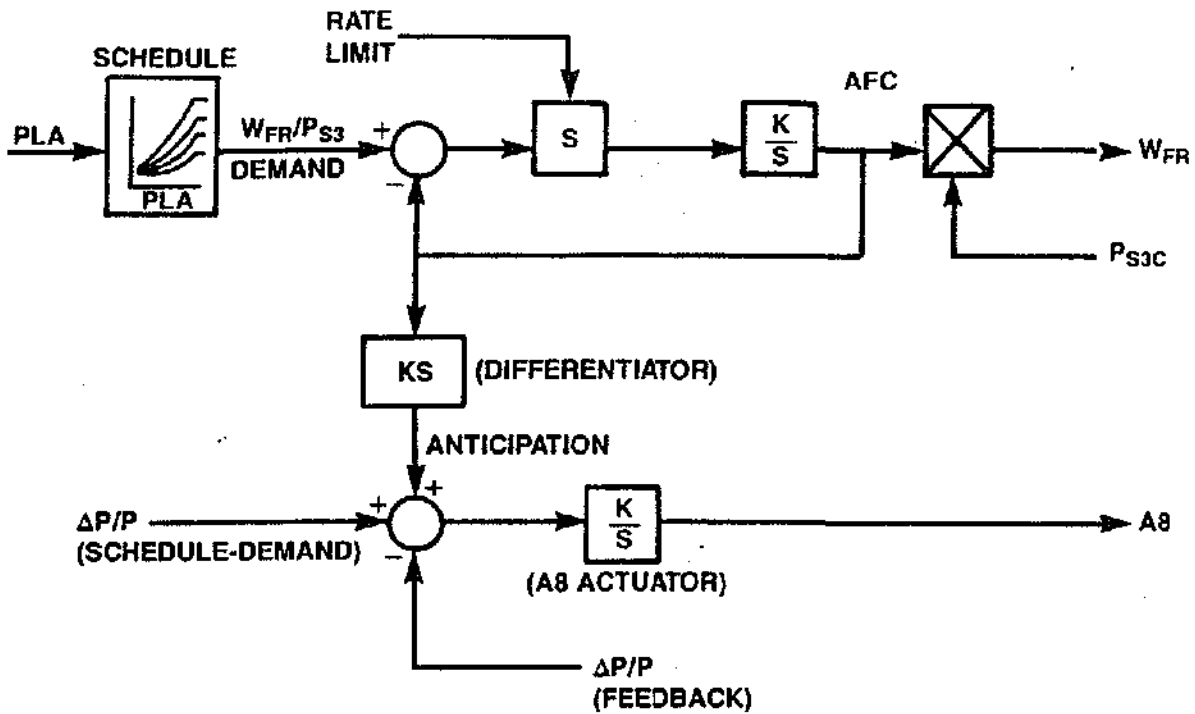


Figure 11.45 A/B Metering Valve Loop and A8 Anticipation

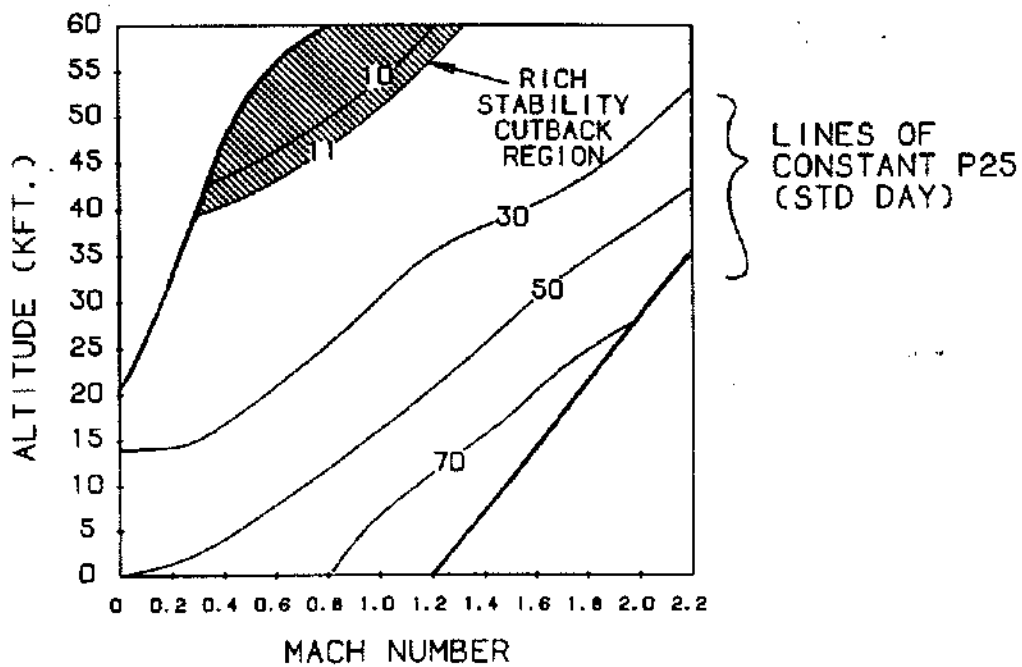


Figure 11.46 Flight Envelope with Rich Stability Cut Back Region Shown

Special Functions Depending on the engine application, the control system provides a variety of special functions to improve the performance and operability of the engine. One of these is main and augmenter ignition control. This is a full automatic system, a typical control logic scheme for main combustor ignition is shown in Figure 11.47. During start, ignition is turned on at 10% NC and off at 59% NC. An auto re-light function is included which energizes ignition when the core decel rate reaches 5% /sec. For air starts the ignition is locked out on decels between 75% and 40% NC to prevent possible start stalls in this region. Augmenter ignition (a separate system) is automatically energized when PLA is demanding A/B and core speed is above 85%. It is automatically turned off as WFR/PS3 ratios reach a certain limit. Special logic also selects A/B ignition when appropriate during blowout decels.

Certain applications require a special increased stability margin mode (ISSM). This may be a function of angle of attack (AOA) of the aircraft (early F16) or be pilot selected under adverse conditions (B-1B). Early model F110-100 electronic controls would reset the max fan speed schedule down 10% and raise the delta P/P schedule to gain more fan stall margin, at high AOA's. The B-1B system, called condition reset is pilot operated when additional fan stall margin is desired. This function resets the delta P/P schedule to the max schedule value, (A8 further open).

During snap decels and subsequent accel's (Bode's) and engine components are hot, and compressor stall margin is reduced. A VSV reset function is incorporated into the F110 family of engines to maintain adequate stall margin under these constraints. This feature resets the VSV schedule closed to provide the additional stall margin. The function remains activated for a specific time period.

Flying at high mach numbers will cause a shock wave in the aircraft inlet. This shock wave effects airflow to the engine. If the engine is not able to use all of the air being "rammed" down the inlet, heavy distortion can occur.

An unstable condition in the inlet causes spillage out around the inlet and an unstable shock wave, this is called inlet "buzz". To avoid inlet buzz, the control system provides an idle speed lock up function. This function is normally activated by aircraft mach number. Once energized the lockup schedule sets a minimum core or fan speed as a function of T25 or T2. This lockup schedule overrides normal speed scheduling.

Fault isolation and protection logic of these engines is becoming increasingly complex. These systems are designed to check the integrity of inputs and outputs of the control system. Based on the severity of the fault; another (redundant) signal might be used, the control may revert to another mode, send a fault message to the cockpit or set a fault flag in the monitoring system for later maintenance. This type of capability is especially important for single engine aircraft. The fault accommodation strategy must be designed to provide minimum degradation of the engine performance, while protecting the aircraft and pilot from unsafe operational effects. Much detailed analysis and design work is required to adequately define this logic.

COMPONENT DESIGN

Controls Engineering is responsible for both the control system design and all of the components in the control system. This covers a wide variety of components included in various systems:

- Main fuel system - pumps, filters, etc.
- Electrical/electronic system - electronic controls, cables, sensors, alternators, etc.
- Turbine and active clearance control systems - valves, timers, etc.
- Main control system - main engine controls, hydro-mechanical sensors, VSV and VBV actuators and valving, etc.

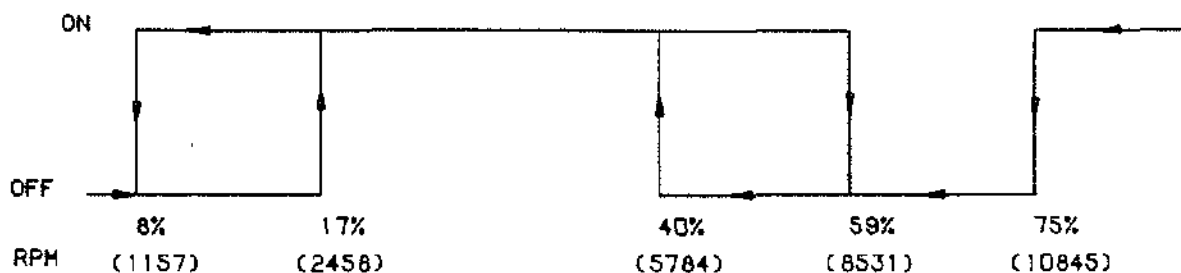


Figure 11.47 F101 Ignition Logic

- Augmentor fuel system - pumps, filters, augmentor fuel control, etc.
- Exhaust nozzle control system - hydraulic pump, filter, actuators, etc.
- Thrust reverser actuation system - drive motors, valves, actuators, etc.

These components are designed internally and externally. Internal designed components are completely designed by Controls Engineering. All of the detailed piece part drawings are provided to a manufacturer to "build to print". Components that fall into this category are: augmentor fuel controls (AFC), turbine clearance control valves (TCCV), active clearance control signal valve (ACCV), altitude sensor, bleed bias venturi and selector valve, hydraulic timer, ninth stage bleed check valve, and A/B pilot burner valve.

The detailed design of externally designed components is accomplished by outside vendors. These components are defined by specifications and source control drawings. The specifications define the component performance requirements, internal and external environments (temperatures, pressures, vibration, etc.), qualification/certification and acceptance test requirements, maintainability, reliability, and quality requirements. The vendor is responsible to prove their component can meet all of the spec. requirements. The source control drawing defines the outer envelope of the part in detail, lists applicable specs and the max component weight. Table 11.5 lists most of the components that fall into this category. Note that they fall into three general categories: hydromechanical (H/M) controls, electronic controls and accessories/sensors. Figures 11.48 and 11.49 show

control component configurations for a military and a commercial engine.

For qualification (certification) an endurance bench test is normally required. For this test a cycle is defined which represents the component's functional operation over a typical flight or a wide range of missions. The cycle is typically "weighted" so that a larger portion of the cycle is spent at the operational points most often "seen" by the component. Depending on the components, a cycle may last seconds or hours. A test setup is designed so that the cycle can be run repeatedly, for a specified total number of hours. The cycle is divided into room, hot and cold temperature portions. Room temperature is just running at ambient conditions, hot will be at the max normal ambient temperature and cold the max operational cold temperature (usually -65°F). There are specified dwell times to assure the component is completely soaked.

All components which carry fuel, oil, or air require contamination testing. The actual type and portions of contamination are specified. This is mixed with the fluid and the component must be capable of operating a specified time under these conditions. Fuel and oil carrying components are usually required to pass a flame test. The component is setup to operate at the minimum flow condition (min. heat rejection). A flame source calibrated to a given output (Btu/hr), is placed in front of the component. The component must survive five minutes without causing a leak that can sustain a flame.

Vibration testing is also required. This normally consists of resonant searches in three planes and subsequent dwell periods at resonant points. Also, sweep cyclic tests are performed over a range of frequencies and "G" lev-

HYDROMECHANICAL CONTROLS	ELECTRICAL CONTROLS & PROCESSORS	ACCESSORIES/SENSORS
MAIN ENGINE (FUEL) CONTROLS CLEARANCE CONTROLS HYDROMECHANICAL UNITS (HMU)	AUGMENTER/FAN/TEMP (AFT) CONTROLS — ANALOG POWER MANAGEMENT CONTROLS (PMC) — ANALOG — DIGITAL DIGITAL ELECTRICAL CONTROL UNIT (ECU) DIGITAL ENGINE CONTROLS (DEC) ENGINE MONITORING SYSTEM PROCESSORS (EMSP)	FUEL PUMPS — CONSTANT DISPLACEMENT — CENTRIFUGAL HYDRAULIC PUMPS FUEL FILTERS HEAT EXCHANGERS FUEL POWERED ACTUATORS SERVOACTUATORS THERMOCOUPLES FEEDBACK CABLES TEMPERATURE SENSORS — ELECTRICAL (RTD'S/THERMOCOUPLES) — HYDROMECHANICAL ALTERNATORS SPEED SENSORS SWITCHES FLAME SENSORS PRESSURE SENSORS OPTICAL PYROMETERS POSITION SENSORS SOLENOID VALVES CHECK VALVES ELECTRICAL CABLES FLOWMETERS STARTERS STARTER CONTROL VALVES THRUST REVERSER ACTUATORS THRUST REVERSER CONTROL VALVES

Table 11.5 External Component Designs

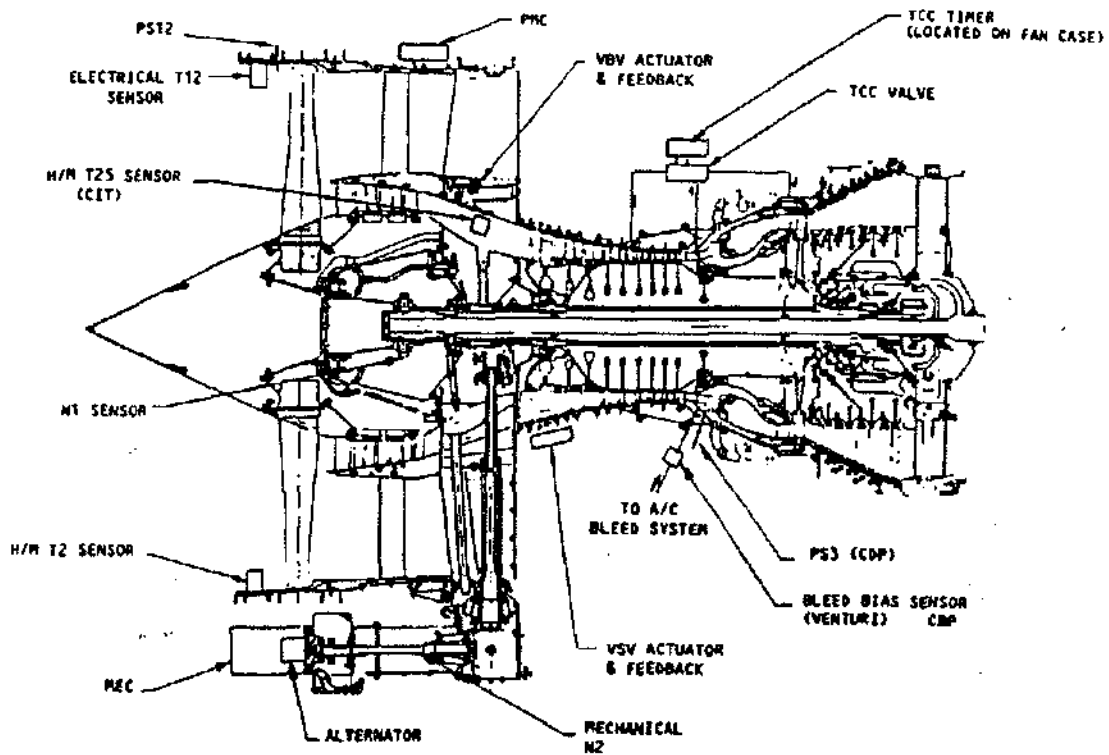


Figure 11.48 CFM56-2 Control Component Locations

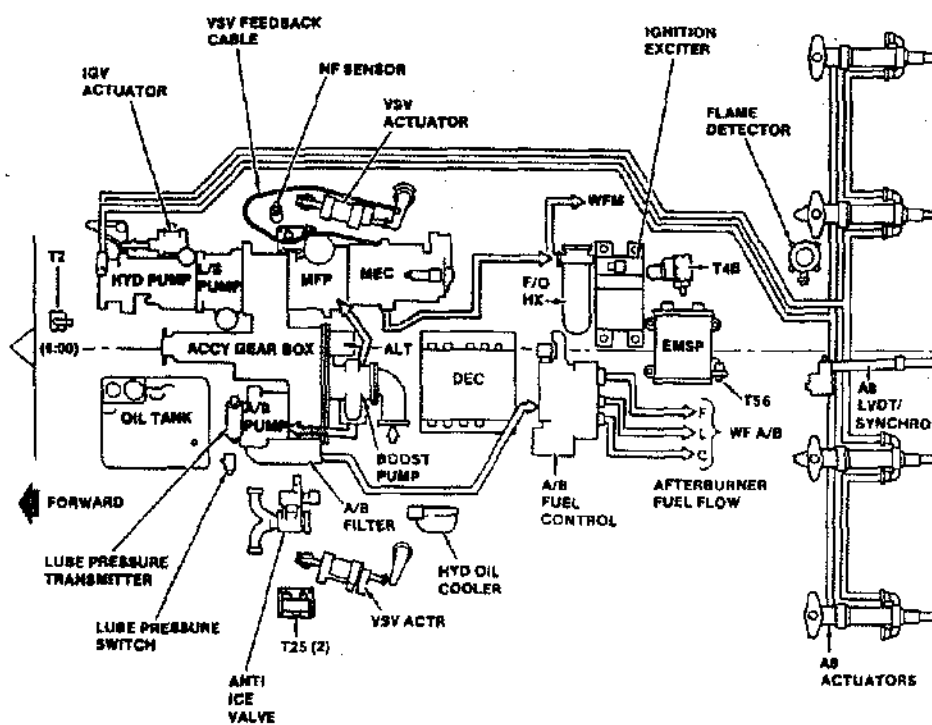


Figure 11.49 F110-129 Control & Accessory Locations

els. Electrical components may also be subjected to electromagnetic interference (EMI), lightning and nuclear exposure testing. These components must be capable of normal operation after exposure to these conditions.

Fuel system components (primarily pumps) are susceptible to cavitation when pressures are low. To prove fuel system components can function under abnormal conditions, where normal fuel supply pressure is not available special tests are run. This is usually called V/L (vapor/liquid) testing. Fuel inlet pressures are reduced to see if the component can pump or function normally and that cavitation doesn't drastically effect component performance. This test is accomplished on individual components and the entire fuel system.

This section has covered some of the design and qualification requirements of the numerous and varied controls components. The next two sections cover some design details and component descriptions.

HYDROMECHANICAL CONTROL

Hydromechanical controls used on jet engines today generally fall into the category of Main Engine Control (MEC) or Augmenter Fuel Control (AFC). This section discusses some basic design concepts used in these types of controls and describes their evolution. Also, a brief description of the HydroMechanical Unit, used on the newest FADEC equipped engines, is included.

Hydromechanical controls, as opposed to other control components, perform computations from sensed inputs and regulate outputs to maintain controlled variables within defined limits. Hydromechanical controls utilize regulated fluid pressures (servo pressures), levers, mechanisms, governors, pistons, and various forms of valves, including torque motor servo valves, to accomplish computation and control of assigned functions.

Two of the most commonly used devices in hydromechanical controls are hydromechanical servos and electro-hydraulic torque motors (or servo valve). An explanation of the operating principles of these two devices follows:

The mechanism shown in Figure 11.50 is a simple hydraulic servo with direct mechanical feedback. With this mechanism, the input lever can be set at a given position and the servo piston will be positioned at a corresponding position.

When the input lever is moved to the right, the lower end of the lever pivots on the left end of the feedback link.

The pilot valve plunger is moved to the right by the input lever and high reference fuel pressure (P_{hi}) is ported to the left side of the piston moving the piston to the right. As the piston is moved to the right, the lower end of the feedback lever is moved to the left and the lower end of the input lever is also moved to the left. The input lever pivots at its upper end, which must be held in each position, and the pilot valve plunger is moved to the left. This action continues until the control land covers the control port (null) cutting off the flow of fuel to the piston. The resulting piston position is indicative of the position of the input lever.

In reverse action, the input lever moves to left and held. The pilot valve plunger likewise moves to the left and the fuel at medium reference pressure (P_{med}) on the left side of the piston can escape to the low reference pressure (P_{lo}). P_{med} on the right side of the piston, being higher than P_{lo} on the left side of the piston, moves the piston to the left. As the piston moves to the left, the lower end of the feedback lever moves to the right, moving the lower end of the input lever to the right. Since the upper end of the input lever is being held in position, the plunger valve is moved to the right. This action continues until the pilot valve plunger moves far enough so the control land is again covers the control port, nulling the pilot valve and stopping the movement of the piston.

A typical electro-hydraulic servovalve, or torque motor, is shown in Figure 11.51. This torque motor is a two stage jet pipe type servovalve, which is generally used in military MEC's and commercial HMU's (FADEC equipped engines). A feature of this type of torque motor system is that once the controlled parameter is driven to the demanded position, the input current to the torque motor moves to a fixed value, or "null" value, indicating that demand has been satisfied. Single stage flapper valve type torque motors (not shown) are generally used in commercial MEC's for PMC speed trim feedback to the hydromechanical governor. This type of torque motor system requires a continuous feedback error signal, proportional to the amount of error in the hydromechanical schedule which is being offset by the electrical trim control.

The torque motor shown in Figure 11.51 receives an electrical feedback error signal from the electronic control. This error may be either positive or negative current (usually measured in milliamps) and, depending on polarity, will cause an electromagnetic force to be generated in the coils proportional to the error signal.

Assume, for the moment, that the electromagnetic force generated causes the armature and jetpipe to deflect to the right. The high pressure supply fuel supplied to the

jetpipe will divert to the right port of the receiver, which raises the pressure on the right end of the spool valve plunger. At the same time the left port of the receiver will sense a lower pressure, which in turn is sensed by the left end of the spool valve plunger. The resulting pressure differential across the spool valve plunger will translate the plunger to the left. As the plunger moves left, the right control port in the spool valve sleeve is uncovered allowing high pressure supply fuel to be ported to the right side of the piston. Also the left control port in the spool valve sleeve is uncovered allowing the left side of the piston to be vented to the low pressure return. The pressure differential across the piston then moves the piston to the left, changing the position of the controlled parameter by a rate equivalent to the error signal. As the piston moves left to the demanded position, the feedback error signal from the electrical control to the torque motor coils will decrease toward null. This action is aided by the feedback spring, which also exerts a restoring force to the jetpipe. When the controlled parameter reaches the demanded value, the torque motor error signal will reach null value.

Use of torque motor servo valves in hydromechanical controls is on the increase in new control system designs. As more computational and scheduling functions are taken over by electronic controls and as new control functions are added, torque motor servo valves function to convert the electrical output signals from the electronic control to fuel valve and actuator positions.

Main Engine Controls (MEC's) Main Engine Controls (MEC's) are electro-hydromechanical controls which utilize fuel as a computational fluid and whose primary purpose is to control the main engine (as opposed to augmentation) functions. MEC's have been used on jet aircraft engines since their inception. As jet engine applications have become more complex, so has the MEC grown in size and number of functions. Early jet engine controls basically provided engine speed governing, start fuel scheduling, transient fuel flow limiting, and overspeed protection. Today's MEC's provide not only these basic functions mentioned, but include a diversity of other functions as well. Figure 11.52 is a schematic of the F101 MEC showing the complexity of a typical present day hydromechanical engine control. Following is a list of the functions performed by today's MEC's:

- Control of compressor variable stator vane (VSV) position
- Control of booster variable bleed valve (VBV) position

- Schedule engine core speed or, in some cases, fan speed directly, using inputs of power lever angle, ambient temperature, and ambient pressure
- Limit minimum and maximum compressor discharge pressure
- Prevent rotor overspeed
- Establish min and max fuel flow limits
- Provide fuel shutoff and pump unloading functions
- Provide hydromechanical switching signals for a variety of engine components, such as turbine clearance control air valves and hydraulic timers
- Provide regulated servo fuel flow to other hydromechanical controls, such as the augmentor control
- Provide interfaces such as solenoids and torque motor servo valves to permit manipulation of fuel flow and other variables from electrical controls
- Provide control system intelligence to electrical controls using electrical transducers (PLA position, fuel metering valve position)
- Provide filtered high pressure fuel to engine actuation systems (VSV's, VBV's, etc.)

Since the MEC requires a core speed input signal and fuel for computation and metering functions, all Even-dale military engine MEC's and most Even-dale commercial engine MEC's are mounted piggy-back on the main engine fuel pump. The speed input and fuel supply/return are provided through the mounting interface.

An example of the use of hydraulic servomechanisms in hydromechanical controls is shown in Figure 11.53, the compressor inlet temperature (CIT) system. This system senses air temperature and positions a three dimensional cam to indicate the temperature being sensed.

The CIT sensor, which is a separate component from the MEC, is installed in the frame assembly in front of the high pressure compressor (see Figure 11.54). The sensor incorporates a helium gas charged sensing coil which is located in the compressor inlet flowpath. When the air temperature increases, the helium gas pressure increases. Conversely when the air temperature decreases, the gas pressure decreases also.

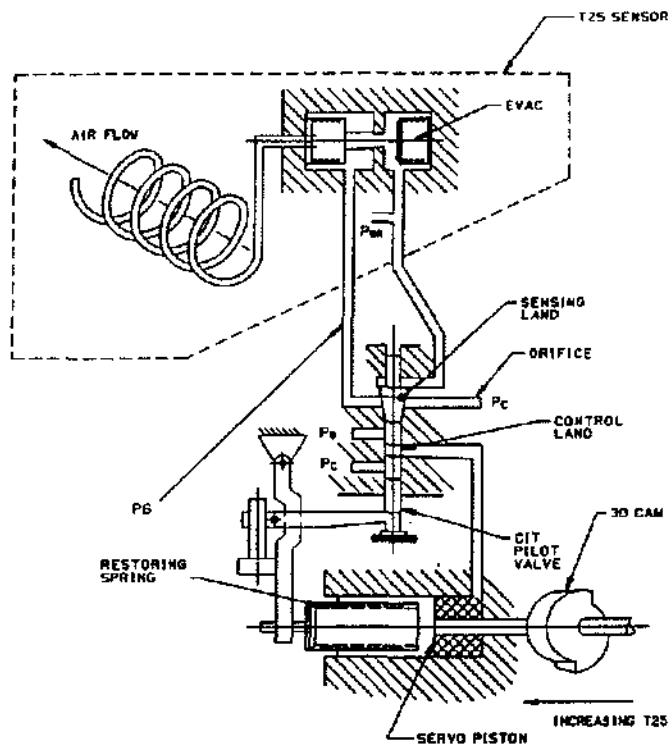


Figure 11.53 CIT Sensor System

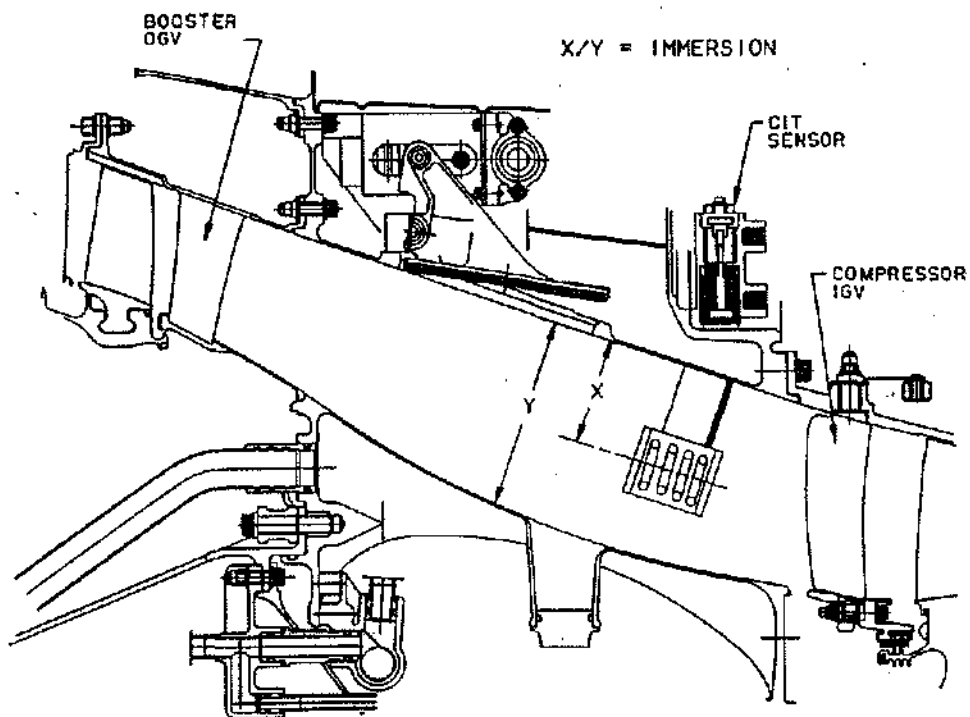


Figure 11.54 (CIT) Sensor Location

The sensing coil is connected to a sensing bellows (see Figure 11.53) which is supplied with fuel at high pressure, P_c , through an orifice which creates a pressure drop. This pressure, called P_6 , increases in the area around the sensing bellows until the bellows contracts and partially opens the valve, allowing P_6 pressure to escape to P_b . P_6 is regulated at a value equal to that required to overcome the spring force from the contracted bellows plus the force of P_b around the reference bellows. If temperature increases, the valve decreases the opening until P_6 pressure increases to a level at which the valve opens.

This P_6 pressure is applied to the bottom of the sensing land of the CIT pilot valve. The force it creates is opposed by restoring spring. P_{br} pressure applied to the top of the sensing land is nullified by the fact that the same P_{br} is also applied to the left side of the reference bellows in the CIT sensor. Any change in P_{br} changes P_6 a like amount.

In a balanced condition, the pilot valve is held at null by the forces of P_6 , P_{br} , and the restoring spring. In this condition, the servo piston and the three dimensional cam do not move. An increase in sensed temperature by the sensing coil causes an increase in P_6 , which moves the pilot valve plunger up. P_c pressure is then ported into the area to the right of the servo piston and the piston and the 3D cam move to the left. The force of the restoring spring increases as it is compressed until it equals the force applied by the increased P_6 pressure. At the same time the piston moves the pilot valve plunger down until it is again at null. Nulling the pilot valve stops the movement of the piston. The system is again balanced and the 3D cam is in a new position indicative of a higher compressor inlet temperature.

When CIT decreases, the action is reversed. As P_6 decreases, the pilot valve plunger moves down, porting the eighth side of the servo piston to P_b . The restoring spring moves the servo piston to the right. The 3D cam moves to the right until the decreased force of the restoring spring allows the pilot valve plunger to re-null. The basic servomechanism principles described above are used in a variety of forms to provide a number of control functions in the MEC.

Hydromechanical Units (HMU's) The HMU is distinguished as being the fuel handling component of Full Authority Digital Electronic Control (FADEC) system. In this system the major computation, logic, and scheduling is accomplished by the digital electronic control unit (ECU). HMU's are currently used on the CFM56-5 and CF6-80C2 and is planned for use on the GE36 (UDF). Figure 11.55 shows a schematic of a typical

HMU used on the -80C2 engine. The HMU's main functions are to convert the electrical output signals from the ECU, i.e. torque motor signals, into servo pressure outputs to various control subsystems. The HMU also provides electrical outputs to the ECU (fuel metering valve position) and redundant core overspeed protection. HMU's receive the following inputs from the ECU:

- Fuel metering valve torque motor current
- VSV torque motor current
- VBV torque motor current
- HP turbine clearance control (HPTCC) torque motor current
- LP turbine clearance control (LPTCC) torque motor current
- Core rotor active clearance control (RACC) torque motor current (-5 only)
- Burner staging (BS) solenoid current (-5 only)
- Fuel metering valve resolver excitation
- Fuel shutoff switch current
- Overspeed governor switch current

The HMU receives a mechanical core speed input signal from the engine accessory gearbox. Aircraft input to the HMU consists of a fuel shutoff solenoid command signal. Outputs from the HMU include:

- Metered fuel flow to the combustor fuel nozzles
- Fuel flow to/from the VSV actuators
- Fuel flow to/from the VBV actuators
- Fuel flow to/from the BS valve
- Fuel flow to/from the HPTCC valve
- Fuel flow to/from the LPTCC valve
- Fuel flow to/from the RACC valve
- Fuel metering valve resolver position
- Fuel shutoff indication
- Overspeed governor function check

As can be seen from the above discussion, while the HMU does not include the major computation and scheduling functions, it is still a major control component of considerable complexity.

Augmenter Fuel Control The augmenter fuel control (AFC) is an electro-hydromechanical component which receives fuel from the augmenter fuel pump and meters

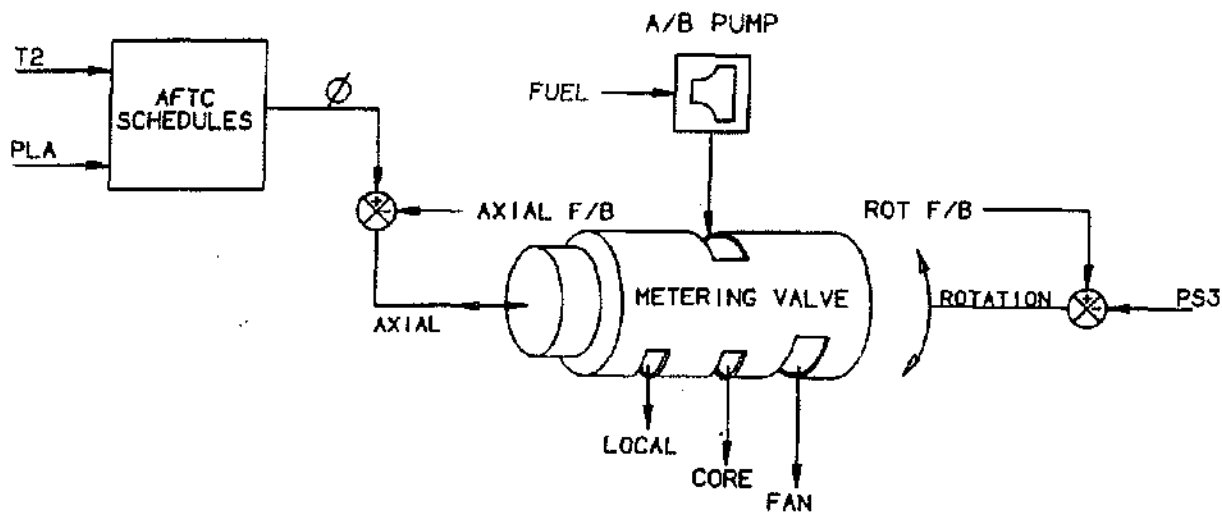


Figure 11.57 AFC Fuel Metering Valve Operation

blow-out sequence can occur. Flow that is too rich could cause augmentser screech.

The metering valve is positioned by an electro-hydraulic servo valve. The servo valve (see Figure 11.56) is a diverter type that is actuated by a torque motor in response to an electrical signal from the electronic control. When the throttle is advanced into the augmentser range, the diverter valve ports servo fuel to the left (open) side of the metering valve piston to overcome the force of a spring, and move the metering valve to the right to increase the axial dimension of the metering valve core and fan window areas. A throttle decrease in the augmentser range signals the torque motor to position the valve to port servo fuel to the spring side of the metering valve so that servo fuel pressure plus spring force causes the metering valve to move to the left, decreasing the axial dimension of the core and fan window area. This valve can deliver a total fuel flow of 78,000 pph.

The PS3 pressure transducer is a pneumatic-hydraulic device that rotates the metering valve in response to changes in PS3, increasing the chordal dimension of the metering valve local, core and fan window areas. It consists of a PS3 sensing bellows and an evacuated bellows attached to opposite sides of a lever

that moves a jet pipe servo. The servo pressures actuate a piston connected to the metering valve by a rack and pinion gear. The force-balance servo loop is completed as spring force, which is generated by the motion of the piston, is balanced by the force generated in the PS3 bellows by changes in PS3 pressure.

The linear variable differential transformer (LVDT) feeds back to the electronic control an electrical signal proportional to the valve position (WFR/PS3). This enables closed loop scheduling of metering valve position. The AFC also houses an augmentser on/off solenoid. An electrical signal from the electronic control energizes the solenoid, sending a fuel pressure signal to the augmentser fuel pump. This signal opens the pump inlet valve and initiates augmentser fuel flow.

A manifold circulation valve distributes fuel to the local, core, and fan manifolds during non-augmented operation to keep them full and thus prevent thrust lags and surges when augmentation is begun. Fuel is circulated from the valve to the bottom of the manifolds, and returned to the valve from the top of the manifolds. It is then returned to the aircraft boost pump discharge. The fuel pressure is low enough so that it does not "crack" the spray bar distribution valve, preventing flow into the augmentser.

OTHER CONTROL COMPONENTS

A wide variety of components fall into the "other" category of controls components. In fact, there are so many different kinds of hardware that a complete book could be written on these components. This category includes pumps, actuators, valves, sensors, starters, electrical cables, filters, heat exchangers, switches and motors. In order to reduce this section to a manageable level, only four major categories of controls components will be discussed. These are: pumps, actuators, valves and sensors. Throughout this section a brief general description will be given for the component class, then some specific component applications.

Pumps Pumps designed for control component applications are normally engine gearbox driven. These pumps supply engine fluids at appropriate pressures to fuel controls and variable geometry actuators. General pump classes or categories include:

- Hydraulic pumps (typically high pressure output piston pumps)

- Fuel boost pumps (high flow, low pressure rise centrifugal fuel pumps which condition the fuel for other engine fuel pumps).
- Main fuel pumps (constant displacement gear element or vane element pumps). Main fuel pumps provide combustor flow, control computation servo flow, and variable geometry actuation flow.

Pump sizing requires detailed fuel system analysis to assure the pump will provide flow and pressure at all flight conditions. An example will be given of the three main classes of pumps (centrifugal, gear and piston). Augmented military engines require a fuel boost pump ahead of the main and augmentor fuel pumps to maintain adequate flow and pressure for the two systems. The F101/F110 boost pump is a single element centrifugal type pump, with a maximum flow capacity of 90,000 pph. The rated pressure rise is 40 psi. Figure 11.58 shows a cross-section and flow paths for this pump.

The engine boost fuel pump receives fuel from the airframe system at airframe boost pressure. It also provides

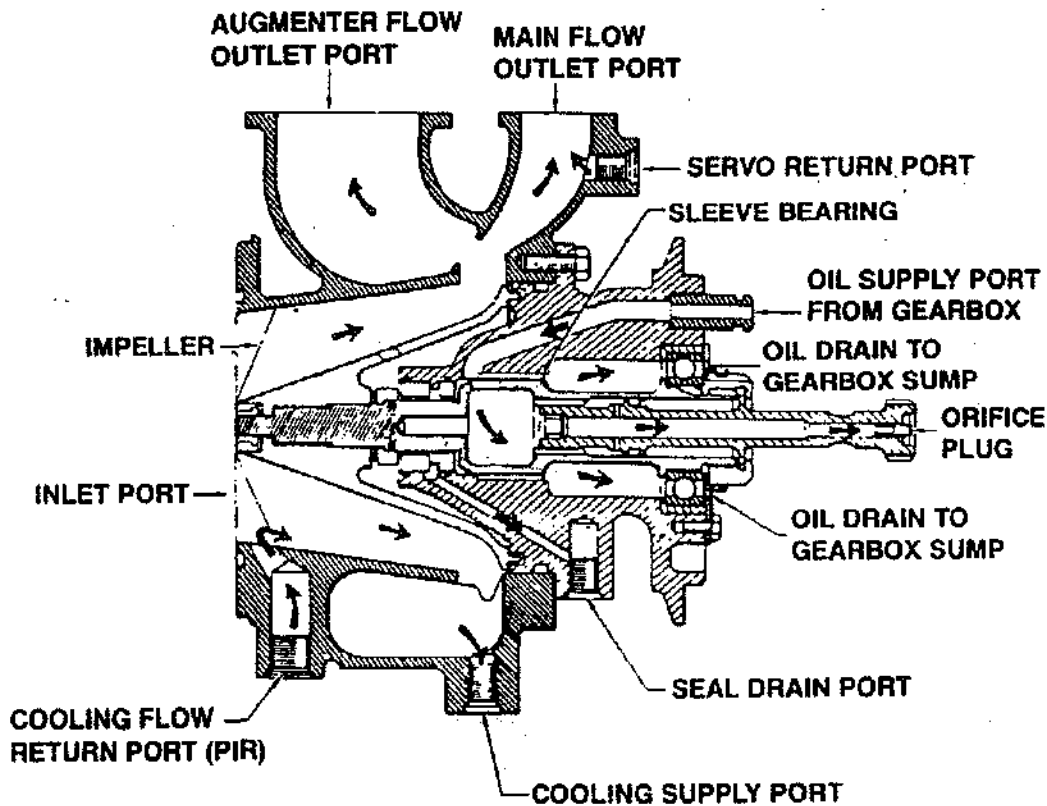


Figure 11.58 F101/F110 Boost Pump Cross-Section

pressure and flow to meet the requirements of the main and augmentor fuel pumps and provides electronics cooling and augmentor manifold recirculation fuel flows. Fuel at aircraft boost pressure enters the pump which boosts pressure to levels adequate to operate the engine at all power levels, and to provide return pressure for augmentor control servo flow, electronics control cooling flow, and augmentor manifold circulation flow during non-augmented operation. Pump pressure rise is sufficient to supply fuel at adequate net positive suction pressure to the main and augmentor fuel pumps over the full range of engine inlet conditions.

The CF6-80C main fuel pump is an example of a constant displacement pump. This means that a fixed volume of fuel is pumped for each revolution of the gears. A schematic of the functional parts of the pump is shown in Figure 11.59. Notice that the MEC bypasses any unneeded fuel flow back to the impeller stage output. The pump consists of a fixed displacement high pressure gear element, an integral centrifugal boost element, an inter-stage strainer with bypass provisions, and a high pressure relief valve. The pump includes provisions to flange mount and support the fuel-oil heat exchanger and the

fuel filter in the high pressure discharge flow path. Ports are provided in the booster flow to provide a cooling flow to the PMC. Additional ports are provided for instrumentation and drainage. Some of the design features of this pump are:

Dimensions	15 L x 10 1/2" w x 11" D.
Weight	35 pounds dry
Spline shaft shear section	3000 - 3700 inch-pounds.
Output	26,5000 p.p.h. Max. flow
Relief valve	1500 psid cracking, 1700 psid max, 1450 psid reseal
Strainer	Photo-etched perforated sheet metal, 0.019 - 0.024 dia. holes.
Bypass valve cracking	4 psid, full flow 16 psid.
Boost pressure	0 - 152 psid.

The pump has a shear section in the drive shaft so that if it binds up the shaft will shear preventing damage to the gearbox. The relief valve is set so that a system overpressure cannot occur. This value is determined by the pressure capability of the weakest component in the fuel system.

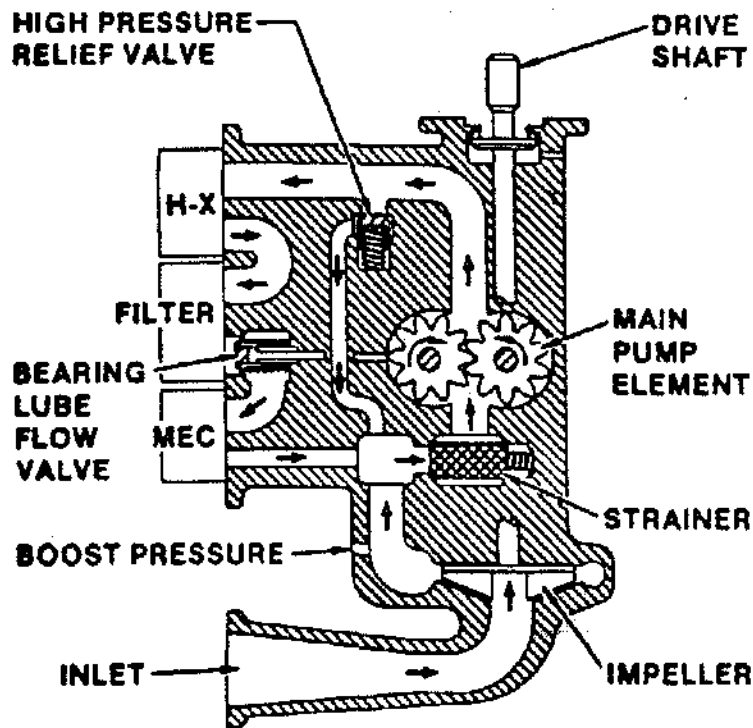


Figure 11.59 CF6-80C Main Fuel Pump Schematic

A common control piston type pump is the F101/F110 exhaust nozzle hydraulic pump. This pump provides the nozzle area control system with hydraulic power for exhaust nozzle positioning (delta P/P loop). Engine oil is the hydraulic fluid. A schematic of the pump is shown in Figure 11.60. This pump is more complex than most because it includes the positioning function for the piston wobble plate and pressure compensation hardware.

The hydraulic pump is an electrically signalled, overcenter piston pump which provides bidirectional hydraulic flow for nozzle actuation at a rate and direction proportional to the magnitude and polarity of the controlling electrical signal. The pump consists of an internal, gear-type, inlet boost pump, an inlet filter, a constant displacement servo supply pump, and a primary piston element with its associated flow control servo. The servo pump provides a constant hydraulic pressure for the servo valve controlling the piston pump flow. All necessary relief, regulation, and pressure-compensating valves are included as integral parts of the pump design. The pump is also equipped with a shuttle valve between the head- and rod-ports to replenish pump flow to, or remove it from the low pressure side of the pump outlet

ports; a destroking device to limit rod-port pressure and temperature rise during excess flow demand with actuators on stroke limits, and output head- and rod-port relief valves.

Oil from the hydraulic compartment of the lube/hydraulic tank enters the hydraulic pump at the inlet port located on the mounting pad. This oil flows to the gerotor boost element, and is pumped through the hydraulic filter to a junction which ports oil to the servo control vane pump and the makeup flow selector valve. Flow from the servo control pump flows to the servo valve, a bidirectional output device, which is controlled by a signal from the electronic control.

Depending upon the polarity and magnitude of the electrical signal from the electronic control, the torque motor flow diverter within the servo valve moves to port servo control flow to either of the two thrust plate control pistons. These pistons control the angle of the thrust plate and consequently the stroke of the high pressure pump pistons. Thrust plate position determines the direction and rate of oil flow to the nozzle actuators. When the thrust plate reaches the desired angle, feedback force

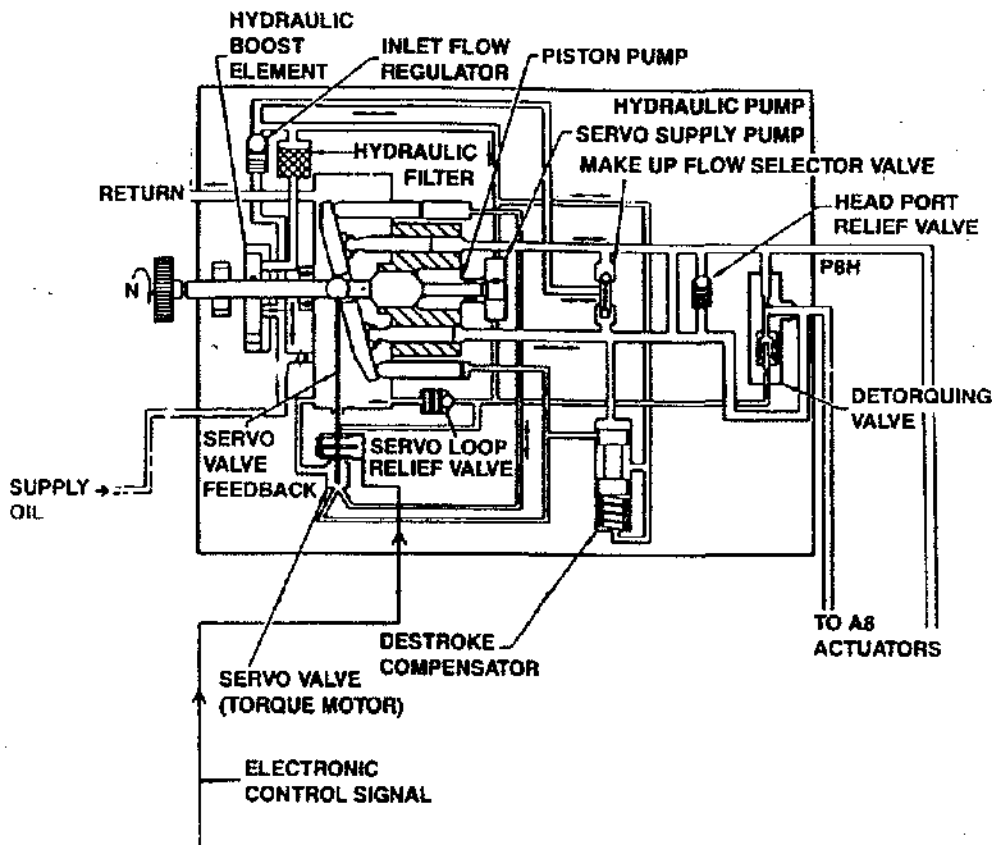


Figure 11.60 Hydraulic Pump Schematic

from the thrust plate feedback spring balances the torque of the torque motor and the jet pipe is nulled. Figure 11.61 shows the piston and barrel operation.

Actuators Actuators provide the force and motion required to move and position engine variable geometry mechanisms. Some actuators are simply pistons in a body (e.g. VSV) with external pressures setting position. Others are more complex with integral electro hydraulic servo valves (EHSV) for electrical signal positioning and LVDT's to provide position feedback for control loop closure. Categories of actuators include:

- Hydraulic (oil powered) piston actuators used primarily in exhaust nozzle actuation (high force requirements)
- Fuel powered piston actuators used in VSV, VBV and IGV actuation systems.
- Motor driven ball screw actuators used in thrust reverser actuation systems.
- Mechanically driven actuators, driven through flex shafts used in thrust reversers and CFM56 VBV's.

System studies are required to correctly size actuators for force and transient slew requirements. Remember,

actuators are the integrators (k/s) in the control loop. An example of an oil driven actuator is the exhaust nozzle (A8) actuator used on augmented engines. The F101 uses six actuators, the F110 uses four. This is a double acting, uncushioned, hydraulic actuator. They can be synchronized by means of a flexible torque carrying cable. One on each engine is equipped with a LVDT for position feedback. A cut away of a synchronous actuator is shown in Figure 11.62. Some of the design features are as follows:

Head-End Piston Area	4.613 sq. in.
Rod-End Piston Area	3.727 sq. in.
Hydraulic Pressures:	
Maximum Rod-Port ΔP (Closed Nozzle)	4400 psid
Maximum Head-Port ΔP (Open Nozzle)	1350 psid
Flow (Maximum Head-End)	24.4 gpm
Output Force per Actuator	
Maximum Compression	6,158 lb
Rated Compression	5,315 lb
Maximum Tension	16,397 lb
Rated Tension	14,907 lb
Actuation Time	Extended 4.0 Sec. Retracted 3.5 Sec.
Stroke	9.62 in.

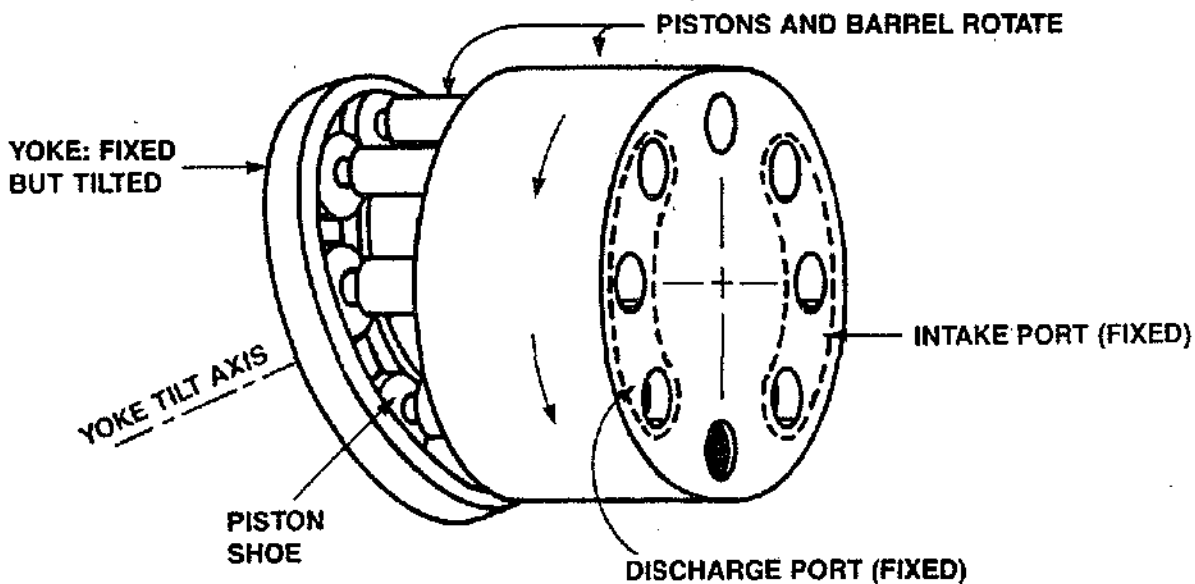


Figure 11.61 Hydraulic Pump Piston Operation

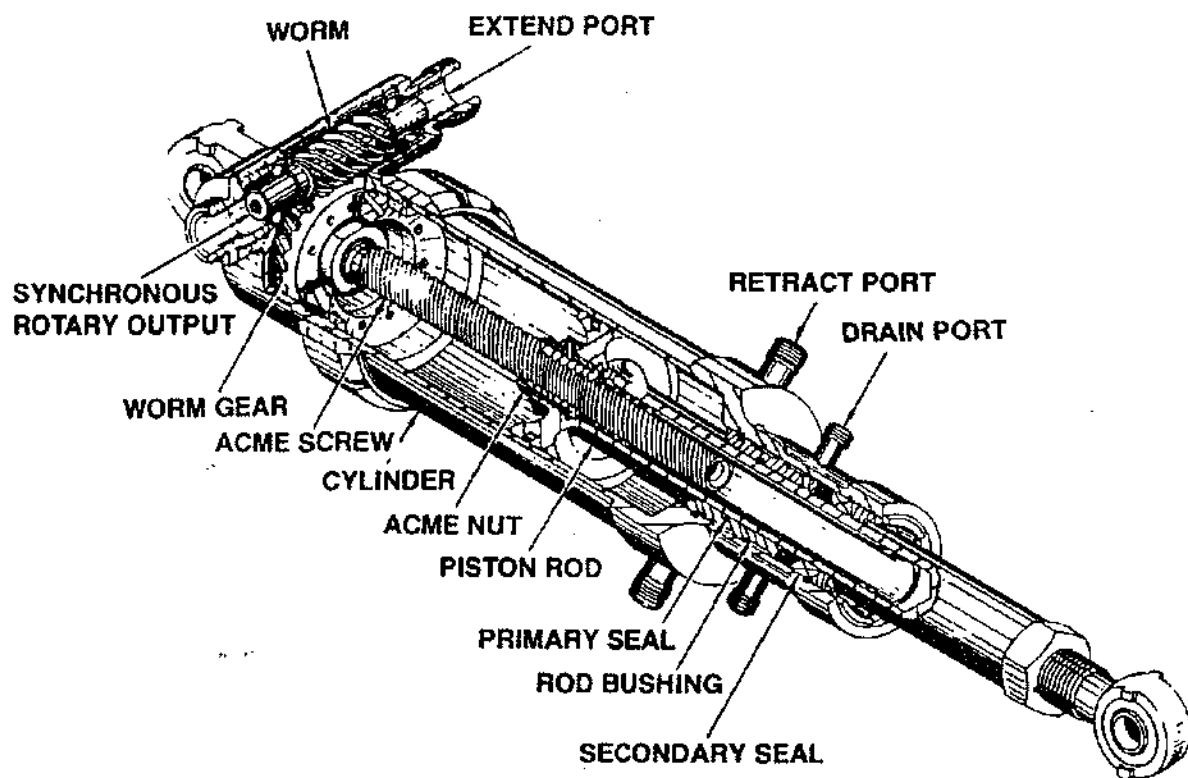


Figure 11.62 A8 Actuator Cutaway

The hydraulic pump supplies high pressure oil to either the rod- or head-ends of the nozzle actuators at the direction of the electronic control which schedules the variable geometry of the exhaust nozzle. As high pressure oil is ported to either end of the cylinders, a pressure differential across the pistons causes the actuators to extend or retract. The pistons of the synchronized actuators move axially in the cylinders rotating the acme screw center shafts, which in turn rotates the wheel gear and worm screw. The flexible shafts, which connect the worm screws, mechanically synchronize the system for even, proportional actuation.

The variable bleed valve (VBV) actuators used on the CF6-80 engine are an example of a simple fuel powered actuator. Two actuators are used to provide the muscle to position and hold the bleed valves at the scheduled position. An adjustable clevis at the end of each actuator is bolted to a bellcrank which moves a 360 degree unison ring and positions the (12) individual bleed doors. This is similar to the IGV actuation system.

Positioning logic is provided by the main engine control (MEC). The main engine control senses VSV feedback cable position to schedule VBV's. The MEC compares

the schedule against the VBV feedback position. If any error is sensed, a pilot valve will port fuel pump discharge pressure to the side of the pistons that will bring the VBV feedback cable into agreement with the schedule. The VBV's are closed at high power and the actuators are retracted. An external view and cross-section are shown in Figure 11.63. Some of the features of the VBV actuators are:

Dimensions	8 1/4" long x 2 1/4" dia.
Weight	3 pounds each
Housing	2618 aluminum with steel rod and piston.

Two fuel ports are cast on the head end. Ports are threaded for adapters and the outer boss is threaded for a shrouded coupling. The head end boss has a drain port emptying into the shroud to drain the shaft double seal cavity. The assembly is able to operate with fuel pressures over 1455 psia. The piston area is 2.45 square inches.

On CF6 engine the thrust reverser is operated by an air driven actuator one on each reverser half. These actuators are called center drive units (CDU) because they

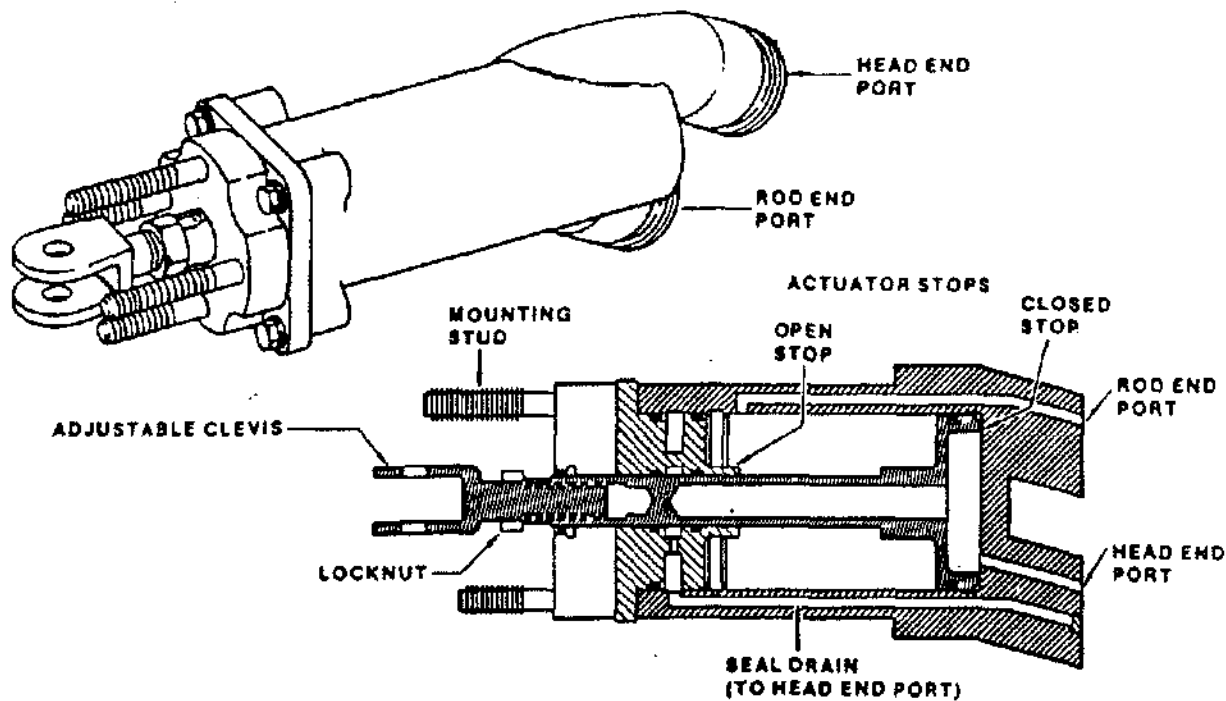


Figure 11.63 CF6-80 VBV Actuator

include the air motor, a directional control valve (for extension and retraction), and a mechanical feedback unit. The CDU also drives flex shafts which extends and retracts two other end actuators required for each reverser half. Figure 11.64 shows a cutaway of a CDU (actuator). This is a complex unit which also falls into the motor and valve category. The actual extension and retraction of the CDU and its end actuators is accomplished by a ballscrew mechanism.

Each ballscrew actuator is spline coupled to its gearbox, clamped by a captive threaded nut and is locked by a splined limit stop collar. The ballscrew is rotated by the gearbox which translates the ballnut. The ballnut is restrained by the torque tube housing, with the rod end bearing and torsion arm engaging a translating cowl clevis pocket. The deployed length is determined by a stop collar pinned to the ballscrew aft end; the deploy limit is reached when the ballnut strikes the stop collar. The rod end bearing adjusts the actuator stowed length.

Engine bleed air is used to drive the air motor which translates the ballscrew actuators via angle gearboxes. The directional control valve (DCV) position (controlled from the cockpit) will port air to extend or retract the actuators. The CDU includes a unidirectional brake which

while engaged will only allow rotation of the air motor in the direction of stow. The brake must be disengaged by the DCV. A position indicating switch is also included to signal deploy and stow, these signals are used in controlling thrust reverser operation.

Valves Valves are used primarily in the control system to direct airflow for other downstream usage. Air valves are used extensively in the CFM56 and CF6-80A and -80C turbine clearance control, compartment cooling and active clearance control systems. In an attempt to improve component efficiencies and reduce SFC as much as possible, new commercial engines have more complicated clearance control systems. These engines may have LP and HP turbine clearance control, bore cooling and compressor clearance control. Operating tip clearances in the core engine are of primary importance. They not only determine steady-state efficiencies, as measured by specific fuel consumption, but have the most significant effect on transient engine performance as measured by peak gas temperatures and compressor stall margin. In a balanced design, they also reduce deterioration by compensating for rapid throttle movements without sacrificing steady-state performance. It's in these systems that air valves are used to direct the airflow as signalled by a controlling source.

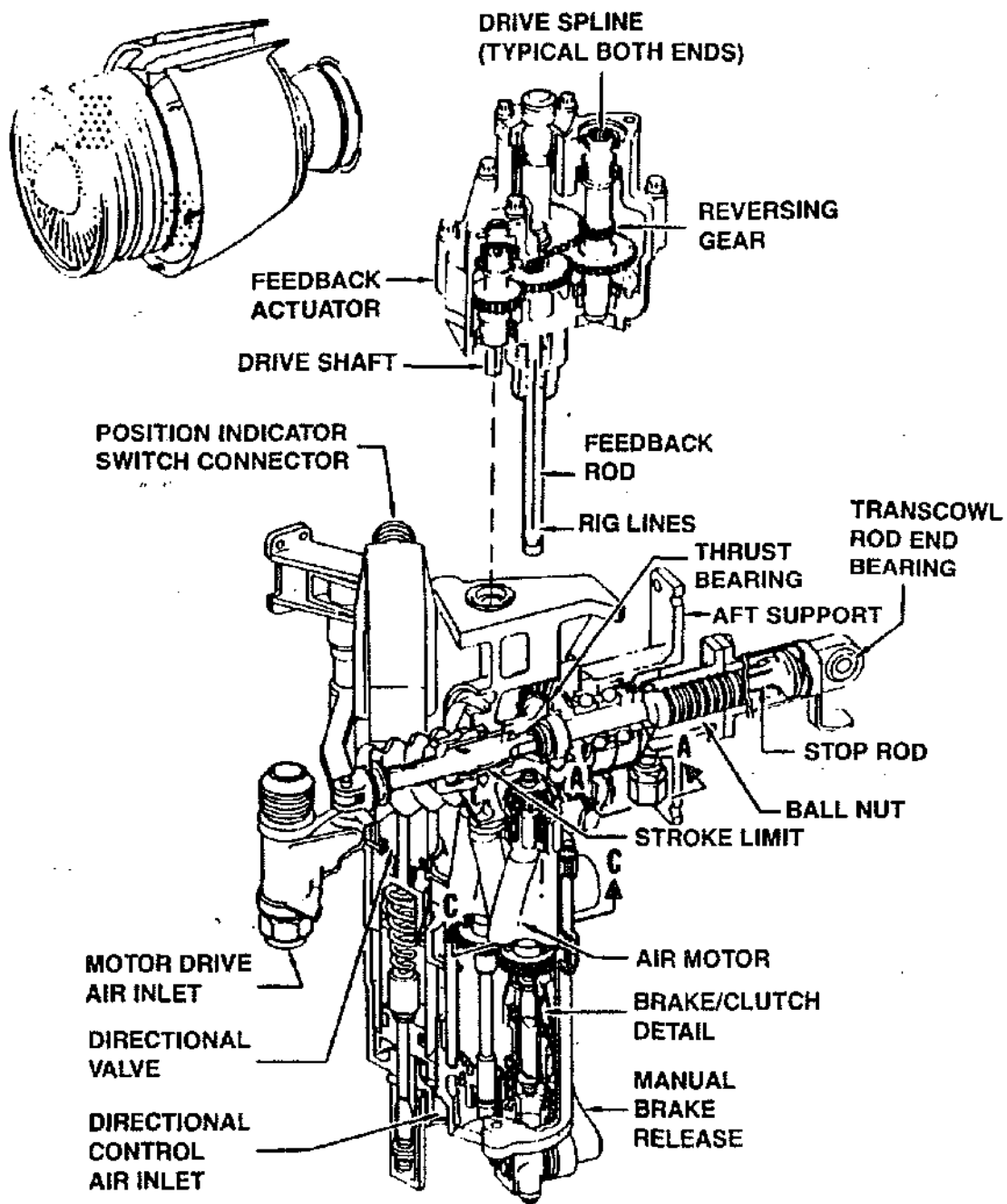


Figure 11.64 CF6-80C T/R Center Drive Unit with Ballscrew Actuator

On the CFM56-2/3 the turbine clearance control valve (TCCV) is used for HPT shroud clearance control. The CFM56 engine high pressure turbine (HPT) clearance control system uses high pressure compressor (HPC) bleed air from stages 5 and 9 to obtain maximum steady-state HPT performance and to minimize exhaust gas temperature (EGT) transient overshoot during throttle bursts. Air selection is determined by fuel pressure signals from the main engine control (MEC). The bleed air is ducted from the valve to a manifold surrounding the HPT shroud. The temperature of the air controls the HPT shrouds relative clearance to the HPT blade tips.

The valve can be set to allow three operational modes: stage 5 air only, stage 9 air only, or a combination of these two. A schematic of the valve is shown in Figure 11.65. During operation fuel circulates through the

valve, to or from the MEC depending upon the pressure differential of the 3 control pressures and the orifice in the hydraulic actuator piston. An orifice, located in the 9th stage air extraction line between the valve and compressor casing extractor manifold, reduces the 9th stage air pressure supplied to the valve to prevent 9th stage air introduction into the 5th stage of the compressor when both valves are open (during climb power).

Another example of a special valve used in clearance control systems is the CF6-80C active clearance control (ACC) signal valve. This valve ports 11th stage (PS3) bleed to two ACC valves and the compressor compartment cooling (CCC) valve. A basic cross-section of this valve is shown in Figure 11.66. This system provides fan discharge air for cooling the core compartment and the turbine cases. At low altitudes the core compartment

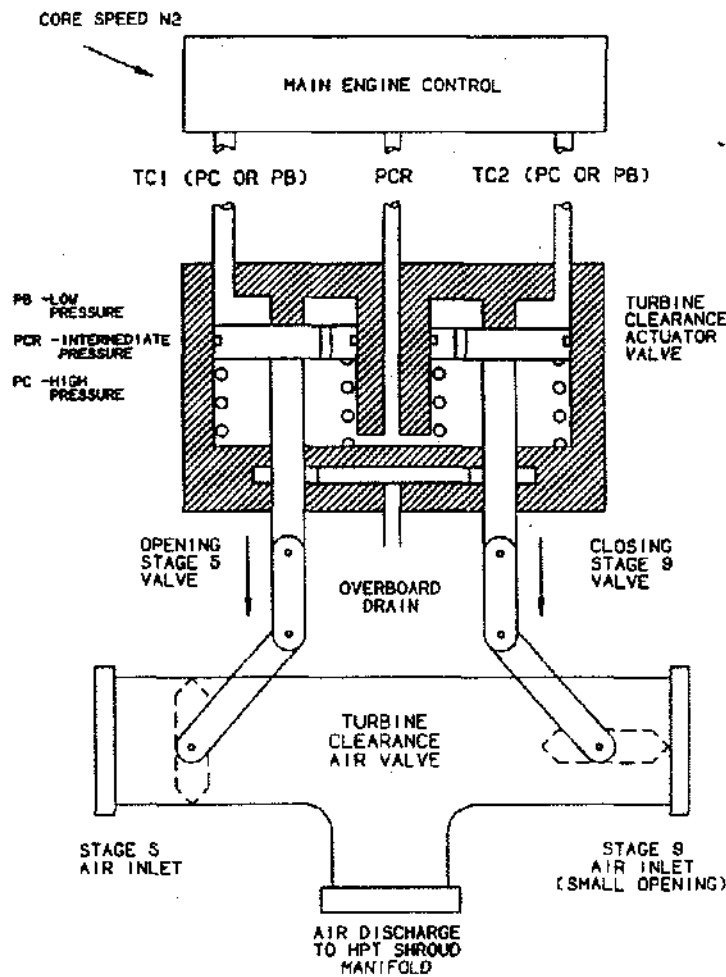


Figure 11.65 CFM56-2/3 Turbine Clearance Control Valve Operation

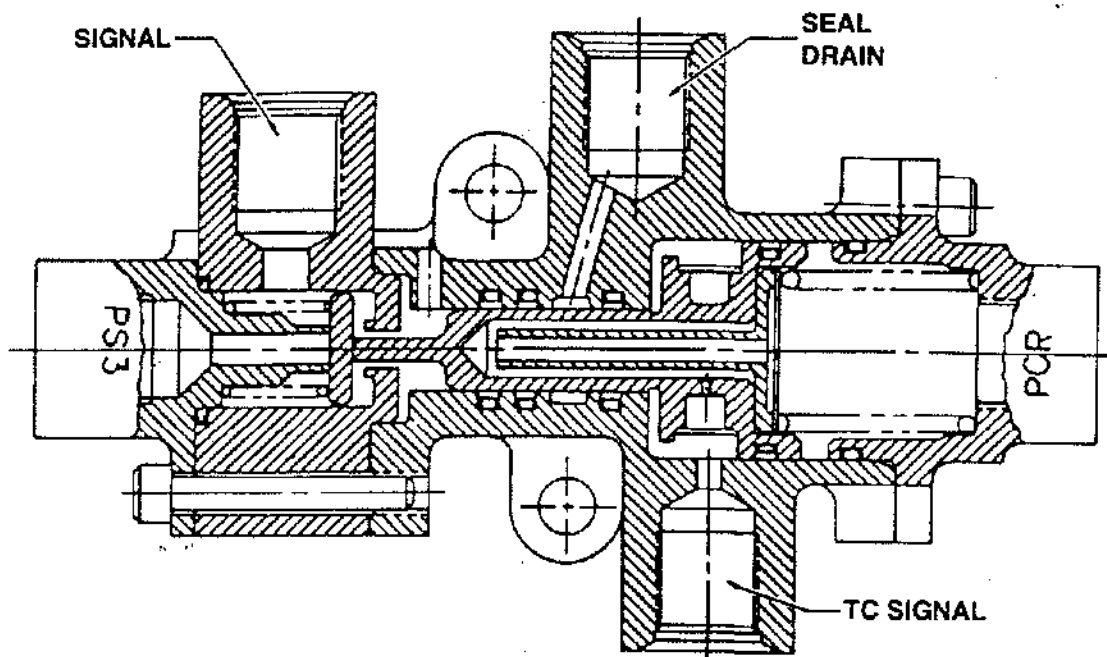


Figure 11.66 CF6-80 Active Clearance Control Signal Valve

requires more cooling and the turbine cases require no cooling. At high altitude the core compartment requires less and the turbine cases require cooling air to close clearances. Increased clearance control airflow causes the cases to cool and shrink. This shrinkage closes blade tip to shroud clearances producing improved efficiency.

The MEC has internal $P_{ambient}$ and $N2$ sensors. These sensors individually control pilot valves arranged in series. Under the proper set of conditions, above 20,000 ft altitude and between 82% and 98% $N2$ speeds, a T_c fuel servo signal of high pressure will be sent to the active clearance control signal (ACC) valve. The ACC valve will then port 11th stage compressor bleed air as muscle to reverse all three valve positions. When the MEC signals of $P_{ambient}$ and $N2$ speed are out of the specified range, the MEC will dump the servo fuel pressure signal which terminates the 11th stage muscle to the air control valves. The valves will revert to their normal spring loaded position.

Sensors measure the parameters which have been selected to schedule the control mode variables. They also provide direct or indirect measurement of the controlled variables to provide feedback (loop closure) for the control system. A variety of sensors are used in most of the control subsystems. There is a wide range of

types and usages for these sensors. Some are used to provide the feedback signal in the control loop, others are inputs to schedule calculations or provide signals for limiting controlled variables, while others may provide signals for cockpit or monitoring systems. If all of the different sensors were given, the list would be quite long. Instead a list of the different categories and types will be given, with some examples. Commonly used sensors include:

- Speed Sensors
 - Hydromechanical Flyweights (Used in MEC's and HMU's)
 - Electrical Tooth Counters (Fan Speed)
 - Alternators (Primary Function is to Provide Electrical Power)
- Temperature Sensors
 - Hydromechanical (Gas Filled Bulb) (Compressor Inlet Temp.)
 - Electrical Resistance Temperature Detector (RTD) (Inlet Temp.)
 - Optical Pyrometers (Turbine Blade Temp.)
 - Thermocouples (Exhaust Gas Temp.)
- Position Sensors
 - Electrical Rotary Variable Differential Transformers (RVDT) (Fuel Metering Valve)

- Electrical Linear Variable Differential Transformers (LVDT) (IGV Position)
- Electrical Resolvers (Pitch Drive Unit)
- Mechanical Cables (VSV Position)
- Pressure Sensors
 - Mechanical Bellows (PS3 Level)
 - Electrical Strain Gauge (Delta P/P System)
 - Electrical Quartz Capsule (Inlet Pressure)
- Flame Sensor (Detects Augmenter Lightoff/Blowout)
- Switches
 - Pressure Activated (Filter Delta P System)
 - Position Activated (Thrust Reverser)

Three different type of sensors will be used as examples. They are a hydromechanical temperature sensor, an electrical speed sensor, and an optical temperature sensor. The F101/F110 hydromechanical fan discharge temperature (FDT) sensor converts fan discharge air temperature (T2.5) into a hydraulic signal which the main engine control uses to establish parameters for the axial positioning of the variable stator vane/acceleration fuel schedule cam and the PLA cam.

This sensor is mounted on the fan frame outer surface. The sensing coil projects through the fan frame into the fan discharge air stream at the entrance to the compressor. The same type of sensor is used to sense inlet temperature (T2) for MEC scheduling on the commercial engines. A signal fuel pressure, proportional to temperature is provided by the sensor, to the MEC. The sensing coil is charged with helium gas. Changes in fan discharge air temperature cause a proportionate change in gas pressure within the sensing coil. This variable pressure acts on the FDT sensing bellows within the sensor which controls the movement of the fuel metering lever. The fuel metering lever is supported by, and pivots through a diaphragm. As the FDT sensing bellows expands and contracts, the fuel metering lever controls (P6) fuel flow from the fuel metering valve. As P6 is bled to bypass pressure (PD), the feedback bellows contracts and pulls the fuel metering lever back against the metering valve to null the signal.

Figure 11.67 shows a schematic of a sensor. Some of the design features of this sensor are:

Temperature	-50 °F to 450 °F steady state
Sensing Range:	-65 °F to 483 °F transient
Fuel Supply Temperature	-65 °F to 325 °F
Ambient Pressure	0.5 to 36 psia
Temperature Rate	-182 °F to +135 °F/second
Air Flow Density	9 to 125 lb/sec/ft ²
Air Velocity	0 to 700 ft/sec.

The CF6-80 N1 sensor is a magnetic speed pickup providing fan speed signals to the electronic control and to the aircraft. Two sensing circuits are electrically isolated and magnetically coupled. The N1 signal to the aircraft is routed independently of the electronic control, but through the common electrical harness. The probe is installed through a tube fabricated in the fan frame strut #3 at 2:00 o'clock. A two bolt, spring loaded mounting flange secures the probe sensor tip under load into its seat in the No. 2 bearing support. A five pin electrical connector provides access to the two windings of the sensor. (See Figure 11.68).

A ferromagnetic toothed wheel is installed on the forward fan shaft with the No. 2 bearing inner race. The magnetic tip containing two separate coils is installed approximately one tenth inch from the teeth of the wheel on the fan shaft. As the fan shaft turns, the teeth interrupt the magnetic lines of force inducing the passing tooth frequency into each of the two separate circuits. A frequency of 38 pulses per revolution is sensed by the indicating and electronic control systems which convert the signals to rpm. One of the 38 teeth of the ferromagnetic wheel is higher. It passes the magnetic tip with a smaller air gap and consequently produces a stronger electrical signal. This 1/Rev. signal is used for tracking the imbalance in the fan trim balance procedure.

The T4B pyrometer is an infrared radiation sensing device consisting of a silicone chip photodiode sensor, an electronics package (a pre-amplifier and thermal compensating resistance network), an optical tube containing two sapphire lens, a fuel cooled heat sink, and a purging system to maintain a clear objective lens. The pyrometer is mounted on the outer bypass duct, and protrudes through the bypass duct, fan stream, outer turbine fairing, and into the first stage LPT nozzle. The objective lens is aimed at the aft side of the HPT blades. (See Figure 11.69). Cooling of the electronics package is accomplished by routing a portion of the engine boost fuel through the heat sink which is encased in the pyrometer's electronic package.

The T4B pyrometer optically scans a portion of the individual HPT blades as the blades rotate through the pyrometer's optical tube viewing path. The infrared emission detected then combines with the narrow band spectral response of the pyrometer's electronic package to produce an output that is an exponential of turbine blade temperature. An added feature is that during engine running the average (DC level) is output, but a raw signal can also be viewed on an oscilloscope. This AC signal shows a temperature level for each blade. If a few blades are running hot (due to plugged cooling passages, etc.), this will be visible on the scope. Photographs can

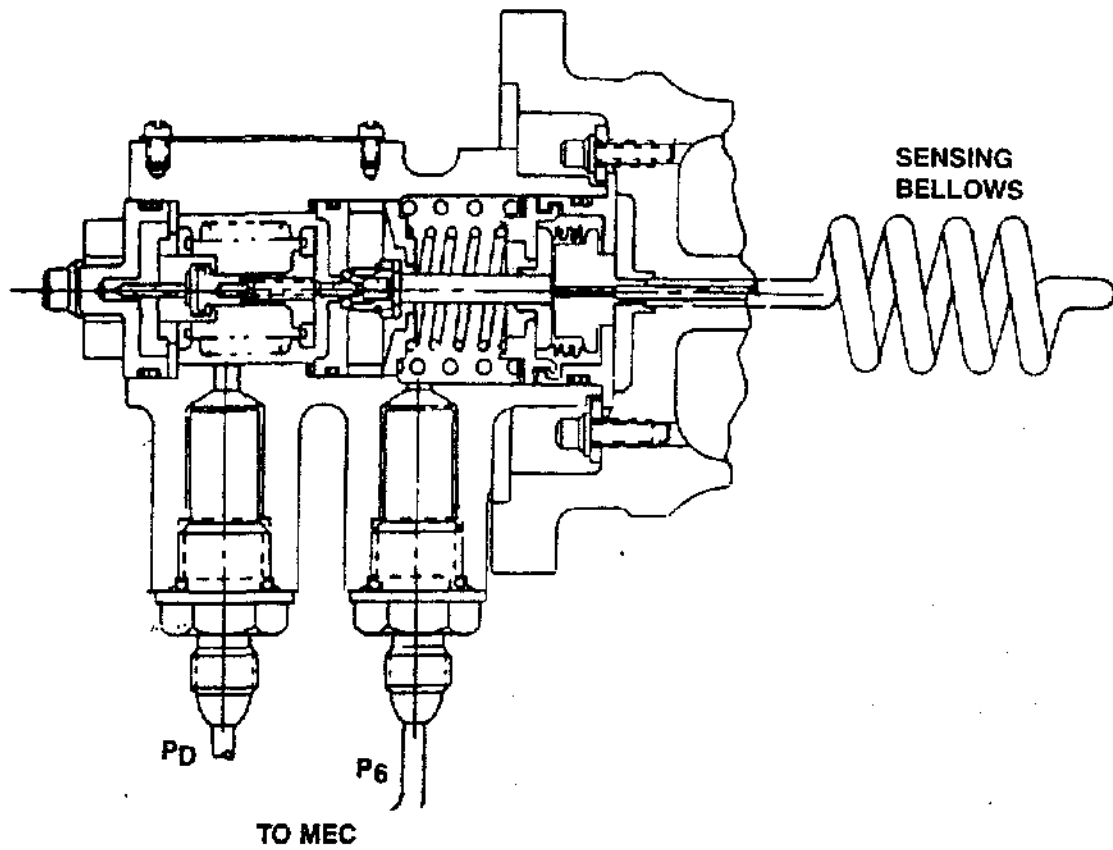


Figure 11.67 T25 (FDT) Sensor Cross-Section

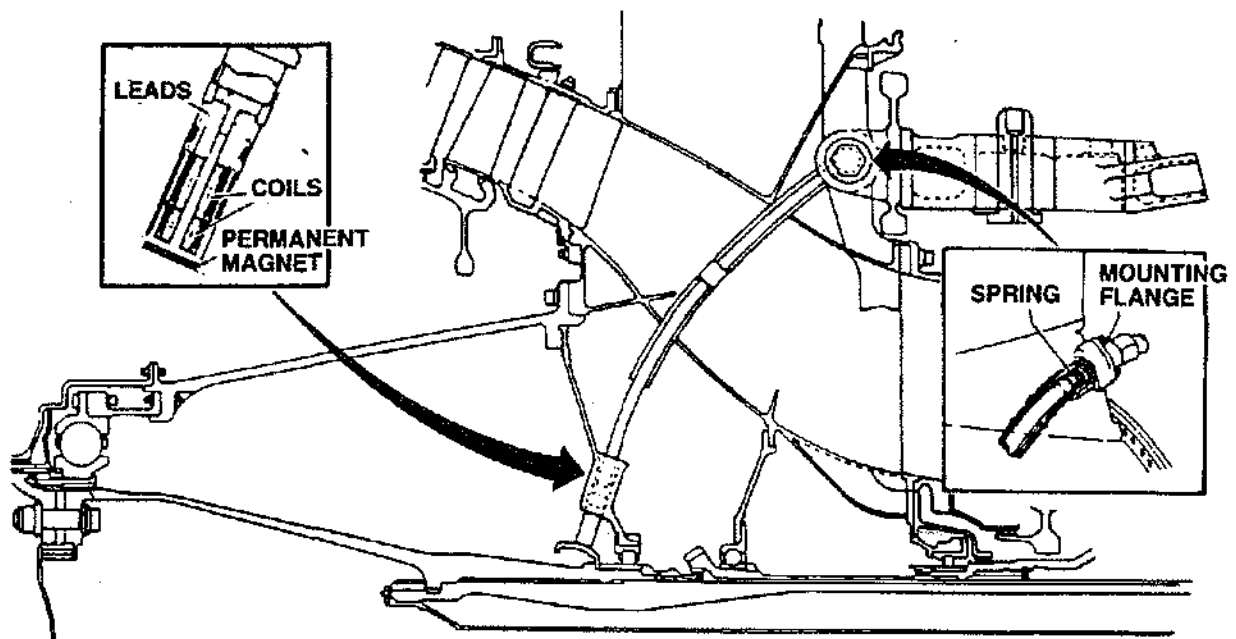


Figure 11.68 CF6-80 N1 Sensor Installation

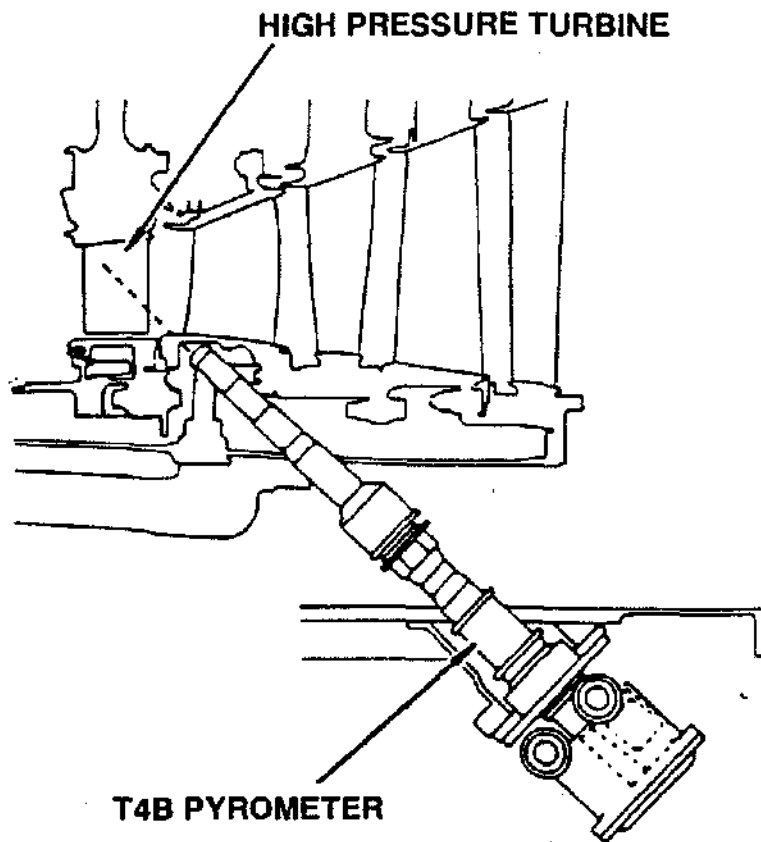


Figure 11.69 F101/F110 T4B Pyrometer Installation

be taken as a record of blade performance during endurance runs. Some of the design features of this device are:

Temperature Sensing Range	1200-2000°F	Output Impedance	50 ohms dc maximum
Excitation Voltage	±15.0, ±0.05 vdc to common	Coolant Temperature	-60 to 220°F normal 242°F max. transient
Ripple	10.0 mv peak-to-peak max.	Coolant Flow	447-916 pph
Power required	1.0 va maximum	Purge Air Max Temperature	800°F
		Purge Air Pressure Ratio	0.6 to 8.0 psid
		Response	8 microseconds from radiation input to voltage output

ELECTRONIC CONTROLS

HISTORY

Electronic controls have been a part of jet engine control systems since the early 1950's. The early applications of electronic controls were somewhat limited in scope due to the electronic technology available at the time. As electronic technology has advanced over the years the implementation of control system strategy and logic ("the brains") has been shifting from hydromechanical implementations to electronic implementations. See Figure 11.70. The majority of control system designs in the future will implement most of the control strategy and logic using digital electronic controls. The degree of redundancy within the electronic control and the control system will vary depending on the specific system reliability requirements. Figure 11.71 provides a graphical description of electronic control trends regarding functional complexity and control system design implementation.

Electronic controls used on jet engines have always been based on the technology of the day. Early usage of electronics in engine controls was bold and daring with the J47-D17 engine in the early 1950's employing a fully electronic mode based on ceramic vacuum tube technology. Unfortunately vacuum tube technology had a difficult time coping with the on-engine environment. Major problems areas were with potentiometers used as feedback sensors and the mechanical integrity of various parts of the vacuum tubes including the heated filaments. Vacuum tube controls were replaced by controls based on magnetic amplifier technology eliminating the vacuum tube reliability problem. The functional scope of the electronic control was decreased on the J73 and J79 engines which used the electronic control to control EGT (exhaust gas temperature) only. Magnetic amplifier electronic controls were also used on the J85, J93, DLD, X211, and T64 engines to control EGT. The development of transistorized controls occurred in the 1960's in response to the displacement of germanium transistor technology with the higher temperature silicon technology which could withstand the on-engine environment.

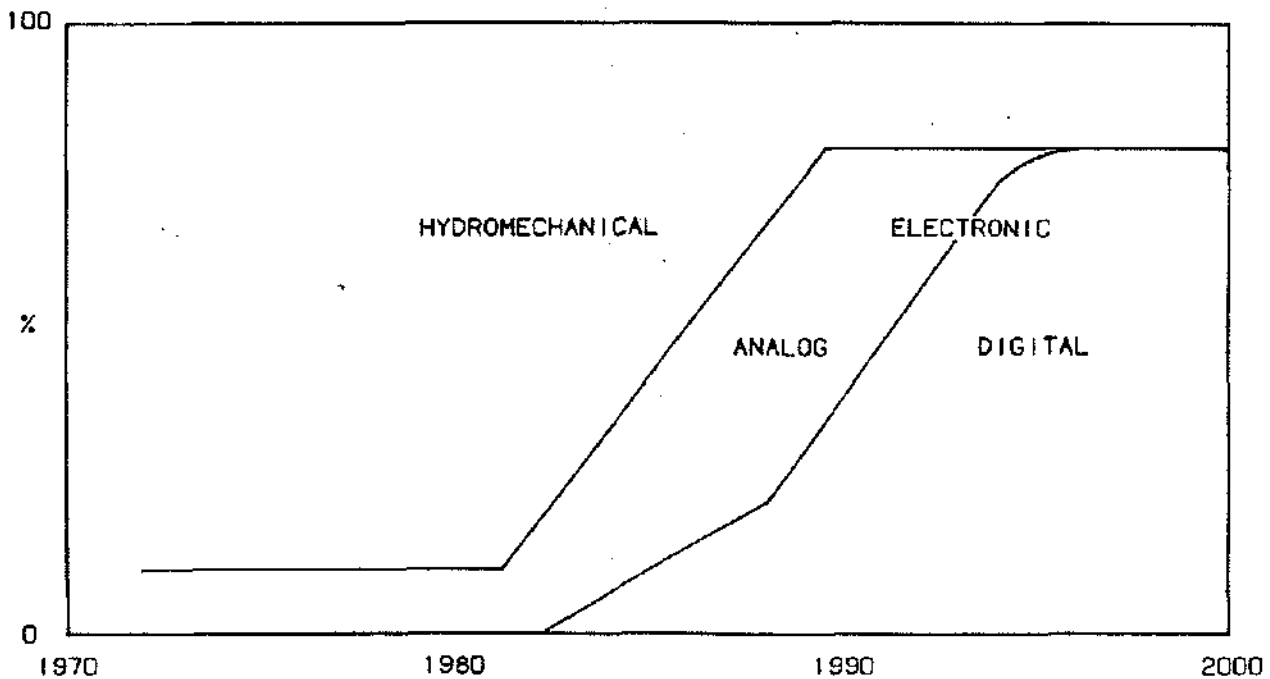


Figure 11.70 Control System Implementation Trends

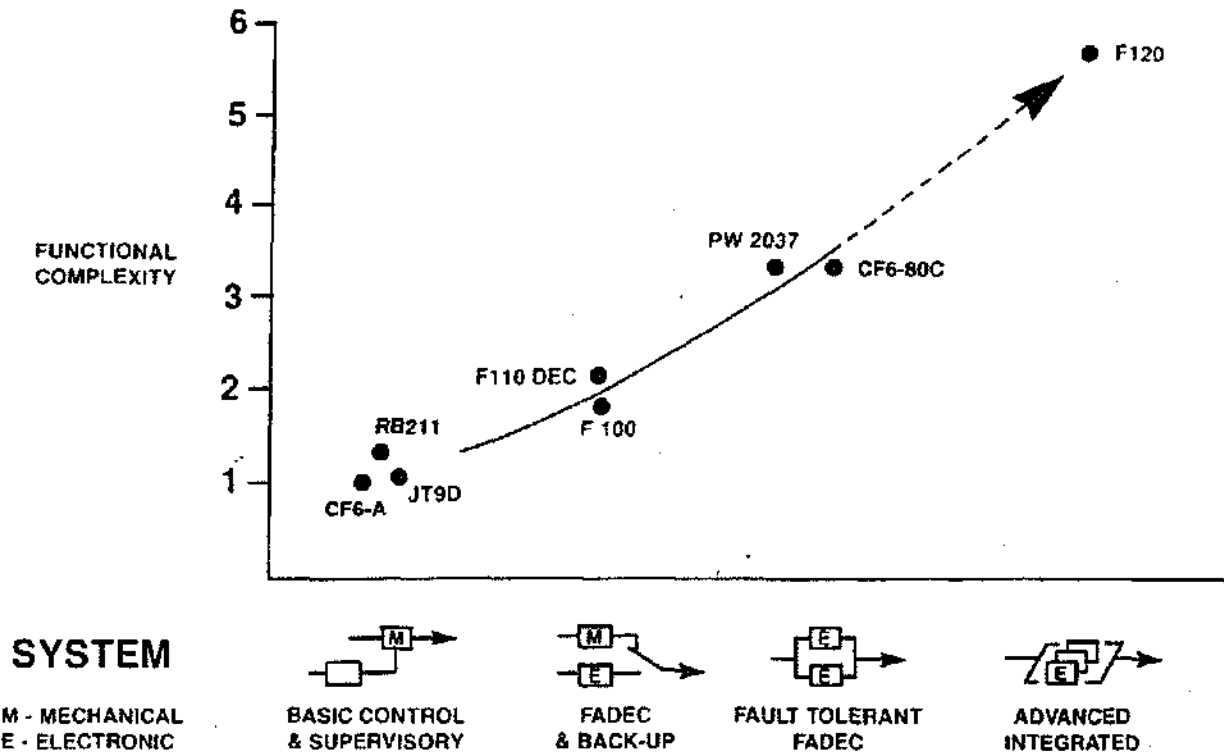


Figure 11.71 Electronic Control Trends

Transistorized electronic controls were developed for the T58 and later versions of the J79. The use of transistor electronics allowed a size reduction and the opportunity to increase the functionality of the control. The next significant electronic technology advancement was the invention of the integrated circuit (IC) in the late 1960's. The integrated circuit combined multiple transistors and resistance elements on one silicon chip. This development brought about the existence and use of operational amplifiers and simple logic functions in electronic controls. All of the electronic control implementation approaches mentioned so far fall within the class of continuous-time implementations typically called "analog" controls.

In analog controls all signals can change continuously with time. Typically each control system parameter would be represented by a voltage where the level of the voltage would correspond to the present value of the parameter. A typical analog electronic control scaling might have 0.000 VDC represent 0% fan speed and 10.000 VDC represent 130% fan speed. These two data points would define the linear relationship between actual fan speed and the voltage in the analog control representing fan speed. The advent of large scale

integrated circuits and bit-slice processors (the ancestors of microprocessors) made possible the creation of a computer of practical size (mainframe computers existed but were hard to fit on the engine!), with practical power requirements (watts instead of hundreds of watts), and memory devices appropriate for use in a hostile environment (solid state memory). With a practical computer now available, digital implementations of electronic controls became viable.

A digital control is a computer-based electronic control. The computer in the digital electronic controls of today is a microprocessor. In a digital control the functionality of the control is determined mainly by the software rather than by the specific circuit design and interconnection as in an analog control. Digital controls provide lower recurring costs and essentially total flexibility in implementing any control strategy which may be desired. This available flexibility has allowed control system designers to successfully incorporate many minor engine control improvements (with minimal recurring cost impact) which previously would have been judged too costly for the benefit gained. Figure 11.72 shows current electronic control production and development schedules.

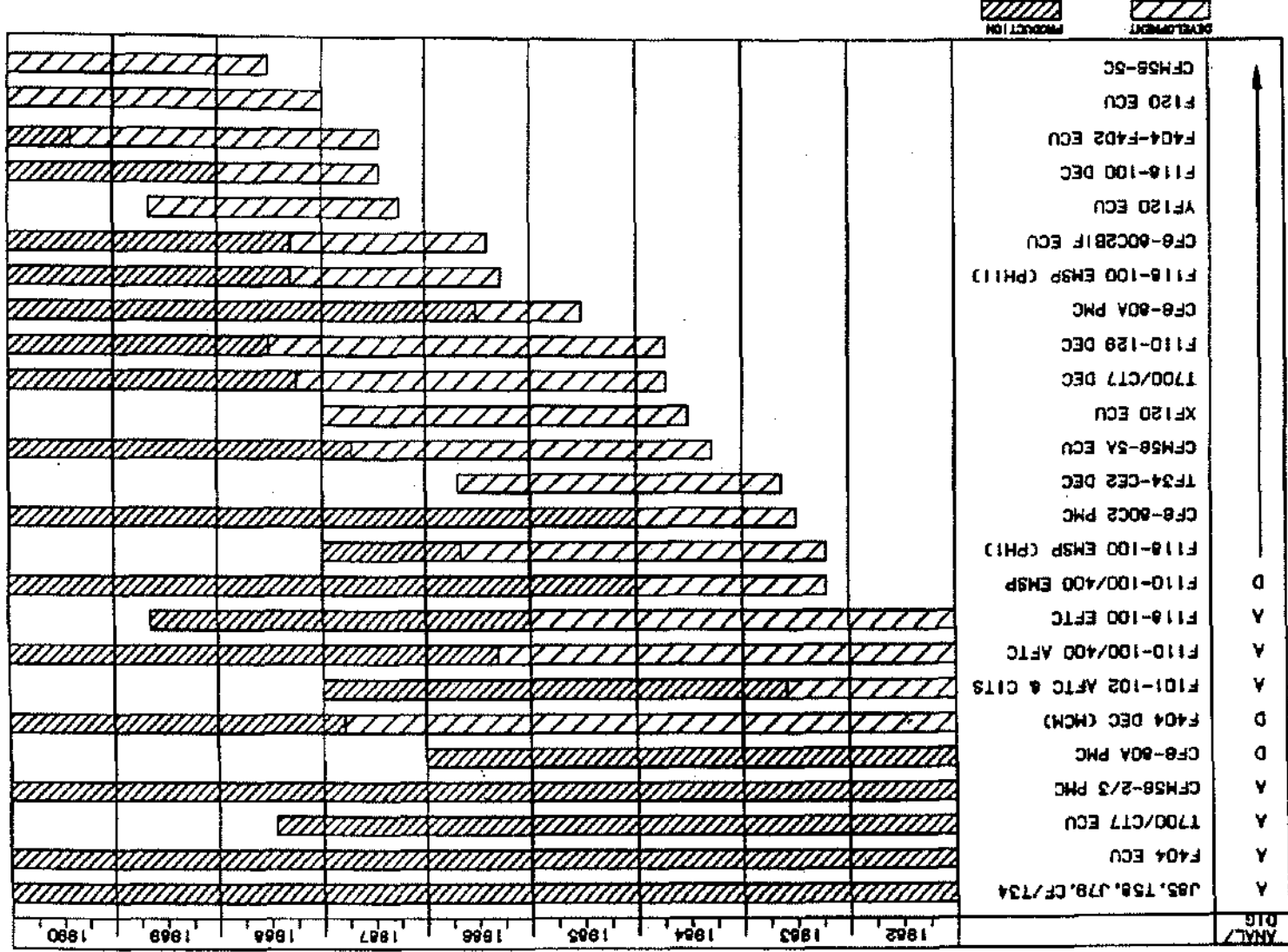


Figure 11.72 GEAE Electronic Control Programs

ENVIRONMENTAL DESIGN FACTORS

Electronic controls are located on-engine because some sensors provide a low level output which cannot successfully be sensed by an aircraft mounted control located many feet away. Therefore, some sensor signal conditioning electronics must be located on the engine. If the signal conditioning electronics must be made to survive when located on the engine, then any other electronics required can successfully be engine-mounted by using the same techniques. This permits the consolidation of all electronics into one chassis located on the engine and interconnected to the various control system components with short cable runs. This eliminates the need for utilization of airframe equipment to interconnect the electronic control to the engine if it were off-engine mounted. The on-engine approach minimizes the length and weight of sensor/actuator to electronic control cabling and helps make the control system an integral part of the engine preserving the traditional well-defined engine-to-aircraft interface.

Temperature The on-engine mounting location brings with it many difficult environmental problems for the electronic control. The electronic control packaging designer has a much more difficult task than for example the packaging designer for your personal computer. The PC typically resides in a rather benign environment in comparison to mounting an electronic device on a jet engine. Temperature is one of the environmental factors which greatly influences the packaging design of the electronic control. The standard temperature range for mil-temp electronic piece parts is -65°F to $+250^{\circ}\text{F}$ case temperature. Thus the packaging designer must take into account the ambient temperatures expected at the electronic control mounting location and the temperature rise expected due to piece part power dissipation within the electronic control.

To lower the ambient temperature environment, electronic controls are typically located as far forward on the engine as possible. On high bypass turbofans this usually results in a mounting location on the fan frame. This tends to be a cooler location because it is physically further away from the hot sections of the engine. The fan frame mounting location usually provides a reasonable amount of volume in which to mount the control. On engines without a large fan frame it is more difficult to find a "cool" (relatively speaking) location with adequate volume available. If the ambient temperature environment and the internal control dissipation result in piece part temperatures which exceed $+250^{\circ}\text{F}$ then some type of cooling is required. This can be as simple as free air convection around a finned chassis or as complex as forced air or forced fuel through a specially designed

chassis. The electronic control is designed to efficiently transmit the heat from each electronic piece part to the chassis heat sink. The chassis heat sink may be cooled by free convection, forced air, or forced fuel. Forced air is the preferred choice if some type of active cooling is required. To date only military controls have utilized fuel for cooling. Fuel "cooling" uses the fuel flowing from the tank as a heat sink to absorb heat from the electronic control. This is accomplished by routing a portion of the low pressure bypass fuel flow through the electronic control chassis. The fuel maintains the electronic control heat sink at a temperature low enough to assure that the electronic piece part temperatures remain adequately below 250°F .

Vibration Another major environmental design factor for the electronic control is the vibration environment. An extreme analogy to mounting an electronic control on a jet engine would be mounting a personal computer on the paint mixing equipment at your local hardware store. Obviously many additional design precautions must be taken to assure that the electronic packaging approach can survive the jet engine vibration environment. As with other engine components mechanical resonances must be avoided to prevent damage to the component.

One resonance aspect always considered when designing electronic controls is the possible "oil can" effect which a circuit board may experience if the electronic packaging approach fails to adequately lower resonance frequencies of the circuit boards adequately. This occurs when the natural resonant frequency of the circuit board as mounted in the electronic control is within the engine's normal vibration range. In this situation it is possible for the board to experience long periods of excitation at a frequency which causes the center portion of the board to undergo a significant physical displacement. If this displacement is large enough and occurs for a long enough period of time, circuit board damage will occur creating a fault. The electronic control is typically mounted to the engine brackets using vibration isolators. The vibration isolators have a low pass filter response to vibration frequencies. The vibration isolation mounts help protect the electronic control from the high "G" forces due to the fan blade passing pulses. The combination of proper packaging design within the electronic control combined with vibration isolation mounting protects the electronic control from the hostile engine vibration environment.

Lightning Electronic controls must have an adequate level of immunity to disturbances caused by lightning strikes to the aircraft and engine. This immunity is achieved through (1) appropriate cable and electronic control chassis shielding, (2) bonding of all electrical/

electronic components to the engine ground plane which is bonded to the aircraft structure, and (3) appropriate circuit design techniques within the electronic control. Special testing is required to assure proper immunity to lightning strike disturbances.

Electromagnetic Interference The electronic control and the entire engine electrical system must have an appropriate immunity to electromagnetic interference (EMI) from sources external to the system. The spectrum of potential effects from EMI spans the range from causing the electronic control to improperly sense input parameters resulting in improper control of the engine to total disruption of the operation of a full authority digital control resulting in an engine shutdown. The engine electrical/electronic system must also limit the amount of EMI which it generates to avoid causing malfunctions in other aircraft equipment.

EMI requirements fall into four general categories: limiting susceptibility to both conducted and radiated interference from sources external to the engine electrical/electronic system and limiting to acceptable levels the conducted and radiated emissions from the engine electrical/electronic system to the external world. Typical EMI sources which the engine electrical/electronic system must be immune to are radio transmitters in use on the aircraft, radio transmitters which the aircraft might typically be near during normal operation, radar transmitters within and external to the aircraft, transmissions from navigational beacons, and transmissions from airport landing guidance systems. Typical sources of EMI within the electronic control are the digital circuitry and switching power supplies. The needed EMI protection is achieved in a manner similar to the means for protecting against lightning disturbances; appropriate shielding of the cables and control, bonding of all electrical/electronic components to the engine structure (which is bonded to the aircraft structure), and appropriate circuit design approaches. Special testing is required to assure that these requirements are met.

Nuclear Radiation Military control systems using electronic controls often require some degree of immunity to nuclear radiation environments (nuclear hardening). This is most easily accomplished by designing the control system with a backup mode of operation which is totally hydromechanical. This allows the designer to ignore the nuclear hardening requirement with respect to the electronic control. The electronic control functions as the primary mode of operation. If the exposure to nuclear radiation renders the electronic control inoperable, then the hydromechanical backup system would take over. Hydromechanical control systems are very immune to nuclear radiation. Whether this design ap-

proach is acceptable depends on the system requirements versus the capability of the hydromechanical control. As engine control strategy becomes more complex with each new program it is more difficult for a hydromechanical backup control system to provide full operational capability. Electronic controls tend to be susceptible to nuclear radiation because of transient upset and permanent degradation which occurs to the electronic parts. Electronic controls can be hardened to both of these effects at levels which are much higher than human beings can withstand for a few minutes. Although it is possible to harden electronic controls, development and recurring costs are considerably higher.

In addition to temperature, vibration, and EMI there are a variety of other environmental factors that must be considered during the design of the electronic control. Some of these include: mechanical shock due to bladeout conditions, humidity, fungus, fluid susceptibility, overpressure immunity, fire immunity, and explosion immunity. Special testing is generally required to assure that all environmental requirements are met.

DIGITAL CONTROLS

Definition A digital control is a computer-based electronic control whose functionality is predominately determined by the specific software program being executed by the computer. The main drivers for digital controls are (a) the ability to self-test, (b) the ability to time share the computational hardware between all functions, (c) the ease with which redundancy can be incorporated, and (d) the ability of a digital system to reconfigure itself. A digital control is not just a computer but also contains analog electronics in order to interface with sensors and actuators which are typically analog in nature, as is the engine we are trying to control. The purpose of the analog electronic circuitry is to signal condition sensor inputs appropriately so they can be converted into digital values (digitized) which can be processed by a computer, and to change digital output values back to analog signals which can then be appropriately "signal conditioned" to interface with analog actuation systems. Digital controls easily handle the standard engine/airframe communications which is typically accomplished via a serial digital communications bus which allows transfer of information between the airframe computers and the engine (digital electronic control). See Tables 11.6 and 11.7 and Figure 11.73 for some general information concerning the dual redundant CFM56-5A electronic control. See Table 11.8 and Figure 11.74, 11.75 and 11.76 for some general information concerning the single channel F110-GE-129 electronic control.

CFM56-5A ECU HARDWARE OVERVIEW

- Dip Brazed 6061-T6 Aluminum Chassis
- Environmentally Sealed Chassis
- Stainless Steel I/O Connectors with Ground Plane
- Forced Air Cooled with Bonded Heatsinks
- Multilayer Motherboards
- Vibration/Shock Isolated
- Captive LRU Mounting Hardware
- Plug-In Multilayer Boards with Interfacial Gasket
- Cam Action Card-Locks Bolted to Board Heatsinks
- 12 Board Test Points Accessible without Extender
- Silicon Rubber Pad in Rear Cover to Seal Test Points and Provide a Board Retention Force
- Locking Thread Inserts for All Covers
- Pressure Transducers Included

Table 11.6 CFM56-5A ECU Hardware Overview

CFM56-5A ECU

• Size	20.73" × 13.25" × 6.4"
• Volume	1758 IN ³
• Typical Power Dissipation	141.6 Watts
• Power Density	0.08 Watts/IN ³
• # I/O Connectors	15
• # Pins/Spare	450/62
• Electrical Circuit Board Area	670 in ²
• # Components	2840
• Weight	52 lbs

Table 11.7 CFM56-5A ECU

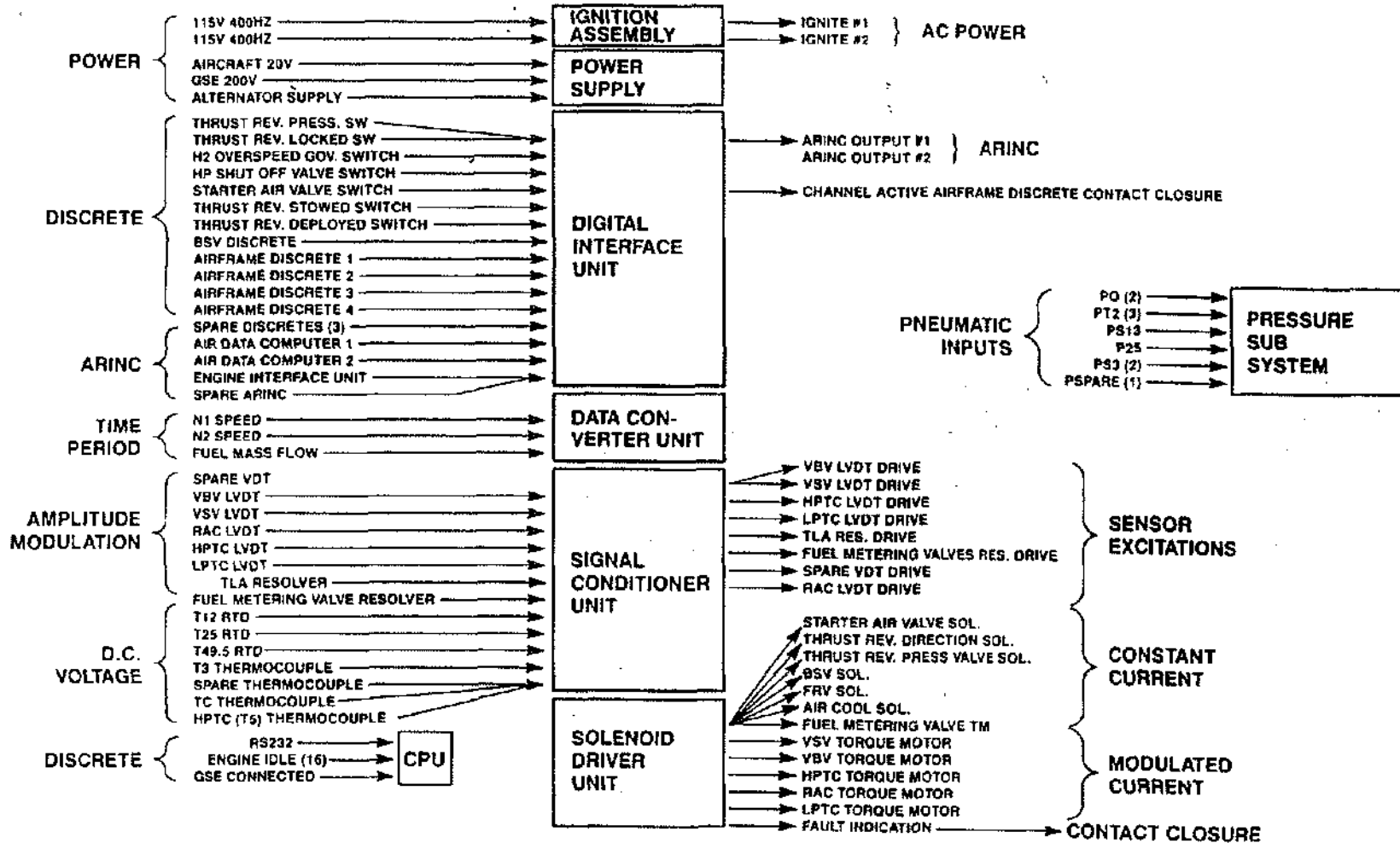


Figure 11.73 CFM56-5A ECU Input/Output Dual Redundant System - Single Channel Shown

F110-GE-129 ECU	
• Size	15.1" x 10.0" x 6.4"
• Volume	885 In ³
• Typical Power Dissipation	85
• Power Density	0.09 Watts/In ³
• # I/O Connectors	12
• # Pins/Spare	307/90
• Electrical Circuit Board Area	562 In ²
• # Components	1850
• Weight	34.5 lbs

Table 11.8 F110-GE-129 ECU

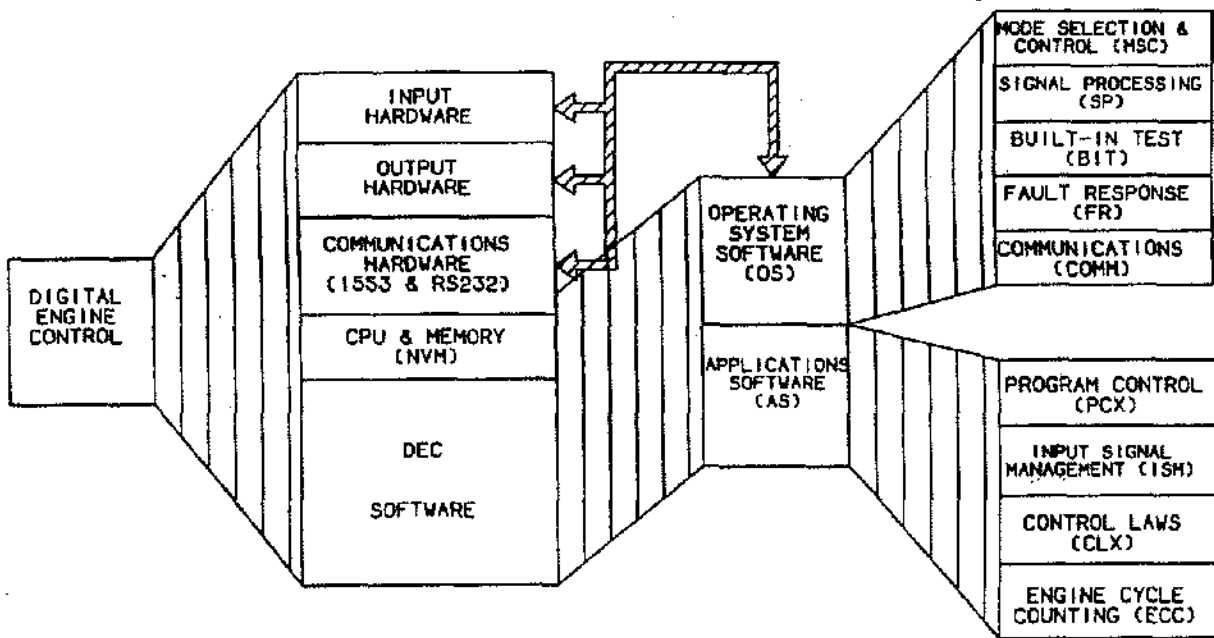


Figure 11.74 F110-GE-129 ECU Architecture

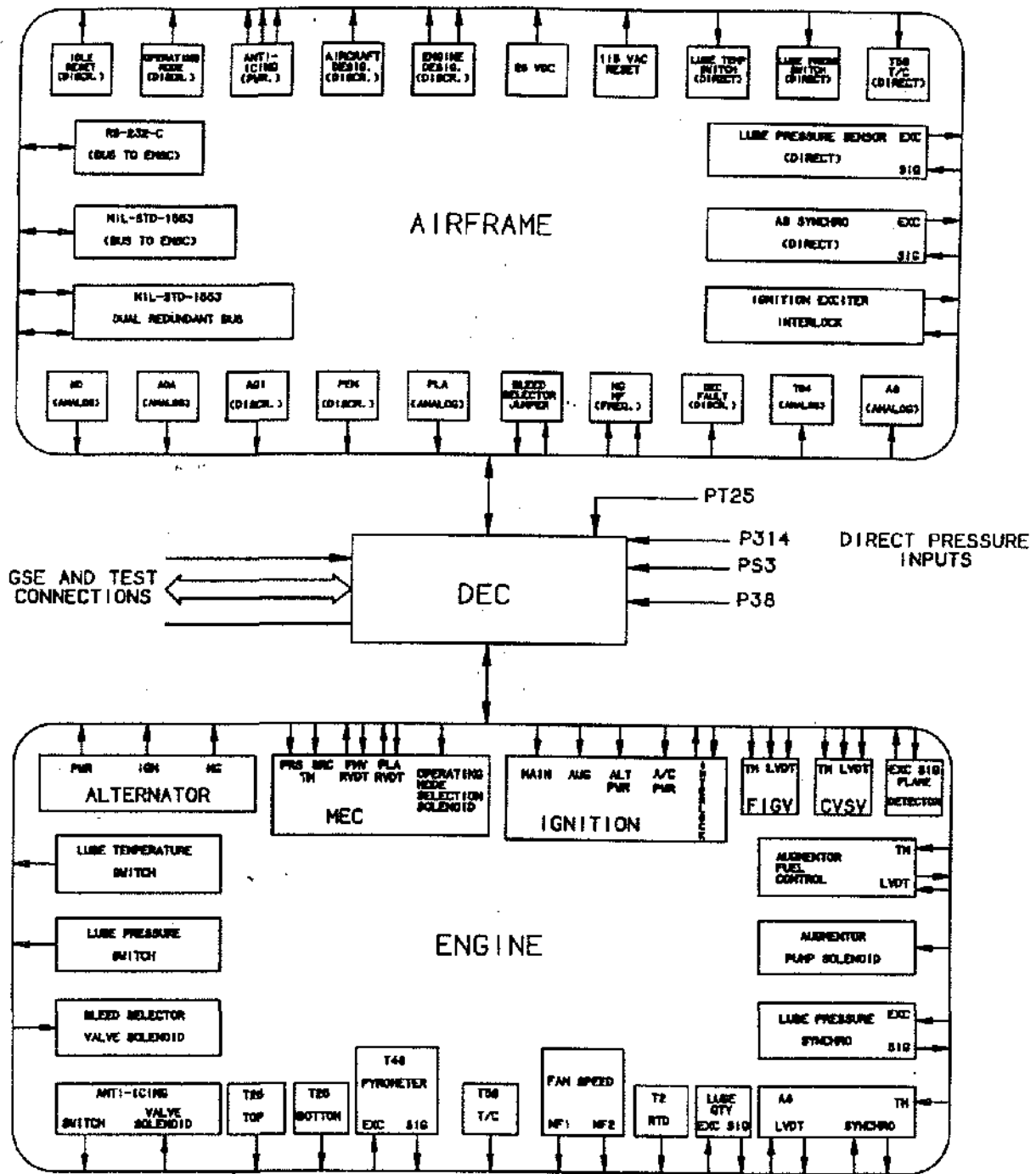


Figure 11.75 F110-GE-129 ECU Input/Output

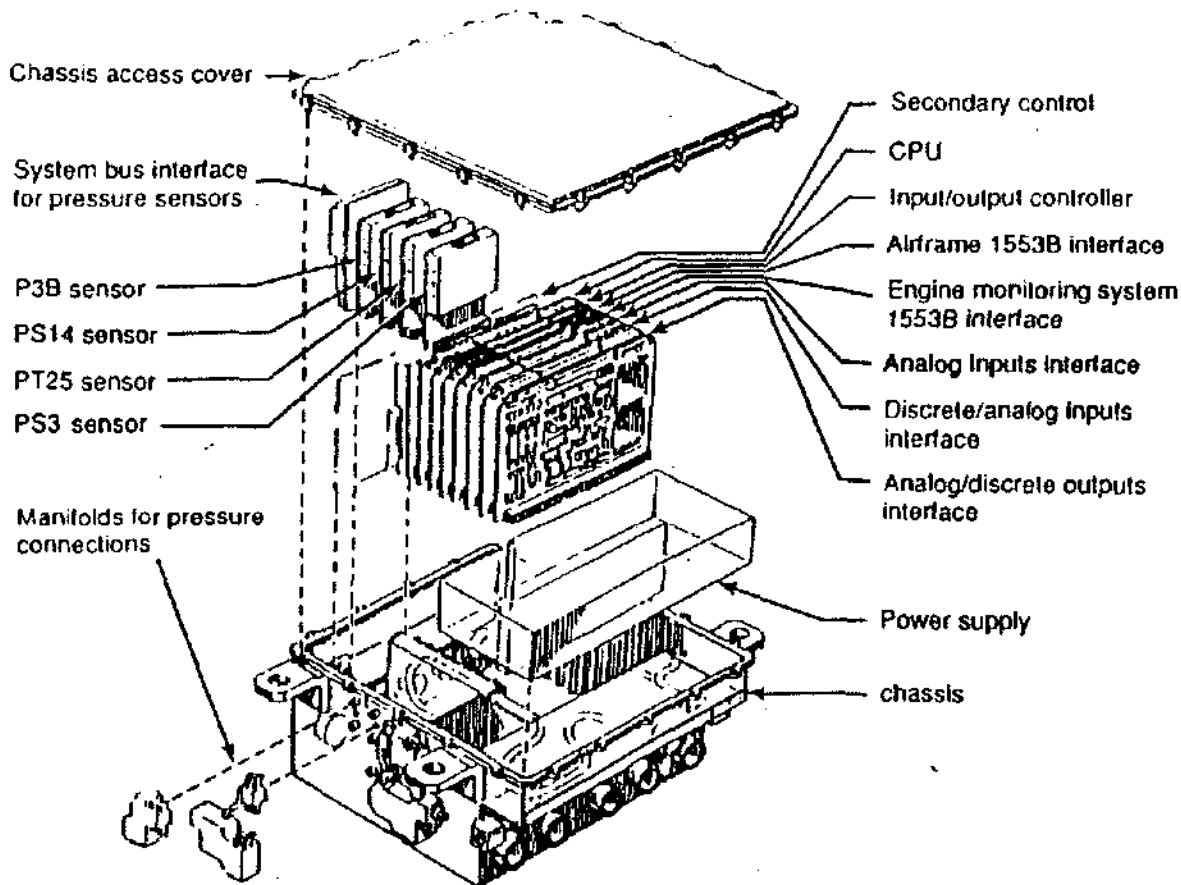


Figure 11.76 F110-GE-129 ECU Mechanical Assembly

Comparison to Analog Analog electronic controls differ from digital electronic controls in several important ways. Analog controls are continuous-time implementations. This means that the calculation process occurs continuously in time just as in an analog computer. In a continuous time implementation there is a circuit associated with every functional aspect of the analog control. Thus if the control system designer suddenly decides he needs to schedule fuel flow as a function of inlet temperature (and previously this was not a requirement), then a new circuit must be added to the analog control with major ramifications on the recurring cost and size of the analog control (not to mention the development schedule).

Digital controls on the other hand are discrete-time implementations; the computer processes information is processed in discrete increments in time. Most of the functionality of the digital control is determined by the software instructions for the computer. The computer hardware is time-shared among all functions which are to be implemented. This feature enables a digital control which experiences a control system requirement change

to typically only require a software change (and not a hardware change). The software change would have minimal recurring cost and size impact to the control. This assumes that the change does not require a new input or output signal to the electronic control. This is not to say that control system requirement changes such as these have no effect on digital controls. They certainly do have an effect and the effect is to increase development cost and cause a slip in the software development schedule. To summarize, if a variable is already an input or output of the digital control, using this input in additional functions or calculating an output differently results in a software change only. Since software resides in memory integrated circuits which are very dense (ability to store a lot of bits in a physically small integrated circuit), the required software change typically has a negligible impact on the digital control recurring cost and size. See Figures 11.77, 11.78 and 11.79 which illustrate the differences between an analog implementation and a digital implementation of a simple control loop. See Figure 11.80 which shows a block diagram of a generic digital electronic control.

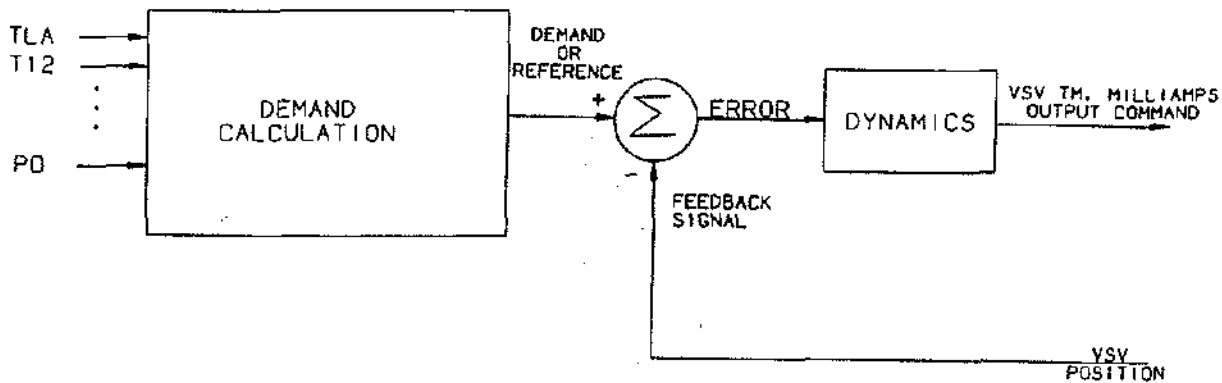


Figure 11.77 Electronic Control Functional Block Diagram

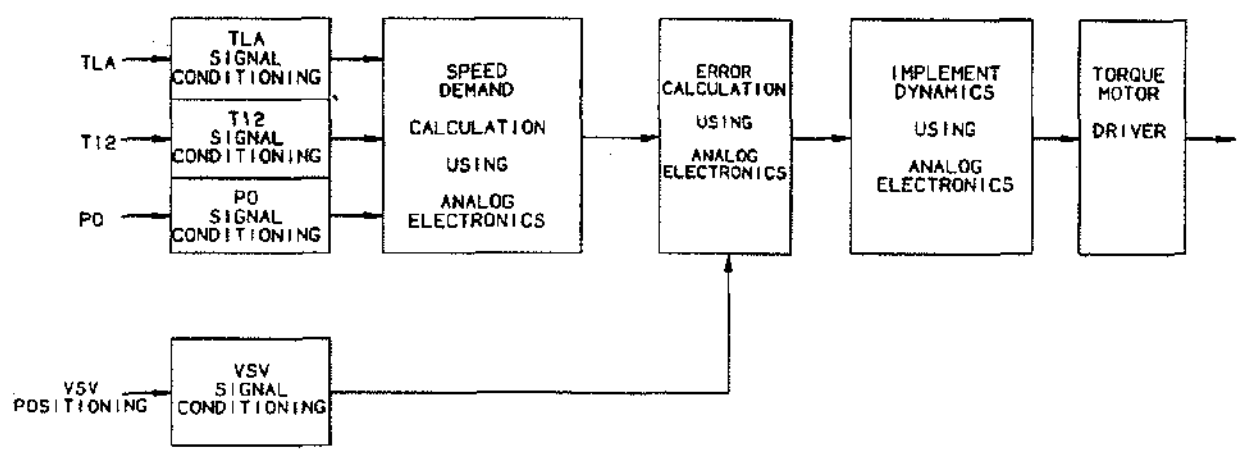


Figure 11.78 Analog Electronic Implementation

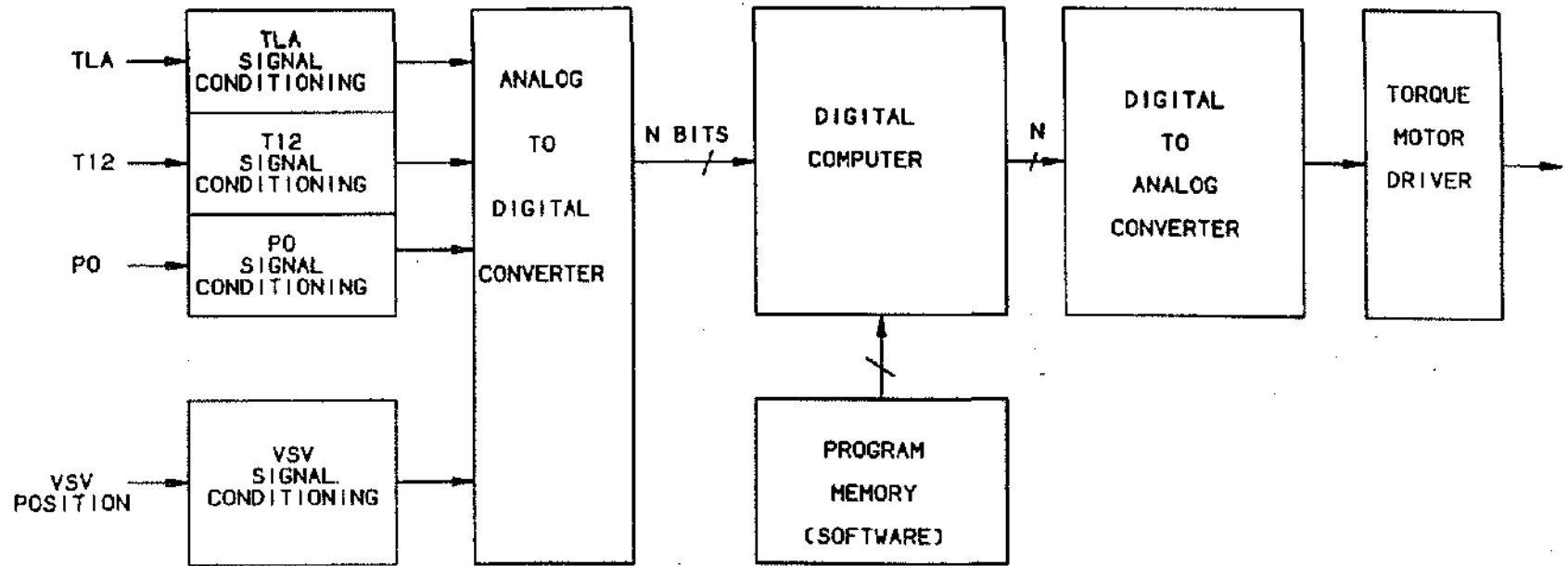


Figure 11.79 Digital Electronic Implementation

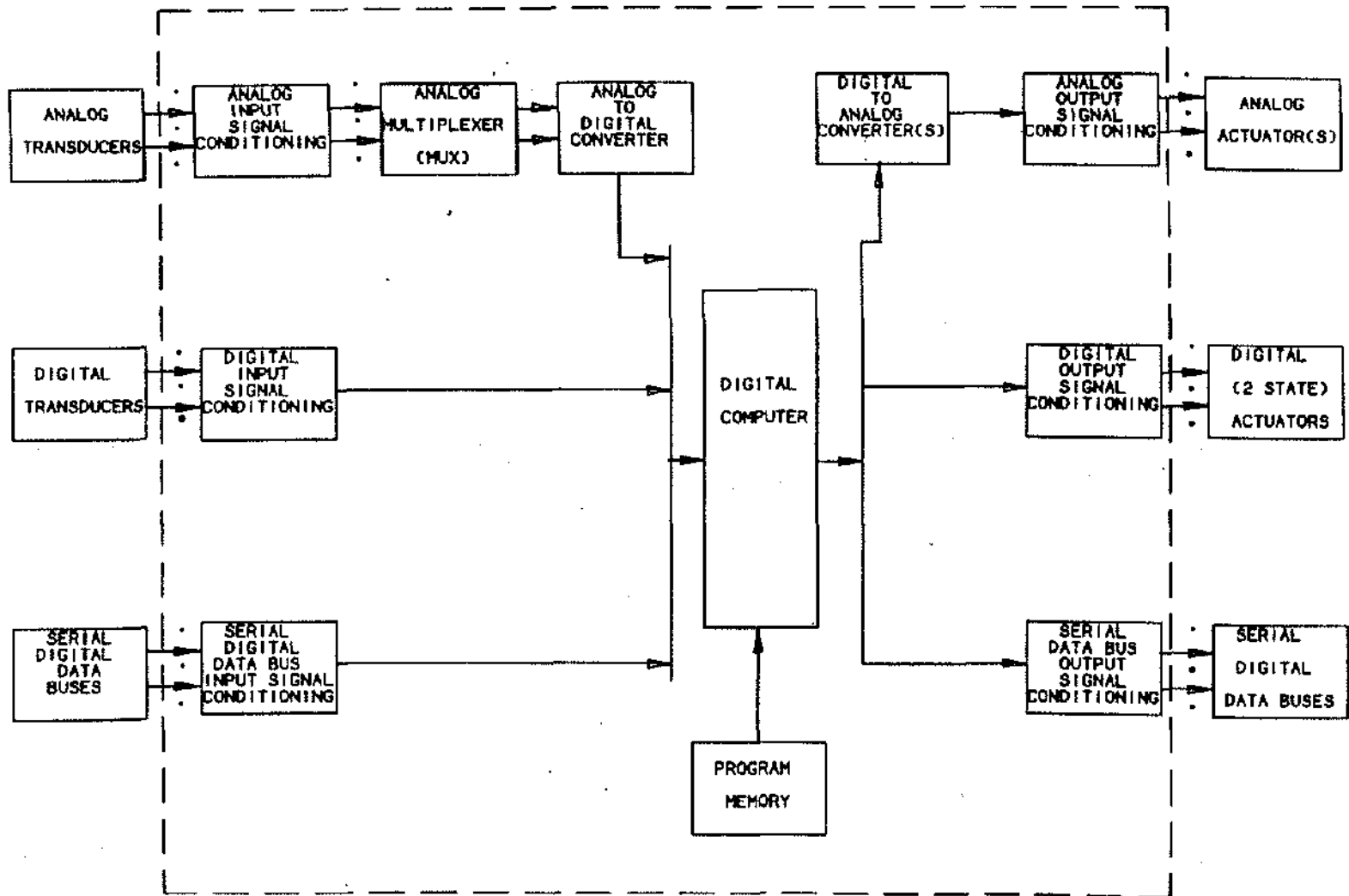


Figure 11.80 Generic Digital Control Block Diagram

Redundancy Management Although analog controls performed significant control functions, they were rarely the component which engine safety depended on. Hydromechanical controls typically performed the functions which assured engine safety. This implies that extreme reliability of operation was not required for the functions typically implemented by analog controls. Thus the internal architecture of analog and early digital controls were typically one-channel systems, that is no multiple redundant electronic channels. This was true whether the electronic control was part of a supervisory control system or a system with hydromechanical backup.

When control system designers started contemplating full authority digital electronic controls with no hydromechanical backup, the question of "How reliable does the electronic control have to be?" had to be re-examined. In a full authority digital engine control (FADEC) system continued engine operation is directly related to the proper operation of the electronic control. Thus the reliability of the full authority digital control needs to be as good or better than the hydromechanical control which it is replacing. Hydromechanical

controls have typically experienced In Flight Shut Down (IFSD) rates of 1-10 per million flight hours. Digital controls typically have larger parts counts and thus lower MTBF's than the analog controls which they were replacing. Standard reliability calculation techniques defined by MIL-HDBK-217D show that based on current electronic piece part reliability data a full authority digital control based on a single electronic channel cannot achieve the required IFSD rate. The natural solution to this problem is to incorporate multiple channels into the digital control.

The typical commercial engine electronic control architecture consists of a two-channel electronic control with no hydromechanical backup. See Figure 11.81 for a simplified control system architecture for the CFM56-5A engine. This configuration meets the IFSD rates required for a commercial multi-engine aircraft. All control related input and feedback sensors are dual redundant with two sensor elements, each feeding one channel of the electronic control. The signals from a dual element sensor are carried to the control in separate engine cables with separate connectors to provide fault tolerance to disconnected cables (includes disconnects

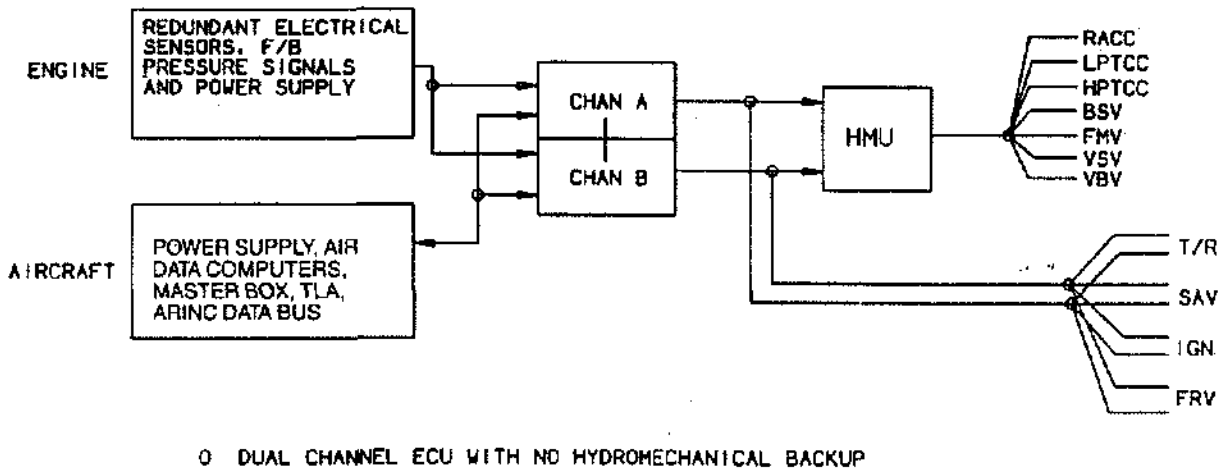


Figure 11.81 CFM56-5A Control System Architecture

due to maintenance oversight or due to damage). Actuators are typically controlled by the electronic control by driving torque motors and solenoids. Torque motors interface between the electronic control and a mechanical servovalve. Torque motors have had dual coils for many years and in a single channel application the coils are paralleled and driven from a single driver. In a two-channel application the torque motor coils are kept separate and each channel of the control drives one of the torque motor coils. Torque motors provide an output which is continuously variable over a certain range. They are typically used as inputs to hydraulic servovalves which are used to position engine variable geometry and fuel metering valves. The arrangement of a torque motor controlling a hydraulic servovalve is called an electro-hydraulic servovalve (EHSV). Solenoids in two-channel systems are also designed with two separate coils where each channel drives one of the coils. Solenoids are used in the control system to provide a two state output. Examples of functions requiring two-state outputs are enabling and disabling of the ignition exciter, control of various thrust reverser solenoids, control of anti-icing valves, and control of the starter air valve.

There are two basic approaches to driving outputs from a multi-channel control. One approach is called active-standby. The nomenclature is indicative of the operational characteristic; one channel drives the outputs while the other channel does not. If the active channel discovers that it has an internal fault, it stops driving the outputs and the standby channel starts driving the outputs. The other basic approach is called active-active. This approach has all channels simultaneously driving some fraction of the required output current. In a two-channel system each channel would supply one half of the required output current. In a three-channel system each channel would supply one third of the output current. If any of the channels discovers an internal fault and stops driving the outputs, the remaining channels appropriately increase their gain to compensate for the missing drive from the channel which went off-line. There are no clear-cut advantages for one approach over the other in every application. Currently the dual redundant controls on the CFM56-5 and the CF6-80C use the active-standby approach. The ATFE demonstrator controls use an active-active-active approach.

The digital data bus inputs to and from the aircraft are dual and carry most of the information which is being exchanged between the aircraft and the engine. Currently several hardwired signals (dedicated wiring for a specific signal in analog form) exist between the aircraft and the engine. There will be fewer and fewer hardwired signals between the engine and the aircraft as redundant data bus systems eliminate the need for hardwired sig-

nals. By putting as much info on the data bus rather than using hardwired signals fewer wires are needed in the aircraft to engine interface thus saving cost and weight. Condition monitoring features are often incorporated into the electronic control. Conditioning monitoring sensors are usually single element sensors since the impact of unavailability of these sensors is not as important as control system sensors. It is significant to note that the hydromechanical portions of the control system (HMU, pumps, valves, actuators) are not dual due to the high degree of reliability which has been achieved over the years.

The typical military engine control system architecture consists of a single channel full authority electronic control with a hydromechanical backup. See Figure 11.82 for a typical military electronic control system architecture with the basic functions. The control system can function in the fully electronic mode (no influence from the hydromechanical control), the full hydromechanical mode (no influence from the electronic control; reduced capability when compared to the fully electronic mode), or in one of several mixed-modes (part electronic and part hydromechanical). All control-related input and feedback sensors are dual redundant and both feed into the single electronic channel. Dual element sensors are used to meet the required reliability requirement for the fully electronic mode. Dual coil torque motors have their coils paralleled and are driven from the single channel. The fully electronic mode is the most comprehensive mode and the control system is designed to operate in this mode most of the time. Dual data buses between the aircraft and the engine have become the standard; typically MIL-STD-1553B buses. Some hardwired signals remain between the aircraft and the engine but will soon diminish in number as military systems become more confident of redundant data bus reliability. In the near future military control systems will make the transition to full authority electronic control systems using electronic controls with multiple channels for redundancy.

Adjustment Capability Digital electronic controls offer additional development flexibility which was not practically obtainable with analog controls. Analog controls usually have limited external adjustments for the primary schedules; implementation is via screwdriver adjustment of a potentiometer which is accessible through the chassis cover of the control. In digital controls many adjustments (up to 500) can be built-in to the software to allow the control system designer to instantaneously change schedules, limits, or any other part of the design (as long as these changes were planned for up front). This allows final definition of some portions of the control design to be determined during engine testing or

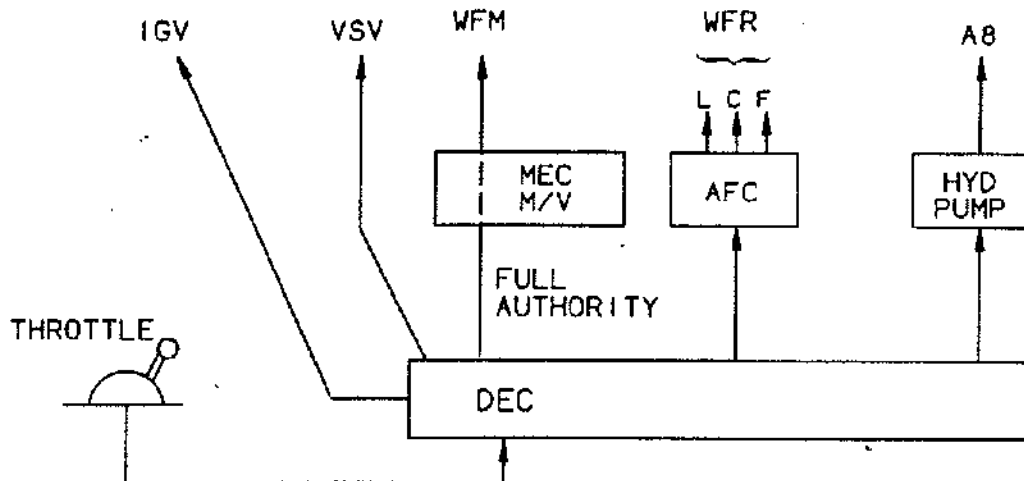


Figure 11.82 Typical Military Control System Architecture

even flight testing without incurring a long test delay due to the time required to change the way the electronic control functions. Adjustments are typically communicated to the electronic control via a serial data bus input. Planned for adjustment capability greatly speeds the ability to alter the control's operation and analyze the effect on the engine. Table 11.9 shows the types of adjustment capabilities present on the F110-GE-129 electronic control.

Maintainability Features Like every computer-based piece of equipment these days, the electronic control has maintenance features which aid in fault detection, fault isolation, and repair verification. Fault detection features (Built-In-Test, BIT) include sensor input range checks, sensor excitation range checks, signal conditioning activity checks, data bus activity and range tests of data bus parameters, power supply voltage checks, analog-to-digital converter accuracy checks, microprocessor instruction set tests, memory device bit-change checks (checksum or RAM pattern tests), real-time software update tests, data bus tests, address bus tests, "software

F110-GE-129 Electronic Control Adjustment Capabilities
Fan IGV Schedule
Core VSV Schedule
Delta P/P Schedule
Augmenter Fuel Schedule (WFR/PS3)
Max Fan Speed Schedule
Max Core Speed Schedule
Max PS3 Reset Modifier
Idle Fan Speed Schedule
Min PS3 Modifier
Start Accel Schedule
Rich Stability Modifier
Decel Schedule
Max Turbine Blade Temperature Limit

Table 11.9

got lost" tests, and output signal conditioning tests (e. g. torque motor current sensed at the controls output pins agrees with software commanded values). See Table 11.10 for a listing and description of the various Built-In-Test features. The control is not only checking itself, it is also checking as thoroughly as possible all other parts of the control system such as sensors, actuators, and cables. The most extensive built-in-test occurs during initialization which occurs when power is first applied to the electronic control. A less extensive built-in-test routine executes continuously during normal operation.

Fault isolation is accomplished by using the results of the fault detection tests. The results of the fault detection tests are typically stored in several software variables designated as system fault diagnostic words. Each bit within the fault diagnostic word corresponds to a specific fault and is set only if the fault has been detected. These fault diagnostic words are stored within the electronic control and are also sent to the aircraft maintenance computer. Based on the specific fault which was detected, the maintenance manual would indicate the most likely faulty LRU's (Line Replaceable Unit) which should be replaced to fix the problem. If the fault detected indicates a problem within the control, additional testing at depot maintenance would probably be required to identify the proper SRU (Shop Replaceable Unit) to replace. Fault information which is detected by the electronic control is stored in non-volatile memory (NVM). NVM is non-volatile RAM; information can be written into and read from the memory like normal RAM but the memory retains the information even after the electrical power is removed from the memory (engine shutdown). Thus NVM allows the control to create a permanent log of finite length containing fault information which can be interrogated at a later time to guide flight line or depot maintenance.

Repair verification is accomplished by verifying the elimination of the fault condition after the suspected component has been replaced. This is accomplished by applying electrical power to the control and seeing that the fault detection capabilities built into the control now indicate no faults are present. Repair verification can easily be handled at the maintenance depot; on a limited basis repair verification can also be accomplished on the flight line (without starting the engine) by supplying the control with airframe power to simulate the typical engine-driven alternator input to the control. Applying airframe power to the control can be used as a pre-flight control system checkout procedure.

Aircraft Bus Interfaces The major communication link between the aircraft and the engine is the serial digital

data bus. Since aircraft avionics and engine electronic controls are computerbased systems, a serial bus communication link similar to that used between remote computer sites is appropriate. The data bus link permits sharing of data between the aircraft and the engine (via the electronic control). This configuration allows increased integration between the engine and various aircraft systems.

Commercial aircraft are using serial bus standard ARINC 429 as the standard avionics interface on current aircraft. ARINC 429 is a broadcast (unidirectional) bus operating at 12.5 kilobit per second rate. For bidirectional communication two buses are required. The ARINC 429 bus is relatively slow and thus must be limited to handling information at a rather slow rate. Typical examples of information coming to the electronic control from the aircraft are altitude, total air temperature, Mach, and total pressure. Typical examples of information going to the aircraft from the electronic control are engine sensor values, rotor speeds, sensed throttle position, cockpit display information, autothrottle commands, aircraft bleed status, and maintenance data.

The standard serial data bus for military aircraft is defined by MIL-STD-1553B. 1553 is a bidirectional bus which has one bus controller and multiple remote terminals or else uses dynamic bus control to allow the various terminals on the bus proper access. 1553 operates at a 1 megabit per second rate and thus is capable of a much higher information transfer rate than ARINC 429. If the data bus is carrying critical info it is typical to use redundant buses to meet the required operational reliability. In the near future buses using electrical or optical technology will be operating at 50-500 megabit per second rates.

Throughput Throughput is a measure of how many operations or functions can be accomplished by a given computer-based design within a certain time period, and is a very important characteristic of any computer-based design. To put it another way it is the amount of processing a given computer can do within a certain time; or the number of instructions per second a given computer can execute. Consider that you need to run a certain Fortran analysis program to solve a problem. Assume the program executes on an IBM PC in 100 CPU-seconds. When you execute the same program on an IBM-AT PC it takes 10 CPU-seconds. Execution the same program on the VAX 11-780 it takes 1 CPU-second. On the CRAY program execution takes 0.1 CPU-seconds. The CRAY has more throughput than the VAX, and the VAX has more throughput than the PC-AT, and the PC-AT has

Test	Description
Input Range Checks	Monitor all sensor and data bus inputs and flag if out-of-range is detected.
Excitation Checks	Monitor sensor excitation and flag if out-of-range is detected.
Activity Checks	Monitor signal conditioning circuitry and data bus inputs; flag if interface stops providing new input samples at proper update rate.
Power Supply Checks	Monitor power supply output voltage levels and flag if out-of-range detected.
ADC Checks	Monitor analog-to-digital conversion of precision reference voltages and flag if out-of-range is detected.
Microprocessor Check	Execute a sample problem with the processor and flag if improper answer is obtained. Absence of stuck or open data and address bus lines is covered by this test.
Memory Check	Checksum program memory and pattern check RAM and flag if error detected.
Update Check	Check time since beginning of minor frame to detect if all tasks completed in time; flag if overrun is detected.
Watchdog Check	Software must properly output to an independent hardware timer every minor frame to assure update rates being met; flag if error is detected.
Torque Motor Driver Check	Compare actual torque motor current with the software command value and flag if they disagree.
Solenoid Check	Compare actual solenoid current with the state commanded by software.

Table 11.10 Built-In-Test Features

more throughput than the PC. Now, since the example uses an analysis type of program (non-realtime) the only difference you the user experience with the various computers is how long you have to wait for the answer. With the PC you had to wait a long time while with the CRAY you received your results almost instantaneously. In both cases you received a valid answer to your problem but depending on the throughput of the computer you used, you received your answer more quickly or less quickly. The above process is used to establish a throughput benchmark for several different computers. A standardized mix of instructions must be used to obtain valid comparisons between different computers. The benchmark provides a comparison of throughput capabilities of several different computers which provides the electronic control designer with information to allow proper selection of a specific computer for a given task (in our case, controlling the jet engine). Throughput capability is determined by the specific computer design. Several factors which influence throughput capability are clock frequency, processor architecture, and semiconductor technology used to implement the processor.

Why is throughput so important for a digital control? The digital control is part of a realtime control system. Realtime control systems require proper functioning of all components of the system or else the control system malfunctions. Only if the algorithms being implemented by the digital control system are executed at the required specific update rates will the system behave as designed. If the required specific update rate is not met, the control system malfunctions. This result is in stark contrast to non-realtime systems which just take longer to get the proper answer.

When a realtime control system is involved in some critical application, it is very important that the computer have adequate throughput to maintain the proper update rates for the various algorithms. When the realtime control system is controlling a jet engine which is part of a commercial aircraft carrying many people or to a military aircraft protecting our freedom, it is vitally important that adequate throughput is available to assure proper control of the engine. Throughput utilization for a given digital computer is typically expressed in percent where 100% utilization would indicate that the current set of tasks given to the computer (or jet engine control in our case) has used up all of the controls ability to execute tasks. 50% throughput utilization would indicate that the current set of tasks being executed by the control requires only half of the controls capability of executing tasks. If no changes are ever to be made to a control system once it is in service, then it is adequate if the throughput utilization of the "final" design is at least

less than 100%. This assures proper operation of the control. But sometimes the "final" design needs to be changed; if new functions are needed it is very advantageous to have enough spare throughput utilization margin to add some appropriate percentage of additional functions. Thus it is desirable for a control to have a throughput utilization of 60-80% when initially introduced into production. This assures that as required changes arise or improvements are desired, there is adequate throughput capability to handle additional tasks.

Resolution Digital controls are computer-based and thus one aspect of the design of the system involves determining the required bit length of words to be used. The bit length of the words in the computer directly relates to how precisely a given parameter can be represented by a digital code in the system. In an analog system resolution is essentially infinite in that there is a voltage level which corresponds to any parameter value. In a digital system there are a finite number of parameter values which can be represented; if N is equal to the bit length of the digital word used by the system, then each parameter range can be expressed by $2^{**}N$ different codes.

Suppose one of the electronic control inputs is inlet temperature. The engine designers specify the inlet temperature range to be -60°C to $+80^{\circ}\text{C}$. To allow the electronic control to identify an out-of-range condition it is necessary for the electronic control to scale the software variable to represent a band of temperatures lower than the lowest expected and higher than the highest expected; adding 10°C out-of-range bands at the high and low ends gives us a range of -70°C to $+90^{\circ}\text{C}$ to be scaled in the electronic control software. If an 8-bit microprocessor is used, we have 256 unique digital codes available (0 to 255) to represent any inlet temperature between -70°C and $+90^{\circ}\text{C}$. The change in inlet temperature represented by the difference between one digital code and the adjacent digital code is called the parameter resolution and is calculated by taking the total range of the parameter and dividing by the number of digital codes available:

$$\frac{90 - (-70)}{256} = 0.625 \text{ C}^{\circ} / \text{count}$$

Now the system designer must decide whether a resolution of $0.625 \text{ C}^{\circ} / \text{count}$ is adequate for proper system operation. If this resolution is inadequate, then a system with longer bit-length words must be used. Each additional bit will increase the resolution by a factor of two. The representation of parameters in software using two's complement arithmetic reduces the resolution achievable with a given word length by a factor of two. Typically

8-bit resolution (0.7813% resolution assuming two's complement arithmetic; $100 \times 2 \times (1/256)$) is inadequate for jet engine control systems while 16-bit resolution (0.00305%) is generally adequate. Usually 12-bit resolution (0.04883%) is marginally adequate for jet engine control systems. Since microprocessors typically come in 8-bit or 16-bit or 32-bit word lengths, the typical choice for an engine control is the 16-bit processor. A 16-bit processor assures that the magnitude of any calculation error related to the finite resolution of the digital processor is insignificant compared to the accuracy and resolution typically provided by analog-to-digital and digital-to-analog converters. In some instances there may be a need for greater resolution than that provided by a 16 bit computer using two's complement arithmetic. In these cases double precision arithmetic might have to be used. Input and output converters with 12 bit resolution are typically used and provide a compatible match with the typical 16 bit computer resolution.

Sampling and Analog-to-Digital Conversion Digital controls are computer-based and thus require digital inputs and naturally provide digital outputs. However, the world is inherently an analog system and thus to allow a computer-based system to be a part of any realtime control system, analog inputs must be digitized (converted into a digital code proportional to the analog value) and digital outputs from the computer must be converted back to analog values to drive analog actuation systems. The terms "sampling" and "analog-to-digital conversion" are used to indicate the process of creating a digital code proportional to an analog signal.

Information theory has provided some important rules which must be followed in order that the digitized samples contain adequate information to prevent misrepresentation of the original analog signal characteristics. An example may help to clarify the misrepresentation which can result if samples are not taken at a fast enough rate. Consider that you are at the amusement park with your child and your child is the only one riding a merry-go-round traveling at exactly 1 RPM. Now assume you are standing at a fixed spot near the merry-go-round and are taking pictures of your child with a camera at exactly 1 minute intervals. Assume the camera freezes any motion and that your child sits perfectly still (I know this is totally unrealistic but bear with me). Now imagine that you have gotten the film developed and you are looking at the pictures. Can you tell how fast the merry-go-round was going? If the merry-go-round speed was 1 RPM and the picture taking interval (sampling interval) was once every minute, all of the pictures will look exactly alike with respect to where your child is physically positioned on the merry-go-round. Since you took a photo every minute and the merry-go-round was going at exactly

1 RPM, your child should appear in exactly the same location in every picture. The set of pictures you have taken is similar to the set of samples that an analog-to-digital converter creates. By looking at the set of pictures you took, you cannot tell if the merry-go-round speed was 1 RPM, or 2 RPM, or even 0 RPM. Thus by this somewhat simplistic analogy we have shown that in sampling a signal, there are some constraints which must be obeyed to avoid misrepresentation of the original signal.

The Nyquist Criteria states that to avoid aliasing (introduction of distortion into the sampled data which cannot be eliminated) the sampling frequency (samples per second) must be higher than twice the highest frequency component present in the signal to be sampled. Directly applying this to a digital control situation we see that signals which can change quickly (have high frequency components) must be sampled more often than signals which change slowly (do not have higher frequency components). From a practical standpoint a sampling rate significantly higher than the Nyquist rate is usually required. It is good design practice to assure that the highest frequency component present in the signal being sampled will not be aliased by the sampling process. This can be accomplished by using a low pass filter with an appropriate cutoff frequency to bandlimit all input signals to the electronic control. As always in engineering a trade-off exists between preventing aliasing of the input signal without introducing excessive phase shift into the transfer function which may cause the control loop to become unstable. Digital controls are designed to bandlimit and then sample each input at an appropriate rate to avoid aliasing. In a jet engine control system position feedback variables from the various control loops and rotor speeds are typically the signals which contain the highest frequency components (capable of changing the fastest) and thus are typically sampled at the highest rates; 10-30 millisecond sampling rates are typical for those inputs requiring fast sampling rates.

Even when sampling is done properly to avoid any signal misrepresentation or aliasing, the sampling process still introduces phase shift on every signal. See Figure 11.83 for a graphical illustration of why sampling or analog-to-digital conversion causes phase shift. The figure shows that an analog approximation drawn through the sampled data curve has been shifted to the right when compared with the original signal. A similar phase shifting process occurs when digital signals are converted back to analog signals. From control system stability considerations, a certain phase margin is required to assure system stability. The phase shift introduced by sampling and the phase shift introduced by the digital to analog conversion process must be taken into account

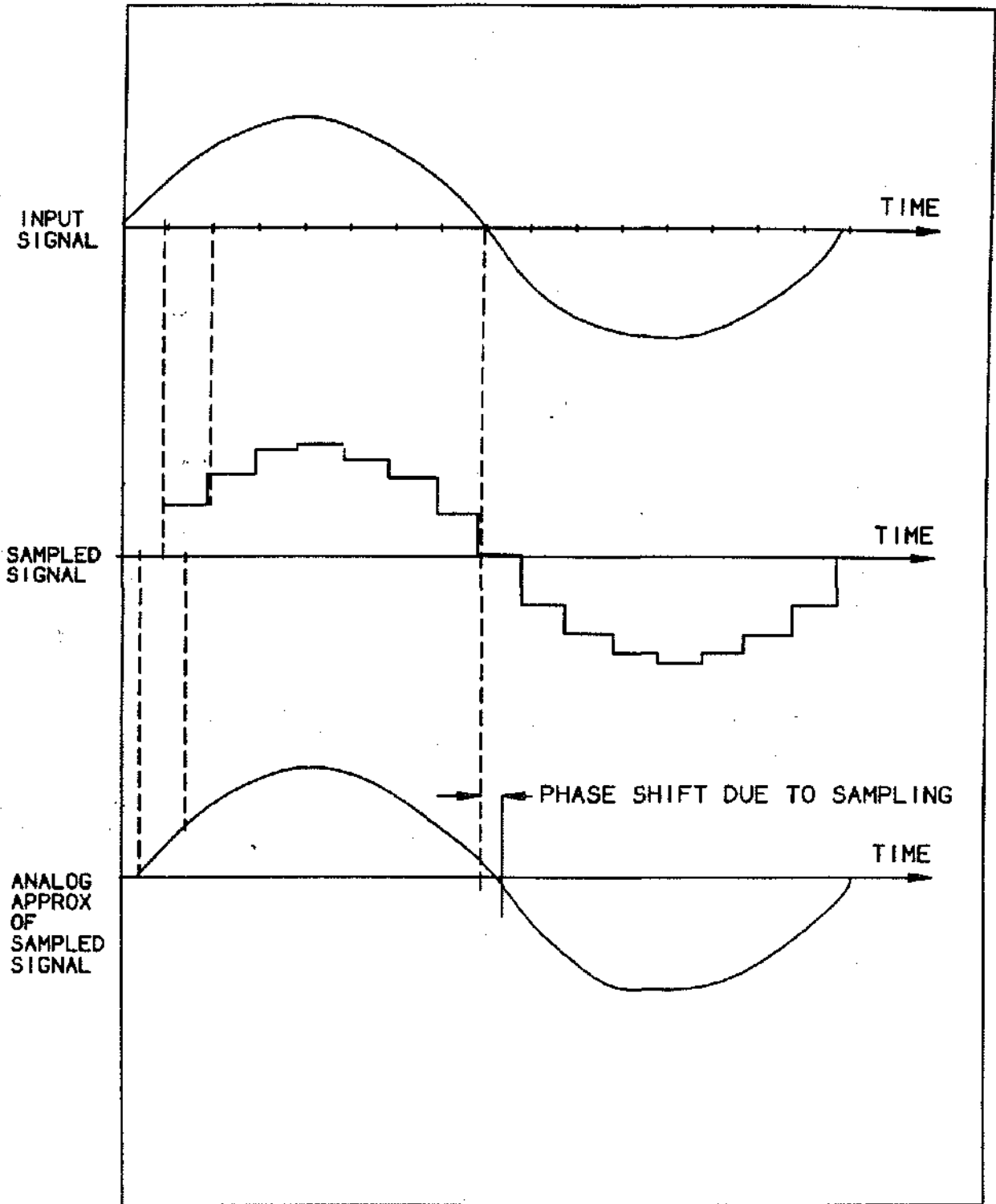


Figure 11.83 Phase Shift Due To Sampling

when designing the overall engine control loops. The faster the digital control samples the inputs, the less phase shift which occurs.

SOFTWARE

Real-Time Software As discussed in the previous section, to prevent misrepresentation or aliasing of the signal when analog signals are digitized the analog signal must be bandlimited (limiting of the highest frequency component allowable in a signal) and then sampled at a certain minimum rate based on the maximum rate of change expected for that particular signal. From a software execution standpoint this implies that any subsequent software calculations (subroutines) to be executed using a given digitized input must be executed at that input's sampling rate or faster or else signal aliasing is again a problem (it does not do any good to sample a signal at the required update rate and then only use every other value in a subsequent calculation). Software which implements real-time control dynamics is typically designed using the discrete-time domain which can be expressed with Z transforms. One basic assumption inherent in Z transforms is that the various terms are time related by integral increments of time. To fulfill this assumption the software must execute routines at periodic intervals. Two basic requirements concerning real-time software are subroutines: (a) execution must execute at periodic rates to assure proper functioning of any Z transform algorithms and (b) any software subroutines must be executed at rates as fast or faster than the sampling rates for any input to that subroutine.

To meet the requirement of executing each software subroutine at a certain rate, a timer is used to signal when it is time to re-execute the software. The timer is typically implemented in hardware and interrupts the computer to force immediate re-execution of the software routines. The timer time period corresponds to the fastest execution rate required. If the fastest execution update rate required is 10 milliseconds, then the hardware timer will interrupt the computer every 10 milliseconds. This time period is typically referred to as the minor frame time. Minor frame times differ from engine to engine but typically range from 10 to 30 milliseconds. At the beginning of the minor frame the software executive directs the computer to execute a certain list of subroutines. The execution of this list of subroutines must always take less than the minor frame time or else the software has failed to meet the periodic execution requirement and the system malfunctions.

So within a minor frame time period the following sequence of events take place. The software executive di-

rects the execution of a predetermined list of subroutines. The subroutines are executed. Subroutine execution is completed before the minor frame time expires. The software enters a wait loop until the minor frame timer interrupts the computer and the software executive directs the execution of another predetermined list of subroutines. (During the wait loop time interval the software is said to be in background and non-realtime tasks which do not have periodic execution rates required such as the built-in-test are performed).

The various software subroutines require different execution rates. Real-time software is rate grouped to accommodate the various required subroutine execution rates. Typically fast execution update rates range from 10-30 milliseconds in length; slow execution update rates range from 40-240 milliseconds in length. See Figure 11.84 for a block diagram of a speed control loop showing the portion of a control loop that can be executed at a fast rate and the portion that can be executed at a slow rate.

Currently electronic controls use fixed point two's complement scaling. Fixed point refers to the fact that every digitized value for a given parameter has the binary point (base 2 equivalent of decimal point) located in a fixed position within the digital word. Floating point scaling reflects a way of representing every digitized value of a given parameter as a mantissa and an exponent which is equivalent to the binary point moving within the digital word. To use floating point scaling requires additional hardware and uses more throughput than when using fixed point scaling. Software programmers in general perceive floating point scaling as easier and less costly to develop. However currently there is no technical necessity for floating point usage in jet engine controls. As floating point capability becomes available for little additional recurring cost, this trade-off will be re-evaluated.

Development Process Development of realtime software for critical applications requires an appropriate management technique to assure proper integrity of the software. The science of software engineering is very young and the appropriate management techniques which need to be employed are still under debate today. The pendulum representing the rigor required for "proper" software development is still swinging and it is not clear where it will come to rest. Originally software development was done by one or several persons. Little formal planning or documentation was necessary since all design communication was within a very small group. As software projects became larger in scope and larger development teams were required to enable project completion on schedule. Several software project

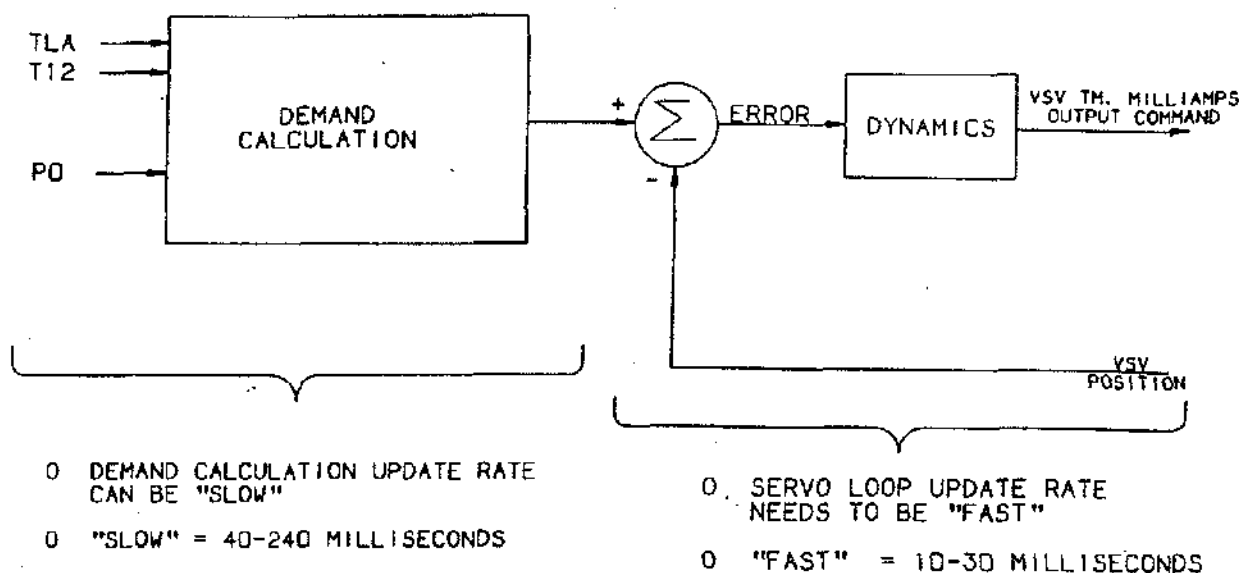


Figure 11.84 Control Loop Update Rate Requirements

"disasters" occurred where the actual cost of software development exceeded the planned cost by factors of 2 to 5 and the projected completion date was missed by years. These occurrences highlighted the need for improved management of software development. The pendulum has been swinging toward a more rigorous approach ever since. Military software development is currently governed by DOD-STD-2167A Defense System Software Development. Commercial software development for avionics is currently governed by RTCA/DO-178A Software Considerations in Airborne Systems and Equipment Certification. Software development techniques are sure to undergo changes in the near future as software engineering wrestles with which management approach results in the best product at the most reasonable cost. Software development tools such as CASE (Computer Aided Software Engineering) are appearing and should help streamline the process while at the same time enforcing the desired software management approach. Software management and development techniques for critical applications such as jet engine controls are sure to reside on the more rigorous side of the software spectrum.

Functional Allocation Software for realtime engine controls consists of the following typical list of tasks: operating system, input signal management/selection, control law calculations, output signal management, built-in-test, and maintenance logic. The operating system consists of the hardware-related software which in-

terfaces to the various signal conditioning circuitry and usually contains the software executive which properly schedules and sequences the various software subroutines. Input signal management/selection is the portion of the software which determines from multiple input sources the one value to be used in control law calculations. Multiple input values are available when sensors are redundant and/or when the aircraft functions as an additional source for some parameters. Control law calculations implement the required control law algorithms. This consists of two basic parts; (1) calculation of the control loop demand (reference) value, and (2) loop closing dynamics (sensing the feedback signal, computing loop error, and calculating the new control loop output value). Output signal management handles redundancy management routines and appropriately controls the condition of all outputs in response to faults discovered by the built-in-test. Built-in-test is the software portion dedicated to exercising the electronic control system to discover any faults which may be present. Maintenance logic is the portion of the software which analyzes the fault data built-in-test generates and decides which LRU has most likely failed. Maintenance logic also communicates with the aircraft maintenance computer to provide fault status information regarding the engine control system. Table 11.11 shows memory usage and throughput usage for the CFM56-5A electronic control. Table 11.12 shows how memory usage has increased on each new electronic control. Table 11.13 describes trends in program memory technology.

TYPICAL ECU SOFTWARE PARTITIONING		
Function	% Of Program Memory Capacity	% Of Throughput
• Operating System	8.7%	12%
• Input Signal Management/Selection	18.6%	23%
• Servo Loop Calculations	28.1%	19%
• Output Signal Management	9.8%	16%
• Built-In-Test	2.6%	1%
• Maintenance Logic/Fault Management	31.9%	5%
	99.7%	75%

2260/18

Table 11.11 Typical ECU Software Partitioning

ELECTRONIC CONTROL MEMORY USAGE							
Revenue Service Date	Control	Processor	Bits/Word	Relative Thruput	Program Memory Capacity	RAM Capacity	Non-Volatile RAM Memory Capacity
1982	CF6-80A PMC	Discrete Design	12	1	8K	1/2K	0
1985	CF6-80C PMC	68000	16	1	24K	2K	1/8K
1988	CFM56-54 FADEC	68000	16	1	64K	8K	1/2K
TBD	GE36 FADEC	68020	32	3-4	128K	8K	1K

2260/23

Table 11.12 Electronic Control Memory Usage

PROGRAM MEMORY TECHNOLOGY

- Digital Controls Are Constantly Expanding To Use More Memory
 - Increased Functionality Requires Increased Software and Hence More Memory

- Program Memory Trend is Toward Reprogrammability
 - ROM Factory Programmed
 - PROM 1 Time User Programmability
 - UVEPROM Ultraviolet Erasable, User Programmable
 - EEPROM Electrically Erasable, User Programmable

- Memory System Design Trends
 - Ability To Reprogram Each Integrated Circuit
 - Ability To Reprogram Each Memory Board
 - Ability To Reprogram The Electronic Control

- Installing New Software Is Becoming Trivial, Designing New Software Is Not.

2260/12

Table 11.13 Program Memory Technology

Chapter 12

LIFE ANALYSIS

by Ken H. Powers

QUALIFICATION/CERTIFICATION, LIFE ANALYSIS

What is life analysis? Life analysis is a system by which several different analytical techniques are combined in order to calculate the life of major rotating parts (Disks, Shafts, etc.) when operating in jet engines.

Why do we conduct life analysis? Typically if one of these major rotating parts fails in a jet engine it will not be contained. Therefore not only will the engine stop functioning but the ejected parts could endanger the air-

craft. The aim of life analysis is to establish a safe operating life for these parts.

There are two distinctly different approaches to life analysis: the commercial and military approaches. The commercial approach is based on the low cycle fatigue properties of the components and assumes that any crack in a part is unacceptable. The military approach is based on the crack propagation properties of the components and assumes defects are present in all parts. Both concepts will be discussed in this chapter and many of the analytical features are common to both systems.

COMMERCIAL LIFE ANALYSIS

The flow chart in Figure 12.1 gives a summary of the process of life analysis.

Thermal Analysis Thermal or heat transfer analysis is conducted using a finite difference program called THTD. The THTD model utilizes boundary conditions based on the predicted performance characteristics of the engine (gas stream pressures and temperatures and cooling air temperatures and pressures). A typical heat transfer model is shown in Figure 12.2.

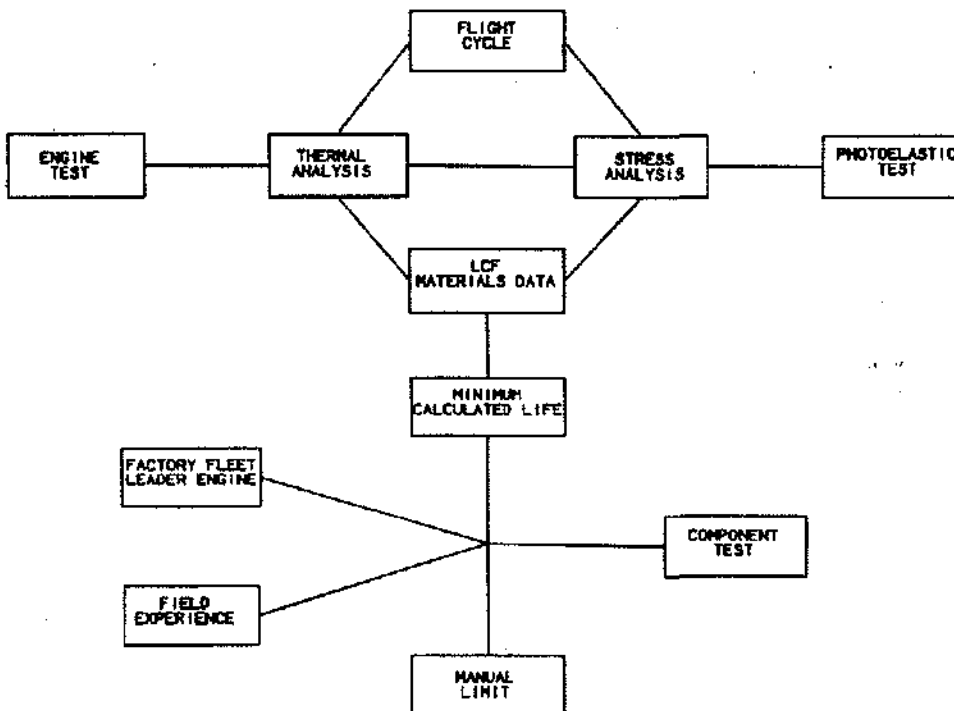


Figure 12.1 Life Analysis Flowchart

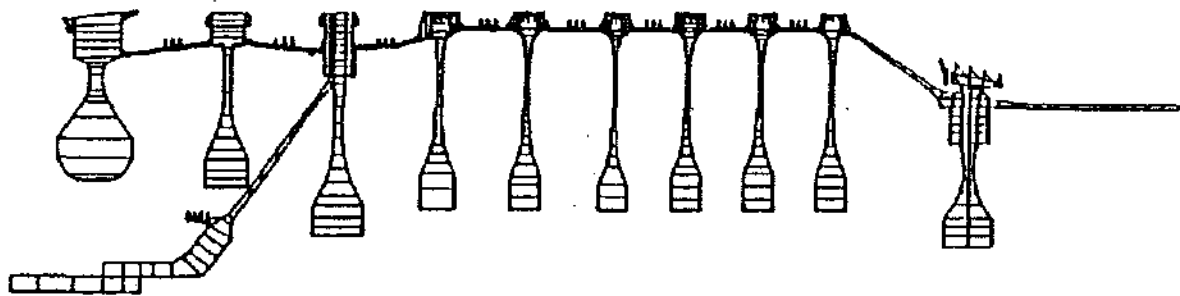


Figure 12.2 THT-D Model of CFM56-3-B1 HPCR

The analysis also takes heat transfer coefficients and boundary conditions from instrumented engines (Figure 12.3) as input. From this input a computer model can be generated which will predict metal temperatures under any flight conditions. The model can be checked out by running a factory instrumented engine for a condition which has been analyzed and comparing the predicted temperatures with the actual measured temperatures. Figure 12.4 shows a typical comparison.

Having established and verified a predictive heat transfer model the output from this can then be used in the stress analysis.

Stress Analysis The first step in the stress analysis of rotating components is to construct a 2 dimensional axisymmetric model of the rotor. This model will contain shells in areas of simple geometry and can include finite elements in areas of concentrated stresses. A typical rotor model is shown in Figure 12.5.

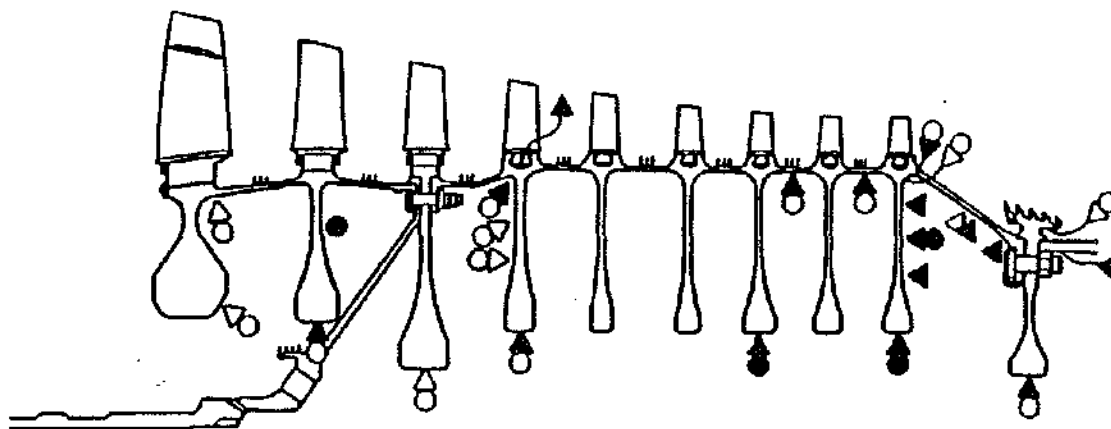
This rotor model then uses metal temperatures input from the heat transfer analysis for specific flight conditions and speeds and pressures from the performance deck also blade and bearing loads are input into the model. From this rotor stresses can be calculated for the

specific flight condition of interest. Stresses may be taken directly from this model or single locations may be modeled separately using 2 dimensional finite elements. This model can then be used for further detailed studies. Figure 12.6 shows details of the large rotor model with a single flange modelled separately.

For complex areas such as bolted joints or disk rims 3 Dimensional finite element models may be constructed. These models would use boundary conditions from the large 2 dimensional rotor model as input. Figure 12.7 shows a fully interactive 3 dimensional stress model of a bolted joint.

Again specific locations within these models can be modelled separately in order to refine the analysis at a specific location and hence obtain more accurate stresses. Typically the small refined models use output from the larger 3 dimensional analysis to provide boundary conditions. Figure 12.8 shows a detailed model of the forward shaft flange shown in Figure 12.7.

In order to verify the analytical results photoelastic testing is sometimes conducted. This uses 'plastic' models which have the property of allowing the stresses in the parts to be 'frozen' in. This testing can take the form of



- ▲ METAL T/C REDUNDANT
- △ METAL T/C
- AIR T/C REDUNDANT
- AIR T/C

Figure 12.3 Instrumentation Locations

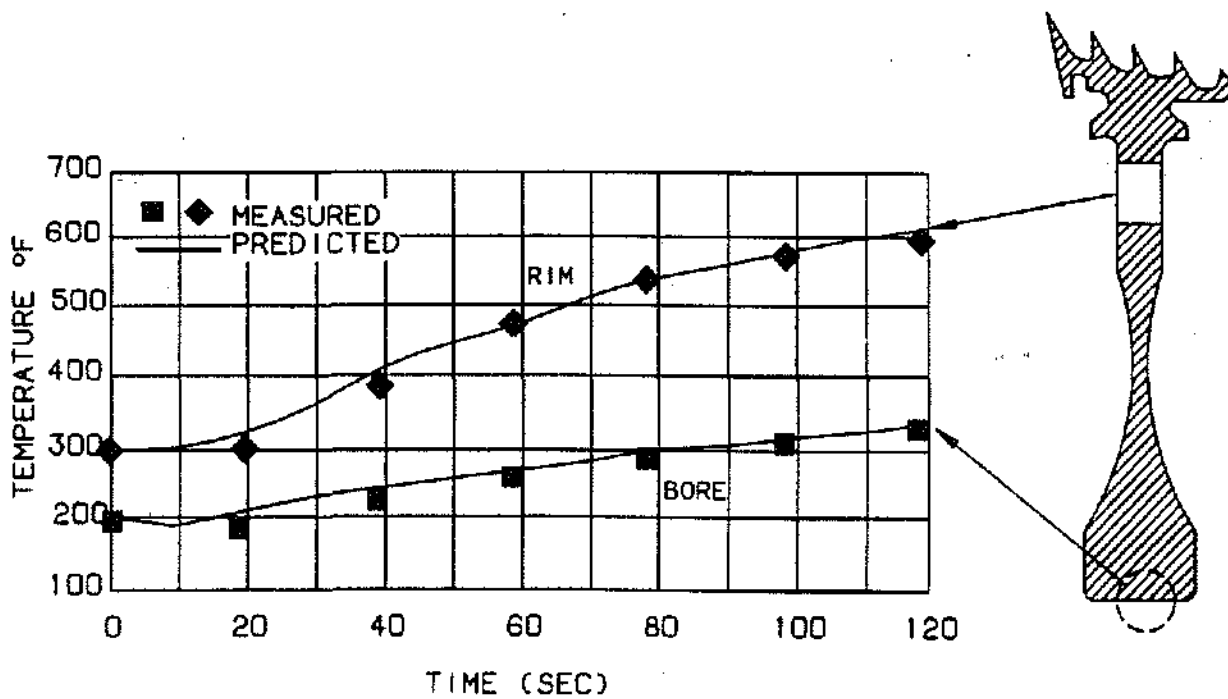


Figure 12.4 Heat Transfer Analysis

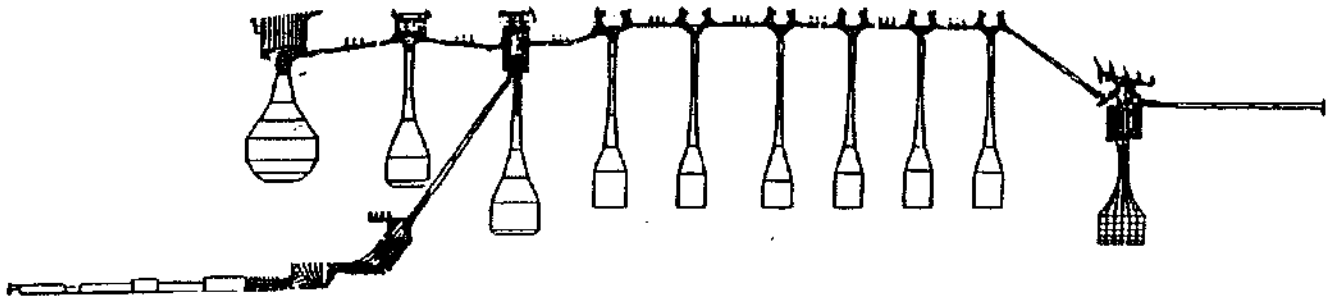


Figure 12.5 CFM56-3 HPCR Axisymmetric Stress Model

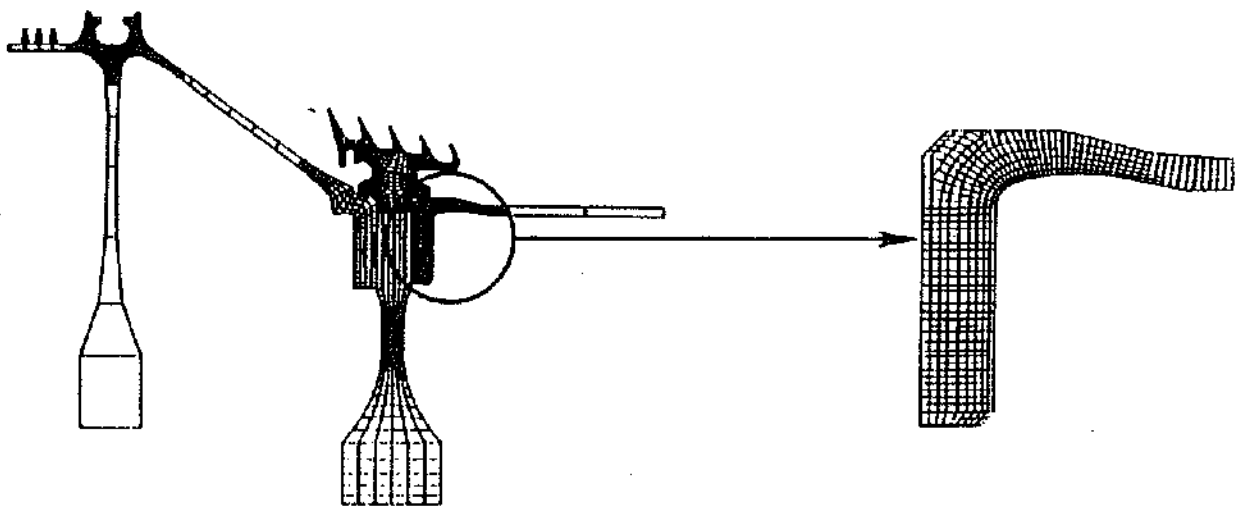


Figure 12.6 Stress Analysis Overview

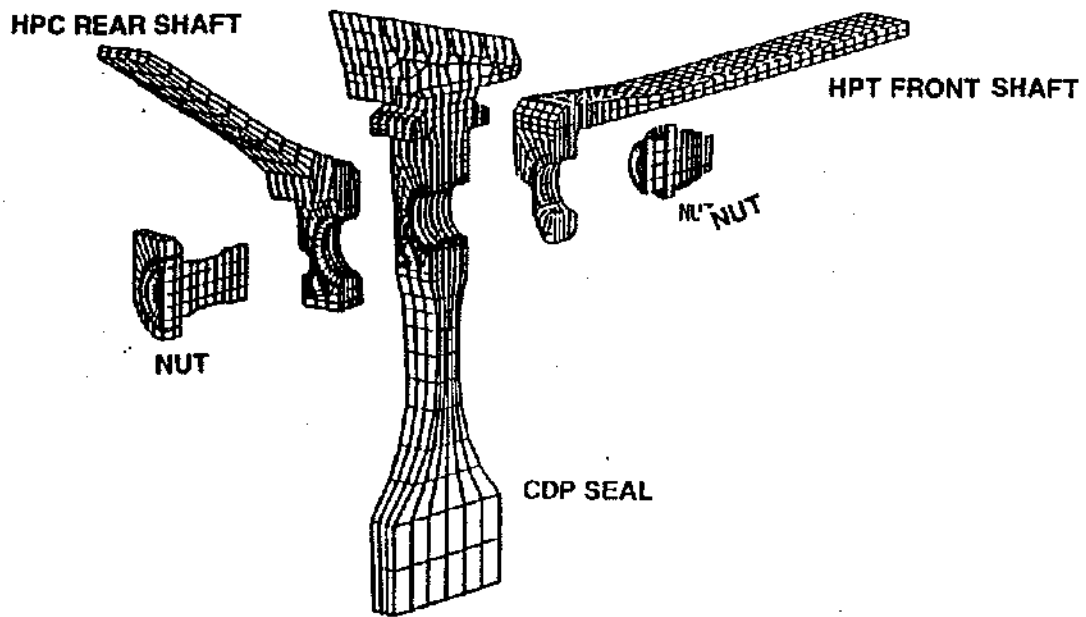


Figure 12.7 3-D Model of CDP Seal Joint

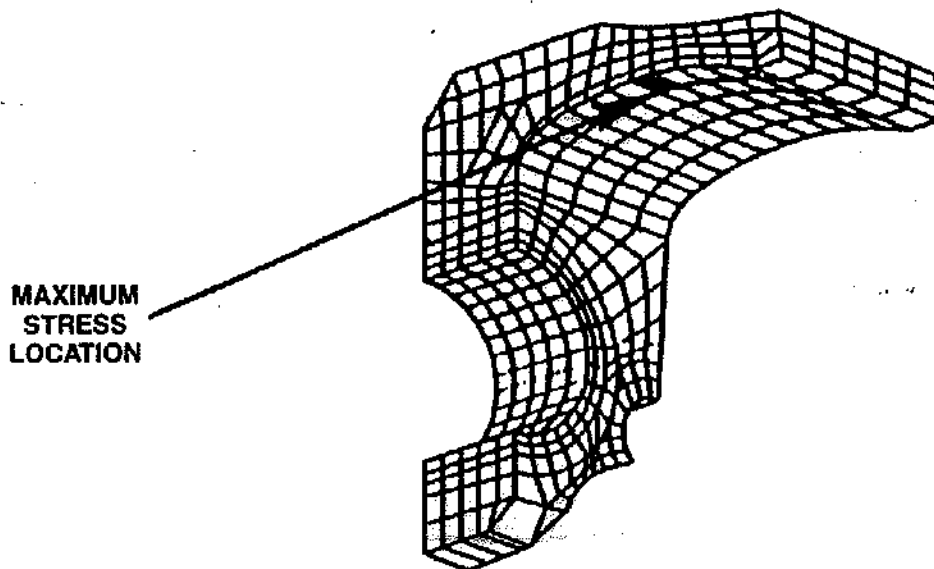


Figure 12.8 Detail of HPT Shaft

either full three dimensional rotating tests (Figure 12.9) or simple 2 dimensional tests (Figure 12.10).

The components of interest are manufactured from the 'plastic' material and then stressed under controlled conditions. The stresses generated cause fringe patterns to appear in the material which can be seen under polarized light. These fringes can be calibrated to give an estimate of the stress concentrations in the part. The stress concentrations developed by this method can be compared with similar values determined by the stress analysis programs in order to verify the analytical technique. Figure 12.11 shows a comparison of the stress contours obtained from a photoelastic test and the stress analysis.

Having established both thermal and stress analytical models the next step is to obtain the flight cycle through which the engine flies in order to identify the critical points at which the analysis needs to be run.

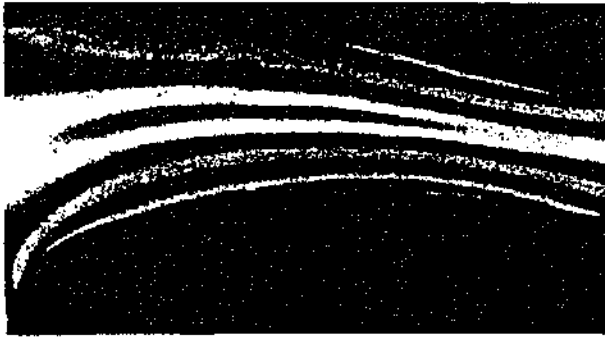
Flight Cycle For a new engine design the flight cycle will be based on engineering judgment and input from the airframe manufacturer on its anticipated usage. The flight cycle thus derived is known as a technical requirements mission and typically assumes a maximum severity operation.



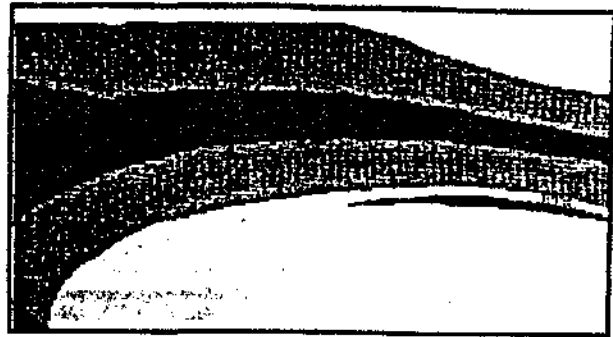
Figure 12.9 3-D Full Sized Photoelastic Model of CDP Seal Joint



Figure 12.10 2-D Photoelastic Model of HPT Forward Shaft Fillet



PHOTOELASTIC MODEL



STRESS CONTOUR PLOT — 2-D ANSYS MODEL

Figure 12.11 2-D Analysis Photoelastic Model and Stress Contour Plot

Once an aircraft/engine is in service, actual flight data is collected by representatives flying in the cockpit on normal revenue flights. This flight data is taken from several operators and an average mission is generated. The data collected in this manner is useful for two reasons, one, it verifies the predicted performance of the engine and secondly it takes account of such things as derated take-off or climb and the amount of time the engines are idling prior to take off (warm up time). The most common way of plotting a flight cycle is as fan speed (N_1) or core speed (N_2) versus time and a typical plot is shown in Figure 12.12.

Once a flight cycle has been determined a program is available which can take simple acceleration and deceleration data from the stress and thermal analysis for the component of interest and 'fly' that component through the flight cycle. The program, called LASTS (Life Analysis Stress Temperature Simulation), will then give the stresses and temperatures throughout the mission for the part analyzed. This program is useful from three standpoints; firstly it gives an independent check of the thermal analysis program THTD secondly it provides a 'quick look' at the stresses being generated in the component and thirdly it identifies the time points in the mission where the detailed stress analysis should be run.

Figure 12.13 shows a plot of temperature throughout the mission for two locations on a part with corresponding individual time point runs from the THTD program. Figure 12.14 shows a plot of stress through the mission showing the time point at which the maximum and minimum stresses occur. These are the points at which the detailed analysis would be run in order to determine the stress range the part is subjected to during a flight.

Once the maximum stress range acting on the part and its operating temperature have been determined the life is established by entering a suitable low cycle fatigue curve with the stress range and determining the cycles of life at this stress.

Materials Data The material data curves used in life analysis are called low cycle fatigue curves (sometimes call S/N curves). Low cycle fatigue is the ability a material has to withstand repeated stress cycles. The curves are obtained by testing specimens made from the particular material under lab controlled conditions of stress and temperature. Curves can be either generic, that is they can be used for any component made from that material, or specific part curves. It is found that a much higher confidence life is obtained by generating curves for a specific part. This is done by machining blanks

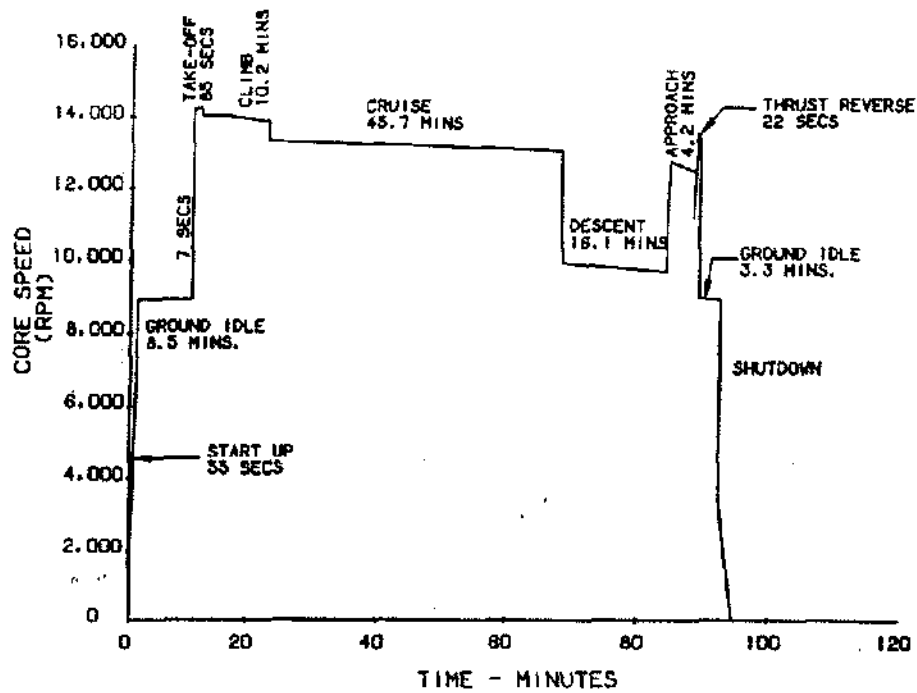


Figure 12.12 CFM56-3-B1 Typical Mission Representation of 20,100 Pound Thrust 737-300 Application

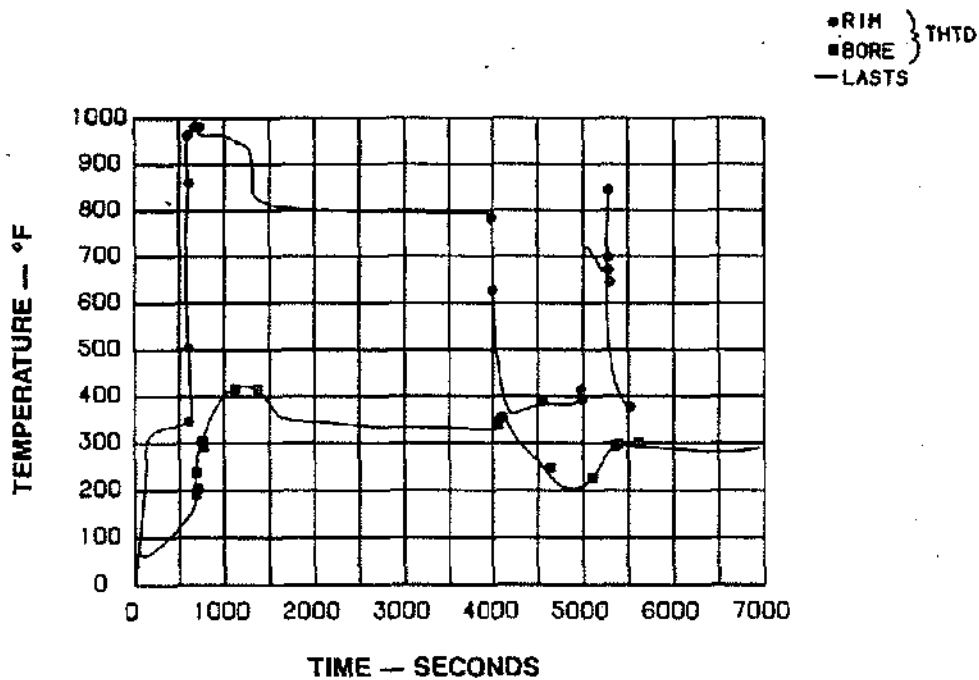


Figure 12.13 Temperature Throughout a Mission

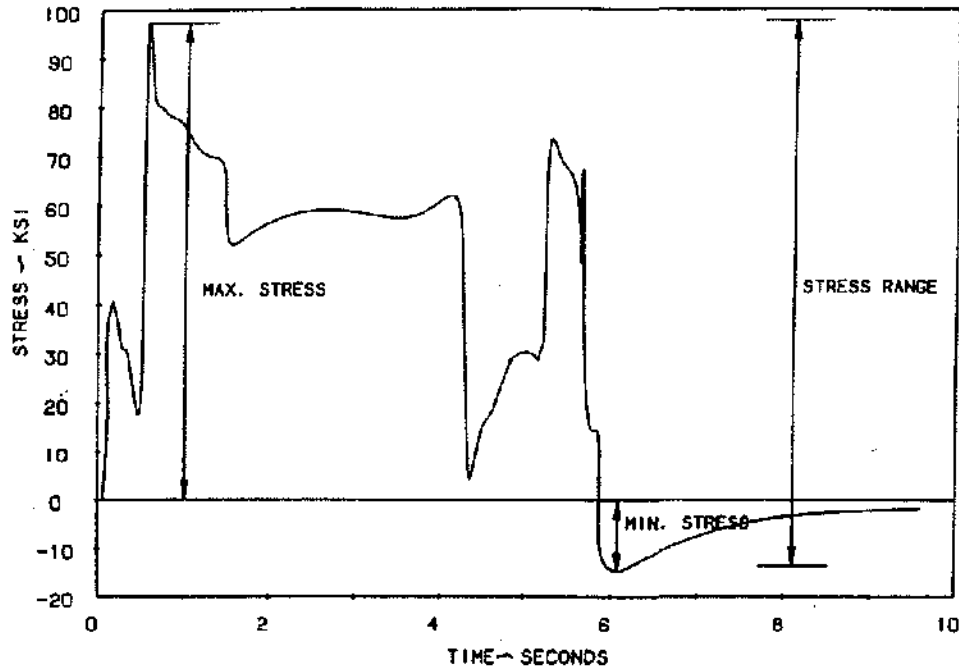


Figure 12.14 Stress Throughout a Mission

from the the actual part forging (Figure 12.15). These are taken in such a manner that they cover all parts of the forging. Specimens will also be taken from several forgings such that a statistically significant sample is taken covering all vendors and any potentially different material populations due to process changes. These blanks are then made into standard test specimens as shown in Figure 12.16. These specimens will than be tested over a range of stresses and temperatures in order to generate a family of curves with cover the total operating range of the part in question. From this data a standard statistical analysis is conducted which calculates a minimum, or minus 3 sigma curve.

Figure 12.17 shows the relationship of the average and minimum curves and the raw data which generates them. *In all life calculations the minimum curve is the only one used.* The life of a location is determined by taking the maximum stress range and entering the minimum curve to determine the minimum calculated life for that location (Figure 12.18).

This calculation is conducted for all the critical locations on a part. Typically these are bores, bolt holes, fillet radii etc. The minimum calculated life of the part is then the lowest of the lives calculated in this manner.

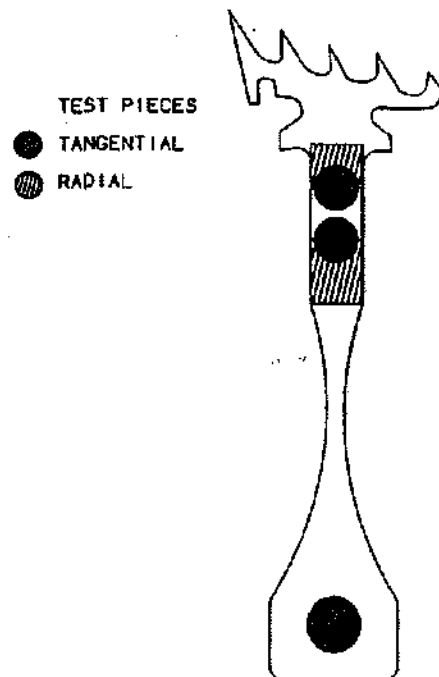


Figure 12.15 Materials Data

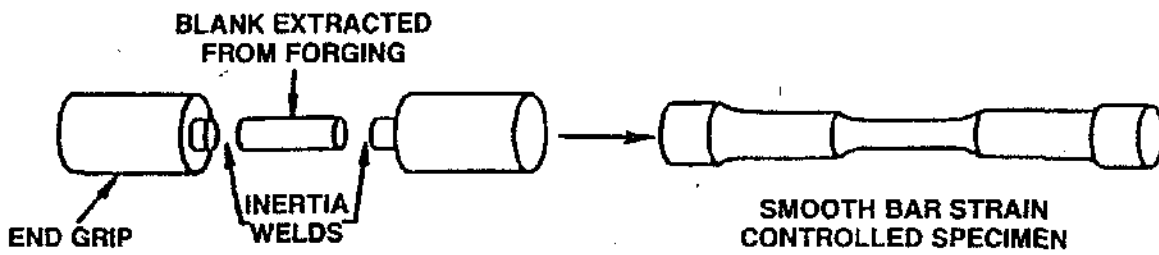


Figure 12.16 Strain Test

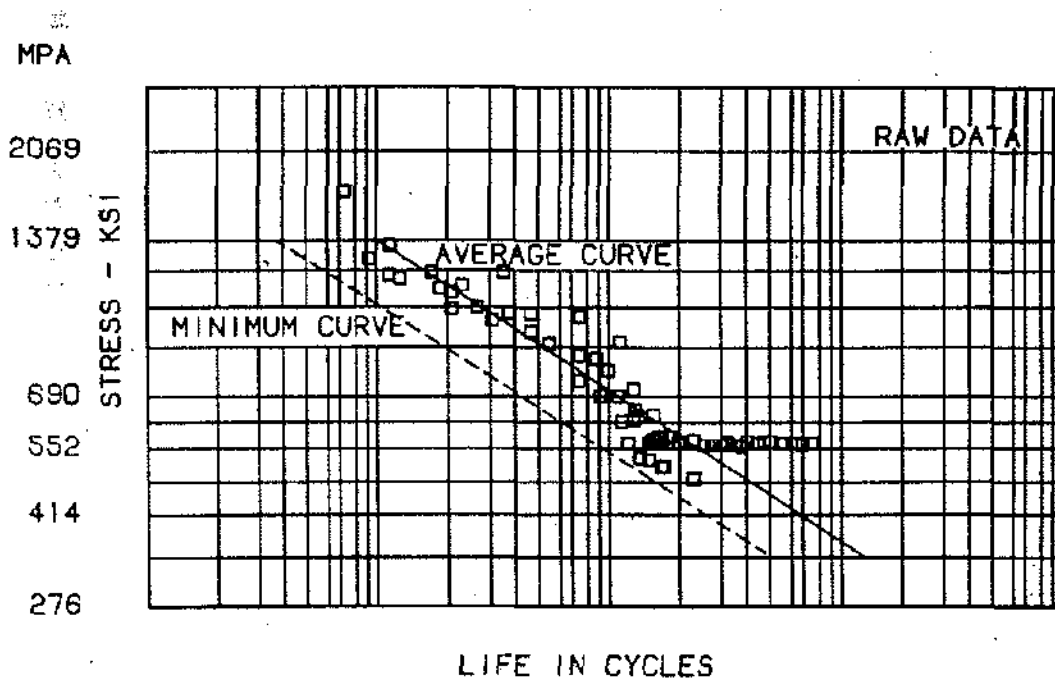


Figure 12.17 Stress Data Showing Average Values and the Minimum Curve that is Used for All Life Cycle Calculation

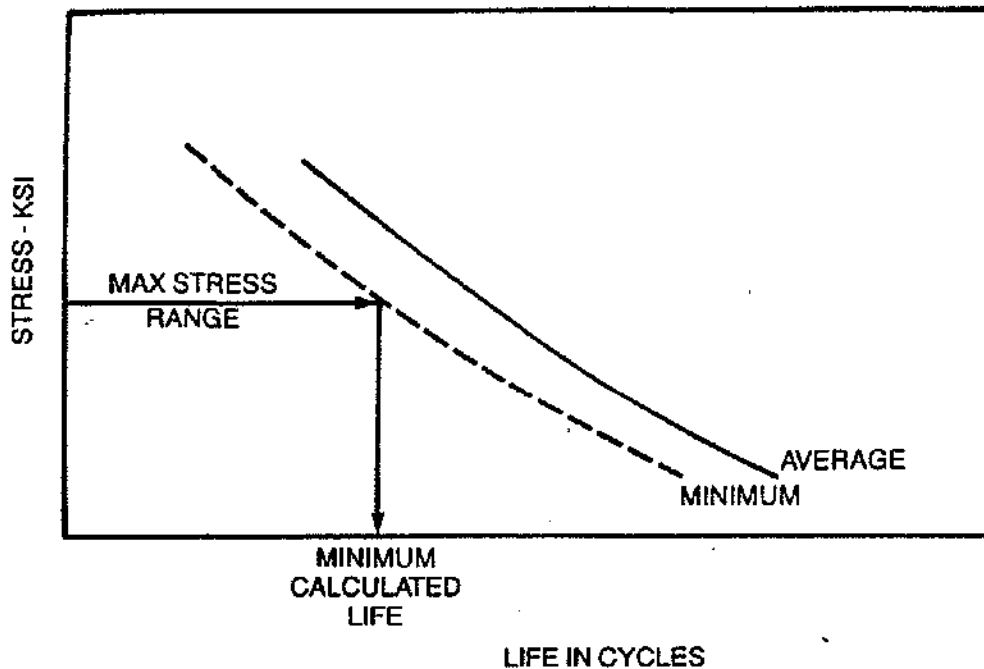


Figure 12.18 Calculated Life from Stress Data

This life is called the minimum calculated life. The number of cycles or flights to which this part can operate in service is usually a portion of the minimum calculated life and is known as the *Manual Limit*. The size of the Manual Limit relative to the minimum calculated life is determined by several factors. These include:

The amount of actual service run parts which have been inspected. Any factory engine running experience, any significant components testing which has been completed and also the quality of the analytical efforts conducted.

The Manual Limit thus determined is required to be approved by the Federal Aviation Administration. It is then communicated to all the airlines operating the engines concerned and they will be required to remove the part at or before the Manual Limit is reached.

This approach is used for determining the safe operating limits for all major rotating parts in GE commercial engines. It has been found to be a safe conservative system and to date has proved satisfactory for continued use in our future commercial engines.

MILITARY APPROACH

The military approach to lifing of major rotating parts is even more conservative than that described for commercial engines. The concept used for military engines is called ENSIP which is an acronym for ENgine Structural Integrity Programs. The USAF philosophy has evolved over several years and came about as a result of a series of incidents which resulted in loss of aircraft and significant numbers of aircraft being grounded. This is obviously totally unacceptable particularly for military operations.

Due to this experience the USAF decided that they wanted to base the operating lives of their components on a fraction of the crack propagation life. The ENSIP philosophy assumes that all parts contain cracks at all critical locations and the life of the part is determined by the propagation life of the minimum detectable crack in the part. This in turn is determined by the inspection capability available for the components.

The basic analysis for military engines is the same as that already described in that the thermal and stress anal-

ysis still needs to be conducted for the mission determined for the particular engine application. The minimum calculated initiation life is still determined for military components and this is exactly the same as the life calculated for commercial engines. In military terminology this is called the *Durability Limit*. Figure 12.19 shows a pictorial representation of this.

The military approach then adds a further step in order to reach this durability limit in the safest possible manner. Typically the military are prepared to overhaul their engines at regular set intervals and a decision was made that at both new production and at every overhaul the parts of the engine would be subjected to full inspection. The length between overhauls would be based on the life of a minimum detectable crack to grow to failure. In fact the ENSIP approach is to take half of this life as the overhaul period. This in theory says that no failures

should ever occur. Figure 12.20 again shows a pictorial representation of this approach.

LIFE ANALYSIS SUMMARY

In summary there are two approaches to calculating the lives of major rotating components. For commercial engines a minimum calculated *initiation* life is determined. A proportion of this is taken to establish a *Manual Limit*. This is the life at which the part is retired.

With military engines this same life establishes the *Durability Limit* which is when the part is retired. However this durability limit is reached by inspecting parts at set safe inspection intervals determined by inspection capability and the crack propagation properties of the material.

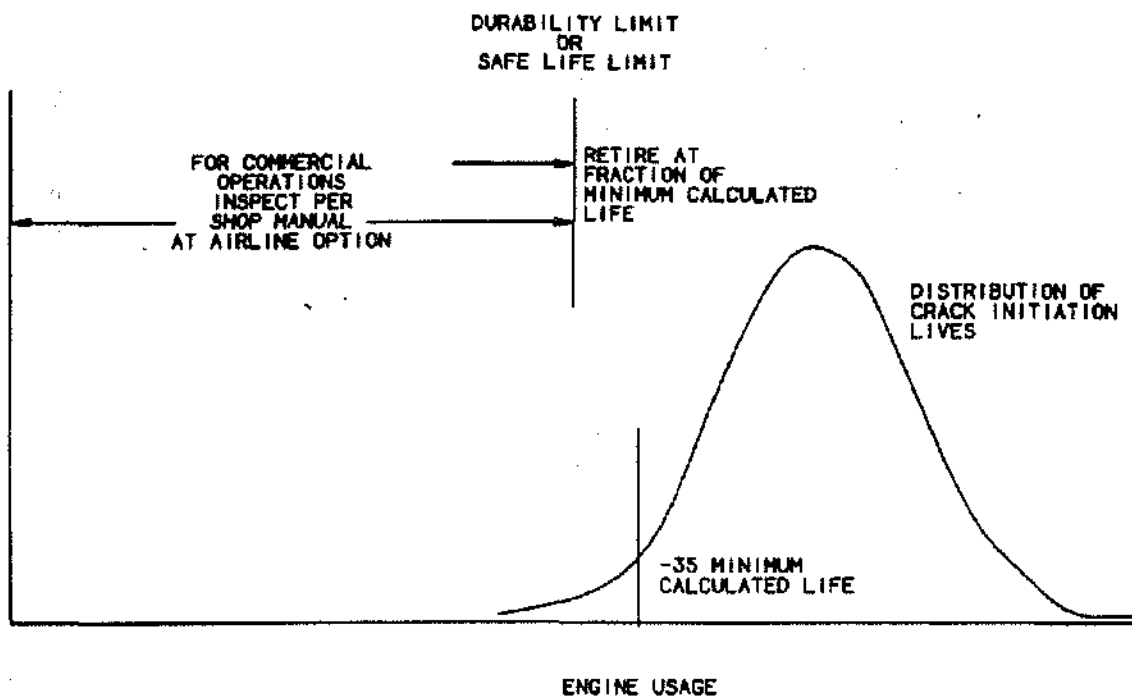


Figure 12.19 Durability Limit Concept and Commercial Engine "Safe Limit" Approach Are Essentially Identical

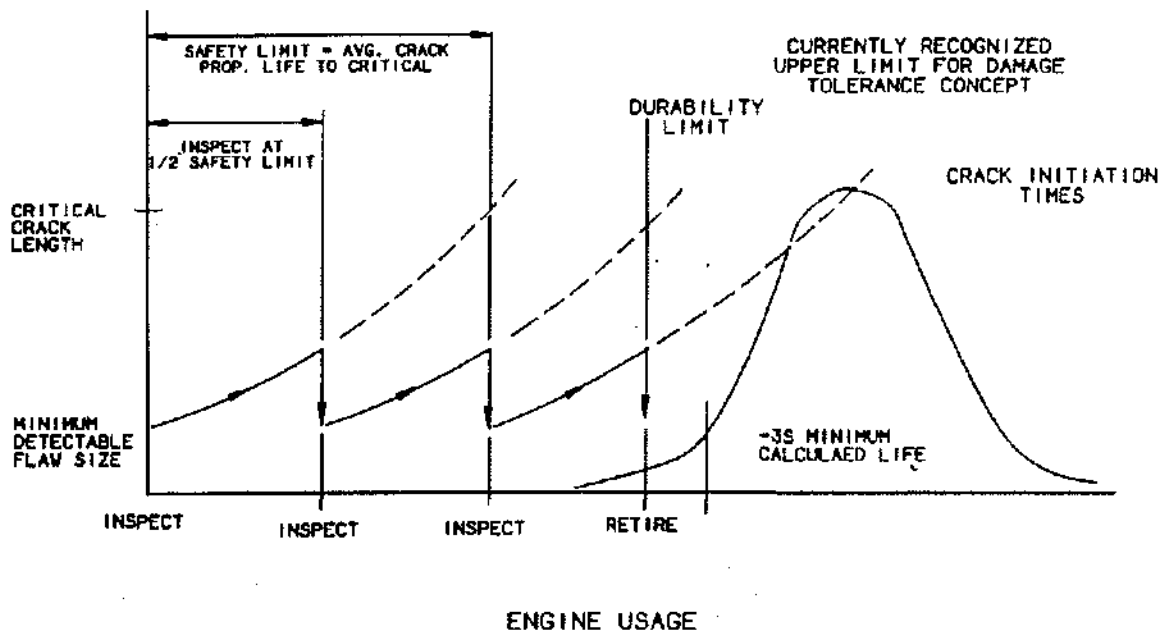


Figure 12.20 Damage Tolerance Approach Forces Periodic Inspection of Critical Features

Chapter 13

PRODUCT SUPPORT

by George Gregg

PRODUCT SUPPORT

Product Support is the intensive support of our product before, during and after its sale. It is the method by which we help our customers insure and be excited about the Reliability, and the Cost of Ownership, of our products which they use, and which leads to the lustrous Reputation of our products in the eyes of those customers.

Product Support is an evolving part of the business, with its requirements and boundaries changing to meet the needs of our customers, the characteristics of the products, and changes in technology. There is no specific list of requirements for Product Support; we usually consider the requirements to be anything which is needed, and is reasonable and attainable, to support the goals of Reliability, Cost of Ownership and Product Reputation held by our customers.

Product Support includes helping the customer plan the maintenance actions and assets needed to maintain the engine while it is in service, and while it is out of service. This involves working with the customer to understand, or to define, his goals for the engine in terms of reliability and cost, and to mutually translate these goals into a plan of the actions, schedules and assets needed to reach those goals. The work usually involves developing excellent rapport with, and knowledge of the customer, the customer's method of managing his business, and the capabilities of the customer. It also requires an intimate knowledge of the engine and its particular capabilities in the environment in which the customer uses it.

The maintenance plans which are developed for commercial engines, in some jurisdictions in the world become the official maintenance plans required by aviation regulatory agencies. The goal-effective maintenance of engines sometimes requires that mechanics, inspectors or other specialized personnel who are involved with engine maintenance must have specialized training in prac-

tices or techniques, or must have more generic training on an engine model to any of several levels of knowledge. A modern Product Support function provides formal classroom training in the required knowledge and skills, both in an Evendale Training School, and in classes and individualized instructions at customers' or common sites.

One subject which is extensively and repeatedly covered in training is the subject of detecting and isolating and correcting faults on installed engines, or trouble shooting. Customers demand that the product be available for use when needed; thus, early identification and correction of faults is mandatory. General and specific training is conducted by Product Support to develop expertise and confidence in trouble shooting. The recent improvements in artificial intelligence and expert Systems will lend themselves to improving both the training and the ease of spreading experts' information on trouble shooting.

During the lifetime of an engine design, product improvements are sometimes developed by GE and made available to the customers. Some of these improvements may be significant and relatively inexpensive to install, and can be planned to be introduced by attrition as their predecessors wear out. Other improvements may be very important to the goals of the customers, and also more expensive to incorporate.

With some improvements, it may be valuable to plan their early introduction even to the extent of removing and retiring otherwise usable parts, because to do this can contribute to the Cost or reliability goals of the customer. Some customers have well developed methods to determine the technical, logistic and financial merits of these more significant product improvements. However, other customers do not have these methods or experience in using them. Product support specialists work with customers to help them understand the technical advantages of product improvements, the logistics planning and execution needed, and the financial costs and advantages. The financial studies must consider the customer's own rules about payback periods, the treatment of the cost of money, national laws concerning interest rates, tax laws, and rules on the capitalization or expense of purchases.

Maintenance cost, which is the cost of the labor, the material and the purchased repairs which are needed to maintain an engine in a condition in which it can meet the goals of the customer, is an important part of the cost of ownership, which is itself a goal-criterion. Product support helps customers develop maintenance cost plans, which may form the basis of a large part of the

customer's budget plans for the engine. During these efforts, product support specialists are often extensively involved in helping the customer forecast how their engines will perform in the study period, what maintenance plans should be used, how product improvements should be incorporated, and what repair or modification programs will be released. All these efforts have an important effect on the maintenance cost, and are significant parts of the customer's planning which goes into committing to the engine budget for the planning period.

An obvious complement of the maintenance cost and budget planning process with the customer is an agreement on what quantities of spare parts will be used by the customer and what quantities will be ordered by the customer. Product support specialists work with the customers to develop these forecasts, and from them to build-up global forecasts of probable sales of parts by part number. This data is necessary to be used in the General Electric spare parts ordering plan, in order to best assure that parts are available when the customer needs them. The corresponding Spare Parts Sales effort, involving forecasting usage and sales, studying trends, ordering stock, receiving and managing customer's orders with personal attention, planning inventory, stocking inventory, managing distribution, and collecting payment, is a very large business in its own right. It is estimated that by 1990, GE Aircraft Engines spare parts sales for commercial engines alone will be almost one-billion dollars annually.

Product support provides customers with specialists who can discuss and give advice on technical concerns on all aspects of the engine and its use. This is an extremely valuable service to the users of our products, especially to those who do not have themselves highly-qualified technical experts. This service may include helping the customer conduct a failure investigation and deciding upon the control plan, and any necessary corrective action. Many product support engineers are employed nearly full time in technical communications with customers.

As an example, consider a typical problem which may develop. A customer, in his engine overhaul shop, is assembling a component of an engine. For reasons which he does not understand, the assembly cannot be done correctly, so that the in-process or final specification requirements are not met.

This may mean that the higher-level assembly cannot be done, because this assembly is not available, nor an alternate one. If the engine which this assembly must support is planned to be needed, and there is a specter of lack of that engine when needed, dramatic actions are

necessary. If the customer's specialists cannot solve their problem, they communicate with Product Support specialists for consultation, and advice. This may take the form of written or telephone communication, to exchange facts and judgments. One of the options is to dispatch the specialist to the customer's shop for hands-on understanding and recommendation on the problem. This may be as near as Tulsa or Tinker, or as far away as Tokyo; the customer receives the support which is needed to make the product successful.

Both military and commercial engines are introduced, operated, maintained, inspected and tested using formally prepared and approved technical publications. The preparation, publication, distribution and auditing of these documentation and management media is an important part of a successful product support function.

Product Support Flight Operations Support specialists, who are experienced aircraft pilots and flight engineers, work with commercial customers to help them better understand the product and the best ways to operate it. They fly in aircraft jump-seats to observe operations, and to counsel aircraft crews. They also conduct seminars to better assure that operations people at airline customers understand the nature and status of elements of the engine and the airplane-to-engine interaction.

The cost of material is a large part of the maintenance cost of an engine. Product support funds and manages a large repair development effort, to provide proven repairs for valuable engine parts, so that customers can better control their maintenance costs and their costs of ownership.

General Electric wants our customers to feel secure in the knowledge that they have a direct face-to-face contact with an experienced, dedicated and professional GE representative who represents their interests with GE. Part of our product support program requires that we recruit, train, position and support these people in every part of the world where we have customers. Thus, in every place in the world where our customers are located, we have field service representatives permanently stationed to provide on-the-spot product support.

There are other facets of product support which are in place. They include providing a system of engines available for lease, helping to plan the organization and arrangement of engine shops, working with the vendors to our customers to satisfy customer's needs, and administering warranties and guarantees.

The list is not complete, because it continues to evolve as the expectations of our customers change. The test is to

determine what the customer wants and needs, and to decide whether we know how to provide it, and if it is reasonable to provide the service. If the answer is yes, it is part of our product support effort. Our competition in both military and commercial engine businesses has realized that we have provided and are continuing to provide superior Product Support, and that we have developed an impressive and valuable basis for differentiation with product support. They recognize that they must compete to be successful, and that product support is one of the competitive fields.

This has forced them to compare themselves to GE on the basis of support of the product, and to start planned drives to improve themselves so that the differentiation is lost. This demands that we stay alert and responsive to the expectations of our customers.

Superior product support is the result of an attitude that says that the business is run by the customer, and that our product is not successful unless the customer is successful with it. In addition, that the success of the customer is measured in his terms and against his goals. Product Support is an investment in winning the future.

MAINTENANCE

Maintenance is defined as the actions necessary to assure the serviceability of the product in the hands of the user. It is made up of the inspections, decisions and corrective actions which are needed to best assure that the engine and its systems can do what they are intended to do.

Maintenance methods and philosophies are often tailored to fit the needs and capabilities of customers, the use of the engine and its environment, and evolving technologies. Several different generic maintenance philosophies can be described; they have emerged as the customers, their needs and engines have emerged and matured.

The original maintenance philosophy was once called the Time Between Overhaul method. Overhaul is defined as the complete disassembly, inspection, repair and assembly of the engine or its parts. This method established hard time milestones, with mandatory observance, at which overhaul must be done. If an interim engine removal is required before the hard time milestone is reached, only the feature which caused the removal is repaired before the engine is returned to service.

The time between overhaul or TBO method has a number of advantages. It is very amenable to pre-planning.

There is little engineering or evaluation work required. The bill of work for engine shop visits is standard. There are also disadvantages. The time milestones are set by the capability of the least capable parts. It is a relatively high cost method, since overhaul is performed on elements which don't need it.

An adaptation of this method recognizes that different major sections of the engine may need inspection and overhaul at different times, because of different inherent capabilities and severity of their respective environments. A usual cleavage of this type would divide the engine into a hot section and a cold section. The latter would include the engine from the inlet to the rear of the compressor stages; the hot section would include the rest of the engine. With this division, the TBO process would be applied separately to the cold and hot sections. Hard times would be established separately for each; for ease of scheduling, the intervals for one part of the engine might be established as whole number integrals of the intervals for the other section. This hot section-cold section TBO method has all the advantages of the simple TBO method. It has a slighter disadvantage in terms of relatively higher cost because it allows more sectional discrimination.

Module conditional restoration is the maintenance method which is most commonly used for free-world commercial engines. It uses the premise that inspection can indicate the need for restoration. For each functional section of the engine, commonly called a module, an established plan specifies the level of disassembly, and inspections done down to that level indicate the amount and type of restoration work to be done. With this system, an engine might not be overhauled in its lifetime. Instead the modules of it might be repaired or overhauled at several intervals which differ from each other.

This method, also called the on-condition method, has advantages. It can achieve maximum utilization of the variation, from maximum to minimum, of the capabilities of parts and systems. It lends itself to effective control of engine costs, because it allows the maximum differentiation between work which needs to be done, and the associated costs, and work which does not need to be done. It usually can result in improved reliability, because it can emphasize and profit from careful review of data, and intelligent decision making. However, it requires a substantial real-time data base. It requires competent and dedicated engineering analysis and evaluation. Every module inspection may require a customized work plan. The apparently erratic nature of some problems requires more sophisticated planning and control to be needed, since there may be little or no warning of an impending problem. On-condition mainte-

nance does has risk elements. Over restoration results in high costs; under restoration causes reduced reliability and high costs. During the terms that an engine is in its initial service with a customer, the very limited empirical data which is available can yield forecasts which are too optimistic or pessimistic.

A refinement of this method, which is intended to help to overcome its disadvantages, is one usually titled inspection thresholds-critical parts. It operates on the premise that, in every part of the engine, there are critical parts, the condition of which is used to determine total module health. These parts are named, and when they are inspected, the inspection results are used to determine the amount and type of work needed for these parts and for the rest of the module. The critical parts often have time milestones, or thresholds, established for them which trigger the process. These thresholds are usually related to the time in service since the last module shop restoration visit. The thresholds may be evolutionary values, resulting from a continuing review of the results of preceding inspections.

The threshold method has several advantages. It reduces the amount, and the cost of, the data required to operate a maintenance system. It requires less engineering analysis and evaluation than does on condition maintenance. There are also disadvantage of the threshold method. It is usually applicable only to engines or systems which are near or at maturity. The integrity of the method depends upon the propriety of the critical parts selection. There is a tendency to judge conditions from that of the average module. It can result in high labor costs. Its use can carry with it the risk that new wear-out modes are not predicted.

Variations of all of these methods are used. Each of them being selected because they seem to fit local needs and abilities the best. Several of them are naturally continuous in nature, in that they require data to be collected and analyzed before changes can be made, which themselves cause changes in conditions and new data to be collected. General Electric is often very involved in helping a customer decide what maintenance philosophy to use and is also often involved in helping to establish a maintenance plan with specific customers.

The maintenance plan is a statement of the goals for a combination of a customer and a product, and the plan to accomplish those goals. In the United States, new commercial aircraft-engine systems are put into initial service using an officially recognized maintenance plan. It is a result of the work of an industry committee, given the title of a Maintenance Steering Group, or M.S.G. These groups are assembled and headed by the Air Transport

Association, the A.T.A. They use a carefully constructed logic analysis approach to decide the types and frequencies of maintenance actions which are mandatory to best guarantee reliability, safety and acceptable cost. They use formal studies done as failure modes and effect analyses, reliability analyses, test data and observations on similar systems. The maintenance plan which they develop for the airplane system becomes the officially approved one which is mandated to be used during the initial service of that airplane system.

As the airplane system develops experience during its initial service, this experience is studied to determine the accuracy and adequacy of the maintenance plan being used to manage the system. Sometimes, airplane subsystems, including engines, are intentionally removed and extensively disassembled and inspected to provide specific data to confirm the plan. The data which is generated during this service experience is used to amend the maintenance plans based upon what has been learned and what the goals are.

The engine is maintained, both on-wing and in the shop, within the framework of specific instructions issued by GE in the form of manuals for maintenance. These manuals are required by the customer in the case of military engines and by the customer and regulatory agencies in the case of commercial engines. Their purpose is to state and explain the requirements to determine airworthiness, and the methods to restore airworthiness. Some commercial customers have the legal authority to change these requirements to fit their own data and goals.

The purpose and format of the manuals are carefully defined by the users. This can lead to brevity. They also are written to explain the maintenance requirement of all of the engines of a model, in use by all customers and in all environments. Hence, they may be cumbersome, overly-comprehensive, and yet incomplete because they cannot explain the innuendo in some details.

For example, it may be important to be sure that the airfoils in a part of the engine do not operate with extensive corrosion damage. The manual for inspection of the part of the engine should give the requirements for inspection for corrosion, the limits of serviceability, and the method of repair, if repair is possible and cost effective. But not all customers may experience corrosion of these airfoils. If the inspection for corrosion is a relatively inexpensive and simple one, it is probably no problem to routinely inspect for it. It is relatively expensive or difficult, the customer who does not experience corrosion does not enhance airworthiness by inspecting for it, and instead, only develops costs which increase the cost of ownership. Instead, that customer is better off if he only stays aware of the concern and monitors for it.

For commercial engines, a medium has been developed to fit the statements for requirements for airworthiness, the manuals, to the localized needs of specific customers. This medium, called the "Workscope Planning Guide" and in some jurisdictions called the official maintenance plan, represents the maintenance plan which is mutually agreed to between a specific customer and GE. It usually states the reliability goals for the engine and its modules and describes the level of inspection, the consequences of inspection, and the methods of repair which can be shown to best deliver reliability and to generate the least cost of ownership. Workscope planning guides have shown that they are excellent active management vehicles for commercial engines.

The future of engine maintenance has interesting prospects. Engines now have, and will probably increasingly have, more complex systems which need maintenance. The capital cost of engines will increase, as will the inherent and the demanded Reliability, while the drive to control and reduce the cost of ownership will become stronger. Making these thrusts merge well with one another will be more difficult. Computerized systems to test engine systems and recommend action, including specifying all of the assets and skills needed are being developed as the needs arise, and some are in use now. Workscope planning guides are amendable to and can be expanded and improved, by applying Artificial Intelligence. The areas of trouble shooting and of repair-problem resolution are fields for the effective use of expert systems.

The entire job of documentation of maintenance of engines will be moved to the electronic format from the present manual one. The move to lease, rather than own, commercial engines will put more strain on the maintenance systems. Maintenance is a mandatory part of the engine use cycle. It is demanding and expensive. General Electric is the leader in cooperating with customers in goal-effective maintenance.

Field Related Problems

Engines are an important part of the system into which they are integrated. As people who design, manufacture and support engines, we often have the parochial view that the engine is the system when, in fact, it is only part of usually complicated systems which must meet goals set by our customers. Whether it is pumping natural gas, powering a tanker aircraft, or propelling a planeload of people on a pleasure trip, the engine must support the system of which it is part so that the goals of its user, our customer, are realized.

Engines are not simple; they often are state-of-the-art machines. In service, they sometimes display problems which range from benign to serious. One of the functions of Product Support is to anticipate concerns, recognize them when they occur, decide which ones are problems or will be problems, develop solutions to the problems, and have the solution available before the problem is real.

The job, simply stated, is to be prophets, and not historians. Readiness planning is an important part of the control and management process. Its purpose is to measure and correct the ability of the product to satisfy the goals of the customer. It will answer questions relating to how well the customer is trained in the understanding, use and maintenance of the engine. It will study the plans and provisions the customer has developed, the facilities he has available, the communications and data systems he uses, and the capabilities of the people. As this is done, product support planning is done to correct deficiencies both at the customer and in GE.

The product is introduced to service at customers with support plans which largely are tailored to the needs of that customer, as indicated by the readiness planning and by explicit agreements with the customer, as well as any other data which is available. The product often gets extra attention early in its customer introduction, until it is reasonably sure that the product, the customer, and the goals are compatible. When the product is operating in the customer's system, it receives close scrutiny by the customer, and by Product Support. For commercial engines, Flight Operations specialists work with airlines to help them tune operating procedures to best realize the goals of the airlines. They also gain data and insights which can be valuable in understanding and solving problems which develop in the field.

Part of the requirements to anticipate concerns is to know and understand what the condition of the engine hardware is in the customer's environment. Analyses are usually used to predict what the lifetimes of parts will be, and how the service lives of parts and systems will be limited. It is important to verify the analyses by assessing the actual conditions of parts and systems as they operate in the field, so that the analyses can be made to agree with observed facts. This is done by performing assessments of the condition of parts, and by collecting and analyzing the data so that it can be used in correlation, and in forming opinions of concerns. These assessments may be formal, done with extensive documentation including video cameras. Others are done by informal surveys, or observations made during the course of other business.

Some of this information is needed to use in formal Life Management programs which are established to best identify and manage the safe useful life of expensive and critical engine hardware. To control the reliability and the cost of ownership of the product, these kinds of parts must be used through all of their safe lives. This means that safe lives must be forecast with accuracy, and the forecasts, usually analytical studies, must be repeatedly reviewed against the data learned in the parts condition assessment programs. As the analysis are done, special tests of used parts, and specialized inspections of field-run parts often must be completed. All of this work is done to develop convergence between analysis and fact, so that the analysis can be solidified and used to predict safe, usable lives.

Some of the work done in Life Management, involving the return of field-run hardware for specialized inspections or tests, requires that expensive hardware be transferred to GE by the customer to use in these programs. Also, when engine failures occur, and when the elements of parts condition assessment require it, expensive customer-owned hardware may be required to be returned to GE by the customer. A system is in place to help to identify the parts, and to financially and physically account for them. This service request system tracks the part from the time it is requested from the customer, through all of the work done with it, including any formal reports on reasons for failures or observations of condition, until it is returned to the customer or the customer is informed that it will not be returned and that compensation will be paid.

An important benefit of the conclusions reached from the data gained from Parts Condition Assessment, and using information as well from all sources, is the valuable data to be implemented in developing maintenance plans, and in doing spare parts forecasting. The data forms the basis for much of the maintenance planning, since it indicates the condition of engine systems and parts. These observed conditions are some of the facts used to develop and to alter maintenance plans. Correspondingly, the same kinds of data are valuable in setting or changing the assumptions used in spare parts forecasting.

When it may become apparent that the engine or its systems will not reach the goals set by the customer, it may be necessary to review and modify the assumptions used to establish a Maintenance Plan and needs for hardware. Sometimes it is necessary to plan that the engine design, or parts of it, should be modified to allow achievement of the goals. This usually results from the realization that the part of the design is not adequate, which leads to an analysis of what must be done to make it adequate. If it is

decided to change part of the design, an integrated program is laid out. It must start with the end date at which the modification must be ready, and work the problem in reverse to show what milestones must be achieved. Also, the modification must be designed, to satisfy the goal-deficiencies of its predecessor without introducing new ones, and without imposing unacceptable cost increases on GE.

As the modification program progresses on its schedule, product support must inform the customers that a modification is being developed, and must inform the customer on all of its important macro details. Some customers want to discuss all of the details, including what technically is planned, test results, relative costs, tooling charges required, and logistic plans. Other customers do little of this, and will do nothing until the design modification is released. When that has been done, the modification program may require selling by product support, to insure that the customers know what the program will do, what it will cost, and how to determine its benefit to their goals. These programs continue for engines, sometimes even well into their mature states.

ENGINE AGING

Engine Aging is the process by which an engine approaches maturity, at which time its reliability and cost of ownership reach stabilized levels in terms of the influence of engine age upon them. A newly-manufactured engine has unused life built into it; at the intervals in service at which work is done on the engine, some of this original life is restored. The amount of original life which is restored is the independent variable which influences the aging characteristic. In turn, the amount of original life which is restored should be the amount which it is cost effective to restore.

The aging characteristic is usually described for the particular fleet of engines being considered. These are usually a fleet of engines, all of the same design, used in the same service, and maintained with the same maintenance plans.

For such a fleet, the aging characteristic curve could usually be shown in Figure 13.1. These expressions are derived analytically, and also developed empirically. The expressions are useful in doing forecasts or simulations of rates for engine removals, costs of ownership, and similar logistic and financial concerns. For example, it is often possible to develop, by analogy or by analysis, a forecast of the mature cost of ownership and the mature reliability of an engine model. If the engine model were sold with a guarantee on the maximum cost of owner-

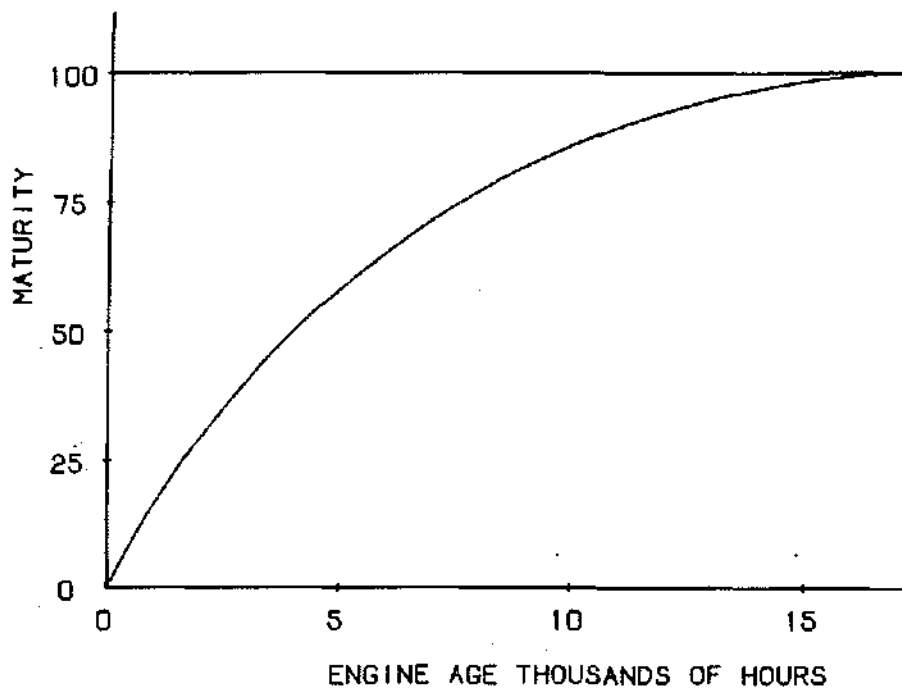


Figure 13.1 Aging Characteristic Curve

ship, or one of its major elements, direct maintenance cost, it is important to know how the costs will build-up to the mature value during the guarantee period.

Consider a commercial engine which is sold with a guarantee which states that for a period of five years the direct maintenance cost, on both an annual and an accumulated basis, will not exceed some value. For a commercial engine which operates 3000 hours per year, the indications are that almost all of the guarantee amounts will accrue during the unstabilized aging period. Using an appropriate aging curve, and analyses of the conditions of the mature characteristics, the transient characteristics can be forecast to use during the guarantee period. These analyses are valuable, and are used, in forecasting cost of ownership, reliability rates, and logistics requirements for assets including material and labor, and others.

After the engine has become mature, it is important to maintain balance between the hours flown in service, and the amount of these hours which are restored. Although hours are cited here, the characteristic cited in some cases might be cycles, or any damaging-inducing characteristic which is definable and measurable.

When engines are purchased, there are usually a number of spare engines purchased to support a fleet of aircraft. The number of spare engines, which are used to operate the fleet while others are in the shop for restoration involving overhaul, is a function of the average amount of time required to restore an engine, and the number of shop visits in a calendar period. When this level of spares is established, the mean time between shop visits becomes an important measure of the balance of the hours flown and the amount of restoration done.

The characteristic which displays this effect is shown in Figure 13.2. There are three characteristics shown. Curve A depicts the effect of over-restoration. The line T-T illustrates the mean time between shop visits which is required to keep spare engines available at adequate protection levels given the shop restoration cycle time. Curve B illustrates appropriate restoration. Curve C illustrates the effect of failure to restore used-up capability. It is obvious that there will not be enough engines available to support the fleet when this characteristic is effective, and consequently, some aircraft will be out of service. If this is unacceptable, the alternatives are to increase the number of spare engines, and restore more used-up life in order to increase the MTBSV. When this

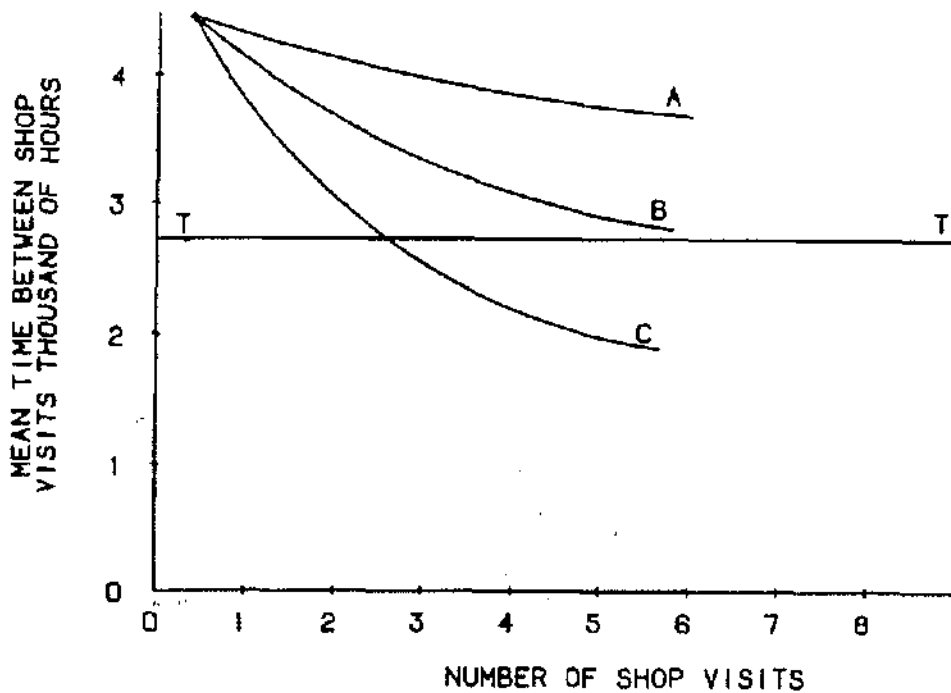


Figure 13.2 Shop Visits and Restoration

situation actually develops in a fleet, drastic measures may be necessary.

If the problem is short term, it may be possible to lease engines from another user to provide the spares support while the engine restoration process is being improved. It also may be necessary to increase the manhours of labor available in the engine shop by working overtime, hiring additional people, and farming-out restoration work. All of these are expensive efforts which cost more than careful management costs. Engine restoration management requires continuing prudent planning and action, often in anticipation of problems.

CONDITION MONITORING

Condition monitoring is an element of the maintenance process. It is the system of inspections and corrective actions which is used for the engine while it is in service, to best assure that it can reach its goals. These goals are usually stated involving reliability, cost of ownership and reputation. Condition monitoring supports these goals by its influences over airworthiness and perform-

ance considerations, and by its ability to help to sense cost thresholds.

Condition monitoring takes several forms. It involves external review and inspection of the engine by flight crews, by ground crews, and by inspectors. It may use the results of analyses of the samples taken from the working fluids of the engine. One of these is the spectrographic oil analysis program, commonly referred to as SOAP. It does spectrographic analysis of oil samples taken from engines, in order to determine whether unusual wear and shedding of engine materials is taking place; some of these wear patterns can be warning of impending failures.

One of the more effective types of condition monitoring is visual inspection of the internal surfaces of the engine by means of borescope devices. Adopted from medical inspection technologies, borescopes range from simple tubular arrangements of light sources and lenses, with mirrors or prisms, to power-flying integrated light sources and television cameras, with television screen and digitized readouts suitable for transmission or storage. Usually used by experienced inspectors, in

response to a need for trouble-shooting, or as a routine, the borescope is a very common inspection technique.

The monitoring of engine trends, primarily thermodynamic and associated parameters, is commonly done to detect changes in performance-related parameters which can illustrate impending problems, or can detect the achievement of performance-related thresholds. Trend monitoring systems can be completely paper and pencil systems, or they can be automatic systems with scanning, recording, alerting, analyzing and taking action all done by crew-aiding systems which supplement ground people.

Some commercial engines are being operated with an automated trend monitoring system; this GE Turbine Engine Monitoring System, GEM, records a number of significant performance-related parameters on an essentially continuous basis. The data record is unloaded at line stations, loaded onto the reservation system for transmission to an analysis station, and there is scanned. Automatic alert levels are set; these point out conditions so that corrective actions can be planned and started. Similar systems are available for military engines. The capability exists to perform these functions continuously with air to ground links that put the situation into real time. The future will include the development and use of expert systems to help to better understand the data and to make the correct decisions.

END USER ASSESSMENT

Product Support is an expensive part of the business. It can be asked: Why do we support the product so extensively and so passionately? Why do we go to such lengths to develop and maintain excited satisfaction in our customers? One of the answers evolves from our pride in our products; we know that they are very good, that they stack-up well against their competition and that they represent our personal best efforts. We know that they can be successful in our customer's fleets, and we want our customers to be successful with them. This pride in our products makes Product Support easier to support financially and personally.

On a more quantitative basis, many Product Support actions are taken because we enter contractual agreements with our customers to provide them. For example, we have contracts with some customers that require us to have spare engines available for them to lease if they need to. These agreements are written into sales contracts because customers specify them. With some customers, we guarantee that their maintenance cost will not exceed a stated value. If it does, GE will pay the customer a large percentage of the amount of the excess.

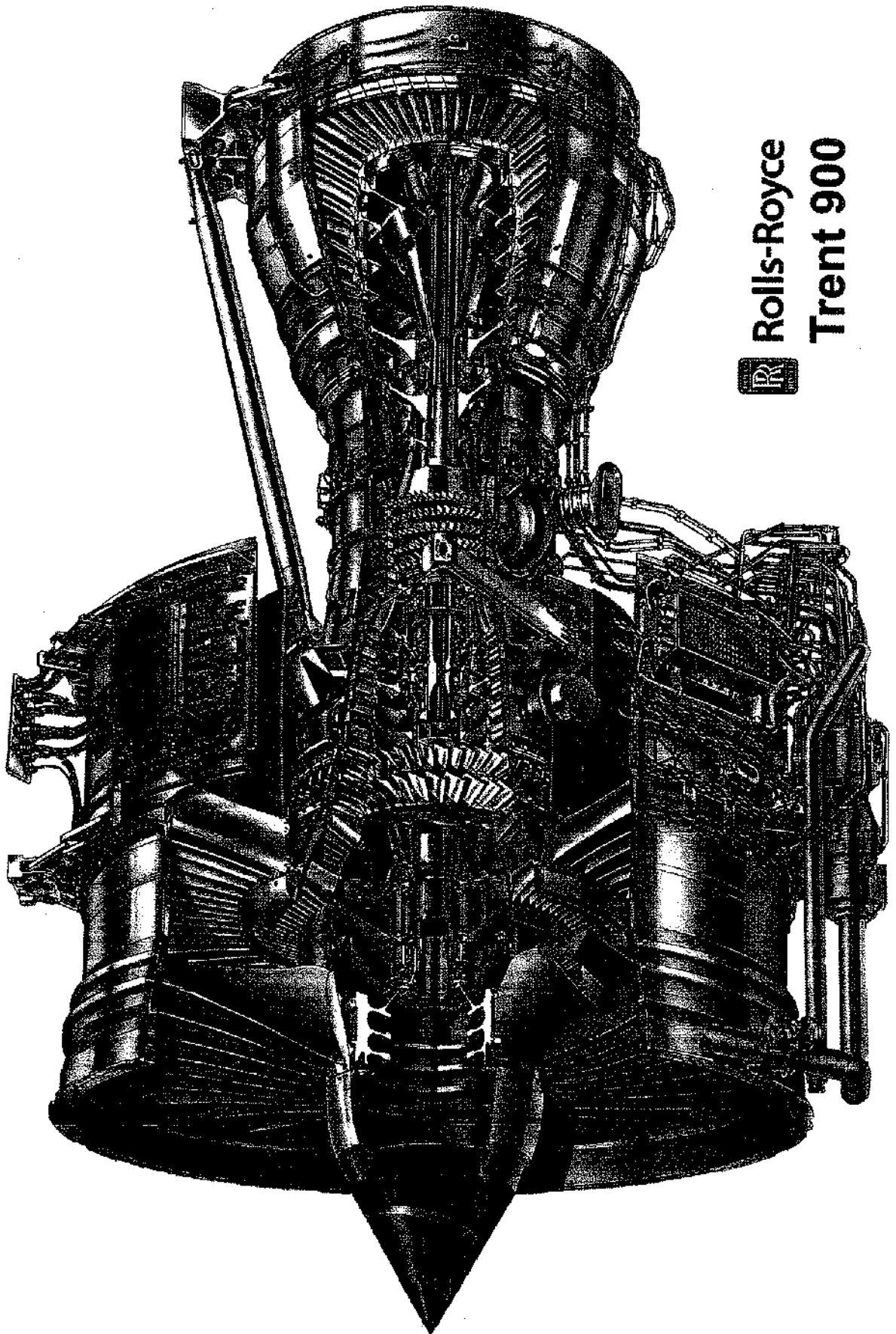
Close and personalized product support gives us better control of the product in the hands of our customers. It helps us to influence our customers to take decisive action when it is needed. It also gives us much better ability to monitor the condition of the product in its user environment, and to get earlier and better prognoses of actions we must take to be successful, and to make our customer successful with our product. There is an unusual synergism which results from personal, comprehensive, and professional product support.

In marketing any product, differentiation is one of the most important facets available. In expensive and technically-refined products, such as our engines, differentiation between the technical merits of the products is often very difficult. It often must use forecasts done by the engine manufacturers themselves, and put into the form of claims which are conflicting and confusing. It is not possible for customers to make comfortable decisions based upon what they can learn confidently, and much product distinction is lost.

In our business, superior product support provides dramatic capability for differentiation. In many competitions, we use our record in product support with incumbent customers, and we develop knowledge of our record in product support with new customers, and find that this provides the winning advantage. Product Support is a long term investment in gaining and keeping customers.

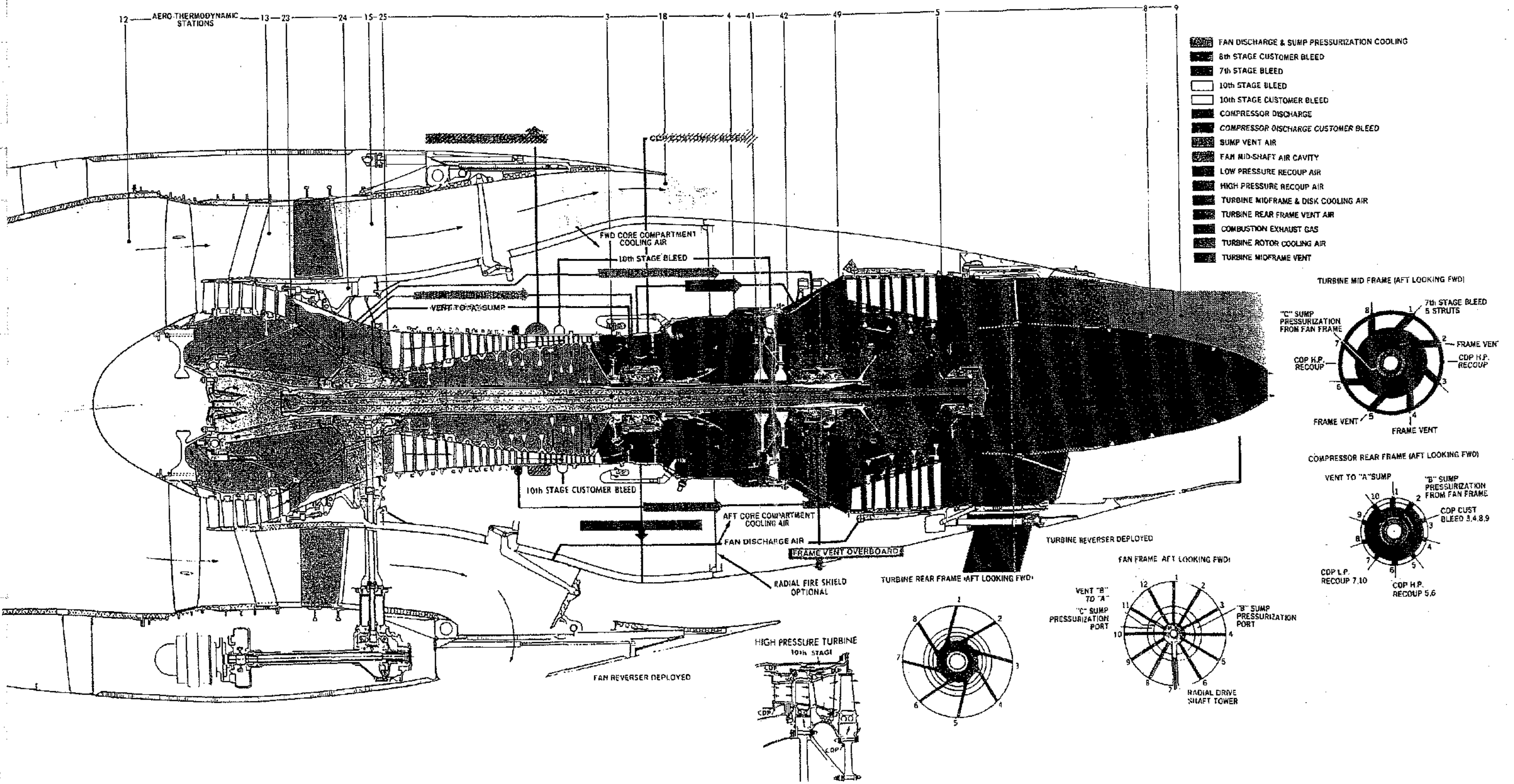
We are always concerned about measuring and directing this investment so that we achieve the most for the least investment. We hear, formally and informally, from our customers who have critical and constructive comments about the way we should support the product. On an annual basis, the customers are interviewed with a specific list of topics discussed to better determine what we need to do to improve our support of that customer. During competitions, much of the same kinds of information are discussed and figure greatly in the market decisions.

During the design phase of modern commercial engines, specialists from prospective and committed airline customers are enrolled in propulsion committees who help GE decide what the engine design should be, and what the support needs must be. All of these data are used to decide on personal Product Support plans, sometimes largely customized to fit the needs and desires of specific customers. Business plans are developed, representatives are trained and assigned, communications are established, and support attitudes are nurtured to make every customer successful, with his goals, with our product.



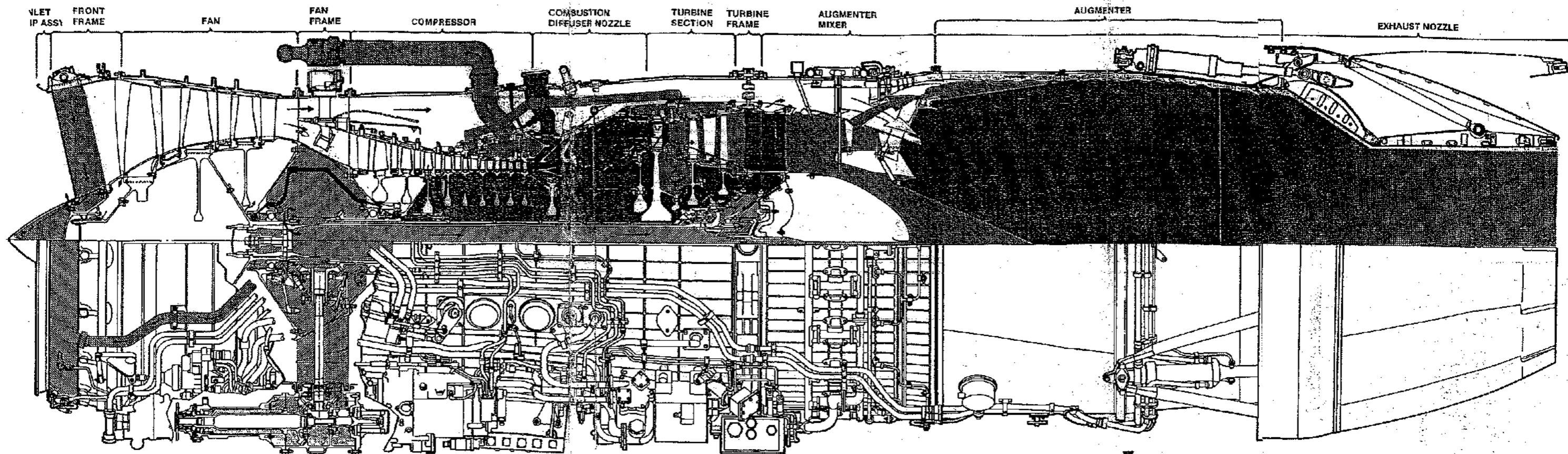
 **Rolls-Royce**
Trent 900

CF6-50 ENGINE AIRFLOW



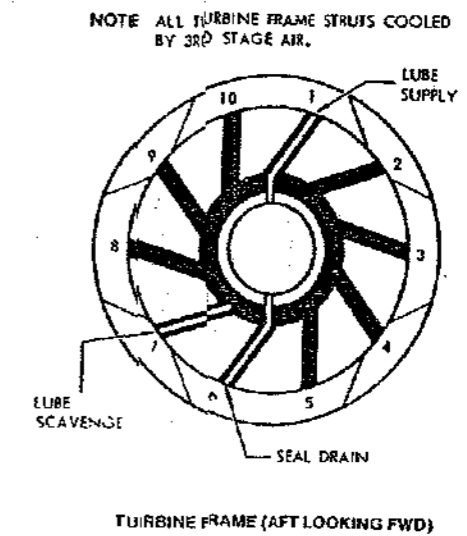
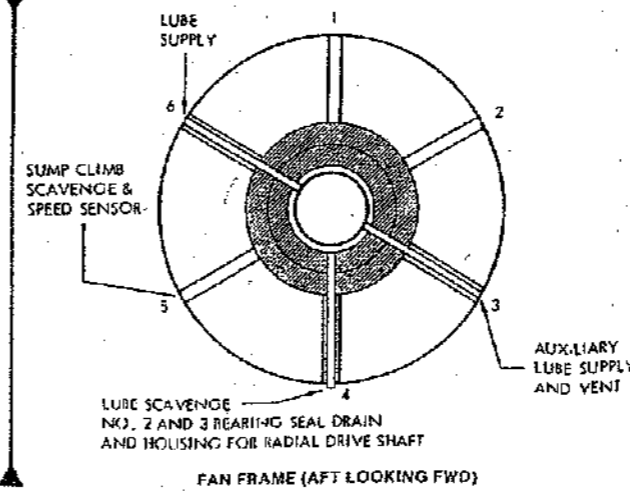
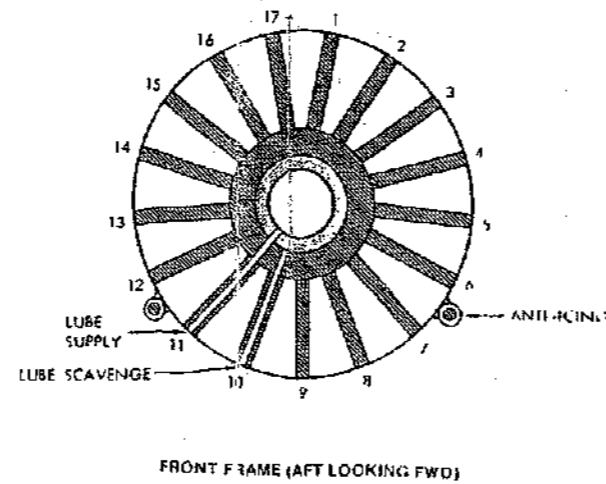
F110-GE-100 ENGINE AIRFLOW *~ 7:10*

GE



LEGEND

- | | | | |
|--|---|--|---|
| | FAN | | THIRD STAGE
(SUMP PRESSURIZATION
COMPRESSOR BORE,
TURBINE COOLING) |
| | FIFTH STAGE
(ANTI-ICING,
EPT COOLING) | | COMBUSTION |
| | NINTH STAGE
COMPRESSOR
DISCHARGE | | CORE GAS |
| | SUMP VENT | | AUGMENTER MIXED
FLOW |



NOTE ALL TURBINE FRAME STRUTS COOLED BY 3RD STAGE AIR.